This is a reproduction of a library book that was digitized by Google as part of an ongoing effort to preserve the information in books and make it universally accessible.

Google™ books

https://books.google.com

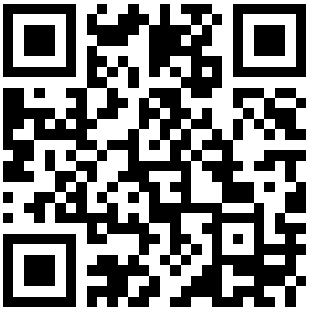

438,367

Digitized by Google

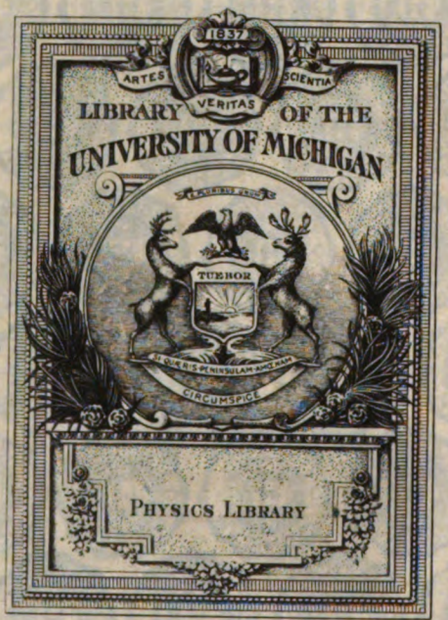


Digitized by Google

Digitized by Google

Digitized by Google

QC
1
.T256
C6

Digitized by Google

Digitized by Google

# THE NATIONAL PHYSICAL LABORATORY

## COLLECTED RESEARCHES

VOL. XVIII, 1924

LONDON:
PUBLISHED BY HIS MAJESTY'S STATIONERY OFFICE.

To be purchased directly from H.M. STATIONERY OFFICE at the following addresses:
Adastral House, Kingsway, London, W.C. 2; 28, Abingdon Street, London, S.W. 1;
York Street, Manchester; 1, St. Andrew's Crescent, Cardiff;
or 120, George Street, Edinburgh;
or through any Bookseller.

1925

*Price* 17*s.* 6*d. Net*

Digitized by Google

Digitized by Google

C.C
1
.T2:6
C6

Teddington, Eng.

THE

# NATIONAL PHYSICAL LABORATORY

## COLLECTED RESEARCHES

VOL. XVIII, 1924

LONDON:
PUBLISHED BY HIS MAJESTY'S STATIONERY OFFICE.

To be purchased directly from H.M. STATIONERY OFFICE at the following addresses:
Adastral House, Kingsway, London, W.C. 2; 28, Abingdon Street, London, S.W. 1;
York Street, Manchester; 1, St. Andrew's Crescent, Cardiff;
or 120, George Street, Edinburgh;
or through any Bookseller.

1925

*Price 17s. 6d. Net.*

Digitized by Google

Digitized by Google

# CONTENTS.

## VOL. XVIII.

Page

I. On the Magnetic Properties of Silicon Iron (Stalloy) in Alternating Magnetic Fields of Low Value. By ALBERT CAMPBELL, B.A., sometime Principal Assistant in the Electricity Department. (Reprinted from the 'Proceedings of the Physical Society of London', Vol. 32, 1920) . . 1

II. On the Self-Inductance of Single-Layer Flat Coils. By S. BUTTERWORTH, M.Sc., sometime Assistant in the Electricity Department. (Reprinted from the 'Proceedings of the Physical Society of London', Vol. 32, 1919) . . . . . 11

III. On the Use of Anderson's Bridge for the Measurement of the Variations of the Capacity and Effective Resistance of a Condenser with Frequency. By S. BUTTERWORTH, M.Sc., sometime Assistant in the Electricity Department. (Reprinted from the 'Proceedings of the Physical Society of London', Vol. 34, 1921) . . . . . 19

IV. Notes on Earth-Capacity Effects in Alternating-Current Bridges. By S. BUTTERWORTH, M.Sc., sometime Assistant in the Electricity Department. (Reprinted from the 'Proceedings of the Physical Society of London', Vol. 34, 1921) . . . . . 29

V. Capacity and Eddy-Current Effects in Inductometers. By S. BUTTERWORTH, M.Sc., sometime Assistant in the Electricity Department. (Reprinted from the 'Proceedings of the Physical Society of London', Vol. 33, 1921) . . . . . 41

VI. Eddy-Current Losses in Cylindrical Conductors with special Applications to the Alternating Current Resistances of Short Coils. By S. BUTTERWORTH, M.Sc., sometime Assistant in the Electricity Department. (Reprinted from the 'Philosophical Transactions of the Royal Society of London', A, Vol. 222, 1921) . . . . . 77

VII. Calculation of a Primary Standard of Mutual Inductance of the Campbell Type and Comparison of it with the Similar N.P.L. Standard. By D. W. DYE, B.Sc., A.C.G.I., Senior Assistant in the Electricity Department. (Reprinted from the 'Proceedings of the Royal Society', A, Vol. 101, 1922) . . . . . 122

VIII. The Measurement of the Electric Intensity of Received Radio Signals. By J. HOLLINGWORTH, M.A., B.Sc., A.C.G.I., A.M.I.E.E., Assistant in the Electricity Department. (Reprinted from the 'Journal of the Institution of Electrical Engineers', Vol. 61, 1923) . . . . . 141

IX. On the Measurement of Amplification given by Triode Amplifers at Audible and at Radio Frequencies. By F. E. SMITH, F.R.S., sometime Superintendent of the Electricity Department, and the late H. G. NAPIER, M.A., formerly Assistant in the Electricity Department. (Reprinted from the 'Proceedings of the Physical Society of London', Vol. 32, 1920) . . 161

X. The Maintenance of a Vibrating System by Means of a Triode Valve. By S. BUTTERWORTH, M.Sc., sometime Assistant in the Electricity Department. (Reprinted from the 'Proceedings of the Physical Society of London', Vol. 32, 1920) . . . . . 175

XI. On the Electro-Magnetic Screening of a Triode Oscillator. By R. L. SMITH-ROSE, Ph.D., M.Sc., A.M.I.E.E., Assistant in the Electricity Department. (Reprinted from the 'Proceedings of the Physical Society of London', Vol. 34, 1922) . . . . . 191

Digitized by Google

Page

XII. The Valve-Maintained Tuning Fork as a Precision Time-Standard. By D. W. Dye, B.Sc., A.C.G.I., Senior Assistant in the Electricity Department. (Reprinted from the 'Proceedings of the Royal Society', Vol. 103, 1923) . . . . . 207

XIII. A Self-Contained Standard Harmonic Wavemeter. By D. W. Dye, B.Sc., A.C.G.I., Senior Assistant in the Electricity Department. (Reprinted from the 'Philosophical Transactions of the Royal Society of London', A, Vol. 224, 1924) . . . . . 229

XIV. The Performance and Properties of Telephonic Frequency Intervalve Transformers. By D. W. Dye, B.Sc., A.C.G.I., Senior Assistant in the Electricity Department. (Reprinted from 'Experimental Wireless', Vol. 1, 1924) . . . . . 273

XV. On an Electro-Magnetic Method for the Measurement of the Horizontal Intensity of the Earth's Magnetic Field. By F. E. Smith, F.R.S., sometime Superintendent of the Electricity Department. (Reprinted from the 'Philosophical Transactions of the Royal Society of London', A, Vol. 223, 1922) . . . . . 317

XVI. A Precision Form of the Kelvin Electrostatic Voltmeter. By E. H. Rayner, Sc.D., M.I.E.E., Principal Assistant in the Electricity Department. (Reprinted from the 'Journal of the Institution of Electrical Engineers', Vol. 59, 1921) . . . . . 345

XVII. The Measurement of Reactive Power. By R. S. J. Spilsbury, B.Sc., A.C.G.I., Assistant in the Electricity Department. (Reprinted from 'B.E.A.M.A.', Vol. 13, 1923) . . . . . 355

XVIII. The Efficiency of Overlapping Joints in Copper and Aluminium Busbar Conductors. By S. W. Melsom, A.M.I.E.E., Principal Assistant, and H. C. Booth, A.R.C.S., Assistant, in the Electricity Department. (Reprinted from the 'Journal of the Institution of Electrical Engineers', Vol. 60, 1922) . . . . . 373

XIX. The Rating of Cables for Intermittent or Fluctuating Loads. By S. W. Melsom, A.M.I.E.E., Principal Assistant, and H. C. Booth, A.R.C.S., Assistant, in the Electricity Department. (Reprinted from the 'Journal of the Institution of Electrical Engineers', Vol. 61, 1923) . 393

XX. Carbon Arcs for Searchlights. By C. C. Paterson, O.B.E., M.I.E.E., A.M.Inst.C.E., sometime Principal Assistant; J. W. T. Walsh, M.A., M.Sc., A.M.I.E.E., F.Inst.P., Senior Assistant; A. K. Taylor, A.C.G.I., M.I.E.E., A.M.Inst.C.E., temporary Research Worker; and W. Barnett, Senior Observer, in the Electricity Department. (Reprinted from the 'Journal of the Institution of Electrical Engineers', Vol. 58, 1920) . . . . . 407

XXI. The Whitened Cube as a Precision Integrating Photometer. By H. Buckley, B.Sc., Assistant in the Electricity Department. (Reprinted from the 'Journal of the Institution of Electrical Engineers', Vol. 59, 1921) . . . . . 437

Digitized by Google

# ON THE MAGNETIC PROPERTIES OF SILICON IRON (STALLOY) IN ALTERNATING MAGNETIC FIELDS OF LOW VALUE

BY

ALBERT CAMPBELL, B.A.,
SOMETIME PRINCIPAL ASSISTANT IN THE ELECTRICITY DEPARTMENT.

Digitized by Google

## ABSTRACT.

Measurements are described of the hysteresis losses in silicon iron sheet and wires in very low alternating magnetic fields at low and telephonic frequencies using an alternating-current method described in a former Paper. The equations giving the hysteresis losses as a function of $B_{max.}$ are deduced in the case of the sheet material at low frequencies for ranges of $H_{max.}$ from 0·0002 to 0·02.

Comparisons are made between sheet material and wires of different diameters, and curves are given showing the great improvement in the permeability of wires when they are annealed.

The behaviour of the material is studied, both by ballistic tests and at telephonic frequencies, as regards the alternating field when direct-current fields of various values are applied at the same time.


Digitized by Google

# ON THE MAGNETIC PROPERTIES OF SILICON IRON (STALLOY) IN ALTERNATING MAGNETIC FIELDS OF LOW VALUE.

By ALBERT CAMPBELL, B.A., Sometime Principal Assistant in the Electricity Department.

[Reprinted from the 'Proceedings of the Physical Society of London', Vol. 32, 1920.]

## 1. *Introduction.*

The behaviour of magnetic materials, and in particular of silicon iron, at very low magnetizations, is of importance in telephony and radio telegraphy, as telephones and transformers in general have iron cores. The following investigation was carried out in 1916 and 1917 for the Board of Invention and Research, and is now published by the kind permission of the Admiralty. The particular silicon iron tested was stalloy, made by Messrs. J. Sankey & Son.

As the hysteresis loss, with which we are here chiefly concerned, falls off more rapidly than the square of the flux-density **B**, it becomes so small at low magnetizations that it is difficult to measure it with accuracy. In Prof. E. Wilson's experiments,* to which we shall allude further below, the lowest value of **H** used was 0·0036. We succeeded in making measurements down to about $\mathbf{H}_{max.} = 0{\cdot}0002$. For this low value the total amount of power measured was of the order of one millionth of a microwatt. In addition to determinations of power loss both at low and telephonic (audio) frequencies, the difference in properties of wire and sheet samples was examined, and investigation was made of the effect of super-imposing on the small alternating field a much larger direct-current steady field.

## 2. *Hysteresis Loss at Low Frequencies.*

The silicon iron in the principal tests was in the form of ring stampings of Messrs. Sankey's stalloy sheet, about 0·4 mm. thick, insulated on one side. A number of these had been made up into a ring of mean diameter 7 cm. and section 3 sq. cm., with 10 windings of 10 turns each and 4 of 200 turns each, being, in fact, one of our small laboratory transformers.

With 10 primary turns and 800 secondary, various ballistic tests were made, but the sensitivity was not sufficient below values of **H** of about 0·02. Accordingly I had recourse to an alternating-current method which is very much more sensitive, and had been found very convenient for similar measurements of the power lost in the iron wrappings of loaded telephone cables. I have already described the method ('Proc. Phys. Soc.', vol. 22, p. 24, 1910), but a brief description here will make matters clearer.

The iron ring is wound with super-imposed primary and secondary turns $N_1$ and $N_2$ respectively, $m$ being the mutual inductance between them. They are connected, as shown

* 'Roy. Soc. Proc.', vol. 80, p. 548, June, 1908.



Digitized by Google

in Fig. 1, through the coils of a mutual inductometer D to a source of alternating current and a vibration galvanometer (G), a sliding contact E allowing a portion Q to be selected from a slide-wire or other suitable resistance connected to the junction of the coils of D. Let the primary current $I_1$ (by tuning or otherwise) be of sine wave form, and let the galvanometer be tuned to its frequency. The galvanometer deflection can now be reduced to zero by adjusting D and E to values M and Q respectively. When the eddy currents in the ring are small we have

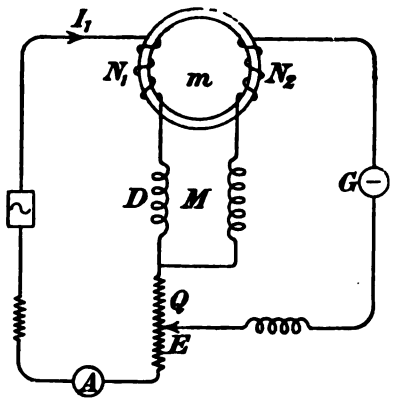

Fig. 1.

$$m = M,$$

and total iron loss

$$= \frac{N_1}{N_2}, QI_1^2.$$

Since $m = 4\pi \times 10^{-9} N_1 N_2 \mu s/l$, where $\mu$ is the permeability, $s$ the section and $l$ the mean circumference of the ring, we can at once find the permeability $\mu$ for various values of $I_1$ (and hence of **H**). The value of **H** is deduced from $I_1\sqrt{2}$, where $I_1$ is the effective value of the sine wave current (measured by the ammeter A).

The low-frequency tests were made chiefly at 10 and 75 ~ per second. At 10 ~ per second the oscillations of the light spot from the vibration galvanometer are easily visible, and extreme accuracy of reading can be obtained by adjusting until no tremor is perceptible.

With $\mathbf{H} = 0{\cdot}004$ at 10 ~ per second, M (and hence $\mu$) could be read with a sensitivity of 1 in 10,000, while the loss could be observed to 1 or 2 per cent. At 75 ~ per second the eddy-current loss forms a considerable fraction of the total power loss, being more than half the total at values of **H** below 0·0004. For both frequencies the eddy-current losses were calculated from the formula

$$h' \doteqdot 1{\cdot}64 \frac{(2a)^2 n^2 \mathbf{B}^2_{\max.}}{\sigma},$$

where $h'$ is in ergs per cubic centimetre per cycle, $\sigma$ is the resistivity (here about 57,000), $2a$ the thickness of the sheet, and $n$ the frequency.

For the upper values of **H** (about 0·01) the hysteresis loss thus derived is in good agreement for the two frequencies. At the lower range of **H** there is some divergence, the higher frequency giving the smaller values. In any case the eddy-current loss is of small importance at 10 ~ per second, and the result which we proceed to give has therefore been deduced only from the observations at this frequency.

Bearing in mind that $\mu$ remains nearly constant over the whole range of **H** dealt with, we deduce $\mathbf{B}_{\max.}$ from $\mathbf{B} = \mu\mathbf{H}$. If $h$ be the observed hysteresis loss (in ergs per cubic centimetre per cycle), when log $h$ was plotted against log **B**, the resulting curve was found

Digitized by Google

to be nearly a straight line. The results are quite well represented by the two following equations :—

| H range. | B range. | Equation. |
|---|---|---|
| 0·0002 to 0·002 | 0·051 to 0·51 | $h \doteqdot 6{\cdot}0 \times 10^{-6}\,\mathbf{B}^{2{\cdot}2}$ |
| 0·002 to 0·02 | 0·51 to 5·1 | $h \doteqdot 6{\cdot}6 \times 10^{-6}\,\mathbf{B}^{2{\cdot}40}$. |

These results refer only to the particular sample tested, for which the permeability $\mu$ over the range of **H** employed is about 254.

Prof. E. WILSON's ballistic tests on stalloy (of initial permeability about 260) for a range of **H** from 0·004 to 0·04 give

$$h \doteqdot 6{\cdot}9 \times 10^{-6}\,\mathbf{B}^{2{\cdot}30}.$$

Our own ballistic tests from $\mathbf{H} = 0{\cdot}015$ to 0·1 gave

$$h \doteqdot 14 \times 10^{-6}\,\mathbf{B}^{2{\cdot}4};$$

but magnetic viscosity effects somewhat complicate tests with slow cycles.

It appears that as **H** is lowered the index of **B** decreases slightly. I have little doubt that the constants will vary very considerably from sample to sample, but I think that the equations given represent the properties of good material ($\mu_0 = 254$). It may be mentioned that the values of the permeability obtained at 10 and 75 ~ per second were almost identical (within 4 parts in 1,000), rising from 254 at $\mathbf{H} = 0{\cdot}00008$ to 264·5 at $\mathbf{H} = 0{\cdot}01$.

### 3. *Power Loss at Telephonic Frequencies.*

By the same method, but using a telephone in place of the vibration galvanometer, similar tests were made both at 500 and 800 ~ per second, the values of the applied $\mathbf{H}_{max.}$ running from 0·0002 up to 0·1. When the logarithm of the total power loss was plotted against log $\mathbf{B}_{max.}$ the resulting curve was in each case an approximate straight line, the line for 500 ~ per second being parallel to but somewhat below that for 800 ~ per second. The hysteresis loss was calculated by the same formula as before, assuming uniform flux density in the material. The (log **B**, log $h$) curves at the two frequencies come to nearly the same straight line. This line is parallel to, but considerably above, the line given at 10 ~ per second, showing the effective hysteresis loss at 500 ~ per second to be about three times that at quite low frequencies. Whether this difference is due to magnetic viscosity, or to want of uniformity of **B** throughout the section of the material (skin effect), or to some omitted correction, is not clear; the point requires further elucidation.

In some of the experiments the material appeared to show a slightly lower initial permeability (*i.e.*, for $\mathbf{H} = 0$) at the higher frequencies, but this was probably due to effects of previous history which are discussed in § 5 below.

Digitized by Google

### 4. *Differences between Wire and Sheet Samples.*

With stalloy as supplied commercially we have noticed that various samples in the form of wire to not show nearly such good magnetic properties as the sheet material. This is unfortunate, as wires have advantages for certain types of core. The cause of the difference was investigated, and it appears to be due to insufficient annealing of the wire. Various samples of wire were annealed in hydrogen (or nitrogen) at a temperature of about 800° C. Some were tested in ring form, others in long, thin bundles placed (with a central search coil) in the middle of a long magnetizing solenoid. In all cases for the lower values of **H** the mutual inductance method was used. The results for the long bundles were corrected for the demagnetizing field due to the ends. The main effect of the annealing was to increase the permeability; the power losses for the same value of **B** did not show any marked improvement. Some of the results for permeability are shown in Fig. 2. The wires marked P and Q had diameters of 0·15 mm. and 0·40 mm. respectively.

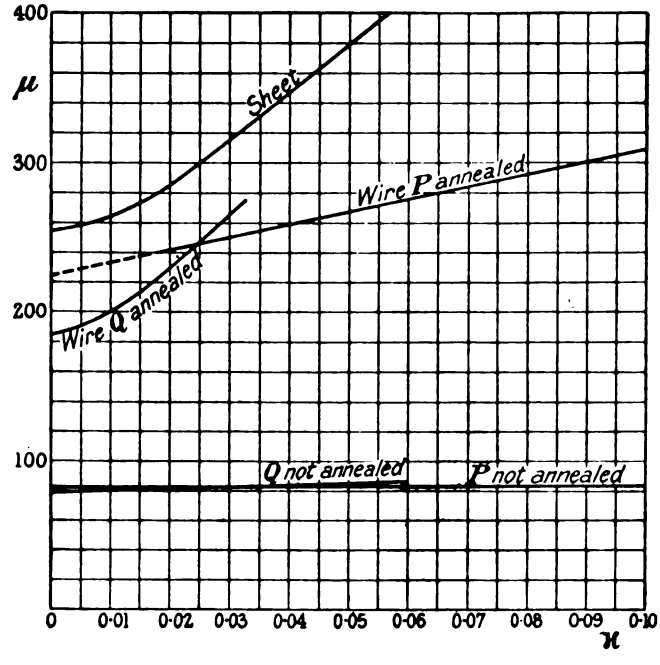


**Fig. 2.**

It will be noticed that the unannealed wires show very constant permeability for small values of **H**. The thicker wire (Q) behaves similarly to unannealed Swedish iron as given by Lord RAYLEIGH, for which $\mu = 81 + 64\,H$. The thinner wire (P) shows much greater constancy in permeability. The annealing makes a very great improvement in the wires, (P) annealed being almost as good as the sheet material. It is interesting to notice that it still retains a slower rate of increase of permeability for change of **H** than is shown by (Q) annealed. The wire (Q) after annealing is very like the very soft Swedish iron for which EWING gives $\mu = 183 + 1382\,H$.

It is clear that for practical purposes, except where constancy of $\mu$ is important, silicon iron wires should be carefully annealed.

Digitized by Google

### 5. *Effect of Super-imposed Direct-Current Field.*

In many cases in practice a core of magnetic material used with alternating magnetization may at the same time be subjected to a direct-current field—for example, in a telephone transformer used with a microphone receiver.

It is of interest therefore to investigate the effect of such a super-imposed field upon the behaviour of the magnetic material as regards the alternating field. For this purpose tests were made on the stalloy sheet and on the unannealed wire (P), both with ballistic galvanometer to represent quite slow frequencies (say, 2 ~ per second), and also at a frequency of 800 ~ per second. As a preliminary to these tests the ordinary permeability curve was determined for each of the materials. As will be seen from the $\mu$ curves in Fig. 3 for sheet and Fig. 4 for unannealed wire, the sheet material shows much higher permeability throughout than the unannealed wire.

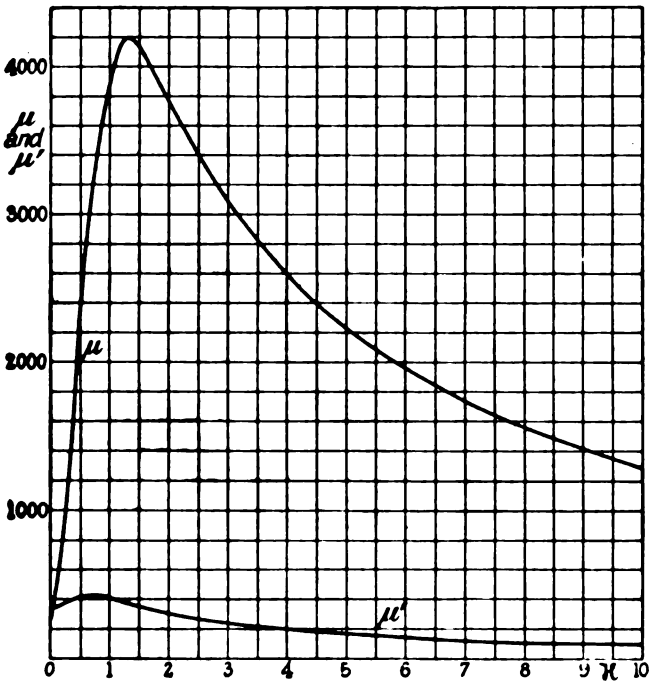


**Fig. 3.—Sheet Material.**

### 6. *Ballistic Tests with Small Super-imposed Cycles.*

In order to examine the effects at quite low frequencies, ballistic tests were made as follows:—The material was first demagnetized by repeated cycles of gradually diminishing **H**, and then brought into a steady cyclic state by many reversals of a given $\mathbf{H}_{max}$. The corresponding $\mathbf{B}_{max.}$ is known from the permeability curve already determined. When in the condition ($\mathbf{H}_{max.}$, $\mathbf{B}_{max.}$), the **H** is suddenly reduced by a small amount $\Delta\mathbf{H}$ by the introduction of a suitable resistance into the magnetizing circuit. By cutting this resistance out and in, a small cycle of amplitude $\Delta\mathbf{H}$ is super-imposed on the main

Digitized by Google

field $\mathbf{H}_{max.}$. This cycle was repeated 20 or 30 times to approximate to a steady state, and then the $\Delta\mathbf{B}$ corresponding to $\Delta\mathbf{H}$ was determined by the throw on a sensitive ballistic galvanometer.

In general $\Delta\mathbf{H}$ was not more than from 0·1 to 0·02 of $\mathbf{H}_{max.}$. The ratio $\Delta\mathbf{B}/\Delta\mathbf{H}$ was taken as the effective permeability $\mu'$ for the small cycle. The values obtained are plotted against $\mathbf{H}$ (the main field) in Figs. 3 and 4. At the lower values of $\mathbf{H}$ (and where the $\mathbf{H}$, $\mu$ curve is rising steeply) the previous history of the material has large effect on $\mu'$, and the experimental results are a little uncertain. For each material, however, the $\mu'$ at the lower values of $\mathbf{H}$ is distinctly approaching the initial permeability $\mu_0$ got by the more direct methods.

An examination of the curves shows that, for small slow cycles, the effective permeability $\mu'$ is considerably increased as the main field is raised. But before $\mathbf{H}$ has reached

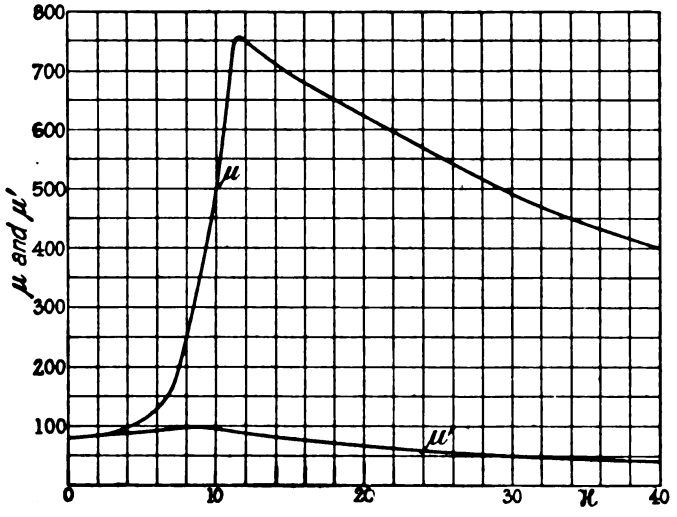


**Fig. 4.—Unannealed Wire.**

the region of maximum $\mu$, $\mu'$ has begun to fall off again, and, as $\mathbf{H}$ goes on increasing, it soon falls below its initial value. There is every reason to believe that when $\mathbf{H}$ has risen to saturation value $\mu'$ will have fallen to the value unity. It is evident that the presence of direct-current magnetization (above the maximum permeability point) may produce very serious reduction in the effective permeability for small cycles. The effect for silicon iron turns out to be very similar to that shown for ordinary hard and soft iron, in the experiments of the late Lord RAYLEIGH.*

### 7. *Tests at Telephonic Frequency.*

The mutual inductance method is easily adapted to measurements with super-imposed direct-current magnetization, which we may designate the "main field". The main

* 'Phil. Mag.', 1887. Reference ought also to be made to Prof. E. WILSON's experiments on the magnetization of stalloy when screened from the earth's field. ('Roy. Soc. Proc.', vol. 90, 1914, and vol. 93, 1917.)

Digitized by Google

field and the small alternating field can be measured quite independently, as shown in Fig. 5.

The part comprising the iron ring G, the mutual inductometer M, the resistance Q (with potential slider) and the telephone T is the same as before, with the addition of the condenser C in the telephone circuit to prevent direct current from getting through the secondary winding of G round the telephone circuit. The small alternating current $I_1$ passing through the primary winding of G is measured by means of the thermo-ammeter A connected through the air-core transformer *a*, the combination being calibrated for the frequency used, which was 800 ~ per second. The source of the alternating current is an electric trumpet buzzer Z linked to the circuit by the variable mutual inductance X. This transformer does not contain iron, in order to ensure that direct current through its secondary coil shall not affect the alternating component. K is an adjustable condenser to give approximate tuning, so that the magnetizing current $I_1$ shall be nearly of sine wave form.

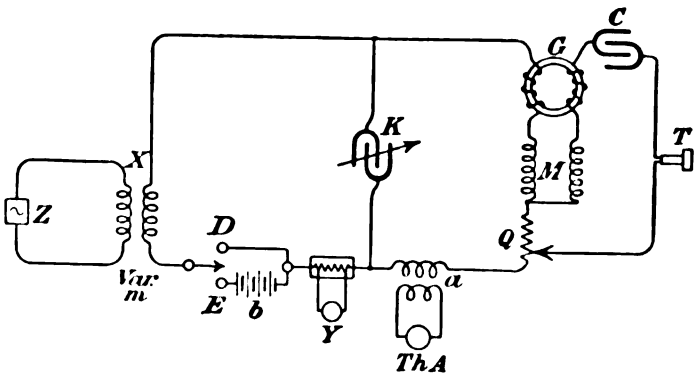


Fig. 5.

The direct-current component $I_0$ is introduced by switching from D to E, thereby bringing the battery *b* into the circuit. $I_0$ is measured by the Weston voltmeter Y with low resistance shunt, giving readings that are entirely unaffected by the presence of the alternating component. In general the alternating component was kept of the order of 3 to 7 milliamperes. For the sheet material this gave cyclic values of **H** from $\pm$ 0·006 up to $\pm$ 0·011. The applied direct-current field $\mathbf{H}_0$ could be varied from 0·06 up to 2·0. Usually $\mathbf{H}_0$ was reversed eight to ten times after any change, in order to attain a fairly cyclic condition.

The effect of the super imposed field on the permeability $\mu'$ was quite marked. As will be seen from the following table (for the sheet material), the changes in $\mu'$ at 800 ~ per second are very similar to those shown in Fig. 3 for very slow small cycles.

Very distinct time effects were observed. With the direct-current field, the value of the effective permeability gradually altered with time, sometimes rising slightly and sometimes falling, according to previous history and the position on the ($\mathbf{H}_0\mathbf{B}$) curve. When the direct-current field was removed, there was also a similar creeping effect,



Digitized by Google

TABLE.

| Time conditions of observation. | $H_0$, direct-current field. | $\mu'$ (for small cycles at 800 ~ per sec.). |
|---|---|---|
| | 0·0 | 260 |
| Immediate | 0·18 | 278 |
| ,, | 0·50 | 313 |
| ,, | 1·00 | 275 |
| ,, | 2·09 | 196 |
| One minute after direct current had been switched off | 0·00 | 247 |
| After standing for 20 hours | 0·00 | 225 |

fairly quick at first (*e.g.*, 4 per cent. change in a few minutes), and observable for several hours afterwards, even when the small alternating field was also removed, except for each moment of test. This latter creeping effect appeared always to bring the condition of the material backwards along the ($\mathbf{H}_0\mu'$) curve in Fig. 3. It did not appear to be due to tremors, for the application of fairly vigorous knocking did not seem to have much effect. The slow changes in $\mu'$ were easily observed, as the method is sensitive to 2 or 3 parts in 10,00. The effective permeability of the unannealed stalloy wire also showed similar alterations due to direct-current field, and these were in general agreement with the $\mu'$ curve of Fig. 4.

In all the experiments the total power loss was measured simultaneously with the permeability $\mu'$. It was found that the power loss was in general altered by the imposition of the direct-current field, but the whole of this change was accounted for by the observed change in permeability.

As already mentioned, the hysteresis loss for small values of **H** is practically the same in the unannealed as in the annealed material. In this connection it is interesting to mention that Mr. N. H. WILLIAMS (' Physical Review ', New Series, vol. 1, May, 1913) has observed that for small cycles of **H** (such as are here considered) there is little difference in the hysteresis losses for soft iron and glass hard steel.

In conclusion I would express my thanks to the Admiralty for kind permission to publish the above research, and to Mr. D. W. DYE for kind help in some of the experiments.

Digitized by Google

# ON THE SELF-INDUCTANCE OF SINGLE-LAYER FLAT COILS

BY

S. BUTTERWORTH, M.Sc.,

SOMETIME ASSISTANT IN THE ELECTRICITY DEPARTMENT.

Digitized by Google

ABSTRACT.

Two formulæ are established for the computation of the self-inductance of single-layer flat coils, one for the case when the inner and outer radii are not very different, and the other for the case of small inner radius. The two formulæ are shown to be consistent and capable of including all possible cases. From the formula a table is calculated which enables the inductance to be expressed in the form $L = Qn^2r^3$, in which $n$ is the number of turns per cm., $r$ the outer radius and Q is a tabulated function of the ratio of the inner and outer radii. Some applications of the table are given.

Digitized by Google

# ON THE SELF-INDUCTANCE OF SINGLE-LAYER FLAT COILS.

By S. BUTTERWORTH, M.Sc., Sometime Assistant in the Electricity Department.

[Reprinted from the 'Proceedings of the Physical Society of London', Vol. 32, 1919.]

1. The extended use of flat inductance coils in high-frequency electrical measurements renders desirable the development of simple formulæ for the predetermination of the inductance of such coils. A modification of Weinstein's formula* for coils of rectangular channel section has usually been employed for this purpose. This formula fails, however, when the inner radius is small.

It is the purpose of the present Paper to extend the modified Weinstein formula, to supply a formula suitable for coils of small inner radius, and to use the two formulæ to compute a table (Table I) for the use of designers of flat inductance coils. Some applications of this table are also given.

2. The method of obtaining the formulæ is one of integration, starting with a suitable formula for the mutual inductance between two coaxial co-planar circles.

Maxwell† has given two elliptic integral formulæ for the mutual inductance between two coaxial circles. When the circles are also co-planar these reduce to

$$M = 4\pi \sqrt{Aa}\,\{(2/k - k)\,K(k) - 2/kE(k)\}, \quad . \quad . \quad . \quad . \quad . \quad . \quad (1)$$

or

$$M = 8\pi A\,\{K(a/A) - E(a/A)\}, \quad . \quad . \quad . \quad . \quad . \quad . \quad . \quad . \quad . \quad . \quad (2)$$

in which K and E are complete elliptic integrals of the first and second kind respectively; $a$, A are the radii of the circles, and

$$k^2 = 4Aa/(A + a)^2.$$

In (2) $A > a$ always.

### 3. *Derivation of Extended Weinstein Formula.*

Let R be the mean radius of the flat coil, 2X be the coil depth, and $n$ be the number of turns per unit of length. Also let $m(x, r)$ be the mutual inductance between two coplanar coaxial circles, whose mean radius is $r$ and radius difference is $2x$. Then by summation of the mutual inductance between the elementary filaments of the flat coil the self-inductance of the latter is

$$L = 4n^2 \int_0^X dx \int_{R-X+x}^{R+X-x} m(x, r)\, dr. \quad . \quad . \quad . \quad . \quad . \quad . \quad . \quad . \quad (3)‡$$

* Weinstein, 'Wied. Ann.', XXI., p. 329, 1884: 'Bull. Bureau of Standards', VIII, p. 127, 1912.

† 'Electricity and Magnetism', vol. 2, p. 701.

‡ For the method of building up this integral, *see* Butterworth, 'Proc. Phys. Soc.', vol. 37. p. 376, 1915.

Digitized by Google

The integral (3) may be evaluated by expressing $m$ in terms of $x$ and $r$. The required expression may be derived from (1) by developing into a series involving only $k'$ the complementary modulus of $k$, for

$$k' = (1 - k^2)^{\frac{1}{2}} = (A - a)/(A + a) = x/r.$$

The suitable series* is

$$M = 4\pi r\left(\Phi_0 + \frac{1^2}{2^2}k'^2\Phi_1 + \frac{1^2 \cdot 1^2}{2^2 \cdot 4^2}k'^4\Phi_2 + \frac{1^2 \cdot 1^2 \cdot 3^2}{2^2 \cdot 4^2 \cdot 6^2}k'^6\Phi_3 + \ldots\right) \quad . \quad . \quad . \quad (4)$$

in which

$$\left.\begin{aligned} \Phi_0 &= \log_e 4/k' - 2 \\ \Phi_1 - \Phi_0 &= \tfrac{1}{1} + \tfrac{2}{1} \\ \Phi_2 - \Phi_1 &= \tfrac{1}{2} - \tfrac{2}{1} \\ \Phi_3 - \Phi_2 &= \tfrac{1}{3} - \tfrac{2}{3} \\ &\ldots\ldots\ldots \\ \Phi_n - \Phi_{n-1} &= \frac{1}{n} - \frac{2}{2n-3} \end{aligned}\right\}.$$

Applying (3) to the first four terms of (4)

$$L = 16\pi n^2 RX\left\{(\lambda - \tfrac{1}{2}) + \tfrac{2}{3}z^2(\lambda + \tfrac{4}{12}) + \tfrac{4}{4}\tfrac{4}{5}z^4(\lambda + \tfrac{9}{5}\tfrac{6}{5}) + \tfrac{1}{1}\tfrac{1}{6}\tfrac{3}{5}z^6(\lambda + \tfrac{9}{8}\tfrac{8}{6}\tfrac{5}{5}\tfrac{7}{2}\tfrac{3}{0}) + \ldots\right\} \quad (A)$$

in which

$$\lambda = \log_e 4R/X, \; z = X/4R.$$

The first two terms of this series constitute the modified WEINSTEIN formula.

The series converges for all possible values of X and R.

In the worst case when the inner radius is zero $X/R = 1$, and the value of the terms in { } of A are then

0·886 0·207 0·012 0·002.

Thus, assuming the four terms evaluated approximate sufficiently closely to the true sum, the WEINSTEIN formula gives a result about 1 per cent. low in the extreme case.

To verify this result a formula is now developed which is suitable for large values of X, that is, for a small inner radius of the flat coil.

4. Using MAXWELL'S second formula {(2) above)} and putting G for K − E, the flux $\Phi$ through a circle of radius $x$ in the plane of the coil is

$$8\pi n\left\{x\int_{r_1}^{x} G(a/x)\,da + \int_{x}^{r_2} aG(x/a)\,da\right\},$$

* BROMWICH, 'Quarterly Journal of Pure and Applied Mathematics', No. 176, p. 363, 1913; BUTTERWORTH, 'Phil, Mag.', vol. 31, p. 276, 1916.

Digitized by Google

in which $r_1$, $r_2$ are the inner and outer radii, or by a change of variables

$$\Phi = 8\pi n x^2 \left( \int_{r_1/x}^{1} \mathrm{G}(\mu)\, d\mu + \int_{x/r_2}^{1} \mathrm{G}(\mu)\, d\mu/\mu^3 \right). \quad . \quad . \quad . \quad . \quad . \quad . \quad . \quad (5)$$

The self-inductance of the flat coil is

$$\mathrm{L} = n \int_{r_1}^{r_2} \Phi\, dx,$$

so that, integrating (5) by parts

$$\mathrm{L} = \tfrac{16}{3}\pi n^2 r_2^3 \int_{\alpha}^{1} (1 - \alpha^3/\mu^3)\, \mathrm{G}(\mu)\, d\mu, \quad . \quad . \quad . \quad . \quad . \quad . \quad . \quad (6)$$

in which

$$\alpha = r_1/r_2.$$

The evaluation of (6) involves integration of K and E with respect to the modulus. The required integrations have been discussed by the author in an earlier Paper.*

Using the notation and results obtained therein, (6) reduces to

$$\mathrm{L} = \tfrac{8}{3}\pi n^2 r_2^3 \{u_1 - 1 - \alpha^3 (1 + v) - u + 2\alpha \mathrm{E} - \alpha (1 - \alpha^2) \mathrm{K}\}, \quad . \quad . \quad . \quad (7)$$

in which

$$u = \int_0^{\alpha} \mathrm{K}\, d\mu, \; v = \int_{\alpha}^{1} \mathrm{K}\, d\mu/\mu,$$

$$u_1 = \int_0^{1} \mathrm{K}\, d\mu = 1{\cdot}831931248 \ldots$$

(7) may be expressed in series by making use of the series for K, E, $u$, $v$, giving

$$\mathrm{L} = \tfrac{4}{3}\pi^2 n^2 r_2^3 [2(u_1 - 1)/\pi + \alpha^3 \{2(u_1 - 1)/\pi + \tfrac{1}{6} - \log 4/\alpha + \sigma\}] \quad . \quad . \quad (\mathrm{B})$$

in which

$$\sigma = 6 \sum_{1}^{\infty} \left( \frac{1 \cdot 3 \cdot 5 \ldots 2n - 1}{2 \cdot 4 \cdot 6 \ldots 2n} \right)^2 \frac{2n + 1}{2n(2n + 1)(2n + 3)} \alpha^{2n}.$$

This formula is most convergent when $\alpha$ is small and is thus suitable for coils having a small inner radius.

5. For the case of zero inner radius formula (B) gives

$$\mathrm{L} = 6{\cdot}96957 n^2 r_2^3,$$

formula (A) gives

$$\mathrm{L} = 6{\cdot}956 n^2 r_2^3,$$

while the first two terms only give

$$\mathrm{L} = 6{\cdot}87 n^2 r_2^3.$$

* 'Phil. Mag.', vol. 29, p. 584, 1915.

Digitized by Google

Thus, in the most unfavourable case for formula (A) the error is of the order 0·2 per cent., while the WEINSTEIN formula gives a result 1·5 per cent below the true value. For the case $\alpha = 0{\cdot}5$

$$L = 4{\cdot}743502 n^2 r_2^3 \text{ by (A)},$$

$$L = 4{\cdot}743500 n^2 r_2^3 \text{ by (B)}.$$

The two formula thus check each other.

For general computation formula (A) is usually the most rapid to work with, while formula (B) may be used as a check formula.

6. For practical calculations we may write

$$L = Q n^2 r_2^3, \quad \ldots \quad (C)$$

and tabulate Q as a function of $r_1/r_2$. This is done in Table I.

TABLE I.

| $r_1/r_2$. | Q. | $r_1/r_2$. | Q. | $r_1/r_2$. | Q. |
|---|---|---|---|---|---|
| 0·00 | 6·970 | 0·35 | 5·996 | 0·70 | 2·528 |
| 0·05 | 6·964 | 0·40 | 5·632 | 0·75 | 1·946 |
| 0·10 | 6·930 | 0·45 | 5·213 | 0·80 | 1·397 |
| 0·15 | 6·845 | 0·50 | 4·743 | 0·85 | 0·8892 |
| 0·20 | 6·728 | 0·55 | 4·231 | 0·90 | 0·4574 |
| 0·25 | 6·544 | 0·60 | 3·682 | 0·95 | 0·1394 |
| 0·30 | 6·300 | 0·65 | 3·105 | 1·00 | 0·0000 |

Self-inductance in centimetres $= Q n^2 r_2^3$.

$r_1$ = inner radius (centimetres). $n$ = turns per centimetre.

$r_2$ = outer radius (centimetres).

7. *Flat Coil of Best Time Constant.*

The (direct current) resistance of a flat coil wound closely with circular wire is

$$4\rho n^3 (r_2^2 - r_1^2) = 4\rho n^3 r_2^2 (1 - \alpha^2),$$

$\rho$ being the resistivity of the wire, so that the time constant is proportional to

$$Q r_2 / n (1 - \alpha^2).$$

Also for a given length and section of wire $r_2^2(1 - \alpha^2)$ and $n$ are fixed, and therefore (by eliminating $r_2$) the time constant is proportional to $Q (1 - \alpha^2)^{3/2}$. By calculating this quantity for various radius ratios we obtain the variation of time constant. It is found (*see* Table II) that the maximum time constant occurs when the inner radius is about

TABLE II.

| | | | | | | | | | | | |
|---|---|---|---|---|---|---|---|---|---|---|---|
| $\alpha = 0{\cdot}0$ | ... | 0·1 | ... | 0·2 | ... | 0·3 | ... | 0·4 | ... | 0·5 | |
| $Q/(1 - \alpha^2)^{3/2} = 6{\cdot}97$ | ... | 7·03 | ... | 7·15 | ... | 7·25 | ... | 7·32 | ... | 7·30 | |
| $\alpha = 0{\cdot}6$ | ... | 0·7 | ... | 0·8 | ... | 0·9 | ... | 1·0 | | | |
| $Q/(1 - \alpha^2)^{3/2} = 7{\cdot}18$ | ... | 6·94 | ... | 6·46 | ... | 5·50 | ... | 0·00 | | | |

Digitized by Google

2/5 the outer radius. The maximum is, however, very flat, the coil having 90 per cent. of the maximum efficiency if $r_1/r_2 < 0{\cdot}7$.

The best time constant for a single-layer *cylindrical* coil is obtained when the length ($b$) is 4/5 of the radius ($a$), and in that case $L = 14{\cdot}90n^2a^3$, $n$ again being the number of times per centimetre. For a flat coil of the best time constant

$$L' = 5{\cdot}632n^2r_2^3.$$

To compare the two cases we require the radius $a$ of the cylindrical coil which can be wound with the same length of wire as the flat coil. This is $a = 0{\cdot}725r_2$, with $r_1 = 0{\cdot}4r_2$.

Using this

$$L = 5{\cdot}666n^2r_2^3.$$

The cylindrical coil is thus slightly better than the corresponding flat coil.

### 8. *Mutual Inductance between Coaxial Co-planar Flat Coils.*

The mutual inductance between two coaxial flat coils in the same plane can be obtained from Table I as follows:—

Let the inner and outer radii of the $\left\{\frac{\text{inner}}{\text{outer}}\right\}$ coils be

$$\left\{\frac{r_1,\ r_2}{r_3,\ r_4}\right\}.$$

Denote the self-inductances of the two coils by $L_\alpha$, $L_\gamma$, and that of the coil which would fill the interspace by $L_\beta$. Denote the mutual inductances between these three coils by $M_{\alpha\beta}$, $M_{\beta\gamma}$, $M_{\gamma\alpha}$. Further, let $L_\alpha$, $L_\beta$ in series have self-inductance $L_A$; $L_\beta$, $L_\gamma$ in series have inductance $L_B$; $L_\alpha$, $L_\beta$, $L_\gamma$ in series have inductance $L_C$.

Then

$$L_A = L_\alpha + L_\beta + 2M_{\alpha\beta}, \qquad L_B = L_\beta + L_\gamma + 2M_{\beta\gamma},$$

$$L_C = L_\alpha + L_\beta + L_\gamma + 2M_{\alpha\beta} + 2M_{\beta\gamma} + 2M_{\gamma\alpha},$$

from which the three M's can be found since the L's are known from Table I.

In particular

$$M_{\alpha\gamma} = \tfrac{1}{2}(L_C - L_A - L_B - L_\beta),$$

or, in terms of Q,

$$M_{\alpha\gamma} = \tfrac{1}{2}n^2\{r_4^3(Q_{r_1/r_4} - Q_{r_2/r_4}) - r_2^3(Q_{r_1/r_2} + Q_{r_3/r_2})\}.$$

A simple case is where there is no interspace, and the inner coil has zero inner radius. Then

$$M = \tfrac{1}{2}n^2R^3\{Q_0(1-\alpha^3) - Q\},$$

in which $\alpha = r/R$, R is the outer radius, $r$ the dividing radius.



Digitized by Google

In order to give some idea of the magnitude of the various inductances, the following table has been calculated from the above formula :—

TABLE III.—Mutual Inductances between Flat Coils.

| $\alpha$. | $L_1/n^2R^3$. | $L_2/n^2R^3$. | $M/n^2R^3$. | $k$. |
|---|---|---|---|---|
| 0·1 | 0·00697 | 6·93 | 0·0162 | 0·074 |
| 0·2 | 0·0557 | 6·73 | 0·0930 | 0·152 |
| 0·3 | 0·1880 | 6·30 | 0·240 | 0·220 |
| 0·4 | 0·446 | 5·63 | 0·446 | 0·280 |
| 0·5 | 0·871 | 4·74 | 0·678 | 0·333 |
| 0·6 | 1·503 | 3·68 | 0·892 | 0·379 |
| 0·7 | 2·39 | 2·53 | 1·025 | 0·421 |
| 0·8 | 3·56 | 1·397 | 1·005 | 0·451 |
| 0·9 | 5·08 | 0·457 | 0·715 | 0·470 |
| 0·92 | 5·23 | 0·317 | 0·611 | 0·474 |
| 0·94 | 5·79 | 0·1910 | 0·495 | 0·470 |
| 0·96 | 6·17 | 0·0942 | 0·356 | 0·465 |
| 0·98 | 6·56 | 0·0272 | 0·192 | 0·454 |
| 1·00 | 6·97 | 0·0000 | 0·000 | 0·000 |

$L_1$ = Self-inductance of inner coil.
$L_2$ = Self-inductance of outer coil.
$M$ = Mutual inductance between coils.
$k$ = Coefficient of coupling = $M/\sqrt{L_1L_2}$.
$r$ = Dividing radius.
$\alpha = r/R$.
$n$ = Turns per centimetre.

Digitized by Google

# ON THE USE OF ANDERSON'S BRIDGE FOR THE MEASUREMENT OF THE VARIATIONS OF THE CAPACITY AND EFFECTIVE RESISTANCE OF A CONDENSER WITH FREQUENCY

BY

S. BUTTERWORTH, M.Sc.,

SOMETIME ASSISTANT IN THE ELECTRICITY DEPARTMENT.

Digitized by Google

## ABSTRACT.

An analysis of the effect of residuals and earth capacities in Anderson's inductance-capacity bridge is made, and it is shown that if balances are obtained

(*a*) by balancing the bridge with *direct* currents ;

(*b*) by making the alternating current adjustments by means of a small series resistance ($s'$) and parallel condenser ($C'$) in the condenser arm ;

then the changes required in $s'$ and $C'$ to hold the balance at different frequencies are equal and opposite to the variations of the effective (series) resistance and capacity of the condenser with frequency.

The assumptions made in obtaining the above conclusions are that the residual inductances and resistances of the " non-inductive " arms of the bridge are invariable with frequency and that the resistance of the inductive arm varies as the square of the frequency. No knowledge of the absolute values of the residuals, etc., is required for the method.

The method is illustrated by results obtained with a condenser of capacity 0·5 $\mu$F, and details are given showing how the chief experimental trouble, viz., drift in D.C. balance owing to temperature variations, may be overcome.


Digitized by Google

# ON THE USE OF ANDERSON'S BRIDGE FOR THE MEASUREMENT OF THE VARIATIONS OF THE CAPACITY AND EFFECTIVE RESISTANCE OF A CONDENSER WITH FREQUENCY.

By S. BUTTERWORTH, M.S.c, Sometime Assistant in the Electricity Department.

[Reprinted from the 'Proceedings of the Physical Society of London', Vol. 34, 1921.]

## I.—*Introduction.*

Although Anderson's bridge has been used frequently in precision measurements of inductance and capacity and the effects of the residual inductances of the arms have been discussed,* a valuable property of this bridge seems to have been overlooked. An examination of the equations of balance of this bridge in which the effects of residuals are included shows that if the balancing adjustments are carried out in a particular manner, the only factors which necessitate a readjustment of balance at various frequencies of current are—

(*a*) the variation of the capacity of the condenser with frequency,

(*b*) the variation of the effective resistance of the condenser with frequency,

(*c*) the variation of the inductance with frequency.

The assumptions upon which the above conclusions are based are that the resistances and residual inductances (or capacities) of the "non-inductive" arms are invariable with frequency and that the resistance of the inductive arm has a term varying as the square of the frequency.

The observed variations of adjustment with frequency may therefore be used to determine the frequency variations of capacity and effective resistance of a condenser, the frequency coefficient of the inductance being supposed given. This frequency coefficient may be determined by a measurement of the self capacity of the inductive coil if the coil is of stranded wire. The absolute magnitudes of the residuals need not be known if the only quantities required are the *variations* of capacity and effective resistance of the condenser.

## II.

Anderson's bridge is shown in Fig. 1(*a*) in which $X_1$, $X_2$, $X_3$, $X_4$ are resistances having small inductances, $X_5$ is an inductive coil and $X_6$ is the condenser under test. If $X_3$ is zero the bridge becomes Maxwell's inductance-capacity bridge (Fig. 1(*b*)). The latter bridge may also be derived from Anderson's bridge by converting the "star" combination $X_1$, $X_2$, $X_3$ to its equivalent "mesh,"†

$$X'_1, X'_2, X'_3 = (X_3X_1 + X_1X_2 + X_2X_3)/X_2, X_1, X_3, \quad . \quad . \quad . \quad . \quad (1)$$

the arm $X'_3$ acting as a shunt across the detector.

* Rosa and Grover, 'Bull. Bureau of Standards', vol. 1, p. 291, 1905.

† G. A. Campbell, 'Trans., Am.I.E.E.', vol. 30, p. 891, 1911.

Digitized by Google

It will first be shown that small constant residuals in the arms $X_1$, $X_2$, $X_3$ convert to small constant residuals in the equivalent arms $X'_1$, $X'_2$, $X'_3$ and then the complete conditions of balance, including residuals, in Maxwell's bridge will be obtained.

Let

$$\mathbf{X}_n = \mathbf{R}_n + j\omega l_n \quad (n = 1, 2, 3).$$

Then

$$\begin{aligned}\mathbf{X}'_1 &= \mathbf{X}_1 + \mathbf{X}_3 + \mathbf{X}_1\mathbf{X}_3/\mathbf{X}_2 \\ &= \mathbf{R}_1 + \mathbf{R}_3 + j\omega\,(l_1 + l_3) + (\mathbf{R}_1 + j\omega l_1)\,(\mathbf{R}_3 + j\omega l_3)/(\mathbf{R}_2 + j\omega l_2) \\ &= \mathbf{R}_1 + \mathbf{R}_3 + \mathbf{R}_1\mathbf{R}_3/\mathbf{R}_2 + j\omega\,\{l_1(1 + \mathbf{R}_3/\mathbf{R}_2) + l_3(1 + \mathbf{R}_1/\mathbf{R}_2) - l_2\mathbf{R}_1\mathbf{R}_3/\mathbf{R}_2^2\}\end{aligned}$$

to the first order of small quantities,

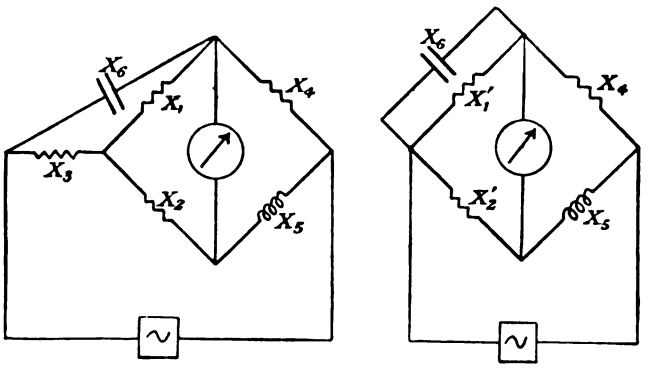


Fig. 1. (*a*) Anderson's Bridge. (*b*) Maxwell's Bridge.

Hence if $l'_1$, $l'_2$, $l'_3$ are the residual inductances of the equivalent arms $X'_1$, $X'_2$, $X'_3$

$$\left.\begin{aligned} l'_1 &= l_1\,(1 + \mathbf{R}_3/\mathbf{R}_2) + l_3\,(1 + \mathbf{R}_1/\mathbf{R}_2) - l_2\mathbf{R}_1\mathbf{R}_3/\mathbf{R}_2^2 \\ l'_2 &= l_2\,(1 + \mathbf{R}_3/\mathbf{R}_1) + l_3\,(1 + \mathbf{R}_2/\mathbf{R}_1) - l_1\mathbf{R}_2\mathbf{R}_3/\mathbf{R}_1^2 \\ l'_3 &= l_1\,(1 + \mathbf{R}_2/\mathbf{R}_3) + l_2\,(1 + \mathbf{R}_1/\mathbf{R}_3) - l_3\mathbf{R}_1\mathbf{R}_2/\mathbf{R}_3^2 \end{aligned}\right\} \quad . \quad . \quad . \quad . \quad . \quad (2)$$

If $l_1$, $l_2$, $l_3$ are invariable with frequency, then to the first order of small quantities $l'_1$, $l'_2$, $l'_3$ are also invariable.

For analytical simplicity it is convenient in certain cases to replace residual inductances by residual capacities. Thus if $l$ is the residual inductance of a resistance R, the equivalent residual capacity acting as a shunt is

$$c = -\,l/\mathrm{R}^2. \quad . \quad . \quad . \quad . \quad . \quad . \quad . \quad . \quad . \quad . \quad . \quad (3)$$

### III.—*Conditions of Balance in Maxwell's Bridge.*

Maxwell's bridge is re-drawn in Fig. 2 with the residuals included.

$\mathrm{R}_1$ is a resistance having residual inductance $l$; $\mathrm{R}_2$ is an inductive coil of inductance L; $\mathrm{G}_2$ is a conductance with residual capacity $c$; $\mathrm{G}_1$ is a conductance shunting the condenser C, its residual capacity being included in C. The condenser C has leakage conductance $g$.

Digitized by Google

If the bridge is earthed at the point E the earth capacities (assumed to be sufficiently represented by condensers connecting the branch points to earth) are either included in $c$, C or are thrown across the whole bridge.

The vector equation of balance when using currents of frequency $\omega/2\pi$ is

$$(G_1 + g + j\omega C)/(G_2 + j\omega c) = (R_2 + j\omega L)/(R_1 + j\omega l), \quad . \quad . \quad . \quad . \quad (4)$$

from which the two conditions of balance are

$$(G_1 + g)R_1 - \omega^2 lC = G_2R_2 - \omega^2 Lc, \quad . \quad . \quad . \quad . \quad . \quad . \quad . \quad . \quad (5)$$

$$CR_1 + l(G_1 + g) = cR_2 + LG_2. \quad . \quad . \quad . \quad . \quad . \quad . \quad . \quad . \quad (6)$$

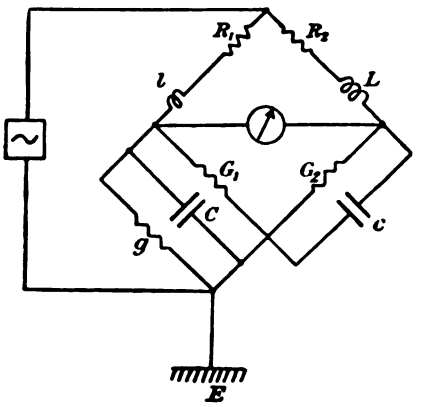


Fig. 2. Maxwell's Bridge, including Residuals.

Now let the parallel combination of capacity C shunted by conductance $g$ be replaced by its equivalent series combination of capacity K in series with resistance $s$, so that

$$g = s\omega^2K^2/(1 + \omega^2s^2K^2), \qquad C = K/(1 + \omega^2s^2K^2). \quad . \quad . \quad . \quad . \quad . \quad (7)$$

Since normally $s\omega K$ will seldom exceed $0{\cdot}001$, we may write to an accuracy $10^{-6}$

$$g = s\omega^2C^2, \qquad K = C, \quad . \quad . \quad . \quad . \quad . \quad . \quad . \quad . \quad . \quad (8)$$

and the two conditions of balance are now

$$G_1R_1 + \omega^2(C^2sR_1 - lC + Lc) = G_2R_2, \quad . \quad . \quad . \quad . \quad . \quad . \quad . \quad . \quad (9)$$

$$CR_1 = LG_2 - lG_1 + cR_2, \quad . \quad . \quad . \quad . \quad . \quad (10)$$

products of residuals being ignored.

## IV.

Apart from the variations of C and $s$ with frequency all the factors in the above equations are invariable with frequency except $R_2$ and L, and for a stranded wire coil we may write

$$L = L_0(1 + \alpha\omega^2), \qquad R_2 = R_0(1 + \beta\omega^2). \quad . \quad . \quad . \quad . \quad . \quad . \quad (11)$$

Suppose now that the condition

$$G_1R_1 = G_2R_0 \quad . \quad . \quad . \quad . \quad . \quad . \quad . \quad . \quad . \quad . \quad (12)$$

Digitized by Google

has been satisfied by balancing with *direct* currents. Then, using (11) and (12) and ignoring products of small quantities, (9) and (10) become

$$C^2sR_1 - lC + L_0c = G_2R_0\beta, \quad . \quad . \quad . \quad . \quad . \quad . \quad . \quad . \quad . \quad . \quad (13)$$

$$CR_1(1 - \alpha\omega^2) = L_0G_2 - lG_1 + cR_0. \quad . \quad . \quad . \quad . \quad . \quad . \quad . \quad . \quad (14)$$

If, therefore, the alternating current balance is secured by having a small adjustable air condenser C′ in parallel with C and a small adjustable resistance $s'$ in series, equations (13) and (14) show that *for all frequencies* $s + s'$ *and* $C(1 - \alpha\omega^2) + C'$ *are constant.*

The variations required in $s'$ and C′ to restore balance at the various frequencies will therefore be equal and opposite to the variations of $s$ and $C(1 - \alpha\omega^2)$.

## V.—*Bridge Details for Effective Resistance Measurements.*

The bridge arrangements when used for the measurement of the variations in effective resistance of ½ microfarad condensers are shown in Fig. 3. The arms corresponding to $X_1$, $X_2$ in Fig. 1(*a*) were similar non-inductive coils each of 100 ohms. The inductive arm was made up of an inductance coil $R_2$, L and a non-inductive 10-ohm resistance. The coil L consisted of a single layer 7/36 stranded wire coil of inductance 780 microhenries

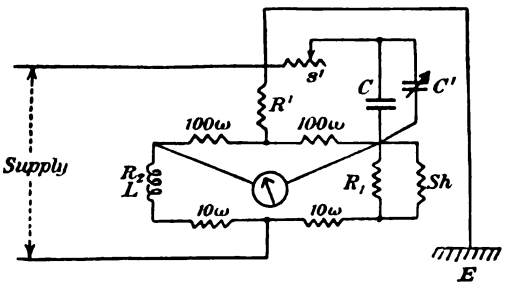


Fig. 3. Anderson's Bridge for Effective Resistance of ½ μF Condensers.

and resistance approximately 2·6 ohms. Its self-capacity, including the connecting leads, was 20 micro-microfarads, so that its increase in effective inductance at a frequency of 2,000 cycles per second was $3/10^6$. The arm adjacent to the inductive arm was made up of a non-inductive 10-ohm coil and a non-inductive copper coil $R_1$ of resistance slightly greater than that of the coil $R_2$. The coil $R_1$ was shunted by a resistance box (Sh.). The inductive coil $R_2$ and the copper coil $R_1$ were enclosed in the same wool-lined box so that their temperature variations would be as nearly as possible identical, the function of $R_1$ being to balance any changes of resistance due to temperature variations of $R_2$. (*See* Section VII.)

C was the condenser under test of nominal value ½ microfarad. It was shunted by an adjustable air condenser C′ whose capacity ranged from 60 to 260 micro-microfarads, and the combination was in series with a constant inductance rheostat $s'$ ranging from 0·1 to 1·1 ohms which could be read to 0·001 ohm. The resistance R′ corresponding to $X_3$ in Fig. 1(*a*) was for purposes of preliminary balancing. It could be adjusted by steps of 0·01 ohm to 100 ohms.

Digitized by Google

## VI.—*Modifications for the Measurement of Variations of Capacity with Frequency.*

The above arrangements required modification when the capacity variations were being studied. Any inductance in the condenser arm will introduce a frequency variation in the effective capacity of this arm, so that the presence of the constant inductance rheostat $s'$ in the condenser arm is a disadvantage. However, the direct current balancing condition is no longer of importance, so that if $s'$ is transferred to the inductive arm $R_2$ and the fine adjustments are made by $s'$ in $R_2$ and C′ in parallel with C, then, since in (14) we may replace $R_0$ by $R_2$ to the order of accuracy required, small variations of $R_2$* will only introduce second order errors in the capacity equation as $R_2$ is associated only with the residual capacity $c$. The capacity arm C may then be made to include only the condenser and its leads, and only a small correction is required for the inductance of the leads.

These modifications were accordingly used when capacity variations were being measured.

## VII.—*Temperature Variations.*

The chief source of trouble in the effective resistance measurements was the difficulty experienced in holding the direct-current balance throughout the alternating-current adjustments, the balance tending to drift because of the large temperature coefficient of the resistance of the inductive coil in $R_2$. This difficulty was largely overcome by the use of the balancing coil $R_1$ of Fig. 3, both $R_1$ and $R_2$ being shielded from stray temperature variations by enclosing them together. It was found necessary also to shield the leads to these coils. For similar reasons the current supplied to the bridge, whether direct or alternating, was made to have the same R.M.S. value. Even with these precautions a small drift in balance often occurred, so that observations were taken in a definite order, and a correction applied for want of D.C. balance. An examination of equation (9) shows that a departure from condition (12) introduces an error in $s$ proportional to $1/\omega^2$, and is thus more serious at the lower frequencies. For this reason it was found advisable to take the lower frequency observations immediately after securing the D.C. balance. Also by deliberately throwing the D.C. balance out of adjustment and observing the change in $s'$ required to re-balance with alternating currents of known frequency, the correction for a given want of balance could be determined. The method is illustrated by the following example.

## VIII.—*Example showing Correction for Drift in D.C. Balance.*

Sh $\fallingdotseq$ 400 ohms. $R_1 \fallingdotseq 3$ ohms.

An increase of 10 ohms in Sh causes an increase in deflection of the D.C. galvanometer of 35 divisions, and to restore the A.C. balance at a frequency of 500 ~ per second requires a diminution in $s'$ of 0·129 ohm.

* It is essential, however, that $R_2$ shall remain of constant *inductance* throughout the adjustments, so that $s'$ must be of the type specified.



Digitized by Google

Hence for a want of balance represented by 1 division of the scale of the D.C. galvanometer the correction on $s' = 0{\cdot}0037$ ohm.

The correction is applied as in the following table :—

| Time. Min. | D.C. observations. | | A.C. observations. | | Deduced. | |
|---|---|---|---|---|---|---|
| | Source. | Galvo. deflections. | Frequency. | $s'$ ohms. | Galvo. zero. | Want of balance. |
| 0 | + | + 2·0 | ... | ... | ... | ... |
| 1 | − | + 4·0 | ... | ... | +2·8 | ... |
| 2 | + | + 1·0 | ... | ... | ... | −1·8 |
| 4 | ... | ... | 500 | 0·520* | ... | ... |
| 6 | + | − 5·0 | ... | ... | ... | −7·5 |
| 7 | − | +10·0 | ... | ... | +2·5 | ... |
| 8 | + | − 5·0 | ... | ... | ... | ... |

Want of balance at moment of A.C. observation = −4·6.

Therefore corrected $s' = 0{\cdot}520 - 0{\cdot}0037 \times 4{\cdot}6$

$= 0{\cdot}503$ ohm.

IX.—*Typical Results for the Change in Effective Resistance of a* 0·5 $\mu F$ *Condenser.*

Preliminary adjustments are made by R′ and Sh, and the remaining adjustments at *all* frequencies by $s'$ and C′ only, observations being taken as in the above table. The following results were obtained in a typical case :—

Condenser I (0·5 $\mu$F).

Bridge current = 30 milliamperes.

| | | | | | |
|---|---|---|---|---|---|
| Frequency ~ per second .. | 500 | 800 | 1,000 | 1,600 | 2,000 |
| $s'$ ohms .. .. .. .. | 0·503 | 0·597 | 0·625 | 0·675 | 0·685 |
| $s$ ohms .. .. .. .. | 0·287 | 0·193 | 0·165 | 0·115 | 0·105 |
| Power factor $\omega sC$ .. | $10^{-4} \times 4{\cdot}5$ | 4·8 | 5·2 | 5·8 | 6·6 |

The values of $s$ have been obtained from the known value of $s$ for this condenser at a frequency of 1,600 ~ per second,† and the law $s + s' =$ constant for all frequencies.

X.—*Typical Results for the Variation in Capacity of a* 0·5 $\mu F$ *Condenser.*

The rheostat $s'$ is removed from the condenser arm, and placed in series in the arm $R_2$. After preliminary adjustments by R′ and Sh the fine adjustments and adjustments

* Mean of source and telephone reversals.

† Butterworth, 'Proc. Phys. Soc.', vol. 33, p. 346, 1921.

Digitized by Google

for different frequencies are made by $s'$ and C′ only. The following results hold for condenser I :—

| Frequency. ~ per sec. | C′* μμF. | $C-C_{1000}$ Uncorrected μμF. | Correction μμF. | $C-C_{1000}$ corrected μμF. |
|---|---|---|---|---|
| 500 | 132 | +46 | + 3 | +49 |
| 675 | 154 | +24 | + 2 | +26 |
| 830 | 164 | +14 | + 1 | +15 |
| 1,000 | 178 | 0 | 0 | 0 |
| 1,170 | 185 | − 7 | − 1 | − 8 |
| 1,510 | 193 | −15 | − 3 | −18 |
| 2,000 | 193 | −15 | −10 | −25 |

The correction in the fourth column is for the variation of the inductive coil L with frequency and for the residual inductance of the leads to the condenser. As regards the latter, if λ is the inductance of the leads, the effective capacity of the whole condenser arm is C $(1 + \omega^2\lambda C)$. In the above observations $\lambda = 0{\cdot}38$ microhenry, so that using $C = \frac{1}{2}$ μF.,

$$\omega^2\lambda C = 30 \times 10^{-6}$$

at a frequency of 2,000 cycles per second. Now the correction due to L (section 5) is $3 \times 10^{-6}$ and (equation 14) acts oppositely to the λ correction, so that the whole correction is $27 \times 10^{-6}$ at 2,000 ~ per second. For a $\frac{1}{2}$ μF condenser this leads to a negative

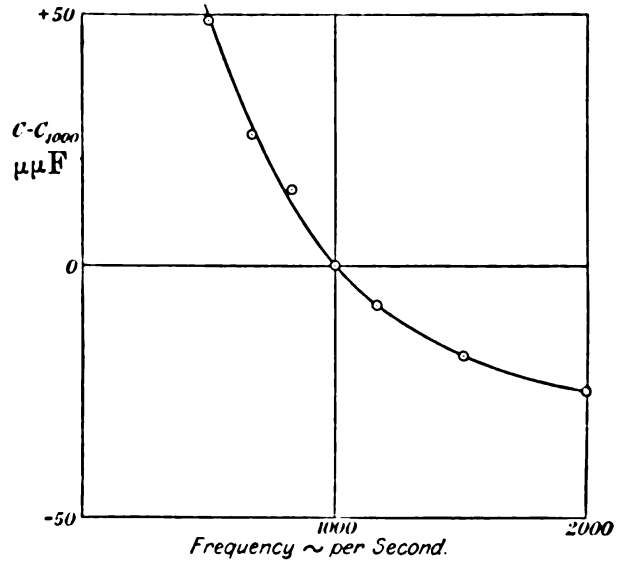


Fig. 4. Change of Capacity of $\frac{1}{2}$ μF Condenser with Frequency.

correction of 13·5 μμF. The corrections for the lower frequencies follow from the square law. The corrected variations are plotted against frequency in Fig. 4. It is seen that the smoothed curve never differs by more than five parts in a million from the observed values.

* Mean of source and telephone reversals.



Digitized by Google

Digitized by Google

# NOTES ON EARTH CAPACITY EFFECTS IN ALTERNATING-CURRENT BRIDGES

BY

S. BUTTERWORTH, M.Sc.,

SOMETIME ASSISTANT IN THE ELECTRICITY DEPARTMENT.

Digitized by Google

## ABSTRACT.

It is shown that an earth capacity acting at any point in the arm of a bridge may be replaced by two earth impedances acting at the ends of the arm together with an impedance in series with the arm. By integration the result is extended to small distributed capacities.

Two methods are given for the elimination of the error due to the end impedances. Complete elimination can only be obtained by the use of shields connected to the ends of the bridge arm.


Digitized by Google

# NOTES ON EARTH CAPACITY EFFECTS IN ALTERNATING CURRENT BRIDGES.

By S. BUTTERWORTH, M.Sc., Sometime Assistant in the Electricity Department.

[Reprinted from the 'Proceedings of the Physical Society of London', Vol. 34, 1921.]

## I.

In precision measurements with alternating-current bridges it is always necessary to eliminate the effects due to the capacity of the various portions of the apparatus with regard to earth. The effect of these capacities is that the network with which we are dealing is not that composed of the visible arms, but includes other arms connecting various points to earth, and therefore different parts of the bridge to each other. Unless these earth paths are allowed for, different balances will be obtained as the bridge-earth conditions are changed. If it may be assumed that the earth capacities are sufficiently represented by condensers connecting the branch points of the bridge to earth, then there are two methods of eliminating the effect of these capacities in bridges which are reducible to one of the Wheatstone bridge type. These methods are described in sections II and III below. The remainder of the Paper deals with the validity of the assumption in regard to earth capacities acting in the middle of an arm and in regard to distributed capacities. It is shown that the elimination is not complete by the two methods adopted. The error due to the incomplete elimination is not, however, serious if the parts of the apparatus are not brought too near to large masses of conductors connected to (or near to) earth, as the earth capacities tend rapidly to a constant value, and therefore behave as practically constant residuals in various bridge measurements. The effect is, therefore, that a different interpretation must be given to the residuals from that usually assumed. The residual inductance of a resistance coil, for example, is not merely that due to the magnetic field and its own intercapacity, but also includes a term which depends on the distributed capacity of the coil to earth. If in all measurements the coil is made to have the same position with regard to earth, no discrepancy will appear when the coil is used in different bridges. This portion of the residual must, however, be taken into account in calculated standards of high resistance.

### II.—*Elimination of Earth Capacities by the "Wagner" Earthing Device.*

The Wagner earthing arrangement as applied to a generalised Wheatstone bridge is shown in Fig. 1. $a$, $b$, $c$, $d$ are the impedances of the arms of the bridge, while $e$ and $f$ are impedances so chosen that the relations $e/f = a/b = c/d$ may be approximately satisfied. The junction between $e$ and $f$ is connected to earth. Assuming that earth capacities or leakages may be represented by impedances connecting the branch points

Digitized by Google

to earth, this earth point causes the paths of the earth currents to pass from the points 1, 2, 3, 4 to the point 5. The paths 5–1, 5–3 will merely modify the impedances $e$ and $f$, but the paths 5–2, 5–4 will produce currents disturbing the balancing conditions if the points 2, 4, 5 are at different potentials. The procedure consists in bringing the points 5, 2, 4 to the same potential by successively adjusting the main bridge and the impedances $e$ and $f$ until the detector indicates balance whether connected to the point 2 or the point 5.*

### III.—*Corrections for Earth Capacities by Alteration of Earth Point.*

Let the symbols in Fig. 2 denote admittances, $\alpha$, $\beta$ being the admittances of the earth paths.

Let two balances be made ($a$) with the admittance C infinite, ($b$) with the admittance $c$ finite. Suppose the balances secured by adjustment of A. Then, if $A_1$ and $A_2$ are the two adjustments of A, while $A_0 = BX/Y$, we have

$$\frac{A_1 + \beta}{B + \alpha} = \frac{X}{Y} = \frac{A_2 + \mu\beta}{B + \mu\alpha},$$

in which

$$\mu = 1 + \frac{A_2 + B}{C}.$$

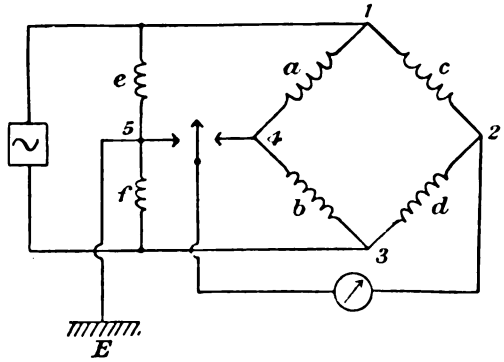


Fig. 1. Wagner Earthing Arrangement.

Hence, eliminating $\beta/\alpha$

$$\frac{X}{Y} = \frac{A_2 - \mu A_1}{B(1 - \mu)} \quad \text{or} \quad A_0 = \frac{A_2 - \mu A_1}{1 - \mu}.$$

If C is chosen to consist of an arm equivalent to $A_2$ and B in parallel, $\mu = 2$ and

$$A_1 = A_0 + (A_2 - A_1).$$

* The device was originally applied for the purpose of eliminating the " head " effect when using a telephone as detector in the comparison of small capacities by the Wien bridge. It has been extended to other bridges, particularly the Carey-Foster bridge, by Mr. D. W. Dye. The scheme given by G. E. Moore (' Electrician ', June 17, 1921) is defective.

Digitized by Google

If $a_0$, $a_1$, $a_2$ are the corresponding impedances and $a_1 - a_2$ is small,

$$a_1 = a_0 + a_2 - a_1,$$

or, regarding $a_0$ as the unknown,

$$a_0 = 2a_1 - a_2.$$

The change in adjustment from $a_1$ to $a_2$ thus doubles the error, and the method, therefore, also gives a measure of the earth capacity effect. It must be remembered in applications that $a_1$ and $a_2$ are vector impedances, and therefore each adjustment is a double adjustment.

This method suffers from the following disadvantages as compared with the Wagner method :—

(*a*) The body must be kept in the same position in both adjustments when a telephone is being used as detector.

(*b*) It is impossible in certain cases to secure a zero balance. This occurs sometimes in the measurement of small capacities by the Carey-Foster method.

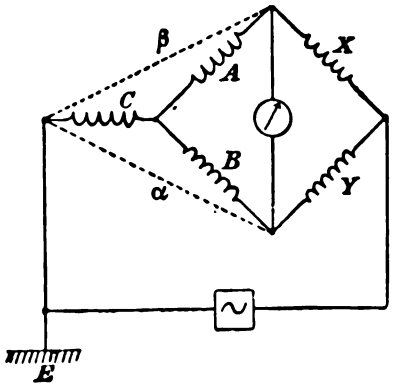


Fig. 2. Correction for Earth Capacity by Alteration of the Earth Point.

The second difficulty may be overcome in the Carey-Foster bridge by using an auxiliary condenser for the zero balance and then placing the condenser to be measured in parallel with the auxiliary condenser.

It has the following advantages over the Wagner method :—

(*a*) Two adjustments only are necessary instead of a series of adjustments.

(*b*) An estimate may be made of the errors due to earth capacities.

The same auxiliary apparatus is required as in the Wagner method, the series arms *e* and *f* of the Wagner arrangement becoming paralleled to form C in the arrangement of Fig. 2.

### IV.—*Earth Capacities in Compounded Arms.*

The assumption that earth capacities may be represented by earth paths from the branch points of the bridge will now be examined.



Digitized by Google

If an arm is made up of several elements, appreciable earth capacities may be located at the junctions of these elements. This is particularly the case when there is a fairly large mass of metal at the junction, as in the case of condensers in series with a resistance or inductance. Even terminals may in certain cases produce an appreciable effect.*

Let an arm consist of two series elements of impedance $\alpha$, $\beta$ having an earth path of impedance $\gamma$ at their junction. Transformation (A)† converts the arrangement to an arm of impedance $\alpha + \beta + \alpha\beta/\gamma$, with two end earth paths of impedances $(\alpha\beta + \beta\gamma + \gamma\alpha)/\beta$,$(\alpha\beta + \beta\gamma + \gamma\alpha)/\alpha$ respectively at the outer ends of $\alpha$ and $\beta$. If one of the methods described has been used to eliminate earth capacities, the effects of the end impedances are eliminated, but there is an uneliminated portion behaving as a residual $\alpha\beta/\gamma$ in series in the arm $\alpha + \beta$.

Thus, let $\alpha$, $\beta$ be two "non-inductive" resistances connected through a massive terminal.

If $c$ is the earth capacity of the terminal, $R_1$, $R_2$ the values of the resistances, the uneliminated earth effect behaves as a residual inductance, $cR_1R_2$.

With resistances of 1,000 ohms, and with $c = 1\,\mu\mu F$, this residual inductance is $1\,\mu H$.

If $\alpha$ is a coil of resistance R and inductance L, while $\beta$ is a condenser of capacity C, then at a frequency $\omega/2\pi$

$$\alpha\beta/\gamma = \frac{c}{C}(R + j\omega L),$$

or the uneliminated portion of the earth capacity at the junction introduces an error in the power factor of the condenser C of an amount $\omega cR$, and causes the inductance to appear too large by an amount $cL/C$.

In illustration, let $c = 50\ \mu\mu F$, $R = 100$ ohms, $\omega = 10^4$. The error in power factor is then $5/10^5$. Large earth capacities at the junction should, therefore, be avoided by shielding the condenser and connecting the shield to that terminal of the branch point which is connected to the condenser.

## V.—*Distributed Earth Capacities.*

Suppose the earth capacity to be small and let it be distributed uniformly throughout the arm. Suppose also that the impedance is distributed uniformly.

Then if $\Gamma$ is the whole earth admittance and X the whole impedance of the arm of length $l$, the earth admittance $\Gamma\delta x/l$ of an element $\delta x$ situated at a distance $x$ along the arm contributes a series impedance $\Gamma X^2 x(l - x)\delta x/l^3$, and end earth admittances $\Gamma(l - x)\delta x/l^2$, $\Gamma x\delta x/l^2$ to the arm, these results being obtained by transformation (A) retaining only first order quantities. With the same approximation the earth paths of all the elements may be treated as acting independently, so that by integration the

* A terminal approximating in size to a sphere of 1 cm. radius has an earth capacity of the order 1 $\mu\mu F$.

† Transformations (A) and (B) are described in the author's Paper on "Capacity and Eddy-Current Effects in Inductometers" ('Proc. Phys. Soc.', vol. 33, p. 312, 1921).

Digitized by Google

whole distributed earth admittance is represented by a series impedance of amount $\frac{1}{6}\Gamma X^2$, and two equal end admittances each of amount $\frac{1}{2}\Gamma$. The former is equivalent to a negative admittance $\frac{1}{6}\Gamma$, acting as a shunt across the arm.

We conclude that the uneliminated portion of the distributed earth capacity behaves as a negative residual capacity in parallel with the arm of an amount equal to $\frac{1}{6}$ the whole earth capacity.

## VI.—*Calculation of Earth Capacity.*

Let a resistance be made of flat strip forming a loop of length $2a$, width $2b$ (Fig. 3).

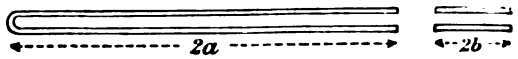


Fig. 3.

If $b/a$ is small the system may be treated as an elliptic disc of semi-axes $a$ and $b$. Now the capacity of an elliptic disc is $a/\mathrm{K}(\sqrt{1 - b^2/a^2})$ where $\mathrm{K}(k)$ is the complete elliptic integral of the first kind to modulus $k$. Further, if the elliptic disc is divided into narrow strips of equal width parallel to the minor axis, each strip will have the same charge when the potential of the whole disc is raised, so that in the limiting case the capacity of the strip is uniformly distributed throughout the length $a$. Further, when $b/a$ is small

$$\mathrm{K}(\sqrt{1-b^2/a^2}) \doteqdot \log_e 4a/b,$$

so that the whole earth capacity of the strip is $a/\log_e 4a/b$ electrostatic units.

In illustration let $a = 10$ cm., $b = 0{\cdot}5$ cm. Then the earth capacity is $10/4{\cdot}4$ cm. $= 2{\cdot}3$ cm. $= 2{\cdot}6$ $\mu\mu$F.

The above result may be applied to give an approximate value of the earth capacity

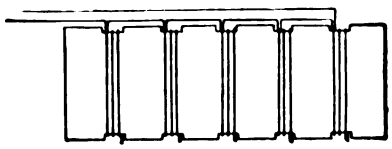

Fig. 4.

of a resistance wound in the manner shown in Fig. 4, a form often adopted to avoid large self-capacities in high-resistance coils. The resistance consists of several separate loops wound on a mica card.

If each segment has a winding length of 3 cm. and winding width of 0·5 cm., the whole earth capacity of each segment would be about 1 $\mu\mu$F, so that if a 1,000-ohm coil is made up of 10 segments each of 100 ohms, the whole earth capacity would be about 10 $\mu\mu$F. When measured on a bridge in which end capacities are eliminated, the uneliminated portion would contribute an inductance of the order 1·7 $\mu$H.



Digitized by Google

## VII.—*Non-uniformly Distributed Capacity.*

The factor $\frac{1}{6}cR^2$ for the residual inductance introduced into a resistance R having earth capacity $c$ has been obtained upon the assumption of uniform distribution. If the distribution is denser towards the outer ends of the coil, the above estimate is too high, while if the capacity tends towards the middle, the estimate is too low. If the coil is of the form of a circular disc, the effect may be calculated. Let a "non-inductive" coil be formed of two oppositely wound disc coils laid over each other.

If $a$ is the radius of the coils, the whole earth capacity is $2a/\pi$ electrostatic units, of which half is associated with one coil and half with the other. The density of distribution at distance $r$ from the centre is proportional to $1/\sqrt{a^2 - r^2}$. Now if $l$ is the length of wire in one coil, and $x$ the length of wire between radii $r$ and $a$, $l/x = a^2/a^2 - r^2$, so that the density of distribution at a wire distance $x$ from the outer end is proportional to $x^{-\frac{1}{2}}$. Hence we write for the capacity per unit length $Ax^{-\frac{1}{2}}$, where since $A\int_0^l x^{-\frac{1}{2}}dx$ is the whole capacity of one coil $(a/\pi)$, $A = a/2\pi\sqrt{l}$.

Again, by the method of section 4, if $\rho$ be resistance per unit length, the residual inductance due to the earth capacity of one coil is

$$\rho^2 A\int_0^l \sqrt{x}\,(l-x)\,dx = \frac{4}{15}\rho^2 A l^{\frac{1}{2}} = \frac{2}{15}\frac{a}{\pi}R^2,$$

R being the total resistance of one coil.

The equivalent outer end capacity is

$$\frac{A}{l}\int_0^l (l-x)\,dx/\sqrt{x} = \frac{4}{3}\sqrt{l} = \frac{2}{3}\frac{a}{\pi},$$

and the equivalent inner end capacity is $\frac{1}{3}\frac{a}{\pi}$.

Now let the two oppositely wound coils be connected at their inner ends. The earth capacities of the combination are equivalent to three earth capacities each of magnitude $\frac{2a}{3\pi}$ joining the ends and centre to earth together with a residual inductance $\frac{a}{15\pi R^2}$ (R now referring to the resistance of the whole combination). By transformation (A) the central earth capacity converts to a series inductance $\frac{a}{6\pi R^2}$, and two end capacities each of magnitude $\frac{1}{3}a/\pi$. Hence writing $c$ for the whole earth capacity so that $c = 2a/\pi$, the whole effect is equivalent to a residual inductance $7cR^2/60$, together with two equal end capacities $\frac{1}{2}c$.

If the outers had been joined, the final system would have been a residual inductance $7cR^2/30$, and equal end capacities $\frac{1}{2}c$.

The effect of interchanging the end connections is thus to double the residual inductance effect.

Digitized by Google

## VIII.—*Distributed Earth Capacities in Inductive Coils.*

Let an earth path of impedance, $\zeta$, be present between two coils having impedances $\xi$, $\eta$ and mutual impedance $m$ {(*a*) Fig. 5}. By transformation (A) the mutual impedance, $m$, may be removed {(*b*) Fig. 5}, and then by transformation (B), the mesh $\alpha$. $\beta$. $\gamma$ {(*c*) Fig. 5} is obtained in which

$$\alpha = \xi + \eta + 2m + \frac{(\xi + m)(\eta + m)}{\zeta + m},$$

$$\beta = \xi + \zeta + 2m + \frac{(\xi + m)(\zeta + m)}{\eta + m},$$

$$\gamma = \eta + \zeta + 2m + \frac{(\eta + m)(\zeta + m)}{\xi + m}.$$

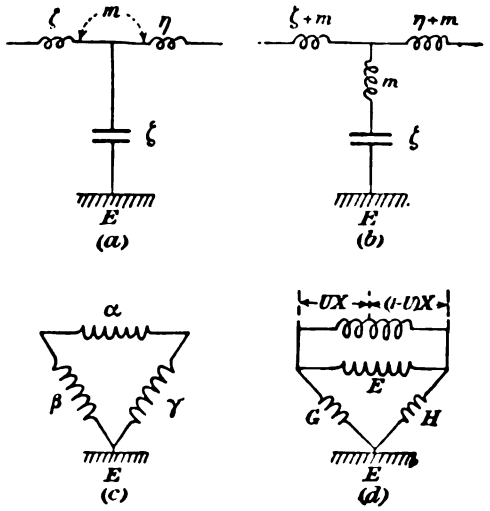


Fig. 5.

If $\zeta$ is large compared with $\xi$, $\eta$, $m$, then to the first order

$$\alpha = \xi + \eta + 2m + \frac{(\xi + m)(\eta + m)}{\zeta},$$

which (again to the first order) is equivalent to the original two coils paralleled by an admittance

$$-\frac{1}{\zeta}\frac{(\xi + m)(\eta + m)}{(\xi + \eta + 2m)^2},$$

while

$$\frac{1}{\beta} = \frac{1}{\zeta}\frac{\eta + m}{\xi + \eta + 2m}, \qquad \frac{1}{\gamma} = \frac{1}{\zeta}\frac{\xi + m}{\xi + \eta + 2m}.$$

In the case of distributed earth capacities there are an infinite number of paths such as $\zeta$, and the above procedure may be applied to each, as to the first order of small quantities each path acts independently.

Digitized by Google

For an element of length $d\lambda$ of the coil, $1/\zeta$ will be of the form $Zd\lambda$ where Z is the earth admittance per unit length of the coil in the neighbourhood of the element. If X is the whole impedance of the coil, $X = \xi + \eta + 2m$, so that, writing $\xi + m = UX$, the whole distributed earth admittances may be replaced, by a shunt of admittance F, together with two end earth admittances G, H; F, G, H having the values

$$F = -\int ZU(1-U)\,d\lambda,$$

$$G = \int X(1-U)\,d\lambda,$$

$$H = \int ZU\,d\lambda.$$

With pure earth capacities Z is of the form $j\omega C$ while U is a complex quantity, being the ratio of the potential difference up to the point $\lambda$ to the whole potential difference between the ends of the coil. Hence except with special types of winding the equivalent

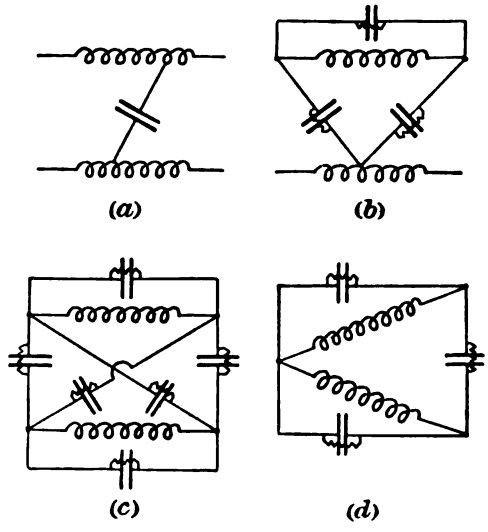


Fig. 6. Replacement of Pure Intercapacity by End System of Leaky Condeners.

end earth admittances and shunt admittance replacing a pure distributed capacity are not pure capacities, but rather behave as capacities having leakage.

## IX.

A similar theory may be developed in regard to distributed intercapacities. The theory is sufficiently illustrated by Fig. 6.

A single pure capacity C {(*a*) Fig. 6} is replaced by three imperfect capacities in (*b*). The capacities $C_2$, $C_3$ are then transformed to the capacity system shown in (*c*) Fig. 6, so that to the first order this system of six leaky condensers is sufficient to represent the distributed capacity effects of two inductive coils.

Digitized by Google

For a single coil suppose the two coils to have a common point. The system then reduces to (*d*), Fig. 6. Finally the two condensers joining the ends to the common point are replaced by their equivalent end condensers, giving a single imperfect condenser across the whole coil, replacing the distributed pure capacity.

## X.

The general conclusions arrived at are that the ordinary methods of eliminating earth capacities do not completely eliminate the earth effect, either if the effect is distributed or if appreciable earth capacities are introduced in the middle of an arm. So long as the whole arm remains a single unit in various bridge measurements no discrepancies will arise unless the earth condition of the arm is considerably altered. If, however, the arm is split in transference from one bridge to another, discrepancies may appear with high resistances and small capacities. By providing shields in these cases, and arranging that the shields are connected to that terminal of the resistance or condenser which is connected to a branch point in the measurements, it ought to be possible to make the observations agree within the limits of errors of observation.

Digitized by Google

Digitized by Google

# CAPACITY AND EDDY CURRENT EFFECTS IN INDUCTOMETERS

BY

S. BUTTERWORTH, M.Sc.,

SOMETIME ASSISTANT IN THE ELECTRICITY DEPARTMENT.

Digitized by Google

## ABSTRACT.

1. A theoretical investigation has been made upon the effects at self and intercapacities and of eddy current losses in mutual inductances for which the coils have a common point. The following are the main conclusions arrived at:—

(*a*) Small capacities introduce variations in the effective self and mutual inductances which change as the square of the frequency.

(*b*) Corresponding variations are introduced in the effective resistances of the coils.

(*c*) The mutual inductance is no longer "pure", that is, the secondary E.M.F. is no longer in exact quadrature with the primary current. The primary and secondary circuits behave as if they have a resistance in common which varies as the square of the frequency.

(*d*) Eddy currents produce impurity and changes of effective resistance which are initially of the same nature as those due to capacity.

(*e*) Eddy current and capacity effects may be so combined that the variations of mutual inductance and of impurity cancel simultaneously, so that it is theoretically possible to obtain a "pure" mutual inductance having no variation with frequency over the whole range of audio frequencies.

2. The conditions of balance of three alternating-current bridges, viz.:—

(*a*) The Heaviside inductance bridge,

(*b*) The Carey-Foster bridge,

(*c*) A modified Campbell frequency bridge,

have been worked out on the basis that the mutual inductance is not pure and the mutual and self-inductances are not invariable with frequency. It is shown how combined observations on these bridges may be used to determine the frequency corrections of a given inductometer.

3. An experimental study has been made upon an inductometer of the Campbell type. The results show that if such an inductometer is used at the higher audio frequencies for the measurements of the effective resistance of coils or of condensers, the inductometer corrections may in certain cases be larger than the quantities measured.

4. A method for automatically correcting an inductometer is suggested in order that it may be used for the measurement of power factors of condensers without having recourse to tables of corrections.


Digitized by Google

# CAPACITY AND EDDY CURRENT EFFECTS IN INDUCTOMETERS.

By S. BUTTERWORTH, M.Sc., Sometime Assistant in the Electricity Department.

[Reprinted from the 'Proceedings of the Physical Society of London', Vol. 33, 1921.]

## 1.

It is usually assumed when mutual inductances are employed in alternating-current bridge measurements that the E.M.F. developed in the secondary coil is in exact quadrature with the primary current. This assumption is practically correct at low frequencies, but at the higher telephonic frequencies a component of secondary E.M.F. which is in phase with the primary current begins to become appreciable.

Mutual inductances in which this in-phase component is developed are said to be "impure," and the magnitude of the in-phase component when unit current flows in the primary may be taken as the measure of the impurity.* Impurity, as defined in this way, is of the dimensions of a resistance, and if it is denoted by $\sigma$, the vector relation connecting secondary E.M.F. $E_s$ with primary current $I_p$ must be written

$$E_s = (\sigma + j\omega M)\, I_p, \quad . \quad . \quad . \quad . \quad . \quad . \quad . \quad . \quad . \quad . \quad (1)$$

M being the mutual inductance, $\omega/2\pi$ the frequency and $j$ the operator rotating through a right angle.

## 2. *Factors producing Impurity.*

In the most general case, the factors bringing about impurity in a mutual inductance composed of coils with air cores are self and intercapacities, leakage, and eddy current losses. If the coils have a common point, impurity might also arise due to a small resistance in common with the primary and secondary circuit, unless proper precautions are taken in regard to the mode of connection. The Carey-Foster bridge used in measurements of the capacity and effective resistance of condensers is particularly liable to error owing to this form of impurity, as the common point of the mutual inductance is a four-branch point. (*See* Fig. 7.) Leakage is usually of little importance with proper insulation. However, a non-uniform distribution of resistance or inductance, combined with distributed capacity, may cause an inductance to behave as if it possessed an end-to-end capacity having leakage. This is readily seen by considering the case of a pure inductance, L, shunted by a capacity C, and connected in series with a resistance R. If C and $R/\omega L$ are small, then the capacity C across L alone is equivalent to a capacity C, having leakance—$2CR/L$, and acting as a shunt across both R and L.

* Silsbee, 'Bull. Bureau of Standards', vol. 13, p. 414, 1916.



Digitized by Google

The effects of self and intercapacity are treated in section 4 for the case where the two coils have a common point. It is there shown that small capacities produce impurities varying as the square of the frequency, and this variation is accompanied by variations of effective resistance and inductance following the same law.

The effects due to eddy currents are considered in section 7 *et seq.* The effects are mainly variations in impurity and effective resistance, the changes in inductance due to eddy currents being small. If the frequency is not too high, the changes in impurity and effective resistance are proportional to the square of the frequency. Thus it is impossible by effective resistance measurements alone to separate the effects due to capacity from those due to eddy currents, but some estimate of the relative importance of the two effects might be obtained by determining the frequency coefficients of the inductances and assuming these to be due mainly to capacity.

### 3. *Preliminary Network Transformations.*

The theory to be given is much simplified if use is made of the following network transformations* :—

(A) Two inductive coils (Fig. 1 (*a*) ), with resistance operators $\xi$, $\eta$ and mutual operator

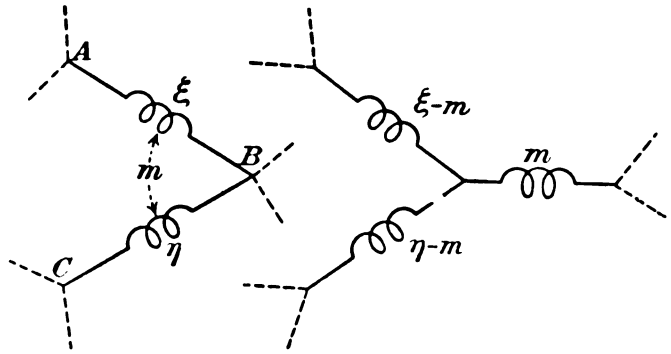


Fig. 1 (*a*). Fig. 1 (*b*).

$m$, and having a common point, may be replaced by three inductive coils having resistance operators $\xi - m$, $\eta - m$, $m$, and no mutual operators radiating as a " star " combination from the common point. (Fig. 1 (*b*).)

In this transformation $m$ must be taken as positive when the directions of winding are such that if current is applied to the combination at the open ends the mutual inductance will oppose the self inductances.

(B) Three arms, OA, OB, OC, having resistance operators $a$, $b$, $c$ respectively, and forming a " star " combination

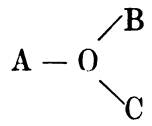


* G. A. CAMPBELL, ' Trans. Am.I.E.E.', vol. 30, p. 891, 1911.

Digitized by Google

may be replaced by a triangular " mesh,"

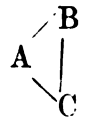


provided that the resistance operators X, Y, Z of the arms BC, CA, AB have the values $(bc + ca + ab)/a, b, c$.

Conversely, the mesh may be replaced by a star, and then

$$a, b, c = (YZ, ZX, XY)/X + Y + Z.$$

If the symbols represent *conductance* operators, the above relations are interchanged.

### 4. *The Effect of Self and Intercapacities in Mutual Inductances.*

Let the two coils have a common point. Let their resistance operators, apart from capacity, be $\xi$, $\eta$, and let their mutual operator be $m$. Suppose the self capacities to be sufficiently represented by condensers of capacities $c_1$, $c_2$ in parallel with the coils $\xi$, $\eta$, and let the intercapacity be represented by a condenser of capacity $c_{12}$, joining the open ends of the coils. The system is then as shown in Fig. 2 (*a*).

By application of transformation (A), the system is converted to that of Fig. 2 (*b*), in which

$$x = m, \quad y = \xi - m, \quad z = \eta - m, \quad . \quad . \quad . \quad . \quad . \quad . \quad . \quad . \quad (2)$$

and $\alpha$, $\beta$, $\gamma$ are the conductance operators of the capacity arms $c_{12}$, $c_2$, $c_1$.

By application of transformation (B) to the star combination $x$, $y$, $z$, the system of Fig. 2 (*b*) is converted to that of Fig. 2 (*c*), in which

$$\alpha' = \alpha + x/\mu, \quad \beta' = \beta + y/\mu, \quad \gamma' = \gamma + z/\mu, \quad \mu = yz + zx + xy. \quad . \quad . \quad (3$$

By the converse of transformation (B), the system of Fig. 2 (*d*) is then obtained, in which

$$\left.\begin{aligned} X, Y, Z &= \frac{x + \alpha\mu,\ y + \beta\mu,\ z + \gamma\mu}{1 + \alpha(y + z) + \beta(z + x) + \gamma(x + y) + \lambda\mu} \\ \lambda &= \beta\gamma + \gamma\alpha + \alpha\beta \end{aligned}\right\}. \quad . \quad . \quad . \quad (4)$$

Finally, by the converse of transformation (A), the system of Fig. 2 (*d*) is converted to that of Fig. 2 (*e*), in which

$$\xi' = X + Y, \quad \eta' = Z + X, \quad m' = X. \quad . \quad . \quad . \quad . \quad . \quad . \quad . \quad (5)$$

Digitized by Google

The result is thus a system in which the capacities have been suppressed, so that $\xi'$, $\eta'$, $m'$ are the modified operators to employ to include the effects of capacity. If $c_1$, $c_2$, $c_{12}$ are small, quantities involving their squares or products may be neglected, and in this case it is found from (2), (4) and (5) that

$$\left.\begin{aligned} m' &= m + \alpha(\xi - m)(\eta - m) - \beta m\eta - \gamma m\xi \\ \xi' &= \xi - \alpha(\xi - m)^2 - \beta m^2 - \gamma\xi^2 \\ \eta' &= \eta - \alpha(\eta - m)^2 - \beta\eta^2 - \gamma m^2 \end{aligned}\right\} \quad . \quad . \quad . \quad . \quad . \quad (6)$$

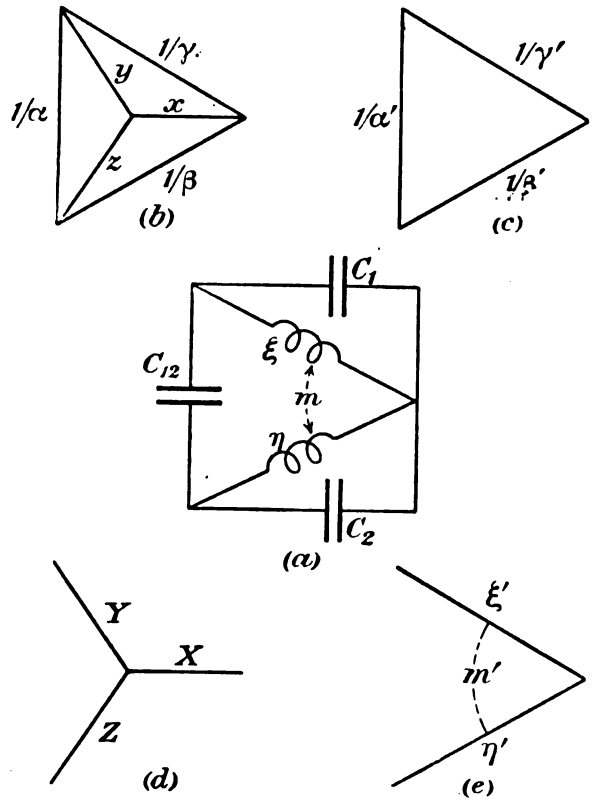


Fig. 2.

Now, in the case of currents alternating with frequency $\omega/2\pi$, resistance operators may be replaced by vector impedances, so that we may then write

$$\left.\begin{aligned} \xi &= R_1 + j\omega L_1, & \eta &= R_2 + j\omega L_2, & m &= j\omega M \\ \alpha &= j\omega C_{12}, & \beta &= j\omega C_2, & \gamma &= j\omega C_1 \end{aligned}\right\} , \quad . \quad . \quad . \quad . \quad . \quad (7)^*$$

in which $R_1$, $R_2$ are the resistances of the coils, $L_1$, $L_2$, M the inductances.

* If leakage is also present $\alpha$, $\beta$, $\gamma$ are of the forms $G + j\omega C$ in which G is the leakage associated with the capacity C.

Digitized by Google

Applying (7) to (6) and separating the real and imaginary parts, the following formulæ are obtained:—

$$m_c = C_{12}R_1R_2 + \omega^2\{C_1L_1M + C_2L_2M - C_{12}(L_1 - M)(L_2 - M)\}, \quad . \quad . \quad (8)$$

$$\sigma_c = \omega^2[C_1R_1M + C_2R_2M - C_{12}\{R_1(L_2 - M) + R_2(L_1 - M)\}], \quad . \quad . \quad (9)$$

$$l_{1c} = -(C_1 + C_{12})R_1^2 + \omega^2\{C_1L_1^2 + C_2M^2 + C_{12}(L_1 - M)^2\}, \quad . \quad . \quad . \quad (10)$$

$$l_{2c} = -(C_2 + C_{12})R_2^2 + \omega^2\{C_1M^2 + C_2L_2^2 + C_{12}(L_2 - M)^2\}, \quad . \quad . \quad . \quad (11)$$

$$r_{1c} = 2\omega^2R_1\{C_1L_1 + C_{12}(L_1 - M)\}, \quad . \quad . \quad . \quad (12)$$

$$r_{2c} = 2\omega^2R_2\{C_2L_2 + C_{12}(L_2 - M)\} \quad . \quad . \quad . \quad (13)$$

In these formulæ $m_c$, $l_{1c}$, $l_{2c}$ are the increases in mutual and self inductance, $\sigma_c$ is the impurity introduced by the capacities, $r_{1c}$, $r_{2c}$ are the added resistances due to capacity.

### 5. *Measurement of Self and Intercapacity.*

If it may be assumed that the variations of self and mutual inductance are due to capacity only, equations (8), (10), and (11) may be used to determine the capacities $C_1$, $C_2$, $C_{12}$.

With both coils in position and having a common point, the effective self inductances of the two coils separately and in series are determined at a number of different frequencies. Then, if for brevity we denote the coefficients of $\omega^2$ in (8), (10), (11) by $k_{12}$, $k_1$, $k_2$ and express $C_1$, $C_2$, $C_{12}$ in terms of these coefficients, we obtain

$$\left.\begin{aligned}(L_1L_2 - M^2)^2 C_1 &= k_1L_2(L_1 - M) - k_2M(L_1 - M) + k_{12}(L_1L_2 - 2ML_1 + M^2)\\ (L_1L_2 - M^2)^2 C_2 &= -k_1M(L_2 - M) + k_2L_1(L_2 - M) + k_{12}(L_1L_2 - 2ML_2 + M^2)\\ (L_1L_2 - M^2)^2 C_{12} &= k_1ML_2 + k_2ML_1 - k_{12}(L_1L_2 - M^2).\end{aligned}\right\} \quad (14)$$

These equations determine $C_1$, $C_2$, $C_{12}$ as $k_1$, $k_2$, $k_{12}$ and may be deduced from the frequency variations of the self and mutual inductances.

The method fails when the coupling is very close, as, for perfect coupling, the three relations employed are no longer independent.

The values of $C_1$, $C_2$ obtained by this method are not necessarily the same as would be obtained when the coils are separated from each other, as the capacities $C_1$, $C_2$ include any intercapacity that may be regarded as acting from the inner end of one coil to the outer end of the other. Also if the common point is altered the values of $C_1$, $C_2$, $C_{12}$ may also change because of the redistribution of the intercapacities.

However, by a systematic alteration of the common points the assumption that distributed intercapacities may be replaced by end capacities may be put to an experimental test.

Digitized by Google

Thus, when the coils are not connected the system is as in Fig. 3, in which the broken lines represent the capacity arms. Four common points are possible, so that 12 combinations of the six capacities—I, II, III, IV, V, VI—may be measured. These are given in the following table :—

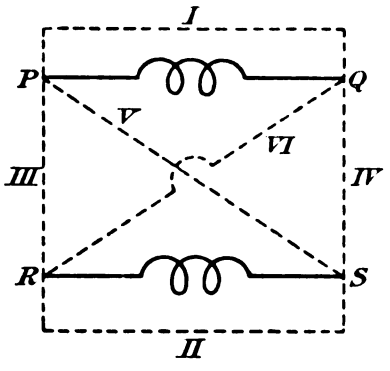

Fig. 3.

| Common Point. | $C_1$ | $C_2$ | $C_{12}$ |
|---|---|---|---|
| PR . . . . | I + VI .. | II + V .. | IV |
| QS . . . . | I + V .. | II + VI .. | III |
| QR . . . . | I + III .. | II + IV .. | V |
| PS . . . . | I + IV .. | II + III .. | VI |

Since the values of $C_{12}$ give the four intercapacities, the remaining observations give four independent determinations of the self capacities I and II respectively. If the end-to-end-capacity theory is adequate, these should be consistent and in agreement with the self capacities as determined when the coils are separated.

### 6. *Conditions for Zero Impurity and for No Variation of Mutual Inductance with Frequency.*

By equation (8) the frequency coefficient of mutual inductance is zero when

$$C_{12} = M(C_1L_1 + C_2L_2)/(L_1 - M)(L_2 - M). \quad . \quad . \quad . \quad . \quad . \quad . \quad (15)$$

By equation (9) the impurity due to capacity is zero when

$$C_{12} = M(C_1R_1 + C_2R_2)/\{R_1(L_2 - M) + R_2(L_1 - M)\}. \quad . \quad . \quad . \quad . \quad (16)$$

If condition (15) is inserted in equation (9) an essentially negative value is obtained for $\sigma_c$, so that a mutual inductance invariable with frequency is always associated with a negative capacity impurity. As, however, the whole impurity includes both capacity and eddy current terms, and as the latter may be positive or negative, it is theoretically possible to construct a mutual inductance invariable with frequency and free from impurity. This conclusion only holds when the common point is such that the two coils in series have their minimum inductance.

The procedure indicated by theory to bring about this result is to secure the condition of invariability of mutual inductance by artificial addition of self or intercapacity and then the condition of zero impurity by introduction of artificial eddy losses.

## Effective Resistances and Impurities due to Eddy Current Losses.

### 7. *Eddy Current Losses in a Long Cylinder.*

Let a long non-magnetic cylinder of diameter $d$ and of material of resistivity $\rho$ be placed in a uniform field alternating with frequency $\omega/2\pi$. Let H′ and H be the maximum

Digitized by Google

values of the components of the field along and perpendicular to the axis of the cylinder. Also write

$$z^2 = \pi\omega d^2/\rho. \quad . \quad . \quad . \quad . \quad . \quad . \quad . \quad . \quad . \quad . \quad . \quad (17)$$

Then it may be shown that the rate of dissipation of energy in unit length of the cylinder due to the eddy currents set up by the alternating field is

$$W_0 = \frac{\rho}{2\pi} G(z)\,(H^2 + \tfrac{1}{2}H'^2), \quad . \quad . \quad . \quad . \quad . \quad . \quad . \quad . \quad . \quad (18)$$

in which for brevity G (*z*) is written for

$$\tfrac{1}{4}z\,\frac{\mathrm{ber}\,z\ \mathrm{ber}'\,z + \mathrm{bei}\,z\ \mathrm{bei}'\,z}{\mathrm{ber}^2\,z + \mathrm{bei}^2\,z} \quad . \quad . \quad . \quad . \quad . \quad . \quad . \quad . \quad . \quad (19)$$

When *z* is less than 1

$$G(z) \doteqdot z^4/64, \quad . \quad . \quad . \quad . \quad . \quad . \quad . \quad . \quad . \quad . \quad (20)$$

When *z* is greater than 4

$$G(z) \doteqdot (\sqrt{2}z - 1)/8, \quad . \quad . \quad . \quad . \quad . \quad . \quad . \quad . \quad . \quad (21)$$

while generally the following table may be used :—

| $z$ = | 0·5 | 1·0 | 1·5 | 2·0 | 2·5 | 3·0 | 3·5 | 4·0 |
|---|---|---|---|---|---|---|---|---|
| $G(z)$ = | 0·000975 | 0·01519 | 0·0691 | 0·1724 | 0·295 | 0·405 | 0·499 | 0·584 |
| $z$ = | 4·5 | 5·0 | | | | | | |
| $G(z)$ = | 0·669 | 0·755 | | | | | | |

## 8. *Eddy Current Losses in a Coil.*

Equation (18) may be applied to determine the eddy current losses in a coil placed in an alternating magnetic field, provided that the values of H and H′ are practically constant over the section of an individual wire, that their variation is slow along the axis of the wire and that the radius of curvature of the wire is large compared with the radius of the wire itself. Then assuming for simplicity that the field is acting transversely so that H′ = 0, the rate of energy dissipation in the whole coil is

$$W = \frac{\rho}{2\pi} G(z) \int_0^l H^2\,dl, \quad . \quad . \quad . \quad . \quad . \quad . \quad . \quad . \quad . \quad (22)$$

where the integration is taken throughout the length *l* of the wire of the coil.

If $H_m^2$ is the mean square value of the transverse field acting on the coil and R is the direct current resistance of the coil, equation (22) may be written

$$W = \tfrac{1}{8}d^2 R G(z)\, H_m^2. \quad . \quad . \quad . \quad . \quad . \quad . \quad . \quad . \quad . \quad . \quad (23)$$



Digitized by Google

### 9. *Coil in Presence of Two Other Coils.*

Let the field H be due to two currents of vector values, $\mathbf{I}_1$, $\mathbf{I}_2$, and of phase difference $\psi$, flowing in two neighbouring coils. The vector fields to $\mathbf{I}_1$ and $\mathbf{I}_2$, which act on an element of the coil, will be of the forms $a_1\mathbf{I}_1$, $a_2\mathbf{I}_2$, and will be inclined in space at an angle $\phi$.

The components of the field along and perpendicular to $a_1\mathbf{I}_1$ are

$$\mathbf{H}_1 = a_1\mathbf{I}_1 + \alpha_2\mathbf{I}_2 \cos\phi,$$
$$\mathbf{H}_2 = a_2\mathbf{I}_2 \sin\phi,$$

so that if $H_1$, $H_2$ are the amplitudes of $\mathbf{H}_1$, $\mathbf{H}_2$, $I_1$, $I_2$ the amplitudes of $\mathbf{I}_1$, $\mathbf{I}_2$, the value of $H^2$ is

$$H^2 = H_1^2 + H_2^2$$
$$= a_1^2I_1^2 + a_2^2I_2^2\cos^2\phi + 2a_1a_2I_1I_2\cos\phi\cos\psi + a_2^2I_2^2\sin^2\phi,$$

and its mean value throughout the whole coil is

$$H_m^2 = \frac{I_1^2}{l}\int_0^l a_1^2\,dl + \frac{I_2^2}{l}\int_0^l a_2^2\,dl + 2\frac{I_1I_2}{l}\cos\psi\int_0^l a_1a_2\cos\phi\,dl. \quad . \quad . \quad . \quad (24)$$

The rate of dissipation of energy in the coil is therefore obtained by using this value of $H_m^2$ in (23).

### 10. *Resistance System imitating Eddy Current Losses.*

Let the two coils (I and II) which carry the currents $I_1$ and $I_2$ have their circuits connected by the resistance system shown in Fig. 4. The rate of dissipation of energy in this resistance system is

$$W' = \tfrac{1}{2}r_{1e}I_1^2 + \tfrac{1}{2}r_{2e}I_2^2 - \sigma_eI_1I_2\cos\psi, \quad . \quad . \quad . \quad . \quad . \quad . \quad . \quad (25)$$

and the system will dissipate the same energy as the eddy currents in the coil just considered provided that

$$\left.\begin{aligned} r_{1e} &= \tfrac{1}{4}d^2\,\mathrm{RG}\,(z)\left\{\frac{1}{l}\int_0^l a_1^2\,dl\right\} \\ r_{2e} &= \tfrac{1}{4}d^2\,\mathrm{RG}\,(z)\left\{\frac{1}{l}\int_0^l a_2^2\,dl\right\} \\ \sigma_e &= -\tfrac{1}{4}d^2\,\mathrm{RG}\,(z)\left\{\frac{1}{l}\int_0^l a_1a_2\cos\phi\,dl\right\} \end{aligned}\right\} \quad . \quad . \quad . \quad . \quad . \quad . \quad . \quad (26)$$

If by the converse of transformation (A) we convert $\sigma_e$ to a mutual operator, the common point may be removed and $r_{1e}$, $r_{2e}$, $\sigma_e$ will then represent the increments of resistances and the impurity introduced by the eddy current losses in a neighbouring coil. If there are a number of neighbouring coils, then since the losses are additive, the eddy

Digitized by Google

current resistances and impurities are sums of expressions such as (26). In particular the neighbouring coils may simply be the coils I and II and the eddy current resistances and impurities are got by performing the integrations in (26) throughout the lengths of wire in the two coils.

The increments in resistance obtained in this way are to be added to the ordinary "skin" increments of resistance, the latter being due to the currents flowing in the individual elements of the coil.

### 11. *Conditions Governing Sign of $\sigma_e$.*

In applying equation (26) some care is required in order to avoid the wrong sign for $\sigma_e$. In Fig. 4, from which the equations have been deduced, the directions of the currents are such that if $I_1 = I_2 = I$ the current I will flow only through the resistances $r_{1e} - \sigma_e$, $r_{2e} - \sigma_e$, so that when the coils are connected in series the total eddy current resistance is $r_{1e} + r_{2e} - 2\sigma_e$. In order, therefore, to make $\sigma_e$ consistent with the defining equation (1), the mutual inductance M between the coils I and II must, under the same conditions, oppose the self-inductances. Now $a_1$, $a_2$ are fields due to unit currents in coils I and II respectively, so that in order to obtain the correct sign for $\sigma_e$ the directions of these unit currents must be so chosen that the mutual inductance opposes the self-inductances. With this convention $\sigma_e$ will be positive if the sum of the eddy current resistances is less than the eddy current resistance of the coils in series and helping.

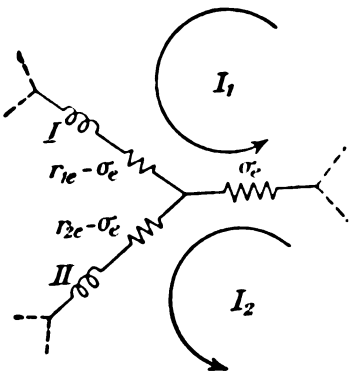

Fig. 4.

### 12.

It is readily seen from equations (26) that the inequalities

$$r_{1e} + r_{2e} > 2\sigma_e$$

$$r_{1e} r_{2e} > \sigma_e^2$$

hold for the eddy current resistances, relations analagous to those between self and mutual inductances.

### 13. *Systems of Parallel Wires.*

The theory finds its simplest application when the coils I and II consist of systems of parallel wires. The results in these cases may be applied to coaxial coils provided that winding sections of the coils and their distance apart are small compared with their radii.



Digitized by Google

In order to illustrate the properties of the impurity $\sigma_c$, consider three parallel wires A, B, C (Fig. 5). Let A be the coil I and B the coil II. Let C carry no current. The impurity introduced by the presence of C will be negative, zero or positive according as the angle of inclination of the fields at C produced by opposite currents in A and B is less than, equal to, or greater than $\pi/2$. If a circular be drawn with AB as diameter,

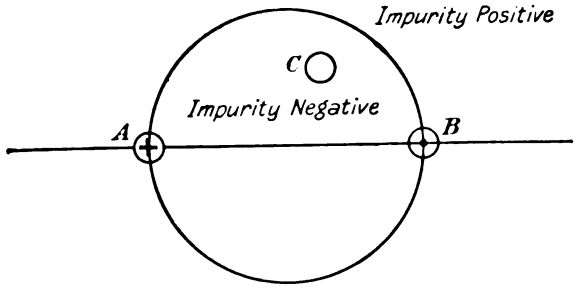


Fig. 5.

then since the two fields are normal at all points on this circle, the impurity due to the presence of C changes sign from negative to positive as C is moved out of the circle. Along the line AB, the fields either help or oppose each other, so that when C is collinear with AB the condition $r_{1r12c} - \sigma_c^2 = 0$ is satisfied. This is a case of perfect eddy current coupling.

The above conclusions still apply when the wires A and B are replaced by bundles of wires, provided that the distance of C is sufficient to warrant the assumption that the currents in A and B act as if concentrated at a point. It is thus possible to counteract an already existing impurity of any sign by introducing a third coil carrying no current in the proper position with respect to the two coils forming the mutual inductance. An example of this use of eddy currents to correct impurity is given in section 19.

### 14. *System of Four Wires.*

Let there be four co-planar wires, two constituting the coil I and two constituting the coil II, spaced at equal distances D. Numbering the wires in order 1, 2, 3, 4, there are three possible combinations, (1, 2), (3, 4) ; (1, 3), (2, 4) ; (1, 4), (2, 3), each giving different effective resistances and impurities. By a simple application of the formula $H = \frac{2I}{r}$ we obtain the following values for $a_1$, $a_2$, $\cos\phi$ for the combination (1, 2), (3, 4).

| Wire | $a_1 D$ | $a_2 D$ | $\cos\phi$ |
|---|---|---|---|
| 1 | 2 | 5/3 | −1 |
| 2 | 2 | 3 | +1 |
| 3 | 3 | 2 | +1 |
| 4 | 5/3 | 2 | −1 |

Using these values in (26) we find

$$r_{1c} = 2{\cdot}472\,\frac{d^2}{D^2}\,G(z)\,R = r_{2c}, \quad \sigma_c = -\,0{\cdot}667\,\frac{d^2}{D^2}\,G(z)\,R,$$

Digitized by Google

in which R is the direct-current resistance of one pair of wires. By similar methods for the combination (1, 3), (2, 4) we find

$$r_{1e} = 1{\cdot}139\,\frac{d^2}{D^2}\,G\,(z)\,R = r_{2e}, \quad \sigma_e = +\,0{\cdot}667\,\frac{d^2}{D^2}G\,(z)\,R,$$

and for the combination (1, 4), (2, 3)

$$r_{1e} = 0{\cdot}361\,\frac{d^2}{D^2}\,G\,(z)\,R, \quad r_{2e} = 3{\cdot}250\,\frac{d^2}{D^2}\,G\,(z)\,R, \quad \sigma_e = 0.$$

In all three cases $r_{1e} + r_{2e} + 2\sigma_e$ has the same value, viz., $3{\cdot}611\,\frac{d^2}{D^2}\,G\,(z)\,R$, which is, of course, the proper value for the proximity resistance of a system of four parallel wires carrying currents in the same direction. The example also shows that the sign and magnitude of the impurity depends upon the interlacing of the wires of the two coils, the tendency being for the impurity to increase positively as the interlacing increases. This point may be further illustrated by a system of 12 equidistant wires, of which six constitute one circuit and six the other circuit. If we write

$$\sigma_e = u_{12}\,\frac{d^2}{D^2}\,G\,(z)\,R,$$

$u_{12}$ takes the following values for different arrangements :—

| Arrangement | $u_{12}$ |
|---|---|
| 1 1 1 1 1 1 2 2 2 2 2 2 | $-\,0{\cdot}80$ |
| 1 1 1 1 1 2 2 2 2 2 2 1 | $-\,0{\cdot}70$ |
| 1 1 1 1 2 2 2 2 2 2 1 1 | $-\,0{\cdot}66$ |
| 1 1 1 2 2 2 2 2 2 1 1 1 | $-\,0{\cdot}65$ |
| 1 1 1 2 2 2 1 1 1 2 2 2 | $-\,0{\cdot}35$ |
| 1 1 2 2 1 1 2 2 1 1 2 2 | $-\,0{\cdot}00_3$ |
| 1 2 1 2 1 2 1 2 1 2 1 2 | $+\,0{\cdot}66$ |

Interlacing the coils will increase intercapacity effects, so that if the coils are used with their common point such that the inductance in series is a minimum, the effect of increasing intercapacity will cause a capacity impurity acting oppositely to the eddy current impurity.

### 15. *Short Single Layer Coils in Contact.*

The eddy current impurity between two short coils of equal radius in end contact may be calculated if their separate effective resistances $r_{1e}$, $r_{2e}$ and their effective resistance $r_s$ in series are known for $r_s = r_{1e} + r_{2e} + 2\sigma_e$.

The value of $r_s$ has been shown by the author in another Paper to be of the form

$$r_s = u_s\,\frac{d^2}{D^2}\,G\,(z)\,R, \quad \ldots\ldots\ldots\ldots \quad (27)$$

Digitized by Google

where R is the direct-current resistance of the whole combination, G (z) is defined in section 7, $d$ is the diameter of the wire, D the distance of consecutive wires and $u_n$ is a factor depending on the number of wires $n$ in the two coils. The following values when plotted against $1/n$ enable $u_n$ to be determined in any case :—

$$n = \quad 1 \qquad 2 \qquad 3 \qquad 5 \qquad 10 \qquad \text{inf.}$$

$$u_n = 0{\cdot}000,\ 1{\cdot}000,\ 1{\cdot}500,\ 2{\cdot}014,\ 2{\cdot}514,\ 3{\cdot}290.$$

The values of $r_{1_e}, r_{2_e}$ are, however, greater than would be estimated by the above method because of the eddy currents induced in one coil by the current in the other. If the number of wires is finite in both coils, the additive term due to the presence of the other coil may be calculated by methods similar in principle to those employed in the case of the four-wire system. When the number of wires is large, this method becomes laborious, but the extreme case of an infinite number of wires may be obtained by integration. Treating the narrow coils as straight-wire systems, the field at any point in the plane of a strip of width $a$ is $2\frac{\mathrm{I}}{\mathrm{D}}\log\frac{a+x}{x}$ where I is the current in each wire and $x$ the distance of the point from the edge of the strip. If the strip representing the other coil has width $b$, the mean square value of the field over this coil is

$$\frac{4\mathrm{I}^2}{\mathrm{D}^2}\cdot\frac{1}{b}\int_0^b \log^2\frac{a+x}{x}\,dx = \frac{4\mathrm{I}^2}{\mathrm{D}^2}\frac{a}{b}f\left(\frac{b}{a}\right),$$

in which

$$f\left(\frac{b}{a}\right) = \int_0^{\frac{b}{a}} \log^2\frac{1+\mu}{\mu}\,d\mu.$$

The values of $f(\mu)$ may be obtained in the form of series. Thus suitable series are

$\mu < 2$

$$f(\mu) = -\mu\log^2\nu + 2\log\nu\log(1-\nu) + 2\sum_1^\infty\frac{\nu^r}{r^2}, \quad . \quad . \quad . \quad . \quad . \quad (28)$$

in which

$$\nu = \mu/(1+\mu);$$

$\mu > 2$

$$f(\mu) = \frac{\pi^2}{3} - \sum_{r=1}^{r=\infty}\frac{(-1)^{r+1}}{r\mu^r}\sum_{s=1}^{s=r}\frac{1}{s(s-r+1)} \quad . \quad . \quad . \quad . \quad . \quad . \quad (29)$$

By (26) the term in $r_{1_e}$ for the coil ($a$), which is due to the eddy currents in ($b$) is

$$\frac{d^2}{\mathrm{D}^2}\mathrm{G}(z)\frac{a}{b}f\left(\frac{b}{a}\right)\mathrm{R}_b = \frac{d^2}{\mathrm{D}^2}\mathrm{G}(z)f\left(\frac{b}{a}\right)\mathrm{R}_a,$$

where $\mathrm{R}_a$, $\mathrm{R}_b$ are the direct-current resistances of $\mathrm{R}_a$ and $\mathrm{R}_b$.

Hence

$$\left.\begin{aligned} r_{1_e} &= \left\{u_n(a) + f\left(\frac{b}{a}\right)\right\}\frac{d^2}{\mathrm{D}^2}\mathrm{G}(z)\,\mathrm{R}_a \\ r_{2_e} &= \left\{u_n(b) + f\left(\frac{a}{b}\right)\right\}\frac{d^2}{\mathrm{D}^2}\mathrm{G}(z)\,\mathrm{R}_b \end{aligned}\right\} \quad . \quad . \quad . \quad . \quad . \quad . \quad . \quad . \quad (30)$$

Digitized by Google

These equations, together with (27) and the tables of $u_n$ and $f(b/a)$ enable the eddy current resistances and impurities of short single-layer coils in end contact to be calculated. In the tables for $f(b/a)$ the values for the case $b/a$ infinite but $n$ finite are calculated from the formula

$$f\left(\frac{b}{a}\right) = \frac{\pi^2}{6} + 1 + \frac{1}{2^2} + \frac{1}{3^2} + \ldots + \frac{1}{(n-1)^2} - \frac{1}{n}\left(1 + \tfrac{1}{2} + \tfrac{1}{3} + \ldots + \frac{1}{n-1}\right),$$

where $n$ is the number of wires in $a$.
When $n$ is also infinite $f(b/a) = \pi^2/3$.

VALUES of $f(b/a)$ in Equations (30).

$n_a$ = number of wires in system $a$.

$n_b$ = number of wires in system $b$.

$b/a < 1$.

| $n_a$ | $n_b$ | $f(b/a)$ | $n_a$ | $n_b$ | $f(b/a)$ |
|---|---|---|---|---|---|
| 2 | 1 | 1·125 | 5 | 1 | 1·042 |
| 3 | 2 | 1·511 | 10 | 4 | 1·704 |
| 3 | 1 | 1·120 | 10 | 3 | 1·523 |
| 5 | 4 | 1·858 | 10 | 2 | 1·265 |
| 5 | 3 | 1·701 | 10 | 1 | 0·858 |
| 5 | 2 | 1·462 | | | |

$n_a = n_b$ = infinity.

| $b/a$ = | 0·2 | 0·4 | 0·6 | 0·8 |
|---|---|---|---|---|
| $f(b/a)$ = | 1·375 | 2·089 | 2·334 | 2·492 |

$b/a > 1$.

| $n_a$ | $b/a = 1$ | 2 | 3 | 4 | 5 | inf. |
|---|---|---|---|---|---|---|
| 1 | 1·000 | 1·250 | 1·361 | 1·423 | 1·463 | 1·645 |
| 2 | 1·472 | 1·743 | 1·859 | 1·923 | 1·963 | 2·145 |
| 3 | 1·715 | 1·992 | 2·108 | 2·172 | 2·209 | 2·395 |
| 5 | 1·970 | 2·248 | 2·365 | 2·429 | 2·470 | 2·652 |
| 10 | 2·218 | 2·497 | 2·613 | 2·674 | 2·710 | 2·901 |
| inf. | 2·606 | 2·886 | 3·002 | 3·067 | 3·119 | 3·290 |

For interpolation $f(b/a)$ may be plotted againt $b/a$ for different values of $n_a$, and against $1/n$ for different values of $b/a$.

Digitized by Google

16.

As an illustration of the application of these results let the coil ($a$) have 20 turns, and the coil ($b$) 30 turns.

Then by graphical interpolation from the tables we find for coil ($a$)

$$f(b/a, n_a) = f(3/2, 30) = 2{\cdot}55,$$
$$u_n(a) = u_{20} \qquad = 2{\cdot}84,$$

so that by (30)

$$r_{1e} = 5{\cdot}39 \times 20\,G(z)\frac{d^2}{D^2}R, \quad . \quad . \quad . \quad . \quad . \quad . \quad . \quad . \quad . \quad . \quad (A)$$

R being the direct-current resistance of one turn of wire.

For coil ($b$)

$$f(a/b, n_b) = f(2/3, 30) = 2{\cdot}24,$$
$$u_n(b) = u_{30} \qquad = 2{\cdot}98,$$

and

$$r_{2e} = 5{\cdot}22 \times 30\,G(z)\frac{d^2}{D^2}R, \quad . \quad . \quad . \quad . \quad . \quad . \quad . \quad . \quad . \quad (B)$$

For coils ($a$) and ($b$) in series, helping

$$f = 0 \; u_n = u_{50} = 3{\cdot}10,$$

and

$$r_{1e} + r_{2e} + 2\sigma_e = r_s = 3{\cdot}10 \times 50\,G(z)\frac{d^2}{D^2}R. \quad . \quad . \quad . \quad . \quad . \quad (C)$$

From (A), (B) and (C)

$$r_{1e} : r_{2e} : \sigma_e = 10{\cdot}8 : 15{\cdot}7 : 5{\cdot}5,$$

$\sigma_e$ being negative.

The absolute magnitudes will depend upon the frequency, the diameter of the wire, and the spacing. If we assume the wire to be of copper of resistivity 1,600 C.G.S. units, and of diameter 1 mm., then by (17) the value of $z$ is unity when the frequency is approximately 8,000 cycles per second, and then $G(z) = 0{\cdot}01519$. Therefore if we take $d/D = 0{\cdot}8$

$$\frac{r_{1e}}{20R} = 5{\cdot}39 \times 0{\cdot}01519 \times (0{\cdot}8)^2 = 0{\cdot}0523,$$

so that at this frequency the value of $r_{1e}$ is 5·2 per cent. of the direct-current resistance of coil ($a$).

The ordinary skin effect for copper wire of diameter 1 mm. at this frequency causes an increase of 0·52 per cent., and this must be added to the above value. If coil ($b$) had been absent the value of $r_{1e}$ would be reduced in the ratio 2·84/5·39, so that slightly less than half of the above increase is due to the presence of the coil ($b$).

For frequencies less than 8,000 cycles per second the eddy current resistances would fall as the square of the frequency, as by section (7) $z^2$ is proportional to frequency, and $G(z)$ is proportional to $z^4$.

Digitized by Google

At greater frequencies the increase is not so rapid, and may be deduced from the values of G ($z$) given in section (7), $z$ being proportional to the square root of the frequency.

In certain applications the values of $r_{1_e}/L_1\omega$, $r_{2_e}/L_2\omega$, $\sigma_e/M\omega$ are of importance, the latter quantity giving the want of quadrature of the mutual inductance. In the above example, if we suppose the coils such that R/L for coil ($a$) is about 1,000, we have $r_{1_e}/L_2\omega = 0{\cdot}001$, and this also gives the order of $\sigma_e/M\omega$. Hence at a frequency of 8,000 cycles per second the secondary E.M.F. will lead the primary current by an angle which exceeds a right angle by about 0·001 radian, *i.e.*, about 3′.

This angle does not increase indefinitely with frequency, as from (27) and (17) $\sigma_e/M\omega$ is proportional to G ($z$)/$z^2$. From the table of values for G ($z$) it is seen that G ($z$)/$z^2$ is maximum when $z = 2{\cdot}6$, and (for the above example) the maximum value for the want of quadrature is about 10′.

It should be noted that for a given spacing factor this maximum angle is independent of the diameter of the wire, but is pushed farther up the scale of frequency as the diameter of the wire diminishes.

### 17. *Short Many-layered Coils wound over Each Other.*

The investigation will be confined to the case in which the winding depth is small compared with the winding breadth, and the latter small compared with the coil radius. The results apply whether the coils are solenoidal or flat.

For a single coil of winding breadth, $b$, having $m$ layers and $n$ turns per layer of wire of diameter $d$, and direct-current resistance $R_1$, the term to be added to the effective resistance due to the increased eddy currents produced by coiling has been shown by the author to be

$$r_e = \tfrac{1}{3}\pi^2\left(\frac{nd}{b}\right)^2 (2m^2 - 1)\, G\,(z)\, R_1. \quad . \quad . \quad . \quad . \quad . \quad . \quad . \quad . \quad (31)$$

If a second coil of M layers is wound over this coil there is a further increase in resistance due to the eddy currents induced in the wire of the second coil.

The components of the field due to the current I in the first coil acting along and perpendicular to the winding breadth have the values $2\pi mn\mathrm{I}/b$, and $2mn\mathrm{I}\log\frac{b-x}{x}/b$ respectively at a point on its surface distant $x$ from the edge. If the second coil has very small winding depth, and is close on the first. the mean square value of the field having the above components may be used in (23) to determine the required additive term.

Since

$$\frac{1}{b}\int_0 \log^2\frac{b-x}{x}\,dx = \frac{\pi^2}{3},$$

the result is

$$r'_e = \tfrac{1}{3}\pi^2\left(\frac{nd}{b}\right)^2 \mathrm{M}m\mathrm{G}\,(z)\,\mathrm{R}_1, \quad . \quad . \quad . \quad . \quad . \quad . \quad . \quad . \quad . \quad (32)$$

remembering that R in (23) refers to the second coil, and is $R_1M/m$.



Digitized by Google

Combining with (31) we have

$$r_{1e} = \tfrac{1}{3}\pi^2\left(\frac{nd}{b}\right)^2 \mathrm{G}(z)\,\mathrm{R}_1(2m^2 + 4\mathrm{M}m - 1). \quad . \quad . \quad . \quad . \quad . \quad . \quad . \quad (33)$$

Similarly

$$r_{2e} = \tfrac{1}{3}\pi^2\left(\frac{nd}{b}\right)^2 \mathrm{G}(z)\,\mathrm{R}_2(2\mathrm{M}^2 + 4\mathrm{M}m - 1), \quad . \quad . \quad . \quad . \quad . \quad . \quad . \quad (34)$$

and for the two coils in series helping (31) immediately gives

$$r_{1e} + r_{2e} + 2\sigma_e = \tfrac{1}{3}\pi^2\left(\frac{nd}{b}\right)^2 \mathrm{G}(z)\,(\mathrm{R}_1 + \mathrm{R}_2)\,\{2\,(\mathrm{M} + m)^2 - 1\}. \quad . \quad . \quad . \quad (35)$$

Solving for $\sigma_e$ with $\frac{\mathrm{R}_1}{m} = \frac{\mathrm{R}_2}{\mathrm{M}}$,

$$\sigma_e = \tfrac{1}{3}\pi^2\left(\frac{nd}{b}\right)^2 \mathrm{G}(z)\,(\mathrm{R}_1 + \mathrm{R}_2)\,\mathrm{M}m. \quad . \quad . \quad . \quad . \quad . \quad . \quad . \quad (36)$$

Comparing with (31) $\sigma_e/r_e = \mathrm{M}(\mathrm{M} + m)/(2m^2 - 1)$ from which it is seen that in the case of equal coils the impurity is slightly greater than the term due to the coiling when the two coils are separate. Since the electro-magnetic coupling is fairly close, the value of $\mathrm{r}_e/\mathrm{L}\omega$ for either coil may be taken as a measure also of $\sigma_e/\mathrm{M}\omega$, the want of quadrature.

It should be noted also that $\sigma_e$ is positive for coils with their widest edges in contact, thus differing from the coils in end contact treated in section 15.

## 18.

Some notion of the magnitude of the eddy current impurities in coils of the type just considered may be obtained by taking wire of a diameter of 1 mm. and a frequency of 8,000 cycles per second. Suppose also that for a single layer $\mathrm{R}_1/\mathrm{L}_1 = 1{,}000$. By the example of section (16) the value of $r_e/\mathrm{L}_1\omega$ for a single layer is of the order 5/10,000. Now as the layers increase L increases as $m^2$, $\mathrm{R}_1$ as $m$, so that by (31) $r_e/\mathrm{L}_1\omega$ will increase as $(2m^2 - 1)/m$. If $m$ is large the value of $r_e/\mathrm{L}_1\omega$ will therefore be $m/1{,}000$, and this may also be taken as a measure of $\sigma_e/\mathrm{M}\omega$. Errors in quadrature due to this cause will therefore amount to one per cent. (34′) at a frequency of 8,000 cycles per second. For lower frequencies and diameters the error is proportional to the frequency and the fourth power of the diameter, so that the formula

$$\frac{\sigma_e}{\mathrm{M}\omega} \doteqdot \frac{mf}{8 \times 10^9} \cdot \frac{\mathrm{R}}{\mathrm{L}}\, d^4$$

may be used to give a very rough estimate of the want of quadrature. In this formula R/L is the time constant of a single layer, $d$ the diameter of the wire in mm., $f$ the frequency in cycles per second, $m$ the number of layers in one of the two equal coils.

Separation of the coils will not necessarily determine the value of $\sigma_e/\mathrm{M}$ as both $\sigma_e$ and M will diminish.

Digitized by Google

19. *Balancing of Impurity and Frequency Coefficient of a Mutual Inductance.*

It will now be shown that it is possible to introduce intercapacity and eddy current losses of such a magnitude as to balance simultaneously an already existing frequency coefficient and impurity in a mutual inductance, provided that the inductance is used with a common point in such a way that the coils are in opposition when in series. Let the two coils be equal and coaxial. Let the radius of each coil be 10 cm., their separation 3 cm., and let there be 240 turns with a square winding section of 1 cm. side. Each coil would then have an inductance of approximately 24 millihenries and their mutual inductance would be approximately 10 millihenries. The frequency coefficient of mutual inductance will be assumed to be positive and of amount 4/1,000 at a frequency of 2,000 cycles per second.* The impurity at the same frequency will be taken to be $+ 0{\cdot}08$ ohm.*

If intercapacity is introduced then by (8) and (9) with $L_1 = L_2 = L$, the frequency coefficient of M is reduced by $\omega^2 C_{12} (L - M)^2/M$ and the impurity by $2R\omega^2 C_{12}(L - M)$. Using the above values of L, M the value of $C_{12}$ required to wipe out the already existing frequency coefficient is approximately 1,280 $\mu\mu$F. This will also introduce negative impurity of amount $0{\cdot}0057R$ ohm. If the resistance of the coils is less than 14 ohms resistance may be added until $0{\cdot}0057R = 0{\cdot}08$, and this will be sufficient to balance the impurity.

If R is greater than 14 ohms, the impurity has become negative by the addition of capacity, and in this case an auxiliary coil of the same radius as the other coils can be placed coaxially with them to introduce positive impurity. Thus suppose the auxiliary coil to consist of wire 1 mm. diameter placed at $1{\cdot}5$ cm. separation from the nearer coil, the positive impurity introduced by the auxiliary coil is $\frac{N^2 d^2}{D_1 D_2} G(z) R'$,

where
$N$ = No. of turns in the inductometer coils = 240.
$a$ = diameter of wire = $0{\cdot}1$ cm.
$D_1, D_2$ = separations of coil from inductometer coils.
= $1{\cdot}5, 4{\cdot}5$ cm.
$R'$ = resistance of auxiliary coil.

Using these values and remembering that $G(z) = 0{\cdot}01519$ at a frequency of 8,000 cycles per second and falls as the square of the frequency, the value of R′ to give $0{\cdot}01$ ohm impurity at 2,000 cycles per second is

$$R' = 0{\cdot}124 \text{ ohm.}$$

This corresponds to about 10 turns of wire of radius 10 cm.

This balancing will hold over the range of frequencies, for which the square law holds. If the diameter of any wire used does not exceed 1 mm., the range is up to 8,000 cycles per second.

* These are the order of magnitude of these quantities in the Campbell type of inductometer.



Digitized by Google

### 20. *Effect of Impurity, etc., in Alternating Current Bridges.*

The effect of impurity in alternating current bridge measurements in which mutual inductances are employed may be included by replacing the mutual impedance $j\omega M$ in the vector equations of balance of these bridges by $\sigma + j\omega M$. In interpreting these

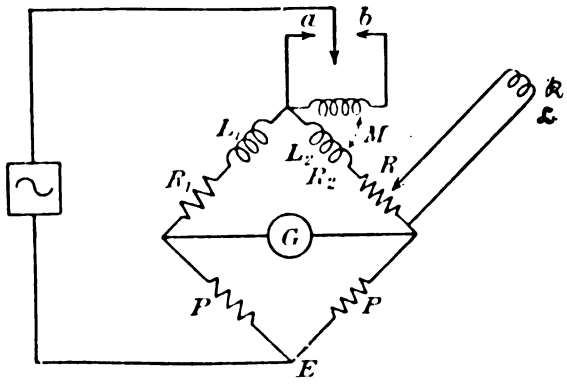


Fig. 6. Heaviside Induction Bridge.

equations account should of course be taken of the variations of inductance and resistance of the various arms with frequency. Three bridges will be considered.

(1) The Heaviside inductance bridge with equal arms.

(2) The Carey-Forster inductance capacity bridge.

(3) A modified Campbell frequency bridge.

### 21. *The Heaviside Inductance Bridge.**

The bridge is shown in Fig. 6. P, P are two similar coils of small residual inductance. $\mathscr{L}$, $\mathscr{R}$ is the inductive coil to be measured by means of the inductometer M. R is a constant inductance rheostat.

Let the procedure be as follows :—,

With the source connected to $a$ and $\mathscr{L}$, $\mathscr{R}$ removed, $L_1$ and R are adjusted for balance. Then with $\mathscr{L}$, $\mathscr{R}$ in position and the source connected to $b$, M and R are adjusted for balance. Let the two values of R be R′, R″.

If residuals and impurities are ignored $\mathscr{L} = 2M$ and $\mathscr{R} = R' - R.''$

As regards residuals, if observations are repeated with the arms P, P reversed the residuals of P, P cancel in the mean. Also, R being of constant inductance the residuals of the other arms cancel when the above procedure is used.

If the mutual inductance has impurity $\sigma$ a simple application of transformation (A) shows that the two conditions of balance are $\mathscr{L} = 2M$, $\mathscr{R} = 2\sigma + R' - R''$.

It should be noted that the value of $R_2$ for the coil $L_2$ only remains the same in the two adjustments provided that the inductive action of M is introduced by the method of transference of the source from $a$ to $b$ *keeping the primary coil of the inductometer in*

* Heaviside, 'Phil. Mag.', p. 173, vol. 23, 1887.

Digitized by Google

*position*. This is the procedure used in the Campbell form of inductometer, the fine adjustment only being made by a moving coil. In inductometers in which the whole of the adjustment is made by a moving coil, the eddy current and capacity conditions may be different in the two balances, so that $R_2$ will have different effective values.

Since for an inductometer of 10 millhenries $\sigma$ may be of the order 0·1 ohm at a frequency of 2,000 cycles per second, neglect of $\sigma$ in the relation between the resistance may introduce errors of order two per cent. in measurements of the effective resistance of 20 millhenry inductances of a nominal resistance of 10 ohms.

## 22. *The Carey Foster Inductance Capacity Bridge.**

The elements of this bridge (Fig. 7) are :—

(*a*) The condenser arm having effective capacity C and effective series resistance S.† Let its vector impedance be $Z = S - j/\omega C$.

(*b*) The inductive arm P, L having vector impedance $\xi = P + j\omega L$;

(*c*) The resistance arm R having residual inductance $l$ and therefore vector impedance $Y = R + j\omega l$;

(*d*) The mutual inductance M having impurity $\sigma$ and acting on the inductive arm. Its mutual impedance is $m = \sigma + j\omega M$.

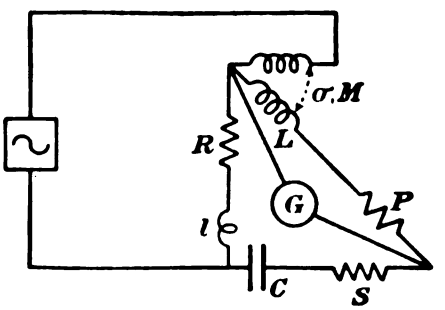


Fig. 7. The Carey Foster Inductance Capacity Bridge.

The condition of balance is readily found by applying transformation (A) to the mutual inductance. The result is a Wheatstone bridge of which the upper arms have vector impedances $m$, $\xi - m$, and the lower arms have vector impedances Y, Z. The vector equation of balance is therefore

$$mZ = Y(\xi - m). \quad . \quad . \quad . \quad . \quad . \quad . \quad . \quad . \quad . \quad . \quad . \quad (37)$$

Inserting the values of $m$, $\xi$, Y, Z and separating real and imaginary parts,

$$M/C + \sigma S = (P - \sigma)R - \omega^2 l(L - M), \quad . \quad . \quad . \quad . \quad . \quad . \quad . \quad (38)$$

$$MS - \sigma/\omega^2 C = R(L - M) + Pl. \quad . \quad . \quad . \quad . \quad . \quad . \quad . \quad . \quad (39)$$

In these equations M, C, $\sigma$, P, L, S may vary with frequency. Also $\sigma$, $l$ and the frequency variations may be taken to be so small that their squares or products may be ignored. Thus in the small terms of (38) and (39) we may assume with sufficient accuracy that the relations

$$M/C = PR, \; S = R(L - M)/M \quad . \quad . \quad . \quad . \quad . \quad . \quad . \quad . \quad (40)$$

will hold.

* A. Campbell, 'Proc. Phys. Soc.', vol. 20, p. 626, 1907. Also 'Phil. Mag.', October, 1907.

† The effective capacity and resistance refer to the whole arm. Thus C includes the equivaent capacities of the leads and any residual inductance in S, while S includes the effective resistance of the condenser and leads as well as any added resistance.

Digitized by Google

In regard to equation (38) if we write $P = P_0 + r$, where $P_0$ is the direct current resistance of P and $C_0 = M/P_0R$ we obtain to the first order of small quantities

$$C = C_0\left\{1 - \frac{r - \sigma L/M}{P_0} + \frac{\omega^2 l\,(L - M)}{P_0 R}\right\}, \quad . \quad . \quad . \quad . \quad . \quad . \quad . \quad . \quad (41)$$

which shows that if we calculate $C_0$ with the value of M proper to the frequency of measurement there is a further frequency correction due not only to residual inductance in R, but also due to the change of the effective resistance of P and to the change of impurity with frequency. The latter correction is less the greater the value of $P_0$, so that different values of $C_0$ may be obtained if measurements are made with different values of $P_0$ keeping $P_0R$ constant. Even if the values of $C_0$ are consistent with various values of $P_0$ this is no proof that $r$ and $\sigma$ are negligible, but merely that they are of the same sign and that $r/L$ and $\sigma/M$ are approximately equal.

Since $r$ and $\sigma$ normally vary as the square of the frequency, it is probably preferable to write (41)

$$C = \frac{M_0}{P_0 R}(1 + \gamma\omega^2), \quad . \quad . \quad . \quad . \quad . \quad . \quad . \quad . \quad . \quad . \quad . \quad (42)$$

in which $\gamma\omega^2$ is the frequency correction peculiar to the particular arrangement of capacity inductance bridge used, and $M_0$ is the geometrical mutual inductance.

It is possible by means of Anderson's bridge to determine the true variation of the capacity of a condenser with frequency so that the value of $\gamma$ may be determined.

Further, by taking observations with different values of $P_0$ keeping $P_0R$ constant, the first correction term in (41) may be separated, and therefore since the residual inductance $l$ of R may be measured we can determine by means of the capacity balance of the Carey-Foster bridge the true variation of M with frequency and the value of $r - \sigma L/M$.

Turning now to the second equation of balance (39) the resistance S includes the series resistance, ($s$) representing loss in the condenser, so that putting $S = S_0 + s$ equation (39) may be written

$$s - \sigma/\omega^2 MC = R\left(\frac{L}{M} - 1\right) + \frac{Pl}{M} - S_0. \quad . \quad . \quad . \quad . \quad . \quad . \quad . \quad . \quad (43)$$

Now L/M may vary with the frequency, but otherwise the quantities on the right-hand side of (43) may be regarded as known.

Writing

$$L/M = L_0/M_0 + \mu\omega^2 \quad . \quad . \quad . \quad . \quad . \quad . \quad . \quad . \quad . \quad . \quad . \quad (44)$$

and

$$s_0 = R\,(L_0/M_0 - 1) + \frac{Pl}{M} - S_0, \quad . \quad . \quad . \quad . \quad . \quad . \quad . \quad . \quad . \quad (45)$$

$s_0$ being capable of being precisely determined, we have

$$s - \sigma/\omega^2 MC - \mu\omega^2 R = s_0. \quad . \quad . \quad . \quad . \quad . \quad . \quad . \quad . \quad . \quad (46)$$

Thus the second equation in the Carey-Foster bridge balance merely gives a relation between three unknown quantities,

Digitized by Google

However, by taking observations with different values of R keeping PR constant, the value of $\mu$ may be determined. If $\sigma$ varies as the square of the frequency equation (46) shows that even if the correction $\mu\omega^2 R$ is applied the apparent series resistance of a condenser as measured by the Carey Foster-method is still in error by a constant amount.

As regards the above determination of the correction $\mu$, a check determination may be made if the variation of the series resistance of a condenser with frequency can be determined independently. This may be done by a proper use of Anderson's bridge.* A comparison of the variations of $s_0$ in equation (46) with those of $s$ then gives the value of $\mu\omega^2 R$, the assumption being that $\sigma/\omega^2 MC$ is constant, or that $\sigma$ varies as the square of the frequency. As has already been pointed out, the four-point contact where the galvanometer and R are connected to the inductometer may cause trouble in regard to the impurity. If this causes a true resistance coupling it will introduce a term varying as $1/\omega^2$ in the apparent series resistance of the condenser, and is thus of importance at the lower frequencies.

### 23. *The Modified Campbell Frequency Bridge.*†

This bridge is shown in Fig. 8, the modification being the addition of an adjustable condenser C′ across the open ends of the inductometer M.

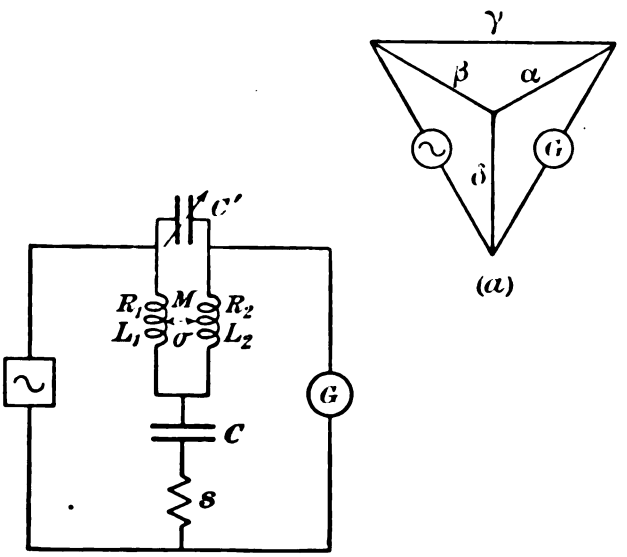


Fig. 8. Modified Campbell Frequency Bridge.

If the mutual inductance and capacity C are both perfect, the only condition of balance is

$$\omega^2 MC = 1. \quad . \quad . \quad . \quad . \quad . \quad . \quad . \quad . \quad . \quad . \quad . \quad (47)$$

* The use of Anderson's bridge for determining the true variation of the series resistance and capacity of a condenser will form the subject of the separate Paper.

† A. Campbell, 'Proc. Phys. Soc.', vol. 21, p. 69, 1908.

Digitized by Google

If these two elements are not perfect a second balance is required. Equation (9) shows that intercapacity may be used to cause the impurity of a mutual inductance to assume a negative value. This suggests the introduction of the condenser C′ in Fig. 8. The addition of C′ will modify the original condition (47). The new conditions are found as follows:—Apply transformation (A) to the mutual inductance to convert it to a "star" combination without mutual inductance. Then apply transformation (B) to the mesh formed by C′ and the two arms of the star which it connects. The result is that the generating and detecting circuits are connected only by a single arm and the conditions of balance follow from the condition that the vector impedance of this arm shall be zero. Thus after transformation (A) the circuits are as shown in Fig. 8 (*a*) in which the vector impedances are

$$\alpha = R_1 - \sigma + j\omega (L_1 - M), \qquad \beta = R_2 - \sigma + j\omega (L_2 + M),$$
$$\gamma = j/\omega C', \qquad \delta = \sigma + s + j (\omega M - 1/\omega C).$$

Applying transformation (B) to the mesh $\alpha$, $\beta$, $\gamma$ the arm common to the generating and detecting circuits will then have vector impedance $\alpha\beta/(\alpha + \beta + \gamma) + \delta$, and the condition of balance is that

$$\alpha\beta/(\alpha + \beta + \gamma) + \delta = 0. \quad . \quad . \quad . \quad . \quad . \quad . \quad . \quad . \quad . \quad (48)$$

Now for small values of $\sigma$ and $s$, $\delta$ will be small compared with $\alpha$ and $\beta$ in the neighbourhood of balance. Hence $\gamma$ must be large, so that to the first order of small quantities (48) becomes

$$\alpha\beta/\gamma + \delta = 0. \quad . \quad . \quad . \quad . \quad . \quad . \quad . \quad . \quad . \quad . \quad (49)$$

Inserting the values of $\alpha$, $\beta$, $\gamma$, $\delta$ the two conditions are

$$\omega^2 MC = 1 - \omega^2 CC'\{R_1R_2 - \omega^2 (L_1 - M) (L_2 - M)\}, \quad . \quad . \quad . \quad . \quad (50)$$
$$\sigma + s = \omega^2 C'\{R_1 (L_2 - M) + R_2 (L_1 - M)\}, \quad . \quad . \quad . \quad . \quad . \quad . \quad . \quad (51)$$

$\sigma$ being ignored where it is multiplied by the small quantity C′.

In regard to equation (50) it should be noted that if the relation

$$R_1R_2 = \omega^2 (L_1 - M) (L_2 - M) \quad . \quad . \quad . \quad . \quad . \quad . \quad . \quad . \quad (52)$$

is satisfied, then to the first order of small quantities, the original condition

$$\omega^2 MC = 1$$

is the condition for this balance. At the usual frequencies for which the bridge is suitable (1,000 cycles per second upwards) the relation (52) is practically $L_1$ or $L_2 = M$. When this condition is satisfied the balances do not react on each other if adjustments are made by C and C′. Otherwise the adjustments may be made independent by inserting a small adjustable resistance (= S, say) in series with the condenser C, and adjusting by C and S.

Digitized by Google

As regards equation (51) it is not necessary to know the separate values of $R_1$, $R_2$, etc., if the following procedure is adopted. Using the adjustments C and S repeat the balances with different values of C′. Then since $\sigma + s + S$ is proportional to C′, the latter when plotted against S will give a straight line cutting the negative side of the axis of S at the value $\sigma + s$. This method may be used if C′ is so large that the approximation used in obtaining equations (50) and (51) is not longer valid. For then by expansion of $\alpha\beta/(\alpha + \beta + \gamma)$ in powers of $1/\gamma$ and extracting the real part we obtain instead of (51) an expression of the form

$$\sigma + s + S = AC' + BC'^2 + \ldots\ldots\ldots\ldots\ldots \quad (53)$$

By using a sufficient number of values of C′ the quantities $\sigma + s$, A, B . . . may be found. The same procedure holds in regard to (50), the equation being of the form

$$\omega^2 MC = 1 + A'C' + B'C'^2 + \ldots\ldots\ldots\ldots\ldots \quad (54)$$

The modified frequency bridge will therefore yield the values of $\sigma + s$ and MC at a known frequency.

## 24. *Determination of Impurity of a Mutual Inductance and Series Resistance of a Condenser by Two Sets of Bridge Measurements.*

It has been shown in section 22 that the value of $s - \sigma/\omega^2 MC$ may be determined by means of the Carey-Foster bridge, and in section 23 that the value of $\sigma + s$ may be found by means of the modified Campbell frequency bridge if the frequency is such that $\omega^2 MC \doteqdot 1$. Hence the two sets of determinations yield $s - \sigma$ and $s + \sigma$ respectively at this frequency and enable $s$ and $\sigma$ to be determined separately. An essential point in this and similar methods is that the common point of the mutual inductance shall be the same in both bridges, as a change in common point will alter the intercapacity relations and, therefore, alter $\sigma$.

## 25. *Measurement of Impurity and Effective Resistance by Combined Observations on the Heaviside Bridge and the Carey-Foster Bridge.*

If observations of the capacity balance are taken on the Carey-Foster bridge with different values of P, keeping PR constant, the results enable $(r - \sigma L/M)$ to be determined, where $r$ is the added resistance in the arm P due to the alternations of the current. Again, from the Heaviside bridge, if $r'$ is the added resistance of another inductive coil (the coil $\mathcal{L}$ of Fig. 6), the measurements give $r' - 2\sigma$. Hence, if two inductometers are used we can measure $r - \sigma L/M$, $r' - \sigma' L'/M'$, $r' - 2\sigma$, $r - 2\sigma'$, the accented letters referring to the second inductometer. These four relations will, therefore, give the required quantities $r$, $r'$, $\sigma$, $\sigma'$.



Digitized by Google

26. *Experimental Study of the Frequency Variations of a Mutual Inductometer.*

The inductometer studied was one of the Campbell type* having a range of 10 millihenries sub-divided by tappings in steps of 0·1 millihenry for coarse adjustment, while fine adjustments were secured by a moving coil having a range somewhat greater than 0·1 millihenry. The scale of the moving coil was capable of being read to 0·1 microhenry, so that an accuracy of setting of one part in 100,000 of the whole range could be secured.

The method of sub-division of the fixed coils is important. This is obtained by twisting 10 equal insulated strands together, connecting in series through tappings, winding as one coil (the primary coil) and adjusting the *whole* to have a mutual inductance of 10 millihenries with regard to the fixed secondary coil. By this method the sub-division into millihenries is found to be correct to a fraction of a microhenry.

This mode of sub-division, however, introduces large capacity effects in the coil because the first and last sections are very close together. When one section only is used, the presence of the remaining nine sections, almost perfectly coupled, causes the system to behave as a 9 to 1 transformer with a capacity load, and thus introduces a large effective self capacity in the coil in use.

27.

The frequency variations to be determined are those of the mutual inductance and the self inductance of the secondary coil, the impurity, and the effective resistance of the secondary coil. These quantities are not usually required for the primary coil, as this coil is in the source arm in alternating current bridges. The methods to be given are independent of any assumption in regard to the perfection of inductive coils and condensers. All that is assumed is that " non-inductive " resistances and the residual inductances of these resistances are invariable with frequency.

28. *Source Employed.*

The source employed was the simple valve circuit, shown in Fig. 9.

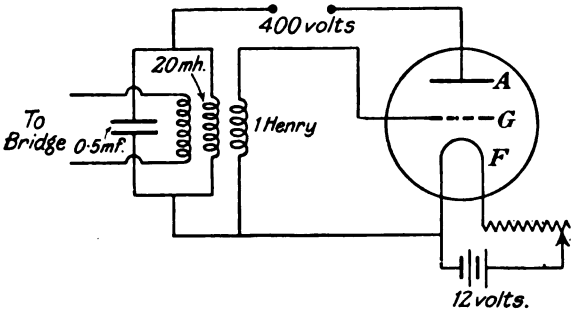


Fig. 9. Source of Alternating Current.

The filament current of the valve was about 4 amperes, and the filament voltage 12 volts, while the anode voltage was 400 volts. The anode inductance was 20 millihenries, and the anode capacity was adjustable continuously to 5 mfds., so that frequency could

* A Campbell, ' Proc. Phys. Soc.', vol. 21, p. 69, 1908.

Digitized by Google

be varied from 500 ~ per second upwards. The grid inductance was about 1 henry and was not usually tuned.

A number of experiments were made using the modified Campbell frequency bridge, partly to test the modification, but mainly to form some notion of the steadiness of the valve source and its reaction to various factors.

With a frequency bridge for which M $\fallingdotseq$ 10 millihenries, C = 0·5 mfd., so that the frequency was about 1,600 ~ per second, it was found that by placing an air condenser (*c*) in parallel with C, and making the final adjustments by this condenser, the sensitivity with a 60-ohms Brown telephone was such as to enable a change of 1 $\mu\mu$F to be detected. This means that the arrangement is capable of holding a frequency constant to one part in a million if the other elements of the bridge can be kept constant to this accuracy.

The following observations illustrate a test of the drift in frequency which occurred during a three-hours' continuous run of the source, the bridge being kept on continuously :

| Time. | Temperatures. | | M Setting $\mu$H. | Readings. $\mu\mu$F. | | | | | |
|---|---|---|---|---|---|---|---|---|---|
| | Source Table. | Bridge Table. | | | | | | | |
| h. m. | °C. | °C. | | | | | | | |
| 5 15 | 18·8 | 20·5 | ... | | | ... | | | Valve on. |
| 5 30 | ... | ... | ... | | | ... | | | Bridge on. |
| 5 43 | ... | ... | 100 10·0 | 129 | 135 | 141 | 147 | 159 | Minute |
| 5 52 | | | | 165 | 170 | 178 | 185 | 190 | readings. |
| 6 15 | 18·7 | 20·5 | 100 12·0 | 132 | 134 | 136 | 138 | 139·5 | |
| 6 20 | | | | 142 | 143·5 | 146 | 148 | 150 | |
| 6 47 | 18·8 | 20·5 | 100 13·0 | 124 | 125 | 127 | 128 | 129 | |
| 6 52 | | | | 129·5 | 131 | 131·5 | 134 | 134 | |
| 7 15 | 18·7 | 20·5 | 100 13·0 | 166·5 | 167 | 167·5 | 167·5 | 168 | Half-minute |
| 7 20 | | | | 168·5 | 169 | 170 | 179·5 | 171 | readings. |
| 7 45 | 18·65 | 20·5 | 100 13·0 | 187·5 | 188 | 188 | 189 | 189·5 | |
| 7 50 | | | | 189 | 189 | 189·5 | 190·5 | 190 | |
| 8 13 | 18·6 | 20·5 | 100 13·0 | 197 | 197 | 196 | 196·5 | 196 | |
| 8 18 | | | | 196·5 | 196·5 | 196·5 | 197 | 197 | |

From the groups of observations of *c* the values of the inductance M which would have secured a balance without change of *c* were deduced for the moments given in the following table, which also gives the drifts at these moments expressed in terms of M.

| Time. | Corrected M. $\mu$H. | Drift per min. |
|---|---|---|
| h. m. | | |
| 5 45 | 100 11·42$_1$ | 0·071 |
| 6 15 | 13·32$_0$ | 0·040 |
| 6 45 | 14·20$_0$ | 0·022 |
| 7 15 | 14·66$_2$ | 0·010 |
| 7 45 | 14·87$_9$ | 0·004$_8$ |
| 8 15 | 14·96$_6$ | 0·000$_8$ |



Digitized by Google

Since for the frequency bridge $\omega^2MC = 1$, the changes in adjustments of M with time are proportional to $1/\omega^2$.

The results are plotted in Fig. 10, the tangential lines representing the observed drifts. The curve B shows the observed drift on a Carey-Foster bridge under similar conditions. The balance for this bridge is practically independent of frequency, so that this curve gives some indication as to what portion of the drift is contributed by the elements of the bridge.

The curve shows the extremely regular behaviour of a valve source when working under favourable conditions.

The whole change in $2\frac{1}{2}$ hours is only 2 parts in 10,000 when expressed in terms of frequency, the change in the last hour being 15 in a million, and during the whole period there was no detectable departure from a regular drift. Other tests were made showing that the source was susceptible to various factors. A change of valve condenser after

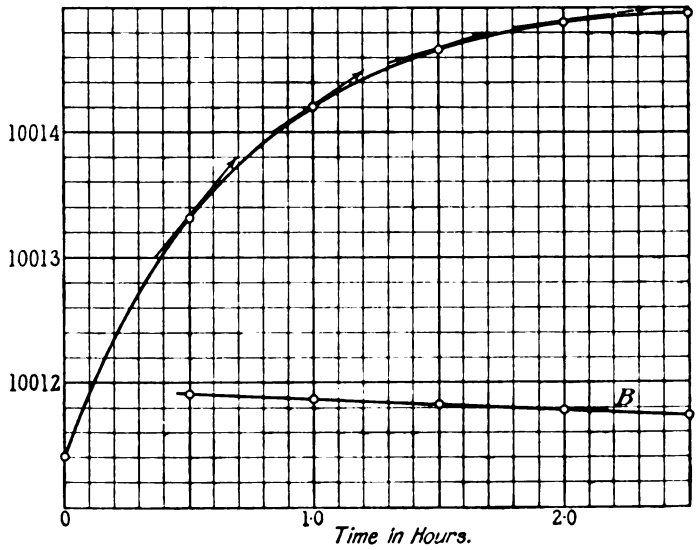


Fig. 10. Drift in Frequency of a Valve Source as indicated by the Modified Frequency Bridge.

the circuit had been brought to a steady state immediately produced a further drift in frequency towards a new state of equilibrium (apart altogether from that due to any change in the value of the capacity). Some condensers produced a drift of opposite sign.

An increase in condenser current of 2 per cent. produced an increase in frequency of two parts in 100,000 and a reduced filament current also increased the frequency by a few parts in 100,000, these changes taking place immediately. By running the valve on full filament current for some time it was found possible to bring about a steady state for a reduced filament current much earlier than is indicated by Fig. 10. The source frequency is also susceptible to variations in load on the bridge, the change of frequency being such as would be expected from the reduced effective inductance of the valve circuit when coupled to the bridge circuit. It is therefore necessary when bridge measurements are being taken which involve extreme steadiness of frequency and also considerable changes in the effective resistance of the bridge to have an auxiliary frequency

Digitized by Google

bridge to hold the frequency constant. The modified frequency bridge has been found very useful for this purpose.

### 29. *Earth Capacities.*

It was found to be necessary to make corrections for earth capacities in certain of the bridge measurements. In bridges of the Wheatstone bridge type (the Heaviside bridge and the Carey-Foster bridge) the Wagner earthing device may be used,* but actually a method of correction was employed involving two measurements with different earth points. This method will form the subject of a separate Paper.

In the case of the frequency bridge, the bridge was connected to earth at the point common to the source, detector and condenser arm as the earth capacities (assumed to be condenser arms connecting the branch points to earth) will either have no effect or act as an added capacity to C (Fig. 8). As this bridge was simply used to measure *changes* in frequency or to determine quantities in which C was involved, only to the first order of small quantities, no appreciable error could arise from this cause.

### 30. *Frequency Coefficient of Mutual Inductance.*

For this purpose a Carey-Foster bridge method was employed, using a condenser of nominal value 0·5 mfd., whose variation with frequency had been determined by Anderson's bridge. The curve of variation for this condenser is shown in Fig. 11 in which the

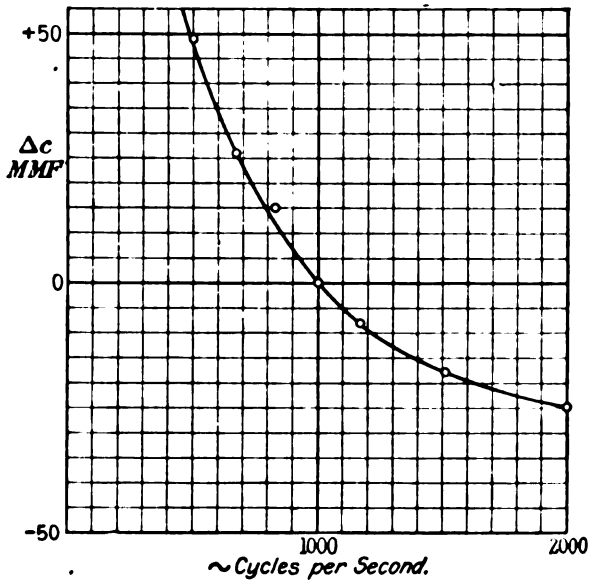


Fig. 11. Change of Capacity of ½ μF Condenser with Frequency.

variations ΔC in micro-microfarads are plotted against frequency. Since the leads to the condenser and the resistance S are included in the condenser arm (Fig. 7), the effect of their residual inductances must be included in the value of C in equation (41). Let

* *See* LAWS, ' Electrical Measurements '.

Digitized by Google

the residual inductance of the condenser arm be $\lambda$. Then if C in (14) is replaced by C $(1 + \omega^2\lambda C)$ the equation becomes

$$C = \frac{M}{P_0R}\left\{1 - \frac{r - \sigma L/M}{P_0} + \frac{\omega^2 l\,(L - M)}{P_0R} - \omega^2\lambda C\right\} \quad . \quad . \quad . \quad . \quad . \quad . \quad (55)$$

Writing $M = M_0\,(1 + \gamma'\omega^2)$, (55) becomes

$$C = \frac{M_0}{P_0R}(1 + \gamma\omega^2), \quad . \quad . \quad . \quad . \quad . \quad . \quad . \quad . \quad . \quad . \quad . \quad (56)$$

in which

$$\gamma\omega^2 = \gamma'\omega^2 - \frac{r - \sigma L/M}{P_0} + \frac{\omega^2 l\,(L - M)}{P_0R} - \omega^2\lambda C, \quad . \quad . \quad . \quad . \quad . \quad (57)$$

and is the frequency correction of the whole bridge outside the condenser.

$\gamma$ may be determined by the variations in the M settings required to balance the known variations in C at different frequencies. Actually coarse adjustments only were made by the moving coil of M, the fine adjustments being made by an air condenser C′ in parallel with C. By subtracting $C'P_0R$ from the reading of M (viz., $M_0$, since the inductometer is calibrated at low frequencies) the value of $M_0$ could be deduced which would give the reading when C′ was absent, and by further subtracting $\Delta C \times P_0R$ (Fig. 11) the value of $M_0$ if C had remained constant at its value at a frequency 1,000 could be obtained.

This procedure gave the following results :—

$P_0 = 400$ ohms. $\qquad$ $R = 50$ ohms.

| Frequency $f \sim$ per second. | $M_0$ setting $\mu$H. | C′ $\mu\mu$F. | $\Delta C$ $\mu\mu$F. | $M_0$ corrected $\mu$H. | $M_0$ deduced $\mu$H. |
|---|---|---|---|---|---|
| 1,650 | 10,025 | 113 | − 20 | $10023{\cdot}1_4$ | $10023{\cdot}1_7$ |
| 1,170 | 10,040 | 202·5 | − 8 | $10036{\cdot}1_1$ | $10036{\cdot}0_8$ |
| 825 | 10,047 | 203·5 | +12 | $10042{\cdot}6_9$ | $10042{\cdot}6_7$ |

The values in the last column are such as to satisfy the law $M_0 = 10049{\cdot}1_7\,\{1 - 9{\cdot}51 \times 10^{-4}\,(f/1{,}000)^2\}$, so that by (56)

$$\gamma\omega^2 = 9{\cdot}51 \times 10^{-4} \quad \text{when} \quad f = 1000.$$

For the resistances used

$$\lambda = 6{\cdot}5\mu\text{H}, \qquad l = 2{\cdot}8\ \mu\text{H}, \qquad L = 26{\cdot}1\ m\text{H}.$$

Using these in (57)

$$\gamma'\omega^2 - \frac{r - \sigma L/M}{P_0} = 9{\cdot}9_1 \times 10^{-4}.$$

Measurements made with $P_0 = 200$, $R = 100$ and $P_0 = 100$, $R = 200$ gave the

Digitized by Google

values $9{\cdot}9_8 \times 10^{-4}$ and $10{\cdot}1_1 \times 10^{-4}$ respectively. By plotting these results against $1/P_0$ the values of $\gamma'\omega^2$ and $r - \sigma L/M$ may be separated leading to

$$\gamma'\omega^2 = 9{\cdot}8 \times 10^{-4},$$
$$r - \sigma L/M = -0{\cdot}003_5 \text{ ohm}$$

at a frequency of 1,000 ~ per second.

31. *Measurements of Impurity and Frequency Coefficient of L/M.*

By the theory given in section 22, if $s_0$ is the apparent series resistance of the condenser in the Carey-Foster bridge as defined by equation (45), $s_0$ is of the form

$$s_0 = a - bR, \quad \ldots\ldots\ldots\ldots \quad (58)$$

when the values of $s_0$ are determined with different values of R, keeping $P_0R$ constant, the values of $a$ and $b$ being by (46)

$$a = s - \sigma/\omega^2 MC,$$
$$b = \mu\omega^2,$$

$s$ being the true series resistance of the condenser C, $\sigma$ the impurity of the mutual inductance M, and $\mu\omega^2$ the frequency correction of L/M. The values of $a$ and $b$ were determined using the condenser already employed in section 30 for three different frequencies. The results are given in the following table, the columns marked "$s_0$ calculated" being obtained from (58), using the best values of $a$ and $b$ for the observations.

TABLE.

Carey-Foster Bridge.
Variation of P and R.

$M_0 \doteqdot 10$ mh. $\qquad L_0 = 26{\cdot}110$ mh.
$C \doteqdot 0{\cdot}5$ μF. $\qquad PR = 20{,}000.$

$f$ = frequency ~ per second.

| R ohms. | $f = 1{,}000$. | | $f = 1{,}600$. | | $f = 2{,}000$. | |
|---|---|---|---|---|---|---|
| | $s_0$ observed ohms. | $s_0$ calculated. | $s_0$ observed ohms. | $s_0$ calculated. | $s_0$ observed ohms. | $s_0$ calculated. |
| 50 | 0·098 | 0·098 | 0·096 | 0·096 | 0·128 | 0·130 |
| 100 | 0·128 | 0·127 | 0·167 | 0·165 | 0·243 | 0·241 |
| 200 | 0·185 | 0·185 | 0·302 | 0·303 | 0·464 | 0·462 |
| $a =$ | 0·069 | | 0·027 | | 0·019 | |
| $-b =$ | 0·00058 | | 0·00138 | | 0·00222 | |
| $-\frac{b}{\omega^2} =$ | $1{\cdot}42 \times 10^{-11}$ | | $1{\cdot}38 \times 10^{-11}$ | | $1{\cdot}40 \times 10^{-11}$ | |

Digitized by Google

Hence, as a mean value

$$\mu = -1{\cdot}40 \times 10^{-11}.$$

A check on this determination may be obtained by combining the results of observations on the Carey-Foster bridge with observations on Anderson's bridge.*

For the Carey-Foster bridge we have equation (46), viz.,

$$s_0 = s - \sigma/\omega^2 MC - \mu\omega^2 R, \quad \ldots\ldots\ldots\ldots \quad (46)$$

and for Anderson's bridge,* if $s'$ is the series resistance used with the condenser,

$$s' = A - s,$$

where A is a quantity independent of frequency involving the remaining residuals in Anderson's bridge.

Hence

$$s_0 + s' = A - \frac{\sigma}{\omega^2 MC} = \mu\omega^2 R,$$

or, since $\sigma$ is proportional to $\omega^2$

$$s_0 + s' = A' - \mu\omega^2 R, \quad \ldots\ldots\ldots\ldots \quad (59)$$

from which $\mu$ may be found by observations at different frequencies.

The results obtained by this method for three different condensers are given in the following table :—

TABLE.

Anderson's Bridge and Carey-Foster Bridge.

For the Carey-Foster Bridge—

M $\doteqdot$ 10 mh. C $\doteqdot$ 0·5 μF. $L_0$ = 26·110 mh. P = 400 ohms. R = 50 ohms.

$$s_0 = R\left(\frac{L_0}{M_0} - 1\right) + \frac{Pl}{M} - S.$$

$s'$ = series resistance in Anderson's Bridge.

| Frequency ~ per second. | —— | Condenser I. | Condenser II. | Condenser III. |
|---|---|---|---|---|
| 1,000 | $s_0$ ... ... ... ... | 0·100 | 0·077 | −0·016 |
| | $s'$ ... ... ... ... | 0·625 | 0·650 | 0·715 |
| | $s_0+s'$ observed ... ... | 0·725 | 0·727 | 0·699 |
| | $s_0+s'$ calculated... ... | 0·726 | 0·726 | 0·700 |
| 1,600 | $s_0$ ... ... ... ... | 0·096 | 0·072 | +0·001 |
| | $s'$ ... ... ... ... | 0·675 | 0·700 | 0·740 |
| | $s_0+s'$ observed ... ... | 0·771 | 0·772 | 0·741 |
| | $s_0+s'$ calculated ... | 0·771 | 0·771 | 0·745 |
| 2,000 | $s_0$ ... ... ... ... | 0·127 | 0·096 | 0·042 |
| | $s'$ ... ... ... ... | 0·685 | 0·715 | 0·751 |
| | $s_0+s'$ observed ... ... | 0·812 | 0·811 | 0·793 |
| | $s_0+s'$ calculated ... | 0·812 | 0·812 | 0·786 |

* The use of Anderson's bridge for determining the true variation of the series resistance and capacity of a condenser will form the subject of a separate Paper.

Digitized by Google

The calculated values of $s_0 + s'$ were obtained from formula (59), using as the values A′ for the three condensers.

$$A' = 0{\cdot}698 \quad 0{\cdot}698 \quad 0{\cdot}672,$$

and for $\mu$ the common value $-1{\cdot}42_5 \times 10^{-11}$, which are the values agreeing best with the observations. This value of $\mu$ differs from the previous determination by 2 per cent.

As regards A′, the capacity of condenser III was a few per cent. higher than those of condensers I and II, which differed only by 2 or 3 parts in 10,000. The differences in A′ are sufficiently accounted for by the changes in the residuals in Anderson's bridge brought about by rebalancing for condenser III.

*Determination of $\sigma$.*

Using the known value of $\mu$ in equation (46) the values of $s - \sigma/\omega^2MC$ at a frequency of 1,600 cycles per second for the three condensers are

$$+ 0{\cdot}025, \quad + 0{\cdot}001, \quad - 0{\cdot}070.$$

Since $\omega^2MC = \frac{1}{2}$ at this frequency, these are the values of $s - 2\sigma$.

Another relation between $s$ and $\sigma$ can be found by the modified frequency bridge (section 23). For this bridge $\omega^2MC \doteqdot 1$, and this condition may be secured by paralleling two of the condensers, say, I and II.

By the usual laws of combination, and by (53) the modified frequency bridge measures

$$(s_1 + s_2)/4 + \sigma.$$

The value obtained with condensers I and II was

$$(s_1 + s_2)/4 + \sigma = 0{\cdot}096.$$

Now,

$$s_1 - 2\sigma = 0{\cdot}025,$$

$$s_2 - 2\sigma = 0{\cdot}001.$$

so that, solving for $s_1$, $s_2$, $\sigma$, $s_1 = 0{\cdot}115$, $s_2 = 0{\cdot}091$, $\sigma = 0{\cdot}045$ ohm. Using this value of $\sigma$ for the condenser III,

$$s_3 = 0{\cdot}020.$$

Since $\sigma$ varies as the square of the frequency, the value of $\sigma$ for the inductometer studied is $0{\cdot}017_5$ ohm, at a frequency of 1,000 cycles per second.

## 32. *Summary of Inductometer Corrections.*

From the results obtained in sections 30 and 31 the corrections for frequency for the inductometer studied are as follows :—

At a frequency of 1,000 ~ per second the mutual inductance has a positive correction of 9·8 parts in 10,000* the self-inductance of the secondary coil has a positive correction

* This result is in good agreement with an earlier determination on the same inductometer by CAMPBELL. 'Roy. Soc. Proc.', vol. 87, p. 406, 1912.



Digitized by Google

of 7·6 parts in 10,000, the impurity is $0{\cdot}017_5$ ohm, and the effective resistance of the secondary coil is greater than its direct current value by 0·042 ohm.

All the corrections vary as the square of the frequency.

These corrections only hold when the mutual inductance has a common point such that when the coils are in series, the mutual inductance opposes the self-inductances.

### 33. *Determination of Impurity by Measurements of Effective Resistance.*

If an inductive coil L is placed in series with a condenser C, a non-inductive resistance and an alternating-current ammeter so as to form a simple circuit, the current induced in the circuit by an E.M.F. E, alternating with frequency $\omega/2\pi$, is $I = E/\{R^2 + (\omega L - 1/\omega C)^2\}^{\frac{1}{2}}$, so that if C is adjusted to resonance with L, the current is a maximum and has the value $I_{max.} = E/R$.

By observing the maximum current with different values of the non-inductive resistance the resistance of the remainder of the circuit may be deduced. The method therefore gives the resistance of the coil and condenser in series. Assuming the condenser to have the same power-factor at all frequencies, then remembering that the value of the capacity is altered for different frequencies, the series resistance of the condenser will increase as the frequency, while if the coil is wound with thin wire the resistance of the coil increases as the square of the frequency, so that the losses in the condenser will become less and less important as the frequency increases. Moreover, at the higher frequencies the resonating capacity may be made so small that an air condenser may be used and thus the condenser losses may be still further reduced.

In order to determine the impurity of a mutual inductance by this method, the two coils are connected at one point (B in Fig. 7A) and the effective resistances measured across the points AB, BC, CA. If at a particular frequency the values of the effective resistances are $R_1$, $R_2$, $R_3$ respectively, then since $R_3 = R_1 + R_2 - 2\sigma$ we have $\sigma = \frac{1}{2}(R_1 + R_2 - R_3)$.

The following values were obtained for a fixed mutual inductance of 10 millihenries, wound on marble with No. 26 d.s.c. wire.

Primary coil L = 21·9 millihenries. D.C.R. = 12·54 ohms.

Secondary coil L = 21·5 millihenries. D.C.R. = 12·25 ohms.

ALTERNATING Current Resistances.

| Frequency. ~ per second. | Primary. | Secondary. ohms. | Series. opposition. |
|---|---|---|---|
| 17,300 | 36 | 34 | 59 |
| 25,000 | 62 | 59 | 99 |
| 33,300 | 105 | 98 | 154 |

Digitized by Google

The resistances are plotted against the square of the frequency in Fig. 12, and from the mean straight lines we find at $f = 1{,}000$ ~ per second, the following corrections :—

| | |
|---|---|
| Primary | 0·081 ohm, |
| Secondary | 0·075 ohm, |
| Series opposition | 0·118 ohm, |

from which the impurity is 0·020 ohm.

The same inductance was tested at a frequency of 1,600 ~ per second upon the modified frequency bridge, using a 1 μF condenser of known power-factor. The deduced impurity at a frequency of 1,000 ~ per second by this method was 0·0207 ohm.

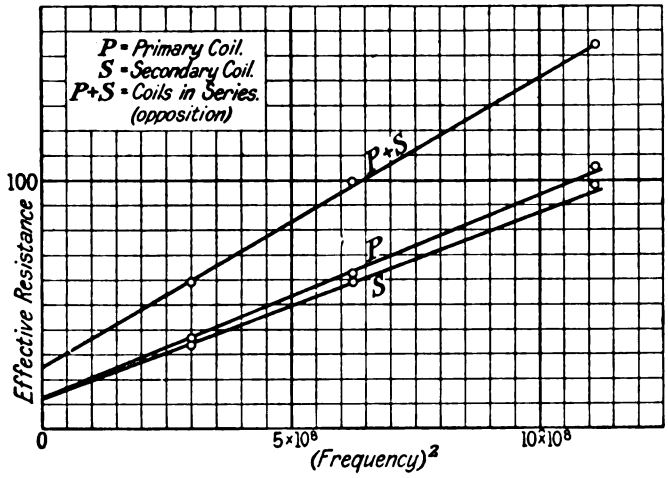


Fig. 12. Effective Resistance of Coils of Inductometer.

### 34. *Errors in Power-Factor Measurements due to Imperfections of Mutual Inductance.*

Equation (46) may be written

$$\omega s_0 C = \omega s C - \sigma/\omega M - \mu\omega^3 M/P,$$

and since $\omega s C$ is the power factor of the condenser, $\omega s_0 C$ will be apparent power-factor of the condenser as deduced from Carey-Foster bridge observations upon the assumption of a perfect mutual inductance. It is seen that the apparent power-factor is subject to two errors, one due to impurity and proportional to the frequency, and the other due to the change of L/M with frequency, and proportional to the cube of the frequency. The latter error depends also on the resistances employed in the bridge. For the inductometer studied, the error due to impurity is $2{\cdot}8/10^4$ at a frequency of 1,000, and tends to make the apparent power-factor low, while the error due to the change of L/M is $0{\cdot}9/10^4$ (when $P = 400$ ohms), tending to make the apparent power-factor too high. These values hold whatever capacity is being measured. Since the power-factor of a good condenser is of the order of a few parts in 10,000, it



Digitized by Google

is clear that the Carey-Foster bridge measures the imperfections of its own mutual inductance, rather than the power-factor of the condenser at the higher telephonic frequencies. However, by a proper use of intercapacity the imperfections of the inductance may be compensated, the compensation holding over the whole range of frequencies for which the eddy current and capacity effects vary as the square of the frequency. A method of compensating a mutual inductance for change of mutual inductance with frequency and for impurity has already been given in section 19. This compensation is suitable for a mutual inductance used for the measurement of self inductance upon a Heaviside bridge, but when using the inductance upon a Carey-Foster bridge for power-factor measurements, what is required is that the impurity shall be zero, and the variation of L/M shall be zero.

Let a condenser C′ connect the open ends of the inductometer. Then by equations (8), (9), (11), the change in the frequency coefficient of $L_2/M$ is $\omega^2 C' (L_2 - M)(L_1 L_2 - M)^2 / ML_2$ and the change in $\sigma$ is

$$- \omega^2 C' \{R_2 (L_1 - M) + R_1 (L_2 - M)\}.$$

For the inductometer studied the values of $L_1$, $L_2$, $R_1$, $R_2$, M were

$L_1 \doteqdot 7$ millihenries, $L_2 \doteqdot 26$ millihenries, $M = 10$ millihenries,
$R_1 \doteqdot 10$ ohms, $R_1 \doteqdot 18$ ohms.

Using these values we find that if $C' = 1{,}100$ $\mu\mu$F the change of $L_2/M$ due to C′ is $+ 2{\cdot}2/10^4$ at a frequency of 1,000 ~ per second, and this will just balance the existing variation of $- 2{\cdot}2/10^4$. Further, with this value of C′ a negative impurity of amount 0·0175 ohm will be introduced if $R_1$ is made equal to 21·5 ohms, so that by adding 11·5 ohms to the primary coil and using an added intercapacity of 1,100 $\mu\mu$F across the whole combination the corrections for this inductometer will be automatically compensated.

The experimental work was carried out at the National Physical Laboratory. I wish to thank a number of my colleagues, particularly Mr. D. W. Dye, for valuable suggestions during the course of the experimental investigation.

Digitized by Google

# EDDY-CURRENT LOSSES IN CYLINDRICAL CONDUCTORS WITH SPECIAL APPLICATIONS TO THE ALTERNATING CURRENT RESISTANCES OF SHORT COILS

BY

S. BUTTERWORTH, M.Sc.,
SOMETIME ASSISTANT IN THE ELECTRICITY DEPARTMENT.

Digitized by Google

## ABSTRACT.

1. The general theory of the eddy-current losses produced in a non-magnetic metallic cylinder when placed in a transverse field of any form is developed, and a series is obtained expressing the eddy-current losses.

From this series conclusions are drawn in regard to the modification of the losses by the want of uniformity of the field over the section of the cylinder. It is shown that in most practical cases a sufficiently good approximation to the losses may be obtained by assuming the field to be uniform throughout the section of the cylinder.

2. The theory is applied to obtain an approximate solution of the problem of the effective resistance of two equal parallel wires carrying equal currents either in the same or in opposite directions. The formula obtained is shown to be in good agreement with KENNELLY'S experimental results.

3. The "uniform-field" theory is applied to determine the effective resistance of parallel wire systems, and by calculating the mean square field acting throughout the section of the coil, formulæ are obtained for the effective resistances of single- and multi-layer solenoidal coils either of solid or of stranded wire. These formulæ are all included in the general formulæ (93), (94), (95) of the Paper.

4. The theoretical results in the case of single-layer solid wire coils at high frequencies are compared with measured values. When the effective resistances are measured by means of a resonance method using an air condenser, the measured values of the effective resistance $R^1$ at a wave-length $\lambda$ may be expressed in the form

$$R^1 = A/\sqrt{\lambda} + B/\lambda^2,$$

as has already been found by Lindemann, while eddy-current theory leads to the expression $R^1 = A/\sqrt{\lambda}$, in which A may be calculated from the coil dimensions. The value of A as calculated is in agreement with the value of A deduced from experiment.

The experimental constant B for a series of coils whose inductance ranges from 30 to 300 microhenries has been found to be approximately proportional to the square of the inductance, and thus the term $B/\lambda^2$ in the measured resistance is such as would be produced by an invariable shunt across the coil.

5. From the theoretical formulæ conditions are deduced in regard to the shape of coil and spacing to employ which will produce the maximum value of $L/R^1$ for a given length of wire of given diameter. For a single-layer coil at high frequencies the best shape to employ is $a/b = 1 \cdot 6$, and the best spacing is $D/d = 2$, where

$a$ = coil radius,
$b$ = coil length,
$d$ = diameter of wire,
D = distance apart of successive wires.

6. Solid wire coils are compared with stranded wire coils, both being wound under the most efficient conditions. It is found that if $s$ = number of strands in the stranded wire coil, the stranded wire coil is superior to the solid wire coil of equal copper section in the approximate ratio $s^{\frac{1}{2}} : 1$.

7. The observed inferiority of stranded wire coils as compared with solid wire coils at high frequencies is due to the lack of internal spacing of the strands of the coils, making the best conditions unattainable. If due regard is paid to proper spacing it should be possible to construct a stranded wire coil superior to a solid wire coil of equal copper section at any frequency.

8. The theoretical conditions for the minimum effective resistance of a many-layered coil of given inductance and resonating with a condenser of given capacity are worked out.

It is shown that if a series of such coils wound with the same diameter of wire are used with a given condenser (say to form a wavemeter circuit), these coils should all have the same radius and length in order to have minimum effective resistance at the same condenser reading.


Digitized by Google

# EDDY-CURRENT LOSSES IN CYLINDRICAL CONDUCTORS WITH SPECIAL APPLICATIONS TO THE ALTERNATING CURRENT RESISTANCES OF SHORT COILS.

By S. BUTTERWORTH, M.Sc., Sometime Assistant in the Electricity Department.

[Reprinted from the 'Philosophical Transactions of the Royal Society of London,' Series A, Vol. 222, 1921.]

## Introduction.

It is well known that a considerable proportion of the effective resistance of inductive coils when used at radio frequencies is caused by the eddy currents set up in the wires of the coils by the alternating magnetic field in which they are situated, and that in extreme cases the alternating current resistance may amount to more than one hundred times the direct current resistance. It is therefore important to have reliable formulæ for the eddy-current resistance of such coils in order to determine the conditions which will reduce the eddy-current losses to a minimum.

The simplest case, that of a long straight cylindrical wire under the action of its own current, has been treated by Kelvin,* Rayleigh,† Heaviside,‡ and others. The general effect is known as the "skin effect", because the current tends to concentrate more and more upon the skin of the conductor as the frequency increases.

The case of two parallel wires forming a go-and-return circuit has been considered theoretically by Nicholson,§ and experimentally examined by Kennelly.‖ Kennelly found that when the wires are close together, the added resistance due to the proximity of the wires may be of the same order as that due to the simple skin effect.

Nicholson's theoretical treatment includes the possibility that the dimensions of the system may be comparable with the wave-length of the disturbance. His formula is very complicated and difficult to apply numerically. A formula {formula (47)} for this case is obtained in section 8 of the present paper. This formula is shown (section 9) to give results in close accordance with Kennelly's observations.

In order to reduce the eddy-current losses solid wire is often replaced by stranded wire in which a bundle of thin separately insulated wires are interlaced symmetrically with each other, the notion being that the sum of the eddy losses in the individual wires

* 'Math. and Phys. Papers', vol. 3, 1889.

† 'Phil. Mag.', vol. 21, 1886.

‡ 'Electrical Papers', vol. 2, p. 64.

§ 'Phil. Mag.', vol. 18, p. 417, 1909.

‖ 'Trans. A.I.E.E.', vol. 35, part 2, p. 1953, 1915. Curtis ('Bull. Bureau of Standards', 1920) has recently published a formula for this case which gives agreement with Kennelly's results.

Digitized by Google

shall be less than the eddy loss in the corresponding solid wire. LINDEMANN* verified this experimentally at certain frequencies, but also found that if a solid wire coil and stranded wire coil were compared at various frequencies, the stranded wire coil increased in resistance more slowly at the lower frequencies but less slowly at the high frequencies, until above a certain frequency the stranded wire coil had a greater effective resistance than the solid wire coil.

HOWE† has treated the problem of straight stranded wire conductors, assuming the eddy losses to increase as the square of the frequency, and from his formulæ has shown that at high frequencies it is difficult to make the resistance of the stranded wire less than that of solid wire of equal section.

In view of the extensive use of stranded wire in the construction of coils for high-frequency currents, it is important that the limitations of stranded wire in reducing effective resistance should be known, so that the present investigation includes the consideration of such coils. From the formulæ obtained, conclusions are drawn in regard to the utility of stranding and in regard to what degree of stranding it is necessary to employ, before any improvement over solid wire coils may be expected.

In formulæ hitherto given for the effective resistance of coils, one or other of the following limitations occur :—

(1) The coil is very long.
(2) The frequency is limited to so low a value that the " square of frequency " law holds.
(3) The coil is wound with wire of square section.

The formulæ deduced in this paper differ from those already established in that—

(1) The dimensions of the winding sections of the coils are small compared with the coil radii.
(2) There is no limitation imposed upon the frequency.
(3) The wire is taken to be circular.

In regard to (1) it is shown that coils of this type have better alternating-current time constants than long coils.

In regard to variation with frequency, the factor governing the upper limit to the application of the square law is the magnitude of $f/R_0$ where $f$ is the frequency and $R_0$ is the direct current resistance per unit length of the wire used. If (in C.G.S. units) $f/R_0$ is less than 0·225 the eddy-current losses vary as $(f/R_0)^2$ to an accuracy of one per cent. At higher frequencies the variation is slower, the ultimate rate of variation being as $(f/R_0)^{\frac{1}{2}}$. A knowledge of these limiting rates of variation enables an immediate explanation to be given of LINDEMANN'S results with stranded wire coils.

A solid wire in a given alternating field has eddy losses which are a function of $f/R_0 = \phi(f/R_0)$ say. If the solid wire is replaced by $s$ strands of the same total metallic

* ' Deut. Phys. Gesell.', p. 382, 1909 ; p. 572, 1910. ' Jahrbuch der Drahtlosen Telegraphie ', p. 561, 1911.

† ' Roy. Soc. Proc.', A, vol. 93, p. 468, 1917.

Digitized by Google

section, the loss per strand in the same field is $\phi\,(f/sR_0)$ and the total loss in the $s$ strands is $s\phi\,(f/sR_0)$.

Thus, as regards the losses due to the general field of the remainder of the coil, we must replace $\phi\,(f/R_0)$ by $s\phi\,(f/sR_0)$ in passing from solid to stranded wire.

At low frequencies $\phi\,(f/R_0) = C\,(f/R_0)^2$ where C is a constant independent of the stranding, so that the respective losses are $C\,(f/R_0)^2$ and $Cs\,(f/sR_0)^2 = C\,(f/R_0)^2/s$.

The effect of stranding at low frequencies is thus to reduce these losses in the ratio $1/s$.

At high frequencies $\phi\,(f/R_0) = C'\,(f/R_0)^{\frac{1}{2}}$ and the losses are $C'\,(f/R_0)^{\frac{1}{2}}$ and $C's\,(f/sR_0)^{\frac{1}{2}} = C's^{\frac{1}{2}}\,(f/R_0)^{\frac{1}{2}}$, or the effect of stranding at high frequencies is to increase the losses in the ratio $s^{\frac{1}{2}}/1$.

Since in inductive coils the general field produces the main losses, LINDEMANN'S results are explained.

## (A). EDDY-CURRENT LOSSES IN A CYLINDER IN AN ALTERNATING MAGNETIC FIELD.

(1) The cylinder is supposed to be non-magnetic and to have electrical conductivity $k$. Its radius is $a$. The magnetic field is perpendicular to the axis of the cylinder and does not vary along the axis; otherwise its form is general. The field alternates with frequency $\omega/2\pi$, and the alternations are so slow that the dielectric current can be neglected in comparison with the conductance current. This means that the wave-length of the disturbance producing the field is large compared with the dimensions of the cylinder. On the other hand, the cylinder is supposed to be long enough to render its end effects negligible.

The procedure is to represent the electric and magnetic forces by rotors* $Ee^{i\omega t}$, &c. The values of these rotors are found at all points in terms of the (given) undisturbed field. Then by application of POYNTING'S Theorem over unit length of the surface of the cylinder, the energy flow into the cylinder is determined.

This energy flow may be regarded as made up of two portions, one continuous and the other alternating. The former portion is the energy dissipated by eddy currents set up in the cylinder.

(2) Take the axis of the cylinder as the axis of a right-handed system of cylindrical co-ordinates $(z, r, \theta)$. With the assumed conditions the electro-magnetic equations are

$$\left.\begin{aligned} -i\omega P = \frac{1}{r}\frac{\partial E}{\partial \theta}, \quad & i\omega Q = \frac{\partial E}{\partial r} \\ \frac{1}{r}\frac{\partial (Qr)}{\partial r} - \frac{1}{r}\frac{\partial P}{\partial \theta} = 4\pi k E \quad & \end{aligned}\right\}, \qquad \ldots\ldots\ldots \quad (1)$$

* These are the rotating vectors used to represent these quantities on the vector diagram. The term is chosen to distinguish them from the space vectors which are also involved in the problem.



Digitized by Google

in which P, Q represent the components of the magnetic force acting along and perpendicular to $r$, and E represents the electric force acting parallel to $z$.

Eliminating P and Q, the equation to be satisfied by E is

$$\frac{1}{r}\frac{\partial}{\partial r}\left(r\frac{\partial \mathrm{E}}{\partial r}\right)+\frac{1}{r^2}\frac{\partial^2 \mathrm{E}}{\partial \theta^2}=4\pi ki\omega \mathrm{E}, \quad . \quad . \quad . \quad . \quad . \quad . \quad . \quad . \quad . \quad (2)$$

the normal solution of which is

$$\mathrm{E}=\mathrm{R}_n\cos n\theta+\mathrm{S}_n\sin n\theta, \quad . \quad . \quad . \quad . \quad . \quad . \quad . \quad . \quad . \quad (3)$$

in which $\mathrm{R}_n$ and $\mathrm{S}_n$ are functions of $r$ both satisfying the equation

$$\frac{1}{r}\frac{d}{dr}\left(r\frac{d\mathrm{R}_n}{dr}\right)-\frac{n^2}{r^2}\mathrm{R}_n=4\pi ki\omega \mathrm{R}_n. \quad . \quad . \quad . \quad . \quad . \quad . \quad . \quad . \quad . \quad (4)$$

Writing $\lambda^2=-4\pi ki\omega$ and putting $x$ for $\lambda r$, (4) may be written

$$\vartheta^2\mathrm{R}_n+(x^2-n^2)\,\mathrm{R}_n=0, \quad . \quad . \quad . \quad . \quad . \quad . \quad . \quad . \quad . \quad (5)$$

in which

$$\vartheta\equiv x\frac{d}{dx}.$$

This is the general differential equation for the BESSEL functions, so that inside the cylinder the appropriate solution of (4) is

$$\mathrm{R}_n=\mathrm{A}_n\mathrm{J}_n(\lambda r), \quad . \quad . \quad . \quad . \quad . \quad . \quad . \quad . \quad . \quad . \quad (6)$$

the second solution being excluded, since the electric force is not infinite at the axis.

Outside the cylinder $k$ is zero, so that the solution of (4) is

$$\mathrm{R}_n=\mathrm{B}_n r^n+\mathrm{C}_n/r^n. \quad . \quad . \quad . \quad . \quad . \quad . \quad . \quad . \quad . \quad (6\mathrm{A})$$

except when $n=0$, in which case

$$\mathrm{R}_0=\mathrm{B}_0\log_e r+\mathrm{C}_0. \quad . \quad . \quad . \quad . \quad . \quad . \quad . \quad . \quad . \quad (6\mathrm{B})$$

In order to maintain the continuity of E and $\frac{\partial \mathrm{E}}{\partial r}$ at the boundary of the cylinder, $\mathrm{A}_n$, $\mathrm{B}_n$, $\mathrm{C}_n$ must satisfy the relations

$$\left.\begin{aligned}\mathrm{A}_n\mathrm{J}_n(\lambda a)&=\mathrm{B}_n a^n+\mathrm{C}_n/a^n\\ \mathrm{A}_n\lambda a\mathrm{J}'_n(\lambda a)&=n\,(\mathrm{B}_n a^n-\mathrm{C}_n/a^n)\end{aligned}\right\}\ n\neq 0$$

$$\left.\begin{aligned}\mathrm{A}_0\mathrm{J}_0(\lambda a)&=\mathrm{B}_0\log_e a+\mathrm{C}_0\\ \mathrm{A}_0\lambda a\mathrm{J}'_0(\lambda a)&=\mathrm{B}_0\end{aligned}\right\},$$

Digitized by Google

or, expressing $A_n$, $C_n$ in terms of $B_n$ and making use of the properties of the BESSEL functions,

$$\left.\begin{aligned} A_n &= 2nB_n a^n/\lambda a J_{n-1}(\lambda a) \\ C_n &= B_n a^{2n} J_{n+1}(\lambda a)/J_{n-1}(\lambda a) \end{aligned}\right\} n \neq 0$$
$$\left.\begin{aligned} A_0 &= B_0/\lambda a J'_0(\lambda a) \\ C_0 &= B_0\{J_0(\lambda a)/\lambda a J'_0(\lambda a) - \log_e a\} \end{aligned}\right\} \quad \ldots\ldots\ldots \quad (7)$$

The general solution of (2) is the sum of the normal solutions of the type (3), so that the electric force may be expressed as a FOURIER series, whose form inside the cylinder is

$$E_1 = B_0 \frac{J_0(\lambda r)}{\lambda a J'_0(\lambda a)} + 2\sum_1^\infty \frac{nB_n a^n J_n(\lambda r)}{\lambda a J_{n-1}(\lambda a)} \cos(n\theta + \alpha_n), \quad \ldots\ldots \quad (8)$$

and outside the cylinder is

$$E_2 = B_0\left(\log_e \frac{r}{a} + \frac{J_0(\lambda a)}{\lambda a J'_0(\lambda a)}\right) + \sum_1^\infty B_n r^n \left\{1 + \left(\frac{a}{r}\right)^{2n} \frac{J_{n+1}(\lambda a)}{J_{n-1}(\lambda a)}\right\} \cos(n\theta + \alpha_n). \quad (8A)$$

The corresponding series for P and Q follow by differentiation using the relation (1).

The combination of the cosine and sine terms into the form $\cos(n\theta + \alpha_n)$ is permissible, since the ratios of the arbitrary constants are the same for both the sine and cosine series. The values of $B_n$ and $\alpha_n$ may be determined when the form of the undisturbed field is given.

(3) *Energy Dissipation in the Cylinder.*—From (8A) and (1) the values of E and Q at the surface of the cylinder are

$$E = B_0\chi_0 + \sum_1^\infty B_n a^n (1 + \chi_n)\cos(n\theta + \alpha_n). \quad \ldots\ldots\ldots \quad (9)$$

$$Q = -\frac{i}{\omega a}\left\{B_0 + \sum_1^\infty nB_n a^n (1 - \chi_n)\cos(n\theta + \alpha_n)\right\}, \quad \ldots\ldots \quad (10)$$

in which

$$\left.\begin{aligned} \chi_n &= J_{n+1}(\lambda a)/J_{n-1}(\lambda a) \\ \chi_0 &= J_0(\lambda a)/\lambda a J'_0(\lambda a) = \tfrac{1}{2}(1 + \chi_2) - \frac{2}{\lambda^2 a^2} \end{aligned}\right\} \quad \ldots\ldots\ldots \quad (11)$$

If $e$, $q$ represent the instantaneous values of E and Q, the rate at which energy flows into the cylinder through a small area $d\sigma$ about the point $a$, $\theta$ is $eqd\sigma/4\pi$ by POYNTING'S theorem, and the integral rate of flow into unit length of the cylinder is

$$\frac{a}{4\pi}\int_0^{2\pi} eqd\sigma. \quad \ldots\ldots\ldots\ldots\ldots \quad (12)$$



Digitized by Google

Now, by (9) and (10), $e$ and $q$ have the forms $\Sigma u_n \cos(n\theta + \alpha_n)$ and $\Sigma v_n \cos(n\theta + \alpha_n)$ respectively.

Using these forms in (12), and remembering that

$$\int_0^{2\pi} \cos(n\theta + \alpha_n) \cos(m\theta + \alpha_n)\, d\theta = 0, \qquad n \neq m,$$

the integral rate of flow becomes

$$\frac{a}{4}(2u_0v_0 + \Sigma u_n v_n) \ldots\ldots\ldots\ldots (13)$$

To determine the products $u_nv_n$, the obvious method is to determine the real parts of the complex coefficients in (9) and (10). The product $u_nv_n$ expressed as a function of time would then be of the form $w_n \cos \omega t \cos(\omega t + \phi_n)$, so that the rate of energy dissipation in the cylinder would be $\frac{1}{2}w_n \cos \phi_n$.

A better method is to make use of the method of conjugates. If U′, V′ are the conjugates* of two complex quantities U, V ; $u$, $v$ their real parts, then

$$u = \tfrac{1}{2}(\mathrm{U} + \mathrm{U}'), \qquad v = \tfrac{1}{2}(\mathrm{V} + \mathrm{V}'),$$

so that

$$uv = \tfrac{1}{4}(\mathrm{U} + \mathrm{U}')(\mathrm{V} + \mathrm{V}').$$

Further, if U, V rotate with time in the same sense, U′, V′ will rotate in the opposite sense, so that UV′ and VU′ will not rotate. The steady portion of $uv$ is thus

$$\tfrac{1}{4}(\mathrm{UV}' + \mathrm{U}'\mathrm{V}).$$

Applying this to the present case, the steady flow into unit length of the cylinder is from (9), (10) and (13)

$$\mathrm{W} = \frac{i}{8\omega}\left\{\mathrm{B}_0\mathrm{B}'_0(\chi_0 - \chi'_0) + \sum_1^\infty n a^{2n}\mathrm{B}_n\mathrm{B}'_n(\chi_n - \chi'_n)\right\},$$

in which as before the accents denote conjugates.

Now $\chi_n$ is a function of $\lambda a$ and $\lambda^2 = +4\pi k i \omega$, so that, putting

$$z^2 = 4\pi k \omega a^2, \ldots\ldots\ldots\ldots (14)$$

$\chi_n$ may be written

$$\chi_n = \phi_n(z) - i\psi_n(z), \ldots\ldots\ldots\ldots (15)$$

from which

$$i(\chi_n - \chi'_n) = 2\psi_n(z),$$

* If $\mathrm{U} = \mathrm{A}\epsilon^{i\psi}$, then $\mathrm{U}' = \mathrm{A}\epsilon^{-i\psi}$ is the conjugate of U.

Digitized by Google

and when $n = 0$

$$i(\chi_0 - \chi'_0) = \frac{4}{z^2} + \tfrac{1}{2}\psi^2(z).$$

Using these expressions in the equation for W with $(B_n)$ for the modulus of $B_n$,

$$W = \frac{1}{4\omega}\left[(B_0)^2\left\{\frac{2}{z^2} + \tfrac{1}{4}\psi_2(z)\right\} + \sum_1^\infty n(B_n)^2 a^{2n}\psi_n(z)\right]. \quad . \quad . \quad . \quad . \quad (16)$$

The energy dissipation in unit length of the cylinder is thus expressed in terms of coefficients $B_n$ depending on the form of the applied magnetic field and of functions $\psi_n$ having argument $z = 2a(\pi k\omega)^{\frac{1}{2}}$. The functions $\phi_n$, $\psi_n$ are discussed in the next section. As regards the coefficients $B_n$, if the components of the magnetic force in the undisturbed field are $P_0$, $Q_0$ these components may be expressed in the forms

$$\left.\begin{aligned} P_0 &= \sum_1^\infty K_n r^{n-1}\sin(n\theta + \alpha_n) \\ Q_0 &= \frac{K_0}{r} + \sum_1^\infty K_n r^{n-1}\cos(n\theta + a_n) \end{aligned}\right\} \quad . \quad . \quad . \quad . \quad . \quad . \quad . \quad (17)$$

at all points outside the cylinder as these expressions are derivatives of a potential function satisfying LAPLACE'S equation and constant along the axis of the cylinder.

Further, by differentiation of (8A), similar expressions to (17) are obtained, when $\lambda$ is made zero—that is, when the disturbance due to eddy-currents in the cylinder is removed. These expressions are identical with (17) if we make

$$B_0 = i\omega K_0, \qquad B_n = i\omega K_n/n.$$

Hence, using $K_n$ in place of $B_n$ in (16)

$$W = \tfrac{1}{4}\omega\left[(K_0)^2\left\{\frac{2}{z^2} + \tfrac{1}{4}\psi_2(z)\right\} + \sum_1^\infty (K_n)^2 a^{2n}\psi_n(z)/n\right]. \quad . \quad . \quad . \quad . \quad (18)$$

(4) *The Functions $\phi_n$ and $\psi_n$.*—These functions are defined by

$$\phi_n(z) - i\psi_n(z) = J_{n+1}(\sqrt{-i}z)/J_{n-1}(\sqrt{-i}z).$$

Series formulæ for these functions have been developed by the author.*

The cases $n = 1$ and $n = 2$ are the most important ones, and in these cases $\phi$ and $\psi$ may be expressed in terms of ber and bei functions as follows :—

Let

$$\left.\begin{aligned} X(z) &= \mathrm{ber}^2 z + \mathrm{bei}^2 z \\ V(z) &= \mathrm{ber}'^2 z + \mathrm{bei}'^2 z \\ Z(z) &= \mathrm{ber}\, z\, \mathrm{bei}'\, z + \mathrm{bei}\, z\, \mathrm{ber}'\, z \\ W(z) &= \mathrm{ber}\, z\, \mathrm{bei}'\, z - \mathrm{bei}\, z\, \mathrm{ber}'\, z \end{aligned}\right\} \quad . \quad . \quad . \quad . \quad . \quad . \quad . \quad (19)$$

* BUTTERWORTH, 'Proc. Phys. Soc. Lond.', vol. 25, p. 294, 1913.

Digitized by Google

Then

$$\left.\begin{aligned} \phi_1(z) &= \frac{2}{z}\frac{W(z)}{X(z)} - 1, & \phi_2(z) &= \frac{4}{z}\frac{Z(z)}{V(z)} - 1 \\ \psi_1(z) &= \frac{2}{z}\frac{Z(z)}{X(z)}, & \psi_2(z) &= \frac{4}{z}\frac{W(z)}{V(z)} - \frac{8}{z^2} \end{aligned}\right\} \quad \ldots\ldots \quad (20)$$

The combinations W/X, Z/X, W/V and Z/V are tabulated.*

In the limiting cases of $z$ very small or very large, it may be shown from the formulæ already cited that $\phi_n$ and $\psi_n$ assume the following simple forms :—

$$z \text{ small} \quad \ldots \quad \left\{\begin{aligned} \phi_n &= -2z^4/(2n)^2\,(2n+2)\,(2n+4) \\ \psi_n &= z^2/2n\,(2n+2) \end{aligned}\right\} \quad \ldots\ldots\ldots \quad (21\text{A})$$

$$z \text{ large} \quad \ldots \quad \phi_n' = -1, \qquad \psi_n' = 2n/\sqrt{2}z. \quad \ldots\ldots\ldots \quad (21\text{B})$$

In regard to the limitations of (21A), the following table of values of $\psi_1$, $\psi_2$ (the functions most generally used) has been calculated :—

| $z$. | $\psi_1$. | $\psi_2$. | $\psi_1/z^2$. | $\psi_2/z^2$. |
|---|---|---|---|---|
| 0·0 | 0·0000 | 0·0000 | 0·1250 | 0·04167 |
| 0·5 | 0·03119 | 0·01041 | 0·1248 | 0·04164 |
| 1·0 | 0·1215 | 0·04149 | 0·1215 | 0·04149 |
| 1·5 | 0·2458 | 0·0918 | ... | ... |
| 2·0 | 0·3448 | 0·1563 | 0·0862 | 0·03908 |
| 2·5 | 0·3770 | 0·2244 | ... | ... |
| 3·0 | 0·3600 | 0·2827 | 0·0400 | 0·03141 |
| 3·5 | 0·3257 | 0·3212 | ... | ... |
| 4·0 | 0·2920 | 0·3389 | ... | ... |
| 4·5 | 0·2643 | 0·3408 | ... | ... |
| 5·0 | 0·2416 | 0·3337 | ... | ... |

For $\psi_1$, (21A) is a good approximation up to $z = 0{\cdot}5$ and a fair approximation up to $z = 1$. For higher values of $n$ the range of (21A) increases.

In regard to (21B), its region of application has not been reached at $z = 5$, but if we take a second approximation we find, when $z$ is large,

$$z^2\psi_1 = \sqrt{2}z - 1, \qquad z^2\psi_2 = 2\sqrt{2}z - 6. \quad \ldots\ldots \quad (21\text{C})$$

These formulæ give the following values for $\psi_1$, $\psi_2$ :—

| $z$ = | 2 | 3 | 4 | 5 |
|---|---|---|---|---|
| $\psi_1$ = | 0·457 | 0·360 | 0·291 | 0·243 |
| $\psi_2$ = | −0·086 | 0·276 | 0·332 | 0·326 |

* Savidge, ' Phil. Mag.', 6, 19, p. 49, 1910. Rosa and Grover, ' Bull. Bureau of Stands.', p. 226, 1912.

Digitized by Google

while the actual values are

| | | | | |
|---|---|---|---|---|
| $\psi_1$ = | 0·345 | 0·360 | 0·292 | 0·242 |
| $\psi_2$ = | 0·156 | 0·287 | 0·339 | 0·334 |

so that if $z$ is greater than 3 the values given by (21c) are fair approximations to the true values. The values of $\psi_1$ and $\psi_2$ from $z = 0$ to $z = 5$ are plotted in fig. 1.

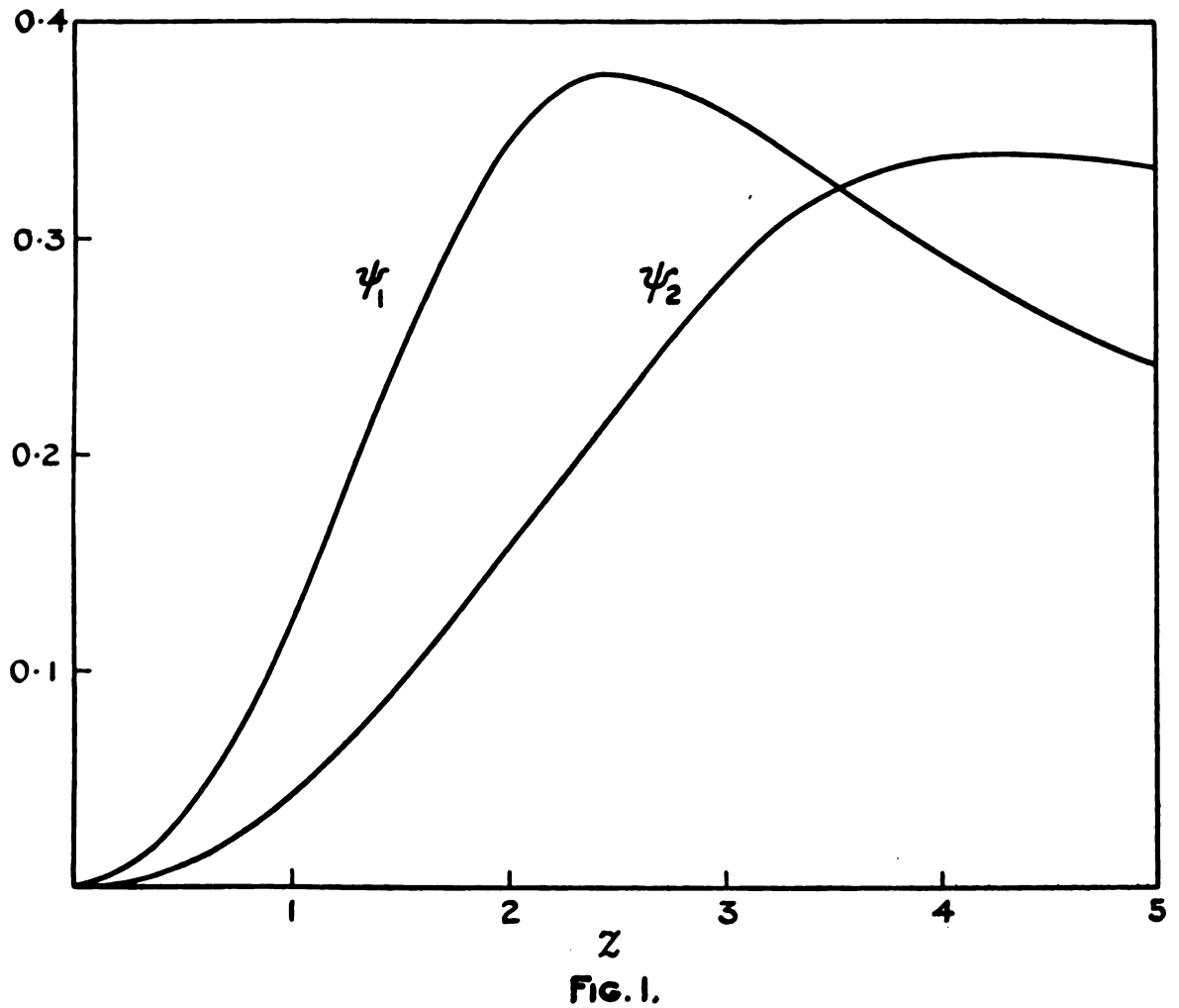


FIG. 1.

(5) *Eddy-Current Losses at Low Frequencies.*—The argument $z$ is related to the radius and conductance of the cylinder and the frequency of alternation of the field by the formula

$$z^2 = 4\pi k\omega a^2.$$

If $R_0$ is the electrical resistance per unit length of the cylinder, the formula may be written

$$z^2 = 4\omega/R_0. \quad . \quad . \quad . \quad . \quad . \quad . \quad . \quad . \quad . \quad . \quad . \quad (22)$$

The frequency $w/2\pi$ will be defined to be *low* when $z$ is less than unity, so that the

Digitized by Google

condition of low frequency is $\omega < R_0/4$. When this holds, formula (21A) applies in regard to $\psi$, so that by (18) the rate of dissipation of energy is

$$W = \tfrac{1}{8}R_0 (K_0)^2 + \frac{\omega^2}{R_0}\left\{\tfrac{1}{96}(K_0)^2 + \sum_1^\infty (K_n)^2 a^{2n}/2n^2(2n+2)\right\}. \quad . \quad . \quad . \quad (23)$$

Now by (17) the terms involving $K_0$ are due to a field whose components outside the cylinder are $Q_0 = K_0/r$, $P_0 = 0$. This field can only be due to a current of magnitude $I = \frac{1}{2}K_0$ distributed symmetrically round the axis and flowing parallel to the axis.

Hence the energy dissipation due to such a current is

$$W_1 = \tfrac{1}{2}R_0\left(1 + \tfrac{1}{12}\frac{\omega^2}{R_0^2}\right)I^2. \quad . \quad . \quad . \quad . \quad . \quad . \quad . \quad . \quad . \quad (24)$$

This is the usual formula for the skin effect at low frequencies.

If a uniform field H is acting on the cylinder, then $H = K_1$, $K_2 = K_3 = \ldots = 0$, so that the energy dissipation due to a uniform field H is

$$W_2 = \tfrac{1}{8}\omega^2 H^2 a^2/R_0 \quad . \quad . \quad . \quad . \quad . \quad . \quad . \quad . \quad . \quad . \quad (25)$$

The remaining terms are due to non-uniformity of the field.

If the external field is expressed in a FOURIER series of the form (17), and if the coefficient of the term $\cos(n\theta + \alpha_n)$ in the series for $Q_0$ has the value $L_n$ at the surface of the cylinder, then this portion of the field contributes an amount

$$\omega^2 a^2 L_n^2/2n^2(2n+2)R_0$$

to the energy dissipation.

The way in which $n$ occurs in this expression shows how unimportant are the higher terms of the FOURIER series in producing eddy losses at low frequencies.

The assumption that the external field is uniform and has its central value will, therefore, in most cases give a good approximation to the actual loss when the frequency is low. In illustration, suppose the external field to be due to a thin wire carrying current I, and stretched parallel to the cylinder at a distance D from the axis. The value of $Q_0$ in the plane common to the axis and the wire is $2I/(D - r)$, or, in ascending powers of $r$,

$$\frac{2I}{D}\left(1 + \frac{r}{D} + \frac{r^2}{D^2} + \ldots\right),$$

so that

$$L_n = \frac{2I}{D}\cdot\frac{a^n}{D^n},$$

and therefore the energy dissipation is

$$\frac{\omega^2 a^2 I^2}{R_0 D^2}\left(\frac{1}{1^2 2} + \frac{1}{2^2 3}\frac{a^2}{D^2} + \frac{1}{3^2 4}\frac{a^4}{D^4} + \ldots\right). \quad . \quad . \quad . \quad . \quad . \quad . \quad . \quad (26)$$

Digitized by Google

In the extreme case in which the wire touches the cylinder, the sum of the series becomes

$$\frac{\pi^2}{6} - 1 = 0{\cdot}64493.$$

Upon the assumption of a uniform field, the first term of the series would be the only one employed; and as this is 1/2, the correction due to non-uniformity of the field is a multiplying factor ranging from 1·00 to 1·29.

If there are two thin parallel wires and the cylinder is situated symmetrically between them, the axes of wires and cylinder being co-planar, the alternate terms of the series (26) vanish, and the losses become

$$\frac{4\omega^2 a^2 I^2}{R_0 D^2}\left(\frac{1}{1^2 2} + \frac{1}{3^2 4}\frac{a^4}{D^4} + \frac{1}{5^2 6}\frac{a^8}{D^8} + \ldots\right) \quad (27)$$

if the currents flow in opposite directions in the two wires, and

$$\frac{4\omega^2 a^2 I^2}{R_0 D^2}\left(\frac{1}{2^2 3}\frac{a^2}{D^2} + \frac{1}{4^2 5}\frac{a^6}{D^6} + \ldots\right) \quad (28)$$

when the currents flow in the same direction.

When the wires touch the cylinder, (27) reduces to

$$\frac{4\omega^2 I^2}{R_0}\left(\frac{\pi^2}{8} - \log_e 2\right) = \frac{4\omega^2 I^2}{R_0} \times 0{\cdot}54005$$

and (28) to

$$\frac{4\omega^2 I^2}{R_0}\left(\frac{\pi^2}{24} + \log_e 2 - 1\right) = \frac{4\omega^2 I^2}{R_0} \times 0{\cdot}10438.$$

The uniform field theory would give $\frac{4\omega^2 I^2}{R_0} \times 0{\cdot}5000$ and zero respectively for these cases.

(6) *Eddy-Current Losses at High Frequencies.*—At very high frequencies

$$\psi_n = 2n/\sqrt{2z} = n\sqrt{R_0/2\omega},$$

so that by (18) the energy dissipation is

$$W = \tfrac{1}{4}\sqrt{R_0\omega/2}\left\{\tfrac{1}{2}(K_0)^2 + \sum_1^\infty K(K_n)^2 a^{2n}\right\} \quad (29)$$

The first term is due to a current $I = \frac{1}{2}K_0$ distributed symmetrically round the axis of the cylinder and flowing in a direction parallel to the axis, and when this is the only factor producing the field the energy dissipation is

$$W_1 = \tfrac{1}{2}\sqrt{R_0\omega/2}I^2. \quad (30)$$

This is the formula for the skin effect at high frequencies.



Digitized by Google

The energy dissipation due to a uniform field H is got by putting $K_1 = H$, $K_2 = K_3 = \ldots = 0$, giving

$$W_2 = \tfrac{1}{4}H^2a^2\sqrt{R_0\omega/2}. \quad . \quad . \quad . \quad . \quad . \quad . \quad . \quad . \quad . \quad (31)$$

If the field is non-uniform, a comparison of (29) with (17) shows that the various harmonic terms in the field produce terms of equal importance in the expression for the eddy-current losses.

The examples of the last section give, for the single thin wire,

$$W = \sqrt{R_0\omega/2}\,\frac{a^2I^2}{D^2}\left(1 + \frac{a^2}{D^2} + \frac{a^4}{D^4} + \ldots\right) = \frac{a^2I^2}{D^2 - a^2} \times \sqrt{R_0\omega/2}, \quad . \quad . \quad (32)$$

and for the pair of wires,

$$W = \frac{a^2D^2}{D^4 - a^4}\,I^2\sqrt{R_0\omega/2} \qquad \text{or} \qquad \frac{a^4}{D^4 - a^4}\,I^2\sqrt{R_0\omega/2}, \quad . \quad . \quad . \quad . \quad (33)$$

according as the currents flow in opposite or the same direction in the two wires.

As regards (32), it is seen that the uniform field theory may be applied if we take as the uniform field the field at the point where the tangent plane through the wire touches the surface of the cylinder.

## (B). Eddy-Current Losses in Two Parallel Cylinders carrying Equal Currents.

(7) If the field acting on the cylinder is due to currents in neighbouring cylinders, then, because of the distortion of the current distribution in these cylinders, the external field acting on the cylinder under consideration is itself variable with frequency, and the assumption that this field is that which would occur if *all* eddy currents are absent will lead to wrong results. The case of two similar parallel cylinders carrying equal currents may be solved by considerations of symmetry.

Fig 2

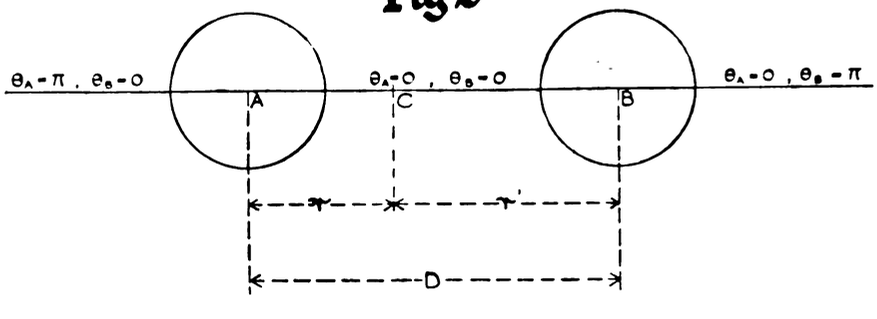


(8) Let the cylinders each have radius $a$, and let the distance of their centres be D. Take two systems of cylindrical co-ordinates (fig. 2), the first system ($r$, $\theta_A$) having A as origin and AB as the line of zero $\theta$, and the second system ($r'$, $\theta_B$) having B as

Digitized by Google

origin and BA as the line of zero $\theta$. Consider the field at the point C external to the cylinders situated on AB and due to two current systems flowing in the two cylinders parallel to the axes and symmetrical in either side of AB. By symmetry $\alpha_n$ of equation (17) is zero; and since $\theta$ is zero, we have from (10), using $K_n$ instead of $B_n$, for the first system of co-ordinates,

$$Q = \frac{K_0}{r} + \sum_1^\infty K_n r^{n-1} \left\{1 - \left(\frac{a}{r}\right)^{2n} \chi_n\right\} \quad . \quad . \quad . \quad . \quad . \quad . \quad . \quad . \quad (34)$$

for the second system

$$Q = \frac{K'_0}{r'} + \sum_1^\infty K'_n r'^{n-1} \left\{1 - \left(\frac{a}{r'}\right)^{2n} \chi_n\right\} \quad . \quad . \quad . \quad . \quad . \quad . \quad . \quad . \quad (35)$$

Also, if the currents are equal and *similarly* directed in the two cylinders,

$$K'n = -Kn;$$

if *oppositely* directed,

$$K'n = +Kn.$$

Further, (34) may be divided into two portions,

$$Q_1 = \frac{K_0}{r} - \sum_1^\infty K_n \frac{a^{2n}}{r^{n+1}} \chi_n \quad . \quad . \quad . \quad . \quad . \quad . \quad . \quad . \quad . \quad (36)$$

and

$$Q_2 = \sum_1^\infty K_n r^{n-1}, \quad . \quad . \quad . \quad . \quad . \quad . \quad . \quad . \quad . \quad (37)$$

the former arising from causes *inside* the cylinder A, and the latter from causes *outside* A, which in this case are located *inside* B, and therefore $Q_2$ has also the value

$$Q_2 = \frac{K'_0}{r'} - \sum_1^\infty K'_n \frac{a^{2n}}{r'^{n+1}} \chi_n \quad . \quad . \quad . \quad . \quad . \quad . \quad . \quad . \quad . \quad (38)$$

Equating (37) and (38),

$$\sum_1^\infty K_n r^{n-1} = \frac{K'_0}{r'} - \sum_1^\infty K'_n \frac{a^{2n}}{r'^{n+1}} \chi_n \quad . \quad . \quad . \quad . \quad . \quad . \quad . \quad . \quad (39)$$

Putting $K'n = \pm Kn$, $r' = D - r$, expanding the right-hand side of (39) in ascending powers of $r$, and equating coefficients of $r^{n-1}$, a series of equations are obtained to determine $K_n$ in terms of $K_0$. Now if I is the total current in either wire, $K_0 = 2I$, so that the method yields the values of $K_n$ completely. Thus, in the case where the currents are similarly directed, $K'n = -Kn$; and on equating coefficients we find

$$\begin{aligned}
K_1 a &= -2I\mu + (K_1 a)\mu^2\chi_1 + (K_2 a^2)\mu^3\chi_2 + \ldots \\
K_2 a^2 &= -2I\mu^2 + 2(K_1 a)\mu^3\chi_1 + 3(K_2 a^2)\mu^4\chi_2 + \ldots \\
K_3 a^3 &= -2I\mu^3 + 3(K_1 a)\mu^4\chi_1 + 6(K_2 a^2)\mu^5\chi_2 + \ldots .
\end{aligned}$$

in which $\mu \equiv a/D$ and is less than 1/2.



Digitized by Google

Solving by successive approximations to the order $\mu^4$,

$$\left.\begin{aligned} K_1 a &= -2I\mu\,\{1+\mu^2\chi_1+\mu^4(\chi_1^2+\chi_2)+\ldots\} \\ K_2 a^2 &= -2I\mu^2(1+2\mu^2\chi_1+\ldots) \\ K_3 a^3 &= -2I\mu^3(1+\ldots) \end{aligned}\right\} \quad \ldots\ldots \quad (40)$$

In the expression for the eddy-current losses (18) the moduli of the complex quantities $K_1$, $K_2$, $K_3$ are required, which, from (40) with $\chi_n = \phi_n - i\psi_n$, are

$$\left.\begin{aligned} (K_1)^2 &= \frac{4I^2}{D^2}\{1+2\mu^2\phi_1+\mu^4(2\phi_2+3\phi_1^2-\psi_1^2)+\ldots\} \\ (K_2)^2 &= \frac{4I^2}{D^4}(1+4\mu^2\phi_1+\ldots) \\ (K_3)^2 &= \frac{4I^2}{D^6}(1+\ldots) \end{aligned}\right\} \quad \ldots \quad (41)$$

Substituting in (18), the energy dissipation per unit length in either cylinder is given by

$$W = \omega I^2\left[\frac{2}{z^2}+\tfrac{1}{4}\psi_2+\mu^2\psi_1\left\{1+\mu^2\left(2\phi_1+\tfrac{1}{2}\frac{\psi_2}{\psi_1}\right)+\mu^4\left(2\phi_2+\tfrac{1}{3}\frac{\psi_3}{\psi_1}+3\phi_1^2-\psi_1^2+\frac{2\phi_1\psi_2}{\psi_1}\right)\right\}\right] \quad (42)$$

When the currents are in opposite directions a similar treatment gives

$$W = \omega I^2\left[\frac{2}{z^2}+\tfrac{1}{4}\psi_2+\mu^2\psi_1\left\{1+\mu^2\left(\tfrac{1}{2}\frac{\psi_2}{\psi_1}-2\phi_1\right)+\mu^4\left(3\phi_1^2-\psi_1^2-2\phi_2-\frac{2\phi_1\psi_2}{\psi_1}+\tfrac{1}{3}\frac{\psi_3}{\psi_1}\right)\right\}\right]. \quad (43)$$

In (42) and (43) the term

$$\omega I^2\left(\frac{2}{z^2}+\tfrac{1}{4}\psi_2\right)$$

is due to the ordinary skin effect. Since $2\omega/z^2 = \frac{1}{2}R_0$, this term may be written $\frac{1}{2}R_0I^2\{1+F(z)\}$ in which $F(z)$ $\{\equiv \frac{1}{8}z^2\psi_2\}$ is plotted in fig. 3 up to $z=5$. When $z$ is greater than 5, then, by (21c),

$$F(z) \doteqdot (\sqrt{2}z-3)/4. \quad \ldots\ldots\ldots \quad (44)$$

This is shown in fig. 3 by the broken line A.

The next term, $\mu^2\psi_1$, is due to the proximity of the two cylinders when they are so far apart that the quantity in { } may be regarded as practically unity. It would have been the term obtained by assuming the current in the second cylinder as concentrated on the axis and producing a uniform field of strength 2 I/D on the first cylinder. Including the proximity effect to this order we may write

$$W = \tfrac{1}{2}R_0I^2\left\{1+F(z)+\frac{d^2}{D^2}G(z)\right\}, \quad \ldots\ldots\ldots \quad (45)$$

Digitized by Google

in which $d$ ($\equiv 2a$) is the diameter of either cylinder, and $G(z) \equiv \frac{1}{8}z^2\psi_1$ is plotted in fig. 3, its limiting value

$$G(z) \doteqdot (\sqrt{2}z - 1)/8 \quad . \quad . \quad . \quad . \quad . \quad . \quad . \quad . \quad . \quad (46)$$

being indicated by the broken line (B).

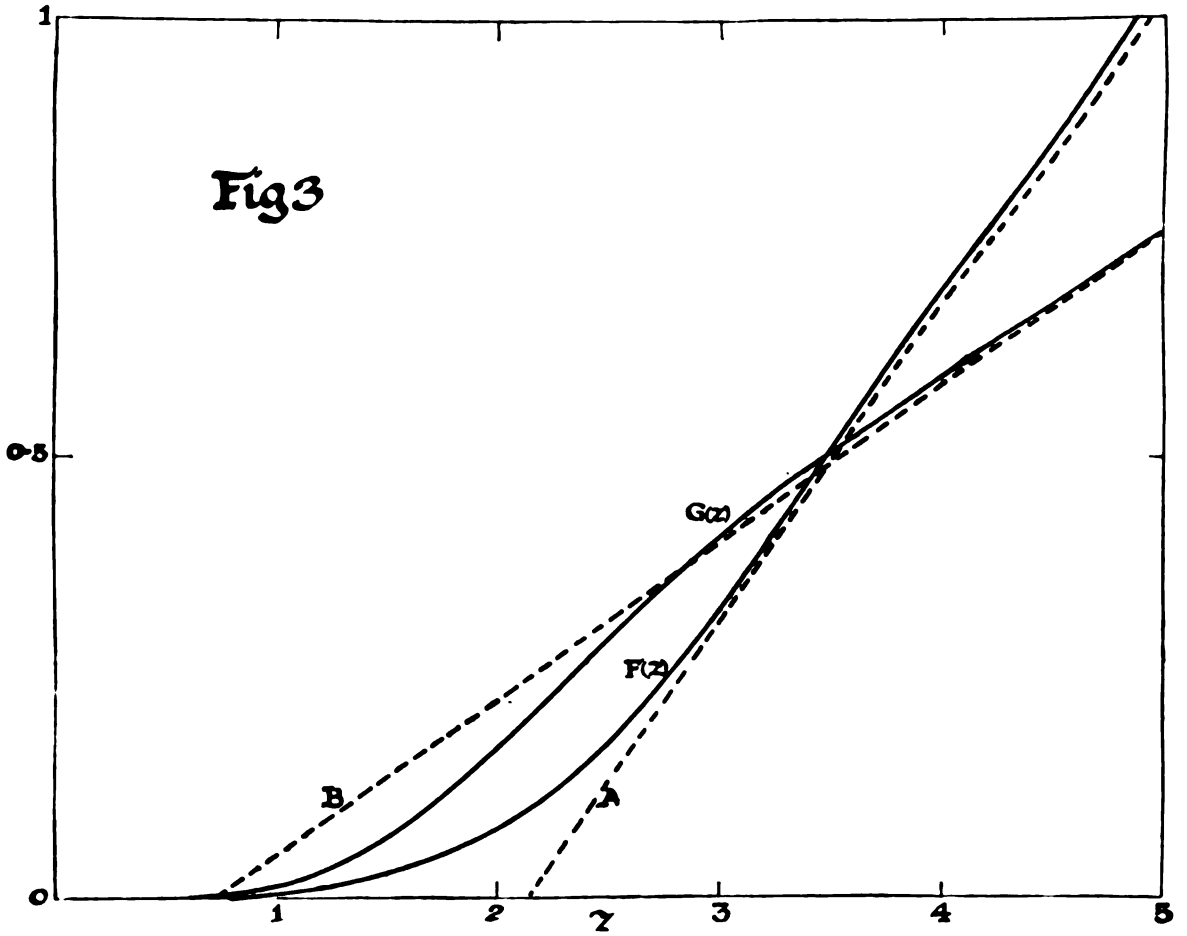


Finally the expression included in { } includes the effect both of disturbance of current distribution due to proximity and of non-uniformity of the field.

At low frequencies, by (21A), $\phi_n$ is negligible and both (42) and (43) give for { }

$$1 + \tfrac{1}{6}\mu^2 + \tfrac{1}{18}\mu^4 + \ldots .$$

This is identical with the result obtained for the thin wire (Equation 26), so that at low frequencies the distortion of distribution due to reaction of eddy currents is quite negligible, and the effect of non-uniformity of the field will give in the extreme case where the cylinders are touching a correcting factor of amount 1·0456 to be applied to the result obtained by the uniform field theory.

At frequencies so high that (21B) holds, the factor { } becomes

$$1 - \mu^2 - 2\mu^4$$

Digitized by Google

when the currents are similarly directed, and

$$1 + 3\mu^2 + 10\mu^4$$

when the currents are oppositely directed; while, if distortion is neglected, its value is

$$1 + \mu^2 + \mu^4$$

by (32). Thus the effects of distortion and of non-uniformity of field are equally important. When the currents are similarly directed the distortion is such as to tend to reduce the losses, and when the currents are oppositely directed the losses are increased.

The term involving $\mu^4$ will contribute less than 1 per cent. at high frequencies if $D > 2{\cdot}5d$ with the currents oppositely directed, and if $D > 2d$ with the currents similarly directed.

To this accuracy we may write for any frequency

$$W = \tfrac{1}{2}R_0\left\{1 + F(z) + G(z)\frac{d^2}{D^2}\left(1 + H(z)\frac{d^2}{D^2}\right)\right\}I^2, \quad (46)$$

in which

$$H(z) = \tfrac{1}{4}\left(\tfrac{1}{2}\frac{\psi_2}{\psi_1} \pm 2\phi_1\right).$$

If we assume the remaining terms to be in geometrical progression (46) may be written

$$W = \tfrac{1}{2}R_0\left\{1 + F(z) + \frac{G(z)}{1 - \frac{d^2}{D^2}H(z)}\frac{d^2}{D^2}\right\}I^2. \quad (47)$$

At low frequencies this formula gives 1·043 as the correction for non-uniformity when the cylinders touch, and will certainly hold to 1 per cent. up to $D = 2d$ at extremely high frequencies.

H (z) is plotted in fig. 4, up to $z = 5$ the curve I holding when the currents are oppositely directed, and II when the currents are similarly directed.

Since the effective resistance R′ of a coil system is such that

$$W = \tfrac{1}{2}R'I^2,$$

the effective resistance (apart from electrostatic capacities) per unit length of a pair of parallel wires is given by the formula*

$$R' = R_0\left\{1 + F(z) + \frac{G(z)}{1 - \frac{d^2}{D^2}H(z)}\frac{d^2}{D^2}\right\}, \quad (48)$$

in which $d$ is the diameter of either wire, D the distance of their centres, and F, G, H are functions of $z\ \{\equiv 2\sqrt{\omega/R_0}\}$ drawn in figs. 3 and 4, and tabulated below.

* At extremely high frequencies it may be shown that ratio of the resistance of a go-and-return system to the skin resistance is given by $D/\sqrt{D^2 - d^2}$. Formula (48) is then 3 per cent. in error when $d = 0{\cdot}8D$.

Digitized by Google

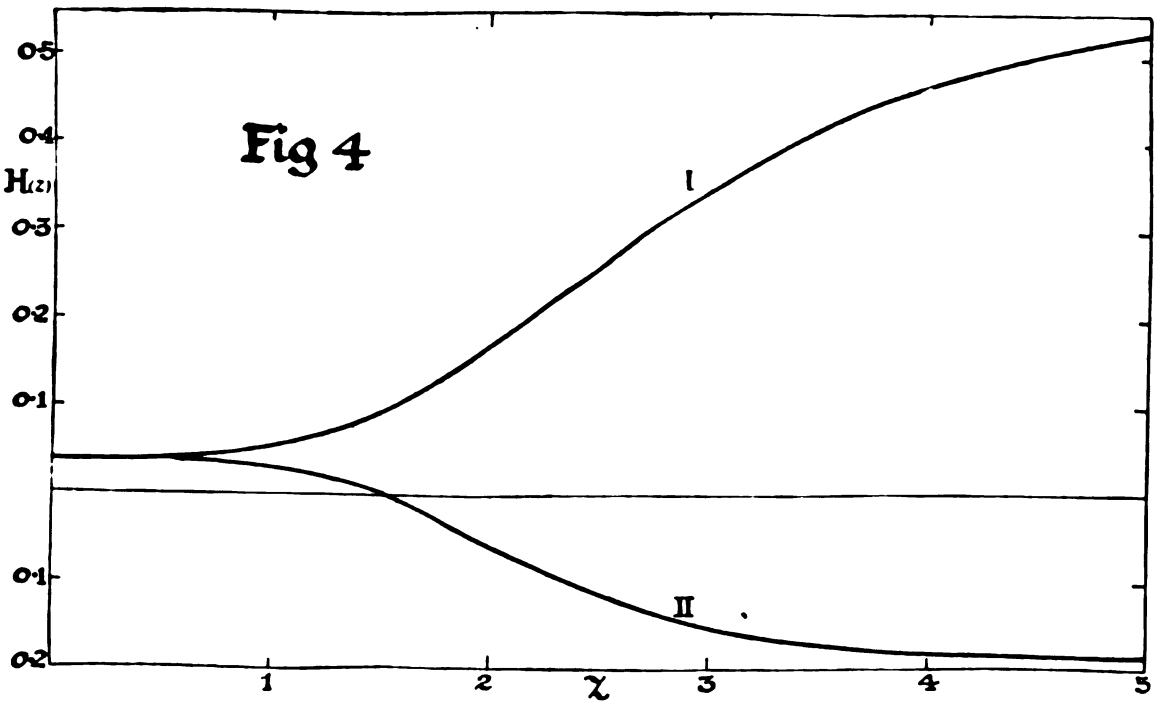


VALUES of F, G, H in Formula (48).

$$z = 2\sqrt{\omega/R_0}\begin{cases}\omega/2\pi = \text{frequency.}\\ R_0 = \text{D.C. resistance of cylinder per centimetre.}\end{cases}$$

| $z$. | F ($z$). | G ($z$). | H ($z$). | |
|---|---|---|---|---|
| | | | I. Currents Opposite. | II. Currents Similar. |
| 0·0 | 0·000 | 0·000 | 0·0417 | +0·0417 |
| 0·5 | 0·000326 | 0·000975 | 0·042 | +0·041 |
| 1·0 | 0·00519 | 0·01519 | 0·053 | +0·033 |
| 1·5 | 0·0258 | 0·0691 | 0·092 | +0·001 |
| 2·0 | 0·0782 | 0·1724 | 0·169 | −0·056 |
| 2·5 | 0·1756 | 0·295 | 0·263 | −0·114 |
| 3·0 | 0·318 | 0·405 | 0·348 | −0·152 |
| 3·5 | 0·492 | 0·499 | 0·416 | −0·170 |
| 4·0 | 0·678 | 0·584 | 0·466 | −0·176 |
| 4·5 | 0·862 | 0·669 | 0·503 | −0·181 |
| 5·0 | 1·042 | 0·755 | 0·530 | −0·185 |
| Large | $(\sqrt{2z}-3)/4$. | $(\sqrt{2z}-1)/8$. | 0·750 | 0·250 |

(9) *Test of Formula* (48) *by Comparison with Experimental Results.*—An extensive series of measurements of the resistance of a go-and-return system of parallel conductors has been made by KENNELLY, LAWS and PIERCE.*

* 'Trans. American Inst. El. Eng.', vol. 35, part 2, p. 1953, 1915.

Digitized by Google

The wire used was copper of diameter 1·168 cm., and the frequencies employed ranged from 60 to 5,000 cycles per second, so that the range of $z$ in formula (48) is from 0·84 to 7·7. The spacing (D — $d$) varied from 0·03 cm. to 60 cm., so that the observations afford a very complete check on the adequacy of the formula.

The resistance of the loop, which for direct currents was of the order 0·01 ohm, was

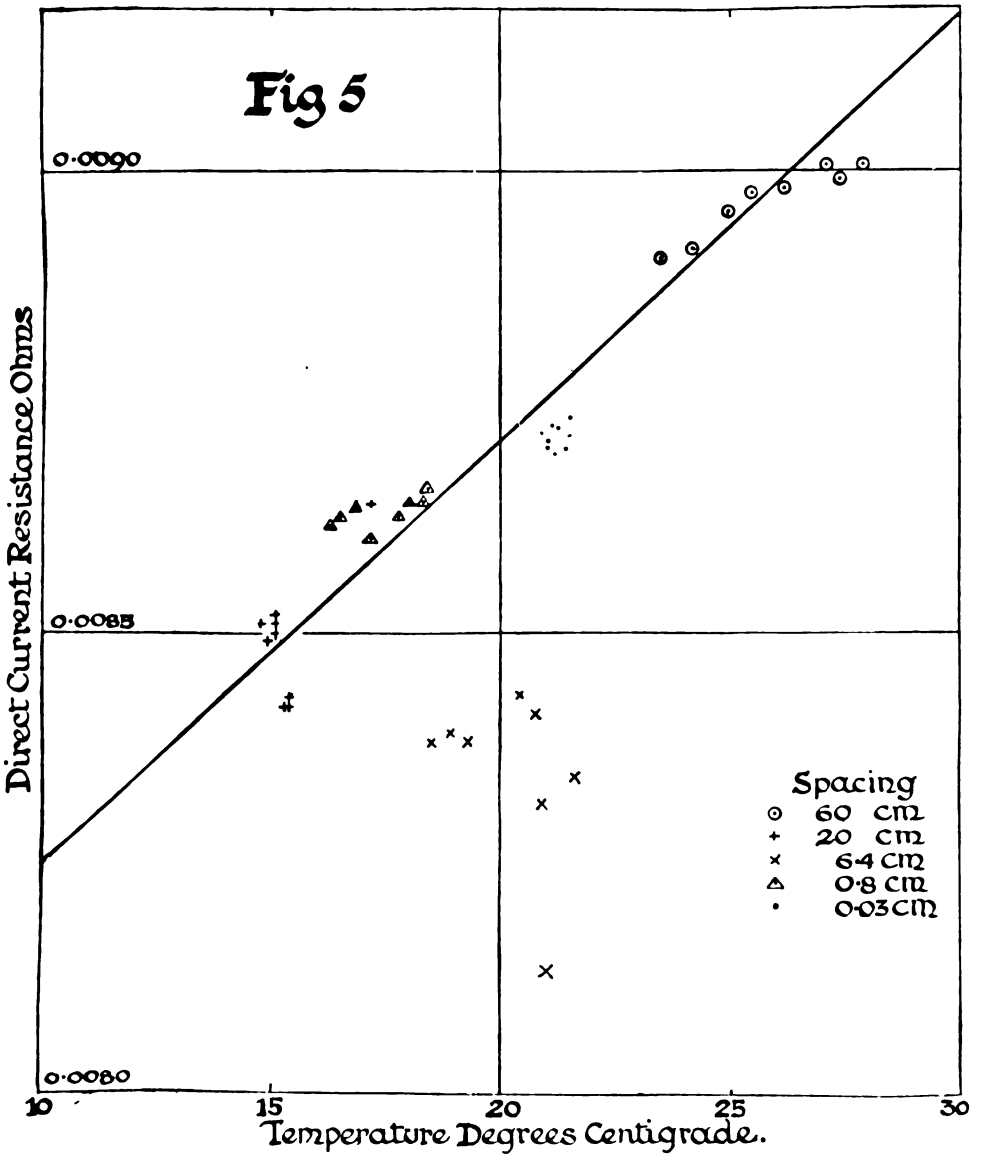


measured by an alternating current bridge. In this method variation of contact resistance would probably be the chief source of trouble. As to whether this effect is appreciable may be judged by a comparison of the tabulated direct current resistances after allowing for temperature variations. In fig. 5 this is done by plotting the resistances on a resistance-temperature diagram. Of the five groups of observations at spacings 60 cm., 20 cm., 6·4 cm., 0·8 cm., 0·03 cm., four show to within half a per

Digitized by Google

cent. a linear increase of resistance with temperature, this increase agreeing with the temperature coefficient of copper. The fifth group, that corresponding to the spacing 6·4 cm., is low. The discrepancy is removed if we suppose the measured resistance in error by 4 per cent. (0·0004 ohm).

In the following tables the ratio of alternating current resistance R′ to the direct current resistance R has been calculated from formula (48) and compared with the observed value. This ratio is not independent of the temperature as the eddy-current resistance varies with temperature in a different way to that of the direct current resistance. The value of $z$ has been calculated using that value of R which corresponds to the temperature of the observation as deduced from fig. 5.

Tables comparing observed values of the effective resistance of two parallel wires with the calculated values :—

$\theta$ = temperature of observation.

$f$ = frequency in cycles per second.

R = direct current resistance.

$R_S - R$ = increase in resistance due to skin effect.

$R_P$ = increase in resistance due to proximity of wires.

$R' = R_S + R_P$ = total alternating current resistance.

TABLE I.—Spacing = 60 cm.

| | | | | | | | | | |
|---|---|---|---|---|---|---|---|---|---|
| θ° C. ... ... ... ... | | 23·5 | 24·2 | 25·0 | 25·6 | 26·2 | 27·1 | 27·4 | 27·9 |
| $f$ ... ... ... ... ... | | 60 | 306 | 888 | 1600 | 2040 | 3065 | 3950 | 5000 |
| Calculated | $R_S/R$ ... ... | 1·0047 | 1·108 | 1·560 | 2·045 | 2·270 | 2·708 | 3·030 | 3·372 |
| | $R_P/R$ ... ... | Negligible | ... | ... | ... | ... | ... | ... | ... |
| | $R'/R$ ... ... | 1·0047 | 1·108 | 1·560 | 2·045 | 2·270 | 2·708 | 3·030 | 3·372 |
| Observed | $R'/R$ ... ... | 1·0038 | 1·111 | 1·587 | 2·042 | 2·279 | 2·694 | 3·034 | 3·361 |
| Difference per cent. ... ... | | +0·1 | −0·2 | −1·4 | +0·2 | −0·4 | +0·5 | −0·1 | +0·3 |

TABLE II.—Spacing = 20 cm.

| | | | | | | | | | |
|---|---|---|---|---|---|---|---|---|---|
| θ° C. ... ... ... | | 17·2 | 15·2 | 15·2 | 15·0 | 14·9 | 15·2 | 15·4 | 15·3 | 15·4 |
| $f$ ... ... ... ... | | 60 | 288 | 868 | 1663 | 2061 | 3063 | 3112 | 3860 | 5040 |
| Calculated | $R_S/R$ ... | 1·0048 | 1·106 | 1·578 | 2·120 | 2·328 | 2·775 | 2·790 | 3·075 | 3·472 |
| | $R_P/R$ ... | 0·00004 | 0·0006 | 0·002 | 0·002 | 0·003 | 0·003 | 0·004 | 0·004 | 0·004 |
| | $R'/R$ ... | 1·0048 | 1·107 | 1·580 | 2·122 | 2·331 | 2·778 | 2·799 | 3·079 | 3·476 |
| Observed | $R'/R$ ... | 1·0058 | 1·106 | 1·584 | 2·120 | 2·313 | 2·755 | 2·781 | 3·067 | 3·446 |
| Difference per cent. ... | | −0·1 | +0·1 | −0·3 | +0·1 | +0·8 | +0·8 | +0·5 | +0·4 | +0·9 |



Digitized by Google

TABLE III.—Spacing = 6·4 cm.

| | | | | | | | | | |
|---|---|---|---|---|---|---|---|---|---|
| 0° C. ... ... | 18·5 | 18·9 | 19·3 | 20·4 | 20·7 | 20·9 | 21·0 | 21·0 | 21·6 | ... |
| $f$ ... ... | 60 | 266 | 582 | 923 | 1465 | 2019 | 1992 | 3028 | 3960 | 5320 |
| Calculated | | | | | | | | | | |
| $R_S/R$ ... | 1·0048 | 1·088 | 1·340 | 1·602 | 1·984 | 2·280 | 2·268 | 2·728 | 3·075 | 3·470 |
| $R_P/R$ ... | 0·0003 | 0·0045 | 0·0099 | 0·0132 | 0·017 | 0·021 | 0·020 | 0·026 | 0·031 | 0·036 |
| $R'/R$ ... | 1·0051 | 1·093 | 1·350 | 1·615 | 2·001 | 2·301 | 2·288 | 2·754 | 3·106 | 3·506 |
| Observed $R'/R$ | 1·0087 | 1·100 | 1·354 | 1·610 | 2·037 | 2·344 | 2·322 | 2·851 | 3·145 | 3·558 |
| Difference per cent.... ... | −0·4 | −0·6 | −0·3 | −1·6 | −1·8 | −1·9 | −1·5 | −3·6 | −1·2 | −1·5 |

This group is abnormal on the resistance-temperature diagram. If we assume R′ and R as measured are *both* too small by a constant amount = 0·04 R, the group becomes normal on the resistance-temperature diagram and gives the following values replacing the observed R′/R :—

| | | | | | | | | | |
|---|---|---|---|---|---|---|---|---|---|
| Corrd. Obsd. $R'/R$ ... | 1·008 | 1·096 | 1·343 | 1·617 | 2·000 | 2·296 | 2·275 | 2·784 | 3·062 | 3·466 |
| Difference per cent.... ... | −0·3 | −0·3 | +0·5 | −0·2 | +0·0 | +0·2 | +0·6 | −1·1 | +1·5 | +1·5 |

TABLE IV.—Spacing = 0·8 cm.

| | | | | | | | | | | |
|---|---|---|---|---|---|---|---|---|---|---|
| 0° C. ... | ... | ... | ... | 16·3 | 16·5 | 16·9 | 17·2 | 17·8 | 18·0 | 18·3 | 18·4 |
| $f$ ... ... | 60 | 239 | 671 | 1068 | 1509 | 1991 | 1988 | 2486 | 3028 | 3880 | 4900 |
| Calculated | | | | | | | | | | | |
| $R_S/R$ ... | 1·0050 | 1·073 | 1·424 | 1·732 | 2·028 | 2·283 | 2·280 | 2·517 | 2·744 | 3·067 | 3·409 |
| $R_P/R$ ... | 0·0052 | 0·061 | 0·187 | 0·254 | 0·314 | 0·382 | 0·380 | 0·424 | 0·477 | 0·550 | 0·620 |
| $R'/R$ ... | 1·0102 | 1·134 | 1·611 | 1·986 | 2·324 | 2·665 | 2·660 | 2·941 | 3·221 | 3·617 | 4·029 |
| Observed $R'/R$ ... | 1·0124 | 1·132 | 1·604 | 1·981 | 2·330 | 2·643 | 2·637 | 2·912 | 3·179 | 3·587 | 3·955 |
| Difference per cent. | −0·2 | +0·2 | +0·4 | +0·3 | +0·5 | +0·8 | +0·8 | +1·0 | +1·3 | +0·8 | +1·8 |

The calculated values are in general too high. A spacing 0·85 cm. would give the following calculated values and differences :—

| | | | | | | | | | | |
|---|---|---|---|---|---|---|---|---|---|---|
| $R'/R$ ... | 1·0100 | 1·131 | 1·602 | 1·973 | 2·326 | 2·646 | 2·641 | 2·920 | 3·197 | 3·589 | 3·998 |
| Difference per cent. | −0·3 | −0·1 | −0·1 | −0·4 | −0·2 | +0·1 | +0·1 | +0·3 | +0·6 | +0·1 | +0·4 |

Digitized by Google

TABLE V.—Spacing = 0·03 cm.

| | | | | | | | | | |
|---|---|---|---|---|---|---|---|---|---|
| 0° C. ... ... ... ... | 21·1 | 21·4 | 21·5 | 21·5 | 21·2 | 21·0 | 20·9 | 21·0 | 21·1 |
| $f$ ... ... ... ... | 60 | 236 | 740 | 1000 | 1473 | 2038 | 3058 | 3918 | 5170 |
| Calculated $R_s/R$ ... ... | 1·005 | 1·068 | 1·464 | 1·658 | 1·995 | 2·31 | 2·74 | 3·06 | 3·46 |
| Calculated $R_p/R$ ... ... | 0·015 | 0·165 | 0·759 | 1·00 | 1·37 | 1·83 | 2·56 | 3·09 | 3·72 |
| Calculated $R'/R$ ... ... | 1·020 | 1·243 | 2·223 | 2·66 | 3·37 | 4·14 | 5·30 | 6·15 | 7·18 |
| Observed R'/R ... ... | 1·017 | 1·244 | 2·231 | 2·688 | 3·460 | 4·272 | 5·522 | 6·449 | 7·512 |
| Difference per cent.... ... | +0·3 | −0·1 | −0·4 | −1·1 | −3·2 | −3·5 | −4·3 | −5·0 | −4·5 |

The calculated values are in general too low, but with so small a spacing R′ is varying rapidly. The formula gives the following values of R′/R when the wires touch :—

| | | | | | | | | |
|---|---|---|---|---|---|---|---|---|
| R′/R ... ... ... ... | 1·021 | 1·253 | 2·288 | 2·75 | 3·52 | 4·35 | 5·64 | 6·57 | 7·71 |
| Difference per cent. ... | +0·4 | +0·7 | +2·6 | +2·2 | +1·7 | +1·4 | +1·8 | +1·6 | +2·7 |

In Tables I and II the skin effect is the only one of importance and very good agreement is obtained. These tables really check the experimental observations, as the skin-effect formula is well established. Tables IV and V form the real test of the proximity effect. It is seen that the small discrepancies are sufficiently accounted for by a slight adjustment (0·5 mm. at most) in the spacing. In Table III the skin effect is predominant, but there is a rather large discrepancy. It is noteworthy that this group also shows a discrepancy on the resistance-temperature diagram, and that both the discrepancies are removed if we assume the measured values of R′ and R to be both in error by 0·04 R.

### (C). Losses in Parallel Wire Systems and in Short Coils.

(10) When the field acting upon the cylinder is uniform and has magnitude H, then by (18) the eddy-current losses per unit of length are given by

$$W = \tfrac{1}{4}\omega a^2 H^2 \psi_1(z),$$

or eliminating $\omega$ by $\omega = z^2 R_0/4$, and putting $\frac{1}{8} z^2 \psi_1 = G(z)$, $2a = d$,

$$W = \tfrac{1}{8} R_0 d^2 G(z) H^2. \quad . \quad . \quad . \quad . \quad . \quad . \quad . \quad . \quad . \quad (49)$$

Consider a system of parallel wires each of diameter $d$ and occupying a square space of side D. Let these wires carry equal currents I in the same direction. Then, if the spacing is not too close, the currents may be supposed to be concentrated on the axes and producing uniform fields acting on the other wires. The field acting upon any wire $s$ may be written $H_s = 2Ik_s/D$ where $k_s$ is a numerical quantity depending upon the distribution of the wires and the position of the wire $s$ in the system. By (49) the eddy-current loss in the wire $s$ due to the field of the neighbouring wires is

$$W = \tfrac{1}{2} R_0 k_s^2 \frac{d^2}{D^2} G(z) I^2 \quad . \quad . \quad . \quad . \quad . \quad . \quad . \quad . \quad . \quad (50)$$

per unit of length.



Digitized by Google

If there are $n$ wires each of length $l$, the total loss due to the proximity of the wires will therefore be

$$\tfrac{1}{2}\mathrm{R}_0 l \frac{d^2}{\mathrm{D}^2}\mathrm{G}(z)\,\mathrm{I}^2 \sum_1^n k_s^2\,;$$

or if the wires are connected in series to give a total direct current resistance $\mathrm{R} = \mathrm{R}_0 nl$, the added resistance due to the proximity of the wires is

$$\mathrm{R}_p = u_n \mathrm{R} \frac{d^2}{\mathrm{D}^2}\mathrm{G}(z), \quad . \quad . \quad . \quad . \quad . \quad . \quad . \quad . \quad . \quad . \quad (51)$$

in which

$$u_n \equiv \frac{1}{n}\sum_1^n k_s^2, \quad . \quad . \quad . \quad . \quad . \quad . \quad . \quad . \quad . \quad . \quad (52)$$

and depends only on the geometry of the axes of the wires.

The total resistance (apart from capacity effects) is got by adding the skin effect to (52) so that the formula for the alternating current resistance R′ of the parallel wire system is

$$\mathrm{R}' = \mathrm{R}\left\{1 + \mathrm{F}(z) + u_n \frac{d^2}{\mathrm{D}^2}\mathrm{G}(z)\right\}. \quad . \quad . \quad . \quad . \quad . \quad . \quad . \quad (53)$$

This formula may also be applied to circular coils if the winding section is small in comparison with the radius. It remains to determine the values of $u_n$.

(11) *Single Layer Systems.*—If all the axes lie in one plane (fig. 6), then, numbering the wires 1, 2, 3....$s$....$n$ from left to right,

$$k_s = \frac{1}{s} + \frac{1}{s+1} + \ldots + \frac{1}{n-s}.$$

From this formula the following values of $k_s^2$ are calculated :—

| $s$ | $n=4$ | $n=8$ | $n=16$ | $n=24$ |
|---|---|---|---|---|
| 1 | 3·25 | 6·70 | 11·00 | 14·00 |
| 2 | 0·25 | 2·10 | 5·06 | 7·30 |
| 3 | 0·25 | 0·61 | 2·82 | 4·63 |
| 4 | 3·35 | 0.06 | 1·61 | 3·14 |
| 5 | | 0·06 | 0·89 | 2·16 |
| 6 | | 0·61 | 0·42 | 1·49 |
| 7 | | 2·10 | 0·14 | 0·98 |
| 8 | | 6·70 | 0·02 | 0·62 |
| 9 | | | &c. | 0·36 |
| 10 | | | | 0·18 |
| 11 | | | | 0·06 |
| 12 | | | | 0·01 |

Digitized by Google

These and similarly deduced results give for $u_n$,

| | | | | | |
|---|---|---|---|---|---|
| $n$ = | 2 | 4 | 6 | 8 | 10 |
| $u_n$ = | 1·00 | 1·80 | 2·16 | 2·37 | 2·51 |
| $n$ = | 12 | 16 | 24 | 32 | inf. |
| $u_n$ = | 2·61 | 2·74 | 2·91 | 3·00 | 3·29 |

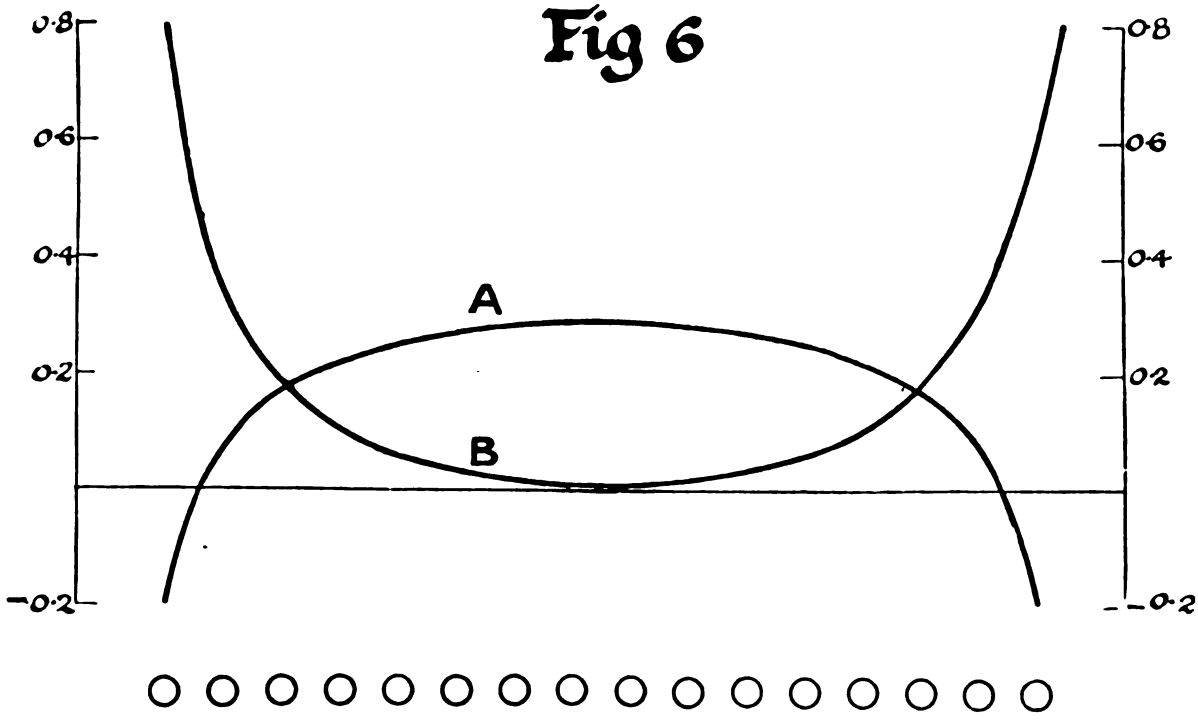


Fig. 6. Single Layer 16-wire System.

Curve A shows the distribution of effective resistance produced by eddy-current losses due to the proximity of the wires.

Curve B shows the distribution of the losses throughout the system.

The value of $u_n$ when $n = \infty$ is obtained as follows. Consider a long strip of width $l$ composed of $Nl$ parallel wires each carrying a current I. The field at a distance $x$ from the edge in this strip is $2NI \log (l - x)/x$, and the mean square field is

$$H_m^2 = \frac{4N^2I^2}{l}\int_0^l \log^2 \frac{l-x}{x}\,dx$$

$$= 16N^2I^2\left(1 - \frac{1}{2^2} + \frac{1}{3^2} - \frac{1}{4^2} + \ldots\right)$$

$$= \tfrac{1}{3}\pi^2N^2I^2.$$

But since $N = 1/D$,

$$H_m^2 = 4N^2I^2u_n,$$

so that

$$\text{Lt } n \to \infty\ u_n = \tfrac{1}{3}\pi^2 = 3{\cdot}2899.$$

Digitized by Google

The tabulated values of $u_n$ when plotted against $1/n$ (fig. 7) enable the value of $u_n$ to be determined for any number of wires.

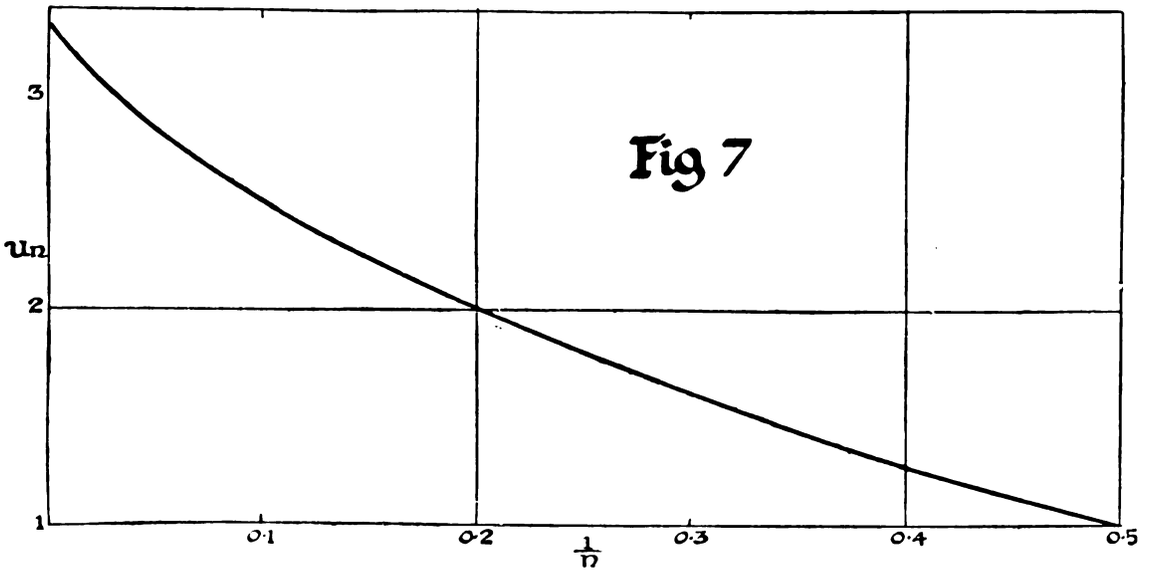


(12) *Distribution of Losses in Single Layer System.*—The energy loss in the wire $s$, due to the fields of the other wires, is proportional to $k_s^2$. From the table for $k_s^2$ it is seen that this is greatest in the end wires. Thus, in the case of four wires, 93 per cent. of this loss takes place in the two outer wires and only 7 per cent. in the two inner wires. For a greater number of wires, if the system is divided into four equal sections the distribution of loss is still such that approximately 93 per cent. of the loss occurs in the two outer sections. This may be of importance in measurements of effective resistance based on the determination of the increase in temperature of the system, and account should be taken of the possibility of a temperature distribution for alternating currents different from that for direct currents.

(13) *Distribution of Resistance in Single Layer System.*—The distribution of eddy-current losses throughout the system does not represent the distribution of effective resistance. In fact the energy required to produce the losses in any wire is supplied by the currents flowing in the other wires, and therefore the other wires behave as if certain resistances were added to them.

In order to determine these equivalent resistances, consider two coils (I) and (II) carrying currents $I_1$, $I_2$ which produce fields acting on a cylinder carrying no current. Ultimately these currents will be assumed equal, so that for simplicity they will be considered in phase. Let the fields in the neighbourhood of the cylinder due to these currents have intensities

$$H_1 = \alpha I_1, \quad H_2 = \beta I_2 \quad . \quad . \quad . \quad . \quad . \quad . \quad . \quad . \quad (54)$$

and let them be inclined at an angle $\phi$.

Digitized by Google

By (49) the eddy-current loss in the cylinder is

$$\begin{aligned} W &= \gamma (H_1^2 + H_2^2 + 2H_1H_2 \cos \phi) \\ &= \gamma (\alpha^2 I_1^2 + \beta^2 I_2^2 + 2\alpha\beta I_1 I_2 \cos \phi) \quad . \quad . \quad . \quad . \quad . \quad . \quad (55) \end{aligned}$$

in which

$$\gamma \equiv \tfrac{1}{8} R_0 d^2 G(z).$$

Now, instead of the cylinder being present, suppose the two circuits carrying the

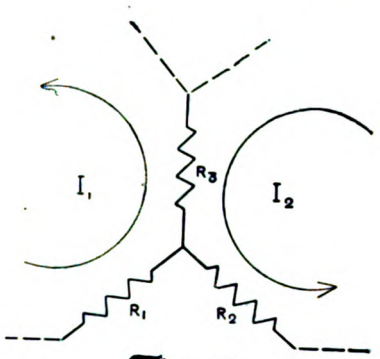


Fig 8

currents $I_1$, $I_2$ to be linked by the resistance system shown in fig. 8. The rate of dissipation of energy by this system is

$$\begin{aligned} W' &= \tfrac{1}{2} \{R_1 I_1^2 + R_2 I_2^2 + R_3 (I_1 - I_2)^2\} \\ &= \tfrac{1}{2} (R_1 + R_3) I_1^2 + \tfrac{1}{2} (R_2 + R_3) I_2^2 - R_3 I_1 I_2, \quad . \quad . \quad . \quad . \quad . \quad (56) \end{aligned}$$

W′ is identical with W if the resistances have the values

$$\left.\begin{aligned} R_1 = 2\alpha (\alpha + \beta \cos \phi) \gamma, \qquad R_2 &= 2\beta (\beta + \alpha \cos \phi) \gamma \\ R_3 = -\, 2 (\alpha\beta \cos \phi) \gamma & \end{aligned}\right\} . \quad . \quad . \quad . \quad (57)$$

In the case $I_1 = I_2$, no current flows through $R_3$, so that the potential differences produced by the eddy losses in the cylinder are then such that they may be represented by the resistances $R_1$, $R_2$ in series with the respective coils.

Applying to a single layer system, suppose we require the resistance to be added to a wire $s$ which would represent the contribution of $s$ to the eddy losses in the whole system. Let the wire $s$ be the coil (I), another wire $r$ be the cylinder, and the remaining wires be the coil (II). $\alpha I$ is the field acting on $r$ due to the current in $s$, $\beta I$ is the field acting on $r$ due to the currents in the remaining wires, so that $(\alpha + \beta \cos \phi) I$ is the nett field acting on $r$ resolved in the direction of $\alpha I$. Since in the single layer system the fields due to individual wires are collinear, $(\alpha + \beta \cos \phi) I$ is the total field in which the wire $r$ is situated. It is to be regarded as positive when the field due to $s$ is the same sense as the total field.

Digitized by Google

Hence if $H_r$ is the whole field acting on $r$, and $H_{rs}$ that portion of the field contributed by the wire $s$, the resistance to be added to the wire $s$ to imitate the eddy losses in the remainder of the system is

$$R_{ps} = \frac{2\gamma}{I^2}\left\{\sum_{r=1}^{r=s-1} H_{rs}\cdot H_r + \sum_{r=s+1}^{r=n} H_{rs}\cdot H_r\right\}. \quad . \quad . \quad . \quad . \quad . \quad . \quad . \quad (58)$$

Remembering that

$$H_{rs} = \frac{2I}{(r-s)D}, \qquad H_r = \frac{2I}{D}\left(\frac{1}{r} + \ldots + \frac{1}{n+r}\right),$$

(58) may be written

$$R_{ps} = u_{ns} R \frac{d^2}{D^2} G(z), \quad . \quad . \quad . \quad . \quad . \quad . \quad . \quad . \quad . \quad (59)$$

where $u_{ns}$ is a numerical quantity depending on the number of wires and the position of $s$.

The general distribution of resistance is sufficiently illustrated by the case of a 16-wire system. The values of $u_{ns}$ for this system are found by the above method to be

| $s =$ | 1 | 2 | 3 | 4 | 5 | 6 | 7 | 8 |
|---|---|---|---|---|---|---|---|---|
| | 16 | 15 | 14 | 13 | 12 | 11 | 10 | 9 |
| $u_{ns} =$ | −0·19 | +0·08 | 0·17 | 0·22 | 0·25 | 0·27 | 0·28 | 0·29 |

The values of $u_{ns}$ when added should give the value of $u_n$ for the whole system. Thus $\sum_{s=1}^{s=16} u_{ns} = 2{\cdot}74$, and this agrees with the tabulated value of $u_n$ for the 16-wire system.

As regards the negative value of $u_{ns}$ for the extreme wires, it must be remembered that the equivalent resistances for each wire are such as to imitate the *potential differences* produced by the eddy losses in the wires, and it is quite possible that the phase relations may produce a rise in potential in phase with the current in *part* of a system. The only condition that is essential is that the value of $u_n$ for the *whole* system shall be positive. Curves A and B of fig. 6 (p. 101) show the distribution of proximity resistance and of loss respectively for a 16-wire system.

## (D). Single Layer Solid Wire Coils.

(14) *Single Layer Coils. Effect of radius of curvature of Coils.*—A single layer circular coil, whose width of winding is small compared with the radius of the coil, differs only slightly from a straight parallel wire system, so that formula (53) will hold for a coil of this kind as a first approximation. The slight differences which occur, due to helicity of winding and owing to the fact that the wire (regarded as a cylinder under the action of a transverse field) is curved, are probably too small to be measurable and the mathematical difficulties too great to make a theoretical treatment possible.

A more important difference is the modification of the transverse field acting on the

Digitized by Google

individual wires. In a straight single layer system the field acting on one wire is perpendicular to the surface of the layer, but in a single layer coil not only is this normal field modified but there also exists a component of the field acting along the surface of the layer. The case where the number of wires in the coil is large will alone be considered.

*Solenoidal Coil.*—Let the mutual inductance (M) between two equal parallel coaxial circles of radius $a$ and separation $b$ be written

$$\mathrm{M} = 4\pi a f(2a/b). \quad . \quad . \quad . \quad . \quad . \quad . \quad . \quad . \quad . \quad . \quad (60)$$

Then*

$$f(\mu) = \log 4\mu - 2 + \tfrac{3}{4}\frac{1}{\mu^2}(\log 4\mu - \tfrac{1}{3}) - \tfrac{15}{64}\frac{1}{\mu^4}(\log 4\mu - \tfrac{31}{30}) + \tfrac{3.5.5}{2.5.6}\frac{1}{\mu^6}(\log 4\mu - \tfrac{3.4.7}{2.10}) + \ldots \quad . \quad . \quad . \quad . \quad . \quad . \quad . \quad . \quad . \quad (61)$$

so long as $\mu > 1$.

From this expression it is readily shown by differentiation and integration that the radial and axial components of the field at the point on the prolongation of the surface of a cylindrical coil distant $\xi$ from the edge are given by

$$\mathrm{H_N} = 2n\mathrm{I}\left\{f\left(\frac{2a}{\xi}\right) - f\left(\frac{2a}{b+\xi}\right)\right\}$$

$$\mathrm{H_T} = 2n\mathrm{I}\int_{2a/\xi}^{2a/b+\xi} \frac{d(\mu f)}{d\mu}\frac{d\mu}{\mu^2}, \quad . \quad . \quad . \quad . \quad . \quad . \quad . \quad . \quad . \quad (62)$$

$n$ being the number of turns per unit of length and I the current.

When $\xi$ is very small, $\mathrm{H_N}$ tends to the value $\mathrm{H_0} - h$, in which

$$\mathrm{H_0} = 2n\mathrm{I}\log\frac{b+\xi}{\xi}, \quad . \quad . \quad . \quad . \quad . \quad . \quad . \quad . \quad . \quad (63)$$

and is the field due to a straight strip of width $b$, while

$$h = 2n\mathrm{I}\left\{\tfrac{3}{4}\frac{1}{\mu^2}(\log 4\mu - \tfrac{1}{3}) - \tfrac{15}{64}\frac{1}{\mu^4}(\log 4\mu - \tfrac{31}{30}) + \tfrac{3.5.5}{2.5.6}\frac{1}{\mu^6}(\log 4\mu - \tfrac{3.4.7}{2.10})\ldots\right\} \quad (64)$$

$\mu = 2a/b$.

$\mathrm{H_T}$ tends to the value

$$\mathrm{H_T} = 2n\mathrm{I}\left\{\frac{\log 4\mu}{\mu} - \tfrac{1}{4}\frac{1}{\mu^3}(\log 4\mu - 1) + \tfrac{9}{64}\frac{1}{\mu^5}(\log 4\mu - \tfrac{7}{6}) - \tfrac{3.5.5}{2.5.6}\frac{1}{\mu^7}(\log 4\mu - \tfrac{3.5.7}{3.10}) + \ldots\right\} \quad (65)$$

$\mu = 2a/b$.

To find the normal and axial components at any point on the surface of the coil,

* Butterworth, 'Phil. Mag.', vol. 31, p. 276, 1916.



Digitized by Google

divide the coil into two portions A and B to the left and right of the point in question. Then the two components of the field are

$$(H_0 - H'_0) - (h - h'), \qquad H_T + H'_T.$$

where the accented letters refer to the field due to the portion B, and the unaccented letters to that due to A. $H_0 - H'_0$ is the normal field for a straight strip, and $h - h'$ the correction on the normal field due to curvature, while $H_T - H'_T$ is the field tangential to the layer due to curvature.

Formulæ (64) and (65) give the following values for $h$ and $H_T$ :—

| $b/2a$ | $h/2n\mathrm{I}$ | $H_T/2n\mathrm{I}$ |
|---|---|---|
| 0·1 | 0·025 | 0·369 |
| 0·2 | 0·079 | 0·595 |
| 0·3 | 0·149 | 0·767 |
| 0·4 | 0·229 | 0·902 |
| 0·5 | 0·313 | 1·010 |
| 0·6 | 0·400 | 1·096 |
| 0·7 | 0·486 | 1·167 |
| 0·8 | 0·569 | 1·225 |
| 0·9 | 0·651 | 1·273 |
| 1·0 | 0·728 | 1·313 |

from which the values of $h - h'$, $H_T - H'_T$ may be calculated for any point on the surface of a coil if $b/2a < 1$.

For the eddy-loss formula we require the mean square field acting on the coils ; that is, denoting $H_0 - H'_0$ by H, $h - h'$ by $H_1$, $H_T + H'_T$ by $H_2$, we require the mean value of

$$(H - H_1)^2 + H_2^2 = H^2 - 2HH_1 + H_1^2 + H_2^2$$

throughout the surface of the coil.

As regards the integrations required in determining this mean value, the integral of $H^2$ leads to the straight system formula ; that of $H_1^2$ and $H_2^2$ may be carried out by approximate methods, since $H_1^2$ and $H_2^2$ are finite throughout the range of integration. The integral of $H \cdot H_1$ is obtained as follows. Choose the length of the coil as twice the unit of length so that $H/2n\mathrm{I} = \log \frac{1+x}{1-x}$ at a point on the surface distant $x$ from the centre. Suppose $H_1$ may be expressed in the form

$$H_1 = \alpha + \beta x + \gamma x^2 + \delta x^3 + \ldots .$$

The integrals required are then of the form

$$\int_{-1}^{1} x^s \log \frac{1+x}{1-x}\, dx.$$

Digitized by Google

When $s$ is even these integrals are zero, and when $s$ is odd have the values

$$\frac{4}{s+1}\left(1+\tfrac{1}{3}+\tfrac{1}{5}+\ldots+\frac{1}{s}\right).$$

Neglecting terms beyond $x^4$ in the series for $H_1$

$$\int_{-1}^{1} HH_1\,dx = 4nI\,(\beta+\tfrac{2}{3}\delta).$$

There is no need to evaluate $\beta$ and $\delta$ for $H_1(x_1) - H_1(-x_1) = 2x_1(\beta + \delta x_1^2)$, which immediately gives $\beta + \frac{2}{3}\delta$ if we put $x_1^2 = 2/3$. Greater accuracy may be obtained by suitably choosing a series of values of $x$, &c., to take into account the higher terms of the series, but the above expression is sufficient for the present purpose.

The evaluation of the integrals by the above methods leads to the following table of values for $u_n$ in applying formula (53) to solenoidal coils of length $b$ and radius $a$.

SINGLE Layer Solenoidal Coils. Radius $= a$. Length $= b$. $u_n$ in formula (53).

| $b/2a$ = | 0·0 | 0·2 | 0·4 | 0·6 | 0·8 | 1·0 |
|---|---|---|---|---|---|---|
| $u$ = | 3·29 | 3·63 | 4·06 | 4·50 | 4·93 | 5·28 |

The assumption $u_n = 3{\cdot}29 + b/a$ will give results which do not differ by more than 2 per cent. from the above values.

*Flat Coils.*—By methods similar in principle to those used in determining the values of $u_n$ for solenoidal coils, the following values of $u_n$ have been found :—

SINGLE Layer Flat Coils. $r$ = inner radius. R = outer radius.

| $r/R$ = | 1·0 | 0·9 | 0·8 | 0·7 | 0·6 | 0·5 |
|---|---|---|---|---|---|---|
| $u$ = | 3·29 | 3·36 | 3·58 | 3·84 | 4·24 | 4·78 |

(15) *Single Layer Coils at High Frequencies.*—When $z$ is greater than 3, F $(z)$ and G $(z)$ assume the simplified forms

$$F(z) = (\sqrt{2}z - 3)/4, \qquad G(z) = (\sqrt{2}z - 1)/8,$$

so that formula (53) becomes

$$R' = \alpha + \beta z, \quad \ldots\ldots\ldots\ldots \quad (66)$$

in which

$$\alpha = \tfrac{1}{8}R\,(2 - u_n' d^2/D^2), \qquad \beta = \frac{\sqrt{2}R}{8}\,(2 + u_n\,d^2/D^2).$$

Now $u_n d^2/D^2$ seldom exceeds 6, so that $\alpha/\beta$ will usually lie between $+0{\cdot}7$ and $-0{\cdot}4$



Digitized by Google

Even when $z$ is as small as 3, $\alpha$ is therefore less than $\frac{1}{4}\beta z$. For most purposes it is sufficiently accurate to take

$$R' = \beta z. \quad . \quad . \quad . \quad . \quad . \quad . \quad . \quad . \quad . \quad . \quad . \quad (67)$$

From the relation $z^2 = 4\omega/R_0$ we may write

$$z = 0{\cdot}0479\sqrt{f/R'_0} = 830/\sqrt{R'_0\lambda}, \quad . \quad . \quad . \quad . \quad . \quad . \quad . \quad (68)$$

in which $f$ is the frequency in cycles per second, $\lambda$ the wave-length in metres, $R'_0$ the resistance of the wire of the coil in ohms per 1,000 yards.

Hence (67) becomes

$$R' = A/\sqrt{\lambda} = A'\sqrt{f}, \quad . \quad . \quad . \quad . \quad . \quad . \quad . \quad . \quad . \quad (69)$$

where A and A′ are given by

$$\left.\begin{aligned} A &= 146{\cdot}7\,(2 + u_n d^2/D^2)R/\sqrt{R'_0} \\ A' &= 8{\cdot}47 \times 10^{-3}\,(2+u_n\,d^2/D^2)\,R/\sqrt{R'_0} \end{aligned}\right\} \quad . \quad . \quad . \quad . \quad . \quad . \quad (70)$$

(16) *Comparison of Formula* (69) *with Experimental Observations.* — LINDEMANN and HÜTER* have measured the effective resistances of a series of single layer coils over a range of wave-lengths to which formula (69) is applicable.

Their method was to bring the coil into resonance with an air condenser at the required wave-length and to measure the effective resistance in this condition by adding a known non-inductive resistance and observing the reduction in current. The method measures the resistance of the whole circuit of which the coil is a part, so that the resistance of the coil may be deduced if the resistances of the non-inductive portions of the circuit are known, and the condenser is assumed to be free from loss.

Their results included four solenoidal coils wound with thick solid wire, and for these coils they found that the effective resistance could be expressed in the form

$$R' = A/\sqrt{\lambda} + B/\lambda^2. \quad . \quad . \quad . \quad . \quad . \quad . \quad . \quad . \quad . \quad (71)$$

The data given by LINDEMANN and HÜTER for these coils enable the value of A in formula (70) to be calculated. The results are given in the following table, which includes also three other coils measured by a similar method at the National Physical Laboratory.

It is seen that the value of A as calculated from formula (70) is in good agreement with the value of A determined experimentally. In the calculation, the value of $u_n$ taken has been the value given in the short table for solenoidal coils in section 14. These values have been deduced upon the assumption of a large number of turns. Calculations based on the value of $u_n$, as deduced from a straight system containing the same number of wires as there were turns in the coil, were found to give a value of A which in every case was lower than the value deduced from observations.

* ' Verh. Deutsch. Phys. Gesellschaft ', vol. 15, p. 219, 1913.

Digitized by Google

TABLE.—Effective Resistance of Single Layer Solenoidal Coils.

| Coil. | Radius *a* cm. | Length *b* cm. | Turns *n*. | Diameter of wire *d* mm. | Direct Current R ohms. | Inductance L microhenries. | Experimental A. | Experimental B. | Calculated A. | Obsr. | Range of Wavelength metres. |
|---|---|---|---|---|---|---|---|---|---|---|---|
| 1 | 15·5 | 1·8 | 7 | 2·2 | ... | 36 | 9·5 | $2·14\times10^4$ | 10·4 | L.H. | ... |
| 2 | $9·7_5$ | 2·6 | 11 | 2 | 0·0382 | 43 | 11·8 | $2·15\times10^4$ | 11·2 | L.H. | 100<br>3500 |
| 3 | 11·3 | 2·0 | 13 | 0·71 | 0·425 | 75 | 25·1 | $7·4\times10^4$ | 25·5 | N.P.L. | 150<br>600 |
| 4 | 10·0 | 6·5 | 18 | 3 | ... | 80 | 14·3 | $7·0\times10^4$ | 13·2 | L.H. | ... |
| 5 | 9·8 | $2·1_5$ | 15 | 1·1 | ... | 84 | 25·5 | $7·0\times10^4$ | 25·6 | L.H. | ... |
| 6 | $11·7_5$ | 1·0 | 13 | 0·71 | 0·444 | 100 | 49·0 | $6·8\times10^4$ | 50 | N.P.L. | 200<br>600 |
| 7 | $8·7_5$ | 7·3 | 40 | 1·62 | 0·193 | 320 | 56 | $1·7\times10^6$ | 55 | N.P.L. | 600<br>1500 |

The direct current resistances were not known in the cases of the coils 1, 4, 5. For the calculation of A, their values were deduced from the dimensions of the coils using the resistivity of copper as given by the known direct current resistance of coil 3.

It was to throw some light upon the properties of the second term ($B/\lambda^2$) in LINDEMANN'S equation that the three coils marked N.P.L. were measured. Coil No. 6, which was wound with D.S.C. wire and held together by wax and silk without any other frame, was measured first to confirm LINDEMANN'S results. The observations are given below for this coil and are typical. In the table, $R_1$ is the measured resistance of the coil. $R'$ is obtained from $R_1$ by multiplying by $(1 - \omega^2LC)^2$, where C is the measured self capacity of the coil. The values of A and B are deduced by plotting $R'\sqrt{\lambda}$ against $\lambda^{-3/2}$ (formula (71)).

COIL No. 6. $L = 100·0$ microhenries. $C = 20\ \mu\mu F$.

| $\lambda$ metres. | $R_1$ ohms. | $R'$ ohms. | $A/\sqrt{\lambda}$. | $B/\lambda^2$. | $R'$ (formula (71)). |
|---|---|---|---|---|---|
| 206 | 7·2 | $5·0_0$ | $3·4_2$ | $1·6_1$ | $5·0_2$ |
| 229 | 6·2 | $4·6_4$ | $3·2_4$ | $1·3_1$ | $4·5_5$ |
| 260 | 5·2 | $4·1_6$ | $3·0_4$ | $1·0^1$ | $4·0_5$ |
| 294 | 4·3 | $3·6_1$ | $2·8_5$ | $0·7_9$ | $3·6_4$ |
| 350 | 3·5 | $3·1_0$ | $2·6_4$ | $0·5_6$ | $3·2_0$ |
| 463 | 2·8 | $2·6_2$ | $2·2_8$ | $0·3_2$ | $2·6_0$ |
| 500 | 2·6 | $2·4_6$ | $2·1_9$ | $0·2_7$ | $2·4_6$ |
| 543 | 2·5 | $2·3_8$ | $2·1_0$ | $0·2_3$ | $2·3_3$ |
| 584 | 2·3 | $2·3_0$ | $2·0_2$ | $0·2_0$ | $2·2_2$ |

Digitized by Google

Coil No. 3 was of bare wire and supported by eight pieces of ebonite upon which equidistant grooves had been cut to keep the wires in position, these ebonite pieces being spaced equally round an octagonal wooden frame. The arrangment involved no metal except the wire of the coil. Coil 3 approximately imitates coil 6, except that the insulation had been removed and the spacing increased. Coil No. 7 was wound on a wooden frame with D.S.C. wire and no wax. It is included in the table to increase the range of inductance and to put a severe test on the curvature correction for $u_n$.

In regard to the second term in formula (71), it is interesting to notice that if B is divided by $L^2$, the result is of the same order of magnitude for all the coils, tested although the inductance increases nine fold. Thus :—

| Coil No. : | 1 | 2 | 3 | 4 | 5 | 6 | 7 |
|---|---|---|---|---|---|---|---|
| $B/L^2$ = | 16·3 | 11·6 | 13·2 | 10·9 | 9·9 | 6·8 | 16·7 |

A leakage of conductance G would contribute a term $\omega^2L^2G$ to the expression for the effective resistance. In terms of wave-length this becomes $3\cdot56\ L^2G/\lambda^2$ if $\lambda$ is in metres, L in microhenries, and G in microhms. In order to imitate the resistance $B/\lambda^2$ by such a leakage the value of 1/G must range from 0·2 to 0·4 megohm to give the values observed for B.

As to whether leakage is the cause of the second term in LINDEMANN'S equation, and as to whether it lies in the coil or the remainder of the circuit is a matter which requires further investigation. There is no doubt, however, that the first term of LINDEMANN'S equations may be closely predicted by formula (69).

(17) *Conditions for Minimum Eddy-Current Losses in Single Layer Coils.* — The inductance of a single layer solenoidal coil of radius $a$ and length $b$ may be written

$$L = 4\pi ab^2X/D^2, \quad . \quad . \quad . \quad . \quad . \quad . \quad . \quad . \quad . \quad . \quad (72)$$

in which D is the distance apart of two consecutive turns and X is a function of $a/b$. The effective resistance of the coil is by (53)

$$R' = R(1+F+u_nGd^2/D^2) \quad . \quad . \quad . \quad . \quad . \quad . \quad . \quad . \quad (73)$$

where F, G depend on the frequency and diameter of wire only, while $u_n$ is a function of $a/b$. The values of X and $u_n$ for the range of $a/b$ 1·0 to 2·4 are given below, the latter being obtained by interpolation from the table of section 14, and the former from RAYLEIGH'S formula

$$X = \log_e 8a/b - 1/2 + b^2/32a^2\ (\log_e 8a/b - \tfrac{1}{4}). \quad . \quad . \quad . \quad . \quad . \quad (74)$$

| $a/b$ = | 1·0 | 1·2 | 1·4 | 1·6 | 1·8 | 2·0 | 2·2 | 2·4 |
|---|---|---|---|---|---|---|---|---|
| $u_n$ = | 4·29 | 4·10 | 3·98 | 3·87 | 3·80 | 3·73 | 3·69 | 3·65 |
| X = | 1·651 | 1·816 | 1·958 | 2·084 | 2·195 | 2·296 | 2·388 | 2·466 |

Digitized by Google

With wire of a given diameter, the value of R′/L depends upon the values of D, $a$, $b$. If the length of wire ($l$) is also fixed, $a$ may be expressed in terms of $l$, D and $b$, since

$$l = 2\pi ab/\mathrm{D}. \quad . \quad . \quad . \quad . \quad . \quad . \quad . \quad . \quad . \quad . \quad (75)$$

Writing $\mathrm{D} = \xi d$, $b = \eta a$ we have from (72), (73), (75)

$$\mathrm{R}'/\mathrm{L} = \mathrm{R}\left(\frac{\pi d}{2l^3}\right)^{\frac{1}{2}} \frac{\xi^{\frac{1}{2}}(1 + \mathrm{F} + u_n\mathrm{G}/\xi^2}{\eta^{\frac{1}{2}}\mathrm{X}}. \quad . \quad . \quad . \quad . \quad . \quad . \quad . \quad (76)$$

The minimum value of R′/L is required for variations of $\xi$ and $\eta$; the former gives the best spacing of the wires with a coil given shape, and the latter gives the best of shape.

*Best Spacing.*—(76) is minimum with regard to variation of $\xi$ when

$$\xi^2 = 3u_n\mathrm{G}/(1 + \mathrm{F}), \quad . \quad . \quad . \quad . \quad . \quad . \quad . \quad . \quad . \quad (77)$$

and then

$$\mathrm{R}'/\mathrm{L} = \tfrac{1}{3}\mathrm{R}\left(\frac{\pi d}{2l^3}\right)^{\frac{1}{2}}\{3\mathrm{G}(1 + \mathrm{F})\}^{\frac{1}{2}} \frac{u_n^{\frac{1}{2}}}{\eta^{\frac{1}{2}}\mathrm{X}}. \quad . \quad . \quad . \quad . \quad . \quad . \quad . \quad (78)$$

Condition (77) shows that at the best spacing the proximity losses are one-third the skin losses. If the best spacing is not employed, then, writing $\mathrm{R}'/\mathrm{L} = \tau$, and letting $\tau_0$, $\xi_0$ be the values of $\tau$, $\xi$ when the spacing is best,

$$\tau/\tau_0 = \tfrac{1}{4}(\xi/\xi_0)^{\frac{1}{2}}\{3 + (\xi_0/\xi)^2\} \quad . \quad . \quad . \quad . \quad . \quad . \quad . \quad . \quad (79)$$

from which the following values are found :—

| | | | | | | | | |
|---|---|---|---|---|---|---|---|---|
| $\xi/\xi_0 (\equiv \mathrm{D}/\mathrm{D}_0) =$ | 0·6 | 0·7 | 0·8 | 0·9 | 1·0 | 1·1 | 1·2 | 1·3 |
| $\tau/\tau_0 =$ | 1·120 | 1·053 | 1·019 | 1·004 | 1·000 | 1·003 | 1·012 | 1·023 |
| $\xi/\xi_0 =$ | 1·4 | 1·5 | | | | | | |
| $\tau/\tau_0 =$ | 1·037 | 1·055 | | | | | | |

*Best Shape.*—Keeping the best spacing, the best shape is that value of $a/b$ which will make $(a/b)^{\frac{1}{2}}\, u_n^{\frac{1}{2}}/\mathrm{X}$ a minimum. The following values are obtained from the table given above for $u_n$ and X :—

| | | | | | | | | |
|---|---|---|---|---|---|---|---|---|
| $a/b =$ | 1·0 | 1·2 | 1·4 | 1·6 | 1·8 | 2·0 | 2·2 | 2·4 |
| $\mathrm{X}/u_n^{\frac{1}{2}}(a/b)^{\frac{1}{2}} =$ | 1·147 | 1·165 | 1·172 | 1·174 | 1·172 | 1·167 | 1·161 | 1·152 |

so that if condition (77) is possible the best shape is $a/b = 1{\cdot}6$, and then

$$\mathrm{R}'/\mathrm{L} = 1{\cdot}872\mathrm{R}\,(d/l^3)^{\frac{1}{2}}\{\mathrm{G}(1 + \mathrm{F})^3\}^{\frac{1}{2}}. \quad . \quad . \quad . \quad . \quad . \quad . \quad . \quad (80)$$

When $z$ is very large, $\mathrm{F} = 2\mathrm{G} = \sqrt{2}z/4$, so that at very high frequencies

$$\mathrm{R}'/\mathrm{L} = 0{\cdot}557\mathrm{R}z\,(d/l^3)^{\frac{1}{2}},$$

or with

$$\mathrm{R} = 4\rho l/\pi d^2, \qquad z^2 = 2\pi^2 f d^2/\rho,$$

$$\mathrm{R}'/\mathrm{L} = 3{\cdot}15\,(f\rho/ld)^{\frac{1}{2}}. \quad . \quad . \quad . \quad . \quad . \quad . \quad . \quad . \quad . \quad (81)$$

Digitized by Google

If the frequency $f$ is not sufficiently high for the approximation to hold, (81) must be replaced by

$$R'/L = \gamma(z)\{f\rho/ld\}^{\frac{1}{2}}, \quad . \quad . \quad . \quad . \quad . \quad . \quad . \quad . \quad . \quad (81A)$$

in which $\gamma(z) \equiv 10{\cdot}6\{G(1+F)^3\}^{\frac{1}{2}}/z$ and has the following values :—

| $z =$ | 1·5 | 2·0 | 2·5 | 3·0 | 3·5 | 4·0 | 4·5 | 5·0 | $\infty$ |
|---|---|---|---|---|---|---|---|---|---|
| $\gamma(z) =$ | 3·68 | 3·61 | 3·53 | 3·48 | 3·43 | 3·41 | 3·39 | 3·37 | 3·15 |

It is seen that $\gamma(z)$ does not vary much throughout a large range of frequency, and if the formula

$$R'/L \doteqdot 3{\cdot}4\{f\rho/ld\}^{\frac{1}{2}} \quad . \quad . \quad . \quad . \quad . \quad . \quad . \quad . \quad . \quad (81B)$$

is used this will represent the best value of alternating current time constant attainable so long as $z$ is greater than 2. Taking for copper $\rho = 1{,}600$ C.G.S., expressing $f$ in terms of wave-length $\lambda$ (in metres), and supposing L to be in microhenries $l$ and $d$ in centimetres,

$$R'/L = 2{\cdot}35/\sqrt{ld\lambda}.$$

Thus A in LINDEMANN'S formula cannot be less than

$$A_{min.} = 2{\cdot}35\,L/\sqrt{ld}.$$

In illustration we have for coils Nos. 1, 2, 3 of the table of section 16,

$$A_{min.} = 7{\cdot}1, \quad 8{\cdot}6 \quad 22$$

while

$$A_{min.}/A_{actual} = 0{\cdot}75, \quad 0{\cdot}73, \quad 0{\cdot}86.$$

The ratio $2{\cdot}35\,L/A\sqrt{ld}$ may be taken as a measure of the efficiency of any coil.

*Condition that Equation* (77) *may be satisfied.* — Since, if the best spacing is used, $a/b = 1{\cdot}6$ is always the best shape, we have from (77), with $u_n = 3{\cdot}87$,

$$(D/d)^2 = 11{\cdot}61G/1+F. \quad . \quad . \quad . \quad . \quad . \quad . \quad . \quad . \quad . \quad (82)$$

This gives the following values for $D/d$ :—

| $z$ = | 1·0 | 1·5 | 2·0 | 2·5 | 3·0 | 3·5 | 4·0 | 4·5 | 5·0 |
|---|---|---|---|---|---|---|---|---|---|
| $D/d$ = | 0·425 | $0{\cdot}88_5$ | 1·36 | $1{\cdot}70_5$ | 1·89 | 1·97 | 2·01 | 2·04 | $2{\cdot}07_5$ |
| $z$ = | 6·0 | 7·0 | 8·0 | 9·0 | 10·0 | inf. | | | |
| $D/d$ = | 2·14 | 2·17 | 2·20 | $2{\cdot}22_5$ | $2{\cdot}24_5$ | 2·41 | | | |

Now $D/d$ must always be greater than unity in practice, so that if $z$ is less than 1·6, close winding is the best. When $z$ exceeds 1·61, spacing rapidly becomes advantageous, the best spacing at very high frequencies being $D = 2{\cdot}4d$. As regards departure from the best spacing, the table of $\tau/\tau_0$ shows that the time constant will vary by less than 1 per cent. from the best value if $D/D_0$ lies between 0·85 and 1·18, by less than 5 per cent. if $D/D_0$ lies between 0·79 and 1·28.

Digitized by Google

If close winding is employed (keeping $a/b = 1{\cdot}6$), the losses at high frequencies will be 42 per cent. greater than when the proper spacing is employed. Fig. 9 summarizes

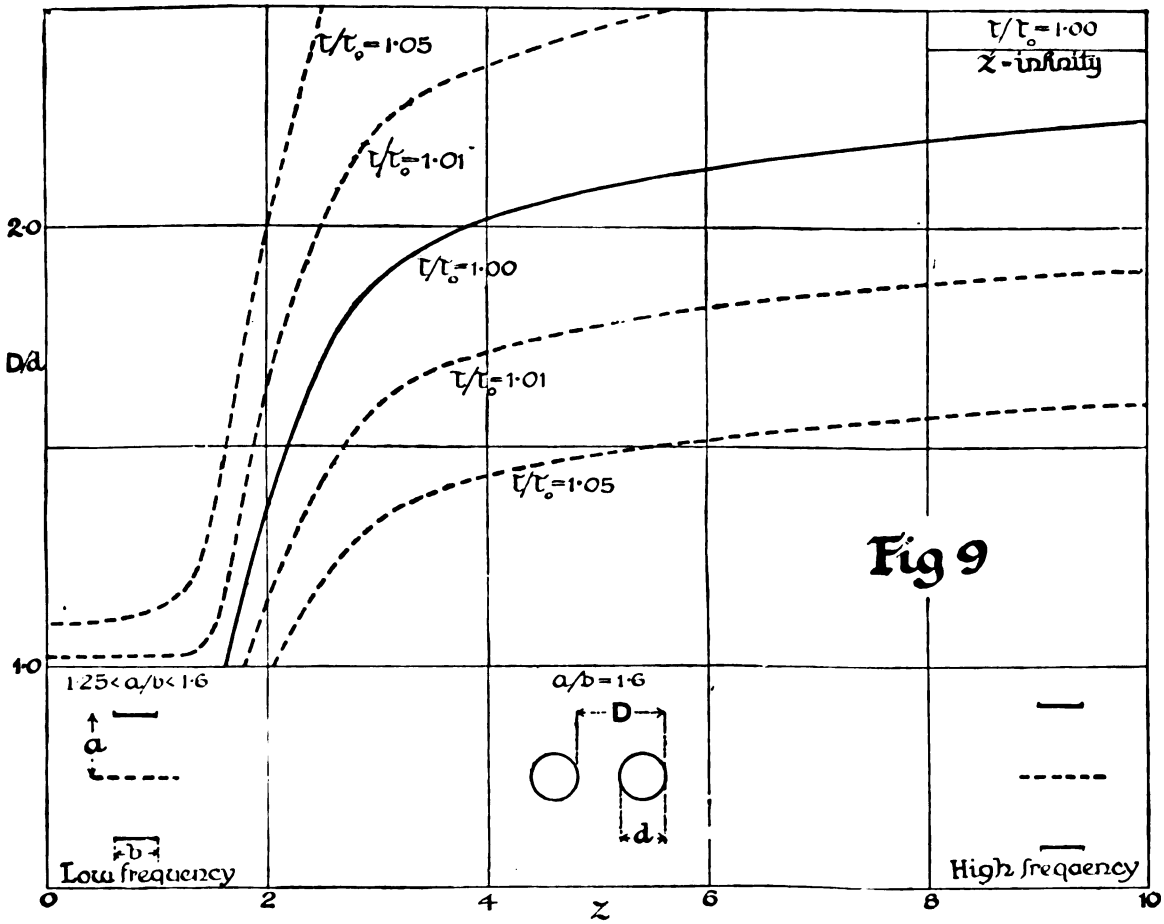


Fig. 9. Single Layer Solenoidal Coils—Solid Wire.

| | | | | | |
|---|---|---|---|---|---|
| R′ | = | Alternating current resistance, | | L = | Inductance. |
| $\tau$ | = | R′/L | , | $\tau_0$ = | Minimum R′/L. |
| $z$ | = | $830/\sqrt{R'_0\lambda}$ | , | $R'_0$ = | D.C. resistance in ohms per 1,000 yards. |
| | | | | $\lambda$ = | Wave-length in metres. |

Frequency *high* if $z > 2$.

At high frequencies best shape is $a/b = 1{\cdot}6$, best spacing (average) is $D/d = 2$.

At low frequencies best shape (average) is $a/b = 1{\cdot}4$ and close winding is the best.

the results of this section. The full curve gives the best spacing, and the broken curves show the limits allowable if losses 1 per cent. and 5 per cent. greater than the minimum losses are permissible. The figure may be used to grade coils for different ranges of frequency.

Thus the 5 per cent. limit will be attained if below $z = 2$ we make $a/b = 1{\cdot}4$* and employ close winding, and above $z = 2$ we make $a/b = 1{\cdot}6$ and space the wire so that

* Between $z = 0$ and $z = 1{\cdot}6$ the best value of $a/b$ rises from $1{\cdot}2_5$ (the steady current value) to $1{\cdot}6$. The value $a/b = 1{\cdot}4$ will never produce a loss exceeding by $0{\cdot}2$ per cent. the minimum loss.



Digitized by Google

$D = 2d$. In estimating, for a given diameter of wire, the wave-length at which spacing should be employed, the formula

$$R'_0\lambda = 172{,}000 \quad . \quad . \quad . \quad . \quad . \quad . \quad . \quad . \quad . \quad . \quad (83)$$

(deduced from (68) with $z = 2$) is useful. Thus, with No. 28 S.W.G. wire, $R'_0$ in ohms per 1,000 yards is 140; so that if $\lambda$ is less than 1,230 metres, spaced winding should be used.

*Flat Coils.*—A similar treatment for flat coils has yielded the following results:—

Spacing becomes advantageous at practically the same value of $z$ (viz., $z = 1{\cdot}6$) as that for solenoidal coils. At any value of $z$ greater than $1{\cdot}6$, the best ratio of inner to outer radius is $r/R = 0{\cdot}60$, and the best spacing is $1{\cdot}04$ times that for solenoidal coils. When both these conditions are satisfied, the eddy-current losses in the flat coil are 5 per cent. greater than those in the solenoidal coil wound in the best way with the same wire. When $z$ is less than $1{\cdot}6$, close winding is the best, and the best ratio of radii varies from $0{\cdot}4$ to $0{\cdot}6$. The value $r/R = 0{\cdot}5$ will therefore be the best ratio to take for a range of working from $z = 0$ to $z = 1{\cdot}6$.

## (E). Single Layer Stranded Wire Coils.

18. *Single Layer Stranded Wire Coils.*—If we replace the solid wire in a coil by a number of insulated parallel filaments of the same copper section and connected in parallel, the direct current resistance of the coil will be unaltered, but for alternating currents the distribution of current between the filaments will not be uniform unless the filaments are interwoven in such a way that they traverse similar paths.

As a non-uniform current distribution will cause increased losses, and twisting will produce increased length in the filaments, it is a matter for investigation as to what gain may be expected by using stranded wire coils.

It will be assumed that each strand traces out a helix about the axis of stranding, the angle of which is $\alpha$. Actually the radius of the helix will vary along a particular strand; but this need not be considered in getting the average result, as we may pass from one strand to its replacing strand, and thus keep at the same distance from the axis throughout the length of the stranded wire. The further assumption that $\alpha$ is constant throughout the section will assure that there are the same number of strands in the same axial length of any layer whatever its distance from the axis.

19. If $r$ is the direct current resistance per unit length of one strand, the skin resistance of each strand in unit *axial* length of the wire is

$$r_0 \sec \alpha \{1 + F(z)\}$$

where $z^2 = \pi k \omega \delta^2$, $\delta$ being the diameter of one strand. Upon this must be superposed the resistances representing the losses due to two fields:—

(*a*) A field $H_1$ due to the strands in the same turn of the coil as that in which the strand

Digitized by Google

in question is situated. This field is normal to the axis of stranding and tangential to the cylinder on which the strand is wound.

(*b*) A field $H_2$ due to the remaining turns in the coil. This field will also be assumed to be normal to the axis of stranding, and will have two components $H_2 \cos 0$ tangentia. to the cylinder and $H_2 \sin 0$ normal to the cylinder, 0 being the angular position of the element under consideration.

Thus an element of one strand is situated in a nett field whose components tangential and normal to the winding cylinder are $H_1 + H_2 \cos 0$, $H_2 \sin 0$. These may further be resolved into components along and at right angles to the direction of the element, viz. :—

$$H_A = (H_1 + H_2 \cos 0) \sin \alpha,$$
$$H_B = (H_1 + H_2 \cos 0) \cos \alpha, H_2 \sin 0.$$

Now, as regards the axial component of the field, it may be shown that if a cylinder is placed with its axis along the direction of an alternating field, the losses in the cylinder are one-half the losses which would occur if the cylinder were placed at right angles to the field.

Therefore the loss in an element $d\lambda$ of one strand due to the fields $H_1$, $H_2$ is by (49)

$$dW = \tfrac{1}{8} r_0 d\lambda \delta^2 G(z) (H_B^2 + \tfrac{1}{2} H_A^2).$$

Now, as we pass along one strand, the value of 0 increases uniformly as we are rotating relative to the field $H_2$. Hence the average loss in one strand is got by replacing $H_A^2$, $H_B^2$ by their mean values throughout a complete cycle of 0 ; that is, $H_A^2$, $H_B^2$ are replaced by

$$\sin^2 \alpha (H_1^2 + \tfrac{1}{2} H_2^2), \qquad \cos^2 \alpha (H_1^2 + \tfrac{1}{2} H_2^2) + \tfrac{1}{2} H_2^2.$$

The loss per unit *axial* length of the stranded wire is thus

$$W = \tfrac{1}{8} r_0 \sec \alpha G(z) \delta^2 \{H_1^2 (1 - \tfrac{1}{2} \sin^2 \alpha) + H_2^2 (1 - \tfrac{1}{4} \sin^2 \alpha)\}.$$

20. Since each strand carries the same current, the value of $H_1$ at a distance $r$ from the axis is $2Ir/a_0^2$, where I is the whole current and $a_0$ the over-all radius of the stranded wire, the number of strands being assumed large.

Again the number of strands crossing an annular belt of width $dr$ in the cross-section of the wire is $2rs\, dr/a_0^2$, $s$ being the whole number of strands. The mean value of $H_1^2$ throughout the section is therefore

$$8I^2 \int_0^{a_0} r^3 dr/a_0^6 = 2I^2/a_0^2 = 8I^2/d_0^2,$$

in which $d_0 = 2a_0$.

The field $H_2$ is the same as that for the corresponding solid wire coil, and the mean value of $H_2^2$ throughout the coil is $4a_n I^2/D^2$, D being the distance apart of consecutive



Digitized by Google

turns. Using these values in W and adding the skin losses, the following formula is obtained for the effective resistance of a stranded wire coil :—

$$R' = R_0 \sec \alpha \left[ 1 + F(z) + s^2\delta^2 G(z) \left\{ \frac{2}{d_0^2}(1 - \tfrac{1}{2}\sin^2\alpha) + \frac{u_n}{D^2}(1 - \tfrac{1}{4}\sin^2\alpha) \right\} \right] \quad (84)$$

in which

$R_0$ ($\equiv r_0/s$) is the direct current resistance per unit length of the equivalent solid wire,
$s$ = No. of strands,
$\delta$ = diameter of each strand,
$\alpha$ = angle of twist,
$d_0$ = over-all diameter of stranded wire,
D = separation of turns in coil ;

while in the calculation of F and G, $z^2 = \pi k \omega \delta^2$.

21. If the twist is so small that $\sin \alpha = \alpha$, (84) becomes

$$R' = R_0 \left[ 1 + F + s^2\delta^2 G \left( \frac{2}{d_0^2} + \frac{u_n}{D^2} \right) + \tfrac{1}{2}\alpha^2 \left\{ 1 + F + \tfrac{1}{2}u_n G \frac{s^2\delta^2}{D^2} \right\} \right] . \quad (85)$$

The correction due to the twist will therefore be less than 1 per cent. if $\alpha < 0{\cdot}14$ radian (8°). In determining the most efficient coil only the main term in (85) need be considered.

22. The quantities fixed will be taken to be the length of wire, the number of strands, and the diameter of each strand. Under these conditions it is clear from (85) that the best value of $d_0$ is $d_0 = D$, as adjustment of $d_0$ will have a negligible effect on the inductance. Then

$$R' = R_0 \left[ 1 + F + \frac{s^2\delta^2}{D^2} G (2 + u_n) \right] . \quad (86)$$

The best value of D and shape of coil then follow by a method identical with that for the solid wire coil, except that $s\delta$ replaces $d$, and $2 + u_n$ replaces $u_n$.

The method gives as the conditions for the best time-constant

$$a/b = 1{\cdot}5 \quad (87)$$

$$(D/s\delta)^2 = 17{\cdot}76 G/(1 + F) \quad (88)$$

and the value of the time-constant is then

$$R'/L = 1{\cdot}111 \gamma(z) \sqrt{f\rho/ls\delta}, \quad (89)$$

$\gamma(z)$ being calculated from the diameter of a single strand using (81A).

23. *Limits of Application.*—The quantity $s\delta^2$ is the diameter of solid copper wire having the same section as the copper section of the stranded wire, so that if it were possible to pack the circle D entirely with copper, $D^2/s\delta^2$ could never fall below unity. Actually the limit is greater than unity, partly because the wire is circular, but also

Digitized by Google

because of twisting and the need for symmetrical distribution. Thus if three wires each of diameter $\delta$ are arranged so that their centres form an equilateral triangle, the diameter of the cylinder in which these wires can be twisted is

$$(1 + 2\sqrt{3})\, n\delta = 2{\cdot}155 n\delta,$$

in which $n$ is a factor greater than unity, introduced to allow for insulation between contiguous wires. Denoting $D^2/s\delta^2$ by $\mu^2$ the value of $\mu$ for the three-wire system is $1{\cdot}244n$. If three three-wire systems are twisted, then, assuming rigidity, the over-all diameter of the resulting nine-wire system is $(2{\cdot}155)^2\, n\delta$, and the value of $\mu$ is $(1{\cdot}244)^2\, n$.

Generally, if the operation is repeated $p$ times, the result is a $3^p$ system for which

$$D = (2{\cdot}155)^p n\delta, \qquad \mu = (1{\cdot}244)^p n.$$

Applying this result to (88), it is seen that, as $G/(1 + F)$ increases with frequency, there is a lower limit of frequency below which the conditions may not be satisfied. If we depart from the condition of best internal space, the resulting increase in $R'/L$ follows a law similar to that for solid wire. If we allow a 10 per cent. variation, the actual value of $\mu$ may range between $0{\cdot}63\ \mu_0$ and $1{\cdot}75\ \mu_0$ where $\mu_0$ is the ideal value of $\mu$, and this may be used to extend the lower limit of the range of application. At the higher frequencies, although $G/I + F$ tends to the finite value 1/2, the spacing required is so large as to give unpractical coils.

If we set as practical limits to $n$ the values 1·1 and 3·3, and allow a 10 per cent. variation, the wave-length limits for copper wire of the usual gauges used in stranding are given in the following table :—

TABLE giving Limits of Application of Formulæ (87), (88), (89).

$\lambda$ = Wave-length in metres.

| Wire No. S.W.G. | | 42 | 40 | 38 | 36 |
|---|---|---|---|---|---|
| No of strands : | | | | | |
| 3 | $\lambda =$ | 0 | 0 | 0 | 0 |
| | $\lambda =$ | 430 | 630 | 960 | 1570 |
| 9 | $\lambda =$ | 10 | 10 | 20 | 30 |
| | $\lambda =$ | 600 | 850 | 1330 | 2150 |
| 27 | $\lambda =$ | 80 | 120 | 180 | 290 |
| | $\lambda =$ | 900 | 1290 | 2030 | 3200 |
| 81 | $\lambda =$ | 140 | 200 | 300 | 500 |
| | $\lambda =$ | 1270 | 1800 | 2800 | 4500 |

Digitized by Google

The shorter wave-length assumes $n = 3{\cdot}3$ and the longer wave-length assumes $n = 1{\cdot}1$. If we introduce a third system with $n = 2{\cdot}2$ for the mid-regions, a choice of one or other of these systems will enable the time-constant (89) to be secured to within 10 per cent. throughout the range of the table. The table shows clearly the transference of the applicability of the results to the regions of lower frequency as the stranding becomes finer. The observed inferiority of stranded wire coils at short wave-lengths is thus due to lack of internal spacing at these wave-lengths.

24. *Comparison of Stranded Wire Coils with Solid Wire Coils.*—Assuming both coils to have the same length of wire, the same total copper section and wound to give the best *time constants*, the ratio of the time-constants is by (81A) and (89),

$$\tau'/\tau = 1{\cdot}111\gamma(z)/s^{\frac{1}{2}}\gamma(s^{\frac{1}{2}}z), \quad \ldots\ldots\ldots \quad (90)$$

since $s\delta^2 = d^2$ and $z$ is proportional to $d$.

In (90) $\tau' = R'/L$ for the stranded wire coil and $\tau$ that for the solid wire. Now, the ratio $\gamma(z)/\gamma(s^{\frac{1}{2}}z)$ lies between 1 and $2^{\frac{1}{2}}$ for all possible values of $z$ and $s$, so that the formula

$$\tau'/\tau \doteqdot 1{\cdot}2/s^{\frac{1}{2}} \quad \ldots\ldots\ldots \quad (91)$$

may be taken as comparing the two cases.

For the 3-system we have therefore

| $s$ = | 3 | 9 | 27 | 81 |
|---|---|---|---|---|
| $\tau'/\tau$ = | 0·91 | 0·69 | 0·53 | 0·40 |

when the same length of wire is used in both coils.

If coils of equal *inductance* are compared, the conditions are different, as the spacing for stranded wire coils is not the same as that for solid wire coils. In fact, throughout the range for which spacing is advantageous,

$$D \doteqdot 2d$$

for the solid wire coils, and for stranded wire coils on the 3-system having the same copper section,

$$D = (1{\cdot}244)^p nd.$$

For coils of the same shape and of radius $a$, the inductance L is proportional to $a^3/D^2$ and the length of wire $l$ is proportional to $a^2/D$. Hence, to keep the inductance constant, $l^3/D$ must be constant. We have then

$$l \propto D^{\frac{1}{5}}, \quad a \propto D^{\frac{2}{5}},$$

and from (89)

$$R'/L \propto D^{-\frac{1}{5}},$$

Digitized by Google

Thus, if accented letters refer to the stranded wire coils, the relative values for equal inductance are

$$(l'/l)^3 = (a'/a)^{3/2} = (1\cdot244)^p\, n/2$$

and

$$\tau'/\tau \doteqdot 1\cdot2/s^{1/4}\{(1\cdot244)^p\, n/2\}^{1/6},$$

in the extreme case, when $s = 81$, $p = 4$, $n = 3\cdot3$, $l' = 1\cdot58l$, $a' = 2\cdot5a$, $\tau'/\tau = 0\cdot32$.

25. *Modification of Formulæ when Strands are few in Number.*—The value of the field $H_1$ was calculated on the assumption of a large number of strands, giving $H_1^2 = 8I^2/d_0^2$. If there are two touching strands each of diameter $\delta$, the field acting on one strand due to a current $I/2$ in the other is $I/\delta$ and $d_0$ (the diameter of the circumscribing circle) is $2\delta$. Hence, for this case, $H_1^2 = 4I^2/d_0^2$. The factor $2/d_0^2$ in the formula (84) must therefore be replaced by $1/d_0^2$. With three strands whose centres form an equilateral triangle of side $\delta$, $H_1^2 = 4I^2/3\delta^2$ and $d_0 = 2\cdot155\delta$, so that $2/d_0^2$ is replaced by $1\cdot55/d_0^2$.

With four strands in square order, the centres form a square of side $\delta$, $H_1^2 = 9I^2/8\delta^2$ and $d_0 = 2\cdot414\delta$; $2/d_0^2$ is replaced by $1\cdot65/d_0^2$. These new values react on the conditions (87), (88), (89); the "shape" condition (87) is practically unaltered. The "spacing" condition (88) gives slightly too high a value for D, viz. :—

| | | | | |
|---|---|---|---|---|
| S | = | 2 | 3 | 4 |
| $D/D_0$ | = | 0·90 | 0·96 | 0·97 |

where $D_0$ is the value calculated by (88) and D the true value.

The factor 1·111 in (89) must be replaced by 1·054, 1·078, 1·084 when $s = 2$, 3, 4. These differences are small, so that the theory may be safely applied even when the strands are few.

## (F). Many Layered Coils.

(26) *Coils of Many Layers.*—Let the winding section of the coil be $b \times c$. Let $c/b$ be small, and let $b$ be small compared with the radius of the coil. Let there be $m$ layers in the depth $c$ and $n$ turns per layer.

The field at any point in the section will have two components $H_b$ and $H_c$ parallel to $b$ and $c$ respectively, which will act independently in producing eddy-current losses.

As regards $H_c$, the field acting on a single wire is the same as that for a single layer coil for which $D = b/mn$. Thus the added resistance due to the action of $H_c$ is

$$\tfrac{1}{3}\pi^2 RG(z)(mnd/b)^2,$$

$d$ being the diameter of the wire and R the direct current resistance of the coil.

As regards $H_b$, each layer behaves as a current sheet having current density $nI/b$. In

Digitized by Google

the immediate neighbourhood of the sheet the component of the field parallel to the sheet is

$$h = 2\pi n \mathrm{I}/b$$

and reverses its direction as we pass through the sheet.

Assuming $h$ to be constant throughout the depth $c$, the field acting on the first layer is $(m-1)\,h$, on the second layer $(m-3)\,h$, and generally on the $r^{\text{th}}$ layer $(m-2r-1)\,h$.

The mean square value for all the layers is therefore

$$h^2\{(m-1)^2+(m-3)^2+(m-s)^2+\ldots\}/m = (m^2-1)\,h^2/3 = \tfrac{4}{3}\pi^2\,(m^2-1)\,(n\mathrm{I}/b)^2.$$

Upon applying this result to (49) it follows that the added resistance due to the action of $\mathrm{H}_b$ is

$$\tfrac{1}{3}\pi^2\,(m^2-1)\,\mathrm{RG}\,(z)\,(nd/b)^2.$$

Adding these resistances to the skin resistance, the formula for the resistance of a many-layered coil is

$$\mathrm{R}' = \mathrm{R}\,\{1+\mathrm{F}+\tfrac{1}{3}\pi^2\,(2m^2-1)\,(nd/b)^2\mathrm{G}\}. \quad . \quad . \quad . \quad . \quad . \quad . \quad (92)$$

The corresponding formula for a stranded wire coil is obtained by replacing F by $\mathrm{F}+2s^2\delta^2\mathrm{G}/d_0^2$ and $d$ by $s\delta$. F and G in this case are calculated, using the diameter of a single strand.

Assuming that the correction for curvature for the many layered coil is of the same form as that for the single layer coil, the following formula includes all the previous formulæ—

$$\mathrm{R}' = \mathrm{R}\,(1+\mathrm{F}+\mathrm{MG}) \quad . \quad . \quad . \quad . \quad . \quad . \quad . \quad . \quad . \quad . \quad (93)$$

in which for solid wire coils

$$\mathrm{M} = u_n\,(2m^2-1)\,(nd/b)^2. \quad . \quad . \quad . \quad . \quad . \quad . \quad . \quad . \quad . \quad (94)$$

and for stranded wire coils

$$\mathrm{M} = 2\,(s\,\delta/d_0)^2 + u_n\,(2m^2-1)\,ns\,\delta/b)^2 \quad . \quad . \quad . \quad . \quad . \quad . \quad . \quad (95)$$

27 *Best Conditions for Many Layered Coils.*—If different coils are wound with the same length and diameter of wire on the same shape of frame, and with the same spacing between the wires but with different radii, then the inductance will vary as $m^4$ while the resistance will be of the form

$$\alpha+\beta m^2,$$

in which

$$\alpha = \mathrm{R}\,\{1+\mathrm{F}-u_n\,(nd/b)^2\mathrm{G}\}, \qquad \beta = 2u_n\,(nd/b)^2\mathrm{G}.$$

At low frequencies F and G are negligibly small, so that increasing the number of layers will always improve the time-constant. At high frequencies the best time-constant is obtained when

$$\alpha = 3\beta m^2.$$

Digitized by Google

which gives

$$6m^2 + 1 = (1 + F)/Gu_n (nd/b)^2. \quad . \quad . \quad . \quad . \quad . \quad . \quad . \quad . \quad (96)$$

Assuming the condition such as to make $m$ large,

$$6 (mnd/b)^2 \doteqdot (1 + F)/u_n G, \quad . \quad . \quad . \quad . \quad . \quad . \quad . \quad . \quad (97)$$

an expression determining the total number of turns ($N = m \times n$). With this value of N we obtain from

$$L = 4\pi N^2 a X\left(\frac{a}{b}\right), \qquad l = 2\pi a N,$$

the relation

$$L^2 = \frac{2l^3}{\pi d} \frac{b}{a} X^2 \left(\frac{1 + F}{6u_n G}\right)^{\frac{1}{2}}$$

for the inductance of the coil, and this leads to the same value for $a/b$ as for single layer coils, viz. :—

$$a/b = 1{\cdot}6, \qquad u_n = 3{\cdot}87 \quad . \quad . \quad . \quad . \quad . \quad . \quad . \quad . \quad (98)$$

When both conditions are satisfied

$$R'/L = 1{\cdot}187\gamma (z) \sqrt{f\rho/ld}. \quad . \quad . \quad . \quad . \quad . \quad . \quad . \quad . \quad (99)$$

When $z > 1$, condition (97) with $u_n = 3{\cdot}87$ shows that $(mnd/b)^2 < 3$ ; and since $nd/b$ is of the order unity, $m$ will not exceed 2. Many layered coils are therefore only of advantage when $z < 1$. When this is the case, $G = z^4/64$ and F is negligible.

Condition (97) may then be written, when $a/b = 1{\cdot}6$,

$$Nd/b = 1{\cdot}66/z^2 ;$$

or, expressing $z$ in terms of wave-length and diameter, and assuming the wire to be of copper of resistivity 1,600 C.G.S. units,

$$N = 2{\cdot}8 + 10^{-4}\lambda a/d^3, \quad . \quad . \quad . \quad . \quad . \quad . \quad . \quad . \quad (100)$$

$\lambda$ being the wave-length in metres, $a$ the coil radius in centimetres, and $d$ the diameter of the wire in millimetres.

For stranded wire coils of the same total copper section the conditions are

$$a/b = 1{\cdot}6$$

$$N = 2{\cdot}8 \times 10^{-4}\lambda a\sqrt{s}/d^3, \quad . \quad . \quad . \quad . \quad . \quad . \quad . \quad (101)$$

while

$$R'/L = 1{\cdot}187\gamma (z) \sqrt{f\rho/ls\delta}, \quad . \quad . \quad . \quad . \quad . \quad . \quad . \quad (102)$$

$d$ being the diameter of the equivalent solid copper, $\delta$ the diameter of one strand, $s$ the number of strands, and $z$ is calculated from the diameter of a single strand.



Digitized by Google

Thus the gain in time-constant by using stranded wire is $1/s^{\frac{1}{2}}$; but, in addition, a larger number of turns, and therefore an increased inductance, may be obtained with stranded wire, while maintaining the best conditions.

28. *Design of Coils of Large Inductance.*—If a coil of large inductance is required to have minimum effective resistance at a specified wave-length the conditions

$$a/b = 1{\cdot}6,$$

$$N = 2{\cdot}8 + 10^{-4}\lambda a\sqrt{s}/d^3, \quad \ldots\ldots\ldots \quad (A)$$

together with the formula for the inductance

$$L = 25{\cdot}5N^2a, \quad \ldots\ldots\ldots \quad (B)$$

determine the radius, shape and number of turns for a given diameter of wire.

Usually these coils are required to resonate with a condenser of given capacity. In this case, if C is the resonating capacity in micro-microfarads,

$$\lambda^2 = 3{\cdot}55 \times 10^{-3}LC. \quad \ldots\ldots\ldots \quad (C)$$

Eliminating L and $\lambda^2$ between (A), (B), (C), we find

$$a^3 = 1{\cdot}4 + 10^8d^6/sC,$$

a relation independent of the number of turns. Thus, whatever inductance is used, the coils must all have the same radius if wound with the same type of wire. In illustration, let the wire consist of nine strands, each of diameter 0·2 mm., and let the resonating capacity be 1,000 $\mu\mu$F.

Then

$$s = 9, \qquad d = \sqrt{s}\delta = 0{\cdot}6,$$

from which

$$a \doteqdot 9 \text{ cm.}$$

Thus, if $L = 20mh$, $N = 297$. As the winding length $b = 5{\cdot}6$ cm., this could be arranged by having 6 layers of 50 turns each. To avoid large self-capacities the winding should be "sliced".

Digitized by Google

# CALCULATION OF A PRIMARY STANDARD OF MUTUAL INDUCTANCE OF THE CAMPBELL TYPE AND COMPARISON OF IT WITH THE SIMILAR N.P.L. STANDARD

BY

D. W. DYE, B.Sc., A.C.G.I.,

SENIOR ASSISTANT IN THE ELECTRICITY DEPARTMENT.

Digitized by Google

ABSTRACT.

A description of the construction of a Campbell form of mutual inductance is given. The accurate dimensions of the windings are shown and the calculation of the inductance is given in detail. In connection with these calculations the new formulæ of L. V. KING are used owing to their great convenience.

The experimental comparisons of this standard with the laboratory standard are then given. From these comparisons and from the comparisons of the calculated values of mutual inductance it is concluded that both standards are accurate to about 1 part in 100,000 in terms of the N.P.L. standards of length.

Unfortunately this standard was destroyed in the great Japanese earthquake of September, 1923.

Digitized by Google

# CALCULATION OF A PRIMARY STANDARD OF MUTUAL INDUCTANCE OF THE CAMPBELL TYPE AND COMPARISON OF IT WITH THE SIMILAR N.P.L. STANDARD.

By D. W. DYE, B.Sc., A.C.G.I., Senior Assistant in the Electricity Department.

[Reprinted from the 'Proceedings of the Royal Society', Series A, Vol. 101, 1922.]

## Introductory.

The standard mutual inductance devised and designed by Mr. A. Campbell and constructed in 1907–8* at the National Physical Laboratory has been one of the foundations of our alternating current measurements since that date.

It will be sufficient here to note that the special feature in the design of the Campbell type of mutual inductance consists in a primary single-layer winding, so proportioned that the field due to it is practically zero over the region occupied by the secondary coil. By this means the dimensions of the secondary coil are rendered relatively unimportant, so that it may be an overwound many-layer winding, whereby a suitably large value of mutual inductance may be obtained.

A number of fundamental measurements have also been made with its help, including a determination of the ohm† and a comparison of self-inductance standards of the Physikalische Technische Reichsanstalt.‡ These measurements give, through various links, an independent check on the accuracy of our standard. From general considerations of the probable accuracy which might be assigned to all the measurements, it appeared possible that the uncertainty of knowledge of the value of this standard might be as great as 1 part in 10,000, *i.e.*, considerably greater than the uncertainty which would be assigned to it from the calculations and length measurements. These latter together might amount to 2 or 3 parts in 100,000.

When, therefore, a similar standard of mutual inductance for the Japanese Government, which was under construction by Mr. R. W. Paul, was approaching completion and had shown great uniformity of the spiral groove finally cut on the marble cylinder at the Laboratory, it was thought that highly accurate measurements should be made of the diameter and pitch of the primary winding and also of the mean diameter and cross-section of the secondary winding in order that the value of the mutual inductance of this standard might be calculated to at least as great accuracy as the original N.P.L. standard. With this end in view the primary winding was done at the Laboratory in order that the necessary measurements of the diameter of the bare copper wire under the tension of winding might be made. The secondary winding was also carried out at

* A. Campbell, 'Roy. Soc. Proc.', A, vol. 79, p. 428, 1907, and N.P.L. 'Collected Researches', vol. 4, Paper V, p. 201, *et seq.*

† A. Campbell, 'Roy. Soc. Proc.', A, vol. 87, 1912, and N.P.L. 'Collected Researches', vol. 9, Paper VI, p. 49.

‡ 'N.P.L. Report', p. 44, 1914–15.

Digitized by Google

the Laboratory in order that the mean diameter of the successive layers of it might be measured as accurately as possible. The calculations were made to the highest accuracy and the full corrections made for departure from mathematical exactness of the actual coils as measured.

The construction of this new standard differs only in minor details from the Laboratory standard; it is not thought that these details can have any measurable effect on the actual value as calculated.

## Winding of the Primary and Secondary Coils and General Remarks regarding the New Mutual Inductance.

The marble cylinder was sent to the Laboratory for measurement in October, 1913, and as a result of the report on these measurements, it was decided to have the two spiral grooves recut and rewound at the Laboratory. This, owing to the war, was delayed until the early part of 1920. It was then taken in hand by the Engineering Department, who recut the spiral and rewound the two coils forming the primary winding. The dimensions and numbers of turns of the two primary windings are as follows:—

| | |
|---|---|
| Approximate diameter .. .. .. .. .. .. .. | 30 cm. |
| Length of coil .. .. .. .. .. .. .. .. | 7·5 „ |
| Distance between inside turns of coils .. .. .. .. .. | 15 „ |
| Number of turns in each coil .. .. .. .. .. .. | 75 |

Some time after winding the primary coils, the cylinder was handed over to the Metrology Department and measured according to the scheme detailed below in section 3 of this paper.

The secondary winding, which is a ring-shaped coil of many layers, was carried out in the Electrical Measurements Department. It is necessary to know the mean diameter represented by the central filament of the cross-section of the secondary, and since this winding consists of twenty layers of silk-covered wire with a layer of paper between each, it was thought that the diameters of the central layers might be reduced slightly by the compression of the outer layers. The diameters of each successive layer can only the accurately measured at the time of winding it, before it is subjected to the compression of the outer layers.

In order to get an idea of the possible change in diameter of the layers due to this cause, holes were cut in the cheeks of the ring-shaped marble bobbin at the ends of three diameters spaced 120° apart. These holes allowed the outer wires in each layer to be seen and to be measured by means of a microscope after the whole coil had been wound. The outer wires at each side of the tenth layer were measured through these holes at the time of winding it and again after the whole twenty layers had been wound. The difference between the mean of the six measurements before and after winding the outer ten layers was within the experimental accuracy of the measurements, being less than 0·01 mm.

Digitized by Google

It may be taken, therefore, that the mean diameter as deduced from the diameters of each layer at the time of winding it represents accurately the mean diameter of the whole winding.

The bottom of the groove in the marble ring was too small to allow the secondary winding to be wound directly on it of the correct mean diameter. A single layer of wire of suitable diameter was, therefore, first wound on and a single layer of paper put over it in order to bring the inside diameter of the secondary winding to such a value as to give the correct mean diameter of the whole coil as nearly as could be determined beforehand.

The finished winding consists of twenty layers of double silk-covered wire ; each layer has twenty-four turns and there is a strip of paper about 0·08 mm. thick between each layer of wire. The odd five turns are in a twenty-first layer wound close together near the cheek of the ring at which the ends come out.

The winding is in four sections, having the following numbers of turns, 96, 144, 144, 96 + 5 turns, thus making 485 turns in all when in series.

## Length Measurements of the Japanese Standard.

### (1) *Primary Winding on Marble Cylinder.*

(*a*) *Description.*—The two windings are referred to as P and Q throughout this paper, in accordance with the diagram, fig. 1, which also indicates the system of numbering adopted for the turns. The top of the cylinder is that end at which the outgoing leads are attached. The overall dimensions of the marble cylinder are—

| | | | |
|---|---|---|---|
| Height | .. | .. | 35 cm. |
| Outside diameter | .. | .. | 30 „ |
| Inside diameter | .. | .. | 18 „ |

Each coil consists of 75 turns of bare wire, having a nominal pitch of 1 mm. and a nominal diameter of 30 cm. The distance $x_0$ is nominally 22·5 cm.

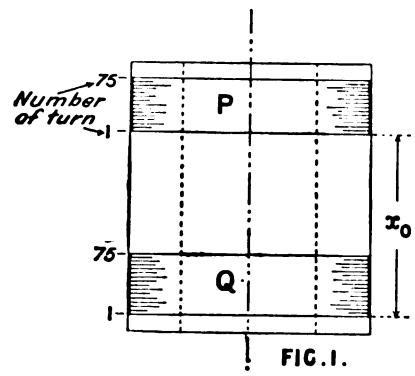

FIG. 1.
Primary windings of mutual inductances.

(*b*) *Measurement of Diameters.*—The diameters over the wires have been compared with the length of the Laboratory 300-mm. Hartmann spherical-ended gauge. The variations in diameter are shown in fig. 2. The continuous portions of the curves, together with the extremeend points, are plotted from the calculated means of readings taken six at a time. The dotted lines completing the curves are partly estimated means.

It will be noted that the first turn of coil P has a diameter about 0·1 mm. less than that of the rest of the winding. This is due to the fact that the groove for this turn was added some time after that for the other turns, with the consequent error noted. The

Digitized by Google

method used in the calculations for correction of variation of diameter takes quite accurate account of this comparatively large local variation in diameter.

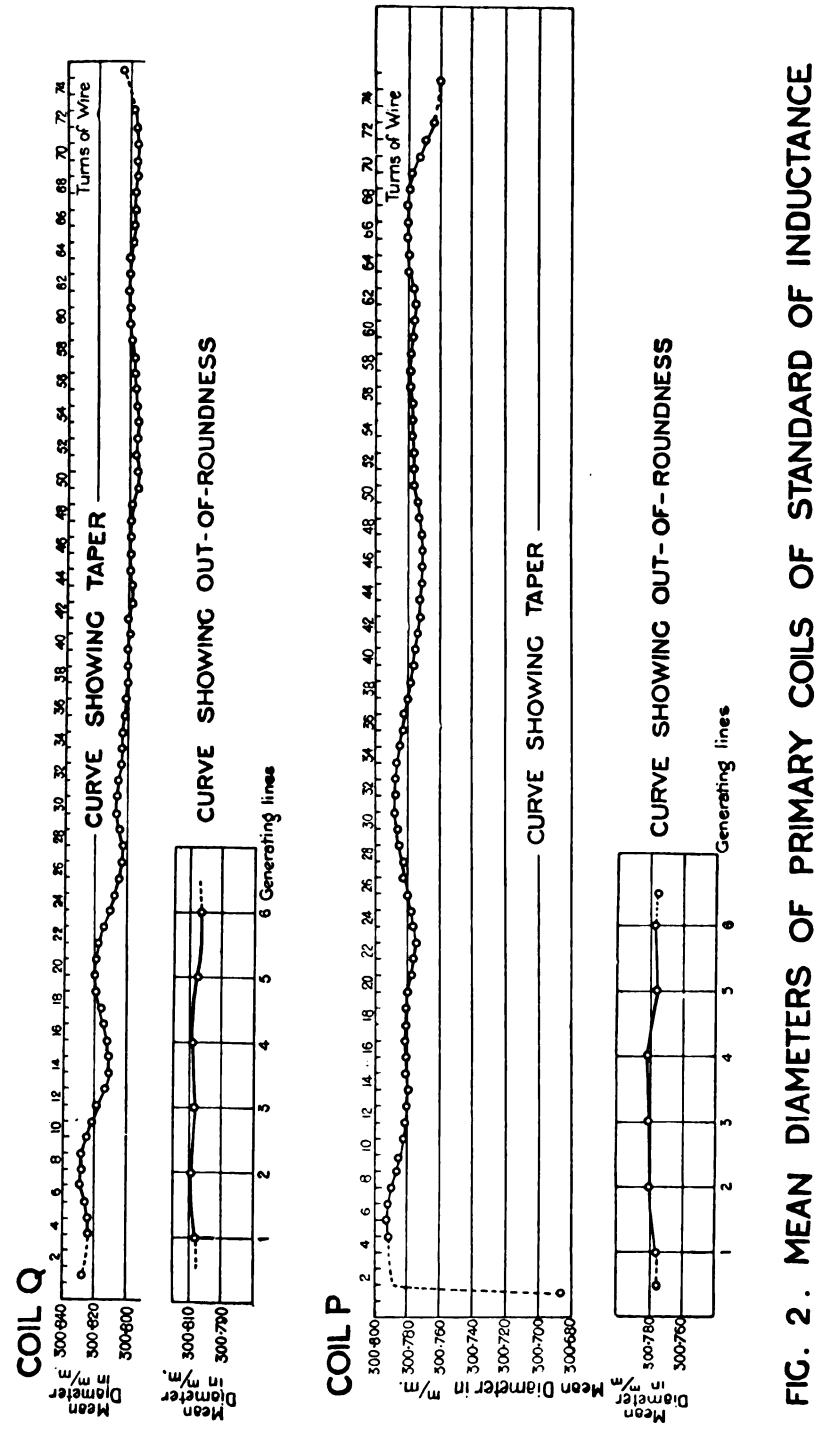


FIG. 2. MEAN DIAMETERS OF PRIMARY COILS OF STANDARD OF INDUCTANCE

The final mean diameters over the wires thus found were :—

Coil P = 300·778$_7$ mm. at 17° C. (omitting first turn).

Coil Q = 300·806$_9$ mm. at 17° C.

Digitized by Google

In order to avoid fractional parts in the differences between the true diameter of each turn and the mean diameter, as given above, nominal mean diameters have been used having the values

Coil P = 300·779 mm.
Coil Q = 300·807 mm.

The differences between these nominal diameters and the actual diameter have been read off from the curves of fig. 2, and are given in section (4), dealing with the corrections for variations from a perfect spiral.

(*c*) *Diameter of Wire.*—The diameter of the wire was measured at about 100 points for each coil, while it was under tension during the process of winding the wire on the cylinder. The mean diameters of wire thus found were

Wire on Coil P = $0{\cdot}620_8$ mm.
Wire on Coil Q = $0{\cdot}621_0$ mm.

(*d*) *Measurement of Pitch.*—The pitch has been measured against the Laboratory line standard Invar No. 27, whose calibration is accurately known. The nominal pitch is 1 mm., and the nominal mean distance from a point on coil P to the corresponding point on coil Q has been taken as $225{\cdot}445_8$ mm. All measurements on both coils are reckoned as from the first turn of coil Q, that is, readings on this turn are taken as correct. The nominal reading on any other turn minus the observed reading gives the variation from nominal pitch. These variations are shown in fig. 3. The continuous portions of the curves, together with the end points, have been plotted from the calculated means of readings taken six at a time, and the dotted portions completing the curves are partly estimated means.

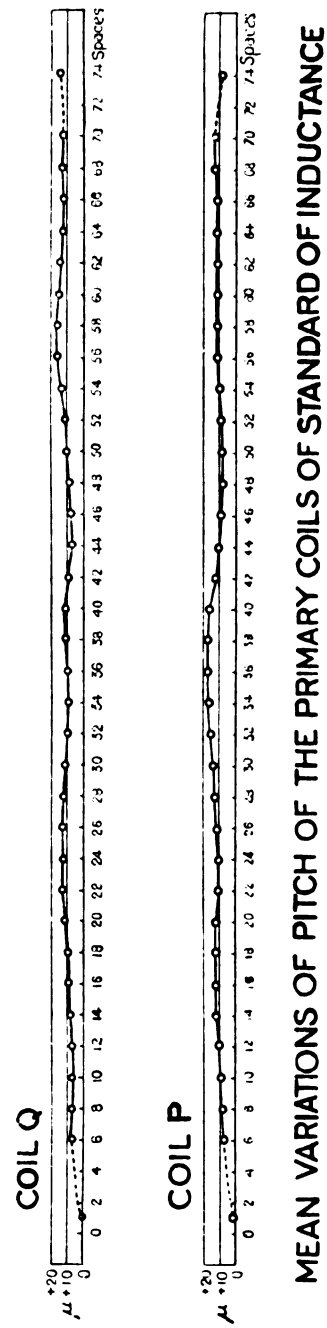


MEAN VARIATIONS OF PITCH OF THE PRIMARY COILS OF STANDARD OF INDUCTANCE
FIG. 3.

In order to correct for these variations in pitch, a zero line of (+ 10 μ = 0·01 mm.) has been chosen for each coil, and the axial displacements of every wire from the perfect spiral were taken from this base line: these, when multiplied by the appropriate $dM/dx$ at that place, give the desired corrections. The change of the zero line for this purpose makes no difference in the fundamental calculations so long as the same change is made in both coils.

(*e*) *Irregularities at the Ends of the Windings.*—The ends of the windings come through small ivory plugs of 5 mm. diameter, which are let into recesses in the marble. The



Digitized by Google

surfaces of these plugs are below the surface of the marble; the wires consequently become chords instead of arcs of circles when passing over this space, and the end of the last turn also bulges outwards somewhat before the wire bends sharply in entering the hole in the plug. A calculation of the effects due to this departure from perfection of shape shows, however, that it is quite negligible. The change in mutual inductance due to a change in diameter of 0·2 mm. of one whole turn of the primary winding is of the order of 0·1 microh., *i.e.*, 1 part in 100,000 of the total mutual inductance.

There are also local irregularities of pitch near the ends of the windings: these also are of negligible effect.

### (2) *Secondary Winding.*

The principle of the Campbell design of mutual inductance is such that the dimensions of the secondary winding are comparatively unimportant. They are, however, sufficiently important to warrant some care in the measurements of mean diameter and dimensions of cross-section of the winding.

The outside diameter of each layer was measured on diameters 120° apart by means of a large micrometer gauge, which was then immediately calibrated against a 17-inch standard spherical-ended gauge. The diameter of the silk-covered wire was also measured at a number of places during winding. The deduced values of mean diameter for each layer are given in Table I, below.

The mean diameter for the whole coil is thus 437·62$_5$ mm. The mean diameter, as measured through the holes by microscope, was 437·63 mm. Since accuracy to 0·01 mm. in diameter is more than sufficient for an accuracy of 1 in $10^4$ in the calculations, the mean diameter has been taken as 437·630 mm.

The axial width of winding = 10·1 mm.

Radial depth of winding = Mean of six measurements through the holes in the marble ring = 9·6$_8$ mm.

TABLE I.—Mean Diameters of Successive Layers of Secondary Winding.

| Layer. | Mean diameter. | Layer. | Mean diameter. | Layer. | Mean diameter. | Layer. | Mean diameter. |
|---|---|---|---|---|---|---|---|
| | mm. | | mm. | | mm. | | mm. |
| 1 | 428·35$_8$ | 6 | 433·28$_3$ | 11 | 438·10$_0$ | 16 | 442·95$_0$ |
| 2 | 429·34$_5$ | 7 | 434·26$_3$ | 12 | 439·08$_0$ | 17 | 443·91$_0$ |
| 3 | 430·33$_7$ | 8 | 435·21$_0$ | 13 | 440·02$_0$ | 18 | 444·90$_0$ |
| 4 | 431·31$_0$ | 9 | 436·18$_0$ | 14 | 440·99$_0$ | 19 | 445·90$_0$ |
| 5 | 432·28$_9$ | 10 | 437·17$_0$ | 15 | 441·98$_0$ | 20 | 446·91$_0$ |

Digitized by Google

(3) *Measurement of Thermal Coefficient of Expansion of the Marble.*

This was measured at temperatures ranging from 13° to 25°, and found to be

$$+ 0{\cdot}000005_9 \text{ per } 1° \text{ C.}$$

(4) *Calculations and Corrections.*

The accurate formula of J. VIRIAMU JONES was used in the fundamental calculations. This formula gives the mutual inductance between a circle and a coaxial helix, having one end in the plane of the circle. A convenient form of this formula* is

$$M = 2\pi n_1 (A + a)\left\{c/k\,(F(k) - E(k)) + \frac{A - a}{x}\,\psi\right\}, \quad . \quad . \quad . \quad . \quad (1)$$

where A = radius of circle, $a$ = radius of helix, $x$ = length of helix, $n_1$ = number of turns in the length "$x$" of the helix.

$$k^2 = \frac{4Aa}{(A + a)^2 + x^2} = \sin^2 \gamma. \qquad c^2 = \frac{4Aa}{(A + a)^2}.$$

F ($k$) and E ($k$) are complete elliptic integrals of the first and second kinds. They were computed by formulas (5) and (6),

$$\psi = F(k)\,.\,E(k_1'\beta) - [F(k) - E(k)]\,F(k_1'\beta) - \frac{\pi}{2}$$

in which F ($k_1'\beta$) and E ($k_1'$ $\beta$) are incomplete integrals of the second kind to modulus $k'$ and amplitude $\beta$

$$k' = \cos\gamma \quad \text{and} \quad \beta = \sin^{-1} c'/k'; \qquad c' = \sqrt{(1 - c^2)}.$$

The values of mutual inductance obtained by the above formula have been multiplied by 485 in every case so as to refer them to a secondary winding of that number of turns.

The calculations have been made in two parts, one for coil P and one for coil Q. The complete curve showing variation of mutual induction with variation in diameter of the secondary winding, has only been made in the case of coil P. It was not essential to obtain the curve shown in fig. 4, but it forms a most valuable check on the calculation of M for the point required and also checks the curve shown in fig. 5 for $dM/dA$.

The dimensions used in the calculations for coil P were $a = 15{\cdot}00791$ cm., $x_1 = 15{\cdot}0223$ cm., $x_2 = 7{\cdot}5223$ cm.

* A. CAMPBELL, 'Roy. Soc. Proc.', A, vol. 79, p. 434, 1907, and N.P.L. 'Collected Researches', vol. 4, Paper V.



Digitized by Google

Five values of A were taken, viz., 21·3915, 21·6915, 21·8815, 22·0915 and 22·3915. The reason these values of A were chosen was that it was thought that the maximum point would be at a radius of A equal to 21·8915 cm., this was afterwards found not to be the case.

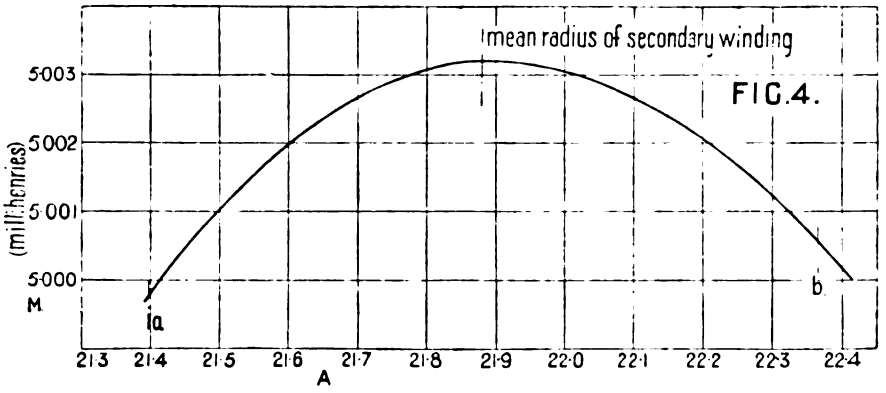


Variation of mutual inductance for variation of diameter of secondary circle.

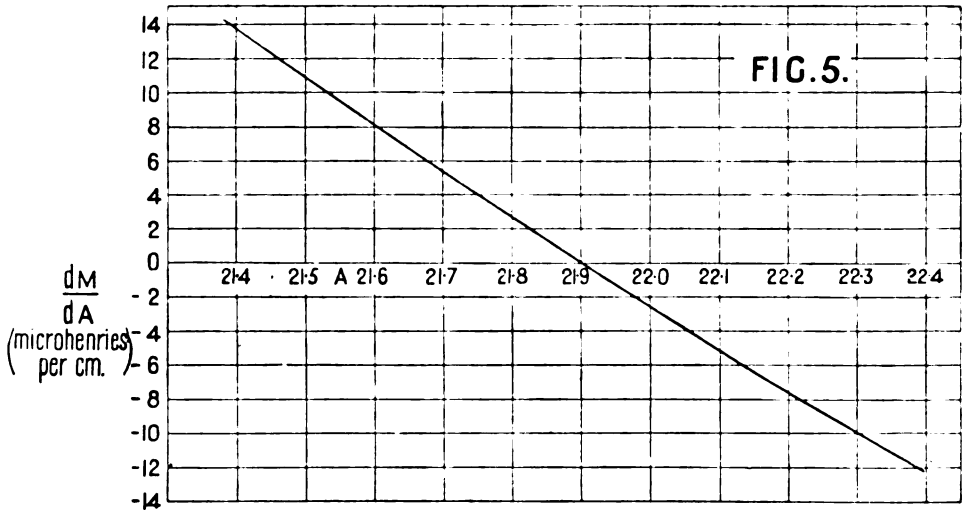


Relation between $dM/dA$ and A for coil P and secondary circle.

The values obtained for the mutual inductances are given in Table II.

TABLE II.—Coil P and Secondary Circle of 485 Turns.

| A (cm.). | M ($x_1$). | M ($x_2$). | M ($x_1 - x_2$). |
|---|---|---|---|
| 21·3915 | 13·45049 | 8·45080 | 4·99969 |
| 21·6915 | 13·31803 | 8·31536 | 5·00267 |
| 21·8815 | 13·23494 | 8·23175 | 5·00319 |
| 22·0915 | 13·14390 | 8·14109 | 5·00281 |
| 22·3915 | 13·01502 | 8·01478 | 5·00024 |

Digitized by Google

The curve connecting A and M $(x_1 - x_2)$ is given in fig. 4. For coil Q the values corresponding to its mean radius of $a = 15{\cdot}0093$ and the mean secondary radius $A = 21{\cdot}8815$ are,

| A. | M ($x_1 = 15{\cdot}0223$). | M ($x_2 = 7{\cdot}5223$). | M ($x_1 - x_2 = 7{\cdot}5000$). |
|---|---|---|---|
| 21·8815 | 13·23758 | 8·23354 | 5·00404 |

The sum of the mutuals to the circle secondary for coils P and Q is, therefore, 10·00723.

For averaging over the space occupied by the cross-section of the secondary winding the formula (2) has been used :—

$$M = M_0 + \frac{1}{a}\frac{dM}{dA}\left(\frac{c^2}{6} + \frac{20B^2C^2 - 9C^4}{360A_0^2}\right) + \left(\frac{B^2 - C^2}{6} + \frac{9C^4 - 20B^2C^2}{360A_0^2}\right)\frac{d^2M}{dA^2} + \frac{10B^2C^2 - 6C^4}{360A_0^2}\cdot\frac{d^3M}{dA^3} + \ldots, \quad (2)$$

where 2 B = radial depth and 2 C = axial length of cross-section of the secondary.

In order to determine $dM/dA$, $d^2M/dA^2$, etc., the curve connecting $dM/dA$ with A was found by calculation and plotting, using the equation

$$\frac{dM}{dA} = 2\pi n_1 n_2 ck\left\{F(k) + \left(\frac{A + a}{2ax}\sqrt{([A + a]^2 + x^2)}\right)\psi\right\} \quad . \quad . \quad . \quad . \quad (3)$$

in which the symbols have the same meaning as in equation (1) ; $n_2 = 485$.

The values obtained for $dM/dA$ in the case of coil P are given in Table III.

TABLE III.

| A. | $dM/dA$ microhenries per centimetre. | | |
|---|---|---|---|
| | $x_1 = 15{\cdot}0223$. | $x_2 = 7{\cdot}5223$. | $x_1 - x_2 = 7{\cdot}5000$. |
| 21·3915 | − 444·11 | − 458·12 | + 14·01 |
| 21·6915 | − 438·96 | − 444·61 | + 5·65 |
| 21·8815 | − 435·67 | − 436·22 | + 0·55 |
| 22·0915 | − 432·00 | − 427·22 | − 4·78 |
| 22·3915 | − 426·72 | − 414·74 | − 11·98 |

The curve connecting A and $dM/dA$ for $(x_1 - x_2 = 7{\cdot}5000)$ is given in fiig 5. To a sufficient accuracy this curve is represented by the equation $dM/dA = -25{\cdot}8\,\epsilon + 4{\cdot}5\epsilon^2$ where $\epsilon$ is the difference between any value of A and that value corresponding to the maximum mutual inductance. In the present case A for the maximum mutual inductance, *i.e.*, when $dM/dA = 0$, is

$A = 21{\cdot}90_1$ cm. for Coil P, and

$A = 21{\cdot}90_4$ cm. for Coil Q ;

when $\epsilon$ is very small we have, therefore, for the whole mutual

$$\frac{dM}{dA} = -51{\cdot}6\epsilon, \qquad \frac{d^2M}{dA^2} = -51{\cdot}6, \qquad \frac{d^3M}{dA^3} = +18{\cdot}0.$$

Digitized by Google

In the present case for coil P, $\varepsilon = -0{\cdot}0195$ cm., and $dM/dA = +0{\cdot}55$; for coil Q, $\varepsilon = -0{\cdot}0225$ and $dM/dA = +0{\cdot}58$ microh. per centimetre.

The only term of any importance in equation (2) is the term

$$\left(\frac{B^2 - C^2}{6} + \frac{9C^4 + 20B^2C^2}{360A_0^2}\right)\frac{d^2M}{dA^2}.$$

Substituting the values B = 0·48 cm., and C = 0·50 cm. (allowing for insulation on the wire) we get, for the correction on the total mutual inductance, due to the finite space occupied by the secondary, the result + 0·170 microh.

We have, therefore, for the case of the mutual inductance with two perfect spirals and a secondary winding of the dimensions given, the value

$$M = 10{\cdot}00740 \text{ millih.}$$

*Corrections for Axial and Radial Displacements of the Primary Winding.*

Each turn of the primary helix is displaced axially and radially from its theoretical position. The most accurate method of determining the corrections due to these displacements is to calculate the $dM/da$ and the $dM/dx$ for each of a number of circles of radius "$a$" and different distances "$x$" from the larger circle A. By plotting these values against $x$, curves are obtained from which the $dM/da$ and $dM/dx$ for each turn of the primary winding may be read off. These values, when multiplied by the respective displacements radially and axially of each of the turns, give the small corrections on M due to them. The sum of all these corrections gives the total correction to be applied. The $dM/da$ and $dM/dx$ for the circles could have been calculated directly from the formulas for these quantities, but only one more calculation for each point is needed if the actual mutual inductances themselves are calculated; moreover, if the new elegant formulas developed from those for complete elliptic integrals are used for the computation of the mutual inductances of the circles,* the labour involved is comparatively light, and no tedious and doubtful interpolation in the tables of elliptical integrals is required.

Starting off with the quantities $a_0$, $b_0$, and $c_0$, which have the values given below, Table IV is constructed.

TABLE IV.

| $a_0$. | $b_0$. | $c_0$. |
|---|---|---|
| $a_1 = \frac{1}{2}(a_0 + b_0)$; | $b_1 = \sqrt{(a_0 b_0)}$; | $c_1 = \frac{1}{2}(a_0 - b_0)$. |
| $a_2 = \frac{1}{2}(a_1 + b_1)$; | $b_2 = \sqrt{(a_1 b_1)}$; | $c_2 = \frac{1}{2}(a_1 - b_1)$. |
| ..... | ..... | ..... |
| $a_n = \frac{1}{2}(a_{n-1} + b_{n-1})$; | $b_n = \sqrt{(a_{n-1} \cdot b_{n-1})}$; | $c_n = \frac{1}{2}(a_{n-1} - b_{n-1})$. |

Then

$$M = \frac{2\pi^2}{a_n}(c_1^2 + 2c_2^2 + 4c_3^2 + \ldots) \quad . \quad . \quad . \quad . \quad . \quad . \quad (4)$$

* L. V. KING, 'On some New Formulæ for the Numerical Calculation of the Mutual Inductance of Coaxial Circles', 'Roy. Soc. Proc.', A, vol. 100, p. 60, 1921.

Digitized by Google

"$a_0$" and "$b_0$" converge with extreme rapidity to the same value. In general, for the cases under consideration, $a_3 = b_3$ to an accuracy of one part in ten million.

$$a_0 = \sqrt{(A+a)^2 + x^2}\,; \qquad b_0 = \sqrt{(A-a)^2 + x^2}\,; \qquad \text{and} \qquad c_0 = \sqrt{(4Aa)}.$$

(*Note.*—$c_0$ is not required in this formula for mutual inductance.)

The expressions for F ($k$) and E ($k$) in terms of the above symbols are

$$F(k) = \tfrac{1}{2}\frac{\pi a_0}{a_n}, \quad \ldots \quad (5)$$

$$F(k) - E(k) = \frac{F(k)[c_0^2 + 2c_1^2 + 4c_2^2 + \ldots]}{a_0}. \quad \ldots \quad (6)$$

In computing the values of M for circles, three cases were taken for each value of "$x$" considered. They were

(1) A, $a$, $x$; (2) A, $a + 0{\cdot}01$ cm., $x$; (3) A, $x + 0{\cdot}01$ cm., $a$.

In these A = 21·8815 cm., $a$ = 15·00791 cm., and $x$ = 7·500 cm.
The difference (2) — (1) gives $\Delta M$ corresponding to $\Delta a = 0{\cdot}01$ cm.
The difference (3) — (1) gives $\Delta M$ corresponding to $\Delta x = 0{\cdot}01$ cm.

In carrying out these computations the constant terms $2\pi^2$ and $n_2 = 485$ have been left out of the calculations till the final additions of the corrections.

The values of $M_1$, $\Delta M_1$ when $\Delta a = 0{\cdot}01$ and $\Delta M_1$ when $\Delta x = 0{\cdot}01$ are given in Table V and curves figs. 6 and 7.

TABLE V. $M_1 = M/2\pi^2$ for Circles Radii A = 21·8815 and $a$ = 15·0079$_1$ with various Values of $x$.

| $x$. | $M_1$ (cm.). | $\Delta M_1$ for $\Delta a = +0{\cdot}1$ mm. | $\Delta M_1$ for $\Delta x = +0{\cdot}1$ mm. |
|---|---|---|---|
| 6·0 | 10·14853 | ... | − 0·00644 |
| 7·5 | 9·13485 | + 0·01217 | − 0·00658 |
| 8·0 | 8·80715 | + 0·01151 | − 0·00649 |
| 9·0 | 8·17523 | + 0·01032 | − 0·00615 |
| 10·0 | 7·57938 | + 0·00932 | − 0·00577 |
| 11·0 | 7·02249 | + 0·00843 | − 0·00537 |
| 12·0 | 6·50508 | + 0·00766 | − 0·00498 |
| 13·0 | 6·02630 | + 0·00699 | − 0·00459 |
| 14·0 | 5·58447 | + 0·00639 | − 0·00426 |
| 15·0 | 5·17742 | + 0·00588 | − 0·00390 |

The values of $\Delta M_1$ corresponding to the position "$x$" of each turn have been read off from these curves and multiplied by the corresponding small differences $u$ and $v$ obtained

Digitized by Google

from the curves, figs. 2 and 3. Since turn 1 on coil P and turn 75 on coil Q are the same distance "$x$" from the secondary winding, the algebraic sum of their radial and

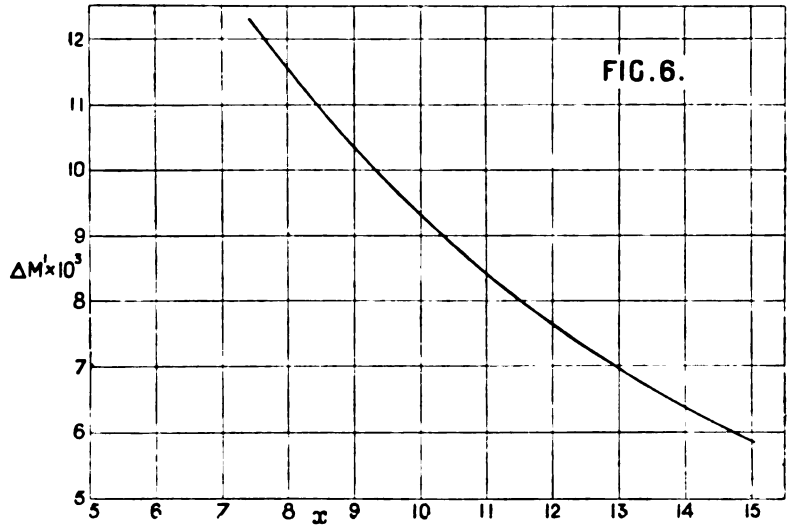


$\Delta M'$ between circles at distance $x$ apart when $\Delta a = 0{\cdot}01$ cm.

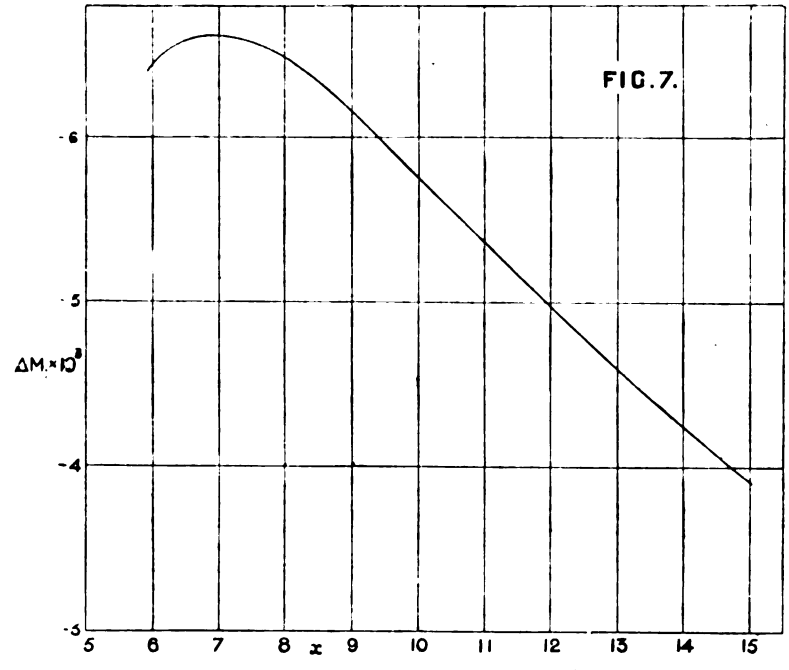


$\Delta M'$ between circles at distance $x$ apart when $\Delta x = 0{\cdot}01$ cm.

axial differences may be taken when multiplying by $\Delta M_1$. A selection of the results of the calculations is given in Table VI, in which turn 1 has the position "outer" on both coils and turn 75 the position "inner" on both coils.

Digitized by Google

TABLE VI.

| Turn. | Sum of radial displacements on P and Q in units of $10^{-3}$ mm. $= u$. | Sum of axial displacements on P and Q in units of $10^{-3}$ mm. $= v$. | The unit is $1 = \frac{10^{-8} \text{ microh.}}{2\pi^2}$. | |
|---|---|---|---|---|
| | | | $u \times \frac{dM_1(a)}{dx}$. | $u \times \frac{dM_1(x)}{dx}$. |
| 1 | + 1 | + 9 | + 5·9 | − 35·0 |
| 5 | + 10 | + 7 | + 61·2 | − 28·2 |
| 10 | + 17 | + 6 | + 108·3 | − 25·2 |
| 15 | + 1 | + 4 | + 6·6 | − 17·5 |
| 20 | + 12 | 0 | + 83·6 | 0 |
| 25 | − 4 | − 6 | − 29·1 | + 28·5 |
| 30 | − 7 | − 3 | − 53·3 | + 14·8 |
| 35 | − 8 | + 6 | − 63·9 | − 30·7 |
| 40 | − 3 | + 5 | − 25·1 | − 26·6 |
| 45 | + 2 | + 7 | + 17·6 | − 38·4 |
| 50 | − 8 | + 1 | + 74·2 | − 5·7 |
| 55 | − 12 | − 4 | − 117·4 | + 23·7 |
| 60 | − 4 | − 4 | − 41·2 | + 24·4 |
| 65 | − 7 | − 4 | − 66·0 | + 25·1 |
| 70 | + 2 | − 8 | + 22·9 | + 51·6 |
| 75 | − 97 | − 14 | − 1178·5 | + 92·0 |

The whole correction for the seventy-five turns of both windings of the primary was found to be—

For radial displacements of the wires = − 0·084 microh.
For axial ,, ,, = + 0·015 ,,

CORRECTION FOR THE FIVE TURNS FORMING THE TWENTY-FIRST LAYER.

The calculations relative to averaging over the cross-sectional area occupied by the secondary winding assume the whole of it to be contained within the rectangle formed by the twenty layers of twenty-four turns each ; the extra five turns necessary to obtain the mutual inductance of 10 millih. are wound close together near the upper cheek of the ring. They may, to a sufficient accuracy, be considered as equivlaent to a five-turn circle displaced radially by + 0·5 cm. and axially by 0·4 cm. from the central filament of the secondary winding.

The corrections due to these displacements are :—

For axial displacement = + 0·041 microh.
For radial ,, = − 0·061 ,,
Net correction = − 0·020 ,,



Digitized by Google

There is, finally, a correction due to one of the coils having slightly more than seventy-five turns; the overlap is 1·2 mm. If the outgoing leads are close together, this extra piece may be considered as equivalent to a positive mutual inductance due to the part NP (Fig. 8) of the circle at one end of the helix together with a negative mutual given by the very open spiral QP formed by the outgoing lead from the end Q. QN is a generator of the cylindrical surface of the winding.

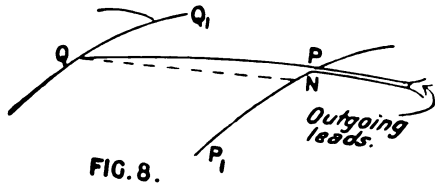

FIG. 8.

Appertaining to overlap at one end of helix.

If the piece NP is considered as at the end of the helix closest to the secondary winding, the positive mutual inductance due to it will be greater than the negative mutual inductance due to the return lead QP; on the other hand, if the small piece is considered as at the end, Q, of the helix its positive value will be less than the negative value of QP. The length measurements of the distance separating the two helices are not quite sufficiently accurate to determine which case is correct.

There is an uncertainty, also, due to the return piece QP being on a different cylinder to the helix, owing to the ends Q and P first going radially inwards through the walls of the hollow marble cylinder. The uncertainty introduced by the ends before they come away together is probably of the order $\pm 3 \times 10^{-6}$.

Summing up the various calculations and corrections we have for the value of the standard,

For perfect Helix P .. .. .. .. M = 5003·19 microh.
„ „ Q .. .. .. .. M = 5004·04 „

| | Microh. |
|---|---|
| Correction for averaging over cross-section of secondary .. .. .. | + 0·170 |
| „ for irregularities of diameter of primary helices .. .. | — 0·084 |
| „ „ pitch of primary helices .. .. .. | + 0·015 |
| „ for five turns on outside of secondary winding .. .. | — 0·020 |

These together give for the final calculated mutual inductance of the standard the value at 17° C.

$$M_{17} = 10{\cdot}0073_1 \text{ millih.}$$

*Probable Accuracy of the Calculated Value of the Standard.*

There are five factors entering into the calculations, each of which represents a series of length measurements. If a probable accuracy is given to these measurements it is possible to assign a probable accuracy to the final result. The factors involved are—

(1) Diameter of primary helices.
(2) Pitch and distance apart of primary helices.
(3) Diameter of secondary winding.
(4) and (5) Width and depth of secondary winding.

Digitized by Google

For the present purpose the helices may be replaced by a circle 10 cm. distant from the plane of the secondary winding.

If it is assumed that the diameter is accurate to $\pm 0{\cdot}001$ mm., and the pitch to $\pm 0{\cdot}002$ mm. for the primary winding; also that the mean diameter of the secondary winding is accurate to $\pm 0{\cdot}1$ mm., and the width and depth of the secondary cross-section is accurate to $\pm 0{\cdot}05$ mm., the following will be the resulting uncertainties in M expressed as parts in a million :—

| | |
|---|---|
| For—Primary diameter .. .. .. .. .. .. | $\pm 6$ |
| ,, length and distance apart .. .. .. .. | $\pm 16$ |
| Secondary diameter .. .. .. .. .. .. | $\pm 0{\cdot}7$ |
| ,, depth and width .. .. .. .. .. | $\pm 8$ each. |

The maximum error is, therefore, 40 parts in $10^6$, but the mean probable error will be of the order 20 parts in $10^6$.

*Comparison with the N.P.L. Standard Mutual Inductance.*

(*a*) *Calculated Value of N.P.L. Standard.*—The original value calculated from measurements of dimensions made when the N.P.L. standard was first constructed in 1908, was

$$M_{15} = 10{\cdot}0178_5 \text{ millih. at } 15^\circ \text{ C.}$$

In 1914, it was thought desirable to check the measurements of the standard. The paraffin-wax coating over the primary windings was dissolved off with petrol, and the pitch and diameter of these were again measured in the Metrology Department. It was found that changes in the dimensions had taken place, but whether these were secular, or due to the waxing or subsequent treatment with petrol, it is impossible to say. The diameters of the two helices were about 5 parts in 100,000 greater, and the axial lengths were all about 1 part in 10,000 greater. The net result of these changes was to make the value of the mutual inductance about 7 parts in $10^6$ smaller. The value at 15° C., as determined from the second set of measurements, was

$$M_{15} = 10{\cdot}0177_8 \text{ millih.}$$

Owing to the uncertainties attaching to the effects of paraffin-waxing, it was decided not to wax either of the windings of the new standard. The windings can therefore be measured without trouble at any future time.

*Comparison.*

The two standards were compared by measuring each on a variable mutual inductometer. In order to avoid capacity effects a frequency of 10 cycles per second was used, at which frequency the sensitivity was about 3 parts in a million.



Digitized by Google

Observations were made alternately, first on one standard and then on the other. Balance on the new standard was, at first, found to be imperfect; this imperfection was traced and found to be due to metal parts in the levelling screws and sockets used to support and adjust the secondary winding. These were replaced by non-metallic parts, and, as a result, the balance was perfect, as far as could be judged on the galvanometer.

The results of four comparisons gave for the difference between the two standards the values

$$10{\cdot}6_2,\ 10{\cdot}7_0,\ 10{\cdot}6_3,\ 10{\cdot}6_0 \text{ microh.}$$

The mean difference at 16° C. may be taken, therefore, as

$$10{\cdot}6_4 \text{ microh. } (\pm 0{\cdot}05 \text{ microh.}).$$

The calculated value of the new standard at 17° C. is

$$M_{17} = 10{\cdot}0073_1 \text{ millih.}$$

If all the dimensions of a mutual inductance change in the same proportion the value of mutual inductance changes in that proportion also. The coefficient of thermal expansion of the marble of the new standard is + 0·000006 per 1° C.

The mutual inductance at any temperature "$t$" will therefore be

$$M_t = M_{17}\,[1 + 0{\cdot}000\,006\,(t - 17)].$$

The N.P.L. standard has the value at 15° C.

$$\text{(N.P.L.) } M_{15} = 10{\cdot}0177_8 \text{ millih.}$$

Correcting the value of the new standard to this temperature we have

$$\text{(New) } M_{15} = 10{\cdot}0071_9 \text{ millih.}$$

The difference between the two calculated values is $10{\cdot}5_3$ microh. The mean measured difference, as given above, is $10{\cdot}6_4$ microh.

This agreement between calculation and measurement may be considered highly satisfactory; it is closer than the various probable errors might lead one to expect.

It appears, therefore, that both these standards are accurate to within about 1 part in 100,000, in their values calculated from the dimensions as measured in terms of the N.P.L. standards of length.

Digitized by Google

# THE MEASUREMENT OF THE ELECTRIC INTENSITY OF RECEIVED RADIO SIGNALS

BY

J. HOLLINGWORTH, M.A., B.Sc., A.C.G.I., A.M.I.E.E.,
ASSISTANT IN THE ELECTRICITY DEPARTMENT.

Digitized by Google

## ABSTRACT.

The first part of the paper is devoted to a discussion of some of the principles on which the measurement of received signals is based, and the practical application of these principles under working conditions is considered.

The latter part describes a system recently developed at the National Physical Laboratory which differs in several details from previous systems. Its operation is described in detail, and some of the possible sources of error and inaccuracy are considered.

Digitized by Google

# THE MEASUREMENT OF THE ELECTRIC INTENSITY OF RECEIVED RADIO SIGNALS.

By J. HOLLINGWORTH, M.A., B.Sc., A.C.G.I., A.M.I.E.E., Assistant in the Electricity Department.

[Reprinted from the 'Journal of the Institution of Electrical Engineers', Vol. 61, 1923.]

## I. *Principles and their Practical Application.*

This problem is one of the most fundamental in radio-telegraphy and has received attention from large numbers of experimenters.

It is one which forces itself on everybody concerned with radio operation, as well as on those interested in the more scientific aspect of the subject. Many theories as to the cause of signal-strength variations have been suggested, and owing to the complexity of the circumstances involved it seems very unlikely that these variations will ever be expressed in a general mathematical form covering all cases; but the work of Austin has shown that, under specified conditions, a workable expression can be obtained.

For this purpose the primary need is a very large number of observations under known conditions, so that the first problem is the production of measuring apparatus the limitations of which are fairly definitely determined.

Prior to the introduction of the thermionic valve the instrumental difficulties in the way of experimenters were enormous. Beyond the small range available if direct-reading instruments were used, the only possibility of measurement was by a method involving some form of crystal detector; and, although the sensitivity of the latter is fair, the uncertainty and difficulty of calibration are a great handicap.

Such a method was indeed used by Austin* in his investigations which led up to the introduction of the Austin-Cohen coefficient; but for the longer ranges, which are the most interesting from the theoretical point of view, some more sensitive form of receiver is essential.

For measurements at very short distances a direct method is practicable. This usually consists of the insertion of a delicate thermal instrument, such as a Duddell thermo-galvanometer, into a tuned aerial or coil circuit the constants of which are known, the instrument being calibrated by direct current.

Such experiments, which have recently been considerably developed by Vallauri† and Pession,‡ serve a rather different purpose, their object being to determine the effective or radiation height of an aerial. For this purpose the measurements must be made at so short a distance from the aerial that the attentuation is negligible, with the

* 'Bulletin of the Bureau of Standards', vol. 7, p. 295, 1911.

† 'Radio Review', vol. 2, p. 77, 1921.

‡ *Ibid.*, p. 228.

Digitized by Google

result that the received signals are comparatively strong. In all cases the problem reduces to the determination of the current induced in an aerial system of known constants, from which either the potential gradient or the magnetic field at the receiving circuit can be calculated. Before the days of continuous waves the problem was further complicated by the decrement. In the resulting calculations the decrements of both the sending and receiving circuits are involved, and the determination of these alone is nearly as difficult as the original problem. With the advent of the triode with its possibilities of amplification and continuous-wave generation, the scope was very much enlarged and new methods became possible. As soon as an amplifier has to be used, however, it becomes necessary to employ some form of substitution method, because the absolute calibration of an amplifier is not at present practicable. This inevitably increases the chances of error, always very numerous, as is known by everyone who has attempted radio-frequency measurements; the result is that any method must appear to be more or less a compromise, and without extended trials and tests it is very difficult to give a decision as to which is the most satisfactory. In many cases practical considerations are of considerable weight, and from this point of view the following requirements must be borne in mind, in addition to all those of a theoretical nature :—

(*a*) The actual operation should be as rapid and simple as possible.
(*b*) Special transmission should be reduced to a minimum.
(*c*) The overall calibration should be effected as closely as possible under working conditions.
(*d*) The set should be moderately portable and capable of adaptation to varying conditions.

(*a*) and (*b*) are strictly practical questions; but they play a very important part in problems of this nature, for the case is rather different from that of a purely scientific measurement in which the whole operation is under the immediate control of the experimenter, who can repeat readings or vary his conditions as often as required. Even if the transmitting aerial be entirely devoted to the experiment its remoteness renders its detailed control difficult, and in many cases altogether impossible, with the result that the measurements must be made either on the routine transmission or on a short, special signal sent for the purpose. Observations seem to show that the first of these is not of much value except for very rough measurement, owing to the continual and irregular variations produced by the keying; and even if it be possible to obtain a reading of some sort at the receiving end, owing to these variations it is difficult to correlate it with the reading of the transmitting-aerial ammeter. If a special signal be used, working conditions demand that it should cause as little interference as possible with the ordinary routine.

This is the chief objection to a method devised by Lieut. GUIERRE,* in which a series of timed signals are required from the transmitting station, they being synchronized with

* 'Radio Review', vol. 2, p. 621, 1921.

Digitized by Google

the signals from the local oscillator. This method certainly enables various other serious difficulties to be overcome; but the organization required for an extended series of measurements on these lines would be very elaborate.

For the same reason it must be possible to obtain the readings rapidly; the set must be capable of being adjusted in working order before the commencement of the special signal, and fine adjustments must be reduced to a minimum. For instance, in the "URSI" signals the whole time available is two minutes, although the preliminary tuning-up of the set in the case of "UA" (Nantes) allows a certain margin for adjustments.

(*c*) and (*d*) are primarily questions of design, though (*d*) involves policy also. In this connection there are two alternatives. Either measurements of as high accuracy as possible may be made, involving a large amount of apparatus and a very highly skilled operator, observation points being, of course, very limited in number; or the apparatus may be in such a form as to permit of multiplication and distribution to a larger number of observers, in order to obtain simultaneous, though rather less accurate, readings. Considering the present state of our knowledge of atmospheric effects at the moment, it appears that the latter method is the one from which the most useful information may be expected, and as it represents approximately the policy of the Radio Research Board, under whose direction the whole of this work is being carried out, this advantage has been borne continuously in mind.

*Technical Considerations.*—The following methods are in use:—

(*a*) Telephone methods.
(*b*) Galvanometer methods.

Under the former heading may be included what is known as the shunted telephone method, in which comparative results are obtained by shunting the telephones until the signal just disappears; but considerable difference of opinion exists as to the accuracy of this method, and in any case it is not high. In all other cases the received signal is balanced, either audibly or visually, against a calibrated, local source of oscillations, from the reading of which the incoming intensity can be calculated in the required form.

Telephones have the advantage of simplicity in use. They can be used in places where a galvanometer is impracticable or undesirable, and are familiar pieces of apparatus. Owing to their power of audible selectivity they can be used when jamming is present, though the accuracy of results obtained under such conditions requires confirmation. They also allow of the easy selection and identification of the station, and messages can be read until the last minute before taking the observation.

On the other hand, an audible method is comparatively insensitive to small variations in intensity. The author has shown* that the minimum change in intensity which can be detected under favourable conditions is about 2 per cent. with spark signals. Experience tends to show that with continuous waves the figure is higher owing to the different quality of the note; and it is probable that 5 per cent. is the lowest which can safely

* 'Radio Review', vol. 2, p. 282, 1921.



Digitized by Google

be assumed for general working. With an audible method a heterodyne is necessary, and it has also been found that telephones have a considerable effect on the amplifier. This will be referred to later.

Galvanometer methods in general involve merely the replacement of the telephones by some form of D.C. indicating instrument. The chief advantage that they afford is greater sensitivity to small variations; but it has been found from experience that they offer several other advantages, among which is the possibility of keeping the signal and its variations under continuous observation. On the other hand, the signal cannot be read directly unless an Einthoven instrument be used, and the power of audible selectivity is lost.

*Fundamental Formulæ.*—Before proceeding to details it will be well to give the simple theory and the equations on which all substitution methods depend. Let I be the current at the base of the transmitting aerial, $\lambda$ the wave-length, and $d$ the distance from the receiving station, assuming propagation over a plane conducting surface through a perfect dielectric; then D, the vertical intensity of the electric field at the receiving station is given by:—

$$D = 120\pi \frac{Ih}{d\lambda},$$

where $h$ is the height of the ideal Hertzian half-oscillator which would produce the same effect as the actual transmitting aerial. It is usual to call $h$ the effective (or radiation) height of the aerial. Its value varies from about 50 per cent. to 75 per cent. of the actual height of the aerial, being dependent upon the form of the latter, the immediate surroundings, and also to a small extent upon the wave-length and various electrical factors. Now, if the potential gradient D be applied to an aerial of effective height $h_1$ and high-frequency resistance $R_1$, the electromotive force induced in it is $Dh_1$, and, consequently, if the aerial be tuned, the resulting current is $Dh_1/R_1$. In the case of a coil of area $a$, and number of turns $n$, the corresponding current is

$$2\pi Da \frac{n}{R_2\lambda},$$

$R_2$ being the high-frequency resistance of the coil (these results are based on the assumption that the wave front is vertical, whereas experience seems to show that this is frequently not the case).* If the wave front be tilted, coil reception will be unaffected, whereas reception by means of an aerial will be changed to an extent depending on the ratio between its horizontal and vertical dimensions. If the polarization be more complex, as often occurs when night effects are present, the intensity of reception in both coil and aerial will be varied, and in such cases the intensity measured has really the value of the equivalent, plane, polarized wave, rather than that of anything possessing an actual physical existence.

* T. L. Eckersley, 'Radio Review', vol. 1, p. 422, 1920.

Digitized by Google

The usual method of calibration is to disconnect the aerial system at intervals and to connect the receiving set to a non-radiating aerial which has the same constants as the receiving aerial and contains a calibrated mutual inductance coupled to a calibrated local oscillating circuit; the latter is then adjusted until equality of signal strength is obtained.

The applied voltage is deduced from the known constants of the local circuit; and, from the formula given above, the potential gradient is derived. This method involves the equalization of the constants of the main and dummy aerials, and the accuracy of this adjustment will be one of the chief factors determining the accuracy of the result. In addition, on switching over to the dummy aerial, any jamming previously present will disappear, thus introducing another uncertain factor into the physiological balancing process. The question of jamming by an extremely powerful station of sufficiently different wave-length to be outside the limit of audibility is one which requires experimental investigation; but it seems likely that under such circumstances, unless the characteristic curve of the receiver can be taken as a perfectly straight line, modification of the position of balance will result.

Unfortunately, with the multiplication of high-power intercontinental stations, the above is becoming a very serious factor in working on weaker signals. These difficulties are largely overcome by the method used by Lieut. GUIERRE, in which the ordinary aerial is used for balancing, the distant transmission being so controlled that its periods of silence synchronize with the working period of the local oscillator. The objections to this system have been referred to above.

## II. *The N.P.L. System.*

*N.P.L. Apparatus.*—The following apparatus has recently been constructed at the National Physical Laboratory with the object of undertaking measurements of this kind. A galvanometer method is used, the idea being to obtain greater sensitivity than is possible with telephones. In general principle it follows standard lines, but it exhibits several important modifications. Its chief features are :—

(*a*) No heterodyne required.
(*b*) No metallic screening necessary.
(*c*) Only one oscillating circuit in use at a time.

The signal from the tuned receiving circuit is applied in the usual way to a multi-valve resistance-capacity amplifier. A galvanometer is connected in the anode lead of the last valve and is made to give zero deflection for the normal anode currrent, a 2-volt cell and adjustable resistance across the galvanometer being used for this purpose. The incoming signal polarizes the grid of the last valve and in this way reduces its anode current, the reduction being indicated by the deflection of the galvanometer.

This is, of course, a standard method adopted by many workers. For calibration purposes the tuned receiving circuit is broken and totally disconnected from the amplifier,



Digitized by Google

which is then joined to the local oscillator through a calibrated untuned coupling coil. The oscillator is next adjusted until the same deflection is obtained as with the signal.

The high-frequency resistance of the receiving circuit is also measured under actual working conditions by the movement of a switch. From this stage the calculation proceeds as before. The method differs from the normal one only in the use of an untuned circuit for calibration and in the internal design of the local oscillator; but in order to obtain reliable results great attention must be paid to a large number of small details.

### *General and Constructional Details.*

(*A*) *The Aerial System.*—The method can be applied equally well to an ordinary aerial or a closed coil. For convenience and portability a closed coil has been adopted, though this is open to several objections, chief among which are the low absorption, especially on long wave-lengths, and the antenna effect. The former is due to the fact that with a vertical potential gradient D the E.M.F. produced in an aerial is $Dh$, whereas with a coil it is $2\pi Dna/\lambda$. On the other hand, the directive property of a coil is often a valuable asset

With regard to antenna effect, the behaviour of the whole coil as an aerial with respect to earth is an old and serious problem. In directional work it is one of the chief objections to the use of a plain revolving coil; but in this case one is working on the minimum of the coil E.M.F., so that the antenna effect is unmodified. In measurements where, of course, the maximum position of the coil is used, it only appears in conjunction with the coil E.M.F., but even then it requires consideration. In theory, since it flows in an untuned path it should be 90° out of phase with the true signal, provided the latter be accurately tuned. Actually, it may not be exactly 90° out of phase, and in this case it would have a component in phase with the signal. Now the characteristic feature of antenna effect in directional work is the great bluntness of the minimum, no sharp zero being discoverable. This effect can be caused only by the out-of-phase component, as the effect of the component in phase with the signal cannot be to blunt the zero but only to shift its position, since the antenna effect does not change sign as the coil passes through its zero position, whereas the coil E.M.F. does. Hence the well-known flat minimum proves that antenna effect has at least a considerable component 90° out of phase with the main signal. In the present case it can also be shown that any component in phase with the signal is small. Consider two positions of the coil 180° apart and not too near the maximum, in which case a signal of fair intensity is obtained. If the antenna effect be exactly 90° out of phase with the main signal the total E.M.F.'s in these two positions will be equal; but if the antenna effect have a component in phase with the signal the total E.M.F.'s in these two positions will not be equal, as the coil E.M.F. changes sign with the rotation through 190°, whereas the antenna E.M.F. does not. Hence the equality of the deflections at any two points 180° apart can be taken as a sign that any antenna effect present is 90° out of phase with the main signal.

Digitized by Google

To verify this, an actual test was made on the Nantes "URSI" signal. The coil was set about 30° from its maximum position, so that a fair signal was obtained, but one which at the same time would be appreciably affected by the antenna E.M.F. A reading of the galvanometer was taken, and the coil was swung rapidly through 180°, when it was found that the galvanometer reading was unaltered. Other tests seem to indicate that the value of antenna effect present on Croix d'Hins (23,450 m.) is about 10 per cent. of the true signal, but accurate measurement on a station is difficult, owing to keying variations; and, of course, the effect cannot be obtained from a local continuous-wave buzzer.

If the above antenna effect be 90° out of phase with the main signal, the actual signal strength will be only $\sqrt{(100^2 + 10^2)}$, *i.e.*, 100·5 approximately, an increase of only half of 1 per cent., which can be safely neglected.

It also seems likely that the absence of an operator and telephones tends to reduce the antenna E.M.F. In this connection the following facts have been noted repeatedly :—

The anode circuit of the last valve contains a double-pole throw-over switch, by means of which it can be connected either to the galvanometer or to the primary of a telephone transformer. When listening-in with the telephones it is often possible to hear, in addition to the station sought, several stations on different wave-lengths, this being effected by correct adjustment of the heterodyne only; but, on changing over to the galvanometer and re-tuning, the required signal comes in with a pure resonance curve having zeros on either side.

Also, when working on the galvanometer, the mere touching of the telephones will produce large variations in the deflection, even though the telephones are isolated from the amplifier both by a transformer and by a double-pole ebonite-insulated switch. Moreover, the amplifier often oscillates violently when the telephones are being used, whereas with the same adjustments it is quite stable on the galvanometer. The above results seem to show that if care be taken with the design and arrangement of the apparatus, the effect of antenna E.M.F. is not serious.

The coil now in use consists of a wooden box frame 5 feet square, wound with 79 turns of 7/26 S.W.G. copper wire spaced $\frac{1}{8}$ inch apart. This is sectionalized by a three-way switch so that either 29, 50, or 79 turns can be used, the coils not in use being completely cut out. With suitable condensers the range covered is from 3,000 to 25,000 m., making allowance for the fact that for work of this type it is essential that a coil should not be worked near its natural wave-length.

Probably, for the measurement of very weak signals, a coil of greater area would be advantageous, but of course it would be less portable.

(*B*) *Amplifier.*—In general this consists of a multi-valve resistance-capacity amplifier of the usual type containing, however, several special arrangements.

Resistance-capacity coupling was adopted for three reasons :—

(*a*) *Larger Effective Wave-Length Range.*—A transformer amplifier, though more efficient over a limited range, cannot be made to cover a large one without the use of interchangeable

Digitized by Google

transformers; and generally it has certain points at which it is very liable to oscillate. As the set is not designed to work below 3,500 m., the question of the inefficiency on short waves of such an amplifier does not arise.

There being no heterodyne effect, audio-frequency amplification is inadmissible.

(*b*) *No Screening required.*—In measurements such as these it would be essential to screen all coils and transformers thoroughly in order to avoid inductive effects from outside stations or from other parts of the circuit, as such inductive effects might be completely altered when the change-over was made from outside station to calibrating circuit.

(*c*) *Stability.*—In dealing with measurements it cannot be too strongly emphasized that the prime necessity is stability of the apparatus. Sensitivity, amplification, and even selectivity must all give place to stability. The amplifier must be kept well away from regeneration, instead of, as is usual, working as near this point as possible. Of the short time available for taking a measurement there is none to spare for fine amplifier adjustments; and, for example, a six-valve set working inefficiently, but stably, is far preferable to a "super-efficient" three-valve pattern. (A great deal of work is being done in order to get the most suitable arrangement combining fair amplification with reliable stability and ease of adjustment, the details of which are rather far from the subject matter of the present Paper.)

The above three reasons have led to the selection of a resistance-capacity amplifier, though under other conditions it is possible that one of another type would be more suitable.

The chief objection to an amplifier of this type is the poor working on low wave-lengths, *i.e.*, with small values of the tuning condenser. This is a side issue of the more important fact that every valve circuit possesses an effective impedance, which forms a load on the oscillating circuit, and so reduces its effective voltage considerably.

This has been discussed in detail by the author in another Paper,* in which it is shown that if the amplifier be considered as equivalent to a high resistance $R_1$ shunted across the condenser (this is not strictly accurate, but avoids considerable mathematical complication) the effective resistance of the equivalent simple circuit is $R + \omega^2L^2/R_1$, R being the ordinary high-frequency resistance of the circuit. Now, under ordinary conditions, with a large inductance and small condenser, $\omega L$ is large, so that it frequently happens that the first term is entirely swamped by the second; and as long as this holds, it actually pays to reduce the number of turns on the receiving coil and to increase the condenser value, since the loss of received energy due to the decreased area-turns is more than compensated for by the reduction in apparent resistance. For instance, the actual deflections of the galvanometer on a fixed signal of wave-length 9,100 m., using the three sections of the coil in turn, were of the same order; whereas the equivalent resistances were 6·5, 36 and 102 ohms, the corresponding D.C. coil resistances being 3·1, 9·0, and 12·1 ohms respectively. It appears from this that any measurement of high-frequency

* 'Wireless World and Radio Review', vol. 10, p. 351, 1922.

Digitized by Google

resistance should include the valve in working condition, especially when the ordinary circuit resistance is low.

The special circuits in the amplifier are confined to the last valve (Fig. 1). Instead of the usual telephones a sensitive galvanometer and shunt are connected in the anode circuit, and across them is placed a 2-volt accumulator with such an arrangement of resistances that the normal anode current can be balanced; the deflection is obtained by the departure from the normal, and the whole is shunted by a 5-$\mu$F condenser. Under these circumstances the effect of atmospherics appears to be small and, as a matter of fact, excellent results have been obtained during a thunderstorm.

The last valve is also run off a separate battery in order to minimize the creep of the zero due to the gradual fall of accumulator voltage on load; and for the same reason the filament resistance is a fixed one of the iron-in-hydrogen pattern. With these precautions, provided that the accumulator be in reasonably good condition, the creep of the zero is negligible except when working at the extreme limit of sensitivity of the galvano-

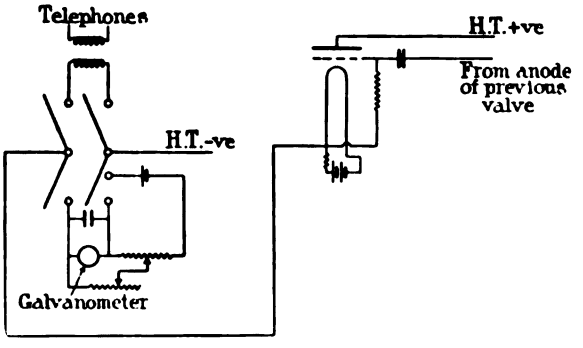


Fig. 1. Connections of the last valve.

meter, a proceeding undesirable for many reasons. A double-pole throw-over switch is also provided so as to allow of the use of telephones for listening-in purposes.

In order to obtain satisfactory results with a balanced system of this type it is essential to use an accumulator and not a primary battery, and the resistances should be of a robust, stud pattern. In fact, such resistances should be used everywhere for work of this nature, as the slightly decreased elasticity, as compared with that obtained in the ordinary sliding, variable type, is more than compensated for by the increased steadiness and reliability.

Between the coil and the amplifier is the usual arrangement of tuning condenser and a throw-over switch (Fig. 2).

The latter connects the amplifier terminals either to the tuned receiving circuit or to the untuned calibrating coil, and by means of two auxiliary contacts the oscillating circuit is completely broken when the switch is in the second position. By a slight rearrangement of connections this switch can be made to introduce a dummy aerial when an audibility method is being used.

*The Calibrated Local Oscillator.*—As has been mentioned above, the local source is

Digitized by Google

connected to the amplifier by an untuned coupling circuit. In this way it is possible to dispense entirely with metallic screening, since there is never more than one oscillating circuit in action at a time.

Screening involves bulky and inconvenient apparatus, since the control must be either inside the screening box or brought out in a very careful manner, and the effectiveness of the operation is always open to doubt. SMITH-ROSE has shown* that in the immediate neighbourhood of a powerful amplifier the most elaborate screening precautions must be taken in order to ensure perfect protection, and that the difficulty increases with the wave-length.

On the other hand, this method involves the necessity of actually measuring the effective high-frequency resistance of the receiving system at each observation; but the set is so arranged that this can easily be done, and the great advantage results that a very severe check on the accuracy and correct working of the apparatus is provided.

In the ordinary systems a dummy aerial, if used, must have the same constants as the receiving system so that the high-frequency resistance problem, though latent, is still present.

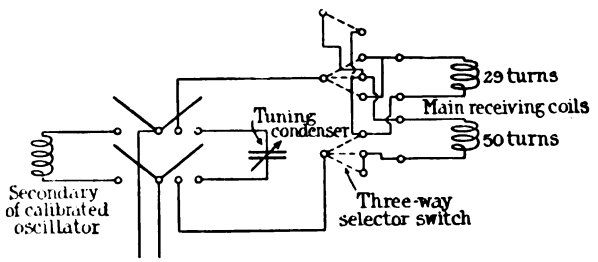


Fig. 2. Tuning condenser and throw-over switch.

Methods which introduce the calibrating oscillation into the receiving aerial avoid this difficulty, but in this case the calibrating cannot be carried out until the transmitting station has stopped, whereas both "UA" and "LY" carry on with their routine work after the special signal.

The oscillator itself has several special features. In the ordinary construction of such oscillators a normal continuous-wave generator is used with a high-pressure supply of 50 to 60 volts, so that the oscillating current is large enough to be measured on a direct-reading instrument. A few turns of the oscillating circuit are led through the primary of a variable mutual inductance; but this arrangement involves the screening of the main part of the oscillator from the mutual inductance. Also it has been found that with the use of such comparatively high voltages there is a danger that an appreciable but indefinite amount of energy may reach the latter valves of the amplifier owing to capacity coupling.

If, however, the whole of the oscillating inductance be used as the primary of the mutual the secondary can be mounted some distance away from it, and this increase in distance and the reduction of the high-tension voltage minimize the risk of capacity coupling.

* 'Proceedings of the Physical Society of London', vol. 34, p. 127, 1922.

Digitized by Google

This method involves actual measurement of the mutual inductance under working conditions, but this is practically essential in any case and is not difficult; whilst, with the control which will be described shortly, it is not necessary to rotate the secondary.

It is impossible to lose sight of the fact that in the normal oscillating circuit the current is not the same throughout. Prof. HOWE has proved this in the case of a simple circuit; and experiments have shown that in an actual oscillator, due to the presence of the reaction coil and other apparatus, the current distribution is much modified from the theoretical form. It is therefore necessary to take a definite point on the circuit as the point of reference and to express everything in terms of the current at this point. This may involve a variation of apparent mutual inductance with wave-length; but as the mutual inductance must be determined experimentally in every case, the net result is merely to necessitate a slight wave-length correction in the apparent mutual inductance when working in the neighbourhood of the natural frequency of the oscillator.

A thermo-junction and galvanometer are connected, therefore, at any convenient point in the oscillating circuit, and all measurements are made with reference to this point. The high-tension voltage is controlled by means of a stud potentiometer so far as fine adjustments are concerned, coarse variations of the secondary E.M.F. being obtained by the use of a selector switch and a set of separate secondary coils. The instrument has been so designed that it can be fitted in a screened box for use with an audibility measurement, experiments having shown that, if the galvanometer have an iron case and be connected to the oscillator by screened leads, the leakage of oscillations is too small to cause trouble.

The secondary of the mutual inductance consists of several coils containing various numbers of turns. As the high-pressure control can be arranged to give a variation of slightly over two to one it is possible, by having several separate secondaries each containing about twice as many turns as the last, to get a very large variation of secondary E.M.F. and to retain the same percentage sensitivity on each range, the latter being an equally important advantage. The present range on 9,000 m. is approximately from 5·0 m.V to 0·05 m.V.

*Calibration of Receiving Set.*—The formula for the results is derived as follows:—

From the second equation in section I above we see that the current in an oscillating circuit with potential gradient D

$$= \frac{D \times 2\pi an}{R\lambda}.$$

Hence, the resonance volts on condenser, *i.e.*, volts applied to amplifier

$$= \frac{D \times 2\pi an\sqrt{(R^2 + \omega^2 L^2)}}{R\lambda}.$$

Under ordinary conditions $\sqrt{(R^2 + \omega^2 L^2)}$ may be replaced by $\omega L$, therefore

$$\text{resonance volts} = \frac{2\pi an D\omega L}{R\lambda} \quad \ldots\ldots\ldots \quad (1)$$



Digitized by Google

Since the local oscillator is then adjusted so as to give the same deflection as the incoming signal, we must have—

Resonance volts = volts applied to amplifier by local oscillator,

= $\omega I_0 M$, where $I_0$ is the current in the local oscillator, and M the mutual inductance between it and the coupling coil.

Hence

$$\frac{2\pi anD\omega L}{R\lambda} = \omega I_0 M. \quad . \quad . \quad . \quad . \quad . \quad . \quad . \quad . \quad . \quad . \quad (2)$$

Therefore

$$D = \frac{I_0 MR\lambda}{2\pi anL},$$

M being the appropriate value of the mutual inductance for the particular wave-length and secondary coil employed.

In connection with the local oscillator the following important point has been found:— Investigations on an oscillating circuit of this form showed that the oscillating current could be expressed in the form $I = A(\lambda + B)(V + C)$, where $\lambda$ is the wave-length, and V the high-tension voltage, A, B, and C being constants.

For some time this law was used to determine the current in order to avoid the use of a thermal measuring instrument, but it was found that the ageing of the valve was liable to affect the values of the constants slightly. It is quite possible that a valve could be artificially aged for this purpose, in which case a simple and rapid method of current measurement would result, but, pending the outcome of experiments to this end, a thermal instrument has been adopted. The immediate importance of the formula lies in the fact that in all cases B appears to be small compared with $\lambda$.

Hence, if $I = A(\lambda + B)(V + C)$

$$\omega IM = A(\lambda + B)(V + C)M \times 3 \times 10^8/\lambda \times 2\pi,$$

*i.e.*, the term involving $\lambda$ is $(1 + B/\lambda)$.

Now, for the shortest $\lambda$ employed, $B/\lambda$ was of the order of 0·1, so that even a 10 per cent. change in the wave-length adjustment of the local oscillator only produces a change of about 1 per cent. in the secondary voltage. Hence, accurate tuning of the local calibrated oscillator is unnecessary; it can be used to heterodyne and to read the incoming signal, and then be used without further adjustment for calibration. This effects a valuable saving of time at a period when every second is of importance.

*Determination of* M.—As has been mentioned above, M is not necessarily the mutual inductance measured by low-frequency methods, but the mutual inductance at working frequency referred to the current at a particular point on the oscillator. It is measured as follows:—

The oscillator is connected as in Fig. 3, the Duddell thermo-galvanometer with an appropriate heater being in the secondary circuit, and an ordinary thermo-junction and

Digitized by Google

galvanometer in the oscillating circuit. The primary voltage must generally be higher than the usual value, in order to give a readable current in the secondary. It is assumed that on any given wave-length the current distribution in the coil is unaltered by this increase in voltage, and this seems probable as there is no grid condenser to alter the potential of the reaction coil. Also, the curve for M (Fig. 4) shows that that function has a practically constant value for the higher wave-lengths, so that the variation of distribution must be small. The resistance and impedance of the secondary are measured by ordinary methods, since its natural frequency is so high compared with those under consideration as to have no measurable effect. In addition, the secondary is of a form in which the increase of resistance with frequency is small, and as a high-resistance heater is generally required in the thermo-galvanometer this variation can be neglected.

Owing to the use of the untuned coupling it is necessary to measure the high-frequency resistance of the circuit for each observation. While this introduces an apparent com-

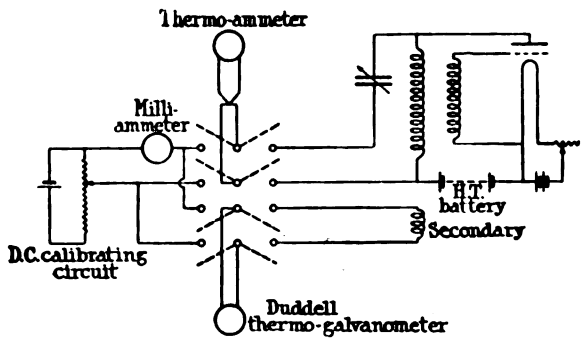


Fig. 3. Diagram showing calibration of oscillator.

plication into the process of taking a reading, it has several very definite advantages, these being :—

(1) No assumptions of uncertain accuracy are made.

(2) A very severe check on the correct working of the apparatus is provided for each reading.

(3) Owing to there being no balancing circuit the number of turns on the coil can be varied at will. This is of value if it is required to take observations of stations on widely different wave-lengths with only a short interval of time between them. In addition, it is sometimes advantageous to have control of the resistance.

As before mentioned, the variable factor in each case is the amplifier itself, owing to its power absorption, and it seems likely that this property must persist even if filter circuits are used, as the power to operate the amplifier must be derived from the receiving circuit either by direct conductivity or by induction. The effect of the amplifier depends, of course, on its adjustment, and it is possible to make the loss excessively small or even negative, so obtaining regeneration.



Digitized by Google

For measurement purposes, however, either of the latter conditions is liable to produce great instability; a slight change in the strength of the incoming signal may completely alter the amplifier characteristics, and where accuracy is required it is far safer to eliminate any regenerative possibility.

In general, the more stable the amplifier the higher its power absorption, so that it is necessary to consider both of these factors; but it must be borne in mind that comparatively high power-absorption does not necessarily mean poor amplification, so that the critical factor is often not sensitivity but selectivity, which brings back the old problem of interference. The absence of a heterodyne destroys the power of audible selectivity, though the accuracy of results obtained when this power has to be exercised requires further investigation.

There is but little difficulty in reducing the total resistance of the circuit to about 10 ohms, which gives a fair degree of selectivity, and the case only becomes serious when an attempt is made to measure a weak station with a high-power station very much nearer to the place of measurement. This can be best illustrated by drawing a tuning curve.

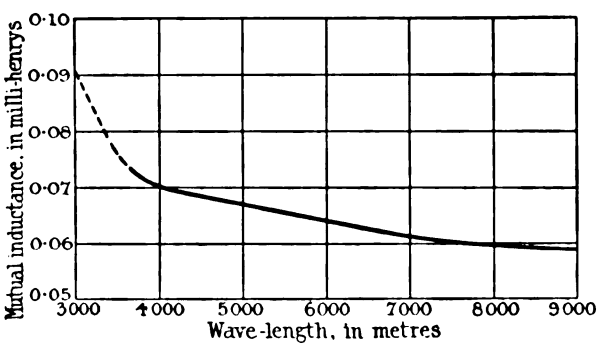


Fig. 4. Value of mutual inductance in calibrated oscillator.

Take, for instance, the case of "GBL" which, with 180 amperes in the aerial, at 8,350 m. may be expected to give an E.M.F. of 400 $\mu$V in the coil at Teddington. Assuming the resistance of the receiving circuit to be 20 ohms and its inductance 10,500 $\mu$H, fig. 5 gives the lower part of the tuning curve, neglecting any antenna effect. It will be seen, therefore, that for a station giving an E.M.F. of 40 $\mu$V, if a measurement of the latter be required to an accuracy of even 20 per cent., the closed range of wave-length is from 7,600 m. to 9,100 m. approximately. Now, suppose a similar measurement to be made by the audibility method. If the heterodyne note of Leafield be just inaudible the small station would give a good working note if its frequency differed from that of Leafield by about 3,000, *i.e.*, if its wave-length were 9,120 m. But at this wave-length the high-frequency E.M.F. of Leafield would be 50 per cent. of that of the incoming small signal, so that unless it were certain that the amplifying power of the high-frequency side of the amplifier were unaltered by a 50 per cent. increase in applied E.M.F., an error would be produced when the circuit was changed over to the calibrating source, in which no such extra E.M.F. was present.

Digitized by Google

Except under such conditions it is an advantage to use a circuit of higher resistance as the tuning is far less critical. Until a galvanometer be used one does not appreciate how critical is the tuning of a circuit or even moderately high resistance, the reason for which being, of course, the comparative insensitivity of the telephones to small changes in intensity. For instance, in fig. 5 a variation of 10 per cent. in intensity is caused by a variation of 0·25 per cent., *i.e.*, 4·5 $\mu\mu$F, in the capacity of the condenser. It is also important to know what error is likely to be produced if accidentally the receiving circuit be slightly out of tune with the signal under measurement. This is most likely to occur for small values of the tuning condenser where the adjustment is finer. Considering, however, the coil data given above, it can be shown by calculation that an error of 1 per cent. in the condenser value, though it reduces the actual galvanometer deflection

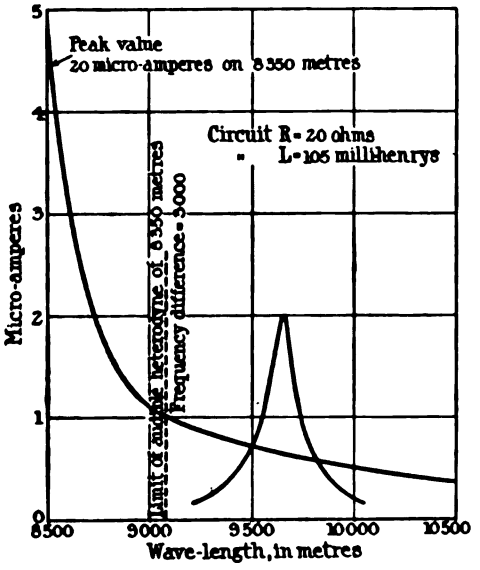


Fig. 5. Tuning curves.

to about 45 per cent. of its maximum value, only reduces the measured value for the potential gradient by 5 per cent.

The actual measurement of resistance is made as follows:—The coil is fitted with a five-way switch by which resistances of 7·46, 18·3, 39·9, and 78·2 ohms can be inserted in the oscillating circuit. A signal, either from a local source or from outside, is tuned, and readings of the galvanometer are taken for all five positions of the switch. The voltages corresponding to these readings are then measured by the local calibrating circuit, the resistance being calculated in the usual way.

From these results very important information can be obtained. Of course, if the resistance of the circuit be unusually high or exceptionally low, the extreme values of the inserted resistance may not give accurate results, but the group has been so chosen as to be suitable for average working. In a particular case the following results have actually been obtained:—By using the five steps and working out the results of individual pairs

Digitized by Google

the following series of values for the high-frequency resistance of the circuit was found: 22·3, 22·9, 22·75, 22·35, 23·8, 23·2, 22·4, 22·3, 21·5, the average of these being 22·6 ohms; the above values are as consistent as may be expected from measurements of this nature under ordinary conditions.

Their close agreement shows the truth of the following statements:—

(*a*) The effective resistance of the amplifier is independent of the signal strength.

(*b*) Since the calculation of these results involves the figures obtained for the various mutual inductances of the secondary coils, these figures must be accurate.

(*c*) Any direct electrostatic coupling to the amplifier is negligible, since the constants in (*b*) were obtained with a thermo-galvanometer and not by means of the amplifier.

In connection with (*a*) it is interesting to note that if the amplifier be forced, this series breaks down abruptly, showing that at a certain point self-oscillation commences. Cases occur in which the values obtained with the larger resistances in series are quite normal, but an abrupt variation occurs when the added resistance is cut out. There appears some evidence in support of the idea that the amplifier resistance varies with the signal strength when close to this state.

A series of this nature is by no means exceptional, but, of course, in order to obtain such a one reasonable care must be taken to get everything into a steady state. In actual working on a definite routine it is seldom necessary to take the entire series, as a single reading is sufficient if it be known that the apparatus is working stably. It is also possible in the case of a special signal to measure the resistance by means of a local source immediately before the transmission commences. This will remain constant throughout the signal, if the duration of the latter be not too great, so that the whole time of reception can be devoted to watching and recording the momentary variations.

It appears from these results that the slight extra complication involved in measuring the resistance is more than compensated for by the very severe test applied to the apparatus in the process; and a definite indication of the accuracy of the result is obtained.

In fact, it appears from experiment that, provided the amplifier be in a stable state, its equivalent resistance on any given wave-length is definitely determined by the adjustments, filament current, high pressure, etc., and that by the measurement of these the total resistance of the coil can be foretold without actual measurement, each time an observation is taken. Of course, owing to possible slight changes in valves, and leaks, it would not be safe to dispense entirely with resistance measurement after having determined it once; but if in the course of a series of observations, through unforeseen circumstances a few measurements of resistance are missed, the values can be obtained from other readings in which the state of the amplifier was the same.

In order to verify the fact that the result was independent of the particular adjustment of amplifier, a local oscillator was set up and its intensity measured. The amplifier was then considerably altered, *i.e.*, the number of valves, high pressure, and filament current were changed, and the local source was measured again. The results differed

Digitized by Google

by less than 1 per cent. The same effect has also been noticed when measuring the "URSI" signals, but, of course, in this case since 24 hours have to elapse between successive readings it is impossible to guarantee that the incoming signal remains constant to this degree of accurcay.

MEASUREMENTS of the URSI Signals from Nantes (UA) made at the National Physical Laboratory.

| Date. | Potential gradient μV/m. | Effective R of set. | Date. | Potential gradient μV/m. | Effective R of set. |
|---|---|---|---|---|---|
| 1922 | | ohms. | 1922 | | ohms. |
| October 25 | 1,100 | 10·5 | December 1 | 1,670 | 17·7 |
| „ 26 | 1,980 | 14·0 | „ 4 | 3,200 | 20·8 |
| „ 27 | 2,190 | 23·0 | „ 6 | 2,310 | 21·0† |
| „ 31 | 1,660 | 16·6 | „ 6 | 2,030 | 21·0† |
| November 1 | 2,100 | 9·8 | „ 7 | 2,050 | 19·4 |
| „ 2 | 4,260* | 14·7 | „ 11 | 1,600 | 21·3 |
| „ 10 | 2,720 | 12·6 | „ 12 | 1,800 | 18·0 |
| „ 14 | 3,270 | 19·4 | „ 14 | 1,730 | 21·7 |
| „ 15 | 1,750 | 9·3 | „ 18 | 1,650 | 14·8 |
| „ 16 | 2,000 | 16·7 | „ 20 | 1,010 | 10·0 |
| „ 17 | 2,250 | 19·2 | „ 21 | 1,360 | 13·0 |
| „ 20 | 1,040 | 30·0 | „ 22 | 2,269 | 15·8 |
| „ 21 | 1,900 | 23·7 | 1923 | | |
| „ 22 | 1,795 | 42·5 | January 3 | 1,720 | 20·0 |
| „ 27 | 2,440 | 16·0 | „ 4 | 2,200 | 21·2 |
| „ 28 | 1,760 | 16·4 | „ 5 | 1,460 | 17·7 |
| „ 29 | 1,420 | 21·4 | „ 8 | 840 | 6·3 |
| „ 30 | 1,950 | 17·6 | „ 10 | 3,100 | 28·0 |

* Obviously an abnormal day. "MSK" (Moscow) was heard loudly on a small set on which it is normally inaudible during the day. Daylight variations of bearing were also reported as excessive.

† An abrupt change of intensity occurred in the middle of the signal.

NOTE.—These figures are the actual readings obtained and are not corrected to the standard aerial current of 180 A for purposes of comparison. The variations are in most cases not more than 2 or 3 per cent.

On the basis of the Austin-Cohen formula the theoretical value of the gradient at the N.P.L. with 180 amperes in the aerial should be 1,760 μV per metre.

Wave-length 9,000 m. Time of transmission 2.15 p.m.

*General Observations.*—The foregoing is primarily a description of the development of a system of signal-strength measurement. Time has not yet permitted of an extended series of actual observations, nor of a critical test against any other method. It is hoped to carry out both of these in the future, as until this is done it is impossible to make any very definite comparisons or to indicate which system is most suitable for any given

Digitized by Google

conditions. It is also hoped to obtain useful information by the incorporation of an Einthoven string galvanometer so as to obtain photographic records of signals, which will assist in deciding another very important question, namely, within what limits of intensity and frequency an average transmission is liable to vary.

MEASUREMENT of the URSI signals from Rome (IDO) made at the National Physical Laboratory.

| Date. | Potential gradient μV/m. | Effective R of set. | Date. | Potential gradient μV/m. | Effective R of set. |
|---|---|---|---|---|---|
| 1922 | | ohms. | 1923 | | ohms. |
| December 12 . . . | 366 | 22·1 | January 11 . . . . . | 282 | 18·8 |
| „ 13 . . . | 455* | 22·0 | „ 15 . . . . . | 220 | 12·5 |
| „ 14 . . . | 210 | 18·2 | „ 16 . . . . . | 383 | 13·6 |
| 1923 | | | „ 18 . . . . . | 354 | 12·5 |
| January 4 . . . | 257 | 5·4 | „ 19 . . . . . | 88 | 2·0 |
| „ 5 . . . | 275 | 1·7 | „ 22 . . . . . | 270 | 11·3 |
| „ 8 . . . | 353 | 20·0 | „ 23 . . . . . | 341 | 13·5 |
| „ 10 . . . | 273 | 5·1 | „ 26 . . . . . | 277 | 13·2 |

* Poor reading.

Aerial current 100 A.

On the basis of the Austin-Cohen formula the theoretical value of the gradient at the N.P.L. is 153 μV per metre.

Wave-length 10,800 m. Time of transmission 5 p.m.

These investigations were carried out for the Radio Research Board, and the author has to acknowledge his indebtedness to the members of Sub-Committee A of this Board, detailed below, for much useful advice and criticism throughout the experiments.

*Members of Sub-Committee A of the Radio Research Board.*—Dr. E. H. RAYNER, M.A. (*Chairman*). Admiral of the Fleet Sir HENRY B. JACKSON, G.C.B., M.C.V.O., F.R.S. (*Chairman of the Board*). Prof. G. W. O. HOWE, D.Sc., Prof. E. H. BARTON, D.Sc., F.R.S., Mr. D. W. DYE, B.Sc., Major J. ERSKINE-MURRAY, D.Sc., Prof. H. M. MACDONALD, F.R.S., Mr. F. E. NANCARROW, Mr. J. HOLLINGWORTH, M.A., B.Sc.

Also he wishes to expresss his indebtedness to his assistant, Mr. H. A. THOMAS, M.Sc., for his valuable aid in all the latter portion of the experimental work.

Digitized by Google

# ON THE MEASUREMENT OF AMPLIFICATION GIVEN BY TRIODE AMPLIFIERS AT AUDIBLE AND AT RADIO FREQUENCIES

BY

F. E. SMITH, F.R.S.,

SOMETIME SUPERINTENDENT OF THE ELECTRICITY DEPARTMENT,

AND

THE LATE R. C. NAPIER, M.A.,

FORMERLY ASSISTANT IN THE ELECTRICITY DEPARTMENT.

Digitized by Google

## ABSTRACT.

The measurement of amplification at audible frequencies which is described is a mutual inductance method, the alternating voltage applied between the filament and grid of the first valve being varied by quickly changing the connections to an air-core transformer having two secondaries at right angles, which secondaries are capable of rotation so as to give any desired ratio of the mutual inductances between the primary and the respective secondaries. The source of alternating voltage is a triode circuit having such capacity and inductance in the oscillatory portion as to give currents of a sonic frequency. The standard intensity of note is such as to enable signals to be read with comfort, and is obtained by adjustment of the source of alternating current. The first note is obtained when the telephone is in the anode circuit of an auxiliary valve, and the second when the telephone is transferred to the anode circuit of the last valve of the amplifying set, changes also being made in the applied alternating voltage, and in the connections between the valve circuits. All these changes are brought about by a six-brush switch in a fraction of a second, so that readings are quickly obtained.

The method is compared with a modifiation of the shunted telephone method, and very good agreement is obtained when the amplifying values are comparatively low. For values of a high order such as 200, it is shown that the two methods are not likely to give the same results, the method described in the Paper being the better one.

In the measurement of amplification of a radio-frequency amplifier an undamped train of oscillations is broken up into groups of sonic frequency by shunting intermittently the condenser in the oscillatory circuit by an inductance of low resistance. A sonic train of oscillations is thus produced.

The receiving circuit is very similar to that used for audible frequency amplification, but the measurement of the amplifying power is made by quickly varying the current at the source, and not by a change of mutual inductance between the two circuits.


Digitized by Google

# ON THE MEASUREMENT OF AMPLIFICATION GIVEN BY TRIODE AMPLIFIERS AT AUDIBLE AND AT RADIO FREQUENCIES.

By F. E. SMITH, F.R.S., sometime Superintendent of the Electricity Department, and the late R. C. NAPIER, M.A., formerly Assistant in the Electricity Department.

[Reprinted from the 'Proceedings of the Physical Society of London', Vol. 32, 1920.]

## 1. *Measurement of the Amplification given by Audible Frequency Amplifiers.*

Triode valves are used for a variety of purposes, but more especially as amplifiers of radio-frequency oscillations, as rectifiers of these oscillations, and as amplifiers of the resulting groups of rectified oscillations, these groups being of audible frequency. In ordinary telephony, triode valves are desired to be amplifiers only, as any rectification leads to distortion.

The quantitative measurement of the amplifying powers of valves is a matter of considerable interest. In the early days of the war, with a three-valve set, voltage amplifications of many thousands and even of a million times were often spoken of, but never met with in our experience.

A set of four valves with their associated transformers is shown in fig. 1. In many such sets the first valve is a rectifier and partial high-frequency amplifier, the other three valves being audible frequency amplifiers. Iron-core transformers are then used between the first and second, the second and third, and between the third and fourth valves. In the figure, the telephone is intended to be in series with the anode of the fourth valve at $D_1D_2$; but sometimes a transformer is interposed, the primary of which is in the anode circuit and the secondary is in circuit with the telephone. For amplification of audible frequencies only, an additional iron-core transformer is used between the source and the grid of the first valve. This is shown in the figure.

Measurements showed, as might be anticipated, that in an amplifier of this kind the transformers play an important part, and it was at times advantageous to substitute other transformers for those supplied with the set.

In amplifying sets for either audible or radio frequencies, but not both, the transformers between valves are similar, and, since an experimental receiving circuit is usually very dissimilar to the connecting circuits between the valves, amplification by a separate valve was first obtained in our experiments, and the intensity of the note produced in a telephone in the anode circuit of this valve was taken as the standard of reference. The valve so used and the transformer associated with it were similar to those in the set. In fig. 1 this reference valve is A, and it is the amplification of the three valves B, C and D which is intended to be measured. The intensity of the standard note was usually adjusted at the source, so that signals could be just read with comfort.

In some early experiments a buzzer was employed as a source of sound, but the noise and general disturbance due to it were very troublesome, and it was displaced by a triode valve set generating oscillations of an audible frequency. The anode oscillatory circuit consists of the inductance $L_s$ and the condenser $C_s$, these being adjustable and of such



Digitized by Google

values that oscillatory currents of almost any audible frequency can be obtained. The great advantages over the buzzer are the constancy of the frequency and intensity of the oscillations, and the fact that no audible note is produced until a telephone circuit is in some way coupled to $L_s$.

A coil, L, is loosely coupled to $L_s$, and the induced currents pass through the primary P of an air-core transformer, M. This transformer has two secondaries, $S_1$ and $S_2$, crossed at right angles and capable of rotating together about a vertical axis. The mutual inductance between the primary and either secondary was measured for various angular

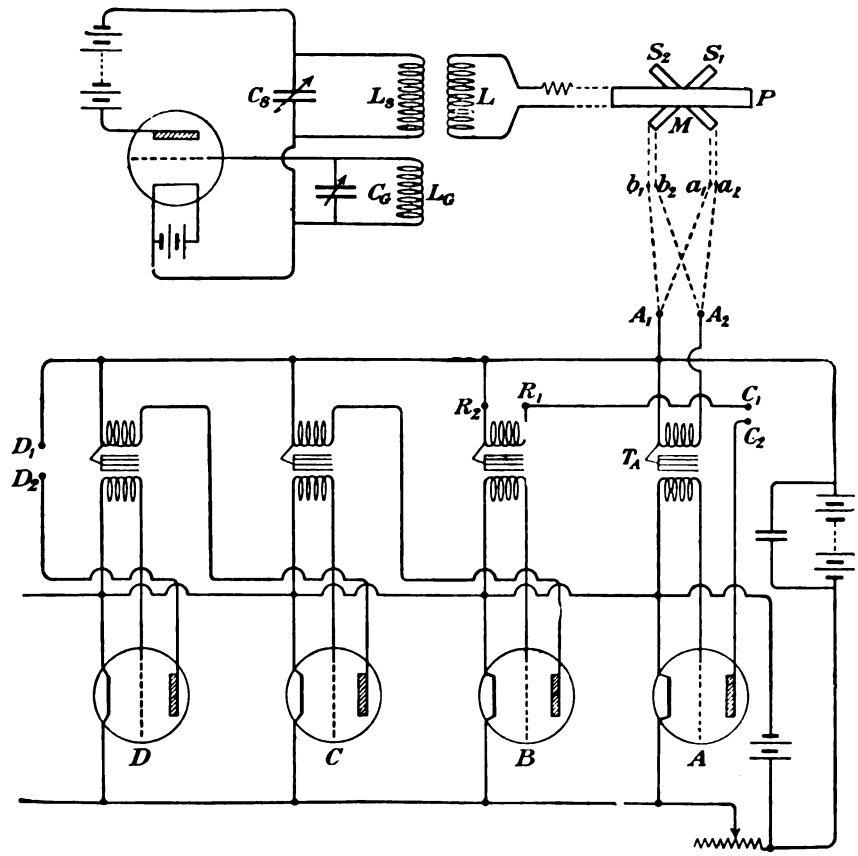


Fig. 1.

positions of the latter by means of a Campbell inductometer. Either of the secondaries may be directly included in the grid circuit of the valve A or a transformer may be interposed. The anode circuit of A includes the primary of a suitable transformer, the secondary of which is in the grid circuit of the valve B. When the telephone (connected to $T_1T_2$, fig. 1B) is included at $C_1C_2$ in the anode circuit of A, the primary of the transformer between the two valves is excluded from the circuit by a short-circuiting piece across $R_1R_2$. In these circumstances, suppose that the secondary $S_1$ of the transformer M is in circuit with the primary of the transformer TA; by means of a turning head (shown in fig. 1B), $S_1$ is now disconnected, and the secondary $S_2$ is substituted, the telephone being simultaneously removed from the anode circuit of A and included at $D_1D_2$

Digitized by Google

in the anode circuit of the last valve; at the same time the short-circuit across $R_1R_2$ is removed. These changes are simultaneously made by a six-brush switch in a fraction of a second. The secondaries $S_1$ and $S_2$ are rotated with respect to the primary P until the intensities of the signals for the two positions of the switch are equal. The ratio of the mutual inductances between P and $S_2$ and P and $S_1$ is then a direct measure of the voltage amplification due to the valves B, C and D.

Amplifications up to 20 are conveniently measured in this way. If it is desired to measure greater amplifications, the number of turns on $S_1$ and $S_2$ may be different, or the

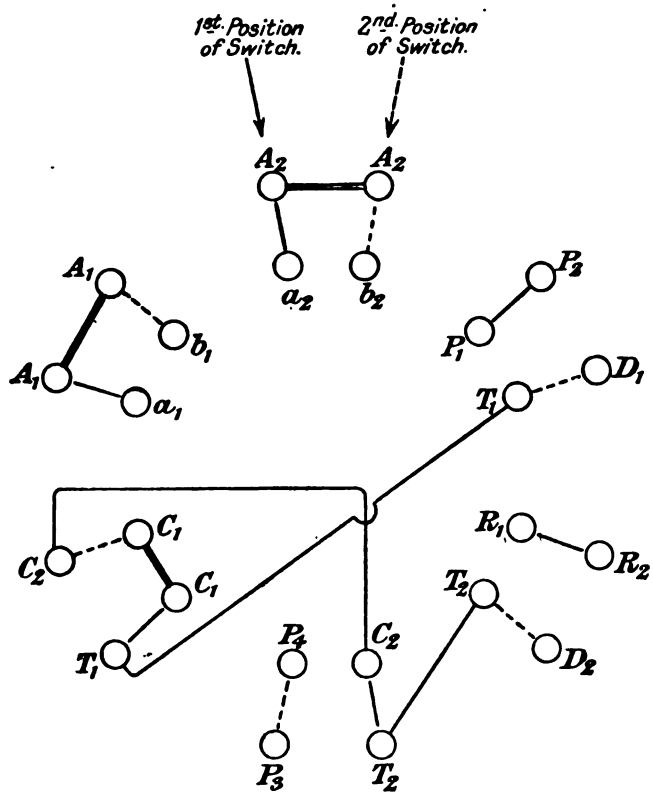


Fig. 1B.

switch may alter the number of turns in the primary P, the current through P remaining practically constant, or the value of the oscillatory current in $L_sC_s$ may be altered. In the last case the ratio of the mutual inductances between P and $S_2$ and P and $S_1$ is the one in which fine adjustments can be made, and has to be multiplied by the ratio of the currents to give the amplification. In this way a series of three selected valves has been found to have an amplifying power as great as 300. Most of our measurements have, however, been made with one or two valve sets, the usual magnification obtained with one valve being from 8 to 12 and with two valves from 20 to 80. The big variation in the latter case is due to variation in the valves employed. If two single valves, each of which will, when the currents and voltages are nicely adjusted, amplify a note 10 times,

Digitized by Google

be used in cascade, the amplification obtained is in general less than 100, for it is usually necessary to adjust the filament current to avoid hissing in the valves. This trouble is, however, much smaller than it was a few years ago.

Fig. 1B shows the connections to a six-brush switch for making the changes referred to. The parts on figs. 1 and 1B, which are indicated by similar letters, were connected together by leads. The telephone is connected to $T_1$ and $T_2$. A single brush connects two studs on a radius, and the angular movement of the switch is limited to the small angle between two pairs of neighbouring studs. When more than 20 volts was applied

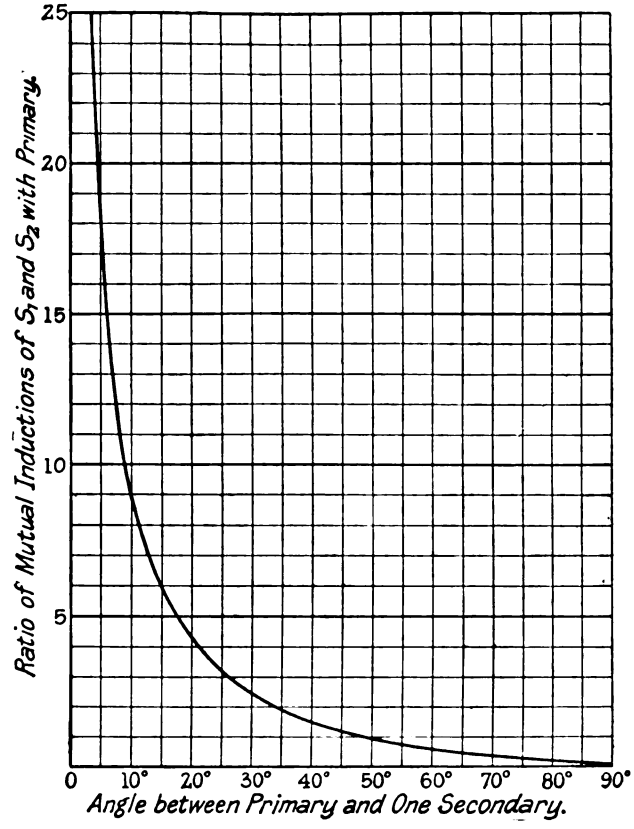


Fig. 2.

to the anode circuits, the telephone was connected to the secondary of a suitable transformer, the primary of which could be placed in an anode circuit by connecting it to the studs $T_1$ and $T_2$ of the switch.

In making measurements the axes of the coils $L_s$, $L_g$ and L were kept vertical and sufficiently far removed from the rest of the apparatus to prevent disturbing effects due to any direct action on the secondaries of the transformer M or any parts of the valve circuits. The axes of the coils of M were horizontal. Loops in leads were avoided, and when P was short-circuited there was a negligible amount of energy passing into the valve circuits from the telephonic frequency circuit.

Fig. 2 gives the ratios of the mutual inductances of the secondaries $S_1$ and $S_2$ with the

Digitized by Google

primary P for angular displacements of the secondaries. For either coil the ratio is a maximum when the plane of the coil is in the plane of the primary.

It will be seen that if the amplification is greater than 20 the angle between one secondary and the primary will be less than 5 degrees. The primary P was therefore divided into three parts, so that the number of turns in circuit with L could be varied, the ratio of turns used being 1 : 10 : 20. In a later apparatus the number of turns on a secondary can be varied.

*Comparison with the Shunted Telephone Method.*

Measurements were made to compare the results obtained by the method already described with those obtained by a shunted telephone method. The latter was a slight modification of the method usually employed, the energy of the current received in the telephone when two or more valves were used being cut down by a shunt until a balance was obtained against the energy of the current derived from one valve. The telephone was not shunted to secure silence. In this shunted telephone method the oscillatory energy in the grid circuit of the first valve was constant, whereas in the method previously described it was varied. If, under the conditions of the experiment, $L_1$ = inductance of the telephone, $R_1$ = resistance of the telephone and $R_2$ = resistance of shunt then

$$\text{Current amplification} = \frac{\sqrt{(R_1 + R_2)^2 + L_1^2\omega^2}}{R_2}.$$

In our experiments the resistances and inductances of the telephone and the shunt were measured at the frequencies employed in the amplification tests. In a particular case, when the frequency was 574 per second, the Sullivan telephone used had an inductance of 1·54 henries and a resistance of 3,900 ohms. The shunt resistance was of negligible self-inductance.

As examples, the following results are given :—

| Valves. | First method. | | | Shunt methods. | |
|---|---|---|---|---|---|
| | Angle of balance. | Ratio of turns in primary P, the current in P being practically constant. | Magnification. | $R_2$ ohms. | Magnification (approximately). |
| $K_1$ . . . . . | 8° | 1 | 12 | 660 | 11 |
| $K_2$ . . . . . | 7½° | 1 | 12½ | 640 | 13 |
| $K_3$ . . . . . | 10° | 1 | 9½ | 740 | 10 |
| $K_3$ . . . . . | 45° | 10 | 10 | 700 | 10 |
| $K_1 + K_2$ . . . . . | 20° | 10 | 45 | 185 | 37 |
| $K_1 + K_2 + K_3$ . . . . | 6° | 10 | 160 | 48 | 140 |
| $F_1$ . . . . . | 12° | 1 | 7½ | 920 | 8 |
| $F_2$ . . . . . | 10° | 1 | 9 | 850 | 8½ |
| $F_3$ . . . . . | 10° | 1 | 9 | 820 | 9 |
| $F_1 + F_3$ . . . . . | 17½° | 10 | 50 | 170 | 40 |
| $F_3 + F + F_3$ . . . . | 7° | 20 | 260 | 33 | 200 |

Digitized by Google

There was some hissing produced when the three valves were used in cascade which rendered it necessary to slightly reduce the filament current.

For the shunted telephone method the number of turns in the primary P was kept constant, and the angular reading of the secondaries was also kept constant at 45 degrees. To facilitate the readings, the six-brush switch was modified as shown in fig. 3. The variable resistance $R_2$ was inserted between the studs marked $T_1$ and $P_3$, and $P_4$ and $T_2$ were connected together. $R_2$ was adjusted until equality of sound was obtained for both positions of the key. The reading of $R_2$ was all that was necessary for the shunt method. For the other method, the switches $K_1$ and $K_2$ were opened, and the secondaries of the transformer M were turned until equality of sound resulted. This gave the reading

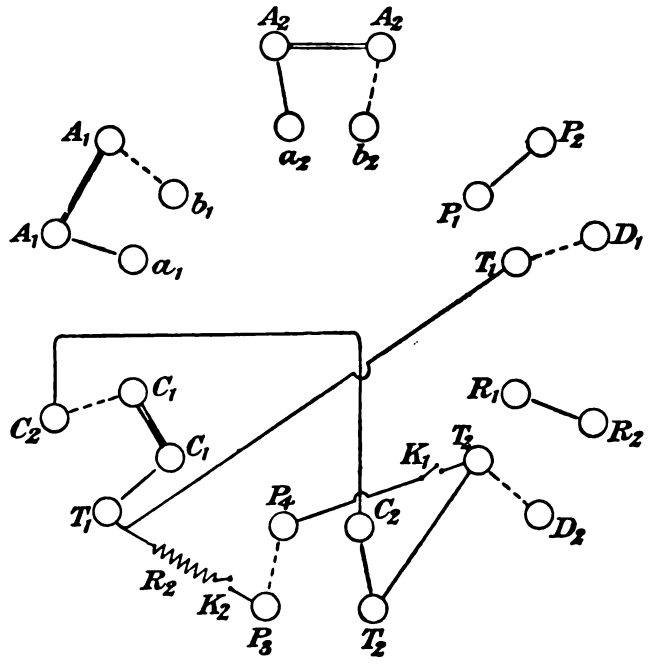


Fig. 3.

for the first method. Thus the comparison of the two methods could be made in a minute or thereabouts.

The two methods are distinctly different. In the first method the amplification is measured by *reducing* the incoming power, while in the second method the incoming power remains *constant*, the amplification being measured by reducing the effect of the amplifying action. If the alternating potentials applied to the valves are within the limits of the grid voltages which correspond with practically straight line portions of the anode characteristics, and if there is negligible grid current, the two methods are likely to agree, but not otherwise. This will be seen from a consideration of fig. 4, which gives the change of anode and grid currents with change of grid voltage over a limited range. In the first method described in this Paper, if when one valve only is used the change of grid voltage

Digitized by Google

on the valve is represented by AB, this will also be (for precisely similar valves), the change of grid voltage on the *last* valve when a number are used, the change of oscillatory voltage on the first valve being reduced in order to achieve this result. In the shunted telephone method the oscillatory voltage on the first valve will still be AB, but that on the second valve will be much larger, and may extend over the bend of the characteristic, so that the ratio of the oscillatory grid voltage to the resultant change in anode current may change considerably from valve to valve. That this is so seems to be evident from the measurements, and since the purpose of an amplifier is not as a rule to make a great noise in the

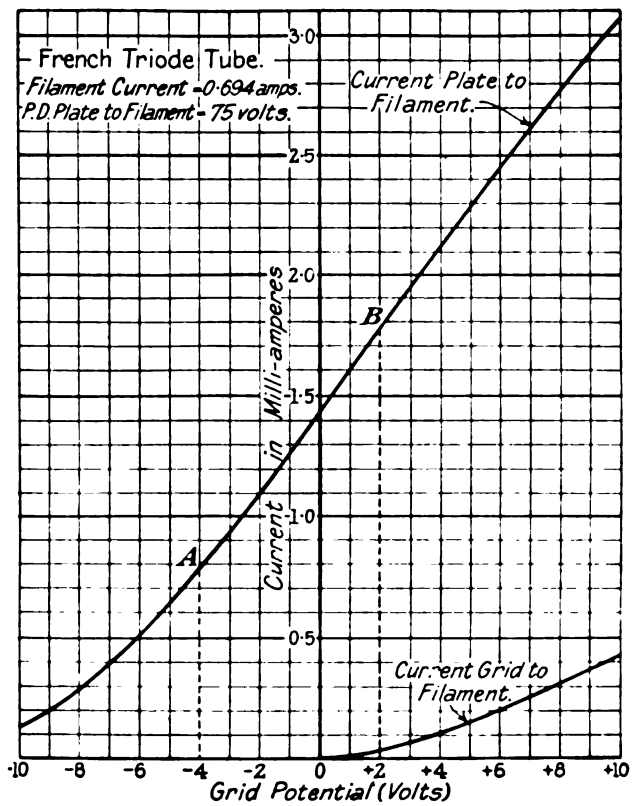


Fig. 4.

receiving telephone, but to amplify either weak or inaudible signals, so as to read messages with comfort, the shunted telephone method does not in general give the results desired.

Fig. 5 gives the anode and grid characteristics of a Telefunken triode valve from a German submarine. It is rather soft, and good results were not obtained with such valves in cascade.

For valves to be satisfactory as telephone relays it is not only desirable for the rate of change of anode current with change of grid potential to be constant over the range worked over, but there should be negligible or constant grid current, or otherwise some rectification and therefore distortion results. This will be referred to in more detail in the next section.



Digitized by Google

### 2. *Measurement of the Amplification of a Radio-Frequency Amplifier.*

Radio-frequency amplifiers differ from those intended for the magnification of audible frequencies, the most conspicuous difference being in the inter-valve transformers, which are either without iron cores or have such in the form of very thin laminated sheets.

The method already described for measuring the amplification of an audible frequency set is not suited for one intended to amplify radio frequencies. The capacity of parts of the circuits with earth results in very irregular distribution of current, and only when extraordinary precautions are taken can the coupling between the coils of any air core transformer be regarded as a true measure of the coupling between the circuits. Measure-

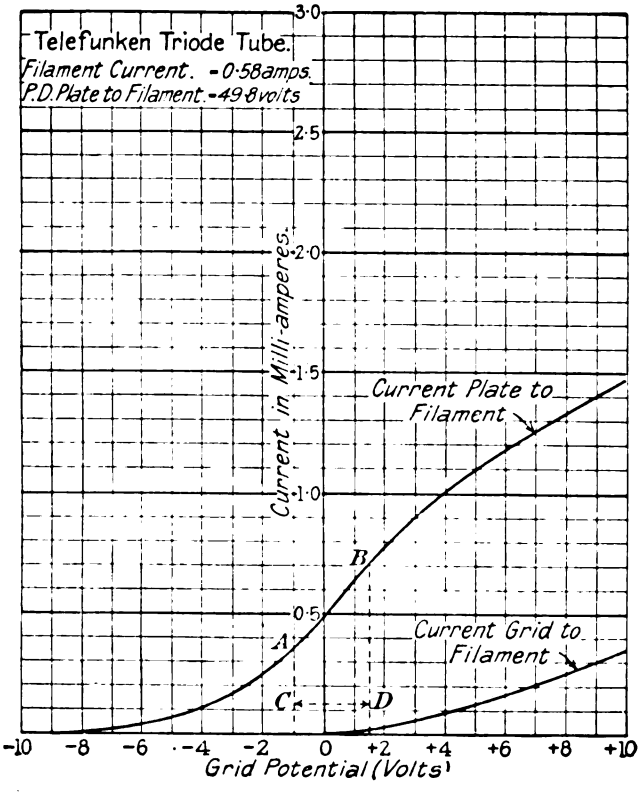


Fig. 5.

ments have been made by a method closely analogous to that for audible frequencies and with fair success; but a simpler method was devised, and this is now described.

The source of radio-frequency oscillations was a single valve, V (fig. 6), with a tuned oscillatory circuit, $L_1C_1$, adjustable so as to give practically any frequency. In general, however, a frequency of one million per second was chosen for our experiments.

Since, after rectification, the amplification of a continuous train of waves of radio frequency produces no note of audible frequency in a receiving telephone, it is necessary either to break up the train into groups of audible frequency or to superpose some effect which will produce the desired result. It is easy to break up the train of waves at the

Digitized by Google

source or at the receiving end, and it is equally easy at the source to superpose on the waves others of telephonic frequency, or at the receiving end to produce interference with a train of waves nearly equal in frequency (heterodyne). For our purpose, it appeared best to break up the train of waves at the source.

The train of oscillations was broken up into groups by throwing the anode oscillatory circuit out of tune at regular intervals corresponding to the period of the audible frequency desired. A rotating shaft S (fig. 6) carried a solid brass disc, from which 24 studs projected into a layer of vulcanized fibre, so that their surface was flush with that of the fibre. A brush made continuous contact with the brass disc, and a second brush made intermittent contact with the studs. On making contact between a brush and a stud the inductance $L_2$ was placed in parallel with the inductance $L_1$ of the anode oscillatory

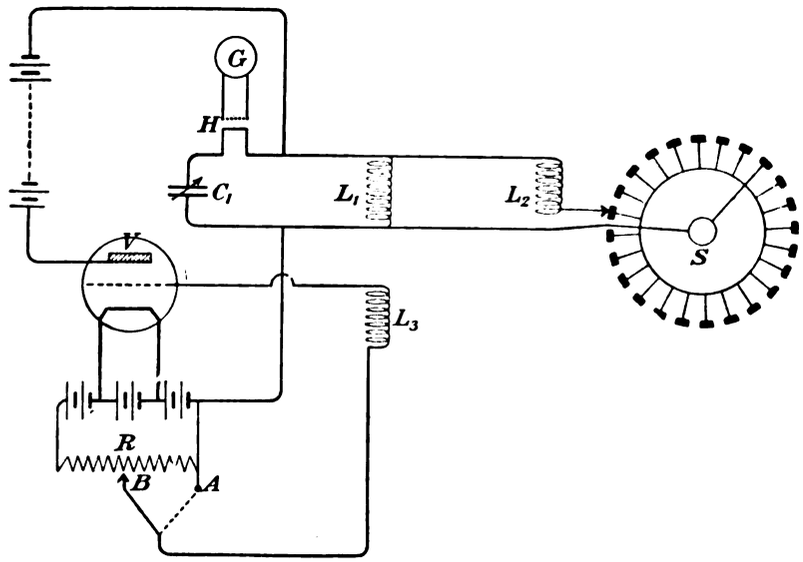


Fig. 6.

circuit, thus throwing the circuit out of tune and stopping the oscillations. This method was adopted in preference to breaking either the anode or grid circuits, as in the latter case the oscillations did not always commence again on make, and an irregular note was given in the telephone of the receiving circuit. Moreover, if the leads carrying a direct current be broken, a further wireless disturbance is set up, as experiment abundantly verified. The plan adopted, however, left nothing to be desired. In the experiments the frequency thus obtained was about 800 per second.

The essence of our method for measuring amplification lies in comparing the intensity of the note obtained from a single receiving valve, plus rectifier, with the intensity obtained from two or more valves plus the same rectifier. The intensities are made equal by adjustment of the incoming energy, but this is not done by a variation of a mutual inductance, as in the method for audible frequencies, but by a variation in the intensity of the radio-frequency current at the source.



Digitized by Google

The arrangement is shown in fig. 6, where V is the generating valve and $L_1C_1$ the anode oscillatory circuit. $L_1$ was of very low resistance. The grid inductance is $L_3$, but there was no tuned grid oscillatory circuit. A heater, H, with separate thermo-junctions, was included in the anode oscillatory circuit, and the current accurately measured. Several heaters were made and carefully adjusted in resistance, so that any one could be substituted for any other one in the oscillatory circuit without any measurable effect on the current or the tuning. The same galvanometer was used throughout the experiments, but several heaters were necessary, as the current was varied from a few milliamperes to an ampere or more. For the heating wires used, the high-frequency resistance was less than 0·5 per cent. greater than the steady current resistance, so that calibration of a combined heater and junction was easy. Variation in the generated current was brought about by altering the grid potential. In general the first grid potential in a measurement corresponded to that of the point A and the second to that of a point B, which was adjustable. The change from A to B was brought about by a switch, and the position B was varied until equal intensity of received notes was obtained when one valve and rectifier was used as receiver for the A position and several valves and the rectifier

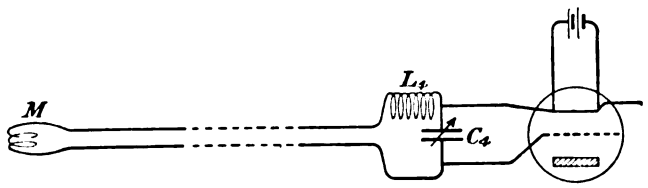


Fig. 7.

for the B position. After obtaining the balance, the oscillatory currents in the anode circuit were read off at leisure. Their ratio was the value desired.

Previous experiments had indicated a small change of wave-length when the grid voltage was varied over a considerable range, and it was necessary to determine to what extent this was a disturbing influence. To do this, another oscillatory circuit was set up and adjusted so that the heterodyne beat frequency was about 780 per second. After an adjustment of the grid voltage of the first valve circuit to reduce the oscillatory current to 1 per cent. of its former value, the heterodyne beat frequency was about 200 per second; but the note which was formerly the higher was now the lower, so that the change in radio frequency of the oscillations in the first circuit was about 980, corresponding to 0·1 per cent. However, in our experiments, the impedance in the receiving circuit $L_4C_4$ (fig. 7) was appreciable, and both measurement and calculation showed the resonance curve to be such that the change in wave-length due to change of grid voltage of the transmitting circuit could have but a negligible effect on our measurements of amplifying power.

Direct radiation from the valve circuit to the amplifier set was in general appreciable even when the distance between the sets was as great as 40 feet. Metal screens and

Digitized by Google

compensating coils greatly reduced the action, and a few measurements were made on the assumption that direct radiation was negligible. However, in the method finally adopted, direct radiation was *not* excluded. The radio receiving circuit consisted of the coil M, the inductance $L_4$ and the condenser $C_4$ (fig. 7). When this circuit was tuned and the oscillatory current in $L_1C_1$ was 1 ampere, the noise in a receiving telephone, after amplification and rectification by three or four valves, could in general be heard very many yards away. It could be reduced by adjustment of the directions of the axes of $L_1$, $L_3$, M and $L_4$, and this was usually done. When the receiving circuit was thrown greatly out of tune the note was scarcely detectable, indicating that the receiving action of the valve leads, &c., was negligible. The axes of the coils $L_1$ and $L_3$ were made vertical, and that of $L_4$ horizontal. The coil M could be turned in any position.

The anode and grid characteristics of all the valves were found previous to any amplification measurements being made, and the grid potentials of the radio amplifying valves were adjusted for favourable amplification but poor rectification. The last valve in a set was of the same type as the others, but the grid potential of it was adjusted for favourable rectification.

Any method for measuring the amplification only of radio frequencies is, however, necessarily difficult, because in practically all cases when the filament currents and anode and grid potentials are adjusted for most favourable amplification there is also some rectification. Referring to fig. 5, the part AB of the anode characteristic may be taken as a straight line, and the rate of change of the anode current with change of grid potential may be regarded as constant. If, therefore, the range of the oscillatory voltage lies within CD, and if these oscillatory voltages be symmetrical about the mid-point, there will be no rectification; but at C the grid current is zero, while at D it is 20 micro-amperes, and it rises with increasing rapidity as the grid potential is increased. If, therefore, the plate of the condenser $C_4$, which is connected to the grid, is charged positively by an amount corresponding to D, there will be a grid current, and therefore a leak; but when it is charged negatively by an amount corresponding to C there will be no grid current and no leak. Thus, it happens that in general the positive half of the incoming wave is cut down by a leak from the grid to a greater extent than the negative half. In other words, the potential variations impressed on the condenser and grid are not only cut down but are slightly rectified by the above action. In radio work, however, this is of little importance, and our measurmeents were made under practical conditions.

For comparison purposes, the standard note was that obtained from one amplifying valve and one rectifying valve, the telephone being included in the anode circuit of the latter or coupled to it by means of a suitable transformer. One or more radio-frequency valves and transformers were then added, and the resultant note reduced in intensity to that of the standard by reducing the current in the main oscillatory circuit. The ratio of the currents was taken as the amplification. The change from one condition to the other was made in a fraction of a second by means of a multiple brush switch, as in the method already described for audible frequencies. No change of tuning was made,

Digitized by Google

and no interference of the main circuits was permissible, except for the adjustment of the grid potential of the valve V. The shunt resistance R was non-inductive. The values obtained with the radio-frequency valves were comparable with those for audible frequency. A few checks on the method were made, of which the following is an example: With two radio amplifiers and a current of 20 milliamperes in the circuit containing $L_1C_1$ a note of very moderate intensity was obtained. The current was increased five times to 100 milliamperes, and the note restored to its original intensity by shunting the telephone, of which the inductance and effective resistance were known at the audible frequency experimented with. The shunt value was such as to give a ratio of currents 4·8. This check was considered very satisfactory.

The writer desires to express his thanks to Mr. ALBERT CAMPBELL and to Mr. D. W. DYE for many suggestions in connection with the measurements.

Digitized by Google

# THE MAINTENANCE OF A VIBRATING SYSTEM BY MEANS OF A TRIODE VALVE

BY

S. BUTTERWORTH, M.Sc.,
SOMETIME ASSISTANT IN THE ELECTRICITY DEPARTMENT.

Digitized by Google

## ABSTRACT.

This Paper gives a mathematical analysis of the arrangement, previously described by ECCLES, whereby the vibrations of a tuning fork are maintained by means of a triode.

In the simplest case, the prongs of the fork vibrate in the field of a permanent magnet, on the pole-pieces of which are wound coils connected in the grid and anode circuits of the valve respectively. From a consideration of the energy relations of the system, it is shown that for the maintenance of oscillations (*a*) the grid and anode coils must be wound in opposite directions, (*b*) there is a certain minimum value of the slope of the grid voltage-anode current characteristic of the valve at its working point.

Following this, the case in which condensers are connected across the two coils is treated on the principle of replacing the dynamical system by its electrical equivalent. In the particular example of similar anode and grid circuits, this system gives rise to three possible oscillations, one with the coils similarly wound and two with the coils oppositely wound. The conditions for maintenance are worked out, and the variation of the obtained frequency in the neighbourhood of the natural frequencies of both the dynamical and electrical systems is illustrated diagrammatically.

Finally, the case in which only one condenser is used is analysed, and a table is given showing the condition of maintenance and the oscillating frequency in the three typical examples.


Digitized by Google

# THE MAINTENANCE OF A VIBRATING SYSTEM BY MEANS OF A TRIODE VALVE.

By S. BUTTERWORTH, M.Sc., Sometime Assistant in the Electricity Department.

[Reprinted from the 'Proceedings of the Physical Society of London', Vol. 32, 1920.]

1. The triode valve has been applied recently by Eccles* for the purpose of maintaining the vibrations of a tuning fork. The circuit employed is shown in fig. 1. V is the triode valve, whose filament F is heated by the battery FB. The anode A is connected through the anode battery AB, and the coil AC to one terminal of the filament. The grid G is connected to the filament through the coil GC. The tuning fork T is permanently magnetised by an auxiliary magnet, on whose pole-pieces the coils AC and GC are wound, the poles of the fork being indicated by *n* and *s*.

The action is as follows: Suppose the fork to have been set in vibration, and consider the moment when the two prongs are moving away from their respective coils. The motion of the pole *s* will induce an E.M.F. in the coil GC, which will raise the potential of

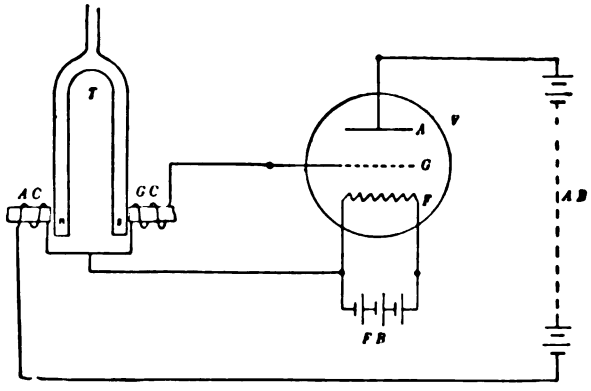


Fig. 1.

the grid, and so increase the current flowing into the valve at the anode. This current leaving by the filament completes its circuit via the coil AC, round which it passes in such a direction as to repel the pole *n*, and thus assist its motion.

The same argument applies to any phase of the motion so that the vibrations are maintained.

The motion is only assisted if the relative directions of winding in the two coils are as in the figure. If the ends of the coils be disconnected from the anode battery and the grid respectively, and the open ends connected to a source of alternating current, the force

* Eccles, 'Proc. Phys. Soc.', vol. 31, p. 269, 1919.



Digitized by Google

exerted by the current flowing through the grid coil would oppose that due to the current in the anode coil if the winding is correct.

2. It is also necessary that the energy supplied by the valve shall be sufficient to balance the energy dissipated by the motion of the fork. If the fork be treated as a system of one degree of freedom, this condition may readily be determined.

Let $A_1$ be the mechanical force acting on the fork when unit current flows in the anode coil. Then, if a current $I_a$ leaves the valve by the anode, the equation of motion of the fork is

$$(\alpha D^2 + \beta D + \gamma)\, y = A_1 I_a, \quad \ldots\ldots\ldots \quad (1)$$

in which $\alpha$, $\beta$ $\gamma$ are the usual mechanical constants, $y$ is the instantaneous deflection, and $D = d/dt$. If $A_2$ is the force per unit current flowing in the grid coil, the voltage induced in the grid coil raises the potential of the grid by an amount

$$v = A_2 D y, \quad \ldots\ldots\ldots\ldots \quad (2)$$

$A_1$ and $A_2$ having the same sign when the coils have the same direction of winding, so that the extra anode current is

$$i_a = -gv = -gA_2 D y, \quad \ldots\ldots\ldots \quad (3)$$

in which $g$ is the slope of the grid voltage — anode current characteristic of the valve at its working point, $g$ being of the dimensions of a conductance and positive in sign.*

Since the normal anode current merely produces a steady deflection, we may, for the purpose of determining the motion, identify $i_a$ with $I_a$, so that (1) becomes

$$\{\alpha D^2 + (\beta + A_1 A_2 g) D + \gamma\} y = 0. \quad \ldots\ldots\ldots \quad (4)$$

The oscillations will increase, remain steady, or decay, according as $\beta + A_1 A_2 g$ is negative, zero, or positive.

Thus, for the maintenance of oscillations, $A_1$ and $A_2$ must be of opposite signs, and

$$g > -\beta/A_1 A_2 = g_0 \text{ (say)}. \quad \ldots\ldots\ldots \quad (5)$$

The conclusion in regard to sign is identical with that arrived at in section 1.

3. The quantity $\beta/A_1 A_2$ is of the dimensions of a conductance, and it is important to form some notion of its magnitude. Suppose the anode and grid coils to have a mean radius of 1 cm., and a square channel section of 1 cm. side; and let them be wound with 10,000 turns of fine wire. The strength of the poles on the fork will be taken as 200 C.G.S. units. Then, assuming the turns concentrated in a single ring of 1 cm. radius, with the pole as centre, the force urging the pole when unit current flows is $4\pi$ megadynes. This gives the order of $A_1$ or $A_2$ if we may treat the fork as if its inertia were concentrated

* The effect of variations of anode voltage upon anode current is discussed in section 18.

Digitized by Google

at the poles. Now, RAYLEIGH* shows that this may be done for the fundamental period, and that the equivalent inertia of one prong is then one-quarter its whole mass, the remainder of the prong acting as a spring devoid of inertia. This gives $\alpha \doteqdot \frac{1}{2}$ (mass of one prong), since both prongs are vibrating. With a fork of reasonable dimensions, the mass of one prong may be taken as of the order 20 grams, and then $\alpha = 10$ grams.

$\beta$ can be found from the rate of decay of the free oscillations and the value of $\alpha$. Thus, suppose the oscillations to fall to $1/e$th of their initial value in one second; then $\beta = 2\alpha = 20$.

Hence, taking $A_1 = A_2 = 10^7$,

$$A_1A_2/\beta = 5 \times 10^{12} \text{ C.G.S. units} = 5000 \text{ ohms},$$

since it is of the dimensions of a resistance.

The condition for maintenance of the above system is, therefore, that 1 volt on the grid should develop an anode current of at least 200 microamperes.

A coil of the above dimensions and turns wound with No. 46 wire would have a direct current resistance of about 4,000 ohms, and its inductance with an air core would be about 4 henries.

For other turns and the same overall dimensions, $A_1$, $A_2$, the resistance and the inductance all increase as the square of the turns.

4. It has been suggested† that a condenser placed in parallel across the anode or grid coil would render the oscillations easier to maintain, and this has proved of value in certain cases. That a condenser might improve matters is to be expected from the principles of resonance, although when a considerable current is flowing in the condenser-coil circuit there is an additional energy loss due to the resistance of the coil. Again, the optimum capacity will not necessarily be that which will make the free frequency of the electrical circuit equal to that of the fork, as the reactive effect due to the motion of the fork is by no means negligible.

5. In the following theory use is made of a principle of electrical equivalence developed by the author‡ in an earlier Paper, in which it was shown that a dynamical system kept in motion by the magnetic action of a current flowing in a coil could be replaced by an electrical system in series with the coil, and of such a nature as to produce the same back E.M.F. as that produced by the motion of the dynamical system.

For the case of a system of one degree of freedom, the equivalent electrical system consists of a parallel combination of inductance, capacity and conductance. In the present problem the only difference is that two coils are acting instead of one. The necessary modifications on the earlier theory are easily made.

* 'Theory of Sound', vol. 1, p. 289.

† 'Proc. Phys. Soc.', (*loc. cit.*). Discussion.

‡ 'Proc. Phys. Soc.', vol. 27, p. 410, 1915.



Digitized by Google

6. If the two coils carry currents, $I_1$ and $I_2$, they act on the dynamical system with forces $A_1I_1$ and $A_2I_2$. The equation of motion is

$$(\alpha D^2 + \beta D + \gamma)\, y = A_1I_1 + A_2I_2, \quad \ldots\ldots\ldots \quad (6)$$

and the back E.M.F. on the respective coils are

$$E_1 = A_1Dy. \qquad E_2 = A_2Dy, \quad \ldots\ldots\ldots \quad (7)$$

so that, eliminating $y$ by means of (6),

$$E_1 = I_1/\xi_1 + I_2/\xi_{12}, \qquad E_2 = I_1/\xi_{12} + I_2/\xi_2, \ldots\ldots\ldots \quad (8)$$

in which

$$A_1^2\xi_1 = A_1A_2\xi_{12} = A_2^2\xi_2 = \alpha D + \beta + \gamma/D. \ldots\ldots\ldots \quad (9)$$

Equations identical with (8) will be obtained if, instead of the dynamical system, we place in series with the respective coils inductances (without resistance) of values $A_1^2/\gamma$, $A_2^2/\gamma$, perfectly coupled with each other, and shunt the former by means of a leaky condenser of capacity $\alpha/A_1^2$ and leakage conductance $\beta/A_1^2$. The leaky condenser may be transferred if desired to the second coil, the values of capacity and leakance being then $\alpha/A_2^2$and $\beta/A_2^2$. This follows from the properties of a perfectly coupled transformer.

7. Applying this principle to the case of the maintained fork, the system may now be taken as purely electrical, the circuits being shown in fig. 2. $l_1$, $l_2$ are the equivalent

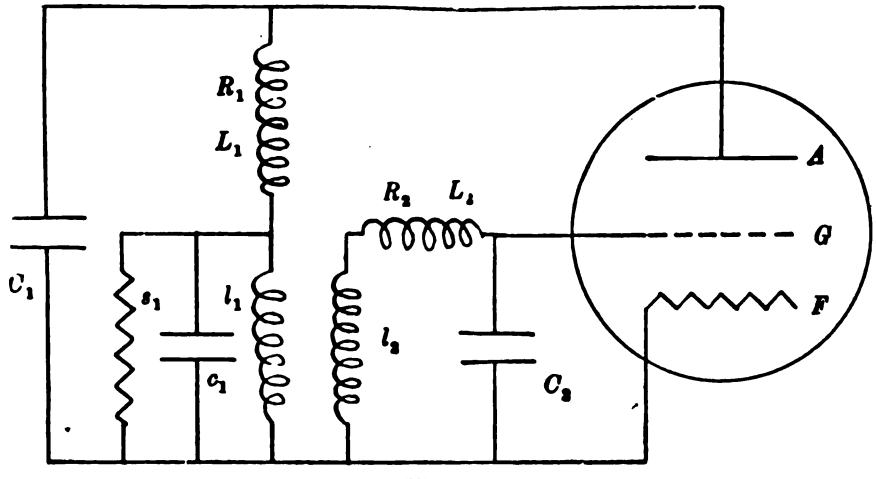


Fig. 2.

inductances of values $A_1^2/\gamma$, $A_2^2/\gamma$ perfectly coupled. $c_1$ is the equivalent condenser $\alpha/A_1^2$, and $s_1$ its leakage conductance $\beta/A_1^2$. $L_1$ is the inductance and $R_1$ the resistance of the anode coil, $L_2R_2$ the inductance and resistance of the grid coil. The condensers whose effects are to be investigated are $C_1$ and $C_2$.

Digitized by Google

The action of the equivalent leaky condenser may be taken into account by first obtaining the equations which hold when the condenser is absent, and then replacing the resistance operators $l_1D$, $l_2D$ and the mutual operator $\sqrt{l_1 l_2}D$ by $1/\xi_1$, $1/\xi_2$, $1/\xi_{12}$, the values of $\xi_1$, $\xi_2$, $\xi_{12}$ being given by (9).

Let $i_1$, $i_2$ be the clockwise currents* circulating in the anode and grid circuits respectively. The grid voltage is $i_2/C_2D$, and the resulting anode current leaving the valve is $-gi_2/C_2D$. This current flows back to the filament via $C_1$, thus impressing an E.M.F. on the anode circuit of amount $-gi_2/C_1C_2D^2$. Hence, if $X_1$, $X_2$ are the resistance operators of the anode and grid circuits, and $m$ is the mutual operator,

$$\left.\begin{aligned} X_1 i_1 &= (m - g/C_1C_2D^2)\, i_2 \\ X_2 i_2 &= m i_1 \end{aligned}\right\}, \quad \ldots\ldots\ldots \quad (10)$$

from which

$$(X_1X_2/m - m + g/C_1C_2D^2)\,\{i_1, i_2\} = 0. \quad \ldots\ldots\ldots \quad (11)$$

Using the explicit values of $X_1$, $X_2$, $m$, viz.,

$$X_1 = R_1 + L_1D + 1/C_1D + 1/\xi_1, \quad X_2 = R_2 + L_2D + 1/C_2D + 1/\xi_2, \quad m = 1/\xi_{12},$$

(11) becomes, with the help of (9),

$$\begin{aligned} &\{(\alpha D^2 + \beta D + \gamma)(C_1L_1D^2 + C_1R_1D + 1)(C_2L_2D^2 + C_2R_2D + 1) \\ &\quad + A_1^2C_1D^2(C_2L_2D^2 + C_2R_2D + 1) + A_2^2C_2D^2(C_1L_1D^2 + C_1R_1D + 1) + A_1A_2gD\} \\ &\qquad\qquad\qquad\qquad\qquad\qquad\qquad\qquad\qquad\qquad \{i_1, i_2\} = 0. \quad (12) \end{aligned}$$

The three possible oscillation frequencies indicated by (12) are obtained by putting $D^2 = -\omega^2$ in the operator, thus giving a complex in $\omega$, of which both the real and imaginary parts must be zero. The real part is a cubic in $\omega^2$, whose three roots determine the frequencies $(\omega/2\pi)$. The imaginary part gives the values of $g$, which will just maintain these frequencies.

8. The solution of (12) in the general case would be difficult, but the case of similar anode and grid circuits is amenable to treatment if the dampings are not too large. Putting $C_1 = C_2 = C$, $L_1 = L_2 = L$, &c., and writing $-\omega^2$ for $D^2$, the equation to determine the frequencies is

$$(\gamma - \alpha\omega^2)(1 - CL\omega^2)^2 - 2A^2C\omega^2(1 - CL\omega^2)(1 + \beta R/A^2) - C^2R^2\omega^2(\gamma - \alpha\omega^2) = 0, \quad (13)$$

and the equation to be satisfied by $g$ (the conditional equation) is

$$\beta(1 - CL\omega^2)^2 + 2CR\{(\gamma - \alpha\omega^2)(1 - CL\omega^2) - A^2C\omega^2(1 + \beta R/2A^2)\} \pm A^2g = 0. \quad (14)$$

* The currents and voltages referred to are the deviations of the currents and voltages from the normal values when oscillations are excited.

Digitized by Google

The positive sign is used when the coils are similarly wound and the negative sign when oppositely wound.

Putting further,

$$\gamma = \alpha\omega_1^2, \quad 1/CL = \omega_2^2, \quad R/L = \mu\omega_1, \quad \beta/\alpha = \nu\omega_1 2\,(A^2/L\alpha), \quad (1 + \beta R/A^2) = \sigma^2\omega_1^2,$$

(13) and (14) become

$$(\omega_1^2 - \omega^2)\,(\omega_2^2 - \omega^2)^2 - \sigma^2\omega^2\omega_1^2\,(\omega_2^2 - \omega^2) - \mu^2\omega^2\omega_1^2\,(\omega_1^2 - \omega^2) = 0, \quad . \quad (15)$$

$$\nu\,\{(\omega_2^2 - \omega^2)^2 + \mu^2\omega^2\omega_1^2\} + \mu\{2\omega_1^2 - \omega^2)\,(\omega_2^2 - \omega^2) - \sigma^2\omega^2\omega_1^2\} \pm A^2 g\omega_2^4/\omega_1\alpha = 0. \quad (16)$$

9. In the case when the free frequency of the circuits is equal to that of the fork (that is, $\omega_2 = \omega_1$), the frequency equation immediately factorises, giving

$$\omega^2/\omega_1^2 = 1, \quad 1 + \tfrac{1}{2}(\sigma^2 + \mu^2) \pm [\,\{1 + \tfrac{1}{2}(\sigma^2 + \mu^2)\}^2 - 1]^{\frac{1}{2}}.$$

Thus, the three possible oscillation frequencies are respectively below, equal to, and above the free frequency of the fork. If, as is often the case, $\sigma$ and $\mu$ are small compared with unity,

$$\omega/\omega_1 \doteqdot 1, \qquad 1 \pm \tfrac{1}{2}(\sigma^2 + \mu^2)^{\frac{1}{2}}.$$

For the root $\omega = \omega_1$, the conditional equation reduces to

$$\mu\,(\nu\mu - \sigma^2) \pm A^2 g/\omega_1\alpha = 0.$$

Now, $\sigma^2 > \nu\mu$, so that for the above condition to be possible the coils must be *similarly* wound. Inserting the values of $\sigma$, $\mu$, $\nu$, and using the positive sign,

$$g = 2R\,(1 + \beta R/2A^2)/L^2\omega^2. \quad . \quad . \quad . \quad . \quad . \quad . \quad . \quad . \quad (17)$$

For the other roots, the conditional equation reduces to

$$(\nu + \mu)\,(\sigma^2 + 2\mu^2)\,\omega^2 \pm A^2 g\omega_1/\alpha = 0.$$

The negative sign must be used, so that these oscillations can only occur when the coils are *oppositely* wound. The *lower* of the two frequencies requires the smaller value of $g$, so that this will be the actual frequency of the oscillation. When $\sigma$ and $\mu$ are small, $\omega \doteqdot \omega_1$, and the condition is then

$$g = (\nu + \mu)\,(\sigma^2 + 2\mu^2)\,\alpha\omega_1/A^2. \quad . \quad . \quad . \quad . \quad . \quad . \quad . \quad . \quad (18)$$

In the typical example of section 3, $\sigma^2 = 0{\cdot}00025$, $\mu^2 = 0{\cdot}025$, $\nu^2 = 10^{-7}$, a free fork frequency of 1,000 cycles per second being assumed. With these values, we find for similarly wound coils (equation 17) $1/g = 50{,}000$ ohms; for oppositely wound coils (equation 18), $1/g = 200$ ohms. The former condition corresponds to 20 microamperes per volt, and the latter to 5 milliamperes per volt. The oscillation with similarly wound coils is, therefore, by far the easiest to maintain. The value of $g$ for the oppositely wound

Digitized by Google

coils will, however, rapidly diminish with increase of L/R, because of the factor $\mu^2$. Also, as will be shown in the next section, a small variation of $\omega_2$ (by capacity adjustment) will cause a gain in ease of maintenance.

10. If the frequency of the electrical circuits is varied over a short range in the neighbourhood of $\omega_1/2\pi$, we may write in (15) and (16)

$$\omega_2^2 - \omega^2 = x\omega_1^2, \qquad \omega_1^2 - \omega^2 = y\omega_1^2 ;$$

and in the case $\sigma^2$, $\mu^2$ small, they reduce to

$$x(xy - \sigma^2) - \mu^2 y = 0,$$
$$\nu(x^2 + \mu^2) + \mu(2xy - \sigma^2) \pm A^2 g/\omega_1 \alpha = 0 ;$$

or, expressing $g$ and $y$ in terms of $x$

$$y = \sigma^2 x/(x^2 - \mu^2), \quad . \quad . \quad . \quad . \quad . \quad . \quad . \quad . \quad . \quad . \quad (19)$$

$$\pm g = -(\alpha\omega_1/A^2)(x^2 + \mu^2)\{\nu x^2 + \mu(\sigma^2 - \mu\nu)\}/(x^2 - \mu^2). \quad . \quad . \quad . \quad (20)$$

Since $\sigma^2 > \mu\nu$, the oscillations which occur when the coils are similarly wound are such that $x^2 > \mu^2$. In this case $g$ is least when $x = 0$, so that the value of $g$ given in (17) is the minimum $g$ for similarly wound coils.

The oscillations which occur when the coils are oppositely wound are such that $x^2 > \mu^2$. A minimum value occurs for $g$ when

$$x^2 - \mu^2 = \mu\sigma\sqrt{2\mu/\nu}, \quad . \quad . \quad . \quad . \quad . \quad . \quad . \quad . \quad . \quad (21)$$

and then

$$g = (\alpha\omega_1/A^2)(\mu\sqrt{2\nu} + \sigma\sqrt{\mu})^2, \quad . \quad . \quad . \quad . \quad . \quad . \quad . \quad . \quad (22)$$

while

$$y = x\sigma\sqrt{\nu/2\mu^3}. \quad . \quad . \quad . \quad . \quad . \quad . \quad . \quad . \quad . \quad . \quad . \quad . \quad (23)$$

In the typical case at minimum $g$

$$x \doteqdot 0{\cdot}32, \quad y \doteqdot 0{\cdot}001, \quad 1/g \doteqdot 15{,}000 \text{ ohms.}$$

11. The value of $x$ in the typical case is thus hardly within the approximation assumed in obtaining (20); $y$ is, however, small.

If we do not assume $x$ small, equation (20) must be modified by replacing $g$ in that equation by $g(1 + x)^2$, $y$ being still supposed small. We have thus really found when $g(1 + x)^2$ is a minimum. The true minimum $g$ will occur for a larger $x$ when $x$ is positive and the value of $g$ will be less than that calculated above. When $x$ is negative, the minimum will occur for a smaller value of $x$, and the value of $g$ will be larger than that for the positive $x$. Thus, of the two possible minima, the best is that for which $\omega_2 > \omega_1$.

12. The full behaviour of the system in the neighbourhood of $\omega_2 = \omega_1$ may be exhibited graphically for given values of $\sigma$, $\mu$, $\nu$, $\alpha\omega_1/A^2$.

Digitized by Google

From equation (19) $y$ is calculated for a suitable series of values of $x$, and $-y$ is plotted against $x - y$. The ordinates then give $(\omega^2 - \omega_1^2)/\omega_1^2$, and the abscissæ $(\omega_2^2 - \omega_1^2)/\omega_1^2$. The graph, therefore, gives the variation of the oscillation frequency from the free frequency of the fork as the free electrical frequency is varied by capacity adjustment.

Similarly, from the (modified) equation (20), $g$ is calculated and plotted against $x - y$. This graph shows the condition for maintenance of the oscillations given in the former graph.

The case used for Figs. 3 and 3A is

$$\sigma = 0{\cdot}012, \quad \mu = 0{\cdot}02, \quad \nu = 0{\cdot}002, \quad A^2/\alpha\omega_1 = 2 \text{ ohms},$$

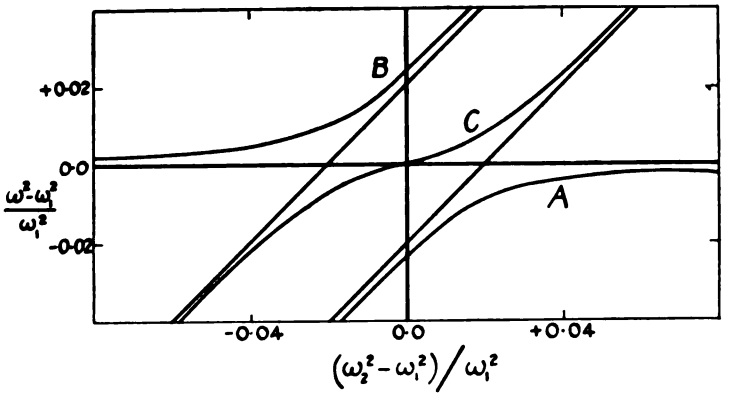


Fig. 3.

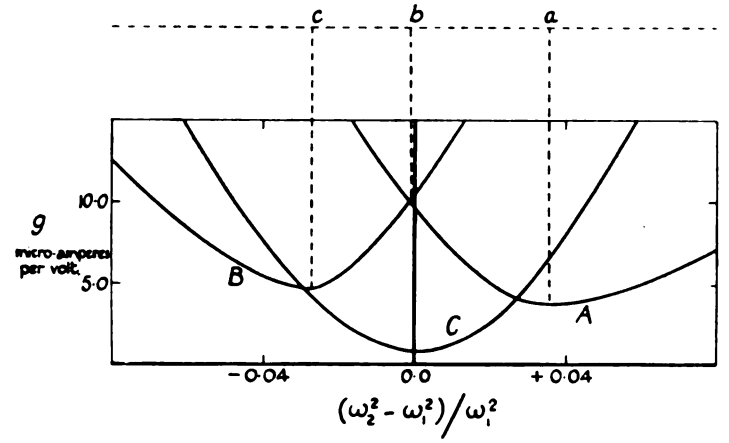


Fig. 3A.

$\omega_1/2\pi$ = free frequency of fork. $\omega_2/2\pi$ = free frequency of circuits. $\omega/2\pi$ = frequency of maintained oscillations.

which corresponds, for example, to

$$\omega_1 = 5{,}000, \quad R = 1{,}250 \text{ ohms}, \quad L = 12{\cdot}5 \text{ henry}, \quad \beta/\alpha = 10,$$
$$\alpha/A^2 = 100 \text{ microfarads}.$$

In fig. 3 the possible oscillations when the coils are oppositely wound are given by the curves A and B. The curve C is for the single oscillation occurring when the coils

Digitized by Google

are similarly wound. In fig. 3A the values required for the three oscillations A, B, C are given by the curves with corresponding letters.

To trace what occurs as the capacity increases we must proceed from right to left along the horizontal axis. With opposite windings and capacities appreciably lower than the resonating capacity, it is the oscillation A which always occurs. This follows from the smaller value of $g$ required to maintain A. Up to the point $a$ the ease of maintenance for both A and B increases. From $a$ to $b$, A becomes more difficult to maintain, while B still increases in ease of maintenance until at $b$ the ease of maintenance of either oscillation is the same. A slight increase of capacity at the point $b$ will make B easier to maintain than A, so that there will be a sudden increase in frequency from that corresponding to A to that corresponding to B. If the frequency difference is suitable, this will be accompanied by beats as A dies down, while B builds up. Beyond the point $b$ it is the oscillation B only which is present, its ease of maintenance being a maximum at the point $c$.

As regards change of pitch with increase of capacity, there is a slow fall in frequency from the free fork frequency, this fall increasing in rapidity as the point of instability is approached. The sudden rise in pitch at the point B is followed by a slow fall towards the free fork frequency.

With similar windings (following the oscillation C), the frequency always remains near that of the electric circuits being lower when $\omega_2 > \omega_1$ and higher when $\omega_1 > \omega_2$. The oscillation is easiest to maintain at the resonating frequency, and its variation with respect to the frequency of the fork is least at this point.

13. When only one condenser is used, equation (12) reduces to

$$\{(\alpha D^2 + \beta D + \gamma)(CLD^2 + CRD + 1) + A_1^2 CD^2 + A_1 A_2 g D\} \quad \{i_1, i_2\} = 0, \quad (24)$$

in which $A_1$ refers to that coil across which the condenser is placed.

Putting $D^2 = -\omega^2$, and using the notation of equation (15), the frequency equation is

$$(\omega_1^2 - \omega^2)(\omega_2^2 - \omega^2) = \tfrac{1}{2}\sigma^2 \omega_1^2 \omega^2. \quad . \quad . \quad . \quad . \quad . \quad . \quad . \quad . \quad (25)$$

The two possible oscillation frequencies, therefore, lie outside the range $\omega_1 \sim \omega_2$, one being above and the other below this range. Since usually $\sigma^2$ is small, the roots ($\Omega_1$, $\Omega_2$) of (25) do not differ much from $\omega_1$ and $\omega_2$, their approximate values being given by

$$(\Omega_1 - \omega_1)/\omega_1 = (\omega_2 - \Omega_2)/\omega_2 = \sigma^2 \omega_1^2 / 4(\omega_1^2 - \omega_2^2), \quad . \quad . \quad . \quad . \quad (26)$$

when $\omega_1$ and $\omega_2$ are not nearly equal, and by

$$\Omega_1 - \omega_1 = \omega_2 - \Omega_2 = \sigma \omega_1 / 2\sqrt{2}. \quad . \quad . \quad . \quad . \quad . \quad . \quad . \quad . \quad (26A)$$

when $\omega_1 = \omega_2$.



Digitized by Google

14. The conditional equation for $\Omega_1$, $\Omega_2$ is

$$\nu(\omega_2^2 - \Omega^2) + \mu(\omega_1^2 - \Omega^2) + A_1A_2\omega_2^2 g/\alpha\omega_1 = 0. \quad . \quad . \quad . \quad . \quad . \quad (27)$$

This may be written

$$g = -\frac{\alpha\omega_1}{A_1A_2\Omega^2} \frac{\mu(\omega_1^2 - \Omega^2)^2 + \frac{1}{2}\sigma^2\nu\omega_1^2\Omega^2}{\omega_1^2(1 + \frac{1}{2}\sigma^2) - \Omega^2} \quad . \quad . \quad . \quad . \quad . \quad . \quad (28)$$

by the substitution

$$\omega_2^2 = \Omega^2\{\omega_1^2(1 + \tfrac{1}{2}\sigma^2) - \Omega^2\}/(\omega_1^2 - \Omega^2) \quad . \quad . \quad . \quad . \quad . \quad . \quad (29)$$

Since (by (29) ) the denominator of (28) has always the same sign as $\omega_1^2 - \Omega^2$, and since the two roots are on either side of $\omega_1$, it follows that $A_1$ and $A_2$ must have the same sign for the higher frequency and opposite signs for the lower frequency in order to make the condition (28) possible. Thus, with the winding of fig. 1, it is always the oscillation of lower frequency which is set up. If the capacity of the condenser is gradually increased, thus diminishing $\omega_2$, the oscillation frequency remains near to and slightly below $\omega_1/2\pi$ so long as $\omega_2$ is greater than $\omega_1$. When $\omega_2$ is less than $\omega_1$, the oscillation frequency remains near to and slightly below $\omega_2/2\pi$.

The effect may be shown graphically by plotting (25) with $\omega_2^2$ as abscissæ and $\omega^2$ as ordinates. The result is a hyperbola whose asymptotes are $\omega^2 = \omega_1^2$, $\omega^2 = \omega_2^2 + \frac{1}{2}\sigma^2\omega_1^2$. That branch of the hyperbola which passes through the origin gives the frequencies of the oscillations which may be set up when the coils are connected as in fig. 1.

The comparative independence of the oscillation frequency of the value of the capacity used may account for the known independence of frequency of a maintained fork of such factors as variation of the steady anode voltage.

In electrically excited oscillations the change in the anode battery will alter (by its change in earth capacity) the effective capacity across the anode circuit. This will have its full effect on frequency in electrically coupled circuits, but practically none in the case of the vibrating fork.

15. The condition for easiest maintenance may be obtained from (27) as follows :—

When $\Omega$ is nearly equal to $\omega_2$, the term involving $\nu$ may be neglected and

$$g \doteqdot \frac{\alpha}{A_1A_2}\frac{R}{L}(1 - \omega_1^2/\omega_2^2). \quad . \quad . \quad . \quad . \quad . \quad . \quad . \quad . \quad (30)$$

For similar anode and grid coils, $\alpha/A_1A_2$ is the equivalent capacity due to the reaction of the system on one coil, and is high (100 microfarads in the typical case). The oscillations are therefore difficult to maintain. When $\Omega$ is in the neighbourhood of $\omega_1$, put $\omega_1^2 - \Omega^2 = v$ in (28), and retain only the first order term. Then $g$ is of the form

$$g = K(v^2 + m^2)/(v + n), \quad . \quad . \quad . \quad . \quad . \quad . \quad . \quad . \quad (31)$$

in which

$$K = -\alpha\mu/A_1A_2\omega_1, \qquad m^2 = \tfrac{1}{2}\sigma^2\omega_1^4\nu/\mu, \qquad n = \tfrac{1}{2}\sigma^2\omega_1^2.$$

Digitized by Google

It is a minimum in regard to variations in $v$ when $v$ satisfies the quadratic

$$v^2 + 2vn - m^2 = 0, \quad . \quad . \quad . \quad . \quad . \quad . \quad . \quad . \quad . \quad (32)$$

and then

$$g = 2\mathrm{K}v = g_1 \quad \text{(say)}. \quad . \quad . \quad . \quad . \quad . \quad . \quad . \quad . \quad . \quad (33)$$

The electrical frequency required for this is found by substituting $v$ for $\omega_1^2 - \omega^2$ in (25). This gives

$$\omega^2 = \omega_1^2 (1 + n/v). \quad . \quad . \quad . \quad . \quad . \quad . \quad . \quad . \quad . \quad (34)$$

Equation (32) has two roots of opposite sign, of which the positive one has the smaller absolute value, and will therefore give the smallest possible value of $g$ in (33). Since it is positive, K must also be positive, or the two coils must be oppositely wound. Further from (31), since when no condenser is present, $v = 0$,

$$\mathrm{K}m^2/n = g_0 = -\beta/\mathrm{A}_1\mathrm{A}_2 \text{ (by (5))},$$

as might otherwise be determined by substitution of the values of K, $m$, $n$. Using this in (33) to eliminate K,

$$g_1 = 2g_0 vn/m^2 = 2g_0 (v/n)(n/m)^2.$$

Now (32) may be written

$$(v/n)^2 + 2(v/n) - m^2/n^2 = 0, \quad . \quad . \quad . \quad . \quad . \quad . \quad . \quad . \quad (35)$$

so that $g_1/g_0$ is a function of the single variable $(n/m)^2$. Denoting this by $\eta$ and using the positive root of (35)

$$g_1 = 2g_0 (\sqrt{\eta + \eta^2} - \eta), \quad . \quad . \quad . \quad . \quad . \quad . \quad . \quad . \quad (36)$$

while (34) becomes

$$\omega_2^2 = \omega_1^2 (1 + \eta + \sqrt{\eta + \eta^2}). \quad . \quad . \quad . \quad . \quad . \quad . \quad . \quad . \quad (37)$$

The oscillation frequency is most simply expressed by

$$\Omega_1^2 = \omega_1^2 (1 + \tfrac{1}{2} g_1/g_0 \,.\, \beta\mathrm{L}/\alpha\mathrm{R}). \quad . \quad . \quad . \quad . \quad . \quad . \quad . \quad (38)$$

In terms of the fundamental constants

$$\eta = \mathrm{R}(\mathrm{R} + \mathrm{A}^2/\beta)/\mathrm{L}^2\omega_1^2. \quad . \quad . \quad . \quad . \quad . \quad . \quad . \quad . \quad (39)$$

It may thus be expressed in terms of two phase angles, $\theta$ and $\phi$, $\phi$ being that of the coil alone and $\theta$ the modified phase angle obtained by adding the leakage resistance of the equivalent condenser of fig. 2 to the resistance of the coil. In fact, $\theta$ is the actual phase angle of the coil when fed with currents of frequency $\omega_1/2\pi$, the reaction of the moving system being taken into account.

In terms of these phase angles

$$\eta = \cot\theta \cot\phi. \quad . \quad . \quad . \quad . \quad . \quad . \quad . \quad . \quad . \quad (39\text{A})$$



Digitized by Google

16. In the typical case (sections 3 and 9) $\eta = 0{\cdot}056$, so that $g_1 = 0{\cdot}38\, g_0$, $\omega_2 = 1{\cdot}14\, \omega_1$; and since $\beta L/\alpha R = 0{\cdot}002$, $\Omega_1 = (1 - 0{\cdot}00019)\omega_1$. Since $1/g_0 = 5{,}000$ ohms, $1/g_1 = 13{,}000$ ohms, so that 1 volt on the grid must now be capable of developing 77 microamperes. The three cases treated may be summarised thus :—

| Condensers used. | $g$ min. microamperes per volt. | Optimum electrical frequency. | Oscillating frequency. |
|---|---|---|---|
| 0 | 200 | ... | 1,000·0 |
| 1 | 77 | 1,140 | 999·8 |
| 2 | 20 | 1,000 | 1,000·0 |

The value of the added condensers is most marked when $\eta$ is small. When this is so, (36) and (37) may be written

$$g_1 = 2g_0\sqrt{\eta}, \qquad \omega_2 = \omega_1(1 + \tfrac{1}{2}\sqrt{\eta}). \quad . \quad . \quad . \quad . \quad . \quad . \quad (40)$$

For higher values of $\eta$, the values of $g_1/g_0$ and $\omega_1^2/\omega_2^2$ may be exhibited graphically. This is done in fig. 4 up to $\eta = 2$. When $\eta > 2$, the addition of a condenser is of little value.

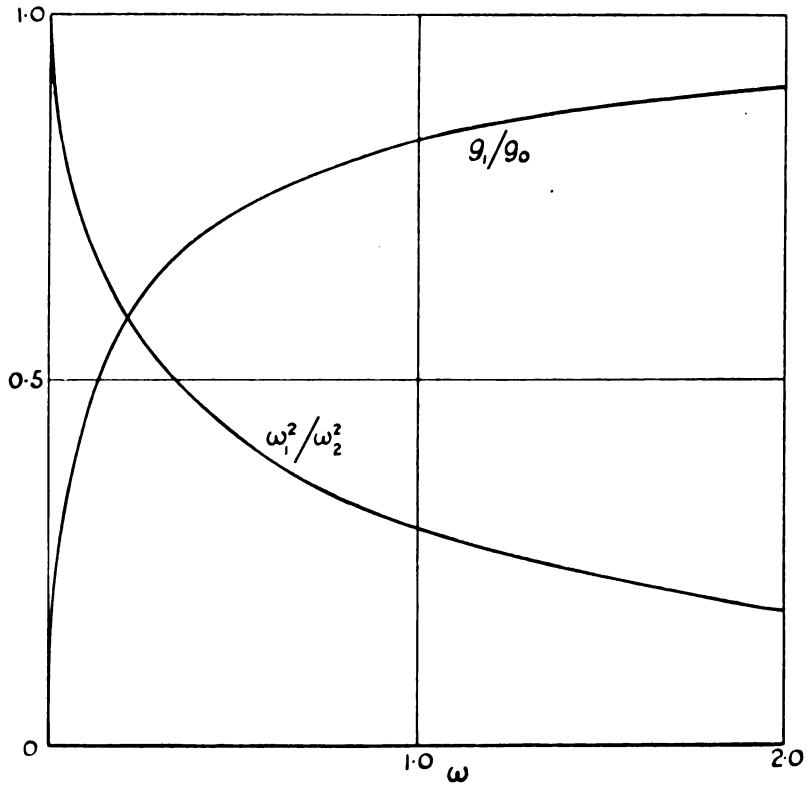


Fig. 4.

Digitized by Google

17. If in (25) and (27) we make the substitutions

$$x = \omega_1^2/\omega_2^2, \qquad y = \omega_1^2/\omega^2$$

we obtain

$$y = x/y = 1 + px, \quad \ldots\ldots\ldots\ldots \quad (41)$$

and

$$q(x-1) - x/y + 1 + z = 0, \ldots\ldots\ldots\ldots \quad (42)$$

in which

$$p = 1 + \tfrac{1}{2}\sigma^2, \qquad q = \alpha R/(\alpha R + \beta L), \qquad z = A_1A_2Lg\sigma/(\alpha R + \beta L).$$

Eliminating $x/y$ between (41) and (42), the latter may be replaced by

$$y + z = (p - q)x + q. \ldots\ldots\ldots\ldots \quad (42A)$$

In these forms, the frequency equation (41) and the conditional equation (42A) admit of a simple graphical solution which holds for all values of the constants.

Taking axes $x$ and $y$, draw the hyperbola (41) and on the same diagram draw the straight line $y = (p + q)x + q$. Then the ordinates of the hyperbola are proportional to the squares of the oscillation periods and the abscissæ to the capacity required to produce them. The vertical distances of the straight line from the hyperbola gives the values of $z$, being positive above and negative below the line. Since $z$ is proportional to $g$, its smallness is a measure of the ease of maintenance of the corresponding oscillation. The

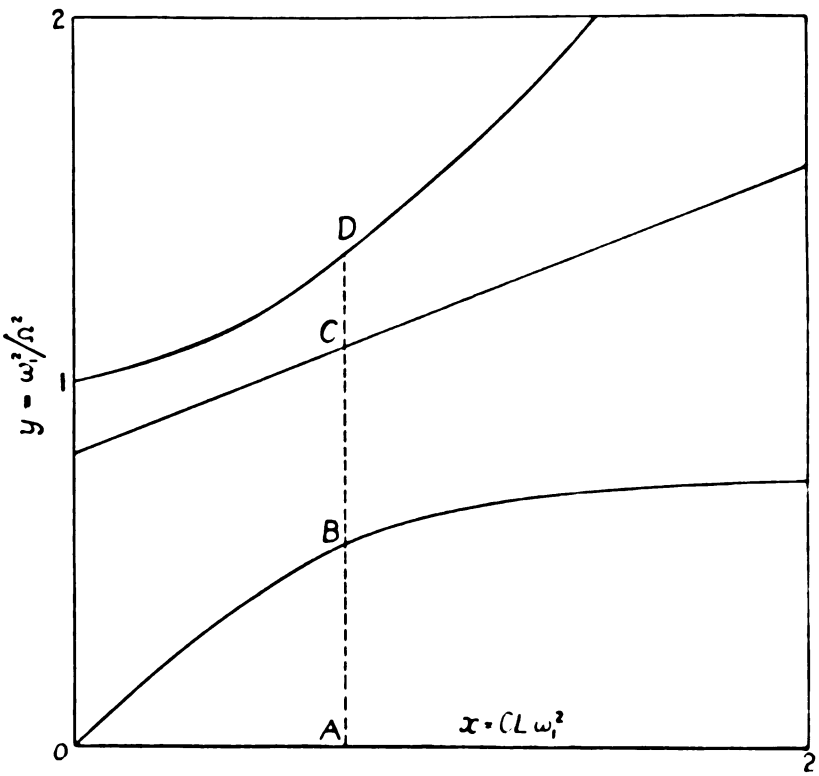


Fig. 5.

Digitized by Google

upper branch of the hyperbola gives the periods when the coils are oppositely wound and the lower branch when they are similarly wound.

This construction is made in fig. 5 for the hypothetical case $p = 1{\cdot}2, q = 0{\cdot}8$. If OA represents the capacity of the condenser, then the square of the two possible periods are represented by AB and AD, the former occurring when the coils are similarly wound. The values of $g$ required are proportional to BC and CD respectively. The figure shows clearly the two optimum capacities and the advantage of using opposite windings.

18. In developing the theory, the effect of fluctuations of the anode voltage upon the anode current has been ignored. If $v$ and $v'$ be the variations in voltage of the grid and anode, the current leaving the valve by the anode varies by an amount

$$i_a = -gv - g'v'.$$

This relation may be written

$$i_a + g'v' = -vg,$$

which shows that if we still suppose the anode to deliver a current $-gv$, but shunt the anode circuits by a conductance $g'$, the current flowing in the anode circuit will have the true value $ia$. The effect of anode voltage upon anode current is exactly as if such a shunt were present.

Digitized by Google

# ON THE ELECTRO-MAGNETIC SCREENING OF A TRIODE OSCILLATOR

BY

R. L. SMITH-ROSE, PH.D., M.Sc., A.M.I.E.E.,

ASSISTANT IN THE ELECTRICITY DEPARTMENT.

Digitized by Google

## ABSTRACT.

The results of the many experiments on screening described in the accompanying Paper show that the most complete method of screening a valve set is to enclose it in a box made of metal of suitable thickness for the frequency used, and to seal hermetically all joints in the box and its lid. The smallest crack or hole is sufficient to allow of the escape of a detectable amount of the high-frequency energy, and it is shown that iron is far more effective than copper of the same thickness in preventing direct penetration of radio-frequency magnetic fields through the metal.

While a practicable means of using an oscillator inside an hermetically sealed screening box is described for work of the highest precision, a much more convenient arrangement for the use of continuous-wave wireless direction-finding is described, with some results which have been obtained with an experimental sample in actual use for this work.

The experiments herein described were carried out at the National Physical Laboratory in connection with investigations undertaken for the Radio Research Board.


Digitized by Google

# ON THE ELECTRO-MAGNETIC SCREENING OF A TRIODE OSCILLATOR.

By R. L. SMITH-ROSE, Ph.D., M.Sc., A.M.I.E.E., Assistant in the Electricity Department.

[Reprinted from the 'Proceedings of the Physical Society of London', Vol. 34, 1922.]

## 1. *Introductory.*

The problem of screening a body or piece of apparatus from a high-frequency electromagnetic field is known to be very much more difficult than the protection from steady electric or magnetic fields. Electrostatic screening may be effectively carried out by completely surrounding the body with a metal covering (a Faraday cage), the thickness of which is immaterial. In cases where transparency of the screen is desirable to permit of inspection of the interior, the screen need not be absolutely continuous, *e.g.*, metal gauze or perforated sheet is effectively used to screen instruments from stray electric fields, or from capacity to external objects. Magnetic shielding of a body may be carried out by surrounding it with a heavy iron screen, which, however, only partially screens by deflecting the magnetic field through the space of greater permeability.

With an alternating magnetic field, however, the shielding effect of the iron is much more complete, and in this case, also, the shielding may be produced by other metals than iron, due to the demagnetisation by the eddy currents induced in the metal by the initial magnetic fields. Simple experiments with oscillation generators give the impression that when the frequency of the alternating magnetic field is very high, the difficulty of the screening is greatly increased. This is, however, a false conception and arises from the fact that the induced E.M.F. in any circuit placed in an alternating magnetic field is directly proportional to the frequency, and thus becomes very large at frequencies of the order employed in radio work. It is essentially this fact, together with the very high magnifications produced by multi-stage triode amplifiers, that leads to some rather surprising results when attempts are made to shield instruments from radio-frequency alternating magnetic fields. That the principles underlying the effective screening of a radio-frequency field have been somewhat misunderstood in the past is borne out by the fact that several experimenters write of employing a Faraday cage for this purpose, the cage often being constructed of wire gauze. The term "Faraday cage" can only strictly be employed in connection with electrostatic screening, and its effect is altered immediately the field is fluctuating or alternating.

## 2. *Object of Present Experiments.*

The present investigation arose from the necessity of a screened local oscillation generator for use in continuous-wave reception on a system of wireless direction-finder. The local oscillations are most conveniently generated by a simple form of triode oscillator



Digitized by Google

operating entirely from a 6-volt battery, and the problem is to protect the receiving coil system from induced local oscillations, which were to be led to the required point in the circuit by a purely conductive connection. The final form of screened triode oscillator may, however, be applied to other purposes than the above. It is, for example, a very necessary appliance for certain methods of measuring the strength of received radio signals.

The transfer of electrical energy from one oscillating circuit to another may take place by either pure mutual induction or by radiation, or by both these factors. In the case under consideration, in which the closed oscillating circuit of the generator is placed comparatively near the receiving circuit, the transfer is almost entirely by mutual inductance, since the radiation will be negligible by comparison. The problem may, therefore, be considered correctly as the limiting of the high-frequency magnetic field around the oscillator by induced eddy currents in the screening body.

### 3. *Preliminary Experiments.*

Some early miscellaneous experiments serve to indicate the difficulty of constructing a perfectly screened oscillation generator. These experiments were carried out with a compact form triode oscillator, using a single R-valve operating entirely from a 6-volt battery, and having a wave-length range of from 1,000 to 10,000 metres. With this instrument and a large-frame coil receiver and a seven-valve amplifier in use at Teddington, the more powerful and near C.W. transmitting stations, such as Horsea and Chelmsford, give a heterodyne note which can be heard several yards away from the telephones, even when the oscillator is placed at the far end of the wireless hut, about 100 feet away. This indicates how very small is the oscillating current required to give a beat note with incoming signals.

When the oscillator and battery were placed inside a thin copper box, with a loose-fitting copper lid, the induced oscillations in the receiving coil were considerably reduced and were only effective in producing a beat note when the oscillator was within 20 feet of the coil.

When the copper box was replaced by a galvanised-iron bin, a similar reduction in the induced oscillations was obtained of about the same order. In both these cases it was observed that the placing of the lid on the box had a considerable effect in the reduction; but the position of the otherwise open end of the box relative to the receiving frame appeared to be immaterial to the strength of the induced signals. A piece of fine brass wire gauze was not so effective as a lid as a solid sheet of material, whether copper or iron.

To obtain much greater sensitiveness in the later experiments and also for more convenience when no suitable incoming signals were received, a second valve oscillator was used, placed inside or near the large receiving coil which was also tuned to the oscillator frequency, thus producing a constant beat note in the telephone receivers when any appreciable oscillation was induced by the generator under experiment. The large

Digitized by Google

receiving coil with tuning condenser and seven-valve amplifier thus acted as an extremely sensitive search-coil method of detecting the presence of any radiated or induced radio-frequency field.

The former oscillator and its battery was next placed inside the copper box, and this in turn was supported on paraffin blocks inside the iron box and with the respective lids in position. In this condition the beat note was only appreciable when these boxes were placed within about 12 feet of the coil. By using a small coil in the amplifier circuit as a search coil, it was found that a considerable increase in the strength of the note was obtained with this coil placed near the aperture between box and lid, indicating that some, at least, of the energy escaped in this direction. Making metallic connection between the copper and iron box had no effect on the strength of the received signal.

Further experiments showed that the copper box provided with well-fitting lid giving about 3-inch overlap was much more efficient in screening than with the lid formerly employed, only $\frac{1}{2}$ inch deep.

### 4. *Experiments on Boxes with Multiple Copper Linings.*

As the combined copper and iron boxes seemed to give hopeful results, as above mentioned, further experiments were carried out with boxes with two and three linings.

One such box was made up as shown in fig. 1, consisting of a wooden box A lined

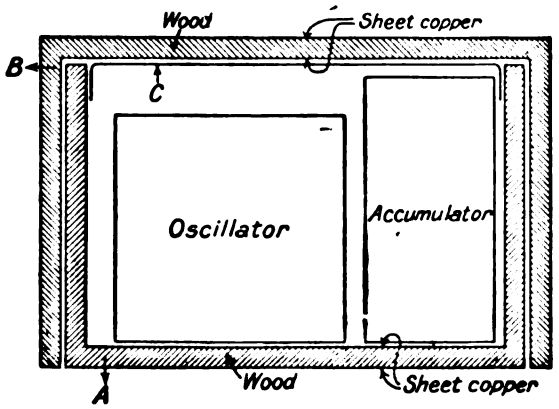


Fig. 1. Simple Screened Oscillator.

A = Double-Copper-Lined Wooden Containing Box.
B = „ „ „ „ Lid.
C = Inner Copper Lid.

inside and outside with thin sheet copper, and supplied with a completely enveloping lid B, similarly double lined.

With this box it was found that putting on the lid made a considerable reduction in the escaping energy from the oscillator, as indicated by the diminution in intensity of the note heard in the telephones. This box appeared, in fact, to be about as good as the combined copper and iron boxes previously tried, but was much more convenient from the point of view that the double-lined lid can be removed at one operation. The



Digitized by Google

diminution effect was continuous as the lid was placed over the box, being a minimum when the box was completely enveloped.

It was subsequently found that the fitting of an auxiliary inner lid, as shown at C, effected a still further reduction in the emitted energy.

Another arrangement consisted of two copper boxes, complete with close-fitting lids, separated from each other by 1-inch wooden strips. This arrangement was found to screen most efficiently when the inner box was inverted, as shown in fig. 2, when it was about the same as the last arrangement used. Again, no difference was experienced on making contact between the two boxes.

At this and subsequent stages of the experiments the need was felt for some simple and fairly accurate means of obtaining a measure of the emitted energy from such a type of partially screened oscillator. What is essentially required is to measure the comparative strengths of the induced energy with the unscreened oscillator, and with the latter enclosed by the various screening arrangements which were used during the present

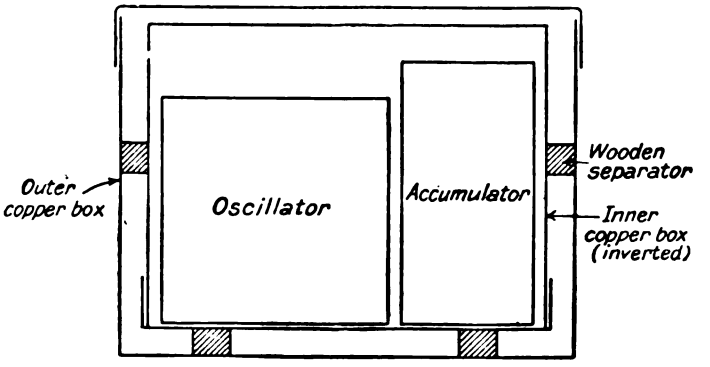


Fig. 2. Triode Oscillator, screened with Two Complete Copper Boxes.

investigation. The shunted telephone method might possibly be used, but the intensity of the note heard in the telephones does not necessarily indicate the amount of energy intercepted by the frame search coil, particularly when the oscillator is unscreened and the induced E.M.F. very large. It was often noticed, for instance, that even when the oscillator was partially screened, the intensity of the note in the telephones increased to a maximum before diminishing, when the oscillator was moved away from the coil. Also the interpretation of the results in terms of the distance of the oscillator from the frame is not simple.

It is possible that a somewhat elaborate arrangement would meet the requirements, involving a very constant amplifier and a means for calibrating it, but this was not considered to be within the scope of the present investigation.

### 5. *Effect of bringing Leads out from Screening Box.*

With a type of double-screened box as used above, the external field, therefore, could be rendered inappreciable when it was at a greater distance than 12 feet from the search coil. In this condition a small coupling coil of a few turns was introduced into the

Digitized by Google

inner copper box, and a flexible conductor brought outside both boxes. So long as this conductor remained entirely within the outer iron box, the beat note was undetectable, but immediately a few inches of it were exposed outside the iron box, even with a closely fitting lid, good beat-note signals were immediately obtained, giving evidence of energy thrown off from these leads. Replacing the flexible wires by a lead-sheathed twin conductor overcame this trouble, which, however, recurred on connecting a small coil to the end of the screened leads, with a view to coupling on to the amplifier. By varying the coupling to the oscillator, this latter " radiation " could be reduced to an extent inappreciable compared with the oscillating energy which could be conveyed through the outer coupling to the amplifier.

### 6. *First Experimental Screened Oscillator.*

Embodying the essential results of the experiments carried out as above, a first experimental oscillator was made up to the author's design by Messrs. H. W. Sullivan. This was in principle, although not in detail, similar to the arrangement shown in fig. 3 below, consisting of a wooden box double lined with sheet copper 1/64 inch thick, fitted

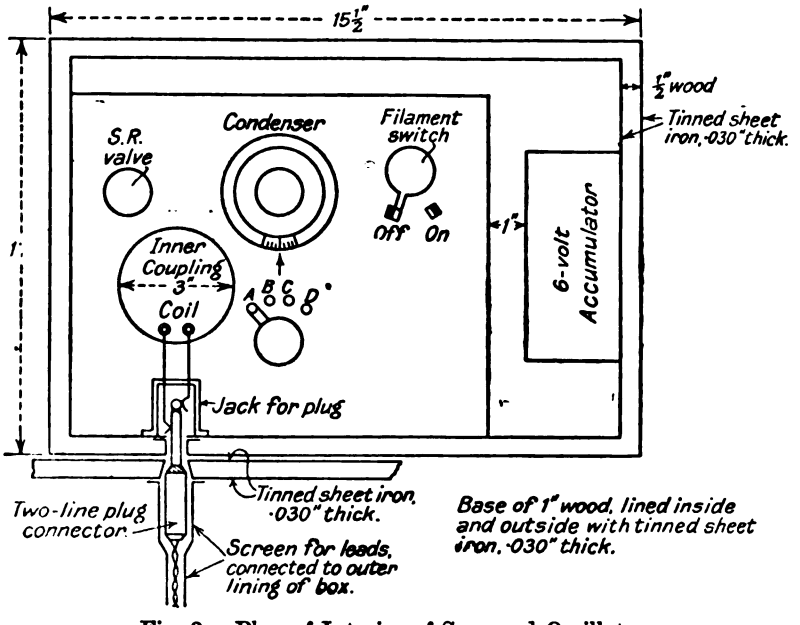


Fig. 3. Plan of Interior of Screened Oscillator.

with an inner copper lid and with a second enveloping lid similarly constructed of wood and double lined with sheet copper. Ebonite connecting pieces were used between the control handles on the top of the lid and the variable condenser and switches for filament current and inductance tappings within the box. The metal parts of the control handles were arranged to make spring contact with the outer coating of copper.

A separate coil was used within the box to couple to the oscillator inductances, and leads from this coil were brought out through the side of the box by a simple telephone

Digitized by Google

jack and plug connection. In the present arrangement, the jack is mounted inside the box and the plug is pushed through holes in lid and box which are only in alignment when the lid is in its final position over the box. The plug is screened by a metal coating in contact with the outer lining of the box and the connections are taken through a metal-sheathed twin flexible conductor to a double-D-shaped coil, forming half of the outer coupling. Leads from the other pair of D-shaped coils are taken to the output terminals mounted on ebonite at the side of the box.

The following points may be emphasised in regard to this screened oscillator arrangement:—

(1) The entire control of the oscillator is obtained from outside, and it need never be opened except for inspection, replacement of valve, or recharging of accumulator. A valve (type SR) consuming only 0·1 ampere filament current is used, which with the accumulator fitted will give continuous operation for about 120 hours.

(2) The opening up of the oscillator, when necessary, is a simple operation. It entails the removal of the connection plug, control handles and the two screening lids.

(3) Fairly close metallic contact is obtained at all points in the paths by which the radio frequency energy may escape from the box, other than by direct penetration through the sides.

(4) No part of the primary oscillator circuit is outside the inner metal lining. The secondary circuit is brought out by a screened conductor to an astatic coupling coil arrangement. The other half of this astatic coupling forms the tertiary circuit containing leads from the direction-finding coil to the amplifier. This coupling forms a convenient means of varying the strength of the local oscillation led to the receiver, varying from a maximum down to zero.

There is thus no part of any tuned circuit common to the inside and outside of the box, and all leads from the inside are carefully screened to reduce to a minimum any energy thrown off by these. With this oscillator in operation, but disconnected from the D.F. receiving circuit, beat-note action could just be detected on the latter, when the oscillator was about 5 feet from the centre of the D.F. coil. In the case of the reception of a C.W. station, this heterodyne action was negligible, compared with the note intensity that could be obtained by connecting up the oscillator to the receiver in the proper manner.

As the pick-up effect from the oscillator by the large frame coil (5 feet by 3 feet 6 inches) is so small, it is reasonable to assume that that picked up by the amplifier will be negligible. The oscillator may, therefore, be placed close up to the amplifier to make the connections between the two as short as possible. As it is essential in the system to have the amplifier at least 5 feet from the D.F. coil, the oscillator can conveniently be placed below or behind the amplifier and so be in a position in which its inductive or radiative action on the frame is quite negligible.

Digitized by Google

### 7. *Use of the Experimental Screened Oscillator for Continuous Wave Direction-Finding Observations.*

With this first screened oscillator, used under the conditions outlined above, a number of observations were taken in duplicate on the few C.W. stations that can be received at Teddington with and without heterodyne. The results, all of which were made in the daytime, are summarised in the following table:—

| Station observed. | Wave-length km. | Without Heterodyne. | | With Heterodyne. | | Difference. A — B. |
|---|---|---|---|---|---|---|
| | | No. of observations. | Mean bearings. (A) | No. of observations. | Mean bearings. (B) | |
| Le Vallois . | 2·2 | 20 | 145·0° | 18 | 145·0° | 0·0° |
| Chelmsford . | 3·8 | 22 | 56·3° | 24 | 56·5° | — 0·2° |
| Horsea . . . | 2·5 | 22 | 220·5 | 22 | 220·8 | — 0·3° |
| ,, . . . | 4·0 | 44 | 219·8 | 50 | 220·0 | — 0·2° |
| ,, . . . | 8·0 | Signals too weak | | 18 | 219·8 | ... |

These observations show that on the stations observed the difference in the mean reading taken, with and without heterodyne, is usually negligible and never greater than the ordinary errors of D.F. observation. The normal position of the oscillator in the above results was 5 feet west of the coil.

A number of observations were also carried out on Chelmsford, with the position of the oscillator varied, and these showed that no serious error is introduced until the oscillator is within 4 feet from the centre of the coil, in which position it is only about 1 foot from the side of the coil during part of its swing.

With the oscillator on the floor immediately underneath the D.F. coil, the error introduced was not more than 0·3°, while with the oscillator placed inside the frame, the error ranged up to 2° in either direction, according to the orientation of the oscillator relative to the frame.

No consistent difference in effect was obtained when the tertiary circuit of the oscillator was connected in either the grid or filament lead of the amplifier, but it may possibly help to balance up the " antenna effect " of the system as a whole if it is introduced into the grid lead.

As a typical example of the effect of " unscreening " the oscillator when connected up in its normal position, the following result may be quoted: With the oscillator fully screened, the error introduced by it was about 0·1°; when the outer lid was removed, this error increased to 4·3°, and with the inner lid also removed, it became 8·3°.

Where it is possible to make the necessary connections, it would be preferable to connect the tertiary circuit of the oscillator in the grid circuit of the rectifying valve of the amplifier to reduce the possibility of reaction from the high-frequency transformers.

Digitized by Google

### 8. *Further Experiments on Screening.*

Using the above screened oscillator in conjunction with the coil receiving set as a very sensitive detector of a high-frequency magnetic field, a number of further experiments were carried out on the screening of the oscillator originally employed :—

(*a*) *Hermetically sealed Copper Box.*

One of the original screening boxes was used, size 12 inches square by 8 inches high, made of sheet copper 25–30 mils thick. All joints at sides and bottom were sweated together with about $\frac{1}{4}$-inch overlap, the box being liquid-tight and probably gas-tight. A well-fitting lid was made for this of similar copper sheet, giving about $\frac{1}{2}$-inch overlap. This lid was actually used as the base with oscillator and battery placed on it, and the box over all. In such condition the external field was easily detectable by the receiving set when the box was within 20 feet of it. A wave-length of 2,400 metres was used, as being fairly free from interference by external signals, and also giving greater possibilities of screening than a longer wave-length.

Without altering any of the adjustments the box and lid were solidly soldered up, using a good thickness of solder to cover up all holes and cracks. In this condition the effect of the syntoniser could still be detected when within 10 feet of the frame. When the box was placed inside the frame the resultant beat note in the telephones could be heard 100 feet away. Also by tilting the box inside the frame a position giving practically dead silence could be obtained in much the same way as is obtained with the oscillator without the screening box. No effect could be obtained by removing the box from the frame and placing it near the amplifier.

The effect of hermetically sealing up this copper box is, therefore, to reduce some of the emitted energy which presumably came from the cracks round the lid, while still leaving a very appreciable amount, apparently passing through the metal, the external field retaining the characteristics of that from the unscreened oscillator.

(*b*) *Hermetically sealed Iron Box.*

A similar experiment to the above was carried out with a box of the same dimensions constructed of tinned iron sheet 28 mils in thickness.

With the oscillator placed inside the box, with a well-fitting lid giving $\frac{3}{8}$-inch overlap, the resulting effects of beat note were about the same as for the copper box. Placing another iron covering over the sides of the box made no appreciable difference, but when the lid as well was covered, the emission was considerably reduced. This seemed to indicate that the major portion of the energy from the inner box was coming from under the lid.

Using the same wave-length of 2,400 metres, the box and lid were solidly soldered up as before, after which no beat note was audible in the telephones. The fact that the oscillator was still in operation undisturbed was proved by making a slit in the box, when a beat note was easily heard in the telephones. A subsequent repetition of this

Digitized by Google

experiment showed that enough energy escaped through a slit ½ inch long to be easily detected. Further experiments indicated the absolute necessity of stopping all holes and cracks and of getting good metallic contact across all the joints, as a " dry soldered " joint may easily be the cause of an external magnetic field.

These experiments indicate, therefore, that it is only possible to screen a valve oscillator completely, as far as the sensitivity of the above apparatus goes, by placing it inside an hermetically sealed box of tinned sheet iron of sufficient thickness to prevent the direct penetration of the high-frequency magnetic field through it. In the latter respect iron would appear to be far superior to copper, which is a result in complete accordance with the theory of the penetration of alternating currents into conductors (skin effect). This theory indicates that iron should be equivalent to about four to six times its thickness in copper. It is, therefore, probable that if experiment (*a*) above were repeated, using a box of ⅛-inch copper sheet, complete screening would also have been obtained.

(c) *Mercury sealed Boxes.*

The process of soldering and reopening metal boxes containing a valve oscillator is very laborious and considerably limits experiments on these lines. It was, therefore, thought that a mercury seal, if of sufficient thickness, would be as efficacious as solder in stopping up holes and cracks.

A suitable tray 2½ inches deep was therefore made on which either the copper or the iron box could be placed giving an all-round clearance of about ½ inch. Placing oscillator and battery in this tray with the iron box over it, the external field was easily detected when within 20 feet of the frame. Filling up the tray with ½ inch of mercury to close all cracks entirely stopped all detectable field, even when the box was placed inside the frame. On raising the box at one side the smallest crack was immediately detected by the note in the telephones.

Using the copper box in the above manner, however, a beat note was still obtained when the mouth of the box was entirely below nearly 1 inch of mercury. This comparison experiment is very striking. With the copper box placed over, the beat note steadily diminishes, and a just detectable drop in intensity is obtained when contact is made with the mercury and the last crack closed up. With the iron box, however, the drop in note intensity to entire inaudibility when contact is made with the mercury is very sudden and a most marked effect.

These experiments were repeated for wave-lengths of 5,000 and 9,000 metres, and the residual effect with the copper box was slightly more noticeable on the latter wave-length, although the initial note-intensity was less, due to the inefficiency of the amplifier at this wave-length. While these results indicate the conditions for effective screening over the range 2,000—10,000 metres, the problem is probably much simpler for shorter waves, but somewhat more difficult for longer waves. A slight increase in thickness of the box would, however, probably be effective up to the greatest wave-lengths at present in use. These results thus confirm fully those previously obtained and indicate that the



Digitized by Google

most complete method of screening a valve oscillator is to enclose it in an iron box of sufficient thickness for the frequency used, and to seal hermetically all joints either with solder or mercury. Where very complete screening is required, therefore, this may be obtained on the above lines, using a plain iron box standing over an iron tray with welded joints, since mercury readily amalgamates with tin and solder. No external controls may be permitted, owing to the aperature necessary for these, but it would not be very difficult, where an approach to ideal conditions is very essential, to remove the box when adjustments are required to be made. One serious disadvantage to this, however, is that the frequency generated by the valve set alters considerably when the box is placed in position over the oscillator. In all the above experiments, this fact always necessitated the continual readjustment of the auxiliary oscillator to retain the beat note within the audible limits.

### 9. *Design of Screened Heterodyne for D.F. Sets.*

The general result of this investigation is that for applying auxiliary oscillations for C.W. reception on the D.F. directional wireless receiver in use, *an almost completely* screened oscillator, similar to the experimental sample used above, is suitable, with certain modifications. These consist in a reduction in the size and weight of the instrument, with the substitution of tinned-iron plate for the copper sheet previously used.

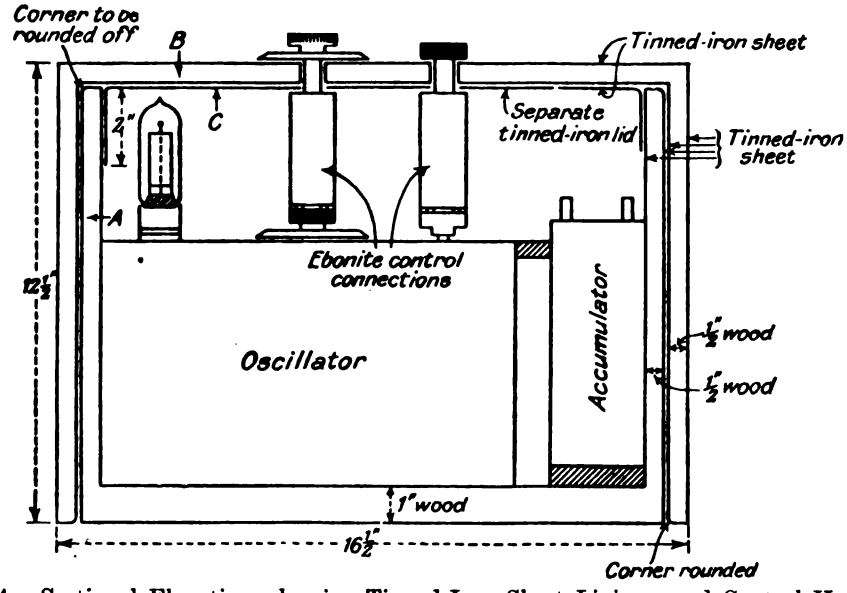


Fig. 4. Sectional Elevation, showing Tinned-Iron Sheet Linings, and Control Handles.

The details of the design of the instrument are shown in the accompanying figs. 3, 4 and 5, which indicate the essential parts of the oscillator and screening box, to the scale of the modified design.

Fig. 3 is a plan view of the interior of the box, showing the positions of the oscillator and battery, with the various switches; also the position of the inner coupling coil and the plug connection. Fig. 4 shows the positions of the screening lids with the method

Digitized by Google

of obtaining external control. The exterior of the top of the box is illustrated in fig. 5, showing the position of the D-shaped coupling coils.

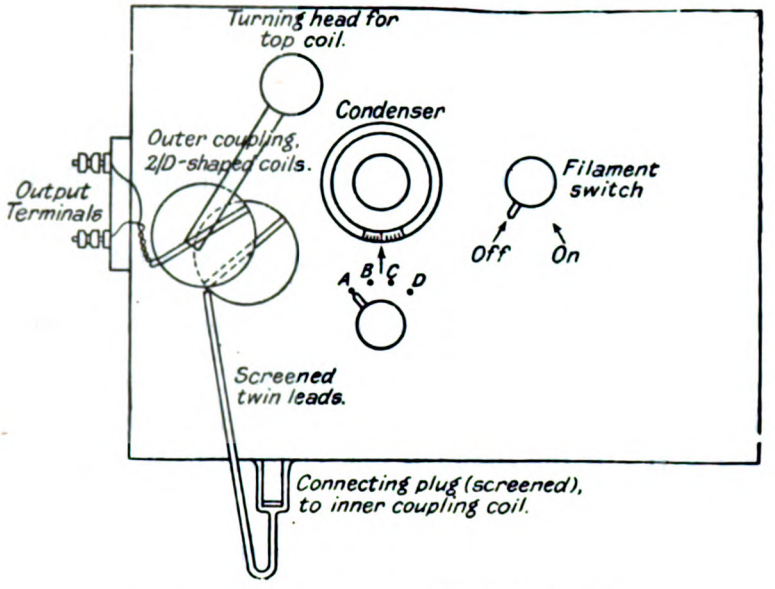


Fig. 5. Plan of Exterior of Screened Oscillator.

10. *Variation of the Screening Effect with Frequency.*

When a sheet of metal is placed in an alternating magnetic field, eddy currents are set up in the conductor, the field from which will tend to counteract the original magnetic field. The penetration of these eddy currents into the conductor will be governed by the ordinary well-known " skin effect " formulæ, and hence the latter will determine the fraction of the original magnetic field which penetrates to any depth in the conductor. The decay factor governing the amplitude of the high-frequency current at a depth " $x$ " below the surface of the metal is $e^{-2\pi\sqrt{\mu f \rho}\cdot x}$, where " $\mu$ " and " $\rho$ " are the permeability and resistivity respectively of the metal and " $f$ " is the frequency of the alternations.

In the present case, this indicates that the field at a depth " $x$ " is reduced to the fraction $a = e^{-2\pi\sqrt{\mu f \rho}\cdot x}$ of its original value at the surface of the metal. Hence, if the strength of the original magnetic field and the limiting value to which this must be reduced be known, the thickness of the metal required for the screen can be calculated.

In the absence of knowledge of the absolute magnitude of the " screened " field the comparative dimensions of the screens for different metals and frequencies may be obtained. For example, for a given frequency the thickness of iron and copper to produce the same values of " $a$ " above may be obtained.

| | | |
|---|---|---|
| For copper | $\mu = 1$ | $\rho = 1{,}600$. |
| ,, iron | $\mu = 300$ | $\rho = 16{,}000$ approximately. |



Digitized by Google

Hence

$$\frac{x_{\text{copper}}}{x_{\text{iron}}} = \sqrt{\frac{1,600}{1} \times \frac{300}{16,000}}$$

$$= \sqrt{30}$$

$$= 5{\cdot}5$$

*i.e.*, it requires 5·5 times the thickness of copper to screen as effectively as a given thickness of iron.

The above expression also shows that the thickness of metal required to produce a given value of "$a$" varies as $\sqrt{\frac{1}{f}}$. In screening a circuit from a stray magnetic field, however, the usual condition is that the induced E.M.F. in the circuit shall be reduced below a certain limiting value. Now the E.M.F. induced in a coil by an alternating field of strength H $\propto f \times$ H. If the circuit is now shielded by a metal sheet, the induced E.M.F. becomes

$$\mathrm{E} = f \times e^{-2\pi\sqrt{\mu f/\rho}\,.\,x} \times \mathrm{H},$$

which is the true equation giving the variation of the screening effect with frequency.

Thus, suppose it is required to determine the comparative thicknesses ($x_1$, $x_2$) of a metal necessary to give the same screening effect at frequencies of 100 and 1,000,000 cycles per second. In this case we have

$$10^2 \times e^{-2\pi\sqrt{\mu 10^2/\rho}\,.\,x_1} = 10^6 e^{-2\pi\sqrt{\mu 10^6/\rho}\,.\,x_2}$$

$$e^{-2\pi\sqrt{\mu/\rho}\,.\,x_1} = 10^4 e^{-2\pi\sqrt{\mu/\rho}\,.\,10^3 x_2}$$

$$-20\pi\sqrt{\frac{\mu}{\rho}}x_1 = \log_e 10^4 - 2000\pi\sqrt{\frac{\mu}{\rho}}x_2.$$

For copper, $\mu = 1$ and $\rho = 1,600$; hence

$$\frac{\pi}{2}x_1 = 50\pi x_2 - 2{\cdot}3 \times 4$$

$$x_1 = 100x_2 - \frac{18{\cdot}4}{\pi}$$

$$x_1 = 100x_2 - 5{\cdot}86.$$

Thus, if a thickness of copper $x_2 = \frac{1}{8}'' = 0{\cdot}32$ cm. is required to give effective screening

Digitized by Google

at $10^6$ frequency, then at a frequency = 100 cycles per second the thickness required to give the same screening effect is

$$\begin{aligned} x_1 &= 100 \times 0{\cdot}32 - 5{\cdot}86 \\ &= 32 - 5{\cdot}86 \\ &= 26{\cdot}14 \text{ cms.} \end{aligned}$$

This example would appear to demonstrate that the difficulties of screening are greatly enhanced at frequencies well below the radio limit—*e.g.*, within the range of audible frequencies, as used in many forms of inductance and capacity bridge measurements.

Since this Paper was written I have learnt that some experimental work on screening has been carried out at the R.A.F. Instrument Design Establishment, Biggin Hill, and at the Army Signals Experimental Establishment, Woolwich ; but no details of this have yet been published. The results of the work at Biggin Hill are already being used, however, in the design of wireless instruments.

Digitized by Google

Digitized by Google

# THE VALVE-MAINTAINED TUNING-FORK AS A PRECISION TIME-STANDARD

BY

D. W. DYE, B.Sc., A.C.G.I.,
SENIOR ASSISTANT IN THE ELECTRICITY DEPARTMENT.

Digitized by Google

## ABSTRACT.

A series of experiments is described on the variation in frequency of a valve-maintained tuning-fork under various conditions of operation.

The quantitites investigated were :—

(i) Temperature coefficient.
(ii) Effect of variation of filament current and anode voltage.
(iii) Effect of variation of grid and anode circuit condensers.
(iv) Effect of variation of polarising magnetic field.
(v) Effect of variation in the amount of energy taken from the output circuit of the fork.
(vi) Effect of adding various circuits in series in the anode circuit of the valve.
(vii) Effect of adding a mass to various parts of the mounting and of tilting the whole fork sideways and up and down.
(viii) Absolute measurement of frequency of the fork.

A number of conclusions are drawn up and suggestions made for further work.


Digitized by Google

# THE VALVE-MAINTAINED TUNING-FORK AS A PRECISION TIME-STANDARD.

By D. W. DYE, B.Sc., A.C.G.I., Senior Assistant in the Electricity Department.

[Reprinted from the 'Proceedings of the Royal Society', Series A, Vol. 103, 1923.]

## Introduction.

The system of driving a mechanical oscillator by means of a triode was first described by Eccles (1).

As applied to the maintenance of vibration of a tuning-fork, the method possesses very great advantages over any previously arranged electro-mechanical method. The complete absence of any attachments to the vibrator, together with the property of perfect self-starting, enables conditions of steadiness in operation to be realised which would not be otherwise possible. One such tuning-fork in use at the N.P.L. controls a multivibrator (2) and so forms the foundation of the radio-frequency standards of the laboratory

In view of the great accuracy of measurement attainable, and of the importance of such a radio-frequency standard, it was thought desirable to make measurements on the controlling tuning-fork under various conditions, in order to ascertain what constancy and reliability might be expected under the conditions of use. The method used was one in which beats between two forks were measured by stop-watch, under conditions such that one fork was kept as invariable as possible, whilst the second fork had adjustments made in the various quantities which might be expected to cause variations in frequency.

## Mounting of the Tuning-Forks.

The forks will be designated A and B throughout the Paper. Fork A had been used for two years for controlling the multivibrator. Fork B was made up specially to carry out this investigation and was almost identical with A, except that the air-gaps between the poles and the prongs of the fork were somewhat larger than on fork A.

The general arrangement of the mounting, also the electrical and physical quantities involved, are given in fig. 1, below, which refers to fork B.

The principal dimensions are as follows :—

*Tuning-fork* (Valentine and Carr)—Prong dimensions: breadth 9·0 mm., depth 13·9 mm., length 86 mm.

Anode winding on bobbin $C_1$ consists of about 9,000 turns of No. 47 d.s.c. wire, having a d.c. resistance of 7,000 ohms.

Grid winding on bobbin $C_2$ consists of about 11,000 turns of No. 47 d.s.c. wire, having a d.c. resistance of about 7,000 ohms. Underneath the anode winding on $C_1$ is an output winding of 2,000 turns No. 44 d.s.c. wire, having a resistance of 290 ohms.



Digitized by Google

The bobbins are fitted on to laminated iron-wire bundles, forming polar projections 1 cm. diameter of the polarising magnet, M. The air-gaps between the poles and the prongs of the tuning-fork are about 0·6 mm. Screws, S, serve to locate the magnet exactly

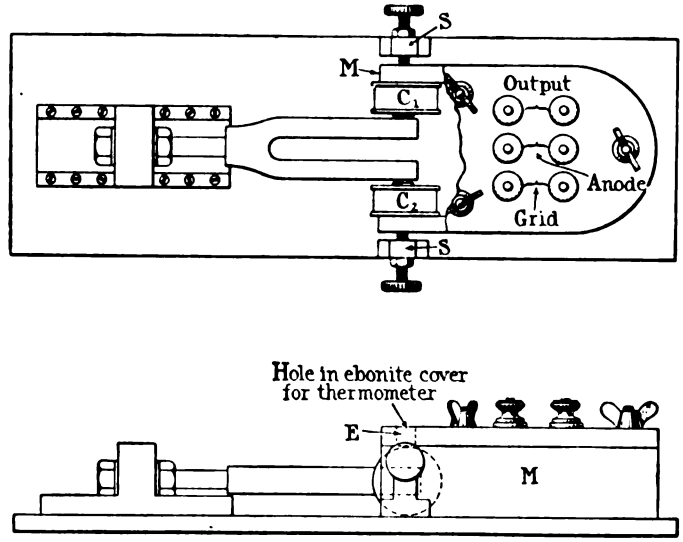


**Fig. 1. Mounting of tuning-fork.**

with respect to the prongs of the fork. An ebonite cover-plate, E, clamps the magnet down on to the brass base and carries the terminals of the anode, grid, and output windings.

Fork A had a fixed condenser of 0·004 mfd. capacity in parallel with the grid winding

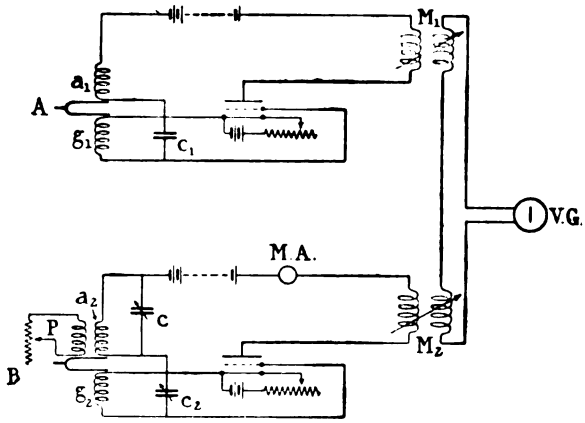


Fig. 2. Circuits for comparison of frequency of tuning-forks.

($C_1$ in fig. 2). On fork B variable condensers were used in parallel with both grid and anode windings.

The forks were encased in padded boxes and rested without constraint, loosely, on cotton-wool, so as not to cause any uncertain nodal points on the base, such as might

Digitized by Google

occur if they rested on a partly solid support. Accurate thermometers, reading to 0·01° C., were mounted so that their bulbs came between the prongs of the forks. The temperature conditions were steady in all the experiments.

The quantities investigated were :—

(*a*) Temperature coefficient.
(*b*) Effect of variation of filament current and anode current and anode voltage.
(*c*) Effect of variation of grid and anode condensers.
(*d*) Effect of variation of polarising magnetic field.
(*e*) Effect of variation of energy taken from the output winding.
(*f*) Effect of adding various circuits in series in the anode circuit as an alternative means of taking out power.
(*g*) Effect of adding a mass to various parts of the mounting and of tilting the whole fork and mounting sideways and up and down.
(*h*) Absolute measurement of frequency.

## Method of the Tests.

The arrangements for varying the quantities and observing the beats were as shown in fig. 2. Each tuning-fork and valve were fed by their own separate batteries, and the beats were observed on a Duddell vibration galvanometer, V.G., tuned to the frequency of fork A. The mutual-inductance couplings, $M_1$ and $M_2$, were small, and the reaction of one fork on the other through these mutuals was found to be entirely negligible. By adjustment of $M_1$ or $M_2$ the amplitudes of the vibration produced by each fork on the galvanometer were made exactly equal, so that when they were opposed during the beat the line came out quite sharply on the galvanometer spot. By this means the rate of the beats was observed with great accuracy. Even when the beats were so slow that they were at the rate of one beat in 200 seconds, zero point could be located in time to within one or two seconds.

We will now turn to the particular quantities studied, in the order given previously in the Paper.

### (*a*) *Temperature Coefficient.*

This is one of the most serious causes of variation of frequency of a tuning-fork. In the case of an ordinary simple tuning-fork, with no attachments, the frequency coefficient is well established for the ordinary low-carbon steels. It is chiefly due to the variation of the modulus of elasticity with temperature. For mild or cast-steel tuning-forks, the temperature coefficient of frequency is never very different from $-1{\cdot}15 \times 10^{-4}$ per 1° C.

In the case of the valve-maintained tuning-fork, B, the coefficient was determined by



Digitized by Google

placing the fork in its padded box in temperature-regulated vaults at various temperatures; the fork was at least 48 hours in a sensibly constant temperature before observations were made. Fork A was kept under practically constant temperature conditions throughout the tests.

The results on both forks are given in Table I below.

TABLE I.

| Fork. | Temperature range, ° C. | Frequency coefficient per 1° C. |
|---|---|---|
| A | 15 — 21 | $-1{\cdot}1_8 \times 10^{-6}$ |
| B | 15 — 21 | $-1{\cdot}2_0 \times 10^{-6}$ |

These values are seen to be in close agreement with the accepted values for a free tuning-fork. The probable accuracy of these coefficients is $\pm 3 \times 10^{-6}$.

(*b*) *Effect of Variation of Filament Current and Anode Voltage*; *and*
(*c*) *Effect of Variation of Grid and Anode Condensers.*

Owing to the interdependence of (*b*) and (*c*) it was necessary to consider these together. The following series of tests were therefore made :—

(I) *Anode Voltage Constant* = 40 volts.

A family of curves was obtained giving change of frequency when anode current was varied by varying the filament brightness. Each curve corresponds to a particular value of grid capacity and a particular value of anode capacity. The families of curves are thus really a series of interlacing families, and are distinguished by different kinds of lines.

The following cases were taken and are shown by the curves of fig. 3, in which the various sets are distinguished by different kinds of lines as follows :—

*Full-line Curves* : Nos. 1, 2, 3 and 4.—Added anode capacity = 0 mfd. Grid capacities of 0·003, 0·005, 0·007 and 0·009 mfd. respectively.

*Dotted-line Curves* : Nos. 5, 6 and 7. Added anode capacity = 0·003 mfd. Grid capacities of 0·003, 0·005 and 0·007 mfd.

*Chain-line Curves* ; Nos. 8, 9, 10, 11, 12. Added anode capacity = 0·005 mfd. Grid capacities of 0·001, 0·0025, 0·0028, 0·003 and 0·005 mfd. respectively.

Two other cases (curves 13 and 14) were also taken with added anode capacity of 0·001 mfd. and added grid capacity of 0·003 and 0·006 mfd.

These curves bring to light a number of interesting facts ; some of these are explained in accordance with the theoretical treatment of the valve-maintained mechanical oscillator

Digitized by Google

as given by BUTTERWORTH (3). There are, however, a number of factors variations of which can cause a change of frequency. These are not included in the mathematical assumptions, for example, the effective resistance of the anode-filament and the grid-filament paths of the valve itself, polarising field, output circuit, &c. These effects are so interdependent on one another that it is almost impossible to arrange the experiments so as to vary only one factor at a time. The changes in frequency due to anode and grid

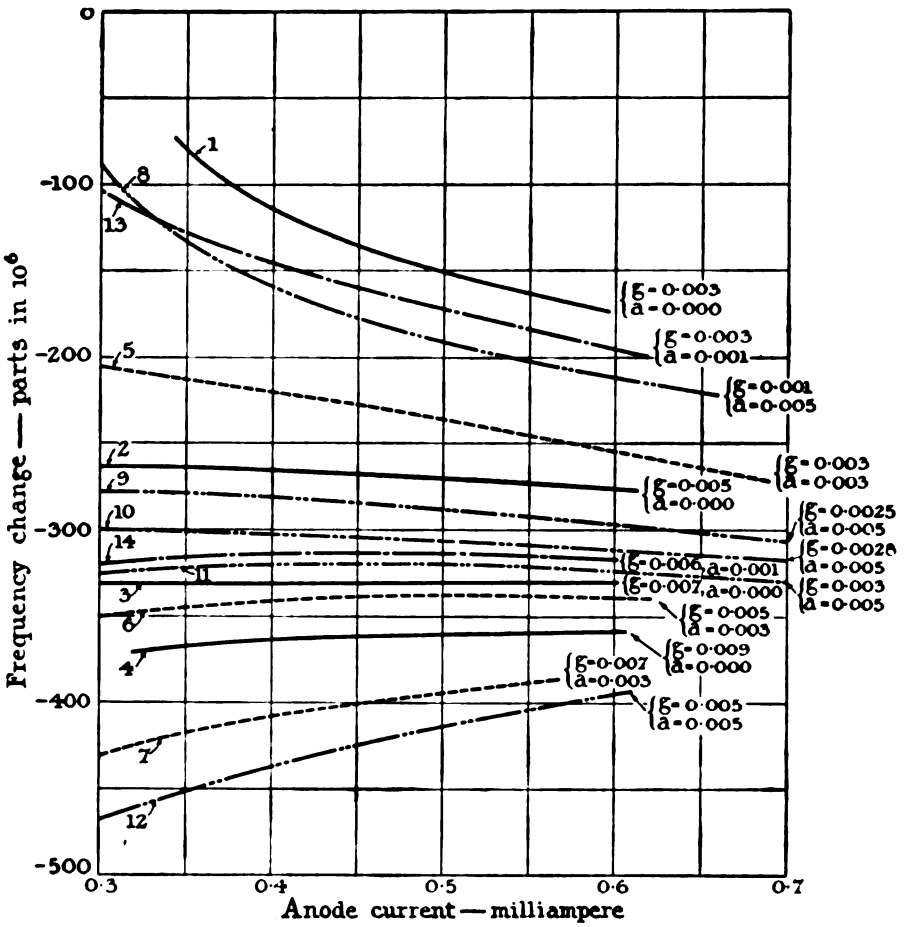


Fig. 3. Variation of frequency with anode current varied by filament brightness.

capacity variations are, however, so large that there is little doubt that they are mainly those developed by BUTTERWORTH and given in equations (19) and (20) in the paper previously referred to. Equation (19), giving variation of operating frequency when the electrical free frequency of the anode and grid circuits is varied, may be written

$$\frac{\omega^2}{\omega_1^2} = 1 + \frac{\sigma^2 x}{x^2 - \mu^2}, \text{ where } x = \frac{C_{res.}}{C_1} - 1. \quad . \quad . \quad . \quad . \quad . \quad . \quad . \quad (1)$$

This equation refers to the case where grid and anode windings are identical, and in which the capacities are varied so as to have always the same value on each winding.

Digitized by Google

The terms have the following meanings :—

$\omega$ = Frequency of steadily maintained vibration.

$\omega_1$ = Free frequency of the fork.

$\alpha$ = Equivalent mass of the fork $\doteqdot \frac{1}{2}$ mass of one prong.

$\beta$ = Damping coefficient in the fundamental equation of motion of the fork.

A = Force acting on the prong due to unit current in the grid or anode winding.

$\mu = R/L\omega_1$ where R and L are effective resistance and inductance of grid or anode windings (windings assumed equal).

$\sigma^2 = \frac{2A^2}{L\alpha\omega_1^2}\left(1+\frac{\beta R}{A^2}\right)$; it is a term analogous to coupling coefficient between electrical circuits.

The various constants of the fork and associated circuits have been approximately measured and are as follows :—

Half mass of one prong = 45 grm. = $\alpha$.

Log dec. of fork as mounted $\doteqdot 0{\cdot}0005$, giving a value for $\beta$ of 45.

Free frequency of fork (nominal) = 1,000 cycles per second.

$A = 4{\cdot}1 \times 10^7$ dynes per unit current (10 amperes) (obtained by observation of the change in the magnetic gap flux due to a small current sent through the anode coil).

The electrical constants were measured and were found to be :—

Added capacity in parallel with the anode winding necessary to give a frequency of resonance at 1,000 cycles per second = 4·2 milli-mfd.

For this test an inducing coil of 0·5 henry was used in series with the anode coil, and an electrostatic voltmeter of about 100 $\mu\mu$F capacity was used as detector of resonance.

If we take the total resonating capacity to be 5 milli-mfd., including the voltmeter and leads and the self capacity of the anode coil, we get for the effective self-inductance of the anode winding the value L = 4·5 henries. The measured effective resistance of the anode winding at a frequency of 1,000 cycles was found to be 27,000 ohms. (The d.c. resistance was about 7,000 ohms.) These measurements were, of course, made with the fork held so that it could not vibrate.

From these two measurements the values of " $\mu$ " and $\sigma^2$ were found to be $\mu^2 = 0{\cdot}95$ and $\sigma^2 \doteqdot 7{\cdot}2 \times 10^{-4}$.

For the grid coil the resonant capacity was found to be 2·6 milli-mfds., giving, on the same assumptions as above, the values of 6·9 henries for effective self-inductance of the grid winding.

The value of $\mu$ assumed by BUTTERWORTH in calculating the curves showing variation of frequency and ease of maintenance was $\mu = 0{\cdot}02$, *i.e.*, nearly fifty times smaller than the experimental value found for this fork. The effect on the curves is to elongate the

Digitized by Google

abscissa scale very greatly. For small values of "$x$" the formula for ratio of frequencies reduces to the very simple one

$$\omega^2/\omega_1^2 = 1 + \sigma^2 x/\mu^2 \quad . \quad . \quad . \quad . \quad . \quad . \quad . \quad . \quad . \quad . \quad . \quad (2)$$

The formula so developed refers to the restricted case where the two electrical circuits are identical, *i.e.*, the capacities across the (assumed equal) grid and anode windings are always equal. The experiments were not carried out in a manner to suit these theoretical assumptions, and so cannot be directly compared with the theoretically calculated values of frequency change.

It will be seen from the curves (fig. 3), that the effects of capacity on grid or anode separately are very similar and in the same direction. Increasing capacity causes a

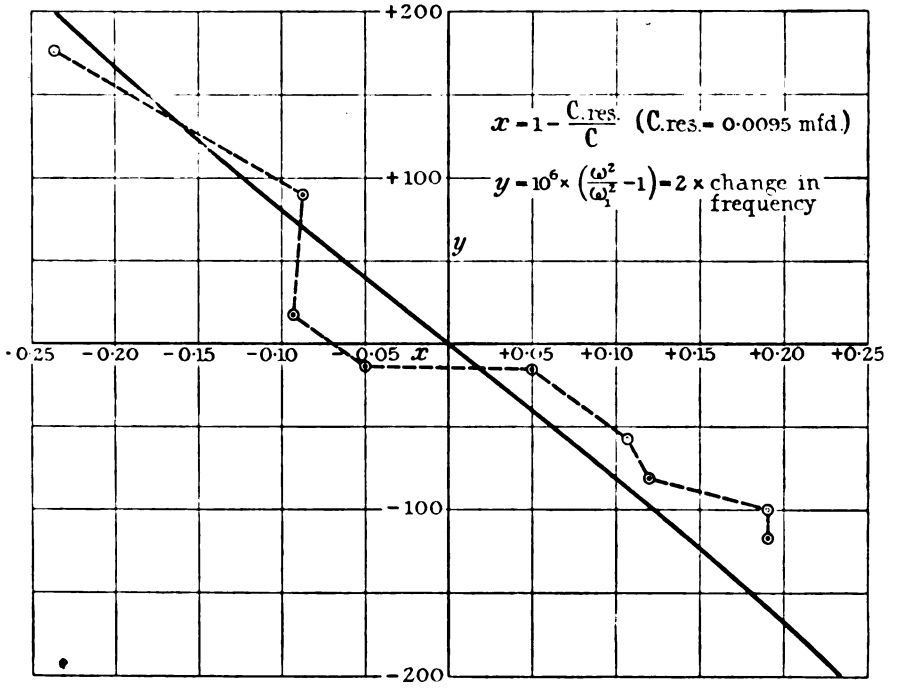


Fig. 4. Effect on frequency of capacities across the windings.

diminution in frequency, which is of the same order for variation of either grid capacity or anode capacity.

Confining attention to the curves in the region where they are nearly horizontal, we can use equivalent values of grid capacities corresponding to a grid winding inductance equal to that of the anode winding. If now we add both capacities together we can calculate experimental values of "$x$" and $\omega^2/\omega_1^2 - 1$. In deducing the values of $x = \frac{C_{res.}}{C_{eff.}} - 1$ the value of $C_{res.}$ has been taken as 0·0095 mfd. These results are plotted in fig. 4.

The curve $\omega^2/\omega_1^2 - 1 = \sigma^2 x/\mu^2$ is also drawn using the independently determined values of $\sigma^2$ and $\mu^2$. The values of $\omega_1^2$ read off from the curves are those corresponding to an anode current of 0·5 milliampere. The irregularity of the experimental curve

Digitized by Google

is not due to errors of observation, but indicates that it is not correct to add together the capacities in the two circuits in the manner described above, or that it is incorrect to assume the same anode current for all the various cases. The rough agreement is, however, all that is intended to be shown.

Turning to these curves it will be seen that a remarkable compensating effect occurs in regard to frequency variation for curve (3). For an anode current variation from 0·25 to 0·6 milliampere, the maximum change in frequency is of the order of one part in a million only. Such an exactness of compensation is probably accidental, since, as will be seen later, changing the valve disturbs this compensation when changes of only a few parts in a million are in question. This condition of compensation is of great value, and indicates that so long as the magnetic, mechanical, and electrical constants of the fork are invariable, then values of the latter can be chosen so that considerable variations of the voltages of the filament and anode batteries are of negligible consequence.

In further pursuance of the quantities governing this condition other combinations of grid and anode capacity were tried, and other similar cases were found as shown by the neighbouring curves. No case could be found, however, so good as that shown in curve No. 3.

(II) *Effect of Varying Anode Voltage.*

An immense number of observations would have been involved in order to have investigated the foregoing capacity and anode current effects at a number of voltages; accordingly, only one capacity case was taken, viz., that case showing compensation,

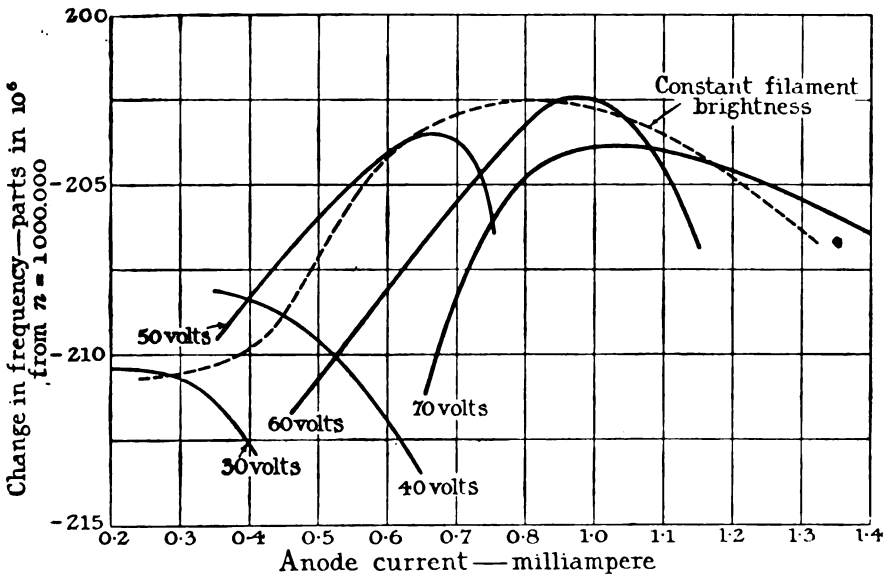


Fig. 5. Anode current : frequency curves for various anode voltages.

where C (grid) = 0·007 mfd., and C (anode) = 0·000 mfd. The results of these experiments are shown in fig. 5. In comparing these curves with those of fig. 3 it must be remembered that the scales are such that the curvature and slopes are magnified

Digitized by Google

fifty-fold. It should be mentioned here that a different valve was used in these experiments.

The voltage variation curves have been taken for one case of grid and anode capacities over the working range of anode current for each case of anode voltage. Variation of anode current was made by insertion of resistance in the filament battery circuit. A dotted curve is shown intersecting all the other curves. This curve represents the change in frequency which occurs when nothing but the anode voltage is allowed to vary. There will, of course, be a whole series of such dotted curves for particular values of filament brightness, but only one such has been taken. These curves show that there is a best voltage from the point of view of variation of frequency with anode current, and also that at this voltage there is a best value of anode current from the ponit of view of variation of anode voltage. In the case of the particular valve used this point occurs with 70 volts on the anode and with an anode current of about 1 milliampere. Under these conditions, a 10 per cent. change in either direction of anode current, or anode voltage, causes less than one part in a million change in frequency.

*Effect of Changing the Valve.*—A variety of different valves were tried, all of the four-pin type, including a Mullard small filament current S.R. valve. The curves for these are given in fig. 6 for one anode voltage and the same condenser case as above. It will

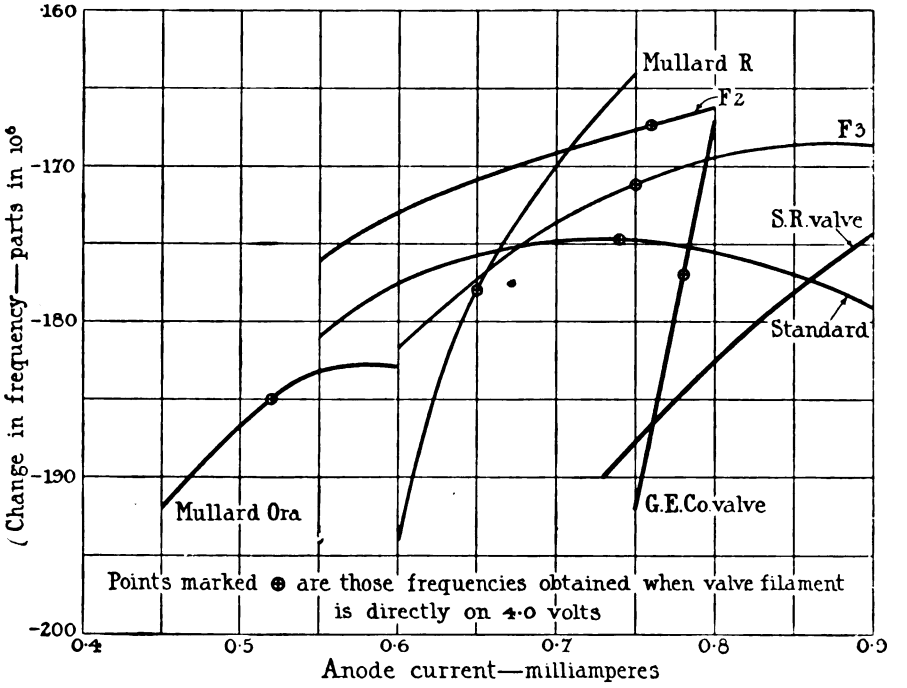


Fig. 6. Effect of using different valves.

be seen that considerable variations can occur in frequency when one valve is changed for another. The points marked thus ⊕ show the frequency obtained for each valve, when any of them (except the S.R. valve) is simply plugged in on a fixed voltage of 4 volts.



Digitized by Google

Judged thus, it will be seen that there is little more than one part in 100,000 change in frequency when one valve is changed for another. The range of the curves represents a variation of 2 to 6 volts on the filament.

### (*d*) *Effect of Polarising Magnetic Field.*

This was known to be considerable and is probably caused by a change in Young's modulus or by a change in the mode of vibration. The method of experiment was very simple. An auxiliary permanent magnet was supported at varying distances from the magnet of the fork. By thus superposing a magnetic field either helping or opposing the main field, a variation of 2 : 1 could be made in the gap flux between the cores and prongs of the fork. The flux was measured by the help of a very thin search coil, which

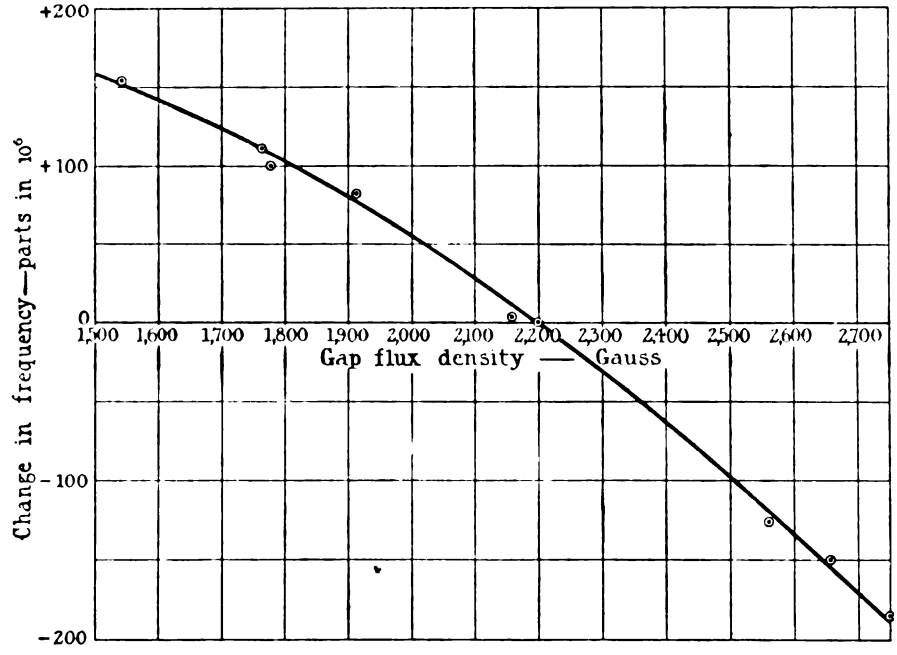


Fig. 7. Effect of polarising field on frequency.

could be withdrawn from the narrow air-gap between the magnet cores and the prongs of the fork. The curve showing change of frequency plotted with gap-flux-density is given in fig. 7. The curve shows that an increase in field strength causes a lowering of frequency and also that this change is greater per unit change of field, with increasing field strength. The normal gap-flux density was B = 2,200. At this point a change of + 1 per cent. in gap flux causes a change of — 6·5 parts in a million in frequency. The change in flux density produced by an anode current of 1·0 milliampere was found by experiment to be about fifty lines per sq. cm. With an anode current of 0·5 milliampere there should, therefore, be a change of fifteen parts in a million on reversal of the connection of both grid and anode windings. An experiment showed that the actual change in frequency was about eleven parts in a million, which is as close agreement as could be

Digitized by Google

expected in view of other effects probably accompanying a reversal of connections. From these results it will be seen that constancy of the polarising field to 1 per cent. is necessary, if constancy to a few parts in a million is desired in frequency. The method of mounting used by ECCLES is probably better, but this method could not be used without constructing special magnets. It was observed that weakening the field down to B = 1,500 made very little difference to the amplitude of the fork.

### (*e*) *and* (*f*) *Effect of taking Power from the System.*

The fork was originally intended to deliver a small amount of electrical power from an output winding underneath the anode winding; as will be seen later it is preferable to take out power by means of circuits added in the anode circuit.

(*e*) *Output Winding on same Core as Anode Winding.*—This case was very simple to deal with. Non-inductive resistances, from $\infty$ to 0, were connected across the output terminals and the effect on frequency observed by beats in the ordinary way. On some occasions the current was measured by a tuned Duddell vibration galvanometer in series, and on other occasions a low reading electrostatic voltmeter was used to measure the voltage across the external resistance.

The first case taken was that corresponding to invariability of frequency with anode current. The conditions were :—

| | |
|---|---|
| Anode volts . . . . . | = 50. |
| Anode current (varied somewhat with load) . . | = 0·7 to 0·85 milliamp. |
| Anode capacity . . . . . | = 0·000 $\mu$F. |
| Grid capacity . . . . . | = 0·007 $\mu$F. |

The curves for this particular case are not given, but they were similar to those given in fig. 8. The change in frequency was about thirty parts in a million for an output of 100 microwatts. The smallness of output was disappointing in view of the relatively large change in frequency.

Tuning of the grid and anode windings was next resorted to in order to increase the power. The case chosen was that corresponding to approximate resonance in both grid and anode windings, viz., anode coil capacity = 0·004 mfd., grid coil capacity 0·003 mfd. The results are shown in fig. 8. Curve A shows change of frequency with change of R and curve B shows output for various values of R. This case showed considerable improvement over the previous one, in that the maximum output was about seven times as great and at the same time the total change in frequency was no greater. Unfortunately the change of frequency is very rapid in the region where R is high. This is just what should be avoided if it is desired to couple the output winding to another amplifying system having an impedance which is high and which might be variable.

(*f*) Experiments were next made using a mutual inductance with primary in the anode circuit and secondary connected to a variable resistance.



Digitized by Google

The first case tried consisted of a 100-millihenries mutual inductance, having primary self-inductance of about 250 millihenries and a secondary self-inductance of 100 millihenries. Its resistance was 40 ohms. Various resistances were again connected across the secondary winding and the changes in frequency observed together with the secondary current. The whole change in frequency was less than one part in a million for a variation of secondary resistance from infinity of 500 ohms. The output was, however, very small, the maximum being only about 100 microwatts. The open circuit secondary voltage was about 0·5. When the primary of the mutual was short-circuited a change of three parts in a million was produced.

A second case was taken using a larger mutual with lower resistance primary and having a condenser across it. This very greatly augmented the power available, as shown

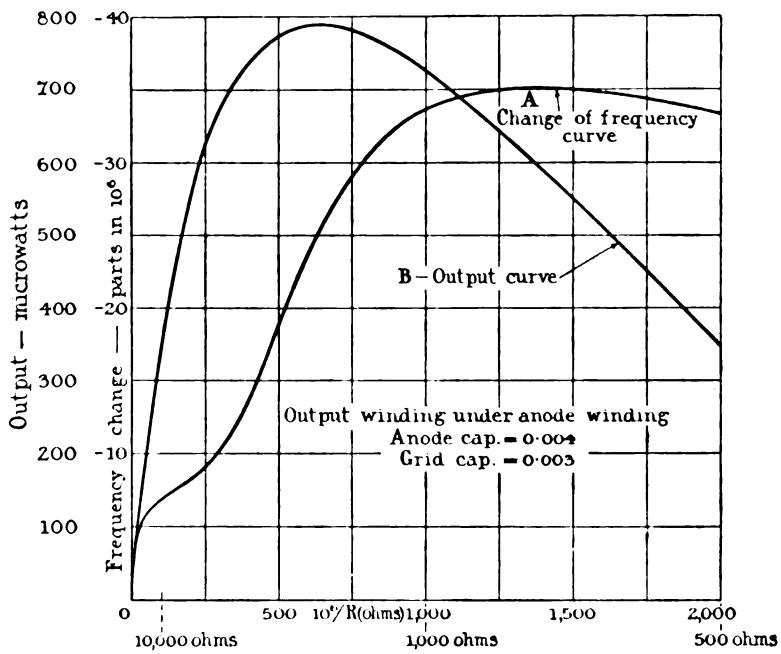


Fig. 8. Change of frequency with variation of electrical load on fork.

by the curve B (fig. 9). Curve A again shows change of frequency for this case. It will be seen that the total change of frequency possible over the whole range of secondary external resistance is no smaller than was the case with output winding on the driving core. The shape of the curve is, however, much better. When the grid-filament circuit of an amplifying valve was connected across the secondary of the mutual it caused a change in frequency of much less than one part in a million.

A number of curves connecting frequency with anode current were taken for various values of secondary resistance in order to determine what effect the tuned circuit had on the isochronism with respect to anode current. These are collected and labelled in fig 10. From an inspection of these it will be seen that the effect of the large added impedance in the anode circuit is to steepen somewhat the curves connecting frequency and anode current.

Digitized by Google

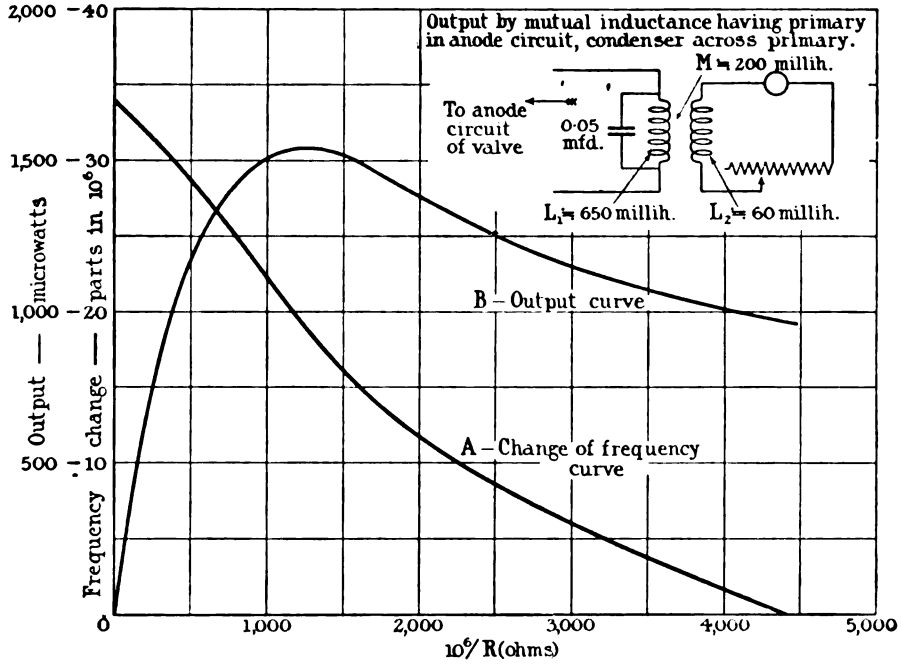


Fig. 9. Change of frequency with variation of electrical load on fork.

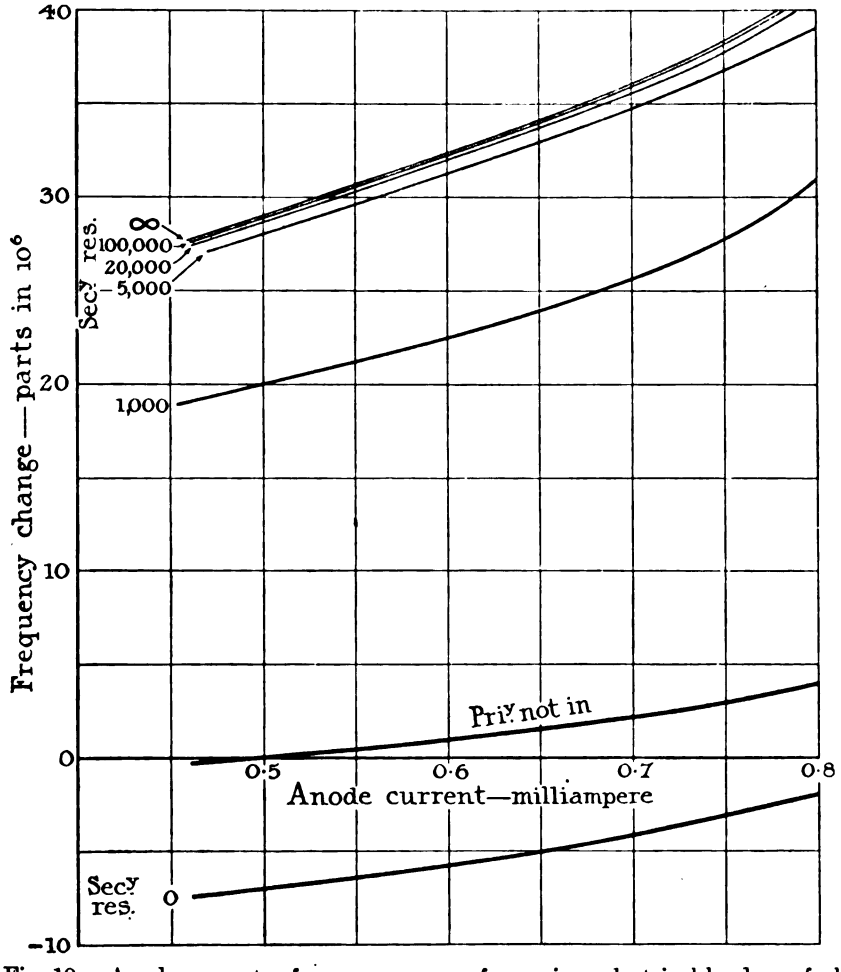


Fig 10. Anode current : frequency curves for various electrical loads on fork.

Digitized by Google

The whole change in frequency due to change of anode current from 0·5 to 0·8 milliampere is only ten parts in a million for any value of secondary resistance from $\infty$ to 0. The relatively large change in frequency produced by the insertion of the large impedance of the tuned mutual circuit is well seen in these curves. If it is specially desired to amplify the power when using the fork as a source, it will clearly be much more efficient to use a bigger mutual inductance. A mutual inductance of about 1 henry might be used giving a secondary voltage of about 12 volts. This applied to the grid filament circuit of an R valve, using 200 volts anode potential, would enable it to give practically all the power of which it was capable.

(*g*) *Effect of adding a Mass to Various Parts of the Mounting and of tilting the Whole Fork Sideways and Up and Down.*

A few simple experiments were tried of the effect of a mass placed in various positions as indicated on the diagram, fig. 11. The mass used was 1 kgrm.

The result of these experiments indicate that the position of the modal surfaces can be

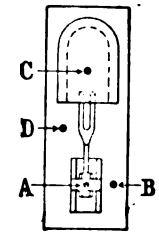


| Position of Mass. | Change in frequency, parts in $10^6$. |
|---|---|
| A | − 8 |
| B | + 15 |
| C | − 7 |
| D | + 32 |

Fig. 11. Effect of mass on base of fork.

appreciably changed by alteration of the effective mass of various parts. The effects are larger at the more flexible part of the base.

The effects of tilting the fork about are shown in the Table (fig. 12). The second and third columns show the position of the fork. The positions are also identified by the number in the first column.

| Position "elevation." Side. | Position "elevation." End. | No. | Change in frequency. |
|---|---|---|---|
| | | 1 | $0 \times 10^6$ |
| | | 2 | $-3 \times 10^6$ |
| 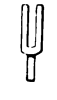 | | 3 | $-7 \times 10^6$ |
| 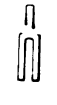 | 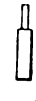 | 4 | $+10 \times 10^6$ |

Fig. 12. Effect of turning fork about.

It is interesting to note, in regard to positions 3 and 4, that a small change in frequency is to be expected on account of gravity. If we consider, as a rough approximation,

Digitized by Google

that the prong behaves as a rigid beam of uniform section freely pivoted at its upper end, then, under the influence of gravity, it would have a frequency of oscillation given by $n_g = \frac{1}{2\pi}\sqrt{\frac{3g}{2l}}$, where $l$ = length of prong. For the case in question, $l = 8{\cdot}6$ cm., giving $n_g = 2{\cdot}1$ complete vibrations per second. The proportional change of $n$ of the fork due to a superimposed vibromotive force, which, acting alone, would give it a frequency $n_g$, is given by

$$\frac{n - n_0}{n} = \pm \tfrac{1}{2}\frac{n_g}{{n_0}^2}.$$

For the case in question $\frac{n - n_0}{n}$ equals $\pm 1 \times 10^{-6}$ according to whether the prongs point upwards or downwards. The effective length of the prong will be less than the true length because of flexure, but the gravity effect will be probably not more than doubled on this account.

The effects observed are therefore much larger than could be accounted for by gravity, but are in the same direction. The effect would be greater on forks of slower frequency, and would be proportional to (length)$^{3\cdot5}$ for forks of constant thickness of prong. The effect of turning a fork of 100 ~ per second from an upright position through 180° might possibly be as great as 1 part in 10,000.

### (*h*) *Measurement of Absolute Frequency of the Fork.*

All the foregoing experiments have been carried out by observing differences between two forks, one of which was kept under as constant conditions as possible. In order to determine the absolute frequency, it is, of course, necessary to compare the vibrations of the fork with time obtained by means of a standard clock giving seconds.

For this purpose a phonic wheel was constructed, and has proved most successful. The wheel is of aluminium, and carries a thin-toothed rim of steel. The mean diameter is about 11 cm., and there are twenty teeth and spaces each about 0·85 cm. circumferential length. The top of the teeth are about 1·5 mm. above the bottom of the spaces. The proportions are therefore as in fig. 13.

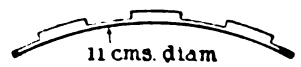

Fig. 13. Steel rim of phonic wheel.

A 50 : 1 worm wheel driven by the phonic wheel carries a small contact pin, which thus closes the circuit through the chronograph once each 1,000 alternations. This wheel and mounting has been very accurately made in one of the laboratory workshops, and the instant of closure of contact is certainly located to 1/1,000 second. The wheel is provided with three magnets from Brown receivers. Two of these serve for running the wheel up to speed as a valve-driven motor on the principle described by Eccles (4). By means of a two-stage amplifier, sufficient energy can be obtained to run the wheel up to a speed of well over 3,000 r.p.m., corresponding to a frequency of about 1,100 per second. The

Digitized by Google

grid magnet can be altered in its phase relation to the driving magnet. There is a third magnet mounted between the other two magnets. This one receives power from the fork by the help of a three-stage amplifier.

The synchronisation is very simply carried out. The wheel is run up to speed controlling its own power. During this process the power from the tuning-fork is weakly applied to the tuning-fork driving magnet. A milliammeter is included in the anode circuit of the valves feeding this magnet.

When the speed reaches that value corresponding nearly to synchronism with the fork, the beats are large on the milliammeter needle. By careful adjustment of speed and

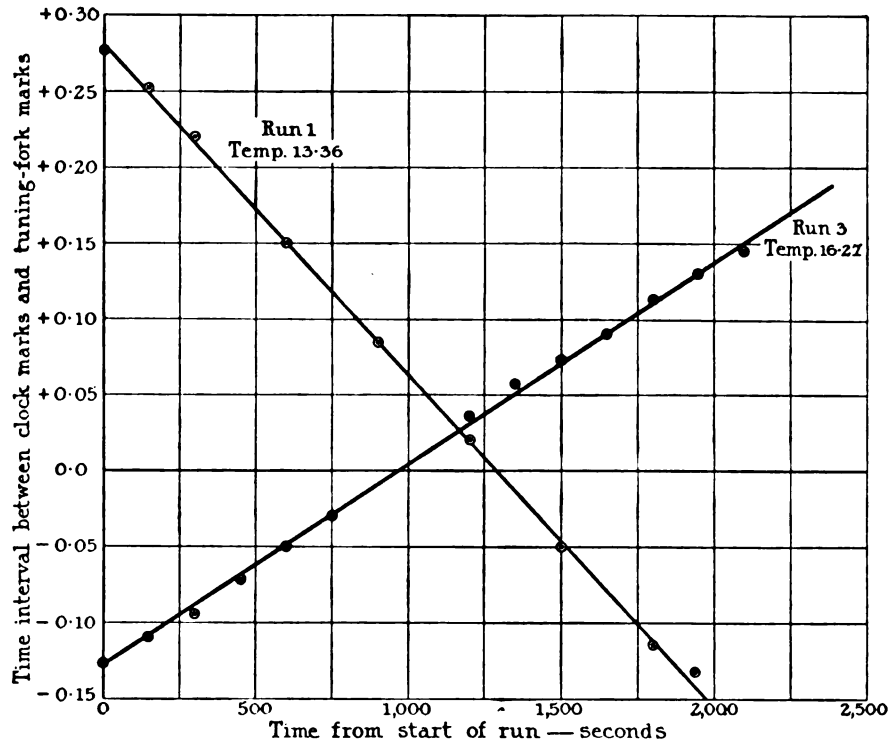


Fig. 14. Chronograph records.

steady increase of current in the tuning-fork magnet, the wheel is pulled into synchronism. The self-driving power is then smoothly reduced to zero, when the wheel then runs as a pure synchronous motor. In this way the tuning-fork records its own frequency directly on the chronograph without any attention and with extreme accuracy.

To obtain the fractional part of a second lost or gained by the fork during a run, time intervals between clock dots and tuning-fork dots, read off from the chronograph record, were plotted against the corresponding number of seconds from the start. This really amounts to straightening out the baseline of clock second dots given by the clock and greatly magnifying the differences between clock dots and tuning-fork dots. The nearest straight line drawn through the points gives the average fractional part of a second lost or gained by the fork during, say, 1,500 seconds. Two such lines are shown in fig. 14,

Digitized by Google

corresponding to runs Nos. 1 and 3 in Table II below. The particulars of three runs, made at intervals of about one month, are given in Table II, and show the great accuracy obtainable.

TABLE II.

| No. | Average temperature. | Fractional part of second gained by fork. | Time for gain given in Column 2. | Deduced frequency. |
|---|---|---|---|---|
| | ° C. | | | |
| 1 | 13·36 | $-0{\cdot}39_2$ | 1 800 | $1000{\cdot}21_8$ |
| 2 | 15·23 | $+0{\cdot}00_7$ | 2 550 | $999{\cdot}99_7$ |
| 3 | 16·27 | $+0{\cdot}29_7$ | 2 250 | $999{\cdot}87_0$ |

It is intended to accumulate chronograph records to see what amount of secular change of frequency occurs, due to ageing of the valve, fork, etc.

*Conclusions.*

A great deal more suggests itself as profitable research, with a view to obtaining the utmost invariability of frequency of valve-maintaining tuning-forks or other mechanical vibrators. In the case of a fork of the design used in this investigation the following points may be noted :—

(*a*) *Temperature Coefficient.*—This effect is by far the one most liable to cause variation of frequency. To obtain constancy to one part in a million, it would be necessary to keep the temperature constant to 0·01° C. By the use of one of the new nickel steels, such as " elinvar," which has a very much smaller change of elasticity with temperature, it is probable that the temperature coefficient could be reduced to one-tenth of that of ordinary steel forks.

(*b*) *Changes in Frequency due to Variations in Voltage and Filament Sources.*—It will be seen from the curves given that these are of no serious consequence. It is, however, desirable to have a milliammeter in the anode circuit. There is a drift in frquency during the first ten minutes after switching on. This is accompanied by small changes in anode current, so that it is desirable to set this current after allowing a quarter of an hour for settling down in cases where the utmost accuracy is desired.

(*c*) *Variations due to Changes in the Electrical Constants of the Driving and Attached Circuits.*—The accidental variations in inductance, capacity, and resistance would be so small as to be quite negligible in their effect on frequency.

The change in frequency which can be produced by intentional variation of grid-circuit or anode-circuit capacity forms a very convenient means of making changes of



Digitized by Google

a few parts in a hundred thousand in frequency. By the use of a variable condenser of 0·001 mfd. range, a smooth reproducible variation of 5 parts in 100,000 can be made in frequency. This is very convenient when using such a source on certain bridges depending on frequency, and when measuring minute changes in capacity in oscillatory circuits.

In order that the attached electrical circuits may have the least effect on frequency if so required, the conditions then are :—

(1) The damping of the fork must be as small as possible.

(2) The dynamical energy associated with the motion of the fork should be large compared with the electrical energy in the circuits.

(3) The damping of the electrical circuits should be large.

(*d*) *The Effect of the Magnetisation of the Fork.*—This is deleterious because it causes increased damping of the fork and introduces stresses and controlling forces which react on frequency. The driving is quite satisfactory with polarising fields of the order of 1,000 c.g.s. units ; this value might possibly be reduced still further without seriously affecting the amplitude. The form of drive adopted by Messrs. E. A. Eckhardt, J. C. Karcher and M. Keiser (5), as in fig. 15, is probably superior from a magnetic point

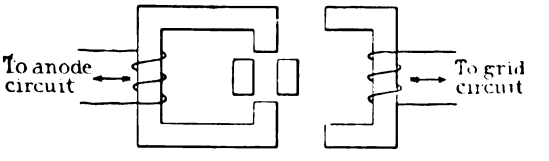


Fig. 15. Self-maintained tuning-fork system of E. A. Eckhardt, &c.

of view. In this system direct magnetic reaction between grid and anode circuits is used, but the author has no experience of the effects on frequency due to changes corresponding to those made in the present investigation.

Electrical capacity coupling to the prongs of the fork would probably be very perfect if the air damping could be sufficiently reduced.

(*e*) *and* (*f*) *Effect of Energy taken from the System.*—The energy is best taken from a circuit in series with the anode of the valve. For certain purposes this energy is sufficient but for a great many others a simple one- or two-stage amplifier is necessary.

(*g*) It is desirable to mount the fork very solidly and then to support the whole on a soft diffused bed, or perhaps on soft pads of rubber.

*General.*—The valve-maintained tuning-fork is capable of operating with a steadiness of frequency which is greater than is necessary for most purposes. The steadiness and invariability, which may be obtained by taking precautions, is very great. Such a time source, though secondary, opens up many possibilities in connection with investigations in which accurate short intervals of time are required. As an example of the use of such

Digitized by Google

a time-standard it may be possible to observe variations in the hourly rate of standard clocks. This is of some importance in connection with absolute measurements of fundamental electrical units.

In conclusion, my best thanks are due to Sir JOSEPH PETAVEL for his kindly interest in the work, and to the Sub-Committee A of the Radio Research Board, in connection with whose researches some of the work was undertaken.

## REFERENCES.

(1) W. H. ECCLES, 'Phys. Soc. Proc.', vol. 31, p. 269 (1919).
(2) H. ABRAHAM and E. BLOCH, 'C. R.', vol. 168, p. 1105 (1919).
(3) S. BUTTERWORTH, 'Phys. Soc. Proc.', vol. 33, p. 345 (1920).
(4) W. H. ECCLES and F. W. JORDAN, 'Phys. Soc. Proc.', vol. 31, p. 151 (1919).
(5) E. A. ECKHARDT, J. C. KARCHER and M. KEISER, 'Phys. Rev.', vol. 17, p. 535 (1921); *see also* 'Journ. Franklin Inst.', vol. 174, p. 61 (1922).



Digitized by Google

Digitized by Google

# A SELF-CONTAINED STANDARD HARMONIC WAVE-METER

BY

D. W. DYE, B.Sc., A.C.G.I.,
SENIOR ASSISTANT IN THE ELECTRICITY DEPARTMENT.

Digitized by Google

## ABSTRACT.

Following a brief introductory survey of the various methods of measuring radiofrequency, the principles of a highly accurate standard harmonic wave-meter are developed.

The essential principle is an arrangement of three-electrode valves, known as multi-vibrator, the invention of H. ABRAHAM and E. BLOCH. The arrangement produces a discontinuous wave, the frequency of which may be adjusted to have any value within very wide limits. When a current of such wave form acts by induction on another circuit, this circuit receives what may be considered as a series of electrical blows at equal intervals of time. If the circuit operated upon is highly resonant, then when its resonant frequency is set so as to be an integral multiple of the frequency of the blows, a large oscillatory current is built up, of a persistent kind and of a frequency whose ratio to that of the blows is quite exact.

In the apparatus developed and described there are two such multivibrators; one of these has a frequency of 1 kilocycle per second and the other has a frequency which is usually 20 kilocycles per second. The most important feature of the wave-meter is the means whereby the frequencies are kept constant. The two multivibrators are kept in harmonic synchronism with each other by the help of the reinforced twentieth harmonic of the low-frequency multivibrator. This is accomplished by the help of a special selector circuit and amplifying valve arrangement, tuned to a frequency of 20 kilocycles per second. The two multivibrators are further both controlled in frequency by means of an electrically maintained tuning-fork, of frequency of 1 kilocycle per second. This complete system therefore forms a source of electrical impulses of extremely steady and accurately known frequencies.

The impulses from either multivibrator can operate on a selector circuit, consisting of a standard variable condenser of special design and a set of six inductance coils of small damping decrement. By this means two complete series of harmonics may be selected, covering a range between 10 and 1,200 kilocycles per second. The frequencies produced do not depend upon the constancy of any electrical circuit. A selective amplifier serves to amplify any selected harmonic and by interference with an external source this latter may be set to exact synchronism with the harmonic.

The Paper is divided into seven main sections as follows :—

(1) Introductory.

(2) to (4) Principles of the multivibrator and experiments therewith to prove its suitability for the purpose in view.

(5) Fundamental principles governing the design of the wave-meter.

(6) General outline of the principal features of the construction, including the design of a condenser to give a uniform frequency scale.

(7) Methods of using the wave-meter and the possibilities connected therewith.

The Paper concludes with a short account of the precautions necessary to ensure certainty in using the wave-meter and some conclusions are given.


Digitized by Google

# A SELF-CONTAINED STANDARD HARMONIC WAVE-METER.

By D. W. DYE, B.Sc., A.C.G.I., Senior Assistant in the Electricity Department.

[Reprinted from the 'Philosophical Transactions of the Royal Society', Series A, vol. 224.]

## Introduction.

The measurement of the frequency and wave-length of electrical oscillations and waves has attracted the attention of many workers since the discovery of the oscillatory character of the discharge from a Leyden jar. The various methods of measurement adopted fall naturally into two classes: (1) Indirect methods, (2) direct methods.

(1) The indirect methods used have been many, but they fall mainly into two sub-divisions:—

(*a*) Those depending upon inductance and capacity in an oscillatory circuit and upon the exact adjustment of one or both of these so as to bring the circuit into the condition of electrical resonance or synchronism with the circuit under measurement.

(*b*) Those depending upon the ratio of currents in two branch circuits, the relative impedances of which vary with frequency. Instruments of this kind can be made direct reading in frequency or wave-length.

(2) The direct methods have been used to measure either frequency or wave-length, depending upon the region investigated; amongst the various methods which have been used may be mentioned:—

(*a*) High-frequency alternators.

(*b*) Photography of luminous discharges after reflection from a revolving mirror.

(*c*) Harmonic methods.

In the case of very high frequencies many measurements have been made by the help of stationary waves on wires. The wave-length is determined as a direct measurement and the frequency is deduced by calculation, using the accepted value of $v$.

Though of much interest, space forbids more than a few passing comments on these various methods of measurement.

The indirect methods depending upon resonance in an oscillatory circuit form the basis of the great majority of wave-meters constructed as portable instruments. The main advantages are ease and certainty of operation and adaptability to the end in view.

Digitized by Google

The accuracy also compares favourably with other electrical instruments whose indications are read off on a scale. The chief disadvantage of such wave-meters is the liability of the calibration to alter with time; this is mainly due to changes in the variable condensers commonly used in such instruments. For certain precise work also the setting of the condenser to the condition of synchronism cannot always be made with sufficient accuracy. There are, however, null methods whereby the condition of resonance may be indicated, and these are more accurate; they have not, as yet, been developed so as to be incorporated into a self-contained wave-meter.

The introduction of the self-generating wave-meter using a triode valve has removed the difficulty of accurate setting to resonance, but the effects of the valve and its associated circuits on the setting for resonance or synchronism may be serious.

Both of these types of wave-meter, however, serve very useful purposes, and for a great deal of work they cannot be displaced by any superior means of measuring frequency or wave-length at present.

By the use of carefully constructed standard inductance coils or loops and standard condensers, a standard of radio frequency accurate to one or two parts in a thousand can be established, but ultimately recourse must be had to a more absolute and direct method of measurement. The increasingly severe requirements for steadiness and accuracy of frequency of transmissions, and of tuning of receiving apparatus, render necessary a greater degree of accuracy and permanence in the wave-meters or other measuring devices than can be achieved in an instrument of the usual oscillatory circuit pattern.

The attention of many workers has therefore been turned to the direct methods of measuring radio frequency. Of these, the high-frequency alternator is the most direct of all, and in those transmitting stations equipped with steadily running high-frequency alternators nothing more is needed than a means of measuring the rate of revolution of the alternator shaft. The limitations of this method are obvious and need not be considered further.

The method of photography of luminous discharges, whilst fulfilling a useful purpose in the history of the development of frequency measurement, is complicated and troublesome to operate. It is further limited entirely to laboratory conditions; the results also are not directly known and are not very accurate on a single observation.

Much attention has been concentrated on harmonic methods of building up or down in frequency, so as to obtain a frequency or series of frequencies which are exact multiples or sub-multiples of some standard frequency which is known or can be measured.

Amongst those who have worked in this field may be mentioned SIMON and BARKHAUSEN (1), of the 'Physikalisch-Technische Reichsanstalt,' who developed the theory of harmonics in the Poulsen arc and showed what conditions governed the suppression or augmentation of harmonics, as desired. LINDEMANN (2) made use of these principles

Digitized by Google

in the calibration of wave-meters; H. DIESSELHORST and R. SCHMIDT (3) also have shown Lissajous figures of harmonics from a Poulsen arc by the help of a cathode-ray tube.

In 1919 MANDELSTAM, in working with buzzer-excited oscillations, observed that an augmentation of the current in the radio-frequency circuit was obtained when the tuning in this circuit brought the radio-frequency into exact harmonic synchronisation with the telephonic frequency of interruption of the buzzer current. There is also a small amount of control exerted by the buzzer-frequency on the radio-frequency when the latter is brought into almost perfect synchronisation with the former. TYKOCINSKI-TYKOCINER (4) carried out a careful investigation on these lines, using a buzzer which gave regular interruptions of telephonic frequency.

The steadiness of operation and adaptability of the three-electrode valve has, however, raised the level of accuracy attainable by harmonic methods to a much higher plane. J. S. TOWNSEND and J. H. MORRELL (5) experimented, at the short-wave end, on the harmonics and overtones of solenoids, using a Lecher wire system and building downwards in frequency harmonically. In a recent Japanese publication also, by AKIRA TSUBOUCHI (6), harmonic standardisation of wave-meters has been accomplished by using a standard circuit consisting of a single-loop inductance and standard condenser of Bureau of Standards pattern. Still more recently G. W. PIERCE (7) has utilised the mechanical resonances of piezo-electric crystal resonators (8) and crystal oscillators to obtain harmonic series of frequencies of known values in terms of the fundamental standard frequencies of the oscillators.

But the multivibrator of H. ABRAHAM and E. BLOCH (9) appears to be the most valuable source of harmonics yet devised for the purpose of producing known radio frequencies and possessed of the necessary steadiness and constancy.

This device forms the principle of the wave-meter about to be described, but before proceeding to this description, a very brief outline of the multivibrator principle may be permitted here in order to make the operation of the wave-meter clear and intelligible. (A complete description of the multivibrator is, of course, given in the Paper by H. ABRAHAM and E. BLOCH (9), mentioned above.)

## 2. PRINCIPLE OF THE ABRAHAM-BLOCH MULTIVIBRATOR.

The scheme of connections is shown in fig. 1, which is symmetrical except for the connections at x in the grid leak path of valve $V_2$. An inducing coil is connected to these terminals for the purpose of applying the electrical impulses to an oscillatory circuit.

Referring to fig. 1, $r_1$ and $r_2$ are two resistances of about 50,000 ohms each in the main anode circuits. The points $P_1$ and $P_2$ are connected to the grids $G_2$ and $G_1$ respectively through adjustable condensers $C_1$ and $C_2$. The grids $G_1$ and $G_2$ are connected



Digitized by Google

through leak resistances $R_1$ and $R_2$ respectively to the filaments. These resistances have the value of about 75,000 ohms each.

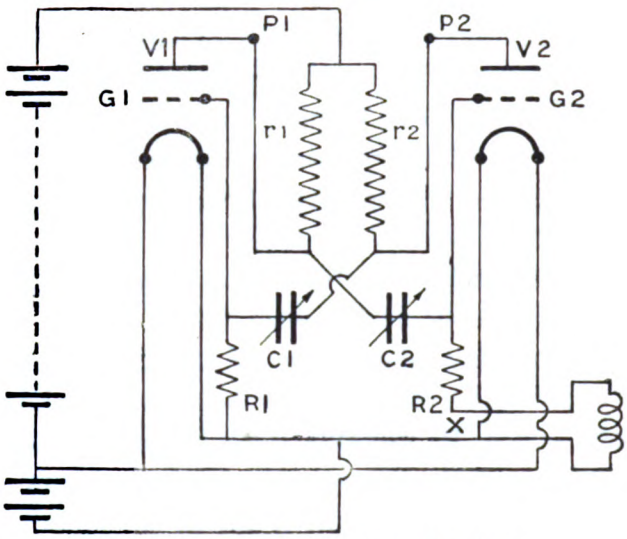


Fig. 1. Abraham-Bloch multivibrator.

The operation is most easily followed by reference to diagram fig. 2, reproduced from actual photographs taken at the National Physical Laboratory on an Einthoven string galvanometer, of a multivibrator operating at a fundamental frequency of about 20 cycles per second.

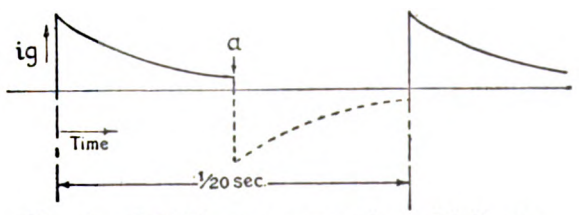


Fig. 2. Grid-filament current in multivibrator.

The curves give current variations in the grid coil on X. The voltage variations between grid and filament will be approximately similar to the current variations. Assume the apparatus to be operating in its steady cyclic state and consider the sequence of events immediately following an inversion at the instant "*a*". The voltage of $G_2$ has become strongly negative and has caused the anode current in valve $V_2$ to suddenly become zero. This negative voltage diminishes towards zero by reason of leakage through $R_2$, of the charge on the condenser $C_2$ and on $G_2$. When the voltage has become small, but before reaching zero value, anode current begins to flow again in valve $V_2$; this causes a diminution of anode voltage at the point $P_2$; this diminution is transmitted *via* condenser $C_1$ to grid $G_1$. The result of this fall in potential of $G_1$ is to cause a decrease in anode current of $V_1$, thus increasing the voltage at the point $P_1$. The consequent rise in grid potential of $G_2$ accelerates the increasing anode current in $V_2$. Finally the potential of grid $G_1$ becomes sufficiently negative as a result of the increased

Digitized by Google

potential fall on $r_2$ to reduce the anode current in $V_1$ to zero. The cycle outlined above now recommences, and may be traced by interchanging the suffixes 2 and 1 wherever they occur above. When the change-over occurs—at such an instant as "*a*"—it is to all intents and purposes quite instantaneous, even in terms of a period of oscillation of 1/1000 second.

The period of the cycle is roughly equal to the sum $C_1 R_1 + C_2 R_2$; thus in the actual multivibrator constructed, $C_1 = C_2 = 0{\cdot}0062$ $\mu$F and $R_1 = R_2 = 75{,}000$ ohms, giving a calculated value, on this basis, of 1/930 sec. for the period, the actual value of which was 1/1000 sec.

The resistances $r_1$ and $r_2$ have not been assumed to have any effect on the frequency at which the apparatus works, but there is little doubt that they do govern the behaviour to a large extent. In the original description of the apparatus by H. ABRAHAM, $r_1$ and $r_2$ were inductive coils wound with high resistance wire for the case of a multivibrator having a fundamental frequency of 1,000 cycles per second. It is, however, not necessary for the resistances $r_1$ and $r_2$ to be inductive. For a multivibrator having a fundamental of the order of 20,000 cycles per second, the coils $r_1$ and $r_2$ are wound with copper wire and the frequency is not very dependent upon the values of C and R.

### *Experiments with the Multivibrator.*

A number of experiments on the multivibrator have been made from time to time by the author with a view to testing its suitability for incorporation into a self-contained and direct-reading standard harmonic wave-meter. The more interesting of these will now be described.

#### (*a*) *Variations in Frequency of the Fundamental.*

Observations were made on the variations in frequency of the fundamental in the absence of control when anode voltage, filament brightness, etc., were varied. The observations were made by counting beats against a standard tuning-fork of a nominal frequency of 1,000 vibrations per second. It was only possible, by this means, to observe the effects over a narrow range of variation, on account of difficulties in counting beats when these are at a greater rate than four or five per second.

Observations on variations in frequency due to change of anode voltage are given in Table I.

TABLE I.

| Anode Battery Voltage. | Beats per second (Multivibrator — Tuning-Fork). |
|---|---|
| 79·0 | + 2·6 |
| 80·0 | 0·0 |
| 81·0 | − 2·1 |



Digitized by Google

It is seen that a change of + 1 per cent. in voltage of the anode battery produces a change in frequency of approximately — 2 parts in a thousand.

Experiments on the effect of altering the filament current were then made and gave the results shown in Table II.

TABLE II.

| Filament Current (through both valves). | Beats per second (Multivibrator — Tuning-Fork). |
|---|---|
| 1·25 | + 2·5 |
| 1·28 | — 0·5 |
| 1·30 | — 2·3 |
| 1·315 | — 3·4 |

Thus the change in frequency due to a + 1 per cent. change in current is about — 1·1 parts in 1,000.

Measurements made, of the drift in frequency, after first switching on showed that after ten minutes the frequency became steady to within a very few parts in ten thousand. Other tests, such as bringing the hand near the apparatus, or altering the coupling between the output coil and an external circuit, were found to cause changes in frequency of the order of 1 or 2 parts in 1,000. When everything is in a steady state, however, the frequency will remain constant to within a few parts in 10,000 for considerable periods of time.

In order to overcome the variations in frequency a system of control was devised using a valve-maintained tuning-fork to hold the multivibrator in synchronism. This feature has been incorporated into the wave-meter in its final form.

*(b) Wave Shape of Harmonic Resonance Curves.*

A multivibrator so controlled was set up and measurements were made on the intensity of current, under its influence, in an oscillatory circuit, consisting of a variable condenser reading to 2,000 $\mu\mu$F, and an inductance coil of about 20 millih. inductance and between 7 and 8 ohms effective resistance at the radio-frequencies concerned. Preliminary experiments using a Duddell thermogalvanometer in series in the circuit

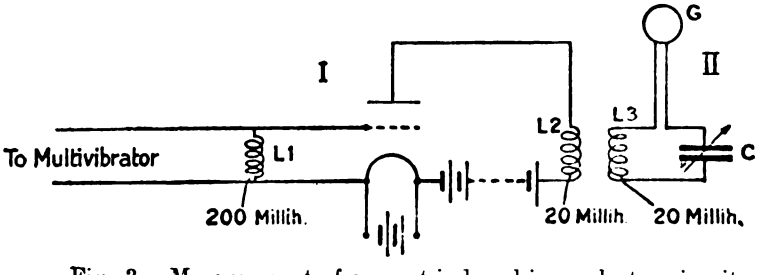


Fig. 3. Measurement of current induced in a selector circuit.

showed that, in order to obtain sufficient deflection, a heater of such resistance would be required as to spoil the sharpness of the resonances. A single stage of amplification was accordingly used on the multivibrator; the circuit was as in fig. 3. The grid

Digitized by Google

filament circuit of the valve was connected to the terminals of an inductance coil of 200 millih. carrying the impulse current from the multivibrator. In the anode circuit was a coil of 20 millih., which induced into the variable selector circuit II containing the Duddell thermogalvanometer G. A series of a great number of observations was made, at selected readings on the condenser, of the galvanometer deflections, covering a range of about 20 harmonics. The induced current in the selector circuit has been plotted in fig. 4 against condenser reading for two series of observations.

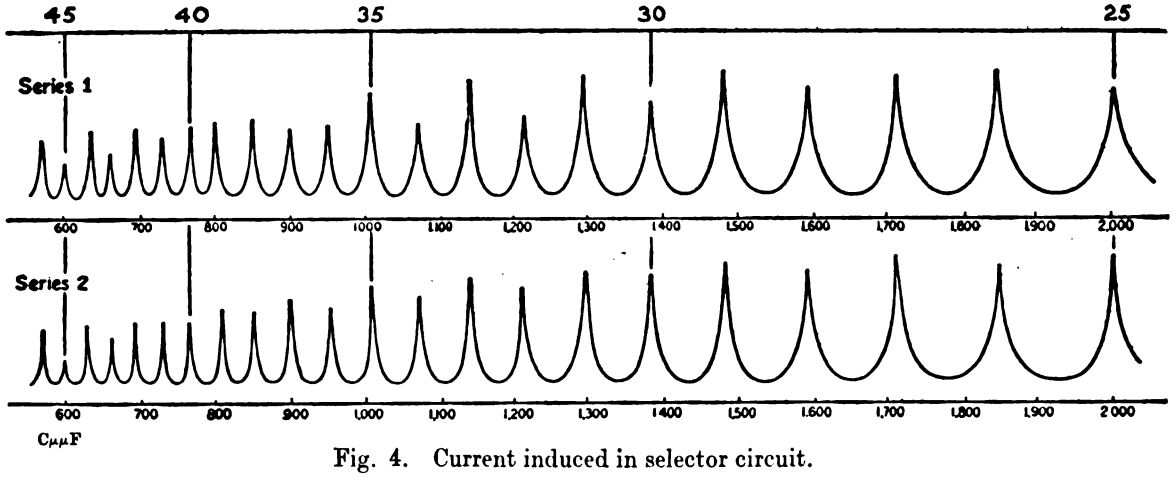


Fig. 4. Current induced in selector circuit.

These interesting curves show the extraordinary sharpness of resonance attained at each reinforcement of a harmonic. An interesting feature of the peaks is that the tips of them fall on two curves, one joining the odd harmonics and the other the even ones. It will be observed that in both series in the region of the 45th harmonic, the even harmonics are stronger than the odd ones, whereas in the region of the 32nd harmonic the position is reversed. The curves joining the peaks are not always the same; there is usually an undulation on each curve, and these undulations intersect one another at certain regions. Considerable variations in the intensities of the harmonics in different regions can be produced by altering the setting of the multivibrator condensers, keeping the variations within the limits of synchronisation by the fork. There is little doubt that the control circuit exerts an influence on the relative intensities of the peaks of the resonances. This is borne out by the differences between the two series of resonance curves shown. Sometimes series 1 would be produced and at other times series 2, when switching on the multivibrator, no alterations whatever being made to the circuits.

It appears that the control voltage from the tuning-fork can operate for two phase relations between its sine wave of voltage and the discontinuous wave of the multivibrator. This is to be expected, since the multivibrator operations are similar in the two symmetrical halves of it and are separated in phase by 180 electrical degrees.

Digitized by Google

Looked at in this way the control may be considered as exerted sometimes on one half of the multivibrator and sometimes on the other half. No more than two series of harmonics could be obtained by switching on and off when everything else was kept constant. It is probable that a more symmetrical control would have been obtained by using a control frequency of 2,000 cycles per second, but this idea was not pursued owing to difficulties in constructing a highly accurate and permanent maintained tuning-fork or other electro-dynamical system at such a frequency. The explanation of the variations in intensity almost certainly lies in the nature of the impact given to the system by the multivibrator. No records of the current in the anode circuit of fig. 3 were taken, but in fig. 5 is reproduced a curve of current in coil L1 in the grid circuit of

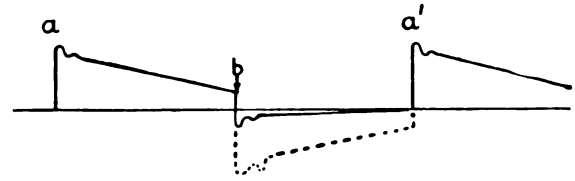


Fig. 5. Current in coil L1 of fig. 3.

the multivibrator. The oscillatory portions at the discontinuities of the curve are due to insufficient damping of the shunted string of the galvanometer.

The same effect was observed when a simple make-and-break circuit replaced the multivibrator.

It will be seen from fig. 5 that a negative impulse is given to the selector circuit by the sudden smaller change in grid current at "*b*". If the positive and negative impacts alternate at exactly equal intervals of time, the odd harmonics will be greater in intensity than the even ones throughout the whole spectrum of harmonics; if, however, "*b*" does not come exactly midway between "*a*" and "*a'*", then a distribution of intensities such as is shown in fig. 3 can be exactly accounted for. Strong support was given to this reasoning by applying a polarising negative potential to the grid of one valve of the multivibrator. This caused a great shortening in the active time of flow of the grid current. The corresponding belt of harmonics—not reproduced—showed abnormal augmentation of intensity of certain harmonics, say, $n$, $n + 2$, $n + 4$, and corresponding reduction of intensity of those of order $n + 1$, $n + 3$, etc. Considerable experimentation was made to try and get approximate equality of successive harmonics over a long range, but no successful way of doing this was found. A condition similar to that given by harmonics 25 to 30 in fig. 4, series 2, could always be obtained by adjustment of the multivibrator condensers for any desired region, but on either side of the belt so obtained the alternately weak and strong characteristic always showed itself. This characteristic of the harmonics, whilst, of course, not desirable, does not in practice introduce any uncertainty into the operation of the apparatus. No measurable change in the setting of the condenser corresponding to resonance at any selected harmonic was observed.

Digitized by Google

In further pursuance of the resonance curves given in fig. 4, some of these have been plotted on very much more open scales of condenser reading and current. Five adjacent harmonics are plotted in fig. 6. The full heavy line curve is the experimental one on harmonics 25 to 29 as measured by the thermogalvanometer. The three dotted resonance

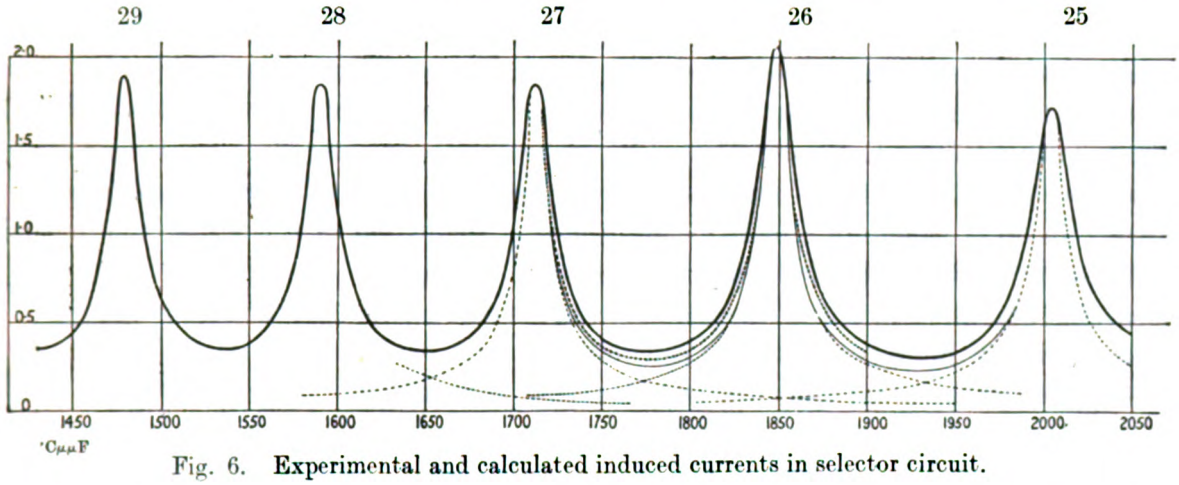


Fig. 6. Experimental and calculated induced currents in selector circuit.

curves are theoretical curves, each giving the variation of current with variation of capacity, which would result for the case of a sine wave of impressed electromotive force of the same frequency as the selected harmonic, and of such value as to give a maximum current at resonance equal to the maximum current actually induced and measured for that harmonic, in the oscillatory circuit under the influence of the induced impulsive electromotive force of the multivibrator. These dotted curves have been calculated, using the well-known equation of the resonance curve for variation of capacity. The most convenient form of equation for this purpose is the exact one

$$I_1 = I_{res.} \frac{\delta \times C_1}{\sqrt{(\delta \times C_1)^2 + (\pi C_2)^2}}, \quad \ldots\ldots\ldots \quad (1)$$

in which $\delta$ = log dec. of the oscillatory circuit per complete period ;

$C_1$ = any capacity value whatever ;

$C_2$ = difference between $C_1$ and the resonance value of capacity without regard to sign.

The value of $\delta$ for the oscillatory circuit was determined both by direct delineation of a resonance curve, using a sine wave source set to the appropriate frequency, and also by calculation from the previously measured effective resistance of the coil and thermo-galvanometer heater. The results agreed to within 1 or 2 per cent. The actual value of $\delta$ was 0·011. Three complete resonance curves are shown for frequencies of 25, 26 and 27 kilocycles per second.

From these curves the thin full-line curve has been constructed, by calculation of the value of

$$\sqrt{I_{25}^2 + I_{26}^2 + I_{27}^2 + \text{etc.}},$$

Digitized by Google

in which $I_{25}$ represents the current at 25 kilocycles per second for any selected capacity, and $I_{26}, I_{27}$, etc., represent the similar quantities for these harmonics at the same capacity.

It will be seen that the resulting curve, although of exactly the same general form as the experimental one, does not exactly fit it, but represents a better case than is found experimentally, since the peaks are sharper and the troughs deeper. The reason for the discrepancy is that, in order to obtain sufficient deflection on the thermogalvanometer, it was necessary to couple the inducing coil L rather more closely than was desirable. The effect of the close coupling is, of course, that the component of current in the coil L at the frequency of any harmonic selected is reduced, as the selector circuit is brought into resonance at that frequency owing to the relatively large current induced in L at resonance. In order to obtain a more accurate idea of the extent of this effect, the mutual inductance between the inducing and selector coils was measured and an estimate of the reduction in current in the selector circuit due to reaction was calculated.

The circuits involved may be considered to a sufficient approximation to be as in fig. 7. We may assume the inducing coil and anode circuit to be a closed circuit in which an electromotive force $e_0$ of value unaffected by circuit II operates.

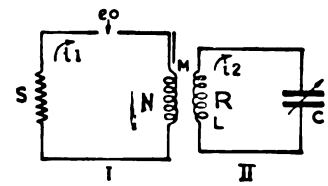


Fig. 7. Simple circuit representing the valve and selector circuit of fig. 3.

Let $i_1$ and $i_2$ be the instantaneous values of current in the two circuits respectively. The letters indicating the constants of the circuits are self-explanatory. Putting $\alpha = j\omega$ we then have

$$i_1 (S + N\alpha) + i_2 M\alpha = e_0, \quad . \quad . \quad . \quad . \quad . \quad . \quad . \quad . \quad . \quad . \quad (2)$$

$$i_2 \left(R + L\alpha + \frac{1}{C\alpha}\right) + i_1 M\alpha = e_0, \quad . \quad . \quad . \quad . \quad . \quad . \quad . \quad . \quad (3)$$

substituting in (2) for $i_2$ its value given by (3) we have

$$i_1 \left[\frac{(S + N\alpha)(RC\alpha + q) + M^2\omega^2 C\alpha}{RC\alpha + q}\right] = 0, \quad . \quad . \quad . \quad . \quad . \quad . \quad (4)$$

in which $q = I - LC\omega^2$.

By the usual process this gives the approximate result

$$\frac{E_0^2}{I_1^2} \doteqdot S^2 + N^2\omega^2 + 2M^2C\omega^4 \left[\frac{SRC - Nq}{R^2C^2\omega^2 + q^2}\right]. \quad . \quad . \quad . \quad . \quad . \quad . \quad (5)$$

This gives approximately

$$\frac{I_1}{I_1'} \doteqdot 1 - \frac{M^2C\omega^4}{S^2}\left[\frac{SRC - Nq}{R^2C^2\omega^2 + q^2}\right] \quad . \quad . \quad . \quad . \quad . \quad . \quad . \quad . \quad (6)$$

where $I_1'$ represents $I_1$ for the case where $M = 0$.

In this expression $N^2\omega^2$ has been neglected as it is small in comparison with $S^2$.

Digitized by Google

The values of the quantities involved are, to a sufficient accuracy :—M (measured) = $1{\cdot}3 \times 10^{-3}$ henry.

$C = 2 \times 10^{-9}$ farad. $\omega = 16 \times 10^4$. $R = 10$ ohms. $S = 5 \times 10^4$ ohms. $N = 2 \times 10^{-2}$ henry.

These values have been inserted in equation 5 and a series of corrected values of $I_2$ calculated for various values of " $q$ ". (It is clear, of course, that $I_2$ will be reduced just in proportion to the reduction in $I_1$.) For the case where $q = 0$, *i.e.*, at the tip of the resonance curve, $I_1$ is less than $I_1'$ by about 9 per cent.

The corrected curve for the experimental case (thick line) is drawn as a thick dotted line, again reducing the results so that the peak has the same value. It is now seen that the trough between the peaks comes much nearer the theoretical one, the difference between the curves is little greater than the inaccuracy of observation, and the whole peak is sharpened up to almost the exact theoretical shape. The desirability of keeping the coupling weak between multivibrator and selector is well brought out by these experiments. The value for the case taken was approximately 0·065, but in the actual wavemeter a very much smaller value has been used and the log. dec. of the selector circuit has been made as small as possible by careful design of the coils—to give as small time constant as possible within reasonable limits of diameter and weight of copper.*

The graphical treatment given above for the effect of an electrical impact on an oscillatory circuit, though very elementary, is sufficient to indicate that under the influence of the successive electrical blows given by the multivibrator the oscillatory circuit behaves substantially exactly as though sine-wave electromotive forces acted upon it, of frequencies and amplitudes having those values which would give the peak values obtained experimentally.

Prof. ABRAHAM has worked out mathematically the case of a system of multivibrator and selector circuit coupled to an amplifier, and has given expressions for the instantaneous quantity " $q$ " on the condenser of the selector circuit as a function of the various electrical constants involved. Omitting the determination of the r.m.s. value of the current in the oscillatory circuit, he has obtained the expression for the electromotive force induced in the amplifier input circuit.

Starting from the expression for the quantity " $q$ " at any instant in the selector circuit, we can easily find the root mean square current in this circuit. This should enable one to obtain the curve given in fig. 6.

The expression for " $q$ " as defined above, and as given by Abraham, is

$$q_2 = Be^{-\alpha t} \cos(\omega t + \psi) \quad . \quad . \quad . \quad . \quad . \quad . \quad . \quad . \quad . \quad (7)$$

in which

$$B^2 = \frac{Q_0^2(\omega^2 + \alpha^2)}{\omega^2(1 - 2e^{-\alpha\theta}\cos\omega\theta + e^{-2\alpha\theta})} \quad . \quad . \quad . \quad . \quad . \quad . \quad . \quad . \quad (8)$$

* Since making these observations it has been found that a value of 30,000 for S more nearly represents the truth. If this value had been used the corrected curve would have almost precisely fitted the experimental curve of fig. 6.



Digitized by Google

and

$$\tan(\psi - \phi) = \frac{e^{-\alpha\theta}\sin\omega\theta}{1 - e^{-\alpha\theta}\cos\omega\theta} \quad \ldots\ldots\ldots (9)$$

also

$$Q_0 = \frac{M}{L_2} q_0 \quad \text{and} \quad \tan\phi = \frac{\alpha}{\omega}$$

where $q_0$ = instantaneous quantity delivered in the operating circuit of the multivibrator,

$\theta$ = time interval between successive blows,

$\alpha = R_2/2L_2$ ($R_2$ and $L_2$ resistance and inductance of the selector circuit),

and $M$ = mutual inductance between the multivibrator coil and the selector circuit coil.

Starting from equation (7), we find for the instantaneous current in the selector circuit

$$i_2 = \frac{dq_2}{dt} = -Be^{-\alpha t}[\alpha\cos(\omega t + \psi) + \omega\sin(\omega t + \psi)] \quad \ldots\ldots (10)$$

which reduces to

$$i_2 = -Be^{-\alpha t}\sqrt{\alpha^2 + \omega^2}\cos(\omega t + \lambda) \quad \ldots\ldots\ldots (11)$$

in which $\lambda = \psi - \gamma$ and $\tan\gamma = \omega/\alpha$.

Calling $I_2$ the root mean square current, we have

$$I_2^2 = \frac{1}{\theta}\int_0^\theta i_2^2\, dt$$

from which

$$I_2^2 = \frac{B^2}{\theta}(\omega^2 + \alpha^2)\int_0^\theta e^{-2\alpha t}\cos^2(\omega t + \lambda)\, dt. \quad \ldots\ldots\ldots (12)$$

This may be written

$$I_2^2 = F^2\int_0^\theta e^{-2\alpha t}\left[\tfrac{1}{2} + \frac{\cos 2(\omega t + \lambda)}{2}\right]dt, \quad \ldots\ldots\ldots (13)$$

giving

$$I_2^2 = \frac{F^2}{4}\left\{-\frac{1}{\alpha}\left[e^{-2\alpha t}\right]_0^\theta - \frac{1}{\sqrt{\omega^2 + \alpha^2}}\left[e^{-2\alpha t}\cos 2(\omega t + \lambda + \xi/2)\right]_0^\theta\right\}, \quad \ldots (14)$$

in which $\xi = \tan^{-1}\omega/\alpha$, whence

$$I_2^2 = \frac{B^2}{4\theta}(\omega^2 + \alpha^2)\left\{\frac{1}{\alpha}(1 - e^{-2\alpha\theta}) - \frac{1}{\sqrt{\alpha^2 + \omega^2}}[e^{-2\alpha\theta}\cos 2(\omega\theta + \lambda + \xi/2) - \cos 2(\lambda + \xi/2)]\right\}. \quad \ldots\ldots (15)$$

In the present case $\alpha = \dfrac{R_2}{2L_2} = n\delta \doteqdot 275$ for the 25th harmonic; but $\omega \doteqdot 2\pi n \doteqdot 15 \times 10^4$, so that $\dfrac{1}{\sqrt{\omega^2 + \alpha^2}}$ is negligible compared to $\dfrac{1}{\alpha}$.

Again, for values of $\alpha$ and $\theta$ of 275 and $1 \times 10^{-3}$ respectively $(1 - e^{-2\alpha\theta})$ becomes 0·4231, and the cosine expression in the second bracket cannot be greater than 1·42,

Digitized by Google

so that the whole second term is always less than about 0·5 per cent. of the term $\frac{1}{\alpha}(1 - e^{-2\alpha\theta})$ and may therefore be omitted. Inserting the value for B and neglecting $\alpha^2$ in comparison with $\omega^2$ we get finally

$$I_2^2 = \frac{Q_0^2}{4\alpha\theta} \cdot \frac{\omega^2(1 - e^{-2\alpha\theta})}{1 + e^{-2\alpha\theta} - 2e^{-\alpha\theta}\cos\omega\theta}. \quad \ldots\ldots\ldots \quad (16)$$

An examination of this expression shows immediately that $I_2^2$ cycles up and down through maximum and minimum values as $\cos\omega\theta$ passes through its limiting values of $+1$ and $-1$, corresponding to values of $\omega$ equal to $\pi k/\theta$, where $k$ is any integral number whatever. The resonance peaks correspond to values of $\omega$ of $2\pi k/\theta$ giving angles, 0, $2\pi$, $4\pi$, etc. The troughs correspond to values of $\omega$ midway between the peaks, so that $\cos\omega\theta = -1$.

The agreement of the theory with experiment is seen by calculating, as an example, the ratio of maximum to minimum current for the 25th harmonic and following trough.

The values of the quantities involved are

$$\alpha = R/2L \doteq 275 \qquad \theta = 1 \times 10^{-3}\ \text{sec.}$$

$$\left(\frac{I_{max.}}{I_{min.}}\right)^2 = \frac{1 + e^{-2\alpha\theta} + 2e^{-\alpha\theta}}{1 + e^{-2\alpha\theta} - 2e^{-\alpha\theta}} = \frac{1{\cdot}577 + 1{\cdot}519}{1{\cdot}577 - 1{\cdot}519} = 53{\cdot}4,$$

whence $I_{max.}/I_{min.} = 7{\cdot}3$.

The value found experimentally is 7·0, taking the ratio between the mean of the peaks of the 25th and 26th harmonics and the intervening trough, and correcting for the mutual effect.

Another case was worked out for the 40th harmonic, at which frequency the effective resistance $R_2$ of the selector circuit is about 14 ohms, giving for "$\alpha$" the approximate value of 350. The calculated ratio of maximum current to minimum current is 5·8, and the observed ratio is about 5, thus, again, giving quite satisfactory agreement, bearing in mind that actual experiment shows the undulation in the peaks as given in fig. 4.

If we examine the formula (16) it is seen that the ratio of maximum $I_2^2$ to the adjacent minimum $I_2^2$ is equal to

$$\frac{1 + e^{-2\alpha\theta} + 2e^{-\alpha\theta}}{1 + e^{-2\alpha\theta} - 2e^{-\alpha\theta}} \quad \ldots\ldots\ldots \quad (17)$$

and that this ratio is only dependent on $\alpha$ and $\theta$. Now $\alpha = R/2L$ is equal to $n\delta$ where $\delta$ = log. dec. of the selector circuit per complete period. But $n = k/\theta$, where $k$ is any integer and $n$ = frequency.

Hence, for the reinforcement ratio of a harmonic as given by (17) we may write

$$\left(\frac{I_{max.}}{I_{min.}}\right)_k \doteq \frac{1 + e^{-2k\delta} + 2e^{-k\delta}}{1 + e^{-2k\delta} - 2e^{-k\delta}} \quad \ldots\ldots\ldots \quad (18)$$

This shows that both $\delta$ and $k$ should be as small as possible. The indication is, too, that as $k$ becomes larger at the higher order harmonics it is desirable for $\delta$ to become smaller.



Digitized by Google

Since, however, there is difficulty in making " $\delta$ " small enough in any case, it is probably the best compromise to design the coils to have minimum decrement somewhere towards the upper range of frequency at which each will be used.

With regard to the factor " $k$ ", from the point of view of reinforcement as defined by equation (18), there is no doubt that it is undesirable to make use of harmonics of too high order. On the other hand, when " $k$ " is, say, only 10, the successive harmonics are 10 per cent. apart in frequency, thus leaving rather a large gap for purposes of interpolation. As will appear later when using a fundamental of 1,000 cycles per second, there are available sub-harmonics in between the main integral harmonics. With a higher fundamental frequency slightly modulated by a lower harmonic frequency, as occurs in the complete wave-meter, one can also obtain sub-harmonics for a considerable distance on each side of the main harmonic and so bridge a large portion of the intervening region between two harmonics.

### 3. Comparison Experiments between Frequencies given by the Multivibrator and those obtained by Calculation from Inductance and Capacity.

It was felt very desirable to make a comparison of the radio-frequencies given by the multivibrator with those obtained by calculation from the inductance and capacity of the resonant selector circuit. The effective inductance and effective capacity of the circuit must, of course, be independently measured in terms of some fundamental standard, and they must be expressed in the same system of units. The circular check thus obtained on all the measurements made becomes of great value in strengthening the general position as regards measurement of frequency, inductance and capacity.

It will be convenient to describe first, very briefly, the measurements on the standard coils and variable condenser before proceeding to the radio-frequency comparisons.

The foundation of the inductance and capacity measurements at the National Physical Laboratory is a standard of mutual inductance calculable from dimensions. This was designed and described by A. Campbell (10). A second similar one was constructed and comparisons were made (11) by the author with the original standard. The results showed that the true value of mutual inductance of the standard in c.g.s. units is probably within one part in a hundred thousand of the value obtained by calculation from the measured dimensions.

The inductance coils were measured with low-frequency current on a mutual inductance bridge with equal arms by the help of a secondary sub-divided standard mutual inductometer carefully calibrated from the primary standard. These measurements presented no special features ; care was taken at every point by reversals of source, galvanometer, ratio arms, etc., to eliminate all cross effects. It is considered that the values of self-inductance of the coils so measured are accurate to five parts in a hundred thousand.

The more difficult calibration of the standard variable air condensers was made by means of a Carey-Foster bridge determining capacity in terms of mutual inductance

Digitized by Google

and resistance. The addition of a Wagner earthing device, first used on this bridge by the author, renders the effects of earth capacities of the various parts of the bridge of negligible account. A diagram of this bridge with the earthing device is given in fig. 8. It is seen that the bridge measures capacity in terms of quantities whose dimensions are $[M]/[R]^2$. In order to be consistent, M and R must be expressed in the same system of units. M, and hence L, is known in c.g.s. units, and since C is also required in the same system it is necessary to know R in these units. The resistance coils used were measured in the ordinary way in international ohms against the Laboratory standards and were corrected to absolute c.g.s. ohms, using the ratio of units determined by F. E. Smith (12). The measurements of capacity are not of such high order as those of inductance, but it is believed that the absolute accuracy of the calibrations at various readings on the condenser is to a few parts in ten thousand. As will be seen later on, only changes of capacity of the condenser are involved in the comparison with the radio-frequency tests, so that uncertainties regarding capacity of the coil and leads to the condenser and of these to earth are thrown on to the effective self-capacity of the coil and do not vitiate the accuracy at all. The mean of differences in capacity between readings on the condenser is probably accurate to one or two parts in ten thousand for the average of twenty observations at different parts of the scale.

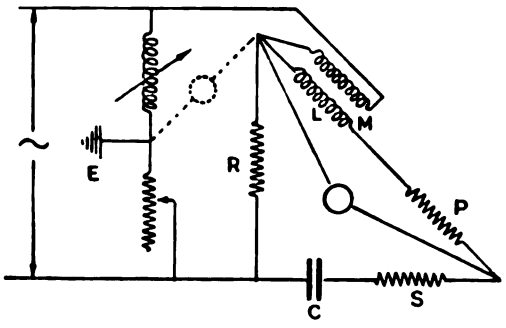

Fig. 8. Carey-Foster bridge with Wagner earth.

Passing on to the radio-frequency tests, the arrangements for these were as given in fig. 9.

Four distinct items of apparatus were used in these experiments, as follows :—

I. The multivibrator M (shown purely diagrammatically) with its controlling tuning-fork F.

The tuning-fork had its own battery for the filament of its valve, so as to be as constant as possible. The multivibrator coil L1 was connected by leads about a metre long, so that circuit II might be well removed from metal parts and coils in circuit I. The coupling between I and II was very loose.

II. This circuit was the standard circuit under observation and was reduced as nearly as possible to an elemental form. The capacity part consisted of the standard calibrated variable air condenser. The inductance part was one of the standard inductance coils which had also been measured at a low frequency. These coils were specially suited to the purpose in view, being very permanent, of highly stranded wire, of small decrement and of small self-capacity.

III. This was a six-valve transformer coupled amplifier for the purpose of detecting the resonances in circuit II. It was very loosely coupled to the standard circuit by

Digitized by Google

the coil L3. The position of this coil was adjusted so as to have no mutual inductance to coil L1.

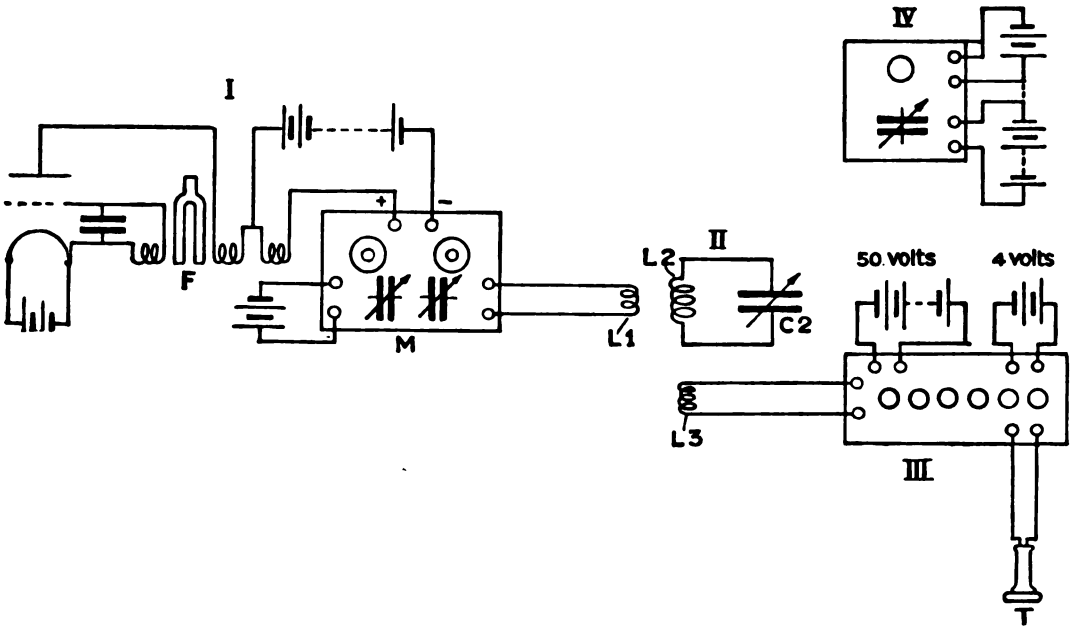


Fig. 9. Arrangement of apparatus for determination of resonant settings of standard selector circuit.

Unit IV was an ordinary heterodyne set with its own batteries, and was provided with fine setting on its variable condenser in order that the interfering beat tone with the chosen harmonic might be adjusted to any desired acoustic frequency.

### *Observation of the Resonances.*

The setting of the condenser to resonance at the chosen harmonics was carried out in four different ways altogether, as follows :—

*Method* 1.—The heterodyne unit IV was not in use and the standard condenser was set until maximum loudness of the 1000 ~ per second note in the amplifier telephone occurred. This note results, of course, from the rectification, by the amplifier, of the modulated wave in the standard oscillatory circuit.

ABRAHAM has shown in his theory of the multivibrator that the setting of the condenser for maximum loudness of the rectified modulated current in the amplifier telephone is not quite the same as that for resonance by maximum loudness of the interference tone with a separate heterodyne source. The correction term is given by $C_1 = C_0 (1 - 5/4\ \delta^2/\pi^2)$ where $\delta$ = log. dec. of the selecting circuit.

In the present case " $\delta$ " was of the order 0·01, so that the correction term is only of the order one part in a hundred thousand, and is therefore entirely negligible.

*Method* 2.—This was a refinement of method 1, in that a Duddell vibration galvanometer tuned to a frequency of 1000 cycles per second replaces the telephone. This

Digitized by Google

means of observing resonance was, of course, very much more accurate than the foregoing. Owing to the very slight uncertainty as to whether the maximum intensity of the 1,000 cycle per second note heard in the amplifier telephone really represented maximum oscillatory current in the standard circuit, it was decided to use methods 3 and 4, requiring the heterodyne.

*Method* 3.—In this method the intensity of the beat tone between the chosen harmonic and the adjusted heterodyne source is caused to have a maximum intensity as judged by loudness in the amplifier telephone.

*Method* 4.—This is a refinement of method 3, in that a Duddell vibration galvanometer tuned to a frequency of about 800 cycles per second was used instead of the telephone, and the heterodyne frequency was accurately set so that the difference tone was at the resonant frequency of the galvanometer. This adjustment had, of course, to be made with great precision. When made, the standard variable condenser of the selector circuit II was set to give maximum deflection on the vibration galvanometer. This last method was the most accurate of all, but was extremely laborious, occupying many hours for a series of 60 harmonics.

### *Determination of the Order of the Harmonics.*

This was really unnecessary in these experiments because the effective values of inductance and capacity were known to an accuracy which left no uncertainty as great as 0·5 per cent. in the value of the frequency of resonance. Since the range of harmonics was over the region 20 to 100, and since they were all observed and carefully counted upwards from, say, the 20th, there was not the slightest doubt regarding the order number of the harmonic.

In order to render this fundamental point doubly certain, the method given by ABRAHAM was also used and found to give absolutely unmistakable location to the harmonic. The method is very simple: a harmonic, say the $n$th, is selected and the heterodyne is set to give a fairly low frequency beat tone of about 400 per second. The succeeding harmonics are then selected one by one and counted, care being taken not to miss one. When the 2 $n$th harmonic is reached, an interference beat tone of 800 per second will be heard against the 2nd harmonic of the heterodyne. The number of intervals counted between "$n$" and "$2n$" is, of course, equal to "$n$" the order number of the harmonic first selected. Some little skill is required in order to select the correct interference tones at each end of the region counted. All the notes, such as $-2400$, $-1400$, $-400$, $+600$, $+1600$, can be heard corresponding to beats between the heterodyne and the successive harmonics $n-2$, $n-1$, $n$, $n+1$ and $n+2$. Similarly at the other end of the scale the notes $-1800$, $-800$, $+200$, $+1200$ can be heard corresponding to the selected harmonics $2n-1$, $2n$ and $2n+1$.

The observations of condenser readings corresponding to resonance for a series of selected harmonics have been dealt with as follows. If resonant capacity is plotted

Digitized by Google

as abscissa and $1/n^2$ as ordinate (where $n$ = frequency), a straight line is obtained cutting the " X " axis at a small negative value of C. This intercept represents the self-capacity of the coil and includes any stray capacities outside the screened condenser. The slope of the line is equal to the effective pure inductance of the coil. If the coil is of finely stranded wire the effective pure inductance so determined should equal the inductance measured at low frequency in terms of the mutual standard. It is not possible to determine the slope with sufficient accuracy by graphical methods, but by the method of least squares quite high accuracy may be obtained.

The formulas for effective pure inductance and effective self-capacity have been developed by HULBERT and BREIT (13). They are, in terms of frequency,

$$L = \frac{10^{18}}{4\pi^2} \frac{N\Sigma\left(\frac{1}{n}\right)^4 - \left[\Sigma\left(\frac{1}{n}\right)^2\right]^2}{N\Sigma C_1 \frac{1}{n_1^2} - (\Sigma C_1)\left[\Sigma\left(\frac{1}{n_1}\right)^2\right]} \quad \ldots\ldots\ldots \quad (20)$$

$$C_0 = \frac{(\Sigma C_1)\left[\Sigma\left(\frac{1}{n_1}\right)^4\right] - \left[\Sigma\left(\frac{1}{n_1}\right)^2\right]\left[\Sigma C_1\left(\frac{1}{n_1}\right)^2\right]}{\left(\Sigma \frac{1}{n_1^2}\right)^2 - N\Sigma \frac{1}{n_1^4}}.$$

These equations assume that the percentage accuracy of condenser reading is proportional to the capacity. This method is very laborious to apply owing to the large amount of arithmetic involved. It has been used in a few cases, but in other cases a method has been used in which an assumed value of L is taken and theoretical capacities calculated corresponding to the frequencies of the harmonics. The difference between these values and the observed value gives a capacity which includes the self-capacity of the coil, etc., and the error of observation. The mean value of these differences is next taken and a second difference representing error of observation found. The sum of these second differences is finally taken. By choosing other values of L and repeating the

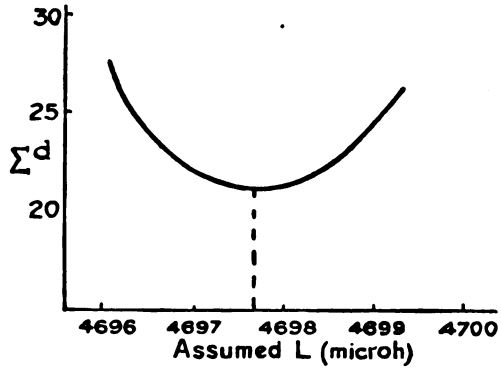


Fig. 10. Deduction of effective inductance of an oscillatory circuit.

process a curve can be obtained between assumed L and ($\Sigma$ 2nd differences). The value of L corresponding to the minimum $\Sigma$ difference gives the best value.

A typical series of such values is shown by the curve in fig. 10.

Digitized by Google

A collection of results is given in Table III which also gives the value of L obtained by comparison against the standard mutual inductance.

TABLE III.

| Coil. | Method of observing Resonance. | Effective Inductance. | Mean Value. | Effective Inductance by Mutual Standard |
|---|---|---|---|---|
| L 307 | 1<br>3<br>4 | 7843·4<br>7843·3<br>7844·8 | 7843.$_8$ | 7844 |
| Ad. 7 | 3<br>3<br>3 | 4698·0<br>4697·7<br>4698·0 | 4697.$_9$ | 4698.$_2$ |
| L 450 | — | 20014 | — | 20017 |

The observations for the coil No. L 450 were those corresponding to the experiments described in section 2, where the relative amplitudes of the harmonics are plotted in fig. 4, and were taken by direct observation of the current peaks as given by the thermo-galvanometer.

In order to check whether a wrong observation had been made, the value of L deduced by the least squares was used to calculate the frequencies by the ordinary formula, using observed values of capacity as written down, and adding to each, of course, the value of self-capacity also determined. In order to give an idea of the accuracy obtained, the observations and calculated values of frequency are given for a complete set of harmonics in Table IV.

TABLE IV.

| Harmonic | C. rdg. $\mu\mu$F. | Calculated Frequency. | True Frequency. | Difference, Parts in 1000. |
|---|---|---|---|---|
| 16 | 4 923 | 16 001 | 16 000 | + 0·06 |
| 17 | 4 358 | 17 001 | 17 000 | + 0·06 |
| 18 | 3 885 | 18 001 | 18 000 | + 0·06 |
| 19 | 3 483.$_5$ | 19 002 | 19 000 | + 0·10 |
| 20 | 3 140 | 20 007 | 20 000 | + 0·35 |
| 21 | 2 849 | 20 996 | 21 000 | − 0·20 |
| 22 | 2 591 | 22 008 | 22 000 | + 0·37 |
| 23 | 2 371 | 22 995 | 23 000 | − 0·23 |
| 24 | 2 178.$_5$ | 23 983 | 24 000 | − 0·73 |
| 25 | 2 006 | 24 978 | 25 000 | − 0·89 |
| 26 | 1 850 | 25 995 | 26 000 | − 0·20 |
| 27 | 1 711 | 27 015 | 27 000 | + 0·55 |
| 28 | 1 590 | 28 009 | 28 000 | + 0·31 |
| 29 | 1 480 | 29 015 | 29 000 | + 0·52 |
| 30 | 1 381 | 30 030 | 30 000 | + 1·00 |



Digitized by Google

Table IV (continued).

| Harmonic | C. rdg. $\mu\mu$F. | Calculated Frequency. | True Frequency. | Difference, Parts in 1000. |
|---|---|---|---|---|
| 31 | 1 290.$_5$ | 31 040 | 31 000 | +1·30 |
| 32 | 1 211 | 32 017 | 32 000 | +0·53 |
| 33 | 1 140 | 32 978 | 33 000 | −0·67 |
| 34 | 1 070 | 34 016 | 34 000 | +0·48 |
| 35 | 1 010 | 34 988 | 35 000 | −0·29 |
| 36 | 951 | 36 030 | 36 000 | +0·82 |
| 37 | 900 | 37 010 | 37 000 | +0·27 |
| 38 | 850.$_5$ | 38 042 | 38 000 | +1·10 |
| 39 | 809 | 38 977 | 39 000 | −0·59 |
| 40 | 765 | 40 047 | 40 000 | +1·17 |

## 4. Crucial Test of the Multivibrator Principle.

In order to place beyond all doubt any question as to the validity of the principle of building-up frequency by harmonic ratios, the following test was carried out:—

Two complete multivibrator assemblages were set up; these will be designated A and B respectively.

Assemblage A consisted of a complete compound multivibrator* having a primary control tuning-fork of a frequency of approximately 1,000 vibrations per second. The 20th harmonic was selected from the low-frequency multivibrator and controlled a high-frequency multivibrator of fundamental of 20 kilocycles per second. From this, any harmonic, say the 12th, could be selected on a selector circuit. A tuned amplifier was loosely coupled to the selector circuit.

Assemblage B was similar to A, but the control tuning-fork had a frequency of approximately 969 vibrations per second. The 19th harmonic of the low-frequency multivibrator was selected and used as control for the high-frequency multivibrator. The fundamental frequency was therefore approximately 18·4 kilocycles per second. A selector circuit enabled one to select any desired harmonic from this high-frequency multivibrator. In both multivibrator assemblages the order of harmonic was determined absolutely, *i.e.*, without assuming any frequencies to be known.

A local source of oscillations was also provided and was of a kind that kept very constant in frequency when adjusted. The capacity part of its oscillatory circuit was provided with an open-scale standard variable condenser in parallel with the main capacity. Calling the capacity reading on this generator condenser C2, the following procedure was carried out. A region of frequency was found in which a selected harmonic of A was close to one of B.

* For a complete understanding of this arrangement it is necessary to refer to sections 5 and 6 and to fig. 11.

Digitized by Google

The frequency of the source was adjusted to exact synchronism with a main harmonic of A and with a number of subsidiary harmonics on either side. (These can be given sufficient prominence by increasing the control of the high-frequency multivibrator by the low one.) The readings on C2 corresponding to these sub-harmonics were noted.

The same procedure was now carried out using B and so obtaining an interlacing series of harmonics. The readings for multivibrator A were then repeated immediately after those taken with B, so as to check any drift in the local source.

A note may be interposed here regarding the observation of harmonics and subsidiary harmonics. The frequency of the fork A may be assumed equal to 1000·00 cycles per second $= n_A$. The frequency of the main harmonic used on the high-frequency multivibrator, for example, the 12th, then becomes $20 \times 12 \times 1000{\cdot}00 =$ 240·00 kilocycles per second. The subsidiary harmonics which can be observed are very many; for example, not only can those corresponding to frequencies of 240,000 $\pm$ $k \times n_A$ be observed, where $k = 1, 2, 3, 4$, etc., but secondary subsidiary intermediate harmonics may also be utilised such as $240{,}000 \pm k \,.\, n_A \pm r \,.\, n_A$, where $r$ is a fraction, such as $\frac{1}{2}$, $\frac{1}{3}$, $\frac{1}{4}$, etc. Thus one can set the source exactly to a frequency such as 241250 without the aid of any auxiliary tuning-forks. The possibility of obtaining fiducial points so close together is very valuable because it removes practically all responsibility of accuracy in the generator condenser C2 when interpolating. Some skill is naturally necessary in interpreting the beats heard, to ensure which sub-harmonic and secondary sub-harmonic is producing the slow beat heard.

Returning now to the method of dealing with the readings on C2, the following procedure was adopted:—

The frequency of the controlling tuning-fork on multivibrator A was assumed equal to 1000·00 vibrations per second. The main harmonic used on the high-frequency multivibrator was the 12th, so that the frequency of this point becomes $20 \times 12 \times 1000{\cdot}00 = 240{\cdot}00$ kilocycles. The other sub-harmonics observed had nominal frequencies, as given in Table V below.

TABLE V.

| Multivibrator A. | | Multivibrator B. | |
|---|---|---|---|
| Nominal Frequency. Kilocycles per Second. | Mean C2 Reading. $\mu\mu$F | Harmonic Observed. | $C_2$ Reading. $\mu\mu$F. |
| 238·00 | 1,579 | — | — |
| 238·50 | 1,397 | 245·50 | 1,582 |
| 239·00 | 1,219 | 246·00 | 1,407 |
| 239·50 | 1,039 | 246·50 | 1,234 |
| 240·00 | 863 | 247·00 | 1,060 |
| 240·50 | 687 | 247·50 | 890.5 |
| 241·00 | 512 | 248·00 | 720 |
| 241·50 | 336 | 248·50 | 550 |
| 242·00 | 166 | 249·00 | 380 |



Digitized by Google

Column 4 gives the condenser readings C2 for the harmonics observed on multivibrator B. In this case the 13th harmonic of the high-frequency multivibrator was used, and this multivibrator was controlled by the 19th harmonic of the low-frequency multivibrator B, having a fundamental frequency of approximately 969 cycles per second.

These harmonics therefore have frequencies of $(13 \times 19)\, n_B \pm k n_B$, as shown in the table ($k = 0{\cdot}5,\ 1{\cdot}0,\ 1{\cdot}5$, etc.). The frequencies of these harmonics were obtained by interpolation in terms of multivibrator A.

If now we divide each interpolated frequency by the harmonic number of B, we should obtain in every case the fundamental frequency of tuning-fork B. The results of these calculations are given in Table VI.

TABLE VI.

| Multivibrator B. | | |
|---|---|---|
| Observed Harmonic. | Interpolated Frequency. Kilocycles per Second. | Deduced Fork Frequency. Cycles per Second. |
| 245·50 | $237{\cdot}98_4$ | 969·38 |
| 246·00 | $238{\cdot}47_3$ | 969·40 |
| 246·50 | $238{\cdot}95_8$ | 969·40 |
| 247·00 | $239{\cdot}44_2$ | 969·40 |
| 247·50 | $239{\cdot}92_1$ | 969·38 |
| 248·00 | $240{\cdot}40_6$ | 969·38 |
| 248·50 | $240{\cdot}90_2$ | 969·42 |
| 249·00 | $241{\cdot}37_0$ | 969·36 |
| Mean temperature, 18·60° C. | | Mean fork frequency = $969{\cdot}39_0$ |

Chronograph runs were taken on the two tuning-forks by the help of a specially constructed phonic wheel suitable for frequencies of the order of 1,000 per second. By this means the frequency of each fork was determined, to an accuracy of one part in a hundred thousand, in terms of the second given by the standard clock of the Laboratory. The values obtained for the forks were :—

By Chronograph .. Fork A at 20° C. = $999{\cdot}96_5$ cycles per second.
,, ,, .. ,, B at $18{\cdot}5_5$° C. = $969{\cdot}34_5$ ,, ,,

The mean value obtained for fork B by the process of stepping up and down through the multivibrators was :—

Fork B at 18·6° C. = $969{\cdot}39_0$ in terms of fork A of nominal value $1000{\cdot}00_0$. Correcting these results for the error of A and to a temperature of $18{\cdot}5_5$° C., we get :—

By multivibrator A .. Fork B at $18{\cdot}5_5$° C. = $969{\cdot}36_0$ cycles per second.

This agreement may be considered very satisfactory and can be considered to remove

Digitized by Google

every trace of uncertainty as to the validity of the harmonic principle of building-up frequency in view of the fact that four harmonic stages intervene in the calculation and measurement of fork B in terms of fork A.

## 5. Fundamental Principles Governing the Design of the Wave-meter.

The experiments and investigations just described gave a great deal of valuable experience and information for guidance in the design of the complete self-contained instrument. Before proceeding to details it is desirable to set down clearly the behaviour of the wave-meter as used to set the frequency of another source or to measure it. This may be summarised as follows :

### (*a*) *For Frequencies up to* 120 *Kilocycles per Second.*

A low-frequency multivibrator unit produces a fundamental frequency of 1 kilocycle per second. The frequency of operation of this multivibrator is directly controlled by an electrically maintained tuning-fork, having a frequency which has been adjusted as closely as possible to 1,000 cycles per second. The impulse from this multivibrator acts by mutual inductance coupling of small amount on a selector circuit, which consists of a special variable condenser and either of three standard radio-frequency inductance coils. By means of directly marked scales any desired harmonic (from the 10th to the 120th) can be selected and reinforced.

The selected and reinforced harmonic is amplified by means of a tuned amplifier. This amplifier also receives a small amount of high-frequency current from any source of undamped oscillations.

This source may be a station or any other generator whose frequency is desired to be known or set to a particular value. We will assume that it is desired to set this source to some exact radio-frequency. The procedure consists in selecting that harmonic whose frequency lies near to that desired for the source. On adjusting the amplifier so that it is sensitive to this frequency, a beat tone will be heard between the selected harmonic and the source (assuming, of course, that the latter is sufficiently nearly adjusted already for this beat tone to be audible). The source can now be set until this beat tone becomes as slow as one in ten seconds, representing to all intents and purposes exact synchronism with the harmonic. Or it may be set to give any desired beat frequency from the selected harmonic representing a radio-frequency such as 50300. In such a case, a beat tone of — 300 cycles per second is heard against the 50th harmonic, when this one is selected, or a beat tone of + 700 per second may be obtained against the selected 51st harmonic, if so desired. For purposes of checking, beat tones of — 1300, — 2300 or + 1700, + 2700 cycles per second may also be observed against the appropriate harmonics. By this system any desired frequency can be obtained up to 120 kilocycles per second, with an accuracy of a few parts in a hundred thousand.

Digitized by Google

*(b) For Frequencies from* 100 *Kilocycles per Second to* 1,200 *Kilocycles per Second.*

For these higher frequencies a second multivibrator is provided. This apparatus is very similar to the low-frequency multivibrator apparatus, but produces a discontinuous wave of fundamental frequency of 20 kilocycles per second.

This apparatus is controlled in frequency by means of the reinforced and amplified 20th harmonic of the low-frequency multivibrator; for this purpose special circuits are incorporated into the apparatus. This high-frequency impulse operates on the selector circuit in the same manner as the low-frequency multivibrator. The same variable air condenser is used, but another set of three coils and scales is provided to suit the range 100 to 1,200 kilocycles per second, corresponding to harmonics 5 to 60. The scales have engraved lines corresponding to every harmonic from 5 to 60, but they are, of course, marked directly in kilocycles per second. The principle of controlling the two multivibrators in tandem from the tuning-fork is one of the most valuable features of the apparatus. The advantages are:—

(1) All the frequencies obtained are an integral number of kilocycles per second.
(2) The responsibility of the accuracy and permanence of the calibration is removed from all the electrical circuits except, in a very minor degree, those immediately associated with the tuning-fork.
(3) The operation of the apparatus is not affected by the presence of the observer, earth capacities, etc.

From the outline given above it will be seen that the complete equipment divides itself naturally into three separate parts:—

(*a*) The compound multivibrator unit.
(*b*) The selector unit.
(*c*) The detector and amplifier unit.

Short general descriptions of these units are now given.

## 6. Description of the Wave-meter.

### (*a*) *The Multivibrator Unit.*

This unit consists of two multivibrators in cascade, together with the intermediate control circuit and the main controlling tuning-fork. The complete scheme of connections is given in fig. 11. For clearness of description this diagram is divided into four sections, lettered A, B, C and D, as follows:—

A. The tuning-fork is valve-maintained and has a fundamental frequency of 1,000 cycles per second. The grid and anode windings are provided with condensers of such values as to make the natural frequency of these circuits approximately equal to that of the fork. A winding L3 underneath the anode winding is provided for the purpose of introducing into the anode battery circuit of the multivibrator the small alternating control voltage which keeps this multivibrator synchronous with the fork.

Digitized by Google

The control thus provided is of such extent that synchronism is maintained over a range of variation in the multivibrator circuits, which in the absence of the control would cause a change in frequency of ± 4 per cent.

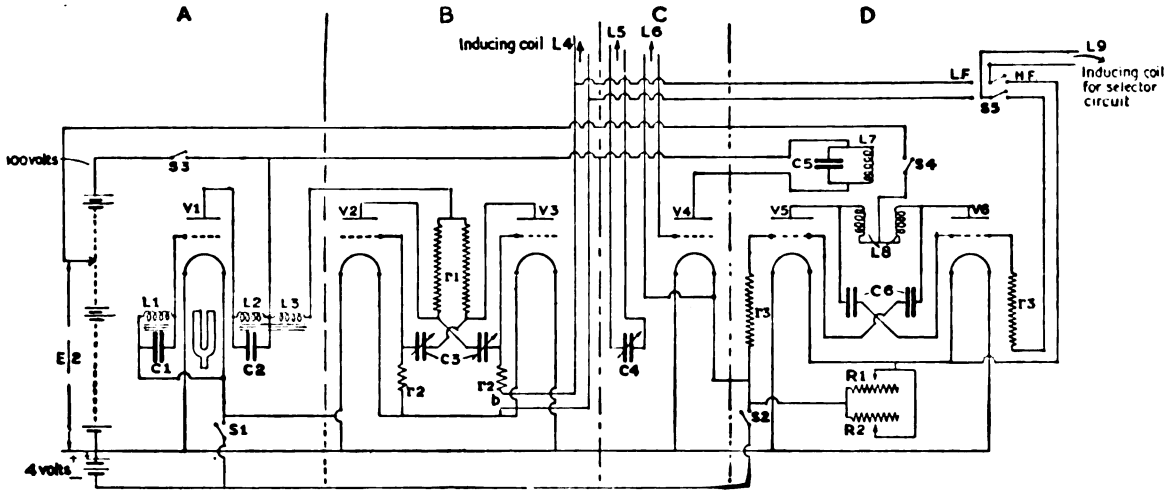


Fig. 11. Arrangement and connections of tuning-fork controlled compound multivibrators.

The conditions governing steadiness of operation of the fork have formed the subject of a previous Paper by the author (13). The present fork is the outcome of the conclusions reached in these experiments.

The fork is constructed of a nickel-iron alloy which has a very small temperature coefficient of elasticity. It has been cut from a wide flat bar of the material in such a manner that a large cross-section of metal is left at the roots of the prongs. The metal here extends beyond the outside surfaces of the prongs, so that they are supported at the root in such a manner that the nodal surfaces are of large area and are close together. The idea has been to reduce as much as possible the axial vibration of the support. Clamps of considerable weight (about 2 kgm.) hold the fork and its auxiliary parts in rigid relationship.

Experiments showed that a want of equality of stiffness of the prongs, or of their effective masses, manifested itself as a rotational oscillation of the base. The prongs were carefully balanced experimentally until this oscillatory vibration was reduced to a minimum. With the fork so constructed and balanced scarcely any vibration of any kind is conveyed outside the fork system. The change in frequency produced by clamping and unclamping the mounted fork at its attachment to the base of the complete apparatus was less than one part in a hundred thousand.

From the point of view of permanence the fork appears to be very satisfactory. During the eighteen months the fork has been under observation, its absolute frequency measured by means of a special phonic wheel constructed for the purpose, has not shown variations from the mean frequency by as much as ± 2 parts in 100,000.

Turning again to fig. 13 we come to the section B.

B. This is the low-frequency multivibrator item consisting of anode resistances $r_1$

Digitized by Google

of eureka wire of 50,000 ohms each, and condensers C3 cross-connecting grids and anodes of the valves V2, V3. These condensers each consist of a fixed mica condenser of 0·006 $\mu$F and a variable air condenser of 0·001 $\mu$F. maximum capacity, in parallel. The leak resistances $r_2$, $r_2$ are also of eureka wire on mica frames and are 75,000 ohms each. A break is made in the circuit of one of these at "*b*", at the filament end; leads from this convey the impulse either to the controlling inducing coil L4 or to the terminals marked "Inducing coil for selector circuit" (top right corner of diagram) for this connection, the change-over switch S5 is to the left-hand side marked LF. Switch S1 is in the 4-volt filament circuit of valves V1, V2 and V3 and switch S3 is in the 100-volt anode battery circuit of these valves and valve V4.

When these switches are closed the tuning-fork and the low-frequency multivibrator are activated. By adjustment of C3 the frequency is brought within the range of synchronisation. This is not critical; the region of holding is for a variation over half the scale of the variable part of C3.

The next portion, C, is the control arrangement for the high-frequency multivibrator.

C. Many different arrangements were tried in order to obtain satisfactory control of the high-frequency multivibrator D.

The real difficulty was that strong control could not be obtained without, at the same time, producing in the high-frequency multivibrator a large modulation from the low-frequency multivibrator. (This effect will be discussed later. There are advantages and disadvantages attending the presence of sub-harmonics in the immediate neighbourhood with respect to frequency of a selected harmonic of multivibrator B.) The final method of control adopted was as follows:—The impulse from the low-frequency multivibrator B is diverted to L4 (at the top of the diagram in the middle) and operates upon a selector circuit consisting of an inductance coil on L5 and a condenser C4. Part of C4 is variable and enables this circuit to select the 19th, 20th or 21st harmonic of B. The 20th harmonic is the one normally selected. This reinforced harmonic induces into a coil L6 connected to the grid filament circuit of the valve V4. In the anode circuit of V4 is the tuned impedance circuit C5, L7 having fixed frequency of about 20 kilocycles per second. A current of a few milliamperes at a frequency of 20 kilocycles results in this circuit. The inductance coil L7 is loosely coupled to the two inductive anode coils L8 of the high-frequency multivibrator D. By this means an electro-motive force, at a frequency of 20 kilocycles per second and with small modulation at 1 kilocycle per second, is impressed on the anode circuits of D and will hold this multivibrator in step over a limited range. If the coupling between L7 and L8 is increased beyond a certain small value, the modulation at 1 kilocycle per second becomes troublesome, but the range of synchronisation is much increased. A compromise has been made whereby the range of synchronisation is the equivalent of a few parts in a thousand in frequency of multivibrator D.

With this amount of control the subsidiary harmonics are just noticeably present when harmonics above the 30th are selected. There is, however, no uncertainty whatever

Digitized by Google

when setting an outside source to exact synchronisation with a main harmonic. The relationship between ease of control and freedom from modulation at the frequency of 1,000 cycles per second was made clearer by subsequent experiments on the high-frequency multivibrator.

D. This is the high-frequency multivibrator, having a fundamental frequency of 20 kilocycles per second. It consists of the following parts :—Anode inductive coils L8, each of which has an inductance of about 0·4 henry. The cross-connecting condensers C6 are fixed mica condensers of 0·004 $\mu$F capacity each. The non-inductive grid and condenser leak resistances $r_3$ are 50,000 ohms each of eureka wire. The inducing coil L9 is connected in series with the right-hand grid resistance at the filament end of it when the switch S5 is to the right in the H.F. position.

The frequency adjustment on this multivibrator is made by adjustment of the filament brightness by means of the coarse and fine resistances, $R_1$, $R_2$ in the filament circuit. By this means the frequency can be brought within the narrow belt of synchronisation with the controlling current in L7. This belt is extremely narrow with regard to filament current in valves V5 and V6, on account of the rather rapid rate of change of frequency on this multivibrator with filament current. This necessitates a stud contact resistance R1 and a smoothly variable rheostat R2, of the kind used on potentiometers.

Adjustment of frequency of this multivibrator to synchronism is, however, not the only condition requisite to satisfactory operation. The characteristics of valves of different kinds differ to such an extent that although the frequency of operation can in general always be brought to the 20-kilocycles region the behaviour is not then always satisfactory. This is particularly the case with regard to the sub-harmonics produced by the modulation of the current in the controlling circuit, and doubtless also by the direct and capacity couplings of the low and high-frequency multivibrators.

In order to throw light on these effects some frequency characteristics were taken, using various types of valve on a separate high-frequency multivibrator. Curves were obtained connecting frequency and filament current for various anode voltages ; observations of anode current were also made. Families of curves were drawn out for a number of different types of valve and for different specimens of the same valve. Pairs of valves had, of course, to be used in the test multivibrator, but observations of filament and anode currents were only made in the circuits of one of them.

In figs. 12 and 13 are shown curves for an ordinary R type (French) receiving valve. The curves of fig. 12 show frequency plotted against filament current for various constant anode battery voltages ; the curves of fig. 13 are derived from those of fig. 12 and show the relation between frequency and anode battery voltage for various constant filament currents.

These curves are similar in general shape to those obtained in the case of a regenerative valve oscillatory circuit of the ordinary kind, as shown by W. H. Eccles and J. H. Vincent (14), also W. A. Leyshon (15). Since, however, the multivibrator is not an oscillatory system in the ordinary sense of the term, it might be expected to show



Digitized by Google

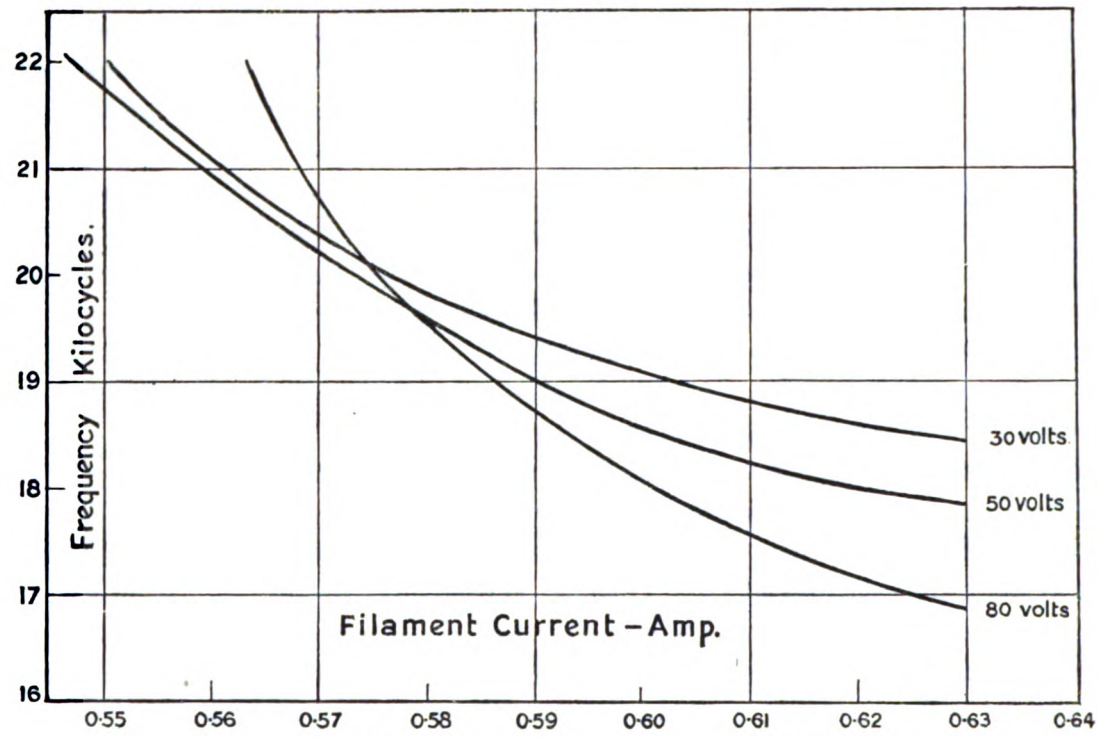


Fig. 12. Variation of frequency of multivibrator with filament temperature.

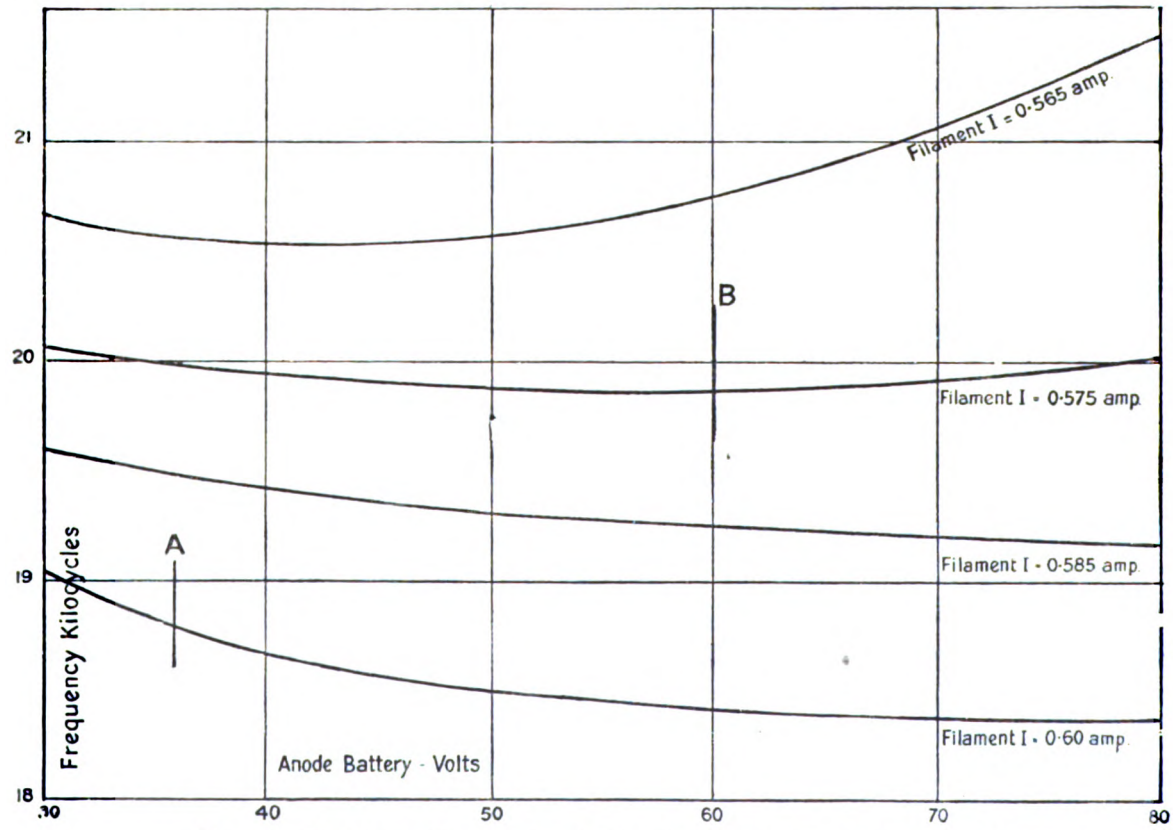


Fig. 13. Variation of frequency of multivibrator with anode battery voltage.

Digitized by Google

reactions of a different nature to those obtaining in an ordinary regenerative oscillator when under the influence of varying conditions in the valve circuits. This is seen to be the case with respect to variations of frequency with variations of anode voltage. In the multivibrator case the curves connecting frequency and anode voltage can show a flat minimum in certain cases, whereas in an ordinary oscillatory system the frequency appears to always diminish with increasing anode voltage (14).

On examination of the curves of fig. 12, it was seen that the filament current adjustment for synchronisation would be less critical by working the multivibrator near the saturation region of the valve at a filament current in the neighbourhood of 0·53 amp. The experiment was therefore tried, on the compound multivibrator, of working the high-frequency multivibrator at the part of the curve where small frequency change occurred with change of filament current. In order to bring this part of the curve into the region of 20 kilocycles per second it was necessary to adjust the number of turns on the anode coils L8. This was done and synchronisation obtained : it was then found, as expected, that the adjustment of filament current did not need to be so precise in order to keep within the belt of synchronisation. Unfortunately, however, this condition carried with it the condition of strong modulation at 1,000 per second. This was so prominent that it was impossible to be certain which of the successive interference beats represented synchronisation with the main harmonic when an outside source was adjusted in frequency.

Further experimenting soon showed that the curves plotted on fig. 13 gave the key to the behaviour of the high-frequency multivibrator. It was found to be always satisfactory when operating at such filament current and anode voltage that the curve connecting frequency and anode voltage was practically horizontal, indicating independence of frequency upon anode voltage over a considerable range of voltage. On adjustment of filament current and anode voltage to such values that the multivibrator was operating at a place such as A on curve IV of fig. 13, the sub-harmonics immediately became prominent. When, however, the conditions were as at B on curve II the behaviour was quite satisfactory.

This property of the multivibrator was found to hold true for five different kinds of valves. Plotting the curves of fig. 13 is the most satisfactory way of choosing the type of valve and of finding the suitable voltage and filament current for that type.

It may happen that none of the curves has a flat portion in the region of frequency of 20 kilocycles per second. In this case the whole family of curves may be shifted upwards or downwards in frequency by adjustment of the turns on the anode coils L8 of the high-frequency multivibrator. The change in frequency produced by this means is nearly proportional to the change in the number of turns. An ideal set of conditions would be that in which the family of curves in fig. 13 were flat and close together. No valve tried gave this condition, but it is possible that a compensating circuit might be so arranged as to bring about the condition of simultaneous invariability with anode battery voltage and filament current.



Digitized by Google

*(b) The Selector Circuit.*

As previously indicated, the object of this circuit is to select any desired harmonic. The two essential properties of the circuit are :—

(i) The proportion of the induced current at the desired frequency corresponding to the harmonic selected, to the currents induced by other harmonics should be as great as possible.

(ii) The selector circuit must be of such design and workmanship that the indication given by the variable part of it must leave no doubt as to which harmonic has been selected.

The circuit consists of a number of fixed inductance coils of small damping and such construction that they will remain invariable to within a few parts in a thousand in value. The capacity part of the circuit consists of a high-class variable air condenser, constructed to be as permanent in calibration as possible. Since harmonics up to the 120th can be selected, it is clear that the permanence of both inductance and capacity must be within about $\frac{1}{2}$ per cent. in order that the pointer of the variable condenser may never be more than, say, 0·25 of the space between two adjacent harmonics away from the engraved line representing a selected harmonic, when the condenser has been set to resonance at that harmonic.

The range of frequencies covered by each multivibrator is about twelve to one. This range requires a ratio of 150 to 1 between $C_{max.} \times L_{max.}$ and $C_{min.} \times L_{min.}$. A little consideration showed that this ratio could most satisfactorily be met by using three inductance coils for each multivibrator and by providing a ratio of maximum to minimum capacity on the condenser of about 7 to 1.

The design of the condenser has been largely determined by consideration of the shape of scales on which the harmonics are read. Since frequencies are read off on the scale the capacity will diminish as the readings increase. The capacity differences between successive harmonics become very small as the higher order harmonics are reached. This would cause, with the ordinary semi-circular shape of moving plate, a serious crowding together of the lines at the upper end. Thus, on such a condenser, if $C_n$ is the capacity corresponding to harmonic "$n$" we then have

$$C_n = Q/n^2$$

where Q = a constant; so that

$$\frac{dC_n}{dn} = -\frac{2Q}{n^3},$$

*i.e.*, the angular interval between two successive harmonics varies inversely as $n^3$.

With a normal size of condenser scale the interval between the 100th and 101st harmonics would become only about 1·5 mm., an amount too small to ensure certainty in the event of the pointer receiving a small accidental displacement. It was, therefore, decided to design the condenser so as to give a uniform frequency scale. This requires

Digitized by Google

a shape of vane somewhat like that for a uniform wave-length scale, or, again, like that for a direct reading decremeter. The equation to the shape of the vane is, however, quite different to either of these.

*Condenser for uniform frequency scale.*

The fundamental equations are :—

$$dn/d\theta = -q = \text{const.}, \quad . \quad . \quad . \quad . \quad . \quad . \quad . \quad . \quad . \quad (24)$$

where $q$ = angular interval between successive harmonics.

$$C = B/n^2 \quad . \quad . \quad . \quad . \quad . \quad . \quad . \quad . \quad . \quad . \quad . \quad (25)$$

where

$$B = \frac{1}{4\pi^2 L}$$

and

$$dc/d\theta = Ar^2 \quad . \quad . \quad . \quad . \quad . \quad . \quad . \quad . \quad . \quad . \quad . \quad (26)$$

where $r$ = radius of moving vane at angle $\theta$, and A = constant determining the capacity of the condenser in suitable units, and thus governing the size of the condenser.

From (25) we have

$$\frac{dC}{dn} = -\frac{2B}{n^3} \quad . \quad . \quad . \quad . \quad . \quad . \quad . \quad . \quad . \quad . \quad . \quad (27)$$

which combined with (24) gives

$$\frac{dC}{d\theta} = +\frac{2Bq}{n^3} \quad . \quad . \quad . \quad . \quad . \quad . \quad . \quad . \quad . \quad . \quad . \quad (28)$$

Equating (26) and (28) gives

$$r^2 = +\frac{2qB}{An^3} \quad . \quad . \quad . \quad . \quad . \quad . \quad . \quad . \quad . \quad . \quad . \quad (29)$$

The integration of (24) may be written

$$n = q\,(\phi - \theta). \quad . \quad . \quad . \quad . \quad . \quad . \quad . \quad . \quad . \quad . \quad (30)$$

Substituting this value of " $n$ " in (29) gives finally

$$r^2 = \frac{2B}{Aq^3} \cdot \frac{1}{(\phi - \theta)^3} \quad . \quad . \quad . \quad . \quad . \quad . \quad . \quad . \quad . \quad . \quad (31)$$

A semi-circular opening must be made in the fixed-plate system to accommodate the spindle and washers of the moving-plate system. If the radius of this opening is " $a$ " equation (31) becomes

$$r^2 - a^2 = \frac{2B}{Aq^3} \cdot \frac{1}{(\phi - \theta)^3} \quad . \quad . \quad . \quad . \quad . \quad . \quad . \quad . \quad . \quad (32)$$

The significance of the constant $\phi$ is that it is that angle (measured from the arbitrarily

Digitized by Google

chosen axis where $\theta = 0$) at which the frequency "$n$" becomes zero; at this angle, therefore, "$r$" becomes infinite. Fig. 14 makes the equation quite clear.

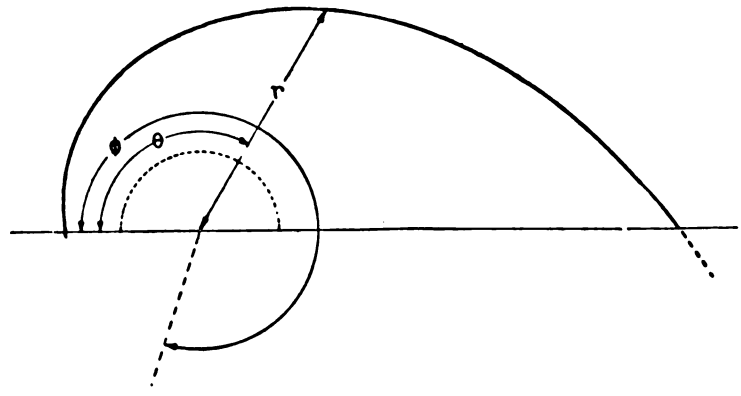


FIG. 14. Shape of vane of condenser giving uniform frequency scale.

The figure is drawn to scale and shows the shape of vane as used on the condenser. Reverting again to equation (31), the expression for C in terms of $\theta$ becomes

$$C_\theta = C_0 + C_0 \frac{\theta(2\phi - \theta)}{(\phi - \theta)^2}, \quad \ldots\ldots\ldots \quad (33)$$

where $C_0$ = capacity when $\theta = 0$. The value of $C_0$ is quite arbitrary. If $C_0$ and $\phi$ are given definite values the condenser is determined. On the other hand, we may let $C_0 = C_{min.}$ and $C_{180} = C_{max.}$ have the values desired and so determine the spacing of the harmonics. In this case $\phi$ will become automatically determined and the shape of vane may be calculated.

In the actual condenser constructed $C_0$ is much larger than the value of the variable part of the condenser at the angle $\theta = 0$. A fixed air condenser is incorporated into the design and is so adjusted, after allowing for the self-capacities of the coils, that the required conditions are satisfied. The small difference between the self-capacities of the coils is of no consequence, since the departure from uniformity of the scales thereby produced is unnoticeable. Each scale has, of course, been marked off experimentally and is direct reading in kilocycles per second.

In order to reduce the effect of stray capacities to a minimum the condenser is shielded in a german-silver box; also, the coils—of disc form—are so arranged that the outer end of each is connected to the screen-connected terminal of the condenser. The only stray capacities which can affect the resonant setting of the condenser are those to the inner end of the coil and to the lead connecting it to the insulated terminal of the condenser. These parts are already largely screened by the outer part of the coil.

It has been necessary to consider in some detail these points regarding the selector circuit, in order to ensure certainty of indication of a selected harmonic. Ultimately, the

Digitized by Google

only degree of permanence required is that the setting of the condenser to resonance at any desired harmonic shall not change adventitiously by an amount exceeding, say, one-quarter of the interval between two adjacent harmonics. In the worst case the capacity change between two adjacent harmonics, *i.e.*, 119th and 120th, is 1·6 per cent. of the total capacity. One quarter of this is 0·4 per cent. The condenser as constructed is not likely to change by this amount; in particular, at this region of its use the main part of the capacity is in the fixed portion of the condenser. Further down the scale (at, say, the 60th harmonic) the capacity is mainly in the variable part of the condenser, but in this region the change in capacity between adjacent harmonics is 3·3 per cent.

It is realised, of course, that when a harmonic has been selected and the condenser adjusted to give maximum loudness of beat tone in the amplifier telephone, even though the condenser pointer is then as much as 0·2 of a division from the line representing the selected harmonic, the frequency obtained is exactly that corresponding to the harmonic. So long as there is no doubt which line on the scale is referred to, there is no doubt regarding the frequency selected.

The chief mechanical features of the design of the condenser are the ribbed aluminium alloy top, to which everything is attached, the quartz washer insulators for holding the bank of fixed plates, and the accurately fitted bearings. The lower bearing does not put any axial constraint on the moving system. The tapering ends of the moving plates are stiffened by the provision of a small lug on each. A thin bolt with separating washers clamps and holds the tips of the vanes so that they are accurately spaced with respect to the fixed plates.

### *The Inductance Coils.*

The design of these is beset with more uncertainties than the design of a condenser. There are so many variables, and the question of permanence has always to occupy such an important place, that they cannot be very simple in construction. The question of obtaining small decrement is mainly one of size and cost. In the present case it was decided to make the coils short in comparison with their diameter and to fix the outside diameter at 20 cms. for all the coils. It was hoped, under these conditions, that all the coils could be so designed that their logarithmic decrements would be in the neighbourhood of 0·01, and that for each coil the region of minimum decrement would fall within the working range of it. Formulas for the calculation of effective resistance of single layer and overwound coils at radio-frequencies have been developed by BUTTERWORTH (16) and more recently by FORTESCUE (17). These formulas are valuable as a general guide to the best proportions and number of strands to use for various coils. The formulas so far developed are not applicable to coils of disc form, or when wound of compact form and short axial dimensions.

There appears room for development of the formulas in this direction. The determination of the components of the magnetic field at any point in the section of the winding

Digitized by Google

is extremely laborious when the coil is of compact form. The extrapolation required to the curves given by FORTESCUE is very uncertain when taken in the direction corresponding to coils having an axial length less than half the mean diameter.

The formulas developed by BUTTERWORTH assume the length and depth of winding to be small in comparison with the diameter; they assume also that the current is distributed uniformly over the section. In practice, however, the dimensions of the cross section are not small, and in the case of coils of less than about 100 total turns, the non-uniformity of current distribution over the cross-section of the winding is of importance.

There is thus some ambiguity as to what value to take for the term *un* in these formulas; this term may have very different values according to whether it is taken from the table for parallel wires or from the table for cylindrical coils, having the ratio of length to diameter chosen for the coil under calculation. It will be found, however, that, provided the correct number of strands is determined and the correct diameter of the individual strand approximated to, it will not then matter very much what the shape of cross-section is, so long as either the length or radial depth or both are not very far from 0·4 times the mean diameter.

If the section can be chosen with a ratio of its two dimensions of the order of 2·5 to 1, a good coil will result. In such a case the winding should proceed uniformly, in such a manner that the layers are many and short, in order that the distributed capacities from layer to layer may be across the minimum inductance. The self-capacity will then become as small as it is possible to make it with the design chosen, and the dielectric losses will also be a minimum.

The coils have been designed on the basis of these general considerations. The best number of strands and the best diameter of wire have not been available in some cases, and also the great desirability of using combs to locate the wires has caused the space factor of the winding to be much smaller than it should have been in the case of coils 1 and 2.

The coils have been constructed on built-up ebonite bobbins in such a manner that the spacing and location of the wires does not depend upon the wire itself. All the coils, except that for use in the region of frequency of $10^6$ per second, have been wound with multiple-stranded silk-insulated wire. The size of the cable has been chosen as large as was consistent with the provision of space for strong enough separating and supporting combs to ensure permanent and accurate location of the wires. Measurements of effective resistance of a variety of types of stranded and solid wire coils of the inductance required by the last coil of the series indicated that a single layer solid copper-strip coil was the best form for frequencies in the region of $10^6$ per second. The form adopted for this coil therefore was that of a flat helix of copper tape.

Measurements of the effective inductance and self-capacity of these coils were made over the range of frequencies at which they are used. The results are given in Table VII.

Digitized by Google

TABLE VII.

| Coil. | Self-Inductance. Millihenries. | Self-Capacity. Micro-microfarads. |
|---|---|---|
| 1 | 100·000 | 25 |
| 2 | 20·000 | 16 |
| 3 | 5·000 | 20 |
| 4 | 0·995 | 13 |
| 5 | 0·202 | 12 |
| 6 | 0·045 | 21 |

Measurements of the effective resistance were also made and the logarithmic decrement calculated for each coil at a number of frequencies. The results of these measurements are given in fig. 15 and show a number of points of interest. As mentioned above, it was hoped to obtain decrements as low as 0·01 for the coils, and at the same time it

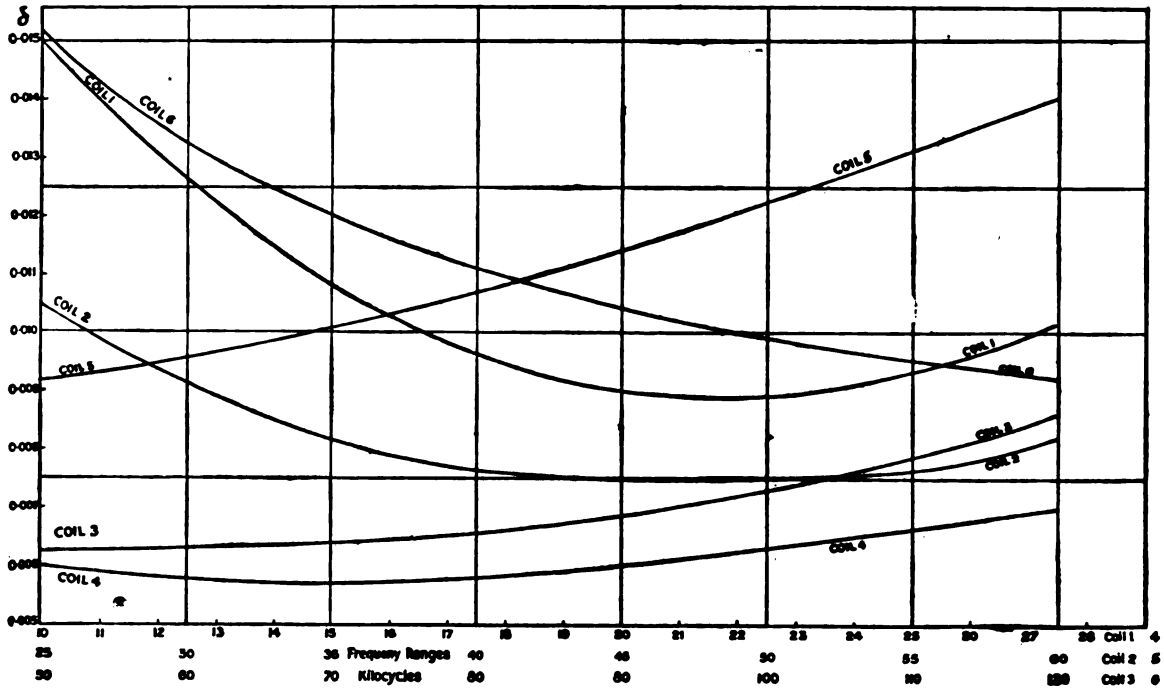


Frequency ranges to be multipled by 10 respectively for coils 4, 5 and 6.

Fig. 15. Log. dec. curves of inductance coils of selector circuit.

was hoped that the minimum decrement would fall within the working range. In the case of coils 1, 2, 3 and 4 these conditions have been realised. Coil 6 shows the typical decrement curve for the solid wire coil, but the curve of coil 5 is not understood. It is probable that a finer strand should have been used in the cable of which it was constructed. Since, however, the cable used already consisted of 81 strands of wire



Digitized by Google

0·12 mm. in diameter, it was not considered of sufficient consequence to obtain still more finely stranded cable.

The inductance coil of the selector circuit, and the coupling coils whereby the selector circuit is coupled to the multivibrator and to the amplifier, are attached at the back of the condenser in such a manner that the coupling coefficients will remain constant. The couplings and the number of turns on the various coupling coils have been chosen experimentally, so as to give the optimum effect in the amplifier telephones without causing any appreciable displacement of the resonant setting of the selector condenser.

### (c) *The Detector Unit.*

This is mounted up as a separate piece of apparatus ; it is of the tuned anode circuit type. The connections are shown in fig. 16. The inducing coil is connected to the grid-filament circuit of the first valve and has no tuning condenser. C1 L1 in the anode

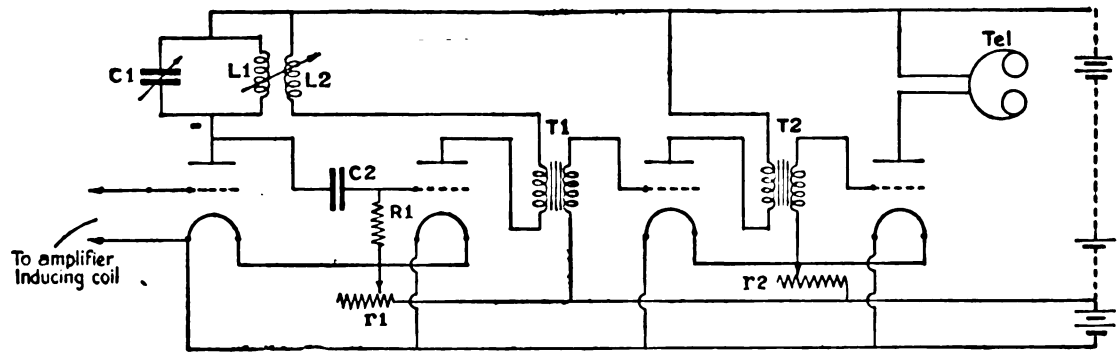


Fig. 16. Connections of selective amplifier.

circuit of the first valve form the tuned anode impedance. $C_1$ consists of fixed and variable condensers reading up to 0·004 $\mu$F. L1 is the inductance, consisting of any one of a set of small-size coils. The range of coils is such that the circuit C1, L1 covers a range from 7 to 2,000 kilocycles per second. The coil L2 provides reaction for the purpose of increasing the selectivity of the apparatus and also to enable it to become self-generating on occasion. Two stages of low-frequency amplification are provided in the usual way.

A selective amplifier is essential when the multivibrator is being used with high-order harmonics, especially on the low-frequency multivibrator. By adjustment of the reaction the effective resistance of the circuit L1, C1 can be greatly reduced. In this condition the amplifier becomes extremely selective and requires very close setting of C1. When the correct adjustment has been found, the neighbouring harmonics to that one selected are rendered relatively weak, so that the interpretation of the interference tones heard is not too dependent on a trained ear.

Digitized by Google

A plan view of the apparatus as set up for use is shown in fig. 17 and indicates the general disposition of the parts.

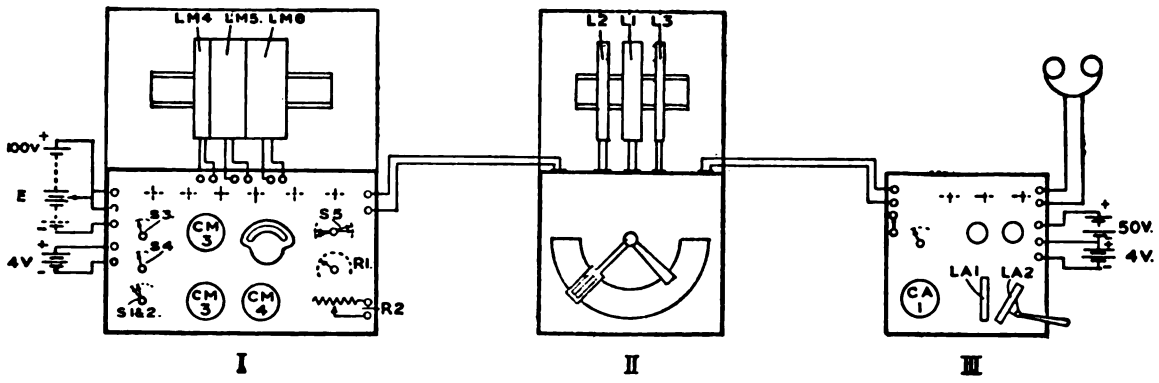


Fig. 17. General disposition of parts of standard wave-meter.

## 7. Methods of Using the Multivibrator Wave-meter.

The wave-meter described has been primarily designed as a fundamental laboratory standard of radio frequency; as such, it has three main uses:—

(*a*) To provide a standard of frequency, whereby a steadily running local oscillator of small power may be set to any desired frequency for the purpose of calibrating wave-meters, and for any other purposes of measurement involving known frequencies.

(*b*) To enable standard waves of constant and known frequency to be transmitted from an aerial for the purpose of broadcasting the standard.

(*c*) To measure the frequency of sustained waves emitted by other transmitting stations.

With regard to (*a*) no difficulties whatever arise; it is merely necessary to provide a valve oscillator of usual type and comply with the conditions for steadiness. The set in use at the Laboratory uses a transmitting valve of about 50 watts rating, run off an anode voltage of 400. The oscillator is set up on a neighbouring table and is provided with a set of interchangeable coils for the oscillatory circuit. An adjustable condenser consisting of fixed sections and a variable air condenser enable overlapping ranges of frequencies to be obtained with each coil. Four coils cover a range from 7 to 3,000 kilocycles per second. The steadiness of frequency is to 1 part in 100,000. Quite loud interference tones are produced in the amplifier telephone when adjusting this set to synchronisation with any desired frequency selected on the multivibrator. No particular coupling to the amplifier is required in general when using such a set; the electrostatic coupling between the oscillator and the amplifier is sufficient on this size of generator. When, however, it is desired to directly calibrate a small oscillator wave-meter or other weak generator, it is necessary to provide a small amount of inductive



Digitized by Google

coupling to the amplifier. This is easily accomplished by inserting a small coil of few turns in series with the amplifier inducing coil and bringing it near the inductive coil of the oscillator under test.

If it is desired to set or to measure a frequency which is considerably removed from a harmonic of the multivibrator, use is made of an accurately calibrated variable condenser in parallel with the main condenser of the oscillator. Fiducial points are found on this condenser corresponding to two or three neighbouring harmonics. Intermediate frequencies are then found by interpolation from a curve connecting variable condenser reading and frequency.

At the lower end of the range of the high-frequency multivibrator between, say, the 6th and 7th harmonics, corresponding to frequencies of 120 and 140 kilocycles per second, it will be seen that the interval is rather large for purposes of accurate interpolation. The gap can be shortened from either end by making use of successive sub-harmonics corresponding to frequencies of, say, 121, 122, 123, 124 and 139, 138, 137, 136 kilocycles per second. The gap can be reduced to about 16 per cent. by this means in the worst case. There is, however, another means of overcoming this trouble, and that is by working the high-frequency multivibrator at a fundamental frequency of 19 or at 21 kilocycles per second, instead of at 20; sufficient range in the tuning of the control circuit has been left to enable the 19th or 21st harmonic to be selected in this circuit from the low-frequency multivibrator for control purposes at these frequencies. Another series of frequencies is thus provided, such as 114, 133, 152 kilocycles per second from a 19 kilocycle per second fundamental; by the further use of sub-harmonics near these main harmonics the gaps may be reduced to about $2\frac{1}{2}$ per cent. in frequency in the worst case.

These subsidiary scales are shown in relation to the main scales in fig. 18. Scales 4A and 5A refer to a fundamental of 19 kilocycles per second, and scales 4B and 5B refer to a fundamental of 21 kilocycles per second.

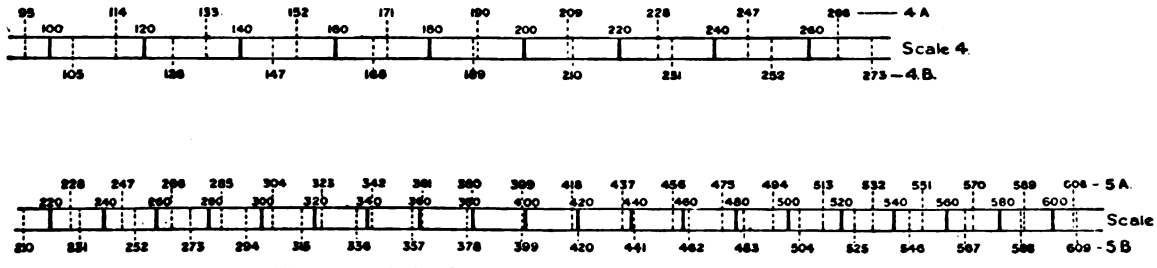


Fig. 18. Subsidiary scales showing spacing of harmonics.

With regard to (*b*), the use of the multivibrator in connection with the transmission of standard waves from an aerial is really a special case of its use in connection with setting the frequency of a source. There are two convenient methods of carrying this out. The simplest of these is to make use of a local generator, such as that mentioned in (*a*), working on a suitable anode voltage. This generator is coupled by capacity

Digitized by Google

coupling to the grid-filament circuit of the transmitting valve. This independent control on the power valve is a very satisfactory means of maintaining a transmission steady in current and frequency. In some actual tests made on an artificial aerial, about 70 watts of high-frequency energy was obtained from a 250-watt valve working on an anode voltage of 2,000. This represents about the maximum power that can be obtained from one valve on this voltage. By a cascade arrangement this power could be made to supply the grid-filament circuit of large valve or bank of valves.

This system of feeding the aerial requires adjustment of the small controlling oscillator and the steadiness obtainable depends upon the steadiness of this oscillator. There is, however, another means of producing steady high-frequency power, and that is to build-up from the multivibrator itself. For this purpose a cascade arrangement of valves is used, with tuned anode impedance in each anode circuit and with capacity coupling between anode and grids of the successive valves. This arrangement was tried; using three stages, enough power was available in the anode oscillatory circuit of the last valve to feed the grid circuit of the 400-volt valve set referred to above; this, in turn, can feed a 2,000-volt valve, thus giving high-frequency power actually controlled in frequency by the multivibrator. The current finally obtained contains a modulation at the tuning-fork frequency, but the amount of this causes no uncertainty regarding the frequency of the amplified harmonic, and this modulation is in some respects of value as it gives some character to the emitted wave.

With regard to (*c*), when measuring the frequency of transmission of a distant station the best procedure is to set a local oscillator to synchronisation, or preferably to a difference tone of 1,000 cycles per second, with the incoming signals, and then to measure the frequency of the local oscillator against the multivibrator by interpolation between two or more calibrated points on the open scale of a variable condenser forming a fractional part of the main capacity of the oscillator.

## 8. Precautions to be taken in using the Apparatus.

The frequencies given by the multivibrator are known with aosolute certainty in terms of the controlling tuning-fork when rightly interpreted; a certain amount of skill in hearing is, however, needed, in order to understand what is actually being heard. For example, owing to the rectification of the amplifier a note of frequency of 1 kilocycle per second is always heard whenever a harmonic of the low-frequency multivibrator is selected and amplified; this note has nothing to do with the interference note heard against an external source. As a consequence, when the external source is varied to the extent of being almost 1 kilocycle per second different from the selected harmonic, a beating is heard between the two notes in the telephone, due respectively to the rectified modulated multivibrator current and to the true interference between multivibrator and external source. There is, therefore, a liability to set the external source to a frequency 1 kilocycle per second different to that intended. In order to

Digitized by Google

ascertain that this mistake has not been made it is very desirable, after having set the external source to supposed synchronisation with a selected harmonic, to then select on the multivibrator selector circuit the two neighbouring harmonics on each side of that chosen. If the external source has been correctly set a loud note of 1 kilocycle per second will be heard when the selector condenser is set to the immediately adjacent harmonic on each side; or, again, a note of 2 kilocycles per second will be heard when the selector condenser is set to the next but one harmonic on each side.

Thus, suppose it is desired to set an external source to a frequency of 60 kilocycles per second. This harmonic is selected on the selector circuit and the amplifier tuned to it. The external source is now set to what is considered synchronism—there will not be complete silence in the telephone when this is done because of the rectified current referred to above, resulting in a note of 1 kilocycle per second—if now the selector circuit is set to 59 or 61 a loud sound at 1 kilocycle per second should be heard. When the selector circuit is set to 58 or 62 the fairly high note of 2 kilocycles per second will be heard and a fainter note of 1 kilocycle per second. If, however, a frequency of 61 kilocycles per second has been set in error on the external source, then, on setting the selector condenser to 61, a fainter note of 1 kilocycle per second will be heard, and on setting it to 59 a frequency of 2 kilocycles per second will be heard as well as the fainter one of 1 kilocycle per second. There is no doubt in judging these notes, so long as enough voltage is induced from the external source into the amplifier, unless the telephone has a natural resonance near to a frequency of 1 kilocycle per second. It may then happen that the 1 kilocycle per second component will drown the true beat tone of 2 kilocycles per second. In general, if Brown telephone receivers are used this effect will not occur, since these telephones have a fundamental natural resonance considerably above 1 kilocycle per second.

One other trouble likely to arise occurs when using the high-frequency multivibrator. Mention has been made of sub-harmonics at intervals of 1 kilocycle per second on each side of the main harmonic selected. These sometimes become prominent because the selector circuit or the amplifier tuning circuit have each not been set sufficiently carefully to the exact position of resonance. If, for example, the selector circuit condenser has been set slightly to one side of the true resonance position, then the sub-harmonics on that side will be reinforced and the true harmonic will be diminished. It is usually satisfactory to set the external source to a beat tone of about 800 or 1,500 per second and then to carefully tune selector circuit and amplifier condenser for maximum loudness of the note.

## 9. Conclusion.

The standard wave-meter here described is essentially a laboratory piece of equipment, but has been designed to be completely portable and not to require any elaborate setting up. In terms of the controlling tuning-fork it is believed that the wave-meter gives a series of frequencies of range and accuracy not hitherto obtained.

Digitized by Google

The fundamental accuracy can be checked at any time by measurement of the frequency of the tuning-fork by any satisfactory method. The accuracy of order of the harmonic can always be checked by the aid of an auxiliary heterodyne set, by making use of its fundamental and second harmonic.

Such a standard has other uses than that of measuring radio-frequencies. It may also be used in connection with measurement of inductance, capacity, and self-capacity of coils. Also very small changes in inductance and capacity may be measured by observing the changes in beat tone produced when the capacity or inductance under observation forms part of a valve-generator circuit.

There are possibilities also in the use of the apparatus, in a modified form, for the purpose of controlling the frequency of transmitting stations to an accuracy not hitherto attained.

In conclusion I wish to express my appreciation of the careful and accurate constructional work carried out by the staff of the workshop. Also to Mr. MARTIN of the Electrical Department for the skilful manner in which he has carried out many—sometimes tedious—observations with the apparatus.

My thanks are due also to Sir JOSEPH PETAVEL and to the members of the Committee of the Radio Research Board on Standards and the Propagation of Waves, established under the Department of Scientific and Industrial Research, under whose auspices the whole work has been carried out and who have shown much interest in the development of the standard.

A complete specification of the wave-meter, with detail working drawings, has been drawn up, copies of which are deposited at the National Physical Laboratory.

An Appendix giving full instructions in the setting up, use and adjustment of the wave-meter has also been prepared.

## REFERENCES.

(1) SIMON and BARKHAUSEN, "On Undamped Electrical Oscillations", 'Jahrb. d. D. Tel.', 1907, vol. 1, pp. 16 and 243.

(2) R. LINDEMANN, "On the Application of the Harmonic Overtones of the Poulsen Arc to the Measurement of Wave-length", 'Verh. Deut. Phys. Gesell.', 1912, vol. 14, p. 624.

(3) H. DIESSELHORST and R. SCHMIDT, "Absolute Measurements of Wave-length of Electrical Oscillations", 'Jahrb. d. D. Tel.', 1907, vol. 1, p. 262; also 'Zeits. f. Instr.', 1909, vol. 29, p. 153, and 'Verh. Deut. Phys. Gesell.', 1909, vol. 11, p. 205.

(4) TYKOCINSKI-TYKOCINER, "The Mandelstam Method of Absolute Measurement of Frequency of Electrical Oscillations", 'Phil. Mag.', 1920, vol. 39, p. 289.

(5) J. S. TOWNSEND and J. H. MORRELL, "Electric Oscillations in Straight Wires and Solenoids", 'Phil. Mag.', 1921, vol. 42, p. 265.

Digitized by Google

(6) AKIRA TSUBOUCHI, "Standardization of Wave-meters", 'Researches of Electrotechnical Laboratory, Tokyo', No. 115, Sept., 1922.

(7) G. W. PIERCE, "Piezo-electrical Crystal Resonators and Crystal Oscillators applied to the Precision Calibration of Wave-meters", 'Proc. Am. Acad. of Arts and Sciences', 1923, vol. 59, p. 81.

(8) W. G. CADY, "The Piezoelectric Resonator", 'Proc. Inst. Radio Engs.', 1922, vol. 10, p. 83.

(8A) M. MERCIER, "Determination of the Speed of Propagation of Electromagnetic Waves along conducting Wires", 'Annales de Physique', vol. 19, p. 248, and vol. 20, p. 5, 1923.

(8B) M. MERCIER, "Harmonic Synchronisation of Electric Oscillators", 'Comptes Rendus', vol. 174, p. 448, 1922.

(9) H. ABRAHAM and E. BLOCH, "Mesure en Valeur Absolue des Périodes des Oscillations Electriques de Haute Fréquence", 'Ann. de Phys.', 1919, vol. 12, p. 237.

(10) A. CAMPBELL, "On a Standard of Mutual Inductance", 'Roy. Soc. Proc.', A, 1907, vol. 79, p. 428; also N.P.L. 'Collected Researches', vol. 4, Paper V.

(11) D. W. DYE, "Calculation of a Primary Standard of Mutual Inductance of the Campbell Type and Comparision of it with the Similar N.P.L. Standard", 'Roy. Soc. Proc.', A, 1922, vol. 101, p. 315; also N.P.L. 'Collected Researches', vol. 18, Paper VII.

(12) F. E. SMITH, "Absolute Measurements of Resistance", 'Phil. Trans.', A, 1914, vol. 214, p. 27; also N.P.L. 'Collected Researches', vol. 11, Paper XIII.

(13) D. W. DYE, "Valve-maintained Tuning-Fork as a Precision Time-Standard", 'Roy. Soc. Proc.', A, 1923, vol. 103, p. 240; also N.P.L. 'Collected Researches', vol. 18, Paper XII.

(14) W. H. ECCLES and J. H. VINCENT, "On the Variations of Wave-length of the Oscillations generated by Three-electrode Thermionic Tubes due to Changes in Filament Current, Plate Voltage, Grid Voltage or Coupling", 'Roy. Soc. Proc.', A, 1920, vol. 96, p. 455.

(15) W. A. LEYSHON, "On the Effect of Changes in Filament Temperature, Grid Potential and Anode Potential on the Frequency of the Oscillations generated by a Thermionic Valve", 'Radio Review', vol. 1, p. 481, 1920.

(16) S. BUTTERWORTH, "Eddy-current Losses in Cylindrical Conductors", 'Phil. Trans.', A, 1921, vol. 222, p. 57; also N.P.L. 'Collected Researches', vol. 18, Paper VI.

(17) C. L. FORTESCUE, "The Design of Inductances for High-frequency Circuits", 'Jour. Inst. Elec. Eng.', 1923, vol. 61, p. 933.

Digitized by Google

# THE PERFORMANCE AND PROPERTIES OF TELEPHONIC FREQUENCY INTERVALVE TRANSFORMERS

BY

D. W. DYE, B.Sc., A.C.G.I.,
SENIOR ASSISTANT IN THE ELECTRICITY DEPARTMENT.

Digitized by Google

## ABSTRACT.

Methods are described for measuring the effective primary inductance and resistance of telephonic frequency transformers.

It is shown that when reactance and resistance are plotted in a convenient manner the result is a circle diagram.

The analysis of the effective components of inductance, capacity and resistance corresponding to the circle diagram is then shown and is developed to include the effects on primary effective reactance and resistance of mutual and secondary capacity, shunt resistance on the secondary and the attachments of a valve grid-filament circuit.

The means of evaluating secondary inductance and self-capacity are shown. The effects of the foregoing quantities on the ratio of the transformer are then examined experimentally and theoretically and the close relationship of ratio to the coefficient of coupling shown.

The results of the complete analysis are applied to the determination of the amplification factor of the transformer and a number of conclusions are drawn therefrom.


Digitized by Google

# THE PERFORMANCE AND PROPERTIES OF TELEPHONIC FREQUENCY INTERVALVE TRANSFORMERS.

By D. W. DYE, B.Sc., A.C.G.I., Senior Assistant in the Electricity Department.

[Reprinted from 'Experimental Wireless and Wireless Engineer', Vol. 1, September, 1924.]

## 1. Introduction.

Intervalve transformers are a very commonly used means of coupling the stages of amplifiers used for various purposes in which it is required to magnify weak currents of telephonic frequency.

Very little information has been published on the properties of such transformers or on the methods of testing their operation and determining the qualities that are desirable in them in order that they may best suit the circuits to which they are applied. One test which is commonly applied is to measure the effective amplification of voltage given by a valve and transformer. This may be expressed as the ratio of the secondary voltage produced by the transformer, when connected to the grid of another similar valve, to the voltage applied to the grid of the first valve in whose anode circuit the primary of the transformer is connected.* This test is very valuable and is a direct measure of the overall performance of a transformer. As a means of comparing various types of transformer also it is probably indispensable. Such a test, however, has very small power of analysing the various factors entering into the overall performance.

It was thought that more insight into the behaviour of such transformers would be obtained by carrying out direct measurements of the effective inductance, resistance and other inherent properties of the windings. The present investigation is an attempt to analyse the transformer experimentally and theoretically under the conditions of use. The results have proved highly interesting and somewhat remarkable, and although it has not been possible to separate completely all the quantities involved, a sufficiently complete analysis has been obtained in a manner which is capable of giving much guidance in design.

## 2. General Considerations.

*Statement of the Case.*

The function of an intervalve transformer is to receive on its primary winding as large a fraction as possible of the alternating voltage set free in the anode circuit in which it is connected. It should then develop at its secondary terminals—connected to the

* F. E. Smith and H. C. Napier, "On the Measurement of Amplification given by Triode Amplifiers, at Audible and at Radio Frequencies", 'Proc. Phys. Soc.', vol. 32, p. 116, 1920; and N.P.L. 'Collected Researches', vol. 18, Paper IX.



Digitized by Google

grid circuit of the ensuing valve—as high a voltage as possible. Further, the ratio of the input voltage to the first valve to that given by the transformer to the ensuing valve should be invariable with regard to frequency and amplitude. It is, of course, realised in making the above statement that the most perfect transformer from this point of view may fail by its very perfection on account of the instability which may be produced and which will result in the self-generation by the system of oscillations of audible frequency constituting one form of the troublesome malady known as "howling". In the present investigation, however, no account is taken of this possibility in any part of the discussion or conclusions.

Referring now to fig. 1, representing a typical use of an intervalve transformer T, we have, applied to the grid of valve $V_1$, an alternating voltage, $e_g$, the source of which, for the moment, does not concern us. As a result of this voltage, a voltage $\mu e_g$ is produced in the anode circuit ABCF; of this voltage a fraction $e_p$ is applied to the primary of the transformer, resulting in a secondary voltage $e_s$ which is applied to the grid-filament circuit of the valve $V_2$. The duty of the transformer is to give a ratio $e_s/e_p$ as large as

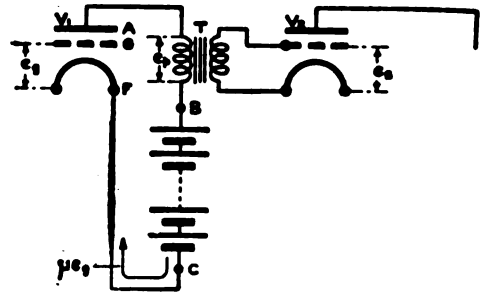

FIG. 1.

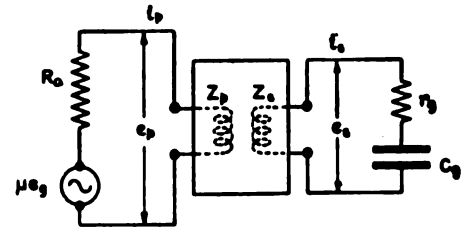

FIG. 2.

possible and to keep this ratio independent of amplitude and frequency. Now the essential electrical quantities involved can be represented as in fig. 2, in which the valve $V_1$ and its batteries have been replaced by a resistance $R_a$ assumed constant and pure and a source of alternating voltage of value $\mu e_g$. The valve $V_2$ is assumed to be replaced by an impedence $Z_g$ consisting of a capacity $C_g$ and a series resistance $r_g$. A variety of quantities enter into the electrical representation of the transformer, but for the moment, as regards the current $i_p$ entering at the terminals, the primary winding can be represented by a simple impedance $Z_p$ and the secondary winding can be represented in a like manner.

The ratio $\frac{e_s}{\mu e_g}$ may now be considered as the product of the two quantities $q$ and $\sigma$, where $q$ is the primary voltage factor and $\sigma$ the ratio of $e_p$ to $e_s$. We have

$$q^2 = \left(\frac{e_p}{\mu e_g}\right)^2 = \frac{Z_p^2}{X_p^2 + (R_p + R_a)^2},$$

in which $X_p$ and $R_p$ are the reactance and resistance components of $Z_p$, while $\sigma$ depends mainly upon the ratio of the numbers of turns of primary and secondary windings. If,

Digitized by Google

therefore, we measure $X_p$ and $R_p$ under various conditions and over a considerable range of frequencies, we can determine the performance of the transformer under these conditions. It is to be anticipated also that a separation of the internal constants of the transformer can to a considerable extent be made by observation of the change in effective primary impedance and in ratio when various external conditions are varied. Since an intervalve transformer contains thousands of turns in its windings, in a confined space, it is to be further expected that the distributed capacities of the windings will play an important part in its behaviour.

The transformer may therefore be considered as a mutual inductance possessing all the parts indicated in fig. 3, in which $R_t$ and $L_t$ represent a tertiary closed circuit imitating the hysteresis and eddy current effects due to the iron core and $C_m$ represents distributed capacity between primary and secondary windings. The meanings of the other quantities are obvious.

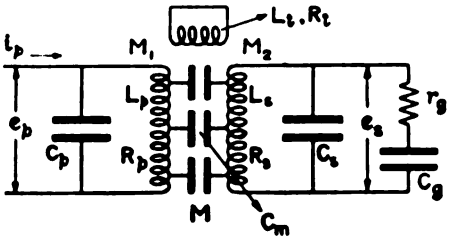


FIG. 3.

The complete solution of this case can be expressed as a determinant, but the reduction of any part of it to a working equation becomes too complicated to enable the bearing of the various factors to be visualised; in addition $L_t$ and $R_t$ are variable with frequency and current, and the effective mutual capacity $C_m$ will depend upon the potential differences between any chosen points on primary and secondary circuits as determined by the complete electrical system including the external circuit. As regards this latter point, in practice the transformer is commonly connected as shown in fig. 4. The impedance of the anode battery between the points A, B is small com-

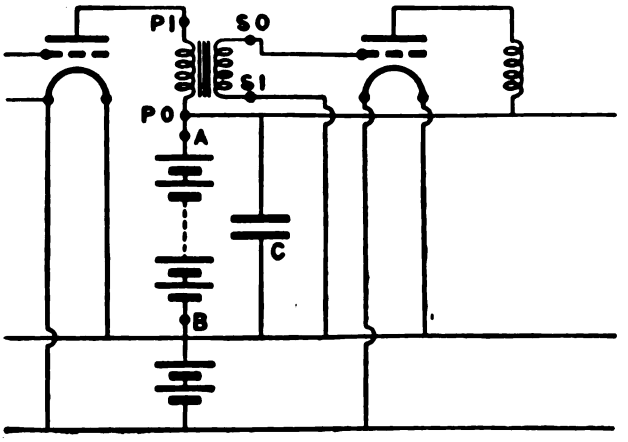


FIG. 4.

pared with the rest of the circuit, even without the condenser C. When this is used, as is common, and has a value of the order 1 or 2 $\mu$F, it virtually amounts to connecting the terminals PO, SI together so far as the alternating voltages are concerned. This

Digitized by Google

results in a simplification of the equivalent circuits of the transformer to those shown in fig. 5, in which also the iron losses have been transferred as a load $Z_s$ (not necessarily invariable with frequency) on the secondary winding. The equivalent grid capacity and resistance have been merged into the secondary capacity and impedance. This diagram represents the simplest form and possesses the smallest number of variables to which an intervalve transformer can be reduced. Before giving the evaluation of the equations connecting the various voltages and currents, it is convenient to describe the methods and some results of the experiments on the measurements of effective inductance and resistance of the primary winding and of the effective ratio of transformation.

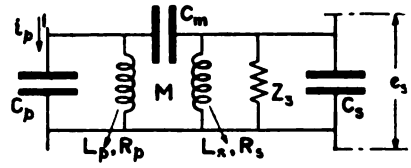


FIG. 5.

## 3. Measurement of Effective Primary Impedance and of Voltage Ratio of Transformer.

The measurement of an inductance of many henries having a resistance of many thousands of ohms is not very easy, especially when these measurements are required at small voltages. Variable mutual or self-inductances of range expressed in henries are not easily available, and, further, if one arm of a bridge is allowed to be of several hundred thousand ohms in impedance, the effects of stray capacities become very troublesome, and the measurements are uncertain unless great precautions are used.

In the light of previous experiments, the method finally adopted consisted of a mutual inductance bridge with four equal arms of 1,000 ohms each. The arrangement is shown in fig. 6. The measurements consist in observing the change in effective inductance

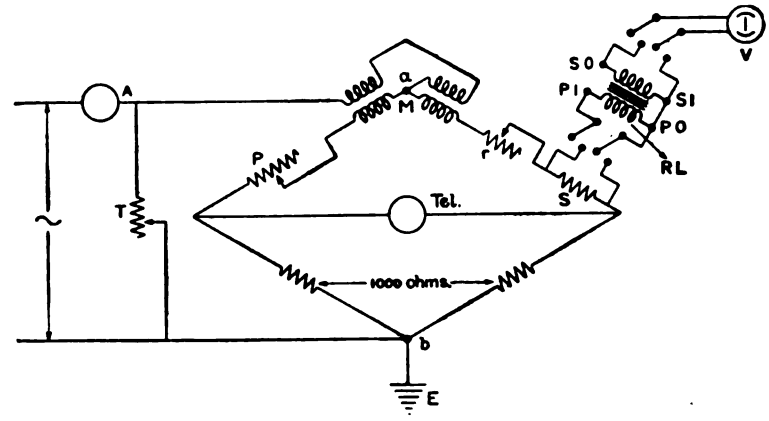


FIG. 6.

and resistance of the non-inductive resistance coil S when shunted by the primary of the transformer. A definite voltage is conveniently applied to the ends of S by the help of the thermoammeter A, and a shunt resistance T across the bridge. The whole bridge resistance between *a* and *b* is almost invariable under all experimental conditions,

Digitized by Google

and is nearly 1,000 ohms. The mutual inductometer is of 10mH range: the variable resistance $r$ requires to be known to 0·01 ohm, and may reach values somewhat greater than 10 ohms. The point $b$ of the bridge is directly earthed, and greatly stabilises it; doubtless a Wagner earth would be superior from the point of view of rendering capacities of the transformer to earth of no consequence, but these effects are of no particular importance in the present investigation, since less than 1 per cent. uncertainty is produced by them.

An Ayrton-Mather low-reading electrostatic voltmeter serves to read or to see the secondary voltage of the transformer. This voltmeter must be disconnected when the observations are made, because of the large effects produced on the effective primary inductance and resistance by the capacity of the voltmeter. As will be seen later, the voltmeter capacity has a negligible effect on secondary voltage. The low-reading voltmeter is rather a luxury in such experiments, but if desired, a valve instrument of the Moullin type could doubtless be used instead.

The procedure consists in observing the values of M and $r$, first with the transformer disconnected from S, and then after shunting it across S. Before making the second observation, the voltmeter is connected to the secondary of the transformer and the bridge current adjusted so as to give the desired primary or secondary voltage. The effective resistance and inductance of a shunt circuit in terms of the change in effective resistance and inductance of the resistance S is given as follows: if the pure resistance S is shunted by R and L in series, and then has an apparent resistance and inductance $S_0$ and $L_0$, then

$$R = \frac{SS_0(S - S_0) - SL_0^2\omega^2}{(S - S_0)^2 + L_0^2\omega^2} = \frac{S^2\Delta S}{\Delta S^2 + L_0^2\omega^2} - S,$$

in which $\Delta S = S - S_0$ and

$$L = \frac{S^2 L_0}{\Delta S^2 + L_0^2\omega^2}.$$

In the equal arm bridge here used $L_0$ is equal to $2(M - M_0)$ where $M_0$ and M are the readings on the inductometer before and after connecting the transformer primary across S, and $\Delta S$ is equal to the difference between the values of $r$ before and after connecting the transformer.

We have, therefore,

$$R = \frac{S^2\Delta R}{\Delta R^2 + (2\Delta M)^2\omega^2} - S \ldots, \quad (1)$$

and

$$L = \frac{S^2 2\Delta M}{\Delta R^2 + (2\Delta M)^2\omega^2}. \quad (2)$$

By choosing Sequal to 1,000 ohms we get a very convenient multiplier of $10^6$, thus enabling the readings to be taken on the 10mH inductometer. In a poor transformer, however,

Digitized by Google

M may be come larger than 10mH. In this case S may be conveniently chosen as 500 ohms.

When the current through the bridge is reduced to such a value that the secondary voltage across the transformer is less than 2, favourable external conditions are required in order to obtain good sensitivity, since there is not then more than about 1 volt on the whole bridge. As will be seen later, a typical transformer may have an effective primary reactance of no less than 500,000 ohms in certain regions of frequency, so that the change in $r$ representing change in S is only about 2 ohms. For an accuracy of 1 per cent., therefore, $r$ must be observed to 0·02 ohm. and this is an arm of 1,000 ohms resistance. Since, however, practically the whole of the bridge consists of 4 manganin coils of 1,000 ohms each, the balance is remarkably stable.

When observing the effects of added capacity across the secondary or as added mutual capacity, a standard low range variable air condenser was used. The effects of resistance across the secondary were also studied, and for this purpose grid leaks previously calibrated at telephonic frequencies were used.

A typical series of observations is given in Table I below, together with the reduced values of $R_p$, $L_p$ and $X_p$, the effective resistance, inductance and reactance of the primary winding.

TABLE I.—Effective Primary Resistance, Inductance and Reactance of Intervalve Transformer with PO and SI common and no connections across the secondary.

| Frequency. cycles per sec. | Observed $r$ difference. | Observed M difference. | $R_p$. | $L_p$. | $X_p$. |
|---|---|---|---|---|---|
| | Ohms. | μH. | Ohms. | Henries. | Ohms. |
| 500 | 4·49 | 5,010 | 3,450 | 9·93 | 31,200 |
| 800 | 2·73 | 1,794 | 7,200 | 10·82 | 54,300 |
| 1,000 | 2·22 | 1,014 | 12,500 | 12·23 | 77,000 |
| 1,200 | 1·93 | 565 | 24,300 | 14·82 | 111,800 |
| 1,400 | 1·88 | 319 | 54,500 | 18·54 | 163,000 |
| 1,500 | 1·85 | + 225 | 85,000 | 21·07 | 198,500 |
| 1,600 | 1·81 | + 156 | 135,300 | 23·84 | 239,600 |
| 1,700 | 1·78 | + 102 | 224,000 | 25·85 | 276,000 |
| 1,750 | 1·76 | + 64 | 345,500 | 25·10 | 276,000 |
| 1,800 | 1·74 | + 42 | 442,000 | 21·36 | + 241,600 |
| 1,850 | 1·74 | + 13 | 557,000 | 8·36 | 97,000 |
| 1,900 | 1·71 | − 10 | 569,000 | − 6·54 | − 78,000 |
| 1,950 | 1·71 | − 30 | 493,000 | − 17·31 | − 212,000 |
| 2,000 | 1·71 | − 46 | 400,000 | − 21·56 | − 271,000 |
| 2,100 | 1·74 | − 85 | 216,000 | − 21·14 | − 279,000 |
| 2,200 | 1·75 | − 116 | 130,000 | − 17·43 | − 241,000 |
| 2,500 | 1·76 | − 187 | 51,000 | − 10·37 | − 163,000 |
| 3,000 | 1·75 | − 256 | 17,000 | − 5·33 | − 100,500 |

The curves corresponding to $R_p$ amd $L_p$ are shown in fig. 7. The changes in them are very great as the frequency passes through the resonant region. In this region,

Digitized by Google

therefore, frequencies near one another must be used if accurate delineation is required; the frequencies must also be known with considerable precision.

It will immediately be seen that these curves are those corresponding to a system having a well-defined resonant frequency. Now one of the properties of such a system is that if we plot effective resistance against the corresponding effective reactance the

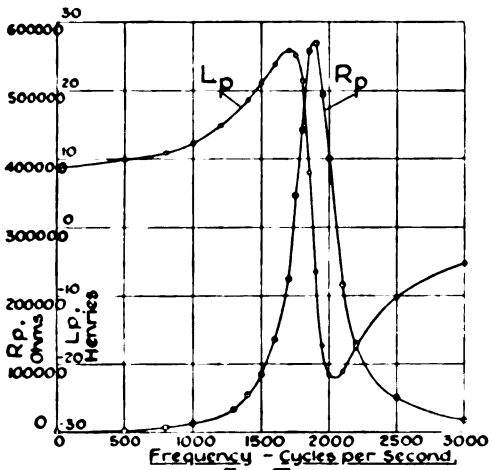

FIG. 7

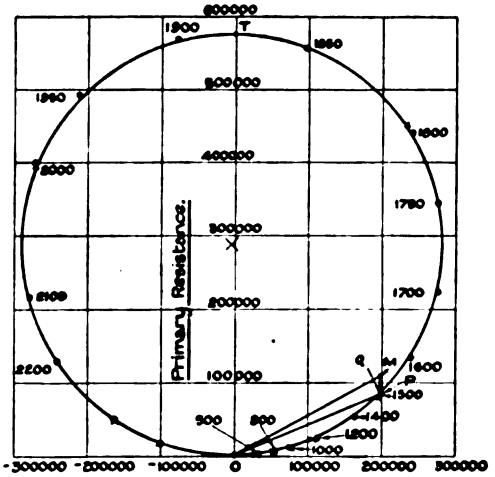

FIG. 8.

points should lie approximately on a circle. In fig. 8 are shown the corresponding values of resistance and reactance plotted—as dots in circles—in this manner. It will be seen that the points lie upon an astonishingly good circle. It is of interest to consider the simplest kind of circuit which can produce a circle when its properties are treated in this manner.

## 4. Circle Diagram and its Relationship to the Properties of a Circuit.

If we take the simple circuit shown in fig. 9 (*a*), we shall find that the equivalent $R_0$ and $X_0$ with respect to the external current $i_0$ have such values as to give a perfect circle when plotted in the manner shown in fig. 8. Thus

$$i_0(R_0 + L_0\alpha) = e_0 = i_1 L a = i_2 S = i_3 \frac{1}{C\alpha}$$

where $\alpha = j\omega$, and $i_0 = i_1 + i_2 + i_3$

whence
$$R_0 = \frac{SL^2\omega^2}{S^2(1 - LC\omega^2)^2 + L^2\omega^2}, \quad \ldots\ldots\ldots\ldots \quad (3)$$

and
$$L_0 = \frac{S^2L(1 - LC\omega^2)}{S^2(1 - LC\omega^2)^2 + L^2\omega^2} \quad \ldots\ldots\ldots\ldots \quad (4)$$

Now if we let $a^2 = (\text{radius of circle})^2 = (R_0 - \frac{1}{2}S)^2 + (L_0\omega)^2$ we get

$$a^2 = \frac{S^2[\{L^2\omega^2 - S_2(1 - LC\omega^2)^2\}^2 + 4S^2L^2\omega^2(1 - LC\omega^2)^2]}{4\{S^2(1 - LC\omega^2)^2 + L^2\omega^2\}^2} = S^2/4.$$



Digitized by Google

For all values of $\omega$, therefore, the points lie on a circle of diameter equal to S, and with its centre on the axis at the point $R_0 = \frac{1}{2}S$. Now such a circle, although approximately representing the transformer primary, cannot quite do so, since the inductance $L_1$ has in practice a resistance R, which is shown by the relatively very small $R_0$ at the point O on fig. 8, corresponding to a frequency 0. Now this resistance R, although of little consequence at frequencies corresponding to the lower portion of the circle, has a considerable influence on the diameter of it. A further effect is to cause the circle to be

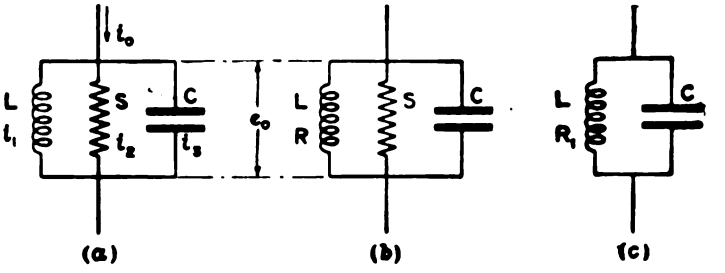


FIG. 9.

displaced horizontally by a small amount, so that its centre lies to the left of the R axis. The experimental results are sufficiently accurate to show this, as will be seen by close inspection of the points. A closer approximation to the experimental and the actual case is given by (*b*) of fig. 9, where an R term is included, and the shunt resistance S now has a different value from that corresponding to fig 9 (*a*).

Calculating the effective values of $R_0$ and $L_0$ for case (*b*) the accurate expressions are

$$R_0 = \frac{S(R^2 + SR + L^2\omega^2)}{(R + S[1 - LC\omega^2])^2 + (L + RSC)^2\omega^2}, \quad \ldots\ldots (5)$$

and

$$L_0 = \frac{S^2\{L(1 - LC\omega^2) - R^2C\}}{(R + S[1 - LC\omega^2])^2 + (L + RSC)^2\omega^2} \quad \ldots\ldots (6)$$

When $LC\omega^2 = 1$, these become to a very close approximation

$$R_{0(max.)} = S - \frac{RS^2C}{L + RSC} = \text{diameter of circle} = \frac{SL}{L + RSC} \quad \ldots\ldots (7)$$

$$L_0 = 0.$$

It is seen that the introduction of the R term has considerably complicated the expressions for $R_0$ and $L_0$, so that the diameter of the circle is no longer equal to S, and the exact evaluation of the four constants L, C, S and R from a series of observed values of $R_0$ and $L_0$ is not quite so easy. It would, in any case, obviously be unwise to attempt to separate L and C at a region of frequency near that at which $LC\omega^2 = 1$. We will,

Digitized by Google

therefore, consider the case where $LC\omega^2$ is not nearly unity, *i.e.*, the lower portion of the circle. Terms containing $R^2$ become negligible, and the expressions reduce to

$$R_0 = R_p = \frac{S(L^2\omega^2 + RS)}{L^2\omega^2 + 2RS + S^2(1 - LC\omega^2)^2}, \quad \ldots\ldots\ldots \quad (8)$$

and

$$L_0 = L_p = \frac{S^2L(1 - LC\omega^2)}{L^2\omega^2 + 2RS + S^2(1 - LC\omega^2)^2}, \quad \ldots\ldots\ldots \quad (9)$$

or

$$X_p = L_p\omega = \frac{S^2L\omega(1 - LC\omega^2)}{L^2\omega^2 + 2RS + S^2(1 - LC\omega^2)^2}, \quad \ldots\ldots\ldots \quad (10)$$

in which $R_p$ and $L_p$ represent the effective resistance and inductance of the primary of a transformer.

The separation of the quantities L, C, S and R will now be considered.

Equation (10) may be written

$$\frac{1}{X_p} = \frac{1 - LC\omega^2}{L\omega} + \frac{1}{S^2} \times \frac{L\omega}{1 - LC\omega^2} + \frac{2R}{SL\omega(1 - LC\omega^2)} \quad \ldots\ldots\ldots \quad (11)$$

Let

$$\frac{1}{X_p} = \frac{1 - LC\omega^2}{L\omega} = P;$$

we then have

$$P + \frac{1}{S^2} \times \frac{1}{P} + \frac{2R}{SL\omega(1 - LC\omega^2)}.$$

We can treat the term $\frac{2R}{SL\omega(1 - LC\omega^2)}$ as a separate correction to be applied afterwards, as will be seen later.

Taking, then, $S^2P = S^2P^2X_p + X_p$ we have

$$P = \frac{1}{2X_p}\left(1 \pm \frac{1}{S}\sqrt{S^2 - 4X_p^2}\right).$$

If, therefore, we choose points having observed values $X_1$ and $X_2$ of $X_p$ at known values of $\omega$ equal to $\omega_1$ and $\omega_2$ as given by the circle, we can write down two equations,

$$P_1 = \frac{1}{2X_1}\left(1 \pm \frac{1}{S}\sqrt{S^2 - 4X_1^2}\right) \quad \ldots\ldots\ldots \quad (12)$$

and

$$P_2 = \frac{1}{2X_2}\left(1 \pm \frac{1}{S}\sqrt{S^2 - 4X_2^2}\right) \quad \ldots\ldots\ldots \quad (13)$$

The significance of the $\pm$ sign in the bracket is that, for points on the circle below the horizontal diameter the sign is $+$, and for values above this diameter the sign is $-$.



Digitized by Google

At the two points on the circle where the horizontal diameter cuts it, the expression under the square root becomes zero.

Now

$$P_1 = \frac{1}{L\omega_1} - C\omega_1 \text{ and } P^2 = \frac{1}{L\omega_2} - C\omega_2$$

so that

$$L = \frac{\omega_2^2 - \omega_1^2}{\omega_1\omega_2(P_1\omega_2 - P_2\omega_2)} = \frac{n_2^2 - n_1^2}{n_1 n_2 (P_1\omega_2 - P_2\omega_1)}, \quad \ldots\ldots (14)$$

and

$$C = \frac{P_1\omega_1 - P_2\omega_2}{\omega_2^2 - \omega_1^2} = \frac{P_1 n_1 - P_2 n_2}{2\pi(n_2^2 - n_1^2)}. \quad \ldots\ldots (15)$$

It has been noted above in equation (7) that the diameter of the circle does not equal S, so that we cannot use the experimentally known diameter in equations (12) and (13) in order to determine $P_1$ and $P_2$.

But if we choose suitable values of $X_1$ and $X_2$, an uncertainty in S can be made of little consequence. The best procedure is first to calculate L and C assuming S to be equal to the diameter of the circle, and then, assuming these values of L and C in the equation

$$S = \frac{LR_{p(\max.)}}{L - CRR_{p(\max.)}} \quad \ldots\ldots (16)$$

—deduced from equation (7)—we can find a more accurate value for S. This new value is then used in equations (12) and (13) in determining $P_1$ and $P_2$. One such stage of successive approximation will give results for L and C which are not in error by $\frac{1}{2}$ per cent.

Suitable points to choose for $X_1$ and $X_2$ are, one on either side of the R axis, at which they have values of the order of one quarter of the diameter of the circle.

An example taken from fig. 8 will illustrate the procedure.

Let the points chosen be

$$n_1 = 1500\,(\omega = 9424) \text{ and } n_2 = 2500\,(\omega = 15700).$$

The corresponding values of $X_1$ and $X_2$ are $X_1 = 198{,}500$ ohms and $X_2 = -163{,}000$ ohms. Using first the value S = 576,000 = (diameter of circle), these give for $P_1$ and $P_2$ the results

$$P_1 = \frac{1}{397000}\left(1 + \frac{1}{576000}\sqrt{576000^2 - 397000^2}\right)$$

and

$$P_2 = -\frac{1}{326000}\left(1 + \frac{1}{576}\sqrt{576^2 - 326^2}\right),$$

whence $P_1 = 4{\cdot}35 \times 10^{-6}$ and $P_2 = -5{\cdot}60 \times 10^{-6}$ so that L = 8·81 henries.

Also C, by formula (15), is equal to

$$\frac{4{\cdot}35 \times 10^{-6} \times 9426 + 5{\cdot}60 \times 10^{-6} \times 15700}{15700^2 - 9424^2} = 814\ \mu\mu\text{F}.$$

Digitized by Google

Using these values of L and C in equation (7A), and assuming the d.c. value of 1,000 ohms for R, we get for S the corrected value, S = 608,000 ohms. The revised values of $P_1$ and $P_2$ become $4{\cdot}43 \times 10^{-6}$ and $-5{\cdot}66 \times 10^{-6}$ respectively, giving for L and C the corrected values

$$L = 8{\cdot}68 \text{ H}$$

and

$$C = 825 \ \mu\mu\text{F}.$$

The analysis yields, therefore, the following effective values for the primary winding :— L = 8·68 H; C = 825 $\mu\mu$F; S = 608,000 ohms; and R (assumed equal to the d.c. value) = 1,000 ohms.

Returning now to the term $\frac{2R}{SL\omega(1 - LC\omega^2)}$ which was neglected in equation (11), we should have used terms of the form

$$\frac{1}{X} - \frac{2R}{SL\omega(1 - LC\omega^2)} \text{ instead of } \frac{1}{X}$$

in equations (12) and (13) when determining $P_1$ and $P_2$. If the values already determined for S and L are inserted in the correction term we shall see that a value of $P_1$ about 0·8 per cent. smaller and a value of $P_2$ about 0·4 per cent. greater should have been used in calculating L and C. If these corrections are applied, it will be found that L will only be increased by 0·3 per cent. and C will be increased by a completely negligible amount. We can therefore safely take the simplified form of equation (11) when calculating L and C.

Using the values of L, C and S thus determined, values of $R_p$ and $L_p$ have been calculated by formulæ (5) and (6) for a number of frequencies. These points are marked by crosses on the circle in fig. 8, and will be seen to give very good agreement with the observed values at these same frequencies. This agreement indicates that L, C and S do not vary much with frequency at the small magnetisation necessary to produce a secondary voltage of 2.

The circle diagram affords a very convenient graphical means of observing the voltages and their phase relations in the primary winding and the associated valve circuit. Thus, at any frequency, such as that given by P on the circle corresponding to $n = 1{,}500$, we may draw PM equal to the anode resistance $R_a$ of the valve ; if now we join OM we have a triangle in which we may consider OM equal to the total voltage $\mu e_g$ in the equivalent circuit of fig. 2. PM is the voltage drop in $R_a$ and OP is the voltage $e_p$ across the primary of the transformer. The phase relationships of these voltages is also shown and the ratio OP/OM gives the fraction $q$ of the voltage $\mu e_g$ which is acting on the primary winding of the transformer.

The circle diagram will be found a very clear and simple method of visualising at a glance the behaviour of a mesh circuit possessing any parallel combination of resistance, capacity, or inductance towards another circuit in which it is placed. The locus of

Digitized by Google

the end of the impedance vector travels round a circle when any one of the four quantities S, L, C or $\omega$ is continuously varied. The circuit need not contain both capacity and inductance, but in such a case only a semi-circle will be obtained; also, for the particular case where $S = \infty$ the circle becomes of infinite diameter and the vector impedances all lie on one line. If we take a common oscillatory circuit with series resistance and infinite shunt resistance, the circle is not quite perfect, since the vector is not zero at zero frequency, but in most cases the diameter is so large compared with the resistance vector that the want of perfection is inappreciable. There would appear to be room for the development of this method of studying the relationship of one circuit to another.*

Returning now to fig. 9, the quantities L, R, S and C require examining. L as analysed above is clearly the true effective self-inductance of the primary winding. R is a term depending upon the copper losses in primary and secondary, and probably has a value in the neighbourhood of $R_1 + R_2/\sigma_0^2$, where $R_1$ and $R_2$ are the d.c. resistances of primary and secondary windings and $\sigma_0$ is the ratio of the turns. C, however, is an equivalent capacity, involving the three capacities of fig. 5 and also $\sigma$, where

$$\sigma = \frac{M}{L_1}.$$

The meaning to be attached to the shunt resistance S was, at first, not at all clear. Before the system 9 (*b*) was tried, it was expected that the various losses in the system would manifest themselves as an augmented R, and a system such as fig. 9 (*c*), in which a single resistance $R_1$ replaced S and R of (*b*) was at first tried. But the value of $R_1$ would then need to be variable with frequency, otherwise the value necessary to give the diameter of the circle would be of the order of 20,000 ohms, and the circle would become a spiral starting at 20,000 ohms at frequency = 0 and finishing at $R_0 = 0$ at frequency = $\infty$. When the system (*b*) was discovered to fit the circle so closely, it became clear that the shunt resistance S must have a physical meaning representing a constant loss in the system for a constant terminal voltage, irrespective of frequency. It is believed by the author that the explanation lies in the nature of the iron losses. The circle has been obtained under the conditions of constant induced voltage of 2 volts on the secondary winding. Now the flux density will therefore be inversely as the frequency, and will in any case be very small. Many measurements made by the author on the total losses in silicon iron at low flux densities and at telephonic frequencies have shown that the main portion of these losses, in the case of sheet material of the usual thicknesses, are eddy current losses. These losses are proportional to $n^2$ and to $\mathscr{B}^2$. Now, for a constant induced voltage under variable frequency, $n \times \mathscr{B}$ will be constant, and hence the eddy current losses will be constant. The hysteresis losses, however, vary as a power of $\mathscr{B}$ which is greater than 2 at low flux densities (below 100), so that this portion of the losses is not invariable but will increase with diminishing frequency, and it is possible that they appear

* A variety of applications of the circle diagram will be found in Dr. Eccles' 'Continuous Wave Wireless Telegraphy', vol. 1, chaps. III and IV.

Digitized by Google

as an augmented R in the primary winding, or that (together with the small secondary losses) they make up a small total not very variable with frequency or small enough not to be separable from the S term. It must be remembered that in the foregoing analysis R has been tacitly assumed equal to 1,000 ohms, *i.e.*, the primary direct current resistance, and then the appropriate S has been determined to make the diameter of the circle come right. If, however, a value of R of 1,200 or 1,300 ohms had been taken, and the appropriate new S calculated, the new circle would be almost indistinguishable from the old one. The methods under examination cannot, therefore, separate hysteresis and eddy current losses in the core of the transformer, but they do give an indication of the value of the total losses.

## 5. Experimental Circle Diagrams. Effects of Capacity connected to the Secondary Winding.

It is clear that information regarding the effective self-inductance and effective self-capacity of the secondary winding will be obtained by observing the effect on L$p$ and R$p$ of added capacity on the secondary winding. There are two methods of carrying out these experiments and each yields information of value; we can

(*a*) Obtain a set of circles each corresponding to a known added secondary capacity $C_2$. This gives all the information available from the experiments, but is rather laborious, since, on each circle, the resonant frequency is in a different region, and so a large number of frequencies must be chosen in order to obtain points around the upper portion of each circle.

(*b*) We can choose a number of fixed frequencies and then find by variation of $C_2$ those values which give resonance on the secondary. We are, by this method, virtually finding the highest point T on each circle. This is easily accomplished experimentally by first obtaining the balance with the transformer disconnected from the bridge. Then, after connecting, adjusting $V_2$ to the chosen secondary voltage and disconnecting the voltmeter in the usual way, we obtain the second balance *without* alteration of M but by adjustment of $C_2$ and $r$. This method is simple to carry out and enables one to evaluate effective secondary inductance and equivalent secondary self-capacity in a direct manner.

Both sets of experiments have been made on the transformer, and are given below.

(*a*) Circle diagrams for various fixed secondary added capacities have been obtained, and are shown in fig. 10. The added capacity consisted of a standard low range variable air condenser set to the successive values of 50, 100 and 150 $\mu\mu$F. It was connected to the terminals SI, SO of the transformer. The four circles are distinguished by their dots to correspond to these capacities and to the case of zero added capacity. It will be seen that the circle for zero $C_2$ is not quite identical with that of fig. 8. It has been found that the diameter and location of the points of the circle are slightly variable from one day to another. It is suspected that this is due to the magnetisation of the iron since

Digitized by Google

other experiments have indicated that the effective permeability and total losses of sheet materials at weak magnetisation are dependent upon the previous magnetic history of the material. For this reason it is desirable, when making these observations, to complete a series at one occasion if information is sought on the relative diameters of the circles. With regard the circles of fig, 10, it is interesting to trace the effect of the factors operating. Reverting to fig. 9 (*a*) it is seen that alteration of C should not have any effect on the diameter of the circle, which for this case is equal to S. But of course it is not C that we are varying, but $C_2$ across the secondary. The introduction of the R term also in (*b*) will explain the reduction in diameter with increasing capacity, and the diameters can be used as a means of evaluating the effective R of the transformer, which may include a part equivalent to some of the iron losses and also a part due to secondary resistance.

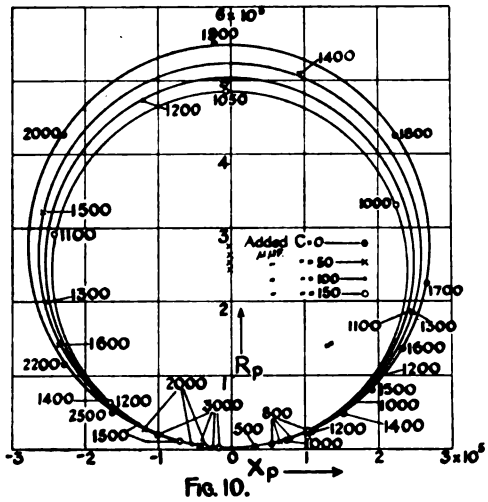

Fig. 10.

We have, as in (7) :—

$$R_{p\,(max.)} \doteqdot \frac{S_1 L_1}{L_1 + R_1 S_1 C_1} \doteqdot S^1 \frac{R_1 S^2 C_1}{L_1 + R_1 S_1 C_1}.$$

If we take the difference $\Delta R_p$ in diameter of two circles corresponding to total equivalent primary capacities $C_a$ and $C_b$ we have

$$\Delta R_{0\,(max.)} = \frac{L_1 S_1{}^2 R_1 (C_a - C_b)}{L_1{}^2 + L_1 S_1 R_1 (C_a + C_b)}$$

(neglecting products of small quantities),

$$\Delta R_{0\,(max.)} = \frac{R_1 S_1{}^2 (C_a - C_b)}{L_1 + R_1 S_1 (C_a + C_b)}$$

Arranging for R, this becomes

$$R_1 = \frac{L_1}{S_1} \frac{\Delta R_p}{S_1 (C_a - C_b) - \Delta R_p (C_a + C_b)} \quad \ldots\ldots\ldots \quad (17)$$

The secondary added capacity when referred to the primary winding will be approximately multiplied by $\sigma_0{}^2$, where $\sigma_0$ is the ratio of the secondary to the primary turns. In this particular transformer $\sigma_0 = 3{\cdot}5$ and $\sigma_0{}^2 = 12{\cdot}25$. If we take the extreme circles we have $\Delta R_p = 63{,}000$ ; $C_a = 826\ \mu\mu F$ and $C_b = 825 + 12{\cdot}25 \times 150 = 2{,}660\ \mu\mu F$.

From these quantities and the known values of $L_1$ and $S_1$ (in this case 8·8 and 582,000 respectively) we find $R_0 = 1{,}060$. The direct current resistance is 1,000 ohms, so that

Digitized by Google

this corroboration may be considered very good in the light of the fact that the effect of R is only in the nature of a correction.

If the values of $L_1$ and $C_1$ are deduced from one of the other circles it is found that the apparent $C_1$ has changed by an amount very nearly equal to $\sigma_0^2 \times$ added $C_2$, but there also occurs a small change in $L_1$ which is not clearly understood, but may be due to the load placed on the transformer or to the fact that a considerably different region of frequency forms the main portion of the circle. The effective $L_1$ is about 1 per cent. smaller for the case of an added secondary capacity of 100 $\mu\mu$F than for the case of no added capacity.

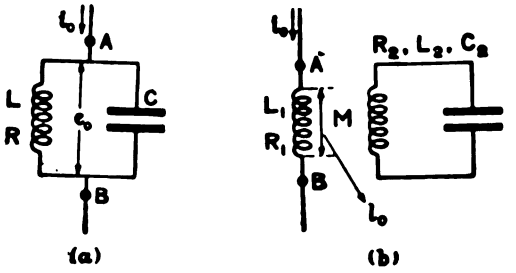


FIG. 11.

We may now compare two simple cases as given in fig. 11 (*a*) and (*b*), in which S has been omitted, since it may be presumed to exist as a separate shunt across AB in both cases. We will compare the $R_p$ and $L_p$ in these two cases.

For (*a*) we have

$$i_0(R_p + L_p\alpha) = i_1(R + L\alpha) = i_2\frac{1}{C\alpha} = e, \qquad i_0 = i_1 + i_2,$$

whence

$$R_p = \frac{R}{(1 - LC\omega^2)^2 + R^2C^2\omega^2}, \quad \ldots\ldots\ldots \quad (18)$$

and

$$L_p = \frac{L(1 - LC\omega^2) - R^2C}{(1 - LC\omega^2)^2 + R^2C^2\omega^2}, \quad \ldots\ldots\ldots \quad (19)$$

or

$$(L_p - L)\omega \doteqdot \frac{L\omega LC\omega^2(1 - LC\omega^2)}{(1 - LC\omega^2)^2 + R^2C^2\omega^2}, \quad \ldots\ldots\ldots \quad (20)$$

in which $R^2C$ has been neglected.

For case (*b*) we have

$$i_0(R_p + L_p\alpha) = e, \qquad i_0(R_1 + L_1\alpha) + i_2M\alpha = e,$$

and

$$i_2\left(R_2 + L_2\alpha + \frac{1}{C_2\alpha}\right) + i_0M\alpha = 0,$$

whence

$$R_p - R_1 = \frac{R_2M^2C_2^2\omega^4}{(1 - L_2C_2\omega^2)^2 + R_2^2C_2^2\omega^2}, \quad \ldots\ldots\ldots \quad (21)$$

and

$$(L_p - L_1)\omega = \frac{M\omega MC_2\omega^2(1 - L_2C_2\omega^2)}{(1 - L_2C_2\omega^2)^2 + R_2^2C_2^2\omega^2}, \quad \ldots\ldots\ldots \quad (22)$$



Digitized by Google

The expressions for $(L_0 - L_1)\omega$ in the two cases are of similar type and become identical if we put $M = \sigma_0 L_1$, $C = \sigma_0^2 C_2$ and $L_2 = \sigma_0^2 L$, where $\sigma_0$ = ratio of secondary to primary turns.

It is seen, therefore, that as far as the effective primary resistance and reactance circle diagram is concerned the effect of capacity connected across the secondary winding is twofold.

Mainly, the points corresponding to given frequencies are shifted round the circle in an anti-clockwise direction so that the resonant frequency is lower; therefore for frequencies below this the impedance is greater, while for frequencies above the resonance the impedance is less than it was before, *i.e.*, the performance of the transformer is improved for low frequencies but made worse for high frequencies.

The second effect of added secondary capacity is to slightly reduce the diameter of the circle, but the effect is of small consequence unless the added capacity is large.

We will now consider the results of experiments using the resonance method (*b*) of adjusting $C_2$ and $r$ (*see* Fig. 6) to obtain a balance at various frequencies without alteration of M from its zero setting. By this means we keep the effective $L_0$ equal to zero. (This method of finding resonance of an oscillatory circuit of large damping is far more sensitive than any methods whereby a maximum voltage or current is obtained in the circuit when brought to resonance. A glance at the curve for $L_p$ on fig. 7 will show how rapid is the rate of change of this quantity at the resonant point.) Fig. 12 (I) shows the straight line obtained when $1/\omega^2$ (resonance) is plotted against added secondary capacity $C_2$. The points are seen to lie on a good line which passes through the C axis at a value of C equal to $-64{\cdot}5\ \mu\mu F$. This quantity, therefore (with a plus sign), corresponds to the virtual effective self-capacity of the secondary winding—it must be corrected by about $-1{\cdot}5\ \mu\mu F$ for the leads connecting the small variable condenser to the secondary winding. The slope of the line gives the true effective secondary inductance. It is in the present case equal to 107 henries. The true primary inductance was shown to be equal to 8·68 henries. The ratio of the two inductances is 12·33 and the square root of this is 3·515. The ratio of turns is 3·50. It is seen, therefore, that the true inductances of the windings are very closely in the ratio of the squares of the numbers of turns.

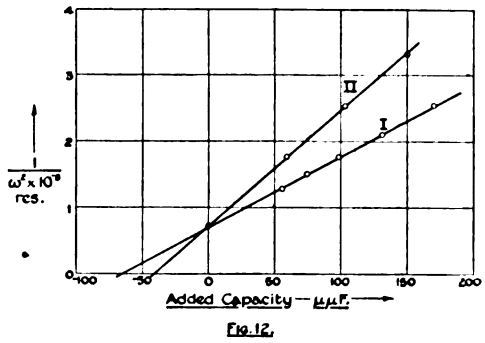

Fig. 12.

If we multiply the virtual effective secondary capacity of $64{\cdot}5\ \mu\mu F$ (as found from the line) by $12{\cdot}25 = \sigma_0^2$ we get the equivalent primary capacity of $774\ \mu\mu F$. The total effective primary capacity was seen to be $825\ \mu\mu F$. The difference of $50\ \mu\mu F$ may be considered as the true primary capacity and is probably not very much in error. The accuracy of this deduced value of $C_p$ cannot, of course, be considered very high, since an

Digitized by Google

error of only 1 $\mu\mu$F in the virtual effective $C_2$ of 63 $\mu\mu$F will produce an error of 12 $\mu\mu$F in $C_p$. In any case the primary self-capacity is of very little practical consequence. The secondary capacity has been called a " virtual " effective capacity, because the value deduced includes the effect, referred to the secondary terminals, of the mutual capacity between the open ends of primary and secondary. This matter will be referred to later when discussing the measurements on the effects of added mutual capacity.

When using this bridge method of determining resonant frequency by variation of $C_2$, we also observe $r$ at the same time, and from it we can immediately deduce the diameter of the circle. For formula (7) may be written

$$\frac{1}{R_p\, max} = \frac{1}{S} + \frac{R_1}{L_1}\sigma_0^2 C_2, \quad . \quad . \quad . \quad . \quad . \quad . \quad . \quad . \quad . \quad (23)$$

and if therefore we plot $\frac{1}{R_p\, max}$ against " added $C_2$ " we should get a straight line whose slope equals $\sigma_0^2 R_1/L_1$ and whose intercept at a value of $C_2$ equal to $-\frac{825}{\sigma_0^2}\left(= -67{\cdot}5\right)$ should give S.

The lower line of fig. 13 shows the results of a series of such observations and indicates that equation (23) is fairly well satisfied. The slope of this line is equal to 1,620, giving $R_1$ the value about 1,150 ohms. It was previously assumed that $R_1$ was equal to the direct current resistance of the primary winding, but it is clear that the copper losses in the secondary winding must appear as an increase in the effective resistance of the primary. The secondary D.C. resistance is very nearly 4,000 ohms. The equivalent of this referred to the primary may be expected to be nearly equal to $4{,}000/\sigma_0^2 = 327$ ohms, thus giving an expected total effective value of 1,327 ohms. The agreement between the calculated and deduced values of $R_1$, whilst not very close, may be considered satisfactory in view of the uncertainties involved in this deduction and the many factors operating.

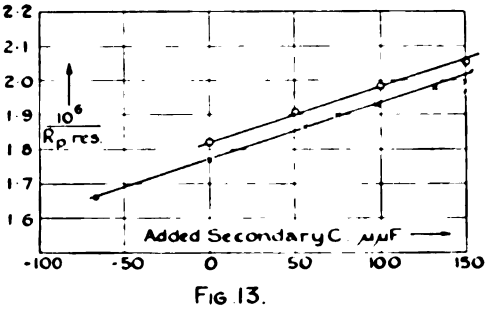

FIG 13.

On fig. 13 another line is also drawn. The points on this line are those corresponding to the actual diameters of the four circles of fig. 10. It will be observed that the slope is practically the same as that of line R, but that the line lies considerably above it. The variation from one day to another in the diameter of a circle has been remarked upon and is not fully understood. The observations by adjustment of $C_2$ were made on a different occasion from that on which the four circles were obtained. The parallelism of the lines, however, indicates that the general theory holds and that only the shunt resistance S is variable from day to day. The matter is of no consequence from the standpoint of performance of the transformer.



Digitized by Google

*Effects of Added Mutual Capacity.*

The experiments on added mutual capacity (between the ends PI, SO on fig. 4) were made in precisely the same manner as those for secondary added capacity. The same standard variable air condenser was used connected to PI, SO, and a similar set of four circles were obtained. The points referred to a secondary terminal voltage of 2·0 in every case. They are shown in fig. 14.

It will be seen that the circles are very similar to those corresponding to added secondary capacity. The points corresponding to any particular frequency are moved round in an anti-clockwise direction and the diameter is reduced as before.

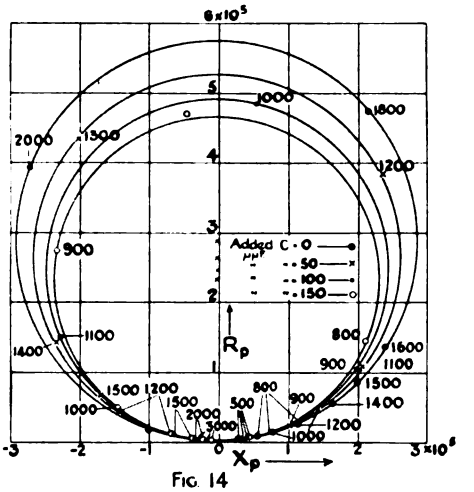


Fig. 14

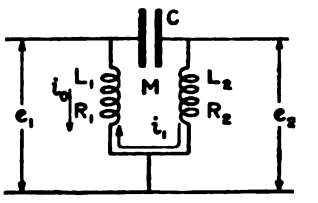


Fig. 15.

It will be observed that the effects of added mutual capacity are more marked than those of added secondary capacity.

If we take the simple case represented by fig. 15, it may easily be shown* that the effect of mutual capacity on effective primary impedance is exactly similar to that of secondary capacity and that it can be represented as an equivalent secondary capacity having the approximate value

$$C_2\,(\text{equivalent}) = C\,(\text{mutual}) \times \left(1 \pm \frac{1}{\sigma_0}\right)^2. \quad . \quad . \quad . \quad . \quad . \quad (29)$$

It is interesting to note the significance of the value and sign of $\sigma_0$. If the transformer has a large ratio, $\frac{1}{\sigma_0}$ will be small and the equivalent secondary capacity will be nearly equal to the mutual capacity. Again, if the direction of the windings is such that the primary and secondary voltages are approximately in the same phase (*i.e.*, M and $\sigma_0$ are negative), then the effect of mutual capacity is less than that due to the same capacity across the secondary. If primary and secondary voltages are in opposite phase, so that the potential difference across the condenser is greater than that across the secondary,

* *See* Note 1, p. 314.

Digitized by Google

mutual capacity produces a greater effect than secondary capacity. In a 1 : 1 transformer having the common point such that M is negative the effect of mutual capacity is negligible, since $\left(1-\frac{1}{\sigma_0}\right)^2$ is zero.

The expression for $L_p$ including the effect of mutual capacity, looks somewhat complicated,* but in the case of a good transformer the term

$$(1-k^2)\left[L_2C\omega^2\left(1\pm\frac{1}{\sigma_0}\right)^2-1\right]$$

is of little importance, sine $k$ is of the order 0·98 and the part in square brackets is considerably less than unity.

To a close approximation, therefore,

$$L_p \doteqdot \frac{\frac{L_2}{\sigma_0^2}\left(1-L_2C\omega^2\left[1\pm\frac{1}{\sigma_0}\right]^2\right)}{R_t^2C^2\omega^2+\left[L_2C\omega^2\left(1\pm\frac{1}{\sigma_0}\right)-1\right]} \quad \ldots\ldots\ldots \quad (30)$$

If we further treat the mutual capacity case in the same manner as that of secondary capacity, by determining the values of $C_m$ corresponding to resonance, we shall expect to find a straight line connecting $1/\omega^2$ (resonance) and added $C_m$, having a slope equal to $L_2\left(1\pm\frac{1}{\sigma_0}\right)^2$ and an intercept equal to $\left(1\pm\frac{1}{\sigma_0}\right)^2$ times that obtained by the line for added secondary capacity. The line actually obtained from the resonances with various mutual capacities is shown on fig. 12 (II). It is seen to be of greater slope than the other line, and must, of course, intersect it at the point C = 0.

The actual slope was found to be 175·5 henries. Dividing by the slope of (1) (= 107 henries) we get $\left(1+\frac{1}{\sigma_0}\right)^2 = 1{\cdot}640$, whence $\sigma_0 = 3{\cdot}57$.

To be strictly accurate, we should have included $k$ in the mutual term, *i.e.*,

$$\text{Effective } L = L_1 + L_2 + 2M = L_2\left(\frac{1}{\sigma_0^2}+1+\frac{2k}{\sigma_0}\right)$$

instead of $\left(1\pm\frac{1}{\sigma_0}\right)^2$.

Taking $k = 0{\cdot}98$ and $\sigma_0 = 3{\cdot}50$ we get Eff. L = 107(1 + 0·082 + 0·560) = 175·6, an agreement which is remarkably good.

(The measurement of $k$ will be discussed later.)

The intercept on the C axis of the line (II) of fig. 12 is at — 40 $\mu\mu$F, which, allowing 1·5 for the leads and multiplying by $\left(1+\frac{1}{\sigma}\right)^2$, gives — 63·2 $\mu\mu$F, a value very close to the value — 63 given by line (I) of fig. 12.

* *See* Note 1, p. 314.

Digitized by Google

It is seen, therefore, from these experiments that the effects of secondary and mutual capacity are interpretable in terms of one another and of the ratio and direction of the windings (as shown by the approximate theory also).

As a result, it is not possible to separate the true effective mutual capacity and the true effective secondary capacity of a transformer by this method. It seems unlikely that any experiments will suffice to effect a separation unless a complete series of measurements is taken, using all four of the possible ways of connecting primary and secondary windings together. If the connection between primary and secondary is charged, other mutual capacities will, of course, be brought into operation.

No attempt has been made in the present investigation to carry out this complete analysis, involving at least six capacities.

An easy way of separating the effective mutual and secondary capacities for the case of one particular common point between primary and secondary is, however, open to those who construct transformers; that is, to wind two transformers precisely similar in every respect, except that the direction of winding of the secondary of one of them is reversed as compared with the other. If the geometry of the windings of the two transformers is identical, then the only quantity changed will be the sign of $\sigma_0$.

We may consider the measured effective $C_2$ as made up in one case of

$$C_2 \text{ eff.}_1 = C_s + C_m\left(1 + \frac{1}{\sigma_0}\right)^2,$$

and in the other case,

$$C_2 \text{ eff.} = C_s + C_m\left(1 - \frac{1}{\sigma_0}\right)^2.$$

The values of $C_2$ eff. obtained on the two transformers will then differ by an amount equal to $\frac{4C_m}{\sigma_0}$, thus allowing $C_m$ and $C_s$ to be separated.

### (c) *Effect of a Shunt Resistance across the Secondary Winding.*

Under some conditions, the grid-filament circuit of a valve has not an extremely high resistance. Also it is not uncommon for a resistance of one or two megohms to be used as a shunt on the secondary winding for the purpose of diminishing distortion. It is interesting, therefore, to analyse the effect of such a resistance. Experiments were made using two grid leaks connected in turn by short leads to the secondary winding. The effective resistance of each was measured at a number of telephonic frequencies by shunting the leak across an air condenser of known value. The change in capacity and power-factor of the condenser was measured by a Carey-Foster bridge. The effective resistance and effective capacity of the leak were thus determined. The changes with frequency were small, the capacity also was only a very few micro-microfarads.

Digitized by Google

In fig. 16 are shown three circles corresponding to secondary resistances of $\infty$, 4.65 megohms and 3·38 megohms respectively. It is immediately seen that the effect on diameter is very marked. This reduction in diameter doubtless accounts for the greater stability and improved performance of transformers when used for telephony and music.

It will be observed that the impedance for low and for high frequencies is not much affected by a secondary shunt of 3 megohms, the main effect being on the impedance in

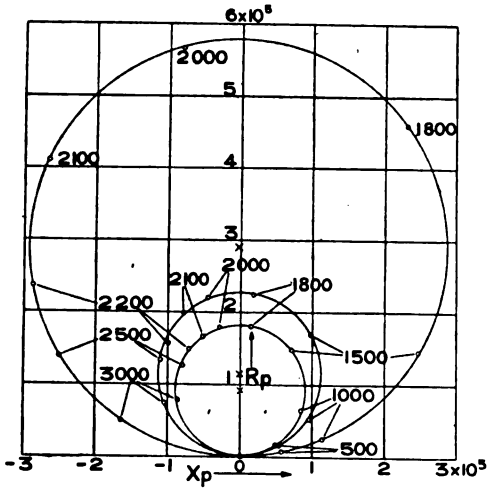

FIG.16.

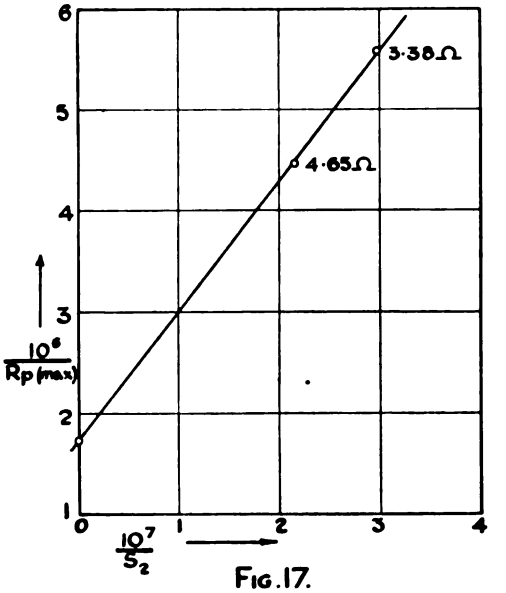

FIG.17.

the resonant region of frequency. Since, even with the shunt, the impedance at resonance is still of the order of 175,000 ohms, a large fraction of the available alternating voltage in the anode circuit will still be received on the primary of the transformer.

If we plot $1/R_p max$ against $1/S_2$, as in fig. 17, we get—as might be expected—a straight line, of which the slope is found to be 12·50.

The square root of this is equal to 3·53, a result of $\sigma_0$ in close agreement with the true value of 3·50.

### (*d*) *Effect of Magnitude of Secondary Induced Electromotive Force.*

Since various stages of amplification are concerned with considerably differing magnitudes of voltages, it was considered desirable to try the effect of varying the magnitude of the applied voltage.

This was carried out as follows: From the circle obtained for a constant induced voltage of 2·0 a few points of frequency were chosen so as to be fairly well distributed round it. At these frequencies observations were taken of $X_p$ and $R_p$ for various values of secondary voltage set by the help of the low-reading electrostatic voltmeter.

Digitized by Google

The results of these observations are shown in fig. 18. A number of interesting deductions can be drawn from the location of the points. The effect of the increased magnetisation necessary to produce an increased secondary voltage is to shift the points round in an anti-clockwise direction, doubtless due to increased permeability as the flux density rises. This effect is smaller the higher the frequency; this is no doubt due to the fact that the portion of the $\mathscr{H}\mathscr{B}$ curve explored at a higher frequency is moved down into a lower region of $\mathscr{H}$ and $\mathscr{B}$ at the higher frequencies, for the same range of voltage. Although the points on the curve for one frequency are more widely separated at the upper region of the circle, the corresponding change in effective $L_p$ is nevertheless smaller. The explanation is, of course, that the scale of frequency is very much opened out over a large part of the circle and closes in towards the zero and $\infty$ points.

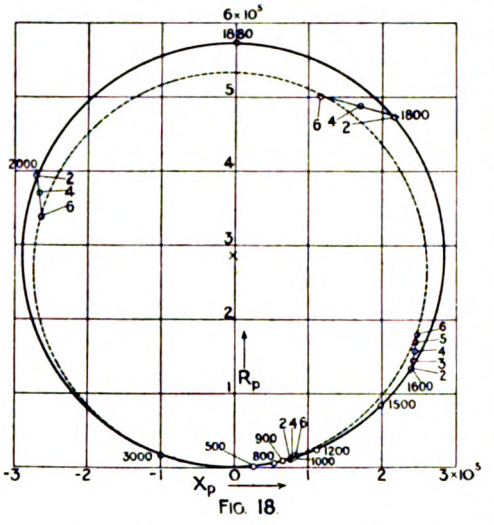

FIG. 18.

The next point to be noticed is that the circle joining the 6-volt points is smaller in diameter than that joining the 2-volt points. The explanation is that the hysteresis losses in the iron, at low densities, vary as a higher power of $\mathscr{B}$ than 2, consequently, as $\mathscr{B}$ diminishes, the shunt resistance representing the total losses will increase. The indication is that over a very large range of amplification of secondary voltage the amplification given by the transformer will not change much, and hence distortion due to variation in intensity should not occur on account of any variability in the constants of the transformer. As will be seen later, the circle may be profoundly modified by variation of applied voltage when a valve is connected to the secondary winding.

### (e) *Effect on Primary Impedance when the Grid-Filament Circuit of a Valve is connected to the Secondary Winding of the Transformer.*

The foregoing experiments must, of course, lead on to an examination of the behaviour of the transformer when performing its normal duty of supplying voltage to the grid-filament circuit of an ensuing valve.

The author has not had time to experimentally penetrate very far into the complicated region exposed by this problem, but it seems probable that the method of attack is a sufficiently powerful one to yield results of considerable value in analysing causes and effects associated with the various factors operating.

Only a very few experiments have been made, but the results are of a surprising nature and show that profound effects may be produced depending upon the conditions in the attached valve circuit.

Digitized by Google

Three cases are given below and are shown in fig. 20. The experimental arrangements were as in fig. 19.

The bridge proper is identical with that of fig. 6, but the arrangements for applying a known voltage to the transformer primary are somewhat different in order to enable

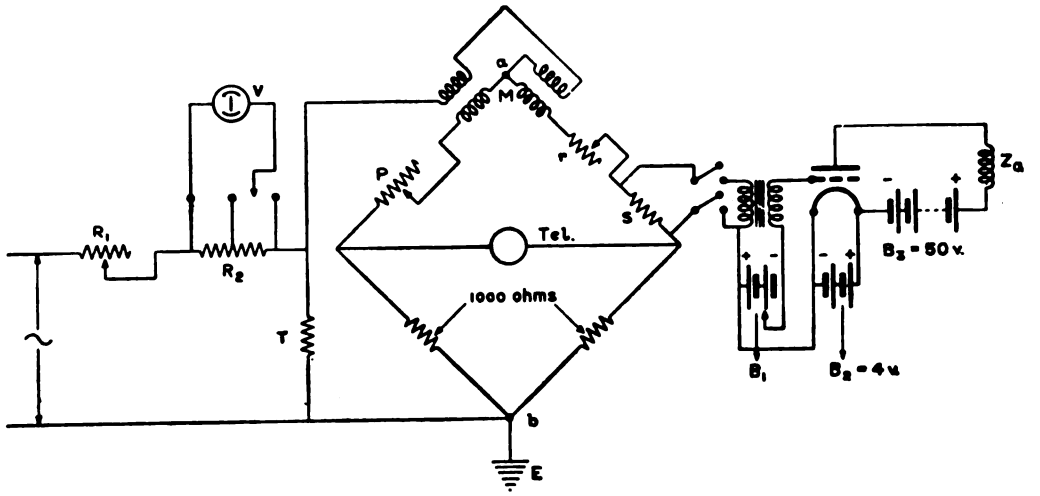


FIG. 19.

smaller voltages to be conveniently measured. For this purpose a non-inductive resistance $R_2$ was used to enable small currents to be measured by the help of the electrostatic voltmeter V. Of this current (from 2 to 5 milliamperes) the major portion passes through the shunt T. The terminal voltage on S can therefore be made a convenient fraction of that on $R_2$. The ratio will not alter appreciably, due to the variations in the bridge,

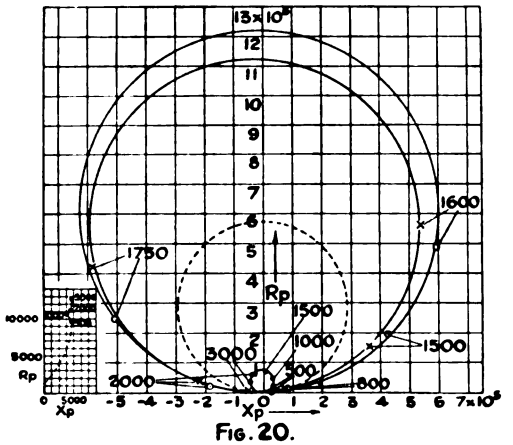


FIG. 20.

since it is almost non-inductive, and except in certain cases the shunting effect of the transformer primary across S is small.

The valve arrangements are indicated on the right of the diagram. The connections were such that a common point existed between primary and secondary windings of the transformer. The battery $B_1$ was for the purpose of maintaining the grid of the valve



Digitized by Google

at a definite negative potential with respect to one end of the filament. The load $Z_a$ in the anode circuit consisted of an inductance coil without iron. Its inductance was 5 henries and its resistance about 1,000 ohms. The self-capacity was small (about 30 $\mu\mu$F) It was placed at a considerable distance from the transformer, and was turned to a position of zero mutual inductance with respect to it. The following trial cases were taken over a range of frequencies from 500 to 3,000 cycles per second :—

(*a*) Grid at — 2 volts steady potential, and a constant applied primary alternating voltage of 0·57 volt r.m.s., corresponding to a secondary voltage of 2.

(*b*) Similar to (*a*) but with constant primary alternating voltage to give a secondary voltage of 0·5 r.m.s.

(*c*) Grid at — 4 volts and a secondary induced voltage of 2 volts r.m.s.

(*d*) Grid at 0 volt and a secondary induced voltage of 0·5 volt r.m.s.

A most remarkable variety of results was obtained, as shown in fig. 20. For the purpose of comparison the normal circle with no connections on the transformer secondary is also shown, dotted. The other three circles are dealt with in order of their diameters, beginning with the smallest.

The following remarks are considered by the author to explain to some extent these results.

(*a*) *Applied Volts* 2, *Grid Volts* — 2.

The circle is very small and somewhat distorted.

Since the applied alternating voltage on the grid has a r.m.s. value of 2 it will cause the grid to become positive during a part of the cycle, so that a heavy load is thrown on the transformer secondary which almost short circuits it during this part of each cycle.

(*b*) *Applied Volt* 0·5, *Grid Volts* — 2.

The grid is always considerably negative with respect to the filament, and consequently the true internal grid-filament resistance is extremely high. Further explanation is needed, however, of the fact that the diameter of the circle is *greater* than that with open secondary. It is believed that the explanation lies in the nature of the load in the anode circuit. Miller* has shown that under certain conditions the input impedance of a valve can consist of a negative resistance and a capacity in series, in the case of an inductive load in the anode circuit. It may be that the increased diameter of the circle is a manifestation of this effect.

(*c*) *Applied Volts* 2, *Grid Volts* — 4.

The circle is again large, although the applied alternating voltage has a r.m.s. value of 2. This is possible on account of the increased negative potential of the grid, which maintains it negative throughout the alternating cycle.

A remark may be permitted here regarding the conditions which should be observed if full use of the transformer is to be made.

* J. M. Miller, "Dependence of the Input Impedance of a Three Electrode Vacuum Tube upon the Load in the Plate Circuit", 'Bulletin Bureau of Standards', No. 5351, vol. 15, p. 367, 1919-20.

Digitized by Google

If it is desired to obtain loud signals or speech, such as to necessitate the application of a few volts to the grid of a valve, then, in order to give the transformer an opportunity to keep a high primary impedance, it will be necessary to apply a considerable negative potential to the grid. Under these conditions, however, the valve will require a high anode potential in order to operate over the steep straight portion of its characteristic.

If it is not desired to use high anode voltage, then a large negative potential cannot be applied to the grid, and a step-up ratio on the transformer cannot be made use of at a loud-speaking stage on account of the heavy load placed on the secondary winding.

(*d*) *Applied Volt* 0·5, *Grid Volt* 0.

The impedance of the transformer no longer gives a circle diagram, but remains almost constant and of very small value. (It is so small as only to be seen on close inspection of fig. 20 as a tiny sloping line near the origin.) The values obtained have been plotted on a much larger scale in the left-hand corner of fig. 20. It is seen that the impedance varies in a somewhat irregular manner, and is so small that it is doubtful whether any gain over a simple resistance or inductance coupling is made in spite of the step-up ratio of the transformer, owing to the smallness of the primary impedance.

These results call for much fuller investigation than the author can at present give them. The measurements under the heading (*b*) are difficult owing to the smallness of the energy available in the bridge. It has been found necessary to carry out the tests represented by the large circle at night under conditions of great quietness and steadiness; doubtless with some experimenting a stage of amplification could be applied to the bridge telephone without impairment of accuracy, so that the measurements could be made without special external conditions.

The possibility of increased diameter of the circle as a result of the conditions in the anode circuit of a valve probably has its counterpart in the howling noises occasioned by self-generation of currents of telephonic frequency. It is clear that the addition of a shunt resistance of one or two megohms on the secondary winding will effectively prevent the diameter of the circle from becoming infinite under conditions where otherwise distortion or howling might occur. No great loss of amplification will result from the use of a shunt resistance of 2 megohms, since this will still allow the circle to have a diameter of over 100,000 ohms in a normal transformer.

Another very convenient method of reducing the diameter of the primary impedance circle is to wind one or two turns of No. 18 or 20 S.W.G. wire round the outside of the secondary and to short circuit this tertiary winding either directly on itself or through a low resistance. Howling or incipient howling causing distortion may be prevented in this manner. The beneficial results which sometimes result from shrouding are probably due to the shroud acting as a closed tertiary winding in this manner and not to magnetic screening.

We must pass on to the consideration of the second part of the function of the transformer, as mentioned in section 2, namely, the effective voltage ratio.



Digitized by Google

## 6. Effective Ratio and Coefficient of Coupling of the Transformer.

The measurement of effective ratio of the transformer is very simple. Referring to fig. 6 (reproduced in this instalment) the method of observation was to observe the main current as indicated on the thermoammeter A. From this, the potential difference on S was readily determined, and hence the primary voltage. The secondary voltage was directly observed by means of the low-reading electrostatic voltmeter. The bridge is so nearly non-inductive that the voltage on S may be computed by means of a simple multiplier from the total current with an inaccuracy much less than 1 per cent. The bridge need not be precisely balance, during this test, and, as will be seen from an examination of the curves of fig. 21, no appreciable correction need be applied on account of the capacity of the voltmeter except at high telephonic frequency. At frequencies of the order of 3,000 cycles per second, the effective ratio of the transformer is increased by about 2 per cent. as a result of the addition of the capacity of the electrostatic voltmeter.

Fig. 21 shows the effective ratio of secondary to primary voltage as a function of added capacity. The curves marked A are those obtained when the capacity is added across the secondary terminals. Those marked B are for added capacity between the free ends of primary and secondary, *i.e.*, added mutual capacity. The capacities used in plotting the curves have been corrected to "total effective capacity", in order that the two sets of curves may appear in their correct relation to one another. These results represent "added capacity" + voltmeter capacity + mutual capacity or self-capacity of the winding, as the case may be. When the curves are so plotted, they are seen to converge with remarkable accuracy on to the point representing the geometrical ratio of the windings, *i.e.*, 3·5. These curves show that marked increase in effective ratio of a transformer can occur as a result of adding capacity across the secondary winding or of adding mutual capacity, and that well-defined maximum ratios occur having values depending upon the frequency. The value of capacity at which the maximum occurs also depends upon the frequency.

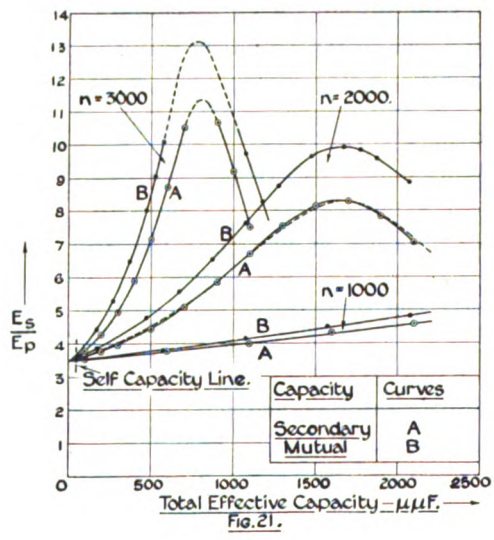

Fig. 21.

These results were at first puzzling, for it must be remembered that the transformer is being operated in a region of frequency far beyond the resonant frequency. The latter occurs at about 2,000 cycles per second at a total effective secondary capacity of the order of 60 μμF (shown by a dotted line near the ratio axis). It will be observed that no marked

Digitized by Google

increase in ratio occurs at the resonant frequency. An insight into this remarkable behaviour is obtained by a simple mathematical consideration of the problem.

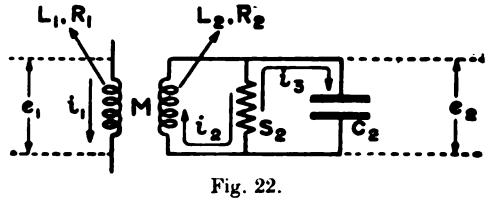


Fig. 22.

It is not quite certain what is the most accurate theoretical representation of the case, involving the fewest variables, but it becomes very involved if we take more than those shown in fig. 22, which represents the case for secondary added capacity. It is certain that the properties of the iron must have some effect on the voltage ratio. These cannot be allowed for if the iron losses are represented, as on previous occasions, by a shunt across the primary winding. They have, therefore, been transferred to the secondary winding as the equivalent shunt resistance $S_2$. This case will also include the case of an external shunt resistance added across the secondary, as is sometimes done.

Taking, then, fig. 22, we have

$$e_1 = i_1(R_1 + L_1\alpha) + i_2 M\alpha,$$

$$i_2(R_2 + L_2\alpha + S_2) + i_1 M\alpha - i_3 S_2 = 0,$$

$$i_3\left(S_2 + \frac{1}{C_2\alpha}\right) - i_2 S_2 = 0,$$

$$e_2 = e_3 \frac{1}{C_2\alpha}.$$

This will be found to give for the instantaneous ratio the expression

$$\frac{e_2}{e_1} = \frac{S_2 M_a}{(R_1S_2 - R_1S_2L_2C_2\omega^2 + R_1R_2 - L_1L_2\omega^2 + M^2\omega^2 - L_1R_2S_2C_2\omega^2) + (S_2L_1 - S_2L_2C_2\omega^2 + R_2L_1 + R_1L_2 + R_1R_2S_2C_2 + S_2M^2C_2\omega^2)\alpha} \quad . \quad (31)$$

From this we find the ratio of the root mean square voltages to be

$$\frac{E_2^2}{E_1^2} = \sigma^2 = \frac{M^2/L_1^2}{\left[1 - \frac{C_2\omega^2(L_1L_2 - M^2)}{L_1} + \frac{R_1R_2C_2}{L_1} + \frac{R_1L_2 + R_2L_1}{S_2L_1}\right]^2 + \left[\frac{R_1}{L_1\omega} - \frac{C_2\omega(R_1L_2 + R_2L_1)}{L_1} + \frac{R_1R_2 - (L_1L_2 - M^2)\omega^2}{S_2L_1\omega}\right]^2} \quad . \quad (32)$$

Let us put $L_1 = L_2/\sigma_0^2$ and $M^2 = k^2L_1L_2 = k^2L_2^2/\sigma_0^2$, where $\sigma_0$ = ratio of secondary to primary turns. The equation then assumes the more convenient form

$$\sigma^2 = \frac{k^2\sigma_0^2}{\left[1 - L_2C_2\omega^2(1 - k^2) + \frac{R_1R_2C_2\sigma_0^2}{L_2} + \frac{R_1\sigma_0^2 + R_2}{S_2}\right]^2 + \left[\frac{R_1\sigma_0^2}{L_2\omega} - C_2\omega(R_1\sigma_0^2 + R_2) + \frac{R_1R_2\sigma_0^2 - L_2^2\omega^2(1 - k^2)}{S_2L_2\omega}\right]^2} \quad . \quad (33)$$

Digitized by Google

Some preliminary calculations show that we can neglect the terms containing the product $R_1R_2$. Writing also $R_1\sigma_0^2 + R_2 = R_t$ we get the more manageable equation

$$\sigma^2 = \frac{k^2\sigma_0^2}{\left[1 + \frac{R_t}{S_2} - L_2C_2\omega^2(1-k^2)\right]^2 + \left[\frac{R_1\sigma_0^2 - L_2C_2\omega^2R_t}{L_2\omega} - \frac{L_2\omega(1-k^2)}{S_2}\right]^2}, \quad . \quad (34)$$

where $R_t = R_1\sigma_0^2 + R_2$.

An examination of this equation reveals immediately why $\sigma$ reaches a maximum value for a frequency or added capacity far beyond the resonant frequency or self-capacity of the secondary circuit. The term $1 - k^2$ is the governing factor. If $k$ is unity, there will be scarcely any variation of $\sigma$ with $C_2$ or $\omega$, since the other terms involving $R_1$, $R_2$ and $S_2$ are small compared with unity. Owing, however, to the fact that $k^2$ is not quite unity, $1 - k^2$ is a small positive quantity such as 0·03. At a value of $L_2C_2\omega^2_0$ equal to about 30, therefore the first bracket becomes zero, and the voltage ratio is determined only by the resistance terms in the second bracket. These can, theoretically, be made as small as we like, so that a large increase in $\sigma$ is possible.

It is generally possible to neglect the terms containing $S_2$, unless a comparatively low resistance shunt is used on the secondary. The expression then reduces to

$$\sigma^2 = \frac{k^2\sigma_0^2}{\left[1 - L_2C_2\omega^2(1-k^2)\right]^2 + \frac{1}{L_2^2\omega^2}\left[R_1\sigma_0^2 - L_2C_2\omega^2R_t\right]^2}. \quad . \quad . \quad . \quad . \quad (35)$$

The corresponding expressions for the case of mutual capacity are somewhat more complicated, but* it may be shown that the effect of mutual capacity is similar to that of secondary capacity, and that the maximum value of $\sigma$ will occur at almost the same frequency or added capacity in the two cases.

It is of interest to find the values of $k$ and R or $S_2$ which will give values of $\sigma$ agreeing with the experimental curves of fig. 21. It will suffice to take the secondary capacity case of (35). Differentiating with respect to $C_2$ we find that $\sigma$ (*max.*) occurs when

$$C_{2\,(\sigma\,max.)} = \frac{\frac{S_2 + R_t}{S_2L_2}\left[L_2^2\omega^2(1-k^2)\right] + \frac{R_t}{L_2S_2}\left[R_1S_2\sigma_0^2 - L_2^2\omega^2(1-k^2)\right]}{L_2^2\omega^4(1-k^2)^2 + R_t^2\omega^2}. \quad . \quad (38)$$

In any case except that of a poor transformer this reduces to

$$C_{2\,(\sigma\,max.)} = \frac{L_2^2\omega^2(1-k^2) + R_tR_1\sigma_0^2}{L_2\omega^2\left[L_2^2\omega^2(1-k^2)^2 + R_t^2\right]}. \quad . \quad . \quad . \quad . \quad . \quad . \quad (39)$$

* *See* Note 2, p. 314.

Digitized by Google

From the curves of fig. 21 the value of $C_2$ is known for any particular case, so that, solving for $1 - k^2$, we shall find that

$$1 - k^2 = \frac{1 + \sqrt{1 + \frac{4R_t C_2}{L_2}(R_1\sigma_0^2 - R_t L_2 C_2 \omega^2)}}{2L_2 C_2 \omega^2} \quad . \quad . \quad . \quad . \quad . \quad (40)$$

In general we can neglect $R_1\sigma_0^2$, so that the expression for $1 - k^2$ reduces to

$$1 - k^2 = \frac{1 + \sqrt{1 - 4R_t^2 C_2^2 \omega^2}}{2L_2 C_2 \omega^2} \quad . \quad . \quad . \quad . \quad . \quad . \quad . \quad . \quad (41)$$

In order to make our theoretical curve for $\sigma$ fit the experimental one at, say, the maximum point, we must substitute the value of $1 - k^2$ back into equation (35).

Taking the approximate form given by (35)

$$P^2 = \frac{\sigma^2}{k^2\sigma_0^2} = \frac{1}{[1 - L_2 C_2 \omega^2 (1 - k^2)]^2 + R_t^2 C_2^2 \omega^2},$$

and putting $R_t^2 C_2^2 \omega^2 = q^2$, we have

$$\frac{1}{P^2(max.)} = [1 - L_2 C_2 \omega^2 (1 - k^2)]^2 + q^2 \quad . \quad . \quad . \quad . \quad . \quad . \quad (42)$$

From (41) we get

$$L_2 C_2 \omega^2 (1 - k^2) = \frac{1 + \sqrt{1 - 4q^2}}{2},$$

which, on substitution in (42) gives

$$\frac{1}{P^2(max.)} = \left(\frac{1 - \sqrt{1 - 4q^2}}{2}\right)^2 + q^2, \quad . \quad . \quad . \quad . \quad . \quad . \quad (43)$$

whence

$$q = R_t C_2 \omega = \frac{\sqrt{P^2(max.) - 1}}{P^2(max.)} \quad . \quad . \quad . \quad . \quad . \quad . \quad . \quad (43A)$$

Substituting this value of $q$ back into (41) gives)

$$1 - k^2 = \frac{1}{L_2 C_2 \omega^2}\left(1 - \frac{1}{P^2(max.)}\right) \quad . \quad . \quad . \quad . \quad . \quad . \quad . \quad (44)$$

Equations (43) and (44) enable the effective values of $(1 - k^2)$ and $R_t$ to be determined from the co-ordinates of the highest points on the experimental curves of fig. 21. This has been done in the case of added secondary capacity at a frequency of 2,000 cycles per second (curve A at 2,000 on fig. 21).

The value of $L_2$ required in equation (44) has been taken as 110 henries and not 107 henries as deduced from the line of fig. 12. This is because the curves of fig. 21 have

Digitized by Google

been obtained for secondary voltages of the order 5, whereas the line of fig. 12 was for a secondary voltage of 2. The circles of fig. 18 show that $L_2$ increases by about 3 per cent. or 4 per cent. for an increase in magnetisation of the core corresponding to a secondary voltage of 5. Taking, then, $L_2 = 110$ henries, and, from the curve $C_2 = 1{,}650$ $\mu\mu$F and $\sigma$ (*max.*) $= 8{\cdot}30$, we find $1 - k^2 = 0{\cdot}0289$, $k^2 = 0{\cdot}971$ and $k = 0{\cdot}985$ and $R_t = 18{,}200$ ohms. Now $R_t = R_1\sigma_0^2 + R_2$. This quantity should, theoretically, have been 16,500, using direct-current values of $R_1$ and $R_2$. On referring back to fig. 13, however, it will be seen that an effective value of 1,150 ohms was found for $R_1$. This value will give almost precisely the value of 18,200 obtained above. There are, therefore, other losses associated with the windings, which cause the effective internal primary resistance to rise.

The values of $1 - k^2$ and $R_t$, deduced above, have been used to calculate theoretically the curve A at $n = 2{,}000$. The line so obtained is drawn dotted on fig. 21. The agreement with the experimental curve is remarkably good and shows that the rise in ratio with increase in frequency or with added secondary or mutual capacity is substantially in accordance with the simple theory given.

In consideration of the curves of fig. 21 we must be careful to keep in mind the effect of added secondary capacity on effective primary impedance as indicated by the circles of fig. 10. An instruction of these shows that the primary impedance is increased at low frequencies and decreased at high frequencies by the addition of secondary capacity.

It is advantageous to both voltage factor and ratio to add secondary capacity so long as we keep on the right hand of the circle, but for frequencies above the resonant frequency the voltage factor will suffer on account of diminished primary impedance. For example, at a frequency of 3,000 cycles per second and with a zero added secondary capacity the primary effective resistance and reactance are 20,000 ohms and — 100,000 ohms respectively. The additionof 100 $\mu\mu$F to the secondary winding reduces these quantities to 2,700 ohms and — 26,000 ohms respectively. We see, therefore, that above the resonant frequency the effect of secondary (or mutual) capacity is to reduce the primary impedance and hence the primary voltage factor $q$, where

$$q^2 = \frac{X_p^2 + R_p^2}{X_p^2 + (R_p + R_a)^2} \quad . \quad . \quad . \quad . \quad . \quad . \quad . \quad . \quad . \quad . \quad (45)$$

On the other hand, the presence of secondary capacity increases the voltage ratio of the transformer, unless the capacity is relatively enormous. For small and moderate values of capacity the voltage ratio of the transformer is given by the expression

$$\sigma = \frac{k\sigma_0}{1 - L_2C_2\omega^2(1 - k^2)} \quad . \quad . \quad . \quad . \quad . \quad . \quad . \quad . \quad . \quad (46)$$

The amplification of the transformer is equal to the product $q\sigma$; it is of interest, therefore, to consider now, as the natural application of the whole of the foregoing analysis, how the amplification depends upon all the factors involved, and, in particular, upon secondary capacity and primary inductance.

Digitized by Google

## 7. Voltage Amplification Curves.

The voltage amplification of a complete stage, consisting of a valve and transformer, may be written $Eg_2/Eg_1$ where $Eg_1$ is the voltage applied to the grid of the valve in front of the transformer and $Eg_2$ is the voltage produced on the grid of the valve beyond the transformer when connected to its secondary winding.

We have, therefore, $Eg_2/Eg_1 = \mu q\sigma$. This is the quantity experimentally determined by the direct method of measurement of amplification, such as that described by Mr F. E. Smith and H. Napier.* The voltage factor $\mu$ if the valve $V_1$ is an independent variable and does not enter into our present considerations at all, except as a mere number.

In the case of the transformer investigated here, the amplification has been directly measured using valves having a voltage factor of about 8·3 and an internal anode-voltage anode-current slope $R_a$ of about 24,000 ohms. The curve obtained is given in fig. 23 as a thin line. The thick line curve has been obtained by calculation of the product of $q$ and $\sigma$ from the calculated values of $X_p$ and $R_p$ and the curves of fig. 21, using the values 8·3 for $\mu$ and 24,000 for $R_a$. In making the calculations allowance was made for the capacity of the leads and valve connected to the secondary winding.

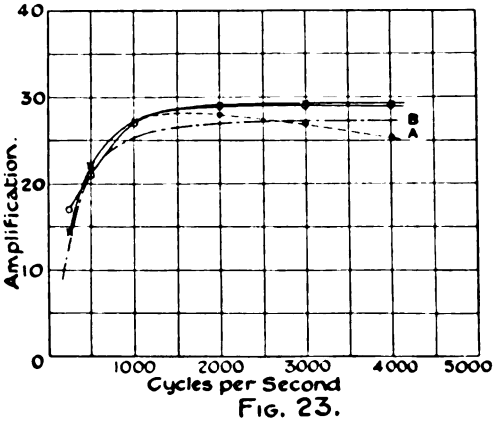

Fig. 23.

The curves fit one another very well except at the low-frequency end, where the experimental curve shows higher amplification than the calculated curve. This is almost certainly due to an increase in effective inductance at frequencies below 500 cycles per second, owing to increased effective permeability in the iron. All the measurements become very difficult at frequencies of the order of 300 per second and the accuracy necessarily falls, but measurements of $X_p$ and $R_p$ at 300 indicated that the inductance was several per cent. greater than that at 500 cycles per second. In calculating the curve, the values of $X_p$ and $R_p$ were calculated from the deduced values of $L_1$, $C_2$, S and $R_1$, as obtained by analysis of the circle. For the present case the simple formulæ (8) and (10) are sufficient for the purpose, but when calculating cases in which considerable secondary capacity is present, or assumed, these formulæ are not sufficiently accurate.

It is desirable to be able to calculate various theoretical amplification curves, starting from assumed constants in the transformer, in order to gain some idea as to the desirable values of these for satisfactory performance. As an example, the theoretical case of zero

* F. E. Smith and H. C. Napier, "On the Measurement of Amplification given by Triode Amplifiers at Audible and at Radio Frequencies", 'Proc. Phys. Soc.', vol. 32, p. 116, 1920; and N.P.L. 'Collected Researches', vol. 18, Paper IX.



Digitized by Google

secondary capacity has been taken for the transformer investigated. The curve has been plotted in fig. 23 as the dotted line B. We see immediately that throughout the whole range of frequency shown, the amplification is lower in the absence of secondary capacity. It is generally considered that secondary capacity is undesirable, but these curves show quite definitely that a certain amount of secondary capacity considerably improves the performance of a transformer.

We must now consider in more detail the formulæ (21) and (22) for $R_p - R_1$ and $(L_p - L_1)\omega$, corresponding to the case given in fig. 11 (*b*). In this case we have left out the shunt S on the primary. This quantity, however, is the main factor deciding the diameter of the circle, and must therefore be taken into account in order to obtain approximately accurate expressions for $R_p$ and $X_p$.

Let $R_{p1}$ and $X_{p1}$ be the effective resistance and reactance of the primary as given by (21) and (22) and let this virtual impedance be shunted by a resistance S.

We then have to a close approximation

$$R_{p0} = \frac{SX^2_{p1}}{S^2 + X^2_{p1}}, \quad \ldots \quad (47)$$

and

$$X_{p0} = \frac{S^2 X_{p1}}{S^2 + X^2_{p1}}. \quad \ldots \quad (48)$$

Now, in the expressions for $X_{p1}$ and $R_{p1}$ the term $R_2$ is the only factor limiting the diameter of the circle in the absence of S across the primary. In a normal case this diameter would be so large, owing to the relative smallness of $R_2$, that we may neglect the effect of $R_2$ in substituting the value of $X_{p1}$ and $R_{p1}$ in the equations for $R_{po}$ and $X_{po}$ so long as S has a value not greater than about $10^6$ ohms.

In this case $R_{p1} = 0$ and

$$X_{p1} = \frac{L_1\omega[1 - L_2C_2\omega^2(1 - k^2)]}{1 - L_2C_2\omega^2}.$$

Substituting these in (47) and (48) we arrive at the final expressions

$$R_{p0} = R_1 + \frac{S_1 L_1^2\omega^2[1 - L_2C_2\omega^2(1 - k^2)]^2}{S_1^2(1 - L_2C_2\omega^2)^2 + L_1^2\omega^2[1 - L_2C_2\omega^2(1 - k^2)]^2}, \quad \ldots \quad (49)$$

and

$$X_{p0} = \frac{S_1^2 L_1\omega(1 - L_2C_2\omega^2)[1 - L_2C_2\omega^2(1 - k^2)]^2}{S_1^2(1 - L_2C_2\omega^2)^2 + L_1^2\omega^2[1 - L_2C_2\omega^2(1 - k^2)]^2}. \quad \ldots \quad (50)$$

These expressions allow a series of cases to be calculated for variations of $S_1$, $L_1$, $L_2$, $C_2$ and $k$. If a shunt resistance $S_2$ is placed across the secondary, or if the grid-filament circuit of the valve imposes a load on the transformer represented by $S_2$, then to a close approximation this load may be transferred to the primary as an equivalent shunt resistance in parallel with $S_1$ and of value equal to $\frac{S_2k^2}{\sigma_0^2}$.*

* *See* Note 3, p. 311.

Digitized by Google

It is obvious that the evaluation of the amplification of the transformer by calculation from its constants involves a considerable amount of arithmetic. Approximations can be made at each end of the frequency scale, but when $L_2C_2\omega^2 = 1$, and when $L_2C_2w^2(1 - k^2)$ is not very small, it is necessary to use the full expressions. Suppose, therefore, we have a transformer of known or assumed constants $L_1$, $R_1$, $R_2$, $\sigma_0$, $S_1$ and $k$: we wish to find its amplification curve when used with its primary in the anode circuit of a valve whose internal anode resistance is $R_a$. We calculate $R_{po}$ and $X_{po}$ by means of (49) and (50). Then $q$ is determined from these and $R_a$, by means of (45). Finally $\sigma$ is calculated by means of (46).

Note that if $L_2C_2\omega^2(1 - k^2)$ is less than about 0·25 it is necessary to use the more exact expression given in equation (35) for $\sigma$. The product $q\sigma$ gives the required amplification factor of the transformer. It is convenient to use exact values of $\omega$ for these calculations. The following typical case is given in full in order to show a convenient arrangement of the calculations so that they follow one another in a simple manner.

The case taken is one in which the constants have been assumed as follows :—

$L_1$ = Primary Inductance = 10 H.

$\sigma_0$ = Turns Ratio = 4.

$C_2$ = Secondary Capacity = 50 $\mu\mu$F.

$S_1$ = Equivalent Primary Shunt Resistance = $5 \times 10^5$ ohms.

$k$ = Coupling Coefficient = 0·985.

$1 - k^2 = 0{\cdot}03$.

$L_2$ = Secondary Inductance = 160 H.

$R_a$ = Anode Impedance of First Valve = $25 \times 10^3$ ohms.

$R_1$ = Ohmic Resistance of Primary = 1,000 ohms.

A number of theoretical cases have been worked out in order to show clearly the effect of variation of some of the constants.

The results of these calculations are given in Tables III to V below.

In all the cases $S_1$ has been taken as $5 \times 10^5$ ohms, $R_1 = 1{,}000$ ohms, $\sigma_0 = 4$, and $L_2 = \sigma_0^2 L_1$.

Some of these results are plotted in figs. 24 and 25. The curves of fig. 24 refer to a theoretical transformer of constant primary inductance of 20 H and show the effect of various secondary capacities and also various cofficients of coupling. The curves of fig. 25 show the effect of various values of primary inductance, and of secondary capacity. These curves show remarkable variations. It has not been possible to test experimentally the cases worked out theoretically, but a considerable number of various types of transformers on the market have been tested for amplification from time to time, and amongst the curves obtained every type shown on figs. 24 and 25 has been found.



Digitized by Google

Amongst the transformers tested for their constants the widest variations in these have been found, thus values of primary inductance between 2 and 15 H; of secondary

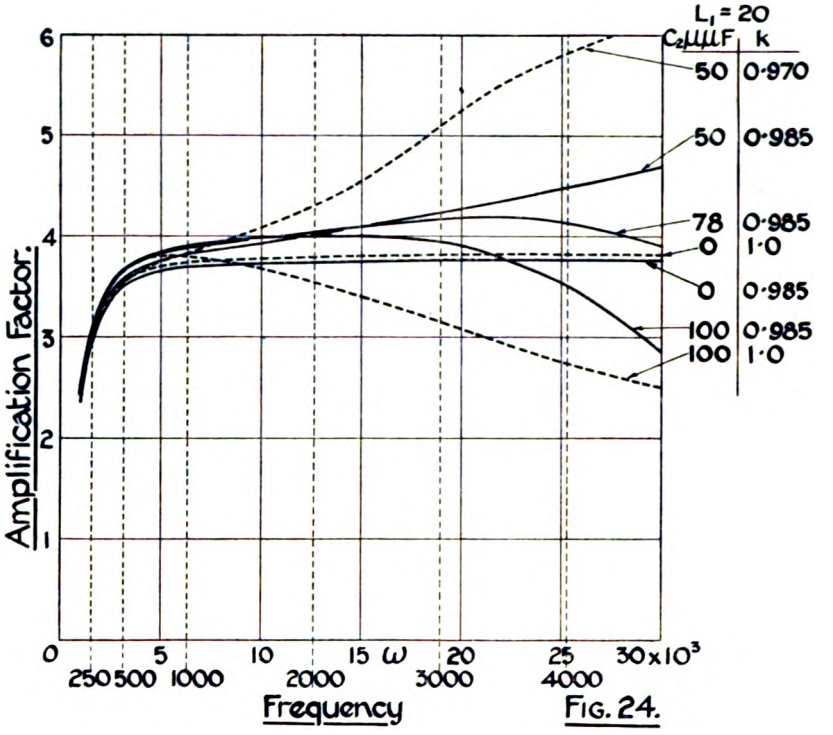


Fig. 24.

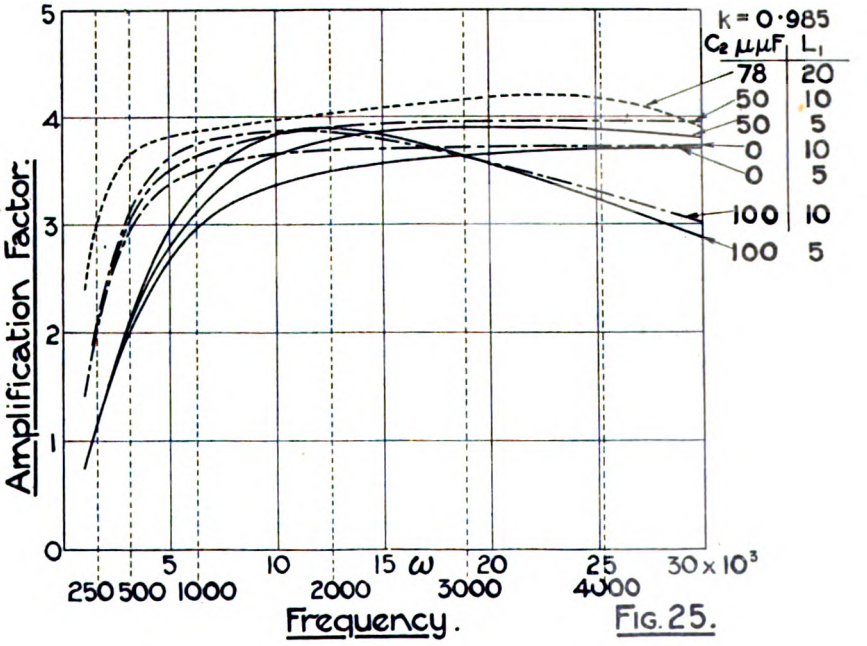


Fig. 25.

capacity between 15 and 1,000 $\mu\mu$F; of $S_1$ between $2{\cdot}5 \times 10^5$ and $12 \times 10^5$ ohms; of $\sigma_0$ between 1 : 1 and 6 : 1; thus indicating considerable differences of opinion or lack of knowledge as to what is desirable under various conditions.

Digitized by Google

TABLE II.—Calculation of Amplification Factor.

| | | | | | | | | |
|---|---|---|---|---|---|---|---|---|
| $\omega \times 10^{-3}$ . . . . . | 1 | 2 | 3 | 5 | 10 | 15 | 20 | 30 |
| $\omega^2 \times 10^{-6}$ . . . . | 1 | 4 | 9 | 25 | 100 | 225 | 400 | 900 |
| $L_2C_2\omega^2$ . . . . . | 0·008 | 0·032 | 0·072 | 0·200 | 0·800 | 1·80 | 3·2 | 7·2 |
| $1 - L_2C_2\omega^2$ . . . . | 0·992 | 0·968 | 0·928 | 0·800 | 0·200 | − 0·80 | − 2·2 | − 6·2 |
| $(1 - L_2C_2\omega^2)^2$ . . . | 0·984 | 0·936 | 0·860 | 0·640 | 0·040 | 0·640 | 4·84 | 38·4 |
| $L_2C_2\omega^2(1 - k^2)$ . . | 0·0002 | 0·001 | 0·002 | 0·006 | 0·024 | 0·054 | 0·096 | 0·216 |
| $1 - L_2C_2\omega^2(1 - k^2)$ | 1·000 | 0·999 | 0·998 | 0·994 | 0·976 | 0·946 | 0·904 | 0·784 |
| $[1 - L_2C_2\omega^2 (1 - k^2)]^2$ | 1·000 | 0·998 | 0·996 | 0·988 | 0·952 | 0·894 | 0·817 | 0·615 |
| $(1 - L_2C_2\omega^2)[1 - L_2C_2\omega^2(1 - k^2)]$ | 0·992 | 0·967 | 0·926 | 0·795 | 0·195 | − 0·757 | − 1·985 | − 4·86 |
| $L_1\omega \times 10^{-4}$ . . . . | 1 | 2 | 3 | 5 | 10 | 15 | 20 | 30 |
| $L_1^2\omega^2 \times 10^{-8}$ . . . | 1 | 4 | 9 | 25 | 100 | 225 | 400 | 900 |
| $S^2(1 - L_2C_2\omega^2)^2 \times 10^{-10}$ | 24·8 | 23·4 | 21·5 | 16·0 | 1·00 | 16·0 | 121 | 960 |
| $L_1^2\omega^2 [1 - L_2C_2\omega^2 (1 - k^2)]^2 \times 10^{-10}$ | 0·01 | 0·04 | 0·09 | 0·25 | 0·95 | 2·01 | ·2 | 5 |
| Denom $\times 10^{-10}$ . . | 24·81 | 23·44 | 21·59 | 16·25 | 1·95 | 18·01 | 124 | 965 |
| $SL_1^2\omega^2 \times 10^{-13}$ . . | 5 | 20 | 45 | 125 | 500 | 1,125 | 2,000 | 4,500 |
| $SL_1^2\omega^2[1 - L_2C_2\omega^2 (1 - k^2)]^2 \times 10^{-13}$ | 5 | 20 | 45 | 124 | 475 | 1,005 | 1,734 | 2,770 |
| $R_{po} \times 10^{-3}$ . . . . | 1·2 | 1·8 | 3·08 | 8·6 | 244 | 57 | 15 | 4 |
| $(R_{po} + R_a) \times 10^{-3}$ . | 26·2 | 26·8 | 28·1 | 33·6 | 269 | 82 | 40 | 29 |
| $R_{po}^2 \times 10^{-6}$ . . . . | 1·4 | 3·2 | 9·5 | 74 | 59,500 | 3,250 | 225 | 16 |
| $(R_{po} + R_a)^2 \times 10^{-6}$ | 686 | 718 | 790 | 1,130 | 72,400 | 7,630 | 1,600 | 835 |
| $S^2L_1\omega \times 10^{-13}$ . . | 250 | 500 | 750 | 1,250 | 2,500 | 3,750 | 5,000 | 7,500 |
| $S^2L_1\omega(1 - L_2C_2\omega^2) (1 - L_2C_2\omega^2[1 - k^2]) \times 10^{-13}$ | 248 | 483 | 695 | 992 | 587 | − 2,840 | − 9,925 | − 36,430 |
| $X_p \times 10^{-3}$ . . . . | 10·16 | 20·2 | 32·2 | 61·0 | 250 | 157·7 | − 79·9 | − 37·7 |
| $X_p^2 \times 10^{-6}$ . . . . | 103·2 | 407 | 1,035 | 3,725 | 62,500 | 24,900 | 6,380 | 1,327 |
| $Z_p^2 \times 10^{-6}$ . . . . | 104·6 | 410 | 1,045 | 3,800 | 122,000 | 28,150 | 6,600 | 1,342 |
| $Z_t^2 \times 10^{-6}$ . . . . | 789 | 1,125 | 1,825 | 4,855 | 134,900 | 31,630 | 7,980 | 2,162 |
| $q$ . . . . . | 0·364 | 0·603 | 0·757 | 0·884 | 0·952 | 0·944 | 0·909 | 0·788 |
| $\sigma$ . . . . . | 3·94 | 3·94 | 3·95 | 3·97 | 4·04 | 4·17 | 4·36 | 5·03 |
| $q \times \sigma$ . . . . . | 1·434 | 2·37 | 2·9 | 3·51 | 3·94 | 3·84 | 3·87 | 3·96 |

TABLE III.—Amplification Factor. (Various Values of $C_2$.)

| $\omega$ | $L_1 = 5$, $\sigma_0 = 4$, $S_1 = 5 \times 10^5$ | | | | | |
|---|---|---|---|---|---|---|
| | $C_2 = 0$ μμF. | | $C_2 = 50$ μμF. | $C_2 = 100$ μμF. | | |
| | $k = 1·0$. | $k = 0·985$. | $k = 0·985$. | $k = 1·0$. | $k = 0·985$. | $k = 0·950$. |
| 1,000 | 0·772 | 0·762 | 0·760 | 0·778 | 0·766 | 0·737 |
| 2,000 | 1·440 | 1·423 | 1·44 | 1·476 | 1·457 | 1·402 |
| 3,000 | 1·980 | 1·955 | 2·02 | 2·10 | 2·07 | 1·990 |
| 5,000 | 2·712 | 2·68 | 2·81 | 2·99 | 2·97 | 2·87 |
| 10,000 | 3·416 | 3·38 | 3·65 | 3·79 | 3·84 | 3·91 |
| 15,000 | 3·62 | 3·58 | 3·87 | 3·68 | 3·84 | 4·20 |
| 20,000 | 3·70 | 3·66 | 3·91 | 3·35 | 3·57 | 4·14 |
| 30,000 | 3·75 | 3·71 | 3·81 | 2·67 | 2·89 | 3·21 |

Digitized by Google

TABLE IV.—Amplification Factor. (Various Values of $C_2$.)

| $\omega$ | $L_1 = 10$, $S_1 = 5 \times 10^5$, $\sigma_0 = 4$. | | | |
|---|---|---|---|---|
| | $C_2 = 0$ μμF. | | $C_2 = 50$ μμF. | $C_2 = 100$ μμF. |
| | $k = 1{\cdot}0$. | $k = 0{\cdot}985$. | $k = 0{\cdot}985$. | $k = 0{\cdot}985$. |
| 1,000 | 1·436 | 1·415 | 1·425 | 1·435 |
| 2,000 | 2·40 | 2·37 | 2·38 | 2·46 |
| 3,000 | 2·86 | 2·92 | 2·99 | 3·07 |
| 5,000 | 3·44 | 3·39 | 3·51 | 3·63 |
| 10,000 | 3·73 | 3·67 | 3·84 | 3·88 |
| 15,000 | 3·77 | 3·71 | 3·94 | 3·80 |
| 20,000 | 3·79 | 3·72 | 3·97 | 3·58 |
| 30,000 | 3·80 | 3·74 | 3·96 | 3·03 |

TABLE V.—Amplification Factor. (Various Values of $C_2$.)

| $\omega$ | $L_1 = 20$, $\sigma_0 = 4$, $S_1 = 5 \times 10^5$. | | | | | | | | |
|---|---|---|---|---|---|---|---|---|---|
| | $C_2 = 0$ μμF. | | $C_2 =$ 25 μμF. | $C_2 =$ 30 μμF. | $C_2 = 50$ μμF. | | $C_2 =$ 70·8 μμF. | $C_2 = 100$ μμF. | |
| | $k$=1. | $k$=0·985. | $k$ 1. | $k$=0·985. | $k$=0·985. | $k$=0·970. | $k$=0·985. | $k$=1. | $k$=0·985. |
| 1,000 | 2·40 | 2·37 | 2·41 | 2·40 | 2·39 | 2·35 | 2·40 | 2·46 | 2·43 |
| 2,000 | 3·24 | 3·20 | 3·27 | 3·23 | 3·25 | 3·21 | 3·29 | 3·32 | 3·28 |
| 3,000 | 3·53 | 3·48 | 3·56 | 3·53 | 3·56 | 3·51 | 3·63 | 3·66 | 3·64 |
| 5,000 | 3·70 | 3·65 | 3·74 | 3·73 | 3·76 | 3·74 | 3·82 | 3·80 | 3·64 |
| 10,000 | 3·78 | 3·73 | 3·82 | 3·87 | 3·93 | 4·08 | 3·98 | 3·68 | 3·98 |
| 15,000 | 3·80 | 3·75 | 3·80 | 4·00 | 4·09 | 4·55 | 4·09 | 3·40 | 4·00 |
| 20,000 | 3·82 | 3·77 | 3·78 | 4·17 | 4·28 | 5·25 | 4·19 | 3·08 | 3·91 |
| 30,000 | 3·82 | 3·77 | 3·68 | 4·67 | 4·70 | 6·16 | 3·91 | 2·50 | 2·85 |

## 8. CONCLUSIONS.

Further experiments are necessary in order to confirm the conclusions stated below, and it is expected that they will be somewhat modified as the result of fuller investigation; but it is believed that in a general sense the conclusions are true and that they will serve as a basis for further work.

(1) Telephonic intervalve transformers may be considered as possessed of inductance, capacity and resistances which are not very variable with frequency or voltage so long as the latter does not exceed a few volts on the secondary.

(2) The transformer behaves towards the circuit in which its primary winding is

Digitized by Google

connected as though it consisted mainly of an inductance, a condenser, and a shunt resistance in parallel. Such a combination has effective reactances and resistances of which the corresponding values at various frequencies when plotted on rectangular co-ordinates give a curve which approximates very closely to a circle; this enables a convenient mental picture of the effective impedance over a considerable range of frequencies to be obtained.

(3) The circle diagrams enable the effects of mutual and secondary capacity and a secondary shunt resistance to be clearly visualised in a manner which allows the voltage factor of the primary winding under given conditions to be seen graphically.

(4) The grid-filament circuit of the valve, to which the secondary winding of the transformer is connected, may produce profound effects on the primary impedance, according to the conditions prevailing in this circuit. In order to allow the transformer to function properly, it is usually desirable to apply to this grid a steady negative E.M.F. with respect to the filament of such value that the grid potential is never more positive than that which it assumes if left free, *i.e.*, that there can never be a thermionic grid current. Under these conditions the grid-filament circuit becomes of very high impedance, consisting of a small capacity and a resistance in series across the secondary winding; and does not seriously react on the primary impedance. Under certain conditions the grid-filament resistance may become negative in sign, and so power may be returned to the secondary winding, thus increasing the diameter of the primary impedance circle and tending to cause instability.

The ensuing conclusions assume that the grid-filament circuit connected to the secondary circuit includes means for keeping the grid at a negative potential.

(5) The addition of a moderate shunt resistance on the secondary winding will, in general, produce greater stability and a flatter amplification curve than would exist in its absence. The amplification will be lowered throughout, but not seriously if the shunt resistance is not smaller than $200{,}000\ \sigma_0^2$ ohms. A turn or two wound over the secondary and short-circuited will produce a similar improvement.

(6) No marked effects occur in either primary voltage factor or ratio of an intervalve transformer as the resonant frequency is passed, but at frequencies above this marked increases in the ratio of the transformer may occur on account of the fact that the coupling coefficient is slightly less than unity. An effect which may be termed a ratio resonance occurs when

$$L_2 C\omega^2 (1 - k^2)^2 = 1.$$

(7) The most important single property of an intervalve transformer is the inductance of the primary winding. At low frequencies (below 300 cycles per second) an amplification as great as 75 per cent. of the maximum cannot be obtained on a step-up transformer unless the primary inductance is in the neighbourhood of 20 H. This value is not usually attained in practice in the writer's experience, but it should not be impracticable if a somewhat larger iron section is used and if the stampings are carefully annealed after all mechanical treatment is finished.

Digitized by Google

(8) The effects of secondary and mutual capacity are, with good approximation, interpretable in terms of one another. Thus, from the standpoint of primary impedance (and hence primary voltage ratio), a mutual capacity $C_m$ may be considered as replaceable by a secondary capacity $C_2$ of such value that

$$C_2 = C_m\left(1 \pm \frac{1}{\sigma_0}\right)^2$$

(the sign depends upon the relative directions of the two windings). From the point of view of ratio, secondary and mutual capacity produce effects which may be interpreted in terms of each other by the relation

$$\sigma_{(C_m)} = \sigma_{(C_2)}\left(1 \pm \frac{1}{\sigma_0}\right)^2,$$

where $\sigma\ (_{C_m})$ is the value of $\sigma$ corresponding to a mutual capacity $C_m$ and $\sigma(_{C_2})$ is the value corresponding to a secondary capacity $C_2$ : it is not correct in this case to consider mutual capacity as replaceable by an equivalent secondary capacity.

At frequencies below that at which $L_2C_2\omega^2 = 1$, the effective primary reactance and resistance are increased by added capacity, and the primary voltage factor thereby improved. Below this limit of frequency, the variation of ratio due to imperfect coupling between primary and secondary is small. The effect of capacity onamplification below this region of frequency is therefore always an increase.

At frequencies between that at which $L_2C_2\omega^2 = 1$ and $L_2C_2\omega^2(1 - k^2) = 1$ the effects are complicated, and involve all the constants of both windings of the transformer. For all frequencies above that corresponding to $L_2C_2\omega^2 = 1$ the primary voltage factor steadily falls. A compensation is, however, afforded by the simultaneous rise which occurs in the ratio. The product, giving the amplification factor, may rise or fall or it may keep constant over a considerable part of the region between that where $L_2C_2\omega^2 = 1$ and $L_2C_2\omega^2\ (1 - k^2) = 1$. The amplification factor may exhibit violent fluctuations in the neighbourhood of the point at which $L_2C_2\omega^2(1 - k^2) = 1$, but above this point it inevitably falls very rapidly and cannot rise again. It is probably desirable to keep this point at a higher frequency than 6,000 cycles per second.

(9) An amplification curve which droops at high frequencies due to the effect of excessive secondary capacity can be improved theoretically by slightly reducing the coupling coefficient. It is not easy to do this in a finished transformer without at the same time reducing the primary inductance, but in the case where an external secondary capacity was used it would be possible to include in the secondary circuit a small external self-inductance. Any reduction in $k$ will cause a corresponding reduction in the ratio at low frequencies. This reduction will, in general, however, never be greater than a few per cent.

(10) By a judicious adjustment of $k$ and $C_2$ to suit each other and the transformer, the amplification ratio can always be improved over that existing in the absence of $C_2$ or when $k$ = unity. This statement may appear contradictory to the usually accepted ideas

Digitized by Google

in intervalve transformers, but escape from this conclusion appears impossible in the light of the theory developed here. This indicates that a certain amount of secondary capacity is advantageous throughout the whole useful range of frequencies. The desirable value falls within that conveniently obtainable in practice unless the ratio of the transformer is exceptionally high. The higher the ratio or the greater the primary self-inductance the smaller becomes the desirable value of capacity. Under these conditions also the coupling coefficient should approach unity more closely. A secondary capacity round about the value $\frac{1,000}{\sigma_0^2}$ in $\mu\mu$F will in general give good results and should bring the resonant frequency to the region between 1,200 and 2,000 cycles per second.

No experiments have been made on the effect of the steady magnetisation of the transformer core as a result of the steady anode current. So long as this magnetisation is not up to the knee of the $\mathscr{H}$ curve the effect of the superposed steady magnetisation will be to increase the effective alternating permeability and will be all to the good. This increase may amount to 50 per cent. or 70 per cent. in primary inductance. If, however, the iron is taken up to the bend in its permeability curve or on to the flat portion above the bend, the effects may be serious, both on account of the introduction of harmonics which will result and also on account of greatly reduced effective alternating permeability. The iron will, however, need to be of quite exceptional quality or the anode current be exceptionably large for such a degree of magnetisation to occur. As an example, consider a well-annealed sample of stalloy. To produce a magnetisation of 6,000 gauss will require a value of $\mathscr{H}$ not less than about 2. If we take the total effective length of the core as 8 cms. we shall require about 12 ampere-turns to produce $\mathscr{H} = 6,000$. Except perhaps in a loud-speaker stage the product of primary turns and anode current is not likely to reach a value of 12 ampere-turns. If a transformer is required to operate under conditions where such a value of ampere-turns is likely to occur, the transformer should be designed with a large cross section of iron and comparatively few turns on the windings, so as to reduce ampere-turns without sacrificing inductance.

It is, however, not certain what characteristics are desirable in a transformer feeding a loud-speaker stage, since information doess not appear to be available concerning the relation between the sound intensity produced and the effective reactance and resistance of loud-speakers under the influence of constant voltage at varying frequencies.

It seems quite certain, however, that intermediate transformers should provide an amplification curve as straight and flat as possible over the longest possible range of audio-frequencies.



Digitized by Google

### Note 1.—The Effect of Mutual Capacity.

We have

$$i_0(Rp + Lp\alpha) = e_1 = (i_0 - i_1)(R_1 + L_1\alpha) - i_1 M\alpha,$$

$$(i_1 - i_0)(R_1 + L_1\alpha + M\alpha) + i_1\left(R_2 + L_2\alpha + M\alpha + \frac{1}{C\alpha}\right) = 0,$$

$$i_1(R_2 + L_2\alpha) + (i_1 - i_0) M\alpha = e_2,$$

whence

$$Rp + Lp\alpha = \frac{(R_1 + L_1\alpha)\left(R_2 + L_2\alpha + \frac{1}{C\alpha}\right) - M\alpha(R_1 + L_1\alpha + M\alpha)}{R_1 + R_2 + L_1\alpha + L_2\alpha + 2M\alpha + \frac{1}{C\alpha}}$$

it will be found that

$$Rp = \frac{R_1\{(M + L_2)C\omega^2 - 1\}^2 + R_2C^2\omega^2\{R_1(R_1 + R_2) + (M + L_1)^2\omega^2\}}{(R_1 + R_2)^2C^2\omega^2 + [(L_1 + L_2 \pm 2M)C\omega^2 - 1]^2} \quad . \quad . \quad . \quad . \quad . \quad (24)$$

and

$$Lp = \frac{L_1 + C\omega^2\left[(L_1L_2 - M^2)\{(L_1 + L_2 \pm 2M)C\omega^2 - 1\} - L_1(L_1 + L_2 \pm 2M) + (R_1^2L_2 + R_2^2L_1 - 2R_1R_2M)C - \frac{R_1^2}{\omega^2}\right]}{(R_1 + R_2)^2C^2\omega^2 + [(L_1 + L_2 \pm 2M)C\omega^2 - 1]^2}$$

$$. \quad . \quad . \quad . \quad . \quad . \quad . \quad (25)$$

Except at very low frequencies $R_1(R_1 + R_2)$ is negligible compared with $(M + L_1)^2\omega^2$. Thus $R_1 = 1000$, $R_2 = 4000$, $M = \pm 30$, $L_1 = 9$, and let $\omega = 2000$. Then

$$R_1(R_1 + R_2) = 5 \times 10^6 \text{ and } (M + L_1)^2\omega^2 = 1600 \times 10^6.$$

We get therefore

$$Rp \doteqdot \frac{R_1\{(M + L_2)C\omega^2 - 1\}^2 + R_2C^2\omega^4(M + L_1)^2}{(R_1 + R_2)^2C^2\omega^2 + [(L_1 + L_2 \pm 2M)C\omega^2 - 1]^2}, \quad . \quad . \quad . \quad . \quad . \quad . \quad . \quad (26)$$

$$Lp \doteqdot \frac{L_1\left[1 + C\omega^2\left\{\frac{(L_1L_2 - M^2)^2}{L_1}([L_1 + L_2 \pm 2M]C\omega^2 - 1) - (L_1 + L_2 \pm 2M)\right\}\right]}{(R_1 + R_2)^2C^2\omega^2 + [(L_1 + L_2 \pm 2M)C\omega^2 - 1]^2}, \quad . \quad . \quad (27)$$

or in terms of $L_2$,

$$Lp \doteqdot \frac{\frac{L_2}{\sigma_0^2}\left[1 + L_2C\omega^2\left[(1 - k^2)\left\{L_2C\omega^2\left(1 \pm \frac{1}{\sigma_0}\right)^2 - 1\right\} - \left(1 \pm \frac{1}{\sigma_0}\right)^2\right]\right]}{(R_1 + R_2)^2C^2\omega^2 + \left[L_2C\omega^2\left(1 \pm \frac{1}{\sigma_0}\right)^2 - 1\right]^2}, \quad . \quad . \quad . \quad . \quad (28)$$

in which $M^2 = k^2L_1L_2$, and $L_2 = \sigma_0^2L_1$.

### Note 2.—Leakage with Mutual Capacity.

The full working is similar to that on p. 301; the accurate resulting expression is:—

$$\sigma^2 = \frac{[\pm k\sigma_0 + L_2C_m\omega^2(1 - k^2)]^2 + [R_tC_m\omega]^2}{\left[1 - L_2C_m\omega^2(1 - k^2) + \frac{R_1R_2C_m\sigma_0^2}{L^2} + \frac{R_t}{S_2}\right]^2 + \left[\frac{R_1\sigma_0^2 - L_2C_m\omega^2R_t}{L_2\omega} - \frac{L_2^2\omega^2(1 - k^2) - R_1R_2\sigma_0^2}{S_2L_2\omega}\right]^2},$$

which again reduces to the approximate form

$$\sigma^2 = \frac{[1 \pm k\sigma_0 + L_2C_m\omega^2(1 - k^2)]^2}{[1 - L_2C_m\omega^2(1 - k^2)] + \frac{1}{L_2^2\omega^2}[R_1\sigma_0^2 - L_2C_m\omega^2R_t]^2}. \quad . \quad . \quad . \quad . \quad . \quad . \quad (37)$$

Digitized by Google

NOTE 3.—TRANSFERRING SECONDARY LOAD TO PRIMARY.

In case it is desired to ascertain in any particular case whether this assumption is valid, the accurate expressions for $Rp_1$ and $Xp_1$ are here given for the case where a secondary shunt $S_2$ of any value is present and no primary shunt is included :—

$$Rp_1 = R_1 + \frac{M^2\omega^2(R_2 + S_2 + R_2S_2C_2^2\omega^2)}{(R_2 + S_2[1 - L_2C_2\omega^2])^2 + (R_2S_2C_2 + L_2)^2\omega^2},$$

and

$$Lp_1 = L_1 + \frac{M^2\omega^2[S_2C_2^2(1 - L_2C_2\omega^2) - L_2]}{(R_2 + S_2[1 - L_2C_2\omega^2])^2 + (R_2S_2C_2 + L_2)^2\omega^2}.$$

The diameter $S'_1$ of the equivalent primary circle is found by putting $L_2C_2\omega^2 = 1$. The expression

$$S'_1 = (Rp_1 - R)_{max.} \doteqdot \frac{S_2M^2}{L_2^2}(1 - R_2S_2C_2^2\omega^2).$$

When the conditions are such that the second term in the bracket is small compared to unity $S'_1 \doteqdot S_2\frac{k^2}{\sigma_0^2}$. This condition will in general be satisfied so long as $S_2$ is not greater than 5 megohms.



Digitized by Google

Digitized by Google

# ON AN ELECTROMAGNETIC METHOD FOR THE MEASUREMENT OF THE HORIZONTAL INTENSITY OF THE EARTH'S MAGNETIC FIELD

BY

F. E. SMITH, F.R.S.,

SOMETIME SUPERINTENDENT OF THE ELECTRICITY DEPARTMENT.

Digitized by Google

## ABSTRACT.

After referring to previous measurements by WATSON, WATANABE, and BARNETT, the construction and working of a magnetometer of the Helmholtz-Gaugain type is described, the principle of which was given by SCHUSTER. The coils of the system carry a current $i$ which produces a horizontal field of intensity $Fi$, greater than H; if the two fields are almost in opposite directions, and the needle is at right angles to the meridian, $H = Fi \cos \alpha$, where $\alpha$ is the acute angle between the two field directions. The coils of the instrument are four in number, each containing 12 turns, of 30 cm. radius, of bare copper wire wound on a marble cylinder capable of rotation round a vertical axis. The needle is 1 cm. long and 5 sq. mm. in section, and is suspended by a quartz fibre. When the needle is deflected, the fibre is turned through an equal angle to remove the torsion. The current $i$ is determined in absolute measure by means of a current weigher. After adjustment of the current, a measurement of H with calculation complete takes less than four minutes, the total probable error being about + 4 parts in 100,000. A full account is given of the construction of the various parts, the measurement of the coils, tests of the uniformity of the field at the needle, calculation of the constant F, examples of measurements of H with the instrument, and comparison of the results with values obtained from a magnetograph and from a Kew magnetometer.


Digitized by Google

# ON AN ELECTROMAGNETIC METHOD FOR THE MEASUREMENT OF THE HORIZONTAL INTENSITY OF THE EARTH'S MAGNETIC FIELD.

By F. E. SMITH, F.R.S., Sometime Superintendent of the Electricity Department.

[Reprinted from the 'Philosophical Transactions of the Royal Society', Series A. Vol. 223.]

## § 1. *Introductory.*

The instrument described in this communication is the outcome of a suggestion made by Sir Arthur Schuster in 1913. The writer was asked to express his opinion on the practicability of the suggestion and the conditions necessary to secure great accuracy in any measurements which might be made. It appeared that the method proposed would allow a determination of H, the horizontal magnetic intensity, to be made in a few minutes and with a probable error of only a few parts in one hundred thousand. The design of a standard instrument was therefore prepared and submitted to Sir Arthur Schuster for approval. Construction of the instrument was commenced in 1914, but owing to the war, it was not completed until late in 1920. In 1919 the writer accepted an appointment with the Admiralty, and as a result, progress with the measurements at Teddington has been slow.

Throughout the work Sir Arthur Schuster has rendered most valuable help, and whatever success has been achieved is largely due to him. From the commencement of the investigation the instrument has been called by me the "Schuster Magnetometer."

## § 2. *Previous Measurements.*

Watson,* in 1902, made the first serious attempt to measure H by an electromagnetic method. In this work the writer collaborated. A large Helmholtz-Gaugain galvanometer was used. The suspended magnet at the centre, together with fibre, torsion head, etc., formed part of a Kew pattern magnetometer. The results were in good agreement with those obtained with a Kew instrument.

Watanabe† has recently published an account of an instrument designed for field work. The dimensions of the coils are not measured, the constant of the instrument being found by comparison with that of a standard Helmholtz-Gaugain galvanometer having coils of single turns. The mean diameter of the latter is 20 cm.

* 'Phil. Trans.', A, vol. 198, p. 431, 1902.

† 'Proc. Phys. Math. Soc. Japan', (3), vol. 2, p. 210, 1920.

Digitized by Google

S. J. BARNETT,* of the Carnegie Institution of Washington, has made measurements with a Helmholtz-Gaugain galvanometer in which the coils are of bare wire wound in spiral grooves in marble. The mean diameter of the coils is 30 cm. The magnets are circular discs of steel, 2 cm. in diameter, which are polished on both sides in order to serve as mirrors. The probable error of the constant of the instrument appears to be about $\pm$ 2 parts in 100,000, and it is stated that the probable error in the value of the current was less than 1 part in 4,000. More precise values of the current are needed. The instrument has been used as a sine galvanometer, and the results obtained agree with those given by a Carnegie Institution magnetometer (somewhat similar to a Kew instrument) within about 1 part in 25,000.

## § 3. *Principle of the Schuster Magnetometer.*

The principle of the new magnetometer was first described by Sir ARTHUR SCHUSTER, in 'Terrestrial Magnetism', March, 1914. Very briefly it is as follows :—

In fig. 1 let AB point accurately to the magnetic north, and let F$i$ represent the direction and magnitude of the horizontal magnetic intensity produced by a current $i$ through a system of coils, the latter being of such size and arrangement that F$i$ is practically uniform throughout a sphere having a diameter equal to, or greater than, the length of a small indicator magnet NS. If F$i$ is greater than H, the earth's horizontal intensity, and if the component of F$i$ along AB is in opposition to H, the indicator magnet may, by a rotation of the coil system, be made to set at right angles to AB. H is then determined by

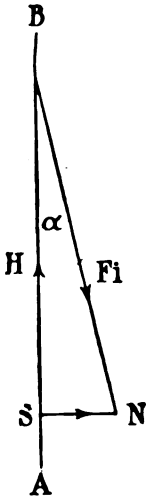

Fig. 1.

$$H = Fi \cos \alpha.$$

If the magnitude of $i$ can be easily adjusted, it may be arranged for $\alpha$ to be very small, when cos $\alpha$ will be nearly equal to unity, and will vary slowly for comparatively large changes in $\alpha$.

The direction AB may be most easily determined by reversing the direction of the current (or by turning the coil system through 180 degrees) and then rotating the system until there is no deflection of the indicator magnet when the circuit is either made or broken.

If F$i$ is less than H and the indicator magnet is caused to set at right angles to F$i$ instead of to H, then

$$H = Fi/\cos \alpha.$$

The horizontal intensity of the earth's magnetic field in the vertical plane containing F$i$ is, then, equal to F$i$, but is in the opposite direction. An instrument of this type may therefore be used to measure the components of H in any direction.

* 'Publication 175 of the Carnegie Inst.' of Washington, December, 1921.

Digitized by Google

## § 4. *Brief Description of Instrument.*

For constructional purposes, as well as to ensure a uniform magnetic field at and near the centre of the system, a Helmholtz-Gaugain arrangement was adopted (*see* fig. 2). The equivalent coils on each side of the centre are of 12 turns, of 30 cm. radius, of $\frac{3}{8}$mm. pitch and of bare copper wire; they are wound on a marble cylinder which, when mounted with axis horizontal, can be rotated about a vertical axis. The magnet at the centre is 1 cm. long and about 5 sq. mm. in cross section; it is supported on a V of aluminium foil by a fine quartz fibre, to which is attached also a reflecting mirror and a damping vane. The damping of the system can be adjusted so that it can be made aperiodic. The magnet is easily removed from its support, and a copper wire of the same weight and of nearly the same dimensions can be substituted. This enables most of the torsion on the fibre to be removed. Reflecting mirrors are attached to the suspended system, to the marble cylinder, and to the case enclosing the magnet. After the magnet has been deflected, the fibre is turned through an equal angle, and no torsion, or change of torsion, in the fibre is therefore possible. The current is determined in absolute measure by means of a current weigher. The leads to and from the magnetometer coils are planned so that the current through them shall have no effect on the magnet. A measurement of H, with calculation complete, occupies (after adjustment of the current) less than four minutes. The total probable error—including error due to uncertainty of the value of the current—is about $\pm$ 4 parts in 100,000.

The horizontal intensity in any direction can be measured, and by a modification of the instrument the vertical intensity can be determined. The modification consists in supporting the coil system with its axis vertical, and spinning a small coil at the centre, the ends of the coil being connected to conductors leading to a vibration galvanometer. For very precise measurements the diameter of the spinning coil, which should consist of a large number of turns, should not exceed 3 cm. The axis of rotation should be at right angles to the axis of the coil system, and the supporting axis should be a metal rod, cut into two parts connected together by an insulator, the ends of the spinning coil being connected to the two parts of the rod. The circuit would be completed through a vibration galvanometer having a frequency equal to that of the spinning coil. The field due to the Helmholtz-Gaugain coils would oppose the vertical field due to the earth, and, when no deflection was obtained with the vibration galvanometer, the two fields would be equal. Careful design of the spinning coil and the vibration galvanometer are needed.

## § 5. *The Marble Cylinder.*

The marble is of fine grain and is from Marmora. It is 61 cm. in diameter and 37 cm. long. Two circular channels, about 2 cm. wide and 0·5 cm. deep, are cut near the ends of the cylinder, and the appropriate twin-screw grooves are cut in these channels



Digitized by Google

to support the wire for the coils. The turning tools used were tipped with bort. Four large circular apertures are made in the cylinder to allow the passage of the main stem and the torsion tube, and to admit light to the mirrors attached to the central system. Two cylindrical holes, parallel to the axis of the cylinder, and at opposite ends of a diameter, permit the introduction of two thermometers, the bulbs of which are centrally situated within the marble.

### § 6. *The Base.*

The base is of gun-metal and consists of a turntable carrying two webs which form a cradle on which the marble cylinder rests. The upper portion of the base, which carries the verniers, rotates about a large central stud, and is supported by a circular race of phosphor-bronze balls. The V ring in which the balls run is in turn supported by a stiff circular spring of phosphor bronze, and it is by adjustment of this spring that a smooth rotational motion is obtained. The turntable is provided with a fine adjustment screw, which operates successfully even when the table is loaded with a weight of 100 kg. There are two verniers 180 degrees apart, and direct readings of angles can be made within 10 seconds. The base was made by Messrs. E. R. Watts & Son, the circular scale being calibrated in the Optical Department of the National Physical Laboratory.

### § 7. *Magnetic Tests.*

When the metal support for the marble cyclinder was cast, three lugs were cast with it, and these, together with samples of all parts of the magnetometer, were carefully tested for magnetic quality.

The principal method of testing was similar to that employed for parts of the current balance* and of the Lorenz apparatus. Soft iron wire and ferrous sulphate were used to calibrate the apparatus, and the sensitiveness was sufficient to detect a difference of about 1 part in 100,000 from unit magnetic permeability. A number of brass rods, tubes and screws were rejected.

In practice, part of the machined surfaces of the webs which carry the cylinder are in a magnetic field having an intensity of about 2·5, and the copper wire carrying the current is of course in a much stronger magnetic field. These parts, together with various small fittings and parts of the concentric cable, were further tested by bringing them within a few millimetres of one of the poles of a suspended magnet. The pole strength of the latter was 100 C.G.S. units, and the strength of the field in which the specimen was placed was calculated to be about 300. The magnet was provided with a deflector mirror, and the deflection could be read within about 1 minute of arc.

* ' Phil. Trans.', A, vol. 207, p. 475, 1908.

Digitized by Google

Digitized by Google

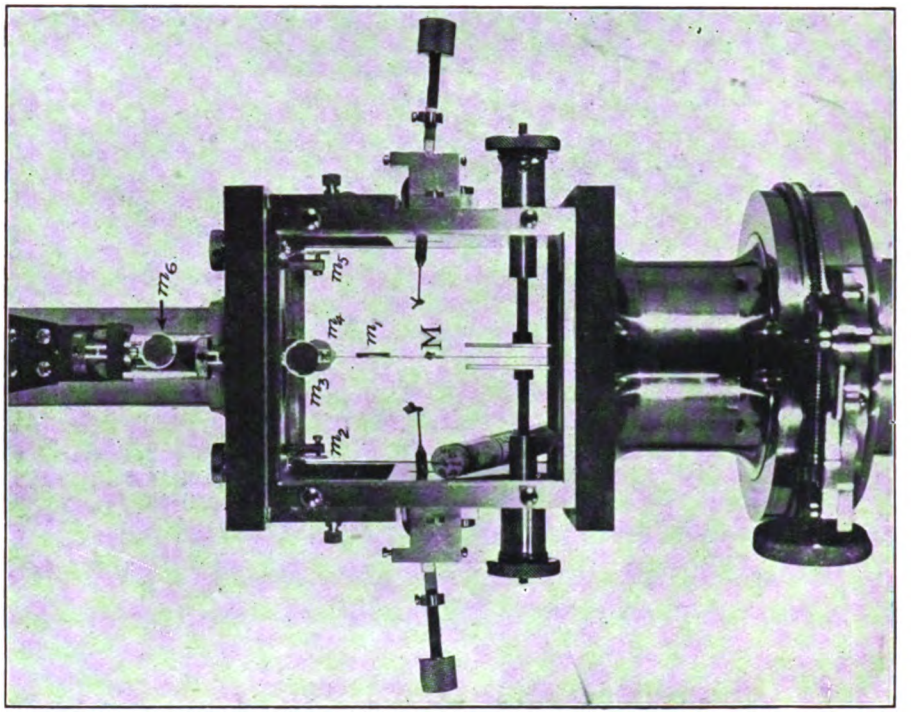


Fig. 3.

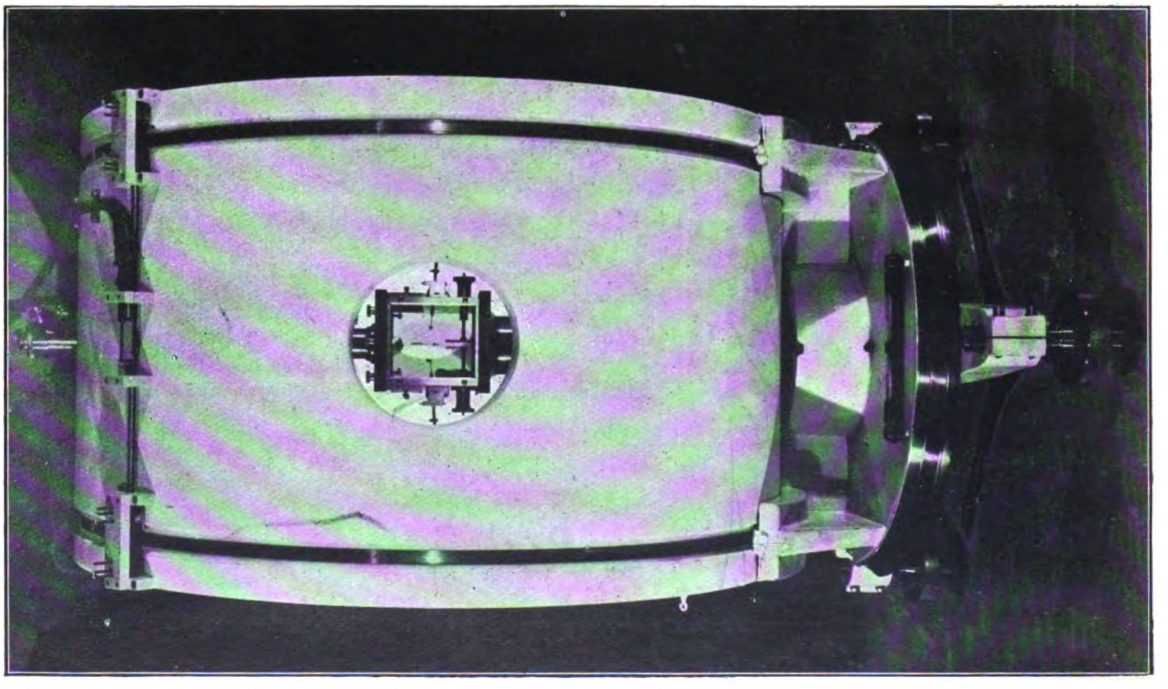

Fig. 2.

[*To face p.* 323.

Digitized by Google

Tested in this way, many metal parts were found to be slightly magnetic, and a considerable number of brass screws were found to be appreciably magnetic.

After completion of the support it was slung so that it could be brought close to a delicate recording magnetgraph and rapidly removed again. Had the resultant change in the horizontal intensity near the indicating magnet been as great as 2 parts in 100,000, it would certainly have been detected. No change was noted.

It is concluded that the permeability of no part of the apparatus differs from unity sufficiently to produce an error of more than 1 part in 100,000.

## § 8. *The Coils.*

The coils are wound with hard-drawn copper wire in tension, the effective load on the wire being 4 kg. During winding, the cylinder was rotated very slowly, and after about one-third of a revolution the motion of the lathe was stopped for measurements to be made of the diameter of the wire. In all, 64 measurements were made. The mean diameter was found to be 0·563 mm. and the maximum variation from the mean was 0·003 mm. A small cylindrical steel gauge, about the same diameter as the wire, was used as a check on the micrometer.

Each half of the coil system consists of two coils, each of which is 60 cm. in diameter, of six turns and $1\frac{2}{3}$ mm. pitch. The two coils form two interwoven helices, the mean planes of which are coincident, but the commencement and end of one coil are 180 degrees apart from the commencement and end of the other. This twin-coil construction, with bare wires, enables the diametral and axial measurements of the coils to be made with great accuracy, and also enables the insulation resistance between neighbouring turns to be measured with ease.

## § 9. *The Suspended System* (fig. 3).

The magnet M, together with a reflecting mirror $m_1$, and a damping vane of aluminium foil, are suspended from a fine quartz fibre 25 cm. long. The suspended portions swing in a square case, of which two opposite sides are of plate glass.

The upper parts of the other sides of the case are also of plate glass, but the lower portions are of brass and carry the adjusting screws for the damping buffers and the rods with V claws at the ends. These claws serve to support the magnet and copper wire, and enable either of them to be placed in the V support. The parts are shown in fig. 3. The damping buffers have their inner surfaces platinized and are not lacquered; also, to eliminate any electrostatic attraction, a glass tube containing a small quantity of radium bromide is introduced into the chamber.

The top of the case is of brass, and in addition to supporting a tube carrying the torsion head and fibre, it supports four reflecting mirrors $m_2$, $m_3$, $m_4$, $m_5$, which, after adjustment,



Digitized by Google

serve to indicate movements of exactly 90 degrees, 180 degrees, etc. A mirror $m_0$ attached to a V strip fixed to the marble cylinder can be used to indicate the angle of rotation of the coil system.

In all there are six mirrors, each of 2 metres radius of curvature. One mirror is attached to the magnet system, one to the marble cylinder, and four (90 degrees apart) to the case containing the suspended parts. Three slit sources of light, approximately 90 degrees apart, are used, and images of these are formed on a circular scale of 2 metres radius. Positions exactly 90 degrees apart are obtained by rotating the case and adjusting the four mirrors, $m_2$, $m_3$, $m_4$, $m_5$ in azimuth until the angle between the images is independent of the mirrors used, *i.e.*, the axes of the mirrors must be 90 degrees apart. As an alternative method to adjust the mirrors, the large circular scale attached to the turntable can be used.

The magnet case is mounted on a stout tubular metal piece, which rotates about a large metal stud, and is supported by phosphor-bronze balls running in a circular race. The main support is a stiff brass tube passing through an aperture in the marble cylinder, and is secured to the base.

The whole of the suspended system, together with torsion head, fibe, damping buffers, mirrors, etc., can thus be turned rapidly about the central stud. A few seconds enables the angle turned through to be adjusted exactly to 90 degrees, 180 degrees, or any other angle previously arranged for. A fine adjustment screw is provided.

Apart from the marble cylinder and its support, the instrument was constructed by Mr. L. Buxton, of the National Physical Laboratory, and the writer wishes to express his appreciation of the skill of Mr. Buxton in work of this character.

## § 10. *Determination of Constants.*

For a precise knowledge of H it is necessary to have an accurate knowledge of the value of the current in absolute measure and of the constant of the coil system.

The uniformity of the magnetic field, the effect of any torsion on the fibre, the possible magnetic effect of the current in the circuit external to the coils, the magnetic permeability of the coil supports and possible electrostatic effects on the suspended system, are also of considerable importance, but merely demand reasonable care in the design and test of the apparatus and in experimental manipulation.

## § 11. *Precision with which the Current can be Measured.*

The value of the current in absolute measure might be obtained by using the magnetometer coils as part of an absolute electrodynamometer of W. Weber's pattern, or they might be used as part of the fixed coils of a current weigher.

The absolute measurement of the current need not, however, be made with the same, or part of the same, instrument. At the National Physical Laboratory there exists an

Digitized by Google

elaborate current balance, which was constructed in 1908. The balance, as a weighing mechanism, is in perfect order; the insulation resistance between the twin coils has fallen, but not sufficiently to introduce an appreciable error in any measurement of current. Certainly, any possible error is less than a few parts in a million. Unfortunately, it is not possible to re-measure the dimensions of the coils, and it is necessary to assume them to have remained constant.

The balance was overhauled and the coils re-set to be co-axial and co-planar. Subsequently a number of absolute measurements of currents were made, a combination of a standard cell and a standard resistance being evaluated. In all, there were twelve determinations, and no single value differed from the mean value by more than 15 parts in 1,000,000. The probable error of the value of the current thus determined is believed to be between 3 and 4 parts in 100,000. In the measurements of H with the magnetometer, the current balance was the basis for the absolute measurements of current.

When the current weigher has been provided with new coils, the probable error associated with the value of the current should be reduced to less than $\pm$ 2 parts in 100,000.

## § 12. *Measurement of the Diameters of the Coils.*

The diameters of the coils were measured twice; once along the rake of the helices so that the measurements related to a single coil, and once with the measuring faces of the machine at right angles to the axis of the cylinder. In the latter case, a measured distance is really the addition of the lengths of the radii of the two twin coils. The measurements were made in 24 axial planes at angular distances of 7·5 degrees apart. These places are numbered, 1, $1\frac{1}{4}$, $1\frac{1}{2}$, $1\frac{3}{4}$, 2, $2\frac{1}{4}$ . . . $6\frac{1}{2}$, $6\frac{3}{4}$, in the tables.

The diameters measured were compared with the length of a 60 cm. Hartmann spherical-ended steel gauge. The pressure exerted by the measuring faces on the copper wire of the coils was between 100 and 140 grammes weight.

The results of the first series of measurements of the diameters are given in Table I. In this series the measurements are related to single coils. The coils on one side of the centre are called $A_1$ and $A_2$, and those on the other side are called $B_1$ and $B_2$.

In Tables I and II the measurements on the coils are summarized in different ways. In Table I the measurements are arranged to show the departure of the coils from the circular form, whilst the mean values given in Table II show the taper of the coils.

Digitized by Google

TABLE I.—First Series (Diameter of Coil — Length of the Hartmann Gauge) at 17° C. Measurements arranged to show Circularity of the Coils. Differences are given in microns (1 micron = 0·001 mm.).

| Mean of 5 or 6 measurements. | | | | Plane. |
|---|---|---|---|---|
| Coil $A_1$. | Coil $A_2$. | Coil $B_1$. | $B_2$. | |
| *485·6 | 482·4 | *488·6 | 476·2 | $1\frac{1}{4}$ |
| 486·4 | *482·6 | 490·4 | *479·2 | $1\frac{3}{4}$ |
| *483·8 | 482·6 | *483·6 | 476·6 | $2\frac{1}{4}$ |
| 486·9 | *479·8 | 480·2 | *473·0 | $2\frac{3}{4}$ |
| *484·6 | 483·6 | *474·4 | 469·1 | $3\frac{1}{4}$ |
| 490·4 | *481·2 | 470·4 | *460·8 | $3\frac{3}{4}$ |
| *487·8 | 485·9 | *461·6 | 457·2 | $4\frac{1}{4}$ |
| 489·2 | *482·2 | 451·4 | *449·6 | $4\frac{3}{4}$ |
| *481·2 | 485·1 | *450·6 | 446·4 | $5\frac{1}{4}$ |
| 484·6 | *477·4 | 453·6 | *445·8 | $5\frac{3}{4}$ |
| *476·4 | 478·1 | *464·8 | 458·7 | $6\frac{1}{4}$ |
| 483·9 | *477·8 | 481·9 | *471·0 | $6\frac{3}{4}$ |
| Weighted mean 485·2 | 481·7 | 471·0 | 463·7 | |
| 483·4 | | 467·3 | | |
| Final Mean = 475·4μ (Coils A and B). | | | | |

TABLE II.—Measurements arranged to show Taper of the Coils. Differences in microns.

| Mean of 6 measurements. | | | | Turn of wire. |
|---|---|---|---|---|
| Coil $A_1$. | Coil $A_2$. | Coil $B_1$. | Coil $B_2$. | |
| 516·1 | 511·9 | 464·4 | 458·7 | $\frac{1}{4}$ to $\frac{3}{4}$ |
| 511·7 | 506·4 | 464·2 | 455·1 | $\frac{3}{4}$ „ $1\frac{1}{4}$ |
| 503·9 | 500·7 | 462·6 | 452·7 | $1\frac{1}{4}$ „ $1\frac{3}{4}$ |
| 493·7 | 492·1 | 460·7 | 454·1 | $1\frac{3}{4}$ „ $2\frac{1}{4}$ |
| 485·7 | 482·6 | 463·9 | 456·1 | $2\frac{1}{4}$ „ $2\frac{3}{4}$ |
| 474·7 | 470·4 | 466·2 | 459·7 | $2\frac{3}{4}$ „ $3\frac{1}{4}$ |
| 463·7 | 461·9 | 472·2 | 465·9 | $3\frac{1}{4}$ „ $3\frac{3}{4}$ |
| 459·6 | 458·2 | 477·4 | 470·7 | $3\frac{3}{4}$ „ $4\frac{1}{4}$ |
| 466·2 | 461·1 | 478·4 | 474·2 | $4\frac{1}{4}$ „ $4\frac{3}{4}$ |
| 476·4 | 473·7 | 483·6 | 476·6 | $4\frac{3}{4}$ „ $5\frac{1}{4}$ |
| 485·7 | 479·4 | 486·4 | 476·6 | $5\frac{1}{4}$ „ $5\frac{3}{4}$ |
| Mean 485·2 | 481·7 | 470·9 | 463·7 | |
| Mean A = 483·4 | | Mean B = 467·3 | | |
| Final Mean = 475·4μ (Coils A and B). | | | | |

* Mean of 5 measurements.

Digitized by Google

The detailed results of the second series of measurements are not given here, but they are shown in figs. 4 and 5, which summarize in a graphical form the results of all

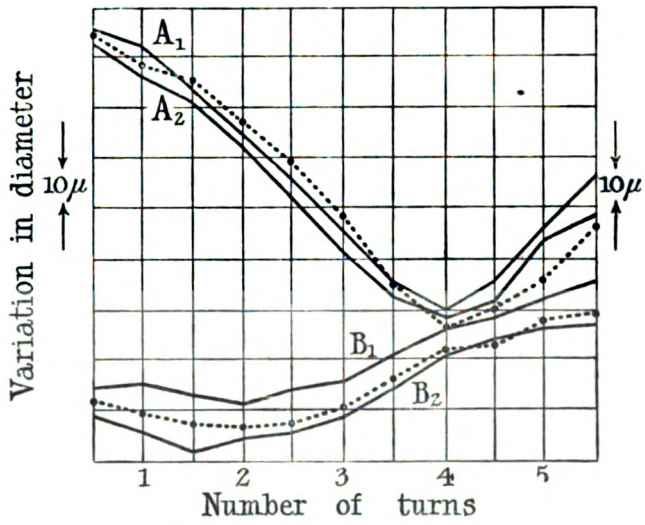


Fig. 4. Showing the taper of the four coils. Length of each coil is 1 cm.

the measurements. Fig. 4 shows the taper of the coils, and fig. 5 shows the departure from the circular form. The dotted lines show the results of the second series of measurements.

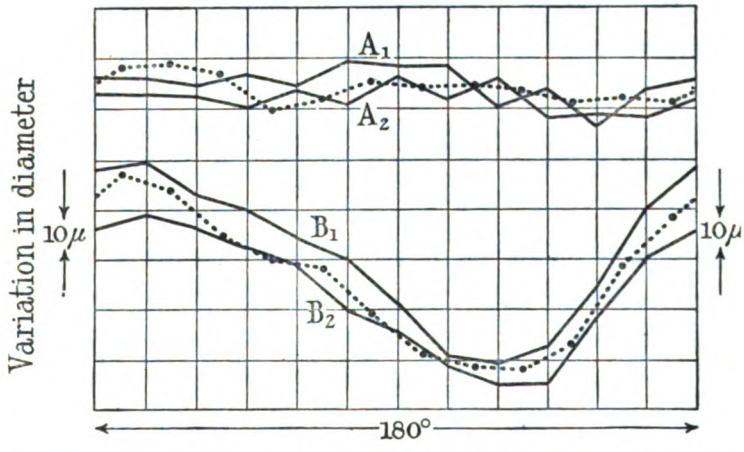


Fig. 5. Showing the departure of the four coils from a circular cross-section.

The mean diameters of the coils at 17° C. measured to the outer limits of the wire are as follows :—

First Series.

| | | | | | |
|---|---|---|---|---|---|
| $A_1$ | 60·0592 | Mean = 60·0591 cm. | $B_1$ | 60·0578 | Mean = 60·0575 cm. |
| $A_2$ | 60·0589 | | $B_2$ | 60·0571 | |

Digitized by Google

Second Series.

| | | | |
|---|---|---|---|
| Coils A ($A_1$ and $A_2$) | 60·0590 cm. | Coils B ($B_1$ and $B_2$) | 60·0573 cm. |

The mean diameters measured to the axis of the wire are :—

| | | | |
|---|---|---|---|
| $A_1$ | 60·0029 cm. | $B_1$ | 60·0015 cm. |
| $A_2$ | 60·0026 ,, | $B_2$ | 60·0008 ,, |

The close agreement between the mean diameters of the four coils bears testimony to the excellent workmanship of Mr. Tribe, who machined the cylinders. The agreement indicates also the degree of precision which can be obtained in this kind of work.

## § 13. *Heating Effect of Current.*

Measurements were made of the diameter of the coils whilst a current of about 0·5 ampere was passing through the coils. For this purpose special agate measuring contact pieces were used in the measuring machine. The two thermometers used in determining the temperature of the marble were placed with their bulbs immediately below the coils. No change in diameter of the coils or in the temperature of the marble was observed during the 30 minutes during which the current was on, or during a subsequent 30 minutes after the current was switched off, other than such as could be accounted for by the change in temperature of the room itself.

## § 14. *Measurement of the Axial Lengths and Pitch of the Coils and the Distance between their Mean Planes.*

The measurements were made on a large pitch-measuring machine, made by Sir W. G. Armstrong, Whitworth & Co.* The micrometer miscroscope attached to the slide of the machine was focussed on the copper wire of the coils, and successive readings were made on each turn. In all, 288 measurements were made along 12 generating lines equally spaced around the cylinder.

The mean lengths of the coils were taken as a basis for calculating the mean pitch, and the mean distance between the pairs of coils was determined by taking the mean of the distances as measured along each generator.

The axial lengths of the coils at 17° C. are as follows :—

| | | | |
|---|---|---|---|
| $A_1$ | = 0·9986 cm. | $B_1$ | = 0·9990 cm. |
| $A_2$ | = 0·9982 ,, | $B_2$ | = 0·9988 cm. |

* *See* " Abs. Measts. of a Resistance by Lorenz Method", ' Phil. Trans.', A, vol. 214, p. 61, 1914.

Digitized by Google

The mean pitch of the coils is 0·083221 cm. Using this figure, the nominal axial reading for any point of a coil can be calculated, and this calculated value, compared with the actual reading of the point, gives the pitch error. Or, symbolically, if $p$ is the mean or nominal pitch and $x$ the reading of the $n$th wire from the first, the pitch error on this wire is given by $x - np$. The mean pitch errors for each turn are given in fig. 6. Coil $A_2$ is asymmetrically displaced by a mean amount of 7 $\mu$ with respect to Coil $A_1$, and Coil $B_2$ is likewise displaced with respect to Coil $B_1$ by 4 $\mu$.

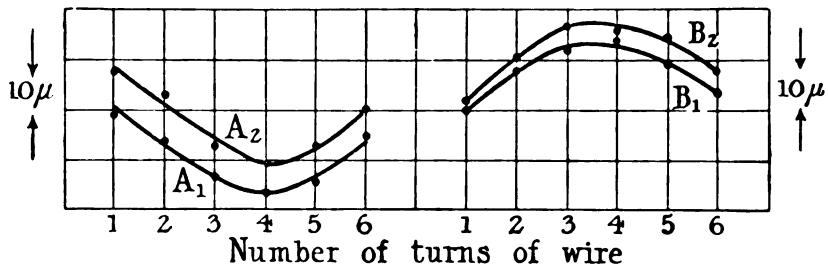


Fig 6. Showing the pitch errors in the four coils.

The shape of the curves points to a periodicity in the pitch error of about half an inch, which corresponds to the pitch of the lead screw of the lathe on which the cylinder was turned. The same periodicity was found in the coils of the Lorenz apparatus.
The distance between the mean plane of the coils $A_1$ and $A_2$ and that of the coils $B_1$ and $B_2$ is 30·0098 cm. at 17° C. The irregularities of pitch existing near the ends of the coils were measured and found to be of negligible importance.

The eight ends of the wires of the four coils are bent into the marble as shown in fig. 9. The effect of this is slightly to increase the diameters of the coils, and these particular parts were therefore specially surveyed with a view to applying a correction. However, the calculated correction is 1 part in 60 millions. Similarly, the axial lengths of the coils and the distance between mid-planes must be slightly affected by these irregularities, but again the calculated correction is ridiculously small.

The ends of all the coils were found to lie in an axial plane within less than 0·5 mm.; as the length of wire in the four coils is a little over 45,000 mm., the correction due to any irregularity is less than 1 part in 90,000.

## § 15. *Thermal Coefficient of Expansion of the Marble.*

Observations were made on certain diameters of the coils at temperatures ranging from 12° to 25° C., the whole room being cooled or heated for the measurements. The thermal coefficient of linear expansion was found to be $7{\cdot}9 \times 10^{-6}$ per 1° C. Thermometers can be inserted so that their bulbs are in a central position in the marble.

I am greatly indebted to Mr. S. Attwell and Mr. Johnson, of the Metrology Department, for making the linear measurements.



Digitized by Google

### § 16. *Calculation of the Constant of the Coil System.*

It is shown later that, for unit current in the circuit, the axial intensity at the centre of a coil system of which each half consists of N turns (the breadth of a coil being comparatively small) is N times that due to unit current in two turns flowing in circles in the mean diametral planes of the coils. The axial intensity at the centre can therefore be calculated from the equation

$$F_z = \frac{4\pi N a^2}{(a^2 + l^2)^{\frac{3}{2}}}, \quad \ldots \ldots \ldots \ldots \quad (1)$$

where N is the number of turns in half of the complete system, $a$ is the mean radius of the coils, and $2l$ is the distance part of the mean planes.

In the present investigation,

$$2a = 60{\cdot}0019 \text{ cm. at } 17^\circ \text{ C.}$$
$$2l = 30{\cdot}0098 \text{ ,, ,, ,,}$$
$$N = 12,$$

and the value of $F_z$ calculated by (1) is $3{\cdot}59595$ cm.$^{-1}$.

Differentiating (1) we get

$$\frac{dF_z}{F_z} = \frac{2l^2 - a^2}{a^2 + l^2} \cdot \frac{da}{a} - \frac{3l^2}{a^2 + l^2} \frac{dl}{l}, \quad \ldots \ldots \ldots \quad (2)$$

or, for $a = 30$ cm. and $l = 15$ cm.,

$$\frac{dF_z}{F_z} = -0{\cdot}4 \frac{da}{a} - 0{\cdot}6 \frac{dl}{l}. \quad \ldots \ldots \ldots \quad (3)$$

Hence, a variation in $a$ of $2{\cdot}5$ parts in 100,000 or in $l$ of $1{\cdot}7$ parts in 100,000, produces a change in the value of $F_z$ of 1 part in 100,000. Also, if the cylinder on which the coils are wound expands uniformly with rise of temperature, then $da/a = dl/l$, and the coefficient of change of $F_z$ with temperature is equal to the temperature coefficient of linear expansion of the marble. The coefficient is $+ 7{\cdot}9 \times 10^{-6}$ for a rise of temperature of 1° C. It is believed that the value of $F_z$ is known within 1 part in 100,000.

### § 17. *Uniformity of Field near the Centre of the Coil System.*

It has been assumed, in the calculation of $F_z$, that the 12 turns constituting each half of the coil system may be regarded as concentrated in the mean planes of the coils. This assumption is justified, because for an axial displacement from the centre equal to half the width (5 mm.) of a coil the change in axial intensity is less than 1 part in a million. In practice, however, the magnet is permanently deflected from the axial

Digitized by Google

position, and it is of importance, therefore, to know if the transverse intensity is also negligible. I have made, therefore, a careful survey of the region in which the indicator magnet may swing.

In the case of two single turns placed co-axial and with their planes parallel, the intensity of the axial magnetic field at the centre for unit current through the turns is

$$F_x = \frac{4\pi a^2}{(a^2 + l^2)^{\frac{3}{2}}}, \quad \ldots \ldots \ldots \quad (4)$$

where $a$ is the radius of a turn and $2l$ is the distance between the planes of the turns.

In the ideal Helmholtz-Gaugain arrangement $l = a/2$, and in such a case the above expression reduces to

$$F_x = \frac{6 \cdot 4\pi}{\sqrt{5}a} = \frac{8 \cdot 99176}{a}. \quad \ldots \ldots \ldots \quad (5)$$

When $a = 30$ cm. and there are 12 turns (supposed to be coincident), $F_x = 3 \cdot 59670_4$ cm.$^{-1}$. The sum of the corrections for $da = 0 \cdot 00095$ cm. and for $dl = 0 \cdot 00490$ cm. is $- 0 \cdot 00075_1$. Hence when $2a = 60 \cdot 0019$ and $2l = 30 \cdot 0098$ the value of $F_x$ is $3 \cdot 59595$ cm.$^{-1}$ as obtained by direct calculation from equation (1).

It follows from equation (5) that if in different instruments it is desired to have the same value of axial field and also to use the same value of current, the number of turns in the coils should be directly proportional to the radii. In England, for an axial intensity of about $0 \cdot 18$ C.G.S. unit, a convenient number of turns is 12 for $a = 60$ cm., 10 for $a = 50$ cm., 8 for $a = 40$ cm., and so on. The current in the coils is supposed to be half an ampere.

Nagaoka has shown* that the axial intensity at any point near the centre can be calculated from the expression

$$F_x = \frac{6 \cdot 4\pi}{a\sqrt{5}}\left\{1 - \frac{18}{125a^4}(8x^4 - 24x^2y^2 + 3y^4)\right\}. \quad \ldots \ldots \quad (6)$$

where $x$ and $y$ are the axial and transverse co-ordinates of the point with respect to the centre.

The transverse magnetic intensity is zero at the centre of the system and at all points in the plane midway between the coils. Its value at a point near the centre can be calculated from the expression

$$F_y = \frac{2304\pi}{625a^5\sqrt{5}} xy\,(4x^2 - 3y^2). \quad \ldots \ldots \ldots \quad (7)$$

It follows from (6) and (7) that the ratio of the transverse to the axial intensity can be calculated at any point. This ratio can be calculated with considerable accuracy by means of the equation

$$F_y/F_x = 0 \cdot 576xy\,(4x^2 - 3y^2)/a^4. \quad \ldots \ldots \ldots \quad (8)$$

* 'Phil. Mag.', vol. 41, 1921.



Digitized by Google

In a system in which $a$ is 30 cm., the above expression reduces to

$$F_y/F_x = (7{\cdot}1\times10^{-7})\,xy\,(4x^2 - 3y^2). \quad . \quad . \quad . \quad . \quad . \quad . \quad . \quad . \quad (9)$$

NAGAOKA has given curves showing regions, near the centre of a system, of equal axial intensity and of negligible transverse intensity. He has shown that, throughout a sphere the radius of which is equal to one-tenth of the radius of a coil, and whose centre is coincident with that of the system, the axial intensity is constant within 1 part in 1,000. In the present investigation, regions have been examined in which the axial intensity is constant within 1 part in a million, 5 parts in a million, and 10 parts in a million respectively. Regions have also been investigated in which the ratio of the transverse to the axial intensities does not exceed these values. A system of two coils, each coil consisting of 12 turns of 1 mm. pitch, has also been investigated. This system is not quite identical with that of the instrument described in this paper, but very nearly so. It is intended to construct any future systems with coils of 1 mm. pitch.

The results are most conveniently given in the form of curves. The regions in which the axial intensity is constant within 1, 5 and 10 parts in a million, respectively, are shown in fig. 7. The curves given in quadrants A, C, are for a Helmholtz-Gaugain

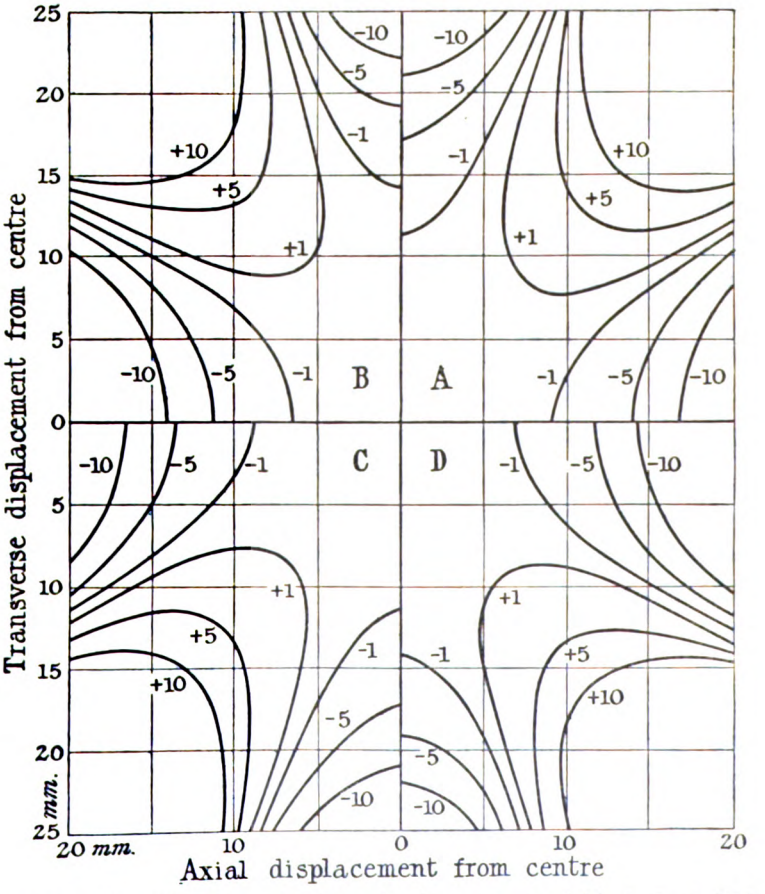


Fig. 7. Showing regions in which the axial intensity is constant within 1, 5, and 10 parts in a million respectively.

Digitized by Google

system, each coil being of 30 cm. radius and consisting of 1 turn only; those given in the quadrants B, D are for a coil system, each coil being of 12 turns each and of 1 mm. pitch, the distance between the central planes of the coils being equal to the radius of either coil. The + and — signs indicate that the intensity is greater and less, respectively, than at the centre.

It will be observed that one result of using coils of appreciable breadth is slightly to reduce the axial distance over which the axial intensity is practically uniform; on the other hand, the transverse distance is increased. The following table gives the principal results:—

TABLE III.

| Variations in axial intensity not exceeding— | Approximate axial distance for system of coils of 1 turn each. | Approximate axial distance for system of coils of 12 turns each. | Approximate transverse distance for system of coils of 1 turn each. | Approximate transverse distance for system of coils of 12 turns each. |
|---|---|---|---|---|
| | mm. | mm. | mm. | mm. |
| $\pm 1 \times 10^{-6}$ | 18 | 14 | 23 | 29 |
| $\pm 5 \times 10^{-6}$ | 28 | 25 | 35 | 38 |
| $\pm 1 \times 10^{-5}$ | 34 | 28 | 42 | 44 |
| $\pm 1 \times 10^{-4}$ | 58 | — | 74 | — |
| $\pm 1 \times 10^{-3}$ | 104 | — | 133 | — |

The axial and transverse distances for variations in axial intensity of $\pm 1 \times 10^{-4}$ and $\pm 1 \times 10^{-3}$ have been calculated for coils of 1 turn, but are not plotted in fig. 7.

The regions in which the *ratio* of the transverse to the axial intensity is less than $1 \times 10^{-6}$, $5 \times 10^{-6}$, and $10 \times 10^{-6}$, respectively, are shown in fig. 8. The curves shown in quadrants A, A are for a system of coils of 1 turn each and of 30 cm. radius; those in quadrants B, B are for coils of 12 turns each, of 30 cm. radius and of 1 mm. pitch. The + and — signs indicate that the magnetic field is not parallel to the axis; in one case, the direction of the transverse component is from the axis outwards, and in the other case the direction is towards the axis. Inspection shows there is no special advantage of the single-turn system. The following table gives the diameters of spheres throughout which the ratio of the transverse to the axial intensities does not exceed 1, 5 and 10 parts in a million respectively:—

TABLE IV.—Diameters of Spheres with Centres at Centre of System and throughout which the Ratio of the Transverse to the Axial Intensity does not exceed the Values in column 1.

| Ratio of transverse intensity to axial intensity. | Coils of 1 turn. | Coils of 12 turns of 1 mm. pitch. |
|---|---|---|
| | mm. | mm. |
| $1.10^{-6}$ | 22 | 22 |
| $5.10^{-6}$ | 34 | 34 |
| $10.10^{-6}$ | 40 | 42 |

Digitized by Google

The differences between the values in columns 2 and 3 are negligible, and of the same order as the probable errors of the approximate method of calculation used for the system of 12 turns. The curves show that the system with single turns is more advantageous for axial symmetry, but at a slight disadvantage for transverse symmetry.

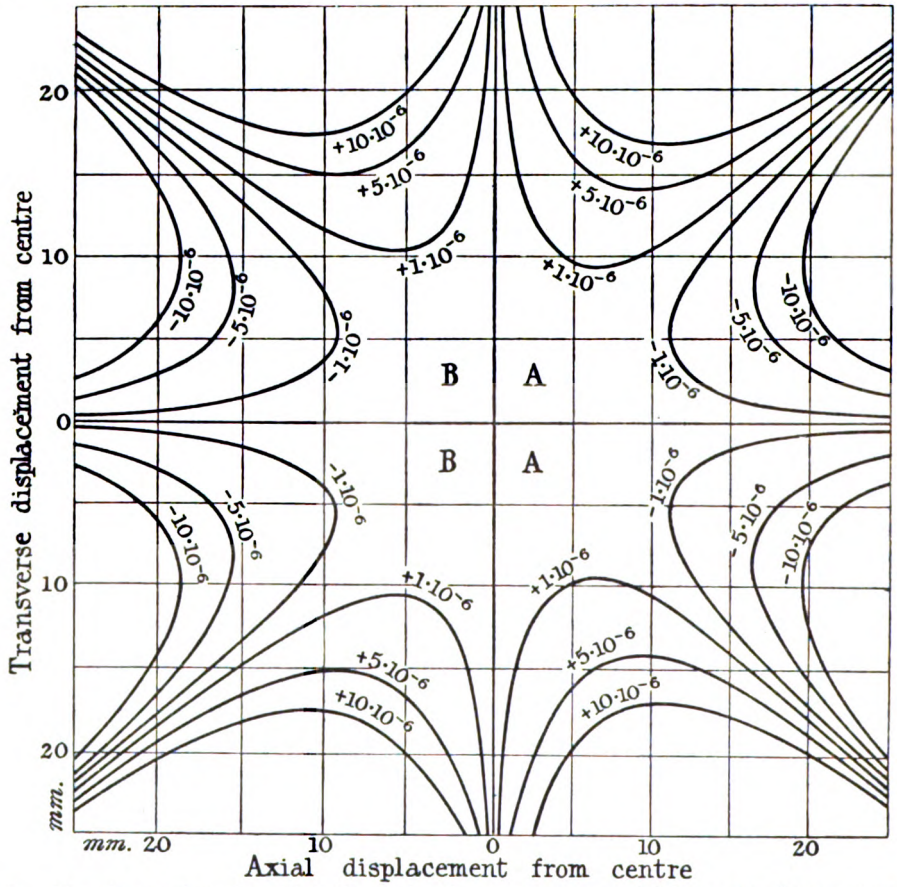


Fig. 8. Showing regions in which the ratio of transverse to axial intensity does not exceed 1, 5, and 10 parts in a million.

The results given in Tables III and IV enable one to determine, for any particular measurement, the maximum length of magnetic needle which can usefully be used, and the precision with which its centre must be made to coincide with the centre of the system. This is so obvious that it is not necessary to give any example except that relating to the present investigation. The magnet used was 10 mm. long, and its centre was certainly coincident with the centre of the coil system within 2 mm. From inspection of Tables III and IV it is apparent that the error due to the lack of uniformity of the magnetic field produced by the current in the coils, combined with the error due to faulty centering, cannot be greater than about 1 part in a million.

Another valuable feature of the Helmholtz-Gaugain arrangement, whether consisting of single turns or of many, is the ease with which two of them can be compared if their centres can be made nearly to coincide. To construct accurately gauged coil systems is very expensive, and such need only be used as standards.

Digitized by Google

The marble cylinder I have used will permit the insertion of another coil system 48 cm. in external diameter so arranged that the two systems are co-axial and have a common centre. If this were done and a small magnet were suspended at the centre by means of a reasonably fine quartz fibre, and if torsion were applied to the latter until the axis of the magnet was about 89 degrees to the meridian, the constants of the two systems could be compared by measuring the currents which, when producing fields in opposition, produced no deflection of the magnet system. For a precision of 1 part in 100,000, approximate coincidence only of the centres is necessary. An axial displacement of 1 cm. combined with a transverse displacement of 1 cm. produces an inappreciable error.

The general conclusion drawn with regard to the accuracy of the constant of the coil system used is that the probable error is not greater than 1 part in 100,000.

## § 18. *Connections to Coils.*

The ends of the wire of each coil are bent into the marble as shown in fig. 9. When the cylinder was in the lathe, and after the twin helical grooves had been cut, four cylindrical holes $e_1$, $e_2$, $e_3$, $e_4$ were drilled to carry the leads of each coil. The holes are

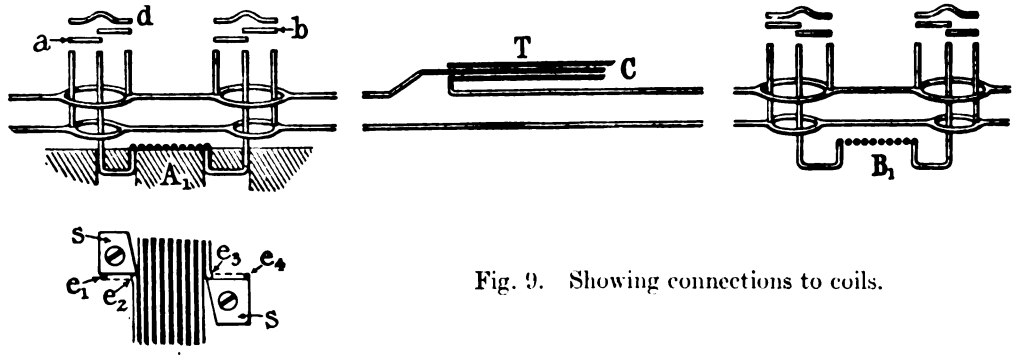


Fig. 9. Showing connections to coils.

slightly greater in diameter than the copper wire, and each hole is about 1 cm. deep. Two pieces of marble of the shape shown by S, fig. 9, were cut from the cylinder and the marble between the holes $e_1$ and $e_2$ and between $e_3$ and $e_4$ was undercut to allow the passage of the wire. When a coil was commenced, or near completion, the wire under tension was carefully bent into this U-shaped channel, and afterwards a piece of marble was fitted into the hole and screwed into position. This piece served as a key.

The single leads from a coil are therefore, by construction, in a plane containing the axis of the cylinder, and should produce no effect. All four coils begin and end in the same axial plane.

Fig. 9 shows the leads to two of the coils (*see* fig. 2 also). C is a specially made concentric cable, of which one end passes through guides which are rigidly secured to the cylinder.

Digitized by Google

The outer tubular conductor of the concentric terminates in a small copper tube T, and from this, in an axial plane, a stiff copper wire is carried by supports to the coil B. A second stiff wire is soldered to the inner conductor of the concentric, and this passes, in the same axial plane as the other wire, towards the coil $A_1$. A third wire, in the same axial plane, passes between the two coils. The short radial leads are stiff copper wires supported by insulating pieces, and connection can be made with the concentric cable by bridge pieces such as *a* and *b*. These bridges are short pieces of copper wire, and are soldered in position. A change from the connections when the *a* pieces are used to those when the *b* pieces are employed reverses the current in a coil. If bridge pieces such as *d* are employed, the current flows through the concentric and all other leads to the coils, except the short radial ones. When such connections are made, there should be no axial magnetic field due to the current.

### § 19. *Effect of Leads and the External Circuit.*

To be certain that the current in the leads and external circuit produces no appreciable effect, the following experiment was made :—

The magnet system was supported by a coarser quartz fibre than that employed in the experiments for measuring the horizontal intensity. The moment of the magnet and the diameter of the fibre were such that about 5,000 degrees of torsion were required to displace the axis of the magnet 89 degrees from the magnetic meridian.

If $\phi$ is the angle through which the upper end of the fibre is turned with reference to the lower end, and $\theta$ is the angle which the magnetic system makes with the meridian. the angle of deflection $\partial\phi$ for an added axial intensity $\partial H$ is given by

$$\partial\phi = \frac{\phi \,.\, \partial H}{(H \{1 + 0{\cdot}0175\phi \cot \theta\}} \quad . \quad . \quad . \quad . \quad . \quad . \quad . \quad . \quad (10)$$

In the case under consideration, if H is 0·18000 and $\partial H$ is 1$\gamma$ the angle $\partial\phi$ is 6 minutes 36 seconds, and the displacement of a reflected spot at 2 metres is 7·7 mm.

Advantage was taken of a " quiet time ", *i.e.*, when there were no sudden variations in H, to short circuit the leads by the bridge pieces *d*, and thus allow the current to flow through the usual circuit with the exception of the coils. Any deflection on make, break, or reversal of the current was less than 1 mm., and it is concluded, therefore, that the effect of the leads and the whole of the external circuit is negligible. Had the effect been such as to necessitate a correction of 1 part in 100,000, the deflection, on reversal, would have been more than 2 mm.

### § 20. *Effect of Torsion on Fibre.*

It is apparent that, when there is torsion on the fibre, the axis of the magnet cannot be in the magnetic meridian. Further, when the coil system is rotated and the current flows through the coils in such a direction that there is no deflection of the magnet,

Digitized by Google

the axis of the coil system will not be in the meridian. With a twisted fibre, therefore, the axis of the coil cannot be set in the magnetic meridian by the "no deflection" method.

When there is torsion on the fibre and no current in the coils, let 0 (fig. 10) be the angle which the axis of the magnet makes with the meridian. If M is the moment of the magnet and H the horizontal intensity, the couple MH sin 0 is balanced by the torsional couple of the fibre. If I is the torsional couple for 1 degree of twist and $\phi$ is the actual angle of torsion,

$$MH \sin \theta = T\phi. \quad . \quad . \quad . \quad . \quad . \quad . \quad . \quad . \quad . \quad . \quad (11)$$

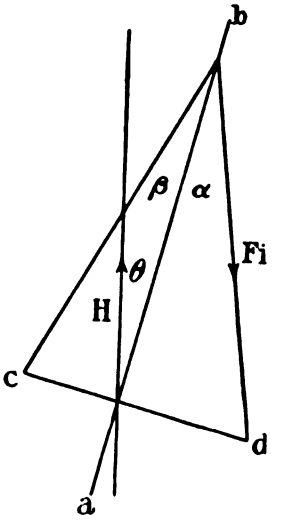

Fig. 10.

When a current $i$ is passed through the coils so as to produce no deflection of the magnet, an axial magnetic intensity F$i$ is produced, which is at an angle 0 with the meridian. In practice, therefore, the direction *ab* must, as a first approximation, be taken as being in the meridian.

When making a measurement, the coil system is next moved through a small angle $\alpha$, and the direction and intensity of the current is changed in order to deflect the magnet through exactly 90 degrees, *i.e.*, into the position *cd*. The condition for equilibrium is

$$MH \cos \theta - T\phi = FiM \cos \alpha. \quad . \quad . \quad . \quad . \quad . \quad . \quad . \quad . \quad (12)$$

The magnet is now deflected from its new position through exactly 180 degrees. To produce this effect the coil system is rotated through a relatively small angle ($\alpha + \beta$). The axis of the magnet is still shown by *cd*, but the poles of the magnet are reversed in position.

The condition for equilibrium is

$$MH \cos \theta + T\phi = FiM \cos \beta. \quad . \quad . \quad . \quad . \quad . \quad . \quad . \quad . \quad (13)$$

From equations (12) and 1(3) we have

$$H = \frac{Fi(\cos \alpha + \cos \beta)}{2 \cos \theta}. \quad . \quad . \quad . \quad . \quad . \quad . \quad . \quad (14)$$

Also

$$2T\phi = FiM(\cos \beta - \cos \alpha). \quad . \quad . \quad . \quad . \quad . \quad . \quad . \quad . \quad (15)$$

Combining (15) with (11) there results

$$\sin \theta = \frac{Fi}{2H}(\cos \beta - \cos \alpha). \quad . \quad . \quad . \quad . \quad . \quad . \quad . \quad . \quad (16)$$

It is apparent that if torsion on the fibre exists, $\alpha$ will not be equal to $\beta$, conditionally that H is constant over the interval of time (less than 1 minute) between the measure-



Digitized by Google

ment of $\alpha$ and $\beta$. It is apparent, also, that the torsion on the fibre can be removed, by adjustment of the torsion head, until $\alpha$ is equal to $\beta$. However, since in practice $Fi$ is equal to H within less than 1 per cent., the value of $\theta$ can be calculated within this limit by the equation

$$\sin \theta = \tfrac{1}{2} (\cos \beta - \cos \alpha). \quad . \quad . \quad . \quad . \quad . \quad . \quad . \quad . \quad . \quad (17)$$

Knowing $\theta$, an adjustment can be made, if necessary, until its value is negligibly small.

For example, in an early set of observations $\alpha$ was 4 degrees 0 minutes, $\beta$ was 4 degrees 30 minutes, and $\theta$ was calculated to be 0 degree 1 minute 7 seconds. Experimentally, it was found that 360 degrees of torsion on the fibre produced a deflection of the magnet, from a position near the meridian, of about 2 minutes; hence the torsion on the fibre was about 200 degrees, which could readily be reduced. However, it was not really necessary to do so, for cos 0 degree 1 minute 17 seconds differs from unity by less than 2 parts in ten millions, and the latter would therefore have been the error in the measurement of H due to 200 degrees of torsion on the fibre.

In general, therefore, after one adjustment, the torsion on the fibre can be neglected. In our experiments, had the torsion been of great importance, the difference $(\alpha - \beta)$ would have been very large indeed. For example, if $\alpha = 2$ degrees and $\beta = 6$ degrees, the value of $\theta$ is 8 minutes only, and the error introduced in the calculation of H by neglecting cos $\theta$ is only 3 parts in one million.

It is concluded, therefore, that any effect of torsion on the fibre cannot, in the present investigation, have produced in any measurement an error so great as 1 part in a million. Some prominence is given to this statement because many experimenters who have seen the magnetometer have expressed surprise at the procedure of suspending a comparatively weak magnet by means of a quartz fibre.

It is important also to note that the first adjustment, *i.e.*, adjusting the axis of the coil to be parallel with the equivalent axis of the magnet, need only be a very approximate one. In practice, such adjustment within less than 1 minute of arc is easily made, but if an error of a quarter of a degree is made, and $\theta$ is taken in error as zero, the error so introduced is only 1 part in 100,000.

If it is desired to measure the direction of magnetic north, the torsional effect is made negligibly small, and the cylinder turned until there is no deflection of the magnet on making the circuit through the coils. The axis of the coil system then lies in the magnetic meridian. In places where the declination is very constant, great sensitiveness can be obtained by arranging the direction of the current to produce an axial field slightly less than, but opposed to, H.

### § 21. *Arrangement of Circuits and Determination of Intensity of Current.*

The arrangement of the circuit is shown in fig. 11. The current, the value of which is desired, passes through a standard resistance R, and is adjusted until the voltage across the potential terminals of R balances that of the standard cell C. A double

Digitized by Google

commutator T, with copper contacts to reduce thermal e.m.f's., is used to reverse the current through R, and simultaneously reverse the connections to the standard cell. The standard resistance is of strip manganin; it is of nominal resistance 2 ohms, and is divided into halves by a potential lead so as to enable comparisons of each half to be made with a standard 1-ohm coil. The temperature of R is maintained constant at 20·0° C. S is a shunt of known value, and is also immersed in oil. The standard cell is one of a series of " acid " cells; they are kept in an oil bath in a constant temperature room. B is a battery of 50 accumulators. The resistance $r$ consists of about 200 ohms of manganin, and is adjustable in steps of 0·1 ohm, 1 ohm, etc., a sliding short-circuiting

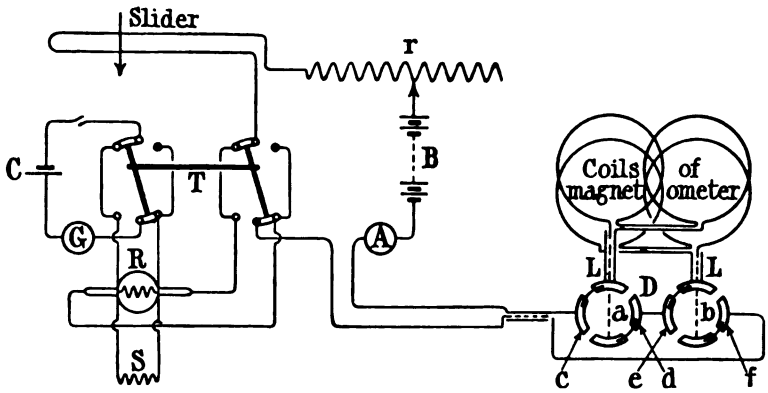


Fig. 11. Circuit.

contact providing the final adjustment. Observations show it is easy to maintain a current constant within less than 1 part in a million.

L L are concentric cables, and lead from a double commutator D to the magnetometer coils. The commutator $a$ reverses the current in two of the coils, one on each side of the centre, and $b$ reverses the current in the other two coils. If the circuit through one half of the system is broken (by placing the cross bar of a turning head in a vertical position) and a conductor placed across $cd$ (or $ef$) the other half of the magnetometer coils can be used as a complete system. A current of about 1 ampere is then required. Measurements of H, using one half of the system, *i.e.*, one coil on each side of the centre, have been made. The results are in complete agreement with those obtained when all four coils are used.

### § 22. *Determination of H.*

After the magnetometer was mounted in position and the cylinder adjusted until its axis was horizontal, the following preliminary experiments were made:—

(1) Determination of effect of leads. The effect was found to be negligible (*see* § 19).

(2) Adjustment of torsion on fibre. The torsion was made negligibly small (*see* § 20).

(3) Adjustment of position of damping buffers until the magnet system was nearly aperiodic in magnetic fields, having an intensity of about H/30.



Digitized by Google

There was no necessity in subsequent determinations to repeat these adjustments, but checks were occasionally made.

The auxiliary current circuit having been completed, the measurement of H comprises the following operations :—

(1) Adjustment of position of the coil system until its axis coincides with the horizontal magnetic axis of the suspended magnet. In this adjustment the axial field due to the coils is approximately in the same direction as the earth's magnetic field. Thirty seconds suffice to make a sufficiently accurate adjustment.

(2) The current through the coils is reversed and the cylinder turned through a few degrees. The torsion tube, etc., are rotated through exactly 90 degrees. The axis of the magnet now tends to set in a direction nearly at right angles to its first position, and is made to do so exactly by adjusting the position of the coil system. Let the angle between the axis of the coil system and the meridian be $\alpha$.

(3) The coil system is swung through a few degrees with a view to making the resultant field reverse in direction. The torsion tube, etc., are rotated through exactly 180 degrees, and the axis of the magnet now tends to set in a direction approximately 180 degrees away from its position in (2). The reversal is caused to be exactly 180 degrees by adjustment of the position of the coil. Let the angle between the axis of the coil and the meridian be $\beta$.

The measurement is now complete, and H is given by

$$H = Fi(\cos \alpha + \cos \beta)/2.$$

F is the constant of the coil system, and $i$ is calculated from the combination value, in absolute measure, of the standard resistance and standard cell.

In practice, the measurements are exceedingly simple and rapidly made. If the current is steady, a complete measurement involving operations (1), (2) and (3) can be conducted within 3 minutes. The following table gives the results of a few observations made on Friday, July 15, 1921, between 1 and 2 a.m. When making these measurements, adjustment (1) was made only at the commencement and end of the observations. It should be noted that the value of the current was intentionally altered so as to vary the values of $i$ and of $\alpha$ and $\beta$. In some measurements, the direction of the current in the circuit was reversed, and the coil swung through 180 degrees approximately, to obtain the proper direction of the axial field.

A sensitive magnetograph for recording the changes in H was in operation simultaneously. A change of $1\gamma$ is represented on the magnetograph charts by a displacement of about 2·5 mm., and the time scale is such that 7 mm. represents 1 minute. The temperature was very constant. The changes in H, as recorded by the magneto-

Digitized by Google

graph, are given in the last column of the table; the value at 1 a.m. is that obtained with the magnetometer.

July 15, 1921.

Temperature of cylinder = 20·5° C.

$F = 3{\cdot}59585$ cm.$^{-1}$.

| Time a.m. | $i$ in C.G.S. units. | $\alpha$. | $\beta$. | $\frac{\cos\alpha + \cos\beta}{2}$ | $H = \frac{Fi(\cos\alpha + \cos\beta)}{2}$ | H as given by magnetograph. |
|---|---|---|---|---|---|---|
| | | ° ′ | ° ′ | | | |
| 1.0 | 0·051598 | 5 18 | 5 12 | 0·99580 | $0{\cdot}18476_1$ | 0·18476 |
| 1.5 | 0·051598 | 5 20 | 5 14 | 0·99575 | $0{\cdot}18475_2$ | 0·18475 |
| 1.11 | 0·051598 | 5 26 | 5 22 | 0·99556 | $0{\cdot}18471_5$ | $0{\cdot}18471_5$ |
| 1.14 | 0·051598 | 5 30 | 5 24 | 0·99547 | $0{\cdot}18470_0$ | $0{\cdot}18470_5$ |
| 1.20 | 0·051428 | 3 6 | 2 57 | 0·99860 | $0{\cdot}18466_7$ | 0·18467 |
| 1.24 | 0·051428 | 3 2 | 2 54 | 0·99866 | $0{\cdot}18468_0$ | 0·18468 |
| 1.27 | 0·051767 | 7 14 | 7 10 | 0·99211 | $0{\cdot}18468_0$ | $0{\cdot}18467_5$ |
| 1.29 | 0·051767 | 7 14 | 7 9 | 0·99213 | $0{\cdot}18468_2$ | 0·18467 |
| 1.32 | 0·051405 | 2 32 | 2 24 | 0·99907 | $0{\cdot}18467_3$ | $0{\cdot}18467_5$ |
| 1.38 | 0·051405 | 2 28 | 2 22 | 0·99911 | $0{\cdot}18468_0$ | 0·18468 |

The dropped figures are for comparison purposes only. It is most satisfactory to note that, with a single exception, the observed and recorded changes agree within the limit (0·5γ) with which the record was read.

As stated in § 21, two coils only, one on each side of the centre, can be used as a complete system. The coils $A_1$ and $B_1$ form one system, and $A_2$ and $B_2$ the other. On a number of occasions the circuit has been arranged to include two coils only, and excellent agreement between the pairs of coils has always been obtained. The following results were obtained in the early morning of November 26, 1921, when the variations in H were very small. The constant of the instrument when two coils only are used is of course one-half of that when four coils are employed.

| Time. | Coils. | $i$. | $\alpha$. | $\beta$. | $\frac{\cos\alpha + \cos\beta}{2}$ | H. |
|---|---|---|---|---|---|---|
| | | $F = 3{\cdot}5960_9$ cm.$^{-1}$. | | | | |
| a.m. | | | ° ′ | ° ′ | | |
| 1.35 | $A_1A_2B_1B_2$ | 0·51428 | 3 35 | 3 33 | 0·99806 | $0{\cdot}18458_1$ |
| 1.39 | $A_1A_2B_1B_2$ | 0·51428 | 3 35 | 3 35 | 0·99805 | $0{\cdot}18457_9$ |
| 1.42 | $A_1A_2B_1B_2$ | 0·51428 | 3 32 | 3 33 | 0·99809 | $0{\cdot}18458_7$ |
| 1.45 | $A_1A_2B_1B_2$ | 0·51428 | 3 32 | 3 35 | 0·99807 | $0{\cdot}18458_3$ |
| | | $F = 1{\cdot}7980_9$ cm.$^{-1}$. | | | | |
| a.m. | | | ° ′ | ° ′ | | |
| 1.53 | $A_1B_1$ | 1·02858 | 3 32 | 3 37 | 0·99805 | $0{\cdot}18458_3$ |
| 1.56 | $A_1B_1$ | 1·02858 | 3 35 | 3 38 | 0·99802 | $0{\cdot}18457_8$ |
| 2.2 | $A_2B_2$ | 1·02858 | 3 32 | 3 35 | 0·99807 | $0{\cdot}18458_7$ |
| 2.6 | $A_2B_2$ | 1·02858 | 3 35 | 3 39 | 0·99801 | $0{\cdot}18457_6$ |
| | | $F = 3{\cdot}5960_9$ cm.$^{-1}$. | | | | |
| a.m. | | | ° ′ | ° ′ | | |
| 2.10 | $A_1A_2B_1B_2$ | 0·51428 | 3 38 | 3 40 | 0·99797 | $0{\cdot}18456_6$ |

Digitized by Google

The magnetograph showed that from 1.35 a.m. to 2 a.m. H had kept constant within about 1γ. At 2.10 a.m. H was less than at 1.35 a.m. by about 2γ.

On a few occasions photographic records have been obtained, and these enable one to read directly the value of H at any given instant. Simultaneously, the ordinary magnetograph with quartz fibre has been run in order to have two records for comparison. The records thus obtained show conclusively that the current has been maintained steady within 1 part in a million. Changes in H are recorded which last less than 3 seconds.

### § 23. *Comparison with Kew Pattern Magnetometer.*

On March 8 and 9, 1921, a comparison was made of the results obtained with a Kew pattern magnetometer and those obtained with the Schuster magnetometer. Dr. CHREE very kindly made some measurements with a Kew instrument set up a few yards away from the new instrument. During these observations, no measurements were made by the electromagnetic method, but a few measurements were made immediately before and immediately after. A magnetograph was run throughout the whole period. The results obtained are given in the following table :—

| 1921. | Time. | Value of H as determined by— | | Difference. |
|---|---|---|---|---|
| | | CHREE. | SMITH. | |
| | | | | γ |
| March 8 . . . . . | 11.3 to 12.22 | 0·18488 | 0·18491 | — 3 |
| „ 8 . . . . . | 12.26 „ 13.22 | 0·18483 | 0·18496 | —13 |
| „ 8 . . . . . | 14.44 „ 16.5 | 0·18487 | 0·18488 | — 1 |
| „ 8 . . . . . | 16.10 „ 17.6 | 0·18480 | 0·18487 | — 7 |
| „ 9 . . . . . | 10.17 „ 11.16 | 0·18460 | 0·18469 | — 9 |
| „ 9 . . . . . | 11.32 „ 12.24 | 0·18469 | 0·18471 | — 2 |
| | | | Mean . . . | — 6 |

Subsequently it was found, on completion of the computation of the P and Q values for the Kew instrument, that the values assigned by Dr. CHREE required a correction, the provisional values being too large by 4γ. The mean observed difference becomes, therefore, 10γ.

Too much importance must not be attached to this result. The horizontal intensity at Teddington fluctuates rapidly in value owing to the local electric railway and tramway systems; disturbances of 15γ are not uncommon. For this reason, precision measurements must be made after 1 a.m. However, it appears to be very unlikely that the probable error of observations during the daytime is as great as 10γ. With the new instrument it is possible to follow changes in H which last for only a few seconds.

In the near future, it is hoped to make a second and more complete comparison.

Digitized by Google

## § 24. *Probable Errors.*

In the absence of artificial disturbances, and natural ones of a rapidly oscillatory character, a convenient value to choose for $\alpha$, the angle between the axis of the magnetometer and the line pointing to the magnetic north, is 2 degrees. In such case an error of 1 minute in the reading of the angle corresponds to an observational error of 1 part in 100,000.

The probable error in the diametral dimensions of the coils is not greater than $3\mu$, and the uncertainty in the distance between the mean planes of the two halves of the system may be taken to be of equal magnitude. From equation (3), § 16, the probable error in the constant of the instrument can be calculated by inserting these dimensional errors for *da* and *dl*. If the diametral and axial errors are of the same sign, their sum is 8 parts in one million.

The total length of wire in the 4 coils is a little over 45,000 mm. The ends of the coils were determined to be in a line parallel with the axis within less than 0·5 mm., and, when the whole of the circuit external to the coils was completed, the axial intensity due to the current in the circuit was less than 1 part in 200,000 of H. It appears safe to conclude, therefore, that the probable error due to the number of turns being slightly greater, or slightly less, than 24, is not so great as 1 part in 100,000.

The detailed probable errors connected with the coil system are therefore

| | | |
|---|---|---|
| Diametral . . . . . | ± 2 | parts in 1,000,000. |
| Axial . . . . . | ± 6 | „ „ |
| Incomplete turns . . . . . | ±10 | „ „ |

Apart from the magnetic quality of the material, the constant of the coil system may therefore be regarded as known, at the temperature of the measurements, within 1 part in 100,000. This probable error is small, but is in accordance with previous experience with bare wire coils wound on marble.

The magnetic tests lead me to believe that the magnetic permeability of the base, etc., does not differ from unity by more than 1 part in 100,000 and, since the metal is in contact with the marble over only a small part of its surface, the probable error due to the base cannot exceed a few parts in a million. Copper wire is often slightly troublesome owing to being drawn through steel dies. No measurable magnetic effect was obtained with the wire used for the coils, but in future work hard-drawn silver wire, drawn through diamond dies, will probably be used.

The errors due to electrostatic effects, to torsional effects on the fibre, and to changes in the magnet, are considered to be not greater than a few parts in a million. It may be that the magnetic axis of the magnet in the earth's field does not exactly coincide with the axis in a magnetic field having an intensity of 0·006 C.G.S. unit or less, and in certain kinds of measurements errors may be thus introduced. In our measurements,

Digitized by Google

however, the only important angular measurements are those when the magnet is turned through 180 degrees, and in these the field intensities are equal.

The remaining source of error is due to an uncertainty in the value of the current. When the current balance was erected at Teddington the probable error of a determination of current in absolute measure was $\pm$ 2 parts in 100,000. Since then the insulation resistance of the coils has fallen considerably, and the dimensions may have altered slightly. The probable error may now be as great $\pm 4$ parts in 100,000.

Finally, we conclude that the probable error of our measurements of H is of the same order as that associated with the current, that is

$$\pm 4 \text{ parts in } 100{,}000.$$

When the coils of the current weigher have been re-wound, the probable error of measurements of H should be reduced to $\pm 2$ parts in 100,000.

## § 25. *Conclusions.*

From the measurements recorded in the previous sections, it is concluded that the type of instrument originally suggested by Sir ARTHUR SCHUSTER can be used to measure the horizontal intensity of the earth's magnetic field with a probable error of the same order as that with which current can be measured. At present this probable error is about $\pm 4$ parts in 100,000, but within a few years it should be reduced to 1 or 2 parts in 100,000. The time occupied in making a measurement and calculating the result is a few minutes only.

My most hearty thanks are tendered to Sir ARTHUR SCHUSTER, F.R.S., to Sir RICHARD GLAZEBROOK, K.C.B., F.R.S., who was Director of the National Physical Laboratory when the magnetometer was commenced, and to Sir JOSEPH PETAVEL, K.B.E., F.R.S., the present Director of the Laboratory. I am indebted also to Mr. S. WATTS, an Observer in the Electrical Department, for much help in making the observations and for aid in the determinations of current intensity.

Digitized by Google

# A PRECISION FORM OF THE KELVIN ELECTROSTATIC VOLTMETER

BY

E. H. RAYNER, Sc.D., M.I.E.E.,
PRINCIPAL ASSISTANT IN THE ELECTRICITY DEPARTMENT.

Digitized by Google

## ABSTRACT.

The paper describes a form of electrostatic voltmeter for precision measurements. The instrument follows the general arrangement of the Kelvin type. The chief modifications are—(1) Very considerable reduction in weight, permitting (2) the use of a bifilar suspension to overcome the effect of elastic fatigue ; (3) a modification of the shape of the needle to produce a more satisfactory " scale law " for both small and large deflections ; and (4) the provision of various mechanical details to facilitate construction and adjustment.

Digitized by Google

# A PRECISION FORM OF THE KELVIN ELECTROSTATIC VOLTMETER.

By E. H. RAYNER, Sc.D., M.I.E.E., Principal Assistant in the Electricity Department.

[Reprinted from the 'Journal of the Institution of Electrical Engineers', Vol. 59, 1921.]

## *Importance and Utility of the Electrostatic Type of Voltmeter.*

In a previous Paper* the methods and apparatus used at the National Physical Laboratory for the measurements of alternating currents have been described. In the Paper it was shown how an electrostatic voltmeter is used not only for the measurement of high and low voltages, but also as a necessary link in the calibration of the standard wattmeter. It is also used for precise measurements of currents up to about 20 amperes, by passing the current through resistances of known value which are capable of giving a potential drop of from 50 to 100 volts. For larger currents resistances giving a drop of about 2 volts are used, across which the primary of a transformer of 1 : 50 or 1 : 100 ratio is connected. The secondary, giving from 50 to 100 volts, is connected to the voltmeter. By either means observations to within 1 or 2 parts in 10,000 can be made. The electrostatic type of instrument has other advantages over those of the dynamometer type. Among these are its independence of ordinary commercial frequencies, and the fact that it takes a very small capacity current which can nearly always be neglected. A further point is that, the moving part being suspended, it is practically frictionless, and great magnification of the motion of the moving part can be usefully employed.

## *Past Experience.*

For many years there have been in use at the National Physical Laboratory Kelvin multicellular voltmeters made by Messrs. Kelvin and White, to which concave mirrors having a radius of 2 metres have been fitted. The readings are taken on a curved scale 8 metres long instead of that under the pointer of the instrument, which is but 10 cm. long. By this means the indications of the instrument working up to 150 volts can be read to 0·01 volt between 50 and 120 volts. Such a great magnification is only practicable because the instrument is suspended by a torsion strip and is frictionless, which would not be the case if it were necessary to use pivots.

Under these conditions, however, certain imperfections become appreciable which

* C. C. Paterson, E. H. Rayner and A. Kinnes, "The Use of the Electrostatic Method for the Measurement of Power", 'Journ. I.E.E.', vol. 51, p. 294, 1913; and N.P.L. 'Collected Researches', vol. 11, Paper VI, p. 115, *et seq.*



Digitized by Google

are quite negligible when the instrument is used in the manner for which it is designed. The most important trouble is due to the elastic fatigue of the suspension. It may take several hours after the application of 100 volts for the deflection to become steady to 0·01 volt, and if, after this steadinss has been obtained, a lower voltage is applied, the " creep " comes out to some extent and the deflection falls steadily for some time. At 100 volts this effect may amount to 0·1 volt or more, and when accurate readings are required, time is taken in calibrating which would not be necessary if an instrument with greater steadiness of deflection were available. Another disadvantage of the ordinary type of instrument is that the moving part is unnecessarily heavy for an instrument which is not intended to be portable, and its time of swing may be shortened by using a lighter moving system. In fact, the time of coming to rest after the application of 100 volts has been reduced from about 50 seconds to 15. These are matters of great importance in practice, as the instrument is used for the testing of all commercial voltmeters, watt-meters and watt-hour meters, and is frequently in use for the whole of the working day.

Preliminary experiments showed that it was practicable to reduce the weight sufficiently to enable a bifilar suspension to be used, and thereby to reduce greatly the effect of the elastic fatigue. As the weight of the moving part supplies most of the controlling force in a bifilar suspension, it is necessary to reduce it as much as possible, if the distance between the supporting wires is not to be too small for satisfactory operation.

### *Description of Instrument.*

Two instruments have been built, reading up to about 130 volts on a scale 8 metres long with a bifilar suspension 400 mm. long and 3·5 mm. apart (*see* fig. 1). For the sake of comparison and possible interchangeability of parts, the vertical distance between the needles was made the same, *i.e.*, 8·7 mm. (11/32 in.), as in the older Kelvin and White instruments. The number of needles for which it is desirable to arrange is a matter for compromise. In spite of the considerable reduction in weight of the moving part, it is amply strong enough to carry a large number of needles. The total weight does not increase as fast as the number of needles, as there are the end fittings to be taken into account, and a large mirror, 20 mm. in diameter, is used. It is also desirable to have a considerable number of needles to provide sufficient motive power to move it quickly. The only disadvantage in using a large number of needles is the increase in capacity of the instrument, but as a good deal of this is extraneous to the moving system, being due to the capacity between inductors and case and to subsidiary apparatus and connecting wires, the capacity does not increase as fast as the number of needles. The number fixed upon is 10. They are made of special aluminium-copper-manganese rolled alloy and are about 0·02 mm. thick. They are threaded on to a wire screwed at both ends. Spindle-shaped distance pieces of aluminium alloy keep them at the correct distance apart. The nuts at the ends have holes through them, by the top one of which the needle system is hung by a hook of wire of square section to the bridge-piece clamping

Digitized by Google

the suspension wires, and to the bottom one the mirror and damping disc are suspended. The disc is immersed in dashpot oil as usually supplied with Kelvin voltmeters. The diameter of the disc is adjusted until suitable damping is obtained. The square section of hooks and parts connected to them provides a four-point contact which prevents relative rotation about a vertical axis.

*Suspending Wires.*—The suspension wires are of tungsten, and are about 0·02 mm. in diameter. This material was chosen as being very strong and easily obtainable in such a small size. It is the finest ordinarily used in vacuum lamps, and was specially annealed by the makers, the Osram-Robertson Lamp Company. The breaking strength of the wires is such that the mechanical factor of safety is well over 100.

*Shape of the Needle.*—The shape of the needle is of great importance in determining the length of scale per volt at various parts of the scale. For the first part of the scale this type of instrument follows approximately a "square" law, the increase of deflection per volt being nearly proportional to the voltage applied. Above half-scale deflection the effect is reversed, due partly to the needle being largely inside the inductors and partly to the presence of the guard plate. Needles of the shape usually provided by Kelvin and White (*see* fig. 2) and others of different shapes, both symmetrical and non-symmetrical, were tried. The shape shown in fig. 3 was finally adopted. The object of these trials was to open out the deflections of the instrument at the top and bottom of the scale, and to keep the rate of change of scale-length per volt small at 100 volts, at which point the instrument is chiefly used. These qualities and other minor desiderata are to some extent antagonistic, and a compromise has to be adopted. Certain commercial electrostatic instruments are made with unsymmetrical needles with the object of greatly increasing the deflections for a certain range of pressure. This can be done by increasing the rate of change of capacity over such

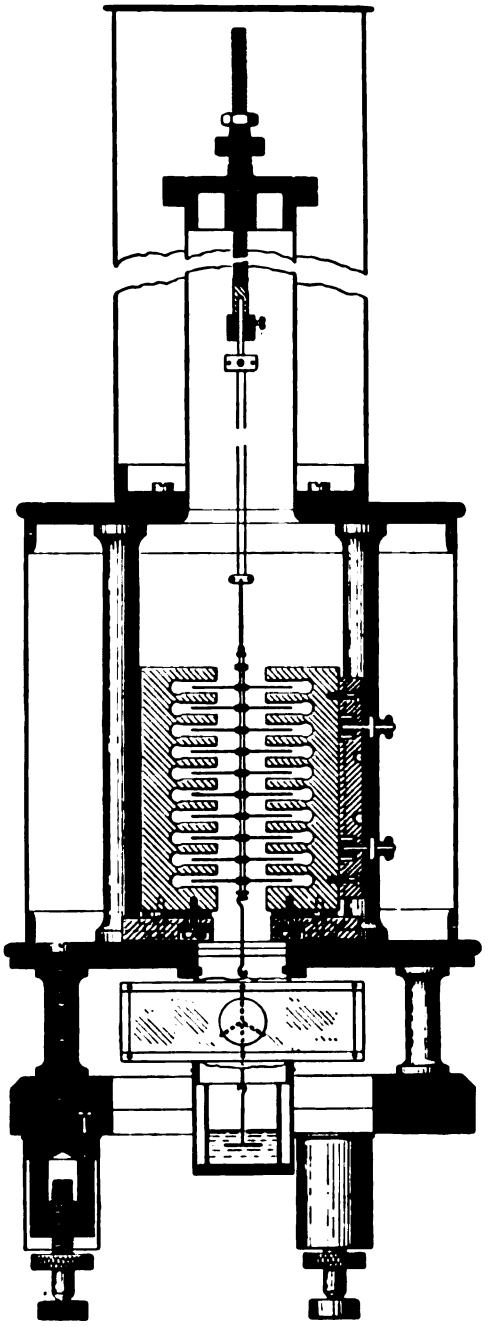

Fig. 1. Sectional elevation of the voltmeter.

Digitized by Google

ranges. The indications of an instrument of this nature are liable to vary considerably with small changes in the initial position of the needle between the inductors. Since permanency in this respect is of first importance, and a symmetrical needle was found to satisfy practical requirements, it was adopted as being simpler to make.

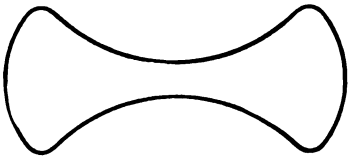

Fig. 2. Type of needle usually adopted in the Kelvin and White voltmeters.

It was found that a needle of the form shown in fig. 3 would give twice as much deflection per volt over the lower part of the scale as that given by needles of the shape usually provided by Messrs. Kelvin and White. At the same time the openness at the top of the scale is also doubled.

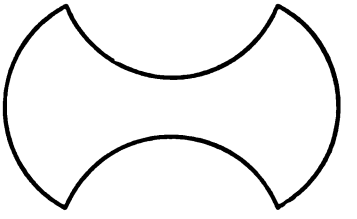

Fig. 3. Form of needle adopted by the author.

*Inductors.*—The inductors are similar in plan to those of the ordinary Kelvin instrument, but, the metal being thicker, the air space is less. This was done so that experiments could be made, if desired, on the effect of cutting the metal fins thinner, but, satisfactory results having been obtained with the proportions as first made, they have not been altered. The inductors are of cast aluminium alloy and are mounted on sliding bases from which they are insulated by amberite discs. These bases slide between guides fixed on the base of the instrument, and a millimetre scale is provided so that they can be set accurately at any desired distance apart, and can be easily separated when it is desired to remove the needle. Two of the guides have holding-down screws with knurled heads for clamping the slides when in position. An ebonite block is mounted on the back of one of the inductors for the support of a fine wire fuse. The current to the inductors passes through a terminal in the base of the instrument which is bushed with amberite, and then through the fuse, the purpose of which is to limit the current in case of an accidental excess of pressure being applied to the instrument. In such cases the needles may be attracted on to the inductors, and so cause a short-circuit. The provision of the fuse will help to prevent the damage to the needles which might occur in such circumstances. A spring support is provided for taking the weight of the needle system at the bottom while the instrument is being assembled, and behind the inductor on the right is a pillar for supporting two horizontal strips of brass. These can embrace the

Digitized by Google

top of the needle system by a scissor motion, limited by a stop. These two details, not shown in the drawing, enable the needle to be disconnected from the suspension without trouble.

*Subsidiary Details.*—The lower part of the base of the instrument consists of a ring supported by three ebonite pillars fitted with levelling screws. The ebonite is protected from light by a metal sleeve. The instrument proper is supported by three metal pillars on a second ring, which can rotate on the lower part of the base. No locking screws are required, as the instrument is not intended to be portable. The three metal pillars are not arranged at 120 degrees, but one of the spaces between them is larger to prevent obstruction of the light reflected from the mirror, which sweeps over an angle of about 120 degrees. The mica window is very thin and of large radius, since even a thin one, bent to sharper curvature, seriously impairs the definition on the scale. Nearly the whole of the instrument, with the exception of tubular parts such as the outer casing and dust cover, is made from aluminium alloy, partly for the sake of lightness and partly because it is an excellent alloy for machining. The main plate has four vertical pillars fixed to it, and these support the upper plate to which the long tube carrying the upper part of the suspension is fixed.

A considerable range of vertical adjustment for different lengths of suspending wires is provided by the screwed spindle, which has a key-way cut in it, and a feather in its housing prevents rotation. The housing can be rotated when it is desired to vary the starting position of the needle in relation to the inductors, and it is clamped by three knurled screws passing through the outer ring at the top of the tube. A split tube and a conical nut clamp the housing tightly round the screwed spindle to ensure rigidity.

An outer brass tube acts as a dust cover and protection for the top of the suspension.

*Source of Light.*—A Nernst lamp, or a gas-filled lamp of 2 to 3 amperes at 10 volts, with an achromatic condensing lens 2 in. in diameter and about 8 in. focus, having a fine wire stretched vertically across the lens, is used as a source of light. The projected and reflected beams are as nearly as practicable in the same horizontal plane. If there is much divergence between them, the motion of the spot of light on the scale will move considerably in a vertical direction towards the ends of the scale. The shape of the scale is such that the ends are much nearer to the instrument than the centre, an arrangement necessary to obtain good definition over the whole length of the scale.*

*Contact Difference of Potential.*—Preliminary experiments with an instrument of Messrs. Kelvin and White, provided with inductors made of sheet aluminium, gave rise to the expectation that with inductors and needle of alloys of very similar composition the difference on reversal of a continuous potential of 100 volts would not exceed a few hundredths of a volt. This was at first by no means the case, the difference on reversal of 100 volts being found to correspond to 2·6 volts, the needle being made of rolled alloy and the inductors of cast alloy. As the usual value for an instrument with aluminium

* Paterson, Rayner and Kinnes, *loc. cit.*; E. H. Rayner, 'Proc. Optical Conv.', 1912; 'Proc. Phys. Soc.', vol. 24, p. 4491, 911-13; and also N.P.L. 'Collected Researches', vol. 10, Paper VIII, p. 197, *et seq.*

Digitized by Google

needle and brass inductors is about 0·35 volt, the result was that the difference, when using similar metals, was nearly eight times that of an instrument having dissimilar metals.

After various experiments it was found that by boiling the inductors for some time in a solution of soap and washing soda this difference on reversal was very much diminished. It may take several weeks to get steady, and the difference may be expected to settle down to the order of 0·1 volt. In one case the difference died slowly down to zero, giving rise to the hope that it would stay there, but it went on farther and became steady at a small negative value.

The reason appears to be that the spaces in the inductors were milled out with a cutter which was kept oiled, and the surface of the metal was never fully exposed to the air, so as to become what one may term " normalized". The removal of the oil by boiling with alkali allowed the natural air-metal interface to be formed, producing a condition of surface much more similar to that of the moving system.

In the case of the two voltmeters which have now been in use for some six years, the value is about 0·04 volt for the one and about four times as much for the other. It is therefore impossible to say beforehand what the value will be, and experiment may be required if it does not come out, at the first attempt, as small in value as is desired. To obtain the smallest possible difference on reversal it might be the best course, since the needles have to be made of very ductile metal, to build up the inductors of sheet metal of the same composition.

*Construction and Manufacture.*—The instruments have been made in the Laboratory, and the author is greatly indebted to Mr. Murfitt, the head of the instrument shop, for the excellence of their construction.

The Director of the National Physical Laboratory is prepared to consider requests for the provision of working drawings of the instrument.

The following appendices give details as to weight and inertia of the moving parts, method of making the needles, and a device for mounting the suspending wires.

## Appendix 1.

### *Details of the Moving System.*

The details of the suspended system are as follows :—

| | | |
|---|---|---|
| Bridge piece clamping suspension wires | 0·16 | gramme |
| Needles (10) | 0·30 | ,, |
| Distance pieces (10) | 0·80 | ,, |
| Spindle and end nuts | 0·33 | ,, |
| Mirror alone | 0·60 | ,, |
| Mirror support | 0·16 | ,, |
| Hook, short | 0·07 | ,, |
| Hook, long | 0·11 | ,, |
| Damper and hook | 0·07 | ,, |
| Total | 2·60 | grammes |

Digitized by Google

APPENDIX 1.—*continued.*

| | |
|---|---|
| Moment of inertia determined by comparing time of swing with that of a mass of known moment . . . | 0·59 |
| Radius of gyration . . . . . | 0·47 |
| Diameter of suspension wires . . . . . | 0·002 cm. |
| Length . . . . . | 40 cm. |
| Separation . . . . . | 0·35 cm. |
| Time of swing (undamped) . . . . . | 4·5 secs. |

## APPENDIX 2.

### *Method of Making the Needles.*

The needles have been made by means of a template of the shape required, made out of brass $\frac{1}{8}$ in. thick. The aluminium foil is placed between the template and a larger brass plate, and is cut out by a sharp knife, using the template as a guide. A more highly finished edge might be produced by using a die-punch, but this would be very expensive. The clearance between needle and inductors is relatively so large that any slight unevenness in the edge is negligibly small in comparison.

To form the template, three holes 7 mm. apart in a line were drilled in it. The outer ones were used for centring it in turn on the face-plate of a lathe by a pump-centre. They formed the centres of the convex parts. The lathe headstock was rotated backwards and forwards about half a turn, the cutting tool being held in the slide-rest. The concave parts were formed as in an ordinary boring operation. The edges have all the same curvature, *i.e.*, 15 mm.

## APPENDIX 3.

### *Assembling the Parts of the Moving System.*

The ideal way of arranging for the assembly of the moving system would be to provide some registering arrangement so that all the needles would come together with their axes of symmetry in the same vertical plane. This could be done by having two vertical pins in one flange of each distance piece, fitting into corresponding holes in the needle and into holes in the adjoining flange of the next distance piece. The only difficulty would be in the smallness of the parts involved. Such arrangement was not found necessary, but since the instruments were constructed, jigs have been developed for doing this, and such a scheme will be used in further instruments. To assist in keeping the needles parallel while tightening up the end nut, the concave edges have been laid on a cylinder of wood of the same curvature (15 mm. radius) and 90 mm. long. The needles, when placed on edge in this manner, are just strong enough to support the spindle and distance pieces. The fit of the cylinder causes them to take the proper position, after which the nut is tightened up. It is convenient to attach a small loop of silk or cotton to the hole in the upper nut to hold it while being put in position in the instrument. Before hooking it to the suspension the thread is cut away.



Digitized by Google

## Appendix 4.

*Method of Mounting the Suspension Wires.*

If the necessity arises for renewing the suspension wires it is important to be able to mount them at a definite distance apart in order to make the deflections of the instrument fit the scale, which has to be divided empirically.

For this purpose a simple jig has been devised for ensuring that the necessary conditions can be easily fulfilled. This is shown in fig. 4. The free end of the wire is clamped under the screw $A_1$. It passes the upper part of the block B, which acts as a temporary holder for the upper suspension clamp K. It then passes a small cylinder $C_1$ which has a comparatively large clearance hole for its fixing screw, and goes over the main part of the upper clamp. At a distance of 40 cm. it passes the lower clamp L and round a screw D which has a cylindrical part turned to 3·5 mm. diameter or other required dimension. It is then crossed over and passes the screw E, which need not be of any

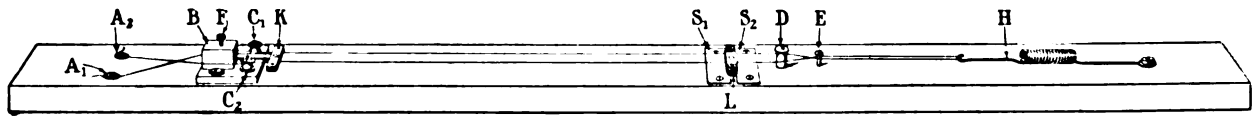


Fig. 4. Form of jig for mounting suspension wires.

special size. The object of this is to keep the wire tight against the cylinder D. It is then looped round a hooked end of a wire spring H. It passes back in a similar manner and is fixed by the screw clamp $A_2$.

The two cylinders $C_1$ and $C_2$ which determine the separation of the top of the suspension wires, are fixed at any desired distance by the fit of a small brass rod turned to the requisite diameter. When this is just a fit between the cylinders the fixing screws are tightened.

Two thin brass strips $S_1$, $S_2$ are screwed to the base board in order to keep the lower bridge-piece square with the wires while screwing it up.

When the wires are taut the parts of the clamps with clearance holes in them are screwed down. The surplus wire is then cut off, the screw F is loosened and the suspension is ready for clamping to the central spindle of the voltmeter. It is desirable to allow for a margin of sensitivity by spacing the wires a few per cent. farther apart than is necessary. The sensitivity is finally adjusted by slipping small weights in the form of rings of thin wire on to the damper spindle.

Digitized by Google

# THE MEASUREMENT OF REACTIVE POWER

BY

R. S. J. SPILSBURY, B.Sc., A.C.G.I.
ASSISTANT IN THE ELECTRICITY DEPARTMENT.

Digitized by Google

ABSTRACT.

The Paper deals with the use of induction-type integrating meters for the measurement of reactive power in supply circuits. Methods for single-phase circuits are first considered, and are shown to involve no theoretical errors. Three-phase systems are then treated, first on the assumption of balanced currents and voltages, and later in the general case, where this assumption is not permissible. It is shown that the majority of the methods are to some extent inaccurate on unbalanced circuits.

Finally numerical results are given for each of the three-phase methods under two typical conditions of unbalance, and the large errors to which some methods are liable are indicated.

Digitized by Google

# THE MEASUREMENT OF REACTIVE POWER.

By R. S. J. SPILSBURY, B.Sc., A.C.G.I., Assistant in the Electricity Department.

[Reprinted from the 'Beama', Vol. 13, December, 1923.]

The wide use of alternating current machinery, and especially of induction motors, has caused supply engineers to take an increasing interest in the measurement of wattless current, that is, that component of current which is at right angles to the voltage vector.

The disadvantages which arise from the presence of this component, such as reduction of the capacity of generators and feeders, and increased losses, are well known, and it is generally accepted that the cost of supplying wattless current should be directly borne by the consumer, and not by the supply authority.

Many meters, some of which are very complex, have been devised to take account of wattless current, or more generally the scalar product of voltage and wattless current, referred to as reactive power. Such meters may measure kilovolt-ampere hours, kilowatt hours plus some fraction of kilovolt-ampere hours, reactive kilovolt-ampere hours, or combinations of these quantities. It is proposed in this article to deal with some theoretical points which arise in meters designed to measure reactive power only. The use of induction watt-hour meters, now almost universal, will be considered, although some of the methods described are equally applicable to other types of watt-hour meter.

## Single-Phase Methods.

Reactive power meters for single-phase circuits depend in general on the use of some special phase angle between the two fluxes which drive the rotor. It can be shown* that the speed or torque of the rotor of a perfect induction meter is given by the equation

$$S = KhH \sin \lambda, \quad . \quad . \quad . \quad . \quad . \quad . \quad . \quad . \quad . \quad . \quad (1)$$

where S is the meter speed, K is a constant, $h$ and H are the values of the operative portions of the fields due to the shunt and series magnets, and $\lambda$ is the phase angle between these two fields. The same expression also gives the torque with an appropriate value of K. Neglecting practical imperfections this may be written

$$S = kVI \sin(\lambda' \pm \phi),$$

where V and I are the voltage and current applied to the meter, $\phi$ is the phase angle between them, and $\lambda'$ is the lag angle of the meter, that is, the phase angle which exists between

* H. G. Solomon, 'Electricity Meters', p. 113, 1906.

Digitized by Google

the driving fluxes when V and I are in phase. Ordinarily $\lambda'$ is adjusted to be 90°, by causing the operative shunt flux to lag approximately 90° behind the voltage. We then have

$$\begin{aligned} S &= kVI \sin(90 \pm \phi) \\ &= kVI \cos \phi, \end{aligned}$$

that is, the meter speed is proportional to the true power, and the meter registration is proportional to the energy which has been absorbed in the circuit.

In order to make the meter speed proportional to the reactive power, it is only necessary to make the lag angle zero instead of 90°. The speed of the rotor will then be given by

$$\begin{aligned} S &= kVI \sin(0 \pm \phi) \\ &= \pm kVI \sin \phi \quad . \quad . \quad . \quad . \quad . \quad . \quad . \quad . \quad . \quad . \quad . \quad (2) \end{aligned}$$

Since I sin $\phi$ is the component of current at right angles to V, this expression is proportional to the reactive power, as previously defined: the instrument is therefore a true reactive power meter. It will be noticed that the direction of rotation of the disc depends upon the sign of the angle $\phi$, that is to say, the direction will be different on circuits of leading and lagging power factor.

The necessary adjustment of the lag angle may be made by winding the shunt coil of the meter on an open iron circuit instead of on the nearly closed one employed in meters for real power: in addition, a non-inductive resistance is connected in series with the shunt coil, and another non-inductive resistance is placed in parallel with the series coil. The result of these adjustments is that the shunt flux lags by a small angle behind the voltage, and the operative series flux lags by an equal small angle behind the current: the two fluxes are therefore in phase when $\phi = 0$.

A variation of this principle consists in using a two-element meter, the two shunt coils being in parallel and the two series coils in series. The upper element of the meter has a lag angle of 90°, and the lower element one of, say, 45°. The torques of the two elements are adjusted to be equal and opposite when the voltage and current are in phase. The torque of the upper element is given by the expression $kVI \sin(90 - \phi)$, and that of the lower element by $k'VI \sin(45 - \phi)$.

Since the torques are equal at unity power factor $kVI \sin 90 = k'VI \sin 45$. That is $k' = \sqrt{2}k$.

Therefore the meter torque is equal to

$$\begin{aligned} kVI \sin(90 - \phi) - k'VI \sin(45 - \phi) &= kVI \sin(90 - \phi) - \sqrt{2}kVI \sin(45 - \phi) \\ &= kVI \sin \phi. \end{aligned}$$

The speed is therefore proportional to the reactive power and the registration is proportional to the time integral of reactive power.

Digitized by Google

It is of interest to note that if the lower element is put out of action, say by breaking the pressure circuit, the meter runs at a speed proportional to the true power: further, if the constant of the meter is adjusted so that it normally reads reactive kilovolt-ampere hours directly, the registration under these conditions will be in true kilowatt hours.

It is not actually necessary, though it is convenient, to adopt lag angles of 90° and 45°. Provided that the adjustment for equal and opposite torques at unity power factor is made, the meter speed will always be proportional to VI sin $\phi$. Certain practical limitations will, however, be obvious.

There are, then, no theoretical errors involved in the use of induction meters to integrate reactive power in single-phase circuits. Nevertheless, it must be borne in mind that the construction of these special meters may present difficulties not encountered in the normal type, and the degree of perfection which has been reached in meters for registering real power may be difficult to attain. As an instance, the fact that reactive power meters may rotate in either direction, according to circuit conditions, may render the problem of compensation for friction difficult.

## Methods for Balanced Three-Phase Circuits.

In three-phase circuits an additional complication is introduced by the possibility of unbalancing. In commercial work the symmetrical three-phase circuit of the text books is in general not obtained: the vectors of the currents in the three phases are not of the same length, and are not separated by angles of 120° and the voltages are, to a less degree, unbalanced and asymmetrical. In considering methods of measuring reactive power, however, we shall first take the case of a perfectly balanced circuit, since the essentials of the various systems are then much more easily seen, and we shall deal later with the effects of unbalancing.

### (1) "*Single Element*" *Method.*

The simplest methods of measuring reactive power in a three-phase three-wire system employs one voltage and one current only. The vector diagram for a balanced system is

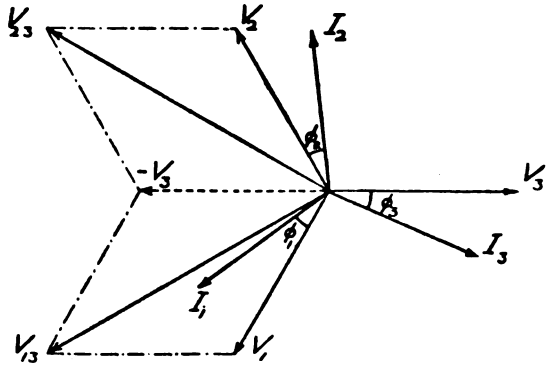


Fig. 1.

given in fig. 1. Here $V_1$, $V_2$, and $V_3$ are the three equal and symmetrical phase voltages, and $V_{13}$ is one of the line voltages, the resultant of $V_1$ and $-V_3$. $I_1$, $I_2$, and $I_3$ are the three

Digitized by Google

equal currents, and $\phi_1$, $\phi_2$, and $\phi_3$ are the equal angles of lag between the phase currents and voltages.

From the geometry of the figure it is evident that the vector $V_{13}$ is perpendicular to the vector $V_2$: hence $V_{13}$ and $I_2$ are separated by the angle $90 + \phi_2$.

If, therefore, we connect a normal induction meter, with 90° lag, to the circuit, energizing the shunt coil by the line voltage $V_{13}$, and the series coil by the current $I_2$, the speed of the meter will be given by

$$\begin{aligned} S &= V_{13}I_2 \cos(90 + \phi_2) \\ &= \sqrt{3}VI \cos(90 + \phi) \\ &= (-)\sqrt{3}VI \sin\phi, \quad \ldots\ldots\ldots\ldots \quad (3) \end{aligned}$$

where

$$\begin{aligned} V &= V_1 = V_2 = V_3, \\ I &= I_1 = I_2 = I_3, \\ \phi &= \phi_1 = \phi_2 = \phi_3. \end{aligned}$$

(The negative sign indicates that $V_{13}$ must be reversed to make the meter run forward on lagging power factor.)

The true reactive power, by analogy from the single-phase circuit, is $3VI \sin\phi$. Hence the rate of registration of the meter is proportional to the reactive power, and by a suitable choice of constant the meter may be made to register reactive kilovolt-ampere hours. This method may evidently be duplicated, using a two-element meter, but there is no advantage in doing this.

### (2) "*Crossed Phase*" *Method.*

This method employs a two-element meter, each element having the normal 90° lag. The connections are given in fig. 2, from which it will be seen that phase voltages and

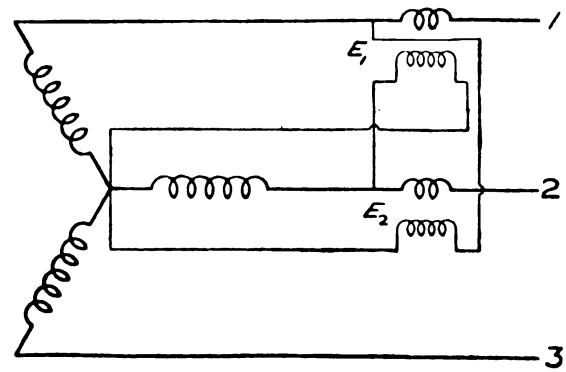


Fig. 2.

not line voltages are used. One element of the meter ($E_2$) is operated by the voltage $V_1$ and the current $I_2$, while the other element ($E_1$) employs the voltage $V_2$ and the current $I_1$: the two elements are arranged to oppose one another at unity power factor.

Digitized by Google

Referring to the vector diagram, fig. 1, we have

$$\begin{aligned} S &= V_2 I_1 \cos(120 - \phi_1) - V_1 I_2 \cos(120 + \phi_2) \\ &= VI(\cos 120 \cos\phi + \sin 120 \sin\phi - \cos 120 \cos\phi + \sin 120 \sin\phi) \\ &= 2VI \sin 120 \sin\phi \\ &= \sqrt{3}VI \sin\phi. \end{aligned}$$

The meter therefore registers at the same rate as in the preceding case, and if a standard meter is employed, its reading must be multiplied by $\sqrt{3}$ in order to obtain the true reactive "energy": this factor is preferably included in the meter constant.

The use of phase voltages in this method is an obvious disadvantage, as only line voltages are, in general, immediately available. The difficulty may be partially overcome for meters employing a potential transformer by bringing out the neutral point of the secondary winding: in low voltage circuits where transformers are not provided a choking coil is introduced, so as to form, with the two meter shunt coils, an artificial star system, which is connected across the three-phase lines.

If, however, the voltages applied to the meter are to be truly representative of the balanced phase voltages, as they must be if the registration is to be correct, it is evidently necessary for the three legs of the transformer, for instance, to have the same ratios and phase angles. Three-phase potential transformers are constructed with asymmetrical iron circuits for the three phases, and this condition is in general not exactly fulfilled. The resulting errors are similar to those due to unbalancing of the circuit, which will be discussed later.

### (3) "*Two-Wattmeter Difference*" *Method.*

It is well known that the real power in any three-phase three-wire circuit may be obtained by algebraic addition of the readings of two-wattmeters, each of which has a series coil connected in one line, and a shunt coil connected between this line and the line containing no series coil.

If, however, the algebraic difference of the two readings is taken, the result is proportional to the total reactive power in the three-phase circuit. A two-element watt-hour meter of normal construction can therefore be used to integrate the reactive power in such a circuit, the two elements being connected so as to be in opposition at unity power factor.

Referring to fig. 1, it will be seen that the torque of the meter element, the series coil of which is connected in line 1, will be proportional to

$$V_{13} I_1 \cos(\phi_1 - 30),$$

while the torque of the element operated by the current in line 2 will be proportional to

$$V_{23} I_2 \cos(\phi_2 + 30).$$



Digitized by Google

The speed of the meter is therefore given by

$$S = \sqrt{3}VI \{\cos(\phi - 30) - \cos(\phi + 30)\}$$
$$= \sqrt{3}VI \sin \phi.$$

The rate of registration is therefore proportional to the reactive power, the constant being the same as in the preceding cases.

### (4) "*Zero Lag*" *Method.*

Assuming the possibility of constructing satisfactory meter elements with zero lag angle, a meter consisting of two such elements may be employed to integrate three-phase reactive power. The connections employed are the same as those given for the two-wattmeter difference method previously described, but the two elements are arranged to assist each other at unity power factor. It has already been shown that an induction meter with zero lag angle runs at a speed proportional to VI sin $\phi$. Referring to fig. 1, the speed of the meter under consideration is seen to be

$$V_{13}I_1 \sin(\phi_1 - 30) + V_{23}I_2 \sin(\phi_2 + 30) = 2\sqrt{3}VI \cos 30 \sin \phi$$
$$= 3VI \sin \phi. \quad \ldots\ldots\ldots \quad (4)$$

Hence the registration of the meter is the true reactive energy.

### (5) "*Composite Voltage*" *Method.*

The principle of this method is the application, to each element of a two-element meter, of a voltage displaced 90° from that employed in a meter measuring real power, this voltage being obtained by compounding one line voltage with part of another. The connections used are given in fig. 3, and the vector diagram of the voltage circuits in fig. 4.

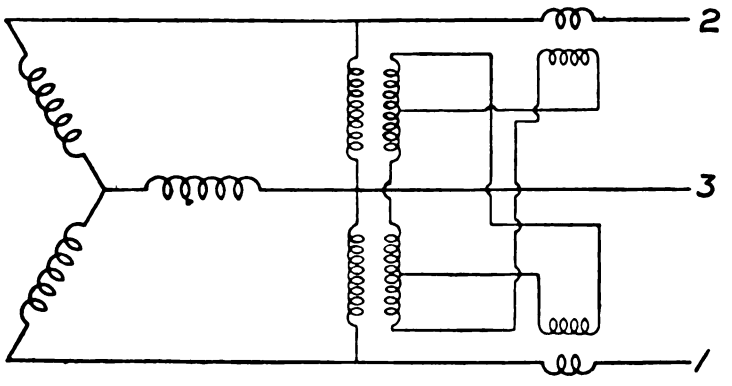


Fig. 3.

It will be seen from the former figure that the voltage applied to the lower element of the meter is the vector sum of the line voltage $V_{23}$ and half the line voltage $V_{31}$, and the current applied is $I_1$: similarly the upper element is operated by $\overline{V_{13} + 1/2\ V_{32}}$, and $I_2$. The two elements are connected so as to oppose each other at unity power factor.

Digitized by Google

When the circuit is balanced the vector diagram shows that the former composite voltage is in the same phase as the phase voltage $V_2$, and is equal to 3/2 $V_2$, while the latter one is in phase with $V_1$ and equal to 3/2 $V_1$.

The equation of a meter working on this method is therefore the same, with the exception of the factor 3/2, as that given under the *crossed phase* method already described,

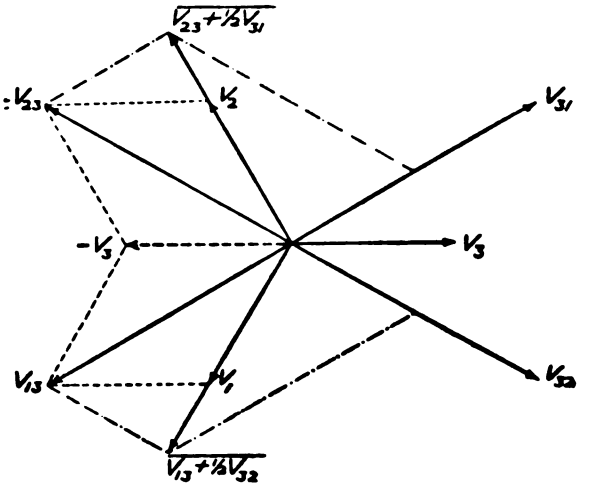

Fig. 4.

since the phases of the voltages and currents supplied to the elements are the same. The meter speed will be given by

$$S = \frac{3\sqrt{3}}{2} VI \sin \phi, \quad . \quad . \quad . \quad . \quad . \quad . \quad . \quad . \quad . \quad . \quad (5)$$

and the registration will be proportional to the reactive kilovolt-ampere hours.

This method, like the *crossed phase* system, requires accurate transformers: in this case the transformers also have to be provided with mid-point tappings on the secondary winding.

## Effects of Unbalancing of the Three-Phase System.

Up to the present we have considered only perfectly balanced three-phase circuits. In practice, however, deviations from this ideal, usually fairly small as regards the voltages, but often large in the case of the currents, are unavoidable. It is therefore necessary to examine the systems of metering reactive power which have been described, and to determine whether they remain accurate when the symmetry of the circuit is upset.

In the first place, however, we shall have to consider what we mean by the reactive power in a three-phase unbalanced circuit. We have defined the quantity for a single-phase circuit as VI sin $\phi$, that is, the product of the magnitudes of the voltage and current and the sine of the phase angle between them, and a similar definition is applied without difficulty to a balanced three-phase system. In an unbalanced system, however, V, I, and $\phi$ may differ from phase to phase: what, then, is the reactive power?



Digitized by Google

Of the several definitions which have been suggested, the most reasonable seems to be that involved in the Campos definition of power factor as

$$\frac{\Sigma VI \cos \phi}{\sqrt{(\Sigma VI \cos \phi)^2 + (\Sigma VI \sin \phi)^2}}$$

Here $\Sigma VI \cos \phi$ is the real power of the circuit, and $\Sigma VI \sin \phi$ is the reactive power.

The definition of reactive power as the algebraic sum $\Sigma VI \sin \phi$, that is

$$V_1 I_1 \sin \phi_1 + V_2 I_2 \sin \phi_2 + V_3 I_3 \sin \phi_3.$$

(taking account of the sign of $\phi$) has the advantages that it is :—

(*a*) Applicable to circuits having any number of phases.
(*b*) Applicable to balanced or unbalanced circuits.
(*c*) Consistent with the accepted method of defining single-phase reactive power.
(*d*) Independent of the point in the circuit at which the reactive power is measured.

For any $n$-phase $n$-wire circuit with given line voltages and currents the value of the reactive power is independent of the position of the neutral point assumed in the calculation. The reactive power can therefore be expressed in terms of the line voltages and currents, and the phase angles between them.

A diagram showing the application of this method to a somewhat violently unbalanced three-phase circuit is given in fig. 5. Here phases one and two have loads with lagging power factors, and phase three has a load with leading power factor, that is to say $\phi_1$ and $\phi_2$ are (say) positive angles, and $\phi_3$ is a negative one.

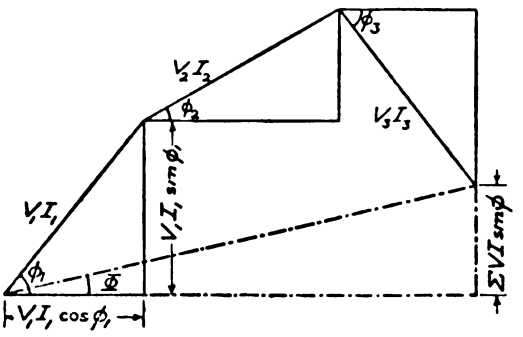


Fig. 5.

In examining the accuracy of the metering methods described, it will be convenient to use analytical methods, as the vectorial method is somewhat clumsy when the circuit is unbalanced. We shall, therefore, obtain the meter speed by integration of the product of the instantaneous voltage and current over a period.

The variables involved are specified as follows :—

$$v_1 = \hat{V}_1 \sin \omega t, \qquad i_1 = \hat{I}_1 \sin (\omega t - \phi_1),$$
$$v_2 = \hat{V}_2 \sin (\omega t - \alpha), \qquad i_2 = \hat{I}_2 \sin (\omega t - \alpha - \phi_2),$$
$$v_3 = \hat{V}_3 \sin (\omega t - \beta), \qquad i_3 = \hat{I}_3 \sin (\omega t - \beta - \phi_3),$$

where $v_1$, $i_1$, etc., are instantaneous values of phase voltage and current, $\hat{V}_1$, $\hat{I}_1$, etc., are maximum values, and $\phi_1$, $\phi_2$ and $\phi_3$ are the phase angles of the three phases. The

Digitized by Google

angles $\alpha$ and $\beta$ specify the relative phases of $v_1$, $v_2$ and $v_3$, and $\omega$ is equal to the circuit frequency $n$, multiplied by $2\pi$.

In the case of a balanced circuit

$$\hat{V}_1 = \hat{V}_2 = \hat{V}_3, \qquad \hat{I}_1 = \hat{I}_2 = \hat{I}_3,$$
$$\phi_1 = \phi_2 = \phi_3, \qquad \alpha = 120^\circ, \qquad \beta = 240^\circ,$$

but in the generalized unbalanced circuit none of these relations holds.

### (1) *Single Element Method.*

From the description of this method already given, it will be seen that the meter is operated by the line voltage $v_{31}$ and the current $i_2$.

The speed of the meter is therefore given by

$$S = \frac{\omega}{2\pi}\int_0^{\frac{2\pi}{\omega}} v_{31} i_2 \, dt$$
$$= \frac{\omega}{2\pi}\int_0^{\frac{2\pi}{\omega}} (v_3 - v_1)\, i_2 \, dt$$
$$= \frac{\omega}{2\pi}\int_0^{\frac{2\pi}{\omega}} \{\hat{V}_3 \sin(\omega t - \beta) - \hat{V}_1 \sin \omega t\}\, \hat{I}_2 \sin(\omega t - \alpha - \phi_2)\, dt.$$

Converting the products of sines

$$= \frac{\omega \hat{V}_3 \hat{I}_2}{4\pi}\int_0^{\frac{2\pi}{\omega}} \{\cos(\alpha + \phi_2 - \beta) - \cos(2\omega t - \alpha - \phi_2 - \beta)\}\, dt$$
$$= \frac{\omega \hat{V}_1 \hat{I}_2}{4\pi}\int_0^{\frac{2\pi}{\omega}} \{\cos(\alpha + \phi_2) - \cos(2\omega t - \alpha - \phi_2)\}\, dt.$$

The terms containing $2\omega t$ have the same value at both limits.

Therefore

$$S = \frac{\hat{V}_3 \hat{I}_2}{2}\cos(\alpha + \phi_2 - \beta) - \frac{\hat{V}_1 \hat{I}_2}{2}\cos(\alpha + \phi_2),$$

substituting effective values for maximum values

$$S = V_3 I_2 \cos(\alpha + \phi_2 - \beta) - V_1 I_2 \cos(\alpha + \phi_2). \quad . \quad . \quad . \quad . \quad . \quad (6)$$

Now we have defined reactive power as $V_1 I_1 \sin \phi_1 + V_2 I_2 \sin \phi_2 + V_3 I_3 \sin \phi_3$, in which expression $V_1$, $V_2$ and $V_3$, the three phase voltages, are quite independent of each other. Further, since the circuit impedances may be given any desired values, one of these voltages may be varied without changing any of the other quantities, $I_1$, $\phi_1$, etc. The right-hand side of equation (6) does not involve $V_2$: it is therefore possible to change this quantity, and so change the value of the reactive power, without altering the meter speed.

Digitized by Google

Hence this method is not in general accurate on unbalanced load. The errors which arise in any particular case may be calculated from the phase voltages and currents by formula (6). Two cases will be considered later.

### (2) *Crossed Phase Method.*

In this method, if the actual phase voltages are applied to the meter, the speed is given by

$$S = \frac{1}{T}\int_0^T (v_2 i_1 - v_1 i_2)\,dt \qquad \text{where} \qquad T = \frac{2\pi}{\omega}$$

$$= \frac{1}{T}\int_0^T \{\hat{V}_2 \sin(\omega t - \alpha)\,\hat{I}_1 \sin(\omega t - \phi_1) - \hat{V}_1 \sin \omega t\, \hat{I}_2 \sin(\omega t - \alpha - \phi_2)\}\,dt$$

$$= \frac{\hat{V}_2\hat{I}_1}{2T}\int_0^T \cos(\phi_1 - \alpha)\,dt - \frac{\hat{V}_1\hat{I}_2}{2T}\int_0^T \cos(\phi_2 + \alpha)\,dt$$

$$+ \text{terms equal to zero.}$$

Therefore

$$S = V_2 I_1 \cos(\phi_1 - \alpha) - V_1 I_2 \cos(\phi_2 + \alpha) \quad . \quad . \quad . \quad . \quad . \quad . \quad (7)$$

This method fails to take any account of the voltage $V_3$, and is therefore unsound in principle.

An interesting case arises when the voltages are balanced and symmetrical, but the currents are not. We then have $V_1 = V_2 = V_3 = V$, and $\alpha = \beta/2 = 120°$.

Therefore from equation (7)

$$S = V\{I_1 \cos(\phi_1 - 120) - I_2 \cos(\phi_2 + 120)\}$$

$$= V\left\{\frac{\sqrt{3}}{2} I_1 \sin\phi_1 + \frac{\sqrt{3}}{2} I_2 \sin\phi_2 - \tfrac{1}{2} I_1 \cos\phi_1 + \tfrac{1}{2} I_2 \cos\phi_2\right\} . \quad . \quad . \quad . \quad (8)$$

Now from Kirchoff's law $i_1 + i_2 + i_3 = 0$, that is

$$I_1 \sin(\omega t - \phi_1) + I_2 \sin(\omega t - \alpha - \phi_2) + I_3 \sin(\omega t - \beta - \phi_3) = 0.$$

Expanding

$$\{I_1 \cos\phi_1 + I_2 \cos(\alpha + \phi_2) + I_3 \cos(\beta + \phi_3)\} \sin \omega t$$
$$- \{I_1 \sin\phi_1 + I_2 \sin(\alpha + \phi_2) + I_3 \sin(\beta + \phi_3)\} \cos \omega t = 0.$$

If this holds for all values of $t$

$$I_1 \cos\phi_1 + I_2 \cos(\alpha + \phi_2) + I_3 \cos(\beta + \phi_3) = 0, \quad . \quad . \quad . \quad . \quad . \quad (9)$$

and

$$I_1 \sin\phi_1 + I_2 \sin(\alpha + \phi_2) + I_3 \sin(\beta + \phi_3) = 0. \quad . \quad . \quad . \quad . \quad . \quad (10)$$

Digitized by Google

Multiplying (9) by sin $\beta$ and (10) by cos $\beta$ and subtracting we have

$$I_1 \sin(\phi_1 - \beta) + I_2 \sin(\alpha + \phi_2 - \beta) + I_3 \sin \phi_3 = 0. \quad . \quad . \quad . \quad (11)$$

Inserting the values of $\alpha$ and $\beta$

$$\frac{\sqrt{3}}{2} I_1 \cos \phi_1 - \frac{\sqrt{3}}{2} I_2 \cos \phi_2 = \tfrac{1}{2} I_1 \sin \phi_1 + \tfrac{1}{2} I_2 \sin \phi_2 - I_3 \sin \phi_3.$$

Therefore

$$-\tfrac{1}{2} I_1 \cos \phi_1 + \tfrac{1}{2} I_2 \cos \phi_2 = -\frac{1}{2\sqrt{3}} I_1 \sin \phi_1 - \frac{1}{2\sqrt{3}} I_2 \sin \phi_2 + \frac{1}{\sqrt{3}} I_3 \sin \phi_3. \quad (12)$$

Substituting the right-hand side of (12) in equation (8)

$$S = V\left\{\left(\frac{\sqrt{3}}{2} - \frac{1}{2\sqrt{3}}\right)(I_1 \sin \phi_1 + I_2 \sin \phi_2) + \frac{1}{\sqrt{3}} I_3 \sin \phi_3\right\}$$

$$= \frac{1}{\sqrt{3}}(VI_1 \sin \phi_1 + VI_2 \sin \phi_2 + VI_3 \sin \phi_3) \quad . \quad . \quad . \quad . \quad . \quad . \quad . \quad . \quad (13)$$

Thus when the phase voltages are balanced and symmetrical the meter speed is proportional to the reactive power, whether the currents are balanced or not. This fact is of some importance because the currents are much more likely than the voltages to be seriously unbalanced.

In practice, the neutral point of the system is usually not accessible, and one of the devices already mentioned has to be employed. Assuming that a transformer is in use, and that its three circuits are identical, it will be seen that the voltages applied to the meter are not the true phase voltages unless the voltages of the system are balanced and symmetrical. If they are not so, the potential of the neutral point of the secondary winding relative to the secondary lines will be at the " centre of gravity " of the triangle formed by the three vectors of line voltage,* which will not in general correspond to the true neutral point of the system. Hence the voltages applied to the meter will not be representative of the phase voltages, and the above treatment is no longer applicable.

The general formula for the reading of the meter under these conditions would be very cumbrous, and it appears best to calculate the error for any given case directly from the known voltages and currents, or to use graphical methods.

It will be observed that if the phase voltages are balanced and symmetrical the " centre of gravity " of the line voltages corresponds to the true neutral point, and the meter will, therefore, read accurately under these conditions on balanced or unbalanced current provided that an accurate potential transformer is employed.

* Russell, ' Alternating Currents ', vol. 1, p. 224, 1904.

Digitized by Google

(3) *Two-Wattmeter Difference Method.*

The meter speed in this method is given by

$$\begin{aligned} S &= \frac{1}{T}\int_0^T (v_1 - v_3)\, i_1\, dt - \frac{1}{T}\int_0^T (v_2 - v_3)\, i_2\, dt \\ &= \frac{1}{T}\int_0^T \{[\hat{V}_1 \sin \omega t - \hat{V}_3 \sin(\omega t - \beta)] \times \hat{I}_1 \sin(\omega t - \phi_1)\}\, dt \\ &\quad - \frac{1}{T}\int_0^T \{[\hat{V}_2 \sin(\omega t - \alpha) - \hat{V}_3 \sin(\omega t - \beta)] \times \hat{I}_2 \sin(\omega t - \alpha - \phi_2)\} dt \\ &= V_1 I_1 \cos\phi_1 - V_2 I_2 \cos\phi_2 + V_3\{I_2 \cos(\alpha + \phi_2 - \beta) - I_1 \cos(\phi_1 - \beta)\}. \end{aligned}$$

By methods similar to those used in the treatment of the crossed phase method it may be shown* that

$$-I_1 \cos(\phi_1 - \beta) = I_2 \cos(\alpha + \phi_2 - \beta) + I_3 \cos\phi_3,$$

therefore,

$$S = V_1 I_1 \cos\phi_1 - V_2 I_2 \cos\phi_2 + V_3 I_3 \cos\phi_3 + 2V_3 I_2 \cos(\alpha + \phi_2 - \beta) \quad . \quad . \quad (14)$$

Assume for the moment that this expression is equal to the true reactive power. Increase $V_1$, which is independent of the other variables, to $V_1(1 + x)$. The reactive power will then change by $x\, V_1 I_1 \sin\phi_1$, by definition, while the speed S will change by $x\, V_1 I_1 \cos\phi_1$. Since the ratio of $\sin\phi_1$ to $\cos\phi_1$ is not constant, these two changes are not in any fixed ratio to one another. Hence the meter will be in error when $V_1$ is increased to $V_1(1 + x)$, if it is correct before the increase. This method is, therefore, not a sound one for unbalanced circuits: as will be shown later, the errors produced by a quite moderate degree of unbalancing may be very serious.

(4) *Zero Lag Method.*

We have seen that a normal induction meter, with 90° lag angle, runs at a speed proportional to the real power, that is to say, to the mean value of the instantaneous product of the applied voltage and current. In the present case, therefore, in which the operative voltage flux of the meter is in phase with the applied voltage, that is, 90° in advance of the normal position, it will be necessary to advance the phase of the voltage by this amount before integration. This is equivalent to employing the cosine instead of the sine function for the voltage, and we therefore have for the speed of the meter

$$\begin{aligned} S &= \frac{1}{T}\int_0^T \{[\hat{V}_3 \cos(\omega t - \beta) - \hat{V}_1 \cos\omega t] \times \hat{I}_1 \sin(\omega t - \phi_1)\}\, dt \\ &\quad + \frac{1}{T}\int_0^T \{[\hat{V}_3 \cos(\omega t - \beta) - \hat{V}_2 \cos(\omega t - \alpha)] \times \hat{I}_2 \sin(\omega t - \alpha - \phi_2)\}\, dt \\ &= V_1 I_1 \sin\phi_1 + V_2 I_2 \sin\phi_2 + V_3\{I_1 \sin(\beta - \phi_1) + I_2 \sin(\beta - \alpha - \phi_2)\}. \end{aligned}$$

* Solomon, 'Electricity Meters', p. 124, 1906.

Digitized by Google

But from equation (11)

$$I_1 \sin(\beta - \phi_1) + I_2 \sin(\beta - \alpha - \phi_2) = I_3 \sin \phi_3,$$

therefore

$$S = V_1 I_1 \sin \phi_1 + V_2 I_2 \sin \phi_2 + V_3 I_3 \sin \phi_3 \quad . \quad . \quad . \quad . \quad . \quad . \quad (15)$$

This method is, therefore, correct on any three-phase three-wire system, whatever the condition of balance of the voltages and currents.

### (5) *Composite Voltage Method.*

Here the meter speed is given by

$$S = \frac{1}{T}\int_0^T \left\{(v_2 - v_3) + \left(\frac{v_3 - v_1}{2}\right)\right\} i_1 \, dt - \frac{1}{T}\int_0^T \left\{(v_1 - v_3) + \left(\frac{v_3 - v_2}{2}\right)\right\} i_2 \, dt.$$

Evaluating this expression in the same way as in the preceding cases we find

$$\left.\begin{aligned} S = V_2 I_1 \cos(\phi_1 - \alpha) - \frac{V_3 I_1}{2} \cos(\phi_1 - \beta) - \frac{V_1 I_1}{2} \cos \phi_1 - V_1 I_2 \cos(\phi_2 + \alpha) \\ + \frac{V_3 I_2}{2} \cos(\alpha - \beta + \phi_2) + \frac{V_2 I_2}{2} \cos \phi_2 \end{aligned}\right\} \quad . \quad (16)$$

In order to test the accuracy of the method we may put $I_1 = 0$, thus eliminating the first three terms of the right-hand side of (16). Of those which remain only the last involves $V_2$, and this term $\left(\frac{V_2 I_2}{2} \cos \phi_2\right)$ should, therefore, be equal or proportional to that term in the expression for reactive power which involves $V_2$, that is, to $V_2 I_2 \sin \phi_2$. This is evidently not the case, and the method is, therefore, not in general accurate when the phase voltages are unbalanced.

When, however, the voltages are balanced and symmetrical the unbalancing of the currents does not affect the accuracy of the meter. This is evident from the fact already noted that under these conditions the results of this method bear a constant ratio to those of the *crossed phase* system, which has been proved to depend only on voltage balance and symmetry.

## Numerical Results.

The equations which express the performances of the various systems of metering reactive power which have been described are necessarily somewhat cumbrous, and while one can determine without much difficulty whether a given system is or is not accurate on unbalanced load, it is not easy to form an idea of the relative merits of those which are



Digitized by Google

not perfectly accurate, that is to say, Nos. (1), (2), (3) and (5). For this reason it has been thought desirable to give the errors for two cases of moderate unbalance.

For the first case the following values have been chosen :—

$$V_1 = 1{\cdot}0000 \quad I_1 = 1{\cdot}0465 \quad \phi_1 = 40^\circ \quad \alpha = 120^\circ$$
$$V_2 = 1{\cdot}0000 \quad I_2 = 0{\cdot}9459 \quad \phi_2 = 40^\circ \quad \beta = 240^\circ$$
$$V_3 = 1{\cdot}0000 \quad I_3 = 1{\cdot}0000 \quad \phi_3 = 35^\circ$$

It will be seen that the voltages are balanced and symmetrical, while the extreme currents differ by approximately 5 per cent. from the mean. Under these conditions methods (2), (4) and (5) will give correct results and need not be further considered. The results given by methods (1) and (3) are set out in Table I. Each method may be applied to the circuit in three ways, and figures are given for each of these. The meter rates have been multiplied by the appropriate factor ($\sqrt{3}$), deduced from the balanced load

TABLE I.

| Method. | Currents employed. | Meter rate. | Error per cent. | Cos Φ from meter. | Error. |
|---|---|---|---|---|---|
| (True value) | — | 1·8543 | — | 0·784 | — |
| Single | $I_3$ | 1·7207 | 7·2 Slow | 0·806 | + 0·022 |
| Element | $I_1$ | 2·0181 | 8·8 Fast | 0·758 | − 0·026 |
| (1) | $I_2$ | 1·8240 | 1·6 Slow | 0·789 | + 0·005 |
| Two-wattmeter | $I_1$, $I_2$ | 2·1213 | 14·4 Fast | 0·742 | − 0·042 |
| Difference | $I_2$, $I_3$ | 1·5268 | 17·7 Slow | 0·838 | + 0·054 |
| (3) | $I_3$, $I_1$ | 1·9150 | 3·3 Fast | 0·775 | − 0·009 |

case, to convert them to reactive volt-amperes. The value of *cos* Φ given is calculated from the true watts and the value of the reactive volt-amperes obtained from the meter rate.

The mean error of method (1), neglecting sign, is 5·9 per cent., and that of method (3) is 11·8 per cent. Considering that the circuit is only moderately unbalanced, these errors must be regarded as very serious, and it does not seem that either method gives results sufficiently accurate to justify its installation.

Where, however, it is decided to us one of the methods, the *single element* meter should be chosen, since it is cheaper, simpler and more accurate* than the alternative. The *two-wattmeter difference* method appears to have nothing to recommend it.

In the second case the circuit chosen has extreme currents differing by approximately

* STUBBINGS has recently shown for the balanced voltage case (' El Review ', vol. 92, p. 816, 1923) that the error of method (1) is always half that of method (3) and of opposite sign.

Digitized by Google

1 per cent. from the mean, and voltages unbalanced to the same extent: the voltages are also slightly unsymmetrical.

The following are the actual values :—

| | | | | |
|---|---|---|---|---|
| $V_1 = 1{\cdot}0100$ | $I_1 = 1{\cdot}0099$ | $\phi_1 = 37°$ | $\alpha = 118°$ | $V_{12} = 1{\cdot}7144$ |
| $V_2 = 0{\cdot}9900$ | $I_2 = 0{\cdot}9898$ | $\phi_2 = 39°$ | $\beta = 238°$ | $V_{23} = 1{\cdot}7234$ |
| $V_3 = 1{\cdot}0000$ | $I_3 = 1{\cdot}0000$ | $\phi_3 = 38°$ | | $V_{31} = 1{\cdot}7580.$ |

The results are scheduled in Table II.

TABLE II.

| Method. | Currents employed. | Meter rate. | Error per cent. | Cos Φ from meter. | Error. |
|---|---|---|---|---|---|
| (True value) | — | 1·8462 | — | 0·788 | — |
| Single | $I_3$ | 1·7727 | 4·0 Slow | 0·800 | + 0·012 |
| Element | $I_1$ | 1·9039 | 3·1 Fast | 0·779 | − 0·009 |
| (1) | $I_2$ | 1·8620 | 0·9 Fast | 0·786 | − 0·002 |
| Crossed | $I_1$, $I_2$ | 1·8647 | 1·0 Fast | 0·785 | − 0·003 |
| Phase (A) | $I_2$, $I_3$ | 1·8580 | 0·6 Fast | 0·786 | − 0·002 |
| (2) | $I_3$, $I_1$ | 1·8159 | 1·6 Slow | 0·793 | + 0·005 |
| Crossed | $I_1$, $I_2$ | 1·8462 | 0·0 | 0·788 | 0·000 |
| Phase (B) | $I_2$, $I_3$ | 1·8462 | 0·0 | 0·788 | 0·000 |
| (2) | $I_3$, $I_1$ | 1·8462 | 0·0 | 0·788 | 0·000 |
| Two-wattmeter | $I_1$, $I_2$ | 1·9932 | 8·0 Fast | 0·765 | − 0·023 |
| Difference | $I_2$, $I_3$ | 1·7308 | 6·3 Slow | 0·807 | + 0·019 |
| (3) | $I_3$, $I_1$ | 1·8147 | 1·7 Slow | 0·793 | + 0·005 |
| Composite | $I_1$, $I_2$ | 1·8462 | 0·0 | 0·788 | 0·000 |
| Voltage | $I_2$, $I_3$ | 1·8462 | 0·0 | 0·788 | 0·000 |
| (5) | $I_3$, $I_1$ | 1·8462 | 0·0 | 0·788 | 0·000 |

It will be noticed that two sets of figures are given for method (2). In (A) the phase voltages are assumed to be applied directly to the meter; in (B) the meter voltages are derived from an accurate star network, as previously described.

As regards methods (1) and (3) it is not necessary to add anything to what has been said above. Method 2 (A) is not greatly in error, but 2 (B) is much preferable under this set of conditions, and would generally be applicable where 2 (A) would not.

Method (5) also gives results which are accurate to 0·01 per cent. In order to test the performance of this method further the following set of conditions was taken :—

| | | | |
|---|---|---|---|
| $V_1 = 1{\cdot}1000$ | $I_1 = 1{\cdot}0465$ | | $\alpha = 120°$ |
| $V_2 = 1{\cdot}0000$ | $I_2 = 0{\cdot}9459$ | $\phi_2 = \phi_1$ | $\beta = 240°$ |
| $V_3 = 1{\cdot}0000$ | $I_3 = 1{\cdot}0000$ | $\phi_3 = \phi_1 - 5°$ | |



Digitized by Google

$\phi_1$ was given various values from 10° to 90°, corresponding to three-phase power factors of 0·99 lag to 0·03 lag: the error was found to vary from 1·7 per cent. slow at the former value to 0·3 per cent. slow at the latter. The error at unity power factor was 0·2 per cent. of the maximum reactive power. (The reading is the same for all of the three possible methods of connection.) This must be considered a good result for a severely unbalanced circuit.

Summarizing the results, the following statements may be made, assuming theoretically perfect meters. Method (4) (*zero lag*) is the only generally exact one which has been discussed: it is suitable when bad unbalance exists and precise readings are required. Methods (2) (*crossed phase*) and (5) (*composite voltage*) are both exact when the voltages are balanced and symmetrical. They show errors due to voltage unbalance, which in the cases investigated are considerable for (2) employing the neutral point, and very small for (5) or for (2) employing an artificial star system or the like. Methods (1) (*single element*) and (3) (*two-wattmeter difference*) are sensitive to voltage and current unbalance and are not satisfactory: (3) is exceedingly unreliable.

Digitized by Google

# THE EFFICIENCY OF OVERLAPPING JOINTS IN COPPER AND ALUMINIUM BUSBAR CONDUCTORS

BY

S. W. MELSOM, A.M.I.E.E.,
PRINCIPAL ASSISTANT IN THE ELECTRICITY DEPARTMENT,
AND
H. C. BOOTH, A.R.C.S.,
ASSISTANT IN THE ELECTRICITY DEPARTMENT.

Digitized by Google

## ABSTRACT.

The object of the investigation was to determine the amount of the contact resistance between the surfaces of an overlapping joint in rectangular straight busbar conductors of copper and aluminium under various conditions of surface preparation and pressure, and hence to ascertain the efficiency of such joints. An efficient joint was regarded as one in which the total resistance, which includes effects due to stream-line distortion, does not exceed that of an equal length of continuous conductor on either side of the joint. As a preliminary it was necessary to determine and allow for the effect of stream-line distortion under various conditions of overlap. Generally full-sized models were investigated, and the two surfaces with varying amounts of overlap were pressed together by means of an hydraulic ram or by bolts or special clamps. Numerical results are deduced and tables and graphs given for the contact resistance per unit of surface area under various conditions of pressure and amount of overlap, and after various modes of cleaning and preparing the surface, including the interposition of tinfoil or the soldering of the two bars together. A series of graphs are given which show the efficiency of copper and aluminium joints in terms of the above defined standard for a wide range of values of busbar sizes and for any value of specific contact resistance likely to occur under practical conditions, and hence the amount of overlap required to obtain an efficient joint. The efficiency of making joints by means of clamps and bolts was also considered and the pressure occurring at such joints estimated by comparison of the contact resistance obtained when the same joint was held together in the hydraulic press. The effect of modifying the numbers, size and position of the bolts used was also investigated.

Digitized by Google

# THE EFFICIENCY OF OVERLAPPING JOINTS IN COPPER AND ALUMINIUM BUSBAR CONDUCTORS.

By S. W. MELSOM, A.M.I.E.E., Principal Assistant in the Electricity Department, and H. C. BOOTH, A.R.C.S., Assistant in the Electricity Department.

[Reprinted from the 'Journal of the Institution of Electrical Engineers', Vol. 60, 1922.]

The typical form of a clamped joint between flat conductors of rectangular cross-section is shown in fig. 1. The data required should enable the resistance of the overlapping

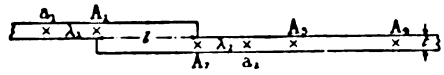

Fig. 1.

portion $A_1$ $A_2$ to be calculated, and the ratio of its resistance to that of an equal length of single conductor of the same cross-section and resistivity to be predetermined.

The problem under consideration divides itself into two heads :—

(1) The increase of resistance due to the stream-line distortion which occurs at the overlap.

(2) The contact or transition resistance between the superposed metal surfaces, and the manner in which this is affected by pressure and area of contact, and the condition or mode of preparation of the surfaces.

## (1) *The Effect of Stream-Line Distortion.*

If the length of overlap is large compared with the thickness of the bar, the metallic resistance of the overlapping portion will obviously be very nearly equal to that of two conductors in parallel. But if the overlap is much reduced this ceases to be strictly true, as, owing to the distortion of the stream lines, the resistance is greater than that of two bars in parallel. It will be obvious that this distortion depends only on the ratio of the overlap to the thickness of the bar, and, provided the two bars are of equal width, it will not be affected by the width ; the current-flow for a straight joint can therefore be regarded as taking place in two dimensions only. To determine the magnitude of this effect a series of experimental observations were made by means of a tinfoil model. A piece of thin, uniform tinfoil was cut into a shape which represented the longitudinal section of an overlap joint (fig. 1). A steady current of suitable strength was passed through the strip, and the voltage-drop $v_1$ between the points $A_1$, $A_2$ was compared by means of a potentiometer or millivoltmeter with the voltage-drop $v_2$ between the two

Digitized by Google

points $A_3$, $A_4$, placed an equal distance apart in the straight portion of the strip. Since the voltage-drop is proportional to the resistance, the factor $\sigma = v_1/v_2$ expresses the increase in metallic resistance due to stream-line distortion. This value is clearly constant whatever the dimensions of the overlap, provided that the ratio of the length $l$ to the thickness $t$ remains the same. To determine $\sigma$ for other values of the overlap ratio $l/t$, the tinfoil was cut away as indicated by the dotted lines in fig. 2. In this way a series

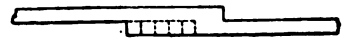

Fig. 2.

of values were obtained for the ratio $l/t$, and for each of these values the resistance ratio $\sigma$ was determined. A sufficient number of values was obtained to enable the curve in fig. 3 to be drawn. This shows graphically the relation between $\sigma$ and the overlap ratio $l/t$. If, for example, the overlap is 10 times the thickness of the bar, the increase of resistance due to distortion effect is only 4 per cent., but if the overlap is 4 times the thickness, the increase is approximately 20 per cent., and, where it is only twice the thickness, it is nearly 50 per cent. As will be seen later, a knowledge of the relation

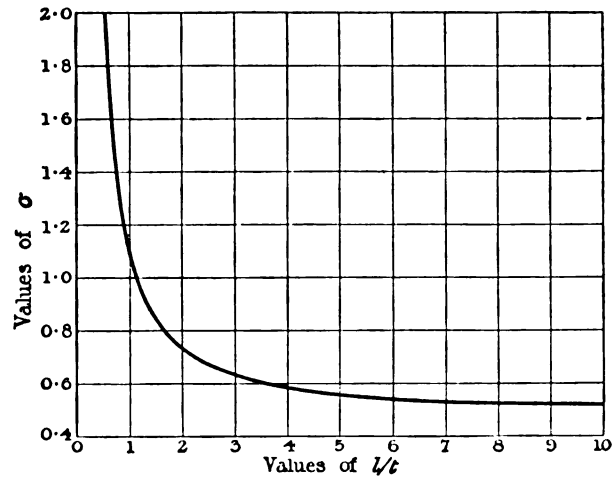


Fig. 3. Showing effect of stream-line distortion in overlapping joints.

between $\sigma$ and the ratio $l/t$ was also necessary in deducing the true contact resistance from the experimental results.

It is perhaps of interest to note that by a slight modification of the procedure it is possible to trace out the equipotential lines over the joint section as represented by the tinfoil model. Another series of lines drawn at right angles to these will then represent the general form of the stream lines of current-flow in an actual joint. This involves the assumption that if there were a joint in the circuit, instead of the metal being continuous, the distribution of the stream lines would not be appreciably affected. As will be shown later, the magnitude of the contact resistance in a satisfactory joint is sufficiently low to justify this assumption.

Digitized by Google

*Tee joints.*—The question of the distortion of stream lines in a T-joint is a much more difficult one, since the distortion is in three dimensions, the compound effect being due to :—

(*a*) Distortion owing to change of direction from the horizontal to the vertical strip, and

(*b*) Distortion produced by the fact that the bars are not in the same plane.

To meet this case, an actual determination was made with a T-joint between two pieces of copper 2 in. × $\frac{3}{8}$ in., the joint being soldered in order to reduce the contact resistance to a low and uniform value. Comparison was then made between the resistance of this joint and that of a straight-on soldered joint having the same amount of overlap and made in a similar way. It was found that the values were not greatly dissimilar.

### (2) *Contact Resistance.*

The contact resistance between a prepared, flat metal surface is dependent on a number of factors, *e.g.*, pressure, the area of the surfaces in contact, and the mode of preparation of the surfaces themselves, all of which require to be investigated.

The assumption commonly made is that a contact between any two surfaces is at three points only, which would lead to the conclusion that if the total pressure remained the same the contact resistance would be independent of the area of the two surfaces pressed together, but all the experiments which were made showed that in copper and aluminium bars clamped together under the pressures used in practice, the contact resistance was more nearly inversely proportional to the area when the pressure per unit area was the same. This is most apparent in the values given for the 1 in. × $\frac{1}{4}$ in. copper bar (Table VIII), where a decrease of overlap resulted in a large decrease in contact resistance. On the three-point contact theory the contact resistance should have remained the same, since the total applied pressure on the assumed three points would have been the same.

With a very small pressure the three-point contact theory would probably apply, but with any appreciable pressure it seems probable that there is some deformation, either by straining or flowing of the metal. In fact, an inspection of the bars after they had been clamped together suggested that this was the case. It will be realized that contact resistance is a function of the thickness of the film of air between the two surfaces. This thickness is, of course, in any case exceedingly small, and a very slight variation of it would affect the value of contact resistance to a very large extent.

The assumption made in interpreting the results given in this Paper, *i.e.*, that the resistance between two surfaces is inversely proportional to the area when the pressure per unit area is the same, may not be absolutely correct, but it appears more nearly to represent the facts.



Digitized by Google

## Experimental Methods.

The values given in this Paper are all based on measurements on actual copper and aluminium bars of various sizes, up to and including bars 6 in. $\times$ $\frac{1}{2}$ in. thick. Kraus* described an ingenious method of determining contact resistance by superposing a number of thin discs of metal in order to magnify the effect. This method appeared to be well suited to laboratory purposes, and seemed good since it would enable the contact resistance to be determined directly. The method was tried, but we failed to obtain any reasonable degree of consistency. Quite apart from this, however, the use of full-scale bars is to be preferred, since it is clear that other factors which affect the result are not operative when a small-scale model is employed. It will, however, be realized that the method adopted involves the evaluation of the contact resistance as a difference between two larger quantities. In any case the contact resistance is a most variable quantity, and the accuracy of the observations was usually much higher than the consistency of individual determinations.

The method generally adopted was to form an overlapping joint by bolting, clamping, or pressing together by means of a hydraulic ram a pair of flat bars of similar cross-section. This also allowed of investigation of the effect of preparing the surfaces under the various conditions obtainable in practice and of other methods of preparation that appeared likely to give better results.

Two contact terminals were fixed at points $a_1$, $a_2$ (fig. 1), each usually at a small distance $\lambda_1$, $\lambda_2$ on either side of the joint. The voltage-drop between these terminals was measured by means of a potentiometer when a known current was flowing through the joints; the resistance was calculated and a correction was then made by subtracting (1) the resistance of that part $\lambda_1$ and $\lambda_2$ of the single conductors which was included between $A_1$ and $a_1$ and $A_2$ and $a_2$; and (2) the resistance of a piece of single conductor equal in length to the overlap multiplied by the appropriate value of $\sigma$ as given by the curve in fig. 3, in order to correct for the effect of stream-line distortion. The residual amount was then considered to represent the contact resistance between the surfaces.

Thus, if the resistivity of the metal is $r$ and if $\lambda = \lambda_1 + \lambda_2$ (the sum of the lengths of single conductor included between $A_1$, $a_1$ and $A_2$, $a_2$ respectively); and if $b$ is the breadth and $t$ the thickness of the bars, then the resistance of this portion will be

$$r\lambda/bt,$$

and, if $l$ is the overlap, the resistance of the overlap portion considered as a solid piece of metal without contact resistance would be

$$\sigma rl/bt,$$

where $\sigma$ is taken from the curve (fig. 3) for the particular value of $l/t$ under consideration.

Then if $R_t$ is the total resistance as measured between the points $a_1$ and $a_2$, the true contact resistance will be

$$R_t - [(\lambda + \sigma l)\, r/bt.$$

* 'Elektrotechnik und Maschinenbau', vol. 38, p. 1, 1920.

Digitized by Google

In order to facilitate the comparison and application of the results obtained, it is further assumed that under such pressures as are used in practice the contact between the surfaces will be fairly complete, and also that the resistance is inversely proportional to the area of the contact surfaces. On this assumption the specific contact resistance or resistance per unit area will be

$$\rho = \{R_t - [(\lambda + \sigma l)\, r/bt]\}\, lb,$$

and this formula was generally employed to deduce the specific contact resistance from the results obtained in the experimental investigations on clamped joints.

In the majority of these experimental determinations the overlap joint was pressed directly into contact by means of an hydraulic ram, which was capable of producing a maximum total pressure of about 10 tons, indicated on an attached pressure gauge. The two ends of the bars which were to form the joint were previously trued up so that when brought together the outer surfaces to which pressure was applied might be very fairly parallel. Flat pieces of ebonite or Stabilit were placed above and below the overlap. These insulated the joint from the plates of the ram, and at the same time their greater plasticity served to equalize the distribution of the applied pressure in the event of the two outer surfaces of the joint not being exactly parallel.

The measurement of the actual resistance of the joint was made under a series of progressively increasing pressures, but in order to obtain more stable conditions the maximum permissible pressure was usually applied several times before a measurement was made. On the assumption that the pressure on the superposed surfaces is evenly distributed, the specific pressure $p$ is equal to the total indicated pressure P divided by the total area of contact, that is, $p = P/lb$.

*Tests on Aluminium Busbars.*

The tests on the aluminium busbars were made on behalf of the British Aluminium Company, whom we have to thank for permission to publish the results.

*Preparation of the Surfaces.*—The contact resistance of aluminium is necessarily influenced to a very large extent by the slight film of oxide normally present on the surface. This oxide forms so rapidly that the usual method of cleaning the bars and immediately clamping them together is not satisfactory. In these experiments the first satisfactory result was obtained with bars the ends of which were cleaned and bolted together under paraffin oil. This is, of course, not a practicable method for ordinary use, but it indicated the nature of the precautions that had to be taken, and led to the evolution of methods which could be readily applied to practical conditions, and which gave equally satisfactory results. Apart from the question of the removal of oxide, the results were affected also by the nature of the surface, *e.g.*, whether it was dead smooth or rough from the file.

The surfaces were therefore tested under a variety of conditions. *i.e.*,—

(1) Bars carefully flatted and left rough ; and

(2) Bars carefully flatted and smoothed ;



Digitized by Google

and in both cases the contact resistance was determined when the surfaces were pressed together—

(*a*) Without further preparation ;

(*b*) After cleaning with emery paper and paraffin, the metal surfaces being cleaned and brought together under paraffin so as to reduce the amount of oxidation to a minimum ; and

(*c*) When cleaned with emery and protected with a thick layer of clean vaseline.

*Numerical Results obtained with the Various Types of Surface.*—The results obtained for contact resistance with the various types of surface at pressures varying from 1,000 to 10,000 lb. per square inch are given in fig. 5 and are summarized in Table I.

TABLE I.

| Nature and condition of service. | Contact resistance : microhms per sq. in. at— | | | |
|---|---|---|---|---|
| | 2,000 lb./sq. in. | 3,000 lb./sq. in. | 4,000 lb./sq. in. | 5,000 lb./sq. in. |
| (1) Flatted rough— | | | | |
| (*a*) Without special cleaning | 15 | 11 | 8 | 7·7 |
| (*b*) Emery paper and paraffin | 5·8 | 4·0 | 3·2 | 2·8 |
| (*c*) Emery paper and vaseline | 5 | 3·7 | 3·4 | 3·2 |
| (2) Flatted smooth— | | | | |
| (*a*) Without special cleaning | | Results extremely variable. | | |
| (*b*) Emery paper and paraffin | 12 | 8 | 6 | 4·8 |
| (*c*) Emery paper and vaseline | 8·5 | 5·5 | 3·5 | 2·5 |

These values represent the mean of a large number of determinations ; at the lower pressures the results of individual observations showed considerable variations, but at the higher pressures these were quite fairly consistent and reproducible. Under practical conditions, as will be shown later, the actual pressure occurring in a bolted joint is approximately equivalent to a value of from 1,000 to 2,000 lb. per square inch, according to the size of the joint and the number and size of bolts used to make the connection, and, in view of the variations at these pressures and the divergencies found when bars not specially machined are used, curve F (fig. 4) has been drawn as representing average values for joints prepared under various conditions, although it is clear that lower values can be obtained if the surfaces are properly prepared.

In order to meet the question of the practical use of busbars where the work of cleaning and preparing the surfaces will have to be carried out on site, a detailed series of observations was made with slight modifications in the mode of preparation. The same bars were used throughout, and the overlap and applied pressure were in

Digitized by Google

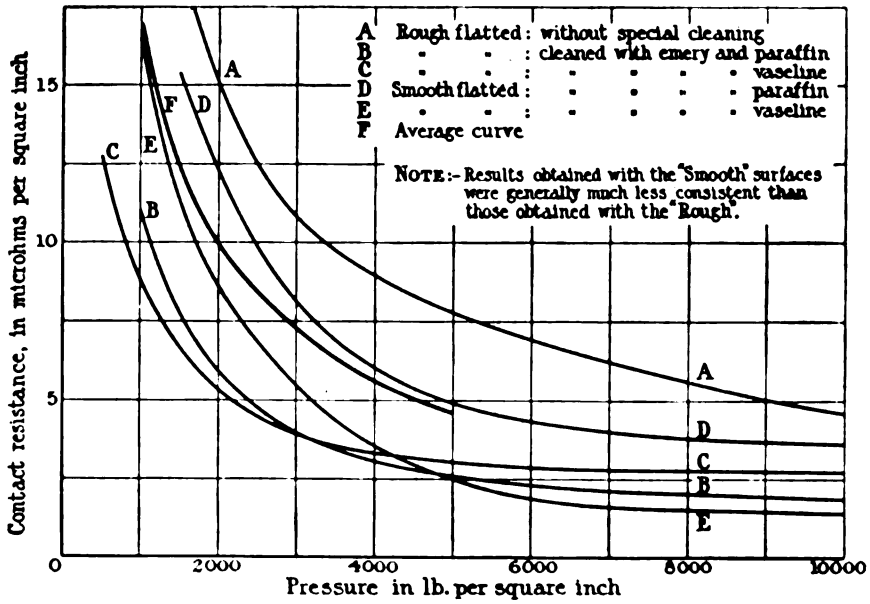
A Rough flatted: without special cleaning
B " " : cleaned with emery and paraffin
C " " : " " vaseline
D Smooth flatted: " " paraffin
E " " : " " vaseline
F Average curve
NOTE:- Results obtained with the "Smooth" surfaces were generally much less consistent than those obtained with the "Rough".
Contact resistance, in microhms per square inch
Pressure in lb. per square inch
0
2000
4000
6000
8000
10000
5
10
15

Fig. 4. Showing variation of specific contact resistance with pressure, for aluminium.

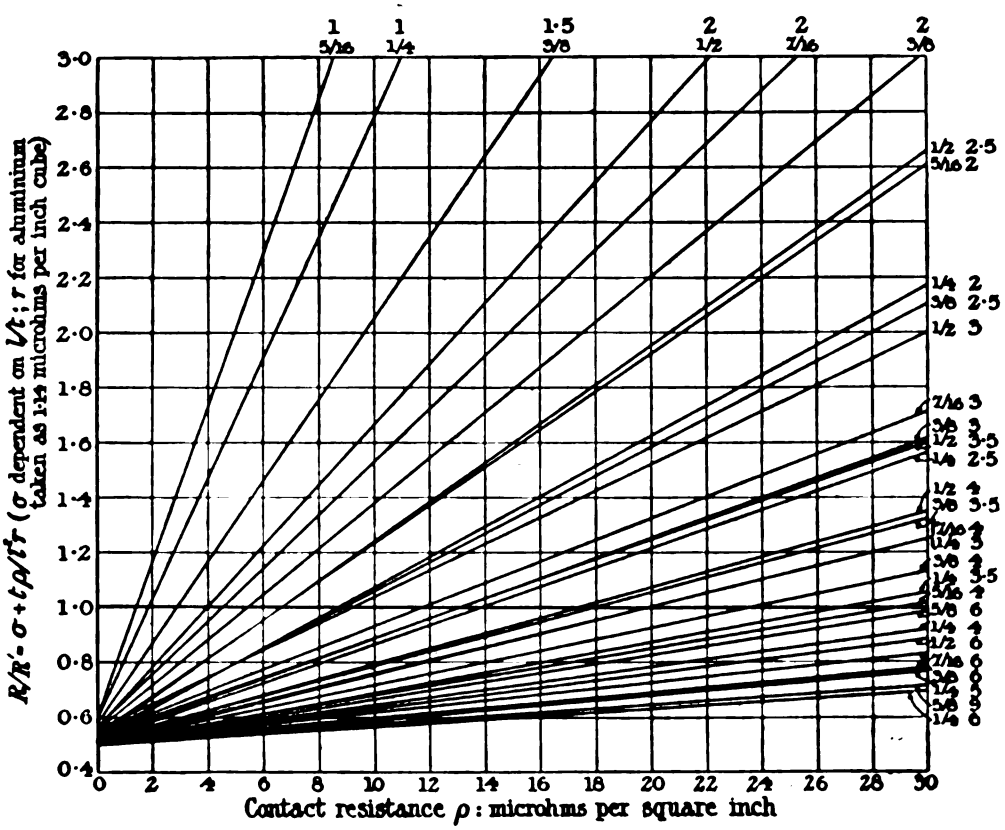


Fig. 5.

Digitized by Google

all cases the same, the pressure being 3,700 lb. per square inch. These results are given in Table II.

TABLE II.

| Test No. | Type of surface. | Contact resistance : microhms per sq. in. |
|---|---|---|
| | *Machine-flatted surfaces.* | |
| 1 | Coated with vaseline ; cleaned with a file and clamped up without removing vaseline . . . . . | 4·8 |
| 2 | Rough-filed dry, coated with vaseline, cleaned with emery paper and clamped without removing vaseline . . . . . | 2·8 |
| 3 | As 2, but with vaseline removed . . . . . | 4·0 |
| 4 | Test 2 repeated . . . . . | 3·2 |
| 5 | Test 1 repeated . . . . . | 3·4 |
| 6 | As 1, but the surfaces left apart for 1 hour before . . . . . | 4·5 |
| 7 | As 6, wiped clean and reassembled . . . . . | 7·4 |
| | *Original surface of the strip, as delivered from the rolls.* | |
| 8 | Wiped with cotton cloth only . . . . . | 15·5 |
| 9 | Smeared with vaseline, rough-filed and clamped without removing vaseline . . . . . | 4·2 |
| 10 | As 9, but with dirty vaseline removed . . . . . | 5·8 |
| 11 | Coated with vaseline, cleaned with emery paper and clamped without removing vaseline . . . . . | 3·0 |
| 12 | As 11, but with vaseline removed . . . . . | 4·2 |
| 13 | Test 11 repeated . . . . . | 5·0 |
| 14 | Dirty vaseline removed and replaced by clean . . . . . | 6·7 |

The only obvious inconsistency in this table is in Test No. 13, where the results are rather higher than would be expected. Generally, however, the results show a remarkable degree of consistency, and it is clear from them that the easiest method of preparation in practical work, *i.e.*, rough cleaning with a file either (*a*) before the vaseline is applied, and cleaning afterwards with emery, or (*b*) coating with vaseline and rough filing, in both cases leaving the dirty vaseline on the bar, is at least as good as, if not better than, any other method.

*Amount of Overlap required.*—In considering the amount of overlap required to make an efficient joint, it is most convenient to express the resistance of the joint as a compound effect made up of the contact resistance and the metallic resistance, as modified by the stream-line distortion. This is best stated in terms of the resistance of an equal length of the straight conductor. Thus, an efficient joint is one in which the total resistance of the length comprising the joint is not greater than that of an equal length of the straight conductor.

Digitized by Google

On the assumption that the contact resistance between two flat metal surfaces is inversely proportional to the area of contact, the total resistance of an overlapping joint is

$$R = r\sigma l/bt + \rho/bl,$$

where the symbols have the meanings already defined (the distortion factor $\sigma$ having the appropriate value for the ratio $l/t$, as given in fig. 3). The resistance of an equal length $l$ of single, straight conductor is

$$R' = rl/bt,$$

therefore the ratio of the two resistances is

$$R/R' = \sigma + (\rho t/l^2 r),$$

that is, a linear function of $\rho$.

In fig. 5, a series of straight-line graphs have been drawn, taking $r$ the resistivity of aluminium as 1·14 microhms per inch cube, which shows the value of R/R′ considered as a function of $\rho$ for series of values of length of overlap $l$ and thickness of strip $t$ as indicated in the top and right-hand side of the figure.

As an example of the use of the graphs, taking the value of contact resistance from curve F in fig. 4 as 10 microhms per square inch for a pressure of 2,000 lb. per square inch, then in the case of a joint in a strip ½ in. thick with an overlap of 3 in., R/R′ = 1·03; for a 4-in. overlap R/R′ = 0·79; and for a 6-in. overlap R/R′ = 0·63. For a pressure of 4,000 lb. per square in., the contact resistance would be 5·6 microhms per square inch, and the values of R/R′ for the same three cases would be 0·79, 0·67 and 0·57 respectively.

In order to show the relative magnitude of the two factors involved in the resistance of an overlapping joint, Tables III and IV have been drawn up. These show the ratio

TABLE III.—Joint Pressure: 2,000 lb. per square inch. $\rho$ = 10 michroms per square inch.

| $l/t$. | R′. | $\sigma$R′. | $\rho/lb$. | | | | $R = \sigma rl/bt + \rho/bl$. | | | | R/R′. | | | |
|---|---|---|---|---|---|---|---|---|---|---|---|---|---|---|
| | | | $t = \frac{3}{8}$ | $t = \frac{1}{2}$ | $t = \frac{5}{8}$ | $t = \frac{3}{4}$ | $t = \frac{3}{8}$ | $t = \frac{1}{2}$ | $t = \frac{5}{8}$ | $t = \frac{3}{4}$ | $t = \frac{3}{8}$ | $t = \frac{1}{2}$ | $t = \frac{5}{8}$ | $t = \frac{3}{4}$ |
| 4 | 4·56 | 2·68 | 6·67 | 5·00 | 4·00 | 3·35 | 9·35 | 7·68 | 6·68 | 6·03 | 2·05 | 1·68 | 1·47 | 1·32 |
| 6 | 6·84 | 3·68 | 4·45 | 3·35 | 2·67 | 2·23 | 8·13 | 7·03 | 6·35 | 5·91 | 1·19 | 1·03 | 0·93 | 0·87 |
| 8 | 9·12 | 4·73 | 3·35 | 2·50 | 2·00 | 1·67 | 8·08 | 7·23 | 6·73 | 6·40 | 0·89 | 0·79 | 0·74 | 0·70 |
| 12 | 13·68 | 6·95 | 2·23 | 1·67 | 1·35 | 1·11 | 9·18 | 8·62 | 8·30 | 8·06 | 0·67 | 0·63 | 0·61 | 0·59 |

R/R′ for a contact resistance of 10·0 microhms per square inch and 5·6 microhms per square inch, corresponding to pressures of 2,000 and 4,000 lb. per square inch respectively.

Digitized by Google

Tables III and IV give the values for the various thicknesses of bar, and overlap ratio $l/t$ for the same values of pressure and contact resistance as in the two cases just quoted. These tables also show separately the magnitude of the two components of the total contact resistance. These are $\rho/lb$, the contact resistance between the surfaces, and $\sigma rl/bt$, the metallic resistance of the joint, allowing for the distortion effect.

TABLE IV.—Joint Pressure: 4,000 lb. per square inch. $\rho = 5{\cdot}6$ michroms per square inch.

| $l/t$. | R′. | $\sigma$R′. | $\rho/lb$. | | | | $R = \sigma rl/bt + \rho/bl$. | | | | R/R′. | | | |
|---|---|---|---|---|---|---|---|---|---|---|---|---|---|---|
| | | | $t = \frac{3}{8}$ | $t = \frac{1}{2}$ | $t = \frac{5}{8}$ | $t = \frac{3}{4}$ | $t = \frac{3}{8}$ | $t = \frac{1}{2}$ | $t = \frac{5}{8}$ | $t = \frac{3}{4}$ | $t = \frac{3}{8}$ | $t = \frac{1}{2}$ | $t = \frac{5}{8}$ | $t = \frac{3}{4}$ |
| 4 | 4·56 | 2·68 | 3·74 | 2·80 | 2·24 | 1·88 | 6·42 | 5·48 | 4·92 | 4·56 | 1·41 | 1·20 | 1·08 | 1·00 |
| 6 | 6·84 | 3·68 | 2·50 | 1·88 | 1·49 | 1·24 | 6·18 | 5·56 | 5·17 | 4·92 | 0·90 | 0·81 | 0·75 | 0·72 |
| 8 | 9·12 | 4·73 | 1·88 | 1·40 | 1·12 | 0·93 | 6·61 | 6·13 | 5·85 | 5·66 | 0·73 | 0·67 | 0·64 | 0·62 |
| 12 | 13·68 | 6·95 | 1·24 | 0·93 | 0·75 | 0·62 | 8·19 | 7·88 | 7·70 | 7·57 | 0·60 | 0·58 | 0·56 | 0·55 |

Tables III and IV are based on a strip 1 in. wide. Their application to bars of other widths may be shown by taking the case of a busbar 3 in. wide and $\frac{3}{8}$ in. thick, with an overlap of 3 in. In this case $l/t$ would be 8. Then, assuming a pressure of 2,000l b. per square inch from Table III, the value of R for $t = \frac{3}{8}$ in. and $l/t = 8$ is found to be 8·08 microhms. Thus, for a bar 3 in. wide, this resistance should be 8·08/3, assuming, of course, the same pressure per square inch in each case, and the total resistance of the joint is 2·69 microhms. The ratio of the resistance of the joint to that of a similar length of straight conductor is the same as that given in Table III, viz., 0·89.

## TESTS ON COPPER BUSBARS.

The properties of copper as regards contact resistance would appear to be somewhat different from those of aluminium. This may be, first, because copper is not so liable to oxidation at ordinary temperatures, and secondly, because it is harder, and on this account its behaviour will not necessarily be the same as that of a more yielding material.

Somewhat the same series of tests were carried out to ascertain the effect of the condition of the surface and the applied pressure, and a series of results, showing the contact resistance under the various conditions, are given in fig. 6. It will be noted that—

(1) As in the case of aluminium, the best results are obtained when the surface is coated with vaseline, although in most cases the results are so low that this method of treatment is not necessary in practice.

(2) The values obtained with a joint pressed together after cleaning with vaseline are as good as when the joint is soldered.

(3) The interposing of layers of tinfoil between the surfaces has a marked effect: one thickness of the foil does not affect the results largely, but with two thicknesses the contact resistance is very much higher.

Digitized by Google

(4) There is no appreciable improvement due to roughening the surface with a file. In one case the results were somewhat better, but in others they were worse than when the surfaces were left smooth and cleaned with emery paper.

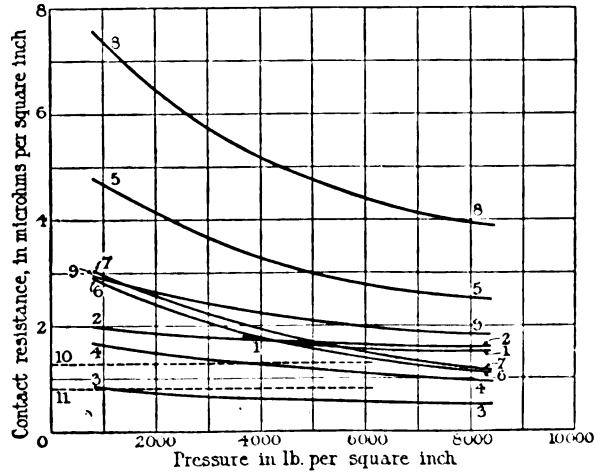


Fig. 6. Showing comparative effect of various modes of preparation. Test taken on 1-in. × $\frac{1}{4}$-in. copper strip without preliminary machining.

1. Rubbed with dry emery paper.
2. Rubbed with dry emery paper, but wiped with cotton waste after rubbing.
3. Rubbed with vaseline and emery paper.
4. Vaseline removed; roughened with file.
5. Vaseline removed; roughened with file.
6. Vaseline removed; roughened with file.
7. One thickness of tinfoil interposed.
8. Two thicknesses of tinfoil interposed.
9. The surfaces previously tinned.
10. The joint soldered.
11. The joint taken apart and resoldered.

Generally, it will be seen that the values shown in the figure are in most cases very low, but in view of the variable nature of contact resistance, too much weight must not be given to what may appear to be large variations.

It will be seen that this particular series was obtained with a strip of copper 1 in. × $\frac{1}{4}$ in.; further tests, however, with sizes up to 6 in. × $\frac{1}{2}$ in. give closely comparable results.

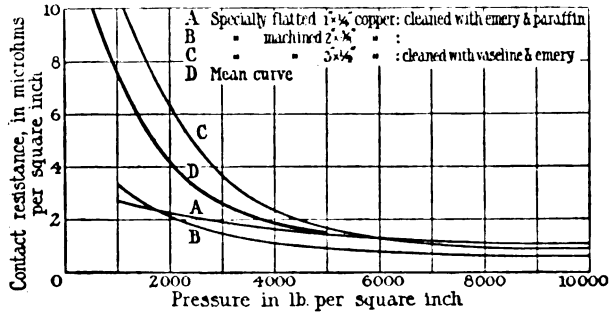


Fig. 7. Showing varieties of specific contact resistance with pressure, for copper.

As with aluminium, however, fairly large variations were found with copper strip straight from the rolls and without special machining, and curve D (fig. 7) has therefore been added as being fairly representative of practical conditions.



Digitized by Google

*Amount of Overlap required.*—The method of determination of the amount of overlap required for an efficient joint will be the same as in the case of aluminium bars, although, of course, two of the factors—resistivity and contact resistance—will be somewhat different. Stream-line distortion will clearly be the same for bars of similar section and overlap. The graphs in fig. 8 have been drawn in the same way as for aluminium, taking the resistivity of copper as 0·68 microhm per inch cube.

Examples of the use of the graphs are as follows :—Taking the specific normal contact resistance of the prepared surfaces shown in curve D (fig. 7), *i.e.*, 4·2 microhms per

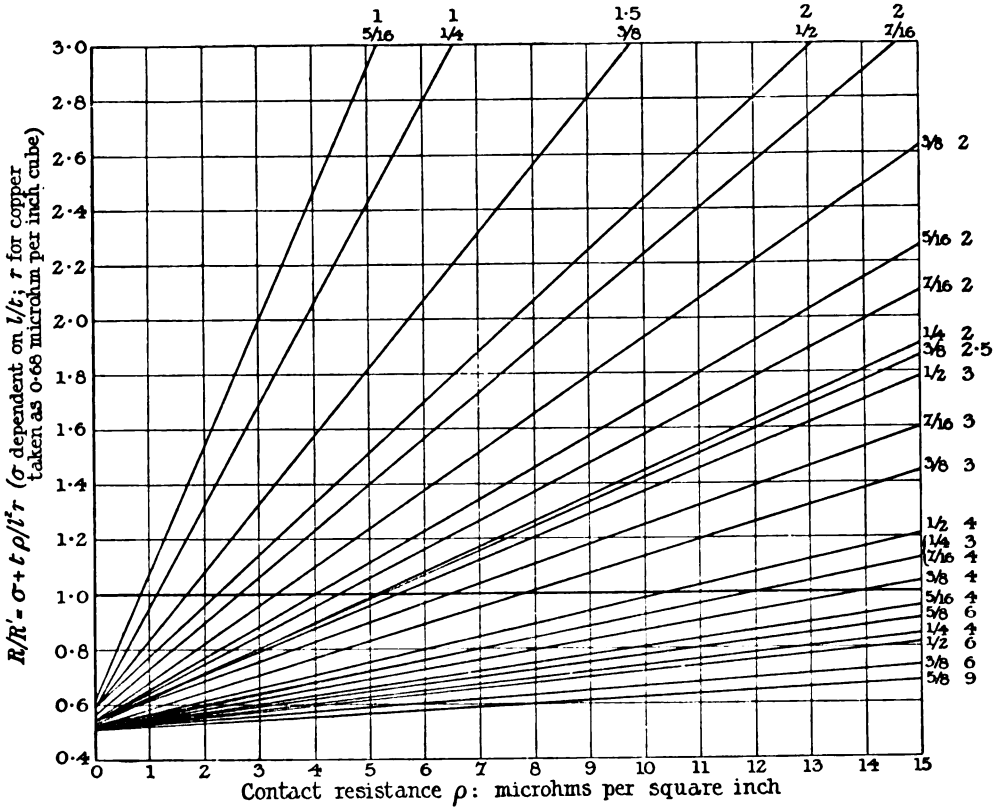


Fig. 8.

square inch with a pressure of 2,000 lb. per square inch, then for a strip ½ in. thick with an overlap of 3 in., the ratio R/R′ = 0·89, and for the same joint with pressures of 3,000 lb. por square inch and 4,000 lb. per square inch, the values would be 0·76 and 0·69 respectively. Tables V and VI give the values for the various thicknesses of bar and overlap ratio $l/t$ for values of contact resistance corresponding to pressures of 2,000 and 4,000 lb. per square inch respectively.

*Clamped Joints.*—The determination of contact and joint resistance with relation to the pressure is not of itself sufficient to solve the problem arising in practice. The further step required is to ascertain the effective pressure exerted by the clamps and bolts used in the ordinary busbar joint.

Digitized by Google

For this determination the surfaces of the bars were prepared under the best conditions, and tests were made alternately with them pressed together in the ram and when clamped or bolted together.

Only two sizes of clamps were available, one suitable for a bar 3 in. wide, and the other for a bar 2 in. wide, and these were tested with aluminium bars 3 in. × $\frac{3}{8}$ in. and 2 in. × $\frac{1}{4}$ in.

The clamps were provided with four steel bolts, one at each corner, the sizes of bolts being $\frac{1}{2}$ in. and $\frac{3}{8}$ in. respectively. During the tests the clamps were insulated from the

TABLE V.—Joint Pressure: 2,000 lb. per square inch. $\rho = 4{\cdot}0$ michroms per square inch.

| $l/t$. | R′. | $\sigma$R′. | $\rho/lb$. | | | | $R = \sigma rl/bt + \rho/bl$. | | | | R/R′. | | | |
|---|---|---|---|---|---|---|---|---|---|---|---|---|---|---|
| | | | $t=\frac{3}{8}$ | $t=\frac{1}{2}$ | $t=\frac{5}{8}$ | $t=\frac{3}{4}$ | $t=\frac{3}{8}$ | $t=\frac{1}{2}$ | $t=\frac{5}{8}$ | $t=\frac{3}{4}$ | $t=\frac{3}{8}$ | $t=\frac{1}{2}$ | $t=\frac{5}{8}$ | $t=\frac{3}{4}$ |
| 4 | 2·72 | 1·60 | 2·67 | 2·0 | 1·6 | 1·33 | 4·27 | 3·60 | 3·20 | 2·93 | 1·57 | 1·32 | 1·17 | 1·08 |
| 6 | 4·08 | 2·20 | 1·78 | 1·33 | 1·07 | 0·89 | 3·98 | 3·53 | 3·27 | 3·09 | 0·97 | 0·86 | 0·80 | 0·76 |
| 8 | 5·44 | 2·82 | 1·33 | 1·00 | 0·80 | 0·67 | 4·15 | 3·82 | 3·62 | 3·49 | 0·76 | 0·70 | 0·67 | 0·64 |
| 12 | 8·16 | 4·16 | 0·89 | 0·67 | 0·53 | 0·445 | 5·05 | 4·83 | 4·69 | 4·60 | 0·62 | 0·59 | 0·57 | 0·56 |

TABLE VI.—Joint Pressure: 4,000 lb. per square inch. $\rho = 1{\cdot}8$ michroms per square inch.

| $l/t$. | R′. | $\sigma$R′. | $\rho/lb$. | | | | $R = \sigma rl/bt + \rho/bl$. | | | | R/R′. | | | |
|---|---|---|---|---|---|---|---|---|---|---|---|---|---|---|
| | | | $t=\frac{3}{8}$ | $t=\frac{1}{2}$ | $t=\frac{5}{8}$ | $t=\frac{3}{4}$ | $t=\frac{3}{8}$ | $t=\frac{1}{2}$ | $t=\frac{5}{8}$ | $t=\frac{3}{4}$ | $t=\frac{3}{8}$ | $t=\frac{1}{2}$ | $t=\frac{5}{8}$ | $t=\frac{3}{4}$ |
| 4 | 2·72 | 1·60 | 1·20 | 0·90 | 0·72 | 0·60 | 2·80 | 2·50 | 2·32 | 2·20 | 1·30 | 0·92 | 0·85 | 0·81 |
| 6 | 4·08 | 2·20 | 0·80 | 0·60 | 0·48 | 0·40 | 3·00 | 2·80 | 2·68 | 2·60 | 0·74 | 0·69 | 0·66 | 0·64 |
| 8 | 5·44 | 2·82 | 0·60 | 0·45 | 0·36 | 0·30 | 3·42 | 3·27 | 3·18 | 3·12 | 0·63 | 0·60 | 0·585 | 0·573 |
| 12 | 8·16 | 4·16 | 0·40 | 0·30 | 0·24 | 0·20 | 4·56 | 4·46 | 4·40 | 4·36 | 0·373 | 0·365 | 0·360 | 0·355 |

bars by means of a thin sheet of hard insulating material. In actual practice they would be in metallic contact with the bars and, in consequence, would improve the joint slightly, but in this case we were endeavouring to make a determination of the much more important factor of pressure and, for the sake of uniformity, it was desirable to eliminate this somewhat uncertain factor.

Taking first the 3-in. clamps, with an overlap of 3 in. in an aluminium bar, the contact resistance was 0·88 microhm, the total joint resistance 2·6 microhms, and the corresponding ratio R/R′ = 0·79. The pressure by ram for an equivalent value would be



Digitized by Google

about 10,800 lb., or 1,200 lb. per square inch. It is interesting to note that with the clamp the joint resistance was only 0·79 time that of an equivalent length of straight conductor, and that even with the higher value of contact resistance indicated by the average curve F in fig. 4, viz., 15 microhms per square inch with a pressure of 1,200 lb. per square inch, the ratio R/R′ would be very nearly 1.

Some tests were made with this clamp before the strips were protected with vaseline and cleaned, and the results may be quoted to emphasize the importance of the preparation of the surfaces. With the bars in their initial condition the contact resistance was 3 microhms and the ratio $R/R' = 1 \cdot 4$, as compared with 0·88 and 0·79 when the surfaces of the bars were properly prepared. It should, however, be noted that with thicker bars the ratio R/R′ would be greater and, under the average conditions quoted, probably more nearly 1·2. In the case of an interleaved joint made with a number of pairs of bars pressed together by a single clamp, it would seem probable that the joint ratio would be the same as that for a single pair of bars under the same conditions of overlap.

With the 2-in. clamps, and the smaller bar with an overlap of 3 in., the contact resistance was 1·7 microhms, the joint resistance 6·9 microhms, and the corresponding ratio $R/R' = 0 \cdot 69$. The same joint tested immediately afterwards in the hydraulic ram showed that the pressure of the clamps was about 2,000 lb. per square inch.

*Bolted Joints.*—The actual pressure exerted by a bolt or by a number of bolts clamping two pieces of metal together has not up to the present been clearly defined. We have, on the one hand, definite information as to the breaking stress for bolts of various sizes, and it was hoped that this investigation would show the actual effective pressure exerted when a bolt, or bolts, were used istead of the hydraulic ram. The assumption was that if two bars previously drilled and prepared were first clamped in the ram with a known pressure, a comparison of the joint resistance under the same conditions with that obtained when the same bars were bolted together would give an approximate indication of the actual pressure exerted by the bolts. The pressures so indicated, however, in some cases exceed the elastic limit of the bolt, and it would appear that with comparatively thin bars the pressure is localized and more effective than with the ram or with clamps. If the bars were very thick and rigid it is probable that there would be no great difference between the two conditions, but with bars of the range of thickness ordinarily used in practice it seems probable that the pressure produced by the bolts may strain the metal to an extent sufficient to bring about a more intimate contact. The effect of bolting two comparatively thin bars together probably results in bending the metal around the bolt to a very slight extent when expressed in actual measurement, but sufficient to affect the contact resistance considerably. When the joint is made with a number of bolts, the slight bending of the strip at or near each bolt possibly produces a lateral motion which of itself would tend, by grinding the surfaces together, to break down the air film.

Taking, first, aluminium with a bar 3 in. wide and $\frac{7}{16}$ in. thick, the following values

Digitized by Google

were obtained under the standard conditions of surface, *i.e.*, roughened and then coated with vaseline and cleaned with emery.

TABLE VII.

| Pressure by | Contact resistance, in microhms. | Joint resistance, in microhms. | Ratio : R/R'. |
|---|---|---|---|
| *Overlap* = 3 *in.* | | | |
| Four $\frac{3}{8}$-in. brass bolts— | | | |
| Initial | 1·4 | 3·18 | 0·97 |
| After 1 day | 1·2 | 2·94 | 0·89 |
| After 2 days | 1·2 | 2·94 | 0·89 |
| After 4 weeks | 1·35 | 3·10 | 0·94 |
| Four $\frac{1}{2}$-in. steel bolts | 1·3 | 3·00 | 0·91 |
| *Overlap* = $1\frac{1}{2}$ *in.* | | | |
| Two $\frac{1}{2}$-in. steel bolts | 2·06 | 3·07 | 1·87 |

Thus with a bar of this thickness and an overlap of 3 in. the predetermined figure obtained by means of the graphs for a pressure of 2,000 lb. per square inch and a contact resistance of 10 microhms per square inch would be R/R' = 0·92, which is in good agreement with the values given above for a bolted joint.

Comparing these results with values obtained with the hydraulic press, it would appear that four $\frac{3}{8}$-in. bolts produce a pressure equal to 2,000 lb. per square inch, and that there was no great difference in this particular case between $\frac{3}{8}$-in. bolts and $\frac{1}{2}$-in. bolts.

*Copper.*—A large number of tests were made with copper bars to determine the effect of bolting in various ways and the effective pressure exerted by bolts.

(1) Taking, first, small strips 1 in. × $\frac{1}{4}$ in. clamped together with a $\frac{3}{8}$-in. steel bolt, the values obtained were as given in Table VIII.

TABLE VIII.

| | | | |
|---|---|---|---|
| Length of overlap, inches | 2 | 1·5 | 1 |
| Contact resistance, microhms | 2·25 | 1·67 | 0·89 |
| Joint resistance | 5·0 | 3·8 | 2·35 |
| Value of R/R' | 0·95 | 0·95 | 0·94 |

With an overlap of 1 in. the pressure, applied by ram, corresponding to the values given above, was 3,000 lb. per square inch.

It will be noted that in this case, although the ratio R/R' was practically constant for

Digitized by Google

any overlap, the contact resistance decreased with the smaller overlap with a consequent increase of pressure per unit area.

TABLE IX.

| Overlap. | Number and size of bolts. | Contact resistance. | Joint resistance. | Value of R/R′. |
|---|---|---|---|---|
| inches. | | michroms. | michroms. | |
| 3 | 2 × ⅝ in. | 0·38 | 0·75 | 1·07 |
| | | 0·36 | 0·73 | 1·04 |
| | | 0·39 | 0·76 | 1·09 |
| | | 0·35 | 0·76 | 0·97 |
| 3 | 2 × ¾ in. | 0·43 | 0·84 | 0·99 |
| | | 0·44 | 0·85 | 1·09 |
| | | 0·45 | 0·86 | 1·10 |
| 6 | 2 × ⅝ in. | 0·54 | 1·26 | 0·90 |
| 6 | 4 × ⅝ in. | 0·29 | 1·01 | 0·72 |
| | | 0·28 | 1·00 | 0·71 |
| | | 0·18 | 0·90 | 0·64 |
| | | 0·37 | 1·06 | 0·74 |
| | | 0·41 | 1·20 | 0·77 |
| | | 0·19 | 0·91 | 0·65 |
| | | 0·35 | 1·14 | 0·73 |
| | | 0·21 | 0·93 | 0·66 |
| | | 0·17 | 0·87 | 0·64 |
| 6 | 5 × ⅝ in. | 0·35 | 1·14 | 0·73 |
| | | 0·5 | 1·28 | 0·82 |
| 6 | 2 × ¾ in. | 0·57 | 1·36 | 0·87 |
| 6 | 4 × ¾ in. | 0·34 | 1·13 | 0·72 |
| | | 0·42 | 1·20 | 0·77 |
| | | 0·47 | 1·23 | 0·79 |
| | | 0·33 | 1·12 | 0·72 |
| | | 0·37 | 1·16 | 0·74 |
| | | 0·29 | 1·08 | 0·69 |
| | | 0·36 | 1·15 | 0·74 |
| 6 | 5 × ¾ in. | 0·29 | 1·08 | 0·69 |
| | | 0·36 | 1·15 | 0·74 |

(2) *An Experiment directed solely to Determine the Pressure exerted by a Bolt.*—Strips of copper 2 in. × ⅜ in. were clamped together by a single ⅝-in. bolt.

| | |
|---|---|
| Length of overlap, inches | 2 |
| Contact resistance, microhms | 0·76 |
| Joint resistance, microhms | 1·70 |
| Value of R/R′ | 0·96 |

With the ram the pressure required to produce the same values was 2,300 lb. per square inch.

(3) Tests were made with a joint of 6-in. × ½-in. copper strip to determine the effect of varying the number of bolts used. The results are given in Table IX.

Digitized by Google

Further tests were made to compare the joint resistance with a single 1-in. bolt and special washers 4 in. in diameter, lent by Dr. FLECK, with the values for a 4-in. × ¾-in. bolt joint. The surfaces of the copper were carefully cleaned and special precautions were taken to ensure that all the bolts were fully tight. The results are given in Table X.

TABLE X.

| Number and size of bolts. | Overlap. | Conditions. | Contact resistance. | Joint resistance. | Value of R/R′. |
|---|---|---|---|---|---|
| | inches | | microhms | microhms | |
| 4 × ¾ in. | 6 | Tightened with ordinary spanner . | 0·62 | 1·35 | 0·94 |
| | | Tightened with long spanner . . | 0·51 | 1·28 | 0·85 |
| 1 × 1 in. | 6 | Tightened with special washers . . | 0·62 | 1·39 | 0·92 |
| 1 × 1 in. | 6 | Tightened with very long spanner | 0·73 | 1·50 | 0·99 |
| | | | 0·71 | 1·48 | 0·98 |
| | | | 0·79 | 1·56 | 1·03 |
| | | | 0·60 | 1·37 | 0·92 |
| | | | 0·71 | 1·48 | 0·98 |
| | | | 0·67 | 1·44 | 0·96 |
| | | | 0·75 | 1·52 | 1·01 |
| | | | 0·79 | 1·56 | 1·03 |
| 4 × ¾ in. | 3·8 | Tightened with ordinary spanner . | 0·21 | 0·71 | 0·73 |
| 1 × 1 in. | 3·8 | Tightened with ordinary spanner . | 0·55 | 1·05 | 1·08 |
| | | | 0·57 | 1·07 | 1·10 |
| | | | 0·57 | 1·07 | 1·10 |
| 1 × 1 in. | 3·8 | Tightened with ordinary spanner . | 0·82 | 1·32 | 1·36 |

While the Paper gives values which it is hoped will be of immediate use, it is clear that further work will have to be carried out on bolted joints, the results of which are somewhat conflicting. With the thinner strips the effective pressure for a given size of bolt is much higher than with the thicker strips, and observations of the surfaces after being clamped together would suggest that there is a slight bending of the material in the immediate neighbourhood of the bolts, which does not occur in the thicker strips. In the latter case, however, it is clear that a 4-in. overlap with four bolts makes a more effective joint than a 6-in. overlap, and also that while there was no great difference between 4-in. × ⅝-in. bolts and 4-in. × ¾-in. bolts, the use of five bolts of either size did not improve matters. The use of a single 1-in. bolt specially tightened and used with large washers designed to spread the pressure over a large surface gave a consistently higher value.

*Heating of Joints.*—Assuming that the conditions necessary for making an efficient joint have been observed, it will be obvious that, since the radiating surface is larger, the temperature-rise at the joint will be less than that of the rest of the conductor.

Some actual observations made with a 3-in. × $\frac{7}{16}$-in. bar, the joints being made by means of the clamps already mentioned, showed that with a given current the temperature-rise at the joint was 22° C., while that of the conductor itself was 33° C. Results with other sizes of bars showed the same order of difference and in the same direction.

Digitized by Google

## Appendix.

*References to Joints and Contacts.*

Binder, L.: "Der Widerstand von Kontakten", 'Elektrotechnik und Maschinenbau', vol. 30, p. 781, 1921.

Fleischbein, H. U.: "Neurungen an Kontakten und Kontakt Materialen", 'Elektrotechnische Zeitschrift', vol. 39, p. 445, 1918.

Harris, F. W.: "Electrical Contact Resistance", 'Electric Journal', vol. 10, p. 637, 1913.

Höpp, W.: "Die Berechnung von Kontakten", 'Elektrotechnische Zeitschrift', vol. 41, p. 205, 1920; "Über den Kontaktwiderstand", *ibid.*, p. 910.

Kraus, F.: "Über den Kontaktwiderstand", 'Elektrotechnik und Maschinenbau', vol. 30, p. 1, 1920.

Richter, R.: "Untersuchungen über die Grösse und Beständigkeit von Kontaktverbindungen", 'Elektrotechnische Zeitschrift', vol. 41, p. 345, 1920.

Smith, I. B.: "Contact Resistance", 'Journal of the Optical Society of America, and Review of Scientific Instruments', vol. 6, p. 500, 1922.

Digitized by Google

# THE RATING OF CABLES FOR INTERMITTENT OR FLUCTUATING LOADS

BY

S. W. MELSOM, A.M.I.E.E.,
PRINCIPAL ASSISTANT IN THE ELECTRICITY DEPARTMENT,

AND

H. C. BOOTH, A.R.C.S.,
ASSISTANT IN THE ELECTRICITY DEPARTMENT.

Digitized by Google

## ABSTRACT.

The extent to which the rating of a cable is affected by an intermittent or fluctuating load as compared with continuous running conditions is investigated theoretically, and formulæ are given by means of which the effect of any type of loading can be calculated.

It is shown by experimental determinations on various sizes and types of cables that the thermal time-constant can be calculated either from a heating or coiling curve of a particular cable, or from the specific heat and mass of the various components of the cable.

Tables are given showing the rating for the cables for which load tables are given in the I.E.E. Wiring Rules, on the same basis as for motors, *i.e.*, ½-hour and 1-hour ratings.


Digitized by Google

# THE RATING OF CABLES FOR INTERMITTENT OR FLUCTUATING LOADS.

By S. W. MELSOM, A.M.I.E.E., Principal Assistant in the Electricity Department, and H. C. BOOTH, A.R.C.S., Assistant in the Electricity Department.

[Reprinted from the 'Journal of the Institution of Electrical Engineers', Vol. 61, 1923.]

The question of the permissible current in cables used for supplying motors or other gear for such purposes as cranes, winches or hoists where the period of full-load current may be comparatively short, alternating with periods when the motor is running light or is shut down, was raised by the Ship Electrical Equipment Committee of the Institution of Electrical Engineers.

Goldschmidt* investigated the case of motors used for such work, and stated that long experience in actual practice has proved that in nearly every case a motor which stands a 1-hour test with a moderate temperature-rise is large enough for crane work. In modern practice, motors for such purposes are rated at ½ hour and 1 hour, depending on the conditions of use.

In the case of cables the time required to attain the maximum temperature is, as a rule, very much shorter than with motors, and it is necessary to consider them separately in order to ensure that the combination of motor and cable will be suitable for a given purpose.

In a previous Paper† the authors gave some results showing the order of increased rating that could be used for cables under intermittent load, the periods of variation being a few minutes, as would be the case in the actual use of a motor. These and other observations have been used in what follows.

For the mathematical treatment of the problem let—

$w$ = rate (in watts) of heat transmission through unit length of the covering of the cable for each degree C. of temperature excess above the surrounding air;

$c$ = heat capacity of unit length of cable per degree C. in watt-second units (joules);

$q$ (or Q) = rate (in watts) at which energy is being developed in unit length of the cable;

$\theta$ = temperature excess (referred to in the calculations below, for brevity, as "temperature");

$t$ = time in seconds.

* 'Journal I.E.E.', vol. 34, p. 660, 1905.

† 'Journal I.E.E.', vol. 47, p. 711, 1911; and N.P.L. 'Collected Researches', vol. 8, Paper VII, p. 113, *et seq.*



Digitized by Google

Then, if we assume that the heat dissipation is proportional to the temperature excess at any moment :—

$$q\,dt = c\,d\theta + w\theta\,dt,$$

or

$$\left(\frac{w}{c}\right)dt = \frac{d\theta}{(q/w - \theta)}.$$

Integrating

$$\left(\frac{w}{c}\right)t = -\log_e(\theta - q/w) + \log_e \mathrm{P},$$

where P = a constant of integration ; whence

$$e^{wt/c} = \frac{\mathrm{P}}{\theta - q/w}.$$

To find P, assume that when $t = 0$ the temperature $\theta$ has the initial value $\theta_1$, then

$$\mathrm{P} = \theta_1 - q/w,$$

$$e^{wt/c} = \frac{q/w - \theta_1}{q/w - \theta},$$

whence

$$\theta = e^{-wt/c}(\theta_1 - q/w) + q/w.$$

If the cable runs for $a$ seconds at Q watts, starting at an initial temeprature $\theta_2$, let the temperature attained be

$$\theta_1 = e^{-wa/c}(\theta_2 - \mathrm{Q}/w) + \mathrm{Q}/w.$$

If the cable then runs for $b$ seconds at $q$ watts, starting at an initial temperature $\theta_1$, let the temperature attained be

$$\theta_3 = e^{-wb/c}(\theta_1 - q/w) + q/w,$$

and if, then, $\theta_3 = \theta_2$ we have

$$\theta_1 = \frac{(\mathrm{Q}/w)(1 - e^{-wa/c}) + (q/w)(1 - e^{-wb/c})\,e^{-wa/c}}{1 - e^{-(a+b)w/c}}.$$

Or, since $\mathrm{Q}/w = \mathrm{M}$, the maximum temperature attained when running continuously at Q watts, and $q/w = m$, the maximum temperature attained when running continuously at $q$ watts, and writing $\gamma$ for $c/w$, where $\gamma$ is the thermal time-constant of the cable,

$$\theta_1 = \frac{\mathrm{M}(1 - e^{-a/\gamma}) + m(1 - e^{-b/\gamma})\,e^{-a/\gamma}}{1 - e^{-(a+b)/\gamma}}.$$

Taking the case of a cable running under crane-load conditions, where the motor runs at full load for $a$ minutes and at light load for $b$ minutes, and so on, intermittently for a

Digitized by Google

long period, the increased rating for the same temperature-rise as would be attained if the cable were loaded continuously at its normal continuous rating of I amperes, can be calculated as follows :—

Let $i$ be the current on light load and $si$ the maximum load current, $s$ being the ratio of the maximum to the light-load current.

Taking the general case of temperature elevation under a fluctuating load of this kind, we have

$$\theta = \frac{M(1 - e^{-a/\gamma}) + m(1 - e^{-b/\gamma})e^{-a/\gamma}}{1 - e^{-(a+b)/\gamma}}.$$

If the watts developed by $i$ amperes be $q = i^2r$, where $r$ is the resistance of unit length of cable at the maximum temperature, then with $si$ amperes the watts developed will be $q = s^2i^2r$. We have, therefore,

$$M = \frac{s^2i^2r}{w} \qquad \text{and} \qquad m = \frac{i^2r}{w},$$

and the maximum temperature elevation will be

$$\theta = \frac{i^2r}{w}\left[\frac{s^2(1 - e^{-a/\gamma}) + (1 - e^{-b/\gamma})e^{-a/\gamma}}{1 - e^{-(a+b)/\gamma}}\right].$$

The maximum temperature elevation for continuous running with I amperes will be $I^2r/w$, and this must equal $\theta$, whence we obtain—

$$si = Is\sqrt{\left[\frac{1 - e^{-(a+b)/\gamma}}{s^2(1 - e^{-a/\gamma}) + (1 - e^{-b/\gamma})e^{-a/\gamma}}\right]},$$

or, if $si = nI$, where $n$ is the rating factor, we have

$$n = s\sqrt{\left[\frac{1 - e^{-(a+b)/\gamma}}{s^2(1 - e^{-a/\gamma}) + (1 - e^{-b/\gamma})e^{-a/\gamma}}\right]}.$$

Thus, if the cable were rated to run at 200 (= I) and if $a = 4$ minutes (240 secs.), $b = 6$ minutes (360 secs.), $\gamma = 1{,}300$ seconds, and $s = 2$, then

$$n = 2\sqrt{\left[\frac{1 - e^{-600/1300}}{2^2(1 - e^{-240/1300}) + (1 - e^{-360/1300})e^{-240/1300}}\right]}$$
$$= 1{\cdot}304,$$

and the maximum permissible current during the full-load period is

$$si = 1{\cdot}304 \times 200 = 261 \text{ amps.}$$

A simpler problem arises out of the decision of the I.E.E. Committee that cables should be rated on the same basis as the motors used, *i.e.*, at a $\frac{1}{2}$-hour and 1-hour rating. For the calculation of the rating factor to suit these conditions, only the initial part of the appropriate heating curve need be considered.

Digitized by Google

On the assumptions made, the temperature of a cable as deduced from the general equation, at any time $t$ after switching on, will be

$$\theta = M(1 - e^{-t/\gamma}),$$

where M is the maximum final temperature.

Let $M_0$ be the final permissible maximum temperature attained when running with the rated current $I_0$. To a first approximation

$$M_0/M = (I_0/I)^2,$$

therefore

$$\theta = M_0 (I/I_0)^2 (1 - e^{-t/\gamma}),$$

whence

$$I = \frac{I_0 \sqrt{(\theta/M_0)}}{\sqrt{(1 - e^{-t/\gamma})}}.$$

If I is greater than $I_0$, but $\theta$, the temperature attained after the interval $t$, is not to exceed $M_0$, we have for the rating factor $n$ :—

$$I = I_0 \frac{1}{\sqrt{(1 - e^{-t/\gamma})}},$$

or

$$n = \frac{1}{\sqrt{(1 - e^{-t/\gamma})}}.$$

For the $\frac{1}{2}$-hour rating, $t$ is 1,800 seconds, and for the 1-hour rating, 3,600.

It will be seen that these formulæ require that the thermal time-constant $\gamma$ should be known. This quantity is the ratio of the heat capacity of the cable to the rate at which heat, measured in the same units, would be transmitted from the cable if the temperature excess were 1 degree C. Regarded from another point of view it is the time that would be required for the cable to reach the maximum temperature corresponding to any current if, with this current passing through the cable, all dissipation of heat to external space were prevented and the heat generated by the current were applied solely to heating the cable.

Thus, if M be the maximum temperature excess attained when the current is running at Q watts, and if $c$ be the heat required to raise the temperature of the cable 1 degree C., then the heat capacity of the cable when raised in temperature M degrees is $Mc$. When it has reached its maximum temperature corresponding to the current carried, and conditions have in consequence become stationary, the heat dissipated per second by the cable, $w$M, is equal to the heat generated, *i.e.*,

$$w\mathrm{M} = \mathrm{Q} = \mathrm{I}^2 r,$$

where $r$ is the resistance and I the current. Therefore the time required to reach the maximum temperature M, if no heat were radiated from the cable, would be

$$\frac{Mc}{Q} = \frac{Mc}{Mw} = \frac{c}{w} = \gamma,$$

Digitized by Google

a quantity which is therefore defined as the " thermal time-constant ", since it will be the same whatever maximum temperature be considered.

The thermal time-constant of a cable can, therefore, be approximately calculated if we know the weight and specific heats of its various components and the final temperature-rise corresponding to a given current.

The temperature of the core will be generally higher than that of the surrounding layers of insulating and other materials. If in order to simplify the calculation it be assumed that the whole of the cable attains the temperature of the core, it would seem as if the value of the thermal time-constant calculated on this assumption should be somewhat in excess of its true value. This error would, however, appear to be very largely compensated for by the fact that in practice a cable is not freely suspended in air, but is in immediate contact with some support, which also shares to some extent in the temperature-rise of the cable. A comparison of the results obtained by calculation of the constant from the dimensions and thermal quantities of the cable with those obtained by the more direct experimental method next to be described would seem to indicate that, within the limits of accuracy required in the evaluation of the constant, the first method affords a satisfactory approximation.

For the calculation of the thermal time-constant from the heating curve we can proceed as follows :—

Since at any time $t$ after switching on, the temperature excess

$$\theta = \mathrm{M}(1 - e^{-t/\gamma}),$$

where M, as before, is the final maximum temperature, we have

$$\log_{10}\left(\frac{\mathrm{M}}{\mathrm{M} - \theta}\right) = t\frac{(0{\cdot}4343)}{\gamma}.$$

If a series of values of $\theta$ are available for various time intervals after switching on, and if we know M the maximum final temperature, then, on plotting the values of $\log_{10}[\mathrm{M}/(\mathrm{M} - \theta)]$ derived from the values of $\theta$, against corresponding values of $t$, we should obtain a straight line passing through the origin, the slope of which line should be equal to $0{\cdot}4343/\gamma$. This affords a criterion as to how nearly the heating curve follows the exponential law here assumed, and also, if the slope be measured in the proper units, a means of evaluating the constant $\gamma$.

In practice, however, this particular method is somewhat difficult in application. Values derived from the first part of the heating curve are liable to error because here the temperature is changing very quickly. In the initial stages of the heating curve the temperature of the core will also be considerably higher than that of the covering, and this would tend to make the value of the thermal time-constant derived from this part of the curve too low.

For the latter part of the curve when $\theta$ is approaching its limiting value M, the term

Digitized by Google

$(M - \theta)/\theta$ becomes uncertain, since $(M - \theta)$ is the difference of two nearly equal quantities, one of which, M, requires a very long and careful observation for its exact determination.

For this reason, therefore, it is preferable to use the cooling curve. For this we have $\theta = \theta_0 e^{-t/\gamma}$, where $\theta_0$ is the initial temperature for $t = 0$. From this it follows that

$$\log_{10}(\theta_0/\theta) = (t/\gamma)\log_{10} e = 0{\cdot}4343t/\gamma,$$

so that if a series of values of $\log_{10}(\theta_0/\theta)$ be plotted against $t$, a straight line passing through the origin should be obtained the slope of which should again be equal to $0{\cdot}4343/\gamma$.

As this does not necessitate the determination of the maximum temperature it is generally the more convenient method.

Some illustrative examples of these three methods of determining the thermal time-constant will now be given. They will also serve to show the sort of consistency obtainable by the various methods and to what extent it is permissible to rely on a calculation of the thermal time-constant derived from the dimensions and specific heat of the cable in place of determinations based on the characteristics of the heating or cooling curves as obtained by direct experiment.

*Example* (1). *A rubber-covered* 0·094 *sq. in. cable.*—In fig. 1 the values of $\log_{10}[M/(M - \theta)]$ are shown plotted against time for (A) the heating curve, and of $\log_{10}(\theta_0/\theta)$ for (B) the cooling curve.

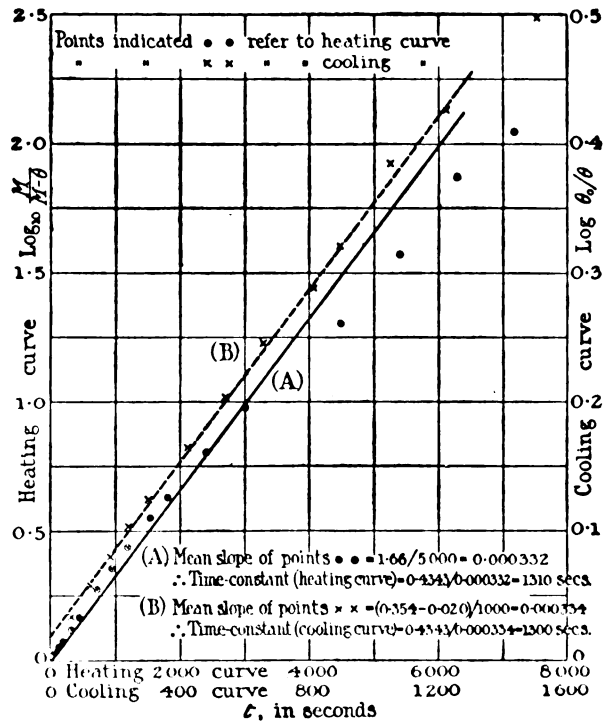


Fig. 1. Determination of the time-constant of a 19/14 S.W.G. rubber-covered cable by means of the heating and cooling curves.

Digitized by Google

The slope of the best mean straight line through these points has been measured and the constant, $\gamma$, obtained by dividing 0·4343 by the slope. The values are :—

(*a*) Heating curve $\gamma = 1{,}310$ seconds.

(*b*) Cooling curve $\gamma = 1{,}300$ seconds.

The evaluation of the thermal time-constant of this cable by means of the dimensions and specific heat is as follows :—

The total heat capacity of the cable is here the sum of two components :—

(1) The heat capacity of the conductor based on weight of copper × specific heat = 2·135 watt-seconds.

(2) The heat capacity of the covering, rubber and braiding = 2·79 watt-seconds.

Hence $c$, the total heat capacity per cm., = 4·925 watt-seconds.

The value for the covering is derived from a direct determination of the specific heat of rubber and braiding made on a small sample taken from the cable. The actual value obtained was 0·39 calorie (= 1·63 watt-second units) per gramme per degree C., and is subject to a possible error of ± 3 per cent. The heat capacity of the covering is obtained by multiplying the value of the specific heat, given above, by the weight of the covering per unit length of cable, which weight was determined on a length of about a yard of covering.

The resistance of unit length of conductor of the 0·094-sq. in. cable at 15·6° C. was $2{\cdot}86 \times 10^{-6}$ ohms, and since for a current of 169 amperes maintained continuously there was a temperature-rise of 21·8 degrees C., the resistance at the higher temperature is

$$r = [1 + (0{\cdot}004 \times 21{\cdot}8)]\,2{\cdot}86 \times 10^{-6} = 3{\cdot}11 \times 10^{-6}\ \text{ohm/cm.}$$

Hence

$$I^2r = wM = 3{\cdot}11 \times 10^{-6} \times 169^2 = 8{\cdot}83 \times 10^{2}\ \text{watt,}$$

and

$$w = \frac{8{\cdot}83 \times 10^{-2}}{21{\cdot}8} = 4{\cdot}06 \times 10^{-3}\ \text{watt.}$$

Thus the thermal time-constant

$$\gamma = c/w = 4{\cdot}925/(4{\cdot}06 \times 10^{-3}) = 1\,210\ \text{seconds.}$$

*Example* (2). *A lead-covered paper-insulated single* 0·1*-sq. in cable* [*see fig.* 2 (A)].—Only the heating curve was available. The value deduced from the slope of the plotted values of $\log_{10}[M/(M - 0)]$ was $\gamma = 1{,}270$ seconds.

For the total heat capacity of unit length of cable we have :—

| | | |
|---|---|---|
| (1) Conductor . . . . . | 2·14 | watt-sec. units. |
| (2) Lead covering . . . . . | 1·59 | „ „ |
| (3) Paper and oil . . . . . | 1·62 | „ „ |
| Total heat capacity $c$ . . . . . | = 5·35 | „ „ |

$$w = \frac{I^2r}{M} = \frac{200^2 \times 2{\cdot}79 \times 10^{-6}[1 + (0{\cdot}004 \times 30)]}{30} = 4{\cdot}16 \times 10^{-3}\ \text{watt,}$$

Therefore

$$\gamma = c/w = 5{\cdot}35/(4{\cdot}16 \times 10^{-3}) = 1{,}290\ \text{seconds.}$$



Digitized by Google

Here again the values for the impregnated-paper insulation were derived from a determination of the specific heat of a sample taken from a cable, the actual values being—

0·37 calorie (= 1·54 watt-second units) per gramme per degree C.

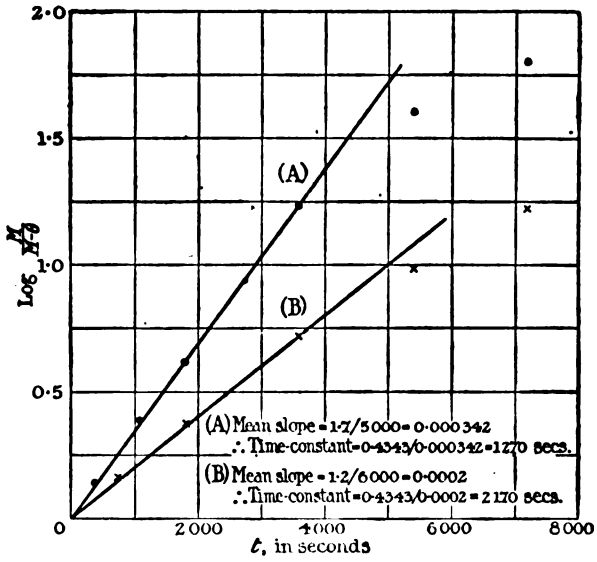


Fig. 2. Determination of the time-constant of two lead-covered paper-insulated cables.
(A) 0·1 sq. in. single. (B) 0·1 sq. in. concentric.

*Example* (3). *A lead-covered paper-insulated concentric* 0·1*-sq. in. cable* [*see fig.* 2 (B)]. —Only the heating curve was available. The value deduced from the slope of the plotted values of $\log_{10}$ [M/(M − θ) was $\gamma = 2{,}170$ seconds. In this case θ was the mean value of the temperature-rises of the inner and outer conductors respectively.

For the total heat capacity of unit length of cable we have :—

| | | |
|---|---|---|
| (1) Conductor (inner and outer) . . . . . | 4·27 | watt-sec. units. |
| (2) Lead covering . . . . . | 2·77 | ,, ,, |
| (3) Paper and oil . . . . . | 4·93 | ,, ,, |
| Total heat capacity per cm. $c$ . . . . . | =11·97 | ,, ,, |

$$w = \frac{I^2 r}{M} = \frac{2 \times 170^2 \times 2{\cdot}7\,[1 + (0{\cdot}004 \times 30{\cdot}6)]\,10^{-6}}{30{\cdot}6} = 5{\cdot}72 \times 10^{-3} \text{ watt.}$$

Therefore

$$\gamma = c/w = 11{\cdot}97/(5{\cdot}72 \times 10^{-3}) = 2{,}100 \text{ seconds.}$$

*Example* (4).—*A high-tension three-core paper-insulated armoured cable on which a number of heating curves both of core and lead sheath were taken, special attention being directed to*

Digitized by Google

*accuracy of the intermediate observations on the curve.*—In fig. 3 are plotted the values of $\log_{10}[M/(M - \theta)]$ against time, (A) referring to the temperature of the core only, and (B) to the average temperature of core and sheath. The values of the thermal time-constant are 7,580 seconds from curve (A), and 7,330 seconds from curve (B), as against the value of 7,100 seconds deduced from the dimensions and thermal constants of the components of the cable. In calculating the heat capacity, the effect of the armouring has been ignored, since it is separated from the lead sheath by tape and obviously cannot be regarded as adding appreciably to the heat capacity of the cable.

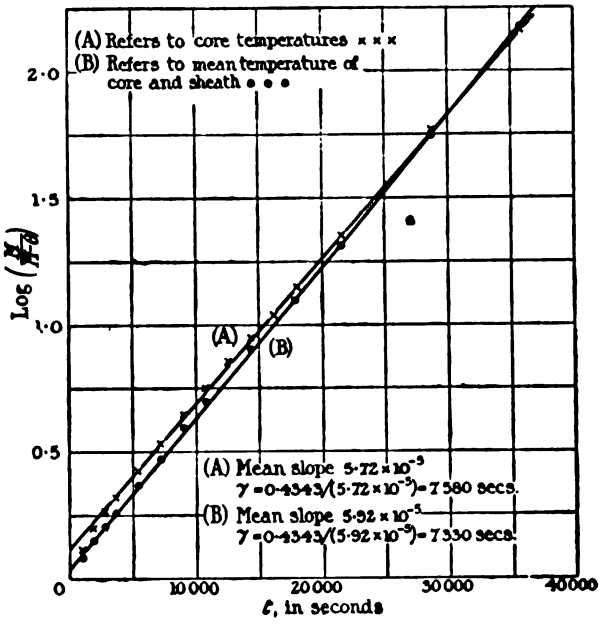


Fig. 3. Determination of the time-constant of a high-tension three-core paper-insulated cable with lead covering and armouring.

In the first example there is a difference of about 7 per cent. between the two determinations, which, however, is not large when the difficulties of the various measurements are taken into account. It is, of course, possible that the difference arises from the fact that the two methods of determination apply to conditions that are not strictly comparable. The heating or cooling curve refers to a cable in contact with the floor (the effect of which is nearly equivalent to that of a wood casing or iron pipe), whereas the calculation from the dimensions and specific heats of the constituent parts of the cable leaves this factor entirely out of account.

The following examples will serve to show the effect on the rating factor of an uncertainty of this order in the evaluation of the thermal time-constant. Taking the formula for the calculation of the rating factor in the case already quoted (p. 400), *i.e.*, a cable which runs for 4 minutes at full load and 6 minutes at half load, it was found that if the thermal time-constant were taken as 1,300 seconds the " full " current could be increased to 1·304 times the normal current for continuous rating. If instead of 1,300 seconds the



Digitized by Google

thermal time-constant were here taken as 1,200 seconds, then the value obtained for the rating factor would be

$$n = 2\sqrt{\left[\frac{(1-e^{-600/1200})}{4(1-e^{-240/1200})+(1-e^{-360/1200})e^{-240/1200}}\right]}$$
$$= 2\sqrt{\left[\frac{0\cdot3935}{(4\times0\cdot1813)+(0\cdot2593\times0\cdot8187)}\right]} = 1\cdot295,$$

a difference of less than 1 per cent.

Take next the formula for the $\frac{1}{2}$-hour rating

$$n = \frac{1}{\sqrt{(1-e^{-T/\gamma})}},$$

where T the working period is $\frac{1}{2}$ hour (= 1,800 secs.). If $\gamma$ = 1,200,

$$n = \frac{1}{\sqrt{(1-e^{-1800/1200})}} = \frac{1}{\sqrt{(1-0\cdot2231)}} = 1\cdot134.$$

But if we take $\gamma$ = 1,300

$$n = 1/\sqrt{(1-e^{-1800/1390})} = 1/\sqrt{(1-0\cdot2503)} = 1\cdot155,$$

a difference of 1·9 per cent. for a variation of 8 per cent. in the thermal time-constant.

Table I gives the time-constants and the direct multiplying factor both for $\frac{1}{2}$-hour and 1-hour rating for low-tension cables of sizes and dimensions as shown in the I.E.E.

TABLE I.

| Cable size (nominal). | Thermal time-constant. | | Multiplying factor for rubber. | | Multiplying factor for paper. | |
|---|---|---|---|---|---|---|
| | Rubber. | Paper. | $\frac{1}{2}$-hour rating. | 1-hour rating. | $\frac{1}{2}$-hour rating. | 1-hour rating. |
| sq. in. | secs. | secs. | | | | |
| 0·0145 | 520 | 700 | 1·02 | 1·00 | 1·05 | 1·00 |
| 0·0225 | 600 | 760 | 1·03 | 1·00 | 1·06 | 1·01 |
| 0·04 | 890 | 900 | 1·07 | 1·01 | 1·09 | 1·01 |
| 0·06 | 1,090 | 1,050 | 1·11 | 1·02 | 1·12 | 1·02 |
| 0·075 | 1,350 | 1,150 | 1·17 | 1·04 | 1·15 | 1·03 |
| 0·1 | 1,520 | 1,320 | 1·21 | 1·05 | 1·18 | 1·04 |
| 0·12 | 1,630 | 1,430 | 1·23 | 1·06 | 1·20 | 1·05 |
| 0·15 | 1,830 | 1,600 | 1·26 | 1·08 | 1·23 | 1·06 |
| 0·2 | 2,190 | 1,850 | 1·34 | 1·11 | 1·27 | 1·08 |
| 0·25 | 2,440 | 2,070 | 1·38 | 1·14 | 1·32 | 1·10 |
| 0·3 | 2,810 | 2,250 | 1·46 | 1·18 | 1·36 | 1·13 |
| 0·4 | 3,390 | 2,620 | 1·57 | 1·24 | 1·43 | 1·17 |
| 0·5 | 3,690 | 2,925 | 1·61 | 1·27 | 1·49 | 1·20 |
| 0·6 | 4,060 | 3,185 | 1·67 | 1·30 | 1·54 | 1·23 |
| 0·75 | 4,100 | 3,520 | 1·68 | 1·31 | 1·60 | 1·26 |
| 1·0 | 4,510 | 3,970 | 1·74 | 1·35 | 1·66 | 1·30 |

Digitized by Google

Wiring Rules, and Table II gives the actual permissible currents for this type of rating, and the sizes of cables which may be used for ratings of ½ hour and 1 hour in place of the sizes at present specified in the Wiring Rules for continuous loading.

TABLE II.

| Cable size (nominal). | Permissible current. | | | Size of cable that will carry same current as for continuous rating, but for— | |
|---|---|---|---|---|---|
| | ½-hour rating. | 1-hour rating. | Continuous rating as in I.E.E. Wiring Rules. | (1) ½ hour. | (2) 1 hour. |
| | | | *Rubber cables.* | | |
| sq. in. | amps. | amps. | amps. | sq. in. | sq. in. |
| 0·0145 | 38 | 37 | 37 | 0·0145 | 0·0145 |
| 0·0225 | 47 | 46 | 46 | 0·0225 | 0·0225 |
| 0·04 | 68 | 65 | 64 | 0·04 | 0·04 |
| 0·06 | 92 | 85 | 83 | 0·06 | 0·06 |
| 0·075 | 113 | 101 | 97 | 0·075 | 0·075 |
| 0·1 | 142 | 124 | 118 | 0·1 | 0·1 |
| 0·12 | 160 | 138 | 130 | 0·1 | 0·12 |
| 0·15 | 191 | 164 | 152 | 0·12 | 0·15 |
| 0·2 | 247 | 204 | 184 | 0·15 | 0·2 |
| 0·25 | 295 | 244 | 214 | 0·2 | 0·25 |
| 0·3 | 351 | 283 | 240 | 0·2 | 0·25 |
| 0·4 | 452 | 357 | 288 | 0·25 | 0·3 |
| 0·5 | 534 | 422 | 332 | 0·3 | 0·4 |
| 0·6 | 641 | 499 | 384 | 0·4 | 0·5 |
| 0·75 | 774 | 604 | 461 | 0·5 | 0·6 |
| 1·0 | 1,036 | 803 | 595 | 0·6 | 0·75 |
| | | | *Paper cables.* | | |
| 0·0145 | 60 | 57 | 57 | 0·0145 | 0·0145 |
| 00·225 | 79 | 75 | 75 | 0·0225 | 0·0225 |
| 0·04 | 113 | 105 | 104 | 0·04 | 0·04 |
| 0·06 | 151 | 138 | 135 | 0·06 | 0·06 |
| 0·075 | 180 | 162 | 157 | 0·075 | 0·075 |
| 0·1 | 225 | 199 | 191 | 0·1 | 0·1 |
| 0·12 | 252 | 220 | 210 | 0·1 | 0·12 |
| 0·15 | 303 | 261 | 246 | 0·12 | 0·15 |
| 0·2 | 376 | 320 | 296 | 0·15 | 0·2 |
| 0·25 | 453 | 377 | 343 | 0·2 | 0·25 |
| 0·3 | 523 | 435 | 385 | 0·25 | 0·3 |
| 0·4 | 663 | 543 | 464 | 0·3 | 0·4 |
| 0·5 | 804 | 648 | 540 | 0·4 | 0·5 |
| 0·6 | 960 | 767 | 624 | 0·4 | 0·5 |
| 0·75 | 1,180 | 930 | 738 | 0·5 | 0·6 |
| 1·0 | 1,548 | 1,211 | 932 | 0·6 | 0·75 |

The thanks of the authors are due to Mr. S. BUTTERWORTH for his kindness in checking the mathematical portions of the work, and to Dr. EZER GRIFFITHS who determined the values of the heat capacity of the dielectric covering materials.

Digitized by Google

Digitized by Google

# CARBON ARCS FOR SEARCHLIGHTS

BY

C. C. PATERSON, O.B.E., M.I.E.E., A.M.I.C.E.,
SOMETIME PRINCIPAL ASSISTANT,

J. W. T. WALSH, M.A., M.Sc., A.M.I.E.E., F.Inst.P.,
SENIOR ASSISTANT,

A. K. TAYLOR, A.C.G.I., M.I.E.E., A.M.I C.E.,
TEMPORARY RESEARCH WORKER,

AND

W. BARNETT,
SENIOR OBSERVER IN THE ELECTRICITY DEPARTMENT.

Digitized by Google

## ABSTRACT.

This Paper describes a series of experiments undertaken—

(*a*) To develop the best method of testing carbons in order to prove their value for searchlights :

(*b*) To compare the relative performances of 13 different types of carbons (not including the flame carbons) :

(*c*) To determine what improvement is possible in the carbons themselves or in the methods of burning them.

Experiments were made with two devices having for their object the control of the arc and its maintenance in the central part of the crater. In general, for any one carbon, the candle-power was found to increase linearly with the current ; further, the efficiency in the candle-power per ampere was found to increase with the diameter of the positive carbon for the same current density.


Digitized by Google

# CARBON ARCS FOR SEARCHLIGHTS.

By C. C. PATERSON, O.B.E., M.I.E.E., A.M.I.C.E., Sometime Principal Assistant, J. W. T. WALSH, M.A., M.Sc., A.M.I.E.E., F.Inst.P., Senior Assistant, A. K. TAYLOR, A.C.G.I., M.I.E.E., A.M.I.C.E., Temporary Research Worker, and W. BARNETT, Senior Observer, in the Electrical Department.

[Reprinted from the 'Journal of the Institution of Electrical Engineers', Vol. 58, 1920.]

1. *Synopsis.*—This Paper describes a series of experiments undertaken at the request of the Admiralty (D.T.M. Dept.) and is published by permission. Their object was—

(*a*) To develop the best method of testing carbons in order to prove their value for searchlights.

(*b*) To compare the relative qualities of existing carbons, other than flame carbons, for producing high-intensity searchlight beams.

(*c*) To determine what improvement can be made either in the carbons themselves or in the methods of burning them.

It was at first proposed to make measurements of illumination at different parts of a searchlight beam under actual working conditions in the open, but the sources of error encountered were so great as to cause this method to be abandoned in favour of an indoor method of test, at any rate for the first series of experiments.

In the Laboratory the carbons were burned in an integrating photometer of cubical form, and simultaneous measurements were made of the average candle-power given by the arc and of the surface brightness of the positive crater. The apparatus is fully described in the body of the Paper and illustrated diagrammatically in fig. 1.

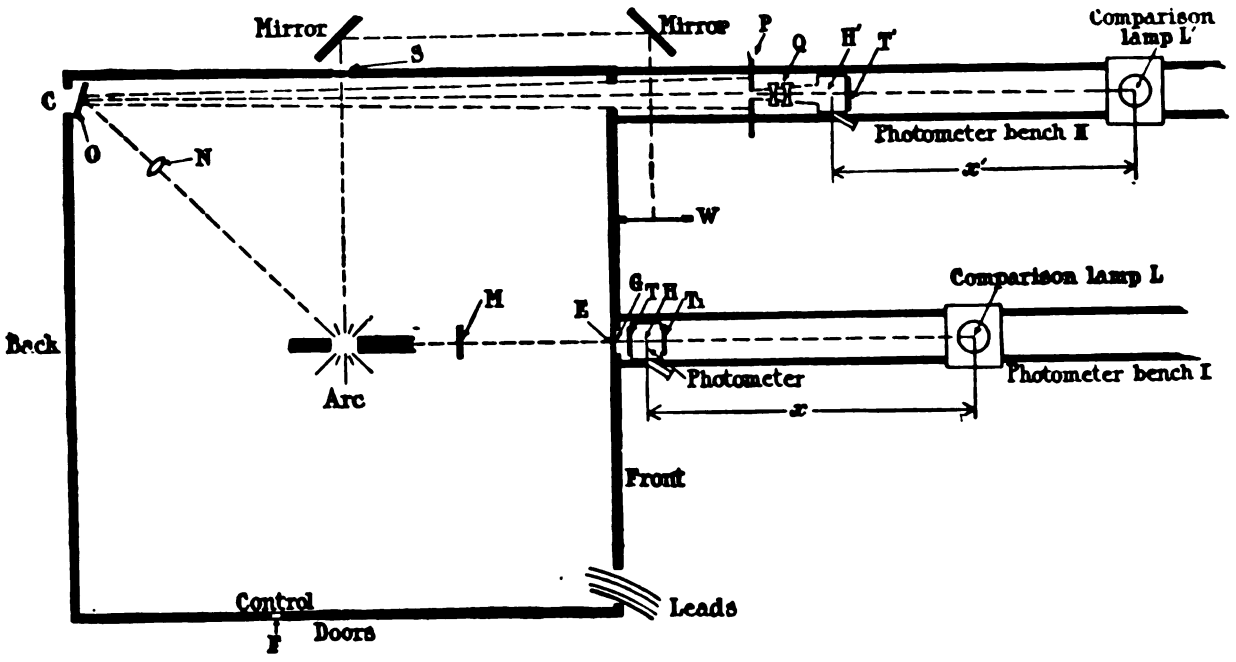


Fig. 1. Diagram of apparatus, etc.



Digitized by Google

By this method a comparison was made of 13 different types of carbons, both those already in use in the British and French Services, and others specially prepared by the General Electric Company. Experiments were made with two devices having for their object the control of the arc and its maintenance in a central part of the crater to ensure even burning of the carbons.

One of these was an electromagnetic device, while the other depended upon a slow rotation of the positive carbon. For high current densities (0·3 ampere per sq. mm. and over) it was necessary to copper both positive and negative carbons. It was found that while change of potential difference on the arc produced no definite detectable change of candle-power, an increase in arc length beyond a certain value produced a decrease both of crater brilliancy and of candle-power. It seems likely that if allowance is made for the light obscured by the negative carbon, the shortening of the arc will be found to produce an increased average candle-power even at short arc lengths, but the exact amount of the obscuration is difficult to determine with accuracy, as is shown in section 19 of the Paper.

In general it seems to be clearly established that for any one carbon the candle-power increases linearly with the current, while the crater brightness also shows a real increase, though its magnitude is not sufficient to determine the form of the relationship in this case.

For the types of carbon considered, and apart from smoothness of running, there seems to be no definite difference of any magnitude either in average candle-power or crater brightness for carbons of the same diameter run at the same current. The efficiency in candle-power per ampere increases, however, for the same current density as the diameter of the positive carbon is increased.

## 1. *Methods of Test.*

2. *Open Air Measurements.*—When the investigation was started it was expected that large differences would be found in the light yielded by the various carbons, and it was proposed to burn them in a searchlight in the open, measuring the intensity of the resulting beam. It was realized that varying atmospheric conditions and differences in the carbons themselves would be disturbing factors, but it was hoped that with careful arrangements for estimating the atmospheric scattering of the light and by taking the average of a large number of readings, these factors would become inappreciable compared with the differences in the light emitted by the carbons themselves. Searchlights were therefore set up, and an 800-yard horizontal course was arranged from the Laboratory across Bushey Park. The measuring station at the other end of the course was fixed, and the projector in use was turned through the necessary angles. These were measured by means of a telescope fixed to the case and sighted on to a distant scale. Arrangements were also made so that an image of the arc was projected on to a screen, and thus it was possible accurately to fix the position of the positive crater with reference to the projector mirror.

Digitized by Google

For measuring the loss of light due to atmospheric scattering, an Ediswan tungsten arc (Pointolite) lamp was used in the focus of a second searchlight mirror and the beam projected along the course to a photometer 300 yards away. The other side of the photometer received a second beam of the same light which had been reflected by optically ground mirrors so that it travelled through a length of the atmosphere some $2\frac{1}{2}$ times as long as the direct beam. It was expected by comparing the intensities of these two beams to obtain a sufficiently accurate estimate of the atmospheric condition to enable corrections to be applied to the illumination measurements. It was found, however, that the actual differences of beam intensity yielded by the different carbons (other than special flame carbons) were relatively small, and that the various sources of uncertainty in the conditions were sufficient to mask such differences completely.

3. *Sources of Uncertainty of Measurements in the Open.*—Before passing to the alternative method of procedure it is desirable to discuss some of the difficulties met with in measurements out of doors.

(*a*) *Scattering of Light by Particles of Moisture.*—Very often the atmosphere in the daytime is exceedingly clear, giving promise of a fine night for measurements, but shortly after dark the illumination in a searchlight beam is found to be falling. When this is first noticed the atmosphere, to ordinary observation, does not appear to be very different, but when the illumination has fallen by some 25 per cent. the scattering of the light becomes noticeable. Two nights both adjudged to be clear have been found to yield differences in illumination of more than 25 per cent. Over the course in Bushey Park a still night in fine weather never remains clear sufficiently long for a proper series of measurements. The atmosphere is also patchy ; at one moment it may be reasonably clear and at another a local cloud of haze may drift over one section of the course. This may readily be seen in misty weather, but the same condition must exist in a lesser degree when the haze is too attenuated to be observed. This accounts for the appreciable up and down variations in brilliancy which were sometimes noticed in the course of a set of readings lasting for, say, 30 minutes.

Probably a clear breezy night gives the best promise of good atmospheric conditions, but a breeze often drops when darkness sets in and bad conditions again prevail.

(*b*) *Draughts in the Searchlight.*—Broken weather with considerable wind, if not actually rainy, causes a bad condition of draught in the searchlight and irregular burning of the carbons.

(*c*) *Position of Positive Carbon in Relation to the Mirror.*—When the arc is burning well there is little difficulty in ensuring that the position of the crater is correct in relation to the mirror, but any slight burning away on one side makes this uncertain and causes the distribution of illumination over the beam to change.

(*d*) *Variations in the Carbons Themselves.*—A given type of carbon does not yield uniform results, nor does one carbon over its whole length. Differences may amount to as much as 35 per cent. It is necessary to obtain the average behaviour of a large number of carbons of any one type before a conclusion can be drawn as to relative merits.



Digitized by Google

(*e*) *Mirror.*—Results, to be comparable, must clearly be made with the same mirror, and apart from it are not likely to have any absolute value.

(*f*) *Measuring Apparatus.*—Measuring apparatus, which is necessarily of a portable character for searchlight tests in the open, must be regarded as liable to an uncertainty of at least ± 5 per cent.

If it were not for atmospheric scattering of the light, the other variables might be eliminated by taking the average of a large number of readings, but the infrequent occurrence of suitable conditions for testing makes this virtually impossible in this climate.

All results of measurements in the open should therefore be subject to very careful scrutiny to see that the above sources of error are negligible compared with the differences of brightness which are being looked for.

4. *Laboratory Measurements.*—In the Laboratory method of test which was adopted in place of tests in the open air with projectors, the carbons were examined alone without any mirror. Two quantities have mainly to be considered :—

(i) The total flux of light emitted by the carbons alone.
(ii) The intrinsic brightness of the positive crater.

Of these the second is the more important for present purposes, since it is a measure of the intensity in the beam of the projector ; for, if the brightness of the crater of one carbon is greater than that of another, the beam will be correspondingly brighter. If, therefore, crater brightness can be accurately measured, we have a direct criterion of the ability of the carbon to yield a high intensity beam, provided the searchlight is adjusted to give a beam of minimum divergence. If, however, a beam of given divergence is obtained, the intensity will be directly proportional to the total flux of light given by the positive crater, whatever its size or brightness. For this purpose, therefore, the more important factor is the total flux emitted towards the mirror, or, what may be taken as proportional to it for ordinary carbons, the average candle-power of the crater in directions embraced by the mirror. It is shown later that for a given current an increase in intrinsic brightness is produced by an increase in current density. Hence it follows that improvements in ordinary searchlight carbons are mainly obtained by reducing the diameter of the positives if the current is to be kept at the same value. This seems to be true for all carbons which depend for their light upon the incandescence of the crater surface. The total flux for a given current also increases with the current density but apparently at a lower rate than the crater brightness.

There is a class of flame carbons such as those used in the Beck, Harrison, or Sperry lamps to which this general statement does not apply. These carbons mainly depend on the light emitted by vapour in the arc and close to the positive ; these carbons are not considered here.

It is, of course, obvious that a quantity which it would be useful to measure in addition to the total flux is the flux emitted within the solid angle embraced by the mirror. The

Digitized by Google

light received by the mirror (together with that obscured by the negative carbon) represents some 70 per cent. of the total light emitted from the positive crater—if this radiates as a true diffusing surface, *i.e.*, as if it were a disc emitting the same total quantity of light as the crater from one of its faces. The proportion of the whole light which actually reaches a given mirror, therefore, depends only on the symmetry of burning of the carbon and the extent of obscuration of the negative carbon. For ordinary purposes it may probably be safely assumed that measurement of total flux bears a very constant ratio to that received by the mirror so long as the crater has not burned unsymmetrically, *i.e.*, in such a way that it shows its incandescent surface when viewed at right angles to the axis of the carbon. There is also the small proportion of the light due to the incandescent tip of the negative and the luminosity of the arc itself, to be taken into account; but the difficulties of making measurements of the light emitted within a given solid angle have resulted in the decision to postpone this and to base the preliminary results given in this Paper on the measurements of total flux, which are more readily obtained. It is intended, however in due course to extend the methods of measurement here described to the investigation of the amount of light emitted within certain solid angles.

5. *General Description of Apparatus.*

(*a*) *Measurement of Total Flux.*—The principle of the integrating globe photometer has been employed, but, following a suggestion by Dr. W. E. SUMPNER* that, to a fairly close approximation, a whitened cube would give as good results as a sphere, this form of integrator has been adopted for the purposes of the present investigation. A cube has great advantages for projector lamp work in that it has a flat floor upon which the lamp can be supported, and it can have doors at the side permitting easy access for adjustment and examination of the lamp. Further, it is much more easy to construct than a sphere, particularly in the large sizes required for projector arc lamps whose average candle-power is of the order of 30,000 candles. It is necessary, however, to choose for the calibration of the cube a standard lamp which has approximately the same distribution of light as the lamp to be tested.

(*b*) *Detailed Description of Parts of Apparatus.*—(i) The integrating cube used in the present investigation has 8 cubic metres' capacity (2 metres side) and is illustrated in sectional plan, fig. 1. The arc lamp is entirely controlled from outside the cube. Two images, in directions at right angles to each other and to the axis of the carbons, are projected through the walls of the cube permitting examination of the arc while burning. The electrical measuring instruments, feeding and locating arrangements, and electromagnetic control (when in use) are manipulated from outside, so that there is no necessity to open the cube except to change carbons. Ventilation is provided by means of adjustable shutters at the sides and top. Readings are taken simultaneously of crater brilliancy and candle-power. The brilliancy is measured by projecting a magnified image of the

* 'Illuminating Engineer' (London), vol. 3, p. 323, 1910.

Digitized by Google

front of the crater along a photometer bench. By the use of a negative lens placed where the image comes to a focus, any small part of the crater image can be isolated and the intensity at this point determined.

The cube is constructed of wood and is mounted on castors. It has doors the full height and width of one side. It is covered inside with asbestos or uralite, and cleaned off so that all inside surfaces are flush and smooth. The roof has a series of sliding shutters 1 ft. wide, so that any required opening can be used. It also has a series of shutters which work horizontally along the centre of the front of the cube, one of which carries the small translucent window E. A similar series of shutters is recommended for ventilation adjustment in the back wall of the cube.

All the inside surfaces are treated with three coats finished with gelatine and zinc white. It is advisable as far as possible to whiten also any objects which have to be in the cube—for instance, cables, lamp-stand, base, etc.

(ii) The diffusing window E. This consists of two plates of special colourless glass, each plate being ground with carborundum powder on both surfaces, and fixed so that the inside face is flush with the surface of the cube wall. Close to the window at G is fixed an iris diaphragm with about 70 mm. opening, permitting adjustment of the illumination on the photometer to a value which will enable the standard lamp to work on a convenient part of the photometer bench. Once fixed, however, the diaphragm opening must not be changed in the course of an experiment or of a calibration, nor must the distance of the photometer head from the window be varied, since the distance between the window and the photometer in these experiments is small, and the illumination at the photometer is therefore not strictly proportional either to the area of the window or to the inverse square of the distance.

(iii) Photometers H, H′, and photometer benches. These are Lummer-Brodhun photometers of the usual contrast type, and ordinary photometer benches about 3 metres long.

(iv) Neutral light filter T. In order to reduce the illumination at the photometer when the arc lamp is burning, a neutral-tinted gelatine filter, T, is placed between the window and the photometer. The transmission value, $t$, of this filter must be known accurately, as it is removed and another substituted during the calibration of the cube. The transmission coefficients therefore become multiplying factors for the candle-power (see para. 6, " Calibration ").

(v) Colour filter $T_1$. A bluish filter is inserted between the photometer and the comparison lamp to render the colour of the light from the latter similar to that from the cube when the arc lamp is in use. The transmission coefficient, $t_1$, of this filter has also to be determined once for all, so that the filter can be removed during the daily calibration of the cube.

(vi) Comparison lamps L, L′. These are ordinary vacuum tungsten-filament lamps operating at about 0·68 candle per watt, mounted on movable carriages, which work along the photometer tracks.

Digitized by Google

(vii) Screen M. The opaque disc M is about 10 cm. diameter, and is placed in the direct line between the arc lamp and the window E and approximately midway between them. No direct light from the source must fall on the window, which only receives light from the inside walls of the cube. During calibration the screen M is moved, if necessary, so as to come between the standard lamp and the window.

(viii) Lens N. The lens N projects an image of the front of the crater (after reflection from the mirror O) through an opening in the cube, on to the white screen P. An ordinary spectacle-trial-case lens 14·3 mm. diameter and 1·5 diopters issued.

(ix) Mirror O. This is a plain back-silvered 4 in. diameter mirror mounted so that it can be tilted or turned about a vertical axis. The operator obtains access to the adjustments through the opening C and thus regulates the position of the arc image on the screen P.

(x) Screen P and lens Q. The screen is a white matt celluloid sheet 3 mm. thick and about 20 cm. square, fixed to a frame which carries the lens Q. P, Q, and the photometer H′ are mounted together in such a manner that their mutual positions cannot change. They are also rigidly attached to the photometer track. The screen P has in it a circular aperture of 10 mm. diameter, bevelled off to a sharp edge. The lens system Q consists of two negative lenses of 16 and 20 diopters. It must be mounted so that the centres of H, Q, and the aperture in P, are accurately aligned on the axis of the beam from the mirror O.

(xi) Colour filter T′. This is another bluish colour filter having a similar function to that of $T_1$.

(xii) The optical system. This comprises the crater, the lens N, the mirror O, and the screen P, and has the following dimensions :—

| | |
|---|---|
| Crater to N . . . . . | 828 mm. |
| N to P . . . . . | 3,440 mm. |

The important dimension is the distance from N to the screen P on which the image of the crater is focussed.

(xiii) Lens S. The lens S casts an image of the arc, viewed from the side, on to the translucent screen W *via* the two mirrors shown.

6. *Calibration for Measurement of Total Flux.*—The cube has to be calibrated in absolute measure for candle-power, and the other optical system for crater brightness in candles per sq. mm. The combined constant of the cube and photometric apparatus is determined by burning in the cube a lamp of known average candle-power (*m.s.c.p.*). If the integrator were spherical it should theoretically give accurate results, however much the distribution of the light from the standard differed from that of the test lamp. The gear inside the cube, however, and particularly the bulky arc lamp and its support, render this assumption dangerous, and a standard source of light should be selected which has approximately the same light distribution as the test lamp.

Digitized by Google

The standard lamp used for calibration of the cube is shown in fig. 2; it is a large 240-volt 1,000-watt vacuum-type lamp made up with a fairly close-fitting opaque hood, with an internal reflecting surface. The type of reflector illustrated serves very well for this purpose. If the distribution of light from this lamp be determined and plotted in a Rousseau diagram, it is found to agree very closely with the Rousseau diagram for the arc lamp.

When calibrating the cube, the arc lamp and all other accessories are left in place and the standard lamp is supported with its axis horizontal in place of the carbons. The positive carbon-holder serves to clasp the socket of the standard lamp in such a position

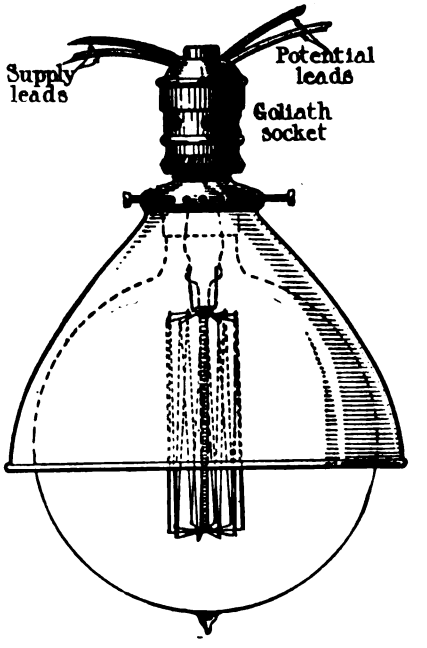


Fig. 2. Standardized lamp and hood, having similar light distribution to the arc lamp, used in calibration of the integrating cube.

The lamp is rated at 240 volts, 1,000 watts.
Average candle power at 240 volts : 422 candles.

that the light is emitted as desired towards the inside back wall of the cube. The method of determining the average candle-power of the hooded standard lamp is in accordance with the usual photometric procedure. The particular lamp illustrated gives an average candle-power of 422 candles at 240 volts with its hood in position.

The burning of the arc lamp inside the cube gradually causes a discoloration of the white walls, and it is therefore necessary to determine the constant of the cube each day by calibration with the standard lamp. The fixing of the large standard lamp for calibration purposes is rather cumbersome, and it has been found convenient to use an ordinary tungsten lamp without hood for the daily calibration, correcting the result by the previously determined ratio between the results given by the two lamps. It so happened that in the N.P.L. cube the two standard lamps gave identical constants. It must not

Digitized by Google

be assumed, however, that this will always be the case, though from the conditions prevailing it is to be expected that the two constants will approximate to the same value.

The comparison lamp L is an ordinary grid filament vacuum lamp operating at 200 volts.

During calibration it is at a distance of approximately 2,000 mm. from the window E. The iris diaphragm G has an opening of 70 mm., and it must be remembered that the neutral filter T and the colour filter $T_1$ are removed during calibration. It is desired to express the constant of the cube in terms of a factor which (when there is a photometric balance) can be divided by the square of the distance $x$, in order to give the average candle-power in absolute units of the source of light in the cube.

(Fig. 3). Let $C_0$ = average candle-power of the standard lamp ;

$t_0$ = transmission coefficient of neutral filter $T_0$ on the comparison lamp side ;

$x_0$ = distance on scale to give balance.

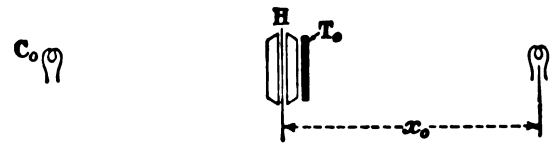


Fig. 3.

Then in balance we have : $C_0/K = t_0/x_0^2$, or

$$K = \frac{C_0 x_0^2}{t_0} \quad . \quad . \quad .

7. *Measurement of Crater Brightness.*—In fig. 4—

A is the crater ;

N is the positive lens (1·5 diopters) of radius $r$, at a distance $a$ from the crater, and of transmission coefficient $n$ ;

O is a mirror of reflection coefficient $m$ ;

P is a xylonite screen with negative system of lenses at Q ;

H′ is a photometer and T′ the colour filter of transmission coefficient $t'$ ;

L′ is a comparison lamp of candle-power C′ at a distance $x'$ from the photometer,

Let B be the normal brightness of the crater in candles per sq. mm. Then the lumens incident on the positive lens from the crater

$$= \text{B (area of crater)}\,\pi r^2/a^2.$$

Therefore lumens transmitted = B (area) $\pi r^2\, n/a^2$.

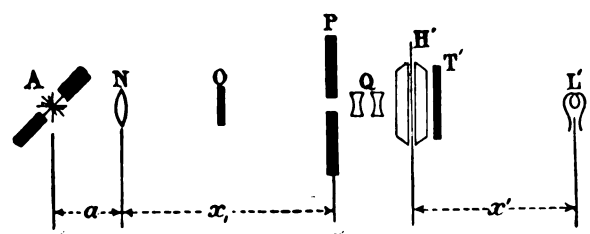


Fig. 4.

Hence the illumination at the image on the screen at P

$$= \frac{\text{B (area of crater)}\,\pi r^2 nm}{a^2\,\text{(area of image)}},$$

but

$$\frac{\text{(area of crater)}}{\text{(area of image)}} = \frac{a^2}{x_1^2}.$$

Therefore the illumination at P $= \dfrac{\text{B}\pi r^2 nm}{x_1^2}$ mm. candles, and the illumination at H′ $= \dfrac{\text{B}\pi r^2 nm}{x_1^2 \text{R}}$ mm. candles, where R = illumination at P ÷ illumination at H′, determined

(*a*) by actual measurement using a portable brightness photometer ;

(*b*) by measurement of magnification and allowance for the absorption of light in the lens system Q ;

(*c*) by substituting for the arc a 500-watt "Pointolite" lamp, the surface brightness of a part of the plate of this lamp having been previously determined in candles per sq. mm. on a standard photometer bench by measurement of the candle-power

Digitized by Google

of the known small area of its surface viewed through a pinhole of accurately determined diameter.

Also, illumination at $H' = C't'/(x')^2$, therefore

$$\frac{B\pi r^2 nm}{(r_1)^2 R} = \frac{C't'}{(x'_1)^2}$$

or

$$B = \frac{C't'(x_1)^2 R}{\pi r^2 nm} \cdot \frac{1}{(x')^2}.$$

8. *Errors in Measurement of Total Flux.*—The probable overall error of the final value of average candle-power is made up of the errors introduced at the different stages of the measurements as follows :—

(*a*) Determination of the average candle-power of the standard lamp used for calibrating the cube. No colour difference is involved in this determination and the value of the candle-power in terms of the unit accepted in England, France and America will be correct to ± 0·75 per cent.

(*b*) Determination of transmission coefficient of the neutral filter T. This causes a reduction of the light to approximately 2½ per cent. There is no colour difference and the result may be taken as correct to ± 1 per cent.

(*c*) Determination of transmission coefficient of the colour filter $T_1$. There is a considerable colour difference here, and the mean of the determinations of several observers must be taken. The error of the final mean may be regarded as correct to within ± 2 per cent.

(*d*) Photometric determination of the constant of the cube. The value obtained is merely the average of a number of ordinary photometric settings and the error may be taken as ± 0·5 per cent.

The probable error in the final value assessed for the constant of the cube may therefore be put at 3·5 per cent., and this covers the probable error of the instruments used as distinct from the errors of observation. To this must be added, for any one carbon, the probable error of the series of observations upon it. This varies according to the individual peculiarities of that type of carbon, and no general figure can be given for all carbons. Some types run more steadily than others, and on some the variations between individual specimens are considerable.

## II. *Results.*

9. *General.*—In Table I is given a list of the carbons which have formed the subject of this investigation. The first seven were originally supplied for a comparison of their light efficiencies with that of a special impregnated carbon developed by Messrs. W. Heape and H. B. Grylls, and described by them in Patents Nos. 126,673 and 128,057 of 1919. Subsequently, and as the result of conclusions drawn from these tests, a series of carbons



Digitized by Google

TABLE I.

| No. | Description. | Diameter. mm. Positive. | Diameter. mm. Negative. | Area. sq. mm. Positive. | Current. Rated. | Current. Amperes per sq. mm. 0·2 | Current. Amperes per sq. mm. 0·3 | Average candles. Rated density. | Average candles. Amperes per sq. mm. 0·2 | Average candles. Amperes per sq. mm. 0·3 | Candles per ampere. Rated density. | Candles per ampere. Amperes per sq. mm. 0·3 | Candles per ampere. Amperes per sq. mm. 0·25 | Candles per ampere. Amperes per sq. mm. 0·3 | Crater brightness. Candles per sq. mm. Rated density. | Crater brightness. Candles per sq. mm. Amperes per sq. mm. 0·2 | Crater brightness. Candles per sq. mm. Amperes per sq. mm. 0·3 | * Minimum arc length. | Candles per watt. Amperes per sq. mm. 0·25 | Candles per watt. Amperes per sq. mm. 0·3 |
|---|---|---|---|---|---|---|---|---|---|---|---|---|---|---|---|---|---|---|---|---|
| 1 | 2 | 3 | 4 | 5 | 6 | 7 | 8 | 9 | 10 | 11 | 12 | 13 | 14 | 15 | 16 | 17 | 18 | 19 | 10 | 21 |
| | *Uncoppered Positives.* | | | | | | | | | | | | | | | | | | | |
| I | Cored | 20 | 9 | 314 | 90 | 63 | 94 | 10,400 | 6,300 | 11,000 | 115 | 100 | 111 | 117 | 180 | 160 | 184 | 14 | 1·8 | 1·9 |
| II | Solid | 22 | 12 | 380 | 60 | 76 | 114 | 5,250 | 7,600 | 13,300 | 87 | 100 | 110 | 116 | 145 | 152 | 170 | 20 | 1·7 | 1·8 |
| III | Impregnated and cored | 23 | 12 | 415 | 110 | 83 | 125 | 12,600 | 8,550 | 14,800 | 114 | 102 | 112 | 118 | 161 | 152 | 164 | 20 | 1·9 | 2·0 |
| IV | Cored | 24 | 16 | 455 | 75 | 91 | 136 | 7,600 | 9,700 | 15,900 | 102 | 106 | 112 | 116 | 155 | 161 | 178 | 27 | 1·6 | 1·6 |
| V | Cored | 28 | 14 | 615 | 110 | 123 | ... | 12,100 | 14,100 | ... | 110 | 114 | 122 | ... | 154 | 162 | ... | 21 | 1·9 | ... |
| VI | Cored | 32 | 16 | 805 | 150 | 161 | ... | 17,100 | 18,800 | ... | 114 | 117 | 125 | ... | 155 | 160 | ... | 24 | 1·7 | ... |
| VII | Solid | 38 | 20 | 1,135 | 150 | 227 | ... | 15,500 | 26,000 | ... | 103 | 114 | ... | ... | 157 | 163 | ... | 30 | ... | ... |
| | *Coppered Positives.* | | | | | | | | | | | | | | | | | | | |
| VIII | Solid | 28 | 16 | 615 | ... | 123 | 185 | ... | 11,800 | 24,000 | ... | 96 | 117 | 130 | ... | 139 | 182 | 35 | 1·7 | 1·7 |
| IX | Impregnated, solid | 28 | 16 | 615 | ... | 123 | 185 | ... | 13,000 | 23,300 | ... | 106 | 118 | 126 | ... | 142 | 174 | 26 | 1·9 | 2·0 |
| X | Solid | 28 | 16 | 615 | ... | 123 | 185 | ... | 14,500 | 25,500 | ... | 118 | 131 | 138 | ... | 150 | 179 | 40 | 1·8 | 1·9 |
| XI | Impregnated, solid | 28 | 16 | 615 | ... | 123 | 185 | ... | 11,400 | 20,900 | ... | 92 | 105 | 113 | ... | 138 | 169 | 26 | 1·6 | 1·7 |
| XII | Cored | 28 | 16 | 615 | ... | 123 | 185 | ... | 9,800 | 22,600 | ... | 80 | 107 | 123 | ... | 130 | 179 | 26 | 1·6 | 1·9 |
| XIII | Cored | 28 | 16 | 615 | ... | 123 | 185 | ... | 9,100 | 22,400 | ... | 74 | 118 | 121 | ... | 174 | 187 | 28 | 1·6 | 1·9 |

* This length is the minimum at which the arc will burn steadily or which will give 7 per cent. obscuration, whichever is the greater.

Digitized by Google

was specially made up and supplied by the General Electric Co., Ltd., with the object of obtaining the best type of carbon for an average burning current of 200 amperes.

Tests were also made with the electromagnetic control device developed by Captain Yorke of the London Electrical Engineers.

The lamp in which the carbons were burned was an old Crompton type for the 90 cm. searchlight with automatic and handfeed gear. During the test all feeding was done by hand by means of a chain and sprocket wheel driven from outside the cube.

It is seen from the table referred to that the rated current densities for the different carbons vary greatly, and while it was of course desirable to obtain data on them at the normal rating, it was obviously necessary to test them at different currents and arc potentials.

10. *Variations of Candle-Power with Potential and Arc Length.*—It was at first thought that the candle-power would vary both with the potential across the arc and with the current, but a careful investigation showed that, while the potential difference and the arc length increased or diminished together, a large change in these quantities within the range of normal working produced no sensible alteration in the average candle-power.

Fig. 5 shows a series of measurements of the average candle-power from 28 mm. impregnated "Apostle" carbons when taking 180 amperes at arc potentials varying from 55 to 72 volts. The points corresponding to arc lengths less than 35 mm. cannot be said to indicate a definite variation of candle-power in either direction. The exact form of

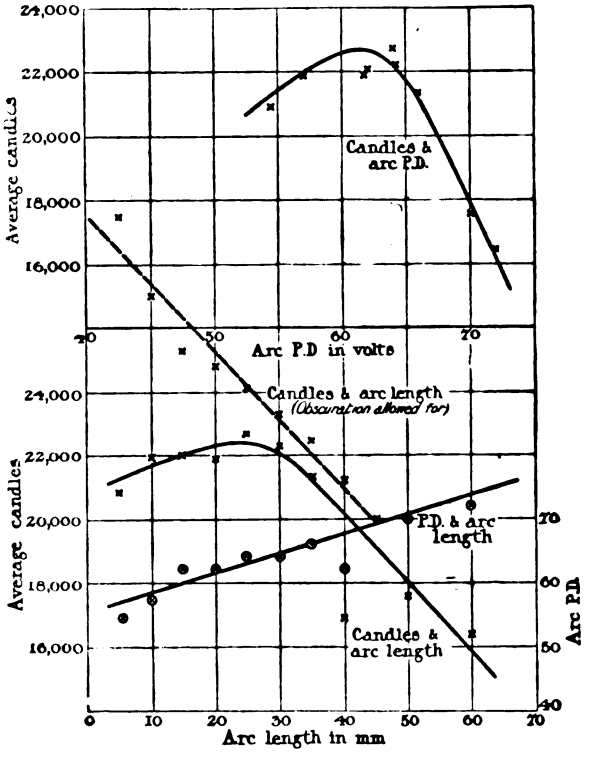


**Fig. 5.** Variation of candle-power with potential difference and arc length (for Carbon IX.)

G.E.C. "Apostle" carbons (+ ve 28 mm. — ve 16 mm.) impregnated, at 180 amperes.

Digitized by Google

this curve may not be repeated in all cases, but it is clear from the observations shown, and others made subsequently, that an increase in arc length or potential difference does not produce any increase in average candle-power. It is true that for different arc lengths there are different degrees of obscuration of the positive by the negative carbon; it is of interest, however, to note that if the obscuration be allowed for and a curve of average candle-power be continued as indicated in the dotted line, the candle-power increases as the arc length is reduced. Mrs. AYRTON* also found that with large currents the candle-power increased as the arc length was diminished. Hence the maximum candle-power *in any given direction not obstructed by the negative* is greater the shorter the arc length.

The fact that candle-power is virtually independent of the arc potential results in a simplification of the problem, since one important variable is thereby eliminated. The arc length can therefore be adjusted to whatever point gives smoothest running, with the proviso that it should not be short enough to cause excessive obscuration, say more than 7 per cent. Although the average candle-power in all directions is not sensibly affected by change of arc length owing to the balance between obscuration and increase of candle-power, the fact that all the obscuration takes place within the solid angle embraced by the projector mirror renders it still important to avoid too short an arc.

The usual practice throughout these investigations was to open out the carbons until the arc ceased to hiss, the resulting arc length usually being greater than the minimum necessary to avoid more than the 7 per cent. obscuration, as indicated above. Certain impregnated carbons, however, run satisfactorily at exceedingly short arc lengths, and for these the arcs were adjusted to avoid excessive obscuration.

11. *Crater Brightness and Current.*—The points on the individual curve sheets showing the relationship between crater brightness and current have been connected by a straight line in order to indicate the general rise of brilliancy with increase of current, but the results are not sufficiently accurate to justify any assumption as to the true form of this relationship. It is clear that if, as seems very probable, the (candle-power)/(current) relationship is linear, and if that of the (crater area)/(current) is also linear, as has been shown by Mrs. AYRTON for small arc lengths and currents, then the (brightness)/(current) relationship must be of the form $(Ai + B) \div (Ci + D)$, and it is actually found that a function of this form suits the observations as well as the straight line indicated on the curves. In fact, using the values of the constants available, the differences between the values given by the two lines are well within the limits of experimental error.

It should be noted that the slope of the reference line in the crater-brightness curves depends on the size of the carbon with which it is compared, and diminishes as its diameter increases. This follows from the explanation given in para. 13.

The general position may therefore be summarized as follows:—

A long arc, for any given carbon, whether from impregnated carbons or not, implies a high potential; and a short arc, a low potential. In order to obtain, under working

* 'The Electric Arc', p. 327.

Digitized by Google

conditions, a given amount of light from a given positive carbon, it is only necessary to pass through it a given current, the voltage across the arc and the arc length required to avoid hissing being immaterial. A positive carbon taking 200 amperes at 70 volts, *i.e.*, 14 kw., will emit the same light as one taking 200 amperes at 100 volts, *i.e.*, 20 kw. From the point of view of light emission from the positive crater, the extra 6 kw. are wasted. In order to ensure, however, that all but a very small proportion of the light directed towards the mirror from the positive carbon misses the negative, it is necessary for the arc length to exceed a certain minimum figure (for a particular diameter of positive and negative carbons), as mentioned in para. 10 above, and to obtain carbons which will take the maximum current through the positive crater at this minimum arc length, thus securing all the light possible with the minimum amount of dissipation of heat at the arc.

12. *Differences in Light Emission.*—The above discussion leaves out of consideration any specific differences there may be in the light emission of different carbons, *i.e.*, in the capacity of one type of carbon to give more light than another for a given current.

The whole investigation shows that, for the types of carbon considered, there is no sensible difference either in average candle-power or in crater brightness for carbons of the same diameter run at the same current. The efficiency in candles per ampere, however, increases somewhat for the same current density as the diameter of the positive carbon is increased; it is reasonable to attribute this, at least in part, to the greater relative cooling surface of the smaller carbons.

13. *Curve Sheets.*—The above conclusions follow from an examination of the curves in figs. 6 to 19. The large curves are for average candles plotted against current; the small curves at the top of the sheet are for crater brightness in candles per sq. mm. plotted against current. Each curve sheet gives for one of the types of carbon the results of a long series of measurements of candle-power and crater brightness at different values of current. The (candle-power)/(current) curve for carbon No. II, when burned with the Yorke electromagnetic control, has been taken as a convenient reference line for purposes of comparison between other carbons, and this has been shown as a broken line on all curve sheets. For crater brightness a dotted reference line has been drawn by connecting two points whose co-ordinates are obtained thus: the abscissæ are the currents corresponding to densities of 0·2 and 0·3 ampere per sq. mm. of the carbon considered, while the ordinates are the crater brightnesses of the reference carbon at the same current densities. It will be seen that the figures of crater brightness agree satisfactorily with those obtained by FORREST.*

Each circle marked on the curves represents the mean of a large number of observations. Usually a series of 10 observations was made at a given current, over a 10-minute period of burning. The current value was then changed and a further series taken after

* 'Electrician', vol. 71, pp. 729 and 1007, 1913.

Digitized by Google

the conditions had settled down at the new current. The first current was then repeated either on the same carbons or on a duplicate set. Usually the results plotted on any curve represent some 5 or 6 pairs of carbons burned in this way.

14. *Individual Variations.*—It has not been thought worth while as a rule to show individual observations on the curve sheets, but for the purpose of illustration this has been done for the (candle-power)/(current) curves in figs. 14 and 15 for the solid coppered carbons. Attention was concentrated on currents of 150, 180, 200, and 220 amperes and, in the case of one of them, of 250 amperes. At each of these currents it is seen that the emission of light from these carbons was liable to vary over a wide range. For instance, at 200 amperes, omitting isolated readings, there is an extreme variation of some 30 per cent. for normal burning conditions.

Smaller carbons appeared generally to vary much less than the larger ones, but in either case no reliable comparison is possible unless the mean of a large number of readings is taken.

## III. *Comments on the Behaviour of Individual Carbons.*

15. *Uncoppered Carbons (Nos. I to VII).*—

(I) Fig. 6.—This was a French cored carbon made by the Sautter, Harlé Company, 20 mm. in diameter, rated at 90 amperes—a relatively high density of 0·29 ampere per

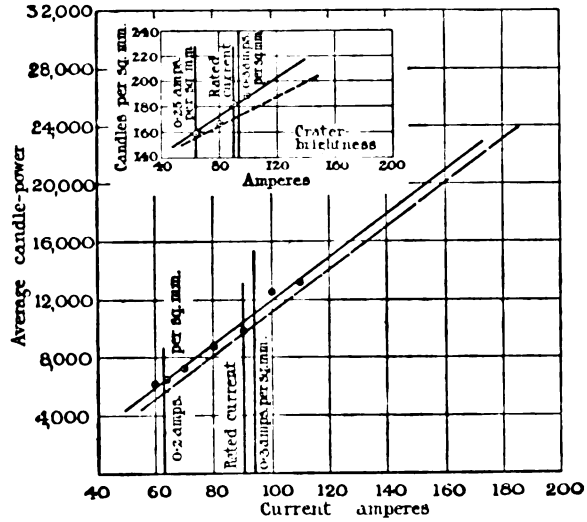


Fig. 6. Candle-power, crater brightness, and current curves (Carbon I).

| *Type of carbon* | + | − | *Rated current.* | *Inclination.* |
|---|---|---|---|---|
| Plain. | 20 mm. cored | 9 mm. solid | 90 amps. | Carbons axial. |

sq. mm. This carbon gave uniformly smooth and flexible running without the use of the electromagnetic device at arc lengths varying from 5 to 30 mm. and at currents varying from 60 to 110 amperes. The potential difference across the arc ranged from 54 to 72

Digitized by Google

volts varying with its length and also, to a small extent, with the current. The efficiency of this carbon (candles per watt consumed in the arc) at a current density of 0·3 ampere per sq. mm. was higher than that of any other unimpregnated carbon, being 1·9 candles per watt at an arc length (14 mm.) giving not more than 7 per cent. obscuration.

(II) Fig. 7.—This was a solid Army carbon (G.E.C. " Apostle " grade) 22 mm. in diameter rated at 60 amperes per sq. mm. On the whole, good running was obtained; without the electromagnetic device currents up to 100 amperes could be taken, and with this device it was possible to run up to 130 amperes. The potential difference across the arc ranged from 50 to 80 volts for arc lengths varying from 10 mm. to 40 mm. and with currents varying from 50 to 120 amperes. The results on this carbon have been used as a reference, as stated in para. 13.

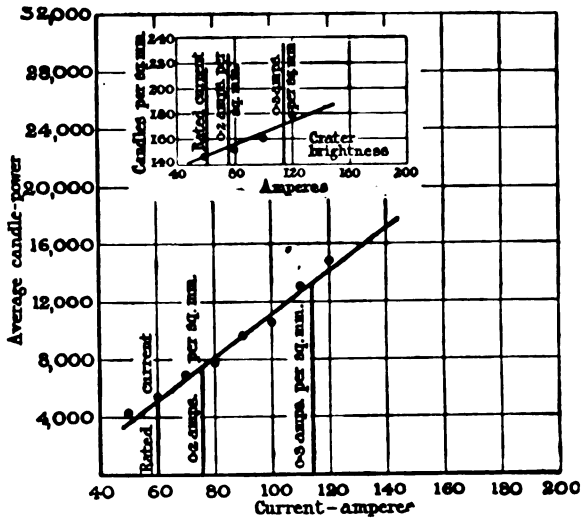


Fig. 7. Candle-power, crater brightness, and current curves (Carbon II).

| *Type of carbon* | + | − | *Rated current* | *Inclination* |
|---|---|---|---|---|
| Plain | 22 mm. solid | 12 mm. cored | 60 amps. | Carbons axial |

(III) Fig. 8.—This was a cored carbon (G.E.C. " Nubia " grade) of 23 mm. diameter, impregnated with the Heape and Grylls special solution. It was rated at 110 amperes or a current density of 0·265 ampere per sq. mm. It was found to give good flexible burning with the electromagnetic device for arc lengths ranging from 3 to 20 mm. and currents varying from 60 to 140 amperes, the potential difference across the arc being 50 to 62 volts.

The efficiency of this carbon at an arc length of 20 mm. (7 per cent. obscuration) was 2·0 candles per watt at a current density of 0·3 ampere per sq. mm.

(IV) Fig. 9.—This was by the same maker as No. I, but possibly of a different composition. It was 24 mm. in diameter, and its rating was 75 amperes, or 0·165 ampere per sq. mm. This also gave good burning without the electromagnetic device, but was



Digitized by Google

not so uniform as the smaller carbon. The arc length ranged from 8 to 23 mm., and the currents from 60 to 140 amperes, the arc potential difference ranging from 50 to 72 volts.

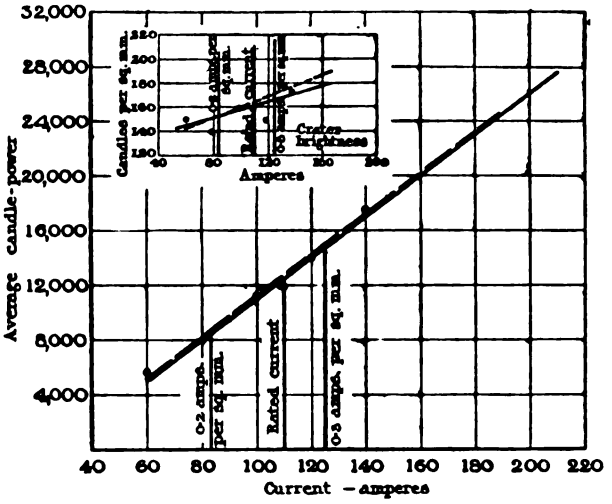


Fig. 8. Candle-power, crater brightness, and current curves (Carbon III).

| *Type of carbon* | + | – | *Rated current* | *Inclination* |
|---|---|---|---|---|
| Impregnated | 23 mm. cored | 12 mm. cored | 110 amps. | Carbons axial |

(V) Fig. 10.—This was a Navy cored carbon (" Apostle " grade) of 28 mm. diameter, its rating being 110 amperes, or 0·18 ampere per sq. mm. This carbon ran very smoothly

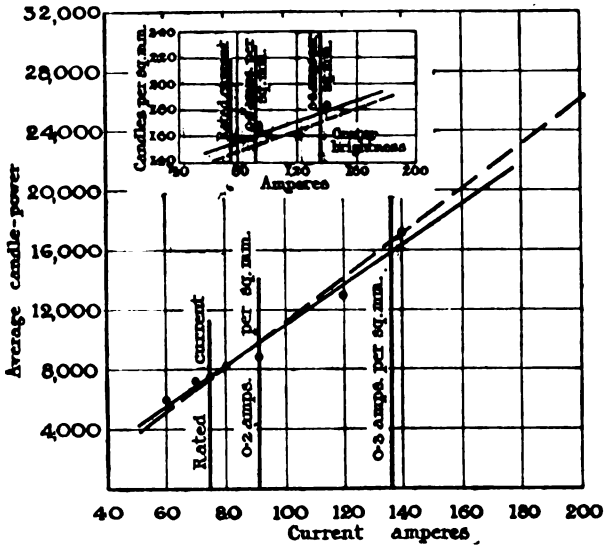


Fig. 9. Candle-power, crater brightness, and current curves (Carbon IV).

| *Type of carbon* | + | – | *Rated current* | *Inclination* |
|---|---|---|---|---|
| Plain | 24 mm. cored | 16 mm. cored | 75 amps. | Carbons axial |

without the electromagnetic device for arc lengths of 14 to 32 mm. and currents varying from 70 to 170 amperes, the potential difference ranging from 55 to 76 volts.

Digitized by Google

(VI) Fig. 11.—This was similar to the foregoing but of 32 mm. diameter. Its rating was 150 amperes, or 0·186 ampere per sq. mm. This carbon did not give very good

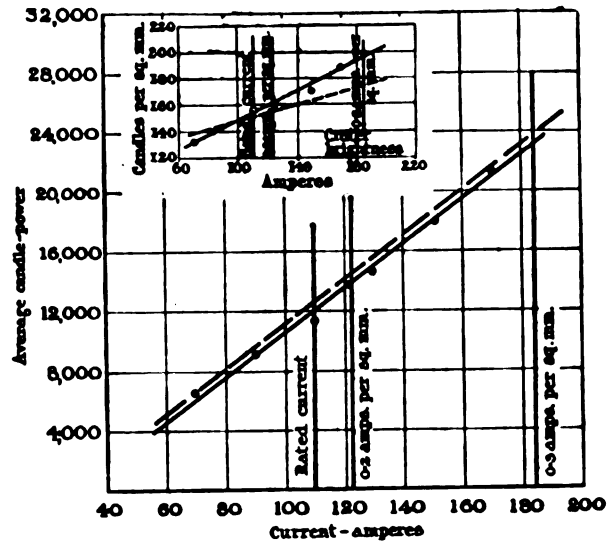


Fig. 10. Candle-power, crater brightness, and current curves (Carbon V).

| *Type of carbon* | + | − | *Rated current* | *Inclination* |
|---|---|---|---|---|
| Plain | 28 mm. cored | 14 mm. cored | 110 amps. | Carbons axial |

running as the arc was difficult to control. The arc length and potential differences ranged from 10 to 35 mm. and from 60 to 86 volts respectively, while the current varied from 100 to 300 amperes.

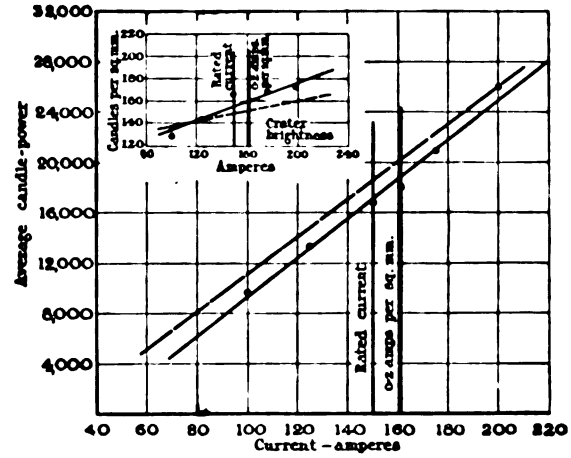


Fig. 11. Candle-power, crater brightness, and current curves (Carbon VI).

| *Type of carbon* | + | − | *Rated current* | *Inclination* |
|---|---|---|---|---|
| Plain | 32 mm. cored | 16 mm. cored | 150 amps. | Carbons axial |

VII. Fig. 12.—This was an Army solid carbon ("Apostle" grade) 38 mm. in diameter, its rating being 150 amperes, or only 0·132 ampere per sq. mm. This arc was



Digitized by Google

often difficult to control and gave irregular results at currents above 200 amperes. The arc length varied from 15 to 30 mm. for currents of 120 to 230 amperes, and the arc

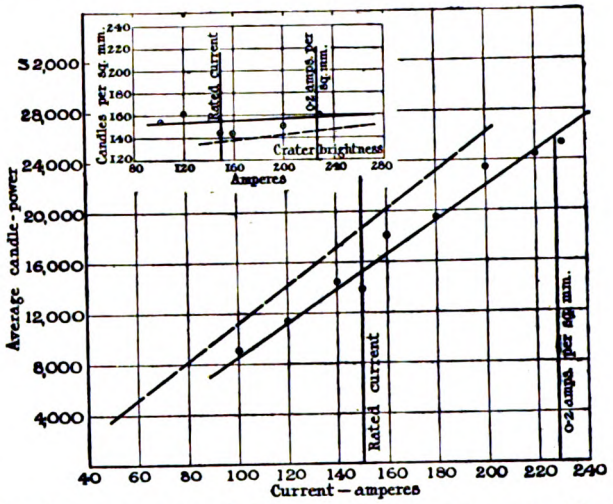


Fig. 12. Candle-power, crater brightness, and current curves (Carbon VII).

| *Type of carbon* | + | − | *Rated current* | *Inclination* |
|---|---|---|---|---|
| Plain | 38 mm. solid | 20 mm. cored | 120–150 amps. | Carbons axial |

potential difference from 60 to 86 volts. It was impossible to get currents exceeding 230 amperes to run steadily.

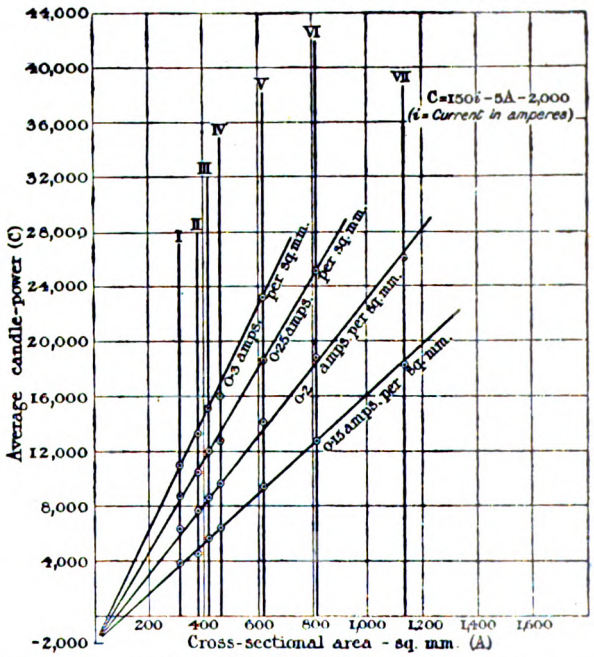
Average candle-power (C)
Cross-sectional area - sq. mm. (A)
C=150i−5A−2,000
(i = Current in amperes)
0·3 amps. per sq. mm.
0·25 amps. per sq. mm.
0·2 amps. per sq. mm.
0·15 amps. per sq. mm.

Fig. 13. Average candles and nominal area of uncoppered positive carbons at four current densities.

16. *General Remarks on Carbons I to VII.*—Fig. 13 gives a set of curves embodying the results of the average candle-power tests on the seven uncoppered carbons referred

Digitized by Google

to above. It is seen that for all these carbons the average candle-power depends only on the current and the nominal area of the positives. The empirical expression obtained for these curves is of the form $c = Ai + Ba + C$, which gives the average candle-power for any carbon in terms of the current and area, where $i$ is the current and $a$ is the nominal cross-sectional area of the positive in sq. mm. For these carbons $A = 150$, $B = -5$, and $C = -2{,}000$.

Hence it is seen that the average number of candles per ampere tends to increase with the area for a given current density. Thus,

$$\text{candles per ampere} = 150 - \frac{5}{i/a} - \frac{2{,}000}{i}$$

and if $i/a$ (*i.e.*, current density) is constant $= p$, then

$$\text{candles per ampere} = 150 - \frac{5}{p} - \frac{2{,}000}{pa}.$$

It appears that no appreciably greater efficiency can be obtained by increasing the diameter of the positive beyond 28 mm., since the rate of increase at this point in candles per ampere for a large percentage change in the diameter is very small.

Further, as a result of this investigation it was found that the maximum current which any uncoppered carbon could carry without overheating was given approximately, for the sizes used, by the empirical formula

$$i_{(max)} = 1{\cdot}8d^{1{\cdot}4}$$

where $d$ was the diameter of the positive in mm. By comparing this with the expression for candles per ampere given above, it was found that the maximum candles per ampere should be obtained with a positive 34 mm. in diameter taking some 250 amperes. This gave 124 candles per ampere, a result almost identical with that obtained with the 28 mm. diameter carbon at 154 amperes, viz., 123 candles per ampere. This is also evident from Table I (*see* cols. 14 and 15).

The fact that the candle-power values for each current density lay regularly on a system of straight lines showed that none of these carbons possessed any noticeable superiority in specific light emission. It may be noted that coppered negatives of smaller diameter could be used with some advantage with Nos. IV and VII, say 12 and 18 mm. respectively, since this would reduce the obscuration of light which would otherwise reach the projector mirror.

All the positives were uncoppered, and it was found that as the current density was increased beyond about 0·3 ampere per sq. mm. the carbons became very hot, especially the larger sizes, and began to disintegrate on the outer surface. For further work at high current densities and to use carbons of 28 mm. diameter, therefore, it was decided to have all the positives coppered.

Digitized by Google

17. *Coppered Carbons (Nos. VIII to XIII).*

(VIII) Fig. 14.—This was a carbon of 28 mm. diameter, of the same grade as No. II but with a copper coating approximately 0·06 mm. thick. The coating enabled this carbon to be run satisfactorily at a higher current density (up to 0·36 ampere per sq. mm.) than solid uncoppered carbons of the same grade. The current ranged from 150 to 220 amperes while the arc length varied from 20 to 65 mm., and the potential across the arc

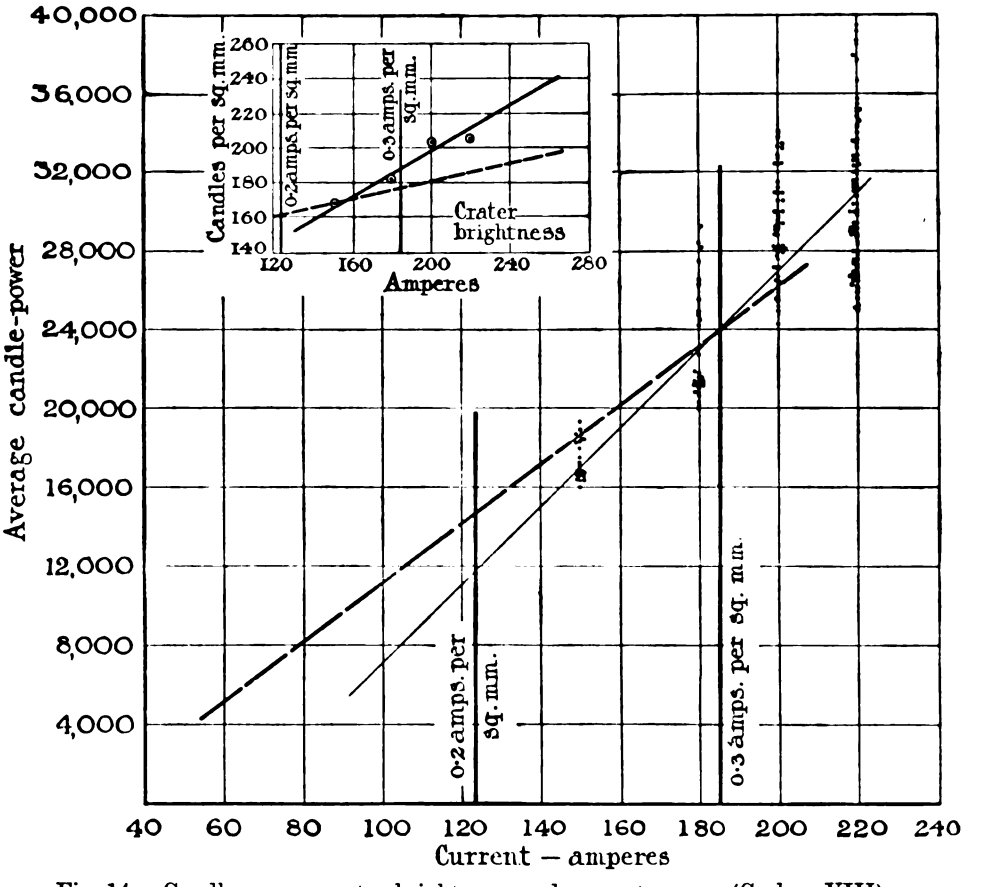


Fig. 14. Candle-power, crater-brightness, and current curves (Carbon VIII).

| *Type of carbon* | + | − | *Rated current* | *Inclination* |
|---|---|---|---|---|
| plain | 28 mm. solid coppered | 16 mm. cored | — | Carbons axial |

from 64 to 98 volts. The efficiency of the carbon at an arc length of 35 to 40 mm. (the minimum for a current density of 0·3 ampere per sq. mm.) was 1·7 candles per watt.

(IX) Fig. 15.—This was a carbon of 28 mm. diameter similar to No. VIII but impregnated with the special Heape and Grylls solution and without any coring.

As in the case of No. III, this carbon gave very good and flexible running with the electromagnetic device which was necessary to keep the arc from wandering. The current ranged from 150 to 250 amperes, the arc lengths from 6 to 60 mm., and the potential difference across the arc from 56 to 78 volts. Hence it followed that this carbon could

Digitized by Google

be run with a very short arc and correspondingly reduced potential difference, though this involved an increased obscuration by the negative carbon (*see* para. 19). This carbon was also run without the electromagnetic device, but with the positive rotating at a uniform speed of about one revolution per 2 minutes while the negative was inclined at an angle of some 25° with the horizontal. The effect of removing the electromagnetic device and adding the rotating device was slight, as the latter kept the crater regular,

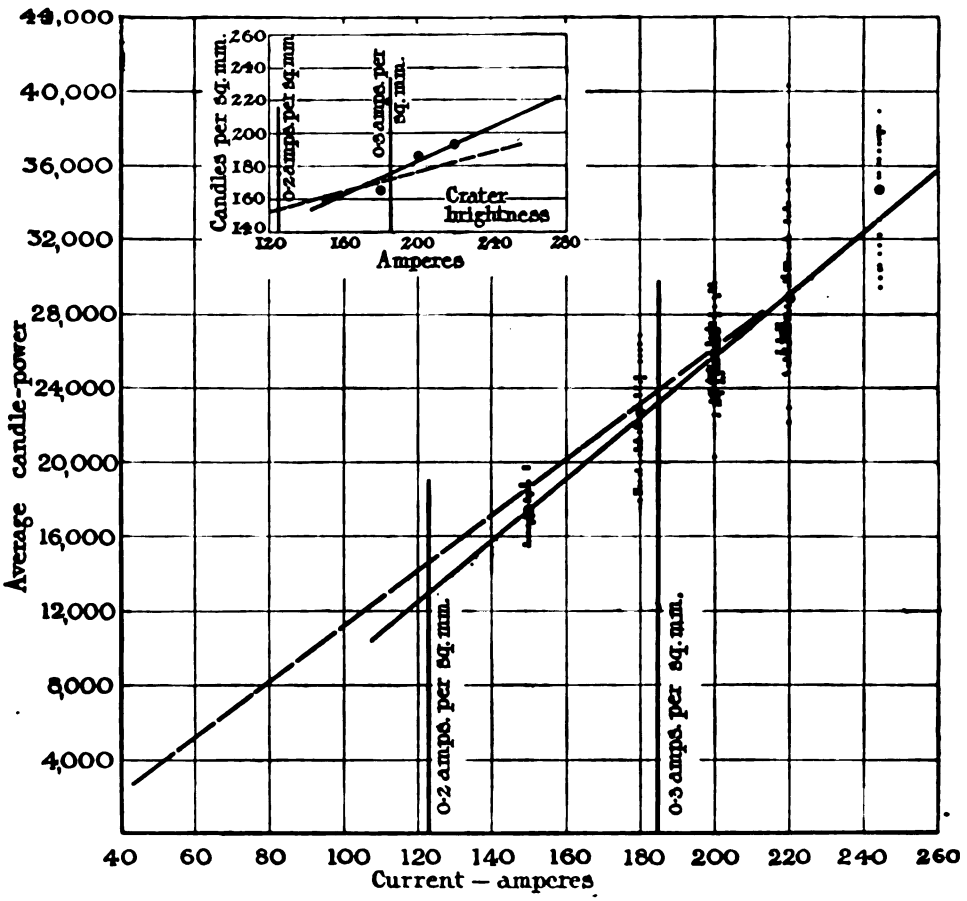


Fig. 15. Candle-power, crater brightness, and current curves (Carbon IX).

| *Type of carbon.* | + | − | *Rated current.* | *Inclination.* |
|---|---|---|---|---|
| Impregnated | 28 mm. solid coppered | 16 mm. cored | — | Carbons axial |

the only difference being that the position of the arc with regard to the crater could not be controlled, though with a short arc this control appeared to be unnecessary.

The efficiency of this carbon was 2·0 candles per watt at a current density of 0·3 ampere per sq. mm. and an arc length of 26 mm. (7 per cent. obscuration).

(X) Fig. 16.—This was a solid carbon of 28 mm. diameter and of a harder grade than No. VIII (G.E.C. " Nubia "). It was run with the electromagnetic device with a range of current of from 150 to 220 amperes, with a potential difference of from 68 to 98 volts

Digitized by Google

and arc lengths of 30 to 70 mm. The results were similar to those obtained with the No. V carbons, except that a higher current density and consequently a higher candle-power

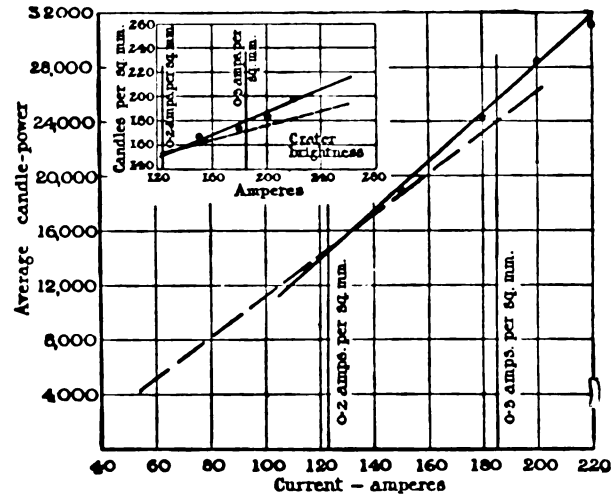


Fig. 16. Candle-power, crater-brightness, and current curves (Carbon X).

| *Type of carbon* | + | – | *Rated current* | *Inclination* |
|---|---|---|---|---|
| Plain | 28 mm. solid coppered | 16 mm. cored | — | Carbons axial |

were obtained. A long and consequently unstable arc was required for currents of 200 amperes and over—in fact some 5 mm. longer than in the case of the No. VIII carbon. It was also found that this grade of carbon tended to chip while burning.

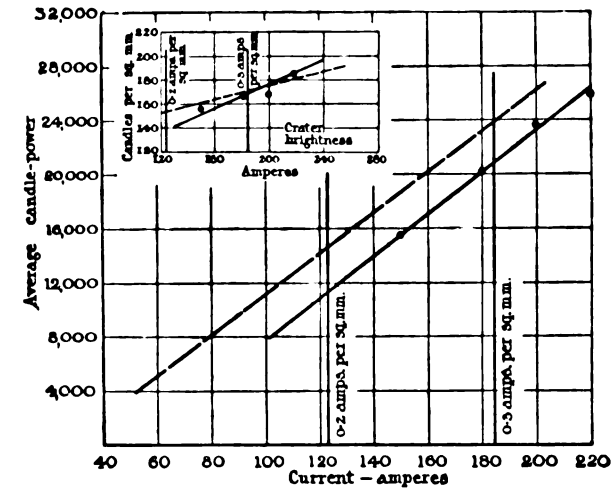


Fig. 17. Candle-power, crater-brightness, and current curves (Carbon XI).

| *Type of carbon* | + | – | *Rated current* | *Inclination* |
|---|---|---|---|---|
| Impregnated | 28 mm. solid coppered | 16 mm. cored | — | Carbons axial |

(XI) Fig. 17.—This was a solid coppered carbon, 28 mm. in diameter and was the same as No. X except that it was impregnated with the special solution. It was run at currents

Digitized by Google

varying from 150 to 220 amperes with a potential difference of from 58 to 68 volts and arc lengths of 14 to 22 mm. There was no difficulty in burning this carbon at any arc

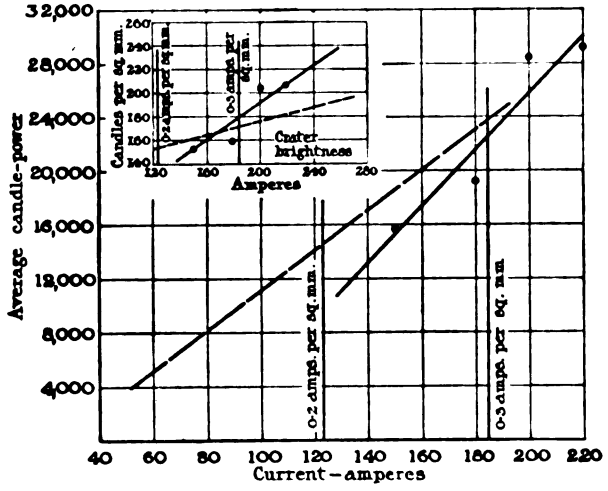


Fig. 18. Candle-power, crater brightness, and current curves (Carbon XII).

| *Type of carbon* | + | − | *Rated current* | *Inclination* |
|---|---|---|---|---|
| Plain | 28 mm. cored coppered | 16 mm. cored | — | Carbons axial |

length and the potential difference only varied slightly with the length and current. The average candle-power, however, was distinctly lower than that of No. IX.

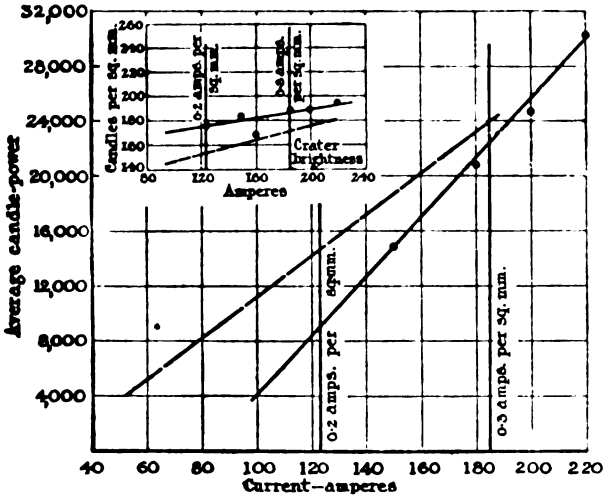


Fig. 19. Candle-power, crater brightness, and current curves (Carbon XIII).

| *Type of carbon* | + | − | *Rated current* | *Inclination* |
|---|---|---|---|---|
| Plain | 28 mm. cored coppered | 16 mm. cored | — | Carbons axial |

(XII) Fig. 18.—This was the same as No. V except that it was coppered. It was run at currents from 150 to 220 amperes and a potential difference ranging from 58 to 86 volts with an arc length of 25 to 42 mm.



Digitized by Google

(XIII) Fig. 19.—This was a cored carbon of 28 mm. diameter and was also run at currents ranging from 150 to 220 amperes and a potential difference varying from 48 to 74 volts with arc lengths of 10 to 40 mm. The running was fairly good, though the candle-power was lower than that of No. VIII for the same current.

18. *General Remarks on Carbons VIII to XIII.*—The thickness of coppering on the carbons VIII to XIII was 0·06 mm. This apparently resulted in an increase in the slope of the (candle-power)/(current) curves, and in shifting the intercepts on the axis of the current. This last was equivalent to an increase in the size of the carbon. It is probable that the relative irregularity of the results was due to the difficulty in maintaining a uniform crater at current densities exceeding 0·3 ampere per sq. mm. Carbon IX had the greatest efficiency in candles per watt, and Nos. IX and XI had the greatest flexibility of burning. At 220 amperes the average candle-power of these six carbons did not differ by more than 13 per cent. from the mean. In all cases the negatives were of 16 mm. diameter and heavily coppered, as it was found that if smaller ones were used the coppering volatilized and the carbon gradually disintegrated and diminished in diameter when the current exceeded 180 amperes.

19. *Obscuration of Light by the Negative Carbon.*—It is clear that at some of the shorter arc lengths employed during the course of the investigation, the proportion of light obscured by the tip of the negative carbon cannot be altogether neglected. The amount of this obscuration can be readily calculated if it be assumed that (i) the positive crater radiates as a circular disc emitting light according to the cosine law (*i.e.*, the radiation in any direction is proportional to the cosine of the angle between that direction and the normal to the radiating surface), and (ii) the negative may be regarded as a circular disc parallel with the positive and at a distance from it equal to the arc length. Of these assumptions the first is probably very close to the truth for all ordinary carbons, as, if internal reflection be neglected, the radiation from a hollow surface is the same as that from a plane of the same apparent area, *i.e.*, a cup-shaped crater gives the same radiation in any direction as a flat crater of the same diameter and of equal surface brightness. The second assumption is open to question on two counts : (*a*) the diameter of the negative carbon becomes considerably reduced at the end, and (*b*) the effect of obscuration by the stem of the negative carbon with its holder is neglected.

Another effect, which tends to offset the result of the reduction in diameter of the negative, is the reduction in the diameter of the positive carbon. These effects, which to a certain extent will counteract one another, will only modify a value that is, in itself, a correction, so that they have not been considered as of sufficient importance to justify the labour of calculation in more than a single case.

Neglecting these corrections, the percentage of the light emitted from a positive crater of diameter D which is obscured by a negative of diameter $d$ at an arc length $a$ is given by the formula :—

$$\frac{50}{D^2}\{(D^2 + d^2 + 4a^2) - \sqrt{[(D^2 + d^2 + 4a^2)^2 - 4d^2D^2]}\}.$$

Digitized by Google

The values of this expression for three different sizes of negative, and at all arc lengths, are given in the curves of fig. 20, where all dimensions are expressed in terms of the diameter of the positive. Thus, for a 28 mm. positive the obscuration values of a 16·8 mm. negative are given by the curve marked $d = 0{\cdot}6$, and thus 7 per cent. obscuration is exceeded in the case of all arc lengths shorter than $1{\cdot}0 \times 28$ mm. $= 28$ mm. There is one other consideration which cannot be neglected. For a 36-inch projector of about

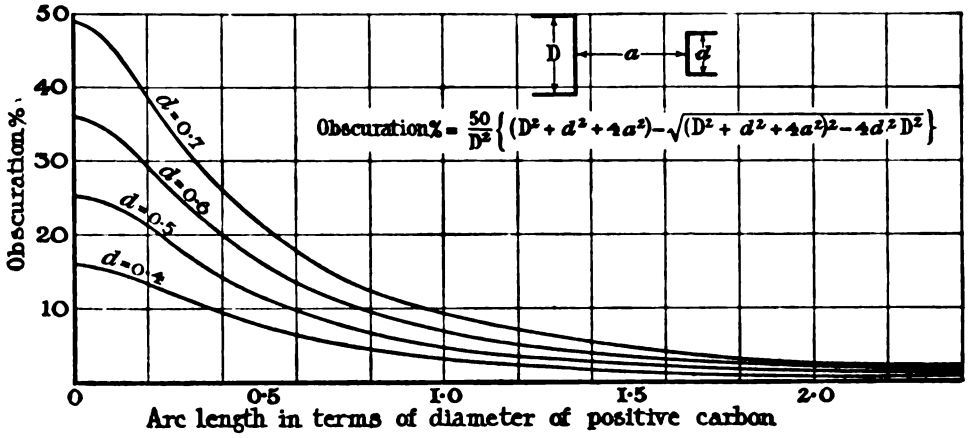


Fig. 20. Curves showing percentage of the total light emitted from a radiating circular disc of unit diameter, which is obscured by a co-axial circular disc of diameter $d$ situated at a distance $a$ from, and parallel to, the radiating disc.

[Note.—All dimensions are in terms of the diameter of positive carbon.]

16·5 inches focal length, only 70 per cent. of the total light from the crater falls on the mirror. All the obscured part of the light is within the angle embraced by the mirror, so that the effective obscuration of the useful light is 1·4 times that given by the formula, *i.e.*, in the example cited above the obscuration is approximately 10 per cent.

The thanks of the authors are due to the Admiralty for permission to make public the results contained in this paper.



Digitized by Google

Digitized by Google

# THE WHITENED CUBE AS A PRECISION INTEGRATING PHOTOMETER

BY

H. BUCKLEY, B.Sc.,

ASSISTANT IN THE ELECTRICITY DEPARTMENT

Digitized by Google

## ABSTRACT.

The Paper indicates how a whitened cube can be made to give accurate results when used in the determination of the average candle-powers of lamps having different polar distributions. As a preliminary, the relative effects of different portions of the interior of the cube in producing illumination on the window are determined, and the results used to calculate the illuminations produced by different types of light distribution. The ratios of these illuminations to that furnished by a uniform point source of unit intensity give apparent average candle-powers in the cube. It is then shown by experiment that candle-powers obtained by the usual methods of integrating photometry agree with these calculated values. Thus it is possible to determine by how much these apparent candle-powers differ from true candle-powers deduced by point-to-point methods, and hence to obtain true candle-powers from experimentally determined apparent values. In the special case when a comparison is made between lamps having identical polar distributions, it is shown that the usual method gives accurate results.


Digitized by Google

# THE WHITENED CUBE AS A PRECISION INTEGRATING PHOTOMETER.

By H. BUCKLEY, B.Sc., Assistant in the Electricity Department.

[Reprinted from the 'Journal of the Institution of Electrical Engineers', Vol. 59, 1921.]

## *Introduction.*

For several years past a 2-metre cube has been in use at the National Physical Laboratory for determining the average candle-power of lamps whose polar distributions have not differed very much from that of the standard lamp with which they are compared. It has been recognized that such results are, to a certain extent, approximate, and it is the object of the present series of experiments to arrive at some estimate of the magnitude of the errors which may be involved in such determinations, and to derive principles which will tend to minimize these errors. The chief reasons which led to the use of the cube, especially of a large-sized one, rather than a sphere, are the greater ease of construction and the increased facility for installing and manipulating such heavy apparatus as arc-lamp projectors, as the whole of one side can be made to open for such purposes.

Dr. Sumpner* first suggested the use of a rectangular box instead of a sphere, and claimed that to a fairly close approximation it would give as good results as the sphere. In the discussion on Dr. Sumpner's paper Prof. G. W. O. Howe described a box with 3-ft. edges which, he stated, acted satisfactorily. He suggested also the use of triangular pieces of cardboard to block up the corners so as to make the box approximate more closely to a sphere.

L. W. Wild,† as a result of this discussion, experimented with a rectangular box, and obtained photometric differences up to 4 per cent. His box was rather small, and his differences would probably be diminished by the use of a larger box.

Grondhal‡ in America has also described experiments with an oblong rectangular box, a box with the corners eliminated, and also a cube with the corners eliminated. He comes to the conclusion that for sources of similar distribution a rectangular box may be substituted for a sphere, and that a cubical box with the corners eliminated is for practical purposes a satisfactory substitute for a sphere, even for dissimilar and asymmetric sources.

## *Theoretical Outline.*

In the case of the Ulbricht sphere the illumination at the window is proportional to the total flux from the source, provided it receives no direct light from this source. In the case of the cube, however, this does not hold, the illumination on the window being a

* 'Illuminating Engineer' (London), vol. 3, p. 323, 1910.

† *Loc. cit.*, p. 549.

‡ 'Transactions of Illuminating Engineering Society', vol. 11, pt. 2, p. 152, 1916.

Digitized by Google

function of the first point of incidence of any part of the flux as well as of the total flux. For the same point of incidence the illumination on the window will be proportional to the total flux, but the proportionality factor, or " contribution coefficient " as it may be conveniently called, varies from point to point in the cube. This variation of the contribution coefficient has been determined for the whole of the cube. If, now, a source of known polar distribution and average candle-power be placed in the middle of the cube, we may calculate the flux falling on each area of the walls, and this, multiplied by the contribution coefficient for that area and summed over the whole surface of the cube, will give a quantity which, when divided by the same summation for a unit point source at the centre, will give the ratio of their apparent total fluxes or, what is proportional to it, the apparent average candle-power of the source when in the cube. We have thus a method of determining in a cube by how much the apparent average candle-powers differ from the actual average candle-power determined by a point-to-point method. This again can be compared with the average candle-power obtained by the usual experimental comparison of two lamps, for one of which this value is known.

*The Present Investigation.*

In the present investigation an Aldis daylight signalling lamp (fig. 1) was used as the source of a constant flux. It consisted of a gas-filled lamp with twin spiral filaments at the focus of a 4-in. Mangin mirror. Only the light emitted towards the mirror was allowed to come from the projector, and this was effected by placing the blackened shield A over the half of the lamp away from the mirror. This resulted in a beam which had a diameter of about 17 cm. at a distance of 1 metre from the projector. The exterior was whitened, as was also the retort stand which held it in position. Throughout the experiments the projector was in the middle of the cube, and it was oriented so that the beam from it fell approximately in the centre of each of the 16 squares into which each quarter side of the cube was divided. Experiments were made on the variations of candle-power of this lamp at different angles of tilt. It was found that these were extremely small and could be neglected. A small screen of about 15 cm. diameter was placed half-way between the projector and the window. It was not necessary in this case, as direct light from the source was never incident on the window, but, as in actual practice it would be necessary, it was placed in position and remained so during all the observations. These observations were not conducted over the whole of each side, as considerations of the symmetry

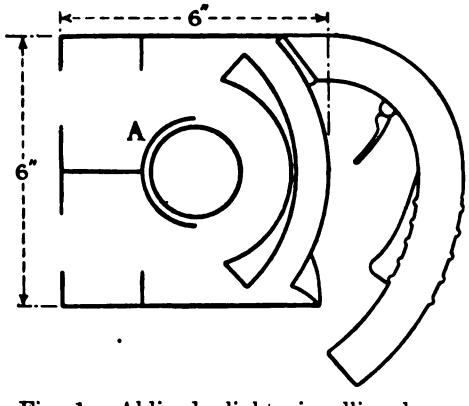


Fig. 1. Aldis daylight signalling lamp (diagrammatic).

Digitized by Google

of the system show this to be unnecessary. In fig. 2, which shows the squares into which each type of wall is divided, it is obvious that the contribution coefficient will be the same for corresponding squares in A, A′, A″, A‴ which are on the wall facing the window ; B, B′ the halves of the sides, top, and bottom farther from the window ; C, C′ the nearer halves of the same walls ; and D, D′, D″, D‴ on the wall containing the window. The observations are the means of two sets of five settings of the photometer by each of two

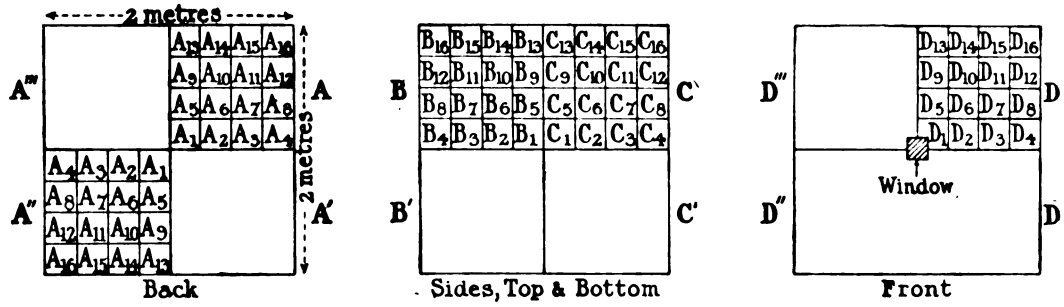


Fig. 2. Types of wall, showing division into small squares.

observers. The illumination on the window was not sufficiently large for convenience in working with a Lummer Brodhun-photometer and comparison lamp of about 20 candle-power, without the use of a mirror in the photometer head. This can be seen diagrammatically in fig. 3, where the mirror (M) is inclined at an angle of about 60 degrees with the axis of the photometer bench. The effect of the mirror is that instead of matching the brightness of the photometer screen as illuminated by the window,

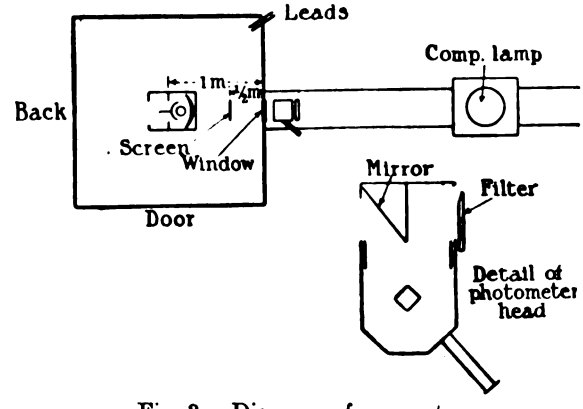


Fig. 3. Diagram of apparatus.

against the bench comparison lamp, the image of the window in the mirror is used, this being six or seven times brighter. On the same side of the photometer as the comparison lamp a blue filter (Wratten photometric 78B of transmission approximately 54 per cent.) was placed, and this gave a fairly good colour match between the gas-filled lamp working at an efficiency of 1·25 candles per watt and the tungsten-filament vacuum lamp at 0·70 candle per watt.



Digitized by Google

Check readings were taken from time to time with the beam incident on the middle of the wall facing the window, and results for other places were corrected to correspond to the slight variation obtained due to changes in the projector lamp.

Now, if L be the total flux in the beam of the projector, C the effective candle-power of the bench comparison lamp with colour filter, and $x$ the distance of this lamp from the photometer at balance.

$$\frac{C}{x^2} = b\mathrm{L}, \text{ where } b \text{ is a constant,}$$

therefore

$$b = \mathrm{C}/\mathrm{L}x^2,$$

so that the contribution coefficient, as $b$ has been called, is proportional to $1/x^2$.

Table I gives the results of the survey of the cube over the back and front. Table II gives the results over the sides, top and bottom.

TABLE I.

| Position. | Reading ($= x$), mm. | $\frac{1}{x^2} \times 10^7$ | Position. | Reading ($= x$), mm. | $\frac{1}{x^2} \times 10^7$ |
|---|---|---|---|---|---|
| $A_1$ | 1,199 | $6{\cdot}96 = \alpha_1$ | $D_1$ | 1,158 | $7{\cdot}46 = \delta_1$ |
| $A_2$ | 1,022 | $9{\cdot}57 = \alpha_2$ | $D_2$ | 1,156 | $7{\cdot}48 = \delta_2$ |
| $A_3$ | 1,068 | $8{\cdot}77 = \alpha_3$ | $D_3$ | 1,180 | $7{\cdot}18 = \delta_3$ |
| $A_4$ | 1,092 | $8{\cdot}38 = \alpha_4$ | $D_4$ | 1,197 | $6{\cdot}98 = \delta_4$ |
| $A_5$ | 1,056 | $8{\cdot}97 = \alpha_5$ | $D_5$ | 1,150 | $7{\cdot}56 = \delta_5$ |
| $A_6$ | 1,031 | $9{\cdot}41 = \alpha_6$ | $D_6$ | 1,168 | $7{\cdot}33 = \delta_6$ |
| $A_7$ | 1,081 | $8{\cdot}55 = \alpha_7$ | $D_7$ | 1,186 | $7{\cdot}11 = \delta_7$ |
| $A_8$ | 1,110 | $8{\cdot}12 = \alpha_8$ | $D_8$ | 1,210 | $6{\cdot}83 = \delta_8$ |
| $A_9$ | 1,049 | $9{\cdot}09 = \alpha_9$ | $D_9$ | 1,172 | $7{\cdot}28 = \delta_9$ |
| $A_{10}$ | 1,061 | $8{\cdot}88 = \alpha_{10}$ | $D_{10}$ | 1,171 | $7{\cdot}28 = \delta_{10}$ |
| $A_{11}$ | 1,100 | $8{\cdot}26 = \alpha_{11}$ | $D_{11}$ | 1,194 | $7{\cdot}01 = \delta_{11}$ |
| $A_{12}$ | 1,118 | $8{\cdot}00 = \alpha_{12}$ | $D_{12}$ | 1,220 | $6{\cdot}72 = \delta_{12}$ |
| $A_{13}$ | 1,072 | $8{\cdot}70 = \alpha_{13}$ | $D_{13}$ | 1,182 | $7{\cdot}16 = \delta_{13}$ |
| $A_{14}$ | 1,088 | $8{\cdot}45 = \alpha_{14}$ | $D_{14}$ | 1,181 | $7{\cdot}17 = \delta_{14}$ |
| $A_{15}$ | 1,124 | $7{\cdot}92 = \alpha_{15}$ | $D_{15}$ | 1,216 | $6{\cdot}76 = \delta_{15}$ |
| $A_{16}$ | 1,136 | $7{\cdot}75 = \alpha_{16}$ | $D_{16}$ | 1,221 | $6{\cdot}71 = \delta_{16}$ |

The variation of $1/x^2$, the contribution coefficient along several lines on the walls, is shown graphically in fig. 4.

For any given polar distribution we can now find a quantity proportional to its apparent total flux or average candle-power in the cube. If F be the flux incident on any small square, and $\alpha$ the contribution coefficient for that square, then $\Sigma(\mathrm{F}\alpha)$ taken over the whole cube is such a quantity. Let $l$ = semi-side of cube = 8 units; let the source be at the middle of the cube, *i.e.*, distant $l$ from the centre of each side, and let $x_1y_1$, $x_2y_2$, etc., be the co-ordinates of the mid-points of the small squares $A_1 \ldots A_{16}$, $B_1 \ldots B_{16}$, $C_1 \ldots C_{16}$, $D_1 \ldots D_{16}$, referred to an origin at the mid-point of the wall over which

Digitized by Google

TABLE II.

| Position. | Reading (= $x$), mm. | $\frac{1}{x^2} \times 10^7$ | Position. | Reading (= $x$), mm. | $\frac{1}{x^2} \times 10^7$ |
|---|---|---|---|---|---|
| $B_1$ | 1,115 | 8·19 = $\beta_1$ | $C_1$ | 1,098 | 8·29 = $\gamma_1$ |
| $B_2$ | 1,108 | 8·14 = $\beta_2$ | $C_2$ | 1,097 | 8·31 = $\gamma_2$ |
| $B_3$ | 1,099 | 8·28 = $\beta_3$ | $C_3$ | 1,120 | 7·98 = $\gamma_3$ |
| $B_4$ | 1,105 | 8·19 = $\beta_4$ | $C_4$ | 1,165 | 7·37 = $\gamma_4$ |
| $B_5$ | 1,101 | 8·25 = $\beta_5$ | $C_5$ | 1,101 | 8·25 = $\gamma_5$ |
| $B_6$ | 1,108 | 8·14 = $\beta_6$ | $C_6$ | 1,114 | 8·06 = $\gamma_6$ |
| $B_7$ | 1,108 | 8·14 = $\beta_7$ | $C_7$ | 1,129 | 7·84 = $\gamma_7$ |
| $B_8$ | 1,098 | 8·29 = $\beta_8$ | $C_8$ | 1,176 | 7·23 = $\gamma_8$ |
| $B_9$ | 1,116 | 8·03 = $\beta_9$ | $C_9$ | 1,126 | 7·88 = $\gamma_9$ |
| $B_{10}$ | 1,115 | 8·05 = $\beta_{10}$ | $C_{10}$ | 1,138 | 7·72 = $\gamma_{10}$ |
| $B_{11}$ | 1,130 | 7·83 = $\beta_{11}$ | $C_{11}$ | 1,152 | 7·53 = $\gamma_{11}$ |
| $B_{12}$ | 1,110 | 8·12 = $\beta_{12}$ | $C_{12}$ | 1,188 | 7·08 = $\gamma_{12}$ |
| $B_{13}$ | 1,119 | 7·99 = $\beta_{13}$ | $C_{13}$ | 1,138 | 7·72 = $\gamma_{13}$ |
| $B_{14}$ | 1,121 | 7·96 = $\beta_{14}$ | $C_{14}$ | 1,156 | 7·48 = $\gamma_{14}$ |
| $B_{15}$ | 1,119 | 7·99 = $\beta_{15}$ | $C_{15}$ | 1,191 | 7·05 = $\gamma_{15}$ |
| $B_{16}$ | 1,125 | 7·90 = $\beta_{16}$ | $C_{16}$ | 1,205 | 6·89 = $\gamma_{16}$ |

the summation is being taken. Then the flux incident on any small square of area $(l/4)^2$

$$= \frac{\text{area} \times \cos(\text{angle of incidence})}{(\text{distance from source to centre of area})^2 \times (\text{c.p. in direction of centre of area})}$$

$$= \frac{l^2}{4^2} \cdot \frac{l}{(l^2 + x^2 + y^2)^{1/2}} \cdot \frac{1}{l^2 + x^2 + y^2} \cdot \Phi_\theta \qquad (\textit{see fig 5})$$

where $\Phi_\theta$ is the candle-power of the source in a direction making an angle $\theta$ with the reference plane of the lamp.

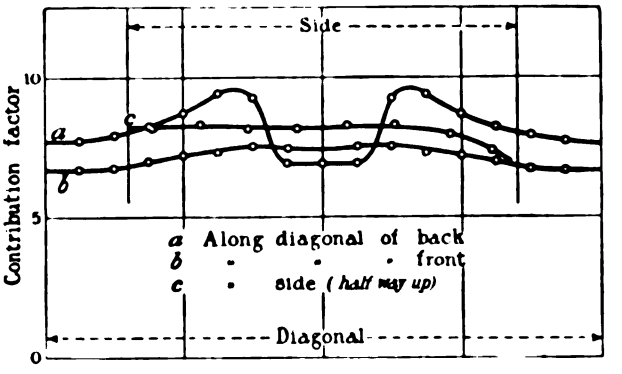


Fig. 4. Variation of "contribution co-efficient" across the cube.

$\Sigma (F\alpha)$ then becomes

$$\frac{l^3}{4^2} \sum \left\{ \frac{\alpha \Phi_\theta}{(l^2 + x^2 + y^2)^{3/2}} \right\}.$$



Digitized by Google

The values of $(l^2 + x^2 + y^2)^{3/2}$ for the mid-points of each of the area $A_1$ . . . $A_{16}$, which are the same as those for corresponding areas in $B_1$ . . . $B_{16}$, $C_1$ . . . $C_{16}$, $D_1$ . . . $D_{16}$, are given in Table III.

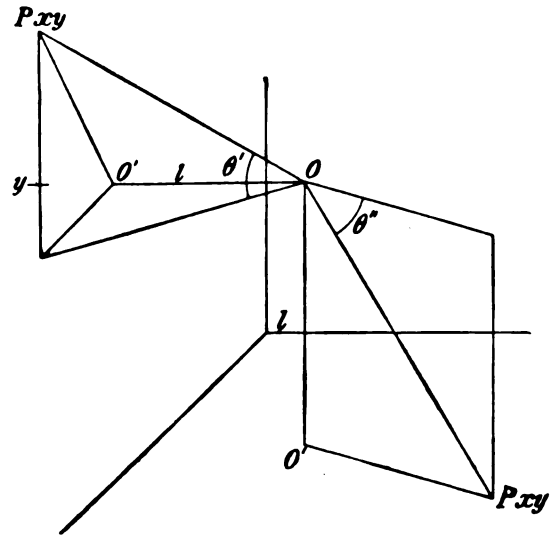


Fig. 5. Geometry of angle of incidence, etc.

TABLE III.

| Area. | $(l^2+x^2+y^2)^{3/2}$ | Area. | $(l^2+x^2+y^2)^{3/2}$ |
|---|---|---|---|
| $A_1$ | 536 | $A_9$ | 854 |
| $A_2$ | 636 | $A_{10}$ | 969 |
| $A_3$ | 853 | $A_{11}$ | 1,218 |
| $A_4$ | 1,218 | $A_{12}$ | 1,621 |
| $A_5$ | 637 | $A_{13}$ | 1,218 |
| $A_6$ | 742 | $A_{14}$ | 1,346 |
| $A_7$ | 969 | $A_{15}$ | 1,621 |
| $A_8$ | 1,346 | $A_{16}$ | 2,062 |

In evaluating the values of $\theta$, which is the angle between the reference plane and the direction of emission of the flux, two cases have to be considered :—

Case (1).—When the direction of emission is incident on a wall of the cube perpendicular to the reference plane.

Case (2).—When the direction of emission is incident on a wall parallel to the reference plane. The former is shown in fig. 5, and it can be seen that

$$\theta' = \text{arc sin } \frac{y}{(l^2 + x^2 + y^2)^{1/2}}.$$

In the latter case (*see* fig. 5)

$$\theta'' = \text{arc sin } \frac{l}{(l^2 + x^2 + y^2)^{1/2}}.$$

Digitized by Google

The values of $\theta'$ and $\theta''$ are given in Table IV for each of the areas $A_1 \ldots A_{16}$, which, of course, have corresponding squares on the other walls.

TABLE IV.

| Area. | $\theta'$. | $\theta''$. | Area. | $\theta'$. | $\theta''$. |
|---|---|---|---|---|---|
| $A_1$ | 7° | 80° | $A_9$ | 32° | 57° |
| $A_2$ | 6° | 68° | $A_{10}$ | 30° | 54° |
| $A_3$ | 6° | 58° | $A_{11}$ | 28° | 49° |
| $A_4$ | 5° | 49° | $A_{12}$ | 25° | 43° |
| $A_5$ | 20° | 69° | $A_{13}$ | 41° | 49° |
| $A_6$ | 19° | 62° | $A_{14}$ | 40° | 46° |
| $A_7$ | 18° | 54° | $A_{15}$ | 37° | 43° |
| $A_8$ | 16° | 46° | $A_{16}$ | 33° | 39° |

### $\Sigma$ (F$\alpha$) *for Various Polar Distributions.*

(1) *A Point Source.*—In this case $\Phi_\theta = \text{const.} = \Phi$, the candle-power of the source. The summation $\Sigma$ (F$\alpha$) is made up of three parts :—

(1) due to the back of the cube ; this equals four times the summation over the small squares $A_1 \ldots A_{16}$

$$= 4\Phi \frac{l^3}{4^2} \sum \left\{ \frac{\alpha}{(l^2 + x^2 + y^2)^{3/2}} \right\};$$

(2) due to the front as above, but over the squares $D_1 \ldots D_{16}$

$$= 4\Phi \frac{l^3}{4^2} \sum \left\{ \frac{\delta}{(l^2 + x^2 + y^2)^{3/}} \right\};$$

(3) due to sides, top and bottom ; this equals 8 times the summations over the small squares $B_1 \ldots B_{16}$, $C_1 \ldots C_{16}$,

$$= 8\Phi \frac{l^3}{4^2} \sum \left\{ \frac{\beta + \gamma}{(l^2 + x^2 + y^2)^{3/2}} \right\}.$$

Now $l = 8$ units, therefore

$$\Sigma (F\alpha) = 128\Phi \sum \left\{ \frac{\alpha + 2(\beta + \gamma) + \delta}{(l^2 + x^2 + y^2)^{3/2}} \right\}$$

$= 100{\cdot}3\ \Phi$ in the particular case of the measurements quoted in Tables I and II.

(2) *A Squirrel-Cage Metal-Filament Vacuum Lamp.*—This lamp had a polar distribution as shown in fig. 6. Measurements were made at the Russell angles (ten in each quadrant) whilst the lamp was rotating, and the average candle-power was deduced as 114·0.

Digitized by Google

The summations in this case consist of four parts due respectively to

$$\text{(1) back} \qquad = 4 \cdot \frac{l^3}{4^2} \sum \left\{ \frac{\alpha \Phi_\theta}{(l^2 + x^2 + y^2)^{3/2}} \right\};$$

$$\text{(2) front} \qquad = 4 \cdot \frac{l^3}{4^2} \sum \left\{ \frac{\delta \Phi_\theta}{(l^2 + x^2 + y^2)^{3/2}} \right\};$$

$$\text{(3) sides} \qquad = 4 \cdot \frac{l^3}{4^2} \sum \left\{ \frac{(\beta + \gamma) \Phi_\theta}{(l^2 + x^2 + y^2)^{3/2}} \right\};$$

$$\text{(4) top and bottom} \qquad = 4 \cdot \frac{l^3}{4^2} \sum \left\{ \frac{(\beta + \gamma) \Phi_\theta}{(l^2 + x^2 + y^2)^{3/2}} \right\};$$

therefore

$$\Sigma (F\alpha) = 128 \sum \left\{ \frac{(\alpha + \delta) \Phi_\theta'}{(l^2 + x^2 + y^2)^{3/2}} \right\} + 128 \sum \left\{ \frac{(\beta + \gamma)(\Phi_\theta + \Phi_{\theta''})}{(l^2 + x^2 + y^2)^{3/2}} \right\}$$

$$= 11{,}336.$$

In calculating these summations the values of $\Phi_\theta'$ and $\Phi_\theta''$ are those read off directly from the polar diagram at the angles given in Table IV. The ratio of this to the summa-

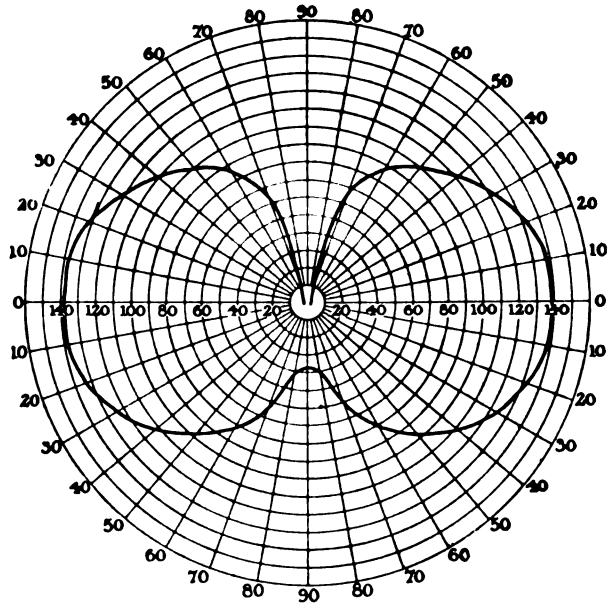


Fig. 6. Polar curve of Osram reference lamp No. 2.

tion for a unit point source gives a result of 113·0. Thus a lamp with the polar distribution shown in fig. 6 behaves in the cube in the same way as does a point source (to a fairly close approximation) and may therefore be used instead of an ideal point source for the purpose of calibrating the cube for measurements of other lamps.

Digitized by Google

(3) *A Squirrel-Cage Metal-Filament Vacuum Lamp with Close-Fitting Shade (axis of lamp vertical).*—This lamp is illustrated in fig. 7, and its polar distribution given in fig. 8.

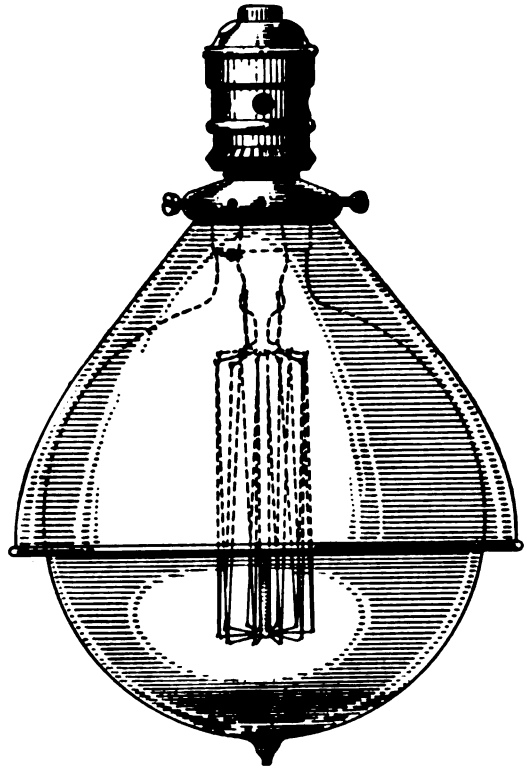

Fig. 7. Standardised 1,000-watt 240-volt lamp, and shade (shade whitened).

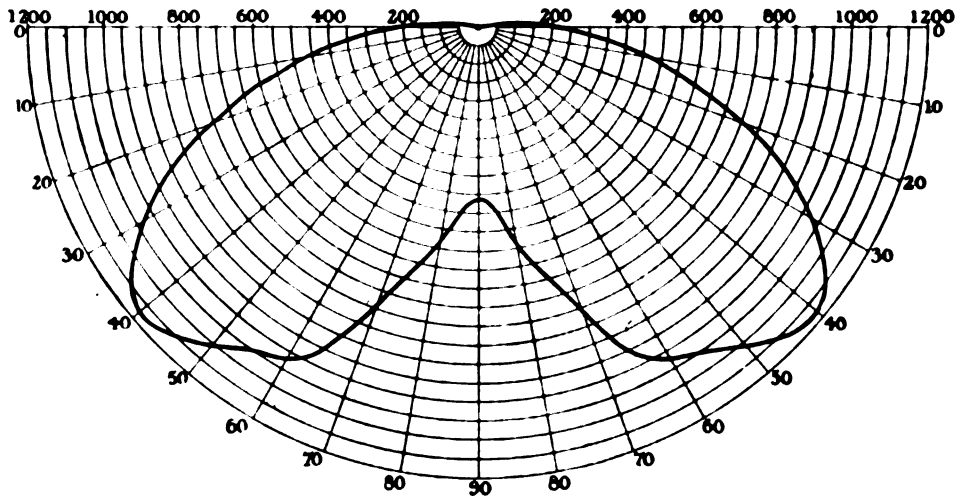


Fig. 8. Polar curve of 1,000-watt lamp (fig. 7).

It was set up with the centre of the edge of the shade at the mid-point of the cube. It was anticipated that a distribution of light of this kind, in which only the lower half of the cube received any direct light, would be one in which the value of $\Sigma$ ($Fz$) would show

Digitized by Google

deviations from proportionality with the average candle-power. In this case the average candle-power as given by a point-to-point method was 422.

As before, the summation consists of four portions

$$\text{(1) back} \qquad = 2\frac{l^3}{4^2}\sum\left\{\frac{\alpha\Phi_{\theta'}}{(l^2+x^2+y^2)^{3/2}}\right\};$$

$$\text{(2) front} \qquad = 2\frac{l^3}{4^2}\sum\left\{\frac{\delta\Phi_{\theta'}}{(l^2+x^2+y^2)^{3/2}}\right\};$$

$$\text{(3) sides} \qquad = 2\frac{l^3}{4^2}\sum\left\{\frac{(\beta+\gamma)\Phi_{\theta'}}{(l^2+x^2+y^2)^{3/2}}\right\};$$

$$\text{(4) bottom} \qquad = 2\frac{l^3}{4^2}\sum\left\{\frac{(\beta+\gamma)\Phi_{\theta''}}{(l^2+x^2+y^2)^{3/2}}\right\};$$

therefore

$$\Sigma\,(F\alpha) = 405{,}25.$$

On comparing this with the summation for a unit point source it can be seen that with this distribution the cube has the effect of making the apparent candle-power 404 instead of 422. Thus from theoretical considerations we may say that lamps having polar distributions similar to (1) that of a point source, (2) that of fig. 6, and (3) that of fig. 8, may be compared among themselves for average candle-power to an accuracy of about 4 per cent., if they are situated in the cube in the same way as the above calculations have assumed.

This statement is capable of experimental verification. The two lamps whose polar curves have been given were introduced into the middle of the cube, and photometric balance was obtained in the usual way. The mirror in the photometer was dispensed with, as the illumination of the window was satisfactory in each case. The means of five observations by each of two observers gave

(1) for the 114·0-c.p. lamp, 1,172 and 1,166 mm. . . . . Mean = 1,169,

(2) for the 422-c.p. lamp, 622 and 616 mm. . . . . Mean = 619.

The comparision should, of course, be made with one lamp behaving as point source. The results of the last section, however, indicate that the 114·0-c.p. lamp is not very far from fulfilling such a condition. Therefore

$$\frac{\text{Average candle-power of 422-c.p. lamp}}{\text{Average candle-power of 114·0-c.p. lamp}} = \left(\frac{1{,}169}{619}\right)^2.$$

Therefore

$$\text{Average candle-power of 422-c.p. lamp} = (1{,}169 \div 619)^2 \times 114{\cdot}0 = 407.$$

This result is very close to that which the summation leads one to expect.

Digitized by Google

Now the summation on the 114·0-c.p. lamp leads to the result that in the cube it behaves as if its candle-power were 113·0 and, if this value is used instead of 114·0, we get a still closer agreement. Therefore

Average candle-power of 422-c.p. lamp = $(1{,}169 \div 619)^2 \times 113{\cdot}0 = 403$.

(4) *A Squirrel-Cage Metal-Filament Vacuum Lamp with Close-Fitting Shade (axis of lamp horizontal and lamp facing the back of the cube).*—The summations are made for the same lamp as that used in the last section. In this position the back of the cube and the halves of the adjoining walls alone receive direct light. The polar curve of this lamp (fig. 8) as thus situated in the cube is very similar to that of an arc, so that the results obtained in this case apply approximately to the case of the arc.

$\Sigma$ (F$\alpha$) consists of two portions (the C and D walls receive no direct light at all).

(1) back $$= 4\frac{l^3}{4^2}\sum\left\{\frac{\alpha\Phi_{\theta''}}{(l^2+x^2+y^2)^{3/2}}\right\},$$

$\theta''$ taking the place of $\theta'$ because the back of the cube is now similarly situated with respect to the lamp as the bottom was previously.

(2) sides, top and bottom (the halves adjoining the back)

$$= 8\,.\,\frac{l^3}{4^2}\sum\left\{\frac{\beta\Phi_{\theta}}{(l^2+x^2+y^2)^{3/2}}\right\}.$$

It should be noted in performing these summations that, since the axis of symmetry of the lamp is now horizontal, the numbering of the small squares from 1 to 16 does not correspond in the cases of the values of $\beta$ and those of $\Phi_{\theta''}$. If the order 1 . . . 16 is maintained for the latter, then the order for $\beta$ is 1, 5, 9, 13 ; 2, 6, 10, 14 ; 3, etc., and the products $\beta\,\Phi_{\theta''}$ are taken $\beta_1\Phi_{\theta_1}$, $\beta_5\Phi_{\theta_2}$, $\beta_9\Phi_{\theta_3}$, etc. Therefore

$$\Sigma\,(\mathrm{F}\alpha) = 128\sum\left\{\frac{\alpha\Phi_{\theta''}}{(l^2+x^2+y^2)^{3/2}}\right\} + 256\sum\left\{\frac{\beta\Phi_{\theta}}{(l^2+x^2+y^2)^{3/2}}\right\}$$
$$= 39{,}800.$$

On comparing this with the summation for the point source, it is seen that the cube has the effect of making the apparent candle-power 397 instead of 422. This is about 6 per cent. less than its known value. This result was tested experimentally. The means of five observations by each of two observers gave

(1) for the 114·0-c.p. lamp, 1,173 and 1,175 mm. . . . . Mean = 1,174,

(2) for the 422-c.p. lamp, 623 and 625 mm. . . . . Mean = 624.

Therefore

Average candle-power of 422-c.p. lamp = $(1{,}174 \div 624)^2 \times 114{\cdot}0 = 403$.



Digitized by Google

If, however, use is made of the result of section (2), which shows that the 114·0-c.p. lamp behaves in the cube as if it had an average candle-power of 113·0, this result is reduced to

$$(1{,}174 \div 624)^2 \times 113{\cdot}0 = 400.$$

This again is very close to the result indicated by theory, so that it can be assumed that a comparison of theory and practice for other positions at the middle of the cube will be accompanied by similar correspondence.

The preceding results and summations have applied only to lamps situated at the middle of the cube. It is important to find whether the same agreement will occur for an eccentric position. The position chosen was half-way between the top of the cube and the middle. It should be remembered, however, that the conditions in this eccentric position are not quite the same as for the central position, as the lamps used in the cube exert some disturbing influence on the "contribution coefficient". This can be seen in fig. 4, where the big dip in curve $\alpha$ is due to the action of the projector in the middle of the cube, and also to the screen. With positions away from the centre it is to be anticipated that this drop in the contribution coefficient will take place roughly at the place where the line through the window and the lamp meets the cube again, and it is probable that the effect on the summations is appreciable in certain cases.

(5) *A Point Source (eccentric position).*—

$$\Sigma(F\alpha) = 100{\cdot}7$$

(6) *A Squirrel-Cage Metal-Filament Vacuum Lamp (eccentric position).*—

$$\Sigma(F\alpha) = 11{,}360.$$

On comparing this with the result for a unit point source it is seen that the apparent average candle-power has become $11{,}360 \div 100{\cdot}7 = 112{\cdot}8$.

(7) *A Squirrel-Cage Metal-Filament Vacuum Lamp with Close-Fitting Shade (eccentric position).*—

$$\Sigma(F\alpha) = 41{,}280.$$

On comparison with the result for a unit point source at the same position the apparent average candle-power becomes 410. On testing this experimentally, photometric balance was obtained at distances of

(1) for the 114·0-c.p. lamp, 1,165 and 1.158 mm. . . . . Mean = 1,161·5,

(2) for the 422-c.p. lamp, 610 and 606 mm. . . . . Mean = 608·5.

Therefore

$$\text{Average candle-power of 422-c.p. lamp} = (1{,}161{\cdot}5 \div 608)^2 \times 114{\cdot}0 = 417.$$

Digitized by Google

On comparing with the result 112·8 as the apparent candle-power of the 114·0-c.p. lamp given by the summation in section (6), we get

$$(1{,}161{\cdot}5 \div 608)^2 = 112{\cdot}8 = 413,$$

and this again is in very close agreement with theory.

*Conclusions.*

These results make it possible for corrections to be applied to the determinations of average candle-power made in the cube in the usual way, *i.e.*, by comparison of the illuminations produced on the window, by the lamp under test, and by a comparision lamp of known intensity. For, instead of the real candle-power of the comparision lamp, its apparent value in the cube is used, and this is given by the ratio of $\Sigma\,(F\alpha)$ for this lamp to the corresponding summation for a unit point source at the same place. The result after the application of the above is then multiplied by the ratio

$$\frac{\text{real candle-power}}{\text{apparent candle-power in the cube}},$$

where this ratio has been calculated for the type of polar distribution exhibited by the test lamp. Thus, if $x$ and $y$ are the distances on the photometer bench for photometric balance with the cube comparison lamp and test lamps respectively, P is the average candle-power of the cube comparison lamp, and Q that of *any* lamp having a similar polar distribution to the test lamp, then the average candle-power of the test lamp

$$= \frac{y^2}{x^2} \times \frac{\Sigma\,(F\alpha)_P}{\Sigma\,(F\alpha)_1} \times \frac{\Sigma\,(F\alpha)_1}{\Sigma\,(F\alpha)_Q} \times Q$$

$$= \frac{y^2}{x^2} \times \frac{\Sigma\,(F\alpha)_P}{\Sigma\,(F\alpha)_Q} \times Q,$$

where the suffixes indicate for which lamp the summation is to be made.

If the polar distributions of the test lamp and comparision lamps are the same, then

$$\frac{\Sigma\,(F\alpha)_P}{\Sigma\,(F\alpha)_Q} = \frac{P}{Q}$$

and the average candle-power of the test lamp

$$= \frac{y^2}{x^2} P,$$

This shows that the cube is quite accurate in comparing light sources of similar distribution.

An application of this theory can be made to the measurement of the total flux in a beam. It is obvious that if a narrow beam of light having a constant flux is incident on



Digitized by Google

the walls of the cube, there will be different illuminations on the window which will vary directly as the contribution coefficient of the point of incidence. Now the greatest and least values of the contribution coefficient are proportional to 9·57 and 6·71 respectively, while the average for the whole cube, when used with a point source, is 7·96. If now the beam is incident at a point where the actual value is equal to the average, we may compare the fluxes in the beam and cube comparision lamp by taking $4\pi$ times the ratio of the inverse squares of the distances from the bench comparison lamp, multiplied by the ratio

$$\frac{\Sigma\,(F\alpha)_P}{\Sigma\,(F\alpha)_1},$$

Fig. 4 shows that the contribution coefficient varies considerably on the back of the cube but is fairly constant on the sides. Fig. 9 shows the same thing in terms of contours. Large portions have a value not far from 8·20, so that a convenient spot on one of these walls can be taken and the result multiplied by $796 \div 820 = 0{\cdot}97$.

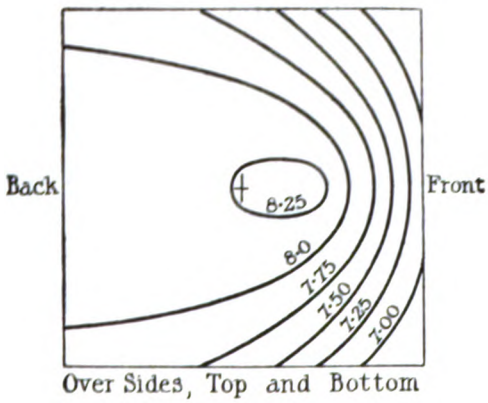


Fig. 9. Variation of "contribution coefficient."

Throughout this investigation the effects of foreign bodies in the cube have been assumed to be small, as they always had an area very small compared with the total area of the inside of the cube. It is proposed in a later paper to deal with this matter and also the effects of ventilating openings (such as have to be used in arc tests) and the non-uniformity of the cube as regards the whiteness of its interior.

*Synopsis of Results.*

(1) The variation in the contribution coefficient over the walls of a 2-metre cube has been determined.

(2) The apparent candle-powers of various light-distributions in the cube have been calculated and found to agree very closely with experiment.

(3) The cube has been shown to be quite accurate with sources having similar distributions.

(4) It has been shown how true average candle-powers may be deduced from the comparison of sources of different polar distribution, thus making the cube an instrument of precision.

(5) An application of the cube to the measurement of the total flux in beams has been indicated.

Digitized by Google

In conclusion I wish to express my indebtedness to Messrs. J. W. T. WALSH and H. C. STURGEON of the National Physical Laboratory, the former for suggesting this work and for his interest in it, and the latter for invaluable assistance in taking the photometric readings and in the somewhat tedious task of performing the summations.

## APPENDIX.

The complete calculations for $\Sigma$ (F$\alpha$) in section (6) are given here to show the method employed. In this case the lamp (Osram, Ref. No. 2, 114·0 candle-power) is midway between the middle of the cube and the top. The projection of the centre of the lamp now comes at the common point of the four squares $A_1$ in fig. 10, which also shows the new system of numbering squares that becomes necessary to avoid possible confusion on this account. A horizontal plane through the centre of the lamp cuts the wall at the double line, and it is about this line that symmetry occurs in the values of $\theta'$. As regards the contribution factor, that is still symmetrical about a horizontal line through the centre of the wall. Thus the values of the contribution factor over the squares $A_1$ . . . $A_8$ below the double line are the same as those over the former squares $A_5$, $A_6$, $A_7$, $A_8$; $A_1$, $A_2$, $A_3$, $A_4$, those over the squares $A_9$ . . . $A_{24}$ are the same as over the former $A_1$ . . . $A_{16}$, while those from $A_1$ . . . $A_8$ above the double line are the same as over the former $A_9$ . . . $A_{16}$. Similar considerations apply to all the vertical walls.

| | | | | | | | |
|---|---|---|---|---|---|---|---|
| $A_8$ | $A_7$ | $A_6$ | $A_5$ | $A_5$ | $A_6$ | $A_7$ | $A_8$ |
| $A_4$ | $A_3$ | $A_2$ | $A_1$ | $A_1$ | $A_2$ | $A_3$ | $A_4$ |
| $A_4$ | $A_3$ | $A_2$ | $A_1$ | $A_1$ | $A_2$ | $A_3$ | $A_4$ |
| $A_8$ | $A_7$ | $A_6$ | $A_5$ | $A_5$ | $A_6$ | $A_7$ | $A_8$ |
| $A_{12}$ | $A_{11}$ | $A_{10}$ | $A_9$ | $A_9$ | $A_{10}$ | $A_{11}$ | $A_{12}$ |
| $A_{16}$ | $A_{15}$ | $A_{14}$ | $A_{13}$ | $A_{13}$ | $A_{14}$ | $A_{15}$ | $A_{16}$ |
| $A_{20}$ | $A_{19}$ | $A_{18}$ | $A_{17}$ | $A_{17}$ | $A_{18}$ | $A_{19}$ | $A_{20}$ |
| $A_{24}$ | $A_{23}$ | $A_{22}$ | $A_{21}$ | $A_{21}$ | $A_{22}$ | $A_{23}$ | $A_{24}$ |

Fig. 10. Division of sides of cube for summation described in appendix.

Now in the expression $\Sigma$ (F$\alpha$), F, the flux on an area, is given by

$$\frac{\text{area} \times \cos \text{(angle of incidence)}}{\text{(distance from source to centre of area)}^2 \times \text{(cp. in direction of centre of area)}}$$

$$= \frac{l^2}{4} \times \frac{l_1}{\sqrt{(l_1^2 + x^2 + y^2)}} \times \frac{1}{(l_1^2 + x^2 + y^2)} \times \Phi_\theta,$$

where $l_1$ = perpendicular distance of the source from a wall of the cube. In sections (1) to (4), $l_1 = l$, but now, if we consider the vertical walls, $l_1 = l$, the bottom $l_1 = 3l/2$ and the top $l_1 = \frac{1}{2}l$. The expressions for $\theta'$ and $\theta''$ also involve $l_1$ thus:—

$$\theta' = \text{arc sin} \frac{y}{\sqrt{(l_1^2 + x^2 + y^2)}},$$

$$\theta'' = \text{arc sin} \frac{l_1}{\sqrt{(l_1^2 + x^2 + y^2)}},$$

Digitized by Google

where $l_1 = l$, $3l/2$ and $\frac{1}{2}l$ for different walls. This will result in modifications to Tables III and IV. These are shown in Tables V and VI respectively.

TABLE V.

| Area. | $[l^2+x^2+y^2]^{3/2}$ | Area | $[(3l/2)^2+x^2+y^2]^{3/2}$ | $[(l/2)^2+x^2+y^2]^{3/2}$ |
|---|---|---|---|---|
| $A_{17}$ | 146 | $A_1$ | 1,767 | 76 |
| $A_{18}$ | 154 | $A_2$ | 1,911 | 133 |
| $A_{19}$ | 170 | $A_3$ | 2,217 | 262 |
| $A_{20}$ | 184 | $A_4$ | 2,703 | 535 |
| $A_{21}$ | 186 | $A_5$ | 1,911 | 133 |
| $A_{22}$ | 194 | $A_6$ | 2,063 | 200 |
| $A_{23}$ | 210 | $A_7$ | 2,374 | 353 |
| $A_{24}$ | 234 | $A_8$ | 2,869 | 636 |
| | | $A_9$ | 1,217 | 272 |
| Values for area $A_1 \ldots A_{16}$ are given in Table III. | | $A_{10}$ | 2,374 | 353 |
| | | $A_{11}$ | 2,703 | 535 |
| | | $A_{12}$ | 3,216 | 855 |
| | | $A_{13}$ | 2,703 | 535 |
| | | $A_{14}$ | 2,869 | 636 |
| | | $A_{15}$ | 3,216 | 855 |
| | | $A_{16}$ | 3,767 | 1,218 |

TABLE VI.—Values of $\theta$.

| Area. | $\theta' = \text{arc sin} \frac{y}{\sqrt{(l^2+x^2+y^2)}}$ | Area. | $\theta''' = \text{arc sin} \frac{3l/2}{\sqrt{[(3l/2)^2+x^2+y^2]}}$ | $\theta'''' = \text{arc sin} \frac{\frac{1}{2}l}{\sqrt{[(\frac{1}{2}l)^2+x^2+y^2]}}$ |
|---|---|---|---|---|
| $A_{17}$ | 48° | $A_1$ | 83° | 71° |
| $A_{18}$ | 47° | $A_2$ | 79° | 51° |
| $A_{19}$ | 44° | $A_3$ | 67° | 38° |
| $A_{20}$ | 40° | $A_4$ | 60° | 30° |
| $A_{21}$ | 54° | $A_5$ | 75° | 51° |
| $A_{22}$ | 52° | $A_6$ | 70° | 43° |
| $A_{23}$ | 49° | $A_7$ | 64° | 34° |
| $A_{24}$ | 46° | $A_8$ | 58° | 28° |
| | | $A_9$ | 67° | 38° |
| Values for areas $A_1 \ldots A_{16}$ are give in Table IV. | | $A_{10}$ | 64° | 34° |
| | | $A_{11}$ | 60° | 30° |
| | | $A_{12}$ | 54° | 25° |
| | | $A_{13}$ | 60° | 30° |
| | | $A_{14}$ | 58° | 28° |
| | | $A_{15}$ | 54° | 25° |
| | | $A_{16}$ | 50° | 22° |

Digitized by Google

The summation $\Sigma(F\alpha)$ consists of four parts—

(1) sides, back and front, below double line,

$$= 2\frac{l^2}{4^2} \cdot l \sum_1^{24} \left\{ \frac{(\alpha + \beta + \gamma + \delta)\,\Phi_\theta}{(l^2 + x^2 + y^2)^{3/2}} \right\};$$

(2) sides, back and front, above double line,

$$= 2\frac{l^2}{4^2} \cdot l \sum_1^{8} \left\{ \frac{(\alpha + \beta + \gamma + \delta)\,\Phi_\theta}{(l^2 + x^2 + y^2)^{3/2}} \right\};$$

(3) bottom

$$= 2\frac{l^2}{4^2} \cdot \frac{3l}{2} \sum_1^{16} \left\{ \frac{(\beta + \gamma)\,\Phi_{\theta'}}{\{(3l/2)^2 + x^2 + y^2\}^{3/2}} \right\};$$

(4) top

$$= 2\frac{l^2}{4^2} \cdot \frac{l}{2} \sum_1^{16} \left\{ \frac{(\beta + \gamma)\,\Phi_{\theta''}}{\{(\frac{1}{2}l)^2 + x^2 + y^2\}^{3/2}} \right\}.$$

Therefore

$$\Sigma(F\alpha) = 64 \sum_1^{24} \left\{ \frac{(\alpha + \beta + \gamma + \delta)\,\Phi_\theta}{(8^2 + x^2 + y^2)^{3/2}} \right\} + 64 \sum_1^{8} \left\{ \frac{(\alpha + \beta + \gamma + \delta)\,\Phi_\theta}{(8^2 + x^2 + y^2)^{3/2}} \right\}$$
$$+ 96 \sum_1^{16} \left\{ \frac{(\beta + \gamma)\,\Phi_{\theta''}}{(12^2 + x^2 + y^2)^{3/2}} \right\} + 32 \sum_1^{16} \left\{ \frac{(\beta + \gamma)\,\Phi_{\theta''}}{(4^2 + x^2 + y^2)^{3/2}} \right\}$$

$$(1) = 6{,}400 \left( \frac{33\cdot02}{536} \times 1\cdot37 + \frac{32\cdot92}{636} \times 1\cdot37 + \frac{31\cdot64}{853} \times 1\cdot37 + \frac{30\cdot46}{1{,}218} \times 1\cdot37 \right.$$
$$+ \frac{31\cdot90}{637} \times 1\cdot31 + \frac{33\cdot39}{742} \times 1\cdot31 + \frac{32\cdot20}{969} \times 1\cdot32 + \frac{30\cdot72}{1{,}346} \times 1\cdot34$$
$$+ \frac{31\cdot90}{854} \times 1\cdot20 + \frac{33\cdot39}{969} \times 1\cdot22 + \frac{32\cdot20}{1{,}218} \times 1\cdot24 + \frac{30\cdot72}{1{,}621} \times 1\cdot27$$
$$+ \frac{33\cdot02}{1{,}218} \times 1\cdot10 + \frac{32\cdot92}{1{,}346} \times 1\cdot11 + \frac{31\cdot64}{1{,}621} \times 1\cdot15 + \frac{30\cdot46}{2{,}062} \times 1\cdot19$$
$$+ \frac{32\cdot27}{1{,}767} \times 1\cdot01 + \frac{31\cdot93}{1.911} \times 1\cdot03 + \frac{30\cdot62}{2{,}217} \times 1\cdot06 + \frac{29\cdot92}{2{,}703} \times 1\cdot11$$
$$\left. + \frac{31\cdot64}{2{,}538} \times 0\cdot93 + \frac{31\cdot06}{2{,}703} \times 0\cdot96 + \frac{29\cdot72}{3{,}042} \times 1\cdot00 + \frac{29\cdot25}{3{,}582} \times 1\cdot04 \right)$$
$$= 6{,}400\ (0\cdot7861) = 5{,}030.$$

$$(2) = 6{,}400 \left( \frac{32\cdot27}{536} \times 1\cdot37 + \frac{31\cdot93}{636} \times 1\cdot37 + \frac{30\cdot62}{853} \times 1\cdot37 + \frac{29\cdot92}{1{,}218} \times 1\cdot37 \right.$$
$$\left. + \frac{31\cdot64}{637} \times 1\cdot31 + \frac{31\cdot06}{742} \times 1\cdot31 + \frac{29\cdot72}{969} \times 1\cdot32 + \frac{29\cdot25}{1{,}346} \times 1\cdot34 \right)$$
$$= 6{,}400 \times (0\cdot4239) = 2{,}710.$$

Digitized by Google

$$(3) = 9{,}600\left(\frac{16\cdot48}{1{,}767}\times 0\cdot22 + \frac{16\cdot45}{1{,}911}\times 0\cdot33 + \frac{16\cdot26}{2{,}217}\times 0\cdot68 + \frac{15\cdot56}{2{,}703}\times 0\cdot84\right.$$
$$+ \frac{16\cdot50}{1{,}911}\times 0\cdot45 + \frac{16\cdot20}{2{,}063}\times 0\cdot60 + \frac{15\cdot98}{2{,}374}\times 0\cdot75 + \frac{15\cdot52}{2{,}869}\times 0\cdot87$$
$$+ \frac{15\cdot91}{2{,}217}\times 0\cdot68 + \frac{15\cdot77}{2{,}374}\times 0\cdot75 + \frac{15\cdot36}{2{,}703}\times 0\cdot84 + \frac{15\cdot20}{3{,}216}\times 0\cdot93$$
$$\left. + \frac{15\cdot71}{2{,}702}\times 0\cdot85 + \frac{15\cdot44}{2{,}869}\times 0\cdot88 + \frac{15\cdot04}{3{,}216}\times 0\cdot93 + \frac{14\cdot78}{3{,}763}\times 0\cdot99\right)$$
$$= 9{,}600 \times 0\cdot0701 = 673.$$

$$(4) = 3{,}200\left(\frac{16\cdot48}{76}\times 0\cdot58 + \frac{16\cdot45}{133}\times 0\cdot97 + \frac{16\cdot26}{272}\times 1\cdot13 + \frac{15\cdot56}{535}\times 1\cdot22\right.$$
$$+ \frac{16\cdot50}{133}\times 0\cdot97 + \frac{16\cdot20}{200}\times 1\cdot08 + \frac{15\cdot98}{353}\times 1\cdot18 + \frac{15\cdot52}{636}\times 1\cdot24$$
$$+ \frac{15\cdot91}{272}\times 1\cdot14 + \frac{15\cdot77}{353}\times 1\cdot18 + \frac{15\cdot36}{535}\times 1\cdot22 + \frac{15\cdot20}{855}\times 1\cdot27$$
$$\left. + \frac{15\cdot71}{535}\times 1\cdot22 + \frac{15\cdot44}{636}\times 1\cdot42 + \frac{15\cdot04}{855}\times 1\cdot27 + \frac{14\cdot78}{1\ 218}\times 1\cdot29\right)$$
$$= 3{,}200 \times 0\cdot9213 = 2{,}945.$$

Therefore

$$\Sigma\ (F\alpha) = (1) + (2) + (3) + (4)$$
$$= 11{,}358.$$

Printed under the authority of His Majesty's Stationery Office
By Harrison and Sons, Ltd., 44-47, St. Martin's Lane, London, W.C. 2,
Printers in Ordinary to His Majesty.
(B 34-2034)z Wt. 19897—1002/1369 625 7/25 H & S Ltd. Gp. 34

Digitized by Google

Physics Lib
JUN 24 1927
QC
1
.T256
C6

Eddington, Eng

THE

# NATIONAL PHYSICAL LABORATORY

## COLLECTED RESEARCHES

VOL. XIX, 1926

LONDON:
PUBLISHED BY HIS MAJESTY'S STATIONERY OFFICE
To be purchased directly from H.M. STATIONERY OFFICE at the following addresses:
Adastral House, Kingsway, London, W.C. 2; 120, George Street, Edinburgh;
York Street, Manchester; 1, St. Andrew's Crescent, Cardiff;
15, Donegall Square West, Belfast;
or through any Bookseller.

1926.

*Price* 18*s.* 6*d. Net*

Digitized by Google

Digitized by Google

THE

# NATIONAL PHYSICAL LABORATORY

## COLLECTED RESEARCHES

VOL. XIX, 1926

LONDON:
PUBLISHED BY HIS MAJESTY'S STATIONERY OFFICE
To be purchased directly from H.M. STATIONERY OFFICE at the following addresses:
Adastral House, Kingsway, London, W.C. 2; 120, George Street, Edinburgh;
York Street, Manchester; 1, St. Andrew's Crescent, Cardiff;
15, Donegall Square West, Belfast;
or through any Bookseller.

1926.

*Price* 18*s.* 6*d. Net*

Digitized by Google

Digitized by Google

Physics
Sotheran
3-30-27
sub.

# CONTENTS.

## Vol. XIX.

Page

I. The Measurement of Thermal Conductivity. By E. Griffiths, D.Sc., F.R.S., Principal Assistant, and G. W. C. Kaye, O.B.E., M.A., D.Sc., Superintendent, Physics Department. (Reprinted from the 'Proceedings of the Royal Society', A, Vol. 104, 1923) . . . . . 1

II. Some Materials of Low Thermal Conductivity. By E. Griffiths, D.Sc., F.R.S., Principal Assistant in the Physics Department. (Reprinted from the 'Transactions of the Faraday Society', Vol. 18, 1922) . . . . . 27

III. The Thermal and Electrical Conductivities of Some Pure Metals. By F. H. Schofield, B.A., B.Sc., Senior Assistant in the Physics Department. (Reprinted from the 'Proceedings of the Royal Society', A, Vol. 107, 1925) . . . . . 37

IV. The Thermal Conductivities of Metal Crystals—I. Bismuth. By G. W. C. Kaye, O.B.E., M.A., D.Sc., Superintendent, and J. K. Roberts, M.Sc., Ph.D., sometime Assistant, Physics Department. (Reprinted from the 'Proceedings of the Royal Society', A, Vol. 104, 1923) 59

V. The Thermal Expansion of Crystals of Metallic Bismuth. By J. K. Roberts, M.Sc., Ph.D., sometime Assistant in the Physics Department. (Reprinted from the 'Proceedings of the Royal Society', A, Vol. 106, 1924) . . . . . 75

VI. New Specific Heat Apparatus. By Ezer Griffiths, D.Sc., F.R.S., Principal Assistant in the Physics Department. (Reprinted from the 'Proceedings of the Physical Society of London', Vol. 33, 1921) . . . . . 91

VII. Apparatus for the Determination of the Heat of Evaporation of Liquids of High Boiling Points. By J. H. Awbery, B.A., B.Sc., Assistant, and Ezer Griffiths, D.Sc., F.R.S., Principal Assistant in the Physics Department. (Reprinted from the 'Proceedings of the Physical Society of London', Vol. 36, 1924) . . . . . 99

VIII. Thermometric Lag with especial Reference to Cold Storage Practice. By Ezer Griffiths, D.Sc., F.R.S., Principal Assistant, and J. H. Awbery, B.A., B.Sc., Assistant in the Physics Department. (Reprinted from the 'Transactions of the Faraday Society', Vol. 18, 1922) . 111

IX. Some Modified Forms of Hygrometers. By Ezer Griffiths, D.Sc., F.R.S., Principal Assistant in the Physics Department. (Reprinted with modifications from the 'Proceedings of the Physical Society of London', Vol. 34, 1922) . . . . . 123

X. An Instrument for Use in Measuring Convected Heat. By A. H. Davis, D.Sc., Assistant in the Physics Department. (Reprinted with modifications from the 'Proceedings of the Physical Society of London', Vol. 33, 1921) . . . . . 171



Digitized by Google

Page

XI. The Convection of Heat in Gases and Liquids—I. Convection of Heat and Similitude. By A. H. Davis, D.Sc., Assistant in the Physics Department. (Reprinted with modifications from the ' Philosophical Magazine ', Vol. 40, 1920) . . . . . 181

XII. The Convection of Heat in Gases and Liquids—II. Natural Convective Cooling of Wires in Gases. By A. H. Davis, D.Sc., Assistant in the Physics Department. (Reprinted from the ' Philosophical Magazine ', Vol. 43, 1922) . . . . . 193

XIII. The Convection of Heat in Gases and Liquids—III. Forced Convective Cooling of Wires in Gases. By A. H. Davis, D.Sc., Assistant in the Physics Department. (Reprinted from the ' Philosophical Magazine ', Vol. 41, 1921) . . . . . 203

XIV. The Convection of Heat in Gases and Liquids—IV. Natural Convective Cooling in Viscous Gases and Liquids. By A. H. Davis, D.Sc., Assistant in the Physics Department. (Reprinted from the ' Philosophical Magazine ', Vol. 44, 1922) . . . . . 213

XV. The Convection of Heat in Gases and Liquids—V. Some Thermal Conductivity Data for Liquids. By A. H. Davis, D.Sc., Assistant in the Physics Department. (Reprinted from the ' Philosophical Magazine ', Vol. 47, 1924) . . . . . 233

XVI. The Convection of Heat in Gases and Liquids—VI. Theory of Forced Convective Cooling in Viscous Gases and Liquids. By A. H. Davis, D.Sc., Assistant in the Physics Department. (Reprinted from the ' Philosophical Magazine ', Vol. 44, 1922, as modified and extended by the subsequent note in Vol. 49, 1925) . . . . . 239

XVII. The Convection of Heat in Gases and Liquids—VII. Experimental Study of Forced Convective Cooling in Viscous Liquids. By A. H. Davis, D.Sc., Assistant in the Physics Department. (Reprinted from the ' Philosophical Magazine ', Vol. 47, 1924) . . . . . 245

XVIII. An All-Metal High-Vacuum Pump System. By Ivor Backhurst, M.Sc., Assistant, and G. W. C. Kaye, O.B.E., M.A., D.Sc., Superintendent, Physics Department. (Reprinted from the ' Philosophical Magazine ', Vol. 47, 1924) . . . . . 275

XIX. A Metal Annular-Jet Vacuum Pump. By Ivor Backhurst, M.Sc., Assistant, and G. W. C. Kaye, O.B.E., M.A., D.Sc., Superintendent, Physics Department. (Reprinted from the ' Philosophical Magazine ', Vol. 47, 1924) . . . . . 287

XX. The Composition of X-Rays from Various Metals. By G. W. C. Kaye, O.B.E., M.A., D.Sc., Superintendent, Physics Department. (Reprinted from the ' Proceedings of the Royal Society ', A., Vol. 93, 1917) . . . . . 293

XXI. X-Ray Protective Materials. By G. W. C. Kaye, O.B.E., M.A., D.Sc., Superintendent, and E. A. Owen, M.A., D.Sc., Senior Assistant, Physics Department. (Reprinted from the ' Proceedings of the Physical Society of London ', Vol. 35, 1923) . . . . . 309

XXII. X-Ray Dosage, with Special Reference to the Barium Platino-Cyanide Pastille. By E. A. Owen, M.A., D.Sc., Senior Assistant, and Phyllis K. Bowes, M.A., B.Sc., sometime Junior Assistant, in the Physics Department. (Reprinted from the ' Journal of the Röntgen Society ', Vol. 17, 1921); also, Note on the Gold Leaf Electroscope. By E. A. Owen, M.A., D.Sc., Senior Assistant in the Physics Department. (Reprinted from the ' Journal of the Röntgen Society ', Vol. 16, 1920) . . . . . 319

Digitized by Google

XXIII. Some Observations on Induction Coil and Transformer Discharges with Coolidge and Gas Tubes. By E. A. Owen, M.A., D.Sc., Senior Assistant, and Phyllis K. Bowes, M.A., B.Sc., sometime Junior Assistant, in the Physics Department. (Reprinted from the 'Journal of the Röntgen Society', Vol. 19, 1923) . . . . . 339

XXIV. Modification of the Powder Method of Determining the Structure of Metal Crystals. By E. A. Owen, M.A., D.Sc., Senior Assistant in the Physics Department, and G. D. Preston, B.A., Assistant in the Metallurgy Department. (Reprinted from the 'Proceedings of the Physical Society of London', Vol. 35, 1923) . . . . . 349

XXV. X-Ray Analysis of Solid Solutions. By E. A. Owen, M.A., D.Sc., Senior Assistant in the Physics Department, and G. D. Preston, B.A., Assistant in the Metallurgy Department. (Reprinted from the 'Proceedings of the Physical Society of London', Vol. 36, 1923) . . . 359

XXVI. X-Ray Analysis of Zinc-Copper Alloys. By E. A. Owen, M.A., D.Sc., Senior Assistant in the Physics Department, and G. D. Preston, B.A., Assistant in the Metallurgy Department. (Reprinted from the 'Proceedings of the Physical Society of London', Vol. 36, 1923) . . . 377

XXVII. The Atomic Structure of Two Intermetallic Compounds. By E. A. Owen, M.A., D.Sc., Senior Assistant in the Physics Department, and G. D. Preston, B.A., Assistant in the Metallurgy Department. (Reprinted from the 'Proceedings of the Physical Society of London', Vol. 36, 1924) . . . . . 395

XXVIII. The Estimation of the Radium Content of Radio-active Luminous Compounds. By E. A. Owen, M.A., D.Sc., Senior Assistant, and Winifred E. Fage, B.Sc., sometime Assistant, in the Physics Department. (Reprinted from the 'Proceedings of the Physical Society of London', Vol. 34, 1921) . . . . . 405

XXIX. On the Measurement of the Radium Content of Sealed Metal Tubes. By E. A. Owen, M.A., D.Sc., Senior Assistant, and Bertha Naylor, B.Sc., Junior Assistant, in the Physics Department. (Reprinted from the 'Proceedings of the Physical Society of London', Vol. 34, 1922) . . . . . 415

XXX. Absorption and Scattering of Gamma-Rays. By E. A. Owen, M.A., D.Sc., Senior Assistant, N. Fleming, B.A., Junior Assistant, and Winifred E. Fage, B.Sc., sometime Assistant, in the Physics Department. (Reprinted from the 'Proceedings of the Physical Society of London', Vol. 36, 1924) . . . . . 423

XXXI. Reverberation Equations for Two Adjacent Rooms connected by an Incompletely Sound-proof Partition. By A. H. Davis, D.Sc., Assistant in the Physics Department. (Reprinted from the 'Philosophical Magazine', Vol. 50, 1925) . . . . . 437

Digitized by Google

Digitized by Google

# THE MEASUREMENT OF THERMAL CONDUCTIVITY

BY

EZER GRIFFITHS, D.Sc., F.R.S.,
PRINCIPAL ASSISTANT IN THE PHYSICS DEPARTMENT,

AND

G. W. C. KAYE, O.B.E., M.A., D.Sc.,
SUPERINTENDENT OF THE PHYSICS DEPARTMENT.

Digitized by Google

## ABSTRACT.

Three types of apparatus of the " plate " type are described for the rapid precision determination of the thermal conductivities of materials of low conductivity. Energy was supplied by electrical means, a measurement of both the energy entering and leaving the test specimen being made. Temperatures were measured by thermocouples. The samples were thin and no guard ring was required. An average time for the attainment of the " steady state " was 30 mins. or less, and the average accuracy of measurement of the conductivity was about 1 per cent.

Among the points dealt with in the paper are the thermal resistance at the bounding faces of a material, the effect of superimposing layers of compressible material, the measurement of the thickness of compressible material, the dependence of the conductivity of timber on structure and moisture content, the variation of the conductivity of rubber with mineral content, etc.


Digitized by Google

# THE MEASUREMENT OF THERMAL CONDUCTIVITY.

By EZER GRIFFITHS, D.Sc., F.R.S., Principal Assistant, and G. W. C. KAYE, O.B.E., M.A., D.Sc., Superintendent of the Physics Department.

[*Reprinted from the* ' Proceedings of the Royal Society ', A, Vol. 104, 1923.]

## I. Introduction.

A knowledge of thermal conductivities has now become of importance in a variety of industries ; for example, in the designing of electrical machinery and in the lagging of refrigerating and high-temperature plants.

While the literature* on thermal conductivity is fairly extensive, little attention has hitherto been paid to the design of apparatus for accelerated precision tests. For example, the ingenious methods of experiment devised by Prof. Lees† in the course of his classical and extensive investigations, while admirably adapted for the particular object he had in view, would be somewhat laborious if the number of specimens to be studied were considerable. Thermal conductivity is a physical constant not capable of ready determination by simple appliances, and in the design of the apparatus described later, our aim has been to produce an equipment which will give the desired data with the minimum expenditure of time and labour.

The present paper is intended to be the first of a series of communications on thermal conductivity from the National Physical Laboratory, in which it is hoped to give the results of determinations on a variety of metals and poor conductors over a range of conditions, together with accounts of the several methods devised for the purpose. The present communication is devoted to a description of the technique developed for testing large numbers of materials of low conductivity, of which relatively small samples can fairly be taken as representative of the parent material. Special attention has been paid to the question of the measurement of the thickness of the specimens. The results of the conductivity measurements are given for a selection of materials and, in particular, for a number of timbers under definite conditions of moisture-content, etc.‡

## II. Description of Apparatus.

Three different apparatus (designated below as Nos. 1, 2 and 3) were designed to meet the various circumstances which arose. They are all modifications of the " plate " or " wall " method, to which the standard equation defining conductivity ($k$)

$$Q = k\,A\,.\,t\,\frac{\theta_1 - \theta_2}{d}$$

* See Schofield, ' Glazebrook's Dictionary of Applied Physics ', vol. 1, p. 429, for a list of references.

† ' Phil. Trans. ', vol. 188, p. 481, 1892 ; vol. 191, p. 399, 1898 ; vol. 208, p. 381, 1908.

‡ We wish to express our appreciation of the valuable assistance which Mr. A. R. Challoner and Mr. D. E. A. Jones have rendered in this work.



Digitized by Google

is directly applicable, Q being the quantity of heat which, when the "steady state" is reached, passes normally in time $t$ through a material of cross section A and thickness $d$, the faces of which are maintained at temperatures $\theta_1$ and $\theta_2$.

As regards the measurement of Q, the samples of material employed were all sufficiently thin compared with the cross section to make the use of a "guard ring" unnecessary. The edge correction could, if necessary, be determined with sufficient accuracy, and in any event its amount was small and usually negligible.

In each type of apparatus the "hot face" was a copper block heated electrically, the energy input being readily measured. The "cold face" was a copper block which was cooled by a stream of water flowing through a copper worm, the energy received being measured by the method of the continuous flow calorimeter. Thus a double measurement of the energy was made, and a valuable check was to hand which served to reveal any anomalies or adventitious losses which might otherwise have escaped detection.

The measurements of the time $t$ and the area A presented no difficulties. The latter was the same in all three apparatus. The thickness $d$ was sufficiently small in some instances to demand special arrangements for its determination. Some difficulty arose as to its measurement in the case of compressible materials like fabrics, for which a definite figure can only be given when the material is under a specific pressure. The question is dealt with in a separate section of the paper.

The temperature measurements ($\theta$) were carried out by copper-constantan thermocouples and presented no special difficulties in themselves. One important question does, however, arise in the case of some materials, and that is the discontinuity in temperature which occurs at the two faces of a material unless there is first-class thermal contact with the adjacent hot or cold copper surfaces. In some cases the difficulty was met by amalgamating the copper plates, but this plan is not always feasible—for example, in dealing with porous materials. The point will be found to have received attention in the paper.

Other features which call for remark were the considerable variation in the physical properties of the various materials tested, *e.g.* the hardness, porosity, compressibility, and, in some cases, the irregular structure. The several modifications of the apparatus devised, which we will now describe, were each adapted in the main for the study of a group of materials possessing the same general characteristics. Each of the apparatus required from 15 minutes to 30 minutes, and less frequently 45 minutes, for the specimens utilised to reach the steady state, so that measurements could be commenced.

The accuracy aimed at in the present measurements was 1 per cent., and this was achieved as a rule, though occasionally 2 per cent. was all that could be claimed. Some of the materials tested were, however, sufficiently indefinite in character to make this figure ample for all requirements.

It is convenient to measure power in watts, so that the above formula becomes

$$k\ (\text{c.g.s.}) = \frac{\text{Q (watts)} \times d\ (\text{cm.})}{\text{A (sq. cm.)} \times (\theta_1 - \theta_2)\ ^\circ\text{C.} \times 4{\cdot}184}.$$

Digitized by Google

In engineering practice in this country the conductivity unit commonly employed is the British Thermal Unit per hour per sq. foot per inch thickness per 1° F. temperature difference. To convert conductivities expressed in c.g.s. units into the British units it is necessary to multiply by 2903.

The use of " thermal resistivity " is found also to be convenient in engineering practice, where the term denotes the ratio of the temperature gradient (in degrees C. per cm.) to the watts conducted per sq. cm. To convert c.g.s. conductivity ($k$) into resistivity it is necessary to divide the reciprocal of $k$ by 4·184.

## (1) *Apparatus No.* 1.

(*a*) *General Description.*—This apparatus was designed for the study of materials which were readily available in the form of discs $\frac{1}{2}$ mm. to 4 mm. thick and about 45 mm. in diameter. The apparatus proved specially convenient for those materials of a slightly compressible nature, such as cardboard and the various hard timbers which could not, moreover, be tested between amalgamated plates owing to the penetration of the mercury into the pores of the material.

The apparatus consists essentially of a hot plate mounted horizontally and midway between and parallel to two cold plates, two samples of the material under test being sandwiched in the intervening spaces (Fig. 1). The hot plate was made up of two copper discs face to face, each 45 mm. ($1\frac{3}{4}$ inches) in diameter and about 1·25 mm. (1/20 inch) thick. Between them was mounted a heating grid made by winding 0·2 mm. platinum wire on a sheet of mica, the resistance when hot being about 8 ohms. The cold surfaces were provided by the ends of two short cylindrical copper blocks, each wound with a spiral of $\frac{1}{8}$-inch diameter copper tubing soldered to the surface of the block. The salient dimensions of the apparatus were those prescribed by the maximum current which could safely be passed through the heating grid, and by the ability of the cooling water to maintain a conveniently measurable temperature gradient across the particular thickness of test material employed.

The surfaces of both hot and cold plates were scraped flat to an accuracy of within 0·00025 cm. (1/10000 inch) over their area. Small holes were drilled into the edges near the flat surfaces, and into these thermocouples were pegged. The arrangement of the thermoelements is dealt with presently.

The water circulation was obtained from a constant head tank, the temperature of which was so adjusted by a submerged thermostatic heating coil that the mean of the inlet and outlet temperatures of the water circulation in the apparatus was approximately equal to room temperature, the object being to avoid the necessity of making correction for heat exchange between the copper blocks and their surroundings. The temperature rise of the water flowing round each block was measured independently by a pair of differential thermojunctions composed of six couples of copper-constantan connected in series and mounted as shown in glass tubes round which the water flowed

Digitized by Google

through spiral guides. When observations were proceeding the apparatus was well wrapped up with asbestos and cotton wool, so as to maintain uniformity of temperature

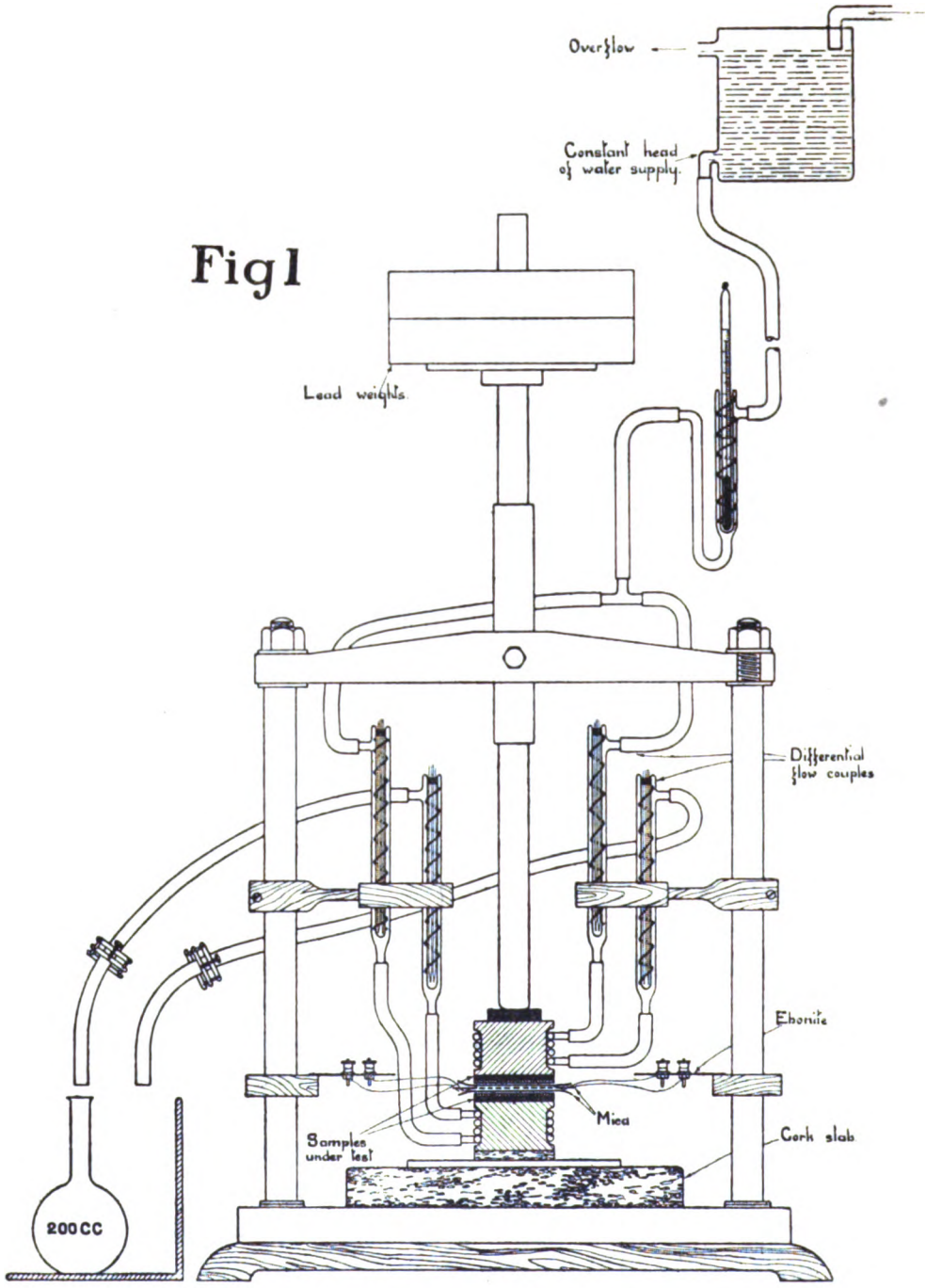


FIG. 1. Apparatus No. 1.

A known pressure was applied to the materials under test by the "dead weight" arrangement shown in Fig. 1.

Digitized by Google

(*b*) *Measurement of the Heat Transmitted through the Material.*—As already mentioned, both the energy input into the heating coil and the energy received by the two cold blocks were measured independently. If the conditions of the experiment are correct, then these two methods of measuring the heat conducted through the specimens should give results in close agreement.

It may be mentioned, however, that experience showed (with all three types of apparatus) that the figure for the useful energy input (E.I.) was usually slightly in excess of that derived from the energy transfer (E.T.) as measured by the water flow. The question is bound up with the control of the temperature of the inlet water and the elimination of the radiation losses from the cold blocks. The greater the care taken in this matter, the more closely did E.T. approach E.I. With proper precautions the agreement reached 1 per cent. or less. In the light of this knowledge, if for any reason (such as small heat flow) the disagreement between E.I. and E.T. somewhat exceeded this amount, the energy input figure (E.I.) was adopted with confidence.

The accuracy attainable when no special care was taken as to radiation losses is illustrated by the details of the several determinations quoted on p. 10. Similar details on p. 15 show closer agreement between E.I. and E.T.

The watts dissipated in the heating coil were measured on the same thermoelectric potentiometer as was used for the temperature measurement. This was effected by the arrangement of volt box and shunts illustrated in Fig. 2, which is self-explanatory.

CIRCUIT FOR N°1 APPARATUS.

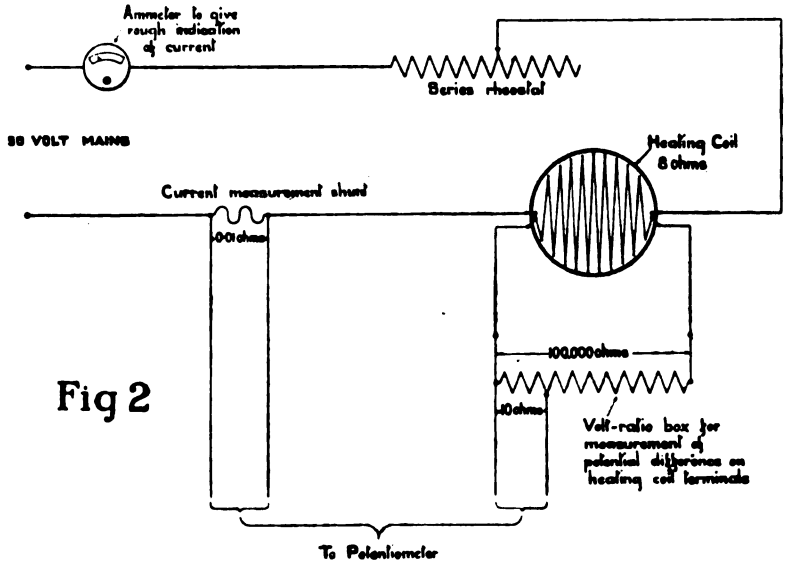
Ammeter to give rough indication of current
Series rheostat
Heating Coil 8 ohms
Current measurement shunt
100,000 ohms
Volt-ratio box for measurement of potential difference on heating coil terminals
To Potentiometer

Fig 2

(*c*) *Temperature Measurements.*—The thermoelements on the hot and cold blocks were so arranged that the difference of temperature between the hot and cold faces, as well as the absolute values, could be measured directly. The arrangement of the circuits for effecting these measurements is shown in Fig. 3.

Digitized by Google

The following typical observations show that the measurements were free from anomaly. The temperatures of the hot and cold surfaces were first measured independently and then differentially. Temperatures are expressed in microvolts. (1° C. = 40 microvolts approximately.)

| | e.m.f. |
|---|---|
| Direct measurements— | |
| Upper face of hot plate | 1738 |
| Lower face of hot plate | 1739 |
| Upper cold plate | 714 |
| Lower cold plate | 706 |
| Differential measurements— | |
| Difference between upper hot and cold plates | 1024 |
| Difference between lower hot and cold plates | 1033 |

Fig 3

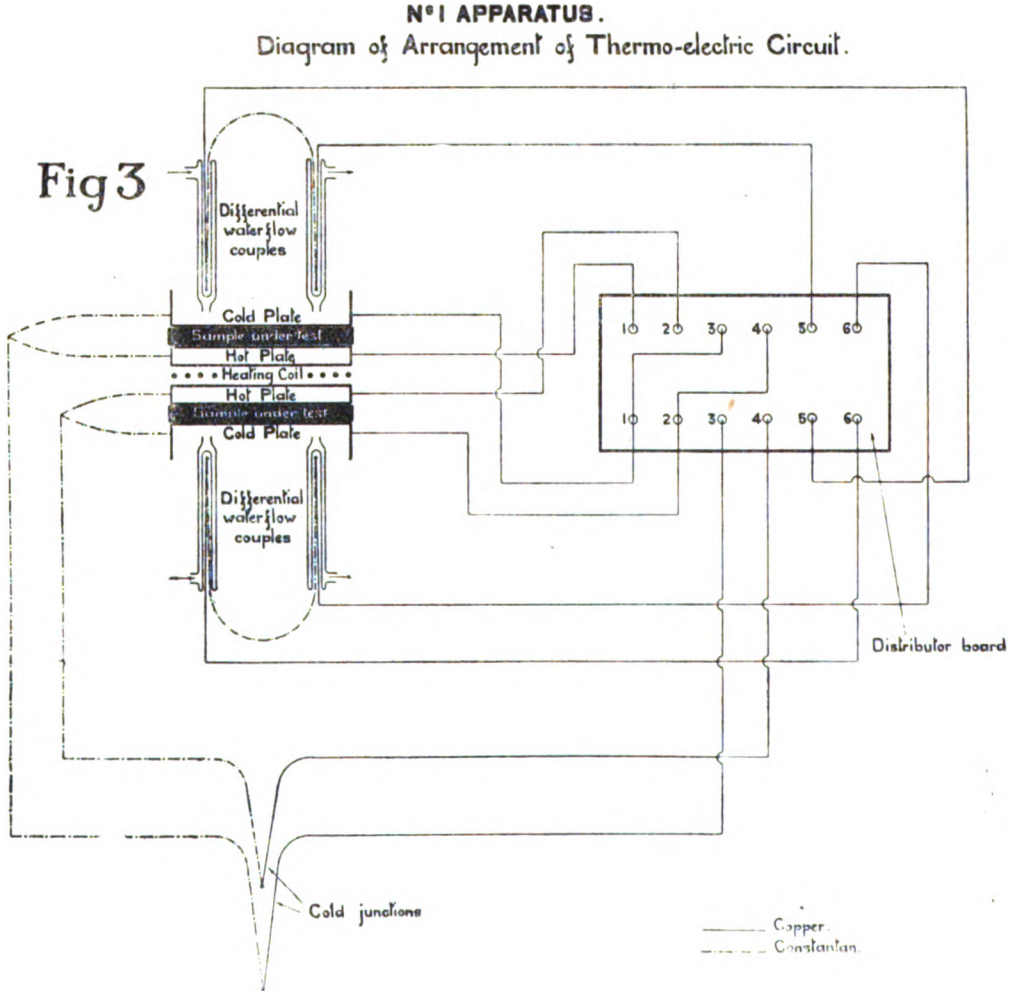


It will be seen that the differences between the hot and cold surfaces, obtained by differential measurements, are in exact agreement with differences calculated from the measured values of the hot and cold plate temperatures.

Digitized by Google

(*d*) *Correction for Heat Loss from Edges of Hot Plate.*—A small correction has to be applied for the heat loss from the edges of the hot plate. This correction was obtained by taking observations with a series of samples of Balsa* wood of various thicknesses. This material had previously been tested in another type of apparatus of the guard-ring pattern and the absolute value of the conductivity determined. This value was then utilised in calculating the amount of energy transmitted through sheets of various thicknesses when tested in the apparatus shown in Fig. 1. The difference between the transmitted energy and the total energy supplied to the heating coil is attributable to loss from the edge of the hot plate into the asbestos and cotton-wool insulation. This correction to the energy input should depend only on the difference of temperature between the hot and cold plates, and if this temperature difference be kept constant the energy correction should be independent of the thickness of the specimen under test, at any rate up to a certain limit. The data quoted below prove the validity of this assumption. The measurements refer throughout to the same sample, the thickness being progressively diminished.

TABLE I.—" Edge-Loss " experiments on Balsa wood samples of various thicknesses.
Constant temperature difference 5·6° C.

| Thickness of Balsa wood in cms. . | 0·356 | 0·316 | 0·245 | 0·195 | 0·156 | 0·103 | 0·066 |
|---|---|---|---|---|---|---|---|
| Correction for edge-loss in watts . . | 0·05 | 0·04 | 0·04 | 0·04 | 0·04 | 0·03 | 0·05 |

(*e*) *Test of Thermal Resistance at Hot and Cold Faces.*—A series of tests were carried out to determine the degree of excellence of the thermal contact at the hot and cold faces. These took the form of ascertaining whether increase of pressure had any effect in decreasing the thermal resistance. The material used for the tests was walnut, the heat flow being across the grain and tangential to the annual rings. The results are tabulated below in Table II.

It is seen that the above results differ among themselves by only 1 per cent. and that there is no definite dependence of conductivity on pressure. Hence it is assumed that with carefully prepared specimens the thermal resistance at the surfaces was negligible, since increase of pressure does not appreciably affect it.

(*f*) *Test of Apparatus No.* 1.—Probably the most searching test that can be applied to the apparatus, particularly as regards the thermal contact at the bounding surfaces, is the comparison of the results obtained when samples of the same material in different

* Balsa is the wood of a tropical tree. It is probably the lightest wood known, the material weighing from 6 to 9 lb. per cubic foot. The thermal conductivity of the dry wood is extremely low, of the order of 0·00011 c.g.s. units, the value depending somewhat on the particular sample.



Digitized by Google

TABLE II.—Dependence of conductivity on pressure.

Mean temperature 20° C.

| Pressure lb./in². | Conductivity c.g.s. units. |
|---|---|
| 33·2 | 0·000327 |
| 46·1 | 0·000329 |
| 61·1 | 0·000328 |
| 52·0 | 0·000327 |
| 46·1 | 0·000330* |
| 37·7 | 0·000328 |
| 33·2 | 0·000326* |
| 23·2 | 0·000329 |

* Denotes repeat readings.

thicknesses are tested. A study of the data in Table III, which are selected as typical, will show that the agreement between the results of tests on three different specimens of walnut, approximately $1\frac{1}{2}$ mm., 1 mm., and $\frac{1}{2}$ mm. thick, is quite satisfactory.

TABLE III.—Thermal Conductivity of various thicknesses of the same material.

The material tested consisted of samples of walnut cut adjacent to one another from the same section of the wood. The heat flow was across the grain and tangential to the annual rings. The experimental results are tabulated in full below :—

Pressure = 21 lb./in². (1·48 kg./cm².).

| | | | |
|---|---|---|---|
| Area of sample, cm². | 15·59 | 15·59 | 15·59 |
| Thickness of samples, cm. | 0·0593 | 0·0913 | 0·1503 |
| Difference in temperature between hot and cold faces, °C. | 4·50 | 5·24 | 6·68 |
| Mean temperature of hot and cold faces, °C. | 20·6 | 21·2 | 18·2 |
| Current in hot-plate heating grid, amps. | 0·637 | 0·559 | 0·494 |
| P.D. at terminals of heating grid, volts | 5·200 | 4·550 | 4·040 |
| Energy dissipated in grid, watts | 3·310 | 2·542 | 1·996 |
| ,, ,, to each face of hot plate, watts | 1·655 | 1·271 | 0·998 |
| Correction for heat loss from edges of hot plate, watts | 0·038 | 0·044 | 0·058 |
| Hence useful energy leaving each face of hot plate, watts | 1·617* | 1·227* | 0·940* |
| Mean rate of water flow in upper and lower cold blocks, ccs. per second | 1·205 | 1·047 | 1·395 |
| Mean temp. rise of water in upper and lower cold blocks, °C. | 0·311 | 0·286 | 0·158 |
| Energy absorbed by water flow in each block, watts | 1·570 | 1·251 | 0·922 |
| Hence thermal conductivity c.g.s. units | 0·000326 | 0·000328 | 0·000324 |

* Used in calculating the conductivity.

(2) *Apparatus No. 2.*

(*a*) *General Description.*—This apparatus was designed primarily for those materials of which the contact resistance at the hot and cold plates is high and for which the use

Digitized by Google

of amalgamated plates becomes necessary. The design of the mounting of the apparatus ensured the exact and easy assembly of the parts when the contact surfaces were flooded with mercury. The same apparatus proved also to be convenient for the study of the variation from point to point in the conductivity over the area of a large sheet of material, such as ebonite or micanite.

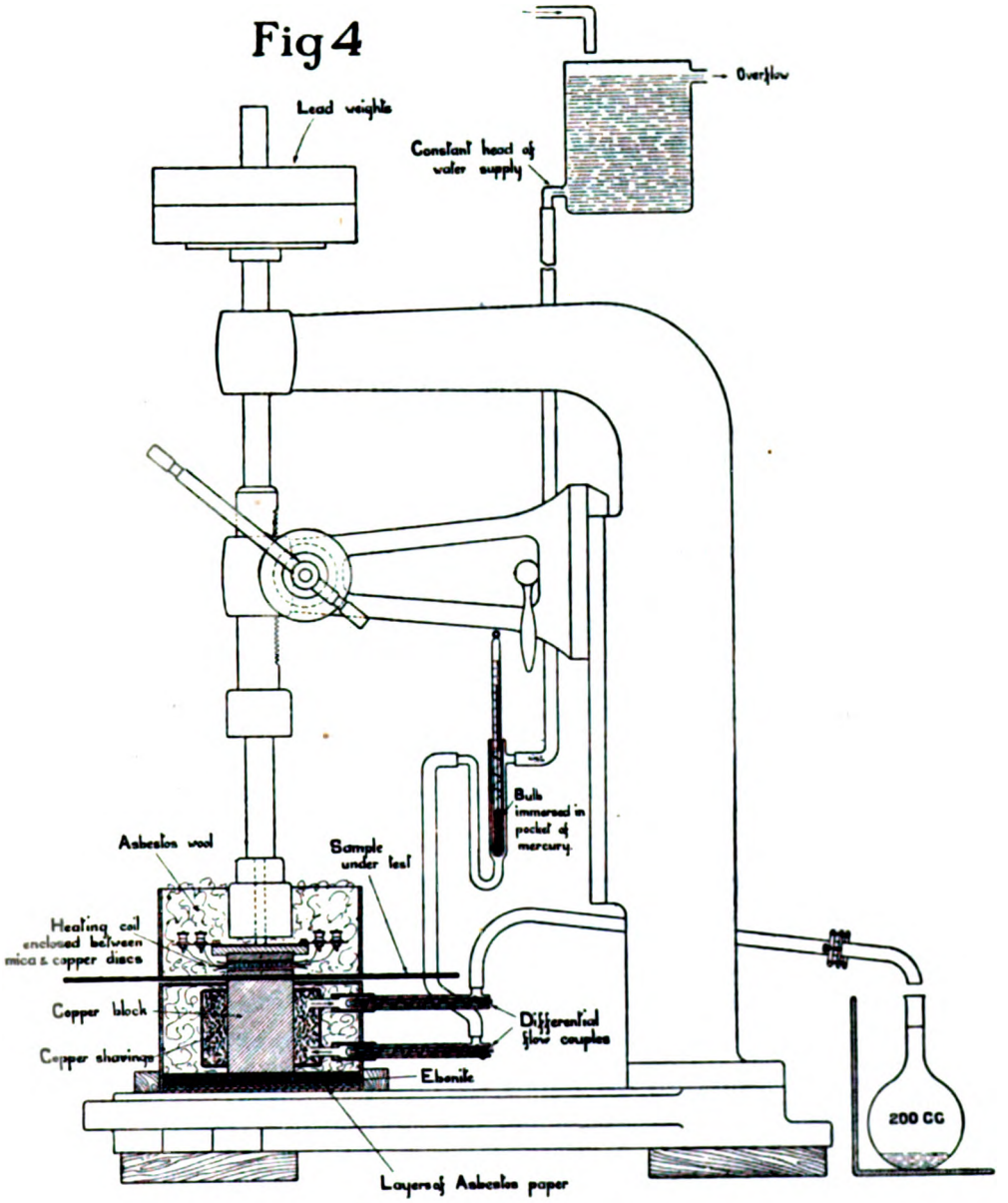


Fig. 4. No. 2 Apparatus.

Manipulative difficulties arising from the use of heavily amalgamated surfaces made it expedient to use only one test sample, mounted horizontally between an upper hot plate and a lower cold plate. Further, the hot and cold faces aligned automatically so



Digitized by Google

that the assembly of the apparatus was facilitated to an extent not possible with apparatus No. 1.

A study of Fig. 4 will show how this was achieved. The hot plate constructed as in apparatus No. 1 is partially embedded in a block of ebonite with the exposed face amalgamated and facing downwards. The complete heating unit is carried on a spindle working in guides, and once it is properly aligned with the cold face, these guides ensure that the hot face always registers exactly with the cold face. This automatic alignment of the two surfaces was essential in the case of point-to-point tests on large sheets, and, of course, was particularly convenient when, as is described later, the degree of amalgamation of the surfaces was such that they were virtually flooded with mercury.

The cold surface was provided by the upper face of a cylindrical block of copper maintained at a constant temperature by a steady circulation of water through a water jacket, much as in apparatus No. 1. The temperature rise of the water was measured as before by a pair of differential flow couples.

A definite pressure was put on the test sample by the dead load shown in Fig. 4, and asbestos and cotton-wool lagging were used as before.

(*b*) *Correction for Heat Leakage into Ebonite Mounting.*—Although it is possible to obtain the conductivity of a sample by observations of the temperature rise of the water flow, its rate of flow, and the temperature gradient through the material, it was deemed advisable to obtain, as heretofore, the energy by measuring the heat input. The watts supplied to the heating coil do not furnish, however, a direct measure of the heat flowing into the sample, since there is also a flow of heat into the ebonite in which the hot plate is mounted.

The magnitude of this flow was determined by observations on a sample of Balsa wood of known conductivity and a table of corrections was drawn up. The magnitude of this correction can be seen from an inspection of the data below in the case of fibre :—

TABLE IV.—Correction for heat loss through the ebonite mounting in No. 2 apparatus.

Material tested : Vulcanised fibre.
Conductivity : 0·00066 c.g.s.
Thickness : 0·19 cm.
Pressure : 21·0 lb./in$^2$. (1·48 kg./cm$^2$.).

| Temp.-diff. between hot plate and lagging (°C.). | Total watts supplied to heating coil. | Correction for heat conducted through ebonite (watts). |
|---|---|---|
| 13·3 | 3·88 | 0·78 |
| 23·3 | 6·57 | 1·25 |
| 54·4 | 15·32 | 2·96 |
| 82·2 | 23·10 | 4·50 |
| 35·0 | 9·46 | 1·89* |

* Denotes repeat reading.

Digitized by Google

(*c*) *Experiments with Amalgamated Surfaces.*—When the surface of the material to be tested is somewhat irregular and hard or unyielding, amalgamated plates proved to be essential to effect good thermal contact between the hot and cold plates and the surfaces of the specimen. Even then it may not be possible to work with specimens of large area, as the following experiment shows :—

An apparatus was built up somewhat on the lines of apparatus No. 1, the two cold plates and the hot plate consisting of thick copper amalgamated plates each measuring 10 cm. × 10 cm. With these as contact plates, tests were made on a sample of material consisting of two sheets of mica each about 0·7 mm. in thickness, but which were known not to be uniform in thickness over their entire area. The results showed that the conductivity obtained was dependent on the pressure applied to the plates. The values for various pressures are given in Table V.

TABLE V.—Effect of pressure on conductivity of mica in large sheets.

Mean temperature 50° C.

| Pressure lb./in². | Apparent Conductivity c.g.s. units. |
|---|---|
| 3·75 | 0·00088 |
| 16·25 | 0·00093 |
| 40·50 | 0·00100 |
| 75·00 | 0·00106 |

This large variation clearly proves that the surfaces of the specimens must be reasonably flat if the mercury on an amalgamated plate is to be relied upon for filling the cavities.

A further complication in these tests was the presence of gas pockets in the mica, which, of course, varied in dimensions with the pressure applied, and, in fact, we were driven to the conclusion from a number of experiments, such as the one described above, that it was not possible accurately to test *large* thick samples of mica. It was found preferable to use thicknesses of the order of 0·025 cm., and in this thickness discs of mica of the necessary size accurate in thickness to 0·00025 cm. (1/10000 inch) can readily be obtained. With specimens of these dimensions the difficulties above described were non-existent. For example, tests were made on a sample of mica supplied in two thicknesses, 0·013 cm. and 0·025 cm. respectively. The results obtained were independent of the pressure and in good agreement, as will be seen in Table VI.

Experiments have also been carried out to ascertain whether the amount of excess mercury used on the amalgamated surfaces had an appreciable influence on the results. The material employed for this test was cardboard.

In the first experiment the amalgamated copper surfaces were flooded with mercury, the specimens inserted, and more mercury gradually added so as to form what were

Digitized by Google

that the assembly of the apparatus was facilitated to an extent not possible with apparatus No. 1.

A study of Fig. 4 will show how this was achieved. The hot plate constructed as in apparatus No. 1 is partially embedded in a block of ebonite with the exposed face amalgamated and facing downwards. The complete heating unit is carried on a spindle working in guides, and once it is properly aligned with the cold face, these guides ensure that the hot face always registers exactly with the cold face. This automatic alignment of the two surfaces was essential in the case of point-to-point tests on large sheets, and, of course, was particularly convenient when, as is described later, the degree of amalgamation of the surfaces was such that they were virtually flooded with mercury.

The cold surface was provided by the upper face of a cylindrical block of copper maintained at a constant temperature by a steady circulation of water through a water jacket, much as in apparatus No. 1. The temperature rise of the water was measured as before by a pair of differential flow couples.

A definite pressure was put on the test sample by the dead load shown in Fig. 4, and asbestos and cotton-wool lagging were used as before.

(*b*) *Correction for Heat Leakage into Ebonite Mounting.*—Although it is possible to obtain the conductivity of a sample by observations of the temperature rise of the water flow, its rate of flow, and the temperature gradient through the material, it was deemed advisable to obtain, as heretofore, the energy by measuring the heat input. The watts supplied to the heating coil do not furnish, however, a direct measure of the heat flowing into the sample, since there is also a flow of heat into the ebonite in which the hot plate is mounted.

The magnitude of this flow was determined by observations on a sample of Balsa wood of known conductivity and a table of corrections was drawn up. The magnitude of this correction can be seen from an inspection of the data below in the case of fibre :—

TABLE IV.—Correction for heat loss through the ebonite mounting in No. 2 apparatus.

Material tested : Vulcanised fibre.
Conductivity : 0·00066 c.g.s.
Thickness : 0·19 cm.
Pressure : 21·0 lb./in². (1·48 kg./cm².).

| Temp.-diff. between hot plate and lagging (°C.). | Total watts supplied to heating coil. | Correction for heat conducted through ebonite (watts). |
|---|---|---|
| 13·3 | 3·88 | 0·78 |
| 23·3 | 6·57 | 1·25 |
| 54·4 | 15·32 | 2·96 |
| 82·2 | 23·10 | 4·50 |
| 35·0 | 9·46 | 1·89* |

* Denotes repeat reading.

Digitized by Google

(*c*) *Experiments with Amalgamated Surfaces.*—When the surface of the material to be tested is somewhat irregular and hard or unyielding, amalgamated plates proved to be essential to effect good thermal contact between the hot and cold plates and the surfaces of the specimen. Even then it may not be possible to work with specimens of large area, as the following experiment shows :—

An apparatus was built up somewhat on the lines of apparatus No. 1, the two cold plates and the hot plate consisting of thick copper amalgamated plates each measuring 10 cm. × 10 cm. With these as contact plates, tests were made on a sample of material consisting of two sheets of mica each about 0·7 mm. in thickness, but which were known not to be uniform in thickness over their entire area. The results showed that the conductivity obtained was dependent on the pressure applied to the plates. The values for various pressures are given in Table V.

TABLE V.—Effect of pressure on conductivity of mica in large sheets.

Mean temperature 50° C.

| Pressure lb./in². | Apparent Conductivity c.g.s. units. |
|---|---|
| 3·75 | 0·00088 |
| 16·25 | 0·00093 |
| 40·50 | 0·00100 |
| 75·00 | 0·00106 |

This large variation clearly proves that the surfaces of the specimens must be reasonably flat if the mercury on an amalgamated plate is to be relied upon for filling the cavities.

A further complication in these tests was the presence of gas pockets in the mica, which, of course, varied in dimensions with the pressure applied, and, in fact, we were driven to the conclusion from a number of experiments, such as the one described above, that it was not possible accurately to test *large* thick samples of mica. It was found preferable to use thicknesses of the order of 0·025 cm., and in this thickness discs of mica of the necessary size accurate in thickness to 0·00025 cm. (1/10000 inch) can readily be obtained. With specimens of these dimensions the difficulties above described were non-existent. For example, tests were made on a sample of mica supplied in two thicknesses, 0·013 cm. and 0·025 cm. respectively. The results obtained were independent of the pressure and in good agreement, as will be seen in Table VI.

Experiments have also been carried out to ascertain whether the amount of excess mercury used on the amalgamated surfaces had an appreciable influence on the results. The material employed for this test was cardboard.

In the first experiment the amalgamated copper surfaces were flooded with mercury, the specimens inserted, and more mercury gradually added so as to form what were

Digitized by Google

TABLE VI.—Conductivity of small specimens of mica.

Mean temperature 50° C.

| Thickness of specimen. cms. | Conductivity c.g.s. units. |
|---|---|
| 0·013 | 0·00135 |
| 0·025 | 0·00137 |

virtually two large flattened drops of mercury. When the hot surface had been lowered into contact, the excess mercury around the edges was removed.

In the second test no special care was taken to flood the surfaces; a few drops of mercury were placed on both copper surfaces, which, of course, were well amalgamated. The experiment was repeated several times, but no difference was observed, as will be seen from Table VII.

TABLE VII.—Amalgamation of surfaces.

Material: Cardboard.

Pressure: 21 lb./in$^2$. (1·48 kg./cm$^2$.).

| State of Amalgamation. | Conductivity c.g.s. units. |
|---|---|
| A | 0·000610 |
| B | 0·000608 |
| A | 0·000612 |
| A | 0·000608* |

A denotes careful amalgamation.

B denotes no special care with amalgamation.

* denotes repeat reading.

(*d*) *Correction for the Temperature Drop through the Mercury Film.*—The thermal conductivity of mercury is only about 1/50th that of copper, so that a correction was necessary for the temperature drop through the two mercury films. This was obtained by direct experiment as follows:—A disc of steel, 0·011 cm. thick, with flat polished surfaces and of the same diameter as the test specimens, was inserted between the amalgamated hot and cold plates and the temperature difference observed for various energy inputs in the heating coil. The temperature drop through the thin steel disc could be obtained by calculation from its known thermal conductivity, so the residue was attributable to the mercury film.

This method of obtaining the correction had the additional advantage that it automatically took into account any resistance at the liquid-solid surface due to microscopic

Digitized by Google

gas bubbles. The magnitude of the correction can be seen from a study of the data in Table VIII.

TABLE VIII.—Temperature drop in mercury film.

| Total Energy Input. Watts. | Observed temp. difference. °C. | Calculated temp. drop through iron sheet. | Temp. drop in mercury film. |
|---|---|---|---|
| 48·15 | 0·52 | 0·07 | 0·45 |
| 179·20 | 2·10 | 0·26 | 1·84 |
| 175·70 | 2·00 | 0·26 | 1·74 |
| 311·00 | 3·40 | 0·46 | 2·94 |

To illustrate the order of magnitude of the quantities dealt with, a typical experiment with this form of apparatus is given below :—

(*e*) *Typical Experiment with Apparatus No. 2 (Amalgamated Surfaces).*

Material : Commercial rubber.
Pressure : 8 lb./in². (0·56 kg./cm².).

| | |
|---|---|
| Area of sample, cm². | 15·59 |
| Thickness of sample, cm. | 0·286 |
| Temperature of hot face, °C. | 62·0 |
| ,, cold face, °C. | 14·1 |
| Correction for temperature drop through mercury film, °C. | 0·1 |
| Hence true temperature difference, °C. | 47·8 |
| Mean temperature of hot and cold faces, °C. | 38·1 |
| Current in hot-plate heating grid, amps. | 0·5819 |
| P.D. at terminals of heating grid, volts | 12·550 |
| Energy dissipated in grid, watts | 7·30 |
| Correction for heat transmitted through ebonite mounting, watts | 2·45 |
| Hence useful energy supplied to hot face of specimen, watts | 4·85* |
| Mean rate of flow of water | 200 cm³. in 160 secs. |
| Mean temperature rise of water, °C. | 0·925 |
| Hence energy absorbed by water flow, watts | 4·84 |

$$\therefore \text{Conductivity} = \frac{4\cdot85 \times 0\cdot286}{4\cdot184 \times 15\cdot59 \times 47\cdot8} = 0\cdot000445 \text{ c.g.s.}$$

* Used in calculating the conductivity.

(3) *Apparatus No. 3.*

(*a*) *General Description.*—This apparatus is a somewhat specialised form of No. 2, adapted in the main for carrying out measurements on materials which are only available in very thin layers (for example, certain fabrics, micas and mica compositions), so that the heat transmitted for an appreciable temperature difference was very considerable. This necessitated the use of a heavier type of heating coil, which was totally enclosed in the block of copper, as shown in Fig. 5.

Digitized by Google

The specimen rested between the upper surface of this block and the lower surface of a water-cooled copper block of the type already described. When the specimen had been inserted between the blocks, pressure was applied by means of a spring plunger

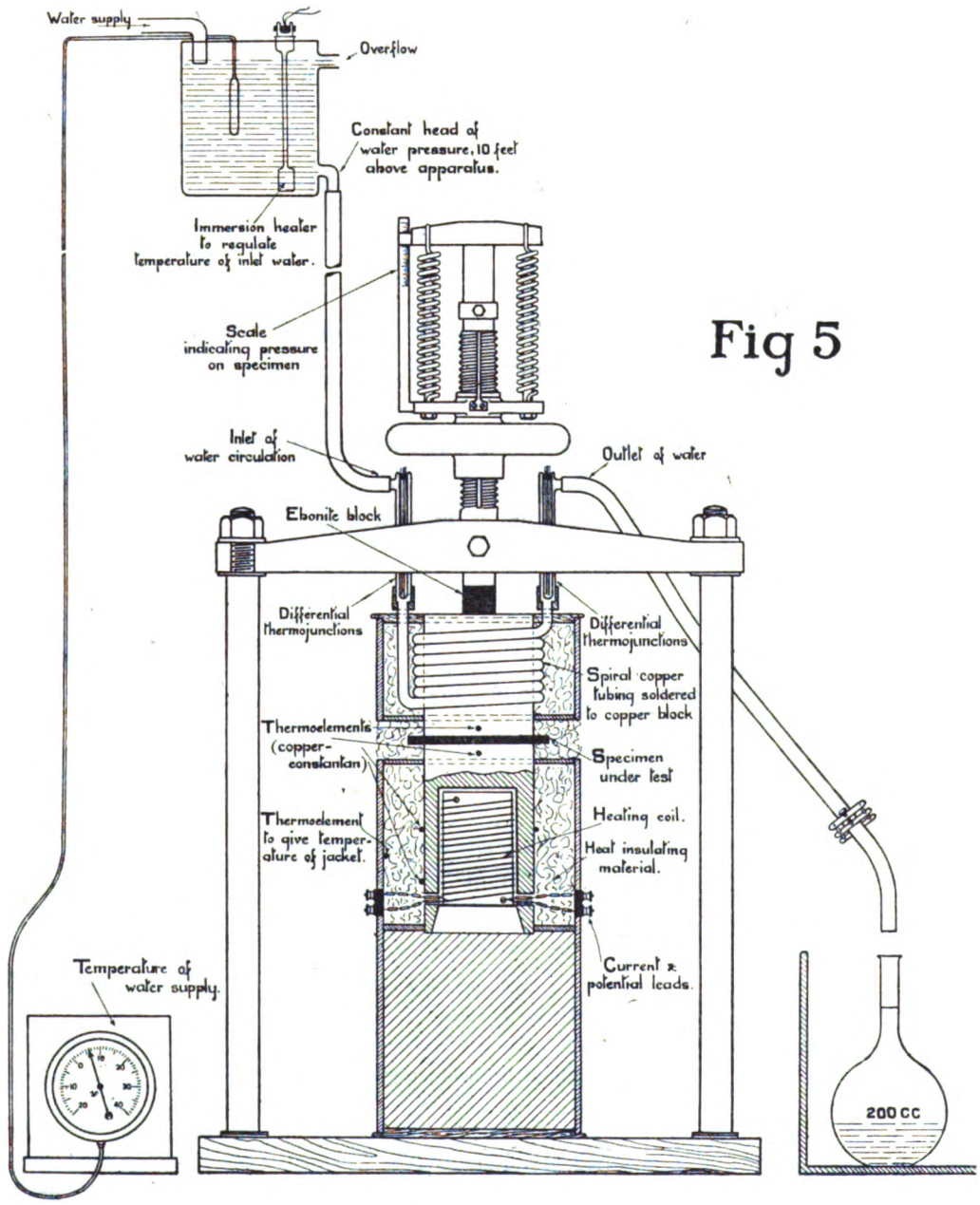


Fig 5

Fig. 5. No. 3 Apparatus.

and the magnitude of this pressure determined by the scale reading. As previously, to reduce stray heat losses both the hot and the cold bars were enclosed in cases packed with insulating material.

Digitized by Google

In the experiments with this apparatus on materials of thickness from 0·002 cm. to 0·05 cm., no attempt was made to separate contact resistance at the surface from the true resistance of the material, as an " overall " coefficient is all that is desired for most purposes.

The same general precautions were taken as with the other two types of apparatus.

(*b*) *Effect of Superimposing Layers on Conductivity.*—Measurements were made of the effect of superimposing layers on the conductivity. The data given in Table IX and Fig. 6 refer to waterproofed silk fabric. The methods of measuring the effective thickness of the superimposed layers under a specific pressure are described later. It will be seen that the conductivity increases considerably as the layers are increased in number.

TABLE IX.—Superimposed layers of waterproofed silk fabric.

Pressure 8 lb./in². (0·56 kg./cm².); unamalgamated plates.

| No. of layers. | Thickness cm. | Mean temp. °C. | Conductivity c.g.s. units. |
|---|---|---|---|
| 1 | 0·012 | 21·0 | 0·000340 |
| 2 | 0·025 | 21·0 | 0·000359 |
| 6 | 0·075 | 21·0 | 0·000415 |
| 9 | 0·111 | 21·0 | 0·000440 |
| 1 | 0·012 | 21·0 | 0·000342* |

* Denotes repeat reading.

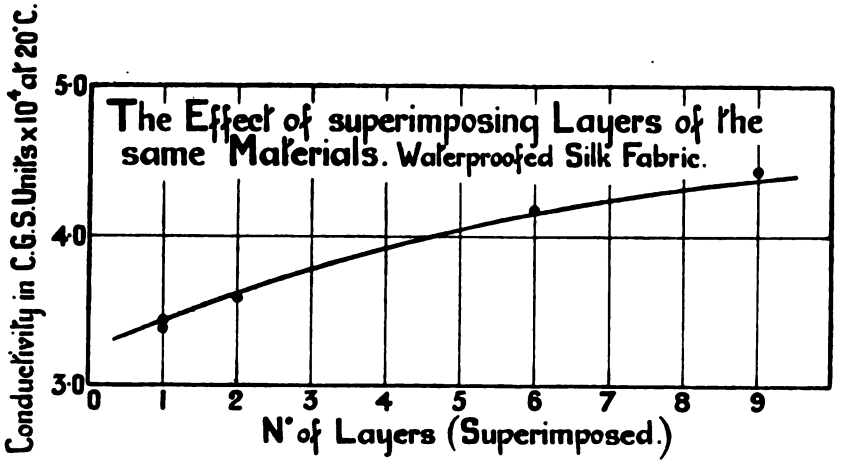


Fig. 6. Effect on conductivity of superimposing layers.

(4) *Measurement of the Thickness.*

(*a*) *Description of Apparatus.*—Considerable attention had to be devoted to the measurement of the thickness of the materials tested, more especially in those cases where this was dependent upon the pressure applied to the surfaces of the specimen.

For the thicker materials the apparatus shown in Fig. 7 was used. It consists essentially of a micrometer head reading to 0·00025 cm. (1/10000 inch) clamped to a vertical pillar,



Digitized by Google

which carries also a fixed table. The specimen to be measured is laid on the table with a disc of steel resting on it. Both the surfaces of the table and the steel disc are accurately ground to plane surfaces. The observations are taken with and without the specimen between the plates. Pressure can be applied by the arrangement of weights as shown in Fig. 7.

It was found that, as would be anticipated, the effect of a gradually increasing pressure on compressible samples for the first time was to produce a permanent deformation, after which loading and unloading gave consistent results. From the pressure-thickness data it was possible to compute the thickness of the material under any load.

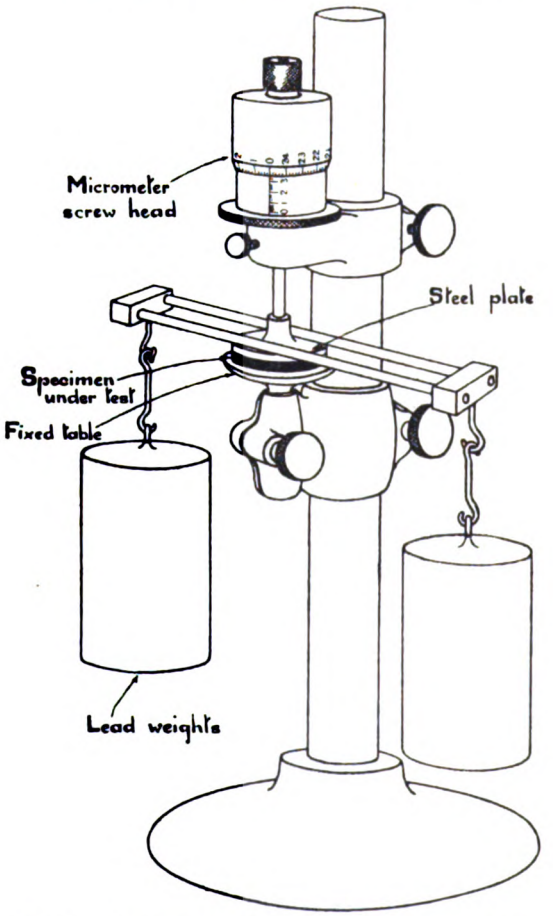


Fig. 7. Apparatus for thickness measurements.

The above apparatus was not sufficiently sensitive for the study of thinner materials, such as paper and fabrics. For such measurements the apparatus illustrated in Fig. 8 was employed, and was an adaptation for the purpose in hand of a measuring machine designed and constructed in the Metrology Department of the Laboratory for the comparison of slip gauges.

The instrument is essentially a large micrometer with one of the headstocks carried on flexible supports. On examination of Fig. 8 it will be observed that the base of the left-hand headstock is supported by means of flexible steel strips at each end of the barrel,

Digitized by Google

a method of support which allows the barrel to move backwards and forwards in a direction parallel to the bed, its axis remaining always parallel to itself. The measuring faces are $\frac{1}{4}$ inch in diameter and are adjusted to be parallel to the order of one-millionth of an inch. The pressure between them is derived from weights suspended from two scale pans hanging on a cross bar, which force is transmitted to the barrel by two bell-crank levers placed one on each side of it. The magnitude of the pressure on the machine can thus be readily adjusted to any definite figure by varying the magnitude of the suspended weights.

The movement of the barrel is magnified partly by mechanical and partly by optical means, so that each division on the indicator scale corresponds to 0·000025 cm. (1/100000 inch). The mechanical part is performed by a 10 to 1 bell-crank lever. It may be mentioned that this lever is not supported on pivots, as the latter, however well made, would

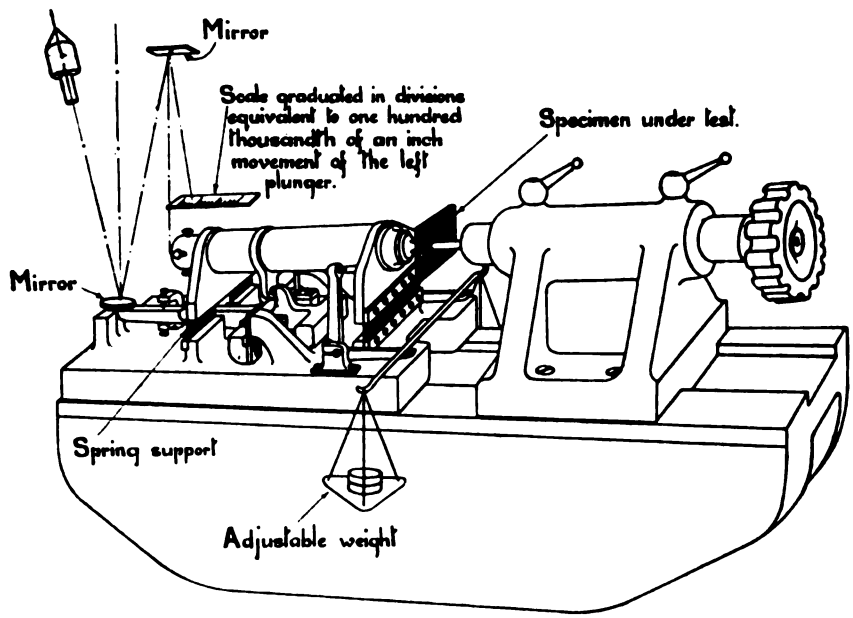
Mirror
Scale graduated in divisions equivalent to one hundred thousandth of an inch movement of the left plunger.
Specimen under test.
Mirror
Spring support
Adjustable weight

Fig. 8. Apparatus for thickness measurements.

introduce some degree of friction or backlash. Instead, the lever has a virtual axis of rotation formed by the line of intersection of the planes of two pairs of steel strips, one pair horizontal and the other vertical, which are fixed to the lever and to the lugs on the base of the left headstock. (The perspective view of the machine in Fig. 8 makes this arrangement clear.) The short arm of the lever, which is vertical, is furnished with a hardened steel ball point, which rests against a flat hardened steel stop projecting from the base of the barrel. The face of this stop is arranged to be vertically above the virtual axis of the lever, so that no sliding contact (with consequent friction) takes place at this contact for small movements of the barrel, the motion being wholly of a rolling nature. The longer arm of the lever is horizontal and the vertical motion of its end is transmitted to a tilting mirror. To prevent undue straining of the suspension springs of the lever, its motion is limited by two stops as shown.

(*b*) *Change of Thickness with Applied Load.*—The above machine was sufficiently sensitive



Digitized by Google

to enable one to observe the changes which occur on loading and unloading a number of times in succession. A typical example is given in Fig. 9, which deals with the case of Balsa wood.

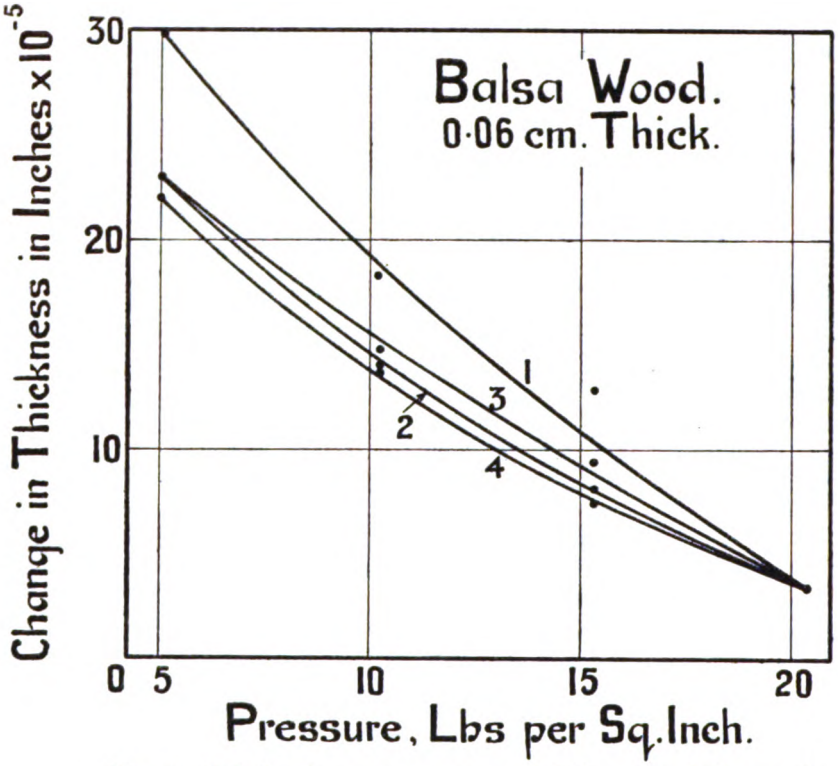


Fig. 9. Relation between pressure and thickness for Balsa wood.

In working out conductivity data, the mean curve through the series of cyclical curves after the first loading was taken, so as to obtain the thickness appropriate to the applied load.

TABLE X.—Thickness of superimposed layers.

Pressure 20 lb./in². (1·41 kg./cm².).

| Silk Fabric. (Thickness of individual sheets.) | Thin Paper. (Thickness of individual sheets.) |
|---|---|
| cm. | cm. |
| $0·0048_3$ | $0·0015_0$ |
| $0·0047_0$ | $0·0025_0$ |
| $0·0042_5$ | $0·0024_6$ |
| $0·0042_0$ | $0·0022_9$ |
| $0·0047_0$ | $0·0024_2$ |
| $0·0042_5$ | $0·0017_8$ |
| $0·0043_2$ | $0·0024_2$ |
| $0·0042_5$ | $0·0021_6$ |
| Total $0·0355_0$ | Total $0·0175_3$ |
| Thickness of the 8 samples superimposed $= 0·0292_1$ cm. | Thickness of the 8 samples superimposed $= 0·0142_8$ cm. |

Digitized by Google

(*c*) *Combined Thickness of a Number of Superimposed Layers.*—The machine illustrated in Fig. 8 was also used to investigate the variation in thickness from point to point over the area of a specimen, and the thickness of a number of superimposed layers, as compared with the thickness of an individual layer. The results obtained in the latter series of experiments are of interest, as illustrating the degree of packing of the materials which takes place when a number of layers are superimposed. The tests were made to ascertain how the thickness of a number of layers of a sample superimposed compared with the sum of the individual thicknesses. The results for silk fabric and paper are given in Table X.

It will be observed that the total thickness of the 8 samples of silk and paper is in each case some 20 per cent. less than the sum of the individual thicknesses, showing that very considerable packing takes place when the single layers are superimposed.

## III. Results.

With the various apparatus described above a large volume of data has been accumulated concerning the thermal conductivity of a variety of materials. A limited selection of results is given below, and it is hoped that in the future the publication of the results for the remaining materials may present no difficulty.

The effect of pressure on the conductivity has already been considered as well as the effect of superimposing layers of certain materials. Considerable attention has been paid to certain timbers, the relation between the conductivity and the direction of the grain and the influence of moisture content having been worked at.

We are indebted to the Superintendent of the Royal Aircraft Establishment, Farnborough, for suitable specimens of a number of the woods, to the Industrial Rubber Products, Ltd., for specimens of commercial rubber, and to Messrs. Henry Wiggins for various specimens of mica. Fig. 10 shows the relation between conductivity and the figure for the percentage of rubber which was furnished by the makers. We understand that mineral matter forms the other constituents of the rubbers. The numerical results are quoted in Table XIII.

A few measurements were made on X-ray protective rubbers, which contain an admixture of lead oxide. No details of the composition were available, and as a rough guide to the amount of mineral matter present, the absorptive values for X-rays were measured in equivalents of lead. As might be anticipated, the conductivity was found to increase with the lead equivalent.

### (1) *The Thermal Conductivity of Timber.*

(*a*) *Direction of Heat Flow and Structure.*—The conducting power of a sample of timber is found to depend on at least two main features of the structure. Firstly, the direction in which heat flow takes place, and, secondly, the coarseness of the grain, of which a notion is afforded by the number of annual rings per inch.

Digitized by Google

There are three approximately perpendicular axes of reference in a specimen of timber which are convenient to adopt :—

(1) Parallel to the grain or, more precisely, the fibres.

(2) Across the grain (or perpendicular to the fibres) and radial to the annual rings.

(3) Across the grain and tangential to the annual rings.

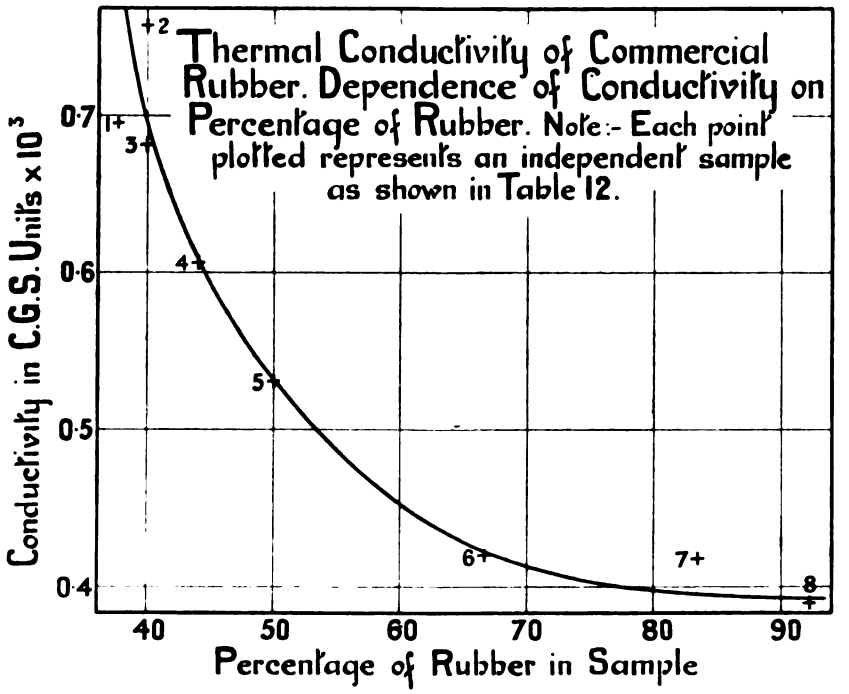


Fig. 10.

Our results (Table XII) go to show that in the case of the woods we have tested, the " longitudinal " conductivity (" with the grain ") is roughly twice that of either of the " transverse " conductivities, and that as regards the two latter, the " radial " conductivity is usually (and very approximately) some 5 to 10 per cent. greater than the " tangential " conductivity.

These results might be anticipated if we recall that in the direction of the grain the heat finds virtually an unbroken path of flow, as the annual rings (if present) consist of rings running longitudinally through the wood in continuous cylindrical bands concentric with the axis of the tree.

When heat flows takes place across the grain and radially to the annual rings, the path of flow, although largely obstructed by the fibres lying across the path, is supplemented by the medullary rays, which consist of bands of honeycomb-like cells radiating from the centre of the tree and interconnecting the annual rings. These medullary rays are invariably present, even though, as in the case of some tropical plants, the annual rings are not.

Digitized by Google

But in the case of heat flow across the grain and tangential to the annual rings, the path of heat flow is obstructed by both the fibres of the wood and the medullary rays, the result being a lower value of the conductivity than in either of the previous cases.

It may be added that the medullary rays do not interfere to any great extent with heat flow along the grain, since they are usually much wider in cross section measured longitudinally than transversely.

As regards the dependence of conductivity on the coarseness of the grain, the coarser the grain the less dense will be the wood, since the fibres are less tightly packed, and the lower the conductivity, as our results confirm.

In Fig. 11 the appearance of the annual rings is shown in the case of the specimen of

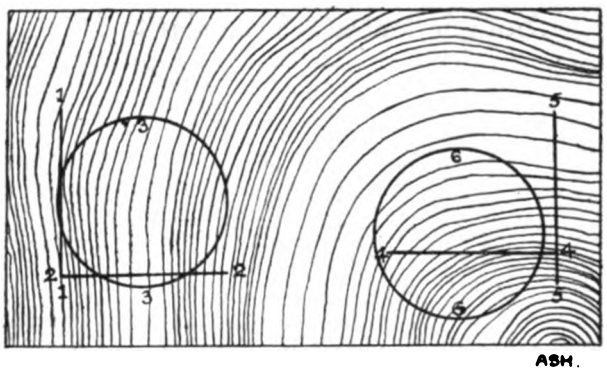


Fig. 11. " Rubbing " of end grain of ash, showing locations of test specimens.

ash. This was prepared by taking a " rubbing " of the end-grain with carbon paper, the facsimile being then either photographed or carefully traced by hand. The method has the advantage of showing the appearance of the grain of the actual specimens employed. The positions from which the various test samples were cut are indicated in the figures. For instance, a circle indicates that a disc $1\frac{3}{4}$ inches in diameter was cut from the position shown, the flow of heat taking place at right angles to the disc. A straight line shows such a disc in section, heat flow taking place perpendicular to that line.

The preparation of the test samples of the requisite thinness and parallelism of faces presented some difficulty at first, more especially when they had to be cut at right angles to the grain. The difficulty was emphasised with the softer woods. The plan eventually adopted was to plane or turn the samples roughly to size and finish off by rubbing with a fine carborundum stone.

(*b*) *The Effect of Moisture Content on Thermal Conductivity.*—The effect of the moisture content on the elastic and other constants of timber is well known, and it was therefore thought that it would be of interest to find out to what extent the moisture content affected the thermal conductivity. Tests were accordingly made on a sample of spruce, the results for which are given in Table XI and Fig. 12, the heat flow being across the grain and radial to the annual rings.

Digitized by Google

TABLE XI.—Moisture Content and Conductivity.

| Moisture Content per cent. | Conductivity c.g.s. units. |
|---|---|
| 3·40 | 0·000292 |
| 5·80 | 0·000302 |
| 7·70 | 0·000308 |
| 9·95 | 0·000318 |
| 17·00 | 0·000340 |

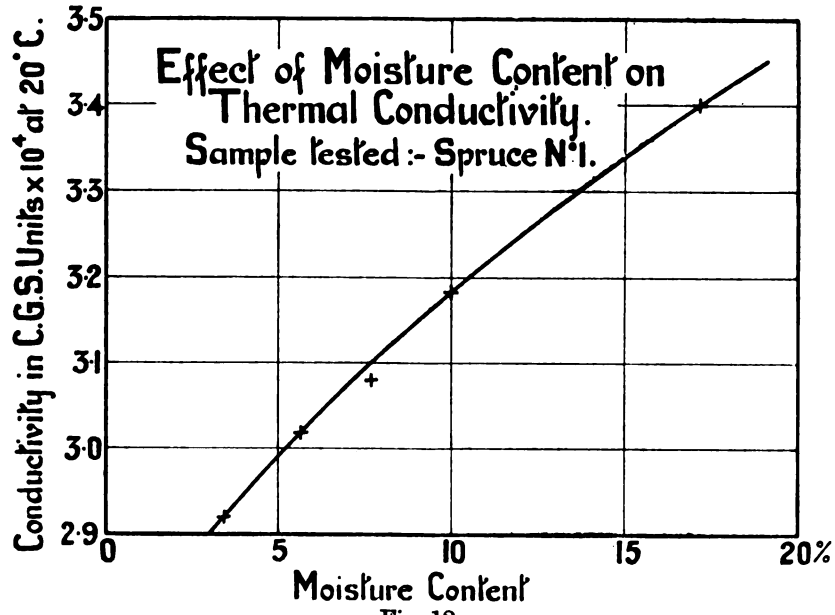


Fig. 12.

It should be mentioned that the sample was gradually dried out in an electric oven maintained at 100° C., measurements of the conductivity being taken with progressively reduced moisture contents. It may be added that the moisture contents are computed on the weight of the dry sample, so that if

$W_1$ be the weight of the sample before heating,

$W_0$ „ „ „ after prolonged heating,

the percentage moisture content $= \dfrac{W_1 - W_0}{W_0} \cdot 100.$

The necessary precautions during weighing were taken, based on the experience of the Aeronautical Inspection Directorate of the Air Ministry.

(2) *Results of Thermal Conductivity of Timbers.*

Timbers tested in No. 1 apparatus (polished surfaces not amalgamated). Pressure = 21 lb./in². (1·48 kg./cm².). The temperature drop across the specimen varied from 3° to 20° C. in different experiments. Not less than five determinations were made on each sample. The positions of the samples corresponding to the numbers in column 3 are as follows :—

Digitized by Google

*Open grain*— (1) Heat flow across the grain and radial to the annual rings.
(2) Heat flow across the grain and tangential to the annual rings.
(3) Heat flow with the grain.

*Close grain*— (4) Corresponding to position (1) above.
(5) ,, ,, (2) ,,
(6) ,, ,, (3) ,,

TABLE XII.

| Timber. | Moisture content per cent. | Position. | Thickness cm. | Mean temp. °C. | Conductivity c.g.s. units. |
|---|---|---|---|---|---|
| Ash (Sp. Gr. = 0·74) . . . . . | 15·5 | 1 | 0·100 | 20 | 0·000365 |
| | | | | 25 | 0·000381 |
| | 15·0 | 2 | 0·102 | 20 | 0·000369 |
| | | | | 25 | 0·000371 |
| | 14·3 | 3 | 0·091 | 20 | 0·000714 |
| | | | | 25 | 0·000725 |
| | 16·0 | 4 | 0·100 | 20 | 0·000464 |
| | | | | 25 | 0·000469 |
| | 16·6 | 5 | 0·100 | 20 | 0·000416 |
| | | | | 25 | 0·000420 |
| | 14·9 | 6 | 0·081 | 20 | 0·000754 |
| | | | | 25 | 0·000771 |
| Mahogany (Sp. Gr. = 0·70) . . | 15·2 | 1 | 0·100 | 20 | 0·000391 |
| | | | | 25 | 0·000398 |
| | 15·2 | 2 | 0·106 | 20 | 0·000351 |
| | | | | 25 | 0·000354 |
| | 14·5 | 3 | 0·108 | 20 | 0·000701 |
| | | | | 25 | 0·000716 |
| | 14·9 | 4 | 0·105 | 20 | 0·000416 |
| | | | | 25 | 0·000419 |
| | 12·7 | 5 | 0·107 | 20 | 0·000387 |
| | | | | 25 | 0·000392 |
| | 15·2 | 6 | 0·153 | 20 | 0·000776 |
| | | | | 25 | 0·000790 |
| Spruce (Sp. Gr. = 0·41) . . . | 17·0 | 1 | 0·147 | 20 | 0·000341 |
| | 16·9 | 2 | 0·150 | 20 | 0·000264 |
| | 15·9 | 3 | 0·151 | 20 | 0·000550 |
| | 16·2 | 4 | 0·150 | 20 | 0·000242 |
| | 16·2 | 5 | 0·159 | 20 | 0·000237 |
| | 15·4 | 6 | 0·152 | 20 | 0·000509 |
| Walnut (Sp. Gr = 0·65) . . . | 12·1 | 1 | 0·146 | 20 | 0·000346 |
| | 11·3 | 2 | 0·150 | 20 | 0·000326 |
| | 11·8 | 3 | 0·154 | 20 | 0·000794 |
| Teak (Sp. Gr. = 0·72) . . . . | 10·3 | 2 | 0·100 | 20 | 0·000314 |
| | | 5 | 0·097 | 20 | 0·000341 |
| Oak (Sp. Gr. = 0·60) . . . . | 13·7 | 2 | 0·154 | 20 | 0·000280 |
| Cedar (Sp. Gr. = 0·49) . . . . | 13·4 | 2 | 0·230 | 20 | 0·000290 |
| Cedar (different sample, Sp. Gr. = 0·48) . . . . . | 12·7 | 2 | 0·200 | 20 | 0·000252 |
| Cedar (East African Pencil, Sp. Gr. = 0·48) . . . . . | 10·6 | — | 0·197 | 20 | 0·000277 |
| Kiri (Japanese, Sp. Gr. = 0·32) | 24·1 | 2 | 0·186 | 20 | 0·000210 |



Digitized by Google

### (3) *Thermal Conductivity of Various Materials.*
### *Summary of Results.*

TABLE XIII.

| Material. | Thickness cm. | Pressure lb./in². | Mean temp. °C. | Conductivity c.g.s. units. |
|---|---|---|---|---|
| Ivory (African) (various samples) ⊥ axis | 0·167 to 0·185 | 113 | 80 | 0·00108 to 0·00125 |
| Ivory (African) (various samples) ‖ axis | 0·178 | 113 | 80 | 0·00137 |
| Quartz ⊥ axis | 0·253 | 21 | 25 | 0·0147 |
| „ ‖ „ | 0·253 | 21 | 40 | 0·0244 |
| Ebonite (various samples) | 0·035 to 0·15 | 21 | 25 | 0·00038 to 0·00044 |
| Vulcanised Fibre | Various | 21 | 50 | 0·0005 to 0·0008 |
| Mica (various samples) | 0·01 to 0·025 | 120 | 50 | 0·0010 to 0·0014 |
| Micanite (commercial) | Various | 21 | 30 | 0·0005 to 0·0010 |
| Cotton fabric | „ | 21 | 40 | 0·00018 to 0·0002 |
| Silk fabric | „ | 21 | 40 | 0·00010 to 0·00012 |
| Paper (rice) | 0·003 | 21 | 40 | 0·00011 |
| Cardboard | Various | 21 | 50 | 0·0004 to 0·0008 |
| Cement, Portland (burnt) | 0·42 | 21 | 55 | 0·0030 |
| Commercial rubber (vulcanised)— | | | | |
| Percentage of rubber— | | | | |
| 38 | 0·385 | 8·4 | 25 | 0·00070 |
| 40 | 0·381 | 8·4 | 25 | 0·00068 |
| 44 | 0·287 | 8·4 | 25 | 0·00060 |
| 50 | 0·387 | 8·4 | 25 | 0·00053 |
| 67 | 0·286 | 8·4 | 25 | 0·00042 |
| 83 | 0·412 | 8·4 | 25 | 0·00042 |
| 92 | 0·324 | 8·4 | 25 | 0·00039 |
| 100* | 0·103 | 34 | 25 | 0·00032 |
| X-ray protective rubber— | | | | |
| Lead equivalent— | | | | |
| 0·35 | 0·173 | 2·5 | 20 | 0·00079 |
| 0·41 | 0·260 | 2·5 | 20 | 0·00087 |
| 0·43 | 0·463 | 2·5 | 20 | 0·00107 |

| | Sp. Gravity. | Moisture Content Per cent. | Mean Conductivity at 20° C. | | |
|---|---|---|---|---|---|
| | | | ‡ | § | ¶ |
| Timber†— | | | | | |
| Ash | 0·74 | 15 | 0·00073 | 0·00042 | 0·00039 |
| Mahogany | 0·70 | 15 | 0·00074 | 0·00040 | 0·00037 |
| Spruce | 0·41 | 16 | 0·00053 | 0·00029 | 0·00025 |
| Walnut | 0·65 | 12 | 0·00079 | 0·00035 | 0·00033 |
| Teak | 0·72 | 10 | — | — | 0·00033 |
| Oak | 0·60 | 14 | — | — | 0·00028 |
| Balsa | 0·1 | 13 | — | — | 0·00011 |
| Waterproofed Balsa | 0·1 | 13 | — | — | 0·00013 |
| Pseudo Balsa | 0·25 | 13 | 0·00029 | 0·00016 | |
| Cedar | 0·48 | 13 | — | — | 0·00027 |
| Fir | 0·6 | 15 | — | 0·00028 | |
| Pitch Pine | — | 15 | — | 0·00033 | |
| Kingia Fibre | 0·3 to 0·6 | — | — | 0·00018 to 0·00025 | |

* Plantation rubber crêpe. † Pressure 21 lb./in². ‡ Parallel to grain.
§ Perpendicular to grain, radial to annual rings. ¶ Perpendicular to grain, tangential to annual rings.

Digitized by Google

# SOME MATERIALS OF LOW THERMAL CONDUCTIVITY

BY

EZER GRIFFITHS, D.Sc., F.R.S.,
PRINCIPAL ASSISTANT IN THE PHYSICS DEPARTMENT.

Digitized by Google

## ABSTRACT.

**The thermal conductivity of the following materials has been determined: expanded rubber (soft and hard), Balsa wood, Kingia Australis fibres, "eel grass" mat, compressed peat, and peat treated with bituminous materials.**


Digitized by Google

# SOME MATERIALS OF LOW THERMAL CONDUCTIVITY.

By EZER GRIFFITHS, D.Sc., F.R.S., Principal Assistant in the Physics Department.

[Reprinted from the 'Transactions of the Faraday Society', Vol. 18, Part 2, 1922.]

*Some Materials of Low Thermal Conductivity.*—From the point of view of the refrigerating engineer, the ideal material for cold storage insulation would be an assemblage of minute gas cells totally enclosed in a light framework impervious to moisture. Hermetical sealing of the cells is essential, for a water-logged material is useless for insulation purposes. Beside the fact that the value of the thermal conductivity of water is about ten times that of the conductivity of the materials usually employed for insulating purposes, the presence of moisture is liable to set up decomposition in substances of organic origin. Consequently many excellent thermal insulators, such as cotton waste and wood sawdust, are ruled out on account of their rapid deterioration in the presence of water.

Another important factor which has to be considered in assessing the value of an insulator, especially for marine work, is the weight per cubic foot of the material. A modern refrigerating ship of 6,400 tons requires about 400 tons of cork.* So a saving of a few per cent. is well worth while.

* The following particulars concerning two ships of the Nelson Line were kindly supplied by Mr. A. R. T. Woods, M.I.Mech.E., M.I.N.A.

Ship built in 1911. Registered gross tonnage 7,490 tons. Insulated throughout:—

*Approx. Weights.*

| | |
|---|---|
| Hull, engines and boilers ... ... ... ... ... ... ... | 4,490 tons. |
| Refrig. machinery and brine piping, etc. ... ... ... ... ... | 610 „ |
| Insulation (silicate cotton) and timber ... ... ... ... ... | 1,050 „ |
| Empty ship, total weight = | 6,150 tons. |
| Total capacity of cargo spaces = | 328,980 cubic feet. |
| „ „ „ „ = | 3,100 tons chilled meat. |
| „ „ „ „ = | 3,300 „ frozen meat. |

Ship built in 1920. Registered gross tonnage, 8,442 tons. Insulated throughout:—

*Approx. Weights.*

| | |
|---|---|
| Hull, engines and boilers . . . . . | 4,624 tons. |
| Refrig. machinery and brine piping, etc. . . . . | 686 „ |
| Insulation, granulated cork . . . . . | 430 „ |
| „ timber . . . . . | 660 „ |
| Empty ship, total weight = | 6,400 tons. |
| Total capacity of cargo spaces = | 414,570 cubic feet. |
| „ „ „ „ = | 3,940 tons chilled meat. |
| „ „ „ „ = | 4,150 „ frozen meat. |
| Silicate cotton packs . . . . . | 22 lb. per cubic foot. |
| Cork (granulated) packs . . . . . | 7 „ „ „ |

Digitized by Google

A material of low weight per cubic foot has the additional advantage that the heat which has to be abstracted in cooling down the stores is less, and this leads to economy of working.

The heat insulators in common use at the present day are slab cork, granulated cork, slag wool, and charcoal. These are so well known as not to need further description,* and the purpose of the present communication is to bring to the attention of refrigerating engineers a few materials which may be worthy of study under practical cold storage conditions, for they possess at least one essential characteristic of a cold stores insulator, namely, low thermal conductivity.

*Expanded Rubber.*—Methods have been devised for the conversion of rubber into a highly cellular form, the resulting product having an exceedingly low density.

When viewed under a low-power microscope, the material shows a structure apparently made up of minute cells bounded by rubber membranes. The cellular structure of the material immediately suggests the possibility of its use as a heat insulator.

The small samples we obtained differed considerably as regards density and presumably this variable can be controlled by the method of manufacture as well as its physical state, whether soft or hard. Samples of the soft variety varied in density from 0·059 to 0·12 c.g.s. units (3·7 to 7·5 lb. per cubic foot), while a hard variety resembling ebonite had a density of 0·17 (10·6 lb. per cubic foot).†

It would be a matter of considerable theoretical interest to ascertain the relation between the density of the sample and its thermal conductivity, but sufficient material has not been available for such tests. The conductivity of some of the material in sheet form has been determined and varied from about 0·00009 to 0·00012 c.g.s. units, the actual value being dependent, apparently, upon the precise method of manufacture, etc.

Now the weight per cubic foot of the samples tested was only about 5 to 7 lb., whereas slab cork weighs 11 to 13 lb., so that when comparisons are made on the basis of the weight of equivalent amounts of insulation, the rubber shows a marked saving.

Tests of the insulating value of expanded rubber clippings when packed into an interspace have also been carried out. The clippings had been prepared from a sheet and measured roughly $\frac{1}{2}$ inch × $\frac{1}{4}$ inch × $\frac{1}{4}$ inch blocks, with considerable variations from the mean. A density determination on some of the fragments gave the value 0·09 ± 0·02, *i.e.*, 5·62 ± 1·25 lb. per cubic foot.

In the test the material was evenly packed on either side of a hot plate measuring 8 inches × 8 inches surrounded by a 2-inch guard ring. The thickness of each layer was $1\frac{1}{8}$ inches.

* Data as to the thermal conductivity of these materials will be found in Special Report No. 5 of the Food Investigation Board entitled 'Report on Heat Insulators', published by H.M. Stationery Office.

† The density of ordinary red rubber vulcanised is variable. Two samples gave 1·31 and 1·77, *i.e.* 82 and 110 lb. per cubic foot respectively.

Digitized by Google

In the first test the packing was light, the material being pressed down slightly. The weight of material per cubic foot under these conditions was 2·6 lb.

The data obtained are given in Table I below.

The material was then taken out of the apparatus and repacked uniformly, but pressing in as much as possible. The weight of material per cubic foot under these conditions was 4 lb. The closer packing has increased the insulating efficiency by 12 per cent. (See Table I.)

TABLE I.—Clippings of Expanded Rubber.

| Date. | Time. | Cold Face Temperatures. | | Hot Face Temperatures. | | Mean Temp. of the Material. | | Conductivities. | |
|---|---|---|---|---|---|---|---|---|---|
| | | °C. | °F. | °C. | °F. | °C. | °F. | C.G.S. Units. | B.T.U.'s per sq. ft. per Hour for 1-in. Thickness and for 1° F. diff. in Temp. |
| **Density of packing, 2·6 lb. per cubic foot.** | | | | | | | | | |
| August 7th | 11 A.M. | 20 | 68 | 50 | 122 | 35 | 95 | 0·000122 | 0·343 |
| ,, 8th | 9 A.M. | 20 | 68 | 50 | 122 | 35 | 95 | 0·000117 | 0·340 |
| ,, 9th | 12 NOON | 20 | 68 | 50 | 122 | 35 | 95 | 0·000118 | 0·342 |
| | | | | | | Probable value | | 0·000118 | 0·342 |
| **Density of packing, 4·0 lb. per cubic foot.** | | | | | | | | | |
| August 13th | 11 A.M. | 20 | 68 | 50 | 122 | 35 | 95 | 0·000105 | 0·305 |
| ,, 14th | 9 A.M. | 20 | 68 | 50 | 122 | 35 | 95 | 0·000107 | 0·311 |
| ,, 15th | 10 A.M. | 20 | 68 | 50 | 122 | 35 | 95 | 0·000105 | 0·305 |
| | | | | | | Probable value | | 0·000106 | 0·308 |

So it would appear that in a granulated form the same insulating efficiency can be obtained with approximately half the weight of this material, as compared with granulated cork and about one-quarter the weight when compared with slab cork.

A somewhat parallel case to this, as regards the difference in weight per cubic foot, granulated and in sheets, is given by cork. In the baked slab form cork weighs about twice as much as the granulated and gives roughly the same insulating efficiency.

Since it is possible to control, in the course of manufacture, the density of the expanded rubber, it would be of interest to ascertain the limit to which the reduction in density can be carried.

Digitized by Google

The material differs markedly from ordinary vulcanised red rubber in its properties, a notable characteristic being its softness. The questions of the durability of the material under rough usage and its chemical stability are ones which merit careful investigation.

Rubber is permeable to water vapour and to many gases, so the gas cells cannot be regarded as hermetically sealed. A sample of the material tested under water for a period of 300 hours showed a progressive increase of weight with time. It cannot yet be stated whether this water absorption is due to water vapour permeating the rubber and forming an adsorbed film on the surface of the cells, or whether it is due to capillary absorption similar to the effect obtained with charcoal. The fact that the action is slow would appear to indicate that it is due to water vapour permeating through the rubber, but it must be remembered that in the case of capillary attraction the action would be slow if the capillaries were close-ended and the water had to dissolve the gas as it flowed along the capillary.

The constitution of the material does not appear to be simply one of gas enclosed in cavities with solid rubber walls, and it is probable that an appreciable amount of gas is adsorbed in the rubber. The determination of the state in which the gas is present in the material is a perplexing chemical problem.

In the present stage of our knowledge concerning this new material, it is difficult to express an opinion as to its value as a practical heat insulator for lining the walls of a store. A long period test on a reasonably large scale is really essential, and the quantity of material necessary for such a test has not yet become available.

*Balsa Wood.**—Balsa is the wood of a large tropical tree growing in Ecuador. It is probably the lightest wood known. The samples we have tested have varied in weight from 5·7 to 8·6 lb. per cubic foot.†

As a structural material it is decidedly weak and liable to damage by blows, etc., but it has the advantage over materials such as cork that it can be worked with ordinary wood-working tools which, however, must be very sharp and run at high speed.

In the natural state the wood is subject to decay, but it is claimed that with preservatives it is possible to make the wood sufficiently waterproof to enable it to be used for cold-storage insulation.

When the material is to be employed in dry situations it can be surfaced with a veneer of hard wood.

The results of tests on several varieties of the material are given in Table II below :—

* There are said to be about nine different species of the timber to which the name "Balsa" is given. The species Ochroma Lagopus belongs to the order Malvaceæ, Sub-order Bombaceæ.

† This may be compared with mahogany, which weighs about 45 lb. per cubic foot.

Digitized by Google

## Table II.—Balsa Wood.

Specimen of 2-in. board weighing 5·75 lb. per cubic foot.

| Date. | Time. | Cold Face Temperatures. | | Hot Face Temperatures. | | Mean Temp. of the Insulating Material. | | Conductivities. | |
|---|---|---|---|---|---|---|---|---|---|
| | | ° Cent. | ° Fahr. | ° Cent. | ° Fahr. | ° Cent. | ° Fahr. | C.G.S. Units. | B.T.U.'s per Hour per sq. ft. for 1-in. Thickness and for 1° F. diff. in Temp. |
| March 4th | 8 P.M. | 11 | 52 | 75 | 167 | 43 | 109 | 0·000112 | 0·326 |
| ,, 5th | 2 P.M. | 10 | 51 | 76 | 168 | 43 | 109 | 0·000114 | 0·332 |
| | | | | | | Probable value | | 0·000113 | 0·329 |
| Specimen of 2-in. treated board weighing 8·6 lb. per cubic foot. | | | | | | | | | |
| July 28th | 5 A.M. | 26 | 79 | 60 | 140 | 43 | 109 | 0·000121 | 0·351 |
| ,, 29th | 11 A.M. | 26 | 79 | 60 | 140 | 43 | 109 | 0·000133 | 0·386 |
| ,, 31st | 10 A.M. | 26 | 79 | 60 | 140 | 43 | 109 | 0·000129 | 0·374 |
| | | | | | | Probable value | | 0·000130 | 0·377 |

*Fibres of Kingia Australis.*—The possibility of using this material was suggested by Mr. R. A Fowler, Forest Produce Laboratory, Perth, Australia, who supplied the following information concerning it:—

It is a fibrous waste from a tree known as "Kingia Australis". This plant is peculiar to Western Australia, where it grows on the poorer soils of the coastal belt. The tree consists of a long cylindrical stem up to about 20 feet high and 1 foot in diameter, surmounted by a tuft of long grass-like leaves. The stems are usually black in outward appearance, owing to charring by forest fires, and are composed of an outer sheath of persistent leaf bases packed very closely together, an inner sheath, 1 inch to 2 inches in thickness, of longitudinal fibres cemented together in a close matrix, and an inner core of closely packed short fibres. The inner sheath of long fibres is the only portion of the plant at present used.

A waste product is obtained in cleaning the fibres from the cementing matrix in the form of dust and fibrous material.

The results of a series of tests on this material are given in Table III below:—



Digitized by Google

TABLE III.—Fibres of Wood, Kingia Australis.

Density of packing, 8·4 lb. per cubic foot.

| Date. | Time. | Cold-Face Temperatures. | | Hot-Face Temperatures. | | Mean Temp. of the Material. | | Conductivities. | |
|---|---|---|---|---|---|---|---|---|---|
| | | °Cent. | ° Fahr. | ° Cent. | ° Fahr. | ° Cent. | ° Fahr. | C.G.S. Units. | B.T.U.'s per sq. ft. per Hour for 1-in. Thickness and for 1° F. diff. in Temp. |
| August 27th | 9 A.M. | 16 | 61 | 32 | 90 | 24 | 75 | 0·000118 | 0·342 |
| ,, 28th | 10 A.M. | 16 | 61 | 32 | 90 | 24 | 75 | 0·000117 | 0·339 |
| ,, 29th | 11 A.M. | 16 | 61 | 32 | 90 | 24 | 75 | 0·000115 | 0·334 |
| ,, 30th | 11 A.M. | 16 | 61 | 32 | 90 | 24 | 75 | 0·000117 | 0·339 |
| ,, 31st | 11 A.M. | 16 | 61 | 32 | 90 | 24 | 75 | 0·000117 | 0·339 |
| | | | | | | | Probable value | 0·000117 | 0·339 |

*Eel-Grass Mats.*—This material is made up of cured eel-grass sewn in between sheets of strong paper. The grass grows in salt water and contains silicon to a large extent. It does not harbour insects or vermin, which is a most valuable characteristic.

TABLE IV.—Eel-Grass Mats.

Density of packing, 9·4 lb. per cubic foot.

| Date. | Time. | Cold-Face Temperatures. | | Hot-Face Temperatures. | | Mean Temp. of the Material. | | Conductivities. | |
|---|---|---|---|---|---|---|---|---|---|
| | | ° Cent. | ° Fahr. | ° Cent. | ° Fahr. | ° Cent. | ° Fahr. | C.G.S. Units. | B.T.U.'s per sq. ft. per Hour for 1-in. Thickness and for 1° F. diff. in Temp. |
| May 8th | 10 A.M. | 15 | 59 | 45 | 113 | 30 | 86 | 0·000109 | 0·318 |
| ,, 9th | 9 A.M. | 15 | 59 | 45 | 113 | 30 | 86 | 0·000108 | 0·314 |
| | | | | | | | Probable value | $0{\cdot}000108_5$ | 0·316 |
| Density of packing, 13·4 lb. per cubic foot. | | | | | | | | | |
| May 16th | 11 A.M. | 19 | 66 | 41 | 106 | 30 | 86 | 0·000117 | 0·341 |
| ,, 17th | 11 A.M. | 19 | 66 | 41 | 106 | 30 | 86 | 0·000117 | 0·341 |
| | | | | | | | Probable value | 0·000117 | 0·341 |

Digitized by Google

The value of eel grass as a thermal insulator appears to have been realised at an early date in the United States, for it is stated that a dwelling house built in 1635 in Dorchester, Mass., was lined with the grass stuffed between the studding, and the material appears to have been in a good state of preservation after a lapse of more than two and a half centuries.

A sample of commercial matting was obtained and tested in two states of packing. The results are given in Table IV.

Whether the material will meet the stringent requirements of the refrigerating engineer is a matter for experiment under service conditions.

*Compressed Peat.*—Peat, variously treated, is being extensively used on the Continent for heat insulation. The chief merit of the material is its cheapness. For cold-storage work the peat is impregnated with a bituminous substance to protect it from the effect of damp. Data concerning tests on "treated" and "untreated" material are given in Table V below.

The heavy weight per cubic foot of the material—20 to 30 lb.—is a disadvantage.

TABLE V.—Compressed Peat.

Weight of specimen, 20 lb. per cubic foot.

| Date. | Time. | Cold-Face Temperatures. | | Hot-Face Temperatures. | | Mean Temp. of the Material. | | Conductivities. | |
|---|---|---|---|---|---|---|---|---|---|
| | | ° Cent. | ° Fahr. | ° Cent. | ° Fahr. | ° Cent. | ° Fahr. | C.G.S. Units. | B.T.U.'s per sq. ft. per Hour for 1-in. Thickness and for 1° F. diff. in Temp. |
| August 7th | 10 A.M. | 23 | 73 | 51 | 124 | 37 | 99 | 0·000175 | 0·509 |
| ,, 8th | 10 A.M. | 23 | 73 | 51 | 124 | 37 | 99 | 0·000176 | 0·512 |
| | | | | | | Probable value | | 0·000176 | 0·512 |
| **Peat Treated with Bituminous Material.** | | | | | | | | | |
| Weight of specimen, 29·5 lb. per cubic foot. | | | | | | | | | |
| August 19th | 11 A.M. | 24 | 75 | 52 | 126 | 38 | 100 | 0·000175 | 0·507 |
| ,, 20th | 11 A.M. | 24 | 75 | 52 | 126 | 38 | 100 | 0·000173 | 0·501 |
| ,, 21st | 10 A.M. | 24 | 75 | 52 | 126 | 38 | 100 | 0·000173 | 0·502 |
| | | | | | | Probable value | | 0·000173 | 0·502 |

A sample obtained from another source gave the value 0·000167 C.G.S. units for the thermal conductivity at 38° C.



Digitized by Google

In conclusion it may be pointed out that the thermal conductivity of insulating materials in general is not an invariable physical constant. So it follows that it is advisable to test samples of various consignments, just as it is desirable to determine the calorific value of a fuel.

The experiments recorded in this paper and Paper 8 on Thermometric Lag constitute a part of the programme of work for the Engineering Committee of the Food Investigation Board.

We desire to record our thanks to the Engineering Committee and to our Director for their interest and encouragement.

Digitized by Google

# THE THERMAL AND ELECTRICAL CONDUCTIVITIES OF SOME PURE METALS

BY

F. H. SCHOFIELD, B.A., B.Sc.,

SENIOR ASSISTANT IN THE PHYSICS DEPARTMENT.

Digitized by Google

## ABSTRACT.

The thermal and electrical conductivity of a number of pure metals has been measured for mean temperatures ranging to a maximum of 700° C. The thermal conductivity of aluminium was found to increase with rising temperature, that of nickel to decrease at first, and then above 500° C. to show an increase. The other metals—namely, copper, magnesium, zinc—showed on the whole slight decreases of conductivity with temperature.

The values of LORENZ's function for copper, magnesium and zinc were practically constant at all temperatures; that for aluminium showed a rise with increasing temperature; that for nickel showed a rise to 300° C., above which temperature it remained nearly constant, except for an abnormal value at 400° C.


Digitized by Google

# THE THERMAL AND ELECTRICAL CONDUCTIVITIES OF SOME PURE METALS.

By F. H. SCHOFIELD, B.A., B.Sc., Senior Assistant in the Physics Department.

[Reprinted from the 'Proceedings of the Royal Society', A, Vol. 107, 1925.]

## I. Introduction.

The relation between the thermal and electrical conductivities of metals has for a long time engaged the attention of physicists. As far back as 1853 Wiedemann and Franz* propounded the law to the effect that the ratio of the two conductivities was the same for all metals. In 1872 Lorenz†, both on theoretical and experimental grounds, sought to establish that the above-mentioned ratio was proportional to the absolute temperature. On the development of the electron theory Drude, H. A. Lorentz, J. J. Thomson and others‡ have, on the basis of various assumptions, arrived at the same conclusion as Lorenz. Up to 1900, however, the experimental values were too uncertain to allow any definite confirmation of the theory. In that year Jaeger and Diesselhorst§ published the result of their investigation, which gave directly the ratio of the conductivities for a number of metals and alloys over the range 18° to 100° C. Lees‖ has since, by an independent method, confirmed the values of Jaeger and Diesselhorst for a number of metals at 18° C. and has carried the investigation down to — 170° C. Meissner¶ has experimented with some pure metals down to — 250° C. and Onnes and Holst** even lower.

The result of these investigations has been to show that between — 100° C. and + 100° C. the value of the function $K/\lambda T$ ( K and $\lambda$ being the thermal and electrical conductivities and T the absolute temperature) is sensibly the same for the pure metals, with perhaps a slight tendency to fall with decreasing temperature. Below — 100° C., however, the function shows an increasingly rapid fall with temperature and a considerable divergence between individual metals. Above a temperature of + 100° C. very few determinations of thermal conductivity have been made, and the object of the present series of experiments has been to measure, in this region, the thermal and electrical conductivities of a number of metals of the highest purity obtainable commercially.

The materials used have been obtained through the kindly offices of Dr. Hutton, the Director of the British Non-Ferrous Metals Research Association, and were presented by

* 'Ann. der Phys.', vol. 89, p. 497, 1853

† 'Ann. der Phys.', vol. 147, p. 429, 1872.

‡ For a critical review of the most recent theories, see Meissner, 'Jahrbuch der Radioaktivität und Elektronik', vol. 17, p. 260, 1920.

§ 'Abh. der Phys.-Tech. Reichsanstalt', vol. 3, p. 282, 1900.

‖ 'Phil. Trans.', A, vol. 208, p. 381, 1908.

¶ 'Verh. Deutsch. Phys. Ges.', vol. 16, p. 262, 1914.

** 'Proc. Acad. Amsterdam', p. 760, 1914.

Digitized by Google

the firms whose names appear below. In setting out the results (see Appendices I to V) it has been thought well to give, in addition to the chemical analysis of the metal, particulars as to the method of preparation and heat treatment. Dr. ROSENHAIN, Superintendent of the Metallurgy Department of the National Physical Laboratory, kindly undertook to advise as to the suitability of the specimens, and arranged for an examination of the aluminium specimen, of which details are included in Appendix I.*

## II. THERMAL CONDUCTIVITY.

### (*a*) *Theory of Experiment and Reference to Previous Work.*

The methods which have been adopted for measuring the thermal conductivity of metals can be classified under two main heads which, for convenience, may be termed "electrical" and "thermal" respectively. Under the former a rod of metal is heated by the passage of an electric current and measurements are made of the thermal and electrical potentials along its length. By this means the ratio of the thermal to the electrical conductivity is obtained. The determination of the latter by a separate experiment then enables the thermal conductivity to be deduced. With various modifications this method has been exploited by JAEGER and DIESSELHORST,† CALLENDAR,‡ MEISSNER† and others. The method probably presents considerable experimental difficulties at high temperatures, and above 200° C. appears to have been tried only by ANGELL,§ who in an ingenious way dealt with the radial, instead of the longitudinal, gradient of temperature in a bar of metal heated by an electric current.

The purely "thermal" methods of measuring conductivity are simple in theory, and generally resolve themselves into a determination of the rate of heat flow through a bar of metal, in which a longitudinal gradient of temperature is maintained.

A method of this description was first used by FORBES in his well-known experiments. FORBES allowed the surface of his bar to be exposed to the atmosphere and determined the heat flow past any point on the bar by the amount given up by radiation and convection from the cooler parts. This procedure gives rise to considerable uncertainty, not only on account of the difficulty of accurate measurement of heat flow in the manner indicated, but also because it involves the necessity of estimating the temperature gradient at a particular point. With modern appliances more convenient and accurate methods of measuring the heat flow are available and, if it is possible to insulate the bar thermally so as to prevent lateral heat loss, the temperature gradient may be measured over a finite distance instead of at a point. Under the conditions indicated the rate of heat flow Q is given by the equation

$$Q = \frac{KA\,(\theta_1 - \theta_2)}{d},$$

* The author is greatly indebted to Mr. CHALLENOR, Observer in the Physics Department, for his skill in constructing and improving the apparatus, and for making the majority of the observations.

† *Loc. cit.*

‡ 'Encycl. Britannica', 11th ed., art. "Conduction of Heat".

§ 'Phys. Rev.', vol. 33, p. 421, 1911.

Digitized by Google

where A is the cross-sectional area of the bar, $\theta_1$ and $\theta_2$ are the temperatures at a distance $d$ apart, and K is the mean conductivity of the metal between the temperatures $\theta_1$ and $\theta_2$, and which is assumed over this range to be a linear function of the temperature.

This is the principle of the method adopted in the present series of experiments. Before describing the details of the apparatus, it is well to refer briefly to those used by some previous workers who have adopted similar methods, particularly for experiments above atmospheric temperature. For example, CALLENDAR and NICHOLSON,* when measuring the thermal conductivity of steel, used bars of considerable cross-section (about 4 inches in diameter) and lagged them with a material of low conductivity. In this way the lateral escape of heat was so reduced as to amount to only a small fraction of that conducted by the metal. The bar under test was heated at one end by steam and cooled at the other end by a flow of water. EZER GRIFFITHS† also used a lagged bar with electric heating at one end and water cooling at the other, and obtained the conductivity of a number of aluminium alloys up to a mean temperature of 250° C. WILKES‡ eliminated lateral heat loss by an application of the guard-ring principle. He surrounded his bar with a coaxial pipe of metal, the annular space between the two being filled with a finely powdered insulating medium to prevent convection currents. At the hot end of the apparatus the bar and pipe fitted into a common end-piece of copper maintained electrically at a constant temperature. At the other end the bar and pipe were cooled independently by water circulations and the cooling was so adjusted that the same longitudinal temperature distribution was induced in the bar and pipe, thus eliminating lateral loss from the former. In the three cases mentioned above, the rate of heat flow (Q) in the test bar was determined by means of a flow calorimeter at the cold end. This method of measuring the heat flow is very accurate and convenient, but it limits the temperature to which the conductivity can be determined, since the value is given for a temperature intermediate between those of the hot and cold ends of the bar, generally the mean of these temperatures. If, however, the heat flow is determined from the energy input at the hot end, the cooler end of the bar may be kept at a higher temperature and the value of the conductivity can be obtained at a correspondingly higher mean temperature. HONDA and SHIMIDU§ worked in this way in determining the conductivity of nickel and various specimens of steel to over 800° C. In their apparatus the test bar was divided into two portions centrally to allow the insertion of a small heating coil, in a very similar way to that subsequently adopted by the author (see Fig. 1, p. 42). This specimen bar was inserted into a pipe and packed with kaolin powder, and the whole apparatus was placed inside a furnace maintained at a steady temperature. In conducting an experiment, energy was switched on in the central heating coil and

* *Loc. cit.*

† Advisory Committee for Aeronautics, Light Alloys Sub-Committee, Report No. 7, November, 1917.

‡ 'Chem. and Met. Eng.', vol. 21, p. 241, 1919.

§ 'Sci. Reports, Tohoku Univ.', vol. 6, p 219, 1917. The author did not have access to this paper until after the conclusion of the experiments described below.



Digitized by Google

was dissipated at a certain rate for about 20 minutes, at the end of which time the steady rate of heat flow was established in the bar. The temperature difference at two points at a known distance apart was then measured by differential thermocouples. Under these conditions a small amount of the energy dissipated in the cental heating coil (estimated at 6 per cent.) was conducted into the kaolin surrounding the bar. This amount could not be directly measured, but, on the assumption that the same fraction of heat generated was always lost by diffusion into the kaolin, relative values were obtained from room temperature up to 900° C. While this assumption may not be strictly valid over very wide ranges of temperature, for moderate ranges, at any rate, the method seems to be admirably adapted to the measurement of changes of conductivity with temperature.

### (*b*) *Details of Apparatus.*

In the present series of experiments the attempt has been made to determine the thermal conductivity in absolute measure by adopting the guard-ring principle. For this purpose a source of heat was applied at the centre of the test bar and a sink at each end in such a way that a steady flow of heat was maintained. The guard ring consisted of a coaxial pipe of metal which surrounded the bar and which, like the bar, was heated centrally and cooled at the ends in such a way as to reproduce as closely as possible the same temperature distribution as that obtaining in the bar.

The details of the apparatus are shown in the accompanying diagrams. Fig. 1 represents a section of the apparatus. The test specimen is seen to be divided into two portions (shown shaded in different directions in Fig. 1) which fit into each other with an over-

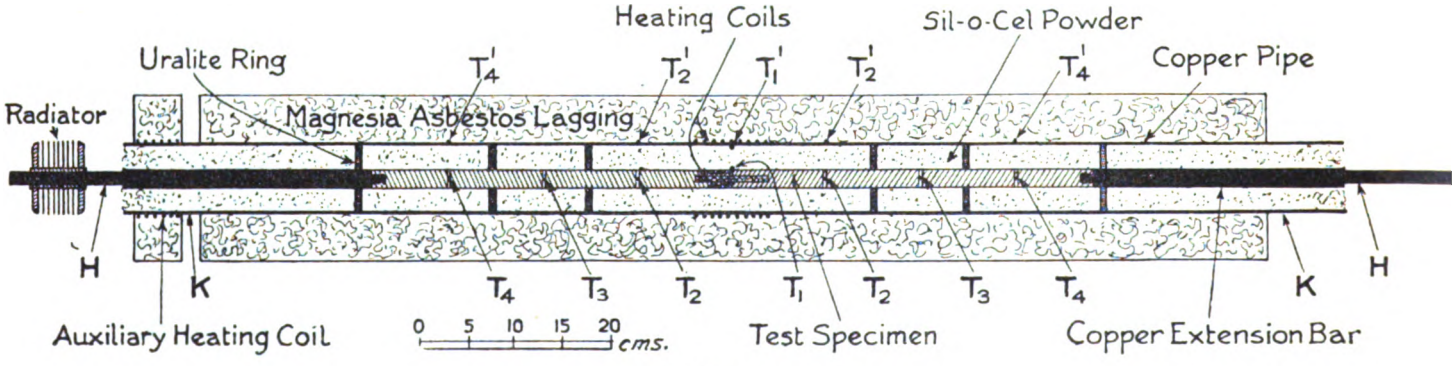


FIG. 1.

lapping joint. Each of these portions is drilled axially to a certain depth, so that when they are brought together an enclosed space is formed, about 7·5 cms. in length, for the reception of a heating unit. For purpose of clearness, the latter is not shown in Fig. 1, but it appears in the enlarged drawing of Fig. 2, and a full description of it is given below. To the ends of the test specimen are screwed copper extension pieces, and the composite bar thus formed is supported by several uralite rings inside a pipe of metal which, in

Digitized by Google

order to facilitate assembly of the apparatus, is cut into halves longitudinally. The temperatures at a series of points along the bar and pipe are measured by means of thermocouples fixed at the positions marked $T_1$, etc., in Fig. 1. These couples are of wires of platinum and 10 per cent. iridium-platinum, 0·2 mm. in diameter. In the case of the bar, all the couples, except the central one, were insulated with capillary tubes of pyrex glass or silica inserted into holes drilled through the bar. The precise arrangement is shown in Fig. 2. In order to fix the couple in position in the rod the capillary

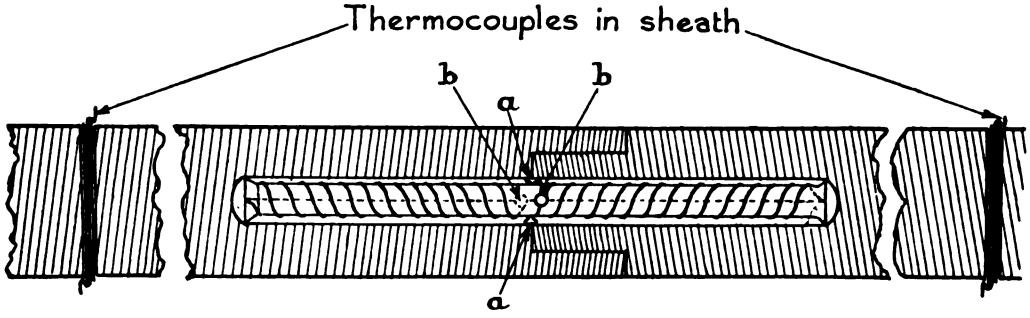


FIG. 2.

tubes were slightly tapered to ensure a tight fit and the wires were bent over the edges of the tubes in the manner shown. The central couple was fixed in a groove, cut in the rod, by means of a binding of platinum wire. In the case of the pipe the couples were attached directly to the metal by means of small pegs.

The central portion of the pipe was heated by means of a coil of platinum wire wound on a wrapping of mica. The length of pipe covered by the winding was equal to that of the cavity in the centre of the test bar, and in assembling the apparatus care was taken to secure that the ends of the two were in alignment. In order to reduce the heat loss from the pipe the whole apparatus was encased in magnesia-asbestos lagging.

The sinks of heat at the ends of the bar and pipe consisted of the exposed ends HH and KK, to which a number of devices for regulating the heat loss could be applied. Thus in Fig. 1 one end of the bar is shown fitted with a movable sleeve to which radiating fins are attached, in order to increase the heat loss. When a still greater loss was required, the ends could be wound with composition pipe, through which water was circulated. If, on the other hand, it was required to reduce the heat loss, the exposed ends could be covered with insulating material, such as asbestos string, or a still greater effect in this direction could be obtained by means of sleeves on which heating coils were wound. An auxiliary heating coil of this kind is shown in Fig. 1 on one end of the pipe.

As has already been indicated, the lateral interchange of heat between the bar and pipe was practically eliminated by maintaining the same temperature distribution in the two, but, in order that this device should be effective, it was necessary to secure that no interference should arise from the heating elements themselves. The respective heating coils were accordingly situated *inside* the rod and *outside* the pipe. The latter has



Digitized by Google

already been described and presented no difficulty, but some experiment was necessary before a satisfactory design was evolved for a heating coil to be embedded in the rod. To secure ease of assembly it was desirable that leads should emerge close together near the centre of the heater, while to obtain the requisite efficiency it was important that there should be no obstruction between the incandescent wire of the heater and the interior surface of the bar.

The design adopted is shown in Figs. 2 and 3, which represent respectively a section of

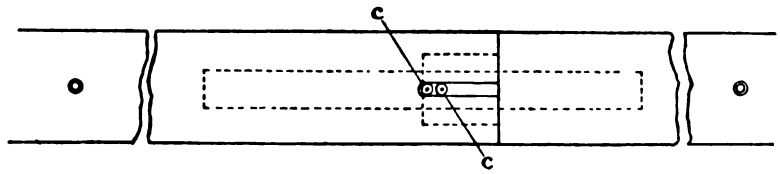


FIG. 3.

the bar and a plan viewed from a position at right-angles to the section. The heater consists of platinum wire, 0·3 mm. in diameter, wound upon a silica tube 5 mm. in diameter. As is shown in Fig. 2, the ends of the silica tube are splayed out to prevent contact of the winding with the interior surface of the bar, and four knobs of silica, *aa* and *bb*, are fused to the tube near the centre. The winding is effected by belaying one end of the wire round the base of the knob *a* and winding spirally from there to the end of the silica tube. The wire then passes through a nick in the splayed end to the interior of the tube and, emerging in a similar way from the other end of the tube, is again wound spirally toward the centre and belayed round the other knob *a*. In order to prevent overheating of the portion of the circuit inside the silica tube, this section consisted of two strands of wire in parallel. The function of the knobs *b* is to prevent the short-circuiting of the complete heating coil owing to a slipping of the windings in the neighbourhood of either of the knobs *a*. Incidentally, the knobs *aa* and *bb* serve to limit any possible sagging of the silica tube at very high temperatures. It will be noticed from Fig. 2 that the internal surfaces of the two portions of the bar, which are exposed to radiation from the heater, are equal.

The assembly was effected by passing the loose ends of the heating coil through the holes *cc* (see Fig. 3) in the right-hand portion of the bar and drawing the heating unit in position. The left-hand portion of the bar, which was provided with a slot for clearing the holes *cc*, was then slid into position. The ends of the heating coil were insulated in the holes *cc* by means of silica tubes, and current and potential leads of platinum were attached to them where they emerged from the tubes.

In the earlier experiments asbestos wool was used for packing the space between the rod and pipe, but the material finally adopted was " Sil-o-cel ", which is a finely powdered diatomaceous earth. This material has the advantage of an extremely low thermal conductivity, while its fine state of division serves to prevent convection currents and reduce the oxidation of the specimen bar.

Digitized by Google

### (c) *Method of Experiment.*

In carrying out an experiment, adjustments were made of the energy supplied to the heating coils at the centres of the rod and pipe and of the energy absorbed at the ends until the desired gradients were obtained. In all cases the gradients in the tube were made to correspond as closely as possible with those of the rod. Typical distributions of temperature for the specimens of nickel and aluminium are shown in Fig. 4. It will be noticed that in each case the gradients in the rod and pipe are approximately straight lines.

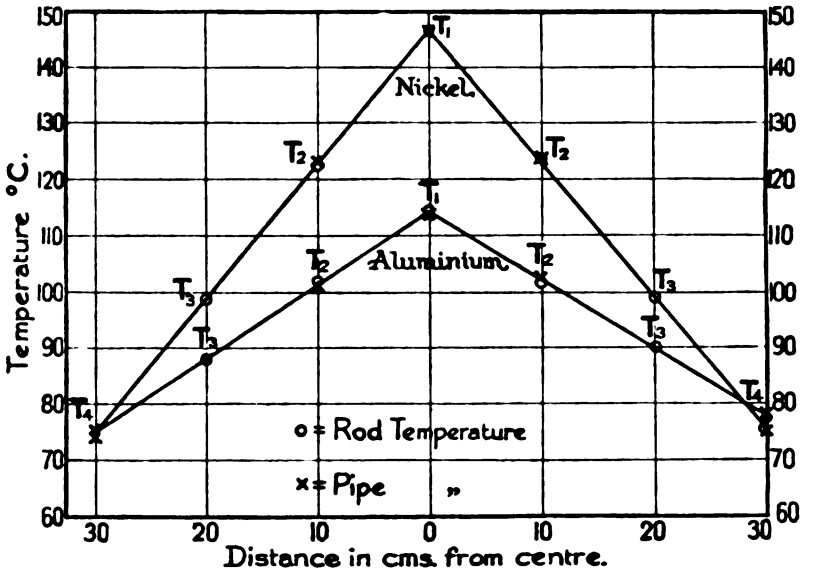


FIG. 4.

A strict linearity of gradient would, of course, be obtained only where the metals composing the rod and pipe had conductivities not varying with temperature; where the lateral heat loss from both rod and pipe were negligible; and where the supply of heat was from sources of zero thickness in a plane at right-angles to the axis. None of these conditions was precisely fulfilled but, as will be seen from Fig. 4, the net effect in producing curvature was negligible. It should, however, be pointed out that the amount of the lateral loss through the lagging from the pipe increased with increasing temperature. The resulting sag which this would tend to produce in the temperature distribution curve of the pipe was counteracted by using a greater thickness of lagging and by increasing the quantity of heat flowing through the metal itself. Consequently, throughout the experiments steeper gradients were employed at the higher temperatures.

As evidence that no systematic error arose from the employment of differing temperature gradients, it may be mentioned that the conductivity measurements for the same mean temperature, but with different temperature gradients, gave results agreeing within the limits of experimental error. (See, for example, the results in Appendix I for a mean temperature of about 150° C. obtained with temperature differences of 28°C., 35° C. and 50° C. respectively.)

Digitized by Google

### (*d*) *Magnitude of Lateral Heat Loss.*

Since the theory of the method presupposes the elimination of lateral heat loss from the specimen, it is important to ascertain the magnitude of any error due to failure to obtain a coincidence of temperatures over the working area of the rod and pipe. Consequently, the following series of experiments were made with the specimen of aluminium. The several temperatures of the rod and pipe were first adjusted to correspond as closely as possible, so as to obtain a value of the true conductivity of the metal. The temperatures along the pipe were then adjusted to differ by a certain amount, either above or below, from the corresponding temperatures of the rod, and when steady conditions had been obtained, the apparent conductivity was calculated. The temperature gradient between the points $T_2$ $T_4$ (Fig. 1) was about 40° C. throughout, and the temperature of $T_3$ approximately 160° C. The results obtained are shown in Fig. 5, and it will be observed that the error due to a mean difference of 1° C. between the rod and pipe was about 1 per cent. It was estimated that the mean temperature difference between corresponding points on rod and pipe could be adjusted to between 1° C. and 2° C., so that this fixes a definite limit to the accuracy of the method. This limit may be stated to be from 1 to 2 per cent. for the aluminium bar working with a temperature gradient of 40° C. Working with higher or lower temperature gradients or with metals of higher or lower conductivity, the accuracy would be correspondingly greater or less.

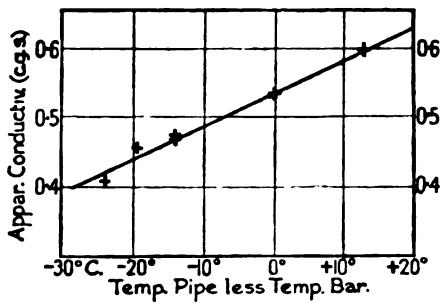

FIG. 5.

As a check on the above conclusion, it is possible to make an approximate estimate of the lateral heat loss from the known conductivity of insulating material. No attempt can be made here to give a mathematical solution of the problem under consideration, namely, the flow of heat between coaxial cylinders with a constant difference of temperature between the corresponding points in planes at right angles to the axis and with a longitudinal gradient in each cylinder, but as an approximation it is proposed to take the case of a constant difference in temperature, but no gradient. The formula for the lateral flow of heat per 1° C. difference would then be

$$H = \frac{2 \cdot 73\, K l}{\log_{10}(b/a)} \text{ cals./sec.}$$

Here $a$ and $b$, the diameters of the rod and pipe respectively, are 1·9 and 7·0 cms.; $l$ is taken as 30 cms., *i.e.* the complete length between $T_1$ and $T_4$, and K, the thermal conductivity of the insulating medium at a mean temperature of 160° C., is about 0·00015 c.g.s. units for " Sil-o-cel ". Hence we get

$$H = 0 \cdot 022 \text{ cals./sec.}$$

Digitized by Google

Now the flow of heat through the aluminium rod for a temperature difference of 40° C. between $T_2$ and $T_1$ at a distance ($d$) apart of 20 cms. is given by

$$H = \frac{\pi a^2 K (\theta_1 - \theta_2)}{4d} = 2 \cdot 95 \text{ cals./sec.}$$

So that the lateral heat loss per 1° C. in the case taken is estimated as 0·7 per cent. of the heat flowing in the rod, a result which is of the same order as that obtained by experiment.

It may be added that the error due to lateral heat loss varies inversely as the square of the diameter of the specimen rod, provided that the ratio of the diameters of the rod and pipe is constant, so that it would be advantageous to use specimens of large diameter. The limit of the dimensions of the present apparatus was decided largely on considerations of convenience and expense.

### (*e*) *Magnitude of Longitudinal Heat Loss.*

The isothermal surfaces in the lagging being adjusted so as to be approximately perpendicular to the axis, it follows that there will be a longitudinal flow of heat in the lagging, which will be contributed mainly by the pipe, but to some extent from the rod. The poorest conductor of all the metals tested, namely, nickel, having a conductivity of the order of 1,000 times that of the insulating material, it was considered safe to neglect the contribution from the rod to the longitudinal heat loss.

## III. Electrical Conductivity.

The measurement of the electrical conductivity of the several metals has been undertaken merely to throw light on its relation to the thermal conductivity. For this purpose an accuracy of 1 per cent. suffices, so that an elaborate investigation has not been called for. The method used consisted in a comparison of the voltage drop on a measured length of the specimen and on a standard resistance arranged in series with it, a constant current being maintained through the two.

Since this method has been adopted by a number of experimenters, a detailed description is not required here, but the following particulars should perhaps be mentioned :—

The current was led into and out of the specimen rod by copper rods 4 mms. in diameter screwed into the test rod. The voltage drop was measured by means of thin potential wires pegged into the specimen at a distance of 22 cms. apart. The specimen was fixed centrally in a tubular furnace 1·8 metres long wound with nichrome ribbon, and its temperature was measured by three thermocouples. The space between the specimen and the furnace tube was packed with " Sil-o-cel " powder. The current, which was supplied from a large storage battery, was of the order of 10 amps. In order to eliminate any thermal E.M.Fs. at the potential points, measurements were made before and after reversing the main current, while the effects of thermal E.M.Fs. in the potentiometer circuit were eliminated by taking readings before and after a simultaneous reversal of the potential leads and the leads supplying the current to the instrument. The magnitude

Digitized by Google

of the difference due to these two sets of reversals seldom exceeded 2 microvolts, and it was estimated that the volt drop was obtained to better than 1 microvolt, a precision amply sufficient to meet the requirements.

No special difficulty occurred in applying this method, except in the case of magnesium, where at temperatures over 300° C. voltaic effects were likely to occur, which were eliminated by the use of potential leads of the same metal as the specimen.

## IV. Discussion of Results.

The detailed results of the measurements of thermal and electrical conductivity are set out in Appendices I to V. The values obtained are also shown in Figs. 6 and 7 and, since the majority of the metals were also investigated by Lees and by Jaeger and Diesselhorst, their values over the respective ranges of — 100° C. to 18° C. and 18° C. to 100° C. have been included for purposes of comparison. Some individual values given by other observers have been shown on the graphs or are referred to in the text below. For the purpose of dealing with the relation of thermal to electrical conductivity, the values of Lorenz's function have been set out in Table I (below).

Table I.—Relation of Thermal and Electrical Conductivity.

| Metal. | Purity. | Observer. | Value of Lorenz's function $K/\lambda T \times 10^8$ (K in watts/cm./°C., $\lambda$ in reciprocal ohms/cm.) at Temperatures of | | | | | | | | |
|---|---|---|---|---|---|---|---|---|---|---|---|
| | | | −100° C. | 18° C. | 100° C. | 200° C. | 300° C. | 400° C. | 500° C. | 600° C. | 700° C. |
| Aluminium ... | 99 | L | 1·81 | 2·13 | | | | | | | |
| | | J. & D | | 2·19 | 2·27 | | | | | | |
| | 99 | A | | | 2·25 | 2·68 | 3·18 | 3·79 | 4·48 | 5·08 | |
| | | K* | | 2·30 | 2·25 | 2·29 | 2·26 | 2·23 | 2·14 | 2·03 | |
| | 99·7 | S | | | 2·23 | 2·36 | 2·44 | 2·53 | | | |
| Copper ... | | L | 2·17 | 2·32 | | | | | | | |
| | | J & D | | 2·29 | 2·32 | | | | | | |
| | | M(1) | | 2·25 | 2·33 | | | | | | |
| | | M(2) | | 2·26 | 2·34 | | | | | | |
| | 99·9 | S | | | 2·31 | 2·36 | 2·34 | 2·37 | 2·34 | 2·35 | |
| Magnesium ... | 99·6 | S | | | 2·31 | 2·32 | 2·30 | 2·33 | | | |
| Nickel... ... | 99 | L | 2·59 | 2·59 | | | | | | | |
| | 97 | J & D | | 2·40 | 2·44 | | | | | | |
| | 97 | A | | | | | 3·10 | 2·67 | 2·24 | 1·81 | 1·42 |
| | 97 | H & S | | | 2·37 | 2·53 | 2·71 | 2·68 | 2·71 | 2·75 | 2·75 |
| | 99·2 | S | | | 2·28 | 2·39 | 2·65 | 2·79 | 2·62 | 2·64 | 2·68 |
| Zinc ... ... | | L | 2·39 | 2·43 | | | | | | | |
| | | J & D | | 2·31 | 2·33 | | | | | | |
| | | K* | | 2·45 | 2·47 | 2·47 | 2·41 | 2·36 | | | |
| | 99·8 | S | | | 2·26 | 2·26 | 2·29 | | | | |

* Konno's values of thermal conductivity are relative to those of Lees at 18°C., and for electrical conductivity he has taken those of Tsutsumi ('Sci. Rep.', vol. 7, p. 93, 1918).

Digitized by Google

In this table the names of the observers have been indicated by initials. Their methods of experiment have differed considerably. Thus, as already stated, an "electrical" method was used by JAEGER and DIESSELHORST, by MEISSNER and, in a considerably modified form, by ANGELL. The other observers worked with "thermal" methods. LEES, who introduced many refinements, obtained his values in absolute units; KONNO was primarily interested in changes of conductivity on melting, and used a relative method, taking LEES' values at 18° C. for his starting points; the method of HONDA and SHIMIDU has already been outlined. Detailed comments on the results are appended under the heads of the several metals.

*Aluminium.*

Like LEES, and JAEGER and DIESSELHORST, in their respective ranges, the author finds that the conductivity of aluminium shows a slight increase with temperature. It will be noticed from Fig. 6 that, at the points of overlap, the values of JAEGER and DIESSELHORST

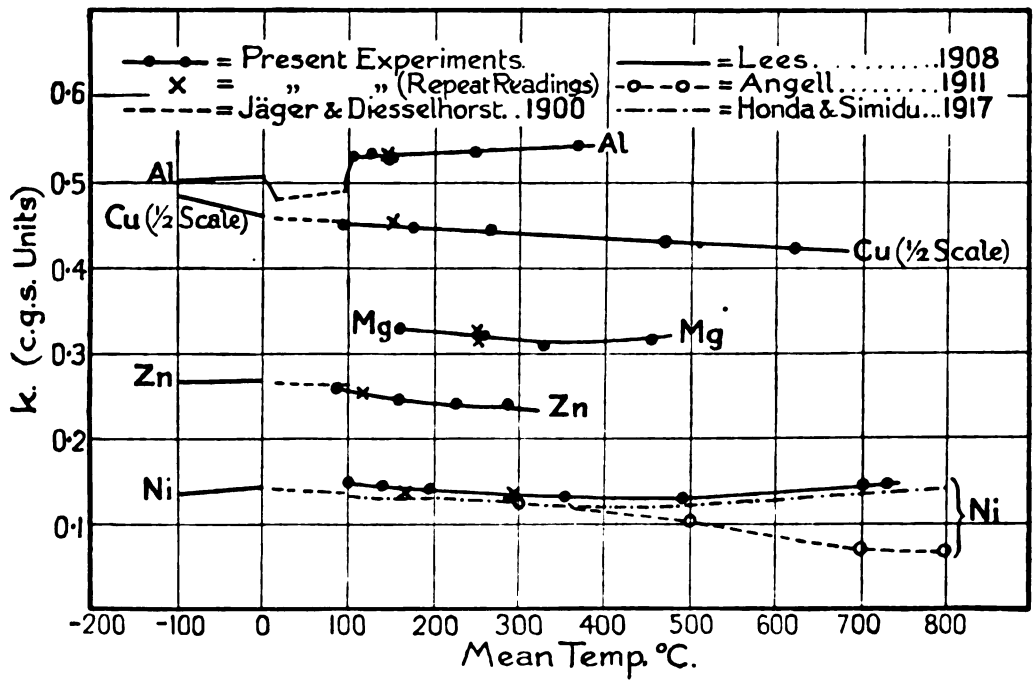


FIG. 6.

are considerably lower than the other two, probably owing to impurity in their specimen. As would be expected, the electrical resistivity found by JAEGER and DIESSELHORST is correspondingly higher (see Fig. 7). Three other sets of values above 100° C. are available, namely, those of EZER GRIFFITHS, ANGELL and KONNO. The first mentioned used material of nearly the same purity as that tested by the author, viz., 99·5 per cent. as against 99·7 per cent., and he gave values for his four specimens ranging from 0·50 to 0·52 at 100° C., and found a slight tendency to increasing conductivity with temperature up to the limit reached (250° C.). This is in very fair agreement with the results of the present



Digitized by Google

experiments. On the other hand, ANGELL gives the value as increasing from 0·49 at 100° C. to 1·0 at 600° C. and KONNO as decreasing from 0·50 to 0·36 over the same range.

As to LORENZ's function, it will be seen that the values of the several observers are in good agreement at 100° C. KONNO gives a nearly constant value throughout, and the others give values rising somewhat with temperature, those of ANGELL showing the greatest change.

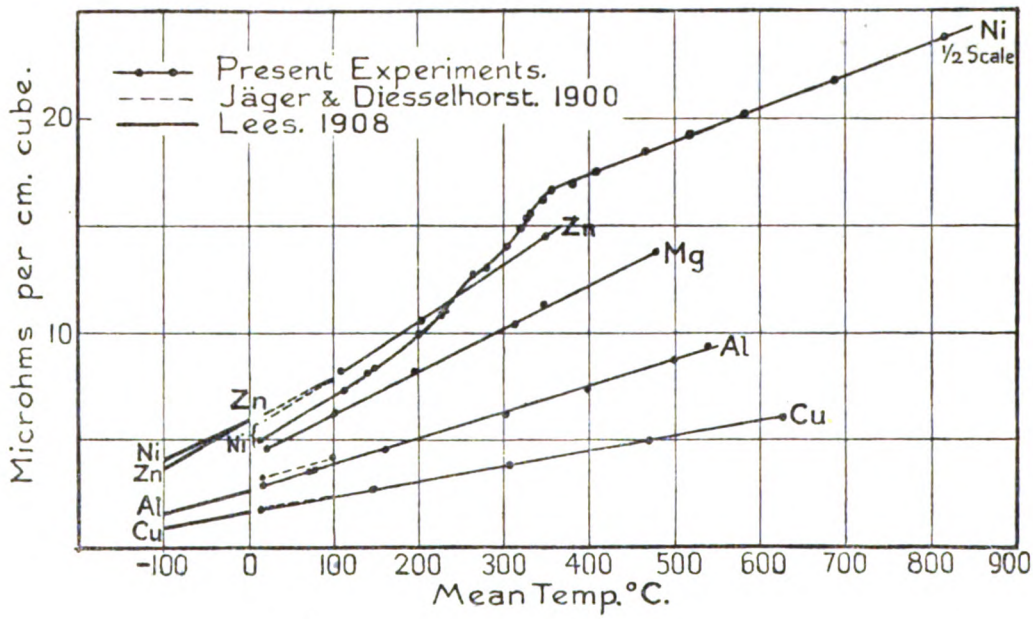


FIG. 7.

*Copper.*

The author's values for the thermal and electrical conductivity show a satisfactory continuity with those of LEES and of JAEGER and DIESSELHORST. The copper used in all three cases seems to have been nearly 100 per cent. in electrical conductivity, according to the international specification.

Further values for copper were obtained by MEISSNER with two specimens of the metal. One of these (No. 1) was better than, and the other (No. 2) equal to, the 100 per cent. standard in conductivity. The respective values obtained are as follows :—

TABLE II.—Thermal Conductivity of Copper.

| Observer. | $K_{18}$. | $K_{100}$. |
|---|---|---|
| Meissner (1) ... ... ... ... | 0·94 | 0·94 |
| ,, (2) ... ... ... ... | 0·92 | 0·92 |
| Lees ... ... ... ... ... | $0·91_8$ | — |
| Jaeger and Diesselhorst ... ... | $0·91_8$ | $0·90_8$ |
| Present paper ... ... ... | — | $0·90_1$ |

Digitized by Google

MEISSNER'S* figure of 0·94 appears to be the highest reliable value yet obtained for copper. SCHOTT† gives 0·98 for a natural crystal of copper, but this value is probably too high, as his figure for pure commercial copper is as large as 0·94.

With regard to LORENZ'S function, it will be seen from the table that there is a good agreement at 100° C. and that the author finds a nearly constant value throughout.

*Magnesium.*

The only previous value traced is that of LORENZ, who gives $0\cdot37_6$ for the thermal conductivity at 100° C. According to the present experiments, the value for the same temperature would be about $0\cdot33_5$.

The values for electrical conductivity are in fair agreement with those of NICOLAI,‡ the latter being on the average about 3 per cent. higher. For LORENZ'S function a nearly constant value is obtained, which does not differ greatly from those found for copper and zinc.

*Nickel.*

As will be seen from Table I, the purity of the specimens used by the several observers varied considerably. In correspondence with the purity, the values given by the present experiments at 100° C. for the thermal and electrical conductivities are somewhat higher than either those of JAEGER and DIESSELHORST, or HONDA and SHIMIDU. The curve for electrical conductivity shows a pronounced change in curvature at the change point at about 350° C. The form of the curve agrees closely with those found by NICOLAI, SOMERVILLE,§ PECHEUX,‖ and by HONDA and SHIMIDU, while the absolute values are in close agreement with that of PECHEUX, whose specimen was of 99·6 per cent. purity, as compared with 99·2 for the specimen used in the present experiments. The author's values for the thermal conductivity show a decrease with temperature between 100° C. and 300° C., thereafter an approximately constant value to 500° C., while the two values obtained in the neighbourhood of 700° C. show a considerable rise. The results of HONDA and SHIMIDU give a generally similar curve, but their method permitted the taking of a large number of values with temperature differences as small as 30° C., so that they were able to trace a definite minimum of conductivity at about 400° C. With the present dimensions of the apparatus described in this paper and a metal of as low conducting power as nickel, it is necessary to use gradients as high as 100° C. to obtain an accuracy of 2 or 3 per cent. Consequently, the point of inflexion in the conductivity curve could not be accurately located. This fact probably accounts for the apparently high value obtained for LORENZ'S function at a temperature of 400° C. It will be observed for Table I that the

* 'Ann. der Phys.', (4), vol. 47, p. 1001, 1915.
† 'Verh. Deutsch. Phys. Ges.', vol 18, p. 27, 1916.
‡ 'Phys. Zeits.', vol. 9, p. 367, 1908.
§ 'Phys. Rev.', vol. 33, p. 77, 1911
‖ 'La Lumière Électrique', vol. 10, p. 232, 1910.



Digitized by Google

value tends to become constant at about 2·6 from a temperature of 300° C. upwards. A similar phenomenon was observed by HONDA and SHIMIDU, while ANGELL found a steady fall in the value with rising temperature.

*Zinc.*

The values obtained for the thermal and electrical conductivity are slightly lower than those of JAEGER and DIESSELHORST at 100° C. Like KONNO, the author finds a nearly constant value for LORENZ's function.

## APPENDIX I.

*Aluminium.*

*Particulars of Specimen* (British Aluminium Co., Ltd.).—The specimen was prepared as follows:—Billets $6\frac{3}{4}$ inches in diameter were cast from a maximum temperature of 700° C., annealed for $2\frac{1}{2}$ hours at 500° C., extruded at temperature of 420° C. to $\frac{3}{4}$-inch diameter, and finally annealed for $2\frac{1}{2}$ hours at 450° C.

In order to test the soundness of the material, transverse and longitudinal sections were taken from the ends of the specimen and were examined in the Metallurgy Department of the National Physical Laboratory. These were reported to be free from the more serious defects of extruded materials, viz., unsoundness, discontinuities between the core and surrounding layers, inclusion of dross and oxidised skin.

Density at 21° C. = 2·70. Purity 99·7 Al.

Thermal Conductivity.

| Mean Temperature $T_3$. | Temperature Difference $T_2-T_4$. | Energy supplied to Bar. | | | Conductivity c.g.s. units. | Mean Conductivity c.g.s. units. |
|---|---|---|---|---|---|---|
| | | Amps. | Volts. | Cals./sec. | | |
| ° C. | ° C. | | | | | |
| 108·7 | 35·7 | 1·360 | 16·60 | 5·38 | 0·528 | 0·528 |
| 128·6 | 51·7 | 1·135 | 28·95 | 7·84 | 0·532 | 0·532 |
| 154·0 | 50·0 | 2·585 | 12·20 | 7·53 | 0·528 | 0·528 |
| 149·4 | 28·1 | 2·030 | 8·70 | 4·22 | 0·526 | 0·526 |
| 148·9 | 28·1 | 2·025 | 8·70 | 4·21 | 0·525 | |
| 149·1 | 28·0 | 2·025 | 8·70 | 4·21 | 0·527 | |
| 254·0 | 46·9 | 2·395 | 12·50 | 7·15 | 0·536 | 0·536 |
| 253·8 | 46·9 | 2·395 | 12·50 | 7·15 | 0·536 | |
| 374·8 | 80·0 | 2·845 | 18·20 | 12·35 | 0·544 | 0·542 |
| 373·3 | 80·5 | 2·840 | 18·20 | 12·35 | 0·540 | |
| 371·6 | 80·3 | 2·830 | 18·20 | 12·30 | 0·537 | |
| 368·8 | 78·3 | 2·820 | 18·20 | 12·25 | 0·547 | |
| 146·4 | 34·8 | 2·150 | 10·20 | 5·24 | 0·527 | 0·528* |
| 149·4 | 35·4 | 2·160 | 10·30 | 5·32 | 0·528 | |
| 149·7 | 35·5 | 2·160 | 10·40 | 5·36 | 0·530 | |

* Repeat reading.

Digitized by Google

Electrical Resistivity.

| Temperature. | Resistivity. | Temperature. | Resistivity. |
|---|---|---|---|
| ° C. | Ohms per cm. cube. | ° C. | Ohms per cm. cube. |
| 16·2 | $2·83 \times 10^{-6}$ | 302·7 | $6·15 \times 10^{-6}$ |
| 16·8 | 2·79 | 304·4 | 6·23 |
| 16·8 | 2·81 | 306·2 | 6·24 |
| 73·0 | 3·45 | 399·0 | 7·39 |
| 77·0 | 3·53 | 500·0 | 8·77 |
| 79·0 | 3·53 | 502·4 | 8·79 |
| 160·0 | 4·47 | 540·7 | 9·31 |
| 161·0 | 4·48 | | |

## Appendix II.

### *Copper.*

*Particulars of Specimen* (T. Bolton & Sons, Ltd., Oakmoor).—The specimen was prepared as follows :—Billets were cast from a mixture of $\frac{1}{3}$ cathodes and $\frac{2}{3}$ electrolytic wire bars immediately after poling. They were rolled hot to 1-inch diameter, drawn cold to $\frac{7}{8}$-inch diameter, machined and polished to $\frac{3}{4}$-inch diameter, and then annealed.

Density at 21° C. = 8·92. Purity 99·9 Cu.

Thermal Conductivity.

| Mean Temperature $T_3$. | Temperature Difference $T_2-T_4$. | Energy supplied to Bar. | | | Conductivity c.g.s. units. | Mean Conductivity c.g.s. units. |
|---|---|---|---|---|---|---|
| | | Amps. | Volts. | Cals./sec. | | |
| ° C. | ° C. | | | | | |
| 93·8 | 19·1 | 2·475 | 8·30 | 4·91 | 0·900 | |
| 96·2 | 20·0 | 2·490 | 8·50 | 5·06 | 0·890 | |
| 95·6 | 19·9 | 2·505 | 8·60 | 5·14 | 0·908 | 0·901 |
| 96·0 | 19·4 | 2·515 | 8·30 | 4·98 | 0·900 | |
| 98·4 | 20·9 | 2·590 | 8·75 | 5·41 | 0·907 | |
| 177·4 | 43·4 | 3·215 | 14·40 | 11·05 | 0·893 | |
| 177·9 | 44·4 | 3·230 | 14·60 | 11·25 | 0·890 | 0·893 |
| 172·4 | 44·0 | 3·225 | 14·60 | 11·25 | 0·897 | |
| 266·0 | 73·6 | 3·755 | 20·80 | 18·65 | 0·888 | |
| 265·7 | 73·6 | 3·750 | 20·85 | 18·65 | 0·890 | 0·888 |
| 265·7 | 74·0 | 3·750 | 20·85 | 18·65 | 0·885 | |
| 473·1 | 93·4 | 3·585 | 26·75 | 22·95 | 0·862 | |
| 473·4 | 94·5 | 3·590 | 26·80 | 23·00 | 0·854 | 0·858 |
| 472·0 | 93·8 | 3·585 | 26·85 | 23·00 | 0·858 | |
| 624·8 | 142·0 | 3·720 | 38·40 | 34·15 | 0·842 | |
| 624·7 | 142·1 | 3·720 | 38·45 | 34·20 | 0·844 | 0·842 |
| 624·7 | 142·3 | 3·720 | 38·45 | 34·20 | 0·839 | |
| 151·8 | 30·7 | 2·060 | 16·10 | 7·93 | 0·905 | 0·905* |

* Repeat reading.

Digitized by Google

Electrical Resistivity.

| Temperature ° C. | Resistivity, Ohms per cm. cube. | Temperature ° C. | Resistivity, Ohms per cm. cube. |
|---|---|---|---|
| 14·0 | $1·69 \times 10^{-6}$ | 470·0 | $4·88 \times 10^{-6}$ |
| 145·0 | 2·59 | 630·5 | 6·00 |
| 144·5 | 2·61 | 630·0 | 6·07 |
| 306·0 | 3·73 | | |

## Appendix III.

### *Magnesium.*

***Particulars of Specimen*** (Magnesium Co., Ltd.).—The specimens were extruded to $\frac{3}{4}$-inch diameter from a billet 5 inches in diameter, annealed at 360° C. for 6 hours, and allowed to cool slowly.

Density at 21° C. = 1·75. Purity 99·6 Mg.

Thermal Conductivity.

| Mean Temperature $T_3$. | Temperature Difference $T_2-T_4$. | Energy supplied to Bar. | | | Conductivity c.g.s. units. | Mean Conductivity c.g.s. units. |
|---|---|---|---|---|---|---|
| | | Amps. | Volts. | Cals./sec. | | |
| 160·4 | 42·1 | 1·940 | 8·00 | 3·71 | 0·328 | 0·328 |
| 157·0 | 42·2 | 1·920 | 8·10 | 3·71 | 0·328 | |
| 156·0 | 40·4 | 1·905 | 7·90 | 3·60 | 0·332 | |
| 153·2 | 39·1 | 1·860 | 7·50 | 3·38 | 0·322 | |
| 264·0 | 74·7 | 2·290 | 11·85 | 6·48 | 0·324 | 0·318 |
| 263·0 | 76·5 | 2·300 | 11·85 | 6·51 | 0·317 | |
| 261·7 | 77·3 | 2·290 | 11·80 | 6·46 | 0·312 | |
| 258·3 | 75·5 | 2·285 | 11·60 | 6·33 | 0·313 | |
| 251·3 | 72·5 | 2·275 | 11·50 | 6·26 | 0·322 | |
| 329·5 | 102·4 | 2·495 | 14·20 | 8·47 | 0·308 | 0·309 |
| 322·0 | 98·6 | 2·460 | 14·00 | 8·23 | 0·311 | |
| 326·4 | 103·8 | 2·510 | 14·30 | 8·58 | 0·308 | |
| 456·0 | 104·8 | 1·510 | 24·50 | 8·84 | 0·314 | 0·314 |
| 456·5 | 104·6 | 1·500 | 24·50 | 8·78 | 0·314 | |
| 254·2 | 70·5 | 1·370 | 18·70 | 6·12 | 0·323 | 0·323* |
| 253·0 | 73·0 | 2·230 | 11·40 | 6·08 | 0·311 | 0·314* |

* Repeat reading with different heating coils.

Digitized by Google

Electrical Resistivity.

| Temperature° C. | Resistivity, Ohms per cm. cube. | Temperature° C. | Resistivity, Ohms per cm. cube. |
|---|---|---|---|
| 20·0 | $4·59 \times 10^{-6}$ | 199·5 | $8·08 \times 10^{-6}$ |
| 101·4 | 6·19 | 314·0 | 10·35 |
| 101·1 | 6·21 | 348·6 | 11·21 |
| 101·1 | 6·18 | 348·0 | 11·04 |
| 199·2 | 8·17 | 480·1 | 13·74 |

## Appendix IV.

### *Nickel.*

*Particulars of Specimen* (H. Wiggins & Co., Ltd.).—The specimen was prepared as follows:—Cast in 3-inch moulds, hot-rolled to $1\frac{1}{2}$ inches diameter, reheated and rolled to $\frac{7}{8}$-inch diameter, close-annealed at 800° C., cold drawn to $\frac{3}{16}$-inch diameter, again annealed, drawn to $\frac{3}{4}$-inch diameter, and finally annealed between 750° C. and 800° C.

Density at 21° C. = 8·79. Purity 99·2 Ni.

Thermal Conductivity.

| Mean Temperature $T_3$. | Temperature Difference $T_2$–$T_4$. | Energy supplied to Bar. | | | Conductivity c.g.s. units. | Mean Conductivity c.g.s. units. |
|---|---|---|---|---|---|---|
| | | Amps. | Volts. | Cals./sec. | | |
| 99·2 | 47·5 | 1·420 | 5·95 | 2·02 | 0·146 | 0·145 |
| 100·8 | 48·0 | 1·420 | 5·95 | 2·02 | 0·145 | |
| 141·6 | 59·8 | 1·490 | 7·00 | 2·49 | 0·143 | 0·144 |
| 141·6 | 59·9 | 1·490 | 7·00 | 2·49 | 0·143 | |
| 141·8 | 60·0 | 1·490 | 7·00 | 2·49 | 0·145 | |
| 196·7 | 75·3 | 1·535 | 7·95 | 2·91 | 0·132 | 0 138 |
| 196·2 | 75·5 | 1·560 | 8·20 | 3·05 | 0·138 | |
| 196·4 | 75·3 | 1·580 | 8·15 | 3·07 | 0·140 | |
| 196·0 | 74·1 | 1·545 | 8·00 | 2·95 | 0·136 | |
| 290·2 | 81·6 | 1·510 | 8·45 | 3·05 | 0·128 | 0·128 |
| 289·7 | 81·5 | 1·510 | 8·45 | 3·04 | 0·128 | |
| 289·2 | 80·9 | 1·510 | 8·45 | 3·04 | 0·129 | |
| 288·4 | 80·8 | 1·510 | 8·45 | 3·04 | 0·129 | |
| 353·6 | 99·4 | 1·610 | 9·70 | 3·73 | 0·129 | 0·128 |
| 355·0 | 100·3 | 1·610 | 9·70 | 3·73 | 0·128 | |
| 357·3 | 100·3 | 1·610 | 9·75 | 3·75 | 0·128 | |
| 357·2 | 100·3 | 1·610 | 9·75 | 3·75 | 0·128 | |
| 491·4 | 105·8 | 1·595 | 10·45 | 3·98 | 0·129 | 0·128 |
| 491·0 | 106·9 | 1·595 | 10·40 | 3·96 | 0·127 | |
| 703·3 | 179·6 | 1·965 | 16·35 | 7·67 | 0·141 | 0·141 |
| 733·0 | 177·3 | 1·975 | 16·70 | 7·88 | 0·147 | 0·147 |
| 166·5 | 65·1 | 1·505 | 7·20 | 2·59 | 0·136* | 0·136 |
| 293·7 | 84·1 | 1·575 | 8·70 | 3·27 | 0·133* | 0·133 |

* Repeat reading

Digitized by Google

Electrical Resistivity.

| Temperature° C. | Resistivity, Ohms per cm. cube. | Temperature° C. | Resistivity, Ohms per cm. cube |
|---|---|---|---|
| 14·0 | $10·04 \times 10^{-6}$ | 320·5 | $29·70 \times 10^{-6}$ |
| 111·0 | 14·60 | 327·8 | 30·75 |
| 142·4 | 16·17 | 331·6 | 31·20 |
| 148·5 | 16·57 | 349·5 | 32·35 |
| 149·2 | 16·62 | 358·8 | 33·50 |
| 200·5 | 19·73 | 383·8 | 33·95 |
| 227·0 | 21·57 | 409·6 | 35·00 |
| 229·5 | 22·10 | 465·2 | 36·85 |
| 265·0 | 25·52 | 519·4 | 38·65 |
| 266·0 | 25·10 | 583·5 | 40·60 |
| 280·0 | 25·90 | 691·1 | 43·60 |
| 304·1 | 28·15 | 820·7 | 47·60 |

## Appendix V.

### *Zinc.*

*Particulars of Specimen* (London Zinc Mills).—The specimen was prepared as follows :— Billets were cast, were rolled at 200° C., sawn into strips and drawn cold.

Density at 21° C. = 7·13. Purity 99·8 Zn.

Thermal Conductivity.

| Mean Temperature $T_3$. | Temperature Difference $T_2$–$T_4$. | Energy supplied to Bar. | | | Conductivity c.g.s. units. | Mean Conductivity c.g.s. units. |
|---|---|---|---|---|---|---|
| | | Amps. | Volts. | Cals./sec. | | |
| °C. | °C. | | | | | |
| 87·5 | 25·0 | 1·520 | 4·90 | 1·78 | 0·256 | 0·258 |
| 87·7 | 25·0 | 1·520 | 4·85 | 1·77 | 0·256 | |
| 87·5 | 25·8 | 1·545 | 5·05 | 1·86 | 0·259 | |
| 87·5 | 25·1 | 1·530 | 4·95 | 1·81 | 0·259 | |
| 87·5 | 26·0 | 1·540 | 5·05 | 1·86 | 0·256 | |
| 87·8 | 25·0 | 1·540 | 5·00 | 1·84 | 0·264 | |
| 160·5 | 54·4 | 1·910 | 8·10 | 3·70 | 0·244 | 0·246 |
| 160·3 | 53·2 | 1·900 | 8·05 | 3·65 | 0·246 | |
| 160·3 | 53·4 | 1·905 | 8·10 | 3·68 | 0·247 | |
| 160·2 | 52·8 | 1·910 | 8·00 | 3·65 | 0·249 | |
| 227·5 | 80·5 | 2·155 | 10·60 | 5·46 | 0·243 | 0·241 |
| 227·1 | 80·0 | 2·160 | 10·30 | 5·32 | 0·239 | |
| 227·1 | 79·9 | 2·145 | 10·60 | 5·44 | 0·243 | |
| 224·5 | 79·5 | 2·150 | 10·45 | 5·37 | 0·242 | |
| 223·5 | 78·3 | 2·130 | 10·30 | 5·25 | 0·240 | |
| 284·1 | 102·6 | 2·325 | 12·40 | 6·89 | 0·240 | 0·238 |
| 288·5 | 102·7 | 2·320 | 12·40 | 6·88 | 0·239 | |
| 290·8 | 103·9 | 2·320 | 12·40 | 6·88 | 0·237 | |
| 291·6 | 104·6 | 2·330 | 12·40 | 6·91 | 0·236 | |
| 117·9 | 47·8 | 1·950 | 7·30 | 3·40 | 0·255 | 0·253* |
| 117·7 | 48·6 | 1·955 | 7·30 | 3·40 | 0·251 | |
| 117·1 | 49·0 | 1·920 | 7·50 | 3·44 | 0·252 | |

* Repeat reading.

Digitized by Google

## Electrical Resistivity.

| Temperature °C. | Resistivity, Ohms per cm. cube. | Temperature °C. | Resistivity, Ohms per cm. cube. |
|---|---|---|---|
| 35·0 | $6{\cdot}08 \times 10^{-6}$ | 105·0 | $8{\cdot}08 \times 10^{-6}$ |
| 107·0 | 8·15 | 200·8 | 10·47 |
| 106·0 | 8·10 | 200·0 | 10·48 |
| 105·0 | 8·09 | 350·2 | 14·50 |



Digitized by Google

Digitized by Google

# THE THERMAL CONDUCTIVITIES OF METAL CRYSTALS.—I. BISMUTH

BY

G. W. C. KAYE, O.B.E., M.A., D.Sc.,
SUPERINTENDENT OF THE PHYSICS DEPARTMENT,

AND

J. KEITH ROBERTS, M.Sc., PH.D.,
SOMETIME ASSISTANT IN THE PHYSICS DEPARTMENT.

Digitized by Google

## ABSTRACT.

Previously all accurate measurements of the thermal conductivity of metals have been made on bars of heterogeneous structure. It was thought desirable to compare the values so obtained with the more fundamental ones given by single crystals.

A " plate " apparatus has been developed which makes it possible to measure thermal conductivities as high as 0·02 c.g.s. with an accuracy of about 1 per cent., using specimens 2 cms. by 1 cm. in area and about 1 or 2 mms. in thickness.

The thermal conductivities of single crystals of metallic bismuth have been determined in directions parallel and perpendicular to the trigonal axis. The values found at 18° C. were, in c.g.s. units :—

| | |
|---|---|
| Thermal conductivity of bismuth parallel to trigonal axis ... ... ... | = 0·0159 |
| Thermal conductivity of bismuth perpendicular to trigonal axis ... ... ... | = 0·0221 |
| Ratio of conductivities ... ... ... ... ... ... ... ... | = 1·39 |

If a random distribution of crystals is assumed, these figures give a mean conductivity of 0·0195, which agrees well with the value 0·0193 obtained on bars by JAEGER and DIESSELHORST in 1899.


Digitized by Google

# THE THERMAL CONDUCTIVITIES OF METAL CRYSTALS.—I. BISMUTH.

By G. W. C. KAYE, O.B.E., M.A., D.Sc., Superintendent, and J. KEITH ROBERTS, M.Sc., Ph.D., sometime Assistant, in the Physics Department.

[Reprinted from the 'Proceedings of the Royal Society', Series A, Vol. 104, 1923.]

## I. Introduction.

Interpretation of the thermal conductivities of metals yields an important test of the validity of any theory of the solid state. In applying the theory it is usually necessary to assume an ordered arrangement of the atoms on a space lattice. Now all the accurate measurements of thermal conductivity of metals have hitherto been made on bars which consist of a random arrangement of aggregations of small crystals possibly held together by inter-crystalline layers of unknown structure and indefinite extent. It seemed important to compare the results so obtained with the more fundamental values yielded from specimens consisting of a single crystal.

Experiments have been carried out in the first instance on bismuth for the reasons that (*a*) it is comparatively easy to obtain large crystals; and (*b*) it is one of the few metals which does not crystallise in the cubic system.* It was thought that any discrepancies between the results for the single crystal and those for the aggregate state would probably be more pronounced in such a case than if a cubic crystal were used.

Experiments by Lownds,† Perrot‡ and Jaeger§ have shown that the thermal conductivities of bismuth crystals in different directions differ considerably, but their work is incapable of furnishing any evidence of the kind required, since all three workers resorted to the well-known method of measuring the ratio of the axes of the elliptical figures formed by melting a low melting-point coating on the surface of the crystal. This ratio, which gives the square root of the ratio of the thermal conductivities in the two directions parallel and perpendicular to the trigonal axis, affords no information as to the absolute value of either of the conductivities.

It might be expected that the less difficult measurements of the electrical conductivity of bismuth crystals in different directions would have thrown light on the subject, but a study of the available literature reveals widely different results by different observers, who again appear to have been interested in the ratio of the two principal conductivities rather than in the absolute values. The question is at present being dealt with at the Laboratory, and we hope to publish results later. It should be mentioned that from

* Bismuth crystallises with rhombohedral symmetry. The arrangement of the atoms in the crystal has been determined by the X-ray method by James, 'Phil. Mag.', vol. 42, pp. 193–96, 1921.

† 'Ann. der Phys.', vol. 9, pp. 677–90, 1902.

‡ 'Arch. Sci. Phys.', (4), vol. 18, p. 445, 1904.

§ 'Arch. Sci. Phys.', (4), vol. 22, p. 240, 1906.

Digitized by Google

the data obtainable it would seem that the ratio of the two principal thermal conductivities of bismuth crystal is not equal to the ratio of the corresponding electrical conductivities*—a point of considerable interest.

## II. Apparatus.

### (1) *Preparation of Specimens.*

The bismuth crystals were prepared by Mr. C. H. M. Jenkins, of the Metallurgy Department, and we are indebted to him for ascertaining the technique of growing individual crystals of the requisite size. The crystals were subsequently annealed for some days. A complete analysis of the crystals revealed only 0·02 per cent. of lead, a trace of iron and no sulphur.

For the purpose of the thermal conductivity measurements, rectangular specimens with parallel faces and true edges are essential. We owe much to the manipulative skill of Mr. H. A. Jones, of the Optics Division, who successfully overcame the difficulties arising from the brittle and "awkward" mechanical characteristics of the bismuth crystals.

### (2) *Thermal Conductivity Apparatus.*

One of the "plate" types of thermal conductivity apparatus designed at the Laboratory primarily for materials of low conductivity† was modified and refined to make it suitable for use in the present case. A diagram of the apparatus is shown in Fig .1, which is self-explanatory. As will be seen, the specimen was mounted horizontally between an upper hot and a lower parallel cold plate. The hot plate consisted of a copper block mounted in an ebonite base and heated electrically by an enclosed heating grid. The cold plate was a copper block round which was soldered a spiral of copper tubing through which a stream of water flowed. When once the apparatus was correctly assembled, it permitted the easy and exact registering of the hot and cold faces. The energy conducted by the test specimen was measured both by the amount supplied to the heating grid and by the amount received by the stream of water.

The apparatus permitted the application of a definite pressure on the faces of the specimen. Experience showed that a pressure of 30 lb. per square inch was sufficient to ensure good thermal contact, and this figure was adhered to throughout the tests.

### (3) *Special Sources of Errors.*

The apparatus, as originally constructed, was designed for specimens of area about 15 square cms. and with thermal conductivities of the order of 0·001 c.g.s. or less.

* See, for example, Lownds, *loc. cit.*, p. 689.

† See N.P L. Collected Researches, vol. 19, Paper 1, p. 1, or 'Roy. Soc. Proc.', A, vol. 104, p. 71, 1923.

Digitized by Google

The largest bismuth crystals obtainable yielded specimens only about 1 cm. × 2 cms. in area, their conductivity being of the order of 0·02. The smaller area and the higher conductivity both increase greatly the difficulty in making accurate measurements·

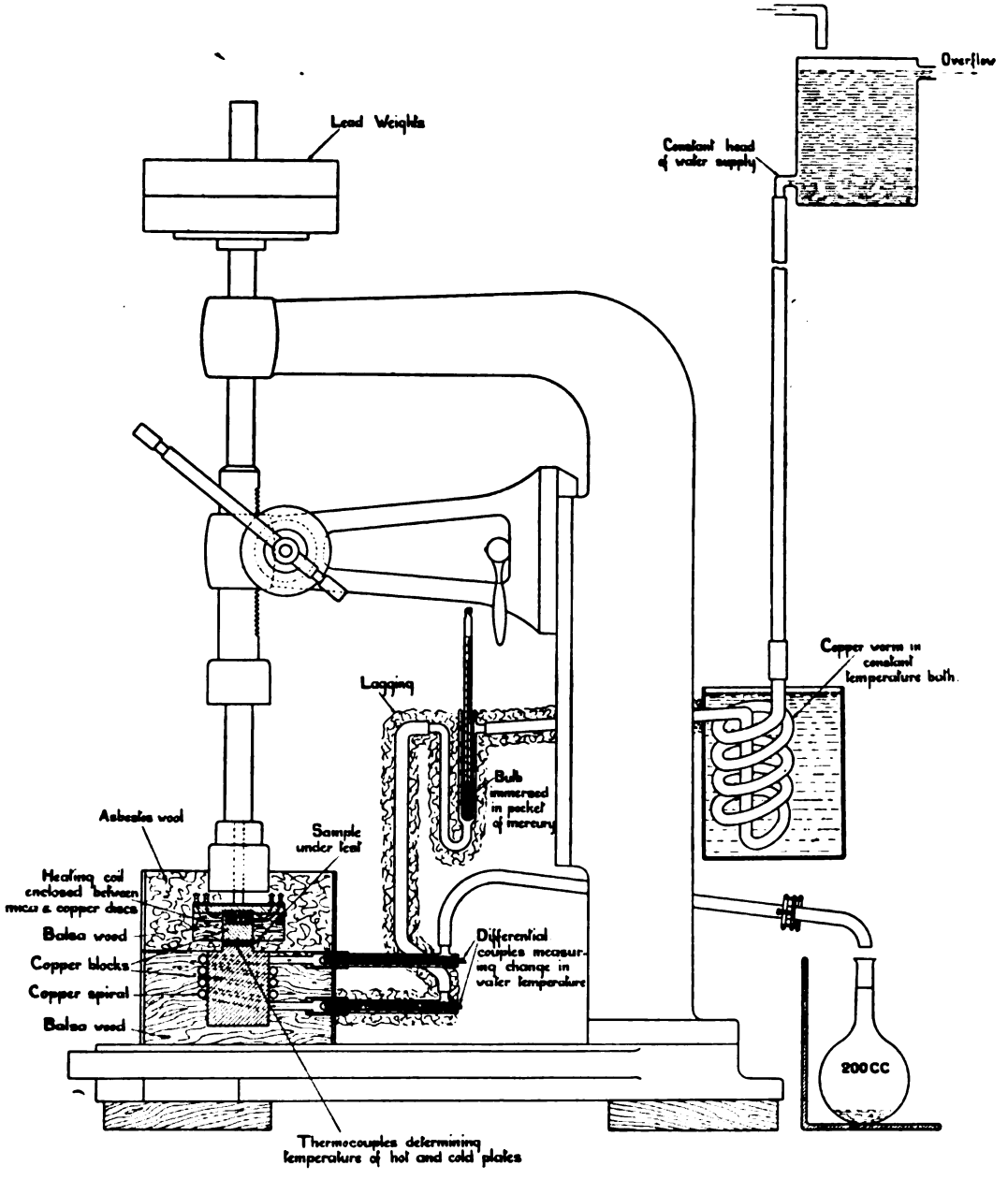


FIG. 1.—Apparatus.

The diminished area means that smaller quantities of energy can be transmitted, and that heat losses become proportionately greater; also, with reasonable rates of flow of the cooling water, the rise of temperature is smaller, and thus any variations in the temperature of the inflowing water cause proportionately greater errors.

Digitized by Google

The higher conductivity has the following effects :—

(*a*) For a given rate of transmission of energy the temperature gradient across the specimen becomes smaller. An upper limit to the power input is fixed by the dimensions of the heating grid.

(*b*) As the temperature gradient is smaller, any fluctuations in the temperature of the cold block, caused by variations in the temperature of the inflowing water, become more important.

(*c*) The temperature drops across each of the two surface films between the copper blocks and the specimen under test become proportionately larger.

(*d*) Uniformity of temperature over the surface of the hot plate becomes more difficult to ensure.

These difficulties were successfully overcome, and, as will be seen later, thermal conductivity measurements could be made with an accuracy of about 1 per cent. The average time for the apparatus to reach the steady state, so that measurements could be taken, was of the order of an hour.

### (4) *Construction of Hot Plate.*

Preliminary experiments were carried out with a hot block of uniform rectangular section of the same area as the test specimens. The heating grid, which was furnished with both potential and current leads, was of platinum wire wound on a mica strip and insulated from the copper block by pieces of mica. The grid fitted in a rectangular slot cut in the copper block and this slot was covered with a plate of copper. The resistance of the current leads was negligible compared to the resistance of the grid itself. In these preliminary experiments the thickness of copper between the heating grid and the specimen under test was only 0·05 cm. Copper-constantan thermocouples, which were pegged in the edge of the copper, indicated that differences of temperature amounting in some cases to more than one degree existed between different parts of the hot plate.

A new hot plate was therefore made, in which the heat from the grid passed through about 0·5 cm. of copper before reaching the surface of the specimen under test. The thermocouples placed near the edge of the hot plate were now found to differ by no more than 4 or 5 microvolts, so that the mean should be correct to about 1 microvolt (*i.e.* 1/40° C.). In any event, it should be noted that any slight error thus introduced in measuring this temperature is eliminated in making the correction for the temperature drop in the surface film between the hot plate and the specimen. (See p. 69.)

### (5) *Thermal Insulation of Hot Plate.*

It was feared that the substantial increase in the thickness of the new hot plate might seriously augment the loss of heat from the sides. In order to minimise this effect, the part of the hot plate projecting from the ebonite mounting was carefully encased in

Digitized by Google

balsa wood, which was arranged to be nearly flush with the lower surface. Balsa is unsurpassed as a heat insulator, and the success of the plan is shown by the fact that, in spite of the tenfold increase in the side area, the power loss at a given temperature was only increased on this score by about 20 per cent.

### (6) *Construction of Cold Plate.*

The cold plate was made of copper rod 1 inch in diameter and about $1\frac{1}{4}$ inches long, round which was soldered a copper cooling spiral. The upper surface, which made contact with the specimen under test, was milled out so that a rectangular piece of exactly the same shape as the specimens projected about 0·1 cm. above the rest of the block. The thermocouples for measuring the cold-face temperature were inserted in the sides of this projection, so that they were as near as possible to the surface of the specimen. The whole cold plate was embedded in balsa wood.

### (7) *Surfaces of Contact.*

The copper surfaces of the hot and cold plate were scraped flat to 1/10,000 of an inch, and the surfaces of the test specimens were made optically flat. In the preliminary experiments the surfaces were flooded with mercury to ensure good thermal contact between the copper and bismuth. It was found, however, that the mercury amalgamated with the bismuth and so destroyed its surface. Apparently the only course open was either to leave the surfaces dry or to use some liquid other than mercury to improve the contact. Choice was ultimately made of glycerine, the conductivity of which, while only 1/30th of that of mercury, is 10 times that of air. This proved satisfactory, as will be shown later.

### (8) *Thermostatic Control of Temperature of Inflowing Water.*

Variations in the air temperature affected the temperature of the inflowing water, and the consequent changes in the temperature of the cold block made it impossible to measure accurately the heat passing into the water. This arose from the fact that (as in all continuous-flow experiments) any change in the heat energy stored in the system affected the rate at which energy was received by the water. These temperature variations also made it impossible to attain steady temperature-distribution in the specimen under test. The inflowing water was, therefore, first passed through a copper worm immersed in a water bath with thermostatic control. The improved temperature steadiness which resulted made it possible to work with the small temperature gradients which obtained with the specimens of bismuth. Further, in spite of the small energy input, an agreement of the order of 1 per cent. was secured between the power input as measured (*a*) by the current and potential drop in the heating grid; and (*b*) by the rate of water flow and rise of temperature of the water. Before the introduction of the refined thermostatic control, the differences between the power measurements by the two methods sometimes amounted to from 7 to 10 per cent.



Digitized by Google

## III. Measurements.

### (1) *Measurement of Power.*

(*a*) ***Power supplied to the Heating Grid.***—The rate at which energy was supplied to the heating grid was determined by measuring by means of a potentiometer the potential drop across the grid itself and across a known series resistance, which latter afforded a measure of the current.

(*b*) ***Loss of Power through Mounting of Hot Block.***—All the energy supplied to the heating grid did not pass through the specimen, but some of it was unavoidably lost through the ebonite and balsa-wood mounting of the hot plate. This loss was determined by making preliminary measurements on a sample of balsa wood of known thickness and conductivity (0·00011 c.g.s.) and of the same area as the test specimens. The total energy supplied to the heating grid was measured in the usual way. The small amount conducted through the sample of balsa wood could be calculated, and the remainder was therefore lost through the mounting of the hot block. The amount so lost was plotted against the difference between the temperatures of the hot plate and the air (Table I; Fig. 2).

Table I.—Power Loss from Hot Plate through Mounting.

| Thickness of balsa wood. | Air temperature. | Hot-plate temperature. | Cold-plate temperature. | Difference between hot- and cold-plate temperatures. | Power conducted through balsa (calculated) ($h_1$). | Power supplied to heating grid ($h_2$). | Power loss from hot plate ($h_2 - h_1$). | Difference between hot-plate temperature and air temperatures. |
|---|---|---|---|---|---|---|---|---|
| Cm. | °C. | ° C. | ° C. | ° C. | Watt. | Watt. | Watt. | ° C. |
| 0·203 | 16·00 | 35·75 | 17·60 | 18·15 | 0·09 | 0·44 | 0·35 | 19·75 |
| 0·203 | 15·70 | 42·90 | 17·65 | 25·25 | 0·13 | 0·66 | 0·53 | 27·20 |
| 0·203 | 15·75 | 64·40 | 17·70 | 46·70 | 0·23 | 1·23 | 1·00 | 48·65 |
| 0·122 | 14·85 | 33·20 | 17·55 | 15·65 | 0·13 | 0·50 | 0·37 | 18·35 |
| 0·122 | 15·15 | 33·85 | 17·55 | 16·35 | 0·14 | 0·50 | 0·36 | 18·70 |
| 0·122 | 15·90 | 62·30 | 18·10 | 44·20 | 0·37 | 1·37 | 1·00 | 46·40 |

The test was carried out with two different thicknesses of balsa wood, the results of which were concordant. In the subsequent measurements on bismuth the corrections for power leakage on this score were obtained from Fig. 2. It should be noted that only the portion of the graph lying between 0° and 10° temperature-excess was actually used in this way, though the observations at higher points were useful in plotting the graph.

(*c*) *Measurement of Power received by Water.*—The heat received by the water was obtained by measuring the rate of flow of the water and the rise of temperature. The

Digitized by Google

latter was measured differentially by six copper-constantan thermocouples in series, arranged so that the inflowing water was circulated round a glass pocket containing the

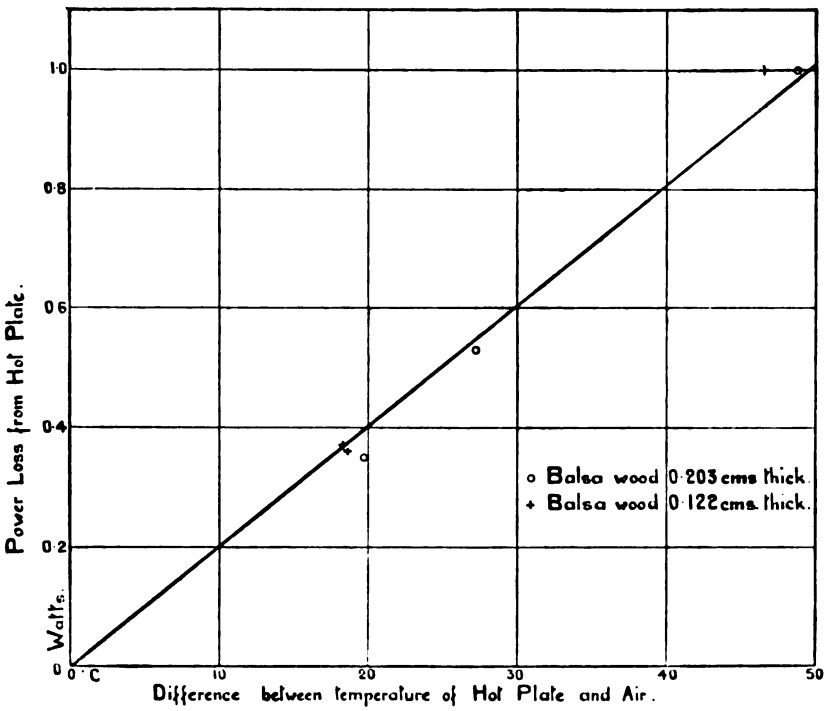


Fig. 2. Power Loss from Hot Plate.

cold junctions and the outflowing water round a similar pocket containing the hot junctions. The actual value of the temperature of the inflowing water was measured on a mercury in glass thermometer.

The heat losses from the water system take place (*a*) from the water tubing between the thermocouples and the cold block, and (*b*) from the cold block itself. For the purpose of determining these heat losses a specimen of balsa wood was inserted between the "hot" and "cold" plates. No current was passed through the heating grid, but the arrangements permitted the temperature measurement of both plates as usual. The heat loss from the tubing was separately determined by "short-circuiting" the spiral round the cold block by a short length of rubber tubing and passing warm water through the system. The temperature drop of the water was measured on the differential thermocouples, and the corresponding heat loss was plotted against difference between mean water temperature and air temperature (Table II; Fig. 3).

The spiral round the cold block was then reconnected to the water system and the heat-loss determined once again with warm water flowing. The difference between the two heat losses when corrected for the loss by conduction through the specimen of balsa wood represents the heat loss from the cold block itself. This latter was plotted against the difference between the temperatures of the block and the air (Table III; Fig. 4).



Digitized by Google

TABLE II.—Power Loss from Tubing between Cold Block and Thermocouples.

| Difference between mean water temperature and air temperature. | Loss of power. |
|---|---|
| ° C. | Watt. |
| 0·80 | 0·04 |
| 1·20 | 0·05 |
| 1·65 | 0·05 |
| 2·20 | 0·06 |
| 2·95 | 0·08 |
| 3·70 | 0·11 |
| 5·30 | 0·24 |
| 6·00 | 0·28 |
| 7·05 | 0·28 |

TABLE III.—Power Loss from Cold Block.

| Temperature differences between cold block and air. | Total power loss from cold block and tubing. | Power loss from tubing (Fig. 3). | Power loss from cold block. |
|---|---|---|---|
| ° C. | Watt. | Watt. | Watt. |
| 1·05 | 0·06 | 0·04 | 0·02 |
| 1·30 | 0·07 | 0·05 | 0·02 |
| 1·70 | 0·10 | 0·06 | 0·04 |
| 3·0 | 0·16 | 0·12 | 0·04 |
| 3·75 | 0·24 | 0·13 | 0·11 |
| 4·10 | 0·27 | 0·14 | 0·13 |
| 6·00 | 0·39 | 0·19 | 0·20 |
| 6·4 | 0·41 | 0·24 | 0·17 |
| 7·2 | 0·48 | 0·24 | 0·24 |

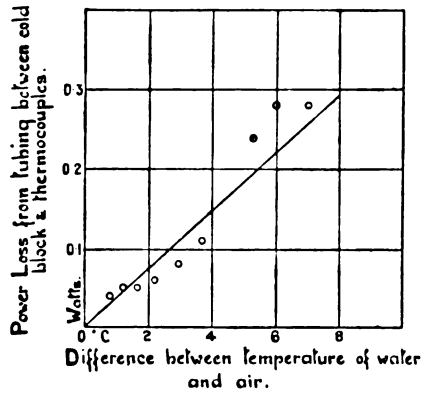


Fig. 3. Power Loss from tubing between cold Block & Thermocouples.

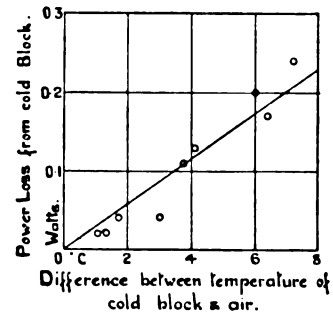


Fig. 4. Power Loss from cold Block.

This temperature difference was measured by a thermocouple with one junction mounted on the side of the cold block and the other just outside the balsa-wood mounting of the cold block.

Digitized by Google

In Figs. 3 and 4 only the parts of the graphs between 0° and 1·5° temperature-excess were actually used; the upper points served, however, to indicate more accurately the true slope of the straight line. The agreement obtained between the power transmitted through the specimen as measured (*a*) by that supplied to the heating grid, and (*b*) by that absorbed by the water, is shown in the last column of Table IV (see p. 70). The mean difference is 1·3 per cent.

(2) *Measurement of Temperature Difference between Hot and Cold Surfaces of Bismuth.*

As already stated, the temperatures of the hot and cold plates were measured by thermo-couples pegged in the blocks as near to the surfaces of the plates as possible. The temperatures so measured had to be corrected for (*a*) the temperature drop through the glycerine film at each of the bounding surfaces between the copper and bismuth, and (*b*) any temperature drop in the copper blocks between the couples and the surfaces. The combined correction was determined by placing between the surfaces of the hot and cold blocks a thin piece of copper of thickness 0·005 cm. and using glycerine to make contact. The temperature difference between the hot and cold plates now gave the drop through the two glycerine films above, as the temperature drop through the thin copper was negligible —being equal to 0·0013° C. for a total drop of 0·35° C., *i.e.* only 1 in 300 of the drop through the films. The results are given in Table V. In Fig. 5 the temperature drop in the films is plotted against power transmitted.

TABLE V.—Temperature Drop in Glycerine Film.

| Hot-plate temperature. | Cold-plate temperature. | Air temperature. | Difference between hot-plate and air temperatures. | Power loss through hot-plate mounting (Fig. 2) ($h_1$). | Total power supplied to heating grid ($h_2$). | Power transmitted through glycerine films ($h_2 - h_1$). | Difference between hot-plate and cold-plate temperatures. |
|---|---|---|---|---|---|---|---|
| ° C. | ° C. | ° C. | ° C. | Watts. | Watts. | Watts. | ° C. |
| 18·00 | 17·65 | 16·70 | 1·30 | 0·03 | 1·87 | 1·84 | 0·35 |
| *18·85 | 18·40 | 16·85 | 2·00 | 0·04 | 2·29 | 2·25 | 0·45 |
| 19·20 | 18·62 | 17·20 | 2·00 | 0·04 | 3·04 | 3·00 | 0·58 |

* This point was determined after the copper specimen had been removed and replaced, the glycerine films being renewed at the same time.

(3) *Measurement of Thickness and Area of Specimens.*

The thickness and area of the specimens were measured with an ordinary micrometer gauge.

## IV. RESULTS.

The results obtained for the conductivity parallel and perpendicular to the trigonal axis are given in Tables VI and VII respectively. In each case the results are arranged so that each group corresponds to one setting of the specimen. The mean values for

Digitized by Google

TABLE IV.—Comparison of Energy supplied by Heating Coil with that absorbed by Water.

| Experiment. | Temperature Measurements. | | | | Power Losses. | | | | | Power Measurements. | | | | |
|---|---|---|---|---|---|---|---|---|---|---|---|---|---|---|
| | Temperature rise in water. | Inlet temperature. | Mean water temperature. | Air temperature. | Difference between mean water temperature and air temperature. | Power loss from tubing (Fig. 3). | Difference between temperature of cold block and air temperature. | Power loss from cold block (Fig. 4). | Total power loss from cold block and tubing. | Rate of flow of water. | Measured power absorbed by water. | Corrected power reaching cold block. | Corrected power leaving hot block. | Percentage difference between $P_w$ and $P_c$. |
| | $\delta\theta$ | — | — | — | — | $L_1$ | — | $L_2$ | $L_1 + L_2$ | $w$ | $w.\delta\theta.J.$ | $P_w$ | $P_c$ | — |
| | ° C. | ° C. | ° C. | ° C. | ° C. | Watts. | ° C. | Watts. | Watts. | cc./sec. | Watts. | Watts. | Watts. | Per cent. |
| Glycerine film correction (Table V). | 0·322 | 17·00 | 17·2 | 16·7 | 0·5 | 0·02 | 0·8 | 0·02 | 0·04 | 1·300 | 1·75 | 1·79 | 1·84 | +2·8 |
| | 0·333 | 17·00 | 17·2 | 16·9 | 0·3 | 0·01 | 0·7 | 0·02 | 0·03 | 1·290 | 1·80 | 1·83 | 1·84 | +0·5 |
| | 0·561 | 17·55 | 17·8 | 17·2 | 0·6 | 0·02 | 0·9 | 0·03 | 0·05 | 1·245 | 2·93 | 2·98 | 3·00 | +0·7 |
| | 0·397 | 17·55 | 17·7 | 16·9 | 0·8 | 0·03 | 1·3 | 0·04 | 0·07 | 1·320 | 2·19 | 2·26 | 2·25 | −0·5 |
| Conductivity of bismuth parallel to trigonal axis (Table VI). | 0·341 | 17·75 | 17·9 | 17·8 | 0·1 | 0·01 | 0·5 | 0·02 | 0·03 | 1·215 | 1·73 | 1·76 | 1·78 | +1·1 |
| | 0·343 | 18·25 | 18·4 | 17·8 | 0·6 | 0·02 | 0·6 | 0·02 | 0·04 | 1·205 | 1·73 | 1·77 | 1·76 | −0·6 |
| | 0·558 | 18·35 | 18·6 | 17·3 | 1·3 | 0·05 | 1·4 | 0·04 | 0·09 | 1·190 | 2·79 | 2·88 | 2·87 | −0·3 |
| | 0·574 | 17·40 | 17·7 | 16·9 | 0·8 | 0·03 | 1·1 | 0·03 | 0·06 | 1·190 | 2·87 | 2·93 | 2·88 | −1·7 |
| | 0·580 | 16·10 | 16·4 | 16·1 | 0·3 | 0·01 | 0·6 | 0·02 | 0·03 | 1·200 | 2·91 | 2·94 | 2·88 | −2·1 |
| | 0·410 | 14·90 | 15·1 | 14·9 | 0·2 | 0·01 | 0·3 | 0·01 | 0·02 | 1·340 | 2·30 | 2·32 | 2·40 | +3·3 |
| | 0·410 | 14·90 | 15·1 | 14·8 | 0·3 | 0·01 | 0·4 | 0·01 | 0·02 | 1·350 | 2·31 | 2·33 | 2·39 | +2·5 |
| | 0·408 | 14·85 | 15·1 | 14·7 | 0·4 | 0·01 | 0·4 | 0·01 | 0·02 | 1·350 | 2·31 | 2·33 | 2·38 | +2·1 |
| | 0·504 | 15·55 | 15·8 | 15·3 | 0·5 | 0·02 | 0·5 | 0·02 | 0·04 | 1·395 | 2·94 | 2·98 | 3·01 | +1·0 |
| | 0·502 | 15·50 | 15·8 | 15·6 | 0·2 | 0·01 | 0·6 | 0·02 | 0·03 | 1·400 | 2·94 | 2·97 | 3·00 | +1·0 |
| | 0·363 | 15·50 | 15·7 | 15·7 | 0·0 | 0·00 | 0·2 | 0·01 | 0·01 | 1·415 | 2·15 | 2·16 | 2·17 | +0·5 |
| | 0·360 | 15·55 | 15·7 | 15·6 | 0·1 | 0·01 | 0·2 | 0·01 | 0·02 | 1·430 | 2·16 | 2·18 | 2·17 | −0·5 |
| Conductivity of bismuth perpendicular to trigonal axis (Table VII). | 0·340 | 15·80 | 16·0 | 15·2 | 0·8 | 0·03 | 1·1 | 0·03 | 0·06 | 1·240 | 1·77 | 1·83 | 1·78 | −2·8 |
| | 0·340 | 15·90 | 16·1 | 15·6 | 0·5 | 0·02 | 0·8 | 0·02 | 0·04 | 1·235 | 1·76 | 1·80 | 1·79 | −0·5 |
| | 0·570 | 15·90 | 16·2 | 15·9 | 0·3 | 0·01 | 0·8 | 0·02 | 0·03 | 1·215 | 2·90 | 2·93 | 2·93 | 0·0 |
| | 0·571 | 16·30 | 16·6 | 15·8 | 0·8 | 0·03 | 0·5 | 0·01 | 0·04 | 1·210 | 2·89 | 2·93 | 2·91 | −0·7 |
| | 0·581 | 16·05 | 16·4 | 16·6 | −0·2 | −0·01 | 0·3 | 0·01 | 0·00 | 1·185 | 2·88 | 2·88 | 2·93 | +1·7 |
| | 0·472 | 14·35 | 14·6 | 14·1 | 0·5 | 0·02 | 0·6 | 0·02 | 0·04 | 1·505 | 2·97 | 3·01 | 3·04 | +1·0 |
| | 0·472 | 15·05 | 15·3 | 15·0 | 0·3 | 0·01 | 0·6 | 0·02 | 0·03 | 1·500 | 2·96 | 2·99 | 3·04 | +1·7 |
| | 0·507 | 14·75 | 15·0 | 15·1 | −0·1 | −0·01 | 0·7 | 0·02 | 0·01 | 1·400 | 2·97 | 2·98 | 3·04 | +2·0 |
| | 0·510 | 14·80 | 15·1 | 15·1 | 0·0 | 0·00 | 0·7 | 0·02 | 0·02 | 1·400 | 2·99 | 3·01 | 3·04 | +1·0 |

Digitized by Google

each group are given in the last column but one. They appear to indicate that small variations may arise, probably due to slightly different thicknesses of the glycerine films. The differences are more pronounced in the case of the thin specimens, as would be expected on this explanation. It should be added, however, that varying the pressure

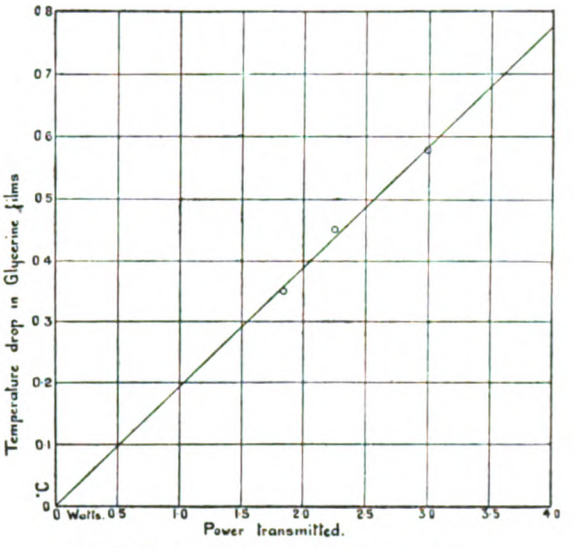


Fig. 5. Temperature drop in Glycerine Film.

from 30 to 60 lb. per square inch produced no sensible alteration of the results. The numbers in the last column but two indicate that for a given setting of the specimen the result does not depend on the power transmitted, while those in the last column indicate that the result does not depend on the thickness of the specimen.

The following are the mean values at 18° C. :—

| | | |
|---|---|---|
| Thermal conductivity of bismuth parallel to trigonal axis .. | = 0·0159 | c.g.s. |
| Thermal conductivity of bismuth perpendicular to trigonal axis .. | = 0·0221 | ,, |
| Ratio of conductivities .. .. .. .. .. .. | = 1·39 | |

The ratio 1·39 may be compared with that found by other experimenters using the method of measuring the ratio of the axes of the elliptical figure formed by melting a low melting-point coating on the surface of a bismuth crystal. Their values were :—

| | |
|---|---|
| Lownds* .. .. .. .. .. .. .. | 1·42 |
| Perrot† .. .. .. .. .. .. .. | 1·37 |
| Jaeger‡ .. .. .. .. .. .. .. | 1·49 |

The thermal conductivity of a rod of ordinary bismuth had been determined by Jaeger

* Lownds, *loc. cit.*
† Perrot, *loc. cit.*
‡ Jaeger, *loc. cit.*

Digitized by Google

TABLE VI.—Thermal Conductivity of Bismuth Parallel to Trigonal Axis.
Area of Specimen 1·023 × 1·842 sq. cms. = 1·88 sq. cms.

| Thickness of specimen of bismuth. | Temperature Drop. | | | | | Power Conducted. | | | | | Conductivity. | | | |
|---|---|---|---|---|---|---|---|---|---|---|---|---|---|---|
| | Hot-plate temperature. | Cold-plate temperature. | Difference between hot- and cold-plate temperatures. | Temperature drop in glycerine films. | Temperature drop in specimen. | Air temperature. | Difference between hot-plate and air temperatures. | Loss of power through mounting of hot block. | Power supplied to heating grid. | Power conducted through specimen. | Conductivity. | Mean conductivity for given power. | Mean conductivity of group. | Mean conductivity of thick and thin specimens respectively. |
| Cm. | ° C. | ° C. | ° C. | ° C. | ° C. | ° C. | ° C. | Watts. | Watts. | Watts. | C.g.s. | C.g.s. | C.g.s. | C.g.s. |
| 0·168 ... ... | 21·32 | 18·58 | 2·74 | 0·34 | 2·40 | 17·8 | 3·5 | 0·07 | 1·85 | 1·78 | 0·0158 | $0·0156_5$ | 0·0157 | $0·0158_5$ |
| | 21·55 | 18·78 | 2·77 | 0·34 | 2·43 | 17·8 | 3·7 | 0·07 | 1·83 | 1·76 | 0·0155 | | | |
| | 23·85 | 19·38 | 4·47 | 0·56 | 3·91 | 17·3 | 6·5 | 0·13 | 3·00 | 2·87 | 0·0157 | 0·0158 | | |
| | 23·08 | 18·65 | 4·43 | 0·56 | 3·87 | 16·9 | 6·2 | 0·13 | 3·01 | 2·88 | 0·0159 | | | |
| | 21·64 | 17·25 | 4·39 | 0·56 | 3·83 | 16·1 | 5·5 | 0·11 | 2·99 | 2·88 | 0·0160 | | 0·0160 | |
| 0·091 ... ... | 18·03 | 15·79 | 2·24 | 0·47 | 1·77 | 14·9 | 3·1 | 0·06 | 2·46 | 2·40 | 0·0158 | | 0·0156 | $0·0159_7$ |
| | 18·00 | 15·74 | 2·26 | 0·47 | 1·79 | 14·8 | 3·2 | 0·07 | 2·46 | 2·39 | 0·0155 | | | |
| | 17·98 | 15·76 | 2·22 | 0·46 | 1·76 | 14·7 | 3·3 | 0·07 | 2·45 | 2·38 | 0·0156 | | | |
| | 19·35 | 16·65 | 2·70 | 0·58 | 2·12 | 15·3 | 4·0 | 0·08 | 3·09 | 3·01 | 0·0164 | | | |
| | 19·35 | 16·65 | 2·70 | 0·58 | 2·12 | 15·6 | 3·8 | 0·08 | 3·08 | 3·00 | 0·0164 | 0·0164 | $0·0163_5$ | |
| | 18·28 | 16·32 | 1·96 | 0·42 | 1·54 | 15·8 | 2·4 | 0·05 | 2·22 | 2·17 | 0·0163 | | | |
| | 18·30 | 16·34 | 1·96 | 0·42 | 1·54 | 15·6 | 2·7 | 0·05 | 2·22 | 2·17 | 0·0163 | 0·0163 | | |

Digitized by Google

TABLE VII.—Thermal Conductivity of Bismuth Perpendicular to Trigonal Axis.
Area of Specimen 1·022 × 1·843 = 1·88 sq. cms.

| Thickness of specimen of bismuth. | Temperature Drop. | | | | | Power Conducted. | | | | | Conductivity. | | | |
|---|---|---|---|---|---|---|---|---|---|---|---|---|---|---|
| | Hot-plate temperature. | Cold-plate temperature. | Difference between hot- and cold-plate temperatures. | Temperature drop in glycerine films. | Temperature drop in specimen. | Air temperature. | Difference between hot-plate and air temperatures. | Loss of power through mounting of hot block. | Power supplied to heating grid. | Power conducted through specimen. | Conductivity. | Mean conductivity for given power. | Mean conductivity of group. | Mean conductivity of thick and thin specimens respectively. |
| Cm. | ° C. | ° C. | ° C. | ° C. | ° C. | ° C. | ° C. | Watts. | Watts. | Watts. | C.g.s. | C.g.s. | C.g.s. | C.g.s. |
| 0·167 ... ... | 18·60 | 16·55 | 2·05 | 0·34 | 1·71 | 15·2 | 3·4 | 0·07 | 1·85 | 1·78 | 0·0221 | 0·0221 | $0·0222_5$ | 0·0222 |
| | 18·47 | 16·40 | 2·07 | 0·35 | 1·72 | 15·6 | 2·9 | 0·06 | 1·85 | 1·79 | 0·0221 | | | |
| | 20·32 | 16·98 | 3·34 | 0·57 | 2·77 | 15·9 | 4·4 | 0·09 | 3·02 | 2·93 | 0·0225 | 0·0224 | | |
| | 20·42 | 17·08 | 3·34 | 0·57 | 2·77 | 15·8 | 4·6 | 0·09 | 3·00 | 2·91 | 0·0223 | | | |
| | 20·62 | 17·23 | 3·39 | 0·57 | 2·82 | 16·6 | 4·0 | 0·08 | 3·01 | 2·93 | 0·0221 | | 0·0221 | |
| 0·0896... ... | 17·55 | 15·38 | 2·17 | 0·59 | 1·58 | 14·1 | 3·5 | 0·07 | 3·11 | 3·04 | 0·0220 | | $0·0218_5$ | 0·0220 |
| | 18·30 | 16·11 | 2·19 | 0·59 | 1·60 | 15·0 | 3·3 | 0·07 | 3·11 | 3·04 | 0·0217 | | | |
| | 18·31 | 16·16 | 2·15 | 0·59 | 1·56 | 15·1 | 3·2 | 0·07 | 3·11 | 3·04 | 0·0222 | | 0·0222 | |
| | 18·31 | 16·16 | 2·15 | 0·59 | 1·56 | 15·1 | 3·2 | 0·07 | 3·11 | 3·04 | 0·0222 | | | |

(a 34–2879)z

Digitized by Google

and DIESSELHORST,* who obtained the value of 0·0193 c.g.s. units at 18° C. This may be compared with the values obtained in the present work by calculating the mean resistance, remembering that resistances and not conductivities are additive, and that the value at right angles to the axis of symmetry must be given double the weight. Thus, if $k$ is the " mean " conductivity,

$$\frac{1}{k} = \frac{1}{3}\left(\frac{1}{0\cdot0159} + \frac{2}{0\cdot0221}\right),$$

therefore

$$k = 0\cdot0195.$$

The agreement of this figure with that of JAEGER and DIESSELHORST indicates that in the case of bismuth metal in the aggregate, the distribution of the constituent small crystals is random, and that the effect on the thermal conductivity of such inter-crystalline layers as may be present is not appreciable. It is hoped to carry out experiments on other metal crystals to see whether this result is generally true.†

* ' Sitzung. der. Kön. Preuss. Akad.', pp. 719–26, 1899.

† We are much indebted to Mr. D. E. A. JONES, for his unremitting and careful assistance in the above work.

Digitized by Google

# THE THERMAL EXPANSION OF CRYSTALS OF METALLIC BISMUTH

BY

J. KEITH ROBERTS, M.Sc., Ph.D.,
SOMETIME ASSISTANT IN THE PHYSICS DEPARTMENT.

Digitized by Google

## ABSTRACT.

An account is given of measurements of the thermal expansion of crystals of metallic bismuth parallel and perpendicular to the vertical axis by comparison with that of crystalline quartz. Both expansion coefficients are practically constant from ordinary temperatures up to 240° C. Bismuth melts at about 270° C.

The constant expansion coefficients over this range are :—

| | |
|---|---|
| Perpendicular to the axis ... ... ... ... ... ... ... | $12{\cdot}0 \times 10^{-6}$ |
| Parallel to the axis ... ... ... ... ... ... ... ... | $16{\cdot}2 \times 10^{-6}$ |
| Mean ... ... ... ... ... ... ... ... ... ... | $13{\cdot}4 \times 10^{-6}$ |

The results are compared with those of GRÜNEISEN and GOENS on zinc and cadmium crystals. At present Bi, Zn, and Cd are the only metallic crystals not crystallising in the regular system which have been studied.

The bending over of the length—temperature curve as the melting-point is approached indicates dissociation of the atoms in the solid. The nature of this dissociation and the general properties of solids near their melting-points are discussed.


Digitized by Google

# THE THERMAL EXPANSION OF CRYSTALS OF METALLIC BISMUTH.

By J. KEITH ROBERTS, M.Sc., Ph.D., sometime Assistant in the Physics Department.

[Reprinted from the 'Proceedings of the Royal Society', Series A, Vol. 106, 1924.]

## Introduction.

A theory of the thermal expansion of regularly crystallising monatomic solid bodies was first proposed by Grüneisen.* An important experimental fact for which this theory accounts is the constancy of the ratio of the coefficient of expansion to the specific heat with varying temperature. There is no theory of the thermal expansion of non-regularly crystallising bodies, and when the present work was started there were no data available as to the temperature variation of the coefficients of expansion of such bodies; it was carried out to supply such data for bismuth crystals and especially to study the behaviour of the crystals near the melting point. Recently Grüneisen and Goens† have given some results which they have obtained for zinc and cadmium crystals, with which the present results are compared.

## Apparatus and Measurements.

### *General Arrangement.*

As only comparatively small crystals of metallic bismuth were available, it was necessary to use an optical method to measure the expansions. I am indebted to Mr. J. Guild, of the Optics Department, for pointing out the advantages of an optical lever method‡ over an interference method for measurements of this kind, and for his advice in the choice of lenses and on the general arrangement of the optical system.

Crystalline quartz was taken as the standard of comparison—the expansion of bismuth relative to it being measured.

The experimental arrangement is shown in Fig. 1. The bismuth and quartz specimens,§ which were the same size and were optically flat, were placed side by side on the surface of the stainless steel block S which was about 3 cms. in diameter. The steel base to which the stainless steel block was screwed was carried by three $\frac{1}{4}$-inch steel rods (only one of which is indicated), as shown in the diagram.

* 'Ann. der Phys.', vol. 39, p. 257, 1912.

† 'Phys. Zeits.', vol. 24, p. 506, 1923.

‡ 'J. Scientific Instruments', vol. 1, p. 198, 1924.

§ The bismuth crystals were kindly made by Mr. C. H. M. Jenkins, of the Metallurgy Department, by the slow cooling of liquid bismuth. The specimens were cut and polished by Mr. H. A. Jones, of the Optics Workshop.

Digitized by Google

A glass plate P, which was slightly wedge-shaped, rested on three $\frac{3}{32}$-inch steel spheres, which were firmly set in a phosphor-bronze plate. The spheres rested on pieces of thin microscope cover-glass placed on the top of the specimens. These prevented the spheres from pressing into the bismuth at the higher temperatures.

The different expansions of the bismuth and quartz specimens caused the angle between

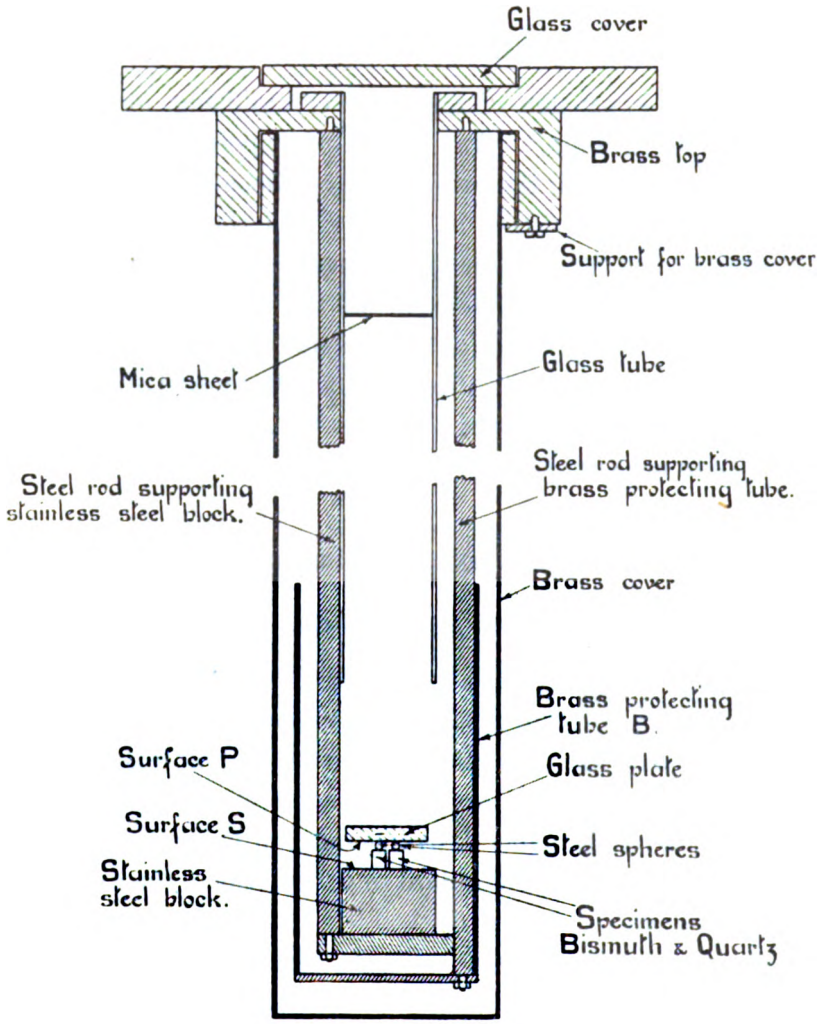


Fig. 1. Apparatus.

the lower surface of P and the surface of S to vary with temperature. This variation was determined by measuring the angle between the reflections of a parallel beam of light from these surfaces. Any effect due to the unequal expansion of the supports was eliminated as it affected both surfaces equally.

A cylindrical brass tube, 7 cms. in diameter and 50 cms. long, closed at the bottom, served as container. This tube was carried on supports attached to the brass top and

Digitized by Google

could be easily removed. A nichrome heating coil was wound over the whole length of the tube and was insulated from it by a sheet of micanite. The whole was lagged with asbestos string. The top of the apparatus was closed by a glass plate.

*Elimination of Convection Currents.*

Convection currents were for some time a serious source of trouble, making the definition so bad that it was not possible to take measurements. They were finally eliminated by the introduction of a small brass tube B, surrounding the specimens, and a glass tube down which the light passed to the reflecting surfaces. As a further precaution, the latter was closed by a thin sheet of mica.

The brass tube B was carried on three steel rods and was closed at the base by resting on a brass plate. It was made to slide up and down, so that it could be removed while the specimens were being adjusted. The specimens themselves were protected from convection currents by this brass tube and by the glass plate P.

*Optical System.*

A ' pointolite ' lamp was used as the source of light. It illuminated a scale consisting of fine lines 5 mms. apart ruled on the surface of a platinised glass plate (see Fig. 2). The

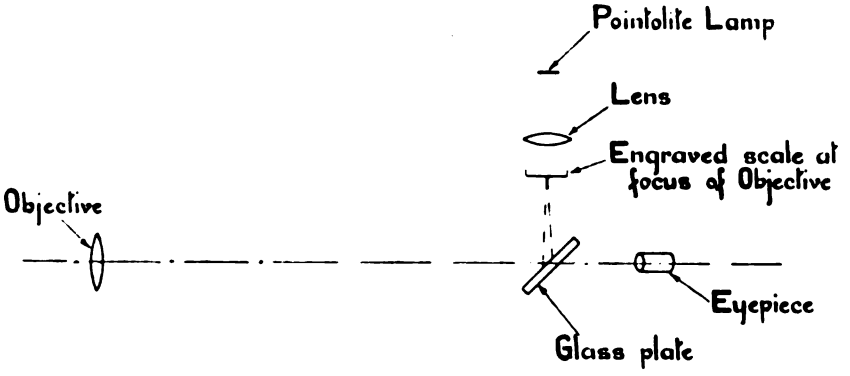


Fig. 2. Plan of Optical System.

light from the scale was reflected through 90 degrees at the surface of a piece of plane glass. The scale was placed at the focus of a telescope objective, which rendered the beam of light parallel before it was reflected by a totally reflecting prism into the apparatus.

On its return it was observed with a micrometer eyepiece.

A short-focus lens was placed between the pointolite lamp and the scale in order to focus an image of the lamp on the surfaces P and S (Fig. 1). This increased the intensity of light and enabled the whole aperture of P and S to be used.*

* See GUILD, *loc. cit.*

Digitized by Google

*Determination of Magnification.*

Let $f$ be the perpendicular distance between the centre of one of the spheres supporting the glass plate P (Fig. 1) and the line joining the centres of the other two, and let $f$ be parallel to the axis of the optical system;

F be the distance of the engraved scale from the object glass;

$e$ be the movement of the light reflected from P (relative to the light reflected from the base S), as measured on the scale in the eyepiece;

E be the distance between the images on the eyepiece scale of two lines 1 cm. apart on the engraved glass scale;

$l_1$ be the change in length of the quartz specimen for a given change in temperature;

$l_2$ be the change in length of the bismuth specimen for the same change in temperature.

$$\frac{l_1 - l_2}{f} = \frac{e}{2\mathrm{E} \cdot \mathrm{F}} \quad i.e., \quad l_1 - l_2 = \frac{ef}{2\mathrm{E} \cdot \mathrm{F}} .$$

F, E, and $f$ had the values

F = 112 cms. E = 6·40 divisions.

$f$ = 0·494 cm. (in some of the experiments $f$ = 0·245 cm., which doubled the sensitivity).

$e$ could be estimated to 0·01 division.

Inserting these in the formula, we see that a relative change of length of

$$l_1 - l_2 = \frac{0{\cdot}01 \times 0{\cdot}494}{2 \times 6{\cdot}40 \times 112} = 3{\cdot}4 \times 10^{-6} \text{ cm.},$$

or considerably less than one-tenth of a wave-length of green light ($\lambda = 5{\cdot}4 \times 10^{-5}$ cm.) could be measured. The expansion of a specimen of bismuth 1 cm. long perpendicular to the axis of the crystal over a range of 30° is $12{\cdot}0 \times 10^{-6} \times 30$ cm., *i.e.* $360 \times 10^{-6}$ cm. Since this can be measured correct to $3{\cdot}4 \times 10^{-6}$ cm., the error using 30° ranges is about 1 per cent.

The value of $f$ was determined in the Metrology Department by placing the phosphor-bronze plate and spheres on a flat steel plate of known thickness and measuring the distance from the lower side of this plate to the top of a cylinder of known diameter which rested between and was supported by spheres. The values of $f$ for the two plates used were 0·494 cm. and $0{\cdot}245_2$ cm. In the case of the latter plate the value was checked by a projection method which gave $0{\cdot}245_6$ cm. These values are correct to about one part in five hundred.

*Temperature Control.*

One junction of a copper-constantan thermocouple, insulated by two strips of mica, was fixed against the outer brass cover at a point about 8 cms. from the bottom. The

Digitized by Google

other junction was in ice and the E.M.F. developed was read on a Weston millivoltmeter. The current through the heating coil was adjusted by hand and the reading of this thermocouple could be held steady to one-tenth of a division (or 10 microvolts), which corresponds to one-quarter of a degree. Any fluctuations in the temperature of the outer case of this order did not have an appreciable effect on the temperature of the specimens.

*Temperature Measurement.**

The temperature of the specimens was measured by a silver-soldered copper-constantan thermocouple held against the block S by a brass clip. It was insulated from S and from the clip by thin strips of mica. The leads were passed up through two glass tubes and then through two holes in the glass cover of the apparatus. The E.M.F. developed was measured on a low-range potentiometer, calibrated by comparison with one of the standard instruments at the Laboratory.

The couple was made from a batch of wire which has been tested over a wide range, and for which calibration curves have been drawn up. The calibration was checked at the steam point before the couple was placed in position and found correct to within a few microvolts. As a further check, the melting-point of bismuth was determined in the apparatus itself by watching the collapse of a specimen which was very slowly heated. Using the calibration curve, the temperature of melting was 272·3°C. BRIDGMAN† gives 271·0° C. as the melting-point. The correction to the calibration curve, therefore, amounts to only 1 part in 200 at this point, and it has been neglected, as the accuracy of measurement of length-changes was not greater than 1 per cent.

Readings were not taken until the temperature had been steady for about ten minutes.

*Test of Apparatus.*

The apparatus was tested and found to be working satisfactorily over the whole range of temperatures by comparing the expansions of two pieces of crystalline quartz, one cut parallel and the other perpendicular to the axis. The results are shown in Fig. 3, in

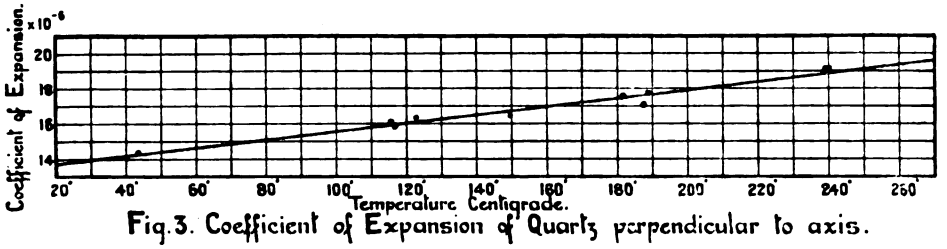


Fig. 3. Coefficient of Expansion of Quartz perpendicular to axis.

which the straight line represents the known variation of the expansion coefficient perpendicular to the axis with temperature, and the points represent the observed values, taking the value parallel to the axis as known. It will be seen that the observed points follow the line satisfactorily.

* Mr. B. J. GIBBS, of the Observer Staff has given valuable assistance by controlling the temperature in many of the experiments.

† 'Phys. Rev.', vol. 6, p. 29, 1915.



Digitized by Google

*Value of Coefficient of Expansion of Quartz.*

The expansion of quartz can be expressed by the formula

$$l_t = l_0 (1 + at + bt^2)$$

where

$l_t$ = length at temperature $t$, $l_0$ = length at 0° C., and $a$ and $b$ are constants.

We have, therefore, at temperatures $t_1$ and $t_2$

$$l_{t_1} = l_0 (1 + at_1 + bt_1^2)$$

$$l_{t_2} = l_0 (1 + at_2 + bt_2^2).$$

Mean coefficient of expansion over this range, or coefficient of expansion at temperature $t = \frac{1}{2}(t_1 + t_2)$,

$$= \frac{l_{t_2} - l_{t_1}}{l_0 (t_2 - t_1)} = a + b (t_1 + t_2) = a + b \cdot 2t.$$

The values obtained by different observers for $a$ and $b$ are given in the following tables :—

Expansion of Quartz Parallel to Axis.

| Observer. | Temperature Range. | $a$ | $b$ | Coefficient of Expansion at 20° C. | Coefficient of Expansion at 270° C. |
|---|---|---|---|---|---|
| Benoit* ... ... | 6° to 80° | $7{\cdot}16 \times 10^{-6}$ | $8{\cdot}00 \times 10^{-9}$ | $7{\cdot}48 \times 10^{-6}$ | $11{\cdot}48 \times 10^{-6}$ |
| Reimerdes† ... ... | 5° to 220° | 6·92 ,, | 8·45 ,, | 7·25 ,, | 11·48 ,, |
| Scheel‡ ... ... | 16° to 100° | 7·14 ,, | 8·15 ,, | 7·47 ,, | 11·54 ,, |
| Randall§ ... ... | 0° to 250° | 7·17 ,, | 8·10 ,, | 7·49 ,, | 11·54 ,, |
| Bein‖ ... ... ... | 16° to 100° | 7·15 ,, | 8·08 ,, | 7·47 ,, | 11·51 ,, |
| Müller¶ ... ... | 0° to 360° | 7·07 ,, | 8·36 ,, | 7·40 ,, | 11·58 ,, |
| Lindman** ... ... | 9° to 270° | 7·01 ,, | 9·25 ,, | 7·38 ,, | 12·00 ,, |

* ' Trav. et Mém. du Bureau Int. Poids et Mes.', vol. 6, p. 3, 1888.

† ' Inaug. Diss. Jena ' (Reference obtained from Randall§).

‡ ' Ann. der Physik', vol. 9, p. 837, 1902.

§ ' Phys. Rev.', vol. 20, p. 10, 1905.

‖ ' Deutsch. Phys. Ges. Verh.', vol. 14, p. 1097, 1912.

¶ ' Phys. Zeits.', vol. 17, p. 29, 1916.

** ' Acta Soc. Sci. Fenn.', vol 46, No. 5, 1916.

Digitized by Google

Expansion of Quartz Perpendicular to Axis.

| Observer. | Temperature Range. | $a$ | $b$ | Coefficient of Expansion at 20° C. | Coefficient of Expansion at 270° C. |
|---|---|---|---|---|---|
| BENOIT* ... ... | 6° to 80° | $13{\cdot}25 \times 10^{-6}$ | $11{\cdot}63 \times 10^{-9}$ | $13{\cdot}71 \times 10^{-6}$ | $19{\cdot}53 \times 10^{-6}$ |
| LINDMAN† ... ... | 9° to 270° | 13·25 ,, | 12·62 ,, | 13·75 ,, | 20·07 ,, |

* *Loc. cit.* † *Loc. cit.*

It will be seen that for the expansion parallel to the axis all the results except those of LINDMAN are in agreement with BENOIT's formula. The weight of evidence justifies the use of BENOIT's values parallel to the axis. His value for the expansion perpendicular to the axis has also been used in view of the probable correctness of his value parallel to the axis and of the comparison of the expansion in the two directions which I have carried out (see above).

The results for bismuth parallel to the axis are deduced from those of BENOIT for quartz parallel to the axis; and for bismuth perpendicular to the axis from those of BENOIT for quartz perpendicular to the axis. If later work should show that BENOIT's values are appreciably in error, the values given in this paper for bismuth can be corrected by adding on to them the difference between the value of the correct coefficient of expansion of quartz and that given by BENOIT's formula for the temperature considered.

## RESULTS.

Three specimens have been tested, of which two were cut from one crystal and the third from another crystal made from a different lot of bismuth. The results for the three specimens agree closely.

### *Expansion Perpendicular to Axis.*

The values obtained for the expansion coefficient perpendicular to the axis at different temperatures are shown in Fig. 4. These points were determined over ranges varying

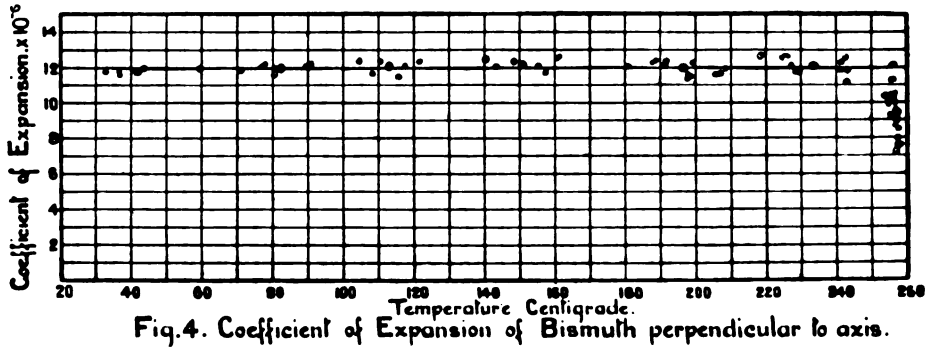


Fig. 4. Coefficient of Expansion of Bismuth perpendicular to axis.



Digitized by Google

from ten to forty degrees. The points are divided into groups and the mean of all the points in each group is indicated by a dark circle. These mean values are given in the following table :—

Expansion of Bismuth Perpendicular to Axis.

| Temperature. | Coefficient of Expansion. |
|---|---|
| 41·8° C. | $11{\cdot}8 \times 10^{-6}$ |
| 81·1 | 12·0 ,, |
| 113·0 | 12·1 ,, |
| 150·8 | 12·2 ,, |
| 196·1 | 12·0 ,, |
| 233·2 | 12·1 ,, |

It will be seen from this table and from Fig. 4 that over a wide range of temperatures the expansion coefficient is constant, but that as the melting-point is approached it decreases rapidly.

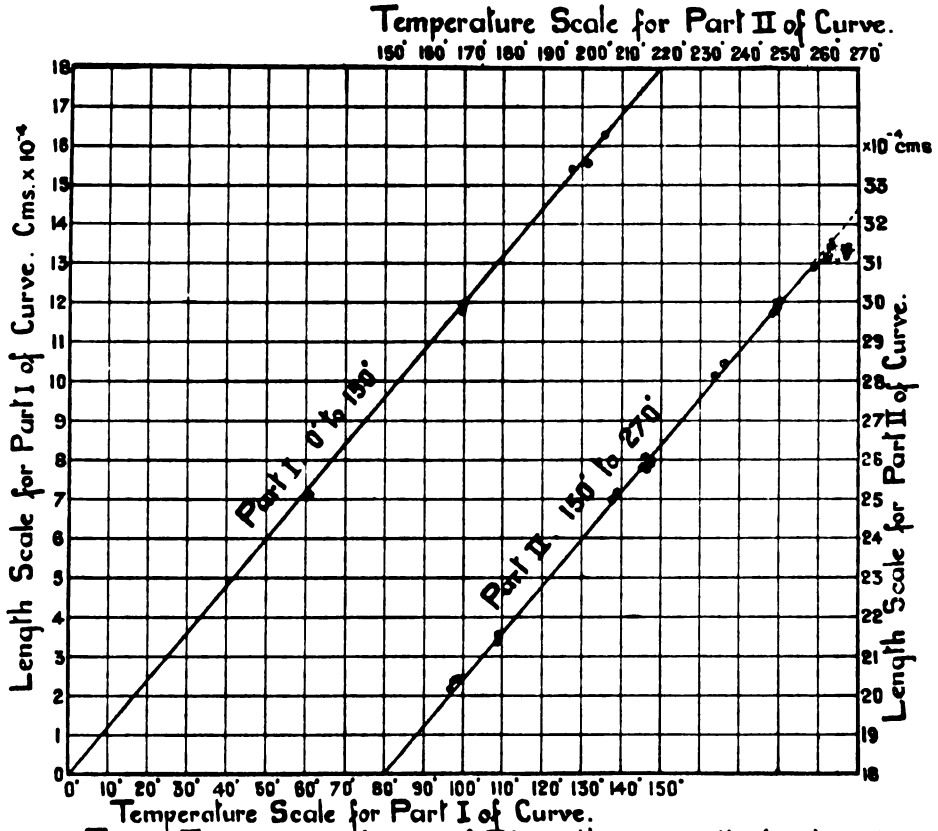
Temperature Scale for Part II of Curve.
150° 160° 170° 180° 190° 200° 210° 220° 230° 240° 250° 260° 270°
Length Scale for Part I of Curve. Cms. x 10⁻⁴
Length Scale for Part II of Curve. x10⁻⁴ cms
Part I. 0° to 150°
Part II. 130° to 270°
0° 10° 20° 30° 40° 50° 60° 70° 80° 90° 100° 110° 120° 130° 140° 150°
Temperature Scale for Part I of Curve.

Fig. 5. Expansion of 1 cm of Bismuth perpendicular to axis.

This rapid change makes it difficult to attach a meaning to experimental values obtained over a range of ten or twenty degrees, and it is convenient to plot length against temperature. This is done in Fig. 5, in which the increase in length of a specimen 1 cm. long at

Digitized by Google

0° C. is plotted against temperature. The straight line is drawn with gradient equal to the mean coefficient of expansion obtained from the above table, namely, $12{\cdot}0 \times 10^{-6}$. In the experiment the change in length for a given temperature change is measured. For plotting this curve the measured change is added to the length shown by the line for the lower temperature of the range, and the value so obtained plotted as the length at the upper temperature.

In order to show that the observed decrease in the coefficient of expansion at the higher temperatures was real, and was not due, for example, to a slow change in the size of the specimen owing to softening and consequent plastic deformation or to some annealing effect, a large number of observations with both rising and falling temperatures were made. There was no systematic difference between the results obtained in the two cases.

After the specimen had been heated to the high temperatures, a series of readings was taken over the range of lower temperatures. Only these measurements are included in Fig. 5. The fact that these values at lower temperatures do not depart systematically from the straight line indicates that no appreciable permanent change in the specimen had been brought about by the heating.

*Expansion Parallel to Axis.*

Similar results for the expansion parallel to the axis are shown in Figs. 6 and 7. In

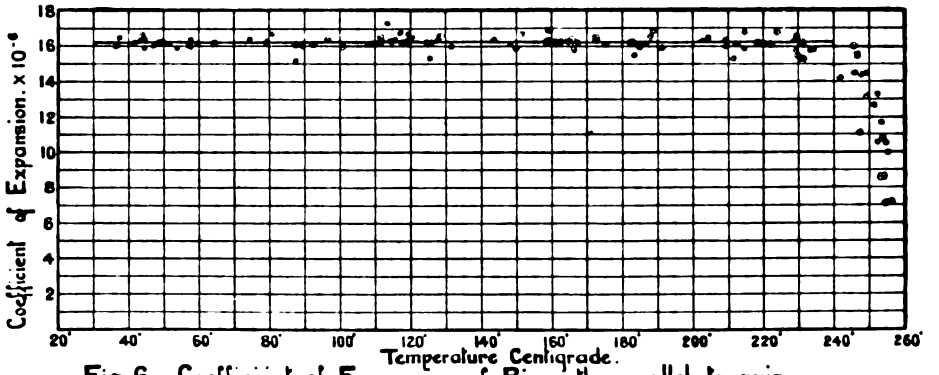


Fig. 6 Coefficient of Expansion of Bismuth parallel to axis.

this case the coefficient of expansion up to about 240° C. is $16{\cdot}2 \times 10^{-6}$. The mean values at different temperatures are given in the following table :—

Expansion of Bismuth Parallel to Axis.

| Temperature. | Coefficient of Expansion. |
|---|---|
| 49·3° C. | $16{\cdot}2 \times 10^{-6}$ |
| 87·6 | 16·1 ,, |
| 119·3 | 16·3 ,, |
| 159·0 | 16·3 ,, |
| 182·5 | 16·2 ,, |
| 221·9 | 16·1 ,, |

Digitized by Google

Combining these two values, we obtain as the mean coefficient of linear expansion of the solid

$$\frac{16{\cdot}2 + 12{\cdot}0 + 12{\cdot}0}{3} \times 10^{-6} = 13{\cdot}4 \times 10^{-6}.$$

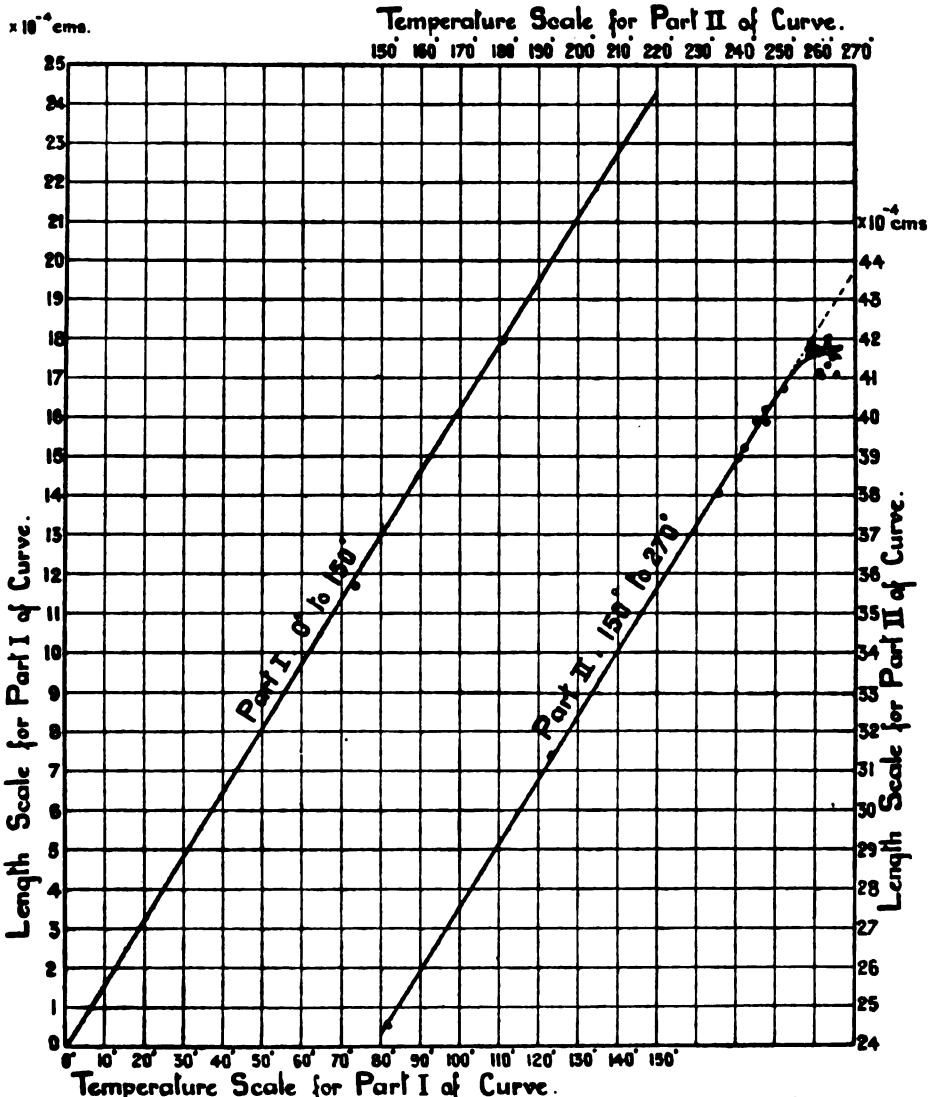
Temperature Scale for Part II of Curve.
Length Scale for Part I of Curve.
Length Scale for Part II of Curve.
Part I. 0° to 150°
Part II. 150° to 270°
Temperature Scale for Part I of Curve.

Fig. 7. Expansion of 1 cm of Bismuth parallel to axis.

The only other determination is that of Fizeau,* who worked only over the range 20° to 80° and obtained for the coefficient of expansion perpendicular to the axis $12{\cdot}4 \times 10^{-6}$, and parallel to the axis $16{\cdot}4 \times 10^{-6}$.

* 'Comptes Rendus', vol. 68, p. 1125, 1869.

Digitized by Google

## Interpretation of Results.

### *Comparison with Results of Grüneisen and Goens.*

In a letter* to 'Nature' I have pointed out the difference between the behaviour of bismuth crystals and the zinc and cadmium crystals examined by Grüneisen and Goens.†

If $\alpha_{//}$ = expansion coefficient parallel to the axis of the crystal,

$\alpha_{/}$ = expansion coefficient perpendicular to the axis of the crystal,

$\alpha$ = mean expansion coefficient,

$c$ = specific heat,

Grüneisen and Goens have shown that for zinc and cadmium crystals both $\alpha_{//}/c$ and $\alpha_{/}/c$ vary with temperature, while in each case $\alpha/c$ is practically constant.

There are very few data on the specific heat of bismuth at higher temperatures, but Richards and Jackson‡ have shown that at lower temperatures the variation with temperature is small. It is, therefore, probable that at higher temperatures it will be practically constant and in this case, since both $\alpha_{//}$ and $\alpha_{/}$ are constant up to about 240° C., both $\alpha_{//}/c$ and $\alpha_{/}/c$ will be constant.

### *Effect of Re-crystallisation.*

After the experiments were completed, the specimens were polished and examined in the Metallurgy Department by Mr. Jenkins. They showed some re-crystallisation round the edges, probably due to strains introduced by cutting. This in some places amounted to 25 per cent. of the thickness of the specimen. If we assume the new growth to be of random orientation, the absolute values of the expansions would be affected by about 5 per cent. However, the points of particular interest, viz., the constancy of both expansion coefficients up to 240° C., and the falling-off in both values above this point, would not be affected in any way.

### *Behaviour near Melting-Point.*

The results show that when bismuth crystals are heated they expand uniformly up to a temperature about 20 or 30 degrees below the melting-point. Above this temperature the straight line showing the relation between length and temperature begins to bend over, anticipating in the solid the large decrease of volume which occurs when melting takes place.

This contraction on melting indicates that dissociated bismuth atoms occupy less volume than those in the solid state. We may suppose that before the melting-point is reached there is a certain number of dissociated bismuth atoms distributed or dissolved

* 'Nature', vol. 113, p. 275, 1924.

† *Loc. cit.*

‡ 'Zeits. Phys. Chem.', vol. 70, p. 414, 1910.

Digitized by Google

in the solid lattice.* Such an arrangement is in some respects similar to those studied by OWEN and PRESTON† and others who have shown that, when a foreign atom is introduced into a space-lattice in a state of solid solution, it displaces one of the original atoms and causes a distortion of the whole lattice, which is either a contraction or an expansion, according as the foreign atom occupies less or more volume than the atoms of the lattice. The distortion is proportional to the number of foreign atoms present.

So in this case the presence of the dissociated atoms, which locally allow closer packing, distorts the bismuth lattice and, as the number increases, causes it to contract so much that it considerably decreases the normal thermal expansion. From a comparison of Figs. 5 and 7 it will be seen that at a given temperature the effect parallel to the axis is greater than that perpendicular to the axis.

*General Consideration of Properties of Solids near their Melting-Points.*

It is now necessary to consider the nature of this dissociation. General considerations would lead us to expect that some process similar to that about to be described would take place. The fact that, as will be shown later, it does not occur is a very remarkable one, and one that must be explained by any complete theory of the solid state.

The idea of an increasing number of molecular aggregates existing in the liquid phase as the temperature is lower is a familiar one, and has long been used‡ to explain such phenomena as the anomalous volume changes of water near its freezing-point. According to this view, the energy is divided among the molecules of the liquid according to statistical laws, and as the temperature is lowered the number of molecules which possess less than the minimum amount of energy required to keep them dissociated increases, and therefore the degree of aggregation increases. Similarly, it would be expected, when a solid is heated, that before the melting-point is reached a certain number of the atoms will possess sufficient energy to dissociate themselves from their neighbours. Distributed in the solid lattice there will be a certain number of these dissociated atoms, and the number of such atoms will increase as the temperature increases. These dissociated atoms can be regarded as in solid solution in the solid lattice.

Such a view would explain the effect which I have observed in the expansion of bismuth near the melting-point. Considerations similar in principle to those given above have been advanced recently by others§ to account for other effects observed near the melting-points of solids.

* It is shown in the next section that a pure solid does not show signs of dissociation below the melting-point, but that very slight traces of impurity are sufficient to make it do so.

† 'N.P.L. Collected Researches,' vol. 19, paper 25, or 'Proc. Phys. Soc.', Lond., vol. 36, p. 14, 1923.

‡ See SUTHERLAND, 'Phil. Mag.', vol. 50, p. 460, 1900.

§ See, for example, BIDWELL, 'Phys. Rev.', vol. 23, p. 357, 1924. Referring to the thermoelectric power and resistance of cæsium which melts at 27·4° C., BIDWELL says on p. 363: "At 0° C. the metal apparently shows evidence of the approaching fusion. This behaviour on approaching the melting-point is characteristic of all the alkali metals, as will be noted in the other curves. It suggests a gradual loosening up of the crystal structure, the lattice, however, holding together and retaining the metal in the solid state until the complete collapse at the melting point".

Digitized by Google

There are, however, experiments on the specific heat of ice near its melting-point which make such a hypothesis untenable. Any effect of the kind described would cause a progressively larger increase in the specific heat of the solid on approaching the melting-point, because it would be necessary to supply the heat of dissociation. DICKINSON and OSBORNE,* however, have shown that over the range " $-40°$ C. to $-2°$ C. the specific heat in 20° calories at a given temperature $\theta°$ C. of the purest ice experimented on is represented within the limit of experimental error by the equation $S = 0{\cdot}5057 + 0{\cdot}0018630\theta$, and that in the range closer to zero, *i.e.* $-2°$ to $-0°{\cdot}05$, the purer the ice the less the specific heat exceeds the value given by this equation ". They have further shown that the departure from the equation can be quantitatively accounted for by an amount of impurity sufficient to lower the initial freezing-point of the whole mass by $0{\cdot}00005°$ C.

The significance of these experiments of DICKINSON and OSBORNE in disposing of any theory of progressive change near the melting-points of pure solids similar to that outlined above has not, I think, been pointed out. We must conclude that the effects observed in my experiments, and any other similar effects on the properties of solids which can be ascribed to the presence of dissociated atoms, are due to the presence of impurities, which lower the melting-point. As an example of this, other workers† on the specific heat of ice, who do not appear to have taken special precautions to ensure the purity of the specimen examined, have obtained an appreciable increase in the specific heat ten or more degrees below the melting-point.

It is a remarkable fact that the melting of a pure solid is so sudden a process, and that below the melting-point, although we should expect on statistical theory a considerable number of molecules to have sufficient energy to dissociate, no such dissociation occurs.

* ' Bull. Bureau of Standards ', vol. 12, p. 49, 1915.

† See, for example, DICKINSON and OSBORNE, *loc. cit.*, p. 51.



Digitized by Google

Digitized by Google

# NEW SPECIFIC HEAT APPARATUS

BY

EZER GRIFFITHS, D.Sc., F.R.S.,
PRINCIPAL ASSISTANT IN THE PHYSICS DEPARTMENT.

Digitized by Google

## ABSTRACT.

The Paper is a description of an apparatus for the determination of the specific heats of materials such as cork, charcoal, etc., which are difficult to deal with by the ordinary methods. The calorimeter is a closed cylinder rotating on a horizontal axis. The heating coil and the thermo-elements project into the calorimeter and are maintained stationary. The material under test fills about one-third of the calorimeter and is mixed by being carried round by the fins attached to the internal surface. To ensure equalisation of the temperature, the material is ground to a state of fine sub-division before test.

By reducing the weights of all parts to a minimum, a calorimeter of 4 litres capacity has been constructed whose water equivalent is of the order of 100 gms. The jacket surrounding the calorimeter is made of copper wound with a heating coil. In an experiment the temperature of this jacket is maintained equal to that of the calorimeter, thus eliminating the corrections for heat loss by radiation and convection.


Digitized by Google

# NEW SPECIFIC HEAT APPARATUS.

By EZER GRIFFITHS, D.Sc., F.R.S.,
Principal Assistant in the Physics Department.

[Reprinted from the 'Proceedings of the Physical Society of London', Vol. 33, 1921.]

The usual "method of mixtures" for specific heat determinations is simple, and gives satisfactory results when the test specimens happen to take the form of metallic blocks. But when materials such as cork, chocolate, concrete, etc., have to be examined, serious experimental difficulties are encountered when an attempt is made to use the above method, so it is better to design an apparatus specially adapted to the work in hand. The apparatus described below was constructed for the study of the thermal capacity of light, bulky materials.

Cork, charcoal, slag wool, and diatomaceous earth are materials extensively used for cold-storage insulation, and it is sometimes necessary to make calculations as to the penetration of heat through a wall when the temperature of one of its faces is suddenly raised.

In the course of an investigation on heat insulators for the Food Investigation Board, it became necessary to determine the specific heats of various heat insulating materials.

An electrical method was employed, because it was desirable to obtain the specific heat over a narrow range of temperature. Heating materials such as charcoal to 100° C. alters the moisture content of the samples, and some preliminary tests proved that the charcoal and diatomaceous earth on heating to 105° C. showed a loss of weight of 6·9 and 8·8 per cent. respectively, due to the water driven off. Hence, any method which necessitated the heating of the sample through a wide interval of temperature was inadmissible.

## Description of Apparatus.

The calorimeter (Fig. 1) was a large cylindrical vessel of thin sheet aluminium. It was carried on a horizontal axis, and rotated at a uniform rate by an electric motor through a gear box. The usual speed of rotation was about one revolution in two seconds.

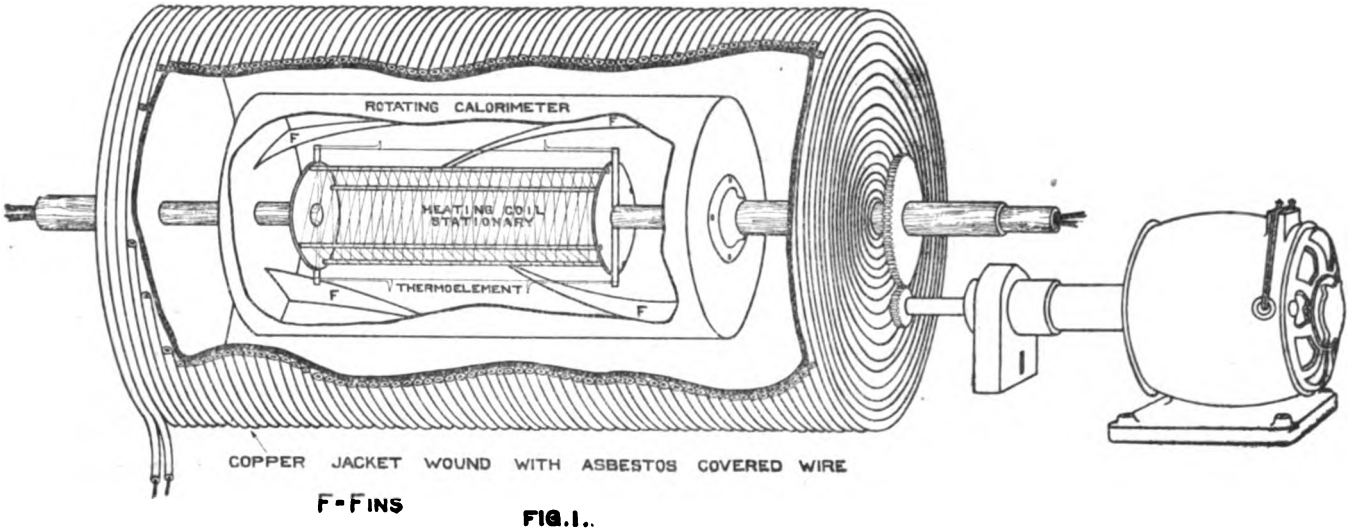


FIG. 1.

Digitized by Google

The material, in the state of fine sub-division, occupied about one-third to one-half the volume of the calorimeter. Helical fins were riveted to the internal surface, which, by the rotation of the cylinder, carried the contents round, and produced a very thorough mixing up of the powder.

A heating coil projected into the cylinder, and it was held stationary. The watts dissipated in this coil were measured by observations of the current and the potential difference at its ends.

Temperature was measured by six thermo-junctions of iron-constantan wire suitably supported so as to give the temperature at various points, but the observed differences were found to be negligibly small.

The rotation of the cylinder carried the material up, and, on reaching various heights, it dropped off the fins and fell through the heating coil on to the thermo-junctions. The helical fins were so arranged that half the set tended to carry the material in one direction by screw motion, and the other half in the opposite direction, the object being to produce mixing of the contents in the longitudinal direction. It was deemed advisable to assist the mixing by arranging the apparatus so that it would be swayed about an axis at right angles to that of the rotation, the effect of this being to throw the material from end to end of the cylinder.

By reducing the weights of the various parts to a minimum, it has been possible to construct the apparatus with a heat capacity of only 103 gram calories, whilst the calorimeter has a cubical capacity of 4,300 ccs. A calorimeter of this volume with such a small thermal capacity would have a relatively big heat loss by radiation and convection if it were allowed to radiate to constant temperature surroundings. This correction was eliminated by arranging the rotating calorimeter within a large copper drum wound with a heating coil. During the experiment the surroundings were heated up at the same rate as the calorimeter by suitably controlling the current through the coil around the drum.

Hence, during the actual experiment, the material under test was heated from one nearly stationary temperature to another, and no account had to be taken of any heat losses.

The heating coil on the drum was made of asbestos-covered resistance wire, the ends as well as the cylindrical portions of the drums being heated. The temperature of the internal face was obtained by means of thermo-junctions.

## Preparation of the Materials for Test.

These materials in their natural state are either granular or of fibrous structure. Consequently it was necessary to reduce them to a fine state of subdivision to ensure that the mixing up during the stirring produced uniformity of temperature throughout the mass. The charcoal and slag wool were ground up in an iron mortar and the iron abraded from the mortar was removed by the aid of a magnet. Cork was somewhat more

Digitized by Google

difficult, but it was found that a meat-mincer effectively reduced it to a state of suitable subdivision. The operation of grinding had to be carried on slowly, otherwise the heat generated was considerable; it was, in fact, found that too vigorous operation caused charring of the cork. The moisture content of the samples was determined during the course of the work.

The procedure in carrying through a test was as follows:—

A quantity of the material was ground to an exceedingly fine powder, weighed and inserted into the calorimeter. This was set in rotation, and after an interval of time the temperature would attain a steady state. The electric supply was then switched on to the heating coil and, a little previously, to the jacket, the appropriate values of the heating currents having been determined from preliminary experiments. The temperatures of both the calorimeter and the jacket then rose at a steady rate, and adjustments of the supply to the jacket were made to keep them approximately equal. After the temperature had risen through about 15°, the supply was switched off and observations of the temperature of the calorimeter continued until the steady state had been reached. From a knowledge of the initial and final temperatures as well as of the total watts supplied during the run, the specific heat of the material is readily calculated. Experience showed that, owing to the fact that the response of the jacket temperature to the heating coil was less rapid than that of the calorimeter, it was necessary to switch on and cut down the supply to the jacket about two minutes before switching on and off the supply to the calorimeter.

The result would be that the rise and the final steady temperature of the jacket would correspond very closely with that of the calorimeter. It was, of course, necessary to maintain a small current through the coil on the jacket to compensate for the heat lost from its surface at the higher temperatures. Tests and calculations were made to determine the small correction for the heating of the charge by the stirring.

Correction was also made for the heat absorbed by the air in the space unoccupied by the charge in the calorimeter. The values of the specific heats given correspond to the material in the closely packed state and, of course, include that of a little air.

A typical series of observations is shown in Fig. 2.

*Specific Heat Results.*

(At mean temperature of 25° C.)

| Material. | Moisture Content. | Specific Heat. |
|---|---|---|
| | Per cent. | |
| Charcoal . . . . . | 6·89 | $0·29_9$ |
| Slag wool . . . . . | 0·02 | $0·17_1$ |
| Diatomaceous earth . . . . . | 2·09 | $0·23_2$ |
| Baked cork (slab) . . . . . | — | $0·43_1$ |
| Granulated cork . . . . . | 3·45 | 0·43 |

Digitized by Google

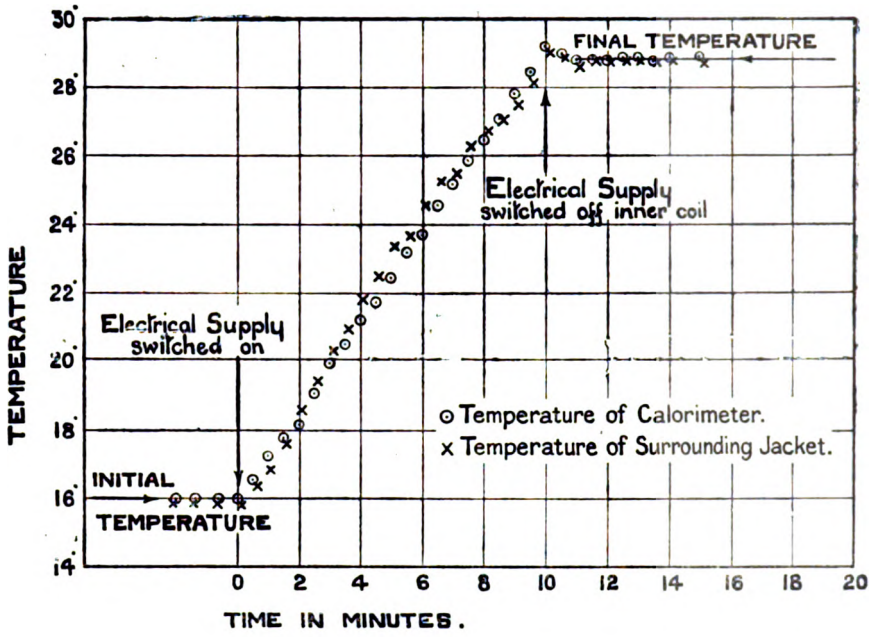


FIG. 2.

During the course of some more recent experiments on the specific heats of materials used in cable insulation, the above apparatus was modified in several details by Mr. R. R. STRAND, Senior Observer in the Heat Division.

To facilitate the adjustment of the temperature of the calorimeter to equality with the jacket, differential thermo-couples were attached to the surfaces of both calorimeter and jacket, and the method of stirring modified so that only a partial rotation is given to the calorimeter. The form of gearing required to effect this is shown diagrammatically in Fig. 3. The worm-driven wheel makes about one revolution in two seconds, and from

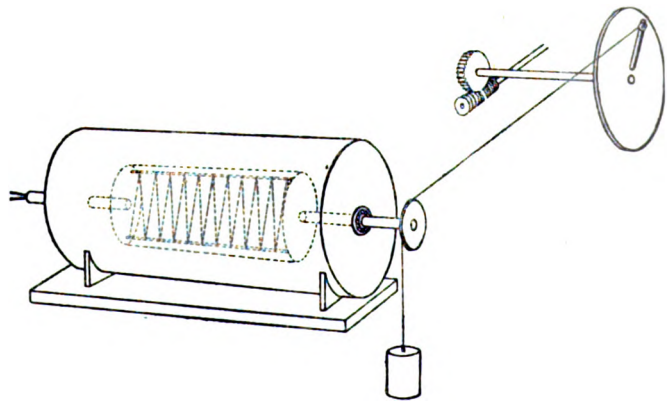

FIG. 3.

the crank pin a string is led over the pulley fixed to the axle of the calorimeter. By suitably proportioning the diameter of the pulley and the radial distance of the crank pin, the magnitude of the angular rotation of the calorimeter can be adjusted.

Digitized by Google

The jacket was wound with flat nichrome tape insulated by very thin micanite so as to obtain quicker response of the temperature of the surroundings to alterations in the energy supply.

In this particular calorimeter the heating coil was made of a flat, open grid of platinum wire occupying the diametrical plane. This coil was also the thermometer.

Initially a minute current was passed through the coil and the potential difference at its ends compared with that at the terminals of a standard coil connected in series with it. This gave the initial temperature rise of the calorimeter due to the stirring alone. The connections were then switched over to the heating supply circuit and the watts dissipated in the heating coil measured in the usual manner. Finally, the connections were switched back to the thermometer circuit and observations taken until the final equilibrium temperature had been attained. The advantage of the resistance thermometer is that it gives the average temperature over the area occupied.

We wish to thank our Director, Sir JOSEPH PETAVEL, for his kind interest and encouragement.



Digitized by Google

Digitized by Google

# APPARATUS FOR THE DETERMINATION OF THE HEAT OF EVAPORATION OF LIQUIDS OF HIGH BOILING POINTS

BY

J. H. AWBERY, B.A., B.Sc.,
ASSISTANT IN THE PHYSICS DEPARTMENT.,

AND

EZER GRIFFITHS, D.Sc., F.R.S.,
PRINCIPAL ASSISTANT IN THE PHYSICS DEPARTMENT.

Digitized by Google

## ABSTRACT.

Two new forms of apparatus for determining the heat of evaporation of liquids of high boiling point are described, and their relative merits briefly discussed.

In the one, the determination is made by a measurement of the amount of liquid vaporised for a given energy supply (radiation loss being eliminated by means of a constant temperature jacket), and in the other, the energy given up on condensing is estimated by means of a continuous flow calorimeter. The latter is thus a modification of the well-known apparatus of BERTHELOT, but particular attention has been paid to the avoidance of defects inherent in earlier types of apparatus.

The apparatus have been tested by determining with them the heats of evaporation of such liquids as alcohol, water and aniline, whose heats of evaporation are well known.

A brief survey of the earlier work is included, and a number of references given.


Digitized by Google

# APPARATUS FOR THE DETERMINATION OF THE HEAT OF EVAPORATION OF LIQUIDS OF HIGH BOILING POINTS.

By J. H. AWBERY, B.A., B.Sc., Assistant, and EZER GRIFFITHS, D.Sc., F.R.S., Principal Assistant in the Physics Department.

[Reprinted from the 'Proceedings of the Physical Society of London', Vol. 36, 1924.]

## Introduction.

During the course of some general investigations, it became necessary to determine the heats of evaporation of some liquids boiling at temperatures from 300° to 400° C.

The high temperatures involved rendered the utilisation of the customary forms of apparatus extremely difficult, so modifications had to be made to meet the special requirements of the case.

The apparatus hitherto employed for latent heat measurements may be broadly classified under two heads: In the one the quantity of heat liberated on the condensation of a definite weight of vapour is measured. In the other the heat which must be supplied to the liquid to produce a certain weight of vapour is measured.

All the earlier forms of apparatus belong to the first class for the simple reason that gas heating was almost universal at the time of their origin, and it is only the development of electrical measurements that has rendered possible the use of the second method.

In this paper it is not necessary to dwell in detail on the historical apparatus, but in passing one must pay tribute to the insight shown by Regnault* in designing his apparatus on a really large scale, and thereby minimising the errors inherent in the first method. We employed this method, and made two modifications which are obvious in the present state of our knowledge of calorimetry, namely, the application of the continuous flow calorimeter and of electrical heating.

This rendered possible the carrying out of an experiment under steady conditions, and, furthermore, the length of the connecting tube between boiler and calorimeter was cut down to a minimum, thereby avoiding premature condensation.

The second method of measurement, in which heat input is the quantity observed, appealed to us on account of the ease with which heat can be measured in the form of electrical energy, and a type of apparatus was devised working on this principle. Existing forms of apparatus did not afford us much help in the design, since they had been developed with a view to tests on liquids of low boiling points.

It may be of interest before passing on to a description of our own apparatus to indicate the development made by previous investigators.

Following on Regnault, Berthelot† is the most noteworthy worker in this field. He produced a laboratory form of apparatus where the liquid was boiled in a bulb and the vapour carried into the calorimeter through a tube projecting up through the centre.

* 'Mém. de l'Inst. de France', vol. 21, p. 638, 1847.

† 'Comptes Rendus', vol. 85, p. 646, 1877.

Digitized by Google

When a ring burner is employed for heating, there is a tendency for superheating of the vapour to take place in this form of apparatus. This apparatus was improved in details by SCHIFF* and LOUGUININE.†

HARKER‡ substituted internal electrical heating for the gas ring and also devised an ingenious form of valve. He emphasised the difficulty due to condensation of the vapour in the tubes and the carrying over of minute liquid particles.

Dr. E. H. GRIFFITHS§ brought the electrical method to a high degree of perfection for determination at temperatures below 100° C. He also made an absolute determination of the latent heat of benzene to serve as standard for Sir WILLIAM RAMSAY and Miss MARSHALL|| in their comparative apparatus for latent heat determinations. Their apparatus consisted essentially of a glass globe similar to a lamp bulb, which was enclosed in a jacket of the vapour of the same liquid as that under test. It was assumed that by this arrangement heat loss or gain by the liquid within the bulb was completely prevented. The electrical energy was not directly measured, but a similar apparatus with benzene was used as a standard, the two heating resistances being in series.

It seems to us that the apparatus could be improved by the use of a double-walled enclosure for the bulb, so as to offer greater thermal resistance to the heat flow should the temperatures within and without the globe not be identical.

In our apparatus this principle was adopted and, furthermore, the heat input was measured as electrical energy, since electrical measurements present nothing like the same difficulties today as they did thirty years ago, when RAMSAY and MARSHALL carried out their experiments.

In addition to the above-mentioned papers, reference might be made to the following:—

TRAUTZ ('Zeits. Elektrochem', vol. 14, p. 271, 1908); HENNING ('Ann. der Phys.', vol. 29, p. 441, 1909); A. C. SMITH ('Edinburgh Proc.', vol. 24, p. 450, 1903); A. W. SMITH ('Phys. Rev.', vol. 33, p. 173, 1911); NAGORNOW and ROTINJANZ ('Zeits. Phys. Chem.', vol. 77, p. 700, 1911); and KAHLENBERG ('J. Phys. Chem.', vol. 5, p. 215, 1901). See also GLAZEBROOK's 'Dictionary of Applied Physics', vol. 1, p. 550.

We turn now to our own apparatus.

## APPARATUS No. 1.

The fundamental principle of this method is the determination, by condensation, of the total heat of the vapour, and the subtraction from it of the total heat of the liquid to just below the boiling point.

* 'Liebig's Ann. Chem.', vol. 234, p. 338, 1886.

† 'Ann. Chim. Phys.', vol. 7, p. 251, 1896, and vol. 13, p. 337, 1898.

‡ 'Mem. Manchester Lit. & Phil. Soc.', (4), vol. 10, p. 38, 1896.

§ 'Phil. Mag.', vol. 41, p. 1, 1896; also 'Phil. Trans.', A, vol. 186, p. 216, 1895.

|| 'Phil. Mag.', vol. 41, p. 49, 1896.

Digitized by Google

This method was found to be extremely convenient, but suffers under the disadvantage that the accuracy attainable is determined by the relative magnitudes of the heat of evaporation and the specific heat of the liquid.

The experiment resolves itself into two parts: (*a*) the determination of the total heat of the vapour, and (*b*) the determination of the mean specific heat.

The apparatus employed for the determination of the total heat of the vapour is illustrated in Fig. 1.

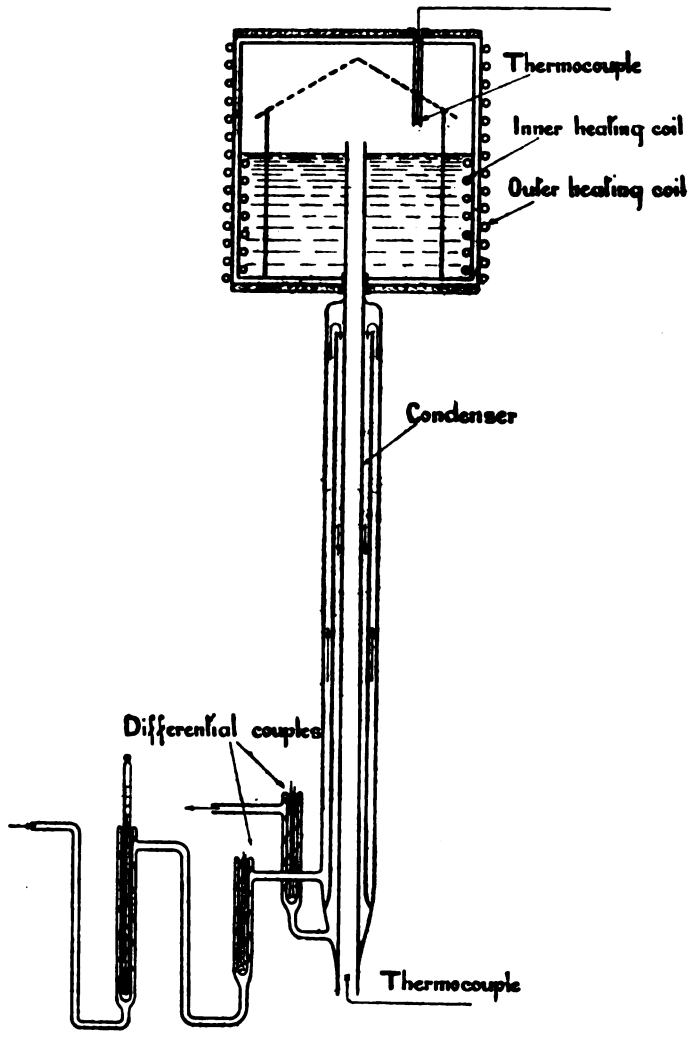


FIG. 1.

## DESCRIPTION OF APPARATUS FOR TOTAL HEAT OF THE VAPOUR.

A continuous flow calorimeter was employed for the measuremement of the heat liberated by the condensation of the vapour and the cooling of the fluid.

Referring to Fig. 1, the large vessel was wound with an external heating coil of

Digitized by Google

approximate resistance 8 ohms, and through the top a thermocouple of copper-constantan projected, which recorded the temperature of the vapour.

To diminish any radiation transfer between the liquid and the top of the boiler, the conical metal shield shown in the figure was placed inside. This was perforated with holes to allow free circulation of the vapour, and supported on a sheet metal cylinder which stood in the vessel. The outside and top of the heater were well lagged with asbestos wool contained in a sheath of asbestos paper. A re-entrant brass tube passed through the base of the heater, and was of such length that it projected above the surface of the liquid. Through this tube was carried a silica tube, extending to about 20 inches below the base. This was surrounded with a water jacket, through which a stream of water was passed at constant head. The water stream was arranged to flow up an outer jacket, when its temperature was approximately that of the air, and down the inner jacket, during which time it took up heat from the liquid, and was almost completely shielded from radiation by the surrounding stream of incoming water. As additional protection the tube was heavily lagged with cotton wool. A thermometer inserted in a U-tube in the pipe line gave the temperature of the water on its entrance to the apparatus, and a set of copper-constantan thermocouples arranged differentially gave the rise of temperature due to the heat absorption. A third thermocouple was inserted in the exit of the silica tube in such a way that the condensed liquid flowing down the latter ran over the junction.

Thus the experiment consisted in steadily boiling the liquid under examination by means of the heating coil, when the vapour produced escaped into the silica tube, and, flowing down this, was condensed ; the heat given up in this process, and in cooling down to the temperature at which it was collected, is absorbed by the water flowing in the surrounding condenser. Hence, when a steady state is reached, we have, if Q is the water flowing per second, $\theta$ its rise (measured by the differential couples), $t_2$ and $t_1$ the temperature of the vapour and of the liquid at its exit from the apparatus, and L its latent heat, $s$ its mean specific heat in the liquid form over the range $t_2$ to $t_1$, and $m$ the mass of liquid condensed per second.

$$Q\theta = m\,[L + s\,(t_2 - t_1)].$$

Here $s$ is known from a separate experiment, and every other quantity is directly measured. Q was determined by taking the time to fill a graduated flask, and it may be remarked that when the time measured was about 80 seconds the extremes of several successive determinations of Q differed by less than 0·6 second.

$m$ was determined by collecting fractions for 30 seconds or 1 minute and weighing.

It will be noted that the value of $s$ required is that over the range $t_1$ to $t_2$ (in these experiments about 30° to 340° C.), whereas that found experimentally was determined over the range 20° to 320° C. approximately. It is not anticipated that the variation of specific heat with temperature is sufficiently large to introduce any appreciable error from this fact.

Digitized by Google

### Description of Apparatus for the Specific Heat of the Liquid.

The method of mixtures was adopted for this part of the experiment in the following form:—

The liquid under test was heated in a thick copper vessel of about 750 cc. capacity, which had a large-bore gas cock silver-soldered in the bottom. This was well lagged with asbestos wool, and immediately before an experiment some liquid was run out, so that contact with the tap would not cool the sample used for the experiment. The vessel was wound with a heating coiling of nichrome strip, of about 4 ohms resistance cold, and this sufficed to heat the liquid inside from room temperature up to 350° C. in about an hour.

The temperature was obtained with a nitrogen-filled mercury thermometer passed through a packing gland in the lid of the vessel. This thermometer was calibrated under the same conditions of immersion as those of the experiment.

### Procedure in Carrying out an Experiment.

By means of the heating coil, the temperature of the liquid was raised to just below the boiling point. Some of the liquid was then run out so as to bring the temperature of the outlet pipe up to that of the liquid. Finally, some of the liquid was rapidly run into the calorimeter. The fluid in the calorimeter was an oil whose specific heat at air temperature was determined by the customary methods.

### Results and Check Experiments.

The working of the apparatus was first tested by determining in it the latent heats of the following liquids, the values for which have previously been determined, and are quoted in the last column for comparison.

| Substance. | Temp. of boiling °C. | $s$. | $\frac{Q\theta}{m}$. | $s(t_2 - t_1)$. | L (cals. per gm.). | L (Kaye & Laby's Tables). |
|---|---|---|---|---|---|---|
| Methyl alcohol . . . . . | 78·9 | 0·61 | 289 | 31 | 258 | 259 |
| Water . . . . . | 100 | 1·00 | 605 | 68 | 537 | 540 |
| Aniline . . . . . | 179 | 0·51 | 183 | 78 | 105 | 104 |

As the order of accuracy aimed at was only about 1 per cent. the agreement is satisfactory.

A further check on the apparatus was obtained by comparison with the results of an alternate method of experiment now to be described.



Digitized by Google

### A Second Method of Use of Apparatus I.

In this series of experiments the converse principle was applied, in that the heat required to evaporate a known mass of liquid was determined, instead of that liberated on condensation of vapour. To adapt the apparatus above described for this purpose another heating coil was wound on a mica cylinder and fixed inside the boiler, suitably insulated from the base and from the central brass pipe. It was of such dimensions that it was completely submerged in the liquid throughout an experiment.

The procedure adopted was to pass a suitable small current until a steady temperature was attained in the liquid, and to repeat this with several values of the current until a curve could be drawn showing watts expended against temperature of equilibrium. When the liquid was at a steady temperature the energy supplied was lost by radiation from the surface of the calorimeter, and by a small graphical extrapolation over a range of about 20° or 30° C. the energy required to maintain the apparatus at the boiling point could be deduced.

In the next stage of the experiment the energy supply was increased considerably so that the liquid was boiling freely. The rate at which it distilled over was obtained by collecting fractions for a known time. In this method there is no question involved of total heat. The energy supplied, less that radiated, is all employed in vaporising the liquid, and hence the calculation of the heat of evaporation involves merely the measurement of the energy supply and the weight of liquid condensed.

One important precaution to be observed in these experiments was to maintain the conditions uniform throughout as regards the thickness of the lagging and the prevention of draughts.

A check experiment was carried out with aniline, and the results are shown below :—

| Mass of aniline in 30 secs. (gms.) | Temperature. °C. | Total Energy Supplied. | | | Energy Radiated (cals.) | Energy entering aniline. (cals.) | Heat of evaporations. (cals. per gm.) | Remarks. |
|---|---|---|---|---|---|---|---|---|
| | | (Volts.) | (Amps.) | (cals.) | | | | |
| — | 50 | 25·0 | 3·44 | 20·5 | 20·5 | — | — | These figures were utilised for drawing the curve of radiation loss against temperature. |
| — | 135 | 29·4 | 3·91 | 27·45 | 27·45 | — | — | |
| — | 140 | 29·6 | 3·92 | 27·7 | 27·7 | — | — | |
| — | 159 | 33·9 | 4·50 | 36·4 | 36·4 | — | — | |
| 17·88 | 183 | 57·16 | 7·51 | 102·6 | 40·8 | 61·8 | 103·7 | The heat of evaporation is given in tables as 104. |

### Accuracy Obtainable.

The examples we have given above represent a rather higher degree of accuracy than we have been able to obtain in tests on certain commercial liquids, owing to the high fraction of the total heat which the specific heat term represented. In our experience

Digitized by Google

it is the determination of the specific heat which is the more troublesome determination to make and the one which appears to be subject to the greater uncertainty.

Thus, for example, we have for one liquid $\frac{Q\theta}{m} = 261 \cdot 3$, $s(t_2 - t_1) = 191 \cdot 4$, whence $L = 69 \cdot 9$. In this case an error of 1 per cent. in the specific heat introduces an error of nearly 3 per cent. in latent heat.

Even for materials of low latent heat we consider that an equal accuracy would be attainable by means of the second method of using Apparatus No. 1 with an internal heating coil. This method, however, is slow, since the radiation correction must be redetermined on each occasion that the lagging is disturbed, and this involves allowing the temperature to become steady at four or five points, each of which may take two to three hours.

## Description of Apparatus II.

The chief objection to the apparatus above described is the necessity for subsidiary experiments to determine either the specific heat of the liquid or the heat required to maintain the calorimeter at the temperature of the boiling point of the liquid.

An apparatus will now be described in which the heat of evaporation is determined directly, without any necessity for determining the total heat to the boiling point; in this respect it resembles the second method above described, but it is superior to that method in economy of time.

The principle was to hold the liquid at the boiling point and then to measure the amount vaporised for a given further expenditure of energy. It is evident that this can only be done if the radiation losses are of negligible magnitude, and to secure this it was found possible to eliminate the radiation entirely by holding the surroundings at the same temperature as the liquid.

The apparatus is shown in Fig. 2. Its main features are a small double-walled vessel to contain the liquid under examination, provided with a condenser tube for the final collection of the condensed vapour. This vessel is closed by a pressed metal lid whose edge is submerged in a layer of molten tin. A well-fitting disc of mica rests on the top edge of the double-walled vessel, so that a thermally insulating stopper is obtained. Surrounding the double-walled vessel is another thick-walled metal enclosure wound with a heating coil, so that it can be maintained at the same temperature as the liquid. A shaft carrying a fan passes through the base of this, the function of the fan being to keep the air in motion, thereby ensuring thermal uniformity within the apparatus. The liquid was heated by means of a submerged coil until the vapour was just slowly distilling over, and the outer jacket was then maintained at this temperature. Equality of temperature was obtained by observing the motion of a galvanometer spot in the circuit of a differential thermocouple with junctions on the wall and in the liquid. To secure uniformity of temperature, the air inside was kept in continual movement, baffle plates being arranged to direct its path all round the double-walled vessel.

Under these conditions there could be but little radiation from the liquid outwards,



Digitized by Google

and the residual effect was allowed for by determining the energy required to produce a very slow rate of evaporation. Hence a careful weighing of the amount vaporised per second at two known rates of energy input gave, by difference, a value for the heat of evaporation that was probably of a high order of accuracy.

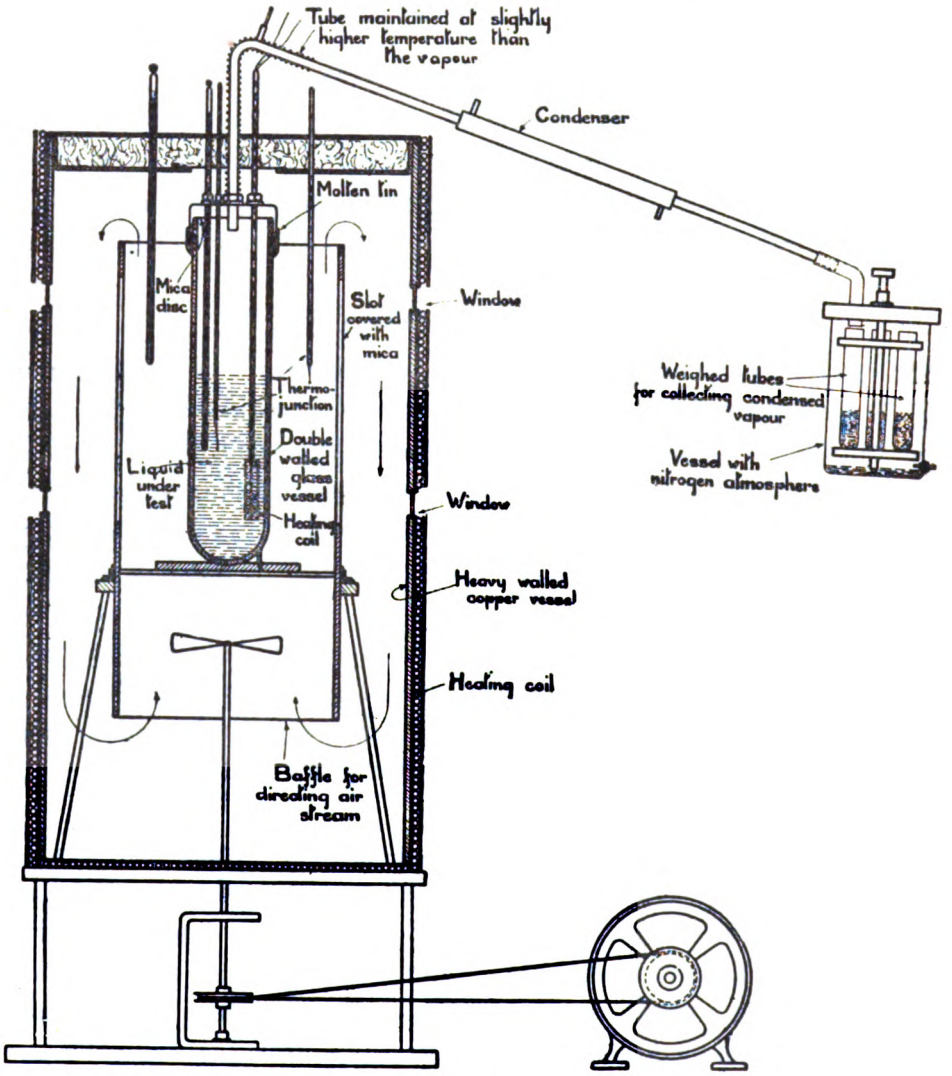


FIG. 2.

It is, perhaps, worth while to point out to what extent the plan here employed to eliminate radiation losses may introduce uncertainty.

We have two cylindrical vessels, one inside the other, of radii $a$ and $b$ at temperatures which are supposed to be equal. Let us suppose, however, that there is an actual difference of 1° C. between them. The heat radiated from the inner will then be (assuming STEFAN'S Law)—

$$2\pi a \times 1{\cdot}374 \times 10^{-12} [(\theta + 1)^4 - \theta^4]$$

$$= 11 \times 10^{-12} \pi a \theta^3 \text{ cals. per sec. per cm. of length.}$$

Digitized by Google

Thus, if the energy supply to the liquid is H cals. per sec. and the true latent heat L, we shall have

$$\frac{(H - 11 \times 10^{-12} \pi a \theta^3)}{L} \text{ gms.}$$

evaporated per sec., and we shall deduce a latent heat of

$$\frac{HL}{H - 11 \times 10^{-12} \pi a \theta^3} = L\left[\frac{1 + 11 \times 10^{-12} \pi a \theta^3}{H}\right]$$

cals. per gm., which is in error by $\frac{11 \times 10^{-10} \pi a \theta^3}{H}$ per cent.

To see what this may mean let us take a few typical values.

| | | | | |
|---|---|---|---|---|
| $a = 30$ cms. | $H = 12$ cals. per sec. | $\theta = 300°$ K. $= 27°$ C. | Error $= 0{\cdot}23$ | per cent. |
| | $= 50$ watts approx. | $= 500°$ K. $= 227°$ C. | ,, $= 0{\cdot}55$ | ,, |
| | | $= 700°$ K. $= 427°$ C. | ,, $= 1{\cdot}08$ | ,, |
| $a = 300$ cms. | $H = 200$ cals. per sec. | $\theta = 300°$ K. $= 27°$ C. | ,, $= 0{\cdot}14$ | ,, |
| | $= 800$ watts approx. | $= 500°$ K. $= 227°$ C. | ,, $= 0{\cdot}33$ | ,, |
| | | $= 700°$ K. $= 427°$ C. | ,, $= 0{\cdot}65$ | ,, |

The above figures, which take account of radiation only, are merely illustrative, since they neglect convection, and, further, assume an emissivity of unity. Nevertheless, they illustrate the order of the error, as radiation is the important factor to be considered at high temperatures.

A source of practical difficulty in the manipulation lay in the necessity for using a "tin-seal" to close the top of the double-walled vessel. We were unable, however, to find any other convenient way of preventing the egress of vapour, so that we had to perform the filling of the seal on each occasion when the melting point of tin was reached (232° C.). In testing inflammable liquids the vapour was apt to take fire on coming into contact with the air in the tube, so that we had to have the end of the condenser tube and collect the condensate in an atmosphere of nitrogen.

Our best thanks are due to Mr. A. R. CHALLONER, of the Observer Staff, for very skilful assistance both in the construction of the various forms of apparatus and in the taking of observations with them.

Digitized by Google

Digitized by Google

# THERMOMETRIC LAG WITH ESPECIAL REFERENCE TO COLD STORAGE PRACTICE

BY

EZER GRIFFITHS, D.Sc., F.R.S.,
PRINCIPAL ASSISTANT IN THE PHYSICS DEPARTMENT,

AND

J. H. AWBERY, B.A., B.Sc.,
ASSISTANT IN THE PHYSICS DEPARTMENT.

Digitized by Google

## ABSTRACT.

(Reprinted from ' Science Abstracts ', Section A, Physics, Vol. 26.)

The authors discuss the magnitudes of some of the possible sources of error in the determination of the temperature of a cold stores in a ship's hold by means of a mercury or spirit thermometer which is carried to the deck for the purposes of reading. The effect of time lag upon the reading of the thermometer is discussed in the case when the temperature is changing rapidly.


Digitized by Google

# THERMOMETRIC LAG, WITH ESPECIAL REFERENCE TO COLD STORAGE PRACTICE.

By EZER GRIFFITHS, D.Sc., F.R.S., Principal Assistant, and J. H. AWBERY, B.A., B.Sc., Assistant, in the Physics Department.

[Reprinted from the 'Transactions of the Faraday Society', Vol. 18, Part 2, 1922.]

Temperature control is a factor of such vital importance to the successful operation of a cold store that the instruments employed should receive the most thorough study. Mercury in glass or spirit thermometers are almost universally used for such measurements and have the merit of extreme simplicity. For distant reading work the resistance and the mercury in steel thermometers have obvious advantages and are now finding applications.

The object of the experiments described below was to obtain numerical data as to the magnitude of some of the possible sources of error in the measurements when mercury or spirit thermometers are employed for taking the temperature of the atmosphere of a ship's hold by withdrawal of the thermometer to the deck for reading. They also give information as to the error introduced by the "time lag" of the thermometer if the temperature of the store happens to be changing rapidly.

Besides the spirit and mercury thermometers generally employed in such measurements, tests were made on a resistance thermometer and a distant reading mercury thermometer.

## Description of the Various Types of Thermometers.

A. *Mercury in Glass and Spirit Thermometers.*—The mercury thermometer shown in Fig. 1 was designed by Mr. A. R. T. Woods, Managing Director of the Nelson Line, with a view to eliminating a most serious source of error in the common type, namely, the rapid change in reading which occurs when a bare thermometer is withdrawn from the hold and read on deck. Mr. Woods states that this error was often accentuated by the observer holding the bulb in the palm of his hand when taking the reading.

In the form shown in Fig. 1 both the bulb and stem are protected by a wooden sheath, while the bulb is lagged by cotton waste. The efficiency of this simple device for overcoming this particular difficulty is demonstrated by the experimental data given later in this report.

Plain mercury and spirit thermometers were also studied, the bulb of the former being $\frac{1}{4}$ inch in diameter and 1 inch long, of the latter $\frac{3}{8}$ inch in diameter and $1\frac{3}{8}$ inches long.

B. *Mercury in Steel Thermometer. Distant Reading Type.*—In this instrument the mercury is contained in a steel bulb, connected by a fine capillary to a Bourdon tube. The temperature is indicated on a dial resembling a steam pressure gauge. The bulb of the thermometer is cylindrical, $\frac{3}{4}$ inch in diameter and 8 inches in length.



Digitized by Google

C. *Resistance Thermometer.*—The " bulb " of this thermometer consisted of a porcelain spool $2\frac{3}{16}$ inches long by $\frac{7}{16}$ inch in diameter, wound with platinum wire, as shown in Fig. 1. After winding, the spool had been dipped in a glaze so as to protect the platinum.

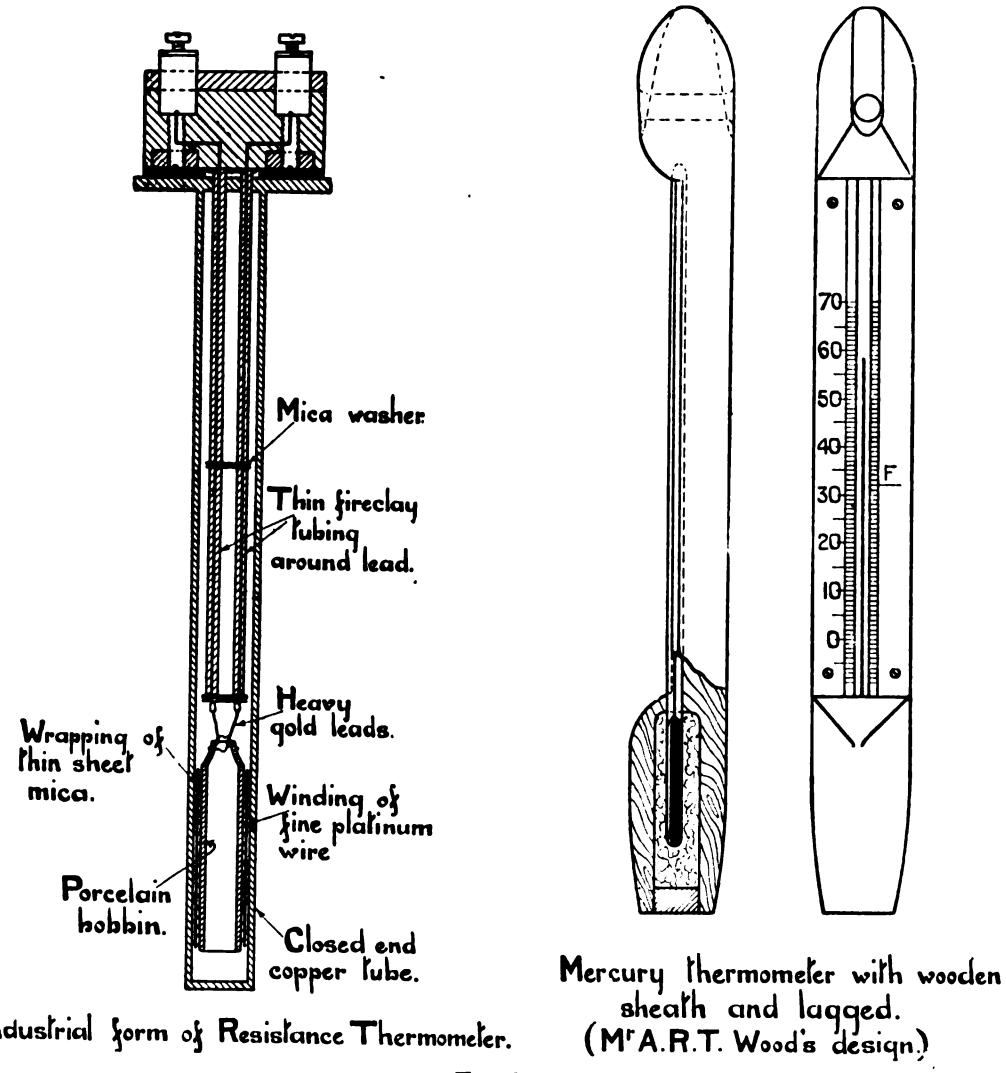


FIG. 1.

The bulb and wires were protected by a closed end copper sheath, the spool being electrically insulated from the metal walls by a wrapping of mica.

In this temperature measuring outfit a number of thermometers were connected to the one indicator and could be plugged in as desired.

## CALIBRATION OF LOW TEMPERATURE THERMOMETERS.

The calibration of the thermometers below 0° C. was carried out in the apparatus shown diagrammatically in Figs. 2 and 3.

Digitized by Google

*Description of Apparatus.*—For plain mercury and spirit thermometers the apparatus shown in Fig. 2 was used. It consists of a Dewar vacuum vessel (not silvered), fitted with a " drawing off " pipe for emptying.

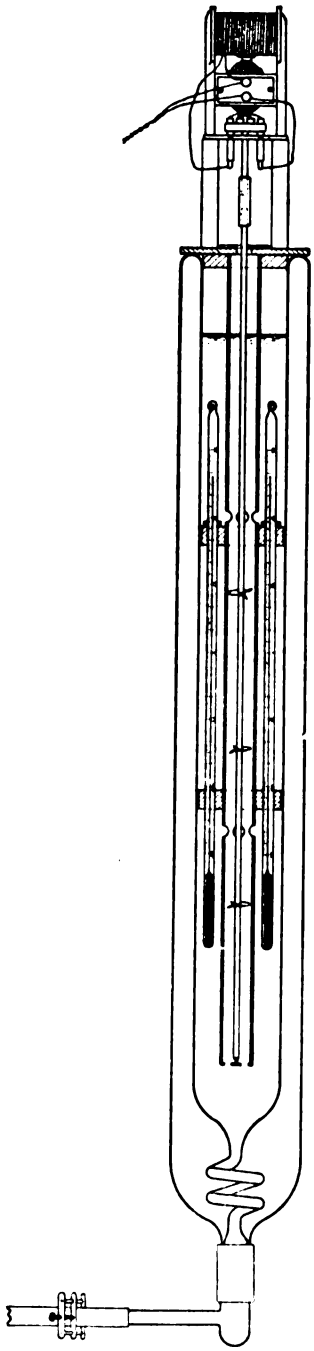

FIG. 2.

A tube projects into the vessel containing a shaft with propeller blades. When the motor is in action the liquid is sucked up the central tube and discharged out through the orifices, thus ensuring a thorough stirring of the contents. The thermometers are carried on clips attached to the tube and are totally immersed, the readings being taken through the transparent walls of the vacuum vessel.

The liquid employed is clean anhydrous ether. The temperature is lowered by adding successive quantities of carbon dioxide snow.*

By means of this apparatus any desired temperature down to — 60° C. may be obtained.

This method was devised about ten years ago by Messrs. KAYE and HIGGINS for the routine test of low-temperature thermometers, and the original vessel still survives.

The distant reading mercury thermometer and the resistance thermometer were calibrated in the apparatus shown in Fig. 3, as they were too large to be inserted into the vacuum vessel.

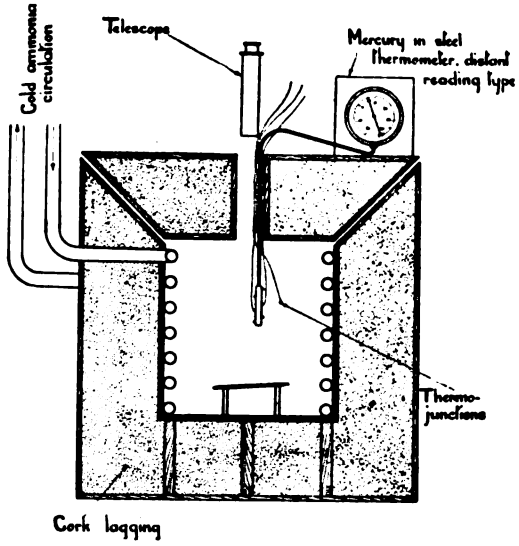


FIG. 3.

This apparatus was also used for finding the " time lag " of the different types. It consists of a box measuring 2 feet by 2 feet by 2 feet, within which is a rectangular spiral

* Carbon dioxide snow is prepared as required by allowing the liquid carbon dioxide, sold in cylinders, to expand into a perforated container.



Digitized by Google

of iron piping. This spiral is connected to the refrigerating plant and, by the circulation of the expanded ammonia, the temperature of the air within the box can be lowered rapidly to a minimum of about — 35° C.

The bulb of the instrument under test projects into this enclosure and has strapped to it a number of thermo-junctions of copper-constantan.

The temperature of the enclosure is maintained steady by observations of the temperature of a thermo-junction suspended freely, as shown in Fig. 3.

It may be remarked in passing that the above methods of calibrating are not applicable to thermometers inserted in pipe lines and which usually have an emergent column. With such thermometers it is desirable to carry out the tests under conditions closely similar to those obtained in practice.

An apparatus which we have found satisfactory for such tests is a small cast-iron box inserted in a pipe line connected through a pump to the cold brine reservoir.

The thermometers are screwed into sockets in the top of the tank and a circulation of cold brine maintained during the test.

## The "Time Lag" of the Different Types of Thermometers.

The apparatus shown in Fig. 3 was used. The procedure was to lower the temperature of the enclosure down to a point corresponding to the lowest scale reading of the thermometer under test and allow it to settle there. The thermometer, initially at room temperature, was rapidly inserted into the enclosure and observations of apparent temperature taken at successive time intervals.

The type of curves obtained will be seen from an inspection of Fig. 4 and, as they are exponential in character, the observations can be shown graphically on a series of straight lines by plotting the logarithm of the temperature excess against the time (see Fig. 5.)

The slope of these lines determines the relative "time lags", *i.e.* the smaller the slope the greater the time taken to settle to equilibrium.

For if the thermometer is at a temperature $\theta$ and the enclosure at U, the rate at which the thermometer takes up heat is proportional to $(U - \theta)$. Thus the rate, $\frac{d\theta}{dt} = \frac{1}{L}(U - \theta)$, where $\frac{1}{L}$ is a constant of proportionality and L has the dimensions of a time.

This equation may be written :—

$$\frac{d\theta}{\theta - U} = -\frac{dt}{L} \text{ which gives, if U = constant,}$$

$$\log (\theta - U) = -\frac{t + a}{L} \quad . \quad . \quad . \quad . \quad . \quad . \quad . \quad . \quad . \quad . \quad (1)$$

To determine $a$, we note that, when $t = 0$, $\theta = \theta_0$.

Digitized by Google

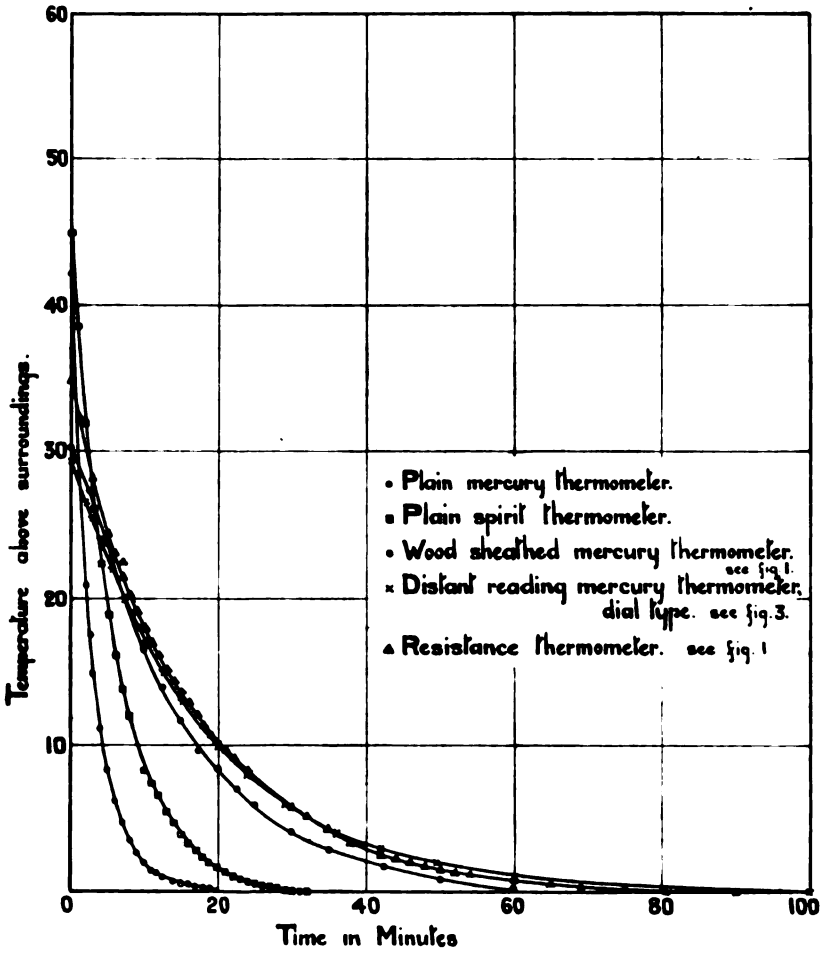


FIG. 4.

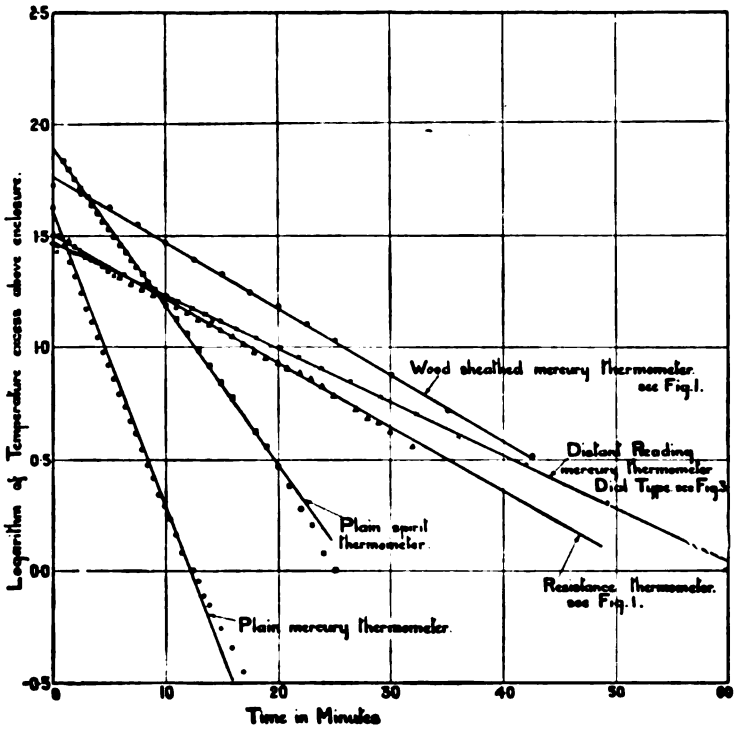


FIG. 5.

Digitized by Google

Thus

$$\log (\theta_0 - U) = -\frac{a}{L}.$$

So that, substituting in (1), we get—

$$\log (\theta - U) = -\frac{t}{L} + \log (\theta_0 - U). \quad . \quad . \quad . \quad . \quad . \quad . \quad . \quad . \quad . \quad (2)$$

It is the quantity on the left which is plotted against $t$ in Fig. 5, and we see, therefore, that the slope of the lines in Fig. 5 is $-\frac{1}{L}$. (In that figure the logs are to base 10, so that the slope has to be multiplied by $0{\cdot}4343 = \log_{10} e$ to obtain $-\frac{1}{L}$.)

Equation (2) gives us—

$$\log \frac{\theta - U}{\theta_0 - U} = -\frac{t}{L},$$

*i.e.* $(\theta - U) = (\theta_0 - U)\, e^{-\frac{t}{L}}$, which shows that the experimental curves are exponential.

Hence, when

$$t = L$$
$$(\theta - U) = (\theta_0 - U)\, e^{-1},$$

*i.e.* the difference is reduced to $\frac{1}{e}$ of its original value.

For this reason L is a convenient constant by which to measure the time lag. A mere statement of its value in seconds or minutes for a particular thermometer is all that is required to determine the behaviour of that instrument under any circumstances as regards time lag.

In particular, if the instrument has been taken from one room to another where the temperature is lower by T°, we can see the way in which it will take up the new temperature.

In a time L secs. it will still have $0{\cdot}368$ T° to fall, and this is reduced to $0{\cdot}000045$ T° in 10 L secs.

*Experimental Results and their Application.*—From the experiments described with the various types of thermometers the values determined for the particular thermometers (in air) are given below :—

| Plain Mercury. (Minutes. | Spirit Thermometer. (Minutes.) | Wood-encased Mercury Thermometer. (Minutes.) | Direct Reading Platinum Thermometer. (Minutes.) | Mercury in Steel Thermometer, Distant Reading Type. (Minutes.) |
|---|---|---|---|---|
| 3·38 | 6·11 | 14·57 | 17·29 | 18·28 |

Digitized by Google

The following table (p. 120), calculated from the above figures, shows the errors introduced in the determination of the temperature of an enclosure such as a ship's hold if the thermometer is first brought to a place where the temperature differs from that of the enclosure by N°, and held there for time $t$ before reading. The corrections are true in Fahrenheit units if N is so expressed and in Centigrade if N is measured in ° C.

It may be worth noting, further, that the constant L has another interpretation, namely, if the temperature of the enclosure is changing uniformly, the thermometer records the temperature which existed L minutes previously. To show this we have to return to the equation previously given, viz.,

$$\frac{d\theta}{dt} = \frac{1}{L}(U - \theta).$$

But U is not now a constant. Say it is $U_0 + rt$, where $r$ = the rate at which the enclosure is rising in temperature in degrees per minute.

Then

$$\frac{d\theta}{dt} = \frac{1}{L}(U_0 + rt - \theta).$$

It may be verified that the solution of this equation is

$$\theta = U_0 + r(t - L) + Ae^{-t/L}.$$

We determine A by putting $\theta = \theta_0$ when $t = 0$, and the equation becomes

$$\theta = U_0 + r(t - L) + (\theta_0 - U_0 + rL)e^{-t/L}.$$

Now, if $t$ is large, the last term becomes negligible, and

$$\theta = U_0 + r(t - L) = U - rL \text{ (since } U = U_0 + rt),$$

which means that the thermometer, however long it has been in the enclosure, records a temperature less by $rL$ than the correct temperature, *i.e.* the temperature which existed L minutes previously.

To give some examples of the use of these figures :—

CASE 1. *Temperature of Ship's Hold rising and Observations taken with a Distant Reading Mercury Thermometer.*—Let us suppose the temperature is required at 12 noon on a certain day and that readings are taken at times 11.50 and 12.10, the values being 39·7° F. and 40·8° F. respectively. Since the lag of this particular thermometer is 18·28 minutes, the hold was at these temperatures at 11 hours 31·72 minutes and 11 hours 51·72 minutes respectively. It is rising at the rate of 1·1° in 20 minutes, and therefore in 8·28 it will rise 0·46° F. Thus, at noon the hold temperature is 40·8° + 0·46° = 41·3° F., whereas the mean of the thermometer readings was only 40·25° F.

CASE 2. *Temperature of Hold Steady : Observations taken by withdrawing a plain Mercury Thermometer.*—Assume that the mercury thermometer has had time to settle to

Digitized by Google

TABLE.—Error Introduced in the Determination of a Temperature if the Thermometer is first held for $t$ secs. at a Temperature N° Higher or Lower.

| $t$ secs. | Plain Mercury Thermometer. | | | | | | Spirit Thermometer. | | | | | Wood-encased Mercury Thermometer. | | | | |
|---|---|---|---|---|---|---|---|---|---|---|---|---|---|---|---|---|
| | N = | 40°. | 55°. | 60°. | 65°. | 80°. | 40°. | 55°. | 60°. | 65°. | 80°. | 40°. | 55°. | 60°. | 65°. | 80°. |
| 0 | | 0·00 | 0·00 | 0·00 | 0·00 | 0·00 | 0·00 | 0·00 | 0·00 | 0·00 | 0·00 | 0·00 | 0·00 | 0·00 | 0·00 | 0·00 |
| 10 | | 1·92 | 2·64 | 2·88 | 3·12 | 3·84 | 1·09 | 1·49 | 1·63 | 1·77 | 2·18 | 0·45 | 0·62 | 0·68 | 0·74 | 0·90 |
| 20 | | 3·76 | 5·16 | 5·64 | 6·10 | 7·52 | 2·15 | 2·96 | 3·23 | 3·50 | 4·30 | 0·91 | 1·25 | 1·36 | 1·47 | 1·82 |
| 40 | | 7·17 | 9·87 | 10·77 | 11·67 | 14·35 | 4·19 | 5·76 | 6·28 | 6·80 | 8·38 | 1·81 | 2·49 | 2·72 | 2·95 | 3·62 |
| 60 | | 10·25 | 14·10 | 15·38 | 16·66 | 20·50 | 6·12 | 7·65 | 9·18 | 10·71 | 12·24 | 2·65 | 3·65 | 3·98 | 4·31 | 5·30 |
| 120 | | 17·87 | 24·58 | 26·81 | 29·06 | 35·74 | 11·30 | 15·51 | 16·95 | 18·36 | 22·59 | 5·11 | 7·02 | 7·66 | 8·30 | 10·22 |
| 180 | | 23·54 | 32·37 | 35·31 | 38·25 | 47·08 | 15·70 | 21·59 | 23·55 | 25·51 | 31·39 | 7·43 | 10·22 | 11·15 | 12·08 | 14·86 |

*Note I.*—If the temperature to be observed is lower than the one in which the thermometer is read, the above corrections should be subtracted from the observed readings.

*Note* II.—The actual values above given are for a particular specimen of each type and would not be true for all thermometers of that type.

Digitized by Google

the temperature of the hold, is withdrawn at 11.50, and read 15 seconds later on deck, which is at 90° F.; withdrawn again at 12.10, but an interval of 20 seconds elapses before the reading is taken. Suppose the readings are 38·8° F. and 39·8° F. Then in the first case the value of N in the table is 90 — 39° = 51° F. and $t$ is 15 seconds. From the table the error is 3·8° F., so that the corrected reading is 35·0° F. For the second observation N is again 50°, but $t = 20$, so the error is 4·80° F. and the corrected value 35·0° F. This example illustrates the danger of assuming that the hold is rising in temperature merely by noting two readings without correcting for the lag error.

CASE 3. *Temperature of Hold rising: Observations taken by withdrawing the Spirit Thermometer.*—The case considered is that of a ship's hold at about 40° F. and the deck at 95° F.

The thermometer is withdrawn at 11.50 and read after a lapse of one minute and then replaced. The reading obtained is 39·7° F. It is then withdrawn again at 12.10 and read after a lapse of 40 seconds, the reading being 40·8° F. On correcting these observations for the rise after withdrawal by means of the above table, we get for the readings in the hold at 11.50 and 12.10 the values 39·7 — 7·65 = 32·05° F. and 40·8 — 5·76 = 35·04° F. respectively.

Now, the reading at 12 noon would appear to be the mean of these, viz., 33·54° F., but owing to the fact that the hold temperature is changing, the lag of the thermometer introduces an error in this also. For each of these temperatures existed L mins. previously (L in the case of this particular thermometer being 6·11 mins.), so that at 11 hrs. 53·89 mins. the hold temperature was 33·54° F. It is rising at the rate of (35·04° — 32·05°) in 20 mins., *i.e.*, 2·99° F. in 20 mins., so that at noon the correct value of the hold temperature was $33{\cdot}54 + 6{\cdot}11/20 \times 2{\cdot}99 = 34{\cdot}45°$ F.

CASE 4. *Conditions identical with Case 3 except that Wood's Pattern Lagged Thermometer was employed.*—Reading in hold at 11.50 corrected by table for the deck temperature

$$39{\cdot}7° - 3{\cdot}65° = 33{\cdot}05° \text{ F.}$$

Reading in hold at 12.10 corrected = 40·8° — 2·49° = 38·31° F.

Rate of rise = 38·31 — 33·05° = 5·26° F. in 20 mins.

Now, the thermometer lags behind the hold by 14·6 mins., therefore temperature of hold = 38·31° F. at a time 14·6 mins. before 12.10, *i.e.* at 11 hrs. 55·4 mins. A.M.

So the reading of the thermometer at 12.10 is still 4·6 mins. behind the true noon temperature of the hold.

$$\therefore \text{ Temperature of hold at 12 noon} = 38{\cdot}31 + 4{\cdot}6 \times \frac{5{\cdot}26}{20} = 39{\cdot}52° \text{ F.}$$

As a rule the temperature of the hold does not change at a notable rate, so the correction for change of temperature of the hold would be of negligible magnitude. Even in the above case it is only about 1°, while that due to the reading being taken on deck is of the order of 6° to 8° F.

The above examples have been constructed to illustrate variations of all conditions,



Digitized by Google

but for comparison of the various thermometers considered the following table is appended, showing the magnitude of the errors of each thermometer under the same conditions :—

*Error in determining the Temperature of a Space introduced by Lag Effects.*—

Rate of rise of store = 6° F. per hour.

Rate of fall for values in brackets ( ) = 3° F. per hour.

The thermometer is taken out at the time when the true temperature is required, and read after 40 seconds in a space where the temperature is 80° F.

| Thermometer. | Reading. ° F. | Error due to Withdrawal. ° F. | Error Due to Rise of Enclosure. ° F. | Total Error. ° F. | Corrected Value. ° F. |
|---|---|---|---|---|---|
| Plain mercury . . . . . | 46·3 | + 7·17 | — 0·34<br>(+ 0·17) | + 6·83<br>(+ 7·34) | 39·5<br>(39·0) |
| Spirit thermometer . . . . . | 43·1 | + 4·19 | — 0·61<br>(+ 0·31) | + 3·58<br>(+ 4·50) | 39·5<br>(38·6) |
| Wood's pattern lagged thermometer | 39·9 | + 1·81 | — 1·46<br>(+ 0·73) | + 0·35<br>(+ 2·54) | 39·5<br>(37·4) |
| Direct reading electrical thermometer . . . . . | 37·8 | — | — 1·73<br>(+ 0·86) | — 1·73<br>(+ 0·86) | 39·5<br>(36·9) |
| Distant reading mercury thermometer . . . . . | 37·7 | — | — 1·83<br>(+ 0·91) | — 1·83<br>(+ 0·91) | 39·5<br>(36·8) |

Digitized by Google

# SOME MODIFIED FORMS OF HYGROMETERS

BY

EZER GRIFFITHS, D.Sc., F.R.S.,
PRINCIPAL ASSISTANT IN THE PHYSICS DEPARTMENT.

Digitized by Google

## ABSTRACT.

The Paper describes experiments made with the object of developing suitable apparatus for the measurement of humidity at low temperatures. The three classical methods—the wet-and-dry bulb hygrometer, the dew-point apparatus, and the hair hygrometer—were studied and so modified that they could be used in a low-temperature room inaccessible to the observer.

The common form of wet-and-dry bulb hygrometer is notoriously unreliable, but the ventilated form is quite satisfactory provided the wind velocity past the bulb exceeds about 3 metres per second. A tubular form of wet-and-dry bulb hygrometer was developed with an electric fan for aspiring the air past the bulbs. A continuously recording, resistance thermometer type was also made, which had a cam device for rapidly dipping and withdrawing the thermometer bulb at periodic intervals from a reservoir of water.

The dew-point apparatus was modified into a form suitable for permanent installation, the cooling of the polished metal surface being effected by pipe connections to the cold brine circulation of the stores.

In another form a silver thimble, cooled by the evaporation of ether, was placed at one end of a long aluminium tube and a telescope at the other. By suitable arrangements of mirrors and lamps both the silver surface and the thermometer column were thrown into the field of the telescope. The end containing the thimble was inserted into the enclosure through a circular aperture. The instrument was portable and self-contained.

A distant reading type of dew-point apparatus was constructed, in which the formation of dew was indicated by the change of reflecting power of the cooled surface. A beam of heat radiation was reflected from the polished surface and concentrated on to a minute thermopile. The thermo-junctions were connected to a pivoted indicator situated at the observation station where the observer controlled the flow of cooling fluid by means of a solenoid valve. The formation of dew resulted in a sharp falling-off of the reflecting power and was indicated by the movement of the pointer of the instrument.

The hair hygrometer was studied under a variety of conditions and the changes in the calibration of this type of instrument, caused by exposure to low and high temperature, etc., were determined.

A very simple form of distant reading hair hygrometer was developed. In this the clockwork drum of the ordinary recorder was replaced by a tubular rheostat. The pointer was pressed into contact with the drum when a reading of the humidity was desired. The two portions of the resistance winding then constituted the two arms of a Wheatstone bridge.

A number of other forms of hygrometers were also studied, notably the one utilising the heating effect on dry cotton when exposed to a humid atmosphere.

A convenient form of apparatus for the calibration of hygrometers over a wide range of humidities is described. It consists essentially of a drum fitted with a heavy glass front making an air-tight joint. The drum contains an electric fan which circulates the air over a dish of desiccating agent. This method of reducing the humidity is more effective than bubbling through strong sulphuric acid and does not produce acid spray. The drying agent can be cut out of communication with the chamber by a ground glass cover operated by a lever projecting out of the drum.


Digitized by Google

# SOME MODIFIED FORMS OF HYGROMETERS.

By EZER GRIFFITHS, D.Sc., F.R.S., Principal Assistant in the Physics Department.

[Reprinted with modification from the 'Proceedings of the Physical Society of London', Vol. 34, 1922.]

## CONTENTS.

1. Apparatus for obtaining Variable Humidity.

2. Standard of Reference in Calibration Work on Hygrometers.

3. Wet and Dry Bulb Hygrometers of the Ventilated Type.

- (*a*) *Determination of velocity of air stream past the wet bulb.*
- (*b*) *Tubular psychrometer.*
- (*c*) *Experiments below* 0° C. *with the ordinary form of Assmann psychrometer.*
- (*d*) *Low-temperature distant-reading psychrometer.*

4. The Dew-Point Hygrometer.

- (*a*) *Temperature difference between the thermometer and silver surface.*
- (*b*) *Estimate of weight and thickness of dew deposit.*
- (*c*) *Industrial forms of dew-point apparatus.*
  - (i) *Wall fixture type.*
  - (ii) *Portable type.*
  - (iii) *Distant reading apparatus.*

5. The Hair Hygrometer.

- (*a*) *Reliability over long intervals of time.*
- (*b*) *Behaviour of the instrument when taken through a complete cycle of humidities.*
- (*c*) *Calibration at low temperature.*
- (*d*) *Influence of change of temperature from that of the room* (15° C.) *up to* 38° C.
- (*e*) *Accuracy of the engraved scale.*
- (*f*) *Relation between extension of hair and relative humidity.*
- (*g*) *Summary of conclusions concerning the hair hygrometer.*
- (*h*) *Distant reading type.*

6. Thermal Effect on Cotton Hygrometer.

- (*a*) *Previous work on heating of cotton by water-vapour absorption.*
- (*b*) *Electrical resistance type.*
- (*c*) *Apparatus utilising the effect for hygrometric measurements.*

7. The Hot-Wire Type Hygrometer.

## Introduction.

Humidity and temperature are two variables which have a profound influence on the physical properties of materials of organic origin. One has only to study such industrial processes as the seasoning of timber, the drying of raw rubber, or the preservation of foodstuffs, to appreciate the necessity for control over both the humidity and the temperature of the surrounding atmosphere.

Digitized by Google

As regards the measurement of temperature, there are available at the present time a variety of reliable instruments which can be adapted to meet most requirements. Such a satisfactory state of affairs does not exist as regards the measurement of humidity. Yet the importance of a knowledge of the hygrometric state of the atmosphere appears to have been recognised from an early date. As far back as 1783 DE SAUSSURE devised the hair hygrometer, while DANIELL invented the dew-point hygrometer in 1827.

The origin of the familiar wet-and-dry bulb hygrometer is not quite certain. It is stated that Sir JOHN LESLIE in 1813 converted his differential air thermometer into a form of hygrometer by keeping one bulb wet and the other dry, and observing the temperature difference.

The simplicity of the wet-and-dry bulb mercury hygrometer has led to the adoption of this instrument to the exclusion of practically all other types of hygrometers in meteorological and industrial work. The conservative attitude of scientific workers in this respect is greatly to be deplored, for it is now generally admitted that the instrument in its elementary form is very inaccurate.

It is a curious fact that no fundamentally new method of hygrometry has since been introduced, and the above instruments have remained the sole physical appliances available for routine tests. It is true that innumerable proposals have been made concerning novel hygrometric devices. Usually, however, such instruments are put forward without receiving adequate experimental investigation, and it often happens that humidity is but one of the many factors in operation.

The investigation described in the present paper arose from an inquiry for suitable apparatus for use in measuring the humidity of the air in cold stores. It was considered that the design of the standard form of laboratory apparatus was unsuitable for this purpose, particularly when it was desired to measure the humidity without actually entering the room.

With the object of meeting these special requirements a study was first made of the three standard methods of hygrometry :—

(1) The ventilated wet-and-dry bulb hygrometer.
(2) The dew-point apparatus.
(3) The hair hygrometer.

In the course of the work other methods of measuring humidity were also studied.

But before passing on to the description of the various appliances for the measurement of humidity it is necessary to consider the means available for adjusting to any desired value the humidity within a closed space. For it is essential in calibration work to be able to vary the humidity over a wide range without being dependent upon climatic conditions.

### 1. APPARATUS FOR OBTAINING VARIABLE HUMIDITY.

The problem of humidity control is not difficult if only comparatively small volumes of air have to be considered, but when it becomes necessary to vary the humidity in a

Digitized by Google

space of, say, 10 cubic metres in capacity, it becomes a troublesome matter, especially if an observer has to enter the room.

Since the experiments were primarily concerned with temperatures near 0° C., a sheet iron enclosure was constructed within a cold stores room. In this enclosure an electric fan was fitted to keep the air in rapid circulation. If a humidity value below normal was required, the air was circulated over granulated calcium chloride. This salt was spread out on lead trays so inclined that the liquid drained off to reservoirs beneath.

With this arrangement it was possible to maintain a humidity as low as 45 per cent. with the observer in the room. The presence of the observer is a serious hindrance to the maintenance of a low humidity at a low temperature, for the quantity of water required to saturate a cubic metre of air at 0° C. is only 4·84 grammes, and the average human being gives off 63 grammes of water per hour when in repose and considerably more when exercising.* Hence it will be realised that very efficient methods of water vapour absorption must be employed if the humidity is to be maintained at a low value.

When it is practicable to carry out experiments in a closed vessel of moderate dimensions, then the problem becomes decidedly simpler. For instance, with some types of hygrometers it is possible to make observations without the necessity of manipulating the instruments or aspirating considerable volumes of air out of the enclosure. Such is the case with the hair hygrometer, the dew-point apparatus, and the refractive index of glycerine method. For some experiments the apparatus shown in Fig. 1 has been found to work admirably.

### *Description of Apparatus.*

The apparatus consists of a sheet metal vessel 14 inches in diameter by 18 inches in length, closed by a piece of plate glass clamped down on a soft rubber packing so as to give an air tight joint. A small electric fan is fixed in the drum, and is switched on when it is desired to mix the air in the vessel before an observation. The humidity of the atmosphere inside the drum is varied by the aid of a lead dish containing strong sulphuric acid. The fan drives the air over the exposed acid surface and the humidity can be rapidly lowered. When the required point has been reached, the dish is closed by a weighted glass cover carried from a rod. This is operated from without the enclosure. The humidity of the atmosphere can be raised by blowing in a little steam or merely by breathing into the drum through a piece of rubber tubing.

Driving the air by means of the fan over the exposed acid surface is a far more effective method of changing the humidity than by pumping the air round through wash bottles containing acid. This latter method was tried, and abandoned on account of its extreme slowness.

* About 1 gramme per kilogramme of adult human body per hour in repose. This quantity is extremely variable; the slightest exercise increases it enormously.—'Recueil de Constantes Physiques', Société Française de Physique, p. 740.

Digitized by Google

Instead of sulphuric acid, caustic potash in the form of sticks can be used as a desiccating agent, and with fresh material, humidities as low as 10 per cent. are readily obtained.

An objection to the use of sulphuric acid is that it decomposes any organic dust which comes into contact with it, and, in the course of the reaction, it seems probable that minute traces of acid gases, such as sulphur dioxide, are generated.

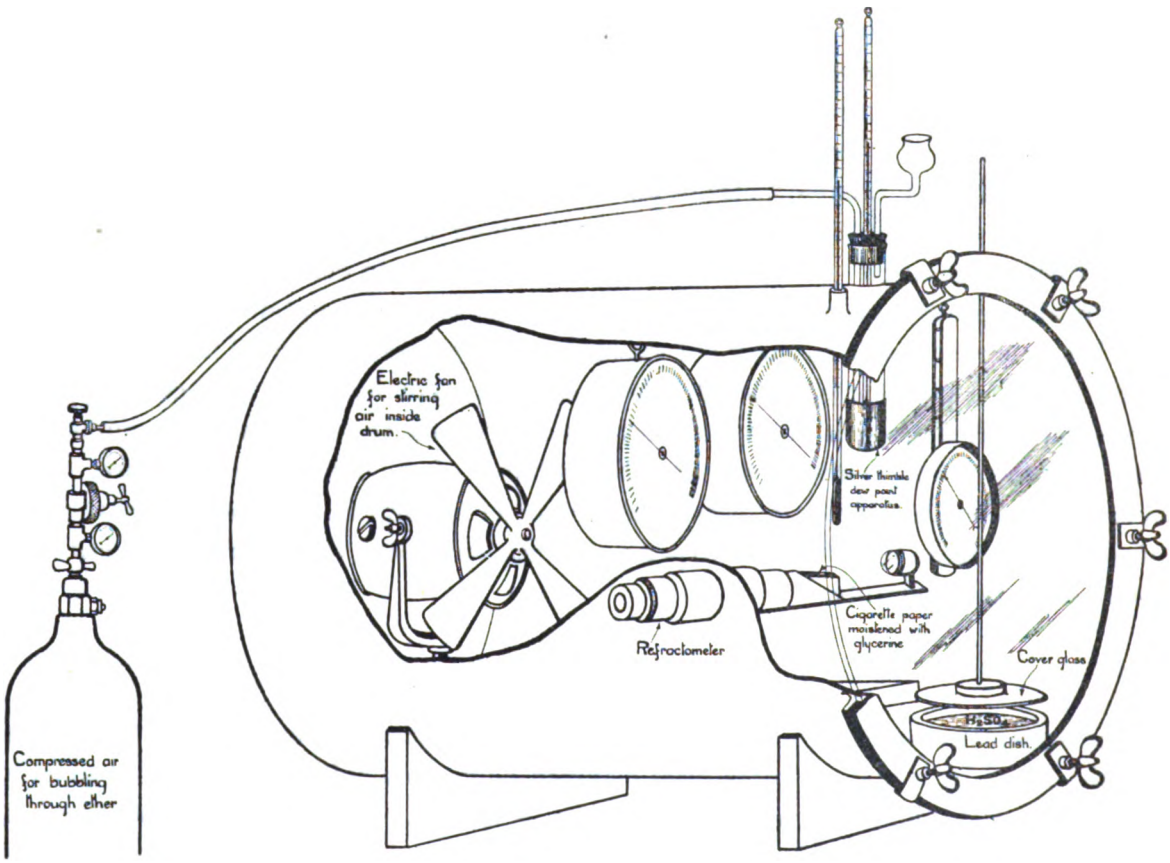


FIG. 1.

While we have not been able, by tests with blue litmus paper, to detect any gas of an acid nature in the atmosphere within the drum, we do not deem it advisable to expose instruments for a prolonged period to air which has been in contact with acid, for the reason mentioned above.

With the simple arrangement illustrated in Fig. 1 humidities down to 5 per cent. can be obtained with ease. To determine the actual value of the humidity a dew-point apparatus is installed as shown in the diagram. This consists of a silver thimble soldered on a piece of glass tubing. Air is bubbled through the ether and the temperature of the appearance and disappearance of the dew observed.

In our experiments this apparatus has worked satisfactorily over the range of temperatures from — 8° C. to + 40° C. When studying the behaviour of the instruments in atmospheres of very low humidities, the dew-point was lowered as far as — 28° C.,

Digitized by Google

a depression of 21° C. below the air in the enclosure. Even with these extreme conditions the method was workable, and under the circumstances it would have been impossible to employ the chemical method.

In addition to the dew-point method a special form of Abbé refractometer was tried, so as to obtain the humidity on a direct reading scale. This instrument will be seen projecting in from the left-hand side. The prism and the telescope are rigidly fixed and the refractive index read from a scale in the eye-piece. The surface of the piece of cigarette paper, moistened in glycerine,* is illuminated by the small bull's-eye electric lamp.

The procedure in making the tests was to bring the air to the desired humidity approximately, close the sulphuric acid vessel (the top of the lead vessel and the plate had been ground to a good fit), and allow the fan to run for some time to mix up the contents of the drum thoroughly. After an interval the fan was stopped, the instrument read, and the dew-point observed.

Another method of obtaining air of a definite humidity is to bubble through $H_2SO_4$ solution of appropriate density. The advantage of this procedure is that it is not necessary to determine the humidity, but only to ensure that the moisture content of the air is that of the partial vapour pressure corresponding to the strength of sulphuric acid solution employed. The usual procedure is to bubble the air at the rate of 50 cc. to 100 cc. per minute through two or three wash bottles in series.

An essential precaution in the use of this method is to pass the air through a tube rather tightly packed with glass wool, so as to remove the particles of sulphuric acid carried over by the air stream.

This tendency of the acid spray to be carried over when bubbling air through the solution is troublesome to overcome. For example, in attempting to obtain air of definite humidity in a large cylindrical vessel by bubbling air through a layer of acid in the bottom, it was found that the air near the top of the vessel and at a distance of 18 inches from the liquid surface was acid in reaction to litmus paper. This feature rendered the method impracticable for the experiments described in this paper.

For studying the humidity equilibria of various substances which can be packed into U-tubes of small capacity, the above method appears to be quite satisfactory, and it might be observed that accurate control of the temperature is not very important, since the moisture content of most organic materials varies but little with moderate changes in temperature, providing the relative humidity is maintained constant.

Reference to Table I shows that for a temperature change of about 10° C. the relative vapour pressure of most of the solutions is practically constant; it must not, however, be supposed that constant humidity conditions will be maintained in a closed space when subject to temperature change unless the temperature of the entire apparatus is

* A solution of glycerine will evaporate or condense water vapour from the surrounding atmosphere until the concentration of the solution is such that it is in equilibrium with the aqueous vapour pressure prevailing. —(GIRAUD).



Digitized by Google

uniform throughout. Local irregularities of temperature produce very serious errors if diffusion is depended upon for equalising the humidity. Hence in precision work it may be assumed that thermostatic control over the temperature of the space is necessary.

TABLE I.—Strength of $H_2SO_4$ required to Give Definite Humidities.

| Relative Humidity. | Per cent. Sulphuric Acid required at | | | |
|---|---|---|---|---|
| Per cent. | 0° C. | 25° C. | 50° C. | 75° C. |
| 10 | 63·1 | 64·8 | 66·6 | 68·3 |
| 25 | 54·3 | 55·9 | 57·5 | 59·0 |
| 35 | 49·4 | 50·9 | 52·5 | 54·0 |
| 50 | 42·1 | 43·4 | 44·8 | 46·2 |
| 65 | 34·8 | 36·0 | 37·1 | 38·3 |
| 75 | 29·4 | 30·4 | 31·4 | 32·4 |
| 90 | 17·8 | 18·5 | 19·2 | 20·0 |

NOTE.—The values given in the above table were computed by R. E. WILSON from the experimental data of REGAULT, SOREL, HELMHOLTZ, BRONSTED and DIETERICI (see 'J. Ind. Eng. Chem.', vol. 13, p. 326,1921).

An analogous method for use at higher temperatures is that employed in the Freas oven. This oven is designed with shelves on which suitable crystals containing water of crystallisation are placed. An air-circulating device is arranged so as to sweep air over these crystals, thus maintaining a humidity content corresponding to the dissociation vapour pressure of the water of crystallisation. An essential condition is that the chemical must be present in both the anhydrous and crystallised forms.

When the moisture content of the air becomes too great, owing to the material in the oven giving off a great deal of moisture, then the anhydrous salt will remove some of it, and be converted to the crystalline form. On the other hand, if the air is too dry, the crystallised form will furnish the moisture required. Adjustment of the salt to the required state is effected by drawing unsaturated air over the chemical when the crystal form is in excess, and saturated air when the anhydrous form is in excess. It is stated that such treatment for an hour or so will prepare a mixture of the chemical in the proper proportion of crystal and anhydrous form for rendering it successful for maintaining constant humidity.

By this method it is possible to obtain a range of humidity up to temperatures as high as 80° C., but, of course, it is advisable to control the temperature by a thermostat arrangement.

In Table II some figures are quoted from the catalogue of Messrs. EIMER and AMEND to indicate the possibilities of the method.

Digitized by Google

TABLE II.—Dissociation Tension with Loss of Water of Crystallisation.

| Temperature ° C. | Tension of Water Vapour. | Tension of Water Vapour. | | | |
|---|---|---|---|---|---|
| | | $CuSO_4$, $5H_2O$ | $MgSO_4$, $7H_2O$ | $ZnSO_4$, $7H_2O$ | $FeSO_4$, $7H_2O$ |
| | mms. | mms. | mms. | mms. | mms. |
| 20 | 17·4 | 6·0 | — | 10·1 | 10·9 |
| 30 | 31·5 | 11·6 | 27·0 | 20·2 | 20·3 |
| 40 | 54·9 | 22·4 | 47·2 | 44·2 | 40·1 |
| 50 | 92·0 | 42·0 | 75·7 | 73·1 | 74·8 |
| 60 | 148·9 | — | 122·5 | 113·9 | 131·3 |
| 70 | 233·3 | — | 186·0 | 170·8 | 205·2 |
| 78 | 327·0 | 234·0 | — | 258·5 | 321·9 |

## 2. STANDARD OF REFERENCE IN CALIBRATION WORK ON HYGROMETRY.

In calibration work it is generally accepted that the chemical method is the ultimate standard of reference.

In our early experiments at low temperatures we found the chemical method exceedingly tedious to operate. There was also the fact that the absolute weight of water, for a given percentage of humidity, was considerably reduced at low temperatures; and difficulties were encountered owing to dew deposition on the weighing tubes, etc. So, although it was possible with care to obtain a reasonable degree of accuracy by this method, we were soon forced to seek for more expeditious appliances for calibration work.

Of the three physical methods of hygrometry, the dew-point apparatus stands out conspicuously as being the one instrument which has a sound theoretical foundation and, further, it has the practical advantage that it is as easy to manipulate at low temperatures as at room temperatures. After a lengthy experience with the various methods under the most diverse conditions, we have come to the conclusion that the dew-point is the most convenient of all methods for low-temperature work, and, consequently, it has been employed as standard of reference for most of the work recorded in this paper.

## 3. WET-AND-DRY BULB HYGROMETER OF THE VENTILATED TYPE.

Whilst the unventilated type of wet-and-dry bulb hygrometer is a notoriously unreliable instrument, it does not appear to be sufficiently well known that by so modifying the construction that air at a definite velocity is drawn past the thermometer bulbs it can be converted into an instrument of satisfactory precision.

This important fact was demonstrated by the Italian physicist BELLI in 1830, and in view of the simplicity of the device it is somewhat surprising that the stationary form of wet-and-dry bulb hygrometer is tolerated at all at the present day.



Digitized by Google

In the familiar equation* for the wet-and-dry bulb hygrometer,

$$p = p_w - \mathrm{AP}(t - t_w),$$

where $t$ = air temperature.

$t_w$ = wet-bulb temperature.

$p$ = pressure of aqueous vapour in the air.

$p_w$ = saturation vapour pressure at the temperature of the wet bulb.

P = barometric pressure.

A = a quantity which for the same instrument and certain conditions is constant, or a function depending in a small measure on $t_w$.

The value of A differs materially according to whether the wet bulb is in quiet or in moving air; it is in this connection that the use of a forced air-stream past the bulb becomes of fundamental importance. In theory the value of A depends upon the size and shape of the thermometer bulb, size of stem, and velocity of the ventilation; so that different formulæ are required for different forms of instruments. But using an air velocity exceeding about 3 metres per second, the differences in the results given by different instruments vanish, and the same tables can be adapted to any kind of thermometer, and to all changes of velocity above that which gives sensibly the greatest depression of the wet-bulb temperature; and with this arrangement there is no necessity to measure or estimate the velocity in each case further than to be certain that it does not fall below the assigned limit.

It is not difficult to obtain sufficient velocity of the air past the bulbs, since all that is necessary is to fix the two thermometers securely on a rod and swirl them round. Espy at a very early date noted the advantage of this procedure, for he states: "When experimenting to ascertain the dew-point by means of a wet bulb, I always swung both thermometers moderately in the air, having first ascertained that a moderate movement produced the same depression as a rapid one".†

The most popular form of ventilated wet-and-dry bulb hygrometer is the Assmann type. In this the two thermometers are fixed alongside each other in two tubes, and a clockwork-driven fan sucks air past the bulbs. Before each series of observations the instrument requires winding up, and the muslin sack around the wet-bulb thermometer needs moistening with distilled water.

* Attempts have been made by various scientists to deduce from theoretical considerations the relation between the vapour pressure of the aqueous vapour in the air and the difference of temperature between the dry and the wet bulbs. Not one of these is satisfactory, and the simplest plan is to use an empirical equation of the above form.

† Smithsonian Meteorological Tables, 4th edition, 1918.

Digitized by Google

Tables* are published covering the temperature range from — 30° C. to + 40° C. for converting the readings into relative humidity; the same operation can be performed graphically.

We have made a large number of observations with this form of hygrometer, and compared its indications with those of a dew-point apparatus. At room temperature its readings agreed with those of the dew-point apparatus within 1 to 2 per cent., but at low temperatures the divergence was greater on account of the disturbance caused by the observer when reading the thermometers at close quarters. The actual data will be found in Columns 4 and 5 of Tables IX and XIII.

The following observations may also be quoted as illustrating the degree of concordance obtained with three ventilated psychrometers obtained from various sources (Continental and British) when compared with a dew-point apparatus. In each case, of course, corrections were applied to bring the mercury thermometer readings to true temperature.

TABLE III.—Psychrometer Readings.

| Instrument No. | Wet-bulb temperature. ° C. | Dry-bulb temperature. ° C. | Relative humidity. |
|---|---|---|---|
| 1 | 13·3°<br>13·5° | 17·3°<br>17·8° | 64 per cent.<br>62 „ |
| 2 | 13·6°<br>13·8° | 17·2°<br>17·9° | 67 „<br>64 „ |
| 3 | 13·6°<br>13·9° | 17·5°<br>18·1° | 65 „<br>63 „ |

*Dew-point Apparatus.*

| Air temperature. ° C. | Dew appears. ° C. | Dew disappears. ° C. | Mean reading. ° C. | Relative humidity. |
|---|---|---|---|---|
| 17·2°<br>17·8° | 10·15°<br>10·55° | 10·35°<br>10·65° | 10·25°<br>10·6° | 63·7 per cent.<br>62·7 „ |

### (*a*) *Determination of Velocity of Air Stream past the Wet Bulb.*

It is always advisable to test an instrument to ensure that the velocity of the air stream past the bulb is of the order of 3 metres per second. This can be effected by connecting on to the tube surrounding the wet bulb a glass tube, and determining the speed of a puff of smoke along the glass tube. An alternative method is to measure the velocity in the extension tube by means of a Pitot tube and sensitive gauge, making corrections for the relative cross-sections of the extension tube and annular space around

* Aspirations—Psychrometer—Tafeln. Published Vieweg, Braunschweig.

Digitized by Google

the bulb. Since only an approximate check is usually necessary, the smoke method is quite effective.

One practical defect of the Assmann design is the possibility of water being squirted over on to the dry bulb when saturating the sack around the wet bulb. This, of course, vitiates the readings.

### (*b*) *Tubular Psychrometer.*

We constructed a modified form of instrument which permitted of observations being taken without the observer entering the room. In this arrangement an electric fan aspired the air past the bulbs contained in a steel tube 2·7 cms. in diameter and 70 cms. long. The complete instrument is shown in Fig. 2. The motor was directly connected to the 100-volt supply, and took 0·1 of an ampère. After once moistening the sack around the wet bulb, the instrument would continue to operate for 40 minutes without attention.

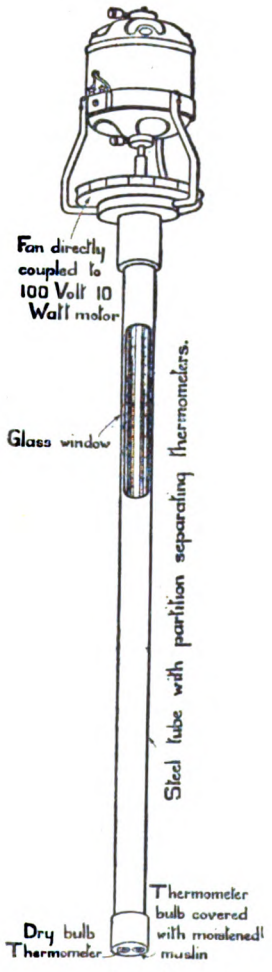
Fan directly coupled to 100 Volt 10 Watt motor
Glass window
Steel tube with partition separating thermometers.
Thermometer bulb covered with moistened muslin
Dry bulb Thermometer

FIG. 2.

### (*c*) *Experiments below* 0° C. *with the ordinary form of Assmann Psychrometer.*

At temperatures below 0° C. the water freezes on to the muslin bag, but the instrument still operates fairly satisfactorily.

In order to obtain the data necessary for the design of a distant reading wet-and-dry bulb instrument, which would act automatically and could be placed at a considerable distance from the recording station, some observations were made with a standard mercury thermometer type of Assmann psychrometer. In these experiments the instrument was set up in the cold stores room and observations taken at intervals for a period of $3\frac{1}{2}$ hours, the observer entering the room occasionally to wind up the clockwork and read the thermometers. Reference to Fig. 3 will show the curves obtained.

Initially, both bulbs were dry, and at approximately the same temperature (about — 3·5° C.). The muslin around the wet bulb was moistened with water, whose temperature was above 0° C., and the fan started. The reading of the thermometer then dropped quite rapidly to — 4·4° under the influence of the air current. It will be observed from an inspection of the data in Fig. 3 that the temperature fell to this value in $3\frac{1}{4}$ minutes. At this point, apparently, the under-cooled water froze and the temperature rose sharply to 0° C. Then the frozen mantle cooled down and acquired an equilibrium temperature about 1° below the dry bulb after an interval of 10 minutes from the time of the initial moistening. From this point forward for a period of about two hours the difference between the two thermometers was practically constant. In Fig. 3

Digitized by Google

the time scale after the first 10 minutes is contracted up so as to include the respective temperatures over a long interval of time. The violent oscillations of temperature were due to the observer going in and out of the cold stores room and disturbing the thermometers when winding the clockwork at intervals of about 10 minutes.

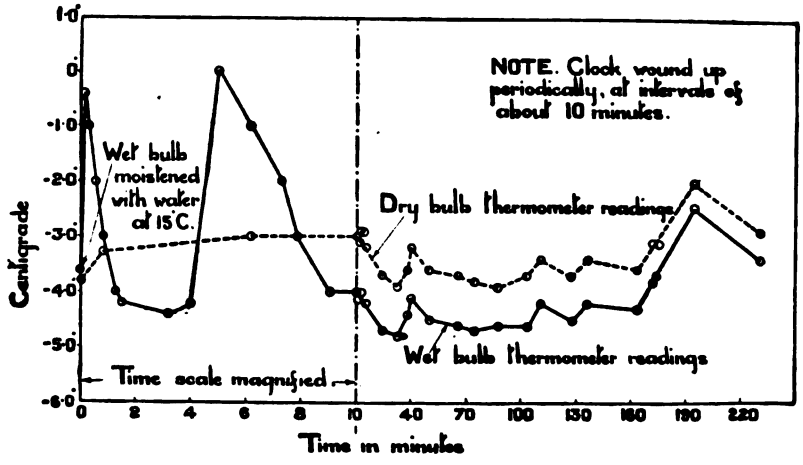
NOTE. Clock wound up periodically, at intervals of about 10 minutes.
Wet bulb moistened with water at 15°C.
Dry bulb thermometer readings
Wet bulb thermometer readings
← Time scale magnified →
Centigrade
Time in minutes

FIG. 3.

*(d) Low Temperature Distant Reading Psychrometer.*

From the results of the above experiment it appeared that saturating muslin in water at intervals of from 1 to 2 hours would suffice, so the problem resolved itself to devising a mechanical device by means of which the wet bulb could be periodically saturated with water. It was, of course, necessary to maintain the water into which the bulb was dipped at a temperature above 0° C. by the use of a small heating coil. It would have been easy to perform the dipping by a clockwork arrangement, but since an electric fan was required for producing an air stream past the bulbs, it was decided to utilise the same motor for operating the dipping mechanism.

The essential condition to be complied with was that, at the desired instant, the thermometer should be plunged into the water fairly rapidly, kept there for a period sufficient to ensure that any residual ice was melted, then withdrawn sharply and restored to its normal position in front of the fan. To effect this motion the arrangements shown in Figs. 4 and 5 were constructed. The resistance thermometer is carried

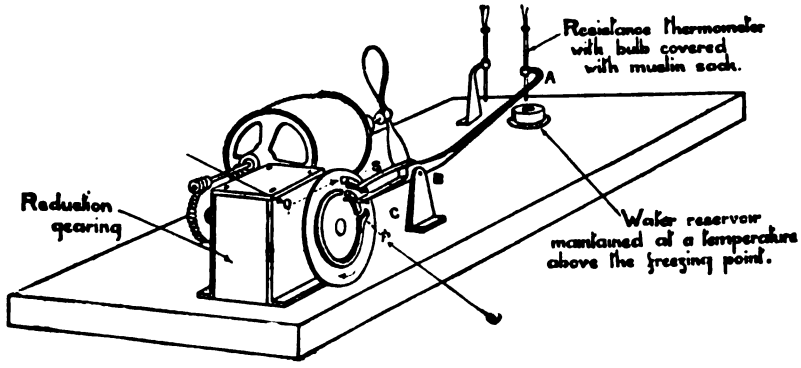
Resistance thermometer with bulb covered with muslin sock.
A
Reduction gearing
Water reservoir maintained at a temperature above the freezing point.

FIG. 4.

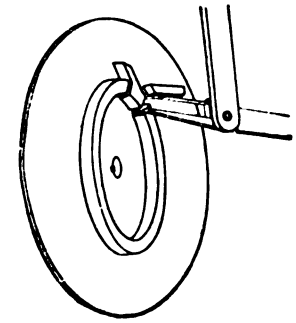

FIG. 5.

Digitized by Google

from the end A of the arm AB. This arm prolongs to C, where it terminates in a small pin projecting out at right angles to the arm. Parallel to this extension BC is a spring S, with a pin projecting at its end. BC and S are situated in front of the face of a disc. This disc is rotated at the rate of one revolution per two hours by means of the reduction gearing from the motor. A square section ring projects out from the plane of the disc, which has two slots cut in it. In the ordinary way, the pin C rides on the inner or outer circumference of this projecting ring. On the face of the disc are two inclined planes O and P. In the course of the rotation the pin at the end of the spring comes into contact with the inclined plane O. It travels up the plane, and the spring is thereby depressed towards the centre of the disc. The compression of the spring tends to rotate the arm AB and, consequently, when the pin C comes opposite the slot it slips through, and end A of the arm AB is raised. Referring to Fig. 4, the arm is shown in the position when the pin C has just slipped through the slot.

During the next period of rotation the pin C rides upon the inner circumference of the ring and the thermometer remains stationary in the air breeze. When the disc has nearly made a complete revolution, the pin projecting from the spring S comes into contact with the inclined plane P, set at such an angle as to pull away from the centre of the disc. Consequently, when the pin C reaches the slot, it passes through from the inner to the outer circumference of the projecting ring. In so doing the point A is depressed, and the thermometer bulb plunges into the water.

For the comparatively short period that the pin C is travelling on the outside circumference of the projecting ring the bulb remains immersed in the water. As the rotation of the disc continues, the pin at the end of the spring travels up the inclined plane O, and the compression of the spring forces the pin C through when it arrives opposite the slot, thus withdrawing the thermometer from the water.

In Fig. 5 the same arrangement is shown in a slightly modified form. Here the pin C rides on the outer circumference of the ring when the thermometer is in the " up " position.

The rest of the apparatus needs no detailed description. The resistance thermometers were constructed with very small compact bulbs, as the amplitude of the motion was limited. The condensation of moisture within the sheaths on the thermometer coils had to be guarded against by careful sealing. In our experiments the wet and dry bulbs were connected up differentially to a thread recorder.

A distant reading hygrometer of this character does not involve much more apparatus than is necessary for the recording of temperature by the use of a resistance thermometer outfit, since the expensive items of both equipments are identical.

### 4. The Dew-Point Hygrometer.

Although numerous attempts have been made to formulate some consistent theory for the wet-and-dry-bulb hygrometer, the nature of the assumptions which have to be

Digitized by Google

made are such that the resulting formulæ will not stand experimental test. The dew-point method, on the other hand, is based on straightforward physical facts, and the theory is so simple that it inspires confidence in the results obtained with the instrument.

For our requirements it was necessary to be able to operate the hygrometer in a somewhat confined space, and we developed, after a few preliminary experiments, the form shown in Fig. 6. The polished silver thimble contains the thermometer and tubes for bubbling air through the ether. This is situated in the lead-lined box cut diagonally as shown. By oscillating the lower half of the box it is possible to ensure that an average sample of air is obtained. The box is then closed and the observer sets the air bubbling and watches the formation of the dew through the double windows in front. The use of a box around a dew-point apparatus has the great advantage that it practically eliminates the disturbing influence of the observer in the vicinity of the apparatus, and this is a most important factor in low-temperature work, for it will be remembered that less than 5 gms. of water will saturate a cubic metre of dry air at 0° C.

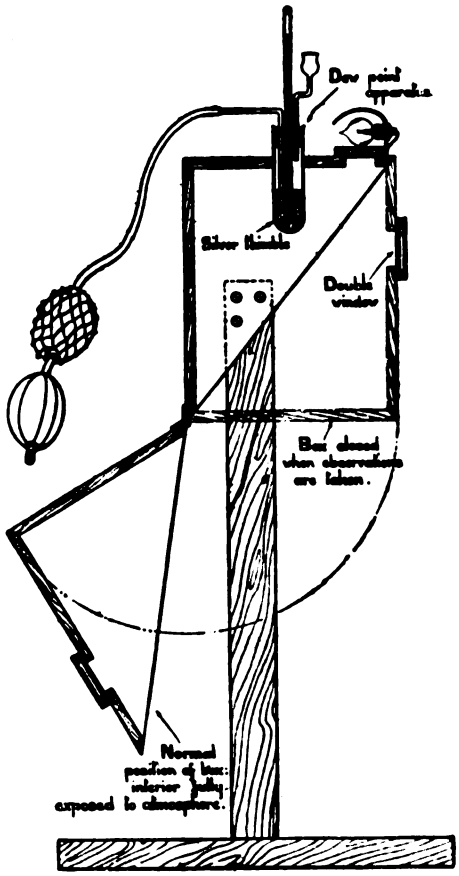
Dew point apparatus
Silver thimble
Double window
Box closed when observations are taken.
Normal position of box: interior fully exposed to atmosphere.
FIG. 6.

The box method has the additional advantage that it eliminates the disturbances of convection currents and draughts in the room.

### (a) *Temperature Difference between Thermometer and Silver Surface.*

A point of importance in connection with the method is the measurement of the difference in temperature between the thermometer in the ether and that of the external surface of the thimble on which the dew is deposited.

To ascertain the magnitude of this a differential couple was made up of copper-constantan. One junction was soldered to the surface of the silver thimble and the other attached to the bulb of the thermometer. The difference of temperature between the two junctions was observed at successive time intervals by means of a potentiometer.

Two forms of apparatus were tested; in the one the silver cup was soldered on as a prolongation of a glass tube, whilst in the other the cup was cemented on to a close glass tube by means of plaster of Paris. This second method of fixing is, of course, not to be recommended, but we have found it employed in apparatus sold for teaching purposes. The glass and plaster are poor heat conductors and often the defect is aggravated by the plaster not being a continuous layer but full of air bubbles.



Digitized by Google

The results obtained in the two experiments are shown graphically in Fig. 7. The upper curves refer to the temperature of the ether during the period of cooling and warming up, while the lower curves are the readings of the differential couples. It will be observed that in the case of the thimble attached by plaster of Paris the surface of the silver is 0·8° C. warmer than the ether when dew forms and about 0·4° C. when it disappears. The soldered thimble, on the other hand, is only 0·28° C. warmer when dew appears and 0·35° C. when it disappears.

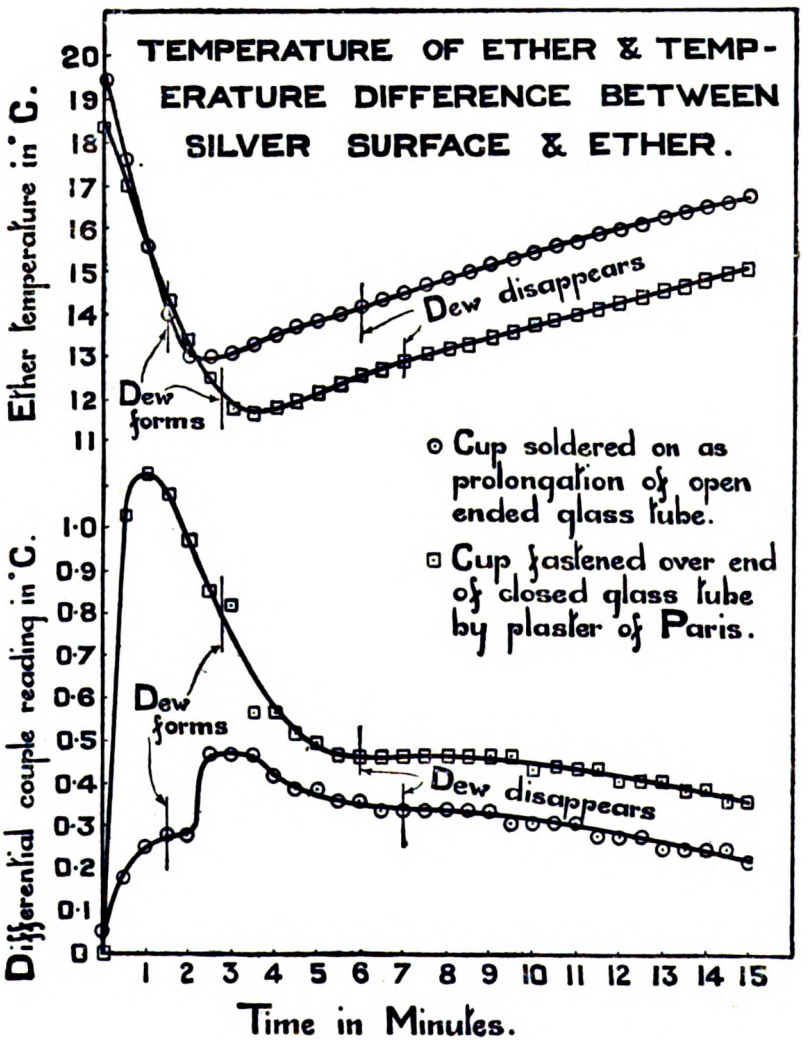


Fig. 7.

We found it advisable in practice to bubble air through the ether at intervals in the period when dew had formed and the temperature was slowly rising until it disappeared. By a little practice it was possible to mix the ether without causing appreciable evaporation.

Digitized by Google

### (*b*) *Estimate of Weight and Thickness of Dew Deposit.*

Another question of considerable interest in connection with the dew-point method is the estimation of the weight of deposit required to give a visible indication of its presence on the surface.

Such estimates were arrived at by several independent methods and observers.*

(1) *By Weighing a Film.*

(*a*) A silver thimble of 17·4 sq. cms. area was weighed, cooled down, exposed to the atmosphere of the room until a deposit appeared, sealed in a weighing-jar and again weighed.

The following results were obtained in a series of experiments :—

TABLE IV.

| Experiment. | Weight of Deposit. |
|---|---|
| 1 | 0·0016 |
| 2 | 0·0013 |
| 3 | 0·0011 |
| 4 | 0·0009 |
| 5 | 0·0008 |
| 6 | 0·0012 |
| | Mean 0·0011 |

Hence the weight of deposit per square centimetre $= 6{\cdot}3 \times 10^{-5}$ gm.

Results of the same order were obtained by another method. In this a film was deposited directly on the balance pan by breathing on it. The change of the equilibrium position of the pointer of the balance was observed by the usual method of oscillations. The pointer deflection scale was calibrated by noting the effect of changes in position of the rider. It was found that with no film the calculated zero would be in a certain position. A film altered the zero and, as the film gradually disappeared, the pointer gradually returned to its old zero. As the day was a wet one the rate of evaporation was not unduly great, being about 0·5 milligram per complete oscillation.

About four-fifths of the balance-pan area was covered with deposit equivalent to an area of 55 sq. cms.

The following results were obtained :—

TABLE V.

| Experiment. | Weight of Deposit. |
|---|---|
| | gm. |
| 1 | 0·005 |
| 2 | 0·006 |
| 3 extra heavy film | 0·008 |
| 4 slight film | 0·002 |

* I am indebted to my colleague, Dr. A. H. DAVIS, for most of the observations on weight of dew deposition.



Digitized by Google

Thus the mass of water deposit per square centimetre lies between $3 \cdot 6 \times 10^{-5}$ gm. and $14 \times 10^{-5}$ gm. for slight and thick deposits respectively.

(2) *By Interference Colours.*

A film was obtained by breathing on a piece of platinised glass. With relatively thick films rather impure colours were visible, such as reddish-brown.

Assuming these to be due to the usual interference effects with thin films, it appears that the thickness in this case is of the order of three or four wave-lengths of light.

So the mass of water per square centimetre of surface would be about

$$24 \times 10^{-5} \text{ gm.}$$

(3) *From Water Vapour in one Breath.*

In normal breathing a person takes 16 breaths per minute, or $2 \cdot 3 \times 10^4$ per day.

The total weight of water breathed out per day on the average is about 10 oz. = 300 gms. Hence the weight of water in one *normal* respiration is

$$\frac{300}{2 \cdot 3 \times 10^4} = 1 \cdot 3 \times 10^{-2} \text{ gm.}$$

One ordinary breath will dew over an area of 100 sq. cms. Hence, assuming all the water in the breath is deposited, the weight per square centimetre becomes

$$13 \times 10^{-5} \text{ gm.}$$

An alternative method of obtaining a similar estimate is to consider a *full* breath.

A full breath includes

| | Cub. ins. |
|---|---|
| Tidal air .. .. .. .. .. | 30 |
| Complementary air .. .. .. .. | 100 |
| Supplementary air .. .. .. .. | 100 |
| Total .. .. .. .. .. | 230 |

This total, together with the 100 cubic inches of residual air which always remains in the lungs, makes up the total lung capacity of 330 cubic inches.

In a normal respiration a person breathes out 30 cubic inches which, as shown above, contains $1 \cdot 3 \times 10^{-2}$ gm. of water.

Assuming a *full* breath to contain a correspondingly larger weight of water, we have for the weight in a full breath

$$1 \cdot 3 \times 10^{-2} \times \frac{230}{30} = 0 \cdot 1 \text{ gm.}$$

Digitized by Google

The area dewed over by a full breath is roughly 1,000 sq. cms. Hence, if all water vapour is deposited, the thickness of the film is $10^{-4}$ cm., and the mass of water vapour per square centimetre is $10 \times 10^{-5}$ gm.

Now 1 cc. of air saturated with water vapour at 20° C. contains $1 \cdot 7 \times 10^{-5}$ gm., and at 0° C. $0 \cdot 48 \times 10^{-5}$ gm. So that we can calculate from the above estimates the volume of dry air that the weight of water in the film would saturate.

TABLE VI.

| Method. | Magnitude of dew film expressed as— | | |
|---|---|---|---|
| | Gms. per sq. cm. | Ccs of dry air that dew on 1 sq. cm. of the surface would saturate— | |
| | | At 20° C. | At 0° C. |
| Weighing :— | | | |
| (*a*) Normal film . . . . . | $6 \cdot 3 \times 10^{-5}$ | 4 | 13 |
| (*b*) Slight film . . . . . | $3 \cdot 6 \times 10^{-5}$ | 2 | 7 |
| (*c*) Heavy film . . . . . | $14 \times 10^{-5}$ | 8 | 29 |
| Interference colours . . . . . | $24 \times 10^{-5}$ | 14 | 50 |
| Respiration :— | | | |
| (*a*) Full breath . . . . . | $10 \times 10^{-5}$ | 6 | 21 |
| (*b*) Ordinary breath . . . . | $13 \times 10^{-5}$ | 7 | 27 |

### (*c*) *Industrial Forms of Dew-Point Apparatus.*

#### (i) *Wall Fixture Type.*

The apparatus shown in Fig. 6 is hardly suitable for routine use in cold stores, so for this purpose we developed the form illustrated in Fig. 8. Here the silver thimble

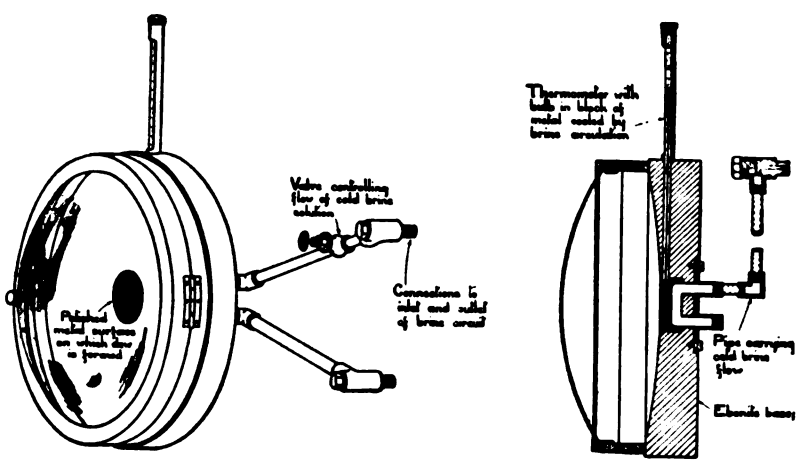

FIG. 8.

is replaced by a nickel-plated block of copper, which can be cooled by the brine circulation used for cooling the stores. The temperature of the copper is determined by means of

Digitized by Google

a thermometer with its bulb fixed as close as possible to the surface of the copper. The manipulation of this instrument is very simple. When an observation has to be taken the observer closes the glass front of the instrument and turns on the brine supply. The temperature at the instant of dewing over is observed and also of the disappearance.

It may be of interest to quote some of the results obtained with this instrument.

TABLE VII.—Test of " Wall Fixture " Type Dew-Point Apparatus.

| Experiment No. | Psychrometer readings. | | Humidity. | Dew-point Apparatus. | | Humidity. |
|---|---|---|---|---|---|---|
| | Dry-bulb thermometer. ° C. | Wet-bulb thermometer. ° C. | | Dew forms. ° C. | Dew disappears. ° C. | |
| | | | Per cent. | | | Per cent. |
| 1 | 15·7 | 12·9 | 73 | 9·5 | 11·7 | 72 |
| 2 | 15·9 | 13·0 | 72 | 10·5 | 11·3 | 72 |
| 3 | 16·0 | 13·2 | 73 | 11·0 | 11·3 | 73 |
| 4 | 16·0 | 13·2 | 73 | 10·9 | 11·2 | 72·6 |
| 5 | 14·1 | 12·1 | 79 | 9·7 | 11·9 | 80 |
| 6 | 14·7 | 13·2 | 85 | 12·2 | 12·3 | 85 |

(ii) *Portable Form.*

It was found desirable to have an instrument which could be taken from place to place and inserted through the circular aperture built in the walls to permit of the insertion of the thermometers. For this purpose the hygrometer shown in Fig. 9 was constructed.

It consists of an aluminium tube 8 feet in length by $2\frac{1}{2}$ inches in diameter. At one end of the tube the dew-point thimble is placed while a telescope is fixed to the other end.

The silver surface is at an angle of about 45° to the axis of the tube, so that it is possible to view it directly from the telescope. This arrangement of the silver thimble has the additional advantage of permitting the apparatus to be operated with the axis of the tube either vertical or inclined with the thimble pointing downwards. The thermometer scale is read by the aid of a small mirror moving along guides, so as to maintain the meniscus of the mercury column in the field of view. Both the mercury column and the silver surface are illuminated by minute " pea " lamps set out of the field of view, a mirror being fixed opposite the silver surface to throw the light on to it.

In the vicinity of the dew-point surface a wide slot is cut in the aluminium sheath to permit of free access of air to the silver surface.

(iii) *Distant Reading Dew-Point Apparatus.*

It will be observed that the dew-point method depends primarily upon the acuteness of vision of the observer to detect the formation of a trace of dew, and whilst it is possible, by the aid of a telescope, to operate the apparatus at distances up to 10 feet,

Digitized by Google

for considerably greater distances it becomes necessary to find some other method of dew detection.

Now the dew-point method is essentially a discontinuous one and a prescribed cycle of operations has to be gone through for each determination of humidity. If these operations could be performed mechanically, without human intervention at any stage, we should have an industrial form of hygrometer possessing a sound theoretical basis.

It was anticipated that the conversion of the dew-point apparatus into a distant reading form would present unique practical difficulties, and our anticipations were fully realised when the attempt was made to produce a continuously recording hygrometer working on this principle.

Some preliminary experiments indicated that a promising line to follow in the design of such an instrument would be to utilise the change of reflecting power of a metallic surface on the formation of dew.

The apparatus illustrated in Fig. 10 shows how this idea was applied in the construction of a distant-reading hygrometer.

The source of radiant energy is a gas-filled tungsten lamp. The energy is reflected from the plane surface on to the concave mirror* and thus concentrated on two minute thermo-junctions connected in series.

The indicator is located at a point convenient for observation and the instrument is worked in a similar manner to the standard form of apparatus; the only difference is that the observer watches the movement of the pointer instead of the surface on which dew forms.

The valve controlling the brine flow is operated by means of a solenoid. Until the dew formation the deflection of the pointer is steady, but simultaneously with the deposition of dew the

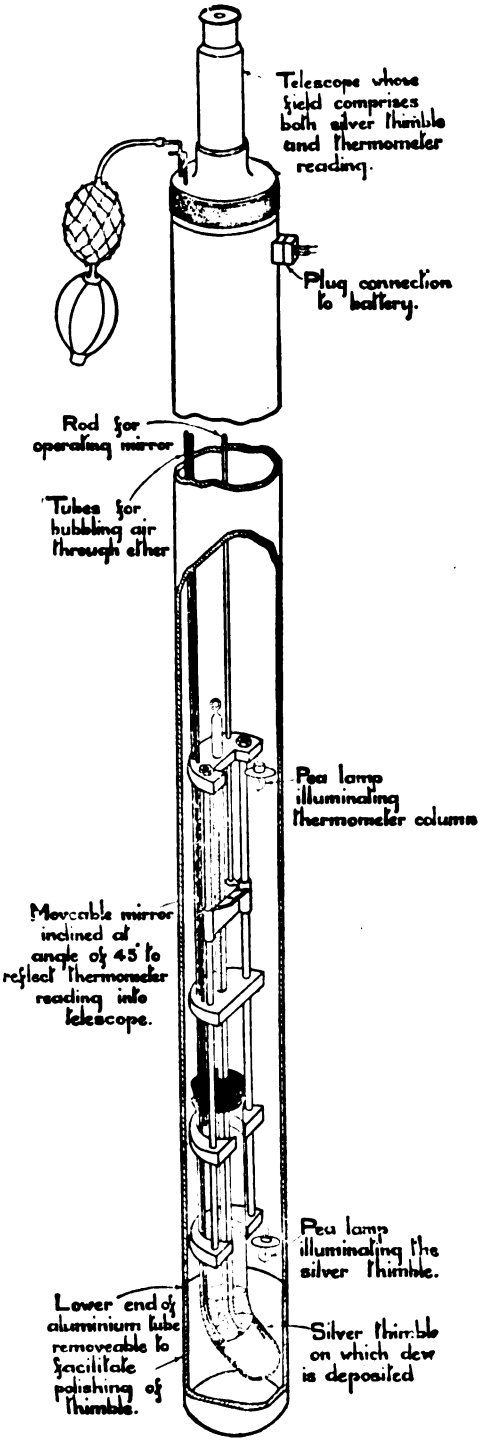
Telescope whose field comprises both silver thimble and thermometer reading.
Plug connection to battery.
Rod for operating mirror
Tubes for bubbling air through ether
Pea lamp illuminating thermometer column
Moveable mirror inclined at angle of 45° to reflect thermometer reading into telescope.
Pea lamp illuminating the silver thimble.
Lower end of aluminium tube removeable to facilitate polishing of thimble.
Silver thimble on which dew is deposited

FIG. 9.

* We are indebted to Mr. R. S. WHIPPLE for presenting us with the concave metallic mirror and thermo-junctions which are standard parts of Féry pyrometers.

Digitized by Google

reflecting power is diminished and the pointer moves rapidly toward zero. The temperature of the surface on which dew forms is then read by means of a thermo-junction.

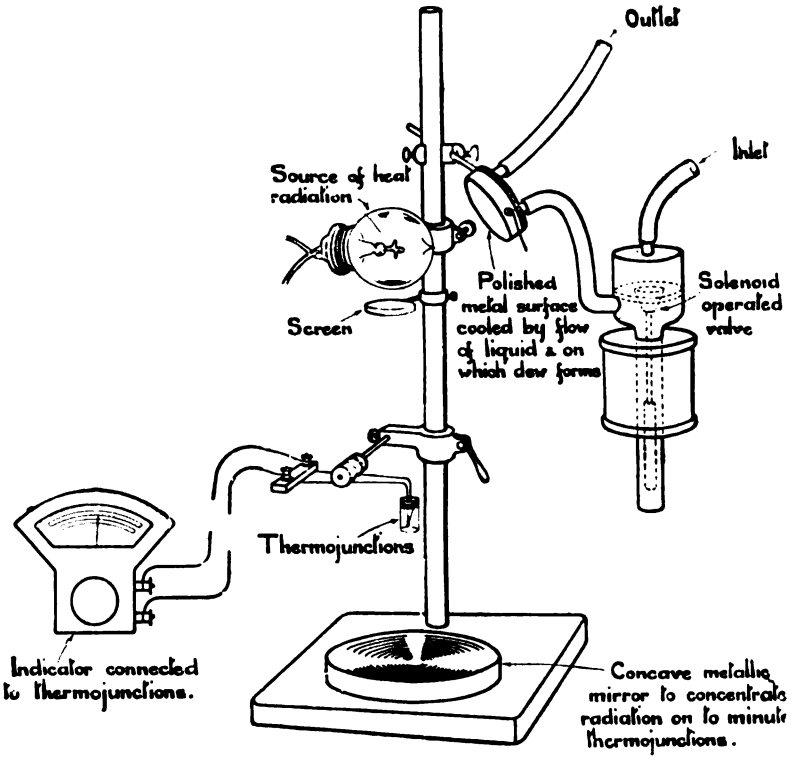
Outlet
Inlet
Source of heat radiation
Screen
Polished metal surface cooled by flow of liquid on which dew forms
Solenoid operated valve
Thermojunctions
Indicator connected to thermojunctions.
Concave metallic mirror to concentrate radiation on to minute thermojunctions.

FIG. 10.

This apparatus functioned satisfactorily and was tested against a psychrometer with the results shown in Table VIII.

TABLE VIII.—Test on Distant Reading Dew-Point Apparatus.
(Typical Experiment.)

| Time. | | Deflection of radiant heat indicator. | Temp. of metallic surface in ° C. | Remarks. |
|---|---|---|---|---|
| Min. | Sec. | | | |
| | 0 | 45·5 | 14·0 | |
| | 30 | 45·7 | 14·1 | |
| 1 | 0 | 45·8 | 14·2 | |
| | 30 | 45·7 | 14·0 | |
| 2 | 0 | 45·5 | 11·1 | |
| | 30 | 45·0 | 9·1 | |
| 3 | 0 | 45·0 | 7·5 | |
| | 30 | 45·0 | 6·5 ←— | Dew forming. |
| | 45 | 41·5 | — | |
| 4 | 0 | 40·5 | 6·2 | |
| | 30 | 39·0 | 6·5 | |
| 5 | 0 | 39·5 | 6·8 | |
| | 30 | 44·5 | 7·1 ←— | Dew disappearing |
| 6 | 0 | 45·0 | 7·5 | |
| | 30 | 45·3 | 7·7 | |

Digitized by Google

If it were possible to work the indicator as a relay for operating the solenoid valve, then it might be possible to maintain the surface always at the dew-point temperature and thus obtain a continuous record of the dew-point in the room.

Hence taking the mean of the temperatures of appearance and disappearance the value found for the humidity is 59·5 per cent.

Taking the temperature of appearance only the value becomes 58·3 per cent.

*Assmann psychrometer readings during the above series* :—

Dry-bulb temperatures = 14·6°, 14·7° C.
Wet-bulb temperatures = 10·2°, 10·4° C.

Hence humidity by psychrometer = 58 per cent.

Experiments have also been made on another method of indicating the occurrence of the dew-point—namely, the change of electrical resistance of a surface on the deposition of dew. The apparatus used consisted of a test tube, on the outside of which were deposited two rings of platinum film with a small gap of one or two millimetres between them. The platinum films were connected to a " megger " or to the secondary of an induction coil with a telephone in series. The test tube was cooled down in the usual way by bubbling air through ether.

When the glass between the films was quite clean the resistance of the gap remained at infinity after the deposition of the dew. With the glass dipped in a solution of an efflorescent salt like sodium carbonate and dried out, the resistance even when dry was too low. Finally, the method was adopted of grinding the glass before deposition of the platinum films. In this case breathing on the surface gave a very rapid fall and rise in resistance as the moisture was deposited and evaporated. When, however, the test tube was slowly cooled down to the dew-point, apparently no very sharp change of resistance occurred, and consequently it was difficult to detect the point at which the dew appeared. One set of observations is shown in Fig. 11.*

The true dew-point obtained by independent methods was at a temperature of 7·7° C. The tube was cooled down to 4·8° C. and then allowed to heat up. It will be noticed that the resistance-temperature curve did not return on itself, but that the resistance remained practically constant till the temperature rose to 7·9° C. (just above the dew-point), when a rise of resistance occurred which became increasingly rapid. In another experiment where the tube was cooled *just* below the dew-point, the curves of rising and falling temperature were much closer.

The reason for the effect obtained with a ground glass surface is not clear; possibly slight chemical decomposition is produced giving traces of soluble salts.

## 5. The Hair Hygrometer.

The two types of hygrometers already described require a certain amount of manipulation and computation before the value of the humidity can be ascertained.

* These observations were taken by Mr. F. H. Schofield, to whom our thanks are due.



Digitized by Google

This may not be of much consequence in laboratory work, but for every-day use a direct reading instrument of simple construction is much to be desired. A hygrometer possessing these characteristics is tolerable even if the accuracy of its indications is somewhat below that demanded in a laboratory instrument.

The hair hygrometer comes within this category. Besides the fact that it is direct reading, it has the additional advantage that it can be used at low temperatures, and so is applicable to cold storage work.

It utilises the principle that most substances consisting of organic tissue are hygroscopic, and change their length when they absorb or part with moisture.

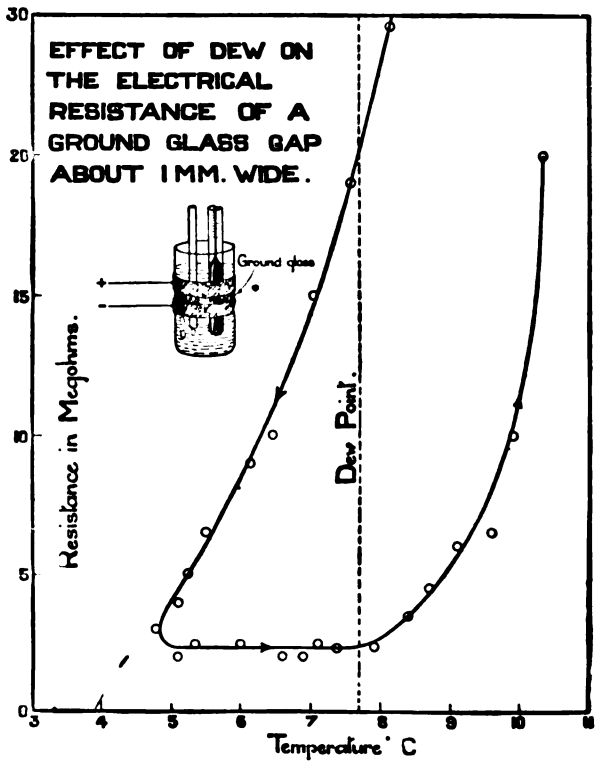


FIG. 11.

Hair, free from grease, increases its length when moistened, and DE SAUSSURE'S hygrometer works on this principle.

His original instrument has been greatly modified in mechanical detail since its invention, and modern forms of the instrument are illustrated in Figs. 12 and 13.

The hair hygrometer seems to have lost its reputation as a reliable instrument, but the evidence as to its unreliability is very meagre, and so far as we have been able to ascertain, no serious scientific study of it has been made since the time of REGNAULT, three-quarters of a century ago.

For the purpose of this inquiry, five instruments were studied :—

One was of the form illustrated in Fig. 12, and will be referred to as type A.

Two were of the form shown in Fig. 13, which will be referred to as type B.

Digitized by Google

One was a recording hair hygrometer, while the other was an instrument which we had arranged for distant reading work (see Fig. 16).

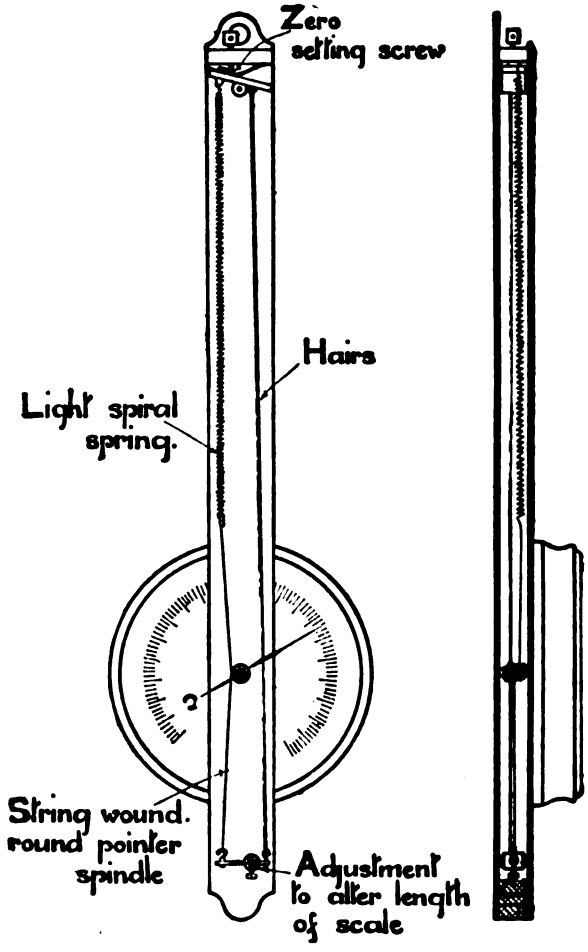


FIG. 12.

It seemed desirable to have quantitative information on the following points, and experiments were made with this object in view :—

(1) The reliability of the instruments over a long interval of time when subject to moderate ranges of temperature and humidity (humidities from 45 per cent. to 95 per cent.).

(2) The behaviour of the instrument when taken through a complete cycle of humidity changes such as from 7 per cent. to 90 per cent.

(3) The influence of temperatures below freezing point of water on the calibration curves.

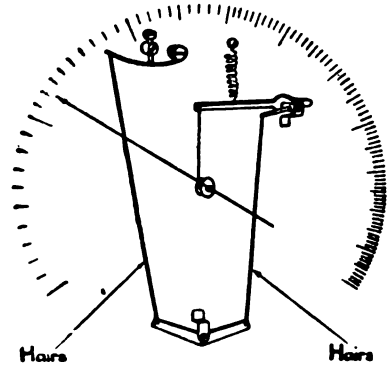


FIG. 13.

(4) The effect of temperature changes above that of the room (for a nearly constant relative humidity of the atmosphere).



Digitized by Google

### (*a*) *Reliability over Long Intervals of Time.*

Systematic observations were made over a period of three months at room temperatures (17° C.) and at temperatures about 0° C.

A range of humidity from 45 per cent. to 95 per cent. was covered, and it was considered that this was sufficient for the range of climatic changes met with in this country.

The dew-point apparatus was supplemented by the use of an Assmann psychrometer as standard of reference for obtaining the true humidity. A comparison of the data given in columns IV and V of Table IX shows the close agreement between the results obtained with these two instruments, although fundamentally different in principle. The agreement is within 2 per cent. for practically all the observations taken at room temperature. The divergence at low temperatures is greater, and is probably due to the fact that the presence of the observer near the psychrometer disturbed the humidity conditions, whereas the dew-point apparatus was shielded by its box.

In the reduction of the observations on the hair hygrometers mean calibration curves have been drawn, and the divergencies of the individual readings from these curves are given.

A study of the data shows that when the instruments have settled down the divergencies are of the order of 4 per cent., with an occasional departure amounting to 10 per cent. The bigger divergencies are possibly due to the lag of the instrument in getting to equilibrium value after a rapid change of humidity, and they generally occurred in all three simultaneously.

At low temperatures it was observed that the hair type of instrument was slow in settling to its final reading, particularly when it was taken from room temperature down to 0° C. For instance, when the instruments were taken into the cold stores it required 2½ hours for the readings to settle to their equilibrium values.

It is, however, somewhat surprising that the calibration at room temperatures holds so satisfactorily at lower temperatures, for the absolute weight of water vapour per unit volume of the atmosphere for a given humidity varies considerably. For example, 85 per cent. humidity at + 15° C. corresponds to 11 milligrammes of water per litre, whilst at 0° C. it corresponds to only 4 milligrammes of water per litre.

It would appear that hair behaves somewhat similarly to flannel, for which the moisture absorption depends on the relative humidity only, and varies but little with temperature.

Digitized by Google

TABLE IX.

| I. | II. | III. | IV. | V. | VI. | VII. | VIII. | IX. | X. |
|---|---|---|---|---|---|---|---|---|---|
| Date. | Time. | Room temperature. ° C. | Humidity by psychrometer. | Humidity by dew-point apparatus. | Mean value of humidity. | Correction to mean calibration curve. | | | |
| | | | | | | Hair hygrometer Type A. | Hair hygrometer. Type B. | | Recording hair hygrometer. |
| | | | | | | | No. 1. | No. 2. | |
| Feb. 5 | 12 noon | 14° | 55 | 55 | 55 | 0 | — | — | − 3 |
| „ 7 | 4 p.m. | 13° | 52 | 53 | 53 | 0 | — | — | − 2 |
| „ 16 | 1 „ | 15° | 62 | 62 | 62 | + 9 | — | — | + 1 |
| „ 17 | 1 „ | 16° | 65 | — | 65 | +11 | — | — | + 4 |
| „ 18 | — | 17° | 95 | 95 | 95 | +11 | — | — | + 7 |
| „ 19 | 10 a.m. | 10° | 73 | 74 | 74 | + 6 | — | — | + 5 |
| „ 21 | 4 p.m. | 15° | 62 | 62 | 62 | + 6 | — | — | + 2 |
| „ 22 | 11 a.m. | 11° | 69 | 69 | 69 | + 4 | — | — | 0 |
| „ 22 | 3 p.m. | 15° | 63 | 62 | 63 | + 6 | + 5 | — | + 3 |
| „ 24 | 3 p.m. | 15° | 66 | 68 | 67 | + 2 | + 2 | — | — |
| „ 26 | 11 „ | 9° | 63 | 64 | 64 | 0 | 0 | — | + 3 |
| „ 28 | 5 „ | 9° | 56 | 57 | 57 | 0 | 0 | — | + 1 |
| Mar. 2 | 12 noon | 6° | 52 | 50 | 51 | − 2 | 0 | — | 0 |
| „ 3 | 12 „ | 6° | 49 | 47 | 48 | − 1 | − 2 | — | − 1 |
| „ 3 | 5 p.m. | 7° | 49 | 48 | 48 | − 1 | − 2 | — | − 1 |
| „ 4 | 12 noon | 12° | 46 | 46 | 46 | 0 | − 1 | — | − 1 |
| „ 4 | 5 p.m. | 13° | 46 | 46 | 46 | 0 | − 1 | — | 0 |
| „ 5 | 12 noon | 14° | 45 | 44 | 44 | + 2 | + 1 | — | 0 |
| „ 7 | 12 „ | 12° | 45 | 45 | 45 | + 1 | 0 | — | 0 |
| „ 7 | 5 p.m. | 13° | 44 | 44 | 44 | + 1 | 0 | — | 0 |
| „ 8 | 12 noon | 9° | 46 | 44 | 45 | 0 | − 1 | — | 0 |
| „ 8 | 5 p.m. | 7° | 47 | 47 | 47 | + 1 | − 1 | — | 0 |
| „ 9 | 5 „ | 4° | 52 | 51 | 51 | + 2 | + 2 | — | + 1 |
| „ 10 | 12 noon | 5° | 47 | 47 | 47 | + 1 | 0 | — | 0 |
| „ 10 | 5 p.m. | 4° | 48 | 47 | 47 | + 1 | 0 | — | − 5 |
| „ 11 | 12 noon | 4° | 52 | 51 | 51 | − 3 | − 4 | — | − 5 |
| „ 11 | 5 p.m. | 0° | 55 | 52 | 53 | − 4 | − 5 | — | − 7 |
| „ 12 | 12 noon | 0° | 54 | 51 | 52 | − 7 | − 8 | −4 | −10 |
| „ 12 | 4 p.m. | 0° | 89 | 89 | 89 | 0 | − 2 | −2 | − 2 |
| „ 14 | 12 noon | 10° | 83 | 84 | 83 | + 2 | + 2 | +1 | + 2 |
| „ 14 | 12 „ | 12° | 79 | 79 | 79 | + 2 | + 2 | +2 | 0 |
| „ 15 | 12 „ | 12° | 72 | 72 | 72 | + 2 | + 1 | +1 | + 1 |
| „ 15 | 5 p.m. | 13° | 73 | 73 | 73 | + 3 | + 1 | +2 | + 1 |
| „ 16 | 12 noon | 12° | 72 | 74 | 73 | + 3 | + 1 | +2 | + 1 |
| „ 16 | 5 p.m. | 14° | 71 | 71 | 71 | + 3 | + 1 | +1 | 0 |
| „ 17 | 12 noon | 12° | 71 | 71 | 71 | + 2 | + 1 | +1 | 0 |
| „ 17 | 5 p.m. | 14° | 84 | 84 | 84 | 0 | 0 | 0 | − 1 |
| „ 18 | 12 noon | 14° | 79 | 80 | 79 | − 1 | 0 | +1 | 0 |

Digitized by Google

TABLE IX (continued).

| I. | II. | III. | IV. | V. | VI. | VII. | VIII. | IX. | X. |
|---|---|---|---|---|---|---|---|---|---|
| | | | | | | Correction to mean calibration curve. | | | |
| Date. | Time. | Room temperature. °C. | Humidity by psychrometer. | Humidity by dew-point apparatus. | Mean value of humidity. | Hair hygrometer Type A. | Hair hygrometer. Type B. | | Recording hair hygrometer. |
| | | | | | | | No. 1. | No. 2. | |
| Mar. 18 | 5 p.m. | 15° | 88 | 87 | 87 | +1 | +1 | + 1 | −1 |
| „ 19 | 12 noon | 15° | 87 | 87 | 87 | +3 | +3 | + 3 | +3 |
| „ 21 | 5 p.m. | 15° | 80 | 80 | 80 | +1 | 0 | 0 | 0 |
| „ 22 | 12 noon | 16° | 82 | 80 | 81 | 0 | −1 | 0 | −1 |
| „ 22 | 5 p.m. | 15° | 68 | 67 | 67 | +1 | −1 | + 2 | 0 |
| „ 31 | 5 p.m. | −1° | 63 | 61 | 62 | −5 | −6 | − 3 | −7 |
| Apr. 1 | 12 noon | 0° | 78 | 75 | 76 | −3 | −5 | − 4 | −7 |
| „ 1 | 5 p.m. | 0° | 92 | 90 | 91 | 0 | −1 | 0 | −3 |
| „ 2 | 11 a.m. | −1° | 87 | 82 | 84 | −4 | −6 | − 4 | −7 |
| „ 2 | 12 noon | −2° | 72 | 69 | 70 | −3 | −2 | − 1 | −3 |
| „ 11 | 12 noon | 15° | 71 | 68 | 69 | −2 | −3 | − 2 | −2 |
| „ 14 | 5 p.m. | 14° | 66 | — | 66 | −1 | −4 | − 2 | −2 |
| „ 20 | 5 „ | 12° | 62 | 60 | 61 | −1 | −4 | − 2 | −3 |
| „ 21 | 12 noon | 12° | 63 | 62 | 62 | −2 | −4 | − 2 | −3 |
| „ 21 | 5 p.m. | 14° | 60 | 57 | 58 | −2 | −5 | − 3 | −4 |
| „ 22 | 5 „ | 15° | 67 | 66 | 66 | 0 | −3 | − 1 | −3 |

A study of the table brings out the interesting fact that the hair hygrometer tends to read higher as time goes on, as is evidenced by the negative sign to the corrections during the latter period of the comparisons. Hence the hair appears to take up a permanent stretch.

In these experiments there were three variables—time, temperature and humidity. The main object of the experiments was to determine the magnitude of the changes to be anticipated for such fluctuations in these variables as would be encountered in practice, leaving for separate experiment the determination of the effect of temperature alone, etc.

It is interesting, however, to note that the results summarised in Table IX clearly indicate that at lower temperatures the instruments read high, and this is in agreement with subsequent observations when temperature and humidity were the only variables.

(*b*) *Behaviour of the Instrument when taken through a Complete Cycle of Humidities.*

For this part of the inquiry a more expeditious method than that adopted by GLAISHER had to be found. In his comparison of the dry-and-wet bulb hygrometer with DANIELL'S hygrometer he obtained his high-temperature points in India, his low and medium temperatures in Toronto, and the remaining odd thousand or so observations at Greenwich during the period 1841 to 1854.

The apparatus illustrated in Fig. 1 was employed for this part of the investigation, and by means of it a wide range of humidity could be covered in a comparatively short interval of time.

Digitized by Google

TABLE X.

| Experiment No. | Date. | Time. | Room temperature. °C. | Humidity by dew-point apparatus. | Correction to mean calibration curve. | | |
|---|---|---|---|---|---|---|---|
| | | | | | Hair hygrometer, Type A. | Hair hygrometer Type B. | |
| | | | | | | No. 1. | No. 2. |
| 1 | May 7th | 12.45 p.m. | 16° | 21 | − 5 | −10 | − 9 |
| 2 | „ 7th | 3.0 p.m. | 19° | 7 | + 2 | − 7 | − 5 |
| 3 | „ 7th | 3.15 p.m. | 18° | 8 | + 3 | − 7 | − 5 |
| 4 | „ 7th | — | 18° | 47 | − 6 | − 9 | − 7 |
| 5 | „ 9th | 9.45 a.m. | 13° | 57 | − 7 | −12 | − 9 |
| 6 | „ 9th | 2.30 p.m. | 19° | 31 | − 8 | −11 | − 9 |
| 7 | „ 9th | 4.45 p.m. | 19° | 77 | − 5 | −10 | − 7 |
| 8 | „ 9th | 4.50 p.m. | 19° | 76 | − 4 | − 9 | − 6 |
| 9 | „ 10th | 10.30 a.m. | 14° | 62 | − 1 | − 5 | − 3 |
| 10 | „ 10th | 11.0 a.m. | 15° | 51 | − 1 | − 5 | − 4 |
| 11 | „ 10th | 11.30 a.m. | 17° | 35 | − 2 | − 5 | − 4 |
| 12 | „ 10th | 12.30 p.m. | 19° | 23 | − 3 | − 7 | − 6 |
| 13 | „ 10th | 2.30 p.m. | 18° | 45 | − 2 | − 4 | − 4 |
| 14 | „ 10th | 3.0 p.m. | 15° | 50 | − 4 | − 7 | − 7 |
| 15 | „ 10th | 4.0 p.m. | 18° | 63 | − 5 | −11 | − 8 |
| 16 | „ 10th | 5.15 p.m. | 19° | 81 | − 6 | −10 | − 8 |
| 17 | „ 10th | 5.35 p.m. | 19° | 83 | − 4 | − 8 | − 6 |
| 18 | „ 10th | 9.15 p.m. | 13° | 72 | − 3 | − 7 | −11 |
| 19 | „ 13th | 2.25 p.m. | 20° | 88 | − 7 | − 8 | − 7 |
| 20 | „ 13th | 3.15 p.m. | 20° | 77 | − 2 | − 6 | − 6 |
| 21 | „ 13th | 3.45 p.m. | 20° | 52 | + 1 | − 2 | − 2 |
| 22 | „ 13th | 4.30 p.m. | 21° | 30 | + 2 | − 5 | − 5 |
| 23 | „ 13th | 5.0 p.m. | 21° | 50 | − 2 | − 6 | − 6 |
| 24 | „ 13th | 5.25 p.m. | 21° | 79 | − 5 | −10 | − 9 |
| 25 | „ 14th | 9.45 a.m. | 15° | 83 | − 5 | −12 | −10 |
| 26 | „ 14th | 10.10 a.m. | 15° | 85 | − 5 | −11 | −10 |
| 27 | „ 14th | 10.35 a.m. | 17° | 70 | − 3 | − 7 | − 6 |
| 28 | „ 14th | 11.20 a.m. | 19° | 52 | + 2 | − 7 | − 6 |
| 29 | „ 14th | 12.0 noon | 20° | 36 | + 3 | − 8 | − 7 |
| 30 | „ 14th | 12.30 p.m. | 21° | 50 | + 1 | − 6 | − 5 |
| 31 | „ 17th | 9.30 a.m. | 13° | 73 | − 5 | −12 | − 9 |
| 32 | „ 19th | 11.5 a.m. | 18° | 89 | − 3 | −10 | − 8 |
| 33 | „ 19th | 11.35 a.m. | 18° | 67 | −11 | − 7 | − 5 |
| 34 | „ 19th | 12.5 p.m. | 19° | 45 | − 1 | − 6 | − 5 |
| 35 | „ 19th | 12.30 p.m. | 19° | 35 | − 2 | − 6 | − 5 |
| 36 | „ 19th | 1.15 p.m. | 20° | 87 | − 3 | −10 | − 9 |
| The following low temperature readings were taken in Smithfield Cold Stores :— | | | | | | | |
| 37 | May 20th | 3.45 p.m. | −6° | 67 | −14 | −23 | −16 |
| 38 | „ 20th | 3.50 p.m. | −6° | 67 | −12 | −22 | −16 |
| 39 | „ 20th | 4.10 p.m. | −6° | 49 | −13 | −22 | −18 |
| 40 | „ 20th | 4.15 p.m. | −6° | 52 | −13 | −20 | −15 |
| 41 | „ 20th | 5.10 p.m. | −5° | 31 | −11 | −13 | −13 |
| 42 | „ 20th | 5.20 p.m. | −5° | 32 | −13 | −14 | −14 |
| 43 | „ 20th | 6.10 p.m. | −5° | 21 | −11 | −13 | −13 |
| 44 | „ 21st | 8.20 a.m. | −9° | 28 | −15 | −17 | −17 |
| 45 | „ 21st | 8.25 a.m. | −9° | 27 | −15 | −17 | −17 |
| 46 | „ 21st | 9.10 a.m. | −7° | 15 | −12 | −16 | −10 |
| 47 | „ 21st | 9.50 a.m. | −5° | 30 | −12 | −13 | −14 |
| 48 | „ 21st | 10.0 a.m. | −5° | 31 | −12 | −13 | −14 |
| 49 | „ 21st | 10.45 a.m. | −6° | 48 | −16 | −21 | −18 |
| 50 | „ 21st | 11.30 a.m. | −5° | 60 | −12 | −20 | −15 |
| 51 | „ 21st | 11.35 a.m. | −5° | 61 | −12 | −20 | − 5 |

Digitized by Google

TABLE X (Continued).

The following low-temperature readings were taken in Smithfield Cold Stores (Contd.) :—

| Experiment No. | Date. | Time. | Room temperature. °C. | Humidity by dew-point apparatus. | Correction to mean calibration curve. | | |
|---|---|---|---|---|---|---|---|
| | | | | | Hair hygrometer. Type A. | Hair hygrometer Type B. | |
| | | | | | | No. 1. | No. 2. |
| 52 | May 21st | 12.0 noon | −6° | 59 | −14 | −19 | −14 |
| 53 | ,, 23rd | 9.30 a.m. | −7° | 87 | − 9 | −18 | −14 |
| 54 | ,, 23rd | 9.35 a.m. | −7° | 86 | − 9 | −10 | −13 |
| 55 | ,, 23rd | 10.25 a.m. | −5° | 49 | −11 | −17 | −13 |
| 56 | ,, 23rd | 10.30 a.m. | −5° | 50 | −11 | −16 | −13 |
| 57 | ,, 23rd | 11.10 a.m. | −4° | 37 | −14 | −16 | −14 |
| 58 | ,, 23rd | 11.15 a.m. | −4° | 38 | −12 | −16 | −14 |
| 59 | ,, 23rd | 11.50 a.m. | −3° | 21 | −11 | −14 | −13 |
| 60 | ,, 23rd | 1.45 p.m. | −6° | 20 | −13 | −15 | −14 |
| 61 | ,, 23rd | 2.30 p.m. | −4° | 34 | −14 | −14 | −14 |
| 62 | ,, 23rd | 2.40 p.m. | −4° | 35 | −13 | −14 | −13 |
| 63 | ,, 23rd | 3.30 p.m. | −5° | 54 | −13 | −19 | −16 |
| 64 | ,, 23rd | 3.35 p.m. | −5° | 54 | −13 | −19 | −15 |
| 65 | ,, 23rd | 4.20 p.m. | −5° | 65 | −15 | −24 | −18 |
| 66 | ,, 23rd | 4.50 p.m. | −5° | 75 | −14 | −24 | −18 |
| 67 | ,, 25th | 9.0 a.m. | −9° | 65 | −13 | −21 | −16 |
| | | Experiments at Room Temperature. | | | | | |
| 68 | May 25th | 5.0 p.m. | 21° | 84 | − 5 | − 9 | − 7 |
| 69 | ,, 25th | 5.20 p.m. | 22° | 65 | − 3 | − 7 | − 6 |
| 70 | ,, 26th | 10.20 a.m. | 20° | 47 | − 3 | − 8 | − 7 |
| 71 | ,, 26th | 11.10 a.m. | 22° | 39 | − 4 | − 7 | − 8 |
| 72 | ,, 26th | 12.0 noon | 23° | 26 | − 2 | − 6 | − 7 |
| 73 | ,, 26th | 12.45 p.m. | 23° | 37 | − 4 | − 0 | − 8 |
| 74 | ,, 26th | 2.30 p.m. | 21° | 49 | − 8 | −12 | −12 |
| 75 | ,, 26th | 3.25 p.m. | 23° | 64 | − 8 | −14 | −14 |
| 76 | ,, 26th | 4.10 p.m. | 22° | 76 | − 8 | −16 | −13 |
| 77 | ,, 26th | 4.55 p.m. | 21° | 78 | − 8 | −16 | −13 |
| 78 | ,, 27th | 10.15 a.m. | 16° | 62 | − 7 | −14 | −12 |
| 79 | ,, 27th | 11.10 a.m. | 20° | 82 | − 6 | −14 | −12 |
| 80 | ,, 27th | 12.30 p.m. | 21° | 62 | − 4 | − 9 | − 9 |
| 81 | ,, 27th | 2.20 p.m. | 22° | 54 | − 5 | −11 | − 9 |
| 82 | ,, 27th | 3.10 p.m. | 22° | 44 | − 4 | − 8 | − 9 |
| 83 | ,, 27th | 4.5 p.m. | 22° | 28 | − 4 | − 9 | − 9 |
| 84 | ,, 27th | 4.50 p.m. | 22° | 45 | − 5 | − 9 | − 9 |
| 85 | ,, 27th | 5.15 p.m. | 22° | 60 | −10 | −17 | −13 |
| 86 | ,, 28th | 10.15 a.m. | 19° | 88 | − 3 | −10 | − 9 |
| 87 | June 1st | 9.45 a.m. | 16° | 65 | − 5 | −13 | −11 |
| 88 | ,, 1st | 10.15 a.m. | 18° | 52 | − 5 | −11 | − 9 |
| 89 | ,, 1st | 11.10 a.m. | 20° | 46 | − 4 | −10 | − 9 |
| 90 | ,, 1st | 11.50 a.m. | 21° | 31 | − 4 | − 9 | − 9 |
| 91 | ,, 1st | 12.30 p.m. | 21° | 42 | − 5 | −10 | − 8 |
| 92 | ,, 2nd | 9.50 a.m. | 17° | 55 | − 6 | −13 | −12 |
| 93 | ,, 2nd | 10.20 a.m. | 19° | 65 | − 8 | −17 | −14 |
| 94 | ,, 2nd | 11.0 a.m. | 19° | 81 | − 5 | −13 | −11 |
| 95 | ,, 2nd | 12.0 noon | 22° | 61 | − 3 | −10 | −12 |
| 96 | ,, 2nd | 12.50 p.m. | 23° | 45 | − 3 | − 9 | − 9 |
| 97 | ,, 2nd | 2.50 p.m. | 23° | 31 | − 3 | −10 | −10 |
| 98 | ,, 2nd | 4.0 p.m. | 24° | 26 | − 4 | − 9 | −10 |
| 99 | ,, 2nd | 5.0 p.m. | 25° | 45 | − 5 | −11 | −11 |
| 100 | ,, 3rd | 9.30 a.m. | 18° | 55 | − 5 | −13 | −12 |
| 101 | ,, 3rd | 10.10 a.m. | 19° | 67 | − 7 | −16 | −15 |
| 102 | ,, 3rd | 10.35 a.m. | 20° | 75 | − 7 | −17 | −14 |
| 103 | ,, 4th | — | 16° | 57 | − 6 | −14 | −13 |

Digitized by Google

When the hair hygometers were placed in the apparatus, and subjected to very low humidities of the order of 5 per cent., a permanent change occurred and the calibration curve shifted in a direction which indicated that the hairs had stretched permanently. The same change, but not to the same extent, occurred in all the hair hygrometers tested.

One of the curves for an instrument type B are reproduced in Fig. 14. The change in the instrument type A (illustrated in Fig. 12) was 3 to 4 per cent. throughout the scale. The calibration curves of the two instruments of type B (illustrated in Fig. 13) changed by 5 and 8 per cent. respectively.

The calibration points repeated themselves, and there was no evidence of appreciable hysteresis effect. The data for these experiments are summarised in Table X (May 7 to 19).

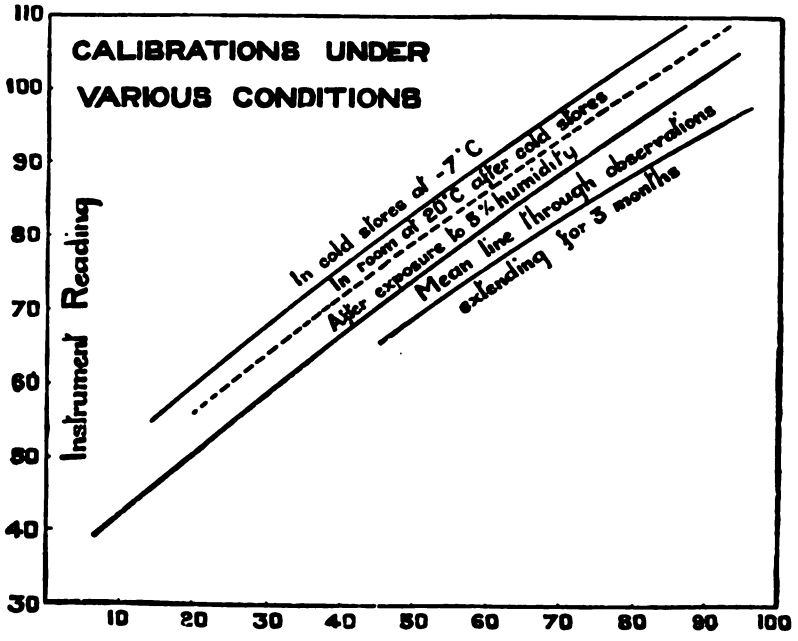


FIG. 14. True percentage Humidity of Atmosphere.

### (c) *Calibration at Low Temperatures.*

The next series was made in a cold store at a temperature of about — 7° C., the same apparatus being employed. This was then taken to the Central Meat Markets Store at Smithfield, and the calibration repeated at low temperatures.

Comparing the results obtained in the cold stores with the previous ones at room temperature, it will be seen that the calibration curve at low temperature for type A has shifted by 8 to 9 per cent.; for type B, No. 1, 10 to 13 per cent., and for No. 2 9 per cent.

On the return of the apparatus to the laboratory the experiments were repeated at room temperature. The results show that instrument type A repeated its original room temperature calibration within the limits of the error of experiment. But a permanent



Digitized by Google

alteration had occurred on exposure to low temperatures with instruments type B, resulting in their calibration curves being displaced (see Fig. 14). These results indicate that subjection to extremes of temperature or humidity causes a permanent "set", but for moderate variations of the conditions the instruments behave fairly satisfactorily.

So far as we could ascertain the only difference between types A and B was that the hairs in B were under greater tension than in A.

(*d*) *Influence of Change of Temperature from* 16° C. *up to* 38° C. (60° F. *to* 100° F.).

In these experiments the temperature was varied in steps up to 38° C., while the indications of the instruments were kept at a fixed value by adjusting the moisture content of the atmosphere. The corresponding humidity was determined by the dew-point apparatus. The data obtained are summarised in Table XI, and graphically in Fig. 15. The first exposure of the hairs to higher temperatures on June 8 gave results

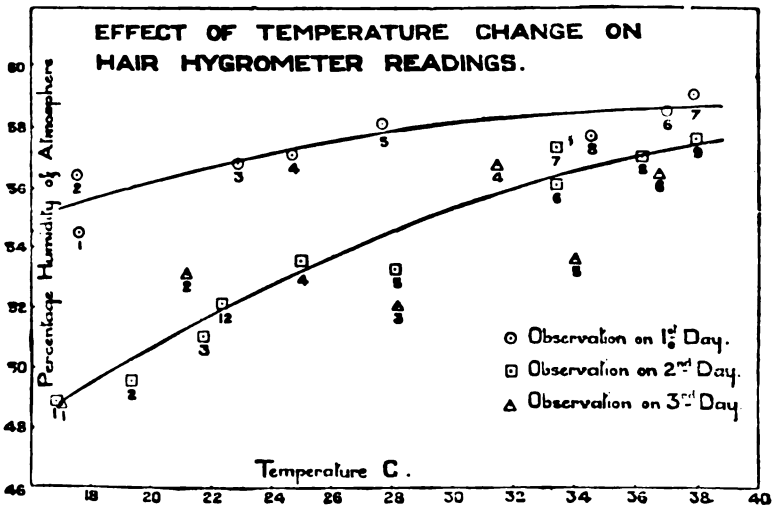


FIG. 15.

which indicate a slight contraction of the hairs with increasing temperatures. That the change is in this direction will be seen by consideration of the fact that the humidity of the surrounding atmosphere had to be raised as the temperature was raised, and the effect of an increase in the humidity of the surrounding atmosphere is to cause a lengthening of the hairs. In the present experiment the lengthening due to increasing the humidity counteracted the contraction due to temperature.

When repeating the observations the next day, June 9, the surprising result was obtained that the hairs had taken a permanent set overnight in the direction of expansion, the change amounting to 6 per cent. since the period of exposure to the higher temperatures. It now required only 49 per cent. relative humidity of the atmosphere at a temperature of 16° C. to give the same instrument reading as on the previous day was equivalent to 55 per cent. relative humidity of the atmosphere. The results on this day and the succeeding day show a well-marked coefficient of *contraction* with temperature,

Digitized by Google

TABLE XI.—Influence of Temperature on Indications of Hair Hygrometers.
(Humidity of atmosphere varied to maintain instrument readings at steady value.)

| I. | II. | III. | IV. | V. | VI. | VII. | VIII. | |
|---|---|---|---|---|---|---|---|---|
| No. of Experiment. | Temperature of atmosphere. °C. | Dew forms. °C. | Dew disappears. °C. | Dew-point temperature. °C. | Humidity. | Hair Hygrometer. Type A. | Hair Hygrometer. Type B. | |
| | | | | | | | No. 1. | No. 2. |
| June 8, 1921. | | | | | | | | |
| 1 | 17·6 | 8·0 | 8·5 | 8·2 | 54·3 | 63·5 | 77·5 | 85·1 |
| 2 | 17·6 | 8·6 | 8·9 | 8·7 | 56·2 | 64·5 | 78·0 | 86·0 |
| 3 | 22·8 | 13·6 | 13·7 | 13·6 | 56·5 | 63·5 | 77·5 | 85·1 |
| 4 | 24·7 | 15·3 | 15·7 | 15·5 | 56·8 | 63·5 | 77·3 | 85·1 |
| 5 | 27·7 | 18·4 | 18·7 | 18·6 | 57·8 | 63·5 | 77·5 | 85·0 |
| 6 | 37·2 | 27·6 | 27·8 | 27·7 | 58·5 | 63·5 | 77·5 | 85·2 |
| 7 | 37·9 | 28·5 | 28·6 | 28·5 | 58·9 | 64·5 | 77·5 | 86·0 |
| 8 | 34·6 | 25·0 | 25·1 | 25·0 | 57·5 | 63·5 | 77·0 | 85·6 |
| June 9, 1921. | | | | | | | | |
| 1 | 16·7 | 5·5 | 6·2 | 5·8 | 48·8 | 63·5 | 77·8 | 85·8 |
| 2 | 19·4 | 8·5 | 9·2 | 8·8 | 49·5 | 63·4 | 77·7 | 85·5 |
| 3 | 21·8 | 10·8 | 11·5 | 11·1 | 50·9 | 63·5 | 77·8 | 85·6 |
| 4 | 25·0 | 14·6 | 15·0 | 14·8 | 53·4 | 63·5 | 77·9 | 85·6 |
| 5 | 28·2 | 17·7 | 17·8 | 17·7 | 53·2 | 63·5 | 77·7 | 85·5 |
| 6 | 33·4 | 23·4 | 23·5 | 23·4 | 55·9 | 63·5 | 77·5 | 85·4 |
| 7 | 33·4 | 23·8 | 23·8 | 23·8 | 57·1 | 63·5 | 77·2 | 85·2 |
| 8 | 36·3 | 26·3 | 26·5 | 26·4 | 56·7 | 63·5 | 77·7 | 86·0 |
| 9 | 38·2 | 28·2 | 28·4 | 28·3 | 57·4 | 63·9 | 76·3 | 84·5 |
| The following three observations were taken directly after cooling down :— | | | | | | | | |
| 10 | 24·2 | 14·8 | 15·0 | 14·9 | 56·3 | 63·6 | 77·8 | 85·6 |
| 11 | 22·9 | 12·7 | 13·0 | 12·8 | 56·4 | 63·5 | 76·8 | 85·0 |
| 12 | 21·7 | 11·2 | 11·6 | 11·4 | 52·1 | 63·5 | 77·2 | 85·3 |
| June 10, 1921. | | | | | | | | |
| 1 | 16·5 | 5·3 | 6·0 | 5·6 | 48·7 | 63·5 | 77·5 | |
| 2 | 22·2 | 11·1 | 11·3 | 11·2 | 49·9 | 63·5 | 77·5 | |
| 3 | 28·3 | 17·3 | 17·5 | 17·4 | 51·8 | 63·5 | 77·2 | |
| 4 | 31·5 | 21·7 | 22·0 | 21·8 | 56·6 | 63·5 | 77·5 | |
| 5 | 35·1 | 24·3 | 24·3 | 24·3 | 53·6 | 63·6 | 77·5 | |
| 6 | 36·8 | 26·5 | 26·9 | 26·7 | 56·3 | 63·5 | 77·3 | |

the magnitude of which is 0·4 per cent. relative humidity per 1° C. It is interesting to note that the *expansion* on exposure to cold stores' temperature works out to be practically the same in numerical value as the contraction on exposure to higher temperatures—*i.e.* an average change of 10 per cent. in the humidity scale for a lowering of 25° C. in temperature. This gives a coefficient of 0·4 per cent. relative humidity per 1° C.



Digitized by Google

The experiments show that the instrument has a true thermal contraction or expansion with increasing or decreasing temperatures.

The most serious defect of this type of hygrometer is the permanent changes on exposure for the first time to big fluctuations of temperature or humidity resulting in elongation of the hairs. It is very curious that the change should always occur in this direction, and it may possibly be due to the fact that the hairs are always under tension by the control springs.

### (*e*) *Accuracy of the Engraved Scale supplied with the Instruments.*

It was somewhat disconcerting to find the scales supplied with the instruments of types A and B to be so much in error. Even when the pointers were adjusted to read correctly at one point of the scale, the divergence at the extreme end amounted to as much as 30 per cent. (see Table XI).

This wide discrepancy was traced to the fact that the maker had attempted to obtain the scale by comparison with a wet-and-dry bulb thermometer of the non-ventilated type.

Recently we obtained from another source an instrument somewhat similar to type A (Fig. 12), but with gravity instead of spring control. On testing this instrument at room temperature over the range 50 to 100 per cent. humidity, the maximum error only amounted to 3 per cent.

### (*f*) *The Relation between the Extensions of the Hairs and the Relative Humidity of the Atmosphere.*

The relation between the linear expansion of the hairs and the relative humidity is given in Table XII.

TABLE XII.—Relation between Extension of Hairs and Relative Humidity of Atmosphere.

| Relative humidity of atmosphere. | Percentage extension of hairs. |
|---|---|
| 10 | 0·40 |
| 20 | 0·67 |
| 30 | 0·91 |
| 40 | 1·11 |
| 50 | 1·29 |
| 60 | 1·45 |
| 70 | 1·58 |
| 80 | 1·70 |
| 90 | 1·81 |

These data have been obtained from the measurement of the lever system of one of the instruments (type B) and the experimental data connecting the angular deflection of the pointer with the relative humidity.

Digitized by Google

In view of the complex structure of the hair it is hardly to be expected that the same relationship will apply even approximately to all instruments of this type.

(*g*) *Summary of Conclusions concerning Hair Hygrometers.*

From the results of the experiments one arrives at the conclusion that, under normal working conditions and subjected to ordinary variations of humidity and temperature, the hair hygrometer shows a tendency to give high readings with lapse of time. This may be due to the fact that the hairs are always under tension, and consequently a permanent set takes place.

In our experience the instruments which behave most satisfactorily are those in which the tension force is small and whose bearings and pivots are so well made that friction is a minimum. There is no doubt that good performance from the hair hygrometer can only be obtained when the design of the instrument is such that the hairs are safeguarded from any undue strain.

The instrument should not be subjected to large variations of temperature, and the calibration should be checked at frequent intervals under conditions identical with those under which it is used.

For this purpose a simple protected form of dew-point apparatus should be installed close to the instrument. Periodic checks could then be made and the hair hygrometer employed merely as an indicator to show the variations in humidity of the atmosphere.

The presence of oil vapour in the atmosphere and of dust is stated to reduce with time the sensitivity of the hairs by preventing free access of the aqueous vapour to the surface, and precautions should therefore be taken to eliminate these disturbances as much as possible.

(*h*) *Distant Reading Form of Hair Hygrometer:*

The hair hygrometer is the simplest of all instruments to convert to a distant reading type. We constructed a distant reading instrument of the form shown in Fig. 16. It

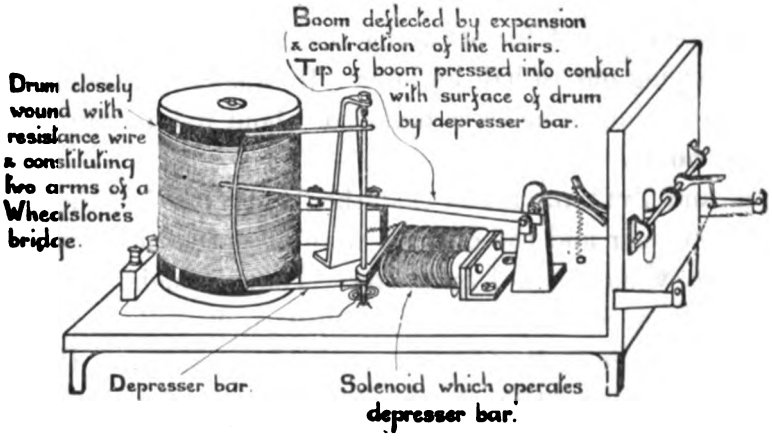
Boom deflected by expansion & contraction of the hairs.
Tip of boom pressed into contact with surface of drum by depresser bar.
Drum closely wound with resistance wire & constituting two arms of a Wheatstone's bridge.
Depresser bar.
Solenoid which operates depresser bar.

FIG. 16.

Digitized by Google

is a standard form of recording hair hygrometer with the clockwork drum removed and replaced by a stationary drum wound with oxidised wire giving a total resistance of 1,000 ohms. A longitudinal strip is cleaned on the surface of the drum so that electrical contact can be effected with the wire. The pointer has a silver contact piece instead of the pen. Above the pointer is fixed a " chopper bar " arrangement operated by an electro-magnet. When a reading of the humidity is desired, the observer switches on the electro-magnet, which brings the pointer into contact with the drum immediately beneath the spot where it is situated.

The resistance drum then constitutes the two arms of a Wheatstone bridge and the pointer is the contact to the galvanometer circuit; the other galvanometer contact is on a similar drum at the observation station. The observer balances the bridge in the usual manner and thus determines electrically the position of the pointer on the drum which is situated at the hair hygrometer.

The behaviour of the instrument was found to be quite satisfactory over a long period of test, but it suffers, of course, from all the inherent defects associated with the use of hair as a fundamental element in the design of a physical instrument.

### 6. Thermal Effect on Cotton Hygrometer.

Orme Masson* in 1904 investigated the change in temperature produced in dry cotton wool when exposed to a damp atmosphere. He employed a mercury thermometer with about 1 gramme of cotton wool wound round the bulb and observed the temperature rise when the instrument was withdrawn from a desiccator to a humid atmosphere.

His experiments showed that the heat production was proportional to the amount of hygroscopic absorption. He suggested the possibility of utilising the phenomenon as a method of measuring humidity, but did not give this aspect of the subject detailed investigation.

Drs. Chattock and Tyndall modified Masson's arrangement by employing thermo-junctions instead of mercury thermometers. By this device they were able to reduce the time of exposure required for attaining the maximum temperature to 15 seconds and the period of drying out to half an hour. In Masson's experiments the maximum temperature was not attained below a period of about five minutes and the drying out occupied about 24 hours.

Drs. Chattock and Tyndall found that the " constant " of their instrument varied in an inexplicable manner and the changes were of such a magnitude as to render the instrument of little value as a hygrometer. They brought the subject before the Engineering Committee of the Food Investigation Board, who requested that the matter should also be investigated further at the Laboratory, as the method seemed to have possibilities as the basis of the design of a distant reading hygrometer.

* 'Roy. Soc. Proc.', vol. 74, p. 230, 1904. Masson and Richards, 'Roy. Soc. Proc.', vol. 78, p. 412, 1906.

Digitized by Google

### (*b*) *Electrical Resistance Type.*

After consideration of the magnitude of the temperature changes to be observed, we decided to abandon the use of thermo-junctions in favour of a resistance thermometer method. This had the additional advantage that the absorbent cotton was distributed evenly over a length of wire instead of being concentrated in a blob around the thermo-junction.

Accordingly a differential resistance thermometer was made of cotton-covered nickel wire wound on a large ebonite rack similar to a resistance thermometer. On one of the coils the cotton covering was left in its natural state, whilst that on the other was shellac varnished. These coils were connected up in the form of a Wheatstone bridge and the arrangement of the coils is shown in Fig. 17. Each coil was composed of about 15 feet of wire of approximately 22 ohms resistance. The mean temperature coefficient of resistance between 0° C. and 100° C. was 0·00516 per 1° C.

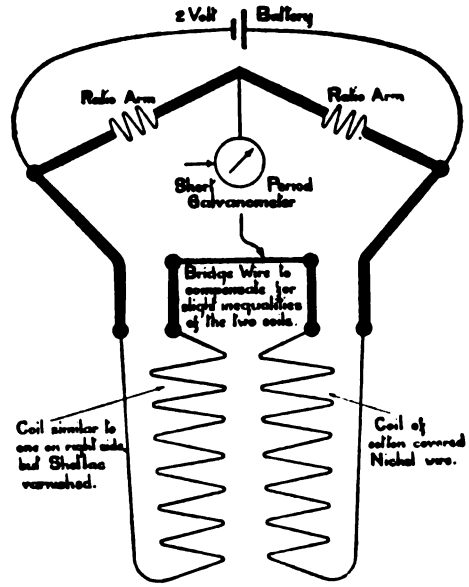
2 Volt Battery
Ratio Arm
Ratio Arm
Short Period Galvanometer
Bridge Wire to compensate for slight inequalities of the two coils.
Coil similar to one on right side but Shellac varnished.
Coil of cotton covered Nickel wire.

Fig. 17.

The function of the varnished coil is to compensate for changes of resistance of the cotton-covered coil due to changes of room temperature, so that the bridge is balanced at all temperatures. If the coils are placed in a dry atmosphere, then on exposure to a humid atmosphere a large deflection of the galvanometer spot is obtained, due to the ready absorption of water vapour by the untreated cotton on the one coil.

The thermal effect on absorption of water vapour occurs with extraordinary rapidity, the maximum deflection being attained within six seconds of the exposure. In order to slow down the effect six additional layers of cotton were wound on the wire, bringing up the external diameter to approximately one millimetre, the diameter of the nickel wire being only one-tenth of a millimetre. This increased the time taken to reach a maximum to about 12 seconds.

With the means at our disposal it was not possible to wind the additional layers of thin cotton so closely and well spaced as to give a perfectly even surface, and consequently it presented a slightly corrugated appearance. This may be an advantage, as it helps to expose more surface to the atmosphere. Having satisfied ourselves that the instrument would work at temperatures below 0° C., experiments were made at room temperatures so as to obtain some information as to the characteristics of the phenomenon.

In the early experiments the coil was carried from a rubber stopper which could be

Digitized by Google

inserted into wide-mouthed bottles containing a dry or a saturated atmosphere. The coil when transferred from the dry to the saturated atmosphere would give consistent readings, but these were quite valueless owing to the fact that the coil absorbed the moisture in its vicinity, and the effect of such absorption was to upset completely the hygrometric conditions of the atmosphere in the vessel.

### (c) *Apparatus utilising the Effect for Hygrometric Measurements.*

To overcome these difficulties the form of apparatus, shown diagrammatically in Fig. 18, was devised. The coil is contained in the central tube and past it is pumped either dry air from the tower on the left, saturated air from the tower on the right, or

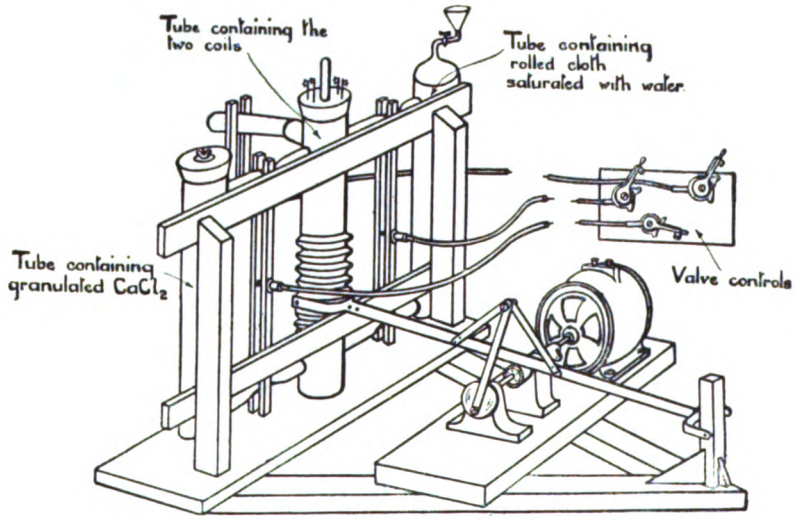
Tube containing the two coils
Tube containing rolled cloth saturated with water
Tube containing granulated $CaCl_2$
Valve controls

Fig. 18.

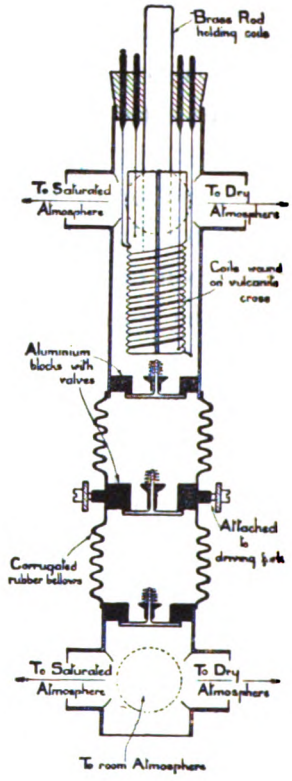


Fig. 19.

air from the room, through an inlet and outlet in front. The pumping device is a corrugated rubber tube made from a motor tyre, and it contains three disc valves of large diameter, as shown in Fig. 19. This method of pumping was adopted in preference to the usual type of piston in order to avoid the necessity of introducing any lubricant between a piston and cylinder which might be carried on to the coil by the air stream; also all generation of heat by friction between moving parts is eliminated. Connections between the towers are made by $1\frac{3}{4}$-inch bore rubber tubing, and both inlet and outlet to a tower can be closed by one movement of a spring-operated crossbar. The general features of the apparatus will be understood from the diagrams. The drying tower

Digitized by Google

contains granulated calcium chloride, while the saturation tower is filled with a roll of brass gauze and muslin interwoven, which is periodically saturated with water.

The procedure in taking the observations is as follows :—The tower containing the coil is placed in communication with the drying tower and air pumped around for a few minutes. The inlet and outlet to the atmosphere of the room is then opened quickly and the drying tower cut off. A typical time-deflection curve for the galvanometer spot is shown in Fig. 20, the maximum deflection corresponding to a temperature change

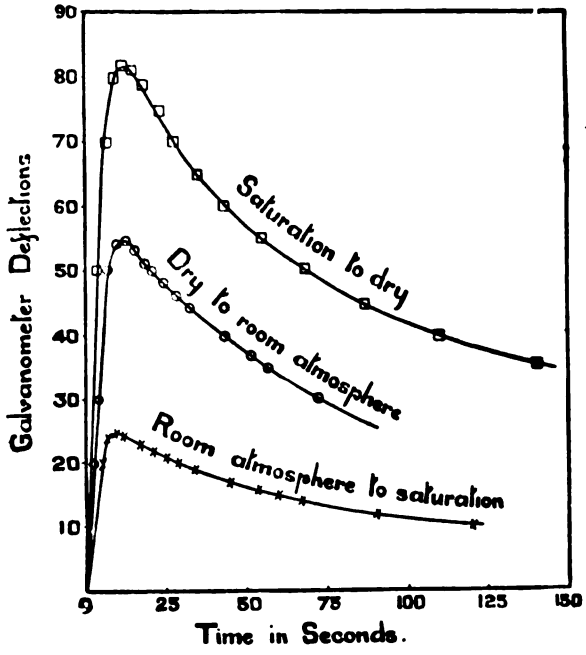


FIG. 20.

of 2·7° C. When the galvanometer spot has returned to nearly zero the communication with the saturation tower is quickly opened and that to the atmosphere of the room closed. A similar form of curve is obtained.

Finally the saturation tower is cut off and communication made to the dry tower. The deflection will now be in the opposite direction since the cotton is being subjected to a dry atmosphere following a saturated one, and is consequently liberating moistnre. Any one of these operations can be carried out in the reverse direction with practically identical results.

Since the natural period of the moving coil system of the galvanometer is a fifth of a second, it closely follows the change of resistance of the coil. It will be observed that the sum of the maximum deflections obtained on exposure from " dry to room " and " room to saturation " successively is nearly equal to the maximum deflection obtained on going direct from " saturation " to " dry ".

The direct transfer gives a slightly larger deflection, owing presumably to the smaller loss of heat during the time it is rising to a maximum. The actual magnitude of the



Digitized by Google

deflection obtained depends upon several factors besides the relative humidity, such as the temperature of the air, velocity of the circulating air stream, galvanometer sensitivity, and the battery current. It was found, however, that the percentage deflection, *i.e.* ratio of {(Dry to Room)/[Dry to Room + Room to Saturation]} was independent of all the above variables, and (within the limits of the errors of experiment) a function of the relative humidity alone (see Table XIII and Fig. 21).

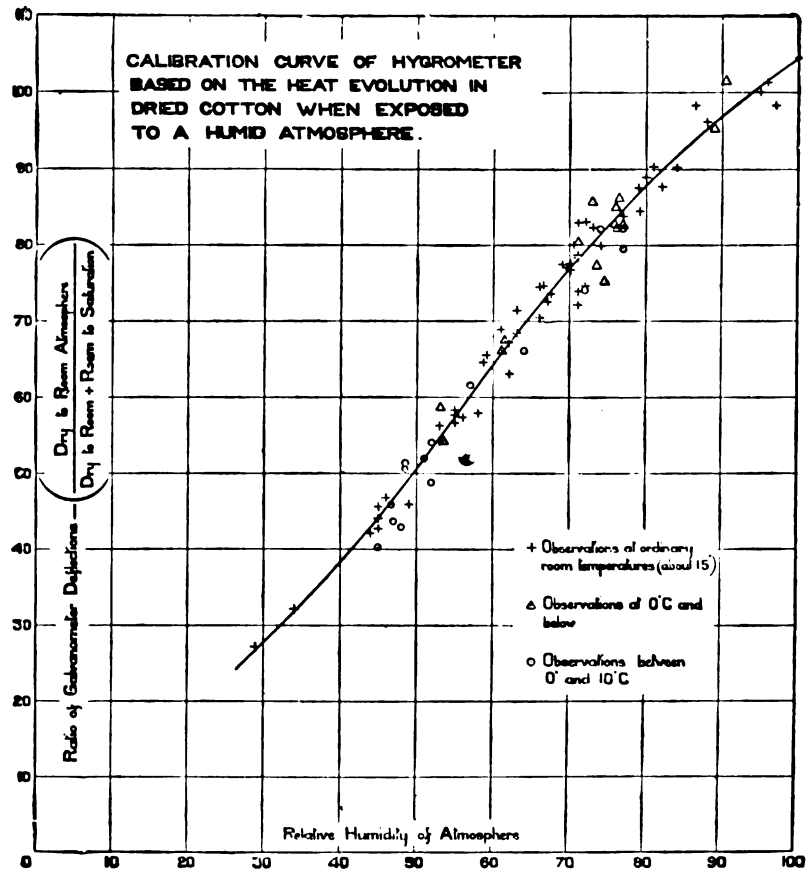
CALIBRATION CURVE OF HYGROMETER BASED ON THE HEAT EVOLUTION IN DRIED COTTON WHEN EXPOSED TO A HUMID ATMOSPHERE.
Ratio of Galvanometer Deflections — Dry to Room Atmosphere / Dry to Room + Room to Saturation
Relative Humidity of Atmosphere
+ Observations at ordinary room temperatures (about 15)
△ Observations at 0°C and below
o Observations between 0° and 10°C
0
10
20
30
40
50
60
70
80
90
100

Fig. 21.

This procedure in taking the observations was found to be much more convenient than attempting to find a " constant " for the instrument, since it reduces the work to merely observing deflections of the galvanometer spot, and the instrument is self calibrating once the form of the curve connecting deflection ratios to true humidity has been determined.

Several features of the curves shown in Figs. 20 and 21 deserve attention. An analysis of the data in Fig. 20 indicates that the rate of cooling is not proportional to the temperature excess: the heat loss is very rapid initially, and then slows downs considerably. In fact it seems that the cotton continues to absorb moisture, thus generating heat, for a considerable time after the maximum effect has been observed. The same applies to the drying out when exposed to air which has circulated through

Digitized by Google

TABLE XIII.—The Thermal (Cotton) Hygrometer.

| I. | II. | III. | IV. | V. | VI. | VII. | VIII. | IX. | X. | XI. | XII. |
|---|---|---|---|---|---|---|---|---|---|---|---|
| Date. | Time. | Temp. room. ° C | Humidity by psychrometer. | Humidity by dew-point apparatus. | Mean humidity. | Deflection :— Dry to room atmosphere. | Deflection :— Room atmosphere to saturation. | Sum of dry to atmosphere + atmosphere to saturation. | Deflection :— Saturation to dry. | Ratio :— Dry to atmosphere / Dry to atmosphere + atmosphere to saturation. | Difference from mean curve through observations. |
| 1920. | | | | | | | | | | | |
| Oct. 15 ... | 10.42 a.m. | 15° | 82 | — | 82 | 67·8 | 9·5 | 77·3 | 71·5 | 87·7 | −2·3 |
| „ 20 ... | 9.31 „ | 12° | 68 | — | 68 | 56 | — | — | 82 | — | — |
| „ 20 ... | 11.50 „ | 13·7° | 63 | — | 63 | 54·5 | 25 | 79·5 | 82 | 68·5 | 0 |
| „ 21 ... | 10.26 „ | 10·5° | 72 | — | 72 | 53·8 | 18·8 | 72·6 | 75 | 74·1 | −5·4 |
| „ 25 ... | 4.44 p.m. | 15·6° | 70 | 72 | 71 | 52 | 20 | 72 | 71 | 72·2 | −5·8 |
| „ 25 ... | 9.15 a.m. | 15° | 57 | 59 | 58 | 40 | 29 | 69 | 71 | 58 | −3·5 |
| „ 26 ... | 10.54 „ | 17° | 54 | 58 | 56 | 44 | 32·5 | 76·5 | 80 | 57·5 | −1·5 |
| „ 26 ... | 2.37 p.m. | 23·5° | 96 | 98 | 97 | 110 | 18 | 128 | 96 | 98·4 | −4·1 |
| „ 27 ... | 3.33 „ | 15° | 69 | 71 | 70 | 56·5 | 17 | 73·5 | 71 | 76·9 | −0·1 |
| „ 28 ... | 11.40 a.m. | 15° | 65·5 | 66·5 | 66 | 48 | 20 | 68 | 69·8 | 70·6 | −1·4 |
| „ 28 ... | 4.34 p.m. | 23° | 100 | 100 | 100 | 110 | −5 | 105 | 88 | 104·7 | +0·2 |
| „ 29 ... | 11.45 a.m. | 14° | 67 | 67 | 67 | 45·5 | 17·2 | 63 | 66·2 | 72·6 | −0·9 |
| „ 29 ... | 3.49 p.m. | 16° | 62 | — | 62 | 42·8 | 25 | 67·8 | 69·3 | 63·1 | −3·9 |
| „ 30 ... | 7.30 „ | 14° | 55 | 55 | 55 | 40 | 30·5 | 70·5 | 68·8 | 56·7 | −0·8 |
| „ 31 ... | 6.30 „ | 12° | 71 | 71 | 71 | 50·6 | 13·7 | 64·3 | 63·1 | 78·7 | +0·7 |
| Nov. 1 ... | 3.30 „ | 10° | 79 | 75 | 77 | 50·4 | 13 | 63·4 | 59 | 79·5 | −5·5 |
| „ 1 ... | 8.30 „ | 9° | 79 | 75 | 77 | 46·6 | 10·1 | 56·7 | 54·5 | 82·2 | −2·8 |
| „ 2 ... | 4.55 „ | 9° | — | 46·7 | — | 23·2 | 27·3 | 50·5 | 54·7 | 45·9 | −0·6 |
| „ 3 ... | 12.30 „ | 13° | — | 28·8 | — | 13·6 | 36·5 | 50 | 53·5 | 27·1 | +0·1 |
| „ 3 ... | 4.50 „ | 15° | — | 34 | — | 19 | 40 | 59 | 62·5 | 32·2 | +0·2 |
| „ 6 ... | 11.30 a.m. | 0° | 76 | 73 | 74·5 | 22·8 | 7·5 | 30·3 | 31 | 75·3 | −6·7 |
| „ 6 ... | 12.45 p.m. | 0° | 75 | 72 | 73·5 | 24 | 7 | 31 | 29·7 | 77·4 | −3·6 |
| „ 9 ... | 3.0 „ | −1° | 75 | 79 | 77 | 24·3 | 5 | 29·3 | 29·4 | 82·9 | −2·1 |
| „ 15 ... | 2.30 „ | 0° | 77 | 75 | 76 | 27·8 | 4·9 | 32·7 | 32·5 | 85 | +1 |
| „ 25 ... | 11.0 a.m. | −3° | 78 | 74 | 76 | 24 | 5 | 29 | 26·5 | 82·5 | −1·2 |
| „ 27 ... | 10.30 „ | −4° | 74 | 72 | 73 | 20·8 | 3·5 | 24·3 | 24 | 85·6 | +5·1 |

(B 34—2879)z Y 2

Digitized by Google

TABLE XIII.—The Thermal (Cotton) Hygrometer (continued).

| I. | II. | III. | IV. | V. | VI. | VII. | VIII. | IX. | X. | XI. | XII. |
|---|---|---|---|---|---|---|---|---|---|---|---|
| Date. | Time. | Temp. room. ° C. | Humidity by psychrometer. | Humidity by dew-point apparatus. | Mean humidity. | Deflection :— Dry to room atmosphere. | Deflection :— Room atmosphere to saturation. | Sum of dry to atmosphere + atmosphere to saturation. | Deflection :— Saturation to dry. | Ratio :— Dry to atmosphere / Dry to atmosphere + atmosphere to saturation. | Difference from mean curve through observations. |
| 1920. | | | | | | | | | | | |
| Dec. 2 ... | 12.30 p.m. | −1° | 76 | 73 | 74·5 | 25·2 | 8 | 33·2 | 29·8 | 75·9 | −6·1 |
| „ 3 ... | 9.45 „ | −1° | 79 | 74 | 76·5 | 25 | 4 | 29 | 27·5 | 86·2 | +2·2 |
| „ 6 ... | — | −2° | 78 | 75 | 76·5 | 22·4 | 4·8 | 27·2 | 27 | 82·3 | −1·7 |
| 1921. | | | | | | | | | | | |
| Jan. 24 ... | — | 15° | 71·7 | 71 | 71 | 51 | 10·4 | 61·4 | 60 | 83 | +5 |
| „ 25 ... | 2.30 p.m. | 17° | 59 | 58·5 | 58·7 | 42·2 | 23 | 65·2 | 69 | 64·6 | +1·6 |
| „ 25 ... | 4.45 „ | 18° | 54·4 | 55·5 | 55 | 39·5 | 29 | 68·5 | 69 | 57·7 | +0·2 |
| „ 26 ... | 2.30 „ | 18° | 53 | 53 | 53 | 39·3 | 30·5 | 69·8 | 71·5 | 56·3 | +1·8 |
| „ 26 ... | 4.55 „ | 19° | 45 | 45 | 45 | 29·2 | 39·4 | 68·6 | 71·8 | 42·6 | −1·4 |
| „ 27 ... | 12.30 „ | 17° | 49 | 48 | 49 | 29 | 34 | 63 | 69 | 46 | −3 |
| „ 28 ... | 4.0 „ | 16° | 75 | 73 | 74 | 53 | 13·3 | 66·3 | 66 | 80 | −1·5 |
| „ 29 ... | 12.0 noon | 17° | 77·5 | 76 | 77 | 57·5 | 11 | 68·5 | 67 | 83·9 | −0·6 |
| „ 31 ... | 4.20 p.m. | 15° | 73 | 71 | 72 | 49 | 16·7 | 65·7 | 63 | 74·6 | −4·9 |
| Feb. 1 ... | 4.55 „ | 13° | 69·5 | 70 | 69·7 | 42·5 | 12·5 | 55 | 55·7 | 77·3 | +0·3 |
| „ 2 ... | 4.30 | 14° | 71 | 71 | 71 | 46 | 14 | 60 | 58·4 | 74 | −4 |
| „ 5 ... | 12.35 „ | 14° | 55 | 55 | 55 | 35 | 25 | 60 | 61·7 | 58·3 | +0·8 |
| „ 7 ... | 4.35 „ | 13° | 52·5 | 53·5 | 53 | 32 | 27 | 59 | 61 | 54·2 | −0·3 |
| „ 16 ... | 1.10 „ | 16° | 62 | 61·7 | 62 | 43 | 21 | 64 | 64·6 | 67·2 | +0·2 |
| „ 17 ... | 1.0 „ | 16° | 96 | — | 96 | 73·5 | −1 | 72·5 | 66·5 | 101·4 | −0·1 |
| „ 18 ... | — | 17° | 95 | 95·4 | 95 | 74 | 0 | 47 | 68·5 | 100 | −1 |
| „ 19 ... | 10.30 a.m. | 10° | 73·5 | 74·4 | 74 | 41·2 | 9 | 50·2 | 51 | 82·1 | +0·6 |
| „ 22 ... | 11.30 „ | 12° | 69 | 68·6 | 69 | 43 | 12·5 | 55·5 | 56·6 | 77·5 | +1·5 |
| „ 26 ... | 11.20 „ | 10° | 63·5 | 64·1 | 64 | 33·2 | 17 | 50 | 49·5 | 66·1 | −3·9 |
| „ 28 ... | 5.0 p.m. | 9° | 56·5 | 57·3 | 57 | 29 | 18·1 | 47 | 49 | 61·6 | +1·1 |
| Mar. 2 ... | 12.40 „ | 6° | 52·5 | 51 | 52 | 23 | 19·5 | 42·5 | 42·3 | 54·1 | +0·6 |
| „ 3 ... | 12.35 „ | 6° | 49·5 | 47·5 | 48·5 | 21 | 20·5 | 41·5 | 42·5 | 50·6 | +1·9 |

Digitized by Google

| I. | II. | III. | IV. | V. | VI. | VII. | VIII. | IX. | X. | XI. | XII. |
|---|---|---|---|---|---|---|---|---|---|---|---|
| Mar. 3 ... | 5.0 p.m. | 7° | 49 | 48 | 48·5 | 22 | 20·8 | 42·8 | 42 | 51·4 | +2·7 |
| „ 4 ... | 5.0 „ | 13° | 46 | 46 | 46 | 24·3 | 27·5 | 51·8 | 52 | 46·9 | +1·4 |
| „ 5 ... | 12.30 „ | 14° | 45 | 45 | 45 | 24 | 30·6 | 54·6 | 53·5 | 44 | 0 |
| „ 7 ... | 12.30 „ | 12° | 45 | 45 | 45 | 22·3 | 26·6 | 48·9 | 49·2 | 45·6 | +1·6 |
| „ 7 ... | 5.0 „ | 13° | 44·1 | 44 | 44 | 22·5 | 31 | 53·5 | 51·2 | 42·1 | −0·9 |
| „ 8 ... | 12.45 „ | 9° | 46 | 44 | 45 | 18·9 | 28 | 46·9 | 47 | 40·3 | −3·7 |
| „ 8 ... | 5.0 „ | 7° | 47 | 47 | 47 | 18·2 | 23·4 | 41·6 | 41 | 43·8 | −3 |
| „ 9 ... | 5.0 „ | 4° | 52·5 | 51 | 52 | 18·2 | 19 | 37·2 | 36·7 | 48·9 | −4·5 |
| „ 10 ... | 5.0 „ | 4° | 48 | 48 | 48 | 16 | 21·2 | 37·2 | 37·5 | 43 | −5 |
| „ 11 ... | 12.30 „ | 3° | 52 | 50 | 51 | 18·5 | 17 | 35·5 | 34 | 52 | 0 |
| „ 11 ... | 5.0 „ | 0° | 55 | 52 | 53·5 | 16·7 | 14 | 30·7 | 31·7 | 54·4 | −1 |
| „ 12 ... | 9.30 a.m. | −1° | 64 | 58 | 61 | 17·7 | 9 | 26·7 | 28·7 | 66·3 | +0·3 |
| „ 12 ... | 12.45 p.m. | 0° | 54 | 52 | 53 | 16·4 | 11·5 | 27·9 | 29 | 58·8 | +4·3 |
| „ 12 ... | 4.0 „ | 0° | 89 | 89 | 89 | 30·2 | 1·5 | 31·7 | 28·8 | 95·3 | −0·7 |
| „ 14 ... | 5.0 „ | 12° | 79 | 79 | 79 | 53·8 | 7·7 | 61·5 | 56·4 | 87·5 | +0·5 |
| „ 15 ... | 12.30 „ | 12° | 72 | 72 | 72 | 46 | 9·3 | 55·3 | 54·5 | 83·1 | +3·6 |
| „ 15 ... | 5.0 „ | 13° | 73 | 73 | 73 | 47 | 10 | 57 | 56·5 | 82·4 | +1·9 |
| „ 16 ... | 12.40 „ | 12° | 72 | 74 | 73 | 46·8 | 11 | 57·8 | 84·3 | 81 | +0·5 |
| „ 16 ... | 5.10 „ | 14° | 71 | 71 | 71 | 49 | 13·4 | 62·4 | 59·6 | 78·5 | +0·5 |
| „ 17 ... | 12.40 „ | 12° | 70·5 | 70·7 | 70·6 | 43·5 | 10·7 | 44·2 | 52 | 80·2 | +2·7 |
| „ 17 ... | 5.0 „ | 14° | 84 | 84 | 84 | 56 | 60 | 116 | 57 | 90·3 | −1·4 |
| „ 18 ... | 12.35 „ | 14° | 78·5 | 79·8 | 79·2 | 51·8 | 9·5 | 61·3 | 57·7 | 84·5 | −2·5 |
| „ 18 ... | 5.0 „ | 15° | 88 | 87·4 | 87·7 | 63·5 | 2·5 | 66 | 64 | 96·2 | +1·2 |
| „ 19 ... | 12.35 „ | 15° | 86·5 | 86·5 | 86·5 | 60 | 1 | 61 | 59·5 | 98·3 | +4·3 |
| „ 21 ... | 5.0 „ | 15° | 80 | 80 | 80 | 55 | 6·8 | 61·8 | 58·5 | 89 | +1 |
| „ 22 ... | 12.30 „ | 16° | 82 | 80 | 81 | 56·4 | 6 | 62·4 | 60 | 90·4 | +1·4 |
| „ 22 ... | 5.0 „ | 15° | 68 | 67 | 67·5 | 45·8 | 16·3 | 62·1 | 61·5 | 73·7 | −0·3 |
| „ 31 ... | 4.50 „ | −1° | 63 | 60 | 61·5 | 22 | 10·6 | 32·6 | 30·4 | 67·5 | +1 |
| Apr. 1 ... | 12.30 „ | 0° | 78 | 76 | 77 | 21·3 | 1·9 | 23·2 | 31·2 | 93·9 | +9·1 |
| „ 1 ... | 5.0 „ | 0° | 92 | 89 | 90·5 | 33·7 | −5 | 28·7 | 31·2 | 101·5 | +4 |
| „ 2 ... | 12.30 „ | −2° | 72 | 70 | 71 | 23 | 5·6 | 28·6 | 28·5 | 80·4 | +2·4 |
| „ 11 ... | 5.0 „ | 15° | 71·5 | 68·5 | 70 | 48·3 | 14 | 62·3 | 63·2 | 77·5 | +0·5 |
| „ 14 ... | 5.0 „ | 14° | 66 | — | 66 | 42·7 | 14·5 | 57·2 | 48·2 | 74·6 | +2·3 |
| „ 20 ... | 5.0 „ | 12° | 62 | 60 | 61 | 36 | 16 | 52 | 52·2 | 69 | +3 |
| „ 21 ... | 12.30 „ | 12° | 63·5 | 62·5 | 63 | 36·5 | 14·5 | 51 | 51·3 | 71·5 | +3 |
| „ 21 ... | 5.0 „ | 14° | 60 | 58 | 59 | 36·5 | 19 | 55·5 | 56 | 65·7 | +2·7 |
| „ 22 ... | 5.0 „ | 15° | 67 | 65·6 | 66·3 | 44 | 15 | 59 | 57 | 74·6 | +2·1 |

Digitized by Google

the $CaCl_2$ tower. Hence it is difficult to calculate the correction for the heat loss during the period the deflection is rising to a maximum. The problem is further complicated by the fact that the observed temperature is that of the wire core, and this may differ appreciably from that of the cotton surface in contact with the air stream. Cotton is a complex organic material concerning which very little is known.

It is probable that the form of the curve shown in Fig. 21 is determined to some extent by the mechanical details of the apparatus. In the ideal case one would expect that the quantity [(Dry to atmosphere)/(Dry to atmosphere + Atmosphere to saturation)] would be proportional to the relative humidity.

When the atmosphere of the room is near saturation one finds that the deflection obtained on exposure of the dry cotton to the atmosphere is equal to or slightly greater than that obtained when the dry cotton is exposed to the air circulated from the "saturation" tower. This is probably due to the fact that the air coming into contact with the resistance coil from the "saturation" tower is below room temperature. When the humidity of the room atmosphere is raised by blowing steam into the air, the temperature rises quite considerably, and it is to be expected that the temperature of the layer of muslin within the saturation tower would lag behind that of the room.

Further, the action of the pumping arrangements tends to produce rarefaction of the air being circulated if there is any resistance to its flow. The conclusion one arrives at after an extended experience with the apparatus is that it is very difficult to obtain results with it when the humidity of the atmosphere is near saturation.

It is conceivable that by further improvements in construction these defects may be remedied.

## 7. The Hot Wire Hygrometer.

Our attention has frequently been drawn to the possibility of applying the hot-wire method for measuring humidity.

Instruments utilising the fact that the thermal conductivity of the surrounding gas determines the heat loss from a wire, under appropriate conditions, have found extensive application as hydrogen and carbon dioxide recorders.

The method is an extraordinarily sensitive one for hydrogen-air mixtures since the thermal conductivity of hydrogen is nearly six times that of air. Koepsel* states that his apparatus is capable of easily detecting the presence of 0·001 per cent. of hydrogen without the use of a very refined measuring apparatus.

During the war Dr. Shakespear† made a portable instrument termed the "Katharometer" for measuring the permeability of balloon fabrics to hydrogen, and his instrument has been applied to a variety of uses.

The katharometer and $CO_2$ recorders are manufactured commercially by the Cambridge Instrument Co., Ltd.

* 'Ber. Deutsch. Physik. Ges.', vol. 10, p. 814, 1908.

† 'Proc. Phys. Soc.', Lond., vol. 33, p. 168, 1921.

Digitized by Google

We are not acquainted with the results of any experiments on the thermal conductivity of water-vapour air mixtures, but from some data we estimated that the effect of the change from absolute dryness to saturation of air at — 10° C. would be to increase its thermal conductivity by 8 parts in 10,000.

As it is desirable to measure humidities to an accuracy of 1 per cent., this will necessitate the measurement of thermal conductivity changes to a few parts in a million.

We inquired of the Cambridge Instrument Co., Ltd., what order of deflections they considered possible with their hot-wire instruments in hygrometric measurements. They stated that at room temperature with a totally suspended type of indicator it would be possible to obtain full-scale deflection for 100 per cent. humidity, but at — 10° C. the deflection would be about 14 millimetres, and with a recorder half this amount.

This decrease in sensitivity is due to the fact that the deflection depends upon the actual weight of vapour present in the air, and not its relative humidity.

A full-scale range of 14 millimetres would not give sufficient accuracy in hygrometric measurements, so it would be necessary to increase it either by the use of a more sensitive indicator or by raising the temperature of the hot wire.

Increasing the galvanometer sensitivity usually results in unstable zero, and increasing the temperature of the wire gives rise to convection currents. So the problem resolves itself into making very accurate resistance measurements when the wire and its insulation are exposed to a humid atmosphere.

One of the troubles of low-temperature work is the frequent deposition of dew, due to temperature changes causing supersaturation, and the formation of a moisture film on the electrical insulation of the wire would be fatal to reliable measurements.

There is also the additional complication of the presence of varying amounts of $CO_2$ in the atmosphere of the stores. It is a well-known fact that apples, etc., give off $CO_2$ and one modern method of storage is to seal the room and allow the $CO_2$ content to rise to 10 per cent. at the expense of the oxygen. Now it appears that volume for volume $CO_2$ has a greater effect on the thermal conductivity of the atmosphere than $H_2O$ vapour. So to eliminate this variable it would be necessary to employ an absorbent for $CO_2$, leaving the water vapour.

The writer is not acquainted with any absorbent for $CO_2$ which will not absorb $H_2O$ at the same time. The alternative method is to estimate by difference: determine the conductivity of the air containing $CO_2$ and the water vapour; then saturate and again find the conductivity.

It must not, however, be concluded that the hot-wire method has no applications in hygrometry. It is conceivable that it will prove to be of great service for humidity measurements at temperatures beyond the range of the classical methods, since the instrument measures the actual percentage of vapour present, and its sensitivity as a hygrometer will increase with temperature at about the same rate as the saturation vapour pressure.

Digitized by Google

ACKNOWLEDGMENTS.

The work described in this paper constitutes a part of a more extensive research carried out on behalf of the Food Investigation Board of the Department of Scientific and Industrial Research.

To the Chairman of the Engineering Committee, Sir ALFRED EWING, and the Chairman of the Insulation Sub-Committee, Sir RICHARD GLAZEBROOK, the author wishes to record his thanks for their continued interest in the work.

The Director of the Laboratory, Sir JOSEPH PETAVEL, has furthered the work by placing every facility at our disposal, and by constructive criticism of the various designs.

Mr. A. SNOW, Junior Observer, has rendered valuable assistance with the experimental work, and Mr. EDGAR A. GRIFFITHS has suggested many features embodied in the instruments.

## BIBLIOGRAPHY.

[This list, it is hoped, contains most of the important Papers bearing on the present discussion, but it is not intended that it should be regarded as exhaustive.]

1. *Apparatus and Methods for Maintaining Definite Humidity.*

"Humidity Control by Means of Sulphuric Acid Solutions, with Critical Compilation of Vapour Pressure Data". R. E. WILSON. 'J. Ind. Eng. Chem.', vol. 13, p. 326, 1921.

"Automatic Regulation of Humidity in Factories". U.S. Forest Products Laboratory. 'Scientific American', Supplement. January, 1920.

"Some Observations on the Influence of Humidity on the Physical Constants of Paper". KRESS and SILVERSTEIN. 'J. Ind. Eng. Chem.', vol. 9, p. 277, 1917.

"The Hygrostat and its Management". R. KEMPF. 'Zeits. Instrumentenk.', vol. 37, p. 193, 1917.

"Apparatus for Recording and Regulating the Humidity of the Air". 'Elektrotech. Anzeiger', vol. 28, p. 207, 1911.

"The Aqueous Pressure of some Hydrated Crystals, Oxalic Acid, Strontium Chloride and Sodium Sulphate". G. P. BAXTER and J. E. LANSING. 'J. Amer. Chem. Soc.', vol. 42, p. 419, 1920.

"Symposium on Drying". 'J. Ind. Eng. Chem.', vol. 13, pp. 427, 460, 1921.

2. *The Wet-and-Dry Bulb Hygrometer.*

"Assmann Psychrometer". 'Meteor. Zeits.', p. 15, 1891.

"The Psychrometric Formula". LOVE and SMEAL. 'Proc. Roy. Soc.', Victoria, vol. 24, Part II, 1911.

"Recent Advances in Meteorology". (Hygrometry). FERREL, p. 380, 1886.

"The Sling Psychrometer in a Balloon". H. A. HAZEN. 'Amer. Meteor. J.', vol. 10, 1893.

"Errors of the Psychrometer". H. A. HAZEN. 'Amer. Meteor. J.', vol. 10, 1893.

"Psychrometer Studies". H. A. HAZEN. 'Amer. Meteor. J.', vol. 11, 1894.

"Psychrometer unter dem Gefrierpunkt". EKHOLM. 'Meteor. Zeits.', vol. 29, 1894.

"Zur Theorie des Assmannschen Aspirations Psychrometers". EKHOLM. 'Meteor. Zeits.', vol. 29, 1894.

"Psychrometer Studies". H. A. HAZEN. 'Amer. Meteor. J.', vol. 11, 1895.

"Das Psychrometer unter dem Gefrierpunkt". H. A. HAZEN. 'Meteor. Zeits.', vol. 30, 1895.

Digitized by Google

" L'Emploi du Psychrometer aux Stations de Second Ordre ". PERNTER. ' Rapport du Comité Météorol. Internat., Séance de Pétersbourg', 1899.

" A New Hygrometer Method". E. B. H. WADE. ' Proc. Phys. Soc.', Lond., vol. 18, p. 137, 1901-2.

" Rational Psychrometric Formulæ ". W. H. CARRIER. ' Amer. Soc. Mech. Eng.', vol 33, p. 1005, 1911.

3. *The Hair Hygrometer.*

" Essais sur l'Hygrométrie ". BENEDICT DE SAUSSURE. Neuchâtel, 1783.

" Errors of Absorption Hygrometers ". S. P. FERGUSSON. Blue Hill Meteorological Observations, 1903-1904. Abstract in ' J. Roy. Meteor. Soc.', vol. 33, p. 67, 1907.

Circular No. 48. (Bureau of Standards). On Standard Methods of Gas Testing, 1916. Appendix J. Determination of Atmospheric Humidity.

Lambrecht's Polymeter. Symon's ' Meteor. Mag.' No. 488.

" Reliability of Hair Hygrometer Records in Balloon Ascents ". E. KLEINSCHMIDT. Beiträge z. Physik d. freien Atmosphäre, 2, p. 99, 1906-1907. Abstract by R. SÜRING. ' Zeits. Instrumentenk.', vol. 27, p. 378, 1907.

4. *Thermal Effect on Cotton Hygrometer.*

" On the Wetting of Cotton by Water Vapour ". ORME MASSON, D.Sc., F.R.S. ' Roy. Soc. Proc.', A., vol. 74, p. 230, 1904.

" On the Hygroscopic Action of Cotton ". ORME MASSON, D.Sc., F.R.S., and E. S. RICHARDS, B.Sc. ' Roy. Soc. Proc.', A., vol. 78, p. 412, 1906.

" Hygroscopic Properties of Textile Materials ". By SCHLOESING. Issued by the Manchester Chamber of Commerce Testing House. Reprinted in ' Textile World Record ', Boston, November, 1908.

5. *Hot Wire Method.*

History of method and references to original papers in " Automatic Methods of Gas Analysis depending upon Thermal Conductivity ". ' J. Ind. Eng. Chem.', vol. 12, pp. 359 and 895, 1920.

" Shakespear Permeameter for Balloon Fabric ". G. BARR. Advisory Committee for Aeronautics, Report No. 504, 1918.

" The Theory of the Katharometer ". H. A. DAYNES. ' Roy Soc. Proc.', A., vol. 97, p. 273, 1920.

6. *Absorption Hygrometers.*

" Absorption Hygrometer ". RIDEAL and HANNAH. ' Analyst ', vol. 40, p. 41, 1915.

" A New Hygrometer ". E. SALVIONI. ' N. Cimento ', vol. 3, p. 390, 1902.

Pettisson's Absorption Method. ' Zeits. Anal. Chem.', vol. 25, p. 467.

" Methods of Gas Analysis ", HEMPEL. 1902 Ed., p. 346.

" Absorption Hygrometer ". EDELMANN. ' Ann. der Phys. u. Chem.', vol. 6, p. 455, 1879.

" Absorption Hygrometer ". SONDERN and MATERN. ' Ann. der Phys. u. Chem.', vol. 9, p. 147, 1880.

" Ein Neues Hygrometer ". SONDERN. ' Meteor. Zeits.', p. 81, 1892.

7. *Miscellaneous Hygrometers and Tests.*

" Report on Hygrometric Methods ". Sir NAPIER SHAW. ' Phil. Trans.', vol. 179, p. 73, 1888.

" Determination of Relative Humidity of the Air by Refractometry ". M. FRANCE GIRAUD. ' J. de Phys.', 5th Ser., vol. 3, p. 900, 1913.



Digitized by Google

"Dew-Point Detection by Electrical Resistance". B. A. Report, Southport, 1903.

"The Foil Hygroscope". INWARDS. Symon's 'Meteor. Mag.', vol. 42, p. 126, 1907.

"A Method in Hygrometry". C. BARUS. 'Science', vol. 16, pp. 33–34, 1902. Suggests possibility of cooling by expansion artificially nucleated air until fog just appears.

"Improved Methods in Hygrometry". A. N. SHAW. 'Trans. Roy. Soc.', Canada, vol. 10, p. 85, 1916.

"A Metallographic Hygroscope". BENEDICKS and ARPI. 'J. Inst. Metals', vol. 7, p. 246, 1912.

"Colloidal Electrolytes". McBAIN and SALMON. 'Roy. Soc. Proc.', A, vol. 97, p. 46, 1920. [Method of preparing dew-point surface.]

Digitized by Google

# AN INSTRUMENT FOR USE IN MEASURING CONVECTED HEAT

BY

A. H. DAVIS, D.Sc.,
ASSISTANT IN THE PHYSICS DEPARTMENT.

Digitized by Google

## ABSTRACT.

THE rate at which an air stream carries off heat from a hot body may be determined if the mass flow and temperature rise of the air can be measured. An instrument is therefore described which has been used to measure the distribution both of temperature and of mass flow in air streams. In this instrument a platinum wire functions both as a resistance thermometer and as a hot-wire anemometer compensated for temperature changes in the ambient air. The compensation is satisfactory provided the temperature changes in the air are not so extreme that its thermal properties differ appreciably from those at normal temperature. Two forms of the instrument are described, one being direct reading and the other of the null type. Particulars are given of the calibration of the instrument in a horizontal wind channel, in a vertical hot-air channel, and when moved slowly downwards in still air by means of a form of ATTWOOD'S machine. An illustration is given of the measurement of convected heat by means of the instrument.


Digitized by Google

# AN INSTRUMENT FOR USE IN MEASURING CONVECTED HEAT.

By A. H. DAVIS, D.Sc., Assistant in the Physics Department.

[Reprinted with modifications from the 'Proceedings of the Physical Society of London', Vol. 33, 1921.]

## Introduction.

Heat losses by convection depend not only on the area of the surface of the body, but also on its form and orientation. If the theoretical calculation were possible in a few ideal cases, in actual practice it would still often be necessary to determine the heat loss by other means. Even in ideal cases the laws of convection are not yet accurately known, and it is desirable to ascertain the circumstances of air temperature and velocity in the vicinity of the cooling body. In this connection the present apparatus was devised to trace convection losses in the air itself.

If air, of density $\rho$ and temperature $\theta$, flowing with velocity $v$, was originally at 0° C., then the air has been supplied with heat which is passing a section normal to the stream at the rate of

$$v\rho s\theta \text{ cals. per sq. cm. per sec.} \quad . \quad . \quad . \quad . \quad . \quad . \quad . \quad (1)$$

$s$ being the known specific heat at constant pressure. The instrument to be described is a hot-wire anemometer measuring $v\rho$,* independent of the temperature of the air, and adapted for use as a resistance thermometer to obtain $\theta$. Thus it determines the rate at which convected heat is passing a given point.

It was constructed in two types, one being a null instrument, the other being direct reading, and so more convenient, but involving an approximation which somewhat restricts its range.

## Preliminary Theory of Hot-Wire Anemometer.

King,† in comprehensive experiments with platinum wires, verified his theoretical formula of the form

$$H/\theta = B\sqrt{(v\rho)} + C, \quad . \quad . \quad . \quad . \quad . \quad . \quad . \quad . \quad . \quad (2)$$

where H = heat loss per unit length of wire,

$\theta$ = *excess* of wire temperature over air-stream temperature,

$v$ = velocity of air,

$\rho$ = density of air,

B and C being constant for a given wire and temperature excess, and having but a small coefficient of change with temperature excess.

* In calibrating the instruments, mass flow $v\rho$ was expressed in terms of the velocity $v_{17}$ at which air at 17° C. would have to move to give the same mass flow.

Thus,

$$v\rho = v_{17}\rho_{17}\,; \text{ and } v\rho s\theta = 0{\cdot}000289\ (v_{17}\theta) \text{ cals./cm.}^2\text{/sec.} \quad . \quad . \quad . \quad . \quad . \quad . \quad . \quad (1A)$$

† 'Phil. Trans.', vol. 214, p. 373, 1914.

Digitized by Google

In his experiments, although the temperature of the wire was altered, that of the ambient air was always about 17° C.; but theoretically there is no reason for appreciable departure from the law through change of actual air temperature, for temperature *excess* is the essential factor. The null instrument was arranged to work at a constant temperature excess, and by experiment in a wind channel to which heated air was supplied, it was found that in these circumstances the relation between H and $v\rho$ was independent of the actual temperature of the air.

## Description of the Null Instrument.

### *Construction.*

The instrument consists essentially of a Wheatstone's net, as is seen from Fig. 1. In the fourth arm of the net TT is the 6-mil platinum wire, which is placed in the air

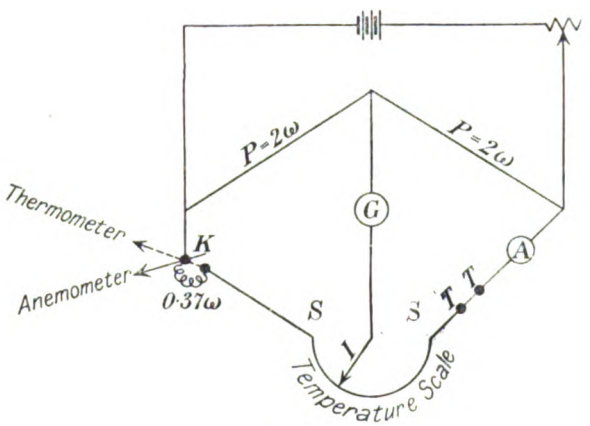


Fig. 1.

stream. An ammeter, A, gives the current through the wire. Manganin is the material of the rest of the bridge, as this has no temperature coefficient. SS is a slide wire. The third arm of the net consists of two coils, one of which can be short-circuited as desired by the key K, which carries an indicating pointer. For convenience, this pointer also controls the sensitivity of the galvanometer and, further, makes about a hundredfold difference to the current in the bridge. The connections, however, are not shown.

### *Method of Use and Theory of Null Instrument.*

Setting the indicator at *Thermometer* closes the key K and passes but a small current through the bridge. The instrument is now a resistance thermometer, the temperature of the air being read directly on the bridge wire scale from the position of the pointer I for balance. The slider is fixed in this position.

Setting the indicator at *Anemometer* now passes a larger current through the bridge and opens the key K, thus increasing the resistance of the arm by 0·37 ohm. Balance

Digitized by Google

can only be restored by heating the platinum wire to a definite temperature excess (108° C.), independent of the initial temperature of the air.* The requisite heating current $i$, which restores balance, is read from the ammeter. If R is the resistance of the wire at its working temperature, we have, using (2),

$$i^2R/\theta = H/\theta = B\sqrt{(v\rho)} + C, \quad . \quad . \quad . \quad . \quad . \quad . \quad . \quad . \quad . \quad (3)$$

or, since $\theta$ is constant,†

$$i^2R = F(v\rho). \quad . \quad . \quad . \quad . \quad . \quad . \quad . \quad . \quad . \quad . \quad . \quad (4)$$

Thus $i^2R$ measures the mass flow of air, and noting that the position of the pointer I already determined along the slide wire gives R, we see that $i^2R$ is readily obtained from one setting of a slide rule, and the mass flow is then known.

Even more conveniently, a three-scale nomogram may be readily constructed in which a thread stretched between the value $\theta$ on one scale and $i$ on another cuts the third scale at a point from which the air velocity is read off directly.

*Calibration of the Instrument.*

As thermometer the instrument was calibrated by direct determination of the ice point and of the steam point, and checked from a knowledge of the constants of the bridge wire and of the platinum wire.

As anemometer it was calibrated in wind channels. For use in measuring convection currents the calibration should extend as far as possible into the region of low speed. Also, when the air speeds become so low that they are comparable with the speed of the natural convection current from the anemometer wire, the instrument should be calibrated under such conditions that the air velocity is in the same direction, relative to the vertical, as in the experiment in which the instrument is to be employed.

The actual instrument worked at 108° C. temperature excess, but some preliminary work was done at air temperatures with an anemometer working at nearly three times this excess, so that the natural convection currents should be more pronounced. In this, instead of using vertically upward currents, the instrument was moved downwards through still air by a modification of ATTWOOD'S machine. The calibration was found to agree with that for horizontal currents in a wind channel, except, perhaps, for speeds lower than 10 cms. per second, and the relation (2) held down to 15 cms. per second, needing slight correction below.

The actual instrument should be reliable at least to these limits, and it was calibrated for various temperatures of air stream in a specially constructed vertical channel, and for room temperatures it was also calibrated in the horizontal 3-foot wind channel of

* This is exactly true when the resistance-temperature law is linear.

† Rigorous constancy of $\theta$ is not essential, for if $\theta$ depends on the initial temperature of the wire, the position of the pointer I determines $R/\theta$, and (3) is used instead of (4) without complication.

Digitized by Google

the National Physical Laboratory. In the horizontal channel the usual laboratory calibration was used for the higher speeds; however, since the pressure head measurements become insufficiently accurate for speeds less than 100 cms. per second, the lower speeds were obtained by observing smoke puffs through a window, and timing them with a stop watch over a distance of about 1 metre.

The special vertical channel is shown diagrammatically in Fig. 2. The entrance contained layers of wire gauze, and a honeycomb grid to break up eddies and to ensure

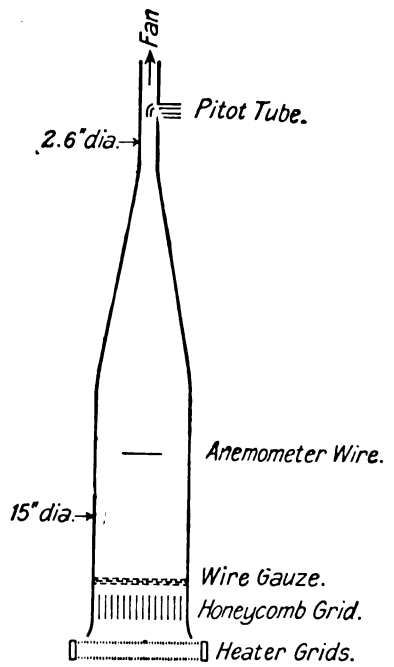


Fig. 2. Vertical hot-air channel.

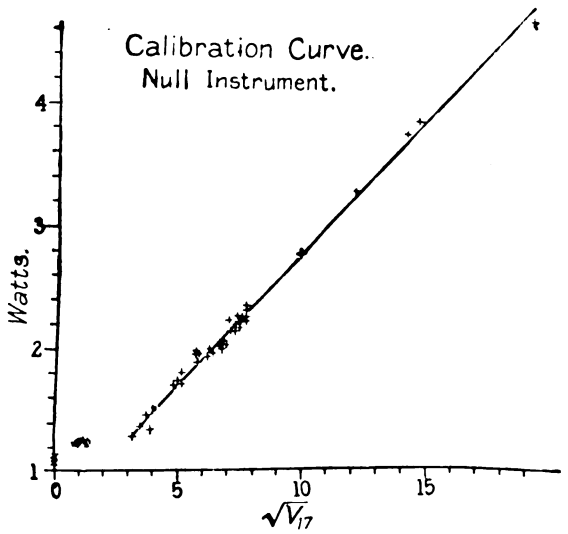


Fig. 3.

an evenly distributed and vertical flow of air. The speeds being too slow for direct measurement with the Pitot tube, this was inserted in a subsequent portion of the channel, of smaller diameter, reached by a section of approximate stream-line shape. For higher temperatures over a range of about 50° C., the air entering this channel was heated by the heater grid. The distribution of velocity across the neck was determined by the Pitot tube, and found to be independent of the temperature of the air stream. It was found that the calibration for ordinary temperatures in the horizontal channel agreed with those for the vertical channel and the hotter air, up to the temperatures reached. The results are shown graphically in Fig. 3. The relation (2) holds down to 9 cms. per second, and is not found to depend on the temperature of the ambient air.

## The Direct Reading Instrument.

Direct reading instruments have already been used,* in which, for ordinary temperatures, the out-of-balance deflection measures the mass flow of air. In the instrument

* Morris, 'Electrician', vol. 69, p. 1056, 1912.

Digitized by Google

here described it has been found possible to allow for the effect of temperature very approximately by choosing for each temperature an appropriate current through the anemometer wire.* The instrument differs from Fig. 1 only in the absence of the 0·37 ohm coil and its key K. The indicator which carried K remains, retaining its other functions, altering the current in the bridge and the sensitivity of the galvanometer. A simple key enables one millivoltmeter to be used either as A or as G, as required.

Setting the indicator at *Thermometer* sends a very small current through the wire. As before, the air temperature is read directly from the balance position of the slider on the slide wire. At the same time a second scale shows the anemometer current appropriate to the temperature.

Setting the indicator at *Anemometer* sends a heating current through the wire, and adjusting this to the appropriate value, the mass velocity of the air is read directly from the galvanometer scale. The reason for this is clear from the theory of the instrument in the anemometer position.

Let P, P, R and $(X + L_\theta)$ be respectively the resistances of the four arms of the bridge and let $L_0$, $L_t$, $L_\theta$ be respectively the resistance of the wire at 0° C., at air temperature $t$° C., and when heated by the current $c$ to 0° C. above air temperature. From the thermometer setting $R = X + L_t$. Then if $g$ be the current through the galvanometer of *high* resistance G, we have

$$g/c = L_0 a\theta/2G, \quad L_\theta = L_t + L_0 a\theta, \quad c^2 L_\theta = 0 \cdot f(v\rho),$$

whence

$$(2G/L_0 a)g = L_t c^3/[f(v\rho) - L_0 a c^2].$$

It will be seen that if $c$ be chosen so that $L_t c^3$ is constant, and if $[f(v\rho) - L_0 a c^2]$ does not vary appreciably for the necessary variations of $c$, then the galvanometer reading is a function of the mass velocity only. The appropriate current $c$ determined by $L_t$, depends on the temperature of the air stream only. For a range of 100° C., only 12 per cent. variation in $c$ is necessary to keep $L_t c^3$ constant. The slight effect of this variation on $[f(v\rho) - L_0 a c^2]$ may be approximately allowed for by choosing the current appropriate to $L_t$ such that the instrument reads quite correctly for one standard velocity $(V_s\rho)$ in the middle of the scale. Thus, instead of making $L_t c^3$ constant, make

$$L_t c^3/[f(V_s\rho) - L_0 a c^2] = \text{constant}.$$

Calculations given in Table I show for two air temperatures, 17° C. and 100° C., the appropriate currents and the galvanometer deflections produced by them for a range of air velocities.

* Since this Paper was first written, MORRIS (' Electrician', vol. 85, p. 227, 1920) has described an instrument for measuring air velocity in mines, in which the conversion of mass velocity to actual velocity is effected for each temperature by appropriate setting of the current. The present Paper shows that such adjustment is needed even to get mass velocities.



Digitized by Google

TABLE I.

| Velocity. $v_{17}$ cm./sec. | Galvanometer deflection. 17° C. $c = 1{\cdot}00$. | 100° C. $c = 0{\cdot}929$. |
|---|---|---|
| 9·0 | 20·1 | 19·6 |
| 42·1 | 10·7 | 10·7 |
| 100 | 7·3 | 7·3 |

The anemometer current varies but little over the range of temperature and the instrument is quite satisfactory.

The actual instrument was calibrated in the wind channels by means of the previously calibrated null instrument. The results are shown graphically in Fig. 4, where it is

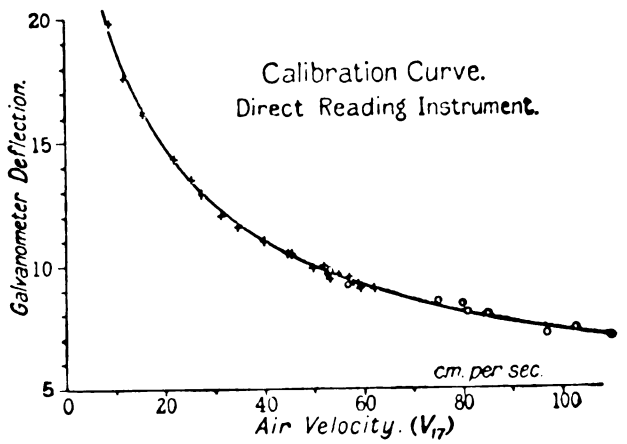


FIG. 4.

seen that the form of the curve agrees excellently with that calculated, and that no dependence on the temperature of the air is revealed. Finally, the scale of equal divisions was removed from the galvanometer, and a direct velocity scale engraved.

Fig. 5 illustrates a portable instrument as supplied to Dr. EZER GRIFFITHS for his study of air currents in the hold of a cargo ship engaged in overseas apple transport. At the side of the main box may be seen the anemometer wire in its holder, and a number of spare wires; these are normally housed within the box.

## EXAMPLE OF MEASUREMENT OF CONVECTION.

The heat loss by convection from unit length of a horizontal cylinder was measured by means of the instrument and checked from a knowledge of the actual watts consumed, after allowing for radiation. Keeping the exploring wire always parallel to the axis

Digitized by Google

of the cylinder, the distributions of velocity and temperature were obtained for the air passing vertically upwards through a horizontal plane about 10 cms. above the cylinder.

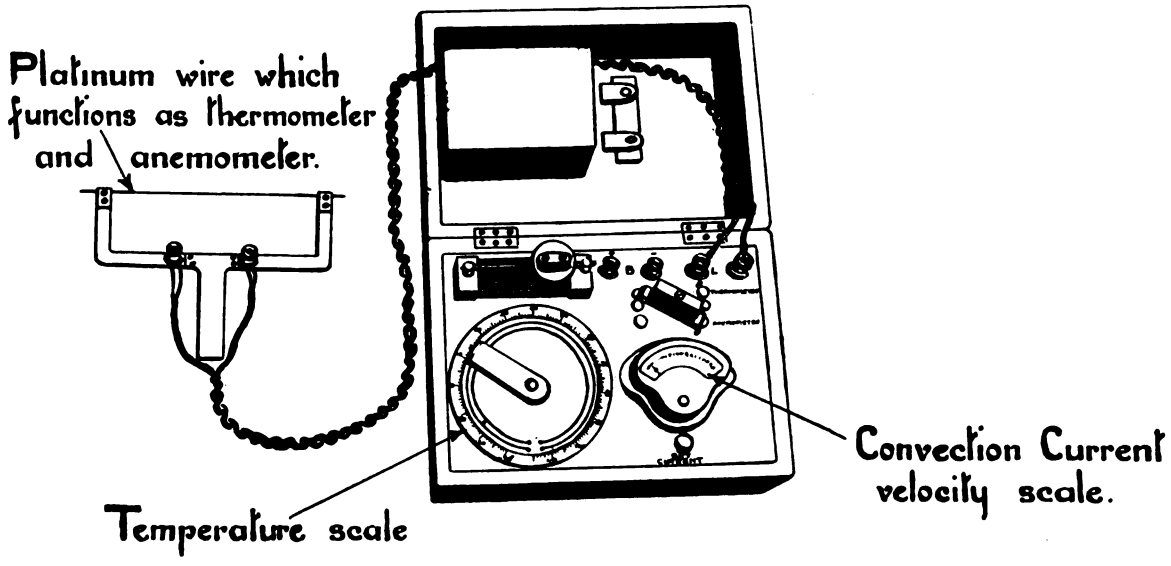


FIG. 5. Portable Direct Reading Hot Wire Anemometer.

In Fig. 6 the curves show for the air stream the temperature excess ($\theta$) above room temperature, the velocity ($v_{17}$), and the product $v_{17}\theta$. The abscissæ represent distances

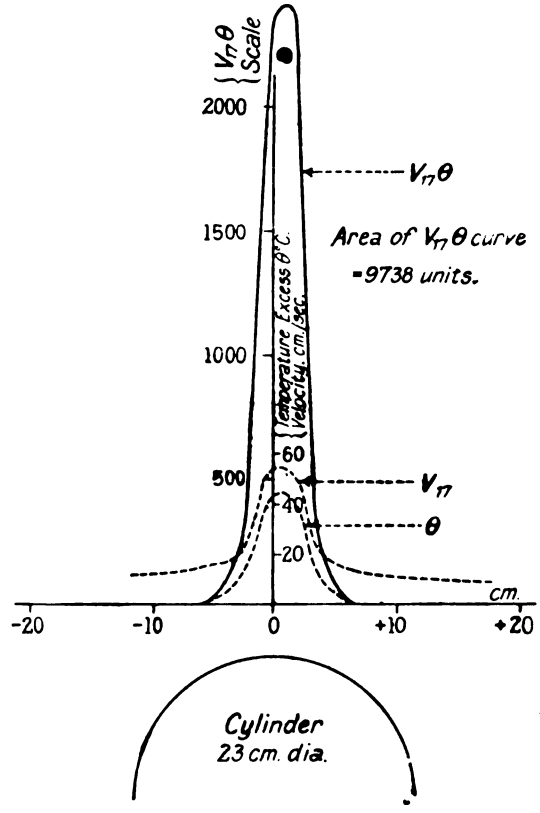


FIG. 6. Convection Current above Horizontal Cylinder.



Digitized by Google

to the right or left of the vertical through the axis of the cylinder. Using (1*a*), the heat ($h$) carried off per unit length of the cylinder is readily seen to be

$$h = 0{\cdot}000289\int(v_{17}\theta)\,dx, \textit{ i.e.}$$
$$= 0{\cdot}000289 \text{ (Area of the } v_{17}\theta \text{ curve)}$$
$$= 2{\cdot}8 \text{ calories per cm. per sec.}$$

The value obtained by other means was 3 calories per cm. per sec., and is in good agreement, considering the sources of error associated with convection measurements using large bodies. Fuller details of the use of the instrument in this manner may be published later.

The combined instrument has been designed and developed for measuring certain convection losses and currents in elucidating the laws of convection of heat—work which has arisen out of and forms part of researches on cold storage insulation being carried out at the National Physical Laboratory, under the direction of Dr. EZER GRIFFITHS for the Food Investigation Board of the Department of Scientific and Industrial Research. The author desires to thank Dr. GRIFFITHS also for advice in the preparation for publication.

Digitized by Google

# CONVECTION OF HEAT IN GASES AND LIQUIDS. I.—CONVECTION OF HEAT AND SIMILITUDE

BY

A. H. DAVIS, D.Sc.,
ASSISTANT IN THE PHYSICS DEPARTMENT.

Digitized by Google

## ABSTRACT.

1. The hydrodynamic basis of convection of heat suggests study by means of models.
2. We have the formulæ :

$$\text{Natural convection} \quad . \quad . \quad . \quad . \quad . \quad . \quad . \quad . \quad . \quad . \quad h = (k\theta/l)\mathrm{F}(c^2gl^3a\theta/k^2),$$

$$\text{Forced convection} \quad . \quad . \quad . \quad . \quad . \quad . \quad . \quad . \quad . \quad . \quad h = (k\theta/l)\mathrm{F}(lvc/k).$$

3. Graphs drawn with $h \div (k\theta/l)$ as ordinate and either $(c^2gl^3a\theta/k^2)$ or $(lvc/k)$ as abscissa should be independent of the size of the object ; consequently, to ascertain the heat-loss for any particular body it should be necessary only to perform the appropriate experiment with a model.

4. For natural convection PÉCLET'S data have been analysed with promising result. The formula would not be applicable to bodies where the fluid expansion caused was no longer negligible as a mere volume change.

5. For forced convection the formula, tested by data given by HUGHES, is very promising. The cooling fluid is not heated so much as in natural convection, and can still be regarded as incompressible for smaller bodies at higher temperatures. The formula is good, even for thin wires, and it is satisfactory to trace in it the hydrodynamic variable determining turbulence.

6. Evidence available in published data indicates that, for heat-loss from a body, an excellent first approximation can be obtained from experiments with a model. The principle of similitude affords a convenient method of expressing experimental results.


Digitized by Google

# CONVECTION OF HEAT IN GASES AND LIQUIDS. I.—CONVECTION OF HEAT AND SIMILITUDE.

By A. H. DAVIS, D.Sc., Assistant in the Physics Department.

[Reprinted, with modifications, from the 'Philosophical Magazine', Vol. 40, 1920.]

## Introduction.

The heat-losses from a hot body may be due to conduction, radiation and convection. While the two former may be calculated, if the constants of the materials and surfaces be known, the loss by convection is complicated by its dependence on the geometrical form of the surface. Although for the simplest forms (spheres, cylinders, etc.) the effect may be calculable, it is obvious that in general it can only be found by experiment, using either the actual object or an object of similar form. It may be remarked here that, mathematically, convection is a combination of hydrodynamics with the Fourier equations for heat-flow, and that in the solution of the purely hydrodynamic problems presented by ships and by aircraft the value of experiments with models has been proved. One is led, therefore, to derive relations applicable to convection from the standpoint of models.

Convective cooling is taken to refer to the total heat transfer from a hot body by the medium of a fluid moving past the surface. Such cooling is said to be "natural" or "free" when the fluid is still, except for the streams set up by the heat from the hot body itself, and is said to be "forced" when the body is immersed in a fluid stream, usually considered to be moving with such velocity that the currents set up by the hot body itself are negligible.

## 1. Natural Convection.

### *Formula.*

Boussinesq has given a mathematical solution of the problem of heat-loss by convection, natural * and forced. † The desirability of conducting experiments and expressing experimental results in a form applicable to models is further indicated by the fact that study of his analysis shows that he is led to consider bodies of similar form. The equations required for this paper may be deduced from his. However, they may also be obtained from the principle of similitude. Rayleigh ‡ has pointed this out for the case of forced convection. It is instructive to work out the case for natural convection from this alternative point of view.

* 'Comptes Rendus', vol. 132, p. 1382, 1901.

† 'Comptes Rendus', vol. 133, p. 257, 1901.

‡ 'Nature', vol. 95, p. 66, 1915.

Digitized by Google

Let the fundamental units be those of mass (M), length (L), time (T), and temperature ($\Theta$). The derived units are given in brackets below. For an inviscid fluid, BOUSSINESQ's equations show that the mean heat-loss "$h$" ($MT^{-3}$) per unit area of a body per unit time depends upon

| | |
|---|---|
| $k$, ($MT^{-3}L\Theta^{-1}$) | thermal conductivity of the fluid. |
| $c$, ($MT^{-2}L^{-1}\Theta^{-1}$) | capacity for heat per unit volume of the fluid. |
| $\theta$, ($\Theta$) | temperature excess of the body. |
| $a$, ($\Theta^{-1}$) | coefficient of density reduction of the fluid per degree rise of temperature. |
| $g$, ($LT^{-2}$) | acceleration due to gravity. |
| $l$, (L) | linear dimensions of the body. |

Since we deal with the capacity for heat per unit volume of the fluid, reflection shows why the density ($\rho$) of the fluid does not enter. The convection currents, essentially gravity currents, depend upon the density of the heated fluid *relative* to that of the cool fluid, and not upon the absolute density.

BOUSSINESQ regards the effect of the thermal expansion of the fluid as negligible except in so far as it alters the weight of unit volume of the fluid—that is, except in so far as "$a$" and "$g$" occur as a product. Consequently, let

$$h = k^u c^v \theta^w (ag)^x l^z ; \quad \ldots\ldots\ldots\ldots \quad (1)$$

then we readily derive :—

| | |
|---|---|
| By mass | $1 = u + v,$ |
| By length | $0 = u - v + x + z,$ |
| By time | $-3 = -3u - 2v - 2x,$ |
| By temperature | $0 = -u - v + w - x ;$ |

whence

$$u = 1 - 2x,\ w = 1 + x,\ z = 3x - 1,\ v = 2x. \quad \ldots\ldots\ldots \quad (2)$$

Substituting in (1) we obtain

$$h = (k\theta/l)\,(c^2 g l^3 a\theta/k^2)^x \quad \ldots\ldots\ldots\ldots \quad (3)$$

Since "$x$" is undetermined, we must write

$$h = (k\theta/l)\mathrm{F}(c^2 g l^3 a\theta/k^2) \quad \ldots\ldots\ldots\ldots \quad (4)$$

Let us consider the assumption that expansion effects of the fluid are negligible except in so far as they alter the weight of unit volume and so set up gravity currents. With

Digitized by Google

large bodies this will be fairly true. But in an extreme case of a hot thin wire, the mere volume changes of the air near the wire may be far from negligible. Indeed, observation of smoke near a hot thin wire shows that the effective diameter of the wire seems several times its true diameter. In this case we shall not expect (4) to hold. Convection data for wires, given by LANGMUIR,* show on test that the relation (8) based on (4) does not hold; and, in fact, LANGMUIR, in his theory, supposes the wire surrounded by a stationary film of fluid, of thickness several times the actual diameter of the wire. For large bodies at moderate temperatures our formula should be satisfactory.

For a viscous fluid we find, on introducing a term $\nu^t$ ($\nu$ being the kinematical viscosity coefficient with dimensions $L^2T^{-1}$),

$$h = (k\theta/l)\,(c^3gl^3a\theta/k^3)^x(c\nu/k)^t. \quad . \quad . \quad . \quad . \quad . \quad . \quad . \quad . \quad (5)$$

For gases, by the kinetic theory, $(c\nu/k)$ = const. Actually it seems constant for a given kind of gas, and varies but moderately from one kind to another. If, analogous to RAYLEIGH'S † treatment of convection in a stream of fluid, $(c\nu/k)$ be supposed constant for all fluids, the result reduces to (3) as before. Viscosity, therefore, has less effect than one might expect.

On reflection this result may be made more or less clear. The kinetic theory of gases shows how increasing the viscosity ($\nu$) of a gas is equivalent to increasing its thermal diffusivity ($k/c$) in the same ratio. Consequently, although increase in viscosity may decrease the speed at which cold gas sweeps over the heated body, still at the same time the thermal diffusivity is increased, and the heat escapes laterally by this means.

### *Examination of Formula.*

$$h = (k\theta/l)\mathrm{F}(c^3gl^3a\theta/k^3). \quad . \quad . \quad . \quad . \quad . \quad . \quad . \quad . \quad . \quad (4)‡$$

The form of the function F may be determined experimentally by finding its variation with " $\theta$ ", say, the other quantities remaining constant. DULONG and PETIT§, PÉCLET,|| and COMPAN¶ have given formulæ in which, for the same body, $h \propto \theta^{1\cdot233}$. Hence

$$\mathrm{F}(c^3gl^3a\theta/k^3) = (c^3gl^3a\theta/k^3)^{0\cdot233},$$

* ' Phys. Rev.', vol. 34, p. 416, 1912.

† ' Nature ', vol. 95, p. 66, 1915.

‡ Equation (4) is present in BOUSSINESQ'S paper in the form

$$h \propto \theta^{4/3}\,(kc^3a)^{1/3} \quad \text{if} \quad l \propto (c^3a\theta/k^3)^{-1/3}, \quad . \quad . \quad . \quad . \quad . \quad . \quad . \quad . \quad . \quad . \quad (4a)$$

which is seen to be equivalent to (4) for

$$k\theta/l \propto \theta^{4/3}\,(kc^3a)^{1/3} \quad \text{when} \quad l \propto (c^3a\theta/k^3)^{-1/3}.$$

From this BOUSSINESQ obtains an equivalent of (6), but limited to the same body so that " $l$ " does not occur. He does not further test the equation.

§ DULONG and PETIT. See ' The Theory of Heat ', by T. PRESTON, edited by J. R. COTTER, p. 510, 1919.

|| See translation of PÉCLET'S paper in ' Practical Laws and Data on the Condensation of Steam in Covered and Bare Pipes.' C. P. PAULDING, 1904. Published by VAN NOSTRAND Co.

¶ ' Ann. Chim. Phys.', vol. 26, p. 482, 1902.



Digitized by Google

whence (5) becomes

$$h \propto \theta^{1\cdot233} k^{0\cdot534} c^{0\cdot466} a^{0\cdot233} g^{0\cdot233} l^{-0\cdot301} \quad \ldots \quad (6)$$

Now we may put $c = c_p \rho$, where $c_p$ is the specific heat of unit mass of the fluid, and for air is known to be practically independent of the density " $\rho$". Hence, for any given body, if " $k$", " $a$", and " $g$ " do not alter, $h \propto \rho^{0\cdot466} \theta^{1\cdot233}$. In excellent agreement with this, DULONG and PETIT found for air $h \propto p^{0\cdot45} \theta^{1\cdot233}$, the pressure "$p$ " being of course proportional to " $\rho$ ". Further, in one experiment with a very small cooling-chamber, COMPAN* found $h \propto \theta^{1\cdot154}$. Similar reasoning in this case gives $h \propto \rho^{0\cdot308} \theta^{1\cdot154}$, and COMPAN found experimentally $h \propto p^{0\cdot30}$ as his mean for this series. This is excellent agreement.

Let us return to the question of models. If, instead of attempting to determine the form of the function in (5), we so choose our models that its value is constant, we have

$$c^2 g l^3 a \theta / k^2 = \text{constant}, \quad \ldots \quad (7)$$

and then for models so chosen in size ($l$)

$$h \propto k\theta / l. \quad \ldots \quad (8)$$

If only the temperature and size of the model are varied, $c$, $g$, $a$ and $k$, the gaseous constants, remaining the same, (7) becomes

$$\theta l^3 = \text{constant}. \quad \ldots \quad (7a)$$

Data are available for testing whether $h \propto k\theta/l$ when $\theta l^3 = \text{const}$. E. PÉCLET has made perhaps the most complete experiments on heat-losses from surfaces (*Traité de Chaleur*, 3rd ed., 1860), and he measured the rate of cooling of metal cylinders and spheres filled with water. He used bodies ranging from 5 to 30 cms. in diameter and 5 to 50 cms. in length, placed in a large water-jacketed metal cylinder about 80 cms. in diameter and 100 cms. high. He worked at various values of temperature excess up to 65°. He found for these bodies

$$h \propto \mathrm{A} \theta^{1\cdot233},$$

where A has the value

for spheres . . . . . $\mathrm{A} = 1\cdot778 + 0\cdot13/r$,

for horizontal cylinders . . . . . $\mathrm{A} = 2\cdot058 + 0\cdot0382/r$,

" $r$ " being radius in metres.

Also a formula is given for vertical cylinders from which the values of A can be calculated for the similar bodies we require of this shape. All spheres are similar; and in a long horizontal cylinder it is obvious that the length does not affect the heat-loss per unit area, so the formula is applicable to models, even although in the actual experiments the ratio of length to diameter may not have been constant.

From PÉCLET'S formulæ heat-losses have, therefore, been calculated for similar bodies

* 'Ann. Chim. Phys.', vol. 26, p. 482, 1902.

Digitized by Google

in the cases mentioned above. Following (7*a*) the models have been so chosen that $\theta l^3 = \text{const.} = 6 \times 10^4$. The result is given in Table I. This choice is such that the first seven models roughly range in temperature excess and size over the region in which PÉCLET's experiments were confined. The eighth model, working at 480° C. excess, is an extrapolation.

TABLE I.—Heat-Loss from Models calculated from PÉCLET'S Formulæ.
(Test of relation $h \propto \theta/l$ for a series of models in which $\theta l^3 = \text{constant}$.)

| Model. | | Relative value of $h \div (\theta/l)$.* | | | |
|---|---|---|---|---|---|
| Temperature, $\theta$° C. | Linear† dimensions, $l$ (*cms.*). | Sphere. | Horizontal cylinder. | Vertical cylinder‡. | Mean. |
| 60 | 10·00 | 1·00 | 1·00 | 1·00 | 1·00 |
| 50 | 10·62 | 0·99 | 1·01 | 0·99 | 1·00 |
| 40 | 11·45 | 0·99 | 1·02 | 0·99 | 1·00 |
| 30 | 12·60 | 0·98 | 1·04 | 0·98 | 1·00 |
| 20 | 14·42 | 0·97 | 1·06 | 0·97 | 1·00 |
| 10 | 18·17 | 0·97 | 1·11 | 0·96 | 1·01 |
| 7·5 | 20·00 | 0·97 | 1·13 | 0·96 | 1·02 |
| 480 | 5·00 | 1·16 | 0·94 | 1·09 | 1·06 |
| 0·94 | 40·00 | — | — | 0·97 | 0·97 |

* Value given, for each shape, relative to value for first model of that shape.

† For spheres and horizontal cylinders "$l$" is the radius, for vertical cylinders it is the height.

‡ Vertical cylinders have height = 5 × radius.

N.B.—In any test of data obtained from empirical formulæ it should be borne in mind that the formula will tend to be most reliable in the central region of the experiments on which they are based, and less reliable at the limits.

This table indicates that instead of the arbitrary form $h \propto A\theta^{1\cdot233}$, where A has complicated empirical values, PÉCLET's results may possibly be presented in the form suggested by (5),

$$h \propto (\theta/l)F(\theta l^3).$$

This could only be decided by a complete study of the whole of his *experimental* results. However, the above shows that it is fairly true for $F(x) = x^{0\cdot233}$. In any case, it would be valuable to express results in a form applicable to models, and if this were found impossible, the fact is worth stating.

An alternative way of testing PÉCLET's data is to plot a curve with $h \div \theta/l$ as ordinate and $\theta l^3$ as abscissa. Of course, only values of $l$ and $\theta$ are taken which fall within the range of the actual experiments.



Digitized by Google

## 2. Convection from a Body in a Stream of Fluid.

### *Formula.*

Convection from a body in a stream of fluid moving with velocity $v$ (natural convection being negligible) has been determined by Boussinesq,

$$h = (k\theta/l)\mathrm{F}(lvc/k), \quad . \quad . \quad . \quad . \quad . \quad . \quad . \quad . \quad . \quad . \quad (9)$$

and Rayleigh has shown the derivation from the principle of similitude.

Since from the kinetic theory of gases, as mentioned above, $c\nu/k$ is constant, (9) becomes $h = (k\theta/l)\mathrm{F}(lv/\nu)$, and $(lv/\nu)$ is the well-known variable in experiments on fluid resistance and flow. This raises the possibility of a useful relation between the thermal and dynamic effects of a fluid stream. It is important apart from this, however; for if heat-loss is affected by change from stream-line motion to turbulence, it is satisfactory to find the equation for heat-loss contains the variable $(lv/\nu)$ which determines turbulence.

A formula given by Russell* for stream-line flow past a cylinder at right angles to the stream is readily seen to be equivalent to (9), where $\mathrm{F}(lvc/k) \propto (lvc/k)^{1/2}$. Although such special approximate forms of the function F calculated for stream-line flow might cease to hold when turbulence set in, the formula (9) would still be satisfactory. One recalls that in dealing with purely hydrodynamic problems of the flow of viscous fluids in cylindrical pipes, Stanton and Pannell† investigated the resistance to flow from the standpoint of similitude. Their results show that although the relation analogous to (9) has a special form for stream-line motion, which apparently alters when turbulence sets in, the general relation holds even for turbulent motion, and is continuous through the transition region.

### *Examination of Formula.*

Experimental work on the heat-losses from bodies in a stream of air has been carried out chiefly on thin wires, but some data are available for larger cylinders. Let us consider these two cases.

(1) *Thin Cylinders.*

Kennelly‡ and Morris§ have investigated the cooling of thin wires in streams of air. King‖ has given, perhaps, the most comprehensive investigation, working over a wide range. He used wires ranging in diameter ($d$) from 0·003 cm. to 0·015 cm. He worked at velocities ($v$) of 17 to 900 cms. per sec., and at temperature excesses ($\theta$) (wire over air)

* 'Phil. Mag.', vol. 20, p. 591, 1910.

† 'N.P.L. Collected Researches', vol. 11, Paper 14, p. 293, or 'Phil. Trans.', vol. 214, p. 199, 1914.

‡ 'Trans. Amer. Inst. Elec. Eng.', vol. 28, p. 363, 1909.

§ 'Electrician', p. 1056, 1912.

‖ 'Phil. Trans.', vol. 214, p. 373, 1914.

Digitized by Google

of 200° C. to 1200° C. As a result he gives a formula, which may be written

$$H/\theta = B\sqrt{(vd)} + C. \quad . \quad . \quad . \quad . \quad . \quad . \quad . \quad . \quad . \quad . \quad (10)$$

H is the heat-loss per cm. of wire, B and C are practically constant. B has a slight coefficient depending on the temperature excess of the wire; C has a larger coefficient, and also depends somewhat on the diameter of the wire. We may note that, in (9), "$h$" refers to unit *area* of the body. If the body is a long cylinder, the length obviously does not affect "$h$". It readily follows for long cylinders (diameter "$d$") that the rate of loss of heat "H" per unit *length* is given by

$$H = (k\theta)F(vdc/k) \quad . \quad . \quad . \quad . \quad . \quad . \quad . \quad . \quad . \quad . \quad (11)$$

Thus KING's results show that the formula (11), which for these experiments reduces to

$$H/\theta = F(vd), \quad . \quad . \quad . \quad . \quad . \quad . \quad . \quad . \quad . \quad . \quad (12)$$

is very satisfactory, but slight corrections seem necessary. The results are in a form which readily shows this, being essentially the evaluation of the constants B and C in his theoretical formula.

(2) *Spheres and Thick Cylinders.*

COMPAN*, using a sphere, verified BOUSSINESQ's approximate equation within narrow limits of temperature and air-velocity, but he did not use bodies of different size. However, HUGHES† has investigated the cooling of cylinders (0·5 to 15 cm. diam.) over a range of air-velocity from 2 to 15 metres per second.

The experimental data are given in a full table in his paper, and curves are given between the heat-loss "H" in calories per cm. of the cylinder and "$v$" the air-velocity, one curve for each value of the diameter ($d$). They have been re-drawn in Fig. 1 in c.g.s. units. The relation between the four curves is not obvious. However, formula (12) suggests that they can be replaced by one curve if "H" is plotted against "$vd$". In Fig. 2 this has been attempted from the experimental data.‡ It is seen that the result is very satisfactory. It is excellent for the three smaller cylinders (0·43 to 1·93 cm.) and quite good for the fourth (5·06 cms.), although the points of the latter all seem displaced somewhat from the line of the former.

Possible sources of this displacement may be mentioned. In the "$vd$" term there is possibility of error in the velocity "$v$". HUGHES' methods of allowing for lack of uniformity of distribution of the air-stream in his channel is open to criticism from a

* 'Ann. Chim. Phys.', vol. 26, p. 482, 1902.

† 'Phil. Mag.', vol. 31, p. 118, 1916.

‡ The points of Fig. 1 are too numerous to plot individually in Fig. 2, and advantage has been taken of the natural groups (of from 2 to 6 points) which occur, and mean values have been plotted.

Digitized by Google

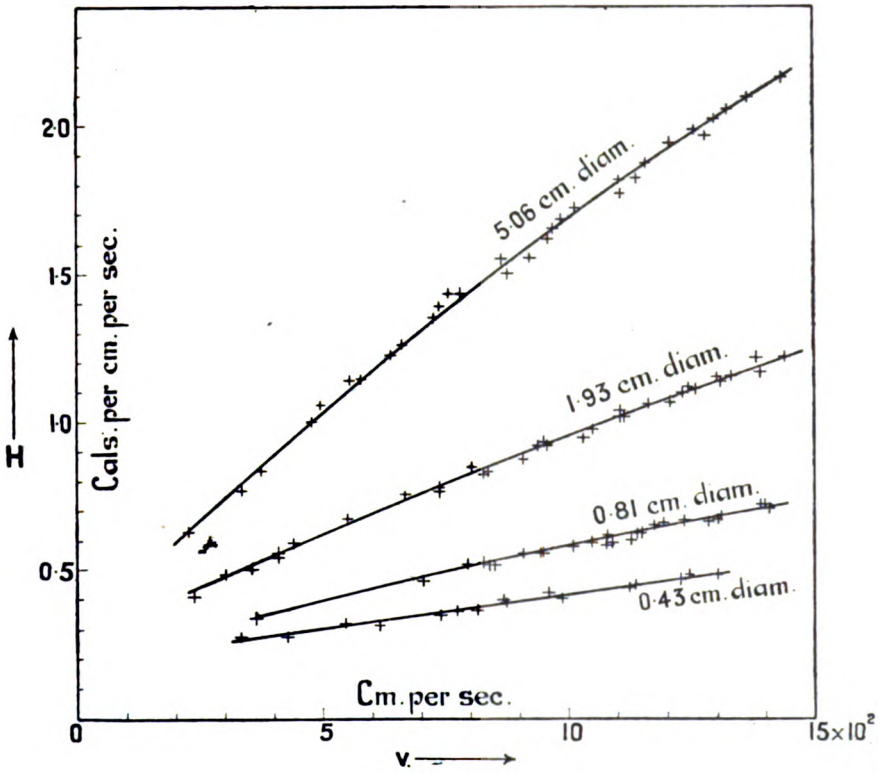


FIG. 1.

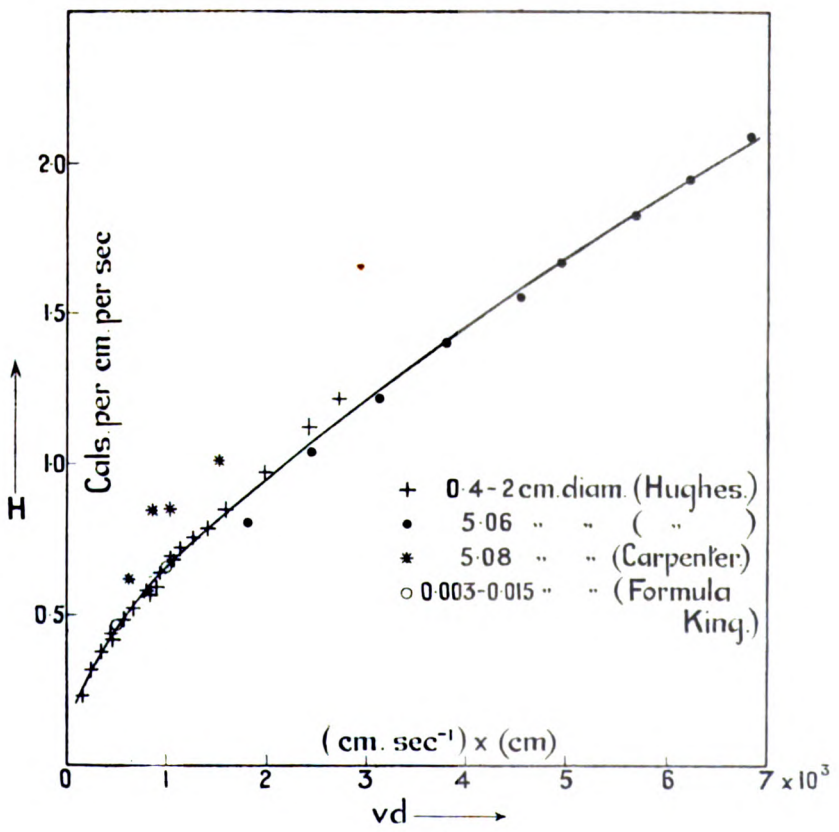


FIG. 2.

Digitized by Google

precision point of view. A Pitot-tube reading is proportional to $v^2$, whereas the heat-loss from small and large cylinders is proportional to $v^{0\cdot55}$ and $v^{0\cdot7}$ respectively. So a value of average velocity, as deduced by HUGHES, from the mean square velocity obtained from Pitot-tube readings, is not strictly applicable. Further, the particular average required depends on which cylinder is in use. It will be noticed that the double series of points on the graph of Fig. 2 come where the high-velocity values of the smaller cylinders are plotted near the low-velocity values of the 5·06 cm. cylinder. One may mention also that experience with wind channels shows that rectilinear stream-line motion is not obtained unless special precautions are taken. The entrance must be of stream-line shape, and a special metal honeycomb should be used at the beginning of the channel proper to break up vortices and ensure rectilinear delivery.

Even if there is actual discrepancy, it is obvious that the law $H \propto F(vd)$ is approximately true. Unless a better theoretical formula can be advanced, this point is worth emphasis in the form in which results are presented, even although a slight correction factor be introduced for deviation with diameter ($d$).

Finally, LANGMUIR,* in his study of convection of heat, quotes from CARPENTER ('Heating and Ventilation of Buildings', Wiley & Sons, 1903) values for a 2-inch steam pipe, sensibly the same size as HUGHES' largest cylinder (5·06 cms.). These convection values, calculated for a temperature excess of 85° C., are plotted as asterisks in Fig. 2, and are seen to lie higher than the mean curve, although the points given by HUGHES lie lower.

(3) *Long Cylinders: Thick and Thin compared.*

HUGHES gave the results for his cylinders in a form $H \propto d^{0\cdot57}v^n$, where $n$ varies with diameter from 0·55 to 0·7, and shows signs of depending also upon the velocity itself. Obviously, this is not a suitable formula for extrapolation. KING, working over a wide range of conditions, gave the formula (10) above. It is better adapted for extrapolation. Particularly, there is no sign of variation with velocity apart from that under the root sign; so we can work with a wire of diameter within KING's range, only extrapolating the velocity.

Let us take, then, two wires approximating to the smallest and to the largest used by KING, of diameter 0·003 and 0·015 cm. respectively. As with HUGHES' cylinders, let them work at 100° C., in air at 15° C., this being apparently the temperature (deduced from his radiation data) at which HUGHES worked. Then, if we choose velocities to give values of "$vd$" similar to those in HUGHES' experiments, we may calculate from KING's constants the appropriate heat-loss (H). We find for both wires

$$\text{when } vd = 500, \quad H = 0\cdot46$$
$$\text{,, } vd = 1{,}000, \quad H = 0\cdot66.$$

* 'Trans. Amer. Electrochem. Soc.', vol. 23, p. 324, 1913.

Digitized by Google

These points have been plotted on the graph of Fig. 2, where remarkable agreement is seen with the curve obtained for cylinders 30 to 1,600 times as thick. The extrapolation is considerable, but we recall that the most satisfactory part of the most satisfactory formula was chosen to stand the strain. It would not seem possible to conduct experiments to test this particular extrapolation, as the velocities are so great that the fine wires would oscillate or break under the mechanical strain.

Digitized by Google

# CONVECTION OF HEAT IN GASES AND LIQUIDS. II—NATURAL CONVECTIVE COOLING OF WIRES IN GASES

BY

A. H. DAVIS, D.Sc.,
ASSISTANT IN THE PHYSICS DEPARTMENT.

Digitized by Google

## ABSTRACT.

(Reprinted from 'Science Abstracts', Physics, Section A, Vol. 25.)

In continuation of previous work the author investigates the apparent discrepancy between published data for the natural or free convective cooling of thin wires and the hydrodynamical theory. The hydrodynamical relation may be expressed in the form $H/k = F(\theta d^3/\nu^2)$, where H represents the heat-loss per unit length per degree temperature excess of the cylinder, $k$ the thermal conductivity of the cooling fluid, $\theta$ the temperature excess of the cylinder of the diameter $d$, and $\nu$ the ratio of the thermal conductivity of the fluid to its thermal capacity per unit volume. Using values of $k$ and $\nu$ appropriate to individual experiments, such values being calculated in the case of thin wires for the mean temperature of the wire and its surroundings, it is shown that the above relation accurately represents the results contained in the published work of Langmuir for the free convection losses from fine platinum wires at temperature excesses from 200° C. to 1600° C., of Ayrton and Kilgour for fine wires, Petavel for the heat-loss from steam pipes up to 1 foot in diameter and from a fine wire in various gases, and of Kennelly. The hydrodynamical formula developed is therefore seen to be in agreement with the published data for fine wires, provided allowance be made for the temperature changes of the properties of the cooling fluid owing to the high temperatures at which such wires have been usually employed.


Digitized by Google

# CONVECTION OF HEAT IN GASES AND LIQUIDS. II.—NATURAL CONVECTIVE COOLING OF WIRES IN GASES.

By A. H. DAVIS, D.Sc., Assistant in the Physics Department.

[Reprinted from the 'Philosophical Magazine', Vol. 43, 1922.]

## (1) *Introduction.*

The object of this paper is to investigate the apparent discrepancy between published data for the natural convective cooling of wires and the hydrodynamical theory of the phenomenon.

"Convective cooling" is taken to refer to the total heat transfer from a hot body by the medium of a fluid moving past the surface. Such cooling is said to be "natural" or "free" when the fluid is still except for the streams set up by the heat from the hot body itself.

The theory involves the dilatability of the fluid, the hydrodynamical equations of motion, the Fourier equations of heat-flow, and the appropriate boundary conditions. From this point of view Boussinesq* has studied both natural and forced convection for similar bodies immersed in an infinite inviscid fluid. His formulæ may also be derived from the principle of similitude by simple consideration of the variables involved, and may be extended to viscous fluids by the same means. The following formula is obtained for the heat-loss by natural convection from similar bodies similarly immersed in viscous fluids.

$$hl/k\theta = \mathrm{F}(c^2gl^3a\theta/k^2)f(c\nu/k), \quad \ldots\ldots\ldots \quad (1)$$

where

$h$ = heat-loss per second per unit area of the body,

$k$ = thermal conductivity of the fluid,

$c$ = capacity for heat of the fluid per unit volume,

$\theta$ = temperature excess of the body,

$a$ = coefficient of density reduction of the fluid per degree rise of temperature,

$g$ = acceleration due to gravity,

$l$ = linear dimensions of the body.

For a given kind of gas $c\nu/k$ appears to be constant as required by the kinetic theory, and the formula becomes simpler

$$h = (k\theta/l)\mathrm{F}(c^2gl^3a\theta/k^2). \quad \ldots\ldots\ldots \quad (2)$$

The formula involves an assumption that $a$ and $g$ always occur as a product, that is, that the expansion of the fluid is negligible, except in so far as it alters the *weight* of unit

* 'Comptes Rendus', vol. 132, p. 1382, 1901.



Digitized by Google

volume, and thus supplies the necessary driving force for the convection currents. This restriction may impose limits to the temperature excess for which the formula is applicable for a given series of bodies.

If only the temperature and size of the model are varied, the gaseous constants ($c$, $a$ and $k$) and gravity ($g$) remaining the same, the formula becomes

$$h = (\theta/l)\mathrm{F}(\theta l^3). \quad \ldots\ldots\ldots\ldots \quad (3)$$

In a previous paper* where this formula was studied, it was shown that in general, both for forced and for free convection, the hydrodynamic formulæ are in very promising agreement with published data, except in the case of free convection from hot thin wires. The present paper investigates this apparent disagreement.

## (2) *Convection Loss from Wires.*

Experimenters have almost invariably conducted wire experiments at temperatures much higher than those used with larger bodies, and this suggests two possible sources of the apparent failure of the theoretical formula. Firstly, it may be that in this extreme case it is no longer legitimate to assume that "$a$" and "$g$" occur only as a product, the mere volume changes of the air now having sensible effect. Secondly, it may be now necessary to allow for the change of the conductivity and specific heat of the fluid due to the temperature rise caused by the hot wire. The present paper shows the remarkable improvement which follows an attempt to allow for this second effect, so that even for thin wires the equation appears to be substantially correct.

The formula may be put in a more convenient form for our purpose. In (1) "$h$" refers to unit *area*, and if the body is a long cylinder, "$h$" is obviously unaffected by the length. It readily follows that for long cylinders (diameter $d$) the heat loss H per unit length per degree temperature elevation is given by

$$\mathrm{H}/k = \mathrm{F}(c^2 g d^3 a \theta/k^2). \quad \ldots\ldots\ldots\ldots \quad (4)$$

Writing $\nu$ for $k/c$ (since $c\nu/k$ is constant for a given kind of gas) and regarding "$a$" † and "$g$" as constant, we have

$$\mathrm{H}/k = \mathrm{F}(\theta d^3/\nu^2). \quad \ldots\ldots\ldots\ldots \quad (5)$$

Consequently, if data for the natural convective cooling of long cylinders be plotted on a graph with $\mathrm{H}/k$ as ordinate and $\theta d^3/\nu^2$ as abscissa, the result should be a single curve independent of the size of the cylinders, and also of their temperature excess, if appropriate allowance be made for the variation of $k$ and $\nu$ with temperature. Further, from the method of its derivation, formula (5) would appear to hold for all fluids for

* Davis, 'N.P.L. Collected Researches', vol. 19, Paper 11, or 'Phil. Mag.', vol. 40, p. 692, 1920.

† The convection currents depend on the density change relative to the density of the *cold* fluid, so that "$a$" must be regarded as applicable to the cold gas, and independent of the temperature of the wire.

Digitized by Google

which $c\nu/k$ is the same. For gases the value of this variable appears to depend on the number of atoms in the molecule, and has the same value for the diatomic gases—oxygen, hydrogen and nitrogen—as it has for air, so that these gases should give convection results in agreement with the curve for air.

### (3) *Method of Examination of Data.*

Published data have been examined in the light of the formula, and to obtain a convenient tabular summary the following general procedure has been adopted :—

The published data have been converted into c.g.s. units, corrected for radiation if necessary, and plotted on a graph from which values have been read off for even values of temperature excess. This gives corresponding values of $\theta d^3$ and H.

To obtain $\theta d^3/\nu^2$ and $H/k$ it was necessary to decide on the values of $k$ and $\nu$ appropriate to the particular experiment. For a hot wire in air at room temperature (15° C.) the appropriate values are neither those for air at the temperature of the hot wire nor those for air at 15° C. As a first approximation the values actually taken were those for air at the mean of these two temperatures.

In cases where the pressure was not atmospheric allowance has been made as before, and in addition it has been assumed that, as indicated by the kinetic theory of gases, both the conductivity $k$ and the viscosity $\eta$ are independent of pressure, and consequently the kinematical viscosity $\nu$ has been taken as inversely proportional to the pressure of the gas.

In following this general procedure certain auxiliary constants have been used, as explained in the following paragraphs :—

(*a*) *Radiation Correction.*—Data for heat-losses are often published in the form of a total loss, radiation being included. LANGMUIR,* who used platinum wires, published his data with the radiation eliminated, and in this paper results obtained by other experimenters for platinum surfaces have been corrected, using his values for the emissivity for radiation. For steam pipes, total heat-losses given by PETAVEL have been corrected by the amount attributed by him to radiation, an amount equivalent to $0{\cdot}4 \times 10^{-12} \times (T^4 - T_0^4)$† calories per sq. cm. per sec., where T and $T_0$ refer respectively to the absolute temperatures of the body and its surroundings.

(*b*) *Convection Constants of Gases.*—Below are given data to express the variation of $k$ and $\nu$ with temperature.

The viscosity ($\eta$) of a gas is given by SUTHERLAND'S formula and the density by $\rho = \rho_0(273/T)$, where T is the absolute temperature; from these the kinematical viscosity $\nu$ ($= \eta/\rho$) has been derived.

The conductivity ($k$) has been calculated from the viscosity ($\eta$) and the specific heat at constant volume ($c_v$), using the formula $k/c_v\eta = \text{constant}$, as given by the kinetic

* 'Phys. Rev.', vol. 34, p. 401, 1912.

† $5 \times 10^{-10}$ ($T^4 - T_0^4$) B.T.U. per square foot per hour.

Digitized by Google

theory of gases. EUCKEN* has shown that the constant has the value 2·50 for monatomic gases and 1·90 for the diatomic gases, hydrogen, oxygen, nitrogen, and also for air. The specific heats at high temperature have been obtained from the data given by M. PIER,† who has given formulæ which, for the above gases, may be written $c_v = A(1 + 0{\cdot}0002T)$, where A depends on the nature of the gas. LANGMUIR‡ adopted this method of calculating conductivity when dealing with heat convection from the point of view of conduction through a film of gas adherent to the hot body.

Thus, for the gases considered,

$$\nu = \eta/\rho, \quad . \quad . \quad . \quad . \quad . \quad . \quad . \quad . \quad . \quad . \quad . \quad . \quad . \quad . \quad . \quad (6)$$

$$k = 1{\cdot}90 c_v \eta, \quad . \quad . \quad . \quad . \quad . \quad . \quad . \quad . \quad . \quad . \quad . \quad . \quad . \quad . \quad . \quad (7)$$

where

$$\eta = KT^{\frac{1}{2}}/(1 + C/T), \quad . \quad . \quad . \quad . \quad . \quad . \quad . \quad . \quad . \quad . \quad . \quad . \quad . \quad . \quad (8)$$

$$c_v = A(1 + 0{\cdot}0002T), \quad . \quad . \quad . \quad . \quad . \quad . \quad . \quad . \quad . \quad . \quad . \quad . \quad . \quad . \quad (9)$$

$$\rho = 273\rho_0/T, \quad . \quad . \quad . \quad . \quad . \quad . \quad . \quad . \quad . \quad . \quad . \quad . \quad . \quad . \quad . \quad (10)$$

and where the constants have the values given in the following Table :—

TABLE I

(c.g.s. units).

| | $10^6$K.* | C.* | A. | $10^3\rho_0$. |
|---|---|---|---|---|
| Air ... ... ... | 15·0 | 124 | 0·161 | 1·293 |
| Hydrogen ... ... | 6·6 | 77 | 2·21 | 0·09 |
| Oxygen ... ... | 17·5 | 127 | 0·145 | 1·43 |

* See Tables by KAYE and LABY, or FISHER, ' Phys. Rev.', vol. 24, p. 385, 1907 ; vol. 29, p. 146, 1909.

Calculation from these data yields the values for $k$ and $\nu$ given in Table II.

TABLE II.

| ° C. | Air. | | Hydrogen. | | Oxygen. | |
|---|---|---|---|---|---|---|
| | $10^4 . k$. | $\nu$. | $10^4 . k$. | $\nu$. | $10^4 . k$. | $\nu$. |
| 0 | 0·55 | 0·13 | 3·7 | 0·9 | 0·58 | 0·14 |
| 17 | 0·58 | 0·15 | 4·1 | 1·1 | 0·61 | 0·15 |
| 100 | 0·72 | 0·23 | 4·7 | 1·6 | 0·75 | 0·24 |
| 200 | 0·86 | 0·35 | 5·7 | 2·4 | 0·91 | 0·36 |
| 300 | 1·01 | 0·48 | 6·5 | 3·3 | 1·00 | 0·50 |
| 400 | 1·14 | 0·62 | 7·4 | 4·2 | 1·20 | 0·66 |
| 500 | 1·27 | 0·78 | 8·2 | 5·3 | 1·33 | 0·83 |
| 1,000 | 1·89 | 1·76 | 11·8 | 11·4 | 1·97 | 1·85 |

* ' Phys. Zeits.', vol. 12, p. 1101, 1911.

† ' Zeits. Elektrochem.', vol. 15, p. 536, 1909 ; vol. 16, p. 899, 1910.

‡ ' Phys. Rev. ', vol. 34, p. 401, 1912.

Digitized by Google

### (4) *Summary of Collected Data.*

Following the procedure explained, Tables III and IV have been compiled summarising a wide range of data for convection losses from cylinders. In the experiments of Table III the wires were used mainly in free air, or in enclosures so large that the free air figure would evidently be obtained. It appears, however, that heat-losses from wires in even a small enclosure (a few centimetres diameter) are not different from those obtained in an unlimited medium. In Table III the results by AYRTON and KILGOUR were obtained using water-cooled enclosures 5·08 cm. internal diameter, and they agree excellently with data for similar wires in practically free air, as given by LANGMUIR and by KENNELLY. Table IV refers to an enclosure of 2·06 cm. diameter, and this is still fairly large compared with the diameter of the wire, and the results for air at one atmosphere agree satisfactorily with the curve derived from data for free air already considered. Results given in the tables are plotted in Fig. 1.

TABLE III.—Natural Convection from Long Cylinders in Air.

(Logarithmic values of $\theta d^3/\nu^2$ and $H/k$ are given.)

| Source. | Diam. cm. | Temperature Excess (° C.). | | | | | | | | | |
|---|---|---|---|---|---|---|---|---|---|---|---|
| | | 30°. | | 100°. | | 200°. | | 600°. | | 1600°. | |
| | | $\frac{\theta d^3}{\nu^2}$. | $\frac{H}{k}$. | $\frac{\theta d^3}{\nu^2}$. | $\frac{H}{k}$. | $\frac{\theta d^3}{\nu^2}$. | $\frac{H}{k}$. | $\frac{\theta d^3}{\nu^2}$. | $\frac{H}{k}$. | $\frac{\theta d^3}{\nu^2}$. | $\frac{H}{k}$. |
| B . . . | 0·0031 | $\bar{5}$·55 | 0·14 | $\bar{5}$·90 | 0·21 | $\bar{5}$·98 | 0·32 | ... | ... | ... | ... |
| A . . . | 0·00404 | ... | ... | ... | ... | $\bar{4}$·32 | 0·25 | $\bar{4}$·22 | 0·20 | $\bar{5}$·74 | 0·24 |
| B . . . | 0·0051 | $\bar{4}$·20 | 0·22 | $\bar{4}$·55 | 0·31 | $\bar{4}$·63 | 0·31 | ... | ... | ... | ... |
| A . . . | 0·00691 | ... | ... | ... | ... | $\bar{3}$·02 | 0·29 | $\bar{4}$·92 | 0·26 | $\bar{4}$·44 | 0·29 |
| B . . . | 0·0074 | $\bar{4}$·69 | $\bar{1}$·99 | $\bar{3}$·04 | 0·24 | $\bar{3}$·11 | 0·25 | ... | ... | ... | ... |
| D . . . | 0·0114 | ... | ... | $\bar{3}$·59 | 0·29 | $\bar{3}$·67 | 0·29 | ... | ... | ... | ... |
| A . . . | 0·01262 | ... | ... | ... | ... | $\bar{3}$·80 | 0·32 | $\bar{3}$·70 | 0·30 | $\bar{3}$·23 | 0·29 |
| B . . . | 0·0152 | $\bar{3}$·62 | 0·30 | $\bar{3}$·97 | 0·34 | $\bar{2}$·05 | 0·36 | ... | ... | ... | ... |
| A . . . | 0·02508 | ... | ... | ... | ... | $\bar{2}$·70 | 0·44 | $\bar{2}$·60 | 0·41 | $\bar{2}$·12 | 0·34 |
| B . . . | 0·0356 | ... | ... | $\bar{1}$·08 | 0·53 | $\bar{1}$·16 | 0·53 | ... | ... | ... | ... |
| A . . . | 0·051 | ... | ... | ... | ... | $\bar{1}$·62 | 0·55 | $\bar{1}$·52 | 0·52 | $\bar{1}$·05 | 0·49 |
| D . . . | 0·0691 | ... | ... | $\bar{1}$·94 | 0·58 | 0·02 | 0·58 | ... | ... | ... | ... |
| E . . . | 0·1106 | ... | ... | 0·48 | 0·63 | ... | ... | ... | ... | ... | ... |
| C . . . | 0·51 | ... | ... | 2·55 | 1·11 | 2·62 | 1·17 | ... | ... | ... | ... |
| C . . . | 5·08 | ... | ... | 5·55 | 1·88 | 5·62 | 1·93 | ... | ... | ... | ... |
| C . . . | 30·48 | ... | ... | 7·88 | 2·61 | 7·95 | 2·67 | ... | ... | ... | ... |
| D* . . . | 0·0114 | ... | ... | $\bar{3}$·00 | 0·26 | $\bar{3}$·07 | 0·23 | ... | ... | .. | ... |
| D† . . | 0·0114 | ... | ... | $\bar{2}$·20 | 0·35 | $\bar{2}$·27 | 0·35 | ... | ... | ... | ... |
| D* . . | 0·0691 | ... | ... | $\bar{1}$·35 | 0·50 | $\bar{1}$·42 | 0·51 | ... | ... | ... | ... |
| D† . . | 0·0691 | ... | ... | 0·55 | 0·67 | 0·62 | 0·67 | ... | ... | ... | ... |

* Air at ½ atmosphere pressure. † Air at 2 atmospheres pressure.

Digitized by Google

TABLE IV.—Convection Loss for Wire in Various Gases at Various Pressures.
Wire diam. 0·1106 cm.

| Source. | Gas. | Pressure Atm. | Temperature Excess (° C.) | | | | | |
|---|---|---|---|---|---|---|---|---|
| | | | 100°. | | 300°. | | 900°. | |
| | | | $\frac{\theta d^3}{\nu^2}$. | $\frac{H}{k}$. | $\frac{\theta d^3}{\nu^2}$. | $\frac{H}{k}$. | $\frac{\theta d^3}{\nu^2}$. | $\frac{H}{k}$. |
| E . . . . | Air . . . | 0·1 | $\bar{2}$·48 | 0·40 | $\bar{2}$·59 | 0·45 | $\bar{2}$·34 | 0·53 |
| | | 1·0 | 0·48 | 0·63 | 0·59 | 0·64 | 0·34 | 0·67 |
| | | 10 | 2·48 | 0·95 | 2·59 | 0·97 | 2·34 | 0·99 |
| | | 100 | 4·48 | 1·47 | 4·59 | 1·44 | 4·34 | 1·39 |
| F . . . . | Hydrogen | 0·1 | $\bar{4}$·82 | 0·34 | $\bar{4}$·91 | 0·34 | $\bar{4}$·69 | 0·38 |
| | | 1·0 | $\bar{2}$·82 | 0·38 | $\bar{2}$·91 | 0·40 | $\bar{2}$·69 | 0·44 |
| | | 10 | 0·82 | 0·60 | 0·91 | 0·68 | 0·69 | 0·62 |
| | | 100 | 2·82 | 1·00 | 2·91 | 1·03 | 2·69 | 0·99 |
| G . . . . | Oxygen . | 0·1 | $\bar{2}$·47 | 0·40 | $\bar{2}$·56 | 0·44 | $\bar{2}$·30 | 0·57 |
| | | 1·0 | 0·47 | 0·66 | 0·56 | 0·66 | 0·30 | 0·67 |
| | | 10 | 2·47 | 0·93 | 2·56 | 0·95 | 2·30 | 0·96 |
| | | 100 | 4·47 | 1·47 | 4·56 | 1·45 | 4·30 | 1·45 |

The sources from which the summary was compiled are briefly indicated below, the distinguishing letters corresponding with those used in the tables :—

(A) LANGMUIR* conducted experiments practically in free air with fine platinum wires at temperature excesses from 200° C. to 1600° C. He carefully corrected for radiation. His results may be represented to a certain degree of approximation by the formula $H \propto d^{1/5}\theta^{1/4}$, which does not agree with (3), where $k$ and $\nu$ are regarded as constant ; the disagreement is brought out even more clearly if $\theta d^3$ is plotted against H.

In Fig. 1 all the LANGMUIR values of Table III are plotted.

(B) AYRTON and KILGOUR† worked with fine wires at more moderate temperature excesses. Table III contains values for all their wires, but for convenience Fig. 1 only shows values for the largest and the smallest. It should be mentioned that one wire (0·0074 cm. diam.) gives results at low temperature excess in poor agreement with the line in Fig. 1. However, study of their curves shows that the behaviour of this particular wire is exceptional.

(C) PETAVEL‡ has given data for the total heat-loss from the oxidised iron surface of steam pipes of various diameters up to 1 foot, a diameter which is ten thousand times the diameter of AYRTON and KILGOUR's smallest wire. Values with radiation eliminated are plotted in Fig. 1.

* ' Phys. Rev.', vol. 34, p. 401, 1912.

† ' Phil. Trans.', A, vol. 183, p. 371, 1892.

‡ ' Proc. Manchester Assoc. Eng.', 1915–16.

Digitized by Google

(D) KENNELLY* investigated the heat losses from wires in very large enclosures at various pressures, thus introducing another experimental variable.

LANGMUIR† has corrected these for radiation, and his corrected values have been used in compiling Table III. The points, if plotted on Fig. 1, are in excellent agreement, but to preserve a clear figure only two points are shown, these corresponding to the extremities of the range.

(E, F and G) PETAVEL,‡ who worked over a wide range of pressure (1/10 to 100 atm.) and up to 1100° C. excess, has given data by means of which the performance of different

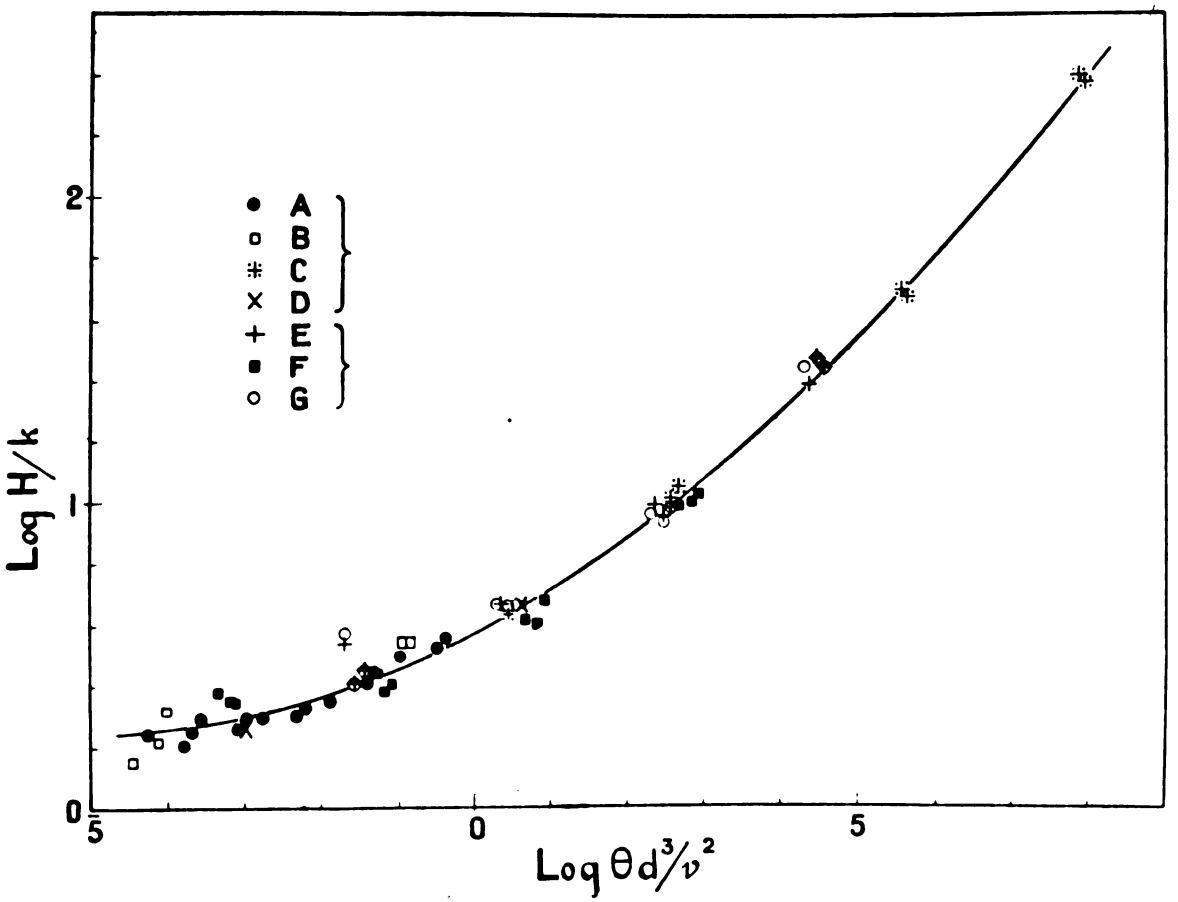


FIG. 1.

gases may be compared. He studied the cooling of 0·1106 cm. wire, using a cylindrical water-cooled enclosure. Values have been plotted on the graph of Fig. 1 instead of on a separate graph. The radiation correction is not large and in its calculation the enclosure temperature has been taken as 300° absolute. E, F and G refer respectively to air,

* 'Trans. Amer. Inst. Elec. Eng.', vol. 28, p. 363, 1909.

† 'Trans. Amer. Inst. Elec. Eng.', vol. 31, p. 1228, 1912.

‡ 'Phil. Trans.', A, vol. 197, p. 229, 1901.



Digitized by Google

hydrogen and oxygen. The point for the case of 1/10 atmosphere and 900° C. temperature excess is seen to lie rather high for each of the gases considered.

### (5) *Conclusion.*

The curve of Fig. 1 shows that very diverse data give points which, in general, all lie on one line independent of the size and temperature excess of the object, and of the nature and pressure of the gas involved. It therefore appears that the hydrodynamical theory of convection represented by our formulæ is substantially satisfactory even in the case of hot thin wires, provided allowance* is made for the temperature change of the properties of the fluid, an allowance brought into prominence by the high temperatures to which wires are usually heated in convection experiments. High temperatures are also used in experiments on *forced* convection from wires, and it is desirable to notice that in this case approximate agreement with the appropriate formula is found even without allowing for the temperature variations of the properties of the fluid, but that agreement is improved when such allowance is made.†

LANGMUIR developed a theory of convection in which bodies are considered to be surrounded by a film of gas through which the heat is transmitted by pure conduction, and with certain assumptions, and allowing for the temperature change of the conductivity of the gas, he obtained results in agreement with experiment for free convection. However, he concludes that "for forced convection the film theory does not seem to apply".‡

It may be counted a superiority of the hydrodynamical theory that the treatment which reconciles theory with experiment for free convection is satisfactory for forced convection also.

Besides testing the hydrodynamical theory, Fig. 1 effects a graphical correlation of diverse convection data for various gases and gas pressures over a wide range of wire diameter and temperature excess. The tendency of the curve appears to be, at its upper extremity, towards the form

$$H/k \propto (\theta d^3/\nu^2)^{1/3} \quad \ldots\ldots\ldots\ldots \quad (11)$$

and at its other end towards

$$H/k = \text{constant}. \quad \ldots\ldots\ldots\ldots \quad (12)$$

Equation (11) would imply that for large bodies the heat loss per unit *area* is independent of the size, and (12) that for very fine wires the heat loss per unit *length* is independent of the diameter. Equation (12) would also imply that the convective cooling of wires, very fine and very slightly heated, is a measure of the conductivity of the fluid, at any rate for fluids of such similar molecular constitution that $c\nu/k$ is the same.

* Only approximate allowance is made in this paper.

† DAVIS, 'N.P.L. Collected Researches', vol. 19, Paper 13, or 'Phil. Mag.', vol. 41, p. 899, 1921.

‡ LANGMUIR, 'Trans. Amer. Electrochem. Soc.', vol. 23, p. 329, 1913.

Digitized by Google

# CONVECTION OF HEAT IN GASES AND LIQUIDS. III.—FORCED CONVECTIVE COOLING OF WIRES IN GASES

BY

A. H. DAVIS, D.Sc.,
ASSISTANT IN THE PHYSICS DEPARTMENT.

Digitized by Google

## ABSTRACT.

In an earlier paper ('N.P.L. Collected Researches', vol. 19, Paper 11, or 'Phil. Mag.', vol. 40, p. 692, 1920) it was shown that BOUSSINESQ's formula, as derived from considerations of similitude by RAYLEIGH, is well borne out by some published results for the cooling of cylinders in a stream of air. For gases the formula may be written $H/k = F(vl/\nu)$, where H is the rate of heat-loss per degree temperature excess by unit length of an infinite cylinder of diameter $l$ when immersed in a stream of gas of which $k$, $v$ and $\nu$ are respectively the thermal conductivity, the velocity, and the kinematical viscosity. Here $(vl/\nu)$ is the familiar hydrodynamical variable determining fluid resistance and turbulence.

The present paper extends the study. In the case of very hot wires some allowance is made for the changed physical properties of the heated gas near the wire. It is then found that a single curve will represent results obtained by various observers, a wide range of air velocity, air pressure, wire diameter and temperature excess being covered.

The formula is further compared with the dynamic relation $(R/\rho v^2 l^2) = f(vl/\nu)$, where R is the fluid resistance per diameter length of the wire, and $\rho$ the density of the fluid. The relation between the thermal and mechanical effects experienced by a wire immersed in a steam was not found to conform generally with the simple formula $H \propto R/v$ advanced by OSBORNE REYNOLDS for fluid flow through a pipe. There appears, however, to be a tendency towards the REYNOLDS relation as the size of the cylinder is increased.


Digitized by Google

# CONVECTION OF HEAT IN GASES AND LIQUIDS. III.—FORCED CONVECTIVE COOLING OF WIRES IN GASES.

By A. H. Davis, D.Sc., Assistant in the Physics Department.

[Reprinted, with modified title, from the 'Philosophical Magazine', Vol. 41, 1921.]

## 1. *Introduction.*

It has been shown* that some published results for the cooling of cylinders in a stream of air agree excellently with Boussinesq's formula, which may be derived from considerations of similitude,† and which may be written in the form

$$H/k = F(lvc/k), \quad . \quad . \quad . \quad . \quad . \quad . \quad . \quad . \quad . \quad . \quad . \quad (1)$$

where

H = heat lost per second per unit length of the wire per degree temperature excess above stream temperature.

$k$ = heat conductivity of the fluid.

$c$ = specific heat of the fluid per unit volume.

$v$ = velocity of the fluid stream.

$l$ = diameter of the wire.

It was pointed out that since for a given gas $cv/k$ is constant ($\nu$ being the kinematical viscosity), the above reduces to

$$H/k = F(vl/\nu). \quad . \quad . \quad . \quad . \quad . \quad . \quad . \quad . \quad . \quad . \quad . \quad (2)$$

Here $vl/\nu$ is the familiar variable in hydrodynamics determining fluid resistance and turbulence, so the equation in this form involves a relation between the thermal and dynamic effects of a fluid stream. The dynamic effect is represented by the formula

$$R/(\rho v^2 l^2) = f(vl/\nu), \quad . \quad . \quad . \quad . \quad . \quad . \quad . \quad . \quad . \quad . \quad (3)$$

where R = fluid resistance per diameter length of the wire,

$\rho$ = density of the fluid.

The present paper extends the investigation of the agreement of the similitude equation with published data for heat loss from cylinders in a stream of air, and determines the relation between the thermal and dynamic effects of the stream in this case.

* Davis, 'N.P.L. Collected Researches', vol. 19, Paper 11, or 'Phil. Mag.', vol. 40, p. 692, 1920.

† Rayleigh, 'Nature', vol. 95, p. 66, 1915.

Digitized by Google

Osborne Reynolds,* considering the heating surface of boilers, pointed out that, from the identity of the two molecular phenomena by means of which convection of heat and of momentum (surface friction) were carried on, their dependence on the conditions of motion would be the same. Formulæ he deduced for cool liquid flowing through a hot pipe indicate that

Heat loss per unit area $\propto$ Temperature difference between fluid and pipe.
$\propto$ Fluid resistance per unit area.
$\propto$ Reciprocal of the velocity of the fluid in the pipe.

Stanton† showed experimentally that for the same pipe and range of temperature the heat transmission varied as $v^{n-1}$, where $n$ is the index of $v$ in the ordinary resistance formula.

### 2. *The Convection Constants of Air.*

Below are given the formulæ taken in this paper to represent the variation with temperature of the convection constants of air. Langmuir,‡ dealing with convection of heat from the point of view of conduction through a stationary film of gas in contact with the hot body, has collected formulæ for the convection constants for various gases. From his paper we have, T being the absolute temperature,

$$\text{viscosity } (\eta) = \frac{(150 \times 10^{-7})\mathrm{T}^{\frac{1}{2}}}{1 + 124/\mathrm{T}}, \quad \ldots \quad (4)$$

$$k = 4{\cdot}6 \times 10^{-6}\mathrm{T}^{\frac{1}{2}} \frac{1 + 0{\cdot}0002\mathrm{T}}{1 + 124/\mathrm{T}} \text{ cals. per cm. per sec. per } ^\circ\text{C.}, \quad \ldots \quad (5)$$

and since for air

$$\rho = 0{\cdot}001293\ (273/\mathrm{T}) \text{ gm. per cc.}$$

it follows that

$$\nu\ (= \eta/\rho) = \frac{(425 \times 10^{-7})\ \mathrm{T}^{3/2}}{1 + 124/\mathrm{T}} \text{ cm}^2\text{. per sec.} \quad \ldots \quad (6)$$

### 3. *The Thermal Relation.*

For convection loss from thin wires in air, the most complete and satisfactory experimental results are those given by King,§ and he obtained to represent them a formula which may be written

$$\mathrm{H}/k = \mathrm{B}\sqrt{(vl/\nu)} + \mathrm{C}, \quad \ldots \quad (7)$$

where $\nu$ has been put for $k/c$. This agrees with the theory advanced by King and with (2), except that B and C vary slightly with the temperature excess at which the wire

* 'Proc. Manchester Lit. and Phil. Soc.', 1874. See also Stanton, 'Report Adv. Committee Aeronautics', p. 45, 1912–13.

† 'Phil. Trans.', A, vol. 190, p. 67, 1897.

‡ 'Phys. Rev.', vol. 34, p. 401, 1912.

§ 'Phil. Trans.', A, vol. 214, p. 373, 1914.

Digitized by Google

works, and that C increases with the diameter of the wire. He gave empirical coefficients which allowed for this, and supposed the slight variation in B and C to be due to the change in the values of the physical constants of air.

To get a relation between $H/k$ and $vl/\nu$ it is necessary to assign values to these physical constants. While throughout this paper the temperature of the air stream is taken as 15° C., the values of $k$ and $\nu$ appropriate to any experiment with a hot wire in the stream are neither those for air at the temperature of the wire nor those for air at the temperature of the cold stream. Consequently, as a first approximation, the values taken are those for air at the mean of these temperatures. The relation between $H/k$ and $vl/\nu$ is then found to be practically independent of the temperature excess. Fig. 1 shows this and will be referred to later. In section 2 are given the formulæ representing the variation of $k$ and $\nu$ with temperature.

With respect to the dependence of C on the diameter $l$ of the wire, it is not possible by rearranging the similitude equation to obtain a term in which $l$ occurs without $v$, nor is this possible by introducing the temperature coefficients of $k$ and $\nu$. It is possible, however, by taking into account the free convection from the wire, as well as the forced convection. It seems improbable that this is the complete solution, for with the higher wind speeds the effect is still appreciable when variation with diameter of the free convection loss must be negligible. The true explanation may lie in the increasing lack of rigidity in the finer wires, which to eliminate end correction were generally of the same length (23 cms.) as the stouter ones. The former, vibrating in the wind and presumably following the changes in air-pressure more closely, might yield less heat. KING himself mentioned the existence of vibration, and that higher air speeds were impossible owing to risk of breakage of the wire at high temperatures.

To cover the whole range of KING's experiments, the heat loss has been determined, using his formula, for two wires (0·003 cm. and 0·015 cm. diameter) working at three different temperature excesses (85°, 500°, and 1,000° C.) in winds of four speeds (20, 100, 500 and 1,000 cms. per sec.). As stated earlier, the values taken for $k$ and $\nu$ have been calculated from the formulæ already given, the appropriate temperature for any case being the arithmetical mean of the temperatures of the hot wire and of the ambient cold stream (15° C.). The results have been plotted in Fig. 1 and give the lower end of the " Thermal Relation " line.

The upper part of the curve has been obtained from data given by HUGHES* for larger cylinders (0·43 to 5·06 cm. diameter), steam-heated, in air (assumed 15° C.) moving with speeds of 200 to 1,400 cms. per sec. These data have been plotted on a graph† having heat loss as ordinate and $vl$ as abscissa; values read off from this curve give points in the upper part of Fig. 1.

Some values intermediate between the two sets above mentioned were obtained from

* ' Phil. Mag.', vol. 31, p. 118, 1916.

† DAVIS *loc. cit.*

Digitized by Google

figures compiled by LANGMUIR* from a study of results given by KENNELLY.† They relate to the high velocity (800 to 1,800 cms. per sec.) values for KENNELLY's largest wire (0·0204 cm.) working at temperature excesses of 51° and 128° C.

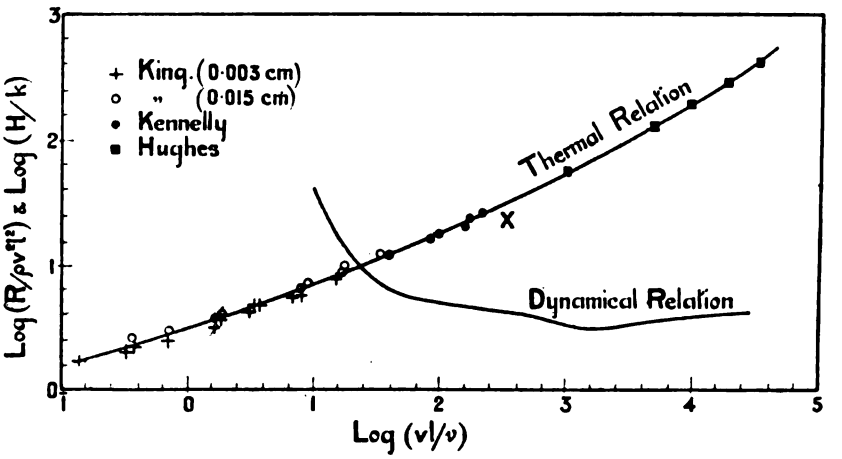


FIG. 1.

The graph thus obtained—" Thermal Relation " of Fig. 1—is excellent, practically independent of the temperature or diameter of the cylinders involved. The data range over air-streams of from ½ to 50 miles per hour, wires of 0·003 cm. diameter up to 5 cm. piping, and temperatures from that of boiling water to a bright red heat.

The curve may be further examined by comparison with the results of experiments by KENNELLY and SANBORN,‡ who investigated the heat loss from a wire in air at various pressures, the wire being mounted on a whirling arm in a special chamber. Table I is calculated from the data given in Table III of their paper. As before, allowance has been made for variation of $k$ and $\nu$ with temperature. It has been assumed that, as indicated by the kinetic theory of gases, both the conductivity $k$ of a gas and its viscosity $\eta$ are independent of pressure. The kinematical viscosity $\nu$ has consequently been taken as inversely proportional to the pressure of the gas. The data of Table I, if plotted on the graph of Fig. 1, agree satisfactorily with the curve there given for air at atmospheric pressure. A slight upward displacement above the line occurs for all the points, but this is undoubtedly due to experimental error, since two of the points relate to ordinary atmospheric pressure, and should agree with KING's results for the same condition.

It is interesting to compare the above results for air with data for the heat loss in a stream of other fluid. WORTHINGTON and MALONE§ have shown that the convection of

* 'Trans. Amer. Inst. Elec. Eng.', vol. 31, part 1, p. 1229, 1912.
† 'Trans. Amer. Inst. Elec. Eng.', vol. 28, part 1, p. 363, 1909.
‡ 'Proc. Amer. Phil. Soc.', vol. 53, p. 55, 1914.
§ 'J. Franklin Inst.', vol. 184, p. 115, 1917.

Digitized by Google

heat from a 0·0256 cm. platinum wire in water follows the same laws as convection in air. Water carries off over 100 times as much heat as air, and they give the following example for the wire :—

| | |
|---|---|
| Velocity of water relative to wire . . . . . | 14·85 cms. per sec. |
| Temperature excess of the wire . . . . . | 30° C. |
| Heat loss from the wire . . . . . | 0·88 cal. per cm. per sec. |

According to tables by KAYE and LABY

$$c = 1, \qquad k = 0{\cdot}00136,$$

hence $$H/k = 21{\cdot}6, \qquad vlc/k = 280.$$

Now for air $k/c\nu = 1{\cdot}3$ approximately, so in Fig. 1 the relation between $H/k$ and $vl/\nu$ for air is a relation between $H/k$ and $1{\cdot}3\ vlc/k$. Plotting the above value for water on the curve regarded in this manner, gives the point X in fair agreement.

TABLE I.—Convection at Various Air Pressures.
Wire diam. 0·0114 cm. $v = 970$ cms. per sec.
Values of $\nu$ given for a pressure of 1 atmosphere ( $= 1{\cdot}012 \times 10^6$ bars).
Room temperature about 20° C.

| Pressure (bars). | 390° C. excess. $\log \nu = \bar{1}{\cdot}56$ $\log k = \bar{5}{\cdot}95$ | | 538° C. excess. $\log \nu = \bar{1}{\cdot}67$. $\log k = \bar{4}{\cdot}00$. | |
|---|---|---|---|---|
| $10^6\times$ | $\log vl/\nu$ | $\log H/k$. | $\log vl/\nu$. | $\log H/k$. |
| 4·0 | — | — | 1·97 | 1·33 |
| 3·95 | 2·07 | 1·36 | — | — |
| 2·02 | — | — | 1·68 | 1·18 |
| 2·00 | 1·78 | 1·20 | — | — |
| 1·02 | 1·48 | 1·08 | 1·38 | 1·05 |
| 0·44 | 1·12 | 0·92 | 1·01 | 0·90 |

### 4. *The Dynamical Data.*

The mechanical pressure on smooth wires placed in a stream of air has been given in the 'Technical Report of the Advisory Committee for Aeronautics for 1913–14'. The data relate to 60° F. and a barometric pressure of 760 mms. The wires range from 0·002 inch to 1½ inch diameter, and were placed in winds of 10–50 feet per second (20–50 feet per second for wires above ¼ inch diameter). The results were exhibited in a non-dimensional curve, and this has been re-drawn in the "Dynamical Relation" line of Fig. 1, where $\log R/\rho v^2 l^2$ is plotted against $\log vl/\nu$.



Digitized by Google

### 5. *Relation between Thermal and Dynamical Effects.*

Fig. 1 gives for definite values of $vl/\nu$ the appropriate values of $H/k$ and of $R/\rho v^2 l^2$, and, using these, Fig. 2 has been drawn showing the relation between $H/k$ and $R/\rho v^2 l^2$ for corresponding values of $vl/\nu$.

In the above form the curves are non-dimensional and general, but it is instructive to draw a curve which shows for corresponding values of $vl$ the relation of the heat loss H to the mechanical resistance R. Strictly, this cannot be done unless $\nu$ is the same in the two cases, and presumably this condition would be satisfied if R were measured not for a cold wire, but for one at the same temperature as that at which H was measured. Failing such measurements, however, the data of Table II approximately satisfy the condition, for here, for an air stream of 15° C., the mechanical pressure R of cold wires is compared with the heat loss H from wires at a temperature (100° C.) not far removed. The table has been drawn up from data already considered, and the results are plotted in Fig. 3. To facilitate comparison with previous work $H/k$ is given instead of H, taking for $k$ the value $5{\cdot}77 \times 10^{-5}$ appropriate to the temperature of the ambient air. Similarly, $R/\rho$ is given. This does not alter the shape of the curve. It may be mentioned that a curve between $H/k$ and $vl/\nu$ plotted from this table is practically identical with that of Fig. 1, where allowance was made for the change of the physical constants with temperature.

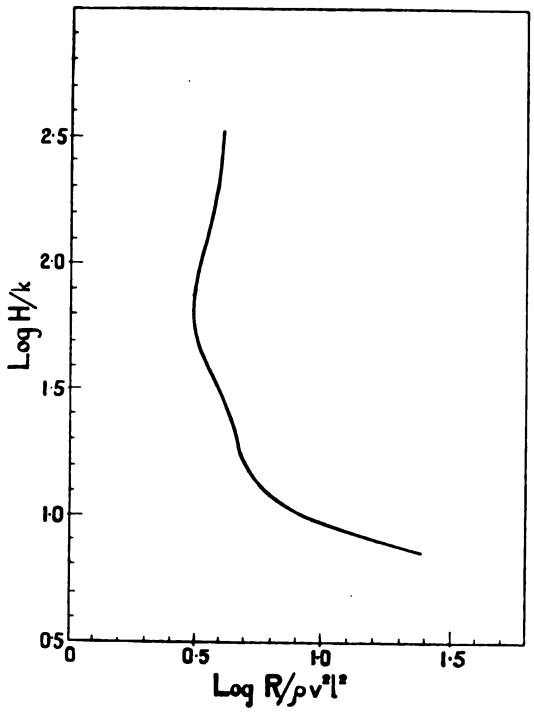


Fig. 2.

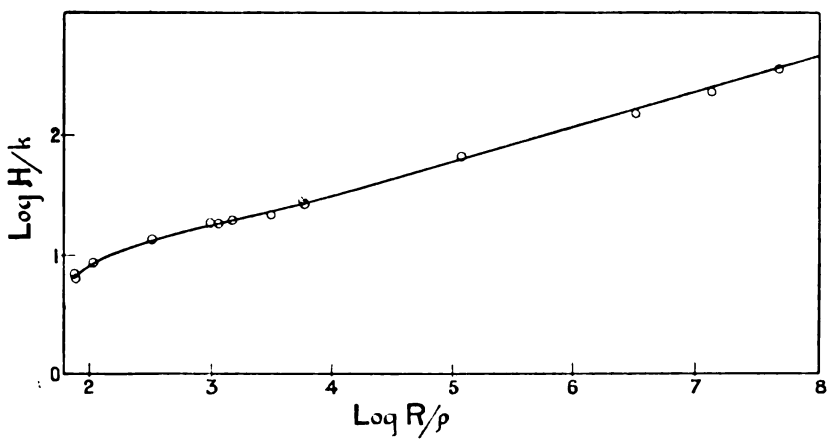


Fig. 3.

Digitized by Google

TABLE II.—Relation between R/ρ and $H/k$.

$\nu = 0{\cdot}145$.* $\log \nu = \bar{1}{\cdot}16$.

$k = 5{\cdot}77 \times 10^{-5}$. $\log k = \bar{5}{\cdot}76$.

| $\log \frac{vl}{\nu}$. | $\log \frac{H}{k}$. | $\log \frac{R}{\rho}$. | Source of data. |
|---|---|---|---|
| 1·015 | 0·81 | 1·88 | KING (0·003 cm.). |
| 1·316 | 0·93 | 2·03 | |
| 1·015 | 0·84 | 1·88 | (0·015 cm.). |
| 1·714 | 1·12 | 2·51 | |
| 2·015 | 1·26 | 3·01 | |
| 3·14 | 1·78 | 5·09 | HUGHES. |
| 3·84 | 2·13 | 6·54 | |
| 4·14 | 2·30 | 7·17 | |
| 4·44 | 2·48 | 7·79 | |
| 4·68 | 2·64 | 8·29 | |
| 2·05 | 1·25 | 3·08 | KENNELLY. |
| 2·26 | 1·31 | 3·50 | |
| 2·40 | 1·41 | 3·76 | |
| 2·10 | 1·26 | 3·18 | |
| 2·40 | 1·42 | 3·76 | |

As stated earlier, the theory of OSBORNE REYNOLDS gives for fluid flow through a given pipe

$$H \propto R/v.$$

This simple relation does not hold for wires in the region considered, for taking the straight-line part of the curve of Fig. 3 it is seen that

$$H \propto R^{0{\cdot}275} \text{ approx.} \quad . \quad . \quad . \quad . \quad . \quad . \quad . \quad . \quad . \quad . \quad (8)\dagger$$

and for this region it may be shown from Fig. 1 that roughly

$$H \propto v^{0{\cdot}55} \text{ and } R \propto v^2.$$

Consequently,

$$H \propto R/v^{1{\cdot}45}. \quad . \quad . \quad . \quad . \quad . \quad . \quad . \quad . \quad . \quad . \quad . \quad (9)$$

There is, however, most probably a tendency for the relation to take the simpler form given by REYNOLDS as the size of the cylinders is still further increased. This follows since R tends to be proportional to the square of the velocity, and since HUGHES found that the heat loss H tends to be proportional to $v$.

* The value taken for ν in the 'Report of the Advisory Committee for Aeronautics' differs slightly but inappreciably from this, and so no allowance has been made for the difference.

† With respect to the reality or otherwise of the unexplained dip in the "Dynamical Relation" of Fig. 1, little effect is made in Fig. 3 by smoothing out the dip entirely. Smoothing appears, however, to make more uniform the tendency of the relation to take the REYNOLDS form as $vl/\nu$ increases.



Digitized by Google

Digitized by Google

# CONVECTION OF HEAT IN GASES AND LIQUIDS. IV.—NATURAL CONVECTIVE COOLING IN VISCOUS GASES AND LIQUIDS

BY

A. H. DAVIS, D.Sc.,
ASSISTANT IN THE PHYSICS DEPARTMENT.

Digitized by Google

## ABSTRACT.

It has been shown in a previous paper that the loss of heat by natural convection from similar bodies immersed in viscous fluid can be expressed by the relation $hL/k\theta = F(c^2g L^3 a\theta/k^2) f(c\nu/k)$ where the symbols have the meaning given below. For gases the relation is simplified since $(c\nu/k)$ is constant, and good agreement has been found between experimental results and the simplified formula. The case of viscous liquids is now considered.

A theoretical investigation is given which shows that in certain cases the general formula takes the special form $hL/k\theta = F(L^3\theta gac/k\nu)$.

To test the accuracy with which this equation may be substituted for the more general one, and to determine the form of the function involving $c\nu/k$, experiments were conducted on the cooling of electrically heated wires immersed horizontally in various liquids. The liquids tested were toluene, carbon tetrachloride, aniline, olive oil and glycerine. If $d$ represents the diameter of the wire and H the heat-loss per unit length of wire per degree temperature excess, the relation between $H/k$ and $(c^2gd^3a\theta/k^2)$ is shown to be given by a family of curves having $c\nu/k$ as parameter. The results obtained can be expressed by the relation $H/k \propto (c^2gd^3a\theta/k^2)^x (c\nu/k)^{-y}$ where $x$ varies from 1/10 to 1/6 and $y$ varies from 1/10 to 1/8. If $x = y$ we obtain $H/k \propto (d^3\theta gac/k\nu)^x$; this equation, which is of the special form indicated above, is shown to be satisfactory by plotting $H/k$ against $(d^3\theta gac/k\nu)$ when one line covers the results for all the fluids considered. The variation of viscosity with temperature is allowed for but temperature variations of other properties are neglected. Apparently, judging from cases so far studied, the cooling power of a fluid may be represented by $h \propto k\,(ac/k\nu)^n$, where $n$ varies from 0 to 1/3, and thus the cooling power of a fluid is mainly determined by its thermal conductivity.


Digitized by Google

# CONVECTION OF HEAT IN GASES AND LIQUIDS. IV.—NATURAL CONVECTIVE COOLING IN VISCOUS GASES AND LIQUIDS.

By A. H. DAVIS, D.Sc., Assistant in the Physics Department.

[Reprinted, with modified title, from the 'Philosophical Magazine', Vol. 44, 1922.]

## *Introduction.*

By general reasoning from the principle of similitude,* introducing certain plausible assumptions, it is possible to obtain the following formula to represent the heat loss by natural convection from similar bodies similarly immersed in viscous fluids.

$$hL/k\theta = F(c^2gL^3a\theta/k^2)f(c\nu/k), \quad \ldots\ldots\ldots \quad (1)$$

where

$h$ = heat loss per unit time per unit area of the body,

$k$ = thermal conductivity of the fluid,

$c$ = capacity for heat of the fluid per unit volume,

$\nu$ = kinematical viscosity of the fluid,

$\theta$ = temperature excess of the body,

$a$ = coefficient of density reduction of the fluid per degree rise of temperature,

$g$ = acceleration due to gravity,

L = linear dimensions of the body.

For gases, $c\nu/k$ is practically constant, and so experiments with them cannot reveal the effects of this term. However, the formula, restricted by its omission, has already been shown for gases to be in good general agreement with experimental results. In the investigation, early work on miscellaneous small bodies has been considered† and also data for moderately heated large vertical surfaces from 2 inches to 9 feet in height.‡ Particular attention has been given to the case of wires and long cylinders,§ owing to the wide range of size, temperature excess, gas nature and pressure for which results were available.

Liquids, however, cover a wide range of values of $c\nu/k$, and so experiments on the cooling of wires in liquids were undertaken to study the effect of this term.

But, further, it was suspected that $g$ and $\nu$ might always occur together in the equation

* Davis, 'N.P.L. Collected Researches', vol. 19, Paper 11, or 'Phil. Mag.', vol. 40, p. 692, 1920.

† Davis, *loc. cit.*

‡ Dept. of Sci. and Ind. Research. Food Investigation Board, Special Report, No. 9.

§ Davis, 'N.P.L. Collected Researches', vol. 19, Paper 12, or 'Phil. Mag.', vol. 43, p. 329, 1922.

Digitized by Google

in the form $g/\nu$, for any steady velocity of the viscous streams will be determined by a balance between the accelerating forces due to gravity and the retardation due to viscosity. The formula would then take the simple form

$$hL/k\theta = F(L^3\theta gac/k\nu). \quad . \quad . \quad . \quad . \quad . \quad . \quad . \quad . \quad . \quad (2)$$

The present paper investigates the possibility of such a simplification, and therefore consists of two main parts—one theoretical, in which more formal consideration is given to convection in a viscous fluid; and the other experimental, where convective cooling of wires is studied for a series of fluids of different viscosity with a view to experimental verification of the formulæ put forward.

## Part I.—Theoretical.

Convective cooling is taken to refer to the total heat transfer from a hot body by the medium of a fluid moving past the surface. Such cooling is said to be "natural" or "free" when the fluid is still, except for the streams set up by the heat from the hot body itself, and is said to be "forced" when the body is immersed in a fluid stream, usually considered to be moving with such velocity that the currents set up by the hot body itself are negligible. The present paper is limited to natural convection.

In 1820 Fourier* stated the equation of heat conduction in a moving fluid, and in 1881 Lorenz,† upon certain assumptions, gave a formula for heat-loss by natural convection for the special case of a vertical plane surface immersed in an infinite viscous fluid. In 1901 Boussinesq,‡ dealing with inviscid fluids, gave a general solution of the problem of natural convection from heated solids in infinite fluid media.

The following investigation follows Boussinesq closely, but introduces the modifications necessary in extending the inquiry to viscous fluids.

Adopting the same mathematical symbols as those already used, let us consider the natural convective cooling of a hot body immersed in an infinite viscous medium and maintained at a certain temperature, $\theta$ degrees in excess of that of the liquid at infinite distance, to which all temperatures are referred.

Let $\rho$ and $\nu$ be respectively the density of the fluid and its kinematical viscosity. For an element of the fluid at the point $x\,y\,z$, let $\tau$, $u$, $v$, $w$, P be the temperature excess (assumed steady, *i.e.*, independent of time "$t$"), the three components of its velocity, and the non-hydrostatic part of its pressure. For elements of the fluid at infinite distance these quantities are all zero.

Let us assume that the dilation of the fluid by heat is negligible except in so far as the weight of unit volume is altered, so that it occurs in the equations only when multiplied by "$g$." Let $g\rho a$ be the reduction in weight produced in unit volume by unit

* 'Mém. de l'Académie', vol. 12, p. 507, 1820.

† 'Ann. der Phys.', vol. 13, p. 582, 1881.

‡ 'Comptes Rendus', vol. 132, p. 1382, 1901.

Digitized by Google

rise of temperature, $g\rho a\tau$ thus being the total reduction effected. The axis of $z$ being vertical, the hydrodynamical equations of continuity and of motion are

$$\left.\begin{aligned} &\frac{\partial u}{\partial x}+\frac{\partial v}{\partial y}+\frac{\partial w}{\partial z}=0, \qquad \frac{1}{\rho}\frac{\partial \mathrm{P}}{\partial x}=-u'+\nu\nabla^2 u,\\ &\frac{1}{\rho}\frac{\partial \mathrm{P}}{\partial y}=-v'+\nu\nabla^2 v, \qquad \frac{1}{\rho}\frac{\partial \mathrm{P}}{\partial z}=-ga\tau-w'+\nu\nabla^2 w, \end{aligned}\right\}. \quad . \quad . \quad . \quad . \quad (3)$$

$u'$, $v'$ and $w'$ being the accelerations of the fluid parallel to the axes.

If $k$ be the thermal conductivity of the fluid and $c$ its heat capacity per unit volume, then $\tau'$, the rate of change of temperature for a given particle with respect to time, is given by

$$\tau'=\frac{k}{c}\nabla^2\tau. \quad . \quad . \quad . \quad . \quad . \quad . \quad . \quad . \quad . \quad . \quad . \quad . \quad (4)$$

Also, the derivative $\tau'$, like the derivatives $u'$, $v'$, $w'$ of the velocities, is obtained by finding the increase in $\tau$ when $x$, $y$, $z$ increase by $u\,dt$, $v\,dt$ and $w\,dt$; in this way we have the quadruple equation

$$(u',\ v',\ w',\ \tau')=u\frac{\partial(u,\ v,\ w,\ \tau)}{\partial x}+v\frac{\partial(u,\ v,\ w,\ \tau)}{\partial y}+w\frac{\partial(u,\ v,\ w,\ \tau)}{\partial z} \quad . \quad . \quad . \quad (5)$$

To the five differential equations (3) and (4) it is necessary to add the following seven boundary conditions, in the first of which, $l$, $m$, $n$, denote the three direction-cosines of the normal drawn from the interior of the fluid to any element of surface of the body.

$$\left.\begin{aligned} &\text{At the surface of the solid} \quad u=v=w=0 \quad \text{and} \quad \tau=\theta,\\ &\text{At infinite distance} \qquad (\mathrm{P},\ u,\ v,\ w,\ \tau)=0. \end{aligned}\right\}. \quad . \quad . \quad . \quad . \quad (6)$$

In words, at the surface of the solid the fluid takes the temperature $\theta$ of the solid, and the velocity is zero.

Following Boussinesq, let us endeavour to replace the independent variables $x$, $y$, $z$, and the functions $\tau$, $u$, $v$, $w$, P by others, $\xi$, $\eta$, $\zeta$, T, U, V, W, $\Pi$, respectively proportional to each of them, but whose ratios are chosen in a manner to eliminate the parameters $\theta$, $ga$, $k/c$, $\rho$, $\nu$.

Let us consider the following substitutions :

$$\left.\begin{aligned} &\xi=\left(\frac{\theta gac}{k\nu}\right)^{1/3}x, \qquad \eta=\left(\frac{\theta gac}{k\nu}\right)^{1/3}y, \qquad \zeta=\left(\frac{\theta gac}{k\nu}\right)^{1/3}z,\\ &\tau=\theta\mathrm{T}, \qquad u=\left(\frac{\theta gak^2}{c^2\nu}\right)^{1/3}\mathrm{U}, \qquad v=\left(\frac{\theta gak^2}{c^2\nu}\right)^{1/3}\mathrm{V}, \qquad w=\left(\frac{\theta gak^2}{c^2\nu}\right)^{1/3}\mathrm{W},\\ &\mathrm{P}=\rho\left(\frac{\theta^2a^2g^2k\nu}{c}\right)^{1/3}\Pi \end{aligned}\right\}. \quad . \quad (8)$$



Digitized by Google

It is readily found that the substitutions eliminate the parameters satisfactorily if $c\nu/k$ is a constant and equal to unity. For liquids $c\nu/k$ may have very large values (glycerine 8,000, etc., see later), but for gases, as indicated by the kinetic theory, it is constant and approximately equal to unity. For gases, therefore, the above substitutions should be fairly satisfactory on this ground.

There is an alternative condition under which the substitutions are satisfactory, even without $c\nu/k$ being a constant. The condition is that the accelerations $u'$, $v'$, $w'$ of the particle shall be negligible compared with $\nu\nabla^2 u$, etc., which would appear to be justifiable for very viscous fluids. It implies that on coming into the region of the hot body a particle of the fluid almost immediately takes up its final velocity and suffers but little subsequent acceleration.

Consequently, the above substitutions appear satisfactory, and the differential equations (3) and (4) take the following form. (U′ V′ W′ may be retained if $c\nu/k = 1$, but otherwise they must be omitted, since $u'$, $v'$ and $w'$ are neglected*).

$$\left.\begin{aligned}
&\frac{\partial U}{\partial \xi}+\frac{\partial V}{\partial \eta}+\frac{\partial W}{\partial \zeta}=0, \qquad T'=\frac{\partial^2 T}{\partial \xi^2}+\frac{\partial^2 T}{\partial \eta^2}+\frac{\partial^2 T}{\partial \zeta^2},\\
&\frac{\partial \Pi}{\partial \xi}=-U'+\left(\frac{\partial^2 U}{\partial \xi^2}+\frac{\partial^2 U}{\partial \eta^2}+\frac{\partial^2 U}{\partial \zeta^2}\right), \quad \frac{\partial \Pi}{\partial \eta}=-V'+\left(\frac{\partial^2 V}{\partial \xi^2}+\frac{\partial^2 V}{\partial \eta^2}+\frac{\partial^2 V}{\partial \zeta^2}\right),\\
&\frac{\partial \Pi}{\partial \zeta}=-T-W'+\frac{\partial^2 W}{\partial \xi^2}+\frac{\partial^2 W}{\partial \eta^2}+\frac{\partial^2 W}{\partial \zeta^2},\\
&\text{where}\\
&(U', V', W', T')=U\frac{\partial(U, V, W, T)}{\partial \xi}+V\frac{\partial(U, V, W, T)}{\partial \eta}+W\frac{\partial(U, V, W, T)}{\partial \zeta}
\end{aligned}\right\} \quad . (8)$$

Also, let us put the equation of the solid in the form

$$f\left[\left(\frac{\theta gac}{k\nu}\right)^{1/3}x, \quad \left(\frac{\theta gac}{k\nu}\right)^{1/3}y, \quad \left(\frac{\theta gac}{k\nu}\right)^{1/3}z\right]=0. \quad . \quad . \quad . \quad (9)$$

* I am indebted to Mr. W. G. Bickley, M.Sc., for the following notes :—

(*a*) If $c\nu/k$ is not equal to unity, equations (8) are mathematically correct if we write $\frac{k}{c\nu}U'$ for U′, etc. Evidently, if $c\nu/k$ is large, the term $\frac{k}{c\nu}U'$ is correspondingly small and may be omitted. Retaining it, however, the solution of (8) becomes

$$\frac{\tau}{\theta}, \frac{u, v, w}{\left(\frac{\theta gak^2}{c^2\nu}\right)^{1/3}}, \frac{P}{\rho\left(\frac{\theta^2 g^2 a^2 k\nu}{c}\right)^{1/3}} = \text{definite functions of } \left\{\left(\frac{\theta gac}{k\nu}\right)^{1/3}(x, y, z); \frac{c\nu}{k}\right\}.$$

The experimental curve shows that the occurrence of $c\nu/k$ in these functions is in such a manner that large variations in $c\nu/k$ have imperceptible effects.

(*b*) Equation (5), and the resulting one (8), would be more general if the term $\frac{\partial(u, v, w, \tau)}{\partial t}$ were introduced on the left-hand side. This would include unsteady motion, but would in no way affect the changes of variables.

Digitized by Google

Thus, if the coefficient $(\theta gac/k\nu)^{1/3}$ changes, this amounts to considering, instead of the actual solid, similar bodies having linear dimensions inversely proportional to this coefficient. Then the direction-cosines $l$, $m$, $n$, of the normal will remain the same at corresponding points, and the boundary conditions become

$$\left.\begin{array}{l}\text{At the surface,} \quad U = V = W = 0 \quad \text{and} \quad T = 1, \\ \text{At the distance } \sqrt{\xi^2 + \eta^2 + \zeta^2} \text{ infinite,} \quad (\Pi, U, V, W, T) = 0\end{array}\right\} \quad \ldots\ldots \quad (10)$$

The system of equations (8) and (10) determine (U, V, W, T, $\Pi$) as the functions of $\xi$, $\eta$, $\zeta$, and substituting in the integrals for the eight new variables their equivalents as given by (7), we have five relations of the form

$$\left\{\frac{\tau}{\theta}, \quad \frac{u, v, w,}{\left(\frac{\theta gak^2}{c^2\nu}\right)^{1/3}}, \quad \frac{P}{\rho\left(\frac{\theta^2 g^2 a^2 k\nu}{c}\right)^{1/3}}\right\}$$

$$= \text{definite functions of } \left(\frac{\theta gac}{k\nu}\right)^{1/3} x, \quad \left(\frac{\theta gac}{k\nu}\right)^{1/3} y, \quad \left(\frac{\theta gac}{k\nu}\right)^{1/3} z. \quad \ldots \quad (11)$$

The flux of heat furnished in unit time by unit area of such a body, equal to that which the contiguous liquid layer communicates to the interior of the fluid, is given by

$$k\left(l\frac{\partial\tau}{\partial x} + m\frac{\partial\tau}{\partial y} + n\frac{\partial\tau}{\partial z}\right).$$

Introducing the new variables, we have then

$$h = k(\theta gac/k\nu)^{1/3}\theta\left(l\frac{\partial T}{\partial\xi} + m\frac{\partial T}{\partial\eta} + n\frac{\partial T}{\partial\zeta}\right). \quad \ldots\ldots \quad (12)$$

At corresponding points of the surfaces $f(\xi, \eta, \zeta) = 0$ limiting the bodies considered, the direction-cosines $l$, $m$, $n$ and the derivatives $\frac{\partial T}{\partial(\xi, \eta, \zeta)}$ have the same values respectively; so the trinomial coefficient is a function of the shape and orientation of the bodies only.

Thus the result may be stated in the following form. For a family of similar bodies similarly oriented, and having linear dimensions L given by

$$L \propto (\theta gac/k\nu)^{-1/3}, \text{ i.e. } (L^3\theta gac/k\nu) = \text{const.},$$

the heat loss per unit area from corresponding points is given by

$$h \propto k\theta(\theta gac/k\nu)^{1/3}, \quad \ldots\ldots\ldots \quad (13)$$

and this will also be true if $h$ represents mean heat loss for the whole model. So for bodies of this shape and orientation we have

$$h = k\theta(\theta gac/k\nu)^{1/3} f(L^3\theta gac/k\nu) \quad \ldots\ldots\ldots \quad (14)$$



Digitized by Google

which may be written

$$hL/k\theta = F(L^3\theta gac/k\nu). \quad . \quad . \quad . \quad . \quad . \quad . \quad . \quad . \quad . \quad (15)$$

This equation is the simplified form of equation (1) it was desired to establish, and it has been put to the test of experiments in a later part of this paper. It is desirable to notice here one point in connection with it.

For a series of fluids for which $c\nu/k$ is constant, the equation may readily be shown to agree with that obtained by BOUSSINESQ for inviscid fluids; *i.e.* BOUSSINESQ'S grouping of variables for inviscid fluids is satisfactory for viscid fluids for which $c\nu/k$ is constant. This equivalent grouping is given by omitting $(c\nu/k)$ from formula (1).

## PART II. EXPERIMENTAL.

### *Formulæ.*

For long horizontal wires of diameter "$d$" it may readily be shown that formulæ (1) and (2) may be rewritten as follows in terms of the heat-loss H per unit length of wire per degree temperature excess:

$$\left.\begin{aligned} H/k &= F(c^2gd^3a\theta/k^2)f(c\nu/k), \\ H/k &= F(d^3\theta gac/k\nu). \end{aligned}\right\} \quad . \quad . \quad . \quad . \quad . \quad . \quad . \quad . \quad (16)$$

When $c\nu/k$ is a constant, the equations are identical in form and, consequently, evidence for diatomic gases already shown elsewhere to be in agreement with one of these expressions is necessarily in agreement with the other.

If $c\nu/k$ is not constant, the second equation is a special case of the first. The experiments now to be described on the cooling of wires in liquids will indicate the form of the $c\nu/k$ term in (16) and also whether the simpler expression is satisfactory.

### *Apparatus.*

The method of experiment consisted in stretching a wire horizontally at a convenient depth in a vessel full of the liquid under examination, and measuring the electric energy supply necessary to maintain a measured temperature difference between the wire and the general body of the liquid. The electric energy supplied was determined from the measured current through the wire, and from its resistance as obtained from a Wheatstone bridge. This resistance also gave the temperature of the wire.

For each of the liquids the cooling of wires of two sizes was studied, the diameters being 0·0083 cm. and 0·0155 cm. respectively. Both were thought to be pure platinum, but tests of the resistance at the temperature of melting ice and that of steam gave a very low value for the temperature coefficient of the finer wire.

Digitized by Google

The apparatus is shown diagrammatically in Fig. 1. The platinum wire TT, immersed in the liquid under examination, formed part of the fourth arm of a Wheatstone bridge, having equal ratio arms PP. By adjusting the slider S the bridge was balanced with a small current (0·01 amp.), thus allowing for slight temperature changes of the fluid. An additional resistance $d$R now introduced into the third arm destroyed the balance, which was then restored by increasing the current through the bridge and thus heating the wire TT until its resistance had sufficiently increased. Correction for the cooling at the ends of the test wire was automatically effected by having in the other arm of the bridge a shorter piece CC of the same wire* also immersed in the liquid under examination. To be effective, this compensating wire must be greater than a certain minimum length. AYRTON and KILGOUR† have given a calculation showing that for a 6-mil wire at about 300° C. temperature excess in still air, the effect of the heavy leads extends about 1 cm. from each end. For finer wires it would be less, and also it would be less if the cooling medium were a liquid, for these carry off more heat than air, so that the end effects become less important. In the present experiments CC was never less than 2 cms., and so the end effect should be entirely eliminated.

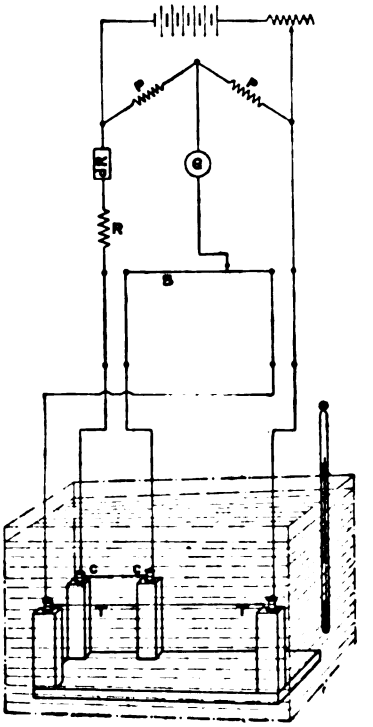

FIG. 1.

The energy dissipated in the uncompensated length ($l$) of TT was calculated from the current ($i$) through the wire and its (hot) resistance R. The temperature excess ($\theta$) of the wire above its surroundings is given by $d\mathrm{R}/\mathrm{R}_0\alpha$, where $\mathrm{R}_0$ is the resistance of the wire at 0° C. and $\alpha$ the temperature coefficient of resistance. The heat-loss H (in calories) per cm. length of wire per 1° C. temperature excess is given by

$$\mathrm{H} = \frac{i^2\mathrm{R}}{4{\cdot}18l} \div \theta, \quad \ldots\ldots\ldots\ldots \quad (17)$$

where

$$\theta = d\mathrm{R}/\mathrm{R}_0\alpha,$$

4·18 being the factor required to convert watts to calories per second.

Details of the wires used are given in Table I.

* CALLENDAR introduced this method of eliminating end effects in resistance measurements, using it for many similar purposes. 'Proc. Phys. Soc. Lond.', vol. 33, p. 137, 1921.

† 'Phil. Trans.', A, vol. 183, p. 371, 1892.

Digitized by Google

TABLE I.—Details of the Wires used.

| Diam. $d$. | $gd^3$. | Uncompensated length. $l$. | $a$. | $R_0$. |
|---|---|---|---|---|
| cm. | | cms. | | ohms. |
| 0·0083 | $5·62 \times 10^{-4}$ | 5·95 | 0·00183 | 2·127 |
| 0·0155 | $36·6 \times 10^{-4}$ | 6·5 | 0·00385 | 0·355 |

The rectangular vessel containing the liquids under examination had a height of 12 cms. and a base of 17 × 10 cms., and the wires (3 cms. apart) were 3·5 cms. below the surface of the liquid. This vessel required rather larger quantities of some of the liquids than were available. A smaller one was found with carbon tetrachloride to give the same result as the larger, and so it was generally used instead. It was 10 cms. high with a base of 16 × 6 cms. It was used quite full and with the wires 5 cms. below the surface of the liquid. In all cases the vessel stood upon an insulated levelling table on a concrete slab on the floor, and no ripples were observable on the liquid surface. It was completely covered in by a draught-proof enclosure of cotton-wool over a cardboard frame, for draughts might by local cooling set up convection currents in the liquid, and might also cause evaporation of the more volatile liquids. A thermometer with 1/10° C. divisions checked the temperature of the fluid.

Table II is a summary of the physical constants of the liquids used. It was compiled from published data in books of physical constants, and since pure liquids were used it is sufficiently exact for present purposes, where (as will be seen later) we are concerned mainly with a small fractional power of the values given. Also, as only moderate heating of the wires was involved, little account has been taken of temperature changes of the physical properties of the liquids, though the point is referred to later.

TABLE II.*—Physical Constants of the Liquids used.

| Liquid. | $10^4k$. | $10^4a$. | $\rho$. | $s$. | $\eta_T$. | $c\nu/k$. | $ac^2/k^2$. | $\eta_{T+25}/\eta_T$ |
|---|---|---|---|---|---|---|---|---|
| Toluene ... ... ... | 3·42 | 10·9 | 0·866 | 0·40 | 0·0062 | 7·24 | 1118 | — |
| Carbon tetrachloride ... | 2·66 | 11·8 | 1·582 | 0·198 | 0·0108 | 8·03 | 1630 | 0·728 |
| Aniline ... ... ... | 4·1 | 8·5 | 1·023 | 0·514 | 0·055 | 69·3 | 1390 | 0·465 |
| Olive oil ... ... ... | 3·92 | 7·0 | 0·916 | 0·47 | 1·17 | 1402 | 842 | 0·363 |
| Glycerine ... ... | 6·8 | 5·3 | 1·26 | 0·58 | 9·3 | 7940 | 611 | 0·42† |

$s$ = specific heat. $\eta$ = viscosity. $\rho$ = density. $c = s\rho$. $\nu = \eta/\rho$.

† $\eta_{T+10}/\eta_T$.

* The majority of these values were obtained from 'Physical and Chemical Constants, etc.', by G. W. C. KAYE and T. H. LABY.

Digitized by Google

The ratio arms were usually 100 ohms each, 1,000 ohms being occasionally used for the larger currents. Equality of the ratio arms was tested by reversing the connections and noticing whether the balance was thereby disturbed.

To eliminate disturbing resistance changes when the heating current was passed, all connecting wires were compensated by similar wires in the opposite arms of the bridge, and the resistances R and $d$R were constructed of manganin, as also was the slide wire S. It was found on test, by removing the platinum wires TT and CC and substituting heavy oil-immersed manganin of the same resistance, that the balance of the bridge obtained with a small current (0·01 amp.) was undisturbed when a heavy current of 1 amp. was passed, and that therefore the compensation was satisfactory. A terminal head on the heavy copper leads to the wires facilitated short circuiting of the platinum wires when subsequent occasional test of the apparatus was required.

It was possible that the heating current might set up thermoelectric effects, but a test showed that these were absent. The method was to switch off the heating current after it had been adjusted to the value necessary to balance the bridge, and no appreciable drift of the galvanometer was then observed while the wires were cooling.

Thermoelectric effects might also have existed through local inequalities of temperature caused otherwise than by the heating current, and these would reveal themselves by drift of the galvanometer on making the galvanometer circuit while the battery circuit was still open. Some slight effect was occasionally found, but it was only important when getting the original balance with the small current; and for this it was eliminated by the familiar device of working with the galvanometer circuit always completed and adjusting the bridge for no deflection when the battery was reversed.

A large storage battery was used at first, and it gave troublesome galvanometer effects due to leakage, discovered and traced by reversal of the battery and galvanometer circuits. To elimimate these a separate 10-volt battery was used, and this and all parts of the apparatus and leads were insulated by standing upon ebonite discs, etc.

The increment resistance $d$R was obtained from a box of manganin coils (resistance 0·01 to 1·0 ohm) provided with mercury cups. A separate test showed that the resistance of the coils was independent of the current. Values of $d$R down to 0·001 ohm were obtained by shunting a resistance of 1 ohm by 1,000 ohms, etc. These values were calibrated directly on a Cambridge resistance bridge, and agreed with calculation. Using a current of 0·01 amp. through the bridge it was possible to obtain the initial balance correct to 0·0001 ohm, or rather less, an amount associated with a galvanometer deflection of 2/5 mm. on reversal of battery. Thus, with a possible error of setting of 0·0001 ohm, values of $d\mathrm{R} = 0{\cdot}1$ would be correct to 1/10 of 1 per cent., and generally the error would be negligible, but with the smallest values of $d$R used (0·001 ohm) the error might be between 5 and 10 per cent., and averages were taken. With the heating current, of course, the bridge was much more sensitive. With the 3-mil wire and a current of $\frac{1}{2}$ amp. a resistance change of 0·0001 ohm in the third arm would cause a galvanometer deflection of 1 cm. Incidentally it was noticed that a change of 1 per

Digitized by Google

cent. in this current value caused a deflection of 13 cms., and this was also approximately the case with the larger wire.

As a further check on the apparatus, the cooling in gases was studied by a volt-drop method instead of using the Wheatstone bridge arrangement. Various experimenters have used this method, measuring the current through a given length of wire and the volt drop along it. To minimise end effects, experimenters have usually used potential leads of very fine wire, attached at sufficient distances from the heavy current leads to eliminate the cooling effects of these latter. This, however, does not eliminate whatever cooling is due to the fine potential leads, and the volt-drop method used in the present experiments is superior in this respect. The method was to pass the current through TT and CC in series, and to measure the respective potential falls by means of a potentiometer. The difference gave the potential drop along the uncompensated length, the end effects being eliminated completely. The current was obtained by passing it also through a standard manganin resistance and determining the volt drop for this also. The resistance TT–CC at the temperature of the air was obtained from the potential drop when a very small current, 0·01 amp., was passing. The results obtained by this check method were within 1 or 2 per cent. of those obtained by means of the Wheatstone bridge. It is not so convenient a method for the liquids, owing to the zero changes which are easily dealt with by the Wheatstone bridge method.

### *Experimental Observations.*

Certain general characteristic effects were noticed during the experiments.

With slight heating of the wire the conditions ultimately set up were usually quite steady, except perhaps for a slight drift with the more viscous liquids due to the fact that the prolonged heating necessary before the steady state was reached gradually increased the temperature of the whole mass of the fluid. However, with greater heating, unsteadiness supervened, the galvanometer deflection and also the current changing spasmodically, as though the convection current had become turbulent or reached some critical condition.

Various measurements were made of the drift mentioned, which was found to be of the order expected from the known energy dissipation in the volume of liquid used. Observations were taken while a heating current was passing, sometimes of the decrease of current necessary as time elapsed to keep the temperature of the wire constant, and sometimes, with constant current, of the ultimate rate of temperature rise of the wire. Observations were also taken of the resistance of the cold wire just before the heating current was passed, and again at such a time after switching off that all local heating of the liquid had been dissipated. In the case of glycerine this dissipation occupied some minutes, and a true drift of 0·001 ohm during an experiment appeared as great as 0·01 ohm when taken too soon after switching off. Results were satisfactorily

Digitized by Google

consistent, and in general were equivalent to a change in $\theta$ of the order of one quarter of 1 per cent. per minute. The less viscous fluids attained the steady state too quickly for this drift to have appreciable effect.

Another effect was noticed with the more viscous liquids. For instance, with the 3-mil wire immersed in olive oil slight heating currents gave a tendency for the galvanometer to drift in a certain direction as though the whole mass were being gradually heated up. With greater heating, however, an opposite drift was observed. This was found to be due to oscillations having a period of a minute or so, which slowly died out and left the usual steady state. Thus, while on switching on a very slight heating current the wire merely rose gradually in temperature to its final value (2° C. excess), reaching this in about three minutes, it was found that for rather greater heating (5° C.) the temperature of the wire first overshot its final value by about 1/8° C., reaching a maximum in about one minute, and then fell gradually to its steady state. With still greater heating (10° C.) two oscillations were noticed, a maximum being reached in $\frac{1}{2}$ minute followed by a minimum $\frac{3}{4}$ minute later, from which the temperature then rose to its final value. These oscillations resemble those of a damped system, the three stages due to different degrees of heating corresponding to three different degrees of damping. The phenomena cannot be attributed to the galvanometer, and must have their origin in the liquid convection currents set up, for the galvanometer normally reached its final deflection in a few seconds, whereas the observed variations occupied minutes.

## *Results.*

The results obtained are given below in tables compiled from smooth curves through experimental points, this making it possible to give them much more concisely than would otherwise have been the case.

It is necessary to state that, in general, results were reproducible to within 5 per cent. With respect to reproducibility, the glycerine series was least satisfactory, but this may have been due to its extremely viscous nature and to the very rapid manner in which its viscosity changes with temperature.

In Table III results are given for the various liquids, showing the relation between the linear emissivity H of the wire in cals. per cm. length per degree temperature excess, and the temperature excess $\theta$.

### (*a*) *Representation in the Form* $H/k = F(c^2gd^3a\theta/k^2)f(c\nu/k)$.

In Table IV these results are represented in the form showing the relation to the equation for inviscid fluids, and $H/k$ is given for various values of $(c^2gd^3a\theta/k^2)$, the value of $c\nu/k$ for the liquid being stated. The heat-losses obtained for air do not appear in this table as they fall under very much smaller values of $c^2gd^3a\theta/k^2$.



Digitized by Google

TABLE III.—Relation between $10^4$H and θ.

[Heat loss (H) in calories per cm. length per 1° C. excess temperature.]

| Liquid. | Wire diam. | $c^2gd^3a/k^2$. | $10^4$H. Temperature excess (θ)° C. 1. | 2. | 5. | 10. | 20. | 50. |
|---|---|---|---|---|---|---|---|---|
| Gases* ... ... ... | 0·0083 | $4·74\times10^{-5}$ | | 0·82 | 0·83 | 0·86 | 0·91 | 1·03 |
| | 0·0155 | $3·09\times10^{-4}$ | | | 0·99 | 1·03 | 1·10 | 1·23 |
| Toluene... ... ... | 0·0083 | 0·624 | | 8·6 | 9·5 | 10·4 | 11·1 | 12·6 |
| | 0·0155 | 4·06 | 9·8 | 10·7 | 12·1 | 13·6 | 15·4 | 18·2 |
| $CCl_4$ ... ... ... | 0·0083 | 0·920 | 6·3 | 6·8 | 7·7 | 8·4 | 9·2 | 10·3 |
| | 0·0155 | 5·98 | 8·1 | 9·1 | 10·5 | 11·7 | 12·9 | 14·9 |
| Aniline ... ... ... | 0·0083 | 0·782 | 7·5 | 8·4 | 9·6 | 10·8 | 12·1 | 14·6 |
| | 0·0155 | 5·08 | 9·9 | 11·0 | 12·3 | 14·1 | 16·2 | 19·4 |
| Olive oil ... ... | 0·0083 | 0·472 | | 5·3 | 6·1 | 6·7 | 7·4 | 8·6 |
| | 0·0155 | 3·08 | | 6·8 | 7·6 | 8·7 | 9·9 | 12·0 |
| Glycerine ... ... | 0·0083 | 0·343 | | 9·6 | 9·4 | 9·5 | 10·3 | |
| | 0·0155 | 2·23 | | 9·9 | 10·7 | 11·9 | 13·5 | 16·2 |

* For gases θ was varied up to 200° C., and the values of $10^4$H obtained for the two wires at θ = 200° C. were 1·34 and 1·60 respectively.

TABLE IV.—Relation between H/$k$ and $c^2gd^3a\theta/k^2$.

| Liquid. | cv/$k$. | Wire diam. | H/$k$. $c^2gd^3a\theta/k^2$. 1. | 2. | 5. | 10. | 20. | 50. | 100. | 200. |
|---|---|---|---|---|---|---|---|---|---|---|
| Toluene . . . . . | 7·2 | 0·0083 | 2·5 | 2·6 | 3·0 | 3·2 | 3·5 | 4·1 | 4·7 | |
| | | 0·0155 | | | 2·9 | 3·2 | 3·6 | 4·1 | 4·6 | |
| $CCl_4$ . . . . . | 8·0 | 0·0083 | 2·3 | 2·6 | 2·9 | 3·2 | 3·5 | 4·0 | | |
| | | 0·0155 | | | | 3·2 | 3·6 | 4·2 | 4·7 | 5·2 |
| Aniline . . . . . | 69 | 0·0083 | 1·9 | 2·2 | 2·5 | 2·8 | 3·2 | 3·8 | 4·3 | |
| | | 0·0155 | | | 2·5 | 2·7 | 3·0 | 3·5 | 4·0 | 4·6 |
| Olive oil . . . . . | 1400 | 0·0083 | 1·4 | 1·6 | 1·8 | 2·0 | 2·1 | | | |
| | | 0·0155 | | | 1·7 | 1·9 | 2·1 | 2·4 | 2·8 | 3·3 |
| Glycerine . . . . . | 7640 | 0·0083 | 1·4 | 1·4 | 1·5 | 1·7 | | | | |
| | | 0·0155 | | | 1·4 | 1·5 | 1·7 | 2·0 | 2·4 | |

It is clear from the table that for a given liquid the relation between H/$k$ and $c^2gd^3a\theta/k^2$ is practically independent of the diameter of the wire.

Digitized by Google

There appears, however, to be a tendency for the finer wire to give values of $H/k$ a few per cent. higher than the other, and this is most probably due to the temperature variation of the properties of the fluids for which no allowance has been made.

In considering the cooling of the wires in gases, where much greater temperature excesses were involved, it was found that approximate allowance of this kind corrected a similar tendency.* It appears on approximate calculation from what data are available (mainly temperature coefficients of viscosity) that in the present experiments the correction to be expected is sensible, and is of the sign and order of magnitude required to bring the results for the two wires into even closer agreement. In Fig. 2 single curves have been drawn representing mean values for each of the liquids.

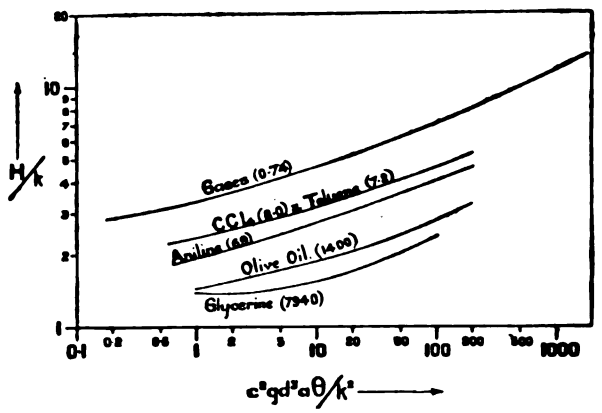


FIG 2.

Although our own figures for gases fall on a very distant region of the graph and so are not shown, a curve has been given to represent gases. It was obtained from the paper already mentioned, where cooling was studied for a wide range of wire diameter and of temperature excess, for various gases—oxygen, hydrogen, and air—over a thousandfold range of gas-pressure.

It is seen that the curves for the different fluids form a family of more or less parallel lines, with $cv/k$ as parameter. The magnitude of the effect of $cv/k$ is not great, for although glycerine has a value more than 10,000 times that for air, the value of $H/k$ for a given value of $c^2gd^3a\theta/k^2$ is only reduced in the ratio 3 : 1. It is satisfactory that toluene and carbon tetrachloride, with values of $cv/k$ so nearly the same, should be represented by one line. The curve for diatomic gases ($cv/k = 0{\cdot}74$) may be shown to agree with published results for cooling of wires in $CO_2$ ($cv/k = 0{\cdot}83$), so that here again it appears that $cv/k$ determines the position of the curve

A logarithmic plot of the relation between $H/k$ and $cv/k$ for various constant values (1, 10 and 100) of $c^2gd^3a\theta/k^2$ yields more or less linear relations; and it appears that

* DAVIS, 'N.P.L. Collected Researches', vol. 19, Paper 12, or 'Phil. Mag.', vol. 43, p. 329, 1922.



Digitized by Google

within the limits of our experiments the complete equation for the cooling of wires in fluids is given by

$$H/k \propto (c^2gd^3a\theta/k^2)^x(c\nu/k)^{-y}, \quad \ldots\ldots\ldots \quad (18)$$

where

$x$ varies from 1/10 to 1/6

and

$y$ varies from 1/10 to 1/8.

It is noticed that $x$ and $y$ have nearly equal values, and if we put $x = y$, equation (6) becomes

$$H/k \propto (d^3\theta gac/k\nu)^x, \quad \ldots\ldots\ldots \quad (19)$$

which is in agreement with the theoretical equation (16). There appears to be no published evidence to show whether this simplified grouping is of more general applicability, but in this connection it is interesting to note that LORENZ, in calculating the convective cooling of a vertical plate in a viscous gas, obtained a result reducible to this form. The assumptions he made led in his special case to the result represented by $x = y = 1/4$. This index is rather higher than those given above, but it is known from an extended curve for gases that for larger cylinders $x$ tends to increase to a value of 1/3.

### (*b*) *Representation of Results in the Form* $H/k = F(d^3\theta gac/k\nu)$.

We now proceed to show graphically the extent to which the present experimental results agree with this theoretical equation.

If satisfactory, results plotted with $H/k$ as ordinate and $(d^3\theta gac/k\nu)$ as abscissa should yield one line independent of the nature of the liquid used. Strictly it is necessary to make allowance for the temperature change in the physical properties of the liquids. Unfortunately, reliable data do not seem to be available for some of the properties, but it appears that the viscosity provides the most rapid change, and its temperature coefficient is usually known.

Consequently, while in this paper temperature variations in the other variables are neglected, an attempt will be made to allow for them in the case of viscosity. As a first approximation, the value taken for the viscosity in any experiment is that appropriate to a temperature intermediate between the temperature of the hot wire and that of the main volume of cold liquid in which it is immersed. If the cooling wire is 50° C. hotter than the cold liquid, the viscosity taken is that for a temperature 25° C. in excess of that of the liquid. The factor $\eta_{T+25}/\eta_T$ is given in Table II, and it is seen that the temperature change is considerable, particularly with glycerine.

From results obtained, and using the above correction for temperature changes in viscosity, Table V and Fig. 3 have been derived, and each liquid is represented on the graph by four points. The extreme points of each set refer to the extremities of the

Digitized by Google

range of the experimental results. They refer respectively to the cooling of the fine wire at 2° C. excess and that of the other wire at 50° C. excess.

TABLE V.—Relation between $H/k$ and $gd^3a\theta c/k\nu$.

| Fluid. | Wire diam. | 2° C. excess. | | 50° C. excess. | |
|---|---|---|---|---|---|
| | | $gd^3a\theta c/k\nu$. | $H/k$. | $gd^3a\theta c/k\nu$. | $H/k$. |
| Air† . . . . . | 0·0083 | $0{\cdot}0_3120$ | 1·41 | $0{\cdot}0_2235$ | 1·66 |
| | 0·0155 | $0{\cdot}0_383$ | | 0·0153 | 1·99 |
| $CCl_4$ . . . . . | 0·0083 | 0·229 | 2·55 | 7·90 | 3·86 |
| | 0·0155 | 1·49 | 3·42 | 51·3 | 5·62 |
| Aniline . . . . . | 0·0083 | 0·0225 | 2·04 | 1·21 | 3·56 |
| | 0·0155 | 1·47 | 2·61 | 7·9 | 4·74 |
| Olive oil . . . . . | 0·0083 | $0{\cdot}0_367$ | 1·34 | 0·047 | 2·18 |
| | 0·0155 | $0{\cdot}0_244$ | 1·73 | 0·30 | 3·07 |
| Glycerine . . . . | 0·0083 | $0{\cdot}0_487$ | 1·18 | $0{\cdot}0_221$* | 1·51* |
| | 0·0155 | $0{\cdot}0_356$ | 1·44 | 0·0134* | 1·99* |

* These refer to $\theta = 20°$ C.

† On the graph of Fig. 3 are also plotted the following values for the wires at 200° C. excess in air :—

| | | |
|---|---|---|
| Wire diam. . . . . | 0·0083 | 0·0155 |
| $gd^3a\theta c/k\nu$ . . . . . | $5{\cdot}12 \times 10^{-3}$ | $3{\cdot}00 \times 10^{-2}$ |
| $H/k$ . . . . . | 1·81 | 2·14 |

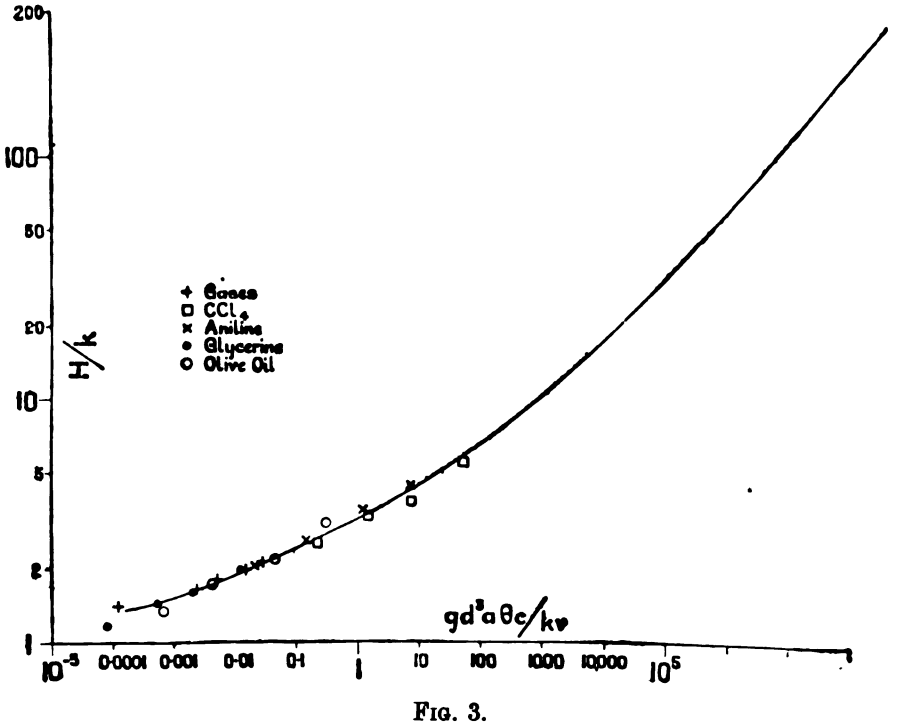


FIG. 3.

Digitized by Google

It is seen that the points all lie very well on one curve, so that equation (16) appears to represent the results of the present experiments very satisfactorily. The upward extension of the curve beyond the points plotted is the representation on the present basis of the upper part of the curve for gases already referred to.

### *The Cooling Power of Fluids.*

It appears from the theoretical considerations and experimental evidence put forward in this paper and previously, that the convective cooling of similar bodies immersed in fluids may be represented by the formula

$$hL/k\theta = F(c^3gL^3a\theta/k^3)f(c\nu/k),$$

and the form of the function $f(c\nu/k)$ is now indicated to be such that we may write the simpler expression

$$hL/k\theta = F(L^3\theta gac/k\nu).$$

It is to be expected that such a grouping of variables is of more general applicability than for the special case of infinite fluids, especially in so far as it can be obtained from the Principle of Similitude. Where liquids by their natural convective motion carry heat from a hot surface and yield it to a cold one, as with the common case of a hot body immersed in a fluid contained in a cooler vessel, one would in general expect approximate agreement with the formula if $\theta$ represented the temperature difference between the two surfaces. A few experiments would soon test the applicability in any doubtful case.

For any circumstances to which the formula applies, the form of the function F may be obtained from an experiment in which only one of the variables (say $\theta$) is altered. We have some knowledge of its form in certain cases. For cooling of large bodies in free air or in enclosures, large compared with the size of the cooling body, we may write

$$hL/k\theta \propto (L^3\theta gac/k\nu)^n,$$

where $n$ is usually about 1/4, but tends to be as great as 1/3 for large bodies or very hot ones, and to be much smaller for fine wires only slightly heated, as in the present experiments. Measurements of the conductivity of fluids have been made by methods involving fine wires, very slightly heated, along the axis of a small metal tube: the validity of this method implies that $n = 0$ in this extreme case.

Since for a given set of circumstances the value of $n$ depends upon the size of the model and upon its temperature excess, it is obvious that the cooling power of a fluid depends upon the circumstances in which it is to be used. Retaining from the above formula only those quantities which relate to the properties of the cooling fluid, we have

$$h \propto k\,(ac/k\nu)^n,$$

Digitized by Google

and for the conditions so far studied $n$ varies from 0 to 1/3, so that the relative cooling power of a fluid may vary between the limits

$$k \text{ and } (ack^2/\nu)^{\frac{1}{4}}.$$

Thus it appears for these conditions that the conductivity of the fluid is the preponderating physical property determining cooling power. This result is probably fairly general, for while it may be possible to devise experimental arrangements in which $k$ does not enter, suitable conditions for its omission seem generally unlikely to be realised, for it evidently enters vitally whenever the temperature of a particle of fluid (and thus the vigour of its motion and the amount of heat it absorbs or yields) depends upon the thermal conductivity of the adjacent layers.

The effect of the physical properties, other than thermal conductivity, appears to be such that high specific heat and high coefficient of expansion have the same degree of importance in facilitating cooling that high viscosity has in restricting it.

I desire to express my thanks to Dr. G. W. C. KAYE and DR. EZER GRIFFITHS for the kind and encouraging way in which the facilities for the present work have been provided, to Mr. W. G. BICKLEY, M.Sc., for critically reading a draft of the theoretical part, and to my wife for assistance with the numerous calculations involved in the reduction of the experimental observations.

Digitized by Google

Digitized by Google

# CONVECTION OF HEAT IN GASES AND LIQUIDS. V.—SOME THERMAL CONDUCTIVITY DATA FOR LIQUIDS

BY

A. H. DAVIS, D.Sc.,
ASSISTANT IN THE PHYSICS DEPARTMENT.

Digitized by Google

## ABSTRACT.

Determinations have been made of the manner in which the thermal conductivity of a number of liquids varies with temperature. The work arose from the fact that the liquids—toluene, carbon tetrachloride, olive oil and aniline—had previously been used in experiments on convective cooling in liquids, and the rate of convective cooling had been found to increase faster than the temperature. In analysing results it had been taken for granted that there was no increase of thermal conductivity with temperature which could contribute appreciably to the effect, but another author deduced that the thermal conductivity of the liquids increased by as much as about 1 per cent. per degree temperature rise. The present determinations, made by means of the GOLDSCHMIDT method over a temperature range of about 20° C. to 75° C., confirmed that the thermal conductivity does not increase with temperature, and the slight variation found was actually a decrease.


Digitized by Google

# CONVECTION OF HEAT IN GASES AND LIQUIDS. V.—SOME THERMAL CONDUCTIVITY DATA FOR LIQUIDS.

By A. H. DAVIS, D.Sc., Assistant in the Physics Department.

[Reprinted, with modified title, from the 'Philosophical Magazine', vol. 47, 1924.]

The author has recently given data* for the cooling of horizontal wires immersed in various liquids, and has correlated them, on the basis of hydrodynamical considerations, with the physical properties of the liquids concerned. In the work it was taken for granted that the thermal conductivities of the liquids were not markedly dependent upon temperature. However, C. W. Rice,† apparently by analysing results for these liquids on the basis of a modification of Langmuir's film theory of convection, has deduced‡ positive temperature coefficients equivalent to about 1 per cent. increase in conductivity per degree temperature rise. Such effects are rather large and are of opposite sign to those the present author had reason to expect. It was desirable, therefore, to carry out direct determinations of thermal conductivity at various temperatures, to supplement the information already given concerning the liquids in question.

Fortunately, apparatus which had been used in the convection experiments was readily adaptable to comparisons of thermal conductivity by the Goldschmidt§ method. and a test was therefore carried out.

## *Apparatus.*

The method consisted in stretching a fine platinum wire along the axis of a narrow horizontal silver tube full of the test liquid, and measuring the electric current necessary to maintain a measured temperature difference between the wire and the walls of the tube. A relative value of the thermal conductivity was thus obtained.

In the actual apparatus the silver tube, 2 mms. diameter and 12·7 cms. long, was fitted tightly into a massive copper cylinder of 5 cm. diameter, so that the temperature was uniform throughout its length. The axial wire was 1 mil (0·002 cm.) in diameter. A shorter length of the same wire, passing through another silver tube in the block, was

* 'N.P.L. Collected Researches', vol. 19, Paper 14, or 'Phil. Mag.', vol. 44, p. 920, 1922.

† 'Phys. Rev.', vol. 21, p. 474, 1923 (abstract).

‡ With regard to the basis of Rice's calculations, it is difficult to see why his equation for film thickness contains the acceleration ($g$) due to gravity, while it omits the volume coefficient of expansion ($a$) of the fluid and the temperature excess of the body. For presumably it is through the vigour of the convection (gravity) currents set up that "$g$" affects the film thickness; and "$a$" is as important as "$g$" in determining these.

§ 'Phys. Zeits.', vol. 12, p. 417, 1911.



Digitized by Google

used for the automatic compensation of any end effects. The whole apparatus was completely immersed in a vessel full of the liquid to be examined, which thus filled the capillary tube. The vessel itself was immersed in a carefully designed water-bath kept well stirred at constant temperature.

Using a Wheatstone bridge arrangement for the necessary resistance measurements, determinations were made of the heat dissipation associated with various small temperature excesses of the wire, ranging from 1° or 2° C. to 10° or 20° C. For moderate heating the results were almost completely independent of the temperature excess, whence it may be inferred that convection currents were inappreciable. The conductivity given later is the value to which results tended as the temperature excess was reduced.

*Results.*

For each liquid, experiments were carried out at two or three temperatures in the range 15° to 80° C. Provided the apparatus was not interfered with mechanically, values for the various temperatures were found to repeat accurately, deviations from the mean curve being generally less than 1 per cent. The relative values of the thermal conductivities of different liquids, however, were not reliable to better than ± 5 per cent., since the constant of the instrument changed within these limits when the apparatus was emptied, cleaned and refilled.

Taking as standard the value given by GOLDSCHMIDT for toluene at air temperatures ($10^4\,k = 3{\cdot}42$) the mean results obtained have been summarised in Table I.

TABLE I.

| Liquid. | Temperature ($t$). | Thermal Conductivity (cals. per cm. per ° C.) ($k$). | Temperature coefficient.† ($\alpha$). |
|---|---|---|---|
| | °C. | | |
| Toluene | 19 | $3{\cdot}4 \times 10^{-4}$ | $-0{\cdot}002$ |
| | 69 | $3{\cdot}1 \times 10^{-4}$ | |
| Carbon tetrachloride | 23 | $2{\cdot}8 \times 10^{-4}$ | $-0{\cdot}003$ |
| | 68 | $2{\cdot}4 \times 10^{-4}$ | |
| Olive oil* | 19 | $4{\cdot}0 \times 10^{-4}$ | $-0{\cdot}000_8$ |
| | 71 | $3{\cdot}85 \times 10^{-4}$ | |
| Aniline | 15 | $4{\cdot}4 \times 10^{-4}$ | $-0{\cdot}000_3$ |
| | 73 | $4{\cdot}35 \times 10^{-4}$ | |

* With olive oil progressive discoloration was noticed as time went on, and the measured values of the thermal conductivity increased from day to day, presumably owing to contamination with copper.

† $k_t = k_0\,(1 + \alpha t)$.

Digitized by Google

It appears that the thermal conductivity does not depend markedly upon the temperature of the liquid, and contrary to the calculations already referred to, the effect is generally a slight decrease as the temperature is raised.

I desire to thank Dr. G. W. C. KAYE for continuing the facilities afforded for the convection work. Mr. R. R. STRAND assisted with the experimental arrangements and observations.

*Note added February*, 1924.

Since this paper was written a more recent contribution by RICE ('J. Amer. Inst. Elec. Eng.', vol. 42, p. 1288, 1923) has been published. His equations have now been modified to include the additional variables referred to above, and in consequence negative temperature coefficients of thermal conductivity have been calculated. These are in better agreement with the experimental values of the present paper.

The new equations, representing the latest development of the film hypothesis, contain all the variables required in a general hydrodynamical theory of convection. Even in a film theory hydrodynamical considerations seem unavoidable, since the size and characteristics of the film need to be explained.

Digitized by Google

Digitized by Google

# CONVECTION OF HEAT IN GASES AND LIQUIDS. VI.—THEORY OF FORCED CONVECTIVE COOLING IN VISCOUS GASES AND LIQUIDS

BY

A. H. DAVIS, D.Sc.,
ASSISTANT IN THE PHYSICS DEPARTMENT.

Digitized by Google

## ABSTRACT.

A theoretical investigation is given of forced convection from a hot body immersed in an infinite stream of viscous fluid. The treatment follows that given by BOUSSINESQ for inviscid fluids. It is assumed that the stream velocity ($v_\infty$ at a distance from the body) is great enough for the effects of natural convection to be neglected. For a family of similar bodies, similarly oriented, having a temperature excess $\theta$ and linear dimensions given by L, it is shown that the mean heat loss $h$ per unit area is given by $hL/k\theta = F(v_\infty Lc/k)$ provided $k/c\nu$ is either equal to unity or is very small. Here $k$, $c$ and $\nu$ refer respectively to the thermal conductivity, the specific heat per unit volume, and the kinematical viscosity of the fluid. The formula should tend to be satisfactory for gases on the one hand and for very viscous liquids on the other, and this has been confirmed by published results for gases and by experiments with viscous liquids, as described in a later paper. If the value of $k/c\nu$ is not restricted we have $hL/k\theta = F\{(v_\infty Lc/k)\,;\ (k/c\nu)\}$.


Digitized by Google

# CONVECTION OF HEAT IN GASES AND LIQUIDS. VI.—THEORY OF FORCED CONVECTIVE COOLING IN VISCOUS GASES AND LIQUIDS.

By A. H. DAVIS, D.Sc., Assistant in the Physics Department.

[Reprinted from the 'Philosophical Magazine', Vol. 44, 1922, as modified and extended by the subsequent note in Vol. 49, 1925.]

In some previous papers* the author has studied the phenomenon of convective cooling, both natural and forced, from the point of view of similitude, and has shown how excellently experimental data for gases agree with a grouping of variables that Boussinesq† deduced by hydrodynamical reasoning for inviscid fluids. The most recent‡ of this series of papers considered for *natural* convective cooling the necessary modifications of Boussinesq's analysis in dealing with the problems of viscous fluids, and the new formula thus obtained was tested experimentally in certain conditions and found to be satisfactory.

The present note develops the theory of *forced* convection in the same way, studying the effect of introducing a viscosity term into Boussinesq's analysis for inviscid fluids.

The problem concerns the cooling of a hot body immersed in an infinite fluid stream maintained at a certain temperature, $\theta$ degrees in excess of that of the fluid at infinite distance to which all temperatures are referred. The fluid stream is rectilinear, and moving with uniform velocity $v_\infty$ at distances from the body sufficiently great. This velocity is supposed to be sufficiently great for the natural convection (gravity) currents set up by the hot body itself to be negligible. We thus neglect the coefficient of expansion of the liquid.

Let $\rho$ and $\nu$ be respectively the density of the fluid and its kinematical viscosity. At a given time $t$, and for an element of the fluid at the point $x, y, z$, let $\tau$, $u, v, w$, P be the temperature excess, the three components of its velocity, and the non-hydrostatic part of its pressure. If $l, m, n$ are three direction-cosines of the general stream of velocity $v_\infty$, we have as boundary conditions:

$$\left.\begin{array}{ll} \text{At infinite distance from the origin} & u, v, w = v_\infty (l, m, n), \quad (\mathrm{P}, \tau) = 0. \\ \text{At the surface of the solid} & (u, v, w) = 0, \quad \tau = \theta \end{array}\right\} \ldots \quad (1)$$

* 'N.P.L. Collected Researches', vol. 19, Papers 11, 13, 12, or 'Phil. Mag.', vol. 40, p. 691, 1920; vol. 41, p. 899, 1921; vol. 43, p. 329, 1922.

† Boussinesq, 'Comptes Rendus', vol. 132, p. 1382; vol. 133, p. 257, 1901.

‡ 'N.P.L. Collected Researches', vol. 19, Paper 14, or 'Phil. Mag.', vol. 44, p. 920, 1922.



Digitized by Google

The hydrodynamical equations of continuity and of motion are

$$\left.\begin{aligned} &\frac{\partial u}{\partial x}+\frac{\partial v}{\partial y}+\frac{\partial w}{\partial z}=0, && \frac{1}{\rho}\frac{\partial \mathrm{P}}{\partial x}=-u'+\nu\nabla^2 u,\\ &\frac{1}{\rho}\frac{\partial \mathrm{P}}{\partial y}=-v'-\nu\nabla^2 v, && \frac{1}{\rho}\frac{\partial \mathrm{P}}{\partial z}=-w'+\nu\nabla^2 w, \end{aligned}\right\} \quad \ldots\ldots (2)$$

$u'$, $v'$ and $w'$ being the accelerations of the fluid parallel to the axes.

Let $k$ be the thermal conductivity of the fluid and $c$ its heat capacity per unit volume, then $\tau'$, the rate of change of temperature for a given particle with respect to time, is given by

$$\tau' = (k/c)\nabla^2\tau \quad \ldots\ldots\ldots\ldots (3)$$

Also we have

$$u', v', w', \tau' = u\frac{\partial(u, v, w, \tau)}{\partial x} + v\frac{\partial(u, v, w, \tau)}{\partial y} + w\frac{\partial(u, v, w, \tau)}{\partial z} + \frac{\partial(u, v, w, \tau)}{\partial t} \quad \ldots\ldots (4)$$

The equations in P, $u$, $v$, $w$ are everywhere quite separate from those in $\theta$, and hydrodynamically the problem is the same as that where $\theta = 0$, the motion of the fluid being determined entirely by the given general stream and the configuration of the immersed body.

Let us endeavour to replace the independent variables $t$, $x$, $y$, $z$ and the functions $\tau$, $u$, $v$, $w$, P by others $t_1$, $\xi$, $\eta$, $\zeta$, T, U, V, W, II respectively proportional to them but whose ratios are chosen to eliminate $\theta$, $k/c$, $\rho$, $\nu$, $v_\infty$.

Let us consider the following substitutions:

$$\left.\begin{aligned} &\xi, \eta, \zeta = (v_\infty c/k)(x, y, z), && (u, v, w) = v_\infty(\mathrm{U}, \mathrm{V}, \mathrm{W}), && \tau = \theta\mathrm{T},\\ &\mathrm{P} = \tfrac{1}{2}\rho v_\infty^2 (c\nu/k)\,\Pi, && t = (k/cv_\infty^2)\,t_1 \end{aligned}\right\} \quad \ldots (5)$$

It is found that these substitutions yield the equations

$$\left.\begin{aligned} &\frac{\partial \mathrm{U}}{\partial\xi}+\frac{\partial \mathrm{V}}{\partial\eta}+\frac{\partial \mathrm{W}}{\partial\zeta}=0, && \mathrm{T}'=\frac{\partial^2\mathrm{T}}{\partial\xi^2}+\frac{\partial^2\mathrm{T}}{\partial\eta^2}+\frac{\partial^2\mathrm{T}}{\partial\zeta^2},\\ &\frac{\partial \Pi}{\partial\xi}=-\left(\frac{k}{c\nu}\right)\mathrm{U}'+\left(\frac{\partial^2\mathrm{U}}{\partial\xi^2}+\frac{\partial^2\mathrm{U}}{\partial\eta^2}+\frac{\partial^2\mathrm{U}}{\partial\zeta^2}\right), && \frac{\partial \Pi}{\partial\eta}=-\left(\frac{k}{c\nu}\right)\mathrm{V}'+\left(\frac{\partial^2\mathrm{V}}{\partial\xi^2}+\frac{\partial^2\mathrm{V}}{\partial\eta^2}+\frac{\partial^2\mathrm{V}}{\partial\zeta^2}\right),\\ &\frac{\partial \Pi}{\partial\zeta}=-\left(\frac{k}{c\nu}\right)\mathrm{W}'+\left(\frac{\partial^2\mathrm{W}}{\partial\xi^2}+\frac{\partial^2\mathrm{W}}{\partial\eta^2}+\frac{\partial^2\mathrm{W}}{\partial\zeta^2}\right), \end{aligned}\right\} \quad (6)$$

where

$$(\mathrm{U}', \mathrm{V}', \mathrm{W}', \mathrm{T}') = \mathrm{U}\frac{\partial(\mathrm{U}, \mathrm{V}, \mathrm{W}, \mathrm{T})}{\partial\xi} + \mathrm{V}\frac{\partial(\mathrm{U}, \mathrm{V}, \mathrm{W}, \mathrm{T})}{\partial\eta} + \mathrm{W}\frac{\partial(\mathrm{U}, \mathrm{V}, \mathrm{W}, \mathrm{T})}{\partial\zeta} + \frac{\partial(\mathrm{U}, \mathrm{V}, \mathrm{W}, \mathrm{T})}{\partial t_1}$$

Digitized by Google

It is seen that the eliminations desired have been effected, except that $k/c\nu$ occurs in certain terms in the equations. For very viscous liquids, however, $k/c\nu$ is very small, and if the terms containing it are neglected, the remaining equations are quite free from the variables it was desired to eliminate. Further, for gases $k/c\nu$ is not a variable but is approximately constant and nearly equal to unity, so for gases the substitutions are satisfactory on this ground.

Considering the matter further for either of the cases for which the eliminations are satisfactory, let us put the equation of the solid in the form

$$f[v_\infty c/k)\,(x, y, z)] = 0. \quad . \quad . \quad . \quad . \quad . \quad . \quad . \quad . \quad . \quad . \quad (7)$$

Thus, if $v_\infty c/k$ changes, this amounts to considering instead of the actual solid, similar bodies having linear dimensions inversely proportional to $v_\infty c/k$. The direction-cosines $l_1$, $m_1$, $n_1$ of the normal will remain the same at corresponding points, and the boundary conditions become :—

$$\left.\begin{aligned} &\text{At the surface,} \quad \mathrm{U} = \mathrm{V} = \mathrm{W} = 0, \qquad \mathrm{T} = 1, \\ &\text{At the distance } \sqrt{\xi^2 + \eta^2 + \zeta^2} \text{ infinite,} \quad \mathrm{U} = l,\ \mathrm{V} = m,\ \mathrm{W} = n. \end{aligned}\right\} \quad . \quad . \quad . \quad . \quad . \quad . \quad (8)$$

The system of equations (6) and (8) determines U, V, W, II, T as functions of $\xi$, $\eta$, $\zeta$, and $t_1$, and substituting in the integrals for the new variables their equivalents, we obtain

$$\frac{\tau}{\theta},\ \frac{u, v, w}{v_\infty},\ \frac{\mathrm{P}}{\rho v_\infty{}^2(c\nu/k)} = \text{definite functions of } [(v_\infty c/k)\,(x, y, z)\,;\ v_\infty{}^2 ct/k]. \quad (9)$$

The flux of heat $h$ furnished in unit time by unit area of such a body, equal to that which the contiguous fluid layer communicates to the interior of the fluid, is given by

$$k\left(l_1\frac{\partial\tau}{\partial x} + m_1\frac{\partial\tau}{\partial y} + n_1\frac{\partial\tau}{\partial z}\right). \quad . \quad . \quad . \quad . \quad . \quad . \quad . \quad . \quad . \quad (10)$$

Introducing the new variables, we have

$$h = (cv_\infty\theta)\left(l_1\frac{\partial\mathrm{T}}{\partial\xi} + m_1\frac{\partial\mathrm{T}}{\partial\eta} + n_1\frac{\partial\mathrm{T}}{\partial\zeta}\right). \quad . \quad . \quad . \quad . \quad . \quad . \quad . \quad (11)$$

At corresponding points of the surfaces $f(\xi, \mu, \zeta) = 0$ limiting the bodies considered, the direction-cosines $l_1$, $m_1$, $n_1$ have the same values, and at corresponding times $t_1$ = const., the derivatives $\dfrac{\partial'\mathrm{T}}{\partial(\xi, \eta, \zeta)}$ at corresponding points have also the same values. Consequently, at corresponding times the trinomial coefficient is a function of the shape and orientation of the bodies only.

Thus, for a family of similar bodies similarly orientated, having linear dimensions L given by

$$\mathrm{L} \propto k/cv_\infty, \text{ i.e. } v_\infty \mathrm{L}c/k = \text{const.}, \quad . \quad . \quad . \quad . \quad . \quad . \quad . \quad . \quad (12)$$



Digitized by Google

the heat loss per unit area at corresponding times from corresponding points is given by

$$h \propto cv_\infty\theta, \quad \ldots\ldots\ldots\ldots\ldots \quad (13)$$

and this will also be true if "$h$" be the mean heat-loss taken at the given instant over the whole surface of the solid.

So for bodies of this shape and orientation we have

$$h = (cv_\infty\theta)\, f\{v_\infty \mathrm{L}c/k\,;\, v_\infty{}^2ct/k\}, \quad \ldots\ldots\ldots \quad (14)$$

which may be written

$$\frac{h\mathrm{L}}{k\theta} = \mathrm{F}\left\{\frac{v_\infty \mathrm{L}c}{k};\, \frac{v_\infty{}^2tc}{k}\right\}. \quad \ldots\ldots\ldots \quad (15)$$

When the conditions have become steady—that is, independent of time $t$,—the formula reduces to

$$\frac{h\mathrm{L}}{k\theta} = \mathrm{F}\left(\frac{v_\infty \mathrm{L}c}{k}\right). \quad \ldots\ldots\ldots \quad (16)$$

And, further, if the conditions do not settle down to complete steadiness, but settle down to periodic fluctuations, then these fluctuations will be similar in form for corresponding cases, and the average value of the heat-loss will be given by (16).

It is desirable to recall two alternative conditions which have been introduced into the proof of the formula. They are that $k/c\nu$ shall be constant or else very small. If these conditions are not satisfied, it may be shown that the formula becomes

$$\frac{h\mathrm{L}}{k\theta} = \mathrm{F}\left(\frac{v_\infty \mathrm{L}c}{k};\, \frac{k}{c\nu}\right), \quad \ldots\ldots\ldots \quad (17)$$

where $k/c\nu$ is expected to be of little importance in the two cases mentioned.

Whether the simpler formula is true for gases on the one hand and for very viscous fluids on the other, and whether $k/c\nu$ is important for intermediate circumstances, is a matter for experimental investigation. It is known that the simpler form is fairly satisfactory for gases, being indistinguishable from the grouping of variables deduced by Boussinesq for inviscid fluids. This is shown graphically in a curve between $h\mathrm{L}/k\theta$ and $v_\infty \mathrm{L}/\nu$, given elsewhere,* for the cooling of wires in a stream of air ($\mathrm{H}/k$ and $vl/\nu$ in the notation of the actual graph). Corresponding data for liquids were not available when this paper was first published, but an isolated result given by Worthington and Malone† for the cooling of a wire in water was in fairly satisfactory accord with the curve mentioned for air. Some further experiments with liquids, however, published later in the following paper, are in good agreement with the considerations set out above. While generally the formula covering the results is of the form (17), it tends to the type (16) for the most viscous liquids used, the heat-loss term tending to vary as $\mathrm{R}(v_\infty \mathrm{L}c/k)^{n\cdot 38}$, where R is a factor representing certain residual effects.‡

* 'N.P.L. Collected Researches', vol. 19, Paper 13, or 'Phil. Mag.', vol. 41, p. 899, 1921. For gases $v_\infty \mathrm{L}/\nu$ and $v_\infty \mathrm{L}c/k$ are practically identical.

† 'J. Franklin Inst.', vol. 184, p. 115, 1917.

‡ This follows since, in the formula of the Abstract of Paper 17, p. 246 of this volume, $m$ and $n$ tend respectively to 0·19 and 0·38.

Digitized by Google

# CONVECTION OF HEAT IN GASES AND LIQUIDS. VII.—EXPERIMENTAL STUDY OF FORCED CONVECTIVE COOLING IN VISCOUS LIQUIDS

BY

A. H. DAVIS, D.Sc.,
ASSISTANT IN THE PHYSICS DEPARTMENT.

Digitized by Google

## ABSTRACT.

Study has been made of the cooling of wires immersed in streams of various liquids. *Theoretical considerations* point to a formula of the type

$$H/k = F(vdc/k;\ k/c\nu),$$

where $H$ = Heat loss per unit time per unit length of the wire per degree temperature elevation,
$k$ = Thermal conductivity of the fluid,
$c$ = Specific heat of the fluid per unit volume,
$\nu$ = Kinematical viscosity of the fluid,
$v$ = Velocity of the fluid stream,
$d$ = Diameter of the wire.

Since $(k/c\nu)$ is practically constant for gases, the present experiments with liquids were undertaken to reveal its importance.

The *apparatus* consisted of a motor-driven whirling arm which carried the test-wire and forced it continually through the liquid contained in an annular circular trough. Observation was made of the temperature of the wire and of the electric energy necessary to maintain a measured temperature difference between the wire and the general body of the liquid. Wires of three sizes were used, and various *liquids* whose physical constants were measured.

The *results* show that the above formula is fairly satisfactory, except that a factor must be included to cover certain small residual effects dependent upon $d$ (and possibly upon $\theta$) and due to some cause, possibly free convection, not fully investigated. It was found that the function F could not be represented by the product of two independent terms in $vdc/k$ and $k/c\nu$ respectively, but that each influences to some extent the effect of the other. The following form was found to be satisfactory :—

$$H/k = R\,.f(k/c\nu).\,F\{(vdc/k) \times (k/c\nu)^{\frac{1}{2}}\},$$

where R represents the residual factors referred to. Curves are given showing the forms of the two functions. If they are represented by power terms thus, $f(x) = x^{-m}$ and $F(x) = x^n$, $m$ and $n$ vary with circumstances but lie within the limits given by $0 < m < 0{\cdot}19$ and $0{\cdot}48 > n > 0{\cdot}38$. For very viscous liquids $m$ tends to $0{\cdot}19$ and $n$ to $0{\cdot}38$, so that $H/k$ then varies as $R\ (vdc/k)^{0{\cdot}38}$.

Concise tables present the experimental results. An estimate was made of the *velocity of the natural convection current* set up by the heated wire.


Digitized by Google

# CONVECTION OF HEAT IN GASES AND LIQUIDS. VII.—EXPERIMENTAL STUDY OF FORCED CONVECTIVE COOLING IN VISCOUS LIQUIDS.

By A. H. DAVIS, D.Sc., Assistant in the Physics Department.

[Reprinted, with modified title, from the 'Philosophical Magazine', Vol. 47, 1924.]

## Introduction.

The subject of the cooling of the surface of a hot body in contact with a moving fluid has received considerable investigation during recent years. For various reasons, diverse experimental methods have been used. Measurements have been made on the one hand of the heat which passes from the walls of a hot tube to the fluid flowing within it, and on the other of the cooling of wires and cylinders when immersed transversely in a fluid stream. In neither case does published information appear sufficient for determining the effect of the nature of cooling liquids: indeed, for the wire method, while air-cooling has been extensively studied, few other data are available at all.

Until liquids have received adequate attention, the laws of convection cannot be fully revealed. For convection of heat is ultimately a molecular phenomenon, which presents complexities in the case of liquids which are almost entirely absent when the gaseous state is considered.

A study has therefore been made of the cooling of wires when immersed in streams of various liquids of known physical properties.

## I. Theoretical Formulæ.

Osborne Reynolds,* from the similarity of molecular motions involved in conduction of heat and diffusion of momentum (skin friction) indicated a relation between surface cooling and skin friction. His theory has received much attention in connection with the turbulent flow in pipes. As Reynolds himself pointed out, its simplest form requires supplementing by an additional factor relating to the transfer of heat through the eddy-free layer near the surface of the tube. G. I. Taylor† has recently calculated this correction from an estimate of the thickness of the film. He made use of the Lorentz criterion for steady fluid motion between two parallel planes moving tangentially to each other. His correction depends upon the ratio of the rates of diffusion of heat and of momentum in the fluid.‡

* 'Proc. Manchester Lit. and Phil. Soc.', 1874. See also Stanton, 'Report Adv. Comm. Aeronautics', p. 45, 1912–13.

† 'Report Adv. Comm. Aeronautics', p. 423, 1916–17.

‡ That is, upon the variable $k/c\nu$ referred to later in this paper.

Digitized by Google

BOUSSINESQ* was the first to give a formal theory of convection, and his analysis combined hydrodynamical equations with the FOURIER equation for heat-flow. With certain assumptions he obtained, for similar bodies similarly immersed in infinite inviscid streams, a general solution which may be written in the form :

$$hl/k\theta = \mathrm{F}(vlc/k), \quad . \quad . \quad . \quad . \quad . \quad . \quad . \quad . \quad . \quad . \quad (1)$$

where

$h$ = heat loss per second per unit area of the hot body,

$l$ = linear dimensions of the body,

$\theta$ = temperature difference between the surface of the hot body and the distant fluid,

$v$ = velocity of the fluid stream,

$k$ = conductivity of the fluid,

$c$ = capacity for heat of the fluid per unit volume.

For horizontal wires of diameter "$d$", transverse to the fluid stream, and of a length sufficient to render the effects of the ends negligible, the above equation may be written

$$\mathrm{H}/k = \mathrm{F}(vdc/k), \quad . \quad . \quad . \quad . \quad . \quad . \quad . \quad . \quad . \quad . \quad (1a)$$

where H = heat-loss per unit time per unit length of the wire per degree temperature excess.

For the case of such thin wires, and for non-turbulent flow, BOUSSINESQ showed the form of the function to be given by a square-root law.† KING,‡ following him, calculated the form

$$\mathrm{H}/k = 1 + (2\pi)^{\frac{1}{2}}(vdc/k)^{\frac{1}{2}} = 1 + 2{\cdot}51\,(vdc/k)^{\frac{1}{2}} \quad . \quad . \quad . \quad . \quad . \quad . \quad (2)$$

for velocities above a (small) critical value. He assumed constant flux of heat across the surface of the wire.

RAYLEIGH,§ in illustration of the use of the Principle of Similitude, derived an extension of the general formula to include viscous fluids. The result may be written‖ :—

$$hl/k\theta = \mathrm{F}(vlc/k\,;\ k/c\nu) \quad \text{or} \quad \mathrm{H}/k = \mathrm{F}(vdc/k\,;\ k/c\nu). \quad . \quad . \quad . \quad . \quad (3)$$

* 'Comptes Rendus', vol. 132, p. 1382, 1901 ; vol. 133, p. 257, 1901.

† BOUSSINESQ, 'Théorie analytique de la Chaleur', vol. 2, 1903. See also RUSSELL, 'Phil. Mag.', vol. 20, p. 591, 1910, where exhaustive references are given.

‡ 'Phil. Trans', A, vol. 214, p. 373, 1914.

§ 'Nature', vol. 95, p. 66, 1915.

‖ This formula may equally well be written $hl/k\theta = \mathrm{F}\{vl/\nu\,;\ k/c\nu\}$. In this form the relation to fluid-resistance formulæ is emphasised. The mechanical resistance R per unit area is given by $\mathrm{R}/\rho v^2 = f(vl/\nu)$. Thus heat-loss and mechanical resistance are closely related, provided allowance is made for complexity of fluid structure by means of a $k/c\nu$ term.

Digitized by Google

NUSSELT* in 1909 had already applied the principle to the problem of heat transfer in tubes, and had obtained a result of the same form. By a further assumption, he reduced his result to BOUSSINESQ's form (equation 1).

Equation (3) forms the basis of the present work, where the effect of the $k/c\nu$ term has been studied. An earlier paper† showed how the expression follows from BOUSSINESQ's method of analysis when a viscosity term is introduced.

## II. EXPERIMENTAL.

### 1. *Introduction.*

Many experiments have been carried out on the heat-transmission to fluids flowing through hot pipes. Comparison with theory is not straightforward, since a certain length of leading-in pipe must be traversed before velocity conditions attain their final distribution.‡ LEPRINCE-RINGUET§ made a study of experiments by many observers (NUSSELT, JORDAN, STANTON, CARCANAGUES, SER, PENNSYLVANIA RRD, and HENRY) and obtained a formula covering all results for air. However, no formula of NUSSELT's simple type would include known values for other fluids, such as certain common gases, steam, and water. STANTON‖ found REYNOLD'S formula to be satisfactory in certain respects, but to need correction presumably for the heat transfer through the eddy-free surface layer. The correction term evaluated by G. I. TAYLOR is a function of $k/c\nu$ and appears promising¶, but apparently more experimental data are required.**

MCADAMS and FROST,†† in a survey of certain experiments on heat transfer in pipes, give a curve covering water and certain oils, in which the heat-loss ($hl/k\theta$) is a function of the hydrodynamical variable ($vl/\nu$). Though the range of viscosity covered appears to be small (about three-fold), this indicates that any other terms in the complete equation are of rather subsidiary importance.

Generally speaking, therefore, experiments with tubes appear to indicate that the complete formula for heat loss contains a $k/c\nu$ term. The omission of this term yields simpler formulæ, which give results which are generally of the right order but which may differ quite appreciably from measured values.

* 'Zeits. Ver. Deutsch. Ing.', vol. 53, pp. 1750, 1808, 1909.

† DAVIS, 'N.P.L. Collected Researches', vol. 19, Paper 14, or 'Phil. Mag.', vol. 44, p. 940, 1922.

‡ See STANTON, 'Report Adv. Comm. Aeronautics', vol. 8, p. 16, 1916–17.

§ 'Comptes Rendus', vol. 152, p. 436, 1911.

‖ 'Report Adv. Comm. Aeronautics', p. 45, 1912–13. See also 'Phil. Trans.', A, vol. 190, p. 67, 1897.

¶ TAYLOR, 'Report Adv. Comm. Aeronautics', p. 423, 1916–17.

** STANTON, 'Report Adv. Comm. Aeronautics', p. 16, 1916–17. See also PANNELL, p. 22 of the same Report.

†† 'J. Ind. Eng. Chem.', vol. 14, p. 1101, 1922.



Digitized by Google

As regards the heat losses from wires and cylinders in a stream of fluid, KING* has made a very comprehensive study of the cooling of fine wires in air, covering a wide range of conditions. He found his results agreed excellently with a formula very similar to his own theoretical equation. A small correction term was necessary, depending upon the temperature excess $\theta$ of the wire; this he supposed to be due to variations in the physical properties of air as the temperature is changed. He found also that the dependence upon the diameter of the wire was rather *greater* than the theoretical formula suggested. His paper contains reference to similar work by other experimenters.

HUGHES† experimented with large steam-heated cylinders up to 5 cm. diameter. His data do not fit KING's special formula, as the variation with velocity ($v^{0\cdot55}$ to $v^{0\cdot7}$) is in excess of that given by a square-root law. However, the more general form of equation (1) appears satisfactory, except that variation with diameter in this case tends to be less than the formula requires. It is noteworthy that this deviation from the formula is in the opposite sense to that found by KING for his wires.

The range of published data is further extended by the results of KENNELLY and SANBORN,‡ who used air at various pressures. Some earlier results by KENNELLY§ cover some of the range later studied by KING, but include additional data for a larger wire.

The present author|| has given a graph upon which results of these experimenters have been plotted, and it appears that equation (1*a*) is fairly satisfactory, viz. :—

$$H/k = F(vdc/k). \quad . \quad . \quad . \quad . \quad . \quad . \quad . \quad . \quad . \quad . \quad . \quad (4)$$

However, since $k/c\nu$ is practically a constant for gases, such experiments cannot reveal the effect of this term. Practically no values are available for liquids, and the need of the present investigation is thus clear.

## 2. *Choice of Method.*

The following general considerations led to the choice of the present method of investigating the cooling powers of streams of liquids. By using wires as the hot bodies size was easily altered, and by adopting electrical heating, measurements of temperature and heat-loss were readily made. By moving the wire through the liquid instead of the liquid past the wire, complications were avoided due to non-uniform flow in tubes and troughs, for in these the flow is greatest in the centre and is not steady until considerable lengths have been traversed. An annular circular track was used; it has various advantages. Since some general circulation of the liquid was, of course, set up, the velocity distribution

* 'Phil. Trans.', A, vol. 214, p. 373, 1914.

† 'Phil. Mag.', vol. 31, p. 118, 1916.

‡ 'Proc. Amer. Phil. Soc.', vol. 53, p. 55, 1914.

§ 'Trans. Amer. Inst. Elec. Eng.', vol. 28, part 1, p. 363, 1909.

|| DAVIS, 'N.P.L. Collected Researches', vol. 19, Paper 13, or 'Phil. Mag.', vol. 41, p. 899, 1921.

Digitized by Google

question was not entirely eliminated, but was only of secondary importance, as it only affected a correction term which had to be applied to the observed speed of the wire.

### 3. *Apparatus.*

The apparatus used consisted of a motor-driven whirling arm which, by suitable attachments, carried the test wire in a vertical position and forced it continually through the liquid contained in the annular circular trough. Observation was made of the velocity of the wire and of the electric energy necessary to maintain a measured temperature difference between the wire and the general body of the liquid. The energy dissipation was determined from the observed current through the wire, and from its resistance as obtained by means of a Kelvin double bridge. This resistance gave also the temperature of the wire.

(i) *The Whirling Arm and the Trough.*—The general arrangement of the apparatus is shown in Fig. 1.

A balanced whirling arm was driven through a worm and wheel (ratio 100 : 1) by means of a 1/10 horse-power electric motor, fitted with ball bearings. The motor was

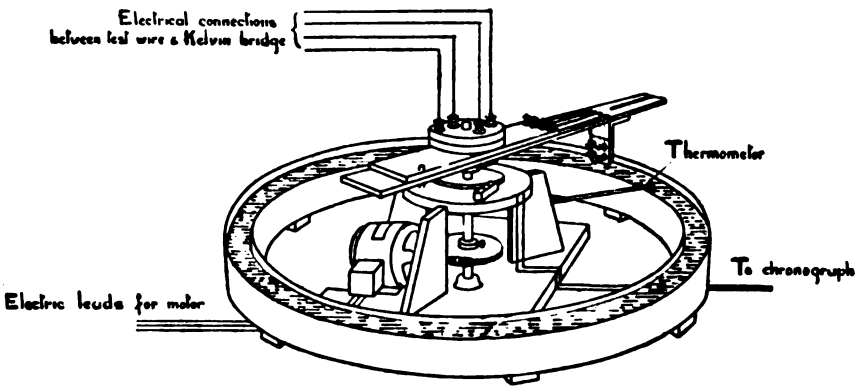


Fig. 1. The Whirling Arm and the Trough.

shunt-wound, and the speed was controlled by means of a series resistance in the armature circuit. To avoid communication of vibration to the rotating arm, the motor was separately screwed down to the concrete floor. Considerable care was taken to ensure uniformity of motion, even at low speeds, throughout a complete revolution of the whirling arm. The motor was driven by means of a storage battery. The rotating arm was fitted with a friction brake to reduce to a minimum the effect of any frictional variations in the bearings. (A thrust ball-bearing took the weight of the rotating arm.) The shaft was accurately vertical, so that the rotating arm had no lowest position at which it would tend to stop during a revolution even if the balance were not exact. A spirit-level, used on the arm at rest, at various positions of revolution, was useful in this connection. All woodwork was painted or varnished to avoid defective alignment arising from warping.



Digitized by Google

The annular circular trough was made from sheet brass (0·16 cm. thick), and was supported separately from the concrete floor to avoid vibrations and ripples. Porcelain supports afforded thorough electrical insulation. The cross-section of the trough was 7 cms. wide and 11 cms. deep. The test wire moved centrally in the trough, the circumference of the circular path being 242 cms. No serious difficulty was experienced on account of any variation in the width of the trough at different parts of the circumference. Some slight imperfection in this respect merely caused the galvanometer-spot to wander slightly from side to side during a revolution of the arm, instead of remaining exactly at zero all the time. Measurements of the general swirl of liquid in the centre of the trough were made at various points of the circumference, but no serious divergences from the mean were observed.

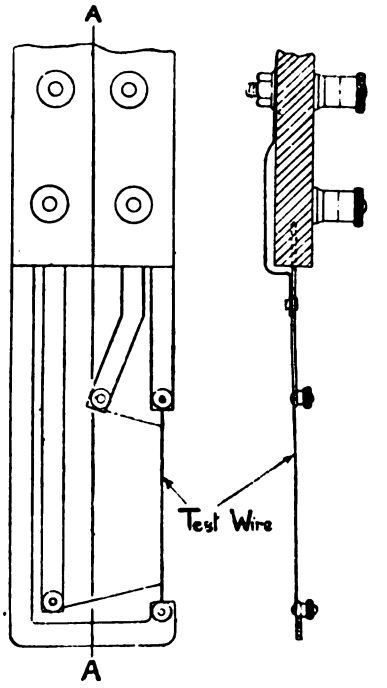

Fig. 2. The Wire Holder.

During the motion of the rotating arm the surface of the liquid was disturbed by the passage of the wire, but the effect was soon damped out and the surface was smooth again before the arm re-passed the same point on its next revolution. The wave behind the arm was especially pronounced for water, but even then, except at highest speeds (about 55 cms. per sec.), the disturbance did not persist for the time taken by the arm in a complete revolution.

Undoubtedly the use of an annular trough rather than a simple circular bath tended to reduce the amount of swirl set up as well as the persistence of these surface-disturbances.

(ii) *The Wire Holder.*—Details of the holder used for the test wire are shown in Fig. 2. It was made from brass strip ($\frac{1}{4}$ in. by $\frac{1}{16}$ in.), together with suitable terminals and an ebonite support. The holder was sufficiently springy to keep the wire gently taut when adjusted to proper length between the terminals. Provision was made for potential and current leads. The strip moved edge-first through the liquid, and the section thus presented was found to be sufficiently stream-line in shape to be satisfactory for the velocities used.

It will be seen from the figure that the two long supporting strips were placed an inch or so behind the test wire. It appears that at the side or in front they would have been more likely to interfere with the stream past the wire. Visual observation of the motion through liquids confirmed the opinion that, upstream, the effects of the strip were limited to only a few millimetres. The arrangement adopted had the additional advantage that the whole of the immersed parts were moving centrally in the trough, so that the velocity distribution in the fluid was simpler, the trough could be made narrower, and economy was thus effected in the quantity of liquid used.

Digitized by Google

(iii) *Electrical Measurements.*—With regard to the electrical measurements, a dual arrangement was fitted up so that two methods could be used. In one a specially-constructed Kelvin bridge was used, and for the other a calibrated potentiometer was available with suitable standard resistances. On account of its greater convenience, the Kelvin-bridge method was almost invariably adopted for each series of observations; but the potentiometer was permanently installed so as to be readily available for checking the bridge, the resistances of its slide wire and coils, and the accuracy of the ammeter. However, for paraffin and for air, a series of potentiometer observations of heat-loss were made, and they agreed satisfactorily with those obtained by means of the Kelvin bridge.

(iv) *The Resistance Bridge.*—Fig. 3 is a diagram of the connections of the Kelvin bridge. The arm X represents the platinum wire under test, which was compared with the variable

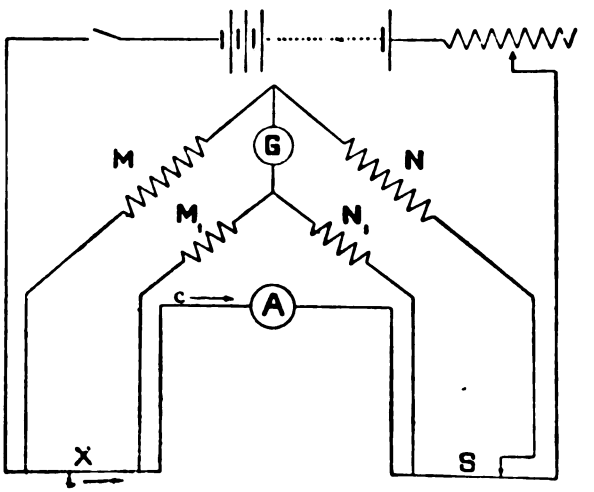


Fig. 3. The Kelvin Bridge Connections.

standard resistance S. This standard consisted of a number of 0·05-ohm coils of heavy manganin wire (S.W.G. 11), together with a 0·1-ohm slide wire 160 cms. long. It had been carefully calibrated by a potentiometer method to read to one ten-thousandth part of an ohm. The ratio arms M, N, $M_1$, and $N_1$ contained accurately adjusted coils of 100 ohms each, together with leads which, although they were of small resistance ($\frac{1}{2}$ ohm), had also been adjusted to sufficient equality (1 per cent.) to avoid appreciable errors which otherwise might have been introduced.

To provide electrical connections to the wire X on the rotating arm, slip rings were utilised, similar to those described by KING,* consisting of stationary copper rings dipping into rotating mercury troughs. The resistance introduced into each arm by the slip-ring apparatus was less than 0·003 ohm, and it remained constant to less than 0·0001 ohm, whether the arm was rotating or still.

* 'Phil. Trans.', A, vol. 214, p. 373, 1974.

Digitized by Google

The ammeter A was a Weston Laboratory Standard instrument. The galvanometer G was a reflecting instrument of the moving-coil type, very free from troublesome zero drift. Its sensitivity was such that 1 microampère gave a deflection of 50 millimetres on a scale at a distance of 1 metre from the galvanometer. The full sensitivity was required only when the initial resistance of the cold wire was determined, and it was suitably reduced when the heating currents were used.

When the bridge was balanced the various resistances satisfied the following formula :—

$$X = \frac{M}{N}S + \frac{AN_1}{A + M_1 + N_1}\left(\frac{M}{N} - \frac{M_1}{N_1}\right). \quad . \quad . \quad . \quad . \quad . \quad . \quad . \quad (5)$$

The current $c$ measured by the ammeter was not exactly the same as that $i$ through the test wire. Strictly a correction was necessary according to the equation

$$i = c\left(1 + \frac{A}{M_1 + N_1}\right); \quad . \quad . \quad . \quad . \quad . \quad . \quad . \quad . \quad . \quad . \quad (6)$$

but A was usually so small that the correction was negligible.

With the bridge out of balance by an amount $dX$ in the test wire, the galvanometer current ($g$) was given approximately by the formula

$$g\left\{2 + G\left(\frac{1}{M} + \frac{1}{N}\right)\right\} = \frac{cdX}{M}. \quad . \quad . \quad . \quad . \quad . \quad . \quad . \quad . \quad (7)$$

(v) *Precautions and Adjustments.*—At the outset the apparatus was well insulated. It was tested by means of an Evershed " Megger " insulation tester, and also by observing whether the galvanometer remained at its true zero when only one pole of the battery was connected to the apparatus.

Thermoelectric effects were practically negligible. The connections of the platinum test wire were all immersed in the liquid in the trough, and were thus at constant temperature. The rest of the bridge connections were of copper or manganin, and these metals together exhibit little thermoelectric activity. Some slight effects were found on one or two occasions, but they were only appreciable when getting the original balance with a small current : they were eliminated by the familiar device of working with the galvanometer circuit always closed, and adjusting the bridge so that no deflection occurred when the battery was reversed. Reversals with the large currents showed no change of balance conditions.

To keep the current as steady as possible the source of supply was a 110-volt storage battery in series with a ballast resistance.

The complete ratio arms M and N, consisting of coils and leads, were accurately adjusted to equality in the following manner :—The coils themselves were tested for equality by reversal of connections, and found to be satisfactory. The potential leads from the coils, which are also in the ratio arms, were brought to equality by adjusting so that the balance of the bridge was not appreciably disturbed if the coils were short-circuited by

Digitized by Google

plug contacts, thus leaving the leads themselves as the complete outer ratios of the bridge. The inner ratio arms were then similarly treated. This procedure ensured that the ratios M/N and $M_1/N_1$ were accurately equal to unity, and so resulted in the simple relation X = S, independent of the intermediate resistance A. It was experimentally verified that increasing A sixfold (from 0·2 ohm to 1·2 ohm) did not affect the reading by more than 1 part in 3,000 (see equation 5). It was easy to make adjustment of this accuracy whenever the test wire was changed, and the apparatus was frequently checked in this and in other ways during use.

As an overall test of the bridge, a standard 0·1 ohm coil was substituted for the test wire. The Kelvin bridge indicated the correct resistance for this, and the reading was the same for large currents (5 amps.) and for very small ones (0·07 amp.); was independent of whether the arm was rotating or not; was not influenced by the speed; and was also independent of the direction of the current employed. This is a stringent test of the suitability of the bridge and slip rings for the currents involved, and of freedom from errors due to leakage or thermoelectricity.

It remained only to substitute the actual test wire and holder for the standard 0·1 ohm coil, and to test for the absence of thermal effects and leaks by observing the behaviour of the galvanometer spot on reversal of the various currents and upon switching off completely.

(vi) *Procedure during an Experiment.*—To obtain a series of observations the usual procedure was as follows:—With the test wire in position, and with a small current through the wire (0·07 amp.), the bridge was balanced by adjustment of the position of the slider along the slide wire. As the heating effect of such a small current was negligible,* this reading gave the resistance of the wire at the temperature of the oil.

The slider position was then altered to increase the reading by a definite amount $dR$. This disturbed the balance of the bridge. With the arm rotating at measured speed, note was made of the increased current through the wire necessary to restore the balance. From the constants of the test wire the increment of temperature associated with the resistance $dR$ was known, and the heat-loss from the wire at this speed was readily calculated.

This procedure was repeated with the same value of $dR$, but with several different speeds. Further series were then taken, until a range of values of temperature excess and velocity had been obtained.

During a series of experiments, the initial temperature of the liquid sometimes drifted slightly. This was allowed for by slight change in the initial slider position, so that $dR$ was maintained constant throughout, and the drawing of a series of curves was facilitated.

It was important to remove stray suspended fluff from the liquid under test, for otherwise readings could not be taken owing to a pronounced drift of the galvanometer reading. It was astonishing how much fine fibrous material could gain entrance to the

* It was satisfactory to find the balance independent of whether the wire was moving or not.

Digitized by Google

liquid, and equally remarkable that the galvanometer spot could indicate so readily when a single fibre, almost invisible, became attached to the moving wire. Consequently all liquids used were passed through filter-paper two or three times, and collected in large clean glass vessels. Before each filling, the experimental trough was very carefully cleaned with suitable agents and swilled out with petrol. A blowpipe-flame was then passed rapidly over the interior to burn off any adherent fibres, and the trough was again washed out, first with filtered petrol and finally with a small quantity of the liquid to be tested. Except when experiments were actually in progress, the trough was kept covered, and at all times unnecessary disturbance of the air of the room was avoided.

Even with these precautions fluff was not completely eliminated, but the trouble was not serious. Consistent results were obtained by cleaning the test wire gently with another wire just before taking readings, after a preliminary run had shown the probable values. Half a minute or more was required in taking a final reading, largely because the steady swirl of liquid could not be attained in less time. At times conditions were obtained which were practically steady (water, for instance), but at others there was sufficient suspended material to give a slight drift. For instance, on one occasion with No. 1 oil and the 6-mil wire there was a drift equivalent to about a $\frac{1}{2}$ per cent. change in heat-loss in one minute, and no further change in the next two minutes. Repeated experiments on this occasion indicated that results for all temperatures of the wire were certainly reproducible to within $\pm 2$ per cent., and usually variations were of the order of $\pm 1$ per cent. or less. If the difficulties increased appreciably, refiltering was resorted to and an improvement thus effected.

(vii) *Measurement of Velocity.*—No difficulty was experienced in determining the velocity of the rotating arm. The periods for one revolution varied from 3 seconds to 25 seconds. An electrical buzzer recorded each revolution, and it was usually sufficient to time with a stop-watch a convenient number of revolutions. A chronograph arrangement connected to a standard clock was available, but was not necessary for general use. A stroboscopic arrangement could have been used for observing the constancy of the actual speed of the motor during a complete revolution of the arm, but was not required, the galvanometer spot being sufficient indication of the state of affairs.

To obtain the velocity of the wire relative to the liquid, it was necessary not only to measure the velocity of the rotating arm, but also to evaluate the correction for the general circulation of the fluid through which the wire moved.

To measure the swirl velocity the test wire was removed from the rotating arm and mounted vertically in a fixed position in the centre of the trough, so that a dummy wire attached to the rotating arm passed within a millimetre or so from it. Heat-losses from the wire in this position were measured with the arm rotating at various speeds, and compared with the losses experienced when it was mounted upon the rotating arm itself. The method of deducing the swirl velocity from the results is as given below.

For a given temperature excess, whether the wire is mounted on the rotating arm or is

Digitized by Google

fixed in the centre of the trough, the heat emitted from it depends only upon the motion of the wire relative to the stream of liquid.

If $V_a$ is the velocity of the wire attached to the moving arm, and if $V_s$ is the velocity of the swirl of liquid set up, the velocity V of the wire relative to the fluid is given by $V = V_a - V_s$.

If the swirl velocity is proportional to the arm velocity causing it, then the relative velocity also will be proportional to $V_a$ and we may write $V_r = kV_a$.

If now we find (from graphs) the new arm velocity $V_{a_1}$, with which the moving wire must move to give the same heat loss as was experienced by the swirl wire, we have $V_s = kV_{a_1}$. Hence the correction factor $k$ may be calculated, and we find $k = V_a/(V_a + V_{a_1})$.

Results obtained are given in Table I, together with check values obtained by another method. The wire data indicate that $k$ is practically constant for a given liquid, and that the mean relative velocity was between 82 per cent. and 88 per cent. of the measured arm velocity. The velocity distribution near the centre of the trough was also found to be fairly uniform, and it did not vary appreciably in different parts of the circumference. In the experiments, conditions were fairly steady except at the moment when the rotating arm passed the swirl wire; precautions were taken to break the galvanometer circuit momentarily as this took place, and the swirl values obtained refer to the general circulation in the centre of the trough.

TABLE I.—Swirl Velocity of Fluid expressed as Percentage of the Measured Wire Velocity.

| Liquid. | Method. | Swirl velocity. For values of arm velocity (cms. per sec.). 10. | 20. | 50. | 70. | Mean value taken. |
|---|---|---|---|---|---|---|
| | | per cent. | per cent. | per cent. | per cent. | per cent. |
| Water ... ... | Wire ... ... | ... | ... | 18 | 18* | 18 |
| | Speck ... ... | 14 | 17 | 21 | 21* | |
| Paraffin ... | Wire ... ... | ... | ... | 16 | 16 | 16 |
| | Speck ... ... | 20 | 20 | 19 | 17 | |
| Oil, No. 1 ... | Wire ... ... | ... | ... | 15 | 17 | 17 |
| | Speck ... ... | 17 | 17 | 17 | 18 | |
| Oil No. 2 ... | Wire ... ... | ... | ... | 15 | 15 | 15 |
| | Speck ... ... | 10 | 14 | 19 | 19 | |
| Oil No. 3 ... | Wire ... ... | ... | ... | 12 | 12 | 12 |
| | Speck ... ... | 10 | 11 | 15 | 16 | |

* For these speeds the surface waves had not subsided before the wire came round again.

The method adopted as a check on the wire method was not so convenient, but it revealed visually the nature of the flow. The arm was set rotating in the usual way,



Digitized by Google

and when the circulation of liquid in the trough was steady, observation was made of the motion of a speck of floating or suspended dust. For some cases tobacco ash was found to be very convenient. The swirl velocity measured was the general drift. The timing of the speck was commenced sufficiently long after the passage of the test wire for the flow to be normal, and was completed just before the returning wire brought the local disturbances round again. Simultaneous observation of floating specks and suspended particles confirmed that there was a central core of liquid $\frac{1}{2}$ inch to $\frac{3}{4}$ inch wide, through which the test wire was moving, where the velocity was practically uniform and independent of depth.

The agreement between these check values and those obtained by the wire method was quite good, as may be seen from Table I, though generally the speck method gives higher results. It will be seen that generally the mean value taken is that given by the wire, although some attention has been paid to the other results. Divergences from the mean are not very systematic, and appear to have an effect on the true velocity of the order of $\pm 2$ per cent.

(viii) *Velocity of the Natural Convection Current from the Wire.*—Experiments were carried out to ascertain to what extent the natural convection current from the heated wire was comparable with the velocity of the wire relative to the liquid.

The principle of the method of measuring the velocity of the natural convection current is simple, and is illustrated in Fig. 4. The heated wire was mounted vertically at a position

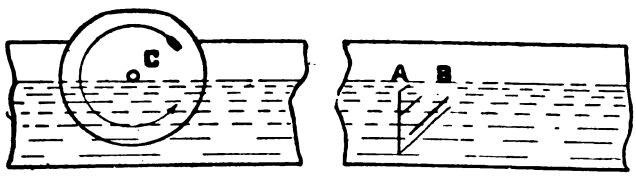


Fig. 4. Arrangements for determining the Velocity of the Natural Convection Streams from the Hot Wire A.

A in the trough. A steady circulation of liquid past the wire was maintained by means of the paddle-wheel C, placed as far away as possible. Convection currents from the wire could then be observed as apparently straight filaments adherent to the wire and trailing behind it at an angle to the vertical depending upon the velocity of the liquid in the trough. Observation was made of the stream velocity at which the filaments were inclined to the vertical at an angle of 45°. In this case, heated particles of liquid were moving so that the vertical component of velocity, due to natural convection, was equal to the horizontal component, which was known from the observed liquid speed.

Errors of refraction in the estimation of the angle of 45° were avoided as follows:—A separate piece of wire B was suitably attached to the apparatus, so that it was immersed in the liquid and extended upwards behind the heated wire at this required angle. Speed adjustments were made until the fluid filaments were parallel to it.

Digitized by Google

These apparent filaments were of course due to the altered refractive index of the liquid which had been heated by the wire. No difficulty was experienced in seeing them with some of the oils. However, with water practically nothing could be detected; so in such cases a speck of soluble dye was attached to the wire at one point. It was quite easy to attach such a speck when desired, introducing it on the end of another piece of wire.

Only the order of the effect was desired, so elaborate arrangements were not adopted. However, by using a transparent trough with plane sides, photographs could be taken and greater precision attained. The results might be of some interest apart from their present application.

The velocities of the natural convection current were measured for water, No. 2 oil, and paraffin. They were more or less proportional to the temperature excess of the wire, and were respectively 0·01, 0·006, and 0·02 cm. per sec. per degree temperature excess of the wire.

The maximum temperature excess used in the main experiments was about 70° C., whence natural convection streams of the order of $\frac{1}{2}$ to $1\frac{1}{2}$ cm. per sec. are to be expected. These should cause but little error in estimating the velocity of the fluid relative to the wire, for being vector quantities directed at right angles to the motion of the wire, they would only increase the slowest speed (10 cms. per sec.) by about 1 per cent. At higher speeds the effect should be quite negligible.

### 4. *The Liquids used.*

(i) *Their Nature and Condition.*—The cooling power of five liquids was studied. These were distilled water, paraffin, and three transformer oils, of which the most viscous resembled olive oil at 15° C. and became practically solid at 8° to 10° C. Thus a wide range of viscosity (and of $k/c\nu$) was covered, and the fluids had the advantage of being of kinds frequently used for cooling purposes. Transformer oils are very carefully refined products. Special care had been taken to ensure that they were dry, clean, and unmixed with other oils or samples, and in a condition satisfying the stringent requirements of their normal use.

Reference has already been made to the care taken to remove fibres of fluff and suspended particles. It was also observed that innumerable bubbles filled the oils when they were freshly poured into a vessel. These would have caused errors in some of the tests, so the liquids were poured carefully and time was allowed for the bubbles to disappear. This delay also allowed the temperature to settle down.

(ii) *Physical Properties of Liquids used.*—The following outlines the various methods used in measuring for these liquids the physical properties concerned in convective cooling. The results obtained are given in Table II.

(*a*)* *Density* ($\rho$).—Determinations of density were made at temperatures of about

* Mr. A. R. Challoner assisted with these observations.



Digitized by Google

15° C., 50° C., and 80° C., an ordinary specific gravity bottle being used. Values for water were taken from tables.

The coefficients of expansion, of importance in natural convection, may be deduced from these results.

TABLE II.—Physical Constants of Liquids used.

| Liquid. | Temp. ° C. | $\rho$. | $10^4 k$. | $\eta$. | $\nu$. | $s\eta/k = c\nu/k$. | $s$. | $c$. |
|---|---|---|---|---|---|---|---|---|
| Water | 12 | 1·00 | 14·0 | 0·0124 | 0·0124 | 8·86 | 1 | 1·00 |
| | 15 | 1·00 | 14·0 | 0·0114 | 0·0114 | 8·15 | | 1·00 |
| | 20 | 0·998 | 14·0 | 0·0101 | 0·0101 | 7·2 | | 1·00 |
| | 40 | 0·992 | 14·7 | 0·0066 | 0·0066 | 4·48 | | 1·00 |
| | 50 | 0·988 | 15·0 | 0·0055 | 0·0056 | 3·67 | | 0·99 |
| | 75 | 0·975 | ... | 0·0038 | 0·0039 | ... | | 0·98 |
| | 80 | 0·972 | ... | 0·0036 | 0·0037 | ... | | 0·97 |
| Paraffin | 12 | 0·814 | 3·0 | 0·0220 | 0·0270 | 38·1 | 0·52 | 0·42 |
| | 15 | 0·812 | 3·0 | 0·0208 | 0·0256 | 36·0 | | 0·42 |
| | 20 | 0·809 | 3·0 | 0·0189 | 0·0234 | 32·6 | | 0·42 |
| | 50 | 0·787 | 2·8 | 0·0110 | 0·0140 | 20·4 | | 0·41 |
| | 60 | 0·780 | 2·7 | 0·0096 | 0·0121 | 18·5 | | 0·41 |
| | 75 | 0·769 | 2·6 | 0·0078 | 0·0101 | 15·6 | | 0·40 |
| | 80 | 0·765 | ... | 0·0075 | 0·0096 | ... | | 0·40 |
| Transformer Oil No. 1 | 15 | 0·844 | 3·2 | 0·140 | 0·166 | 205 | 0·47 | 0·40 |
| | 20 | 0·841 | 3·2 | 0·116 | 0·138 | 170 | | 0·40 |
| | 50 | 0·821 | 3·1 | 0·046 | 0·056 | 70 | | 0·39 |
| | 60 | 0·814 | 3·1 | 0·036 | 0·044 | 54 | | 0·38 |
| | 75 | 0·804 | 3·1 | 0·027 | 0·033 | 40 | | 0·38 |
| | 80 | 0·801 | ... | 0·026 | 0·032 | 39 | | 0·38 |
| Transformer Oil No. 2 | 12 | 0·876 | 2·9 | 0·442 | 0·505 | 732 | 0·48 | 0·42 |
| | 15 | 0·875 | 2·9 | 0·384 | 0·438 | 633 | | 0·42 |
| | 20 | 0·872 | 2·9 | 0·303 | 0·347 | 500 | | 0·42 |
| | 50 | 0·852 | 2·9 | 0·090 | 0·106 | 149 | | 0·41 |
| | 60 | 0·846 | 2·9 | 0·063 | 0·074 | 104 | | 0·41 |
| | 75 | 0·836 | 2·85 | 0·041 | 0·049 | 69 | | 0·40 |
| | 80 | 0·833 | ... | 0·035 | 0·042 | ... | | 0·40 |
| Transformer Oil No. 3 | 12 | 0·918 | 3·0 | 0·981 | 1·07 | 1500 | 0·46 | 0·42 |
| | 15 | 0·915 | 3·0 | 0·745 | 0·816 | 1142 | | 0·42 |
| | 20 | 0·912 | 3·0 | 0·506 | 0·555 | 776 | | 0·42 |
| | 50 | 0·894 | 2·9 | 0·121 | 0·135 | 191 | | 0·41 |
| | 60 | 0·888 | 2·9 | 0·084 | 0·095 | 134 | | 0·41 |
| | 75 | 0·879 | 2·9 | 0·059 | 0·067 | 93 | | 0·40 |
| | 80 | 0·876 | ... | 0·052 | 0·060 | 83 | | 0·40 |

(*b*)* *Viscosity* ($\eta$) *and kinematical viscosity* ($\nu = \eta/\rho$).—Determinations of viscosity were made at various temperatures. Values for water were taken from published tables. For the more viscous oils a Redwood (No. 1 type) viscometer was used in accordance

* Mr. A. R. CHALLONER assisted with these observations.

Digitized by Google

with customary practice at the National Physical Laboratory.* Essentially the method consists in determining the time taken for 50 ccs. of the oil at the test temperature to flow out of an oil cup through a suitable capillary jet, the initial level of the oil having been accurately adjusted to a certain standard position. In this way " kinematical viscosity " is determined, from which the other coefficient may be calculated.

For paraffin, the Redwood instrument is not suitable, as the flow would be turbulent. In this case the viscosity was measured by comparison with water in an Ostwald viscometer.† This consists of a marked U-tube, the connecting piece being of capillary dimensions. The liquid under test stands initially at different levels in the two limbs, and the time is noted which elapses while the liquid meniscus passes certain marks on the tube.

It is desirable to notice (see Table II) that very considerable viscosity changes arise when the temperature of a liquid is altered.

(*c*) *Specific Heat* (*s*) *and* (*c*).—The specific heat (*s*) determined for each oil was the mean value over the range 20° to 100° C. It was obtained by the method of mixtures, a measured quantity of the oil under test at a temperature of 100° C. being poured into a calorimeter containing a standard oil at 20° C. The specific heat of the oil chosen as standard had been determined at air temperatures by introducing a copper block at 360° C. into a measured quantity contained in a calorimeter. The standard oil was found to have a specific heat at air temperatures indistinguishable from its mean value over the range 20° to 100° C. Values obtained were reproducible to an accuracy of about 2 per cent.

The capacity for heat (*c*) per unit *volume* of a liquid is given by the equation $c = s\rho$.

(*d*) *Thermal Conductivity* (*k*).—Thermal conductivities of the fluids were determined by means of an apparatus similar to that described by GOLDSCHMIDT.‡ The method consists of stretching a fine platinum wire along the axis of a small horizontal silver tube full of the test liquid, and measuring the electric current necessary to maintain a measured temperature difference between the wire and the walls of the tube. This gives a relative value for the conductivity of the oil, for it appears that with fine wires, small tubes, and but slight heating, the disturbing effects of convection currents are negligible. This is not surprising, since the cooling of a fine wire immersed horizontally in a bath of fluid tends to depend only upon the conductivity of the fluid in these conditions.

In the actual apparatus the silver tube, 2 mms. diameter and 12·7 cms. long, was fitted tightly into a massive copper cylinder of 5 cms. diameter, so that the temperature was uniform throughout its length. A 4-mil paltinum wire, with current and potential leads attached to its ends, was adjusted to pass axially through the tube. Since the current leads were helical copper springs they prevented sagging of the test wire when heated.

* HIGGINS, 'N.P.L. Collected Researches', vol. 11, Paper 1, 1914, or 'Petroleum World', June and July, 1913.

† I am indebted to Dr. G. BARR, of the Dept. of Metallurgy and Metallurgical Chemistry of the N.P.L. for this determination.

‡ 'Phys. Zeits.', vol. 12, p. 417, 1911.

Digitized by Google

The apparatus* was completely immersed in a quantity of the liquid to be examined, which thus filled the capillary tube.

Measurements were made of the heat dissipation associated with various small temperature excesses of the wire, ranging from 1° or 2° C. to 20° C. For this the Kelvin bridge was used in the manner already described. However, since only slight heating was used, the initial current was reduced to 0·01 ampère so that its heating effect should be negligible in these new conditions. The currents used for heating ranged up to about 1 ampère.

Thermal conductivities were calculated on the assumption of radial flow of heat between the wire and the inner surface of the silver tube. For moderate heating results so calculated increased as the temperature excess was raised, showing that convection currents had become appreciable. For slight heating, however, results were practically constant. The conductivity given in the tables is the value to which results tended as the temperature excess was reduced to zero.

The experiments were carried out with the liquids at two temperatures, about 20° C. and 80° C. respectively. No allowance was made for end effects, but probably the length of wire used (12·7 cms.) was sufficient to render these of little importance.

(*e*) *The Ratio* ($k/c\nu$).—On the kinetic theory of gases the thermal diffusivity ($k/c$) bears a ratio to the kinematical viscosity† ($\nu$), which is constant for a given kind of gas, and depends upon the number of atoms in a molecule. For liquids, owing to complexity of structure, such constancy does not hold, and a wide range of value is covered. It is to be expected on general grounds that this fundamental ratio between the factors determining the fluid flow and the heat transfer will be important in determining the cooling power of fluid streams. Consequently, for each of the liquids, $k/c\nu$ has been evaluated for a series of temperatures. It is the factor determining the complexity of a fluid when thermal and viscous actions are involved together, *i.e.* in convection of heat.

### 5. *The Wires used.*

The wires used were of specially pure platinum, and were of three sizes, being about 4, 6, and 8 mils‡ in diameter. Mean details are given in Table III.

Potential leads of 4-mil platinum wire were welded to the test wire at a distance from its ends. The length of wire between these leads was easily measured. Diameters were measured by means of a micrometer screw gauge reading to one ten-thousandth part of an inch.

Before the wires were cut up into lengths for mounting in the holder of the rotating arm, temperature coefficients of resistance were determined for annealed samples. Lengths of about 30 cms. were used, and resistances were determined at the temperatures of melting ice, and of the vapour of water boiling under normal atmospheric pressure.

* This apparatus was available, having been constructed previously by Dr. Ezer Griffiths.

† Diffusivity of momentum.

‡ 1 mil = 0·001 inch.

Digitized by Google

TABLE III.—Details of the Wire used.

Total length between current terminals = 6·08 cms.

Mean length between potential leads = $l$ cms.

Resistance per unit length at 0° C. = $R_0/l$ ohms per cm.

| Wire. | Diam. | $l$. | $R_0/l$. | $\alpha$. |
|---|---|---|---|---|
| | cm. | | | |
| 4-mil . . . . | 0·0102 | 4·8 | 0·118 | 0·00386 |
| 6-mil . . . . | 0·0152 | *4·75 | 0·0564 | 0·00380 |
| 8-mil . . . . | 0·0204 | 4·98 | 0·0294 | 0·00387 |

* Lengths 3·15 and 6·08 cms. were used in the end correction test.

Sulphur points had previously been determined. For these measurements use was made of a Callendar and Griffiths resistance bridge reading to 0·0001 ohm. However, in one case, using the Kelvin bridge arrangement, a check measurement was obtained for a portion of wire mounted in the normal manner in the holder of the whirling arm. The wire was immersed in a stirred oil bath at a few fairly steady temperatures, and the temperature coefficient of resistance thus obtained agreed to within 2 per cent. with the more accurate determination previously made.

During cooling experiments with the arm rotating, the finer wires tended to stretch slightly, presumably owing to the strains set up. This was most readily detected by the change in resistance of the wire at 0° C., a quantity which was regularly calculated from the measured resistance at the temperature of the oil. Necessary allowances for such changes were made in the heat-loss calculations. The effect, however, was slight, and in the whole life of a wire did not amount to more than 1 per cent. increase in length.

Throughout the experiments care was taken to keep the wire bright and free from adherent fluff, etc. If by accident it was over-heated, it became blackened with carbonised oil. On these occasions the wire was removed from the liquid, and the deposit was burnt off by heating the wire electrically to a dull redness. Naturally, after this procedure, particular attention was paid to alterations in resistance.

(i) *Calculation of Heat-Loss from the Wire.*—The heat-loss from the wire during an experiment was calculated from the current "$i$" flowing through it, and from its hot resistance R, as measured on the Kelvin bridge. Results were converted from watts to calories per second, using 4·184 as the conversion factor. They were expressed in the form of heat-loss per cm. length per degree temperature elevation.

(ii) *Calculation of the Temperature Excess of the Wire.*—The temperature excess of the wire was calculated from the increment of resistance $dR$: on the platinum scale it is given by $\theta = dR/R_0\alpha$, where $R_0$ is the resistance of the wire at 0° C., and $\alpha$ is the temperature coefficient of resistance. Corrections to the Centigrade scale involve increasing the above value by about 1 per cent. for values of $\theta$ up to 20° C. and by 1/5 per cent. for $\theta = 60°$ C. Such corrections are almost negligible, being greatest for the low values of

Digitized by Google

$\theta$, where the experimental errors were greatest. They may be obtained conveniently from tables showing the relation between the two scales.*

(iii) *Correction due to Radial Temperature Gradient in the Wire.*—There is also a small correction due to the fact that, through its immediate proximity to the liquid, the surface of the wire becomes slightly cooler than the core. Calculation on certain assumptions shows the temperature difference between the core of the wire and its surface to be proportional to the rate of surface cooling.† In the notation of this paper it is given by $H\theta/4\pi K$, where K ($= 0{\cdot}166$ cal. per cm. per degree) is the thermal conductivity of the platinum of which the wire is composed. The mean temperature of the wire as obtained by resistance measurements is thus in excess of the surface temperature by an amount $d\theta$ given by $d\theta/\theta = H/8\pi K = 0{\cdot}24\,H$. From the tables of H, given later, we find that for water the relative error $d\theta/\theta$ is appreciable only for the highest speeds, and that for all other liquids it is invariably less than 1/3 per cent. No correction for this effect has therefore been made.

(iv) *Correction for Conduction by the Potential Leads and Terminals.*—The wire was clamped to the holder by two terminals about 6·1 cms. apart and the potential leads (4-mil) were attached at about $\frac{1}{2}$ cm. from the clamped ends. It was considered that at this distance the terminals would have no cooling effect on the test portion of the wire, and that the potential leads were sufficiently thin to be negligible in this respect.

If the terminals exert any appreciable cooling, measured heat-losses should depend upon the distance of the potential leads from the ends. With the liquids no such dependence was found. Direct test with oil No. 1 gave practically identical results, whether the potential leads were attached to the wire at the clamping terminals, at $\frac{1}{2}$ cm. from them, or at double this distance. Even with air as the fluid (where end cooling would be of much greater relative importance owing to the much smaller rates of surface cooling) differences were not very systematic and were limited to $\pm 5$ per cent.‡

It was inferred from these experiments that the heat lost by conduction to the terminals and potential leads was negligible in comparison with that carried off by the liquid streams.

## 6. *Results.*

(i) *Tables and Curves showing Heat-Losses obtained with Each of the Liquids.*—The results obtained in the experimental work were expressed in terms of the heat-loss H per centimetre length of wire per degree Centigrade temperature excess. Observations were taken for various velocities of rotation, and for a series of values of temperature excess.

To present results in convenient comparative tables, it was necessary to obtain by interpolation values appropriate to certain selected velocities and temperatures. In

* Harker, 'N.P.L. Collected Researches', vol. 1, Paper 2, or 'Phil. Trans.', A, vol. 203, p. 343, 1904.

† King, 'Phil. Trans.', A, vol. 214, p. 373, 1914.

‡ Greatest values were indicated when the potential leads were attached at the extreme ends of the wires.

Digitized by Google

this connection a graph is given, Fig. 5, which shows experimental points obtained for one of the oils, and the smooth curves from which representative results were read off. As regards temperature excess, it will be seen that the values deviated but slightly from

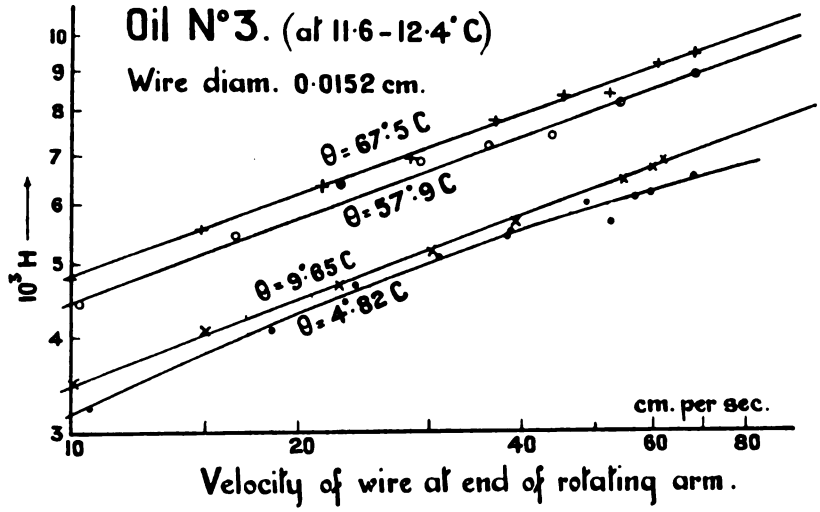


Fig. 5. Specimen Experimental Results.

a convenient series, viz., 5°, 10°, 60°, and 70° C. The small adjustments necessary to give heat-losses corresponding to these exact values were obtained by further curves. The procedure with this oil is typical.

Tables IV (i–v) give results compiled in the above manner, and the values given bear a very close relation to actual points obtained in the experimental work. They present in some 200 orderly values the results of four or five times this number of observations.

TABLE IV.—Heat-Losses ($10^5$ H) from Wires in Liquid Streams.

(H = calories per cm. per sec. per 1° C. temperature excess of wire.)

| Diameter of wire. | Mean temperature of water. | Temperature excess of wire. | $10^5$ H. For values of relative velocity (cms. per sec.). 10. | 20. | 40. | 60. | 70. |
|---|---|---|---|---|---|---|---|
| | | | (i.) Distilled Water.* | | | | |
| cm. | ° C. | ° C. | | | | | |
| 0·0204 | 11 | 8 | 2070 | 2900 | 4060 | 4950 | 5340 |
| | | 20 | 2200 | 3090 | 4300 | 5250 | 5650 |
| | | 35 | 2560 | 3460 | 4800 | 5830 | 6300 |

* WORTHINGTON and MALONE give a value $10^5$ H = 2960, when $d$ = 0·0256 cm., $\theta$ = 30° C., and $v$ = 14·85 cms. per sec. ('J. Franklin Inst.', vol. 184, p. 115, 1917).



Digitized by Google

Table IV. (continued).

| Diameter of wire. | Mean temperature of oil. | Temperature excess of wire. | $10^5$ H. For values of relative velocity (cms. per sec.). | | | | |
|---|---|---|---|---|---|---|---|
| | | | 10. | 20. | 40. | 60. | 70. |
| | | (ii.) Paraffin Oil. | | | | | |
| cm. | ° C. | ° C. | | | | | |
| 0·0152 | 17·6 | 5 | 460 | 622 | 840 | 993 | 1055 |
| | | 50 | 487 | 677 | 940 | 1140 | 1230 |
| 0·0204 | 11 | 5 | 500 | 697 | 978 | 1190 | 1280 |
| | | 50 | 572 | 798 | 1110 | 1350 | 1455 |
| | | (iii.) Transformer Oil No. 1. | | | | | |
| 0·0152 | 16 | 5 | 384 | 515 | 693 | 825 | 875 |
| | | 10 | 400 | 532 | 705 | 827 | 880 |
| | | 20 | 428 | 570 | 757 | 890 | 950 |
| | | 40 | 450 | 603 | 795 | 944 | 1010 |
| | | 60 | 467 | 625 | 835 | 1000 | 1068 |
| 0·0204 | 15 | 5 | 480 | 644 | 855 | 1014 | 1076 |
| | | 10* | 483 | 646 | 863 | 1024 | 1095 |
| | | 20 | 505 | 684 | 910 | 1070 | 1138 |
| | | 40 | 550 | 745 | 990 | 1160 | 1237 |
| | | 60† | 588 | 786 | 1040 | 1225 | 1305 |
| | | (iv.) Transformer Oil No. 2. | | | | | |
| 0·0102 | 11 | 5 | 315 | 425 | 553 | 630 | 660 |
| | | 50 | 383 | 512 | 688 | 814 | 870 |
| 0·0152 | 11 | 5 | 358 | 468 | 610 | 713 | 758 |
| | | 10 | 382 | 492 | 650 | 765 | 812 |
| | | 20 | 395 | 520 | 687 | 808 | 860 |
| | | 40 | 430 | 565 | 740 | 870 | 923 |
| | | 60 | 458 | 598 | 778 | 906 | 960 |
| 0·0204 | 14 | 5 | 440 | 578 | 760 | 890 | 944 |
| | | 50 | 542 | 727 | 972 | 1155 | 1230 |
| | | (v.) Transformer Oil No. 3. | | | | | |
| 0·0512 | 12 | 5 | 335 | 450 | 568 | 640 | 660 |
| | | 10 | 363 | 468 | 600 | 695 | 737 |
| | | 60 | 474 | 600 | 765 | 880 | 930 |
| 0·0204 | 16 | 5 | 406 | 535 | 702 | 825 | 877 |
| | | 10 | 417 | 548 | 720 | 847 | 900 |
| | | 20 | 468. | 612 | 800 | 940 | 1000 |
| | | 40 | 512 | 672 | 890 | 1050 | 1118 |
| | | 60 | 560 | 738 | 970 | 1140 | 1210 |

* A series at 10° C. excess taken much earlier and with a different wire gave smoothed results indistinguishable from these at the lower velocities, and falling to about 3 per cent. lower at 70 cms. per sec.

† An earlier series at 60° C. with a different wire gave smoothed values indistinguishable from these.

Digitized by Google

A trial was made of representing these results on graphs in which heat-loss was plotted as ordinate against the square root of the velocity as abscissa. In general, the lines obtained were slightly curved, so that the results could not be conveniently expressed

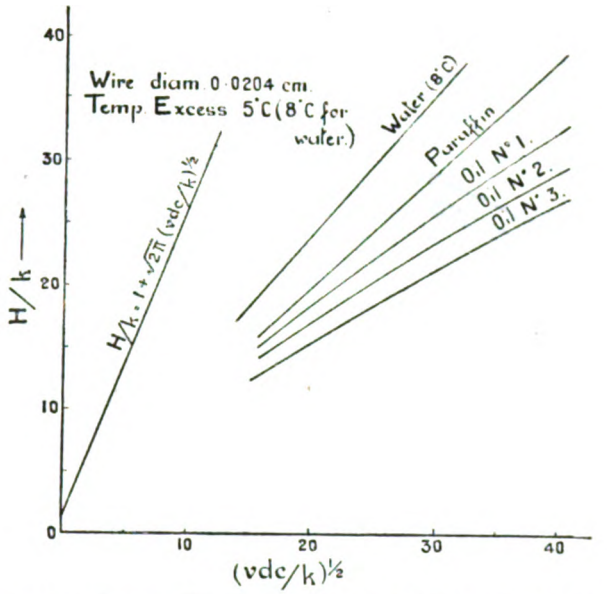


Fig. 6. Results for Viscous Liquids compared with Formula for Inviscid Fluids.

by a formula similar to that found for gases (equation 2). Fig. 6 shows a series of results plotted on a graph of this form.

On plotting logarithmically, however, excellent straight lines were usually obtained, and results were studied from this point of view. Fig. 7 shows families of curves obtained for each of the liquids used. It is immediately evident that for a given liquid the lines are practically parallel, the slope having no marked dependence upon the diameter of the wire or upon its temperature excess. There is possibly a tendency for the slope to be greater for the larger wires, but otherwise occasional irregularity of slope or of curvature appears to be due to experimental error, for with different liquids it is not associated consistently with any particular set of conditions.

Parallel lines are also obtained on plotting results with temperature excess ($\theta$) as abscissa. This may be seen from the curves shown in Fig. 8. Thus the effect of temperature is to introduce a factor dependent only upon the nature of the liquid used.

(ii) *Empirical Relations.*—If we accept the families of curves of Figs. 7 and 8 to be parallel lines, rectilinear in the former case, we find the following general formula covers the results :—

$$H = Mv^n(1 + a\theta + b\theta^2), \quad . \quad . \quad . \quad . \quad . \quad . \quad . \quad . \quad . \quad (9)$$

where $n$, $a$, and $b$ depend only upon the liquid used, while M depends also upon the diameter of the wire.

The values of "$a$" and "$b$" are given later in Table V. Undoubtedly they are



Digitized by Google

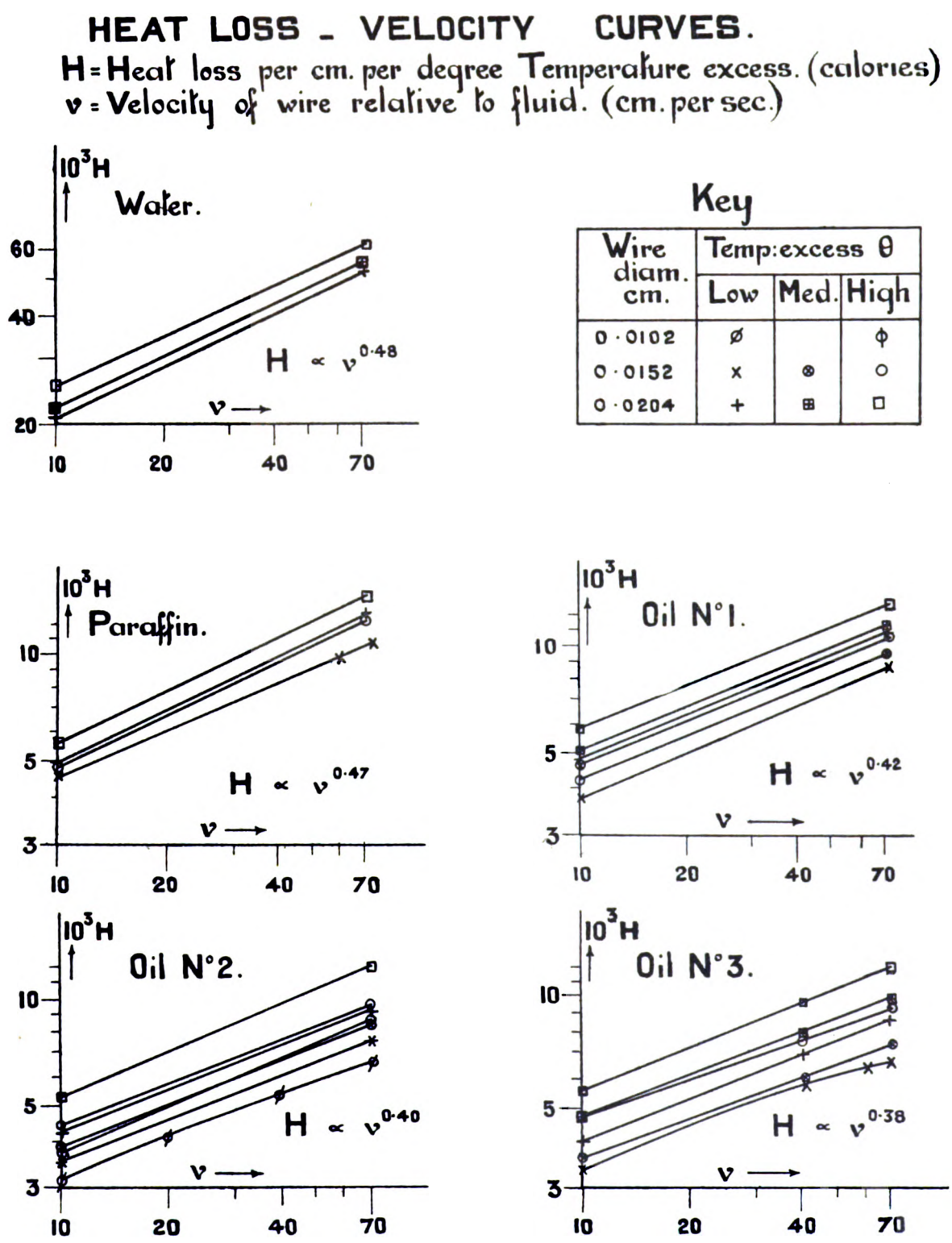


Fig. 7.

Digitized by Google

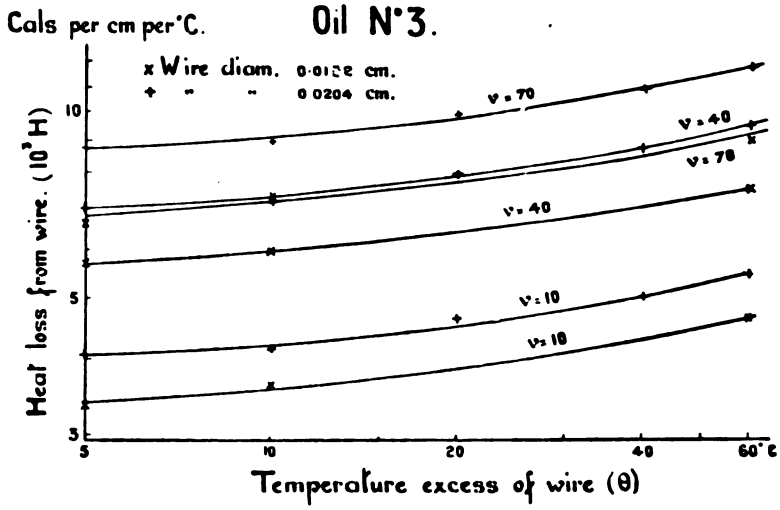


Fig. 8. Specimen Curves. Heat Loss—Temperature Excess.

intimately connected with the rate at which the physical properties of the fluids vary with temperature. Since our theoretical formulæ are restricted to cases where the physical properties remain constant, discussion will be devoted mainly to cases where the temperature excess " θ " is so small that changes in the properties of the fluids are inappreciable. In these circumstances equation (9) becomes

$$H = Mv^n. \quad . \quad . \quad . \quad . \quad . \quad . \quad . \quad . \quad . \quad . \quad . \quad (10)$$

Trial of a more general relation of the form*

$$H/k = N(vdc/250k)^n$$

showed N to depend upon both $vdc/k$ and $k/c\nu$, so that the effects of these two terms are inter-related. While in the present experiments " $n$ " exhibits no appreciable variation with $vdc/k$, being given by

$$n \text{ varies as } (k/c\nu)^{0\cdot03-0\cdot04}, \quad . \quad . \quad . \quad . \quad . \quad . \quad . \quad . \quad . \quad (11)$$

published values for gases cover a much wider range and indicate that

$$n \text{ varies as } (vdc/k)^{0\cdot066}. \quad . \quad . \quad . \quad . \quad . \quad . \quad . \quad . \quad . \quad (12)$$

Now to a certain degree of approximation equations (11) and (12) can be combined in the form

$$n \text{ varies as } \{(vdc/k) \times (k/c\nu)^{\frac{1}{2}}\}^{0\cdot066}, \quad . \quad . \quad . \quad . \quad . \quad . \quad . \quad (13)$$

* In the experiments the minimum value of $vdc/k$ for each liquid was about 250. By writing $vdc/250k$ instead of $vdc/k$ the advantage is gained that N has a definite physical meaning. It is the lowest value of $H/k$ actually measured, instead of being the extrapolated value associated with $vdc/k = 1$.

Digitized by Google

and it was decided to test whether the new variable thus revealed would express completely the inter-relation of $vdc/k$ and $k/c\nu$.

(iii) *Formula covering all Results.*—It was then found possible to express our experimental results in a formula of the type

$$H/k = A \,.\, B \,.\, C \,.\, F\{(vdc/k) \times (k/c\nu)^{\frac{1}{3}}\}^*, \quad . \quad . \quad . \quad . \quad . \quad . \quad . \quad (14)$$

where A $(= 1 + a\theta + b\theta^2)$ depends upon the temperature excess of the wire and the nature of the fluid, and is undoubtedly connected with the rate at which the physical properties of the fluid vary with temperature.

B represents a small residual effect of wire diameter, additional to that covered by the "$vd$" term. It depends somewhat upon the nature of the liquid.

C $[= f(k/c\nu)]$ is dependent only upon the nature of the fluid. It varies as $(k/c\nu) - m$, where $m = 0$ for gases and increases to about 0·19 in the region of the viscous oils.

The formula is of the general form expected (3), except for the small corrections represented by the terms A and B. The particular grouping of variables within the brackets correlates the various slopes of the lines in Fig. 7 with the curvature observed when study is made of an extended $vdc/k$ curve for gases.

TABLE V.—Values of A and B.

$A = 1 + a\theta + b\theta^2$, where $\theta$ = temperature excess of wire.

| Fluid. | $10^3a$. | $10^5b$. | Values of B | | |
|---|---|---|---|---|---|
| | | | For wire diam., cm. | | |
| | | | 0·0102 | 0·0152 | 0·0204 |
| (Air)* . . . . . | ... | ... | (0·91–0·94) | (0·95–0·97) | 1 |
| Water . . . . . | 2·64 | 12 | ... | ... | 1 |
| Paraffin . . . . . | 2·94† | ... | ... | 0·98 | 1 |
| Oil No. 1 . . . . . | 7·25 | − 5·08 | ... | 0·92 | 1 |
| Oil No. 2 . . . . . | 10·7 | − 8·42 | 0·93 | 0·90 | 1 |
| Oil No. 3 . . . . . | 13·5 | − 9·52 | ... | 0·90 | 1 |

* Calculated from KING's results.

† Mean value obtained from results at temperature excesses 5° and 50° C.

(*a*) *The Dependence of* A *upon Temperature Variations in the Physical Properties of the Liquid.*—The physical property of the liquid which depended most upon temperature was the viscosity. In some cases the cold oil was as much as ten times as viscous as hot

* $\{(vdc/k) \times (k/c\nu)^{\frac{1}{3}}\} = \{(vdc/k) \times (vd/\nu)\}^{\frac{1}{3}} = \{(vd/\nu) \div (k/c\nu)^{\frac{1}{3}}\}$.

Digitized by Google

oil at the temperature of the wire. Such variations may be too great to be covered by a simple correction applied to a theoretical formula based upon assumptions of constancy. The temperature effect has therefore been left in the empirical form given above, $k$, $c$, and $\nu$ having the values appropriate to the cold fluid.

It is worth notice, however, that the effect is generally rather greater than can be allowed for in the final formula by supposing the physical properties of the fluid to be those appropriate even to the temperature of the hot wire. Generally, for 60° C temperature excess of the wire, about 10 per cent. increment in heat-loss has still to be accounted for.

## ERRATUM.

Page 270, line 11. *For* "$(k/c\nu)-m$" *read* "$(k/c\nu)^{-m}$."

(B34/3830)z 22198—1495 625 2.27 H & S Ltd. Gp. 34

acceleration due to gravity. A term $cga^4\upsilon/\kappa\nu\tau$ (or its equivalent), found by the author to cover free convective cooling in viscous liquids, may then be expected in the complete equation. If B owes its origin to this new correction term, its dependence (Table V) upon the nature of the liquid ($ca/k\nu$) is thus explained. Some associated dependence upon the temperature excess $\theta$ is also to be expected, and this may explain the residual relation between A and $\theta$ not previously accounted for. It may also explain why, in KING's results, his diameter term is associated with a residual $\theta$ term much larger than that which operates upon the velocity group.

While the term B may have its origin in natural convection effects, other possibilities must not be overlooked. As previously stated, the diameter effect indicated by HUGHES'

* Results were not corrected for swirl, but comparisons were made at definite arm velocities. The actual magnitudes of heat-loss were almost identical with those calculated from KING's formula, provided the swirl velocity in the trough was about 12 per cent. of the arm velocity. Such a figure is reasonable, since values of 10 per cent. to 20 per cent. were obtained when liquids were used. KING found a 5 per cent. swirl in a large room.

† If, in addition to the free convection variables, the density of the fluid is also separately introduced [it is already included to some extent in $c(=s\rho)$ and $\nu(=\eta/\rho)$] a term results which contains $d$ without either $\theta$ or $v$. RICHARDSON has discussed the relation borne by such a term to KING's results ('Proc. Phys. Soc. Lond.', vol. 33, p. 405, 1920).

Digitized by Google

results for large cylinders is in the opposite sense to that found in the present experiments with fine wires. The distribution of heat flux across the boundary may have been different in this case.

(*c*) *Relation between* C *and the Nature of the Liquid.*—

$$C = f(k/c\nu) \quad . \quad . \quad . \quad . \quad . \quad . \quad . \quad . \quad . \quad . \quad . \quad (15)$$

Fig. 9 shows the manner in which C depends upon the value of $k/c\nu$ for the liquid used. It was obtained for the 8-mil wire and for small values of temperature excess by plotting $H/k$ as ordinate against $\{vdc/k \times (k/c\nu)^{\frac{1}{4}}\}$ as abscissa. A series of curves was thus obtained parallel to neighbouring portions of the extended curve for air, but displaced by

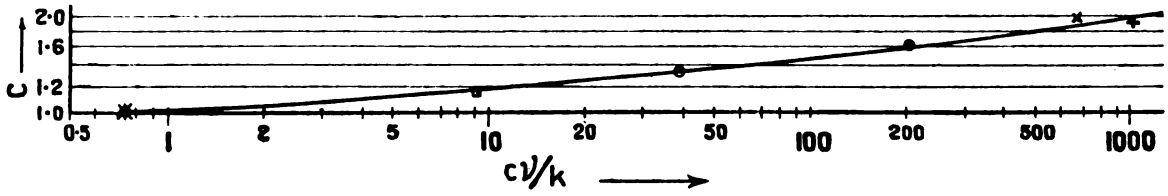


Fig. 9. Relation between C and $c\nu/k$.

amounts depending upon the nature of the liquid used. Measurement was made of the amounts of displacement, that is, of the factors C necessary to bring all the curves into coincidence with that for air. It is seen that a smooth relation is indicated between C and $k/c\nu$. Values read off from Fig. 9 are given in Table VI.

Table VI.—Relation between C and $k/c\nu$.

| $k/c\nu$. | $c\nu/k$. | C. |
|---|---|---|
| 1 | 1 | 1·02 |
| 0·1 | 10 | 1·17 |
| 0·01 | 100 | 1·46 |
| 0·001 | 1000 | 1·98 |

(*d*) *Curve showing Correlation effected.*—Fig. 10 has been drawn to show the extent to which the final formula (14) represents the results of the experimental work. Ordinates give the value of $[H/k] \div [A \,.\, B \,.\, C]$ and abscissæ represent $[vdc/k \times (k/c\nu)^{\frac{1}{4}}]$. Values for A, B, and C are those given above.

The points shown represent the experimental values for liquids as given in Tables IV (i–v). For convenience only a selected number of points have been plotted, and these refer only to small temperature excesses, but each wire is represented by high (70 cms. per sec.) and low (10 cms. per sec.) velocities for each of the liquids used.

Digitized by Google

The line drawn is part of the mean curve* for gases referred to earlier, re-drawn on the present basis, taking for air $k/c\nu = 1{\cdot}35$.† In the region shown, $H/k$ . A . B . C . varies as $[vdc/k \times (k/c\nu)^{\frac{1}{2}}]^n$, where $n$ varies from 0·38 to 0·48.

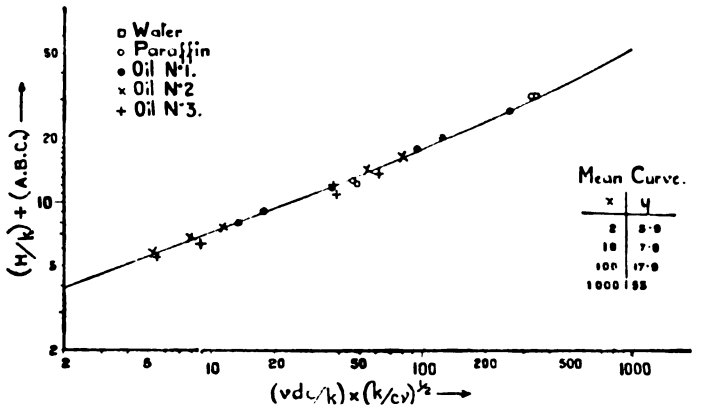


FIG. 10. Representative Results for all Fluids plotted on One Curve

The figure shows that equation (14) satisfactorily represents our results. It is as far as possible of the type suggested by theoretical considerations, but is empirical as regards the actual form of the functions given.

I desire to express my thanks to Dr. G. W. C. KAYE, Superintendent of the Physics Department of the National Physical Laboratory, for the helpful manner in which all the facilities for the work have been provided. Mr. R. R. STRAND, Senior Observer, helped with the constructional work and rendered very valuable assistance with the experimental observations.

* The curve is the mean for gases obtained by the method described elsewhere. No correction terms in B or in $(1+a\theta+b\theta^2)$ have been used, but temperature changes in the properties of air have been approximately allowed for by taking values of $k$, $c$, and $\nu$ for temperatures intermediate between that of the cold air and that of the hot wire. Little difference in the mean curve is obtained if the constants are evaluated for a temperature equal to that of the hot wire.

† $c$ refers to unit volume and constant pressure. If the constant volume value is taken, a slight alteration in the form of the function $f$ is all that is necessary to give a curve practically as good as the present one. All values of $f(x)$ for $x$ greater than 9 have to be reduced by 30 per cent. and the alteration in $f(x)$ for lower values of $x$ falls to zero as $x$ approaches 1·90, the new value of $k/c\nu$ for air.



Digitized by Google

Digitized by Google

# AN ALL-METAL HIGH-VACUUM PUMP SYSTEM

BY

IVOR BACKHURST, M.Sc.,
ASSISTANT IN THE PHYSICS DEPARTMENT,

AND

G. W. C. KAYE, O.B.E., M.A., D.Sc.,
SUPERINTENDENT OF THE PHYSICS DEPARTMENT.

2 N 2

Digitized by Google

## ABSTRACT.

A two stage mercury-vapour pump system constructed wholly of steel has been devised, which consists of a jet pump and a condensation pump in series. The system requires a fore-vacuum of 4 mms. to afford the highest vacua obtainable by a mercury condensation pump. There are no moving parts, vapours are pumped as efficiently as gases, no drying reagents are required, and glass work and rubber joints are eliminated. Above 0·03 mms. pressure the speed (using GAEDE'S definition) is constant at 300 ccs./sec.; below this pressure the speed increases rapidly to a constant value of 6000 ccs./sec.

A short résumé of existing vacuum pumps is given in this paper. The following approximate speeds are quoted :—

| | ccs./sec. |
|---|---|
| Gaede rotary oil pump . . . . . | 100–150 |
| Gaede rotary mercury pump . . . . . | 100 |
| Gaede diffusion pump . . . . . | 100 |
| Gaede molecular pump . . . . . | 1400 (max.) |
| Langmuir condensation pump . . . . . | 3000–4000 |


Digitized by Google

# AN ALL-METAL HIGH-VACUUM PUMP SYSTEM.

By IVOR BACKHURST, M.Sc., Assistant, and G. W. C. Kaye, O.B.E., M.A., D.Sc., Superintendent of the Physics Department.

[Reprinted from the 'Philosophical Magazine', Vol. 47, 1924.]

## I. Introductory.

The two conspicuous advances in the more recent history of high-vacuum production are doubtless (*a*) the use of liquid air and charcoal, a method due, as is well known, to the late Sir James Dewar; and (*b*) the invention of the condensation pump by Langmuir.

The charcoal and liquid air method was the standard method of producing high vacua from its discovery in 1904 until the development of the condensation pump in 1916. The charcoal method is capable of affording extreme vacua, but at the lower pressures the method is normally slower than the condensation pump.

The different types of high-vacuum pumps available at the present time may be conveniently divided into four classes :—(1) oil-sealed pumps; (2) mercury-sealed pumps; (3) high-speed mechanical pumps; (4) mercury-vapour pumps.

### (1) *Oil-Sealed Pumps.*

These are mechanical and fall into two divisions :—

(*a*) *Piston.*—The earlier vacuum pumps were all of the piston type and in the Geryk (1)* pattern are still much used.

(*b*) *Rotary.*—The rotary oil pumps first designed by Gaede (2), although probably foremost for medium vacuum work, are not generally adapted for pressures above 1 mm. or so, but rather are used to obtain pressures of the order of 0·001 mm. when supported by a piston pump capable of reducing the pressure directly from atmospheric to about 0·1 to 2 mm. The rotary pumps are, however, slow in dealing with vapours and the oil is apt to become contaminated. The vibration they occasion is considerable, and it is important to protect them against water vapour by the use of drying-tubes. The provision of a by-pass tap and a trap is advisable to assist in preventing overflow of oil in the event of the back-pressure rising or a sudden leak developing in the apparatus to be exhausted. The speed, as defined by Gaede (see p. 282), is from 100 to 150 ccs./sec.

* See Bibliography at end of paper.

Digitized by Google

### (2) *Mercury-Sealed Pumps.*

The simplest pump of the mercury-sealed type is the *Sprengel* (3) which depends on liquid-jet action and, according to KAHLBAUM, is capable of reaching a pressure lower than $10^{-5}$ mm.

The *Töpler* (4) pump, a simple piston pump in which mercury is used as the piston, is capable of doing nearly as well, and was formerly almost exclusively employed in laboratories devoted to electric discharge-tube research. Both this and the Sprengel pump require constant attention and are extremely slow, and, on this account, they are now comparatively little used.

The *Gaede* (5) rotary mercury pump, consisting essentially of an Archimedean screw having its axis horizontal and immersed in mercury to a level somewhat above the axis, is faster than either of the above and requires little attention when motor driven. Its speed is about 100 ccs./sec. It requires a fore-vacuum of about 10 mms. and a by-pass for the supporting pump is necessary. Vapours are pumped very slowly and drying-tubes are required. Although the rotary mercury pump has been used in many modified forms since it was designed in 1905, it has given place in factory work during the last few years to the rotary oil pump.

### (3) *High-Speed Molecular Pumps.*

The molecular pump, invented by GAEDE (6), consists of a grooved cylinder, designed to rotate at about 10,000 revs./min. with a clearance of the order of 0·01 cm. inside a cylindrical casing in which are narrow radial extensions protruding into the grooves. On either side of the extensions are inlet and outlet ports connected in series fashion. The pumping action depends on the fact that in confined spaces at low pressures the collisions of a molecule with the boundary walls are much more frequent than with other molecules. It follows that if one of the walls is in motion, the molecules tend to take up rapidly the direction of this motion. At low pressures the pump maintains a definite ratio between the pressures on either side of it, the value of the ratio for a given speed of rotation and the same gas or vapour depending only on the dimensions of the pump. The value of the ratio may be as much as 100,000. The speed of pumping for air may reach 1400 ccs./sec. at about 0·01 mm. pressure, but falls off rapidly at lower pressures.

*A type of molecular pump, incorporating a number of improvements, has been designed by HOLWECK (13).

### (4) *Mercury-Vapour Pumps.*

(*a*) *Diffusion Pump.*—The mercury-vapour diffusion pump, also first designed by GAEDE (7), is a true diffusion pump, mercury vapour and air diffusing through a narrow slit in *opposite* directions. The vapour, after passing the slit, is condensed and returned

* Added January, 1924.

Digitized by Google

to the boiler, while the air passing through to the opposite side of the slit is carried away by the supporting pump. The high vacuum is thus on the condenser side of the slit. A great disadvantage is that for efficient operation the pressure of the vapour at the slit must be only slightly in excess of that of the fore-vacuum, so that the temperature of the mercury must be carefully regulated. The pump is also slow, the speed not generally reaching 100 ccs./sec. The advantages of the diffusion pump are that there is no theoretical limit to the lowest pressure attainable, and also that vapours are dealt with as well as gases. These advantages are, however, common to all the various forms of mercury-vapour pumps.

(*b*) *Condensation Pumps.*—In the form of "condensation" pump devised by LANGMUIR (8), a blast of mercury vapour is directed tangentially against a water-cooled surface, along which the gas to be pumped is driven. The action depends on the energy of the mercury molecules "reflected" from the cooled surface being too small and non-directive to interfere with the direct blast. The pump is extremely fast, its speed being 3000–4000 ccs./sec. Moreover, the temperature-control is not critical. A fore-vacuum of 0·001 to 0·01 mm. is generally used, the upper limit being about 0·1 mm., and, as already mentioned, the theoretical limit of the pressure obtainable is zero.

Several modifications of the Langmuir type of pump, making use of the jet principle (as in a steam ejector), have proved very successful, such as CRAWFORD'S (9) parallel-jet pump, and the two-stage pumps of STIMSON (10) and VOLMER (11), on the rapidity of which we have no quantitative information. In a two-stage pump the pressure of the fore-vacuum need not be less than a few millimetres, so that a simple piston oil-pump is the only auxiliary required. In each of these modifications the conditions require a fine annular clearance round the jet. So far, jet pumps, owing to difficulties in design, have been constructed only of glass or silica, and have not, to our knowledge, been made of metal. The fragility of a glass or silica pump system, while not so important in a research laboratory, is, however, an admitted disadvantage from the industrial point of view.

## II. DESCRIPTION OF APPARATUS.

The pump system about to be described is of the two-stage type, constructed wholly of metal and consisting of (A) a mercury-vapour jet pump in series with (B) a mercury-vapour condensation pump. It may perhaps be urged that there is no real demarcation between the two types of pumps, but the terms are convenient.

### (A) *Mercury-Vapour Jet Pump.*

The essential features of the first-stage vapour pump are shown in Fig. 1, which is drawn to scale and is almost self-explanatory. The pump is made of steel, mainly from tubing, and all joints are welded.* Our experience is that, unless welding is carried out

* Brazing is objectionable since it causes gradual contamination of the mercury, while the brazing itself is liable to become porous.

Digitized by Google

by a welder fully accustomed to this class of work, the resulting joints are apt to be porous. We have found that the best remedy for this is thorough nickel-plating.

The boiler is lagged with asbestos board and wool. The condenser is surrounded by a water-jacket, as shown, and in addition it was found essential to cool the return tube R, which can be conveniently done by the use of coils of " compo " tubing. Two or three turns of cooling spiral are also wound round the tube B on the medium vacuum side. When the pressure in the pump has been reduced to 4 mms. or less by means of a piston pump, the jet pump is set in operation by turning on the circulating water and setting a

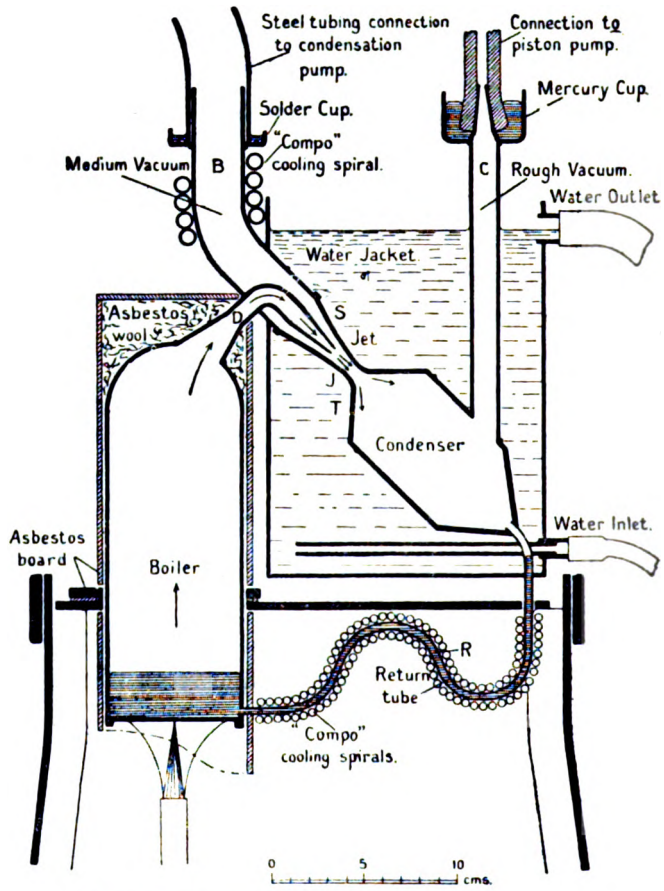


Fig. 1. Mercury-Vapour Jet Pump.

small Bunsen burner under the boiler, the latter containing about $1\frac{1}{2}$ kgs. of mercury. A pointed flame prevents excessive bumping, and in practice a $\frac{3}{8}$-inch diameter Bunsen burner, working under a gas pressure of 4 cms. of water, is found to be convenient. If the pressure at C is about 2 mms., the pressure at B will be reduced to less than 0·001 mm.

The action of the pump is as follows : Vapour leaves the boiler by the tube D, which is stream-lined as far as is practicable, and decreases in cross-section up to the nozzle at J. The mercury vapour issues as a divergent jet, the outer portions of which strike against the water-cooled throat T. Gas or vapour diffusing from the annular space

Digitized by Google

S is caught in the jet and carried into the condenser, and so to the piston pump, while the condensed mercury returns to the boiler through the tube R. The action of the pump is mainly that of the ejector, but utilises also the condensation principle.

In determining the dimensions of the jet pump, the following points have received attention :—

(1) The boiler is designed to be of sufficient cross-section to allow an adequate rate of evaporation without recourse to excessive temperature and vapour pressure.

(2) The height of the boiler is determined by the necessity of allowing for :—

(*a*) Vertical height of the condenser.

(*b*) Difference of level between mercury in return tube near condenser and mercury in the boiler.

(*c*) Sufficient depth of mercury in the boiler.

(3) The tube leading to the nozzle and the nozzle itself are everywhere stream-lined as far as practicable.

(4) The slope of the nozzle, throat, and condenser is everywhere arranged to be sufficient to ensure the flow of condensed mercury to the return tube.

(5) The clearance between the throat and nozzle has to be small, although the cross-sectional area of the nozzle could be increased considerably beyond that shown, providing that the boiler were capable of supplying a sufficient stream of vapour.

(6) The neck has to be prolonged sufficiently beyond the nozzle to avoid the return of air past the jet.

(7) The water-cooling is extended well back behind the mouth of the nozzle to promote efficient operation.

(8) The surface-area and volume of the condenser and the cross-section of the return tube have to be adequate.

### (B) *Mercury-Vapour Condensation Pump.*

The second-stage vapour pump is shown to scale in Fig. 2, and is substantially as designed by LANGMUIR. It is made of steel tubing, the joints being welded and the whole nickel-plated. Since the pressure of the vacuum produced by the jet pump is as low as 0·001 mm., it is possible for the clearance between the deflector and the surrounding pump cylinder to be made wide, over 1 cm., so that the high speeds possible with this type of pump can be secured to advantage. An interior-cooler, which is provided in the upper half of the pump cylinder, effectively increases the area of condensation.

The two pumps are connected by steel tubing of $1\frac{1}{4}$-inch bore, the joints being made conveniently and quickly by the use of solder cups, which have been found to behave satisfactorily over a period of some months.



Digitized by Google

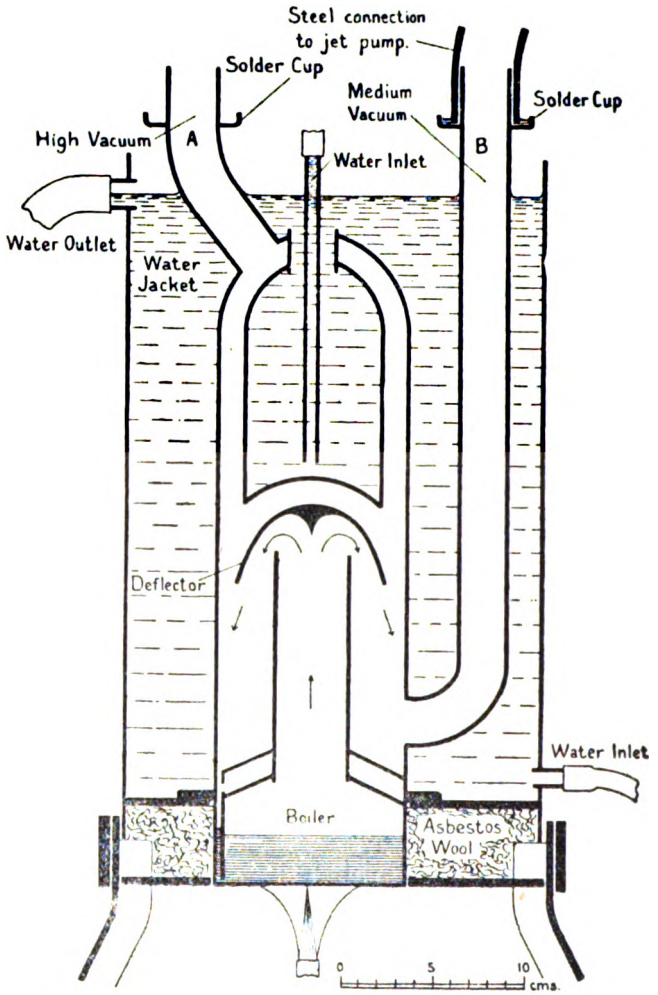


Fig. 2. Mercury-Vapour Condensation Pump.

## III. Speed of the Pump System.

The speed of a vacuum pump has been defined by Gaede in the following way :— If at any instant ($t$) the pressure in the vessel being exhausted is $p$, then

$$-\frac{dp}{dt} = kp,$$

where $k$ is a constant over a limited range of $p$. Since the time taken for exhaustion varies inversely as V, the volume being exhausted, we can write

$$-\frac{dp}{dt} = \frac{S}{V} \cdot p,$$

or, on integration,

$$S = \frac{V}{t_2 - t_1} \log_e \frac{p_1}{p_2}.$$

Digitized by Google

If the vessel being exhausted is immediately adjacent to the pump, then S is the speed of the pump and is measured in ccs./sec. of gas at the pressure obtaining at the instant considered.

Determinations have been made as to the way in which S varies with the pressure for the metal-pump combination under discussion. The values were obtained by means of a constant-flow apparatus, using KNUDSEN'S (12) general equation

$$F = aP + b\frac{(1 + c_1P)}{(1 + c_2P)}$$

for the flow of a gas through tubing of circular cross-section. F is the flow in ccs./sec., measured at a pressure of 1 dyne/cm.$^2$ for 1 dyne/cm.$^2$ pressure-difference between the ends of the tube; P is the average pressure in the tube in dynes/cm.$^2$, and $a$, $b$, $c_1$, and $c_2$ are constants for a given tube when air is the gas considered.

The flow-tube employed connected two spherical bulbs of about 8 cms. diameter, one of which was joined to the low-pressure end of the pump system and the other was connected to the high-pressure end of the pump system through a drying-tube. In this way the pumps were used to circulate dry air through the flow-tube, without occasioning any flow to the supporting oil pump, so that the latter in no way contributed to the pump-speed measured by this method. The pressures in the bulbs were read, as soon as a steady state obtained, by means of two McLeod gauges connected one to each bulb. For pressures less than about 150 dynes/cm.$^2$ the flow-tube was 42 cms. long and 1 cm. diameter; for higher pressures the flow-tube was 36 cms. long and 0·5 cm. diameter. The connecting tubing between the low-pressure bulb and the pump system was 14 cms. long and 2·71 cms. diameter.

To consider the case of the flow-tube for the lower pressures, the flow Q* through the tube under a pressure-difference $(p_1 - p_2)$ is given by the equation

$$Q = F(p_1 - p_2) = \left\{3{\cdot}24\ P + 279{\cdot}2\frac{(1 + 0{\cdot}1903\ P)}{(1 + 0{\cdot}2360\ P)}\right\}(p_1 - p_2).$$

Also $Q = S'p_2$, where S′ measures in ccs./sec. of air at pressure $p_2$ the pumping speed at pressure $p_2$ of the system comprising the pumps and connecting tube. The true pump speed S is obtained from this, as follows:—

If the pressure at the pump end of the connecting tube is $p_3$, and F′ is the flow through the tube for unit pressure-difference at its ends, then we have

$$Q = F'(p_2 - p_3) = S'p_2 = Sp_3,$$

or

$$\frac{1}{S} = \frac{1}{S'} - \frac{1}{F'}.$$

* Q is measured in ccs. per sec., the volume measurements being referred to a pressure of 1 dyne/cm.$^2$.



Digitized by Google

F′ can be obtained from KNUDSEN'S equation, being in this case

$$F' = 524\ P' + 13730\ \frac{(1 + 0{\cdot}516\ P')}{(1 + 0{\cdot}639\ P')}.$$

For low values of P′, F′ is nearly constant, while for higher values $\frac{1}{F'}$ is very small compared with $\frac{1}{S'}$, so that P′ may be taken as being equal to $p_2$ without making appreciable error.

In this way values of S have been found for various values of P′. In seeking a graphical representation of the results, it is more convenient and illuminating to plot S against log P′, and this has been done in Fig. 3. The graph clearly shows that the speed of the

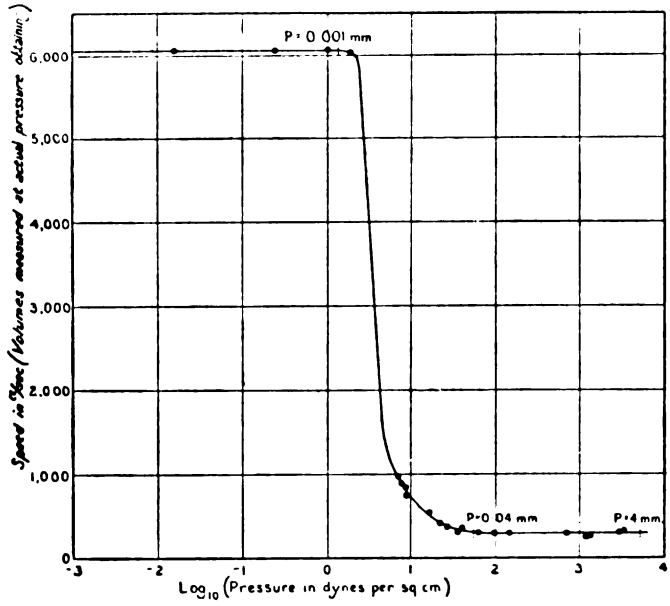


Fig. 3.

pump system at pressures from 4 mms. to 0·03 mm. is constant and equal to 300 ccs./sec., this being due to the jet pump alone. Below this pressure the condensation pump begins to operate and the speed increases rapidly to 6,000 ccs./sec. at 0·0015 mm. pressure, and remains constant at this value for lower pressures. This may be regarded as a minimum figure which normally obtains without undue care as to the conditions. However, by careful adjustment of the temperature for any particular pressure, it has been found possible to increase this value to as much as 10,000 ccs./sec.

## IV. ADVANTAGES OF THE PUMP SYSTEM.

The advantages of this type of two-stage pump system may be summarised as follows:—

(1) The speed of pumping is extremely high.

(2) Pressures of the order of $10^{-6}$ mm. or less (*i.e.* the lowest pressures obtainable by any type of pump) are possible when supported by a simple piston oil pump.

Digitized by Google

(3) There are no moving parts, so that there is a complete absence of vibration, mechanical wear, and noise.
(4) Vapours are pumped as efficiently as permanent gases.
(5) No drying or other reagents are required.
(6) The system is very robust and dependable since glasswork and rubber joints are eliminated.
(7) The temperature control is not critical and the system requires little or no attention while running.
(8) There is a continuous passage from supporting pump to high vacuum, so that no by-pass is necessary. The occurrence of a sudden leak in the apparatus under exhaustion or the failure of the supporting piston pump will not occasion the overflow of liquid from the pumping system.
(9) The running costs are low.
(10) The weight is much less than that of the usual rotary oil-pump combination, so that the system is more readily portable when occasion demands.

The all-metal pump system described in this paper, which has in the main been designed and tested by I. Backhurst, was made in the workshops of the National Physical Laboratory. Much help in the construction and testing of the pumps has been given by Mr. J. Balmanno and Mr. W. H. Sewell, of the Observer Staff of the Laboratory.

The investigation, which is being continued, has been carried out in part in connection with work in progress for the Radio Research Board of the Department of Scientific and Industrial Research.

## BIBLIOGRAPHY.

(1) The Geryk pump is described and illustrated in 'An Introduction to the Mechanics of Fluids', 1915, p. 197. By E. H. Barton. Published Longmans, Green & Co.
(2) K. T. Fischer. 'Verh. Deutsch. Phys. Ges.', vol. 7, p. 383, 1905.
G. Meyer. 'Verh. Deutsch. Phys. Ges.', vol. 10, p. 753, 1907.
(3) Winkelmann. 'Handbuch der Physik', vol. 1, part 2, p. 1314.
G. W. A. Kahlbaum. 'Ann. der Phys. u. Chem.', vol. 53, p. 199, 1894.
L. Zehnder. 'Ann der Phys.', vol. 10, p. 623, 1903.
A. Beutell and P. Oberhoffer. 'Chem.-Zeit.', vol. 43, p. 705, 1919.
H. P. Waran. 'Proc. Phys. Soc. Lond.', vol. 34, p. 120, 1921–22.
J. J. Manley. 'Proc. Phys. Soc. Lond.', vol. 34, p. 86, 1921 22.
G. Ranque. 'Comptes Rendus', vol. 172, p. 1653, 1921.
(4) E. Besselhagen. 'Ann. der Phys. u. Chem.', vol. 12, p. 425, 1881.
A. Stock. 'Ber. Deutsch. Chem. Ges.', vol. 38, p. 2182, 1905.
E. Grimsehl. 'Phys. Zeits.', vol. 8. p. 762, 1907.
U. von Reden. 'Phys. Zeits.', vol. 10, p. 316, 1909.
A. Stock. 'Zeits. Electrochemie', vol. 23, p. 35, 1917.
(5) W. Gaede. 'Verh. Deutsch. Phys. Ges.', vol. 7, p. 287, 1905
W. Gaede. 'Phys. Zeits.', vol. 6, p. 758, 1905.
W. Gaede. 'Verh. Deutsch. Phys. Ges.', vol. 9, p. 639, 1907.
W. Gaede. 'Phys. Zeits.', vol. 8, p. 852, 1907.

Digitized by Google

(6) W. Gaede. 'Ann der Phys.', vol. 41, p. 337, 1913.
(7) W. Gaede. 'Ann. der Phys.', vol. 46, p. 357, 1915.
(8) I. Langmuir. 'Gen. Elec. Rev.', vol. 19, p. 1060, 1916.
I. Langmuir. 'J. Franklin Inst.', vol. 182, p. 719, 1916.
I. Langmuir. 'Phys. Rev.', vol. 8, p. 48, 1916.
(9) W. W. Crawford. 'Phys. Rev.', vol. 10, p. 557, 1917.
(10) H. F. Stimson. 'J. Washington Acad. Sci.', vol. 7, p. 477, 1917.
(11) M. Volmer. 'Ber. Deutsch. Chem. Ges.', vol. 52, p. 804, 1919.
M. Volmer. Brit. Pat. 149313, 1919.
(12) M. Knudsen. 'Ann. der Phys.', vol. 28, p. 75, 1909.
(13) 'Rev. d'Optique', vol. 50, p. 274, 1922.

A good bibliography is contained in a series of articles in the 'General Electric Review' by Dushman on "The Production and Measurement of High Vacua", commencing in vol. 23, p. 493, 1920, which includes most of the earlier references given above. These articles are now published in book-form under the above title.

In Glazebrook's 'Dictionary of Applied Physics', vol. 1, p. 24, a useful list of references will also be found.

Digitized by Google

# A METAL ANNULAR-JET VACUUM PUMP

BY

IVOR BACKHURST, M.Sc.,
ASSISTANT IN THE PHYSICS DEPARTMENT.

AND

G. W. C. KAYE, O.B.E., M.A., D.Sc.,
SUPERINTENDENT, PHYSICS DEPARTMENT.

Digitized by Google

## ABSTRACT.

The mercury-vapour jet pump of steel, described in a previous paper, presents certain difficulties of construction, and accordingly a modification has been devised which is without welded joints. The pump is similar to the Langmuir type, but has additional inner tubes which together with a narrow annular jet enable it to work against higher back pressures. The pump represents an attempt to combine the advantages of the jet and condensation principles in a single and readily accessible unit. Backed by an ordinary piston oil pump, it constitutes a complete and efficient high-vacuum outfit. If mercury vapour is an objection, a liquid air trap must be employed. The pump will readily produce a vacuum of the order 0·00001 mm. mercury or less when working against a back pressure of 1 mm. mercury. The speed is high, the actual value, which varies between 1,000 and 7,000 ccs./sec., depending on the pressure in the vessel being exhausted, and also on the value of the back pressure against which the pump is working.


Digitized by Google

# A METAL ANNULAR-JET VACUUM PUMP.

By IVOR BACKHURST, M.Sc., Assistant, and G. W. C. Kaye, O.B.E., M.A., D.Sc., Superintendent, Physics Department.

[Reprinted from the 'Philosophical Magazine', Vol. 47, 1924.]

The all-metal mercury-vapour jet pump described in a previous paper* presents certain difficulties of construction on account of the welded joints; and accordingly a modification has been devised in which these are avoided. This is made of steel, and embodies in its design features characteristic of both the condensation and jet pump.

## *Description.*

Fig. 1, which is drawn to scale, shows the details of the construction. As will be seen, the boiler occupies the lower third of the pump, the upper two-thirds being surrounded by a water-jacket. The outer casing of the pump is made from one piece of weldless steel

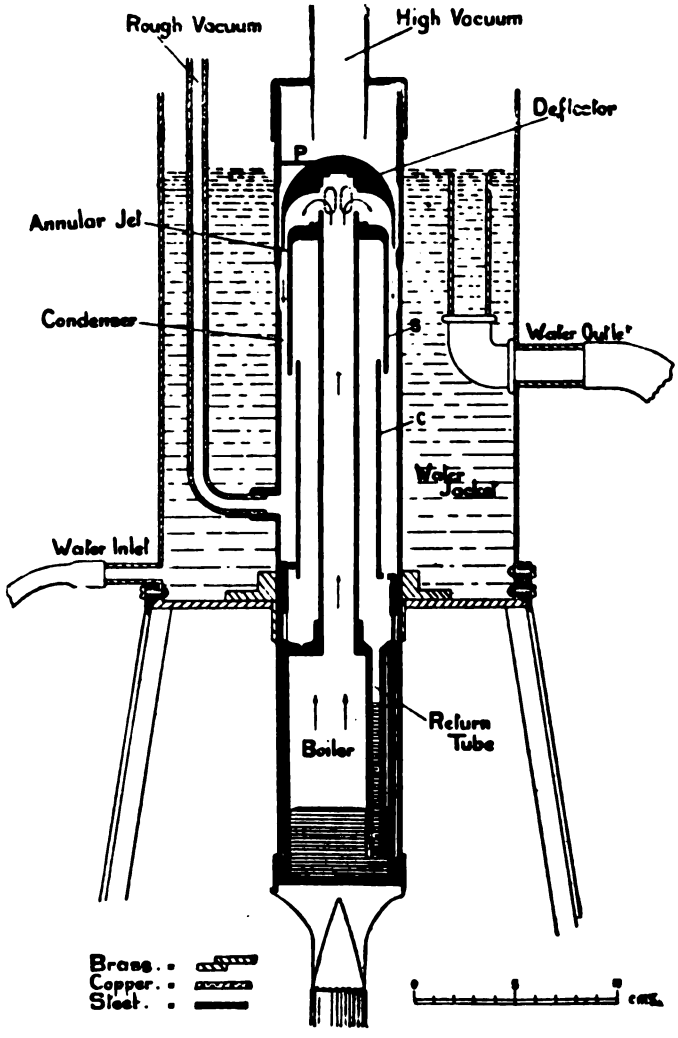


Fig. 1. Annular Jet Pump.

* Backhurst and Kaye, 'N.P.L. Collected Researches', vol. 19, Paper 18, or 'Phil. Mag.', vol. 47, p. 918, 1924.



Digitized by Google

tube. The lower end is closed by a steel cap, which is tightly screwed on, the joint being rendered air-tight by thorough copper and nickel plating. The screwed joint between a second steel cap on the upper end and the connecting tube to the high-vacuum is similarly plated, the cap being sealed to the pump by means of wax or solder. The re-entrant projection of the connecting tube into the pump tends to check the escape of mercury vapour to the high-vacuum system.

On removing the cap, all the inner parts of the pump may be lifted out together and can then be readily unscrewed apart. This construction makes cleaning exceptionally easy. The deflector and sleeve S may be screwed up or down to the positions giving maximum speed over the pressure-range desired. S is fixed by means of a lock-nut (shown) and the deflector is screwed down on to a washer (shown) of the right thickness to serve as a distance piece. When the deflector is adjusted so that its lower edge is level with the shoulder of the outer casing, the best position is obtained for general work. The curves shown in Fig. 2 were obtained with the deflector in this position. Three distance pins, P, screwed into the deflector, maintain it concentric with the casing.

The outer casing has two shallow grooves cut on its inner surface, one opposite the deflector, so forming a " shoulder " for the annular jet, the other just below the jet for the purpose of increasing the efficiency of the water cooling. The amount of mercury required in the boiler is about 70 ccs. (2 lb.).

*Action.*

The action of the pump is as follows :—Mercury vapour from the boiler passes up the centre tube and through holes at the top to the annular space between the deflector and the sleeve S, from which it issues as a jet and entrains gas diffusing from the annular space between the deflector and the outer casing. In the region between the casing and sleeves S and C, condensation of the vapour takes place, the condensed mercury falling through the hole in C, which is immediately above the return tube to the boiler. The sleeve C serves to prevent any mercury vapour which may leak from the boiler through the annular crevice and the several screwed joints just above the boiler from interfering with the vapour jet between S and the outer casing on which the pumping action depends. At the same time it prevents the condensing vapour from this jet from coming in contact with the hot central tube. Since the lower and wider part of C is in contact over an appreciable area with a water-cooled part of the outer casing, and, further, is separated from the top of the boiler by three pins (shown in Fig. 1), it remains comparatively cold, so that the condensed mercury falling on the sloping channelled part of C is not largely re-evaporated, as would happen were it to fall directly on the top of the boiler. It is therefore possible to use a large Bunsen burner and operate the boiler at a comparatively high temperature without any likelihood of failure due to overheating. In this way the blast of vapour obtained is sufficient to supply the annular jet, which has a width of 1·75 mms. and an actual jet area of 2·85 sq. cms. On account of the greater efficiency of the annular jet compared with the circular form, much higher speeds are

Digitized by Google

obtained over the usual jet-pump pressure-range. At lower pressures also the pump is still able to operate, functioning then as a condensation pump, though its speed as such is necessarily restricted by the narrow width of the jet.

The pump could readily be adapted for electrical heating instead of gas.

## *Speed.*

In Fig. 2 are curves showing the way in which the speed, as defined by GAEDE*, varies with the logarithm of the pressure at which the pump is working. For any particular

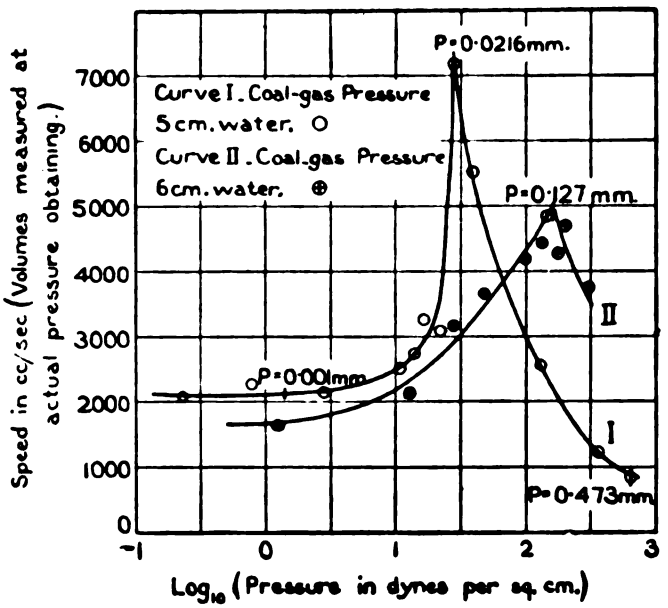


FIG. 2.

setting of the annular nozzle the pressure at which maximum speed is obtained depends on the working temperature of the boiler. If this temperature is increased, the maximum in general occurs at a higher pressure. Curves I and II were obtained using a 1-inch diameter Meker burner supplied with gas at pressures of 5 and 6 cms. of water respectively, the general arrangement of the speed-testing apparatus employed being similar to that previously described.† In the present case the dimensions of the flow-tube for the speed tests were: length 59·0 cms., diameter 1·0095 cms.; and of the tube connecting the latter with the pump, length 18·0 cms., diameter 2·25 cms. Throughout the experiments the supporting vacuum was maintained at 0·9 mm. mercury. The speed values found using another flow-tube 38·3 cms. long and 0·5077 cm. in diameter served as a check.

It will be seen from the curves that at pressures between 0·001 and 0·5 mm. mercury the speed varies between 1000 and 7000 ccs./sec., so that the pump is well suited to

* See 'N.P.L. Collected Researches', vol. 18, Paper 18, or 'Phil. Mag.', vol. 47, p. 925, 1924.

† *Loc. cit.*



Digitized by Google

support a high-speed condensation pump. It is also suitable for maintaining a vacuum in a tube such as a " gas " X-ray tube, liquid air not being required, as the presence of mercury vapour does not interfere with the working of such a tube. When only moderately low pressures are required (as in the " gas " tube), an adjustable leak of air as by a needle-valve or fine capillary is a convenient means of attaining the desired pressure.

It was found that the pump did not operate to advantage for back pressures exceeding 1 mm. mercury. Under this figure the performance of the pump, both as to speed and vacuum attained, is but little dependent on the back pressure.

We wish to acknowledge the assistance given by Mr. J. BALMANNO and Mr. W. H. SEWELL, of the Observer Staff of the Laboratory.

The investigation was carried out in part in connection with work for the Radio Research Board of the Department of Scientific and Industrial Research.

Digitized by Google

# THE COMPOSITION OF THE X-RAYS FROM VARIOUS METALS

BY

G. W. C. KAYE, O.B.E., M.A., D.Sc.,
SUPERINTENDENT OF THE PHYSICS DEPARTMENT.

Digitized by Google

## ABSTRACT.

The X-rays from a bulb excited by low voltages (10,000 to 50,000 volts) are rich in the characteristic radiation of the anticathode. In the case of iron, nickel and copper, the amount of K-radiation lies between 80 and 90 per cent. In the case of platinum the proportion of L-radiation is from 40 to 60 per cent. Evidence of characteristic radiations softer than the K- and L-radiation has been obtained.


Digitized by Google

# THE COMPOSITION OF THE X-RAYS FROM VARIOUS METALS.

By G. W. C. KAYE, O.B.E., M.A., D.Sc., Superintendent of the Physics Department.

[Reprinted from the 'Proceedings of the Royal Society', A, Vol. 93, 1917.]

In a paper published in the 'Philsophical Transactions'* in 1908, the writer described some experiments on the X-rays emitted by a variety of metals when used as anticathodes in an X-ray bulb. Among the results established was the homogeneity of a large proportion of the X-rays when the bulb was very "soft". The absorption curves of the several homogeneous radiations revealed their identities with the characteristic "secondary" radiations which Barkla and Sadler had then recently discovered.

The experiments described in the present paper are an extension of the above, and were carried out partly at the Cavendish Laboratory in 1908 and partly at the National Physical Laboratory just prior to the war. The writer's military duties have prevented the continuation of the work, and the results are now put on record in the hope that they may help to further the progress of the subject, to which the more precise method of the crystal-spectrometer has given a great impetus from a different point of view.

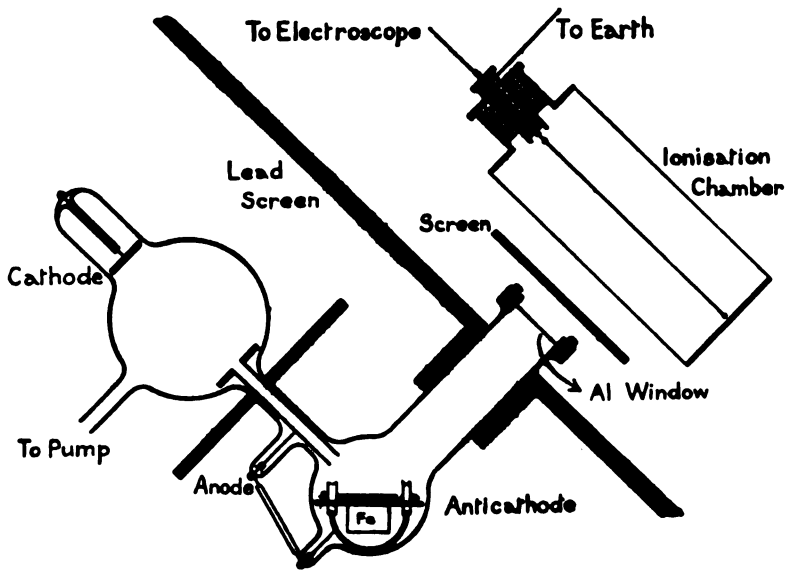


Fig. 1.

*Apparatus.*

The apparatus employed is sufficiently explained by Fig. 1, which is approximately to scale. As in the earlier experiments, the various anticathodes were mounted on a trolley, which could be magnetically propelled. A coil-discharge was employed, the applied voltage being indicated by an alternative spark-gap between polished balls

* Series A, vol. 209, p. 123.

Digitized by Google

2·5 cms. in diameter. For balls of this size and spark-gaps in the neighbourhood of 1 cm., the expression

$$V = 30{,}000d + 2000$$

gives approximately the voltage V, corresponding to a spark-length of $d$ cm.

The X-rays passed out of the tube through an aluminium window (2 cms. diameter and 0·0065 cm. thick), and were received by an ionisation chamber, the front face of which was about 3 cms. from the window. The depth of the chamber was 4 cms.; the sides were of thin aluminium leaf. A Wilson tilted electroscope was employed to measure the ionisation currents.

The quality of the X-rays was tested by absorption screens inserted between the window and the ionisation chamber. Metal leaf was used for the thinnest screens.

For details of the various experimental precautions, the writer's earlier paper on the subject may be consulted. In the present paper the radiations dealt with are those from iron, nickel, copper, aluminium, and platinum.

### *Logarithmic Absorption-Curves.*

The absorption-coefficient $\lambda$ of a substance is defined by the expression $I_d = I_0 e^{-\lambda d}$, where $I_0$ is the initial intensity of an X-ray beam and $I_d$ the intensity after transmission through a screen of the substance of thickness $d$. Accordingly, if the thickness of screen (as abscissa) is plotted against $\log_{10} (I_d/I_0)$, the slope of the tangent to the curve at any point gives (when multiplied by 2·3) the value of $\lambda$ at that point. For ordinary heterogeneous X-rays, $\lambda$ diminishes as $d$ increases, but, if the rays are homogeneous, the graph is a straight line.

### *Analysis of the Log-Absorption Curves.*

The method employed in the present experiments was gradually to cut down the X-rays until the log-absorption curve showed that the residual rays were homogeneous or nearly so. This "end-radiation" was subtracted (graphically) from the whole radiation by producing backwards the final straight part of the absorption curve. A new log-absorption curve was then plotted, employing as ordinate the log of the intensity-difference derived as above. The resulting graph proved in practice to be either (*a*) a straight line throughout its length, or (*b*) a curve merging into a straight line as the thickness of screen increased. In the latter event the process of subtraction was applied again.

The underlying notion was to ascertain whether by such analysis the absorption curves could be made to reveal the presence of characteristic radiations. The justification for the method depends upon its success, for it is possible to express, with very fair accuracy, almost any normal type of absorption curve as the sum of two or three exponentials. If such components have a physical reality, they will be found to recur in the different absorption curves under varying conditions.

Digitized by Google

With low discharge voltages on the tube, the dilution of the characteristic rays by general radiation is slight, and the existence of an appreciable amount of a characteristic radiation is usually betrayed before analysis by a perceptible flattening of the absorption curve over part of its course. But with higher voltages the conditions change, and the method is not so easy unless the accuracy of the measurements and of the graphical analysis is high. The present experiments are not offered as final, but they do, at any rate, indicate that by such means the detection of component radiations is possible provided they are present in appreciable amounts. That such homogeneous components may be expected is shown by the fact that the lines in high-frequency spectra are now known to be not nearly so limited in number as was at first believed.

In those cases where the method of graphical analysis is profitable, there is never any difficulty in "spotting" the K and L characteristic radiations; their absorption-coefficients always come out sufficiently near to the accepted values. Incidentally, the method also reveals the proportion of each radiation present in a beam of rays.

In all the log-absorption curves illustrated in this paper, the original curve is indicated by a heavy line, and the resulting components by thin lines. Most of the radiations were analysed by screens of aluminium, platinum, and copper. In general, the curves for platinum screens are similar to those for aluminium screens; those for copper screens do not always share their common characteristics.

### *Iron Radiation.*

Figs. 2, 3, 4 show the log-absorption curves of iron radiation in screens of aluminium, platinum, and copper respectively. In each case the voltage applied to the X-ray tube was 23,000.

*Aluminium Screens.*—The absorption curve (Fig. 2) is practically straight for screens

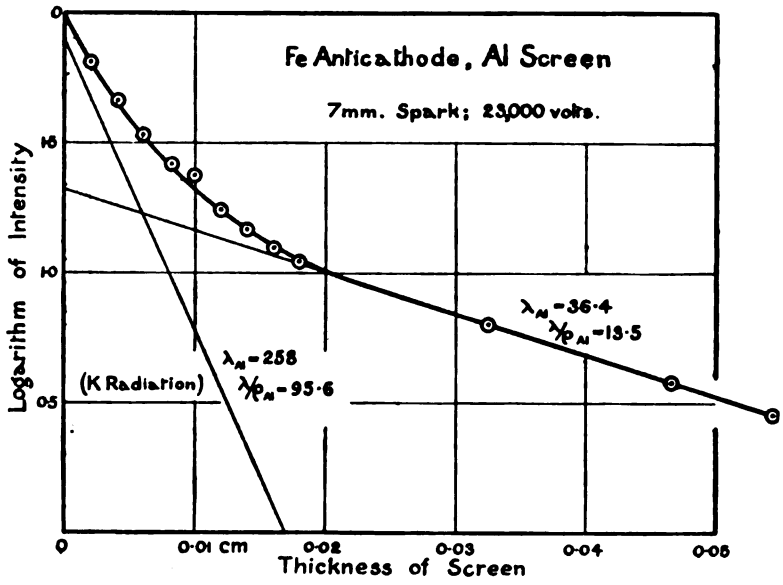


FIG. 2.



Digitized by Google

thicker than 0·02 cm. There is about 20 per cent. of this homogeneous end-radiation ($\lambda/\rho_{Al} = 13{\cdot}5$ c.g.s.), and analysis reveals that the remaining 80 per cent. consists of iron K-radiation ($\lambda/\rho_{Al} = 95{\cdot}6$).

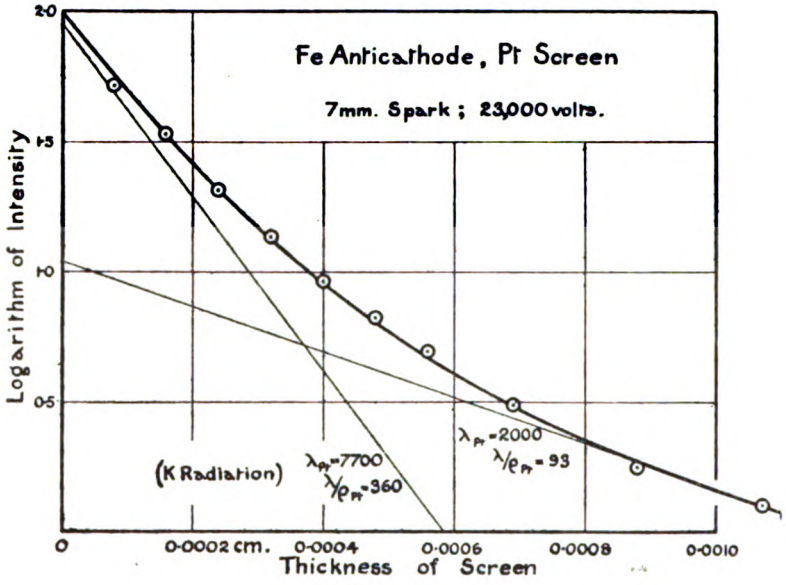


FIG. 3.

*Platinum Screens.*—Fig. 3 similarly displays the absorption curve and its resolutes for screens of platinum. There is about 90 per cent. of Fe K-radiation ($\lambda/\rho_{Pt} = 360$) and 10 per cent. of an end-radiation with $\lambda/\rho_{Pt} = 93$.

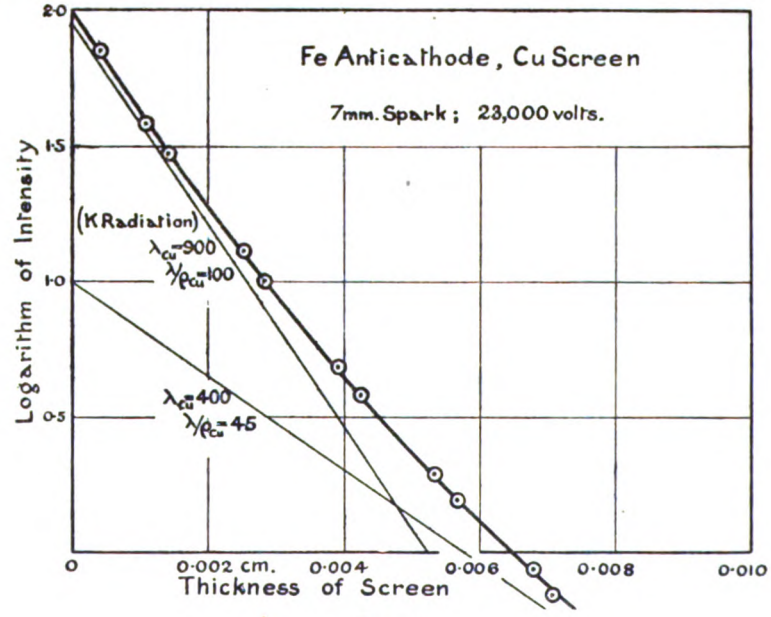


FIG. 4.

*Copper Screens.*—The analysis of the log-absorption curve (Fig. 4) again gives about 90 per cent. of Fe K-radiation ($\lambda/\rho_{Cu} = 100$) after deducting 10 per cent. of a harder end-radiation with $\lambda/\rho_{Cu} = 45$.

Digitized by Google

Figs, 2, 3, and 4 are thus very similar to each other and lead to almost identical results.

*Nickel Radiation.*

Figs. 5, 6, 7 are a corresponding set of curves for nickel radiation, again with an applied voltage of 23,000.

*Aluminium Screens.*—Just as with iron radiation, two components represent the absorption curve (Fig. 5), viz., 86 per cent. of nickel K-radiation ($\lambda/\rho_{Al} = 68$) and 14 per

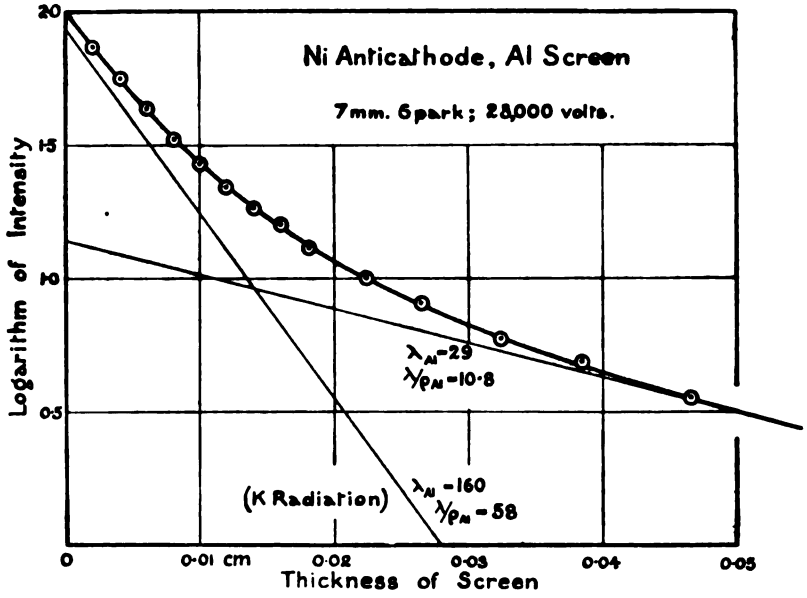


FIG. 5.

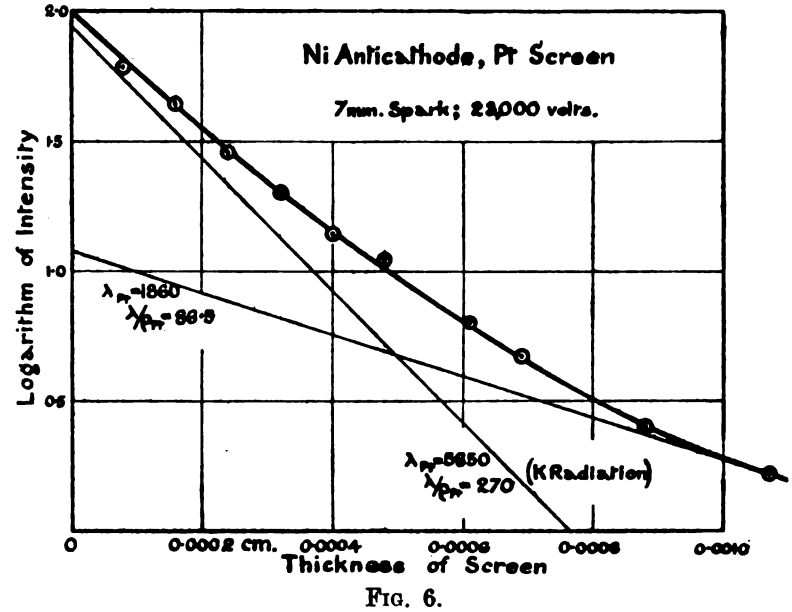


FIG. 6.



Digitized by Google

cent. of end-radiation with $\lambda/\rho_{Al} = 10{\cdot}8$). This agrees closely with RAWLINSON'S figures,* who analysed nickel radiation generated under a voltage of 30,000, into 79 per cent. of K-radiation and 21 per cent. of rays with $\lambda/\rho_{Al} = 10{\cdot}4$.

*Platinum Screens.*—The absorption curve (Fig. 6) is like that for aluminium screens, and we find after subtracting 12 per cent. of end-radiation with $\lambda/\rho_{Pt} = 86{\cdot}5$ that the remaining 88 per cent. is entirely Ni K-radiation ($\lambda/\rho_{Pt} = 270$).

*Copper Screens.*—Thus aluminium and platinum screens absorb iron and nickel radiations in similar fashion, but we now find that copper screens treat the two radiations very differently. With nickel radiation, the absorption curve (Fig. 7) is, except for the thinnest

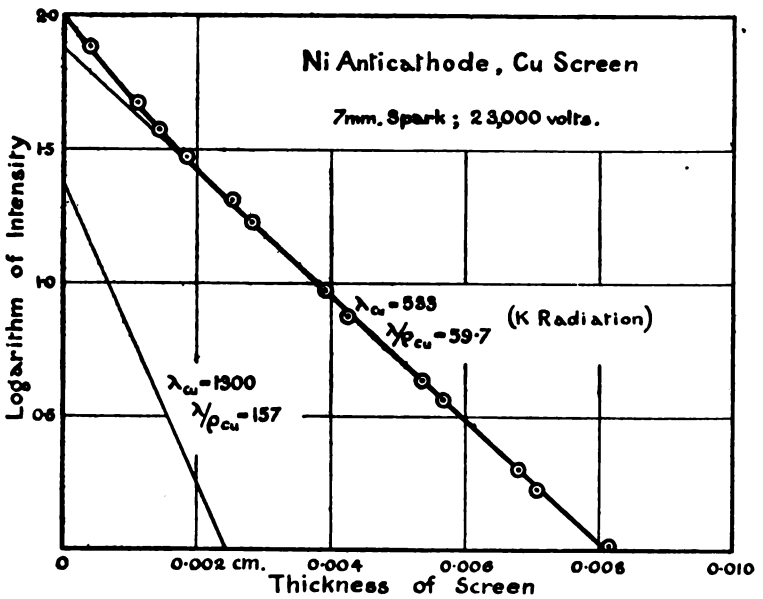


FIG. 7.

screens, straight throughout its length, revealing about 75 per cent. of Ni K-rays. Not even when the radiation was reduced to $\frac{1}{2}$ per cent. was there any trace of the end-radiation of Figs. 5 and 6, and we are led to infer that the end-radiation has been abnormally absorbed and transformed into copper K-radiation, the absorption-coefficient of which does not differ very greatly from that of nickel K-radiation.

On the other hand, a soft component ($\lambda/\rho_{Cu} = 157$) has now made its appearance to the extent of 25 per cent. This may be another characteristic radiation for which Al and Pt screens are specially absorbent. It is very probably mixed with the softer copper radiation ($\lambda/\rho_{Cu} = 100$) referred to below, which has been excited in the screen by the Ni rays from the bulb. Iron radiation is a good deal softer than Ni radiation, and the consequent inability of the Fe radiation to excite any such copper component would be an explanation of its absence in the corresponding absorption curve in Fig. 4.

* 'Phil. Mag.', vol. 28, p. 274, 1914.

Digitized by Google

*Copper Radiation.*

Figs. 8, 9, and 10 give the graphs for copper radiation. The applied voltage in each case was again 23,000.

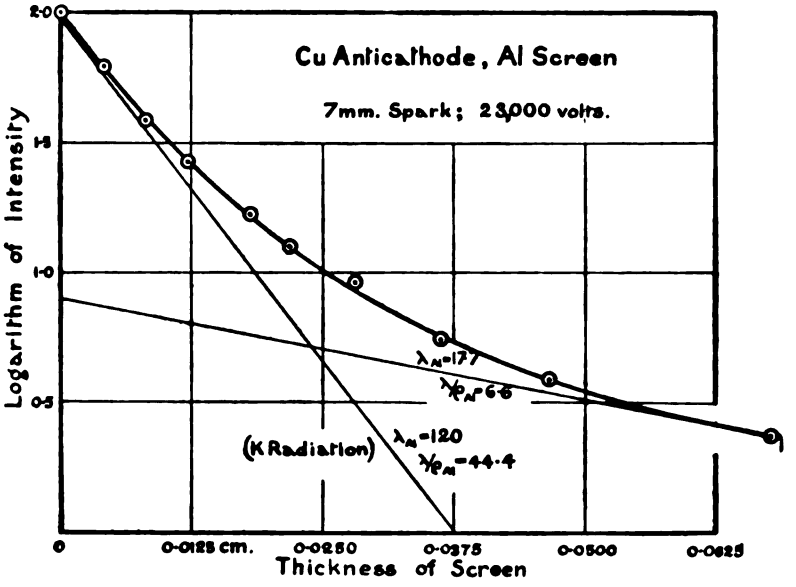


FIG. 8.

*Aluminium and Platinum Screens.*—Figs. 8 and 9 show the log-absorption curves of Cu radiation in Al and Pt respectively. Subtracting 8 per cent. of end-radiation reveals

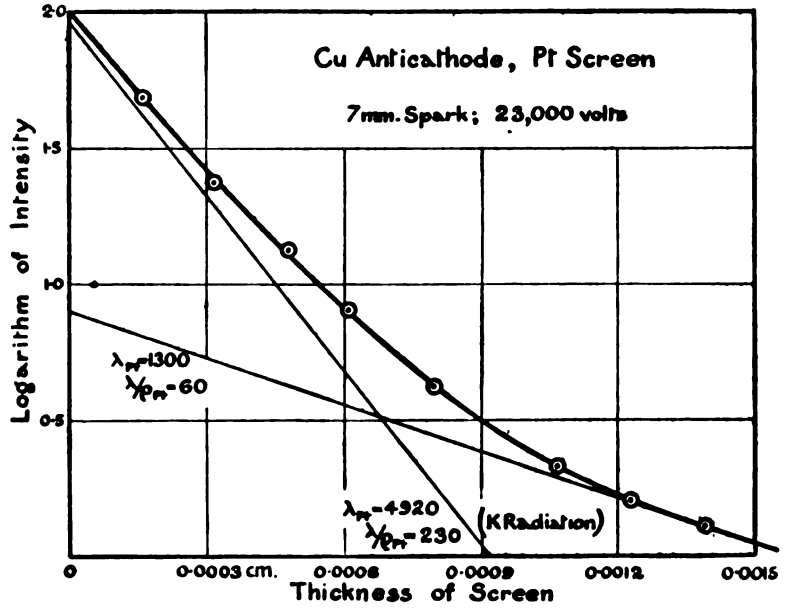


FIG. 9.

in each case the copper K-radiation as making up the rest of the rays. The curves are, therefore, precisely similar in type to Figs. 2 and 3 for Fe radiation, and 5 and 6 for Ni radiation.

Digitized by Google

*Copper Screens.*—If now we turn to Fig. 10, we find that copper screens treat nickel and copper radiations very similarly. Just as with Ni radiation (Fig. 7), but unlike Fe radiation (Fig. 4), the end-radiation completely disappears and is replaced by Cu K-radiation. At the same time a new and softer component appears with a $\lambda/\rho_{Cu}$ of about 100.

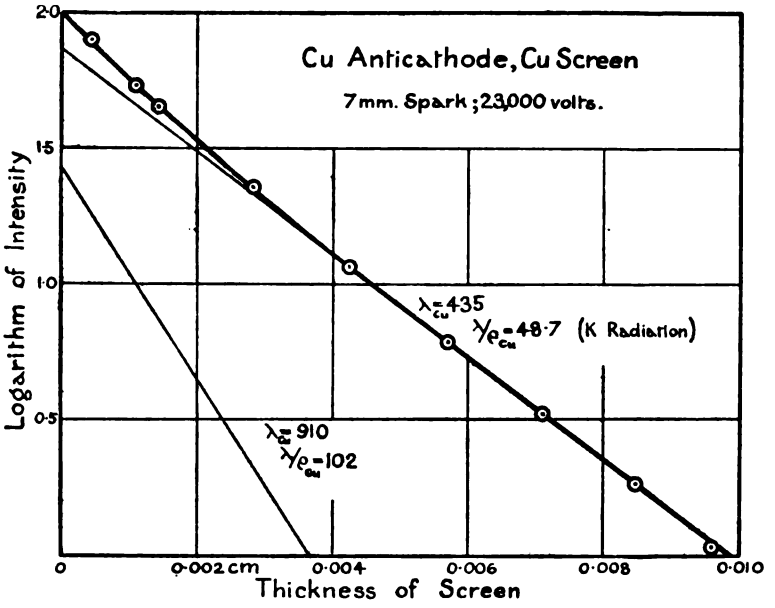


FIG. 10.

Fig. 11 shows the corresponding curve with a higher voltage (45,000) on the tube. Both the preceding radiations are again revealed after subtracting a small amount of end-radiation.

The experiment was repeated for a number of applied voltages. In each case the two radiations were found to be present. Table I gives the results, and it will be seen that the proportion of K-radiation increases with the voltage while that of the softer radiation diminishes. It would certainly be of great interest to extend the limits of voltage employed. According to WHIDDINGTON, at voltages below about 10,000 no K-radiation is generated, and it is a matter for enquiry to see if the softer characteristic component here referred to plays a prominent part under such conditions. The calculated wavelength of this softer component is about $2 \times 10^{-8}$ cm. So far as I know, it has not been detected spectroscopically.

TABLE I.

| Spark. | Volts. | Radiation. | | |
|---|---|---|---|---|
| | | $\lambda/\rho_{Cu} = 100$. | $\lambda/\rho_{Cu} = 53$, K-radiation. | End-radiation. |
| mms. | | per cent. | per cent. | per cent. |
| 2·5 | 10,000 | 32 | 68 | 0 |
| 7 | 23,000 | 26 | 74 | 0 |
| 10 | 32,000 | 24 | 76 | 0 |
| 17 | 45,000 | 16 | 82 | 2 p.c. of $\lambda/\rho_{Cu} = 7$. |

Digitized by Google

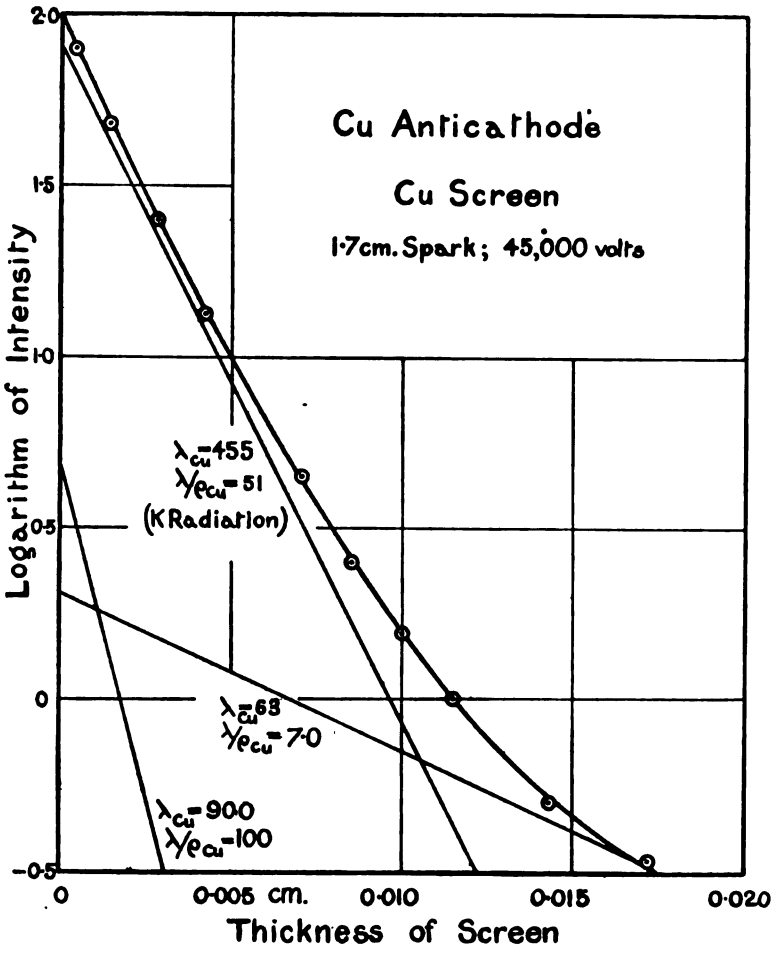


FIG. 11.

*Aluminium Radiation.*

Figs. 12, 13, 14 give the absorption curves for Al radiation when passed through Al, Pt, and Cu screens. The voltage is 23,000.

*Aluminium Screens.*—The absorption curve (Fig. 12) may be analysed approximately into 50 per cent. of end-radiation ($\lambda/\rho_{Al} = 15{\cdot}5$), and 50 per cent. of a radiation having $\lambda/\rho_{Al} = 94{\cdot}3$. Both values are rather low as there is a small proportion of penetrating radiation present. For example, the rays which remain after passage through a 1 mm. screen of Al have a $\lambda/\rho_{Al} =$ of about 1.

*Platinum Screens.*—Subtracting end-radiation ($\lambda/\rho_{Pt} = 95$) amounting to about 25 per cent. of the total radiation, the remaining 75 per cent. may be represented by a straight-line radiation having $\lambda/\rho_{Pt} = 285$.

*Copper Screens.*—Subtracting the end-radiation (15 per cent. in all) with a $\lambda/\rho_{Cu} = 26$, the remainder can be represented by a homogeneous radiation with $\lambda/\rho_{Cu} = 108$.

The above results on aluminium radiation are offered only as tentative.

Digitized by Google

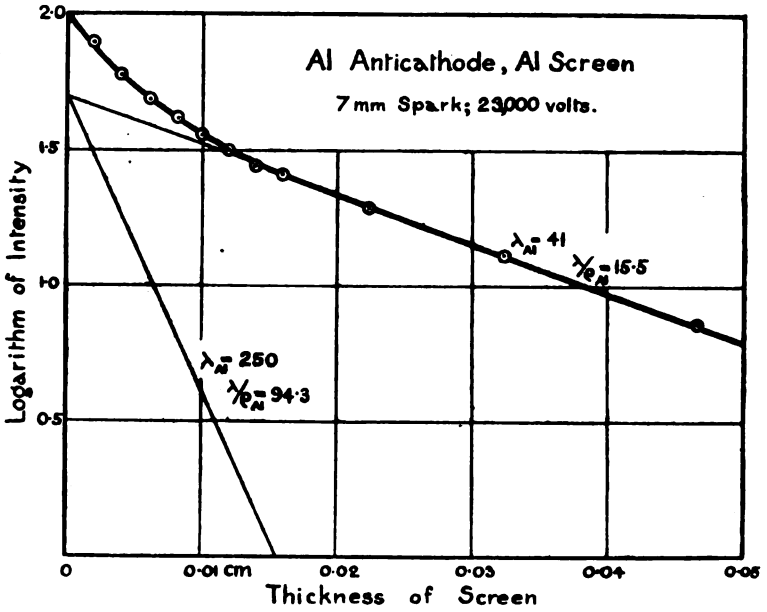


FIG. 12.

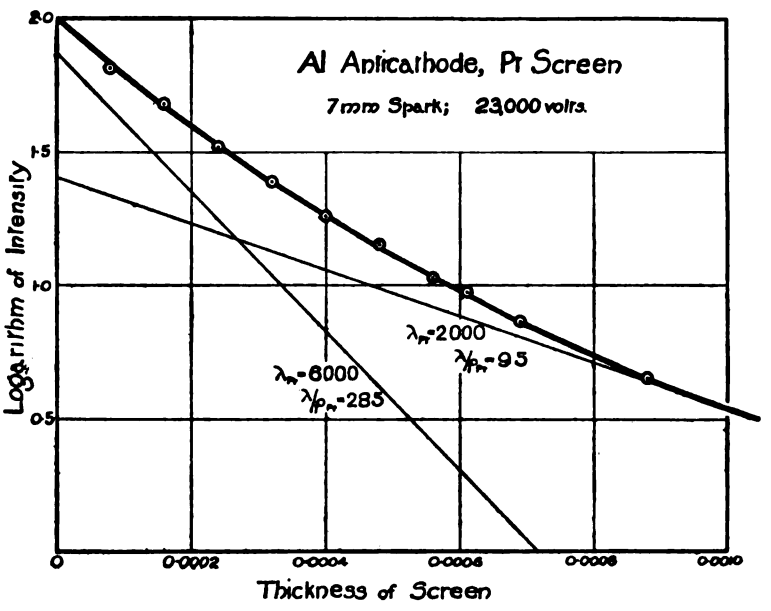


FIG. 13.

*Platinum Radiation.*

Figs. 15, 16, 17 deal with platinum radiation generated under a voltage of 23,000.

*Aluminium Screens.*—Fig. 15 betrays little indication of homogeneity until 10 per cent. of end-radiation ($\lambda/\rho_{Al} = 5{\cdot}6$) is deducted, when a component consisting of 60 per cent. of Pt L-radiation ($\lambda/\rho_{Al} = 23{\cdot}7$) clearly reveals itself. Admixed with this is 30 per cent. of another and softer component which betrays its existence with the thinnest screens. Further analysis shows that this latter radiation is homogeneous and has a $\lambda/\rho_{Al} = 70$ (approx.).

Digitized by Google

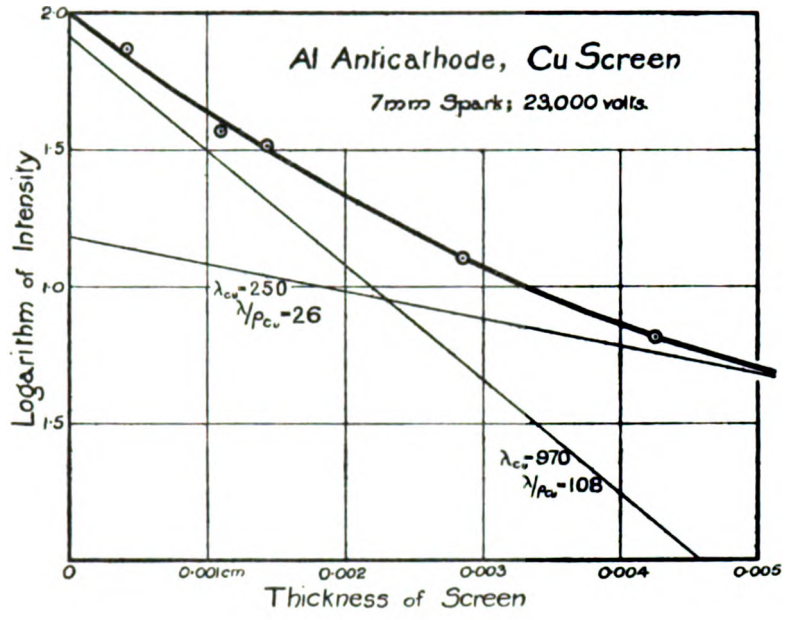


FIG. 14.

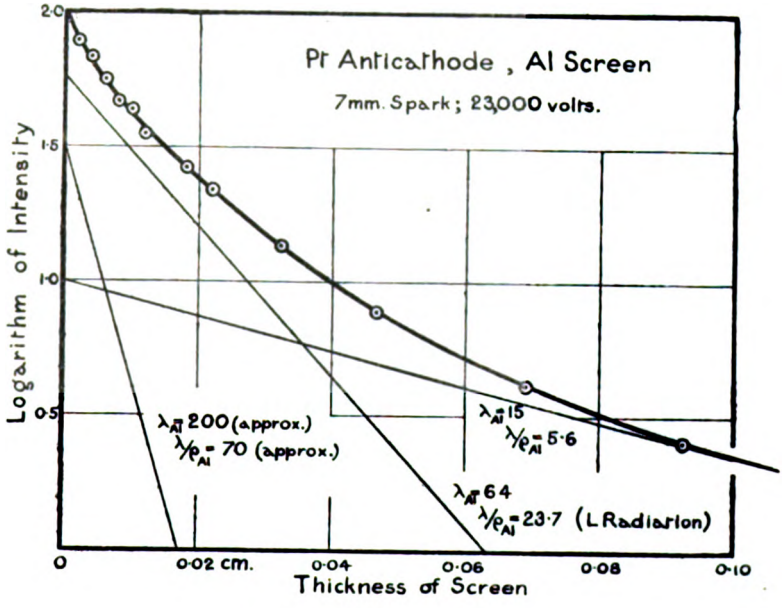


FIG. 15.

*Platinum Screens.*—In Fig. 16 the end-radiation has disappeared, and the homogeneity of much of the radiation is apparent. There is no evidence of the presence of a harder type of ray even though the initial intensity is cut down to nearly $\frac{1}{2}$ per cent. The curve is readily resolvable into 60 per cent. of Pt L-radiation ($\lambda/\rho_{Pt} = 109$) and 40 per cent. of a softer homogeneous component with $\lambda/\rho_{Pt} = 330$.



Digitized by Google

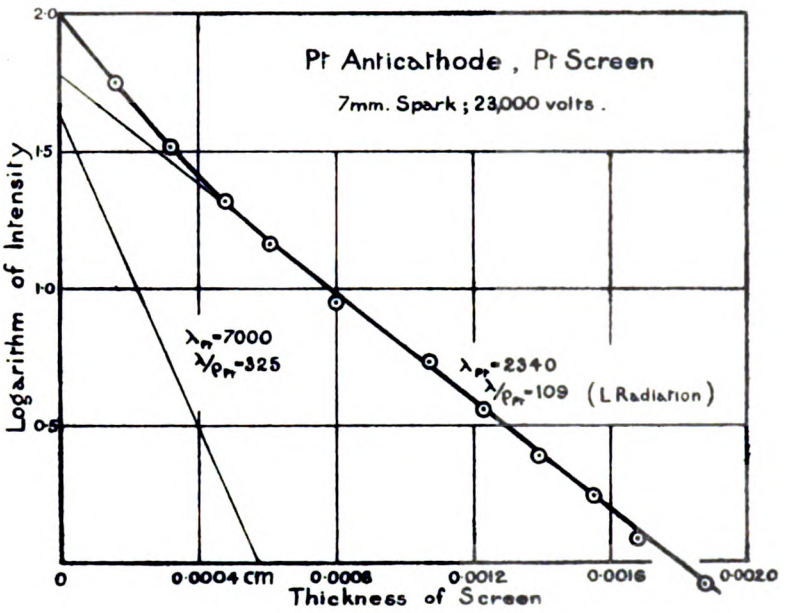


FIG. 16.

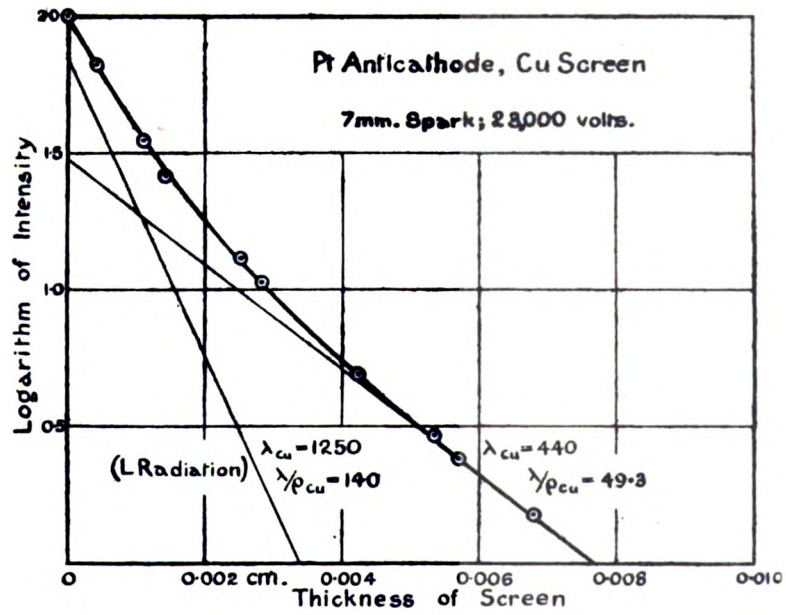


FIG. 17.

Thus both Al and Pt screens agree in indicating the existence of two homogeneous beams in Pt rays, one the L-radiation, the other with an absorption coefficient three times as large.

Absorption curves obtained at higher and lower voltages, using Pt screens, disclosed the two components in each case. The results, which are given in Table II, show that with a low voltage on the tube more than half the X-rays consist of the softer component.

Digitized by Google

An increase in the voltage leads to an increase in the amount of L-radiation, and a decrease in that of the softer radiation. Calculation gives a wave-length for the latter of about $2{\cdot}5 \times 10^{-8}$ cm.

TABLE II.

| Spark gap. | Volts. | Radiation. | |
|---|---|---|---|
| | | $\lambda/\rho_{Pt} = 330$. | $\lambda/\rho_{Pt} = 110$, L-radiation. |
| mms. | | per cent. | per cent. |
| 4 | 14,000 | 63* | 37 |
| 7 | 23,000 | 40 | 60 |
| 10 | 32,000 | 37 | 63 |

* Probably another and even softer component present as well.

*Copper Screens.*—In Fig. 17 the absorption curve is built up of 30 per cent. of end-radiation ($\lambda/\rho_{Cu} = 49$) and 70 per cent. of Pt L-radiation ($\lambda/\rho_{Cu} = 140$).

We have here an example of the importance of the choice of screen. for whereas a Pt screen allows nothing harder than the L-radiation to pass, a Cu screen allows nothing softer than the L-radiation to pass. This behaviour on the part of copper has been noticed by BRAGG* in his spectroscopic work; he remarks that the A peak of Pt is completely wiped out by a copper screen.

### *Ordinary X-Ray Bulbs.*

A good many attempts have also been made to resolve the absorption curves obtained by using Al screens and ordinary X-ray bulbs (with platinum anticathodes) excited by considerable voltages. The writer's experience goes to show that in such cases the end-radiation, even after it is cut down to $\frac{1}{2}$ per cent. or less, is never really homogeneous. It may, however, be taken as such for the purposes of approximate analysis. Such analysis almost always reveals the presence of Pt L-radiation. In the case of one tube worked at 30 mm. spark, there was 40 per cent. of L-radiation in the rays transmitted through the glass walls of the bulb; in the case of another at 85 mm. spark, 37 per cent. Most tubes also reveal the presence of a component having $\lambda/\rho_{Al} = 7{\cdot}4$, in proportions which increase with the voltage, at any rate, within a moderate range.

The extent of the work was not competent to throw doubt on the prevailing view that the bulk of the X-rays from a bulb worked under voltages such as obtain in medical practice consists of other than general heterogeneous radiation.

The writer has perforce had to content himself with little more than setting down observations. For the preparation of the diagrams he is greatly indebted to Mr. W. F. HIGGINS, M.Sc.

* 'Roy. Soc. Proc.', A, vol. 89, p. 434, 1913.



Digitized by Google

Digitized by Google

# X-RAY PROTECTIVE MATERIALS

BY

G. W. C. KAYE., O.B.E, M.A., D.Sc.,
SUPERINTENDENT OF THE PHYSICS DEPARTMENT,

AND

E. A. OWEN, M.A., D.Sc.,
SENIOR ASSISTANT, PHYSICS DEPARTMENT.

Digitized by Google

## ABSTRACT.

The protective values expressed in terms of the equivalent thickness of lead have been measured for a variety of materials. Numerically, 1 mm. of the material in question is equivalent to the following thicknesses of sheet lead in millimetres :—

| | |
|---|---|
| Lead glass | 0·12 to 0·20 |
| Lead rubber | 0·25 to 0·45 |
| Bricks and concrete | About 0·01 |
| Woods | 0·001 or less |
| Baryta plaster | 0·05 to 0·13 |
| Steel | 0·15 |

The above figures relate to tungsten X-rays generated by 100,000 volts.


Digitized by Google

# X-RAY PROTECTIVE MATERIALS.

By G. W. C. KAYE, O.B.E., M.A., D.Sc., Superintendent, and E. A. OWEN, M.A., D.Sc., Senior Assistant, Physics Department.

[Reprinted from the 'Proceedings of the Physical Society of London', Vol. 35, 1923.]

## Introductory.

The steady addition to the already lengthy list of casualties to hospital and other X-ray workers led to the formation nearly two years ago of an X-ray and Radium Protection Committee (under the chairmanship of Sir Humphry Rolleston) which drew up a series of recommendations for the better protection and general improvement of the working conditions of the X-ray operator. These recommendations have resulted in a large number of X-ray protective materials being submitted for test to the National Physical Laboratory, which from the outset agreed to work in co-operation with the Committee, and has inspected the X-ray departments of many hospitals from the point of view of the Committee's recommendations.

It is well known that the absorption of an atom is greatest for those X-rays which have wave-lengths slightly shorter than one or other of its characteristic radiations, and partly with this in mind it was thought that it would be of value to ascertain the protective efficiencies of the various materials which are commercially available for the purpose of affording protection to the radiologist. Among these are sheet lead, lead impregnated rubber, lead glass, and various wall compositions such as barium-sulphate plasters, etc. The choice of one or other is normally dictated by considerations such as dielectric strength, portability, electrical and thermal conductivity, and not least by price.

Protection may be afforded in a variety of ways in practice; for example, by mounting the tube in a surrounding tube box suitably designed to permit the freedom of movement desired, or where this is impracticable the operator and his controls are situated behind a screen or wall which is constructed to give the necessary protection. Less frequently and conveniently the operator is "armoured" and wears protective aprons, gloves, face mask, or goggles.

To the inexperienced the practice of speaking of percentage absorption may be misleading and calculated to give a wrong impression of the value of a protective material. It is not always realised how rapid the rate of absorption is with thin layers, and how slow with thicker layers. For example, in the case of tungsten X-rays generated at 120,000 volts, a sheet of lead only 0·1 mm. thick absorbs as much as 80 per cent. of the radiation, whereas a sheet 2 mms. thick only increases this figure to 99·4 per cent.

For simplicity, therefore, the Protection Committee recommended that the protection afforded by a material should always be referred to in terms of the equivalent thickness

Digitized by Google

of lead. This use of lead as a standard of reference, while not wholly free from objection, is very convenient for the approximate accuracy which suffices in practice, especially in dealing with composite or laminated materials, as the lead values of the several layers can be regarded as additive. The Committee laid down certain thicknesses of lead which it regarded as the minima which should be employed under specified conditions; and, in view of the very unsatisfactory conditions which prevail in the majority of X-ray installations in this country, we have been led to put on record some of our measurements in this connection.

## Apparatus.

The method of test adopted by the Laboratory is the very simple one of measuring by an ionisation method the absorption of a beam of X-rays by a material of given thickness, and then ascertaining the thickness of lead sheet which produces the same degree of absorption. A Coolidge tube with a tungsten target is usually employed for the purpose, and, to avoid any possible anomaly arising from selective absorption, comparisons are conducted with at least two different exciting voltages. The size of the pencil of rays utilised is dictated by the absorptive qualities of the specimen to be measured. An obvious convenience is the provision of a series of lead sheets graded in progressive order of thickness, which can be rapidly piled at will.

Fig. 1 shows in plan the details of an apparatus employing a balance method, which proves a useful alternative to the direct method referred to above. The diagram is self-explanatory, but one or two points may be mentioned. The two ionisation chambers

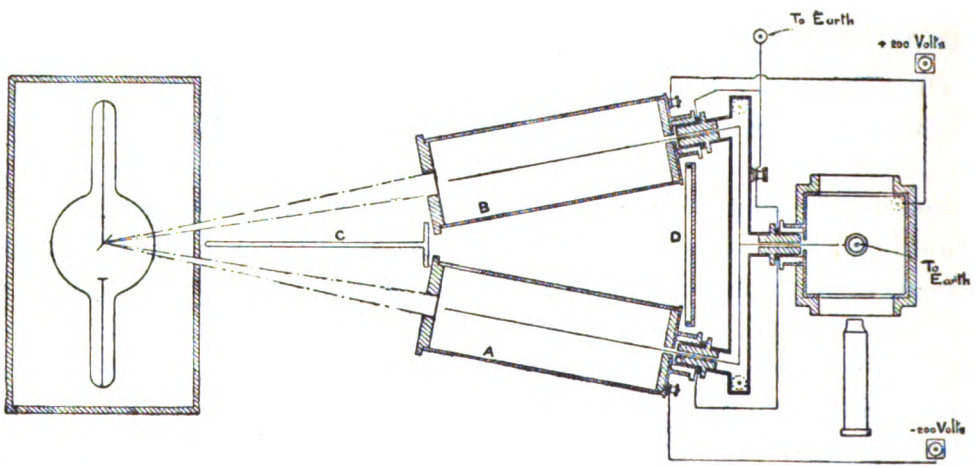


Fig. 1.

A and B are exactly alike and placed as symmetrically as possible with respect to the target of the X-ray bulb. The near ends are closed with aluminium sheet 0·5 mm. thick. The various insulating plugs are of ebonite with sulphur ring insertions and earthed guard rings. The sides of the electroscope are of lead 3 mms. thick. The gold-leaf system is initially earthed. The outer case of the electroscope is raised to 200 volts.

Digitized by Google

whilst the outer cases of the two ionisation chambers are raised to + 200 and — 200 volts respectively. Suitably disposed lead screens C and D prevent anomalies rising out of scattered or stray radiation.

The whole system is mounted on a wooden stand provided with levelling screens and means of lateral adjustment, so that the position of exact balance of ionisation between the two chambers can readily be found. When this has been secured, the test sample is placed in front of one of the ionisation chambers, and the thickness of lead in front of the other chamber rapidly altered until balance once again results.

The above two methods serve in general, but there are certain protective articles the shape of which makes it difficult to test the protection afforded in all directions. To cope with these exceptional cases, a third apparatus has been constructed consisting of a small exploring ionisation chamber connected by a flexible conductor to a gold-leaf electroscope.

## Results.

The table given on the following page contains the " lead equivalents " for a variety of materials, *i.e.* the thickness of lead equivalent in absorbing power to unit thickness of the material. The results are mostly for X-rays generated by 100,000 volts, but the values hold over a considerable range of some 20,000 or 30,000 volts on either side of this figure. The values are ordinarily diminished by from 5 to 10 per cent., when the voltage is 50,000. In the case of those materials which have feebly absorptive properties it was found convenient to compare them with lead through the intermediary of aluminium.

Provision is now being made for the measurement of lead equivalents at voltages ranging up to 200,000. It is intended also to extend the investigation to include gamma rays from radium.

*Walls and Screens.*—We have included a number of samples of building and other materials, as a knowledge of the various protective figures is not without value when buildings intended for radiological purposes are being erected. It will be remarked that the lead values of bricks and concrete are mostly of the order of 0·01. Thus, the lead equivalent of a 300 mms. (12-inch) solid concrete floor is about 3 mms.; rather more for ferroconcrete. The majority of the woods have lead values of 0·001 or less.

With reference to iron, it will be noticed that its lead value is 0·15, and thus 20 mms., (about $\frac{3}{4}$ inch) of steel plate would be required to give protection equal to 3 mms. of lead, the figure recommended by the Protection Committee for exciting voltages over 100,000. The densities of steel and lead being about 7·8 and 11·4, the steel sheet would be four times as heavy as the lead. It so happens that this ratio is roughly that of the present cost by weight of lead and steel sheet,* so that there is nothing in it on the score of cost. It may be noted, however, that lead would increase its protective ratio somewhat at deep therapy voltages. An objection to iron is its rusting tendencies.

* About 40*s.* per cwt. for lead; 10*s.* per cwt. for steel.



Digitized by Google

| Material. | Density. | Lead Equivalent. |
|---|---|---|
| Lead Rubber— | | |
| (60 different samples) | 3 ·7 to 6·5 | 0·25 to 0·45 |
| Lead Glass— | | |
| (40 different samples) | 3·2 to 4·1 | 0·12 to 0·20 |
| Metals— | | |
| Aluminium | 2·7 | 0·01 |
| Brass | 8·4 | 0·25 |
| Steel | 7·8 | 0·15 |
| Miscellaneous— | | |
| Water | 1 | 0·004 |
| 50 per cent. lead, 50 per cent. litharge | ... | 0·3 |
| Ordinary rubber | 1·2 to 1·7 | 0·02 to 0·05 |
| Concrete— | | |
| 4 stone chippings, 2 washed sand, 1 cement | 2·1 | 0·012 |
| 4 clinker, 1 cement | 1·5 | 0·010 |
| 4 granite, 1 cement | 2·1 | 0·013 |
| Roman mortar | 1·5 | 0·009 |
| 20 chalk, 1 cement | 1·6 | 0·011 |
| 6 sand, 1 lime | 1·8 | 0·009 |
| Coke breeze | 1·0 | 0·004 |
| Bricks— | | |
| Fletton brick (red) | 1·6 | 0·010 |
| Stock brick (yellow) | 1·4 | 0·008 |
| Diatomaceous brick | 0·6 | 0·003 |
| Protective Wall Plasters— | | |
| (1) 55 per cent. Native $BaCO_3$, 45 per cent. $CaSO_4$ | 2·0 | 0·091 |
| (2) 33 per cent. $BaSO_4$, 33 per cent. sand, 33 per cent. cement | 1·5 | 0·048 |
| (3) 33 per cent. coarse Ba $SO_4$, 33 per cent. fine $BaSO_4$, 33 per cent. cement* | 2·3 | 0·12 |
| Woods— | | |
| Ash | 0·73 | 0·0013 |
| Balsa | 0·096 | 0·0001 |
| Bass | 0·48 | 0·0005 |
| Fir | 0·52 | 0·0008 |
| Mahogany | 0·49 to 0·68 | 0·0006 to 0·0011 |
| Oak | 0·65 | 0·0008 |
| White Pine | 0·47 | 0·0006 |
| Pitch Pine | 0·53 to 0·56 | 0·0008 |
| Spruce | 0·41 to 0·43 | 0·0004 to 0·0006 |
| Teak | 0·58 to 0·76 | 0·0006 to 0·0011 |
| Walnut | 0·64 | 0·0008 |

* Mixture suggested by Mr. P. J. NEATE.

Incidentally, sheet lead is commercially described and sold by its weight per superficial foot, "2 lb. lead" referring to sheet lead weighing 2 lb. per sq. foot. In this connection the following table may be useful :—

Digitized by Google

| Weight. | Thickness. | Weight. | Thickness. |
|---|---|---|---|
| 2 lb. lead | 0·8 mm. | 7 lb. lead | 3·05 mm. |
| 3 „ | 1·25 „ | 8 „ | 3·5 „ |
| 4 „ | 1·7 „ | 9 „ | 3·95 „ |
| 5 „ | 2·15 „ | 10 „ | 4·3 „ |
| 6 „ | 2·6 „ | 11 „ | 4·75 „ |
| | | 12 „ | 5·2 „ |

There is some tendency at the present time to employ baryta and other plasters in lieu of lead. We give the lead equivalents of three of these plasters. It may be remarked, to take the case of mixture No. 2, that 60 mms. (nearly 2½ inches) thickness will be required to give the protection of 3 mms. of lead, and that the weight of the plaster is nearly three times that of the lead. These figures would be more favourable for plaster No. 3. We have no knowledge of the costs of these plasters as compared with lead, nor of the cost of the labour involved in erection.

Certain plasters have been devised containing iron turnings. They possess no special merit as regards absorption, and the tendency to rust is a disadvantage.

*Tube Boxes.*—Protective tube boxes, if constructed of lead, have to be of dimensions sufficiently generous to prevent sparking between the bulb and the box. If, however, the tube box is required to be in close proximity to the bulb, the former commonly takes the form of a lead-glass bowl, or, alternatively, a wooden box with several layers of lead-rubber lining or wrapping. The open glass bowl is open to grave criticism: it is constructed of lead glass, usually affording, as our measurements show, a total protection of from 0·5 to 0·7 mm. lead; but in many directions, owing to its design, it affords no protection whatever. In our experience, where this type of shield is alone employed, it is often possible to take a radiograph of the hand in any part of a room where a tube is working. The bowl should be provided with some kind of cover and the material increased in effectiveness.

The type of double hemispherical shield supplied for radiator Coolidge tubes is much better, in that it completely encloses the tube. The different shields (whether tinted blue or yellow) which we have tested have a lead equivalent of about 0·2, the total protection provided ranging between 1·2 and 1·5 mm. lead. The Protection Committee recommends not less than 2 mms. for exciting voltages below 100,000. We refer again to the question of lead glass in connection with protective windows, etc.

Different makes of lead rubber differ in protective value by 100 per cent., and the importance of this fact should be stressed. Care should be taken that the lead rubber is not cut away locally when the box is being constructed.

The choice of lead rubber or lead glass in preference to lead sheet is usually dictated by the fact that the former are electrical insulators, at any rate to a limited extent. The resistivity of lead rubber is usually of the order of several thousand megohm



Digitized by Google

centimetres. The insulating value may be greatly improved by including a layer of micanite, ordinary rubber or other suitable insulator among the layers of lead rubber.

Measurements of the dielectric strength have been made in the Electricity Department of the Laboratory on a considerable number of samples. Two circular electrodes $1\frac{1}{2}$ inches in diameter with rounded edges were placed in contact with opposite sides of the material, an alternating potential of approximately sine wave form being applied and steadily increased from zero until the material punctured. For good specimens of lead rubber the breakdown voltage was about 5,000 to 12,000 R.M.S. volts per millimetre thickness. In other cases the values were a good deal less, and on occasion the material acted as a conductor. For lead glass the values ranged from about 5,000 to 9,000 R.M.S. volts per millimetre.

One other point may be referred to. In a prolonged run, especially with a Coolidge tube, a great deal of heat has to be got rid of, and it is usually advisable to provide for ventilation of the tube box; in that event the openings should be properly safeguarded from a protection standpoint. A knowledge of the thermal conductivity of the several protective materials may be useful in this connection. Measurements at the Laboratory show that the values of the thermal conductivity at room temperature are as follows in c.g.s. Centigrade units :—

| | |
|---|---|
| Woods (various) . . . . . | About 0·0003 |
| Ordinary rubber . . . . . | „ 0·0008 to 0·0011* |
| Lead rubber . . . . . | „ 0·0003 to 0·0007 |
| Lead glass . . . . . | „ 0·002 |
| Lead . . . . . | „ 0·08 |

If considerations of weight are of first importance, then lead sheet is almost always the lightest among the protective materials commonly employed for tube boxes. For example, the protective values of lead rubber range between about 0·25 and 0·55, and the densities between about 3·7 and 6·5. On the average, lead rubber is about 10 per cent. heavier than sheet lead affording the same protection, though it may be as much as 25 per cent. and as little as 5 per cent.

Similarly with lead glass the protective values commonly lie between 0·12 and 0·20, and the densities between 3·2 and 4·1. On the average, lead glass is about twice as heavy as sheet lead affording the same protection, the figures ranging from about 1·75 to 2·5.

These results (as with those for the screen materials) are, of course, predictable, as it is known that a heavy atom is ordinarily much more absorbent than a light. For the same reason in the case of two composite materials, each containing a mixture of atoms and having the same density, the one containing a higher proportion of heavy atoms will usually have a higher absorption factor. With lead rubber the lack of propor-

* Depending on the mineral content.

Digitized by Google

tionality between density and lead value is sometimes pronounced, and of two samples the one with the lower density may have the higher lead equivalent.

Diaphragms of the iris type are often fitted to tube boxes. The leaves are usually much too transparent. They should provide protection equal to not less than 3 mms. of lead, and the simpler rectangular diaphragm with two motions is a more practical job.

*Protective Glass Screens or Windows.*—As already mentioned, the lead values of lead glass range between about 0·12 and 0·20 per mm. But glass with the highest values, while perfectly mouldable into protective bowls and the like, is inadmissible for fluorescent screens and windows on account of the impossibility of producing it in flat sheets free from streakiness and colour. Such sheets are rarely more than 4 to 6 mms. thick, and to get the minimum protection recommended by the Protection Committee for fluorescent screens or windows it may be necessary to pile several sheets, a proceeding which is impracticable, as it becomes impossible to see through them.

One has to turn to glass of lower lead content, and this can be obtained in sheets, perfectly flat, of great clarity and almost colourless. The lead value is about 0·12 per mm., but as sheets up to 18 mms. thick can be obtained, the requisite protection is readily afforded, though at the cost of greater weight.

*Miscellaneous Materials.*—Among these are included aprons, gloves, face masks and goggles, of which the minimum protective value recommended by the Protection Committee is $\frac{1}{2}$ mm. lead. The Committee were deterred from recommending a higher figure by considerations of weight and convenience. For obvious reasons lead rubber and lead glass are almost solely utilised in the manufacture of the above articles. The linings of chamois leather or stockingette often employed, while having no appreciable lead value for the primary rays, are doubtless useful in absorbing the softer characteristic rays of lead.

Digitized by Google

Digitized by Google

# X-RAY DOSAGE WITH SPECIAL REFERENCE TO THE BARIUM PLATINO-CYANIDE PASTILLE

BY

E. A. OWEN, M.A., D.Sc.,
SENIOR ASSISTANT IN THE PHYSICS DEPARTMENT.

AND

PHYLLIS K. BOWES, M.A., B.Sc.,
SOMETIME JUNIOR ASSISTANT IN THE PHYSICS DEPARTMENT.

ALSO

# A NOTE ON THE GOLD-LEAF ELECTROSCOPE

BY

E. A. OWEN, M.A., D.Sc.,
SENIOR ASSISTANT IN THE PHYSICS DEPARTMENT.

Digitized by Google

ABSTRACT.

(1) The intensity of a beam of X-rays emitted by a Coolidge tube has been measured by the ionisation method and by the change of tint of a barium platino-cyanide pastille.

(2) The results obtained by the ionisation method corroborate those obtained with the pastille in every instance.

(3) The product of the ionisation per minute given by the electroscope and the time of dose given by the pastille is a constant. This relation is independent of the current through the tube, type of interrupter, frequency of interruption, interval between " break " and " make ", and voltage of primary current.

(4) The ionisation (I) per minute may be represented by the formula—

$$I = K' n^a V^2 \left(\frac{C}{C + \psi}\right),$$

where $n$ is the frequency of interruption of the primary current, V the voltage on the tube, C the mean current through the tube, K' a constant whose value depends upon the distance of the pastille from the anti-cathode, and $\psi$ a function whose value is nearly constant.

(5) A short outline is given of a method of standardising the barium platino-cyanide pastille.

Digitized by Google

# X-RAY DOSAGE WITH SPECIAL REFERENCE TO THE BARIUM PLATINO-CYANIDE PASTILLE.

By E. A. OWEN, M.A., D.Sc., Senior Assistant, and PHYLLIS K. BOWES, M.A., B.Sc., sometime Junior Assistant in the Physics Department.

[Reprinted from the 'Journal of the Röntgen Society', Vol. 17, 1921.]

# Also A NOTE ON THE GOLD-LEAF ELECTROSCOPE.

By E. A. OWEN, M.A., D.Sc., Senior Assistant in the Physics Department.

[Reprinted from the 'Journal of the Röntgen Society', Vol. 16, 1920.]

## I. Introduction.

Different methods have been employed to measure the intensity of a beam of X-rays. They depend upon the various effects produced by the rays, such as ionisation, production of heat, fluorescence of certain salts, chemical change or certain electrical effects, such as the change of the resistance of selenium. The results obtained by these different methods have not so far been thoroughly correlated. It will be our object in a series of investigations, of which this is the first contribution, to attempt to do this. In each case a comparison will be made with the ionisation method which is at present the most accurate means of measuring the intensity of a beam of X-rays. The present paper deals with the barium platino-cyanide pastille. This method was chosen first because it seems to have been, up to now, the most popular amongst radiologists. Our object then will be to compare the results obtained by the ionisation and by the pastille methods, and thereby arrive at some definite information regarding the behaviour of the barium platino-cyanide pastille as a dose meter, the conditions under which it should be used to give the best results and the accuracy of the measurements that can be made with it.

The results will also help to throw some light on the performance of an induction coil outfit as regards efficiency in the production of X-rays when operating a Coolidge tube, and the part played by the interrupter in this outfit.

## II. Apparatus.

The apparatus used in the present investigation is shown in Fig. 1. The standard Coolidge tube was enclosed in a lead box in the side of which was a circular hole 13 mms. in diameter. Situated about 70 cms. away was a screen of lead, 6 mms. thick, with a

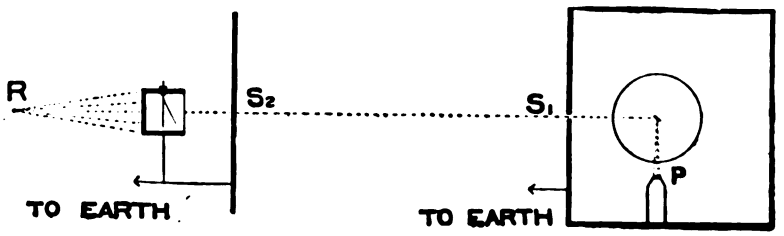


Fig. 1.



Digitized by Google

small hole ($S_2$) in it 1 mm. in diameter placed in line with the anticathode and the hole ($S_1$) in the lead box. The bulb was kept in a fixed position and could be removed when desired and replaced again in exactly the same position by means of the slide which carried it.

The pastille P was placed inside the lead box at a distance of about 12 cms. from the centre of the anticathode; this would mean that it was about 3 cms. from the outside wall of the tube. It was placed on a small lead disc mounted on an ebonite pillar about 8 cms. high. During an exposure the pastille was covered with a small cap of black paper which shielded it from the light emitted by the incandescent cathode. It was necessary to take this precaution because the light would tend to retard the change of colour produced by the X-rays and the pastille would register an erroneous time of dose. Besides cutting off the light rays, the black paper cover helped to shield the pastille from the heat rays emitted by the bulb, whose anticathode became white hot when heavy currents were employed. Overheating of the pastille causes dehydration of the salt and thereby a change of colour which would again lead to erroneous results. The distance of 3 cms. allowed in the present arrangement between the pastille and the glass wall of the tube, together with the additional protection of the paper cover, sufficed to guard against this source of error.

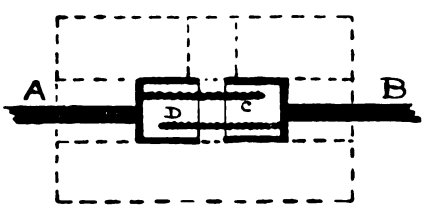

Fig. 2.

The electroscope used was of the ordinary type with special design for supporting and charging the leaf system. A description of the instrument will be found in the Note at the end of this paper. The insulation of the leaf system in the description given consisted of a broad sulphur ring let into ebonite. This method of insulation proved satisfactory and was employed throughout the present investigation. An improvement has recently been made in this direction by using a plug of sulphur. The drawback to using sulphur alone is that it is very brittle and is easily broken. The following simple method has been devised of strengthening the sulphur:—Two metal cups are turned out, having rods A and B attached to their outer surfaces, as in Fig. 2. To the inside of each of the cups is screwed a stiff piece of wire situated about a sixth of the diameter from the centre. The cups are placed so that their edges are about 3 or 4 mms. apart in a cylindrical receptacle which divides longitudinally into two parts. Sulphur is then poured in to fill the cavity and to keep it molten the whole is gently warmed, and rocked to and fro until the air bubbles are all displaced. The whole is allowed to cool and the core removed, which can then be turned in the lathe without fear of breakage. It should also be mentioned that small holes were bored in the sides of the metal cups so as to ensure a firm grip of the sulphur. The " re-inforced " sulphur plug is very strong and its insulation factor is high.

The faces of the electroscope were covered with lead 6 mms. thick, except that through which the X-rays entered; this was covered with a sheet of aluminium 0·5 mm. thick.

Digitized by Google

The opposite end of the electroscope was lined inside with a sheet of aluminium, this precaution being taken to diminish the production of corpuscular radiation as much as possible.

In the case of the heaviest ionisation currents measured, saturation current was obtained in the electroscope when the potential gradient was 40 volts per centimetre, but a potential gradient of 70 volts per centimetre was employed throughout the investigation, so as to allow a liberal margin of safety. The sensitivity of the electroscope was constant over the whole of the scale and its natural leak was about 1 scale division per hour, the correction for this leak being so small that it could be neglected.

To compare the readings of the electroscope from day to day it was necessary to calibrate the instrument by means of a constant source of radiation. A small sealed tube containing a known quantity of radium in radioactive equilibrium was employed for this purpose. The tube was placed at R (Fig. 1), 26 cms. from the electroscope and the rate of fall of the leaf measured each day at the beginning and at the end of the observations. The ionisation produced was due entirely to the $\gamma$ radiation emitted by the radium, the $\beta$ radiation being absorbed in the lead face of the electroscope. The readings showed that the rate of fall of the leaf remained remarkably constant from day to day, and during the course of one day's observations the difference between the readings at the beginning and at the end was always less than 1 per cent.

The change of tint of the pastille after exposure to the rays was measured by means of a Corbett tintometer supplied with Lovibond tints. The tints supplied with the instrument ranged from tint A to tint 2B; additional tints were obtained so that in the neighbourhood of the B-tint the tints changed by steps of 1/10th of a B-dose. This B-tint corresponds to the full epilation dose as measured by the Sabouraud Noire pastille. Two sets of tints are supplied with the instrument—one for use with artificial light and the other for use with daylight. It was considered advisable to use artificial light in making the comparisons so as to be independent of the variation in daylight from day to day; this variation is very marked during the winter months. There is, of course, a change in the quality of the light emitted by a carbon filament lamp with time, but the change is a slow one; in the case of the 8 candle power lamp used for twelve months in the present investigation it was inappreciable.

Although the change of colour of a pastille cannot be gauged as accurately as the deflection of a gold-leaf electroscope can be read, yet after some practice in comparing tints it is possible to obtain readings correct to about 5 per cent.—an accuracy of 10 per cent is readily attained. Comparisons of tints could be more accurately made if the two surfaces to be compared were brought into contact with each other instead of being separated, as is the case in the tintometers at present in use. If this point were attended to, the value of the tintometer as a measuring instrument would be greatly enhanced.

A rectifying device such as a point-plane gap or a rectifying valve placed in series with the tube gave the same results as those obtained when the Coolidge tube was used alone.



Digitized by Google

## III. Time of Dose and Mean Current through the Tube.

The first point investigated was the relation existing between the time of dose as given by the pastille and the mean current through the tube when the voltage on the tube, the frequency of interruption and the voltage of the primary current are kept constant.

The mean current through the tube was measured on an ordinary moving coil milliammeter. During this part of the work the interrupter used was of the Sanax type. The amount of mercury was adjusted in it so that contact was just made when the spindle carrying the rotating disc was turned to the zero mark of the graduated dial of the instrument. The interrupter was run, however, with the spindle turned to mark 7 of the dial,

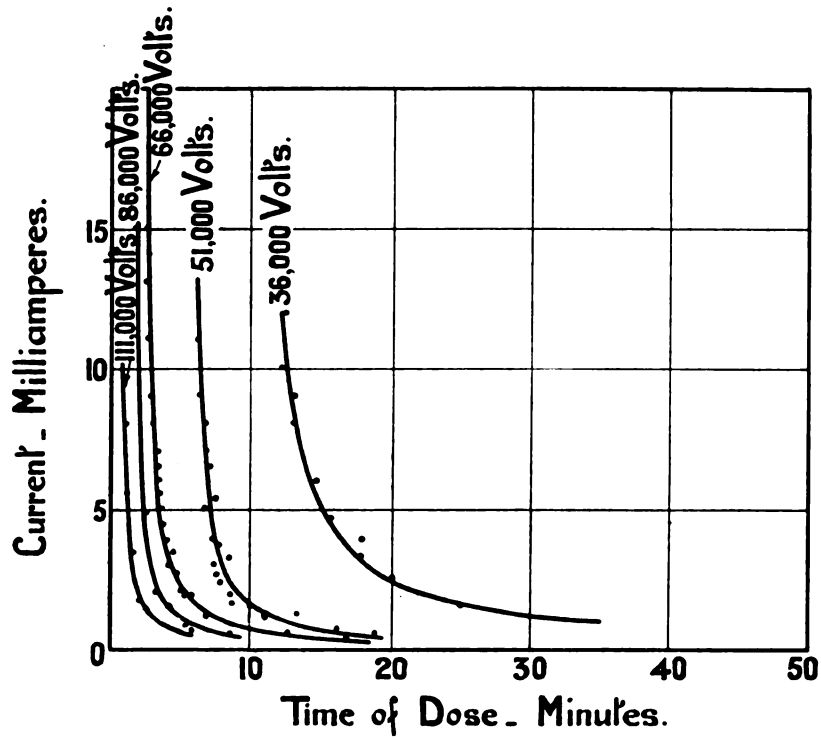


Fig. 3.

*i.e.* midway between no contact and longest time of contact. Oscillographs of the potential wave form of the coil which will be referred to later enabled the speed of the interrupter to be measured with accuracy; in the present instance it was found that 92 interruptions of the primary current were made per second.

The voltage on the tube was measured by means of an alternative spark gap which had been standardised to give readings in kilovolts.

The curves shown in Fig. 3 refer to different voltages ranging from 36 to 111 kilovolts. Each curve was obtained singly, that is, the voltage on the tube was kept constant whilst the current through the tube was varied; odd points on the curves were obtained, however, at later dates. The procedure was to expose the pastille for a certain length of time

Digitized by Google

approximating to a dose whilst observations were taken at the same time on the electroscope. The change of colour of the pastille was measured with the tintometer and the time of the full B-dose calculated.

As the current through the tube increases the time of dose as given by the pastille diminishes, but after a certain point has been reached the decrease in the time of dose is small compared with the increase in the current. Starting with very low currents a small rise in current has a great effect upon the time of dose; for instance, in the case when the applied voltage on the tube is 36 kilovolts an increase of current from 1 ma. to 1·5 ma. lessens the time of dose from 35 minutes to 26·5 minutes. For higher currents, however, the same increase of current produces a smaller change in the time of dose until finally any further increase produces no appreciable effect.

The curves are all of the same form, and may be represented by the equation

$$Ct = a(C + b), \quad . \quad . \quad . \quad . \quad . \quad . \quad . \quad . \quad . \quad . \quad . \quad (1)$$

where C and $t$ are the mean current and the time of dose respectively, and $a$ and $b$ are constants for each individual curve; the value of $a$ varies rapidly as we change from one curve to another, whereas the value of $b$ is approximately constant. It is readily seen that $t = a$ is an asymptote to the hyperbola given by equation (1), so that the value of the time of dose tends to the value of the constant $a$ as the current is increased. As the voltage on the tube increases the limiting value of the time of dose decreases until, for a voltage of 111 kilovolts, the asymptote has moved almost to the current axis.

The above results may be presented in slightly different form. In Fig. 4 the current

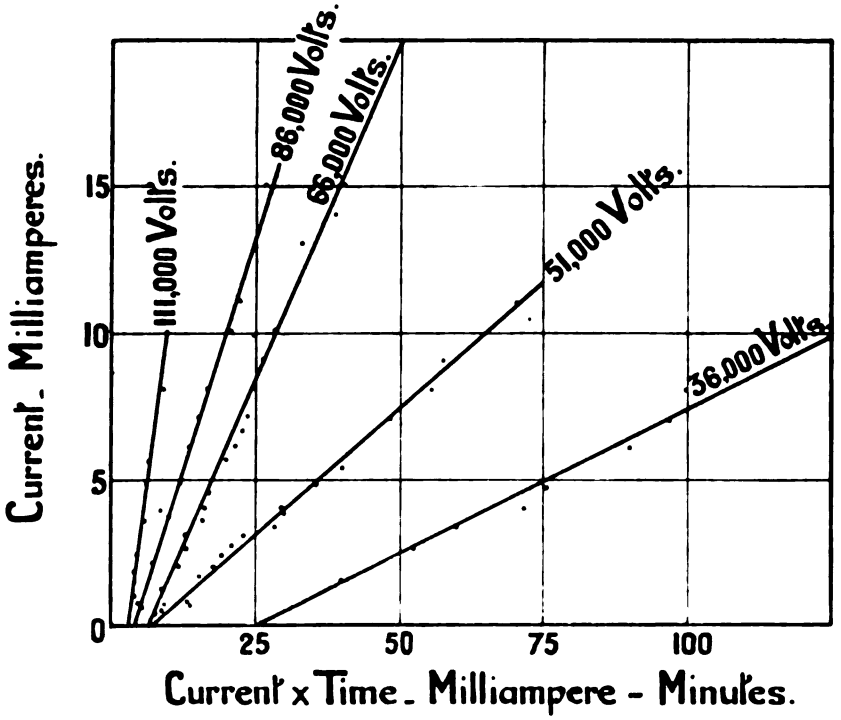


FIG. 4.

Digitized by Google

through the tube is plotted against milliampere-minutes, *i.e.* the product of the current and time of dose, a unit often used by radiographers. We have now, as we should expect from equation (1), a series of straight lines. For the lowest voltages examined the value of the milliampere-minutes necessary for the dose increases rapidly with increase of current. LEVY and STENNING* using a voltage of 66 kilovolts found the same increase in milliampere-minutes necessary to turn the pastille to the B-tint when the current was increased. Other investigators have made the same observation. The above curves show in addition that when the voltage on the tube is increased the value of the product milliampere-minutes increases less rapidly with the current. Whereas a change in current from 1 ma. to 5 ma. when the voltage is 36 kilovolts produces a change of 40 milliampere-minutes, the same alteration of current when the voltage is 111 kilovolts produces a change of only about 2·5 milliampere-minutes. Hence as the voltage increases the product milliampere-minutes tends to become independent of the current; it would be absolutely so if the curves were rectangular hyperbolæ referred to the axes.

One point that is brought out clearly in the curves is the mistake that is often made by radiographers of assuming that the number of milliampere-minutes necessary for a given dose of X-rays is constant. This is not the case with an induction coil outfit and is only approximately true when the voltage is very high. It is not safe, even with the highest voltages used in practice, to assume that the number of milliampere-minutes necessary for a given dose is constant.

The observed points for currents lower than 1 ma. depart quite noticeably from the straight lines; in each case the number of milliampere-minutes is greater for a given current than that given by the curves. Oscillograph curves of the secondary potential wave form showed that the actual potential in the secondary was not as high as that indicated by the alternative spark gap. This would account for the irregularity mentioned.

It was of interest to find how closely we could compare the tints without the aid of the tintometer. A series of observations was accordingly taken by comparing in daylight the colour change of the pastille with the artificial tint attached to the book from which the pastilles were taken. The observations corroborated those previously taken with the tintometer for large currents, but for small currents the two results disagreed by as much as 15 per cent.

The above curves show that a coil outfit works very efficiently as regards production of X-rays whatever the value of the mean current through the tube when the applied voltage is high.

## IV. TIME OF DOSE AND VOLTAGE ON THE TUBE.

The curves in Fig. 3 give some information of the variation of the time of dose with voltage on the tube when the mean current is kept constant. Values of the time of dose

* 'J. Röntg. Soc.', vol. 13, p. 13, 1917.

Digitized by Google

given by these curves for constant mean currents show a definite relation to the values of the voltage, but as only five points could be obtained in this way a fuller investigation was carried out by varying the voltage on the tube, keeping the current constant and measuring the time of dose in each case. The curve given in Fig. 5 was obtained

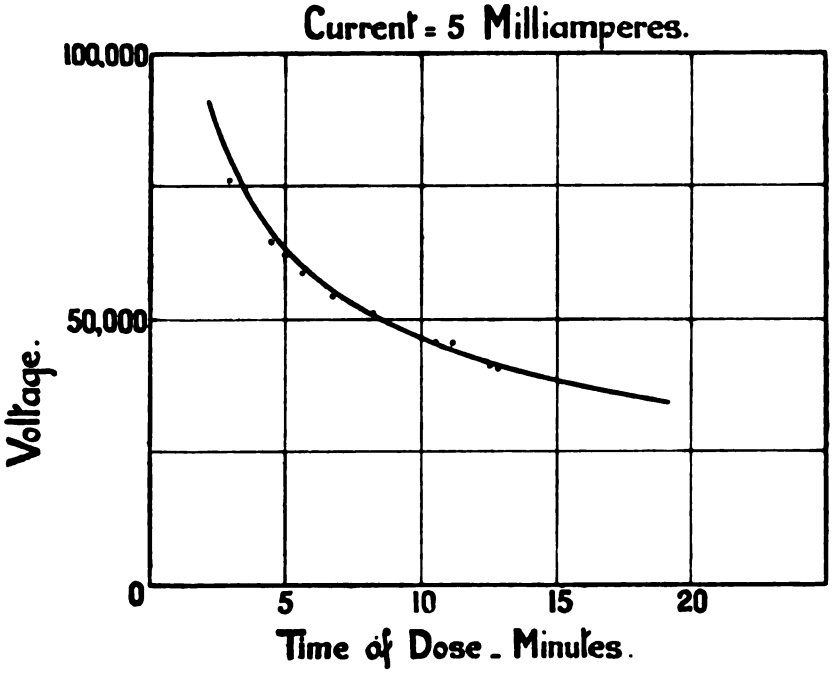


FIG. 5.

when the mean current through the tube was kept at 5 ma. This curve, however, does not give the same values of time of dose as those derived from the five curves in Fig. 3, as the experimental conditions were slightly different in the two cases. It will be seen that the deviations of the observed values from the mean curve are very small. Plotting the logarithms of the corresponding values of time of dose and voltage we get a straight line from which we deduce that for voltages employed here, *i.e.* up to about 90 kilovolts, the time of dose is approximately inversely proportional to the square of the voltage on the tube,

that is, $$t = K/V^2, \quad . \quad . \quad . \quad . \quad . \quad . \quad . \quad . \quad . \quad . \quad . \quad (2)$$

where K is a constant.

## V. IONISATION CURVES.

Simultaneously with the observations carried out on the pastille measurements were made of the ionisation produced in the electroscope. During an exposure the leaf of the electroscope was kept constantly under observation. As a rule it moved so slowly along the scale that observations on it could be taken every minute, and in this way it was possible to detect any variation which might occur in the output of the bulb from

Digitized by Google

time to time. It was found that for the lower voltages the rate of fall of the leaf was steady, but for higher voltages there were always irregularities observed. These were due to variations in the voltage, which had consequently to be measured at frequent intervals during the course of an exposure.

The relation between ionisation and current through the tube for different applied voltages is shown in Fig. 6, the abscissa being the average number of scale divisions

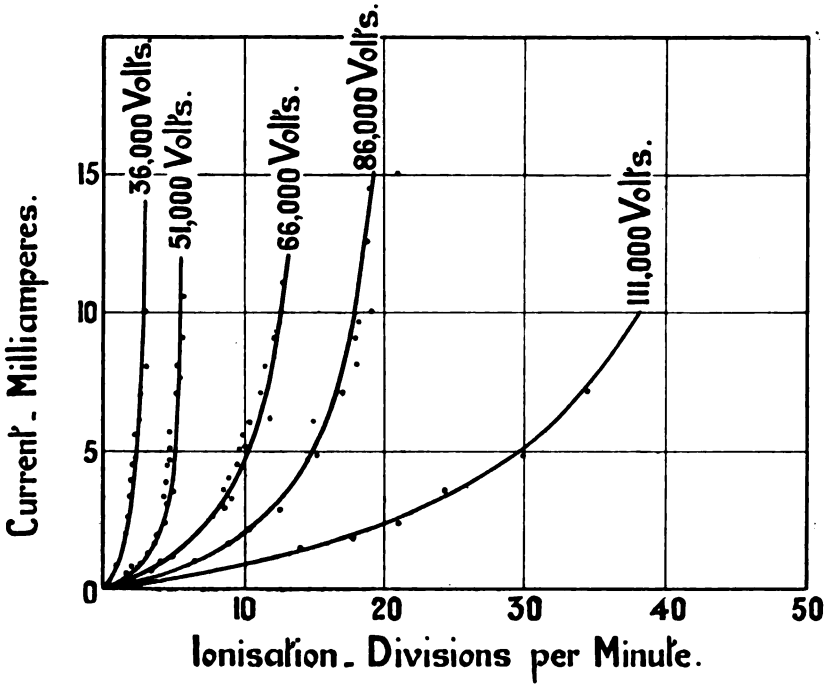


FIG. 6.

traversed by the leaf per minute. Considering the curves singly we find that as the mean current through the tube increases the ionisation increases, rapidly at first, and then more slowly, tending for the lower voltages to reach a steady value for the higher currents. The voltage on the tube has a very marked influence upon the amount of ionisation produced. For instance, when the voltage on the tube is 36 kilovolts, the ionisation produced with a current of 5 ma. is about 2·5 divisions per minute. When the voltage is increased to 86 kilovolts, the ionisation has increased for the same current to 14·8 divisions per minute, that is, the ionisation varies directly as the square of the voltage approximately. This result was also directly obtained when the current through the tube was kept constant and readings were taken of the ionisation when the voltage was varied (Fig. 7).

Other investigators employing different methods have found that the intensity of a beam of X-rays emitted by a bulb is directly proportional to the square of the voltage. BEATTY* found the relation to hold when a beam of X-rays produced by cathode rays

* 'Roy. Soc. Proc.', vol. 89, p. 314, 1913.

Digitized by Google

of definite velocity was completely absorbed in a long ionisation chamber. KRÖNCKE* found the same relation in the case of a gas tube operated with a transformer outfit. Later, ULREY,† using a Coolidge tube, analysed the beam into its component radiations by means of the Bragg X-ray spectrometer, and by summing up the energies of the individual components arrived at the whole energy in the beam, and again found the relation between voltage and intensity of the radiation to hold. In the last two cases the ionisation was that produced at a definite point in the beam, and was not the total ionisation as in the first case cited. Since the relation appears to hold whether we examine the beam at a point or as a whole, we arrive at the conclusion that the energy of a heterogeneous beam at a point is proportional to the total energy in the beam.

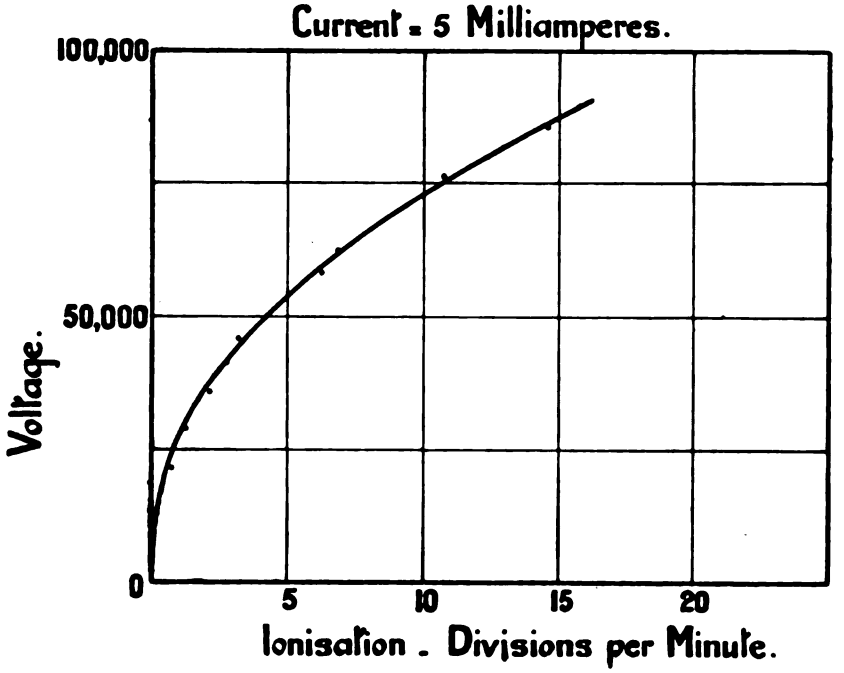


FIG. 7.

This is strictly true for homogeneous radiation, but it is not at once evident that it is so for a heterogeneous beam. Some observers have found that the total energy of a heterogeneous beam is proportional to the cube of the voltage,‡ but this has been put down to the fact that characteristic radiations are excited in this case, which would account for a greater increase of energy with voltage than that given by the square law. This point needs further investigation, and it is our intention as a next step to employ a long chamber such as was used by BEATTY, and compare under exactly similar conditions the effect produced in it directly with that produced in a short chamber.

* 'Ann. der Phys.', vol. 43, p. 687, 1914.

† 'Phys. Rev.', vol. 11, p. 401, 1918.

‡ WEEKS, 'Phys. Rev.', vol. 10, p. 564, 1917; BIQUARD, 'Comptes Rendus', vol. 168, p. 851, 1919.



Digitized by Google

It should be emphasised that the ionisation curves just described give the same information exactly as that deduced from the pastille curves in reference to the energy of the X-ray beam emitted by the bulb under different conditions of current and voltage.

## VI. Results obtained with Different Types of Interrupters.

Three types of interrupters were examined, namely, (1) the Sanax interrupter, in which a disc carrying the contacts rotates owing to friction between its edge and mercury which is contained in a rotating reservoir, the current being broken twice in each revolution of the disc; (2) the mercury-jet gas interrupter. Here contact is made by the squirting of a jet of mercury against vertical contact pieces; and (3) the dipper interrupter, in which two vertical rods fixed to the axis of the motor dip into mercury, breaking the current twice in each revolution of the axis of the motor. The Wehnelt interrupter was not examined. Apart from this type the above are fairly representative of the interrupters at present in use. The voltage on the tube was kept constant at 66 kilovolts. The gas interrupter gave the same type of curves as the Sanax interrupter, the only difference being that for a given current through the tube, the time of dose was longer with the former than with the latter, which is accounted for by the lower speed of the gas interrupter. The dipper break showed considerable unsteadiness, however, and it was impossible to obtain smooth curves with it. This irregularity was explained by the aid of potential wave oscillograph records. The potential peaks with the Sanax and gas interrupters are uniform and occur quite regularly at each break of the primary current, whereas with the dipper break the peaks are very irregular (Fig. 8). On the plate there is only one peak approaching the maximum value, whereas there should be at least two. Other oscillograph records showed the same irregularities. It is now obvious why a smooth curve could not be obtained in this case; in one second there may perhaps be only one high potential peak, whilst in the next there may be several, so that the bulb would not be emitting X-rays at a constant rate, and consequently both the time of dose and ionisation per minute would vary. The irregularity in the dipper break is probably due to the fact that the mercury surface is set oscillating and the suddenness of the interruption of the primary current is not the same throughout an exposure.

The effect of irregular time of contact is brought out very clearly in the last oscillograph in Fig. 8. This is a record of the potential wave form when the spindle of the Sanax interrupter was turned to indication 4 of the dial—this gave a smaller time of contact than that obtained when the indication was 7, to which the first oscillograph refers. It is evident from the curve that the rotating disc of the interrupter was not mounted symmetrically on its axis. There is an appreciable interval of time between make and break in the one case, whilst in the other the make and break occur almost simultaneously, so that in this case the contact piece just grazed the surface of the mercury. The potential corresponding to the length of the alternative spark is therefore only obtained at the

Digitized by Google

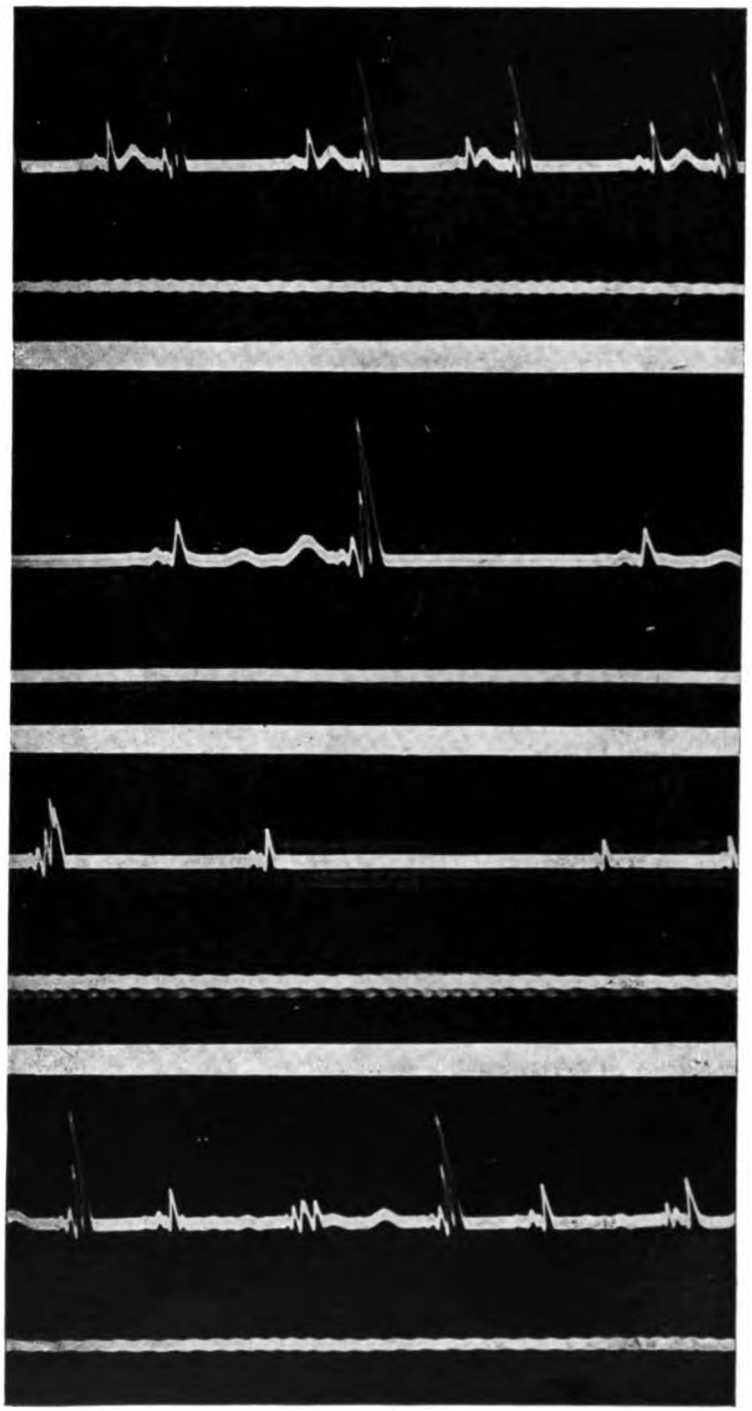


FIG. 8.

*To face p.* 330.]

Digitized by Google

Digitized by Google

one break, the effect of which would be to lower the efficiency of the outfit as regards the production of X-rays. This conclusion was borne out by the values of the time of dose and ionisation which were actually measured for various currents passing through the tube.

## VII. Effect of Frequency of Interruption and Voltage of Primary Current.

The effect of the frequency of interruption of the primary current was investigated by means of the Sanax interrupter, whose normal speed was higher than that of the gas interrupter. The actual frequency of interruption was measured by the aid of potential wave oscillograph curves which were photographed on the same plate as the sine wave

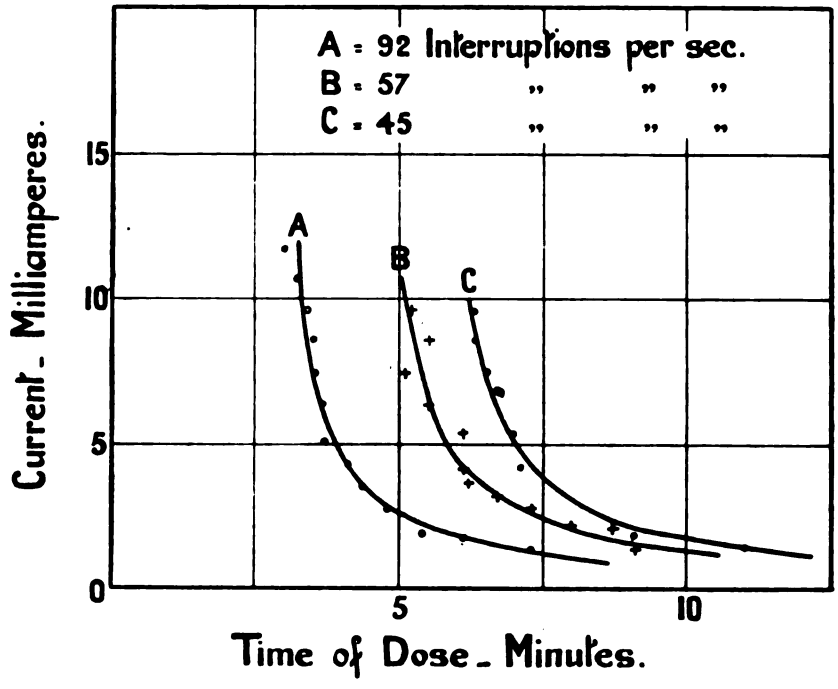


Fig. 9.

of a tuning fork of 700 frequency. Three speeds were examined, giving respectively 92, 57 and 45 interruptions per second, the voltage on the tube being always kept at 66 kilovolts. The curves (Figs. 9 and 10) show that the faster the speed of the interrupter the greater the amount of X-radiation emitted by the bulb. Examining the curves more closely and confining our attention to constant values of current, we find that for large currents the time of dose varies approximately inversely as the frequency of interruption. For smaller currents, however, the time of dose decreases less rapidly with the frequency than that given by the above relation; in other words, the efficiency of X-ray production increases at a more rapid rate with increase of frequency for large than for small currents.



Digitized by Google

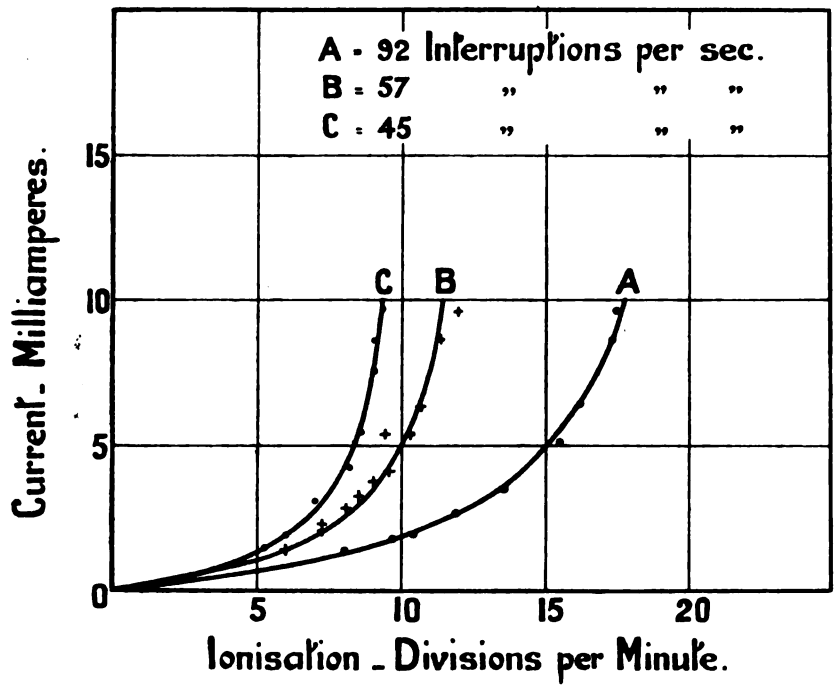


FIG. 10.

From the curves we deduce that the time of dose varies with the frequency ($n$) according to the relation

$$t = K/n^{\alpha} \quad . \quad . \quad . \quad . \quad . \quad . \quad . \quad . \quad . \quad . \quad . \quad . \quad (3)$$

the value of $\alpha$ being always less than unity and depending upon the current passing through the tube. In the present case the values of $\alpha$ were found to be approximately 0·7, 0·8, 0·9 when the values of the mean current were 2 ma., 5 ma. and 10 ma. respectively.

With definite secondary potential and current it was found that if the voltage on the primary is altered the time of dose and the ionisation also change. This was found to be the case both with the Sanax and the gas interrupters; in each case the curve obtained with 100 volts on the primary was different from that obtained with 200 volts. It was possible, however, to bring the two curves to coincide by altering the interval between the " break " and " make " of the primary current. In the case of the Sanax interrupter it was found that the quantity of oil, as well as the quantity of mercury, had a marked effect on the curves and it was essential to adjust both of these to bring the curves to coincide.

## VIII. TIME OF DOSE AND IONISATION.

Hitherto ionisation and time of dose have been expressed in relation to the mean current passing through the tube. By combining these results a relation may be arrived at between ionisation and time of dose which is independent of the current. Plotting the reciprocal of the ionisation per minute corresponding to the time of dose when the voltage on the tube is 66 kilovolts, the curves in Figs. 11 and 12 are obtained. These

Digitized by Google

two curves refer to different Coolidge bulbs. The results observed with different interrupters are included in Fig. 11, whilst Fig. 12 includes observations taken when the frequency of interruption, voltage of primary current and interval between "break"

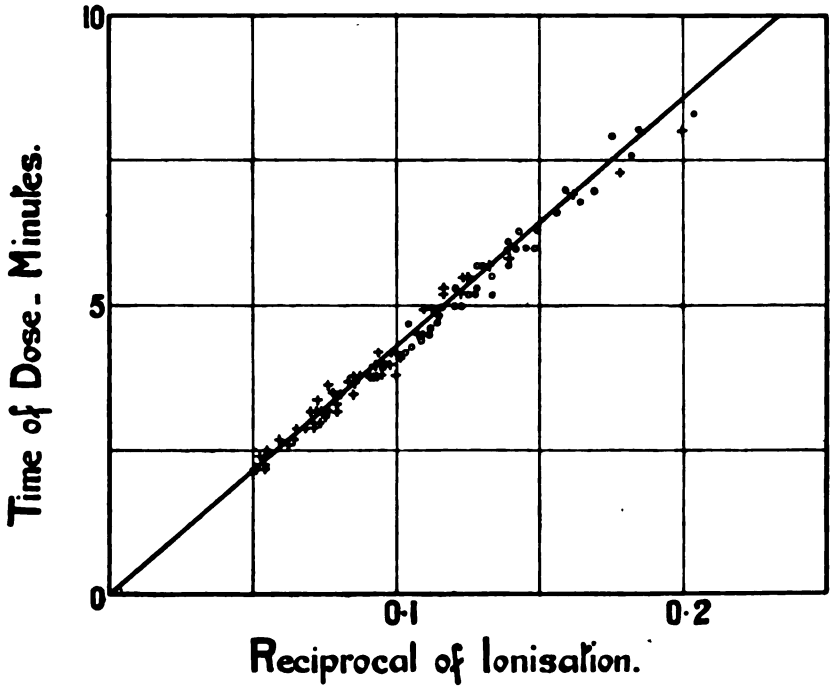


Fig. 11.

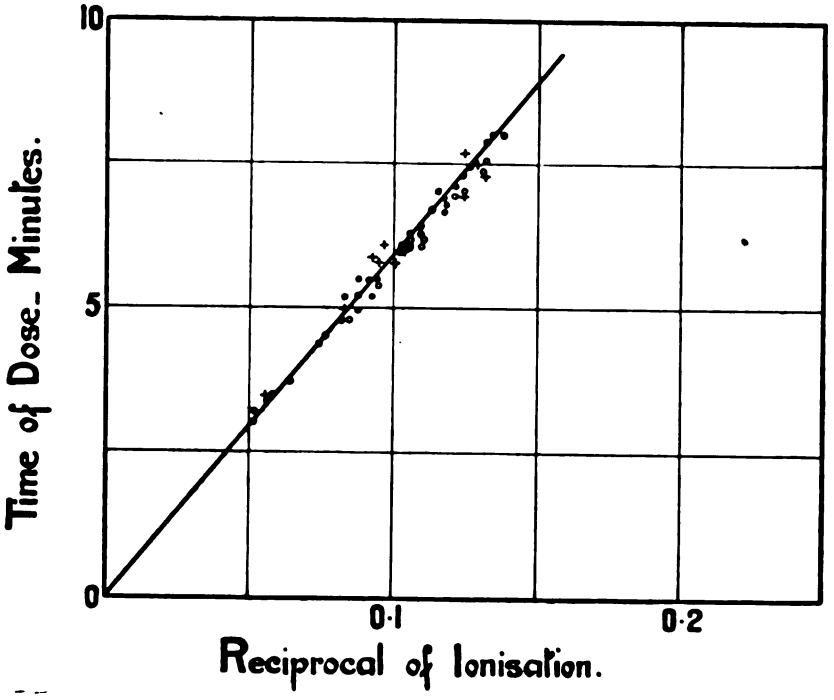


Fig. 12.

Digitized by Google

and " make " were altered. In each case the time of dose varies directly as the reciprocal of the ionisation per minute. Hence the product of the time of dose and the ionisation per minute is always the same, however the current through the tube, frequency of interruption, interval between " break " and " make " and primary voltage vary,

$$i.e. \quad It = \text{constant}. \quad . \quad . \quad . \quad . \quad . \quad . \quad . \quad . \quad . \quad . \quad (4)$$

This relation is strictly true when the voltage on the tube is kept constant; it is also approximately true when the voltage is varied, but it is desirable to make further observations on this point.

The fact that the time of dose as registered by the barium platino-cyanide pastille bears this definite relation to the ionisation produced in the electroscope shows that the pastille is a reliable dose-meter when care is taken to compare the colour changes produced. In the present investigation different batches of pastilles were employed varying greatly in age—some had been at the Laboratory for a few years, whilst others were bought at more recent dates. The total number investigated would be about 200. These were also used over and over again. After being exposed they were submitted to subdued daylight and allowed time to recover to their normal tint. We found that one pastille could be used eight or ten times before any difference could be detected in the colour—after recovery—from that of the normal unexposed pastille. When any difference was found it was considered advisable to discard the pastille rather than use it and make a correction for the difference in colour from the normal.

Combining relations (1), (2) and (3) above we have

$$t = \mathrm{K} \cdot \frac{1}{n^{\alpha}\mathrm{V}^2}\left(1 + \frac{\psi}{\mathrm{C}}\right), \quad . \quad . \quad . \quad . \quad . \quad . \quad . \quad . \quad . \quad . \quad (5)$$

where $t$ is the time of dose, V the voltage, C the mean current, $n$ the frequency of interruption of the primary current, $\alpha$ has a value less than unity and varies with the value of the mean current, K is a constant whose value depends upon the distance of the pastille from the anticathode and $\psi$ is a function whose value is nearly constant. The expression for the ionisation per minute in terms of these quantities then becomes

$$\mathrm{I} = \mathrm{K}' n^{\alpha}\mathrm{V}^2\left(\frac{\mathrm{C}}{\mathrm{C} + \psi}\right), \quad . \quad . \quad . \quad . \quad . \quad . \quad . \quad . \quad . \quad . \quad (6)$$

where I is the ionisation produced in the electroscope per unit time.

Secondary current oscillographs taken under the various conditions employed will probably help to explain the above results. It is hoped to take these at a later date.

## IX. Standardisation of the Pastille.

The above results lead to a simple method of standardising the barium platino-cyanide pastille in terms of the standard Sabouraud pastille. The method of procedure would be as follows :—The electroscope is standardised by means of the gamma radiation

Digitized by Google

emitted by a known quantity of radium. The variation of the indications of the instrument could in this way be corrected for from day to day. The pastille is placed in the same position relative to the anticathode of the bulb that the standard pastille occupied when the installation was standardised. It is then exposed for an interval of time necessary to produce the required amount of ionisation in the electroscope—the product $It$ signifies a constant deflection of the electroscope leaf for the full dose. The tint of the pastille is next examined by means of the tintometer and the fraction of the dose that it measures is obtained. From these observations the dose given when the pastille changes colour to the full B-tint can be calculated and stated in terms of the standard Sabouraud pastille dose.

We would suggest that the same standard tint be used with all pastilles. It is well known that one set of pastilles may have a tint which differs from that of another, and the different tints supplied may lead to confusion when the pastilles are put into use. This difficulty would be got over if one standard B-tint were universally employed. We would emphasise that the best results are obtained with the pastille when the tintometer is used to compare the tints. The accuracy of observation is much lower when the comparison of tints is carried out in daylight by means of the dummy tint usually supplied with the pastilles without the aid of a tintometer.

The National Physical Laboratory is now in a position to test pastilles along the lines briefly outlined above.

## A NOTE ON THE GOLD-LEAF ELECTROSCOPE.

By E. A. OWEN, M.A., D.Sc.,
Senior Assistant in the Physics Department.

[Reprinted from the 'Journal of the Röntgen Society', Vol. 16, 1920.]

Many designs of gold-leaf electroscope have been employed in radium and X-ray measurements. The following is a description of an instrument of robust construction which has been found very satisfactory in practice :—

The rod, to which the gold leaf is attached, is screwed into a small cylinder of ebonite until the flange F bears tightly against its bottom surface. Into the top surface of the ebonite cylinder is screwed a shorter brass rod which passes through the ebonite plug of the electroscope. The whole is held firmly in position by means of a nut forming the lower part of the terminal A.

The top of the charging rod B, which is covered with ebonite, is fitted with a terminal which is permanently connected by means of a short piece of flexible wire to the terminal A. In its normal position the rod is held up by the upper spring shown in the figure, this being stronger than the lower spring, which is normally in a state of compression. When B is pressed downwards the lower spring expands, and continues to do so until

Digitized by Google

the sleeve L comes into contact with the flange F. Further pressure on B does not increase the pressure on the flange, and, since the lower spring is a light one, the pressure exerted by the sleeve on the flange is very small.

The chief point to look to in an electroscope is the insulation of the leaf system. Ebonite is a poor insulator and it deteriorates rapidly with exposure to a damp atmosphere. The best material to employ as insulator would be sulphur or amber; the former is ruled out in this case on account of its weakness mechanically, whilst the latter is at present difficult to obtain and suffers from the same defect as sulphur, though not to the same degree, in that it is not mechanically strong. The insulating properties of ebonite can be greatly improved by the old method of letting sulphur rings into it. The sulphur has to be handled carefully, kept clean, and the rings made as wide as possible so as to

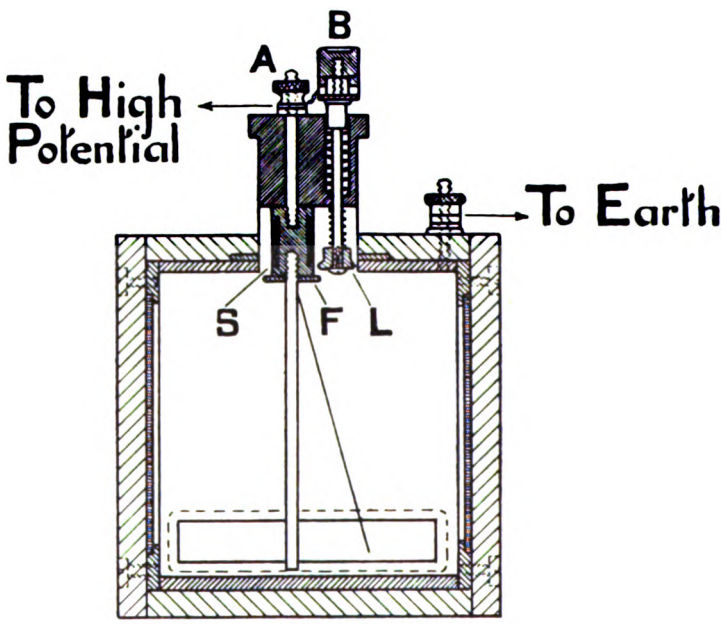


present a good surface. This method was tried in the present case and found satisfactory; a sulphur ring S, about $\frac{1}{16}$ inch in depth and $\frac{1}{2}$ inch in width was let into the ebonite cylinder carrying the gold-leaf system. The sulphur is firstly heated so as to just melt. It is then worked carefully into the recesses of the ring, and before it completely sets, turned in the lathe. In this state it does not chip so readily as it does in a later stage after it has become harder. The sulphur is not touched after the tool employed to turn it to proper size has done its work. The cylinder is immediately mounted as described, kept in the dark and guarded against the deposition of dust.

The terminal A is permanently connected to a high potential, the actual value of the potential depending upon existing conditions. In a particular instrument at present in use at the Laboratory the leaf is about 4·5 cms. long; the end of the leaf falls through 0·11 mm. in one hour when the potential on A is kept at 280 volts, while a change of

Digitized by Google

potential of 1 volt on the leaf moves it through 0·51 mm.* It has maintained this rate of natural leak and sensitivity for about four months and has worked throughout that period entirely satisfactorily. The amount of soakage in the ebonite insulation is small and reliable readings may be taken with the instrument in about five or ten minutes after the leaf is initially charged. The sensitivity of the instrument is constant over the whole scale of the microscope, so that readings may be taken indiscriminately over any part of the scale. That is a well-known property of this type of electroscope.

For γ-ray measurements the whole of the electroscope is covered with lead about 5 mms. thick; for X-ray measurements, the two end faces are removed and the rays pass into and out of the instrument through aluminium windows of suitable thickness.

The instrument as at present constructed is practically airtight. The internal dimensions of the larger size of instrument are about 3¼ inches square by about 2 inches deep from side to side. The relative dimensions of the different parts may be obtained from the diagram, which is drawn to scale. A small electroscope of this type, of about 2 cm. cube internal capacity, gave good results. In this case a high-power microscope is needed to follow the motion of the leaf; the saturation potential may, however, be as low as 40 volts, which in some cases is an advantage.

If the instrument is desired for use in conjunction with a separate ionisation chamber, a wire can be attached to the flange F and brought out through an opening in the case to the electrode of the ionisation chamber. For use in α- and β-ray measurements it is advisable to be able to remove the floor of the instrument, leaving only a thin aluminium window for the rays to pass through on their way to the electroscope from below.

* With a 1½-inch objective and a tube length of about 7 inches (objective to micrometer scale), giving an initial magnification of 5, and a micrometer scale graduated into tenths of a mm., this natural leak would be 0·1 division per min., and the sensitivity 25·5 divisions per volt.



Digitized by Google

Digitized by Google

# SOME OBSERVATIONS ON INDUCTION COIL AND TRANSFORMER DISCHARGES WITH COOLIDGE AND GAS TUBES

BY

E. A. OWEN, M.A., D.Sc.,
SENIOR ASSISTANT IN THE PHYSICS DEPARTMENT,

AND

PHYLLIS K. BOWES, M.A., B.Sc.,
SOMETIME JUNIOR ASSISTANT IN THE PHYSICS DEPARTMENT.

Digitized by Google

## ABSTRACT.

An account is given of an investigation which was carried out to determine the relation between the intensity of the radiation emitted by and the current passing through a Coolidge or gas tube when operated by either an induction coil or a high-tension transformer.

The intensity of the radiation emitted by an X-ray tube when the applied voltage is kept constant is not in all cases proportional to the mean current passing through the tube.

Considerations of voltage and current wave forms point to the conclusion that, for a given voltage and when the maximum current is in phase with the maximum voltage, the intensity of radiation emitted by an X-ray tube, whether of the gas or of the hot cathode type, is roughly proportional to the maximum (or peak) current passing through the tube. This is true both for coil and for transformer discharges.


Digitized by Google

# SOME OBSERVATIONS ON INDUCTION COIL AND TRANSFORMER DISCHARGES WITH COOLIDGE AND GAS TUBES.

By E. A. OWEN, M.A., D.Sc., Senior Assistant, and PHYLLIS K. BOWES, M.A., B.Sc., sometime Junior Assistant, in the Physics Department.

[Reprinted from the 'Journal of the Röntgen Society', Vol. 19, 1923.]

## Introduction.

In an investigation on the intensity of X-rays emitted by a Coolidge tube when operated on an induction coil outfit,* the authors found that when the voltage on the tube was kept constant the intensity of the radiation emitted was not directly proportional to the mean current passing through the tube. Other observers have found under different conditions of experiment that there is a direct proportionality existing between these two quantities. The main object of the present work was to endeavour to account for these differences. With this end in view the investigation has been extended to include both Coolidge and gas tubes when operated by induction coil and transformer respectively.

## Conditions of Experiment.

The arrangement of the apparatus was the same as that previously employed. The electroscope was standardised as before by the use of a tube of radium in radioactive equilibrium. The sensitivity of the instrument kept remarkably constant, only a slight variation being noticed during the course of several months. The sensitivity was also constant over the whole range of the scale of the instrument.

The voltage across the X-ray tube was kept constant at 66 kilovolts, as measured with an alternative spark-gap either between two spheres or between point and plane. The mean current through the tube was measured by means of a moving coil milliammeter and ranged up to about 15 milliamperes.

The X-ray tube was completely enclosed inside a thick lead box and its electrodes could be connected in turn either to the terminals of an induction coil or to those of a transformer. The coil was worked with a gas mercury jet-break which gave about 50 interruptions per second. The number of cycles executed by the transformer was also about 50 per second, each alternate half wave being rectified so that 100 current loops passed through the tube per second. In this case also only about half the loop was picked up by the selector disc.

Both the Coolidge and the gas X-ray tubes employed were fitted with tungsten anticathodes.

## Results.

(*a*) *Relation between Mean Current through the Tube and X-Ray Intensity.*—The results obtained are graphically represented in Fig. 1. It will be observed that for each

* 'N.P.L. Collected Researches', vol. 19, Paper 22, or 'J. Röntg. Soc.', vol. 17, p. 107, 1921.

Digitized by Google

combination of X-ray tube and high-tension generator, except that of Coolidge tube operated by an induction coil, the intensity of radiation emitted is directly proportional to the mean current through the tube. The results obtained now with Coolidge tube on induction coil discharge corroborate those previously recorded under these

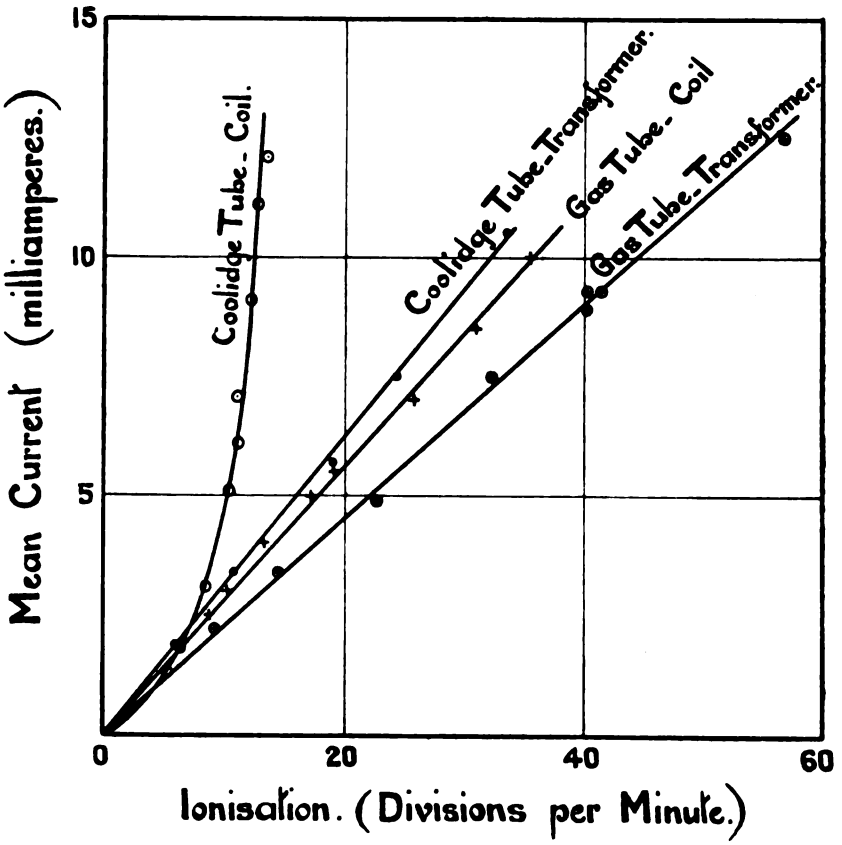


FIG. 1.

conditions. For small currents through the tube, the intensity of the radiation emitted is approximately directly proportional to the mean current, but for larger currents the intensity becomes independent of the mean current, tending towards a limiting value.

It should be pointed out that the above curves give no definite information regarding the relative output of gas and Coolidge tubes, the reason for this being that the ionisation produced in the electroscope depends upon the positions of the anticathodes of the two bulbs relative to the apertures defining the X-ray beams. A slight movement of the anticathode relative to these apertures would alter the value of the ionisation considerably. No particular care was taken that the anticathodes of the two tubes employed were similarly situated in all respects with regard to the aperture, although this may have been approximately the case. Further, the current wave of the transformer was selectively rectified, whilst that of the coil was not.

The only definite conclusion that can be drawn from the curves regarding the X-ray

Digitized by Google

output is that for large secondary currents the Coolidge tube on coil discharge is not as efficient in the production of X-rays as the other combinations of X-ray tube and high-tension generator experimented with in the present work.

(*b*) *Quality of the Radiation emitted.*—The quality of the radiation emitted by the two types of X-ray bulbs under coil and transformer discharge was examined by measuring the absorption of the radiation in sheets of aluminium of different thicknesses. The absorption curves obtained in this way are shown in Fig. 2. Comparing the radiation emitted by the gas tube with that emitted by the Coolidge tube under similar conditions

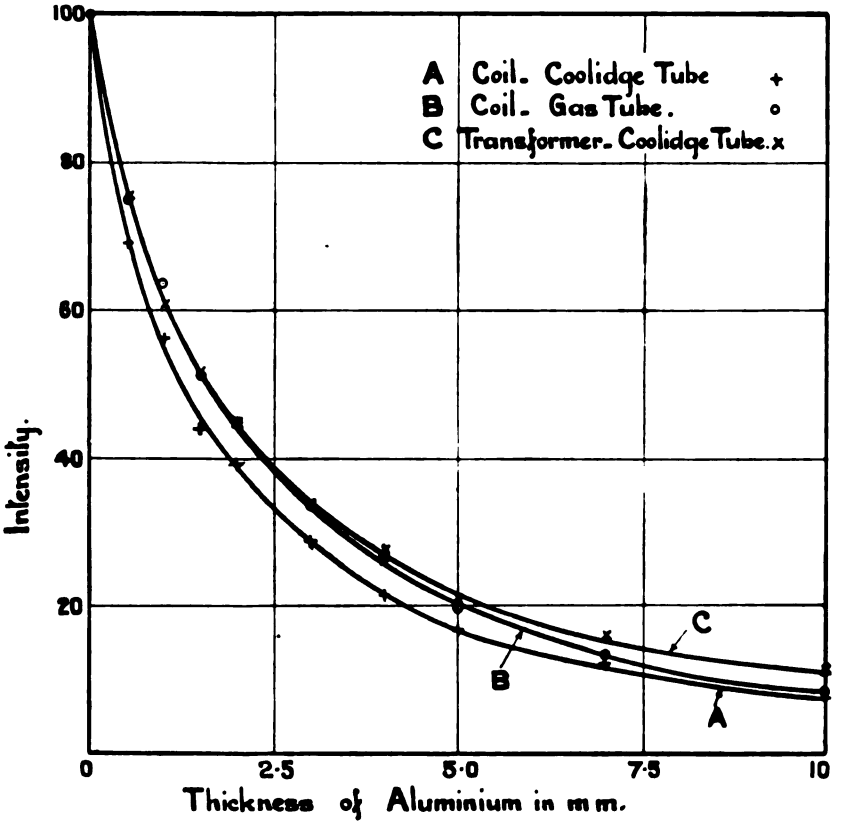


FIG. 2.

of discharge on a coil outfit, it will be observed that the former contains a higher percentage of penetrating radiation than the latter (Curves A and B). In this case a Morton rectifier was fitted to the mercury interrupter. By adjusting the rectifier so that the current passed through the Coolidge tube only during the interval embracing the region of maximum current, it was possible to displace the absorption curve in this case so as to coincide almost with that obtained with the gas tube.

In the particular case of the transformer employed, in which the half-waves were selectively rectified so that only part of the current wave in the region of the maximum passed through the tube, the absorption curve obtained with the Coolidge tube coincides almost with that observed with the gas tube under coil discharge (Curve C). The

Digitized by Google

corresponding curve with the gas tube is not included, because the tube unfortunately gave out before the curve could be obtained with it. It is, however, the comparison of the two types of bulbs on coil discharge that is mainly of interest in the present investigation.

(*c*) *Current and Voltage Wave Forms.*—The current and voltage wave forms of the discharge through a Coolidge tube when operated on a coil outfit were especially considered. The current wave form was determined by means of a Duddell oscillograph placed in series with the X-ray tube and the voltage wave form by means of a Taylor-Jones electrostatic oscillograph placed across the electrodes of the tube. The curves obtained with these instruments are diagrammatically represented in Fig. 3. The current curve

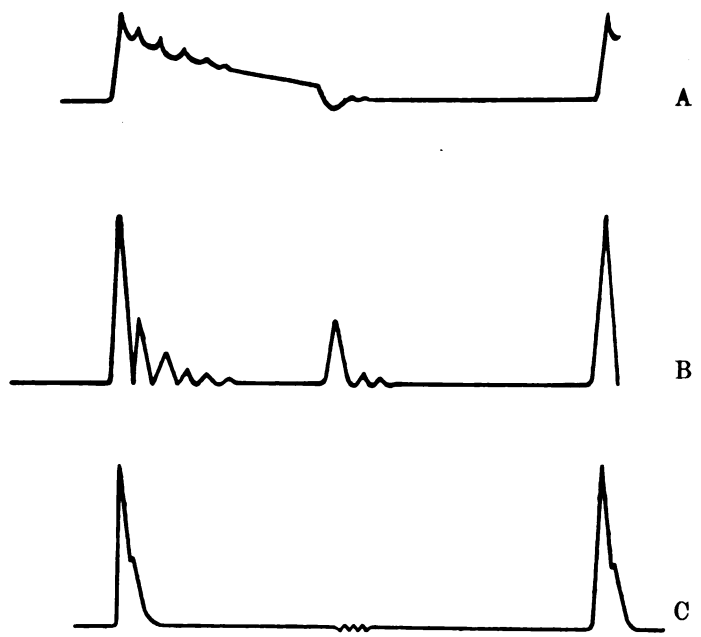


Fig. 3.

(A) shows that the main maximum is reached after a short interval from the instant of the " break " of the primary current. Afterwards the current slowly decays and at " make " suddenly drops to zero value. There are also superposed on the decaying portion of the curve a number of rapid oscillations which are due to the highly damped free oscillations of the coupled system. Below the current wave is shown the voltage wave (Curve B), which consists of one high peak followed by several smaller ones. In the actual oscillograph small variations of voltage were observed throughout the interval between " break " and " make ".

Taylor-Jones* has shown that rays which produce most effect on a photographic plate are given off by a tube operated on a coil outfit when the applied voltage is near

* ' Theory of the Induction Coil ', p. 159.

Digitized by Google

its maximum. CODD* has also observed that this effect occurs in the region of maximum current. It is probable that X-rays are emitted by a Coolidge tube corresponding to the smaller maxima observed in the voltage wave, but that these are of too long a wave length to affect a photographic plate or for some of the peaks even to penetrate the walls of the tube. In the case of a gas tube, however, the current wave form of which is shown in Curve C,† Fig. 3, the voltages corresponding to the smaller maxima will be too low to cause a discharge to pass. These different effects with Coolidge and gas tubes are due to the different mechanism of production of X-rays in the two cases. In the former, so long as a difference of voltage exists between the electrodes, a current will pass through the tube, whereas in the latter the applied voltage must be high enough to produce ionisation by collision before a discharge will take place. Hence, in a gas tube X-rays are produced throughout the interval that the discharge passes through the tube, whilst in the Coolidge tube the current wave may be divided into two parts—(1) the region of the main maximum when penetrating X-rays are emitted, and (2) the decaying portion when practically no X-rays are produced. This point has already been emphasised by CODD. This difference between the two cases would account for the difference in quality of radiation which has already been mentioned, the Coolidge tube emitting a radiation which on the whole is less penetrating than that under similar conditions of coil discharge emitted by the gas tube.

Similar remarks hold for transformer discharge. In this case, however, only the region of the maximum of the wave was picked up by the selector disc, so that the softer constituents of the radiation would be cut out from the X-ray beam. This is in agreement with the absorption curves observed.

(*d*) *Relation between Maximum and Mean Current.*—We are greatly indebted to the late Prof. SALOMONSON of Amsterdam for supplying us with a number of current oscillograph curves which give us the relation between maximum and mean current in the case of a Coolidge tube operated by an induction coil. The oscillographs were taken at his laboratory under precisely the same conditions as those obtaining in the present investigation. On measuring up the curves it was found that the calculated mean current closely followed the indictions of the milliammeter. Plotting the mean current against the maximum current in each case, the curve shown in Fig. 4 was obtained. It shows that, as the mean current is increased, the maximum current (that is, the current corresponding to the first high peak of the current wave) does not increase in proportion to it, but tends towards a constant limiting value. This curve shows very much the same characteristics as that observed between mean current and intensity of radiation (see Fig. 1), which suggests that the maximum current (or the region of maximum current), is the factor that decides the X-ray output. This is in agreement with the result of CODD already referred to, which was arrived at by the photographic method.

* 'Induction Coil Design', p. 36, Fig. 53.

† 'CODD, 'Induction Coil Design', p. 31, Fig. 44.



Digitized by Google

Assuming that the above relation between mean and maximum current is typical for the Coolidge tube operated on a coil outfit, and that it can be applied to the case under investigation, we find by combining it with the observed relation between mean current

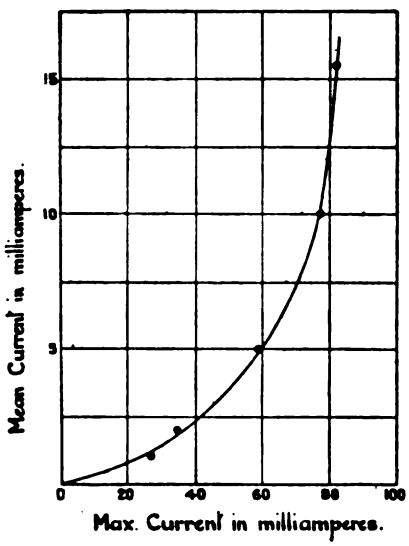


FIG. 4.

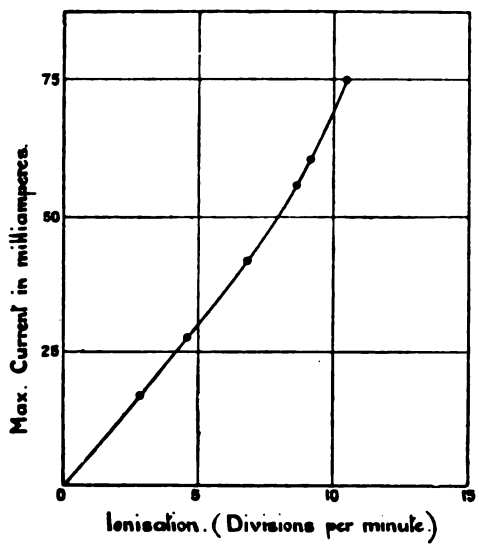


FIG. 5.

and intensity of radiation, that the X-ray output is roughly proportional to the maximum current passing through the tube (Fig. 5). Exact proportionality is not obtained, probably because the ionisation measurements included radiation corresponding to the second and subsequent peaks of the voltage wave, and not that corresponding to the main maximum alone.

The proportionality between mean current and intensity of radiation observed in the case of a Coolidge or gas tube worked on a transformer (see Fig. 1), is readily explained on the above conclusion if the voltage and current curves of the latter are in phase and of approximately sine wave form. For in this case the maximum current is proportional to the mean current so that, if the X-ray intensity bears a linear relation to the maximum current, it will also bear a similar relation to the mean current.

We have seen in the case of a gas tube operated by a coil that the current wave rises rapidly to its maximum value and then falls almost equally rapidly to zero value. We are dealing here with a curve which can be analysed into two sine waves, the area of the one being so small compared with that of the other that it may be neglected to a first approximation.* The area of the curve will then be proportional to the maximum and the same result as in the case of the transformer follows.

* If the value of the two maxima bear a constant ratio to each other, which we are led to believe is the case from voltage oscillograph curves taken on various occasions, the area of the curve will be strictly proportional to the main maximum.

Digitized by Google

(*e*) *Conclusions.*—(1) The intensity of radiation emitted by an X-ray tube is not in all cases proportional to the mean current passing through the tube when the applied voltage is kept constant.

(2) Considerations of voltage and current wave forms point to the conclusion that for a given voltage and when the maximum current is in phase with the maximum voltage, the intensity of radiation emitted by an X-ray tube, whether of the gas or of the hot cathode type, is roughly proportional to the maximum (or peak) current passing through the tube. This is true both for coil and for transformer discharges.



Digitized by Google

Digitized by Google

# MODIFICATION OF THE POWDER METHOD OF DETERMINING THE STRUCTURE OF METAL CRYSTALS

BY

E. A. OWEN, M.A., D.Sc.,
SENIOR ASSISTANT IN THE PHYSICS DEPARTMENT,

AND

G. D. PRESTON, B.A.,
ASSISTANT IN THE METALLURGY DEPARTMENT.

Digitized by Google

ABSTRACT.

Plates of aluminium, iron, copper, lead and magnesium have been examined by means of the Bragg X-ray spectrometer employing radiation direct from a molybdenum anticathode. The maxima observed in the spectra are sufficiently intense to measure with accuracy, and the crystalline structure of the materials examined are readily determined. A few of the results obtained by the method are included in the paper as typical examples.

Digitized by Google

# MODIFICATION OF THE POWDER METHOD OF DETERMINING THE STRUCTURE OF METAL CRYSTALS.

By E. A. OWEN, M.A., D.Sc., Senior Assistant in the Physics Department, and G. D. PRESTON, B.A., Assistant in the Metallurgy Department.

[Reprinted from the 'Proceedings of the Physical Society of London', Vol. 35, 1923.]

## I. Introductory.

The powder method of determining the structure of crystals, independently developed by Hull* and by Debye and Scherrer,† has had a wide application and has been extensively employed by Hull in particular for the examination of the structure of metal crystals. For this method the material under examination is reduced to a fine powder, a small quantity of which is placed in a tiny glass tube situated in the path of a beam of X-rays which has been rendered monochromatic by passing it through a suitable filter. The rays reflected at the different faces of the small crystals in the tube appear on a photographic film upon which they fall as a series of irregularly spaced lines, the positions of which suffice to solve the structure of the material.

W. H. Bragg‡ has recently shown that the structure of powdered materials can also be solved by the aid of the X-ray spectrometer. The powder in this case is pasted on a flat sheet of cardboard and the whole mounted on the table of the spectrometer in the position usually occupied by the face of a single crystal. Unfiltered radiation direct from a rhodium anticathode falls on the powder, both the $\alpha$ and the $\beta$ lines of the K series spectrum of rhodium being reflected in turn into the ionisation chamber. If the structure is not too complicated, the presence of the two lines is an advantage rather than a disadvantage in that the reflection of the one line serves as a check upon the other. The advantage of this method over the photographic method is twofold—the time of exposure is very much shortened and the relative intensity of the lines in the spectrum is directly observed. In order to obtain a readable impression of the spectrum upon a photographic plate an exposure of about 300 milliampere-hours is required, whereas with the X-ray spectrometer the spectrum can be plotted in an hour or two, using only about 1 milliampere through the bulb.

The present paper is an account of a further development of the method of determining the structure of metal crystals. Instead of reducing the metal, the crystalline structure of which is required, to a fine powder, a plate of the metal is taken and examined by means of the X-ray spectrometer in a manner similar to that adopted by Bragg. The few results given below show that the structure can be solved by this means in a

* 'Phys. Rev.', vol. 10, p. 661, 1917.

† 'Phys. Zeits.', vol. 17, p. 277, 1916; vol. 18, p. 291, 1917.

‡ 'Proc. Phys. Soc. Lond.', vol. 33, part 4, p. 222, 1921.

Digitized by Google

comparatively short time with only small currents passing through the bulb. The examples chosen serve to illustrate the application of the method to the solution of the structure of crystals belonging respectively to cubic and hexagonal systems.

## II. Method of Procedure.

A plate of metal, either cast or rolled and measuring about 5 cms. by 2·5 cms., is subjected to heat treatment necessary to produce throughout its volume a mass of small crystals—crystals about 1 mm: or less across are suitable for the purpose. The plate is etched to remove the deformed surface layer of crystals or any oxide that may have formed, and is then smeared over with vaseline to prevent further oxidation. It is mounted on the spectrometer with one of its large surfaces adjusted so as to fall just over the centre of the crystal table.

The spectrometer is provided with an 8-inch circle graduated to read directly to 5 seconds of arc. The width of the chamber slit is kept at 2 mms., which corresponds to about one degree of arc, whilst the bulb and crystal slits are opened wide enough to allow a beam of rays to fall upon the plate just sufficient to cover it from side to side.

During a few preliminary observations the metal plate is fixed at any angle with the X-ray beam and readings are taken of the ionisation for different positions of the chamber. One or two of the main maxima are located in this way. The chamber is then fixed in the position to receive one of these maxima, whilst the plate is rotated through a range of angle and the position of the plate determined at which maximum ionisation occurs in the chamber. Having determined this position, the plate is set at that angle and both chamber and crystal table are rotated together, the former at twice the rate of the latter.

These preliminary observations determine the position of the plate at which there is the smallest amount of absorption of the radiation for the face corresponding to the particular maximum chosen. We are assuming that this condition obtains also approximately for all the other faces of the crystals, since the number of crystals in the area of the plate irradiated is very large and there will be as many crystals on the average whose 100 planes, for example, are in the surface of the plate as there are crystals presenting 111, 110 or any other plane. That this assumption is justified is proved by the relative intensity of a line reflected at a large angle when the plate is kept fixed and when it is rotated in the manner stated, the intensity in the latter case being found to be much greater than that in the former. In the present investigation no particular attention has been directed to the relative intensities of the lines in the spectra, the main object being to locate the lines over a wide range of crystal planes.

## III. Results.

The five metals, magnesium, aluminium, iron, copper and lead, have been examined in detail. The curve obtained by the above method for iron is shown in Fig. 1, the radiation employed being that from a molybdenum anticathode for which $\lambda_\alpha = 0{\cdot}711$ Å

Digitized by Google

and $\lambda_\beta = 0{\cdot}629$ Å. The curves show the actual readings of intensity plotted against chamber angle, readings being taken at half-degree intervals. The exposure for each reading was about 8 seconds. The Coolidge bulb employed was operated at 80,000 volts and had a current of 1 milliampere passing through it.

When reflection takes place at a crystal face the relation $n\lambda = 2d \sin \theta$ must be satisfied, where $\lambda$ is the wave-length of the radiation reflected, $d$ the distance between successive planes parallel to the face, and $\theta$ the angle of reflection. In the case of crystals of cubic structure, $d$ for all faces is proportional to the length of the side of the elementary cube. Thus we have $n\lambda = 2ka$ . sin $\theta$, where $k$ is a constant characteristic of the set of planes at which reflection occurs. The values of $k$ for different sets of planes in any one of the

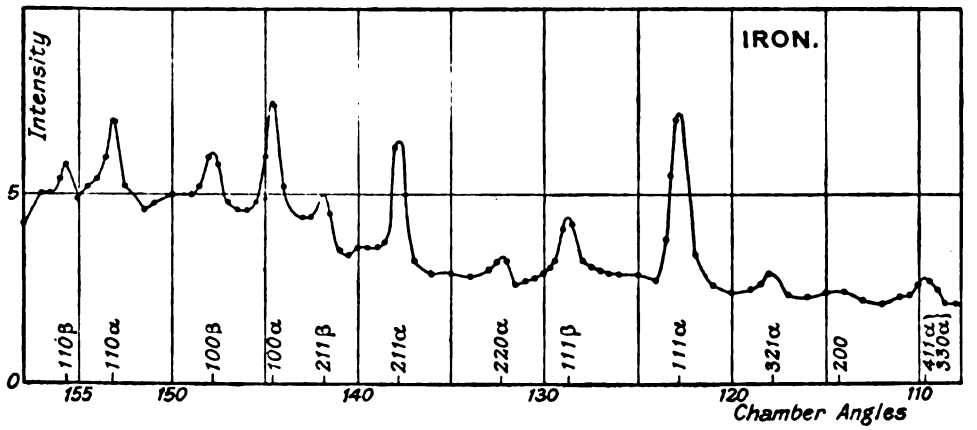


FIG. 1.

three possible cubic structures are fixed so that if we plot the reciprocal of $a$ against sin $\theta$ we get a series of straight lines passing through the origin, each straight line corresponding to one definite face of the crystal. The graphs for the face centred cube and for the centred cube are shown in Figs. 2 and 3 respectively. In these graphs both the $\alpha$ and the $\beta$ lines are included, the former being the full and the latter the broken lines. If the structure of the crystal is cubic, the lines in its spectrum should fit somewhere on one of these graphs. To test this the sines of half the chamber angles of the lines in the spectrum were set out on a slip of paper, which was passed over the graphs, the zero line of the one coinciding with the zero line of the other. We have shown in Figs. 2 and 3 where the best fit occurs in each case. Aluminium, copper and lead fit on the graph for the face centred cube and iron on that for the centred cube. The magnesium spectrum does not fit on any of these graphs and will have to be considered separately. In the case of each of the other four metals the fit is good and, with one or two exceptions, *all* the lines are accounted for.

From the position at which each spectrum fits the graph, we deduce at once the length of the side of the elementary cube. To obtain a more accurate determination of this quantity, its value was calculated independently for each line in the spectrum. The



Digitized by Google

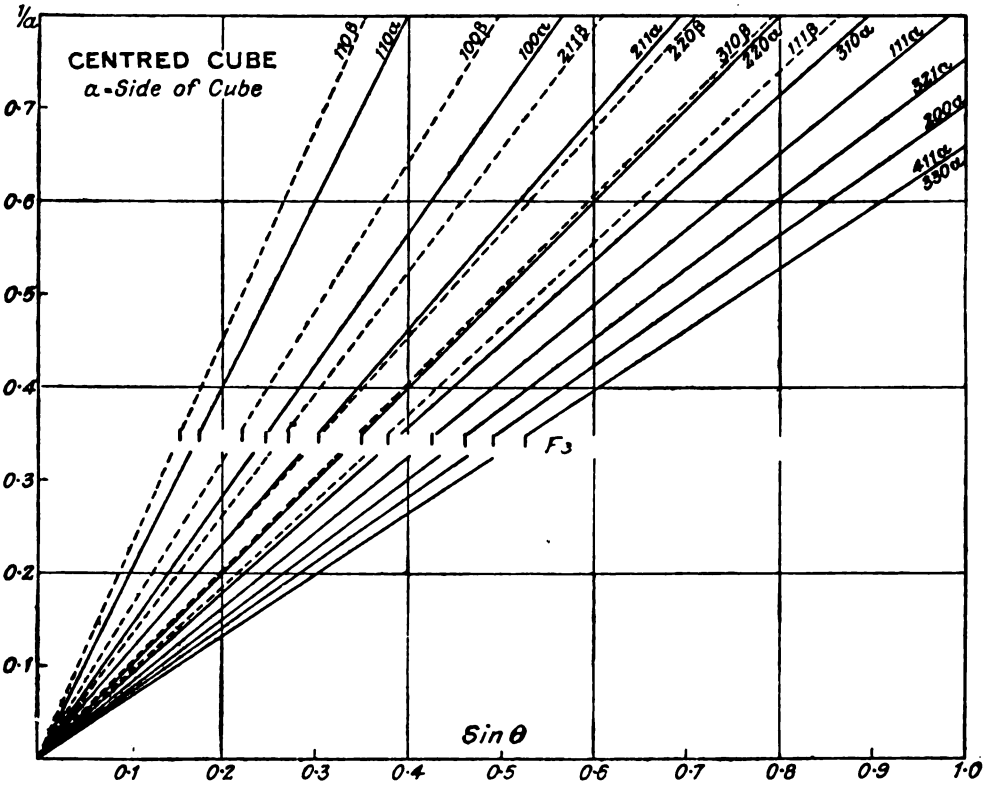


FIG. 2.

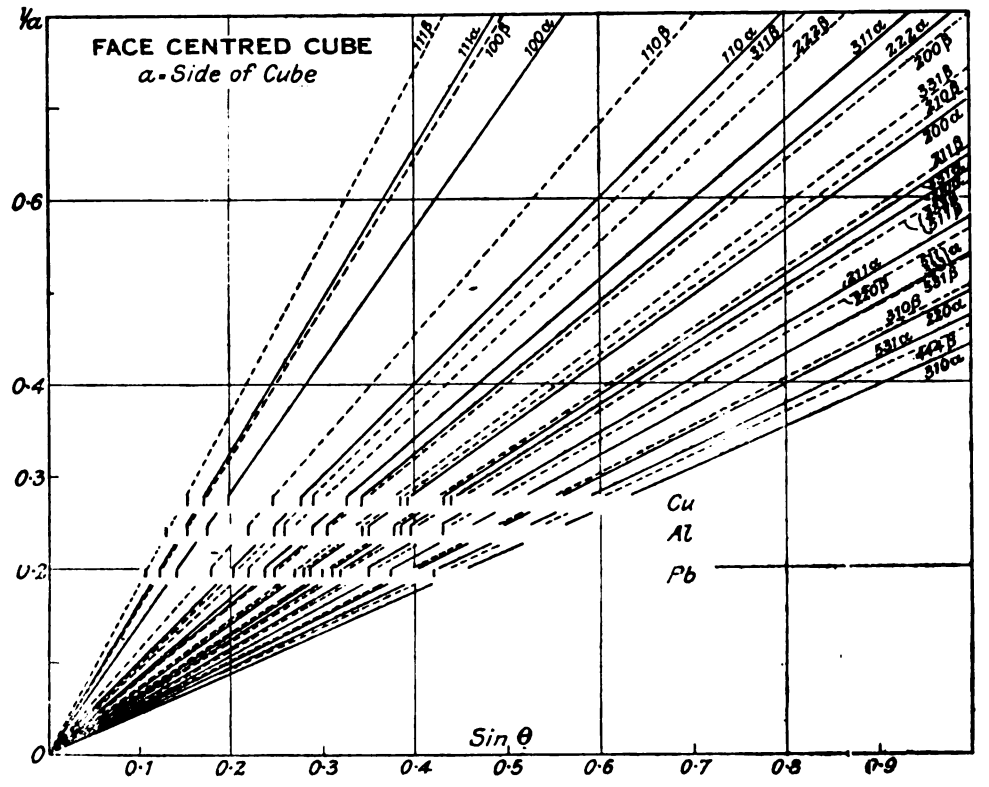


FIG. 3.

Digitized by Google

values calculated for iron are tabulated below and serve as an example of the order of agreement obtained.

TABLE I.—Electrolytic Iron.

| Reading of Maximum. | θ. | sin θ. | Form. | $k \equiv d/a$. | Side of Elementary Cube ($a$). |
|---|---|---|---|---|---|
| 155·6° | 8·85 | 0·1539 | 110β | 0·707 | 2·867 Å |
| 153·1° | 10·1 | 0·1754 | 110α | 0·707 | 2·867 |
| 147·8° | 12·75 | 0·2207 | 100β | 0·500 | 2·828 |
| 144·6° | 14·35 | 0·2478 | 100α | 0·500 | 2·869 |
| 141·8° | 15·75 | 0·2714 | 211β | 0·408 | 2·870 |
| 137·8° | 17·75 | 0·3048 | 211α | 0·408 | 2·909 |
| 132·3° | 20·5 | 0·3502 | 220α | 0·3535 | 2·872 |
| 128·7° | 22·3 | 0·3795 | 111β | 0·2885 | 2·849 |
| 122·8° | 25·25 | 0·4266 | 111α | 0·2885 | 2·888 |
| 117·9° | 27·7 | 0·4648 | 321α | 0·2672 | 2·863 |
| 114·2° | 29·55 | 0·4932 | 200α | 0·250 | 2·882 |
| 109·7° | 31·8 | 0·5270 | (411α) (330α) | 0·2358 | 2·863 |
| | | | | Mean value of $a$ = 2·869 Å. | |

The results obtained with the four metals, aluminium, iron, copper and lead, are summarised in Table II. Included in the table are the values of the number of atoms ($n$) associated with each elementary cube calculated from the observed mean values of $a$. In the last column are inserted for comparison the values of $a$ found by HULL with the powder method. The greatest difference between these values and those obtained by the method described here is about 1 per cent. The calculated values of $n$ in the next to the last column of the table are in accordance with the lattice assigned to the different elements, namely, that for a centred cube, two atoms, and for a face centred cube, four atoms, are associated with each elementary cube.

TABLE II.

| Element. | Structure. | Length of side of elementary cube ($a$). | $n \equiv \frac{\rho a^3}{m}$. | Values of $a$ as measured by HULL. |
|---|---|---|---|---|
| Al | Face Centred Cube . . . . . | 4·041 Å | 3·98 | 4·05 Å |
| Fe | Centred Cube . . . . . | 2·869 | 2·015 | 2·86 |
| Cu | Face Centred Cube . . . . . | 3·628 | 4·06 | 3·60 |
| Pb | Face Centred Cube . . . . . | 4·983 | 4·11 | 4·92 |



Digitized by Google

## IV. Magnesium.

The procedure in the case of magnesium had to be somewhat modified in order to include crystals of different axial ratios. Considering, for instance, crystals of the close packed hexagonal type, a graph was drawn for each set of planes in the crystals giving the relation between the logarithm of the reciprocal of the axial ratio ($c$) and the logarithm of the reciprocal of the distance between consecutive planes, assuming the side of the hexagon to be unity. Such a graph will be independent of the wave length of the radiation reflected, and can, therefore, be used both for the $\alpha$ and for the $\beta$ lines. The graph shown in Fig. 4 is that for a close packed hexagonal lattice. It can be used for crystals over a wide range of axial ratio.*

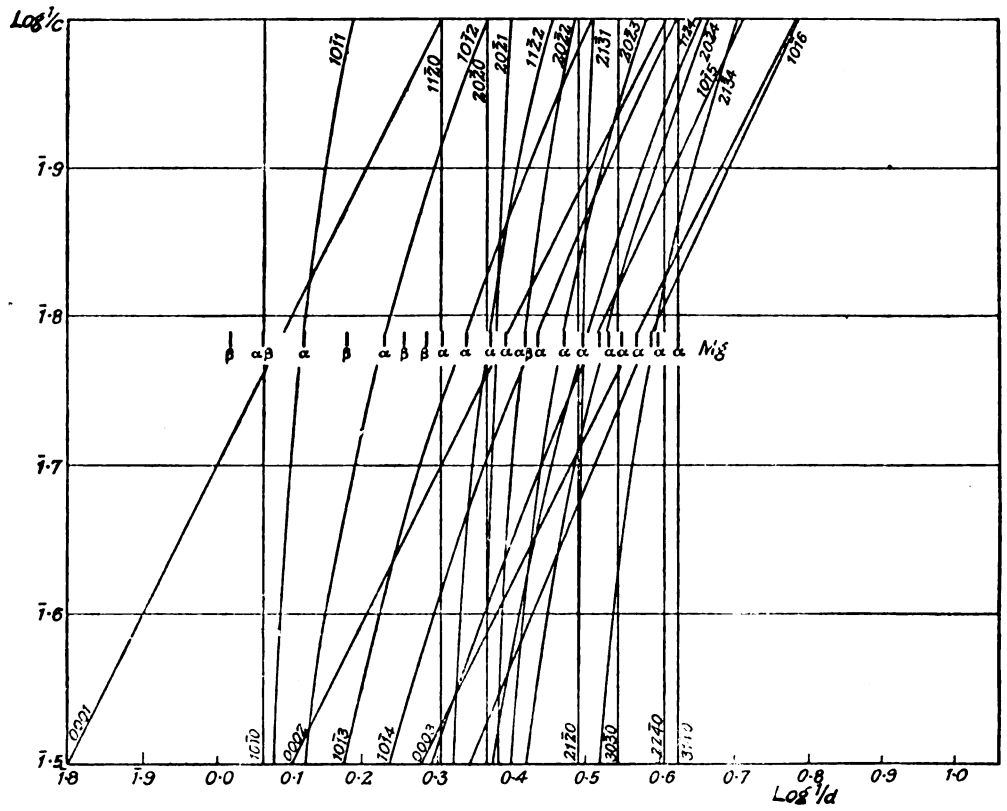


Fig. 4.

It should be mentioned that the magnesium plate examined was cut from a rod of the metal about 2·5 cms. wide. The specimen was polished and etched before the X-ray examination was conducted, but in this case it was not especially heat-treated previously, as in the other cases already considered.

The lines observed in the spectrum of this metal were very prominent, and as many as 22 lines were measured, including both $\alpha$ and $\beta$ lines. The logarithm of the sine of the

* A graph similar to this has been employed by Hull, the only difference being in the choice of the ordinates (see Hull, 'Phys. Rev.', vol. 17, p. 549, 1921).

Digitized by Google

TABLE III.—Magnesium.

| Reading of maximum. | θ. | Log sin θ. | Form (Miller-Bravais). | $d$. | $d/a$ ($c = 1{\cdot}631$). | Length of side of hexagon ($a$). |
|---|---|---|---|---|---|---|
| 160·2° | 6·65 | $\bar{1}{\cdot}0633$ | $10\bar{1}0$ β | $a\frac{\sqrt{3}}{2}$ | 0·866 | 3·116Å |
| 158·5° | 7·4 | $\bar{1}{\cdot}1099$ | $10\bar{1}0$ α | $a\frac{\sqrt{3}}{2}$ | 0·866 | 3·187 |
| | | | $10\bar{1}1$ β | $a/\sqrt{\frac{4}{3}+\frac{1}{c^2}}$ | 0.7649 | 3.162 |
| 156·4° | 8·45 | $\bar{1}{\cdot}1673$ | $10\bar{1}1$ α | $a/\sqrt{\frac{4}{3}+\frac{1}{c^2}}$ | 0·7649 | 3·161 |
| 154·1° | 9·6 | $\bar{1}{\cdot}2222$ | $10\bar{1}2$ β | $a/\sqrt{\frac{4}{3}+\frac{4}{c^2}}$ | 0·5937 | 3·151 |
| 151·7° | 10·8 | $\bar{1}{\cdot}2727$ | $10\bar{1}2$ α | $a/\sqrt{\frac{4}{3}+\frac{4}{c^2}}$ | 0·5937 | 3·186 |
| 150·4° | 11·45 | $\bar{1}{\cdot}2980$ | $11\bar{2}0$ β | $a/2$ | 0·500 | 3·142 |
| 148·5° | 12·4 | $\bar{1}{\cdot}3318$ | $10\bar{1}3$ β | $a/\sqrt{\frac{4}{3}+\frac{9}{c^2}}$ | 0·4605 | 3·156 |
| 147·4° | 12·95 | $\bar{1}{\cdot}3506$ | $11\bar{2}0$ α | $a/2$ | 0·500 | 3·171 |
| 145·2° | 14·05 | $\bar{1}{\cdot}3850$ | $10\bar{1}3$ α | $a/\sqrt{\frac{4}{3}+\frac{9}{c^2}}$ | 0·4605 | 3·181 |
| 142·7° | 15·3 | $\bar{1}{\cdot}4215$ | $11\bar{2}2$ α | $a/\sqrt{4+\frac{4}{c^2}}$ | 0·4263 | 3·159 |
| 141·5° | 15·9 | $\bar{1}{\cdot}4378$ | 0002 α | $ac/4$ | 0·4077 | 3·181 |
| 139·3° | 17·0 | $\bar{1}{\cdot}4660$ | $20\bar{2}2$ α | $a/2\sqrt{\frac{4}{3}+\frac{1}{c^2}}$ | 0·3824 | 3·178 |
| | | | $20\bar{2}3$ β | $a/\sqrt{\frac{16}{3}+\frac{9}{c^2}}$ | 0·3388 | 3·150 |
| 137·8° | 17·75 | $\bar{1}{\cdot}4840$ | $10\bar{1}4$ α | $a/\sqrt{\frac{4}{3}+\frac{16}{c^2}}$ | 0·3689 | 3·161 |
| | | | $21\bar{3}1$ β | $a/\sqrt{\frac{28}{3}+\frac{1}{c^2}}$ | 0·3209 | 3·190 |
| 134·8° | 19·25 | $\bar{1}{\cdot}5181$ | $20\bar{2}3$ α | $a/\sqrt{\frac{16}{3}+\frac{9}{c^2}}$ | 0·3388 | 3·183 |
| 132·5° | 20·4 | $\bar{1}{\cdot}5424$ | $21\bar{3}1$ α | $a/\sqrt{\frac{28}{3}+\frac{1}{c^2}}$ | 0·3209 | 3·177 |
| 130·0° | 21·65 | $\bar{1}{\cdot}5669$ | $10\bar{1}5$ α | $a/\sqrt{\frac{4}{3}+\frac{25}{c^2}}$ | 0·3053 | 3·156 |
| 128·7° | 22·3 | $\bar{1}{\cdot}5794$ | $20\bar{2}4$ α | $a/2\sqrt{\frac{4}{3}+\frac{4}{c^2}}$ | 0·2968 | 3·154 |
| 127·0° | 23·15 | $\bar{1}{\cdot}5945$ | $30\bar{3}0$ α | $a\sqrt{3}/6$ | 0·2886 | 3·133 |
| 124·9° | 24·2 | $\bar{1}{\cdot}6127$ | 0003 α | $ac/6$ | 0·2718 | 3·190 |
| 122·7° | 25·3 | $\bar{1}{\cdot}6308$ | $10\bar{1}6$ α | $a/\sqrt{\frac{4}{3}+\frac{36}{c^2}}$ | 0·2593 | 3·207 |
| 121·5° | 25·9 | $\bar{1}{\cdot}6403$ | $21\bar{3}4$ α | $a/\sqrt{\frac{28}{3}+\frac{16}{c^2}}$ | 0·2553 | 3·188 |
| 117·5° | 27·9 | $\bar{1}{\cdot}6701$ | $31\bar{4}0$ α | $a\sqrt{\frac{3}{52}}$ | 0·2402 | 3·168 |
| | | | | | Mean value of $a = 3{\cdot}17$ Å | |

Digitized by Google

angle of reflection of each line in the spectrum was plotted on a slip of paper, and passed over the graph (Fig. 4) as previously until a position was found at which the lines fitted. In this case it is difficult to decide which are the $\alpha$ and which are the $\beta$ line reflections. In order to ascertain this, a filter of zirconium was placed in front of the chamber slit, and a small portion of the spectrum again examined. In this way the $\beta$ lines were almost entirely cut out, leaving only the $\alpha$ lines.

Of the 22 lines in the spectrum, 18 were found to be $\alpha$ lines and four $\beta$ lines. The value of the axial ratio taken was that obtained from the $\alpha$ lines alone, and was found to be 1·631. The length of the side of the hexagon was calculated for each set of planes in the crystal both for the $\alpha$ and for the $\beta$ lines. These values are included in Table III, the mean value being 3·17 Å.

As a further test on the structure, we may calculate the number of atoms associated with each elementary cell. The volume of the elementary triangular prism is $\frac{\sqrt{3}}{4}a^3c$, where $a$ is the side of the hexagon and $c$ the axial ratio. Then $n$, the number of atoms associated with each elementary triangular prism $= \frac{\sqrt{3}}{4} \cdot \frac{a^3c\rho}{m}$, where $m$ is the mass of the atom and $\rho$ the density of the material.

Hence,
$$n = \frac{\sqrt{3}}{4} \times \frac{(3\cdot17)^3 \times 1\cdot631 \times 1\cdot74}{24\cdot13 \times 1\cdot663} = 0\cdot98.$$

There is, therefore, one atom associated with each elementary cell, which conforms to the requirements of a hexagonal lattice of the close packed type.

A point which needs further explanation is the absence of the 0001 line in the observed spectrum curve. This fact was also noted by HULL, but on fuller investigation of a number of single crystals he found the line to be present. In the present instance the region of the spectrum where the line should appear was examined in greater detail, observations being taken at 10′ intervals instead of 30′ intervals. In this case the line was clearly indicated, although its intensity was small.

The above measurements suffice to show the utility of the method. It promises to be a valuable asset to the metallurgist and has an advantage over the powder method in that it allows the specimen, after being polished and etched for microscopical examination, to be used directly on the X-ray spectrometer. In addition, there is in this case no possible distortion of the crystals with consequent increased absorption of the radiation.

We desire to express our indebtedness to the Metallurgy Department of the Laboratory for their assistance in the preparation of the specimens.

Digitized by Google

# X-RAY ANALYSIS OF SOLID SOLUTIONS

BY

E. A. OWEN, M.A., D.Sc.,
SENIOR ASSISTANT IN THE PHYSICS DEPARTMENT.

AND

G. D. PRESTON, B.A.,
ASSISTANT IN THE METALLURGY DEPARTMENT.

Digitized by Google

## ABSTRACT.

(1) The atomic structure of solid solutions of copper-aluminium, aluminium-magnesium, and copper-nickel has been examined by the X-ray spectrometer. In each case it was found that the solute atom replaces an atom in the lattice of the solvent, the substitution being accompanied by a distortion of the lattice.

A saturated solution of aluminium in copper shows that the aluminium expands the copper lattice from 3·60 Å to 3·65 Å. The effect of adding nickel to copper was to produce a contraction of the lattice, the contraction being approximately a linear function of the atomic percentage of either constituent. The addition of 8 per cent. magnesium by weight to aluminium causes the average parameter of the aluminium lattice to increase from 4·05 Å to 4·10 Å. The addition of 8 per cent. aluminium by weight to magnesium decreases the average parameter of the hexagonal lattice of magnesium from 3·17 Å to 3·15 Å, and increases its axial ratio from 1·63 to 1·66.

(2) An examination of the eutectic alloy of aluminium and copper showed that this alloy consists of a mixture of two distinct substances with different space lattices. The one substance being $CuAl_2$ and the other a substance the space lattice of which could not be distinguished from that of pure aluminium.

(3) The intermetallic compound $CuAl_2$ was found to possess a simple tetragonal lattice of side 4·28 Å and axial ratio 0·562, the copper atoms being at the corners and the aluminium atoms at the centres of the four small faces.

(4) The atomic structure of the compound CuAl resembles that of a solid solution of aluminium in copper, but the distortion is considerably greater. The material was found to have a face centred trigonal lattice of side 3·89 Å and an angle between the axes of 94·6°, the 111 planes being composed alternately of aluminium and copper atoms.


Digitized by Google

# X-RAY ANALYSIS OF SOLID SOLUTIONS.

By E. A. OWEN, M.A., D.Sc., Senior Assistant in the Physics Department, and G. D. PRESTON, B.A., Assistant in the Metallurgy Department.

[Reprinted from the 'Proceedings of the Physical Society of London', Vol. 36, 1923.]

## I. Introductory.

In an attempt to explain the hardness of solid solutions from the consideration of crystal structure, Rosenhain* advanced the view that crystals of solid solution of metal B in metal A are built on the same space lattice as crystals of pure A, the sole difference being that a certain number of individual atoms of A are replaced by atoms of B. The substitution of B atoms for A atoms is accompanied by a slight distortion of the A lattice in the neighbourhood of the B atoms, the extent of the distortion depending upon the relative sizes of the two atoms.

There is another way in which atoms of B may enter into the A lattice. Instead of replacing an atom of the solvent A, the solute atom may take up its position in the interstices between the atoms of the A lattice. There is experimental evidence to show that both of these arrangements actually occur.

Bain,† in an extensive investigation which included the examination of a number of different series of solid solutions, arrived at the conclusion that the arrangement of the atoms was in each case similar to that assumed by Rosenhain. The alloys examined were solutions of tin, zinc, manganese or aluminium in copper; iron or zinc in silver; tungsten, molybdenum, chromium or managanese in iron. McKeehan‡ found that in the silver-palladium and the silver-gold series of alloys the atoms in the crystals of both the pure metals and the alloys are arranged on face centred lattices, and that in the silver-palladium series in particular the parameter is nearly a linear function of the atomic per cent. of either component.

The work of Westgren and Phragmen§ on the crystal structure of steel points to the conclusion that the carbon atoms are located in the interstices of the iron lattice.

In all the above investigations the photographic X-ray method of analysis was employed. The present paper gives an account of a series of experiments on different alloy systems carried out with the Bragg X-ray spectrometer, the intensity of the reflections being measured by means of an ionisation chamber. The object of the experiments was to obtain further data regarding the structure of solid solutions, and to attempt, if possible, to increase the accuracy of measurement with a view to differentiating the more easily between what may be termed the "substitutional" and the "interstitial" atomic arrangements.

* 'Roy. Soc. Proc.', A, vol. 99, p. 196, 1921.

† 'Chem. and Met. Eng.', vol. 25, p. 663, 1921; vol. 28, p. 21, 1923; vol. 28, p. 65, 1923.

‡ 'Phys. Rev.', vol. 20, p. 424, 1922.

§ 'J. Iron and Steel Inst.', vol. 105, p. 241, 1922.



Digitized by Google

From a knowledge of the specific volume of a solid solution, together with the data obtained from X-ray analysis, it is possible to distinguish between these two types of solution. The argument is based upon the assumption that the introduction of a solute atom into the space lattice of a metal distorts the lattice, and that the X-ray spectrometer measures the average spacing between successive layers (no longer planes) of atoms. If we are dealing with a face centred cubic lattice, then the side of the cube $a$, the density $\rho$, and the atomic mass M associated with each point of the lattice are connected by the relation

$$\frac{4M}{a^3} = \rho. \quad \ldots\ldots\ldots\ldots\ldots \quad (1)$$

If the solution is of the substitutional type and there are $N_2$ atoms of a metal of atomic weight $M_2$ dissolved in $N_1$ atoms of a metal of atomic weight $M_1$, then the average mass associated with each point of the lattice will be

$$M_s = M_1 + \frac{N_2}{N_1 + N_2}.(M_2 - M_1). \quad \ldots\ldots\ldots\ldots \quad (2)$$

On the other hand, if the solution is interstitial, there will be associated with each point a mass

$$M_i = M_1 + \frac{N_2}{N_1}.M_2. \quad \ldots\ldots\ldots\ldots \quad (3)$$

Provided there is a sufficient atomic percentage of dissolved material, it is possible by the X-ray spectrometer to detect and measure the change in the parameter of the space lattice of the solvent metal. A comparison of the observed value of the parameter with the values calculated from the observed density on the substitutional and interstitial theories suffices to decide in the cases investigated, with one exception, between these two possible atomic arrangements.

## II. Experimental.

The method of procedure has been described by the authors* in a previous paper. A plate of metal to be examined, about 2 cms. wide, polished and etched, and containing throughout its volume small crystals (the smaller the size of the individual crystals the better for the purpose of the experiment) is placed on the table of the X-ray spectrometer. A beam of radiation from a molybdenum anticathode is allowed to fall on this plate, and the intensity of the "reflected" beam is measured in the usual way. To arrive at the correct angles of reflection, two corrections have to be applied to the observed readings on account of (1) the flatness of the plate, and (2) the penetration and the

* Owen and Preston, 'N.P.L. Collected Researches', vol. 19, Paper 24, or 'Proc. Phys. Soc. Lond.', vol. 35, p. 101, 1923.

Digitized by Google

consequent absorption of the radiation in the plate. It is desirable to consider these two corrections in detail.

(1) *Correction for Flatness of Specimen.*

The conditions of reflection of a beam of X-rays diverging from a point S (Fig. 1) are such that if there are situated at points A, M, B, concyclic with S, suitably orientated crystals, the reflected rays will converge to a focus at S′ on the circle SAMB. If a flat plate is used, then evidently the ray SA striking it at A′ will be reflected along A′Q parallel to AS′, so that the energy from the point S is spread out over the region QS′. As the slit of the ionisation chamber is moved across this region, a maximum intensity will be recorded when the edges of the slit coincide with Q and S′, so that to obtain the proper angle of reflection we will have to add to the observed angle one-half of the angle QMS′.

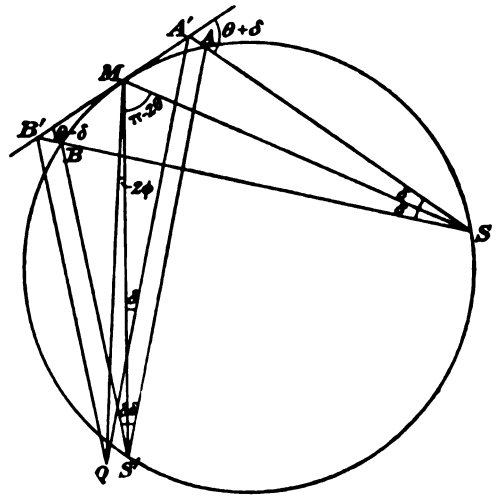


Fig. 1.

If $2\delta$ is the angular divergence of the beam of X-rays and if $l = SM$, then

$$A'M = l\delta/\sin(\theta + \delta) \quad \text{and} \quad B'M = l\delta/\sin(\theta - \delta),$$

and from the triangles A′QM and B′QM

$$\frac{\sin A'QM}{l\delta/\sin(\theta+\delta)} = \frac{\sin QA'M}{QM} \quad \text{and} \quad \frac{\sin B'QM}{l\delta/\sin(\theta-\delta)} = \frac{\sin QB'M}{QM},$$

or, since $QA'M = \theta - \delta$ and $QB'M = \pi - \theta - \delta$,

$$\sin A'QM = \frac{l\delta \sin(\theta-\delta)}{QM \sin(\theta+\delta)} \quad \text{and} \quad \sin B'QM = \frac{l\delta \sin(\theta+\delta)}{QM \sin(\theta-\delta)}. \quad . \quad . \quad (4)$$

From the parallelism of AS′, A′Q, and BS′, B′Q

$$A'QM + B'QM = 2\delta.$$

Provided A′QM and B′QM are small, which in practice is the case, from (4) we have

$$\frac{A'QM}{B'QM} = \frac{\sin^2(\theta-\delta)}{\sin^2(\theta+\delta)},$$

whence

$$A'QM = \frac{2\delta \sin^2(\theta-\delta)}{\sin^2(\theta+\delta) + \sin^2(\theta-\delta)}$$



Digitized by Google

Referring to the figure, the lines A′Q and MS′ intersect at an angle equal to $\delta$, so

$$QMS' = 2\phi = \delta - A'QM$$

or

$$\phi = \frac{\delta}{2} \cdot \left( \frac{\sin^2(\theta + \delta) - \sin^2(\theta - \delta)}{\sin^2(\theta + \delta) + \sin^2(\theta - \delta)} \right).$$

For small values of $\theta$ the length of the specimen A′B′ may be insufficient to obstruct the whole beam of divergence $2\delta$. When this is the case the quantity $\delta' = \frac{A'B' \sin \theta}{2l}$ must be substituted for $\delta$ in computing the value of $\phi$, whenever $\delta'$ is less than $\delta$. Thus, for the instrument used in the present work when the bulb slit is set at 2 mms. $\delta = 34'$ and consequently for a specimen 2 cms. wide, $l$ being 15 cms., for values of $\theta$ up to 8° (when $\delta'$ becomes approximately equal to $\delta$) the expression given for $\delta'$ is substituted for $\delta$. The following table shows the values of $\phi$ computed from the above expression for a few values of $\theta$ for a specimen 2 cms. in width :—

TABLE I.

| $\theta$ | $\phi$. |
|---|---|
| 5° | 2·5′ |
| 8° | 2·5′ |
| 10° | 2·0′ |
| 15° | 1·2′ |

(2) *Correction for Depth of Penetration.*

Suppose AB (Fig. 2) to be the surface of the specimen and S a point in the bulb slit—then the rays diverging from S and reflected by crystals lying in the circle AMB will converge to a focus at S′. The distance traversed in the metal by a ray such as SNS′ varies from zero at A and B to 2ML/sin $\theta$, so as an approximation we may suppose that the average value of this quantity for all the rays diverging from S is ML/sin $\theta$. If now we further suppose that the intensity at S′ is proportional to the length AMB, we can find the value of ML for which the intensity is a maximum.

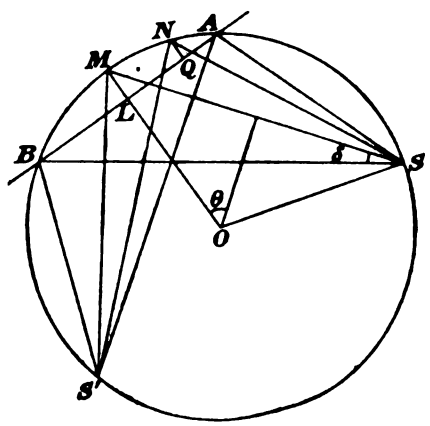


FIG. 2.

Writing ML = $x$, SM = $l$; OS = R and ∠ASM = $\delta$, we have

$$AM = 2R\delta = \frac{l\delta}{\sin \theta}.$$

Subject to the above assumption, the intensity at S′ is

$$I = Ke^{-\frac{\mu x}{\sin \theta}} \cdot \frac{2l\delta}{\sin \theta}.$$

Digitized by Google

Moreover

$$\delta = \sqrt{\frac{x}{2R}} \text{ approximately,}$$

so that

$$I = Ke^{-\frac{\mu x}{\sin\theta}} \cdot \frac{2l}{\sin\theta} \cdot \sqrt{\frac{x}{2R}}.$$

Differentiating with respect to $x$ and equating to zero, we have

$$x = \frac{\sin\theta}{2\mu}.$$

This gives the value of ML for which the intensity is a maximum. The required correction is the angle subtended by ML at S′, *i.e.*

$$\phi' = \frac{ML \cdot \cos\theta}{l} = \frac{\sin 2\theta}{4\mu l}.$$

In the case of aluminium, $\mu$ is 13 for $K_\alpha$ radiation of molybdenum, so that with the instrument previously referred to where $l = 15$ cms. the value of $\phi'$ is about 4 minutes of arc when $\theta = 45°$. When $\theta$ is 10°., $\phi' = 1{\cdot}5$ minutes. For the heavier metals such as copper, nickel, iron, the correction is very much less than the experimental error as $\mu$ increases rapidly with atomic weight.

Both of the above corrections are small over the range of angles employed in the present investigation, but they have been applied to the observations tabulated below.

## III. Results.

### (1) *Aluminium-Copper Alloys.*

(*a*) *Alloys Rich in Copper.*—A series of solid solutions of aluminium in copper, containing 2, 4, 6 and 8 per cent. of aluminium by weight, was examined. It was found that there was a general shift of the lines in the observed spectra towards the origin, showing that the lattice is expanded by the presence of the aluminium atoms (Fig. 3). The form of the lattice, however, was still that of the face centred cube characteristic of copper. The reflection of the $K_\alpha$ radiation of molybdenum from the 110 and 311 planes was examined in detail, the maximum being fixed to within 3′ of arc for the whole series. The angles of reflection and the values of the corresponding parameters of the lattices are given in Table II.

Table II.

| Form. | Copper. | | 2 per cent. Al. | | 4 per cent. Al. | | 6 per cent. Al. | | 8 per cent. Al. | |
|---|---|---|---|---|---|---|---|---|---|---|
| | θ | *a* | θ | *a* | θ | *a* | θ | *a* | θ | *a* |
| 110 . . | 16° 9′ | 3·599 | 16° 4′ | 3·617 | 16° 0′ | 3·633 | 15° 58′ | 3·635 | 15° 54′ | 3·653 |
| 311 . . | 18° 58′ | 3·612 | 18° 55′ | 3·621 | 18° 48′ | 3·642 | 18° 48′ | 3·642 | 18° 47′ | 3·646 |
| Mean value | | 3·605 Å | | 3·619 Å | | 3·638 Å | | 3·639 Å | | 3·649 Å |

Digitized by Google

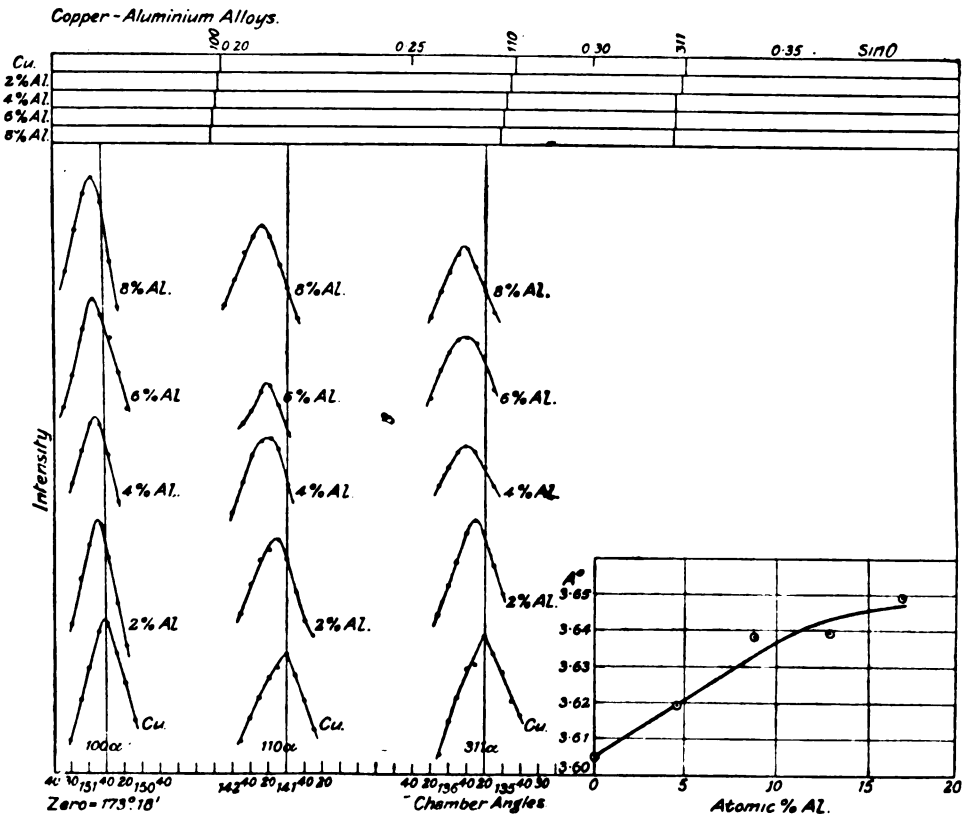


FIG. 3.

The lattice constant increases from 3·60 Å for copper to 3·65 Å for the alloy containing 8 per cent. aluminium.

In Table III the values of the densities of the alloys are compared with values calculated on the assumption that the aluminium atom replaces a copper atom on the distorted lattice, the side of the cube found by the X-ray analysis being supposed to be the average spacing in the material.

TABLE III.

| Per cent. Al. | $\frac{4M_s}{a^3}$ gms. per cc. | ρ observed. | Diff. | $\sqrt[3]{\frac{4M_s}{\rho}}$ | $a$ observed. | Diff. |
|---|---|---|---|---|---|---|
| 0 | 8·96 | 8·93 | +0·03 | 3·608 Å | 3·605 Å | −0·003 |
| 2 | 8·63 | 8·63 | 0·00 | 3·618 | 3·619 | +0·001 |
| 4 | 8·27 | 8·33 | −0·06 | 3·629 | 3·638 | +0·009 |
| 6 | 8·06 | 8·04 | +0·02 | 3·642 | 3·639 | −0·003 |
| 8 | 7·80 | 7·74 | +0·06 | 3·659 | 3·649 | −0·010 |

The appropriate value of $M_s$, the average atomic weight, was calculated by the aid of equation (2) for each specimen. The differences between the observed and calculated values of ρ are not greater than 0·8 per cent., which, in view of the fact that the

Digitized by Google

experimental error has been cubed, is very fair agreement. The alternative of supposing the aluminium atom to be situated in the interstices of a distorted copper lattice gives too high a value for the density. If the calculation were based on the observed value of the density, a lattice the average parameter of which is 3·89 Å would be required in the case of 8 per cent. aluminium alloy. The fact that we find in this case a lattice the parameter of which is 3·65 Å, and that the calculated density is in good agreement with the observed density would indicate that the solution is of the substitutional type.

(*b*) *Alloys Rich in Aluminium.*—No shift of the spectrum could be detected in specimens of aluminium-copper alloy containing 0·5, 1·0, 1·5, 2·0, 3 and 4 per cent. copper respectively. The aluminium lattice persists throughout the series, the amount of distortion, if any, being within the limits of experimental error. In the 0·5 per cent. specimen some lines are unaccounted for at the small angle end of the spectrum and in the 1 and 1·5 per cent. alloys 311 appears to be a doublet.

The reflections of $K_\alpha$ radiation of molybdenum from the 110 and 311 planes were observed in detail for the first four of the series. The results are given in Table IV. The figures show that there is no change of the lattice constant within the error of experiment. Neither is it possible in this case to distinguish between the substitutional and the interstitial arrangement of the atoms from a comparison of the densities.

TABLE IV.

| Form. | Aluminium. | | 0·5 per cent. Cu. | | 1·0 per cent. Cu. | | 1·5 per cent. Cu. | | 2·0 per cent. Cu. | |
|---|---|---|---|---|---|---|---|---|---|---|
| | θ | *a* | θ | *a* | θ | *a* | θ | *a* | θ | *a* |
| 110 . . | 14° 21′ | 4·039 | 14° 23′ | 4·029 | 14° 21′ | 4·039 | 14° 19′ | 4·048 | 14° 21′ | 4·039 |
| 311 . . | 16° 53′ | 4·042 | 16° 53′ | 4·042 | 16° 55′ | 4·033 | 16° 51′ | 4·051 | 16° 54′ | 4·038 |
| Mean value | | 4·040 Å | | 4·036 Å | | 4·036 Å | | 4·050 Å | | 4·039 Å |

(*c*) *Aluminium-Copper Alloy containing* 30 *per cent. Copper by Weight.*—An alloy containing 70 per cent. aluminium and 30 per cent. copper by weight is of interest, as its composition is nearly that of the eutectic alloy. An examination of a small plate of this material by the X-ray spectrometer gave a spectrum containing 18 lines, the sines of the observed angles of reflection being given under the heading $AC_{30}$ in Table V. For the sake of comparison the lines of aluminium and those of the compound $CuAl_2$, the structure of which is described below, are also included. The lines in the observed spectrum of $AC_{30}$ may be divided into two groups - the one group containing aluminium lines and the other group containing $CuAl_2$ lines. The eutectic alloy would thus appear to consist of a mixture of aluminium and the intermetallic compound $CuAl_2$. In the

Digitized by Google

preceding section it was concluded that with the accuracy so far attained with the present method of analysis it is impossible to distinguish between pure aluminium and a saturated solid solution of copper in aluminium. The limit of solid solubility being in the neighbourhood of 1 atomic per cent. of copper the distortion of the aluminium lattice is too small to be detected with certainty. Thus, although the lines in the spectrum of $AC_{30}$ which are not attributable to $CuAl_2$ appear to be due to a lattice identical with that of pure aluminium, they may be due to a saturated solid solution of copper in aluminium. A metallurgical study of the alloy shows that this is actually the case. The definite conclusion arrived at from the present analysis is that the eutectic alloy consists of a mixture of two distinct substances arranged on different space lattices, the one substance being $CuAl_2$ and the other a substance whose space lattice cannot be distinguished from that of pure aluminium.

TABLE V.

| Aluminium. | | $AC_{30}$. | $CuAl_2$. | |
|---|---|---|---|---|
| Form. | Sin θ. | Sin θ. | Sin θ. | Form. |
| ... | ... | ... | 0·074 | 100β |
| ... | ... | ... | 0·083 | 100α |
| ... | ... | 0·100 | 0·104 | 110β |
| ... | ... | 0·118 | 0·117 | 110α |
| 111β | 0·131 | 0·132 | ... | ... |
| 111α | 0·152 | 0·150 | 0·148 | 001α |
| ... | ... | 0·166 | 0·165 | 200α |
| 100α | 0·175 | 0·176 | ... | ... |
| ... | ... | 0·187 | 0·185 | 210α |
| 110β | 0·221 | 0·218 | ... | ... |
| 110α | 0·248 | 0·246 | ... | ... |
| 311β | 0·259 | 0·257 | ... | ... |
| ... | ... | 0·276 | 0·279 | 301α |
| 311α | 0·290 | 0·291 | 0·293 | 002α |
| | ... | 0·299 | 0·301 | 320α |
| 222α | 0·307 | 0·311 | ... | ... |
| ... | ... | 0·332 | 0·334 | 400α |
| ... | ... | 0·347 | 0·343 | 330α |
| 331α | 0·385 | 0·385 | ... | ... |
| 210α | 0·395 | 0·393 | ... | ... |

(*d*) *Structure of $CuAl_2$.*—The results given in Table VI were obtained with a cast flat plate of material containing the proper proportion of copper and aluminium. The observed lines agree approximately with a close-packed hexagonal structure, the side of the hexagon being 4·95 Å and the axial ratio 0·866. This structure had to be rejected because the first and second order reflections from the $11\bar{2}0$ planes and the third order from $10\bar{1}0$, which should be present, were missing. An alternative structure was found to be provided by a simple tetragonal lattice of side 4·28 Å and axial ratio 0·562 (see

Digitized by Google

TABLE VI.—$CuAl_2$.

| Intensity. | 2 θ. | Sin θ. | Form. | *d*. | $a$ ($c = 0{\cdot}562$). |
|---|---|---|---|---|---|
| 1·1 | 8·5 | 0·0741 | 100β | $a$ | 4·25 Å |
| 4·0 | 9·5 | 0·0828 | 100α | $a$ | 4·27 |
| 0·9 | 12·0 | 0·1045 | 110β | $a/\sqrt{2}$ | 4·26 |
| 3·2 | 13·4 | 0·1167 | 110α | $a/\sqrt{2}$ | 4·29 |
| 1·0* | 16·9* | 0·1478 | 001α | $ac$ | 4·26 |
| 1·2 | 17·1 | 0·1487 | 200β | $a/2$ | 4·24 |
| 5·3 | 19·0 | 0·1650 | 200α | $a/2$ | 4·29 |
| 7·5 | 21·3 | 0·1849 | 210α | $a/\sqrt{5}$ | 4·29 |
| 2·6 | 26·9 | 0·2325 | 220α | $a/2\sqrt{2}$ | 4·30 |
| ... | 30·2* | 0·2605 | 002β | $ac/2$ | 4·30 |
| 3·3 | 30·5 | 0·2630 | 310α | $a/\sqrt{10}$ | 4·26 |
| 15·0* | 34·1* | 0·2932 | 002α | $ac/2$ | 4·29 |
| 1·8 | 35·0 | 0·3007 | 320α | $a/\sqrt{13}$ | 4·24 |
| 0·5 | 39·0 | 0·3338 | 400α | $a/4$ | 4·24 |
| 2·1 | 40·1 | 0·3428 | 202α | $a/3\sqrt{2}$ | 4·22 |
| ... | 43·5 | 0·3705 | 420α | $a/2\sqrt{5}$ | 4·27 |
| ... | 49·3 | 0·4171 | 440β | $a/4\sqrt{2}$ | 4·27 |
| 0·01* | 52·7* | 0·4439 | 003α | $ac/3$ | 4·26 |
| ... | 62·7* | 0·5202 | 004β | $ac/4$ | 4·31 |
| 2·0* | 71·6* | 0·5850 | 004α | $ac/4$ | 4·31 |
| ... | 19° 0′ | 0·1650 | 200α | $a/2$ | 4·29 |
| ... | 19° 18′ | 0·1677 | 101α | $a\Big/\sqrt{1+\frac{1}{c^2}}$ | 4·31 |
| ... | 21° 22′ | 0·1840 | 210α | $a/\sqrt{5}$ | 4·30 |
| ... | 21° 38′ | 0·1877 | 111α | $a\Big/\sqrt{2+\frac{1}{c^2}}$ | 4·29 |

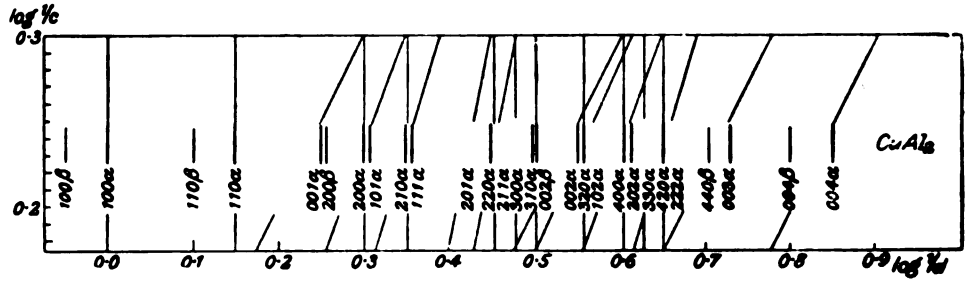


Fig. 4.

Fig. 4). The intensities of the reflections from the 001 planes were so small, however, that it was considered desirable to examine the reflections from these planes more in detail. We were able to do this by the use of a number of single crystals of $CuAl_2$ in the form of rods about 3 mms. diameter and 3 or 4 cms. in length which Dr. HANSON, of the Metallurgy Department, kindly prepared for us. These were cut perpendicular to their length and mounted together so as to provide a surface about 1 cm. square for examination. In this way we were able to detect with certainty the first four orders of reflection



Digitized by Google

from the 001 planes; the angles marked with asterisks in the first column of Table VI were obtained with this specimen. The relative intensities of the observed spectra were as follows:—

$$I_1 : I_2 : I_3 : I_4 = 7 : 100 : 0{\cdot}7 : 14.$$

These agree tolerably well with the calculated intensities, viz., 2·2 : 100 : 0·2 : 10, on the assumption that planes of copper and aluminium occur alternately. The spacing of the 001 planes calculated from the above observations gave the value 2·40 Å. A tetragonal structure of sides 4·28 Å and 2·40 Å having a copper atom at each corner and an aluminium atom at the centre of each of the four small faces is found to account satisfactorily for the observed intensities. A unit cell of the material is shown in Fig. 5.

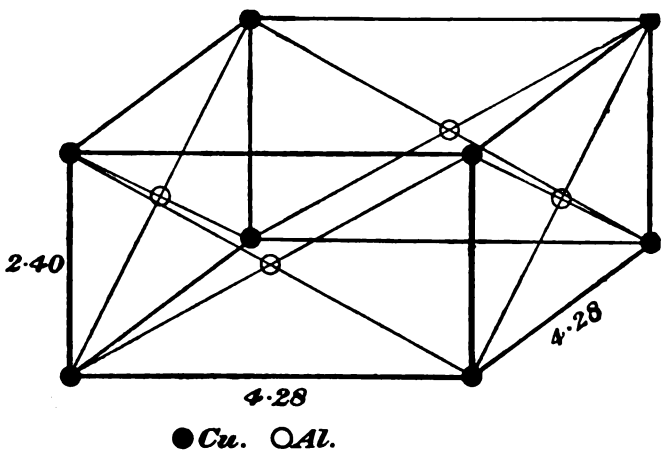


FIG. 5.

In this arrangement the 100 planes are alternately composed of CuAl and Al. The first and third orders will accordingly be weak, the second and fourth strong. The spectrum curve showed this to be the case. A similar agreement between theory and experiment was obtained for other planes in the crystal. Further, the molecular weight of the compound is 117·77 and the density is 4·36, so that the number of molecules associated with each cell is—

$$n = \frac{\rho a^3 c}{M} = 0{\cdot}988,$$

which is, within experimental error, in accordance with the value unity required by the above structure.

(*e*) *Structure of CuAl.*—A small specimen of material, containing equal atomic percentages of copper and aluminium, was investigated. The intensities of the reflections were small, but by repetition it was found possible to arrive at the figures given in Table VII. The lines in the spectrum were found to fit on a plot representing a face centred trigonal structure with the axes inclined at an angle of 94·6°.

Digitized by Google

TABLE VII.—CuAl.

| 2 θ. | Sin θ | Form. | *d*. | *a*. |
|---|---|---|---|---|
| 9·4 | 0·0819 | ... | ... | ... |
| 15·8 | 0·1374 | $\bar{1}11\beta$ | 0·5907 × *a* | 3·88 Å |
| 17·8 | 0·1547 | $\bar{1}11\alpha$ | 0·5907 | 3·88 |
| 19·8 | 0·1719 | $111\alpha$ | 0·5290 | 3·89 |
| 21·3 | 0·1849 | $100\alpha$ | 0·4965 | 3·86 |
| 25·2 | 0·2181 | $\bar{1}10\beta$ | 0·3675 | 3·92 |
| 28·6 | 0·2470 | $\bar{1}10\alpha$ | 0·3675 | 3·90 |
| 31·5 | 0·2714 | $110\alpha$ | 0·3367 | 3·88 |
| 33·8 | 0·2907 | $\bar{3}11\alpha$ | 0·3120 | 3·90 |
| 35·3 | 0·3032 | $3\bar{1}1\alpha$ | 0·3018 | 3·87 |
| 35·9 | 0·3082 | $\bar{2}22\alpha$ | 0·2953 | 3·88 |
| 42·7 | 0·3641 | $200\alpha$ | 0·2483 | 3·91 |
| | | | | Mean *a*=3·89 Å |

$$\eta = 94{\cdot}6^\circ$$

$$2d_{100} = 3{\cdot}86 \text{ Å}$$

$$M = 90{\cdot}67 \times \frac{1{\cdot}663}{1{\cdot}008} \times 10^{-24} \text{ grammes.}$$

$$\rho = \frac{M}{a^2 d_{100} \sin \eta} = 5{\cdot}13 \text{ gms. per cc.; } \rho \text{ (observed)} = 5{\cdot}25 \text{ gms. per cc.}$$

As will be seen from the table, the calculated values of "*a*", the side of the rhomb, do not differ from their mean value by as much as 1 per cent. The average value of the side of the rhomb is 3·89 Å, which corresponds to a density of 5·13 gms. per cc., on the assumption that there are two molecules of CuAl associated with each face centred unit rhomb. The observed value of the density is 5·25 gms. per cc., which would require a lattice of side 3·86Å. The intensities of the reflections are too small to justify deductions as to the position of the atoms on the lattice, but if the occurrence of a line at 9·4° may be taken as indicating the presence of a spacing double that of the 111 spacing of this arrangement, then it suggests that the 111 planes are alternately composed of copper and aluminium atoms. The 100 and $\bar{1}11$ planes would then be composed of equal numbers of copper and aluminium atoms and no "half" order reflections would be expected. The structure could be produced from the lattice of aluminium by a contraction from 4·05 to 3·89 Å and a distortion of the cubic axes until they are inclined at 94·6°, or from the copper lattice by the same angular distortion of the axes accompanied by an extension from 3·60 to 3·89 Å in the side of the cell. The average distortion produced by the substitution of an aluminium atom for a copper atom on the copper lattice has been given in another section of this paper. It was there found that the value of the parameter of the lattice reaches a maximum of 3·65 Å with about 12 atomic per



Digitized by Google

cent. of dissolved aluminium. The structure of CuAl suggested here bears a very clo resemblance to the type of solid solution suggested by TAMMANN* and referred to BAIN.† The distortion of the lattice in this case is, however, more marked than in t cases cited, for example, by BAIN, in which atomic ratios of 3 to 1 are considered.

### (2) *Alloys of Aluminium and Magnesium.*

An alloy containing 8 per cent. magnesium by weight gave a spectrum which wa similar to that of aluminium, *i.e.* a face centred cube, but the lattice showed a sma

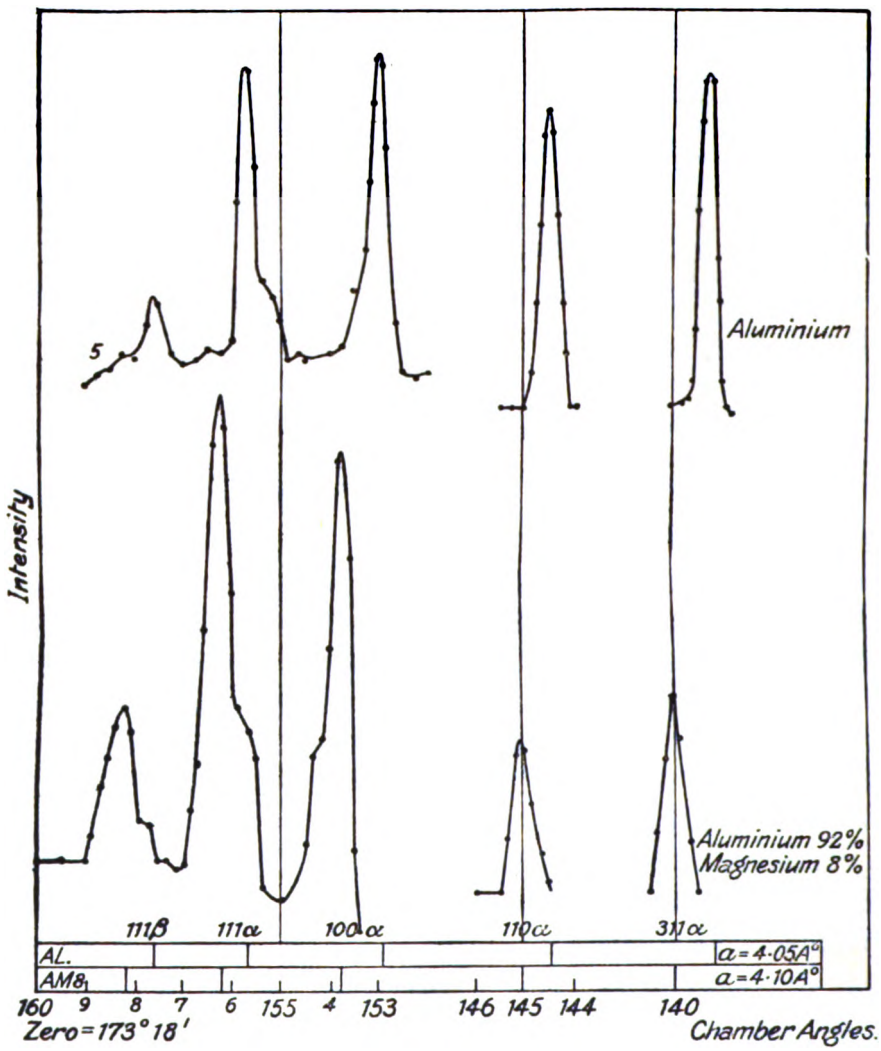


FIG. 6.

expansion. A series of measurements were made of the lines reflected from the 111, 100, 110 and 311 planes (Fig. 6). The results are shown in Table VIII. In Fig. 6 the

* 'Zeits. Anorg. Allgem. Chem.', vol. 107, pp. 1–239, 1919.

† 'Chem and Met. Eng.', vol. 25, p. 663, 1921 ; vol. 28, p. 21, 1923 ; vol. 28, p. 65, 1923.

Digitized by Google

position of the aluminium lines is shown on the same graph as those observed in the present case.

TABLE VIII.

| Form. | θ. | Sin θ. | *a*. |
|---|---|---|---|
| | ° ′ | | |
| 111β | 7 35 | 0·1319 | 4·129 Å |
| 111α | 8 33 | 0·1487 | 4·121 |
| 100α | 10 0 | 0·1736 | 4·078 |
| 110α | 14 7 | 0·2439 | 4·104 |
| 311α | 16 39 | 0·2865 | 4·097 |

The value of "*a*" may be taken as 4·106 Å with a possible error of 0·5 per cent. The density of the alloy is 2·57 gms. per cc. and, on the substitution theory of solid solution, this gives a value 4·10 Å for the average spacing of the lattice. Interstitial solution would require a spacing of 4·23 Å to give the observed density, or a density of 2·81 gms. per cc. to give the observed value of the lattice.

We may conclude, therefore, that the magnesium atoms replace aluminium atoms on the space lattice, producing a distortion of the lattice from 4·05 to 4·10 Å.

A second alloy of aluminium and magnesium containing 92 per cent. by weight of magnesium was found to possess a spectrum similar to that of magnesium, characteristic of a close packed hexagonal lattice. In order to ascertain which of the two constants, the side *a* of the hexagon or the axial ratio *c*, was affected by the introduction of the aluminium atom, careful measurements were made of the reflections from the $10\bar{1}0$, 0001, $10\bar{1}1$ and $20\bar{2}2$ planes of the material (Fig. 7). The reflections from these planes were very sharp. They are shown graphically in Fig. 7. The observed angles of reflection are given in Table IX, together with the values of these angles after the correction for penetration has been made. The values of the experimental error given are the maximum possible and the probable error in the value of sin θ is not more than 0·2 per cent. in each case.

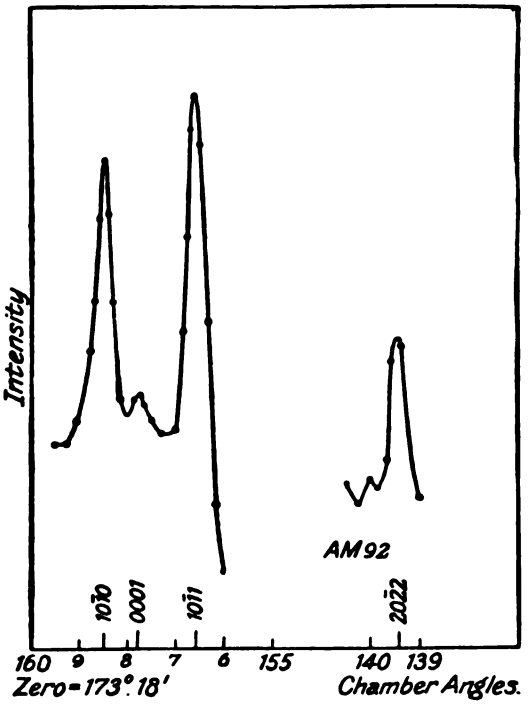


FIG. 7.

Digitized by Google

TABLE IX.—$AM_{93}$.

| $\theta_1$ observed. | $\theta_2$ corrected. | Sin $\theta_2$. | $d$. | Form. |
|---|---|---|---|---|
| 7° 24′ ± 1′ | 7° 27′ | 0·1297 ± 0·0003 | $\frac{a\sqrt{3}}{2}$ | $10\bar{1}0$ |
| 7° 45′ ± 1′ | 7° 48′ | 0·1357 ± 0·0003 | $\frac{ac}{2}$ | 0001 |
| 8° 22′ ± 1′ | 8° 25′ | 0·1464 ± 0·0003 | $a/\sqrt{\frac{4}{3}+\frac{1}{c^2}}$ | $10\bar{1}1$ |
| 16° 57′ ± 2′ | 17° 0′ | 0·2924 ± 0·0006 | $a/2\sqrt{\frac{4}{3}+\frac{1}{c^2}}$ | $20\bar{2}2$ |

$a = 3{\cdot}151$ Å

$c = 1{\cdot}660$

$\rho$ (calcd.) $= 1{\cdot}80$ gms. per cc.

$\rho$ (observed) $= 1{\cdot}79$ gms. per cc.

The specimen may be taken to have been correctly centred on the instrument, since the value of the sin $\theta$ for $10\bar{1}1$ differs by less than 0·2 per cent. from the value of sin $\theta$ for $20\bar{1}2$. From the observation on $10\bar{2}0$, the value of "$a$" is calculated directly and gives the result 3·151 ± 0·007Å. Using this value of "$a$" and taking sin $\theta_{10\bar{1}1} = 0{\cdot}1463$ (the mean of the values obtained from the first and second order spectra), the value of "$c$" is found to be 1·660 ± 0·007. As a check on these figures, we have the value of $d_{0001} = \frac{ac}{2} = 2{\cdot}614$ in good agreement with the observed value $d_{0001} = \frac{\lambda_a}{2\sin\theta_{000\bar{1}}} = 2{\cdot}608$, where $\lambda_a = 0{\cdot}70783$ Å.

For pure magnesium $a = 3{\cdot}17$ Å and $c = 1{\cdot}63$, so that the introduction of the aluminium atom into the magnesium lattice produces a slight contraction of the side of the hexagon, but increases the average distance between the successive hexagonal planes.

The observed density of the specimen is 1·79 gms. per cc. Calculating the density on the assumption that the aluminium atom replaces a magnesium atom on the lattice, the figure 1·80 is obtained. If the aluminium atom were accommodated in the interstices of the lattice, a density of 1·94 would be required to account for the observed spacings, alternatively to account for the observed density, with $a = 3{\cdot}151$ Å, interstitial solution would require the axial ratio to be equal to 1·81, while the substitutional hypothesis yields the figure 1·68 in agreement with observation. There appears, therefore, to be no doubt that the aluminium atom enters into solution by replacing a magnesium atom, the side of the hexagon being decreased from 3·17 to 3·15 Å and the distance between successive hexagonal layers being increased from 5·17 to 5·23 Å.

Digitized by Google

### (3) *Copper-Nickel Alloys.*

The results obtained with alloys of copper containing 10, 20, 30 and 40 per cent. of nickel by weight are included in Table X. It will be observed that the addition of nickel produces a small contraction in the copper lattice, the amount of the contraction being approximately a linear function of the atomic percentage of either component (see Fig. 8).

TABLE X.

| Form. | 10 per cent. Ni. | | 20 per cent. Ni. | | 30 per cent. Ni. | | 40 per cent. Ni. | |
|---|---|---|---|---|---|---|---|---|
| | Sin θ | $a$ | Sin θ | $a$ | Sin θ | $a$ | Sin θ | $a$ |
| 111β | 0·1512 | 3·593 Å | ... | ... | ... | ... | 0·1522 | 3·579 |
| 111α | 0·1708 | 3·588 | 0·1711 | 3·582 Å | 0·1720 | 3·565 Å | 0·1716 | 3·573 |
| 100α | 0·1962 | 3·609 | 0·1968 | 3·595 | 0·1973 | 3·586 | 0·1974 | 3·585 |
| 110α | 0·2784 | 3·594 | 0·2784 | 3·594 | 0·2807 | 3·566 | 0·2804 | 3·570 |
| 222α | 0·3412 | 3·592 | 0·3418 | 3·585 | 0·3421 | 3·583 | ... | ... |
| Mean values . . . | | 3·595 Å | | 3·589 Å | | 3·575 Å | | 3·576 Å |
| Per cent. Ni. | ρ gms./cc. | $M_s$ | $\sqrt[3]{\frac{4M_s}{\rho}}$ | $a$ | Diff. | $\sqrt[3]{\frac{4M_i}{\rho}}$ | | |
| 0 | 8·93 | 63·57 | 3·608 Å | 3·605 Å | −0·003 | 3·608 Å | ... | ... |
| 10 | 8·94 | 63·04 | 3·596 | 3·593 | −0·003 | 3·736 | ... | ... |
| 20 | 8·95 | 62·53 | 3·587 | 3·589 | +0·002 | 3·884 | ... | ... |
| 30 | 8·95 | 62·04 | 3·576 | 3·575 | −0·001 | 4·061 | ... | ... |
| 40 | 8·92 | 61·53 | 3·571 | 3·576 | +0·005 | 4·279 | ... | ... |

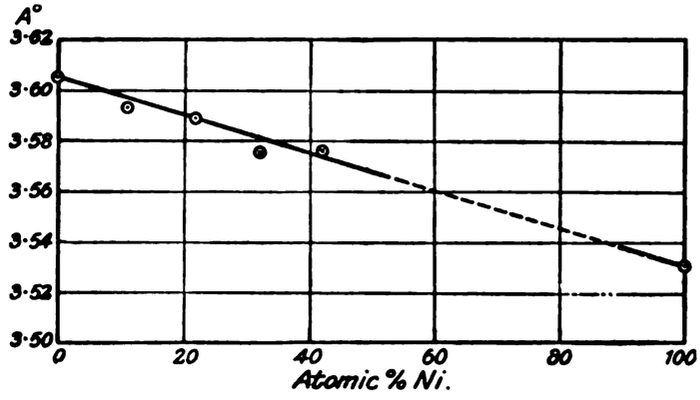


FIG. 8.

The value of the parameter of the lattice calculated from the density (as determined from rolled and annealed specimens) on the assumption that solution by substitution takes place is again in good agreement with the value of the parameter measured directly

Digitized by Google

by the spectrometer. The last column of the lower half of Table X contains the valu of the parameter calculated on the interstitial theory. The departure of these figur from the observed values is very marked.

## IV. Conclusions.

The foregoing results show that in solid solutions of copper-aluminium, aluminiun magnesium, and copper-nickel the solute atom replaces an atom in the lattice of th solvent. This substitution of atoms is accompanied in the cases examined by a dis tortion of the lattice, but the type of the lattice remains unaltered throughout a series c solid solutions until the limit of solid solubility is reached. In none of the cases examine was it found that the interstitial arrangement of atoms occurred, with the possibl exception of copper-aluminium alloys rich in aluminium. In these alloys the atomi percentage of copper was so small that the accuracy of measurement was not sufficien to decide definitely between the two possible atomic arrangements.

Attention should be directed to the fact that in the lattice suggested for the inter metallic compound $CuAl_2$, the centres of the aluminium atoms are separated by 2·40 Å which is smaller than the diameter of the atom (2·86 Å) deduced from the structure o pure aluminium. Similarly, the distance between the copper atoms, which is also 2·40 Å is smaller than the atomic diameter of copper (2·54 Å) obtained from the pure element A possible explanation of these results is that the atoms share electrons and are brough closer together than would otherwise be the case.

The facts accumulated as to the structure of CuAl appear to indicate that this materia is of the same nature as the solid solutions examined in this investigation. The trigona lattice assigned to it is in reality a distorted lattice of the same type as that of the constituent elements; it is similar, in fact, to the distorted lattice obtained in the case of copper-aluminium alloys rich in copper, but with a much more pronounced distortion. It is interesting to note that the material does not separate as CuAl on solidification from the molten metal, but forms by diffusion in the solid state during prolonged annealing.

The results obtained with solid solution of aluminium in magnesium require explanation. One explanation which immediately suggests itself is that the aluminium atom in this instance is elongated, and that it takes its place in the magnesium lattice with its major axis along the hexagonal axis. It may be mentioned in this connection that Hull and others have found it necessary to assign shapes other than spherical to atoms to explain results obtained with certain crystals. We are at present extending the investigation to other alloys in the hope of obtaining further data on this point.

We wish to take this opportunity of thanking Dr. Rosenhain and the staff of the Metallurgy Department for supplying the specimens and for giving helpful advice throughout the course of the investigation.

Digitized by Google

# X-RAY ANALYSIS OF ZINC-COPPER ALLOYS

BY

E. A. OWEN, M.A., D.Sc.,
SENIOR ASSISTANT IN THE PHYSICS DEPARTMENT,

AND

G. D. PRESTON, B.A.,
ASSISTANT IN THE METALLURGY DEPARTMENT.

Digitized by Google

## ABSTRACT.

(1) Alloys containing up to 38 per cent. zinc constituting the α brasses are found to possess a face centred cubic lattice, the parameter increasing from 3·608 Å for pure copper to 3·696 Å for an alloy containing 38 per cent. zinc. Solution takes place by the substitution of zinc atoms for copper atoms.

(2) (*a*) The X-ray analysis of a brass containing 48·5 per cent. zinc by weight showed that the β brasses possess a centred cubic structure, the side of the unit cube being 2·946 Å.

(*b*) Specimens quenched from 550° C. and annealed below 470° C. gave identical spectra and showed no sign of the presence of the α phase. The evolution of heat observed at 470° C. is not accompanied by a change of crystal structure, and is similar to the α–β transformation in iron. It is not accompanied by a breaking up of the β constituent into a mixture of α and γ.

(*c*) Specimens containing 43·7 per cent. zinc by weight were examined. The first annealed at 750° C. and quenched showed the reflections due to β brass only. The second annealed at 500° C. and quenched, and the third annealed at 400° C. consisted of a mixture of the α and β phases. The results of X-ray analysis are in agreement with the constitutional diagram of SHEPHERD.

(3) The γ phase is found to crystallise on a rhombohedral hexagonal lattice of side 4·136 Å and axial ratio 0·6495.

(4) The ε phase gave a spectrum characteristic of a close-packed hexagonal lattice of side 2·718 Å and axial ratio 1·585.

(5)—(*a*) The zinc-copper system crystallises on a rhombohedral hexagonal lattice from copper to γ brass, and on a close-packed hexagonal system from ε (or possibly δ) brass to zinc. The observed parameter of the lattice of ε brass suggests that the copper atom causes the zinc atom to rotate about an axis perpendicular to a $11\bar{2}0$ plane, until the zinc atoms in successive 0001 planes are separated by a distance equal to the side of the lattice of pure zinc. Fusion would then take place at about the same temperature in both cases.

(*b*) The very low value of the density previously ascribed to an alloy containing 10 per cent. copper is not confirmed. The value found for the density of this alloy is 7·35 gms./cc. The observed density of the alloys examined is in good agreement with the value computed from X-ray data.

(*c*) The hardness of the brasses attains a maximum in the region of γ brass, where the atomic volume curve shows the greatest departure from the straight line joining the atomic volumes of copper and zinc. The hardness of the α phase is ascribed to local distortion and that of the β phase to the difference in type of lattice. The relatively very great hardness of γ brass is due to the small atomic volume and loss of symmetry.

(*d*) The fact that the atomic volume curve consists of two straight lines suggests the existence of an allotrope of zinc with an atomic volume of 13·92 $Å^3$. Consideration of the value of the parameter of the lattice of the β phase suggests that this phase is due to an allotropic modification of copper, with an atomic volume of 12·79 $Å^3$.


Digitized by Google

# X-RAY ANALYSIS OF ZINC-COPPER ALLOYS.

By E. A. OWEN, M.A., D.Sc., Senior Assistant in the Physics Department, and G. D. PRESTON, B.A., Assistant in the Metallurgy Department.

[Reprinted from the 'Proceedings of the Physical Society of London', Vol. 36, 1923.]

## I. Introduction.

The determination of crystal structure by means of X-rays provides a method of studying the constitution of metals and alloys which should yield valuable information concerning the changes which take place when we pass from one region of an equilibrium diagram to another. The method has been applied by the authors to the study of the zinc-copper series, and it is proposed in this Paper to give an account of the results so far obtained.

The observations of different metallurgists on this system of alloys are in general agreement, but there are differences of opinion as to certain details. Particularly is this so concerning the change which accompanies the thermal effect observed at 470° C in the range of alloys containing 40 to 63 per cent. copper. In the early stages of the investigation on the zinc-copper series Roberts-Austen,* who was the first to observe the effect, attributed it to an eutectoid change. After the work of Shepherd† on the series, it was doubtful whether the effect actually occurred, as he failed to detect it. Later, however, Carpenter and Edwards‡ made a careful thermal analysis of the series, proving beyond question the existence of the effect. They attributed it to the breaking down of the constituent into a mixture of $\alpha$ and $\gamma$. This explanation was disputed by Hudson,§ who brought evidence to show that the thermal effect observed was due to a polymorphic change of $\beta$ to $\beta'$. Evidence in support of this conclusion has recently been published by Hiroshi Imai,|| who employed the electric resistance method of measurement.

We have been able by the X-ray method to investigate this point in detail and, in addition, to carry out a general survey of the whole system. Owing to the complicated nature of the zinc end of the series (see Fig. 1), it is somewhat difficult to prepare some of the alloys in suitable form for X-ray measurement. Observations have, however, been made on the $\gamma$ and $\epsilon$ phases in addition to the $\alpha$, $\beta$ and $\beta'$.

The zinc-copper alloys have already been examined by X-ray analysis by Bain¶ and Mary Andrews.** Particular attention was paid by the former to the $\alpha$ phase, whilst

* 'Fourth Report to the Alloys Research Committee', 1897.

† 'J. Phys. Chem.', vol. 8, p. 421, 1904.

‡ 'J. Inst. Metals', vol. 5, p. 127, 1911.

§ 'J. Inst. Metals', vol. 12, p. 89, 1914.

|| 'Sci. Reports', Tohoku Univ., vol. 11, p. 313, 1922.

¶ 'Chem. and Met. Eng.', vol. 25, p. 663, 1921; vol. 28, p. 21, 1923; vol. 28, p. 65, 1923.

** 'Phys. Rev.', vol. 21, p. 245, 1921.



Digitized by Google

the latter carried out a general survey of the whole series. In both cases the photographic X-ray method of analysis was employed. For this method the material under examination is usually reduced to a fine powder, a small quantity of which is placed in a tiny glass tube situated in the path of a monochromatic beam of X-rays.

In the present work a plate of the material under investigation is used and the reflections from crystal faces measured by the Bragg ionisation spectrometer. An account of the method of procedure has already been published by the authors.*

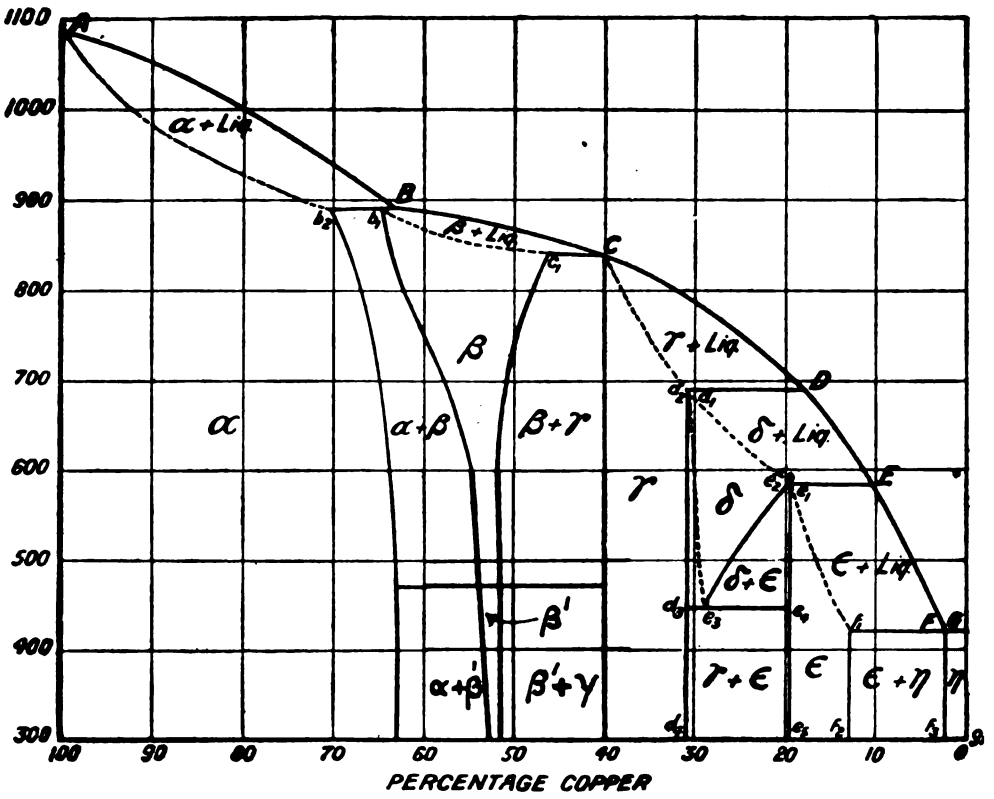


FIG. 1.

## II. RESULTS.

(1) *Alloys containing up to* 38·7 *per cent. Zinc by Weight.*—These alloys, which constitute the α brasses, were prepared from chilled castings 1 inch in diameter, which had been annealed at 530° to 540° C. for 1 hour. The castings were rolled to a thickness of 0·25 inch and again annealed for 2½ hours at 550° to 600° C. Finally, they were rolled to a thickness of 0·125 inch, annealed at 600° C. for 30 minutes and quenched in water. The specimens were polished and etched and presented a surface of at least 1 cm. square for examination by the X-ray spectrometer.

* 'N.P.L. Collected Researches', vol. 19, Paper 24, or 'Proc. Phys. Soc. Lond.', vol. 35, p. 101, 1923.

Digitized by Google

The results of the X-ray examination of five alloys containing up to 38·7 per cent. zinc are given in Table I. The actual observations are plotted in Fig. 2. All the alloys gave spectra characteristic of the face centred cubic structure of copper, the addition of the zinc causing an expansion of the lattice which is shown by the general shift of the lines in the spectra towards the origin as the amount of zinc is increased. The addition of 38·7 per cent. zinc alters the parameter of the copper lattice from 3·60 Å to 3·696 Å.

TABLE I.

| Form. | 11·35 per cent. Zn. | | 20·77 per cent. Zn. | | 27·09 per cent. Zn. | | 30 per cent. Zn. | | 38·73 per cent. Zn. | |
|---|---|---|---|---|---|---|---|---|---|---|
| | θ | *a* | θ | *a* | θ | *a* | θ | *a* | θ | *a* |
| 111β | ° ′ 8 38 | 3·634 Å | ° ′ 8 33 | 3·667 Å | ° ′ 8 35 | 3·656 Å | ° ′ ... | ... | ° ′ 8 30 | 3·689 Å |
| 111α | 9 42 | 3·638 | 9 39 | 3·667 | 9 39 | 3·656 | 9 37 | 3·666 Å | 9 33 | 3·695 |
| 100α | 11 14 | 3·633 | 11 8 | 3·665 | 11 10 | 3·365 | ... | ... | 11 0 | 3·710 |
| 110α | 16 0 | 3·633 | 15 54 | 3·653 | 15 51 | 3·664 | ... | ... | 15 44 | 3·691 |
| 311α | 18 52 | 3·629 | 18 47 | 3·645 | 18 42 | 3·660 | 18 39 | 3·670 | 18 30 | 3·699 |
| 222α | ... | ... | ... | ... | ... | ... | 19 32 | 3·667 | ... | ... |
| Mean values . . | | 3·633 Å | | 3·657 Å | | 3·658 Å | | 3·668 Å | | 3·696 Å |

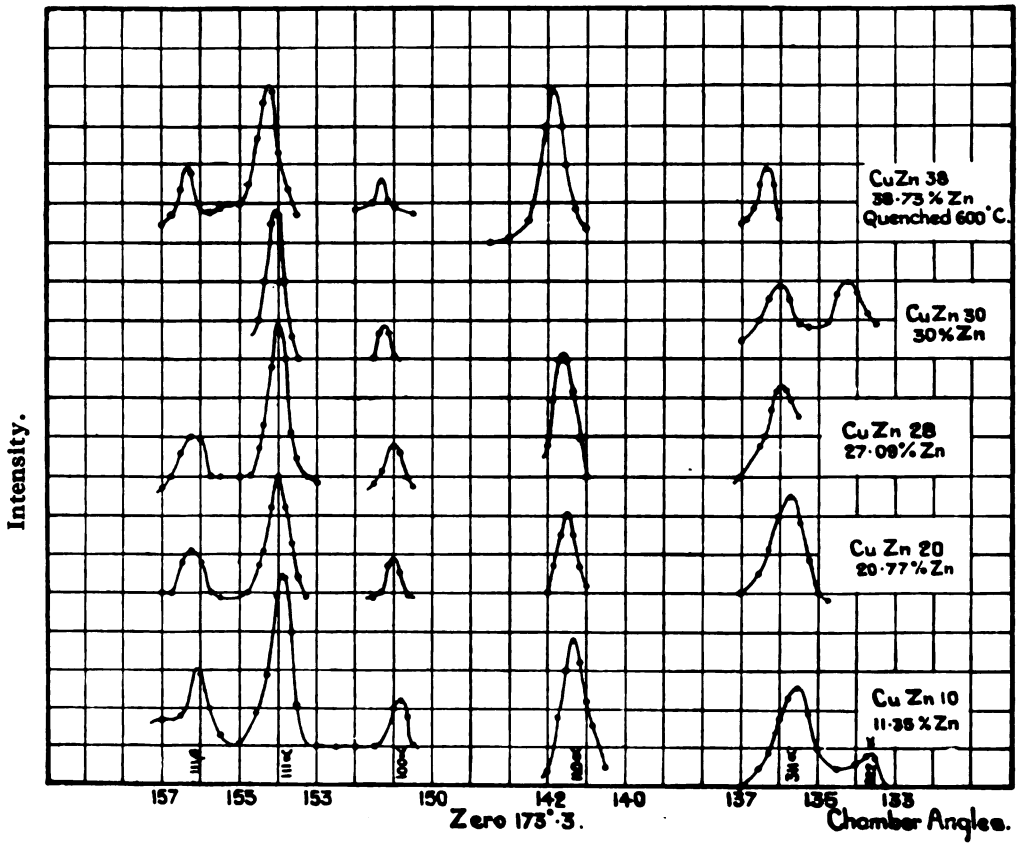


FIG. 2.

Digitized by Google

TABLE II.

| Per cent. Zn. | ρ (gms./cc.). | $M_s$. | $\sqrt[3]{\frac{4M_s}{\rho}}$. | $a$. | Diff. |
|---|---|---|---|---|---|
| 0 | 8·93 | 63·57 | 3·608 Å | 3·605 Å | −0·003 |
| 11·35 | 8·80 | 63·78 | 3·629 | 3·633 | 0·004 |
| 20·77 | 8·67 | 63·90 | 3·651 | 3·657 | 0·006 |
| 27·09 | 8·57 | 64·06 | 3·667 | 3·658 | −0·009 |
| 30·00 | 8·54 | 64·19 | 3·673 | 3·668 | −0·005 |
| 38·73 | 8·43 | 64·29 | 3·694 | 3·698 | 0·004 |

The figures in Table II show that solution takes place by the substitution of a zinc atom for a copper atom. The average weight $M_s$ is computed from the composition of the alloy by use of the relation

$$M_s = \frac{100}{\frac{x}{M_1} + \frac{100 - x}{M_2}},$$

$x$ being the percentage of zinc by weight, $M_1 = 65{\cdot}37$, and $M_2 = 63{\cdot}57$, being respectively the atomic weights of zinc and copper (O = 16).

As will be seen from the table, the values of $\sqrt[3]{\frac{4M_s}{\rho}}$ do not differ from the observed values of $a$, the parameter of the lattice, by as much as 0·25 per cent. These results are in agreement with the observations of the authors on other solid solutions which have already been published.*

(2) *Alloys containing* 48·5 *per cent. Zinc.*—The alloy containing 48·5 per cent. zinc lies in the region of β brasses. Two specimens were examined; the first specimen was heated for 10 minutes at 550° C. and quenched in water, the second specimen was heated for 5 minutes at 500° C., slowly cooled during half an hour to 450° C., quickly cooled to about 400° C., and then quenched in water. According to the constitutional diagram (Fig. 1), the first specimen should consist of the pure β phase, and the second specimen of either the pure β′ phase or a mixture of the α and γ according to whether the view of DESCH and of HUDSON or that of CARPENTER and EDWARDS is the correct one regarding the change which takes place at 470° C.

Two samples of the first specimen were examined and found to possess a spectrum corresponding with a centred cubic structure of side 2·950 Å. This is in good agreement with the value of the parameter, 2·945 Å, calculated from the observed density of the material. The sines of the angles of reflection for the two samples are given in Table III. In neither sample could we find an indication of the presence of a face centred lattice.

* 'N.P.L. Collected Researches', vol. 19, Paper 25, or 'Proc. Phys. Soc. Lond.', vol. 36, p. 341, 1923.

Digitized by Google

TABLE III.—48·5 per cent. Zinc, quenched from 550° C.

| I. | | | II. | | |
|---|---|---|---|---|---|
| Sin θ. | Form. | *a*. | Sin θ. | Form. | *a*. |
| 0·1573 | 110β | 2·832 Å | 0·1504 | 110β | 2·962 Å |
| 0·1719 | 110α | 2·912 | 0·1694 | 110α | 2·954 |
| 0·2122 | 100β | 2·969 | 0·2130 | 100β | 2·957 |
| 0·2380 | 100α | 2·974 | 0·2385 | 100α | 2·968 |
| 0·2622 | 211β | 2·943 | 0·2622 | 211β | 2·943 |
| 0·2932 | 211α | 2·956 | 0·2940 | 211α | 2·949 |
| 0·3379 | 220α | 2·962 | 0·3387 | 220α | 2·955 |
| 0·3795 | 310α | 2·949 | 0·3738 | 310α | 2·994 |
| 0·3995 | 321β | 2·949 | 0·4139 | 111α | 2·961 |
| 0·4486 | 321α | 2·951 | 0·4501 | 321α | 2·942 |
| Mean value . . . . . | | 2·950 Å | | | 2·958 Å |

$$\rho = 8{\cdot}32 \text{ gms./cc.} \qquad M_s = 64{\cdot}45 \times \frac{1{\cdot}663}{1{\cdot}008}\, 10^{-24} \text{ gms.}$$

$$a \text{ (calc.)} = \sqrt[3]{\frac{2M_s}{\rho}} = 2{\cdot}945 \text{ Å.} \qquad a \text{ (obs.)} = 2{\cdot}950 \text{ Å.}$$

The second specimen (two samples of which were examined) which had been slowly cooled to a temperature below 470° C. gave the results shown in Table IV. The spectrum

TABLE IV.—48·0 per cent. Zinc, annealed below 470°C.

| I. | | | II. | |
|---|---|---|---|---|
| Form. | Sin θ. | *a*. | Sin θ. | *a*. |
| 110β | 0·1501 | 2·968 Å | 0·1513 | 2·944 Å |
| 110α | 0·1691 | 2·959 | 0·1702 | 2·941 |
| 100β | 0·2124 | 2·966 | 0·2147 | (2·934) |
| 100α | 0·2393 | 2·957 | 0·2393 | (2·957) |
| 211β | 0·2613 | 2·953 | 0·2630 | (2·934) |
| 211α | 0·2940 | 2·949 | 0·2948 | 2·941 |
| 220α | 0·3404 | 2·941 | 0·3395 | 2·948 |
| 310α | 0·3778 | 2·963 | ... | ... |
| 321β | 0·4011 | 2·939 | ... | ... |
| 111α | 0·4163 | 2·944 | ... | ... |
| 321α | 0·4601 | 2·942 | ... | ... |
| Mean value . . . . | | 2·953 Å | | 2·946 Å |

$$\rho = 8{\cdot}32 \text{ gms./cc.} \qquad M_s = 64{\cdot}45 \times \frac{1{\cdot}663}{1{\cdot}008} \times 10^{-24} \text{ gms.}$$

$$a \text{ (calc.)} = \sqrt[3]{\frac{2M_s}{\rho}} = 2{\cdot}945 \text{ Å.} \qquad a \text{ (obs.)} = 2{\cdot}949 \text{ A.}$$

Digitized by Google

is again characteristic of the centred cube and cannot be distinguished from that of the β phase. The similarity between the two spectra is evident from Fig. 3. The reflections

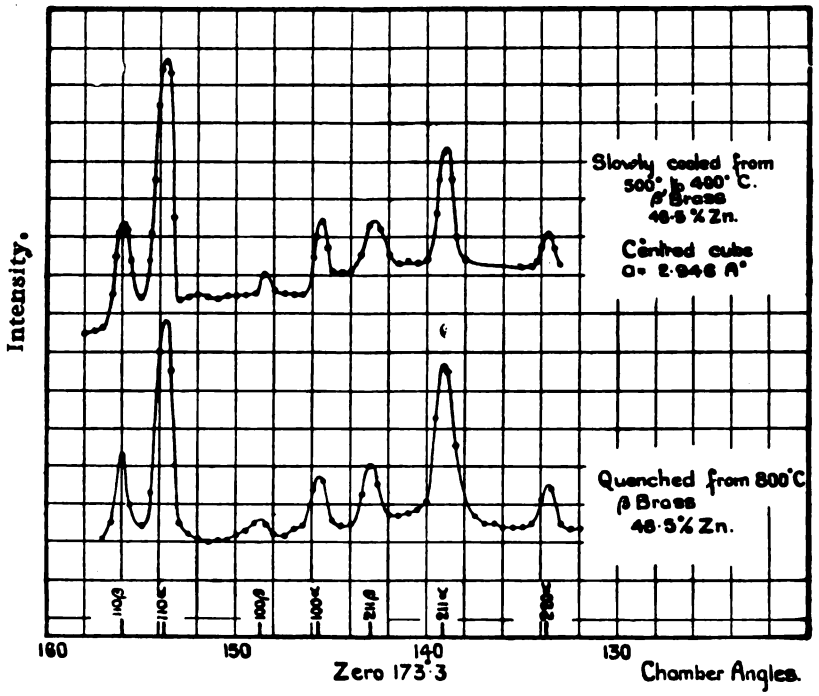


FIG. 3.

of the $K_\alpha$ and $K_\beta$ radiations from the 110 faces and of the $K_\alpha$ radiation from the 100 and 211 faces were carefully examined and gave a value 2·946 Å for the parameter. The observed density was the same as for β brass, which requires a parameter 2·945 Å. We conclude from these observations that there is no change of crystalline structure during the heat evolution observed at 470° C. According to the constitutional diagram suggested by CARPENTER and EDWARDS, this brass should contain about 50 per cent. α and 50 per cent. γ. Although very careful examination was made of the regions of the spectrum in which lines belonging to a face centred cube of the required parameter should appear, no trace of any reflection could be detected in these regions. In case, however, the method was not sensitive enough to detect the presence of the α structure if it existed in the samples ot β′ brass examined, measurements were made on three alloys from a region a little removed from that of β′. They contained 43·7 per cent. zinc and were quenched from different temperatures. The first was annealed for 2 minutes at 750° C., the second annealed for 1 hour at 500° C., and the third annealed for 3 hours at 400° C., quenching in water in each case. According to the constitutional diagram (Fig. 1), the first of the above should contain pure β, the second a mixture of α and β, and the third a mixture of α and β′. The second and third should be indistinguishable, since the structures of β and β′ are crystallographically identical.

Digitized by Google

The results of the X-ray measurements on the second and third of the above specimens are shown in Tables V and VI respectively.

TABLE V.—No. 45B. 43·7 per cent. Zinc, annealed for 30 minutes at 500° C.

| 2 θ. | Sin θ. | α Brass. | | β Brass. | |
|---|---|---|---|---|---|
| | | Form. | *a*. | Form. | *a*. |
| 17·5 | 0·1519 | | | 110β | 2·932 Å |
| 19·1 | 0·1661 | 111α | 3·690 Å | | |
| 19·6 | 0·1707 | | | 110α | 2·944 |
| 22·1 | 0·1918 | 110α | 3·691 | | |
| 24·8 | 0·2147 | | | 100β | 2·934 |
| 27·9 | 0·2410 | 110β | 3·697 | 100α | 2·937 |
| 30·3 | 0·2613 | | | 211β | 2·953 |
| 31·4 | 0·2706 | 110α | 3·699 | | |
| 34·4 | 0·2957 | | | 211α | 2·932 |
| 35·3 | 0·3032 | | | 220β | 2·939 |
| 37·0 | 0·3173 | 311α | 3·699 | | |
| 39·7 | 0·3395 | | | 220α | 2·949 |
| Mean value . . | | | 3·695 Å | | 2·940 Å |

TABLE VI.—No. 45C. 43·7 per cent. Zinc, annealed for 3 hours at 400° C.

| 2 θ. | Sin θ. | α Brass. | | β′ Brass. | |
|---|---|---|---|---|---|
| | | Form. | *a*. | Form. | *a*. |
| 17·2 | 0·1495 | 111β | (3·649) Å | 110β | 2·980 A |
| 19·1 | 0·1659 | 111α | 3·695 | | |
| 19·55 | 0·1696 | | | 110α | 2·950 |
| 22·0 | 0·1908 | 100α | 3·710 | | |
| 27·9 | 0·2410 | | | 100α | 2·937 |
| 30·5 | 0·2630 | | | 211β | 2·934 |
| 31·1 | 0·2697 | 110α | 3·711 | | |
| 34·3 | 0·2948 | | | 211α | 2·941 |
| 37·1 | 0·3181 | 311α | 3·688 | | |
| 39·8 | 0·3404 | | | 220α | 2·941 |
| Mean value . . | | | 3·701 Å | | 2·941 Å |

In each case a mixture of the two constituents α and β or β′ was observed. The remaining specimen gave a spectrum characteristic of a centred cube without any trace of the α constituent. The observations taken between chamber angles of 150° and 155° are plotted in Fig. 4. These suffice to show the different appearance of the spectra, and the absence of reflections from the 100 and 111 faces of the α constituent in the spectra of specimens quenched from 750° C.

These observations show that if the α constituent were present in the alloy containing



Digitized by Google

48·5 per cent. zinc which had been annealed at a temperature below 470° C., it would have been detected in the analysis.

We therefore conclude from the results of the present investigation that the crystalline structures of the β and β′ phases are identical both as regards type and dimension of lattice and that the thermal effect which occurs at 470° C. in alloys containing 48·5 per cent. zinc is not accompanied by the breaking up of the β constituent into a mixture of α and γ.

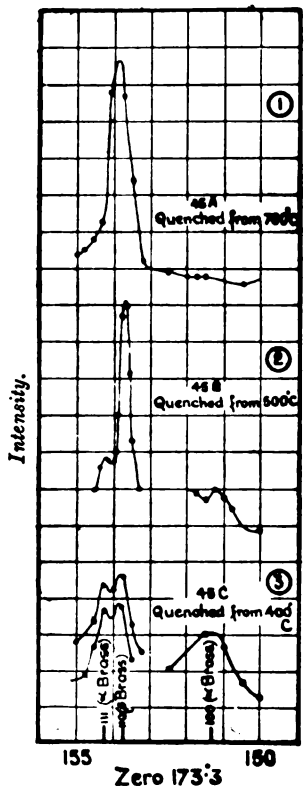


Fig. 4.

(3) *Alloy containing* 67·2 *per cent. Zinc.*—Alloys containing 60 to 70 per cent. zinc form the region of γ brasses. The specimens examined were annealed for 2 hours at 500° C. and quenched in water. The X-ray reflections were found to be very weak, the five specimens which were examined all suffering from this defect. With only a limited number of lines available, the solving of the structure presented some difficulty.

In the initial examination of the spectrum five lines could be detected with certainty—three of these being $K_\alpha$ reflections and two $K_\beta$. The α-lines occurred at angles 19·7° 27·8° and 34·6°, the sines of half these angles being in the ratio :—

$$0{\cdot}1713 : 0{\cdot}2402 : 0{\cdot}2974 = 1 : \sqrt{1{\cdot}96} : \sqrt{3{\cdot}02},$$

or very nearly as $1 : \sqrt{2} : \sqrt{3}$, which are the ratios required for the sines of the angles of reflection from the 100, 110 and 111 planes of a simple cube, or from the 110, 100 and 211 planes of a centred cube. Assuming that the alloy has a simple cubic structure and taking M, the average atomic mass, to be $\frac{64{\cdot}77 \times 1{\cdot}663}{1{\cdot}008} \times 10^{-24}$ gms., the density is calculated to be 12·06 gms./cc.—an impossible value. On the alternative assumption that the structure is a body centred cube of side 2·92 Å, the calculated density becomes 8·60 gms./cc. The observed density is 8·0 gms./cc., this figure being the mean of several determinations carried out on different specimens and by different methods, including weighing the powdered material in paraffin, as water was found to attack the alloy. The figure 8·0 gms./cc. is the density to be expected from an alloy of this composition from the density curve in Fig. 5. The disagreement between the calculated and observed density is about 7½ per cent. This would require an error of 2½ per cent. in the value of the parameter—a discrepancy which is too great to be due to experimental error. With a view to fixing the parameter with greater certainty, a detailed survey of the spectrum was made in the region of the second order reflection of 110α, the most intense line of the spectrum. A reflection of small intensity at an angle of

Digitized by Google

40·2° was found, the corresponding sine being 0·3437, which is in good agreement with the value 0·1713, previously found for the sine of the angle of the first order reflection. The error is, therefore, not in the measurement of the parameter, and a structure other than the centred cube must be found to account for the observed density of the alloy.

An alternative structure was found in a close-packed hexagonal lattice of side 2·92 Å and axial ratio 1·225, the $10\bar{1}1$, $11\bar{2}0$ and $20\bar{2}1$ planes providing reflections with the sines of the angles in the ratio $1 : \sqrt{2} : \sqrt{3}$. In this case the calculated density 8·1 gms./cc was in close agreement with the observed value. The difficulty encountered with this structure was that the $11\bar{1}0$ line, which should be present, was missing, and a close examination of the spectrum in this region failed to reveal its presence.

In view of the uncertainty as to the type of lattice present, an additional number of specimens was examined and the reflections recorded in Table VII, though of small intensity, were found to be present.

These figures do not agree with the reflections to be expected from the hexagonal lattice considered above, but may be accounted for by a rhombohedral lattice of side 4·136 Å and axial ratio 0·6495—a structure which requires a density of 8·06 gms./cc. in agree-

TABLE VII.—γ Brass. Rhombohedral Hexagonal.

| 2 θ. | Sin θ. | Form. | *d*. | *a* ($c = 0{\cdot}6495$). |
|---|---|---|---|---|
| 17·4 | 0·1513 | $11\bar{2}0\beta$ | $a/2$ | 4·163 Å |
| 19·1 | 0·1662 | $10\bar{1}1\alpha$ | $a\Big/\sqrt{\frac{4}{3}+\frac{1}{c^2}}$ | 4·100 |
| 19·7 | 0·1713 | $11\bar{2}0\alpha$ | $a/2$ | 4·130 |
| 27·8 | 0·2402 | $20\bar{2}1\alpha$ | $a\Big/\sqrt{\frac{16}{3}+\frac{1}{c^2}}$ | 4·090 |
| 28·6 | 0·2470 | $10\bar{1}2\beta$ | $a\Big/\sqrt{\frac{4}{3}+\frac{4}{c^2}}$ | 4·194 |
| 30·5 | 0·2630 | $10\bar{1}0\beta$ | $a/2\sqrt{3}$ | 4·148 |
| 32·8 | 0·2823 | $10\bar{1}2\alpha$ | $a\Big/\sqrt{\frac{4}{3}+\frac{1}{c^2}}$ | 4·123 |
| 34·1 | 0·2932 | $21\bar{3}1\alpha$ | $a\Big/\sqrt{\frac{28}{3}+\frac{1}{c^2}}$ | 4·130 |
| 34·6 | 0·2974 | $10\bar{1}0\alpha$ | $a/2\sqrt{3}$ | 4·121 |
| 38·0 | 0·3265 | $20\bar{2}2\alpha$ | $a\Big/2\sqrt{\frac{4}{3}+\frac{1}{c^2}}$ | 4·185 |
| 40·2 | 0·3437 | $22\bar{4}0\alpha$ | $a/4$ | 4·118 |
| | | | Mean . . . . . | 4·136 Å |

$c = 0{\cdot}6495$. $a = 4{\cdot}136 \times 10^{-8}$ cm. $M_s = 64{\cdot}77 \times \frac{1{\cdot}663}{1{\cdot}008} \times 10^{-24}$ gms.

$$\rho = \frac{6M_s}{\sqrt{3}a^3c} = 8{\cdot}06 \text{ gms./cc.} \qquad \rho \text{ (obs.)} = 8{\cdot}00 \text{ gms./cc.}$$



Digitized by Google

ment with observation. The centred cubic structure considered above which failed to account satisfactorily for the observed density is equivalent to a rhombohedral lattice of side 4·13 Å and axial ratio 0·6125, while β brass is a centred cube of side 2·946, *i.e.* a rhombohedral structure of side 4·16 and axial ratio 0·6125 $\left(=\frac{\sqrt{3}}{2\sqrt{2}}\right)$. The structure here assigned to γ brass is not very different from either of these, but the change in axial ratio reduces the number of trigonal axes of symmetry from four for the cubic structure to one for the rhombohedral.

It is hoped to continue the investigation of the structure of this material using specimens of different compositions throughout the range of the γ phase.

*Alloy containing* 80·1 *per cent. Zinc.*—This specimen of ε brass was annealed for five hours at 550° C. before quenching in water. X-ray analysis yielded a spectrum, the details of which are included in Table VIII. The structure which satisfactorily fits the

TABLE VIII.—Brass, 80·09 per cent. Zinc. Annealed for 5 hours at 550° C.

| 2 θ. | Sin θ. | Close-packed hexagonal. | | $a$ ($c = 1{\cdot}585$). |
|---|---|---|---|---|
| | | Form. | $d$. | |
| 17·3 | 0·1504 | $10\bar{1}0\alpha$ | $\frac{a\sqrt{3}}{2}$ | 2·718 Å |
| 19·0 | 0·1650 | $0001\alpha$ | $\frac{ac}{2}$ | 2·707 |
| 19·7 | 0·1711 | $10\bar{1}1\alpha$ | $a\Big/\sqrt{\frac{4}{3}+\frac{1}{c^2}}$ | 2·724 |
| 25·6 | 0·2215 | $10\bar{1}2\alpha$ | $a\Big/\sqrt{\frac{4}{3}+\frac{4}{c^2}}$ | 2·733 |
| 30·0 | 0·2588 | $11\bar{2}0\alpha$ | $a/2$ | 2·735 |
| 31·8 | 0·2740 | $11\bar{2}2\beta$ | $a\Big/\sqrt{4+\frac{4}{c^2}}$ | 2·718 |
| 33·7 | 0·2898 | $10\bar{1}3\alpha$ | $a\Big/\sqrt{\frac{4}{3}+\frac{9}{c^2}}$ | 2·708 |
| 35·8 | 0·3074 | $11\bar{2}2\alpha$ | $a\Big/\sqrt{4+\frac{4}{c^2}}$ | 2·723 |
| 38·4 | 0·3289 | $0002\alpha$ | $\frac{ac}{4}$ | 2·715 |
| 40·3 | 0·3445 | $20\bar{2}2\alpha$ | $a\Big/2\sqrt{\frac{4}{3}+\frac{1}{c^2}}$ | 2·704 |
| 42·5 | 0·3624 | $10\bar{1}4\alpha$ | $a\Big/\sqrt{\frac{4}{3}+\frac{16}{c^2}}$ | 2·710 |
| | | | Mean . . . . . | 2·718 Å |

$a = 2{\cdot}718 \times 10^{-8}$ cm. $c = 1{\cdot}585$. $M_s = 64{\cdot}97 \times \frac{1{\cdot}663}{1{\cdot}008} \times 10^{-24}$ gms.

$$\rho = \frac{4M_s}{\sqrt{3}\ .a^3c} = 7{\cdot}77 \text{ gms./cc.} \quad \rho \text{ (obs.)} = 7{\cdot}6 \text{ gms./cc.}$$

Digitized by Google

experimental observations is a close-packed hexagon of axial ratio 1·585 and parameter 2·718 Å. The observed and calculated densities are respectively 7·6 gms. per cc. and 7·8 gms. per cc., which show fair agreement.

## III. Conclusions.

(1) *Atomic Structure.*—The results obtained by X-ray analysis of the zinc-copper system summarised in Table IX are in agreement with the constitutional diagram of Shepherd as modified by Desch and Hudson. The figures quoted in the table for zinc are due to Hull.*

Table IX.

| Phase. | Composition. | | Structure. | Parameter. | Axial ratio. |
|---|---|---|---|---|---|
| | Atomic per cent. zinc. | Per cent. zinc by weight. | | | |
| Cu | 0·0 | 0·0 | Face centred cubic . . . . . | 3·608 Å | |
| α | 11·07 | 11·35 | „ . . . . . | 3·629 | |
| α | 20·27 | 20·77 | „ . . . . . | 3·651 | |
| α | 26·54 | 27·09 | „ . . . . . | 3·667 | |
| α | 29·42 | 30·0 | | 3·673 | |
| α | 38·05 | 38·73 | „ . . . . . | 3·692 | |
| β | 47·95 | 48·5 | Centred cubic . . . . . | 2·946 | — |
| | | | Rhombohedral hexagonal . | 4·17 | 0·6125 |
| β′ | 47·95 | 48·5 | Ditto . . . . . | 4·17 | 0·6125 |
| γ | 66·6 | 67·2 | Rhombohedral hexagonal . . | 4·136 | 0·649 |
| [δ | 75·0 | 75·5 | Close-packed hexagonal . . | 2·776 | 1·475] |
| ε | 79·5 | 80·1 | „ . . | 2·718 | 1·585 |
| Zn | 100·0 | 100·0 | „ . . | 2·670 | 1·860 |

The changes which occur in the lattice are perhaps most easily visualised by remembering that a face centred cube of side $a$ is equivalent to a rhombohedral lattice of side $a/\sqrt{2}$ and axial ratio $\sqrt{6}$. Thus the copper lattice is a rhombohedral one of side 2·54 Å and height $2{\cdot}54 \times \sqrt{6} = 6{\cdot}23$ Å, successive (0001) planes of copper following one another at intervals of $\frac{6{\cdot}23}{3} \simeq 2{\cdot}08$ Å. The addition of 38 atomic per cent. zinc expands the rhombohedral lattice to one of side 2·62 Å and height 6·41 Å, the axial ratio remaining unchanged. The centred cubic lattice of the β brasses is equivalent to a rhombohedral lattice of side 4·17 Å, *i.e.* $a\sqrt{2}$, and axial ratio $\frac{\sqrt{3}}{2\sqrt{2}}$, so that the height of the unit hexagonal prism is 2·55 Å. Thus, from this point of view the difference between the α, β and γ brasses is not one of difference of type of lattice, but only of relative dimensions. The

* 'Phys. Rev.', vol. 17, p. 571, 1921.

Digitized by Google

side of the hexagonal prism increases from 2·62 Å for an $\alpha$ brass containing 38 atomic per cent. zinc to 4·17 Å for a $\beta$ brass containing 48 atomic per cent. zinc. The difference between the $\beta$ and $\gamma$ brasses is much less marked as far as the dimensions of the lattice are concerned, the axial ratio increasing from 0·6125 to 0·649 and the side of the hexagonal prism decreasing from 4·17 Å to 4·13 Å. The structure in this case, however, loses symmetry, the cubic lattice of the $\alpha$ and $\beta$ phases having four trigonal axes of symmetry, while the rhombohedral lattice of the $\gamma$ phase has only one.

Passing on from the $\gamma$ to the $\varepsilon$ region, the lattice changes from rhombohedral to hexagonal close-packed, which is also the lattice of pure zinc. For $\varepsilon$ brass the side of the hexagonal prism is 2·72 Å and the height 4·31 Å, and for pure zinc the corresponding figures are 2·67 Å and 4·97 Å.

It appears, then, that we may regard the zinc-copper alloys as being built on two hexagonal lattices, those between copper and $\gamma$ brass following the rhombohedral and those between zinc and $\varepsilon$ brass (or possibly $\delta$ brass) following the hexagonal close-packed arrangement.

The spectral curves do not supply sufficient information to enable us to place the atoms in their respective positions in the lattice. The difficulty is enhanced owing to the fact that zinc and copper are of so nearly equal atomic weights. We may, however, be allowed to direct attention to certain points of interest in connection with some of the lattices. If we follow HULL and assume that zinc atoms are prolate spheroids, which in pure zinc are arranged with their circular sections parallel to the 0001 planes and their major axes perpendicular to these planes, then the closest distances of approach of the atoms are 2·67 Å and 2·92 Å, the former being the side $a$ of the hexagonal lattice and the latter the quantity $a\sqrt{\frac{c^2}{4}+\frac{1}{3}}$. In $\varepsilon$ brass $a = 2{\cdot}72$ Å and $c = 1{\cdot}585$, so that $a\sqrt{\frac{c^2}{4}+\frac{1}{3}} = 2{\cdot}67$ Å, the diameter of the circular section of the zinc atom. This suggests that the presence of the copper atoms causes the zinc atoms to rotate about an axis perpendicular to a set of $(11\bar{2}0)$ planes, thus preserving the closest distance of approach between zinc atoms which obtains in the pure zinc lattice. We might, therefore, expect that the forces of cohesion would fail to be sufficient to maintain the zinc atoms in contact at about the same temperature for zinc and for $\varepsilon$ brass. It is of interest to note that, according to the constitutional diagram of SHEPHEPD, brass containing about 13 per cent. copper (at the end of the $\varepsilon$ region rich in zinc) begins to melt at a temperature sensibly the same as the melting point of zinc.

The atomic proportion of copper to zinc in $\varepsilon$ brass is as 1 to 7. Atoms in this proportion can be fitted into a hexagonal close-packed lattice with very little distortion if we assume the (0001) planes to consist alternately of zinc atoms and of copper and zinc atoms in the ratio of 1 to 3. In the latter planes the copper atoms would take up their positions on a hexagon of side $2a$, the zinc atoms occupying the remaining positions.

In $\delta$ brass the ratio of the number of copper atoms to the number of zinc atoms is 1 to 3. If it be assumed that the lattice is close-packed hexagonal, the average mass

Digitized by Google

($M_a$) associated with each point in the lattice will be $64{\cdot}92 \times \frac{1{\cdot}663}{1{\cdot}008} \times 10^{-24}$ gms. The density of the material deduced from the observed curve of density in Fig. 5 is 7·84 gms. per cc.; so that the average atomic volume $\left(\frac{M_a}{\rho}\right)$ is 13·2 cubic Ångströms. If the addition of the necessary number of copper atoms to ε brass to produce δ brass causes a further rotation of the zinc atoms (such as was assumed in connection with the change from zinc to ε brass) so that the major axes of the zinc atoms fall along the sides of the hexagon joining two copper atoms, the side of the hexagon becomes 2·776 Å. In this case the axial ratio $c\left(=\frac{4M_a}{\sqrt{3}a^3\rho}\right)$ works out to be 1·475. On this arrangement the closest distance of approach of zinc and copper atoms in the $(11\bar{2}0)$ plane will be 2·604 Å, which is in close agreement with the sum of the radius of the copper atom (1·274 Å) and the minor axis of the zinc atom (1·335 Å). We were unable in the present investigation to make any direct measurements on δ brass, owing to its being unstable at ordinary temperatures. The hexagonal close-packed structure suggested here is a possible one, but the evidence in support of it is incomplete, and further work is necessary to establish it.

(2) *Density.*—The values of the densities calculated from the results of the X-ray analysis of the α, β, γ and δ phases are in good agreement with the observed values of the densities. Previous work on the densities of zinc-copper alloys carried out by BAMFORD* is in agreement with the results recorded here for alloys up to 60 per cent. zinc; for alloys of higher zinc content, however, there is disagreement. BAMFORD records a very low density (6·8 gms. per cc.) for a brass containing about 10 per cent. copper by weight. This is in the (ε + η) region, and on this account we were unable to make a determination of the density by direct X-ray measurement. It was considered that an independent observation of the density would, however, be desirable. A 1-inch chill casting weighing about 1 kg. and containing 10·2 per cent. copper by weight was accordingly prepared. A piece weighing about 100 grammes was sawn off the lower end of the casting and gave a density of 7·35 gms. per cc. This value is about that to be expected from the constitutional diagram, because in this region the metal exhibits a duplex structure, being a mixture of the ε and η phases, and the specific volume of the material will be the sum of the specific volumes of the constituent phases taken in the proper proportions. We conclude, therefore, that the low value of the density of brass containing 10 per cent. copper given by BAMFORD is not the true crystal density.

It is probable that the directly observed densities of the alloys containing 76, 80 and 90 per cent. zinc are on the low side, as the materials were distinctly porous, so that the figure obtained from the X-ray data for ε brass may be nearer the true density than the smaller directly observed value, in spite of the fact that the experimental error in the

* 'J. Inst. Metals', vol. 26, p. 155, 1921.

Digitized by Google

value of the parameter is trebled in the computation of the density. The density-composition curve (Fig. 5) has accordingly been provisionally drawn between the two values of the density observed for the alloy containing 80 per cent. zinc. This brings the whole curve in this region slightly above the observed values of the densities.

(3) *Hardness.*—The atomic volume curve shown in Fig. 5 consists very approximately of two straight lines meeting in the region of the γ brass.* We have at present no evidence to show what changes of atomic volume take place within the regions of phases other than the α phase, and have drawn a smooth curve through the determined points.

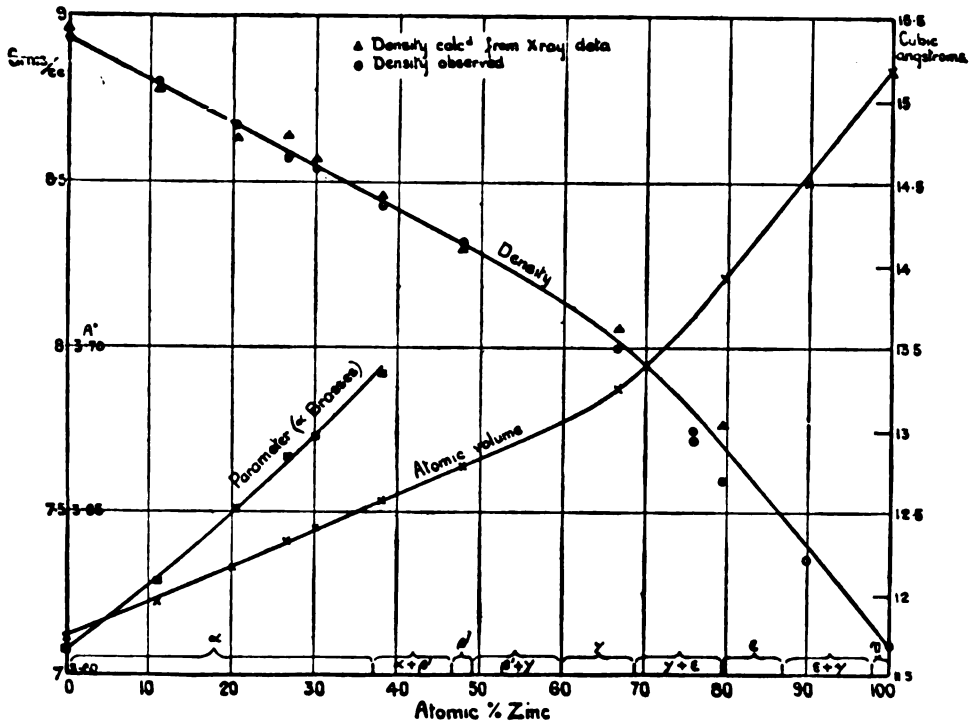


FIG. 5.

The γ brasses lie in the region where there is the greatest departure of the curve from the straight line joining the atomic volumes of copper and zinc. This implies that there is here a maximum of distortion, the atoms "sharing electrons" or being "compressed", so that they occupy a smaller volume than in either of the pure metals. Assuming that the hardness of a material, that is, its resistance to slip, depends upon the amount of distortion obtaining,† we should expect that the hardness of the zinc-copper alloys

* The intersection occurs at 68 per cent. zinc, or very nearly $CuZn_2$. It is doubtful whether the inference that a compound of this composition exists is justified. (*Cf.* DESCH, 'Intermetallic Compounds', 1914, p. 40. Published by Longmans, Green & Co.

† There is ample experimental evidence that hardness is closely related to atomic or molecular volume. For instance it has been observed that a series of isomorphous chemically similar substances exhibit degrees of hardness inversely proportional to their molecular volume. (See A. E. H. TUTTON, 'Crystallography', vol. 1, p. 536.)

Digitized by Google

would increase from the copper end to the region of γ brass, and then diminish as we proceed to the zinc end of the series. This conclusion is supported by experiment. The results of MURRAY* on the hardness of the brasses, as measured by the Shore scleroscope, show that β brass is about twice as hard as pure copper, and that γ brass is about four times as hard as β brass, while ε brass is of about the same hardness as β brass.

There is yet another point of interest which may be considered in reference to the hardness of these alloys. It has been found that the α phase is face centred cubic, and the β phase centred cubic. If we suppose that slipping takes place on the hexagonal (0001) planes, there would be more resistance offered to slip on these planes in the centred than in the face centred cubic lattice, and so on this account alone the β phase would be harder than the α phase. With regard to the relative hardness of β and γ brasses, the former has four axes of trigonal symmetry, whereas the latter has only one. This loss of symmetry coupled with the fact that in γ brass we have the maximum amount of distortion will probably account for the great hardness of γ brass as compared with the hardness of the other alloys in the series.

The increase of hardness of alloys in the α phase with increasing zinc content is accounted for by the local distortion caused by the introduction of the atoms of zinc into the copper lattice.† The same explanation obtains for the relative hardness of zinc, η and probably ε brass.

(4) *Allotropy.*—We have observed that the atomic volume curve may be considered in two parts represented by straight lines meeting in the region of γ brass. Along the one limb the crystal structure of the alloys follows the rhombohedral arrangement, whilst they follow the close-packed hexagonal arrangement along the other. If the atoms of copper and zinc existed in the brasses without loss of volume, the average atomic volume would be the straight line joining the atomic volume of copper and the atomic volume of zinc. If we produce the line representing the atomic volume of the α and β phases, it will meet the zinc ordinate of the graph at a point which will give an atomic volume of 13·92 Å$^3$. This hypothetical zinc atom, when mixed with different proportions of copper, will cause the average atomic volume to increase proportionately to the amount of zinc present.‡

If we assume that this atom crystallises on a face centred lattice, the parameter will be 3·82 Å and the closest distance of approach of the atoms will be 2·70 Å. This is 1 per cent. greater than the minor diameter of the zinc atom. It would therefore appear that the zinc atom, when it is associated with copper atoms up to a concentration of that of γ brass, behaves as a sphere of radius 1·35 Å.

If we assume that the prolate spheroidal shape of the ordinary zinc atom is due to

* 'J. Inst. Metals', vol. 2, p. 199, 1909.

† See W. ROSENHAIN, 'Roy. Soc. Proc.', A, vol. 99, 1921, and 'Trans. Amer. Inst. Mining Met. Eng.', 1923.

‡ *Cf.* NERNST, 'Theoretical Chemistry', 1923, p. 127. Published by Macmillan.



Digitized by Google

the presence of the two valence electrons, then it would appear that when zinc is added to copper the latter deprives the zinc of these electrons, adding them to its own in the endeavour to form a stable ring.

One, if not two, allotropic modifications of zinc have been observed,* and it has been stated that a cubic form has also been noticed.

ROSENHAIN† has suggested that the β and γ phases of the copper-zinc system are due to an allotropic modification of copper, and it is to be observed that the cubic diagonal of the β brass lattice is exactly equal in length to the diagonal of the face of the cube in the lattice of pure copper. That is to say, that spheres of the size of copper atoms could be packed into the lattice of β brass without any distortion, but would require to be held in position by external constraints or a rearrangement of the atomic field of force. The atomic volume of copper (diameter of atom, $D = 2{\cdot}552$ Å) is in the face centred state $V = \frac{1}{4}(D\sqrt{2})^3 = 11{\cdot}74$ Å$^3$, and in the body centred state $V' = \frac{1}{2}\left(\frac{2D}{\sqrt{3}}\right)^3 = 12{\cdot}79$ Å$^3$. The atomic volume thus increases by $1{\cdot}05$ Å$^3$, while the volume of the supposedly spherical atom is in both cases $\frac{4}{3}\pi\left(\frac{D}{2}\right)^3 = 8{\cdot}67$ Å$^3$. The zinc atom has been considered to be a prolate spheroid of semi-axes $r_1 = 1{\cdot}335$ and $r_2 = 1{\cdot}502$ Å, so that the volume of this atom is $\frac{4}{3}\pi r_1^2 r_2 = 11{\cdot}21$ Å$^3$. Taking the compressibility of copper to be $0{\cdot}54 \times 10^{-6}$ per megabar, a tension of $16{\cdot}5 \times 10^4$ megabars would be required to increase its volume from $11{\cdot}74$ to $12{\cdot}79$. A pressure of this magnitude applied to zinc (compressibility $1{\cdot}4 \times 10^{-6}$ per megabar) would reduce a volume of $11{\cdot}21$ Å$^3$ to $8{\cdot}62$ Å$^3$, which is almost exactly the volume at its disposal in β brass.

We wish to express our best thanks to Dr. ROSENHAIN and the staff of the Metallurgy Department for helpful advice throughout the course of the investigation. We are particularly indebted to Miss G. W. FORD, B.Sc., of the Metallurgy Department, for her most competent assistance in the preparation of the specimens.

* Miss K. E. BINGHAM, 'N.P.L. Collected Researches', vol. 16, Paper 11, or 'J. Inst. Metals', vol. 24, p. 333, 1920.

† Inst. Metals, May Lecture, 1923, 'J. Inst. Metals', vol. 30, p. 3, 1923.

Digitized by Google

# THE ATOMIC STRUCTURE OF TWO INTERMETALLIC COMPOUNDS

BY

E. A. OWEN, M.A., D.Sc.,
SENIOR ASSISTANT IN THE PHYSICS DEPARTMENT,

AND

G. D. PRESTON, M.A.,
ASSISTANT IN THE METALLURGY DEPARTMENT.

Digitized by Google

## ABSTRACT.

The two intermetallic compounds $Mg_2Si$ and AlSb have been examined by the X-ray spectrometer with the following results :—

$Mg_2Si$.—A face centred cubic lattice of silicon atoms of side 6·391 Å symmetrically intermeshed with a simple cubic lattice of magnesium atoms of side 3·19 Å. There are eight magnesium atoms situated within each face centred cube of silicon atoms, dividing the four cubic diagonals in the ratio 1 : 3 and 3 : 1. Density from X-ray data $1·95 \pm 0·05$ gm./cc. The magnesium atoms are separated by the same distance as in the pure metal. The sum of the " radii " of silicon and magnesium atoms is equal to the distance between these atoms in the compound.

AlSb.—A face centred cubic lattice of antimony of side 6·126 Å intermeshed with an identical lattice of aluminium atoms ; the corner of the latter dividing the cubic diagonal of the former in the ratio of 1 : 3. Density from X-ray data $4·23 \pm 0·04$ gms./cc. The molecular volume of the compound is greater than the sum of the atomic volumes of its constituents. The increase in volume observed by the method of X-ray analysis agrees with that obtained by other methods of measurement. The volume of the lattice on which the antimony atoms are arranged is 4 per cent. less than the volume of the face centred rhomb found in pure antimony. The molecular volume of the compound is accordingly 4 per cent. less than twice the atomic volume of antimony. The closest distance of approach of aluminium and antimony atoms is 2·65 Å, which is less than the sum of their " radii " as determined from the pure metals.


Digitized by Google

# THE ATOMIC STRUCTURE OF TWO INTERMETALLIC COMPOUNDS.

By E. A. OWEN, M.A., D.Sc., Senior Assistant in the Physics Department, and G. D. PRESTON, B.A., Assistant in the Metallurgy Department.

[Reprinted from the 'Proceedings of the Physical Society of London', Vol. 36, 1924.]

Very few intermetallic compounds have hitherto been examined by X-ray methods. Generally their study is somewhat difficult on account of the small intensities of the reflected beams and the difficulty of measuring the intensities of the reflections. The compounds, the structures of which were examined in the present investigation, presented no particular difficulty in this respect. The procedure, which we need only outline briefly here, as it has already been described in detail in a previous paper,* is to mount on the spectrometer table a plate of the material containing crystals as small as can be produced. The plate is fixed in the position in which it gives the maximum amount of reflection for one definite line in the spectrum. In this position there will be a number of the small crystals at the proper orientation to reflect the radiation of the wave-length employed. Also, if each position of the plate is equally possible on account of the random distribution of the crystals, the particular position chosen will be the one in which there is the least amount of absorption and the best focussing of the radiation.

The plate is then rotated at half the rate of rotation of the ionisation chamber. The spectral curves obtained in this way show a number of definite maxima, the bases of which are generally situated on a smooth curve representing the distribution of intensity in the general radiation. The intensities of the maxima have been determined by subtracting the ordinate of the smooth curve from that of the peak in each case. Although the intensity of the peak thus obtained is not always accurate as it is sometimes difficult to decide the course of the smooth curve with certainty, yet it provides in most cases sufficient information to guide one in the allocation of definite positions of the atoms in the lattice.

To determine the crystal structure of any material, we have first of all to determine the type of lattice present. This is done in the usual way by plotting the lines observed in the spectrum and fitting them on suitably prepared graphs. The number of atoms associated with each unit of the lattice has to be such that the density calculated from the X-ray data agrees with the observed density of the material. Finally, it is necessary to measure the intensities of the peaks in the manner outlined above and thereby arrive at the relative intensities of the different order spectra. This enables us to fix the atoms in their respective positions in the lattice. For the first of these determinations it is essential that the plate should consist of a large number of small crystals, so that within the region examined each crystal plane shall be represented. Since the plate is rotated at the proper rate, the same set of crystals gives the maxima for different orders of

* Owen and Preston, 'N.P.L. Collected Researches', vol. 19, Paper 24, or 'Proc. Phys. Soc. Lond.', vol. 35, p. 101, 1923.

Digitized by Google

reflection from a particular crystal plane. For comparison of the intensities of different orders of reflection from the same set of planes, a random orientation of crystals is not required, but this would be essential if we wished to compare the intensity of reflections from different crystal planes.

An account is given in the present paper of the results obtained by the above method with the two compounds $Mg_2Si$,* and AlSb.

(1) $Mg_2Si$.—A specimen of the compound $Mg_2Si$ yielded a spectrum, the lines in which were found to be characteristic of the reflections from a face centred cube of side 6·391 Å. The observations are given in Table I, and the full spectrum is plotted in Fig. 1.

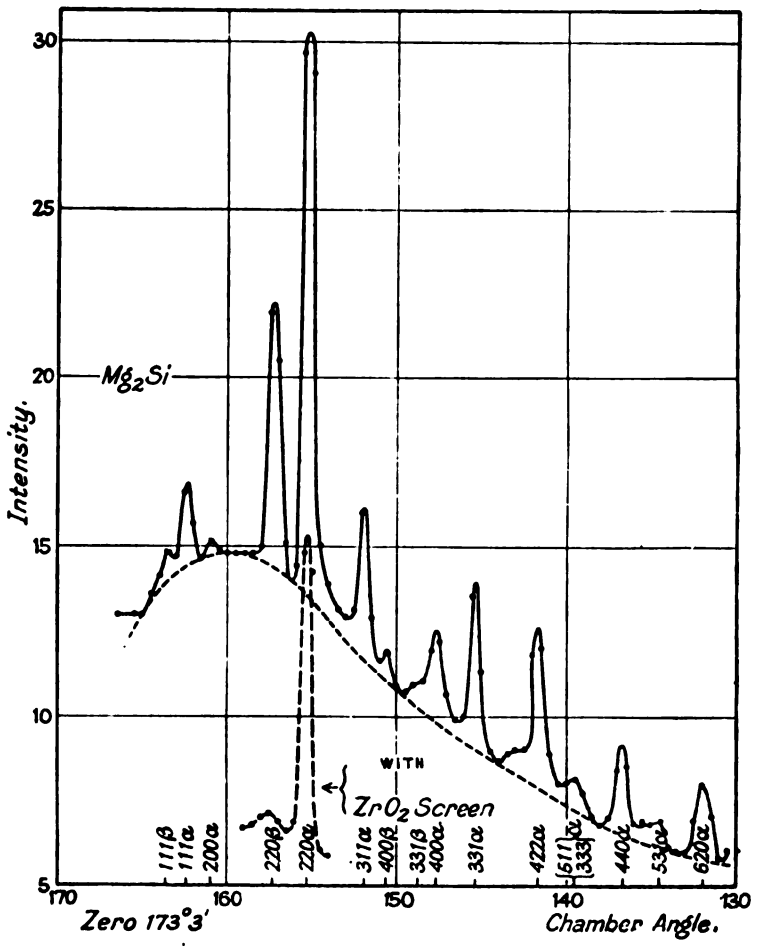


Fig. 1.

The observed density can be accounted for on the assumption that there are four molecules associated with each unit cube. This requires a density of 1·94 gms./cc. while the observed value was 1·88 gms./cc. The specimen, however, was porous and

* Although silicon is a non-metal it forms compounds of such distinctly metallic character that it may be grouped for the present purpose with the metals.

Digitized by Google

TABLE I.—$Mg_2Si$. Face Centred Cube.

| Intensity. | Form. | 2 θ. | Sin θ. | $a$. |
|---|---|---|---|---|
| 0·8 | 111β | 9·7 | 0·0846 | 6·488 Å |
| 2·4 | 111α | 10·9 | 0·0950 | 6·454 |
| 0·4 | 200α | 12·3 | 0·1072 | 6·588 |
| 7·5 | 220β | 16·0 | 0·1392 | 6·400 |
| 17·0 | 220α | 18·05 | 0·1570 | 6·375 |
| 4·0 | 311α | 21·3 | 0·1849 | 6·349 |
| 0·6 | 400β | 22·8 | 0·1977 | 6·372 |
| 0·5 | 331β | 24·5 | 0·2122 | 6·470 |
| 2·7 | 400α | 25·6 | 0·2215 | 6·390 |
| 5·0 | 331α | 27·9 | 0·2410 | 6·401 |
| 4·6 | 422α | 31·5 | 0·2714 | 6·389 |
| 0·8 | {333 / 511}α | 33·6 | 0·2890 | 6·377 |
| 2·6 | 440α | 36·5 | 0·3131 | 6·395 |
| 0·8 | 531α | 38·7 | 0·3313 | 6·339 |
| 2·2 | 620α | 41·3 | 0·3524 | 6·352 |
| | | | | Mean $a = 6·391$ Å |

$$M = 76·92 \times \frac{1·663}{1·008} \times 10^{-24} \text{ gms.}$$

$$n = 4.$$

$$\rho = \frac{4M}{a^3} = 1·94 \text{ gms./cc.}$$

$$\rho \text{ (obsd.)} = 1·88 \text{ gms./cc.}$$

impure, containing an excess of magnesium. The discrepancy of 3 per cent. between the observed and calculated density may be due to this cause, an excess of 3 per cent. magnesium being sufficient to account for the difference. We may thus place silicon atoms at the corners and face centres of a cube of side 6·391 Å and have to dispose of eight magnesium atoms in each cube in such a manner as to account for the observed intensities. The most symmetrical arrangement is to suppose the magnesium atoms to be situated at the corners of a cube of side $\frac{6·391}{2} = 3·19$ Å, the atoms being situated at the centres of the eight small cubes into which the cube of side 6·391Å may be divided.

In such an arrangement the (110) planes would all be identical, containing magnesium and silicon atoms in the ratio 2 : 1, and the reflections would be normal. This is approximately the case, and they are also very intense. The (100) spacing would be halved and, accordingly, the spectra of odd order would be weak. The first order was very weak, and the third was not detected. Alternate planes of Si and $Mg_2$ would give theoretical intensities $I_1 : I_2 : I_3 = 0·7 : 3 : 0$, while the observed intensities are in the ratio 0·5 : 3 : 0. The (111) planes are also abnormal. The distance between successive planes of silicon atoms is divided by two planes of magnesium atoms, dividing the spacing in the

Digitized by Google

ratio of 1 : 3 and 3 : 1. The second-order reflection should theoretically be about one-fifth as intense as the first, while the third-order reflection would be too weak to detect. The second order was, in fact, not detected. The absence of reflection from the (210) planes is also to be expected from the above structure.

The intensities of the reflections from the different faces are, therefore, in general accord with the theoretical values calculated on the assumption that the silicon atoms are arranged on a face-centred cubic lattice with magnesium atoms at the centres of the eight small cubes into which the unit cube of the face-centred lattice may be divided. A unit cell of the structure is shown in Fig. 2.

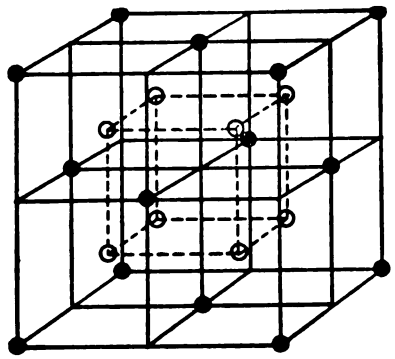

FIG. 2.

The closest distance of approach of magnesium and silicon atoms is $6{\cdot}39 \times \frac{\sqrt{3}}{4} = 2{\cdot}77$ Å. The "radius" of the magnesium atoms is 1·58 Å and that of the silicon atom 1·18 Å, or the sum of their radii is 2·76 Å. The atoms thus do not approach one another any more closely than they do in the pure metals.

The magnesium atoms are assembled on a simple cubic lattice of side 3·19 Å in the compound, while in the pure metal they behave as spheres of diameter 3·17 Å, the lattice being close-packed hexagonal of axial ratio 1·63. The simple cubic lattice found in the compound is very nearly of the dimension required by spheres of this diameter. The presence of the magnesium atoms causes a separation of the silicon atoms; whereas in pure silicon the nearest distance of approach is 2·36 Å, in the compound $Mg_2Si$ the smallest distance between two silicon atoms is 4·5 Å, or nearly double that in the pure element.

(2) AlSb.—The spectrum obtained with the compound AlSb is shown in Fig. 3. Twenty peaks were located and were found to correspond to the lines of a face-centred cubic lattice of side 6·126 Å, as shown in Table II. To account for the observed density four molecules must be associated with each cube. In order to fix the positions of the atoms in the lattice, we have the intensities of the first four orders of the 111 reflections, the first three orders of 100 and the first two orders of 110, as follows :—

| | $I_1$. | $I_2$. | $I_3$. | $I_4$. |
|---|---|---|---|---|
| 111α } 200β } . . . . . | 7·3 | 2·6 | 2·5 | 1·1 |
| 200α . . . . . | 2·5 | 1·7 | 0·8 | ... |
| 220α . . . . . | 4·1 | 1·1 | ... | ... |

Digitized by Google

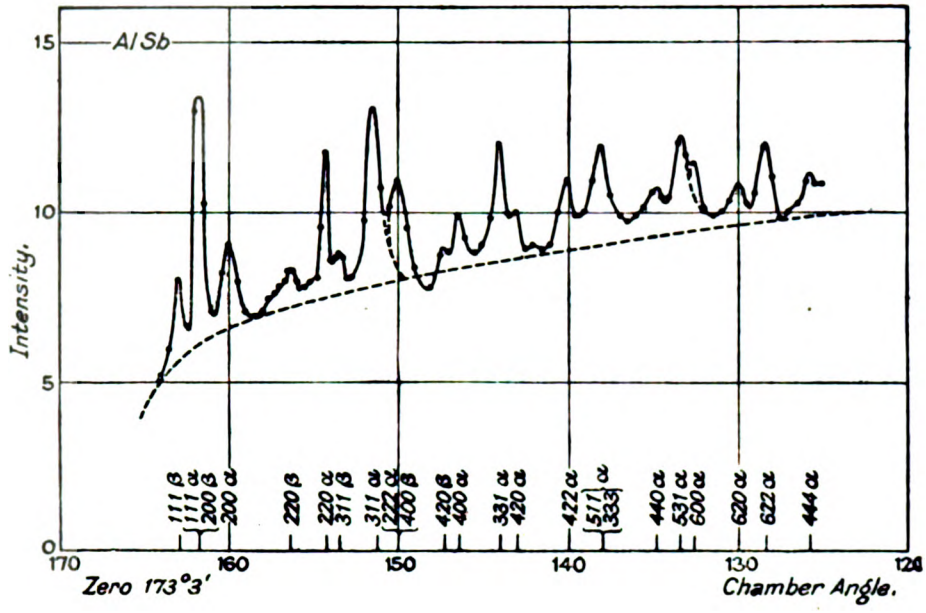


FIG. 3.

TABLE II.—AlSb. Face centred Cube.

| Intensity. | Form. | 2 θ. | Sin θ. | *a*. |
|---|---|---|---|---|
| 2·5 | 111 β | 10·3 | 0·0898 | 6·061Å |
| 7·3 | {111 α, 200 β} | 11·5 | 0·1002 | 6·151 |
| 2·5 | 200 α | 13·2 | 0·1149 | 6·186 |
| 1·0 | 220 β | 16·9 | 0·1470 | 6·050 |
| 4·1 | 220 α | 19·2 | 0·1668 | 6·167 |
| 1·2 | 311 β | 19·8 | 0·1719 | 6·067 |
| 5·0 | 311 α | 22·1 | 0·1917 | 6·151 |
| 2·6 | {222 α, 400 β} | 23·4 | 0·2028 | {6·070, 6·121} |
| 0·7 | 420 β | 26·0 | 0·2250 | 6·250 |
| 1·7 | 400 α | 26·8 | 0·2317 | 6·137 |
| 3·5 | 331 α | 29·3 | 0·2529 | 6·128 |
| 1·3 | 420 α | 30·2 | 0·2605 | 6·102 |
| 1·9 | 422 α | 33·2 | 0·2875 | 6·095 |
| 2·5 | {511, 333} α | 35·2 | 0·3024 | 6·106 |
| 1·1 | 440 α | 38·3 | 0·3280 | 6·130 |
| 2·6 | 531 α | 39·9 | 0·3412 | 6·162 |
| 0·8 | 600 α | 40·6 | 0·3469 | 6·148 |
| 0·9 | 620 α | 43·3 | 0·3689 | 6·094 |
| 2·1 | 622 α | 45·0 | 0·3827 | 6·160 |
| 1·1 | 444 α | 47·5 | 0·4027 | 6·115 |

$a = 6{\cdot}126 \times 10^{-8}$ cm. $\quad M = 147{\cdot}3 \times \frac{1{\cdot}663}{1{\cdot}008} \times 10^{-24}$ gms.

$\rho$ (obsd.) $= 4{\cdot}34$ gms./cc. $\quad n = \frac{a^3\rho}{M} = 4{\cdot}10.$



Digitized by Google

The intensities of the observed orders of the (110) reflections are in the normal ratio of 3 : 1, so that spacings in this direction are as in a face centred cube, successive planes being identical. The ratio of the intensity of the β radiation to the α radiation is approximately as 1 : 3, so subtracting one-third of the intensities of 100α from the figures in the first line, we have for the 111 planes—

$$I_1 : I_2 : I_3 : I_4 = 6{\cdot}5 : 2{\cdot}0 : 2{\cdot}2 : 0{\cdot}9.$$

The last figure is estimated on the assumption that $I_4$ for (100) is approximately one-tenth of $I_2$. Remembering that the spacing of the (511) planes is one-third of the spacing of the (111) planes, the apparently great intensity of the (333) reflection is accounted for. The intensities of the (100) reflections are abnormal—the first order is not interfered with by reflection from other planes, the third order falls very close to the position of 444β and the figure 0·8 may, therefore, be about 30 per cent. too large, while the second order is to some extent interfered with by the β reflection from the (210) planes.

If we assume that the antimony atoms are situated on a face centred cube and that the (100) spacings are halved by planes of aluminium atoms, calculation shows that the (100) intensities to be expected are as 10 : 7·5 : 1. The observed intensities are as 10 : 7 : 3, which is sufficiently good agreement to justify the assumptions made as to the position of the atoms. A structure similar to that of zinc blende (a diamond lattice), with the aluminium atoms arranged on a face centred lattice displaced one quarter of its length along the cube diagonal, would require the intensities of the (111) reflections to be in the ratio 60 : 10 : 6 : 6, while the observed intensities are as 60 : 18 : 20 : 8. The relatively great intensity of the third order reflection is due to the superposition of the reflection from the 511 planes, as already stated. The discrepancy between the observed and calculated intensities of the second-order reflections may be due to error in estimating the intensity of the (222) line, as it falls rather near to the comparatively intense reflection from (311). The figure 18 above may quite well be as low as 15, so that the differences between the observed and calculated values do not make the structure suggested impossible.

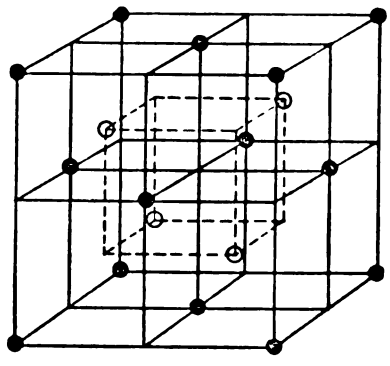

Fig. 4.

The evidence indicates that the compound consists of a face centred lattice of antimony of side 6·126Å intermeshed with an identical lattice of aluminium—the latter having one of its corners situated at a point which divides the cube diagonal in the ratio 1 : 3. A unit cell of the material is shown in Fig. 4.

Antimony is built on two intermeshed face centred rhombohedral lattices* of side

* James and Tunstall, 'Phil. Mag.', vol. 40, p. 233, 1920.

Digitized by Google

6·20 Å, the angle between the edges of the rhomb being 86° 58′. A corner of one rhomb is situated very nearly at the centre of the other rhomb, so that the structure approximates to a simple rhomb of side 3·10 Å. In the compound AlSb the side of the face centred cube is 6·126Å, so that the antimony lattice contracts slightly, and the angle increases by 3° 2′ to 90°. One of the antimony lattices is now replaced by a lattice of aluminium, and the construction point moved along the cubic diagonal towards one corner of the cube. Thus the forces between the atoms of antimony and aluminium are such as to produce a displacement of one lattice relative to the other. The forces involved are, in fact, so great that the compound AlSb is capable of existing in the liquid state,* and does not melt until a temperature of over 900° C. has been reached, while antimony melts at 630° C. In pure antimony the closest distance of approach of atoms is 2·87 Å. In the compound AlSb antimony and aluminium atoms are separated by 2·65 Å. The diameter of the aluminium atom is 2·86 Å, so that the aluminium and antimony atoms approach one another closer than the atoms in the pure metals.

A further point of interest is that this compound is one of those whose molecular volume is greater than the sum of the atomic volumes of its constituent elements. The sum of the atomic volumes of Al and Sb is 46·3 Å$^3$, whilst the molecular volume of the compound AlSb is 57·5 Å$^3$, an increase of about 24 per cent., which agrees with the value obtained by direct measurement.† Now the antimony lattice is practically unchanged in volume by the substitution of aluminium atoms for one set of antimony atoms, so that the whole increase of molecular volume is due to the fact that the aluminium atoms are constrained to lie on a face centred lattice of side 6·126 Å instead of on one of side 4·05 Å, as found in the pure metal, the molecular volume of the compound being 4 per cent. less than twice the atomic volume of antimony.

In conclusion, we wish to express our indebtedness to Miss G. W. Ford and Miss M. L. V. Gayler, of the Metallurgy Department, for the preparation of the specimens.

* Desch, ' Intermetallic Compounds ', 1914, p. 80. Published by Longmans Green & Co.
† Desch, *ibid.*, p. 41.



Digitized by Google

Digitized by Google

# THE ESTIMATION OF THE RADIUM CONTENT OF RADIO-ACTIVE LUMINOUS COMPOUNDS

BY

E. A. OWEN, M.A., D.Sc.,
SENIOR ASSISTANT IN THE PHYSICS DEPARTMENT,

AND

WINIFRED E. FAGE, B.Sc.,
SOMETIME ASSISTANT IN THE METALLURGY DEPARTMENT.

Digitized by Google

## ABSTRACT.

(1) The absorption of $\gamma$-radiation in zinc sulphide has been measured by different methods, and in each case its value was found to be approximately the same.

(2) No indication was observed of the occurrence of an abnormal absorption when the radio-active salt was mixed with the sulphide.

(3) A table has been compiled giving the values of the ratio of the true to the apparent radium content for tubes of different diameters filled with radio-active luminous compound. This table applies to the case of a compound the apparent density of which is 2·03 gms. per cc.

(4) The values of the absorption of $\gamma$-radiation from radium have been measured in different salts, particular attention being paid to the barium salts with which radium is often found in combination.


Digitized by Google

# THE ESTIMATION OF THE RADIUM CONTENT OF RADIO-ACTIVE LUMINOUS COMPOUNDS.

By E. A. OWEN, M.A., D.Sc., Senior Assistant, and WINIFRED E. FAGE, B.Sc., sometime Assistant, in the Physics Department.

[Reprinted from the 'Proceedings of the Physical Society of London', Vol. 34, 1921.]

The apparent radium content of a sample of luminous compound may be directly measured by means of any one of the γ-ray methods. To arrive at the true content, it is necessary to know how much of the radiation is absorbed in the salt. This absorption has been measured by Paterson, Walsh and Higgins,* who found that different values were obtained according to whether it was measured before or after mixing the radium with the responsive base—the base employed being hexagonal zinc sulphide. The value of the absorption coefficient of γ-radiation in the sulphide under the conditions of experiment was found to be about three times as much after mixing as it was before mixing with the radium. It was suspected that this difference was due to a selective effect which occurred in the one case but not in the other. This, however, was not definitely proved. The object of the present investigation was to obtain further information on this point. The absorption coefficient of γ-radiation in zinc sulphide has been re-determined by a number of different methods, and, in addition, data regarding the absorption of other salts have been obtained.

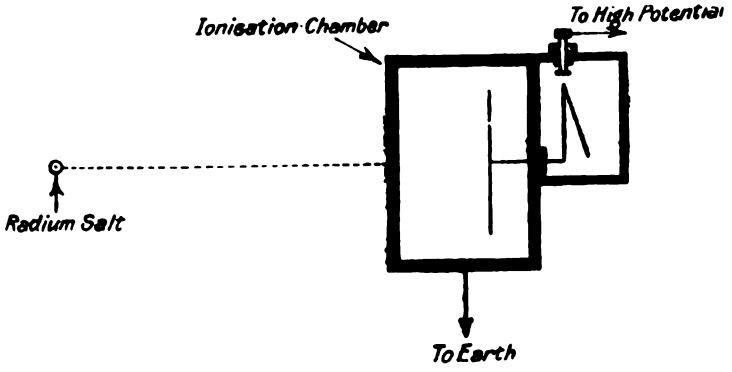


Fig. 1.

## Apparatus.

The most convenient method of measuring the γ-ray activity of a radium salt is the Direct Method. This is one of the methods in constant use at the Laboratory, and has always been employed to measure the radium content of luminous compounds. The apparatus consists of a combined ionisation chamber and gold-leaf electroscope as shown in Fig. 1. The sample whose radium content is desired is placed some distance in front of the ionisation chamber. The distance between the sample and the chamber

* 'N.P.L. Collected Researches', vol. 15, Paper 17, or 'Proc. Phys. Soc. Lond.', vol. 29, p. 215, 1917.

Digitized by Google

is decided by the amount of radium which the sample contains—about 30 divisions per minute is a convenient rate of fall of the leaf. The face of the ionisation chamber is covered with lead 0·5 cm. thick, so that only γ-radiation enters the chamber. To diminish the effect of stray radiation the windows of the electroscope are shielded with lead, and the walls of the chamber and the electroscope are made of lead 0·6 cm. thick. The amount of radium in a sample is measured by comparing it with a standard tube of known content, the experimental conditions during the observations being in each case exactly similar. The time taken by the leaf to fall over a constant number of divisions of the scale is measured both for the standard and for the sample. After correcting these times for the natural leak of the leaf system, which should be determined at the beginning and at the end of the observations, the corrected times are inversely proportional to the radium contents of the standard and sample, and thus the radium content of the sample is directly determined.

### Methods of measuring the Absorption of the Rays in the Sulphide.

The absorption of the radiation in zinc sulphide has been measured in the following ways :—(1) The sealed tube containing the radium which is eventually to be mixed with the sulphide is first measured. The zinc sulphide is placed in a glass cell of known thickness, and the radium placed very close to the face of it, remote from the chamber. Observations are taken with the cell empty and with it full, and from the knowledge of the apparent density of the material in the cell the mass-absorption coefficient under the conditions of experiment is calculated. (2) The sulphide is put into a glass tube of known diameter. The radium tube is then placed on the axis of this tube and its radium content again measured. (3) The contents of the radium tube are intimately mixed with a known quantity of the sulphide and placed in a glass tube of known diameter. The values of the radium content before and after mixing give sufficient data to calculate the absorption coefficient of the radiation in the sulphide. (4) The luminous compound made for the third of the above methods is placed in a glass cell of known thickness and the absorption of the radiation from another tube of radium measured in it by the first method.

### Absorption of γ-Radiation in Soda Glass.

A preliminary investigation was carried out on the absorption of different kinds of soda glass. It was necessary to know this figure in order to correct for the absorption of the radiation in the walls of the glass vessels containing the compounds. A number of determinations of the absorption coefficient ($\mu$) in soda glass, under the conditions of experiment, gave the value 0·105 cm.$^{-1}$.

### Obliquity Correction.

In the first of the above methods of measurement the cone of the rays passing into the ionisation chamber, which was 14 cms. in diameter internally, has an appreciable angle at

Digitized by Google

the vertex. The semi-angle in the present case varied from about 4° to about 17°, and for the larger angles a correction had to be made for the obliquity of the radiation. This was calculated by means of the following formula, due to SODDY and RUSSELL* :—

$$\frac{I}{I_0} = \frac{e^{-\mu t} - \cos\theta e^{-\mu t/\cos\theta} + \mu t\,[Ei(-\mu t)] - \mu t\,[Ei(-\mu t/\cos\theta)]}{(1-\cos\theta)},$$

where $I_0$ and 1 are the intensities of the radiation before and after traversing the salt.

A full curve was drawn, showing the relation between $\frac{I}{I_0}$ and $\mu t$, for given values of $\theta$, from which the value of $\mu$ could be obtained for any intensity ratio measured.

## RESULTS.

Two radium standards were employed in the work, the one (Standard A) containing about 15 mgms. and the other (Standard B) 2·5 mgms. of radium element. The following table shows the variations that were obtained in the values of the absorption coefficient with the two standards when placed at different distances in front of the ionisation chamber :—

TABLE I.

| Standard A. | | Standard B. | |
|---|---|---|---|
| Semi-angle θ of cone of rays. | μ (cm.$^{-1}$). | Semi-angle θ of cone of rays. | μ (cm.$^{-1}$). |
| ° ′ | | ° ′ | |
| 8 19 | 0·100 | 16 31 | 0·095 |
| 7 27 | 0·099 | 13 45 | 0·101 |
| 5 50 | 0·099 | 11 46 | 0·100 |
| 5 6 | 0·101 | 10 17 | 0·101 |
| 4 31 | 0·103 | 9 7 | 0·100 |
| 4 1 | 0·097 | 8 12 | 0·102 |

The values of the absorption coefficient given in the table have been corrected for the obliquity of the rays. The mean value of $\mu = 0{\cdot}100$ cm.$^{-1}$.

Another determination of $\mu$ by the same method for a different sample of sulphide gave the value 0·103 cm.$^{-1}$. The average value of the apparent density of the zinc sulphide employed for these determinations was 2·03 gms. per cc. so that the mean value of the mass absorption coefficient is 0·050.

A determination of the absorption coefficient, when the radium tube was placed axially inside a wider tube filled with zinc sulphide, gave the value $\mu = 0{\cdot}098$ cm.$^{-1}$.

The radium was now carefully mixed with a known quantity of the sulphide. This was

* ' Phil. Mag.', vol. 19, p. 725, 1910.



Digitized by Google

carried out by the dry method, and it may be of interest to indicate the procedure adopted. The contents of the radium tube were transferred into an agate mortar; it was difficult to remove all the salt from the tube as some of it adhered to the walls, even when the tube was gently tapped. The final cleaning was carried out by putting a little zinc sulphide into the tube and rubbing it on the inside walls by means of a small camel-hair brush. The operation was repeated five or six times, using only a small quantity of sulphide in each operation, until all the material clinging to the walls was removed. Having now transferred the radium with the small quantity of zinc sulphide used in the cleaning process into the mortar, it was ground for about 20 minutes into a fine powder. A small quantity of zinc sulphide was afterwards added, say about 1 gramme, and mixed with the radium by means of a spatula, taking care not to apply much pressure to the sulphide so as to avoid breaking up the crystals, which should be kept as large as possible for the best luminous effect. More sulphide was added and again thoroughly mixed with the salt already in the mortar. If the quantity of zinc sulphide is not too large it may all be added little by little to the radium, stirring constantly and keeping about 2 grammes of sulphide in hand for final washings of camel-hair brush, spatula, and funnel used to transfer the compound from mortar to the tube in which it is sealed. It is advisable not to fill the tube, so that the salt may be well shaken for final mixing. In this way a very homogeneous mixture was obtained.*

The compound was finally sealed in a glass tube whose internal diameter was 14·1 mms. and whose thickness of wall was 0·85 mm. The growth of activity of the compound was kept under observation for about five weeks, after which period it had reached a state of radio-active equilibrium. The maximum value of its activity was found to be equivalent to 2·314 milligrammes radium element, whilst the activity of the radium tube before mixing with the sulphide was equivalent to 2·519 milligrammes. Calculating the value of $\mu$ to a first approximation from the simple formula $I = I_0 e^{-\mu t}$, where $t$ is 7·05 mms., we have, after correcting for the absorption in the glass, $\mu = 0{\cdot}107$ cm.$^{-1}$. There will undoubtedly be a slight loss of radium during the process of mixing the compound which will tend to increase the value of $\mu$. A loss of 0·5 per cent. of the salt during mixing would in the present case alter the value of $\mu$ from 0·100 cm.$^{-1}$ to 0·107 cm.$^{-1}$, so that we may say that the above figure is in fair agreement—allowing for experimental error—with the value obtained by the other methods.

The fourth method of measurement, in which the luminous compound was removed from the sealed tube, placed in a glass cell and the absorption of the radiation from another radium tube in it measured, gave 0·100 cm.$^{-1}$ for the value of $\mu$.

There is, therefore, no appreciable difference between the values of the absorption coefficient of the radiation in zinc sulphide when measured by any one of the four methods described. The two values of $\mu$ obtained by PATERSON, WALSH and HIGGINS may be

* The authors are indebted to Mr. F. H. GLEW for the details of this method of preparing luminous compound.

Digitized by Google

explained if it be assumed that the compound when finally measured had not reached a state of radio-active equilibrium. It is possible for a radium salt to reach a steady maximum value of activity and yet not be in a state of true radio-active equilibrium. This may occur if the containing tube is imperfectly sealed, so that there will be a constant small leakage of emanation. The rate of production of emanation by the radium and the rate of leakage of emanation from the tube will, after a time, reach a steady state, giving a fictitious state of equilibrium. The maximum value of the activity will in this case be smaller than the value attained when the salt is in a state of true radio-active equilibrium, so that if the luminous compound were not properly sealed in its enclosure, the value of the absorption coefficient of the radiation measured by the third of the above methods would be too great.

## The Ratio of the True to the Apparent Radium Content of Tubes of Luminous Compound of Different Diameter.

The most reliable value of the absorption coefficient of $\gamma$-radiation in zinc sulphide is that measured by the first of the above methods, which gave the mean value 0·101 cm.$^{-1}$. Knowing this figure and assuming that the radium is distributed uniformly throughout the body of the sulphide, we can calculate the ratio of the true to the apparent radium content of tubes of different diameter filled with luminous compound. Suppose the tube containing the compound is cylindrical and of internal radius $a$ cm. If I is the measured intensity of the $\gamma$-radiation emitted by the tube and $I_0$ the intensity if no absorption had taken place, it can readily be shown,* if the correction due to the obliquity of the rays be neglected, that

$$\frac{I}{I_0} = \frac{1}{\mu a\sqrt{\pi}} \sum_{r=1}^{r=\infty} (-1)^{r+1} \frac{(2\mu a)^r}{\underline{|r+1}} \cdot r \cdot \frac{\Gamma\frac{r}{2}}{\Gamma\frac{r+1}{2}}$$

$$= C_0 + C_1(\mu a) + C_2(\mu a)^2 + \ldots\ldots,$$

where $\mu$ is the coefficient of absorption of the rays per centimetre thickness of compound. The values of the constants $C_0$, $C_1$, $C_2$ . . . are given in the following table :—

Table II.

| Coefficient. | Value. | Coefficient. | Value. |
|---|---|---|---|
| $C_0$ | +1·000000 | $C_7$ | −0·001642 |
| $C_1$ | −0·848826 | $C_8$ | +0·000347 |
| $C_2$ | +0·500000 | $C_9$ | −0·000067 |
| $C_3$ | −0·226354 | $C_{10}$ | +0·000012 |
| $C_4$ | +0·083333 | $C_{11}$ | −0·000002 |
| $C_5$ | −0·025869 | $C_{12}$ | 0·000000 |
| $C_6$ | +0·006944 | | |

* See Paterson, Walsh and Higgins (*loc. cit.*). There is a misprint in the general term of the series as given in their paper, but the values of the constants are the same as given here.



Digitized by Google

Since the value of the absorption coefficient for soda glass is approximately the same as that for zinc sulphide, we may, without serious error, calculate by means of the above series the ratio of the true to the apparent (or measured) radium content for tubes of different *external* diameters on the assumption that $\mu = 0{\cdot}101$ cm.$^{-1}$. The values calculated in this manner are given in the following table :—

TABLE III.

| External Diameter of containing tube in cms. | $\frac{\text{True Content}}{\text{Apparent Content}}$ |
|---|---|
| 0·5 | 1·02 |
| 1·0 | 1·04 |
| 1·5 | 1·07 |
| 2·0 | 1·09 |
| 2·5 | 1·11 |
| 3·0 | 1·13 |

ABSORPTION OF γ-RADIATION IN OTHER SALTS.

The absorption of γ-radiation was also measured in a number of other salts, special attention being paid to barium salts, with which radium is closely associated. The measurements were made by the first method outlined above. Each salt was powdered in a mortar and its apparent density determined from the weight of the salt required to fill the glass cell in which the absorption was measured. The thickness of material traversed by the rays was 1·12 cm. The following table contains a summary of the results obtained :—

TABLE IV.

| Salt. | Apparent Density in gms. per cc. | Absorption Coefficient cm.$^{-1}$. | Mass Absorption Coefficient. |
|---|---|---|---|
| ZnS . . . . | 2·03 | 0·101 | 0·050 |
| $BaSO_4$ . . . | 2·41 | 0·079 | 0·050 |
| $BaCl_2$ . . . | 1·58 | 0·100 | 0·053 |
| $BaCO_3$ . . . | 1·88 | 0·046 | 0·055 |
| PbO . . . . | 4·21 | 0·294 | 0·070 |
| $Bi_2O_3$ . . . . | 2·89 | 0·206 | 0·071 |
| $U_2O_5$ . . . . | 3·93 | 0·315 | 0·080 |

The mean value of the mass absorption coefficient in the barium salts may be taken as 0·053. By the aid of this value and a knowledge of the apparent density of a barium

Digitized by Google

salt containing a small percentage of radium, a table similar to Table III above may be compiled, giving the ratio of the true to the apparent radium content of the salt for tubes of different diameters.

It should be noted that the above values of the absorption coefficients hold when the radiation passes through 0·5 cm. of lead on its way to the chamber. Since $\gamma$-radiation from radium is heterogeneous, the values of the absorption coefficients would be different for other thicknesses of lead in front of the ionisation chamber.

Digitized by Google

Digitized by Google

# ON THE MEASUREMENT OF THE RADIUM CONTENT OF SEALED METAL TUBES

BY

E. A. OWEN, M.A., D.Sc.,
SENIOR ASSISTANT IN THE PHYSICS DEPARTMENT,

AND

BERTHA NAYLOR, B.Sc.,
JUNIOR ASSISTANT IN THE PHYSICS DEPARTMENT.

Digitized by Google

## ABSTRACT.

Tables have been compiled giving the corrections that have to be applied to the observed radium content of sealed platinum and silver tubes to obtain their true radium content. Two cases have been considered, namely, (1) that in which the active deposit is uniformly distributed throughout the volume of the tube such as in a full tube of salt, and (2) that in which the active deposit is uniformly distributed over the inner wall of the tube, such as in a tube containing a minute quantity of highly concentrated salt.

The results show that when the wall thickness is kept constant, the correction increases with the external diameter of the tube. Also for the same increase of external diameter, the increase of correction is more pronounced for the " empty " than for the full tube.


Digitized by Google

# ON THE MEASUREMENT OF THE RADIUM CONTENT OF SEALED METAL TUBES.

By E. A. OWEN, M.A., D.Sc., Senior Assistant, and BERTHA NAYLOR, B.Sc., Junior Assistant, in the Physics Department.

[Reprinted from the 'Proceedings of the Physical Society of London', Vol. 34, 1922.]

Radium salts are often sealed in platinum or silver tubes for convenience and safety of application in practice. The measurement of the radium content of such tubes presents a difficulty owing to the uncertainty which exists regarding the correction that has to be applied for the absorption of the radiation in the walls of the tubes. An approximate correction is usually made by measuring the absorption of the radiation in flat sheets of the metal and calculating its value for a thickness equal to that of the wall. This, however, gives only an approximate correction even when the internal diameter of the tube is small, and it may be much in error for tubes of larger diameter. The correction to be applied depends not only upon the thickness of the wall and the diameter of the tube, but also upon the distribution of the active deposit in the tube; the active deposit may be distributed throughout the whole volume as in a tube filled with salt, or it may be mainly on the walls as in a tube containing a small quantity of highly concentrated salt which occupies only a small amount of space inside the tube.

There is, in addition, the absorption of the radiation in the salt itself which may be considerable for a tube of large diameter.* The correction due to this cause will be omitted here and attention paid only to the corrections arising from the absorption of the radiation in the walls.

The two metals, platinum and silver, will be considered, as they are the metals most frequently met with in this connection.

Two cases arise which can be completely worked out, namely, (1) the case when the tube is full of finely powdered salt and the active deposit may be assumed to be distributed uniformly throughout the whole volume; and (2) the case when the salt is highly concentrated and the amount of space occupied by it is negligible compared with the internal volume of the tube. In this case the active material will be assumed to be uniformly deposited over the walls of the tube.

In actual practice the majority of cases will be those in which the tubes are only partly filled with salt, so that the correction to be applied to the observed radium content in order to obtain the true content will be intermediate between the results arrived at in the above two cases.

* See Owen and Fage, 'N.P.L. Collected Researches', vol. 19, Paper 28, or 'Proc. Phys. Soc. Lond.', vol. 34, p. 27, 1921.



Digitized by Google

### (1) Case of the Full Tube.

It will be assumed that the tube is situated so far from the measuring chamber that an approximation to a beam of parallel rays is obtained. Let O (Fig. 1) be the axis of the tube placed at right angles to the direction OC which passes through the centre of the surface of the measuring chamber, and let I be the measured intensity of the radiation in the direction OC, and $I_0$ the true intensity if there had been no absorption. Consider an element of area $dx\,dy$ at P. The intensity of the radiation emitted from this element in the direction OC is,

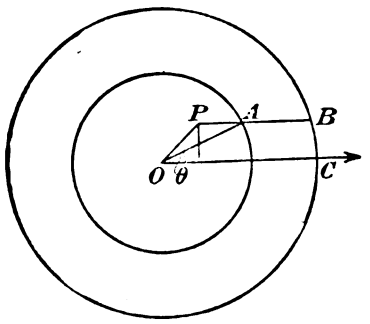


Fig. 1.

$$\frac{I_0}{\pi a^2} \cdot dx\,dy \cdot e^{-\mu \cdot AB}$$

where $$AB = \sqrt{b^2 - y^2} - \sqrt{a^2 - y^2},$$

$a$ and $b$ being the internal and external radius of the tube respectively, and $\mu$ the absorption coefficient of the radiation in the metal of the tube. The total intensity of the radiation in the direction OC is, therefore, given by

$$I = \frac{I_0}{\pi a^2} \int_{y=-a}^{y=+a} \int_{x=-\sqrt{a^2-y^2}}^{x=+\sqrt{a^2-y^2}} e^{-\mu(\sqrt{b^2-y^2}-\sqrt{a^2-y^2})}\,dy \cdot dx$$

$$= \frac{2I_0}{\pi a^2} \int_{-a}^{+a} \sqrt{a^2-y^2} \cdot e^{-\mu(\sqrt{b^2-y^2}-\sqrt{a^2-y^2})}\,dy.$$

Putting $y = a \sin \phi$, this becomes

$$\frac{I}{I_0} = \frac{2}{\pi} \int_{-\pi/2}^{+\pi/2} \cos^2\phi \cdot e^{-\mu a(\sqrt{(b/a)^2 - \sin^2\phi} - \cos\phi)} \cdot d\phi, \quad \ldots\ldots\ldots \quad (1)$$

which gives the ratio of the apparent to the true radium content of the tube.

### (2) Case of the "Empty" Tube.

In this case the active deposit which emits the hard $\gamma$ radiation, whose intensity is measured when estimating the radium content of the tube, is assumed to be entirely distributed over the walls. If I and $I_0$ have the same significance as before, the intensity of the radiation emitted in the direction OC from a small element of the surface at A is

$$\frac{I_0}{2\pi a} \cdot a\,d\theta \cdot e^{-\mu \cdot AB}$$

where

$$AB = a\left(\sqrt{\left(\frac{b}{a}\right)^2 - \sin^2\theta} - \cos\theta\right)$$

and $\theta$ is the angle which OA makes with OC.

Digitized by Google

Then the total intensity of the radiation in the direction OC is given by

$$I = \frac{I_0}{2\pi a}\int_0^{2\pi} a \cdot e^{-\mu \cdot AB} d\theta,$$

so that

$$\frac{I}{I_0} = \frac{2}{\pi}\int_0^{\pi/2} e^{-\mu a(\sqrt{(b/a)^2 - \sin^2\theta} - \cos\theta)} d\theta. \quad . \quad . \quad . \quad . \quad . \quad . \quad . \quad . \quad (2)$$

The values of the integrals appearing in equations (1) and (2) may be obtained graphically after substituting the proper values for $\mu$.

The measurement of the coefficient of absorption ($\mu$) was carried out on the same apparatus that is employed to standardise samples of radium preparations. This consists of a combined ionisation chamber and electroscope,* the radiation entering the chamber through a lead sheet 5 mms. thick. The source of radiation in the present instance was placed as far as was convenient from the chamber so as to obtain an approximation to a beam of parallel rays. Also the sheets of platinum and silver employed for measuring the absorption coefficient were small—a little larger than that necessary to shield the whole tube from the chamber, the axis of the tube being placed at right angles to the surface of the chamber. In this way the secondary radiation emitted by the absorbing screens was reduced to a minimum. Large sheets would tend to give a value of the absorption coefficient which would be too low on account of the increased amount of scattered radiation superposed upon the primary radiation transmitted by the screen.

The values of the absorption coefficient showed little variation with thickness of screen over the ranges of thickness employed, namely, up to about 0·5 mm. for platinum and 2·0 mms. for silver. The following mean values were obtained :—

| | $\mu$ mm.$^{-1}$. |
|---|---|
| Platinum . . . . . | 0·124 |
| Silver . . . . . | 0·036$_6$ |

It should be borne in mind that these values apply to radiation emitted by radium in radioactive equilibrium which has passed through 5 mms. of lead before entering the measuring chamber.

The above values of $\mu$ were substituted in the exponentials appearing in equations (1) and (2), and the expressions under the integrals evaluated for different values of $a$ and $b/a$. For each combination of values of these two quantities, a series of values for each expression was obtained for different values of angle, and curves were drawn on a large scale, whose areas were measured by means of a planimeter capable of giving the results to about 1 in 1000. A summary of the results obtained in this way is tabulated in Tables I and II. They give the percentage correction which has to be added to the

* Owen and Fage, *loc. cit.*



Digitized by Google

observed radium content in order to obtain the true radium content of tubes of various external diameters and thickness of wall. For the empty tube no further correction is needed, but for the full tube an additional correction has to be made for the absorption of the radiation in the salt itself.

TABLE I.—Platinum Tube.

| External diameter in millimetres. | Full tube. | | | Empty tube. | | |
|---|---|---|---|---|---|---|
| | Thickness of wall in millimetres. | | | Thickness of wall in millimetres. | | |
| | 0·3 | 0·4 | 0·5 | 0·3 | 0·4 | 0·5 |
| 1·5 | 4·3 | 5·3 | 6·6 | 4·9 | 5·9 | 7·0 |
| 2·0 | 4·4 | 5·5 | 6·9 | 5·3 | 6·4 | 7·6 |
| 3·0 | 4·5 | $5·7_5$ | $7·1_5$ | 5·7 | 7·1 | 8·3 |
| 4·0 | $4·5_5$ | 5·9 | 7·3 | 6·0 | 7·4 | 8·8 |
| 5·0 | 4·6 | $5·9_5$ | 7·4 | $6·2_5$ | 7·7 | 9·1 |
| 6·0 | $4·6_5$ | 6·0 | $7·4_5$ | $6·4_5$ | 7·9 | 9·4 |
| 8·0 | 4·7 | $6·0_5$ | 7·5 | $6·7_5$ | 8·3 | 9·9 |
| 10·0 | $4·7_5$ | 6·1 | 7·6 | $7·0_5$ | 8·6 | 10·3 |

TABLE II.—Silver Tube.

| External diameter in millimetres. | Full tube. | | | Empty tube. | | |
|---|---|---|---|---|---|---|
| | Thickness of wall in millimetres. | | | Thickness of wall in millimetres. | | |
| | 0·5 | 1·0 | 1·5 | 0·5 | 1·0 | 1·5 |
| 1·5 | $2·0_5$ | ... | ... | $2·2_5$ | ... | ... |
| 2·0 | $2·1_5$ | ... | ... | 2·5 | ... | ... |
| 3·0 | 2·2 | 3·9 | ... | $2·7_5$ | $4·1_5$ | ... |
| 4·0 | 2·2 | $4·0_5$ | 5·8 | 2·9 | 4·5 | 6·1 |
| 5·0 | $2·2_5$ | 4·1 | 6·0 | 3·0 | 4·7 | 6·5 |
| 6·0 | 2·3 | 4·2 | 6·1 | 3·1 | 4·9 | 6·8 |
| 8·0 | 2·3 | 4·3 | 6·2 | 3·2 | 5·2 | $7·2_5$ |
| 10·0 | 2·4 | $4·3_5$ | 6·3 | $3·3_5$ | 5·5 | 7·6 |

The tables show that when the wall thickness is kept constant, the correction increases with the external diameter of the tube. Also for the same increase of external diameter, the increase of correction is more pronounced for the empty than for the full tube. This is to be expected in view of the nature of the distribution of the active deposit in the two cases.

Digitized by Google

When the internal diameter approaches zero, it will be noted that equations (1) and (2) both become

$$\frac{I}{I_0} = e^{-\mu b}, \quad \ldots \ldots \ldots \ldots \quad (3)$$

so that the correction tends towards the value obtained for a flat sheet for both empty and full tubes as the internal diameter diminishes. The values of the corrections when the internal diameter is nearly zero are given in Table III :—

TABLE III.

| | Platinum tube. | | | Silver tube. | | |
|---|---|---|---|---|---|---|
| | Thickness of wall in millimetres. | | | Thickness of wall in millimetres. | | |
| | 0·3 | 0·4 | 0·5 | 0·5 | 1·0 | 1·5 |
| Percentage correction | $3{\cdot}6_5$ | $4{\cdot}8_4$ | $6{\cdot}0_1$ | $1{\cdot}8_1$ | $3{\cdot}6_0$ | $5{\cdot}3_5$ |

It was of interest to test the above calculations on a few practical cases. A glass tube full of radium salt was measured, and found to contain 269·0 milligrammes of radium element. This tube was afterwards divided up between six platinum tubes of 3·0 mms. external diameter and 0·5 mm. thickness of wall. Each of these tubes was filled with the salt and hermetically sealed. After the state of radioactive equilibrium was reached the tubes were measured, and the total apparent content was found to be 252·5 milligrammes radium element. The correction to be applied to this to obtain the true content, according to Table I above, is + 7·1 per cent. of the observed content, *i.e.* 18·0 milligrammes, so that the true radium content becomes 270·5 milligrammes radium element. This figure agrees within about 0·6 per cent. with the radium content of the original tube before it was divided up.

In another case a glass tube contained 121·6 milligrammes radium element before being divided up between eleven platinum tubes as follows: Two tubes of 3 mms. external diameter and 0·5 mm. wall; three tubes of 2·5 mms. external diameter and 0·5 mm. wall; and six tubes of 1·6 mms. external diameter and 0·3 mm. wall. The sum total of the contents of these tubes, after the appropriate correction had been added in each case, was found to be 122·5 milligrammes of radium element, which agrees within about 0·7 per cent. with the radium content of the original tube.

This agreement is good in view of the possibility of slight loss during sub-division and the accumulation of small experimental errors in the measurements of the tubes.

Digitized by Google

The correction for the absorption of the radiation in the salt itself which would be greater for the original tube than for all the small tubes added together, would tend to bring the two figures in each case into still closer agreement.

The above two cases suffice to show that the figures given in the above tables are sufficiently accurate for most practical purposes.

*Note added 7th March*, 1922 :—

Table IV contains the results calculated for tubes of soda glass. The value of the absorption coefficient ($\mu$) for soda glass was found to be 0·010 mm.$^{-1}$. The figures given in the table, as in the foregoing tables, are the percentage corrections which have to be added to the observed radium content to obtain the true radium content of the tubes.

TABLE IV.—Soda Glass Tube.

| External diameter in millimetres. | Full tube. | | | Empty tube. | | |
|---|---|---|---|---|---|---|
| | Thickness of wall in millimetres. | | | Thickness of wall in millimetres. | | |
| | 0·5 | 1·0 | 2·0 | 0·5 | 1·0 | 2·0 |
| | Per cent. | Per cent. | Per cent. | Per cent. | Per cent. | Per cent. |
| 3 | 0·5 | ... | ... | 0·5 | ... | ... |
| 5 | 0·6 | 1·2 | 2·2 | 0·6 | 1·2 | 2·2 |
| 10 | 0·7 | 1·2 | 2·4 | 0·7 | 1·3$_5$ | 2·5 |
| 15 | 0·7 | 1·3 | 2·5 | 0·8 | 1·5 | 2·7 |
| 20 | ... | 1·3 | 2;6 | ... | 1·6 | 2·9 |
| 25 | ... | 1·3 | 2·6 | ... | 1·7 | 3·1 |

Digitized by Google

# ABSORPTION AND SCATTERING OF GAMMA RAYS

BY

E. A. OWEN, M.A., DSc.,
SENIOR ASSISTANT,

N. FLEMING, B.A.,
JUNIOR ASSISTANT,

AND

WINIFRED E. FAGE, B.Sc.,
SOMETIME ASSISTANT IN THE PHYSICS DEPARTMENT.

Digitized by Google

## ABSTRACT.

(1) The absorption and scattering of gamma-rays from radium filtered through 23 mms. of lead have been measured in magnesium, aluminium, zinc, tin and lead.

(2) *On the assumption that the mean effective wave-length of the radiation employed is* 0·021 Å, the experimental results are consistent with the following statements :—

(i) When gamma-rays traverse matter, the characteristic radiations of the absorbing medium are excited.

(ii) The atomic fluorescent absorption coefficient of gamma-rays depends upon the wave-length of the incident radiation and the atomic number of the absorber according to the law $\frac{\tau}{\rho} . \omega = K\lambda^3 N^4$, which holds for X-rays.

(iii) The radiations which accompany this fluorescent absorption are the characteristic radiations of the K, L, M, . . . series of the absorbing elements.

(iv) The absorption of gamma-rays in light elements is due almost entirely to scattering.

(v) The pure atomic scattering absorption coefficient is proportional to the atomic number of the absorber.

(vi) In addition to fluorescent and scattering absorption, a true absorption exists, the atomic coefficient of which is proportional to the atomic number.

(3) COMPTON'S formulæ, deduced from his Quantum Theory of Scattering, would account for the experimental results if the wave-length of the incident radiation were 0·020 Å. JAUNCEY'S formulæ would require the wave-length to be 0·029 Å.


Digitized by Google

# ABSORPTION AND SCATTERING OF GAMMA-RAYS.

By E. A. OWEN, M.A., D.Sc., Senior Assistant, N. FLEMING, B.A., Junior Assistant, and WINIFRED E. FAGE, B.Sc., sometime Assistant, in the Physics Department.

[Reprinted from the 'Proceedings of the Physical Society of London', Vol. 36, 1924.]

In an investigation on the scattering and absorption of gamma-rays, Ishino* found that the greater part of the total absorption in light elements was due to scattering, and that there existed also in all the elements examined a true absorption which was approximately directly proportional to the atomic number of the absorbing element. It is of interest to enquire into the nature of this true absorption and to obtain, if possible, further data concerning the whole phenomenon of the absorption by matter of radiation of short wave-length. Such data have an important bearing upon the theories of electromagnetic radiation and of atomic structure.

A brief reference to some preliminary measurements on the absorption of gamma-rays from radium and the conclusions drawn therefrom was made in the annual report of the National Physical Laboratory for 1921. The main result arrived at was that part of the absorption, especially in the heavy elements, was due to the excitation of the characteristic radiation of the absorber. Further measurements have confirmed this conclusion, and, in addition, data have been obtained concerning the scattering of the radiation.

## Description of Apparatus.

The apparatus initially employed differed from that used by Ishino in that a rectangular chamber, the electrode of which was connected to a Wilson tilted electroscope, measured the ionisation current instead of an ordinary electroscope. With this apparatus results of the same order of magnitude as those recorded by Ishino were obtained for the absorption and scattering, although our measurements gave lower values for what he termed the true absorption. The apparatus was capable of a fair degree of accuracy, but it was considered that the form of the apparatus was such that the results obtained with it could not be easily interpreted, the chief drawback being that the rectangular chamber did not measure the ionisation produced by radiation emitted in all directions from the radiator. The apparatus finally adopted is shown in Fig. 1. Here the rectangular ionisation chamber is replaced by a spherical one, the insulated electrode of which is connected through an earthing key to a pair of the quadrants of a Dolezalek electrometer having a comparatively low sensitivity—about 1,000 divisions per volt on a scale placed about a metre in front of the instrument.

The results of different observers on the absorption of gamma-rays have shown variation according to the disposition of the apparatus employed. This is probably to be

* 'Phil. Mag.', vol. 33, p. 140, 1917.



Digitized by Google

accounted for by the different amount of scattered radiation which entered the ionisation chamber. In view of this, it was deemed advisable to give the following details concerning the experimental arrangement adopted here, so that, if desired, the experiments can be repeated by other observers.

The source of gamma radiation is a tube of radium 40·3 mms. in length and 6·4 mms. in diameter, containing the equivalent of 172 milligrammes of radium element in radioactive equilibrium. It is embedded at A (Fig. 1) in a lead block measuring 20 by 20 by

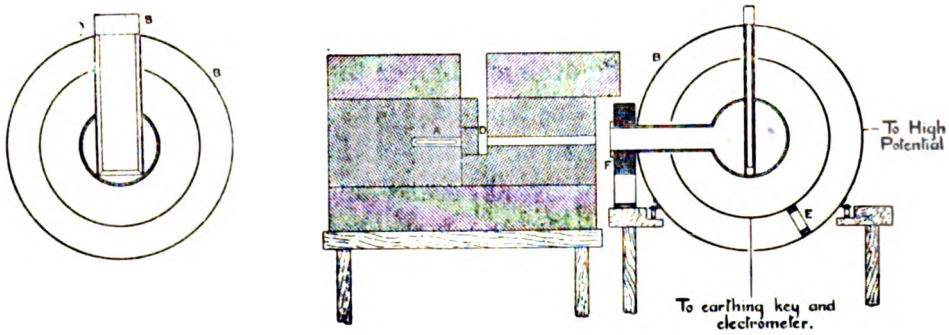


FIG. 1.

30 cms., which is made up in sections overlapping each other and fitting closely together. The mean distance of the tube from the end of the block remote from the ionisation chamber is 12·5 cms. The gamma-rays are filtered through 23 mms. of lead before reaching a rectangular hole 1 cm. square and 12 cms. long, in which the radiation is formed into a narrow beam. This hole is accurately machined, and a rod of lead fitting it closely can be inserted to block it up. In front of the 23 mms. lead filter and extending to the top of the lead block, is a space D, about 6 mms. wide and 3 cms. broad, into which the absorbing screens are placed.

The spherical ionisation chamber B is constructed from three copper spheres of diameters 9 cms., 18 cms., and 25·5 cms. respectively. The inner sphere is lined with lead 2·8 mms. thick, and is connected to the outer sphere. It is fixed to a brass tube of internal diameter 2·5 cms., held in an insulated metal clamp at F. The middle sphere which constitutes the insulated electrode is held in position by a rod of ebonite E, into which a wide sulphur ring is inserted to increase the insulation. This is connected to the electrometer by means of an earth-guarded wire passing through a hole in the outer sphere. The potential of the inner and outer spheres is 240 volts. The absorbing screens are inserted at the centre of the inner sphere by means of a carrier which moves in a slide S (8 mms. by 5 cms. in cross-section), extending to the top of the outer sphere. To obtain consistent readings when the screens are in this position, it was found that the portion of the slide between the inner and the outer spheres had to be completely covered in. When a skeleton slide was employed, the readings were unsteady for some time after the

Digitized by Google

screens were lowered into position. The precaution of covering in the slide, as indicated above, remedied this defect.

## Method of Procedure.

The ionisation currents in the spherical chamber were measured when different thicknesses of absorbing screen were placed inside the blocks and inside the spheres respectively. In the first position all the secondary radiation excited in the screens is cut away from the ionisation chamber, whereas in the second position a portion of the secondary radiation enters the chamber. For convenience the intensity of the radiation in the two cases will be denoted by $I_1$ and $I_2$.

The natural leak of the apparatus is an important factor for which allowance must be made. The apparatus is so arranged that the lead blocks can be removed and replaced again in the same position relative to the chamber. This allows the lead rod to be inserted into the rectangular hole defining the beam of radiation, so that a measurement of the natural leak can be made with the radium in position. The leak measured in this way differs appreciably from that observed when the radium is removed to a great distance.

The four metals—aluminium, zinc, tin and lead—were investigated in detail. The procedure in taking readings was to observe the time taken by the electrometer leaf to deflect through a definite angle with no absorbing screen and with increasing thicknesses of absorbing screen within the blocks or within the spheres.

## Results.

The relative ionisation currents observed with different thicknesses of absorbing screen are given in Table I. The figures are corrected for natural leak, and represent the means of a large number of observations.

When the values of $I_1$ and $I_2$ are plotted against thickness of absorbing screen, it is found that for the small thicknesses examined the resulting curves are exponential within the error of observation, so that the results may be represented by the formulæ :—

$$I_1 = {}_0I_1 e^{-\mu_1 t} \text{ and } I_2 = {}_0I_2 e^{-\mu_2 t}, \quad \ldots\ldots\ldots \quad (1)$$

where $t$ is the thickness of the absorbing screen in centimetres. The values of $\mu_1 t$ and $\mu_2 t$ calculated from the above formulæ are shown in Figs. 2 and 3* plotted against the thickness $t$. From these straight lines the mean values of $\mu_1$ and $\mu_2$ given in Table II were obtained. The values of the mass and atomic absorption coefficients are also included for reference in the same table. The value of $\mu_1$ for magnesium appearing in this table was obtained with a single sample of the material.

* The values for zinc are not shown in these figures. They are omitted to avoid confusion, as they are very nearly the same as those for tin.



Digitized by Google

TABLE I.

| Aluminium. | | | Zinc. | | | |
|---|---|---|---|---|---|---|
| Thickness of screen in cm. | $I_1$ (inside lead block). | $I_2$ (inside spheres). | Thickness of screen. in cm. | $I_1$. | Thickness of screen. in cm. | $I_2$. |
| 0·0 | 100 | 100 | 0·0 | 100 | 0·0 | 100 |
| 0·105 | 98·1 | 99·4 | 0·05 | 97·6 | 0·052 | $99·1_5$ |
| 0·210 | 97·3 | 98·9 | 0·102 | 96·2 | 0·104 | 98·2 |
| 0·315 | 95·2 | 97·9 | 0·204 | 92·2 | 0·207 | 97·1 |
| 0·42 | 93·9 | 97·7 | 0·306 | 88·5 | 0·310 | 95·2 |
| 0·525 | 92·3 | 97·3 | 0·408 | 85·1 | 0·414 | 94·0 |
| | | | 0·510 | 81·4 | 0·517 | 92·8 |

| Tin. | | | Lead. | | | |
|---|---|---|---|---|---|---|
| Thickness of screen. in cm. | $I_1$. | $I_2$. | Thickness of screen. in cm. | $I_1$. | Thickness of screen. in cm. | $I_2$. |
| 0·0 | 100 | 100 | 0·0 | 100 | 0·0 | 100 |
| 0·050 | $98·1_5$ | 99·3 | 0·053 | 96·3 | 0·050 | $98·9_5$ |
| 0·100 | 96·3 | 98·5 | 0·104 | 92·8 | 0·101 | 97·4 |
| 0·200 | 92·3 | $97·0_5$ | 0·202 | 85·8 | 0·198 | 94·1 |
| 0·300 | 89·5 | 95·5 | 0·305 | 80·4 | 0·299 | 92·0 |
| 0·400 | 85·2 | 94·5 | 0·403 | 73·9 | 0·395 | 88·9 |
| 0·500 | 82·0 | 92·7 | 0·518 | 68·9 | 0·497 | 86·8 |

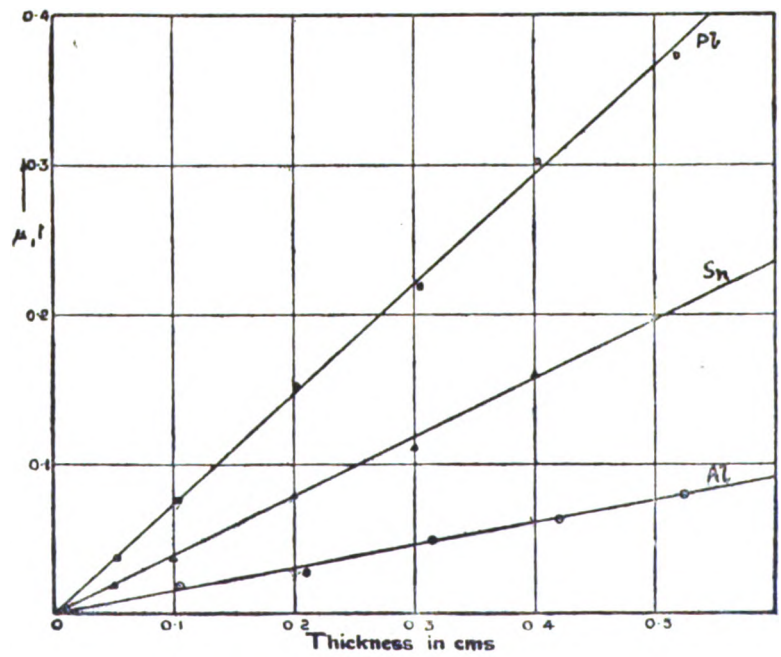


FIG. 2.

Digitized by Google

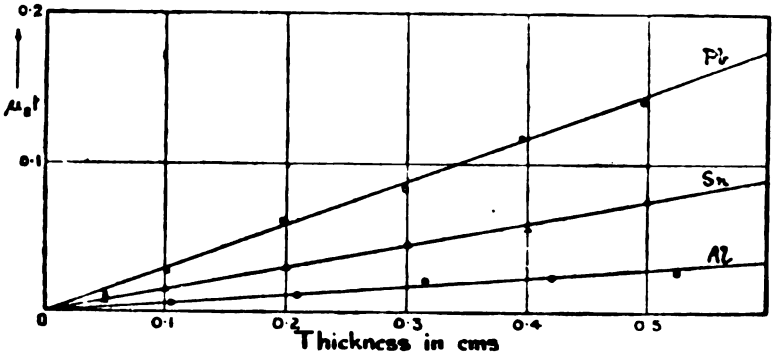


FIG. 3.

TABLE II.

| Absorbing screen. | At. No. of absorber. | $\mu_1$. | $\mu_2$. | $\frac{\mu_1}{\rho}$. | $\frac{\mu_2}{\rho}$ | $\frac{\mu_1}{\rho}$. $w+10^{24}$. | $\frac{\mu_2}{\rho}$. $w\times10^{24}$. |
|---|---|---|---|---|---|---|---|
| Mg | 12 | $0\cdot098_5$ | ... | 0·0566 | ... | 2·2 | ... |
| Al | 13 | 0·151 | 0·056 | 0·0559 | 0·0207 | 2·5 | 0·93 |
| Zn | 30 | 0·403 | 0·151 | 0·0567 | 0·0213 | 6·1 | 2·3 |
| Sn | 50 | 0·383 | 0·148 | 0·0525 | 0·0203 | 10·3 | 4·0 |
| Pb | 82 | 0·720 | 0·292 | 0·0633 | 0·0257 | $21\cdot6_5$ | 8·8 |

In previous work on this subject $\mu_2$ has been taken as a measure of the true absorption coefficient, and has been found to be approximately directly proportional to the atomic number of the absorbing element. It will be observed from Fig. 4, in which the values of the atomic absorption coefficients given in the last two columns of Table II are plotted against atomic number, that a linear relation does not exist between $\mu_2$ and N. Neither is this true for $\mu_1$ and N, the departure from proportionality being even more marked in this case. To explain these results, it is evident that we must take a different view of the absorption phenomenon of gamma radiation from that previously adopted.

## THEORETICAL.

It has been fairly well established, both experimentally and on theoretical grounds, that for X-rays the atomic fluorescent absorption coefficient is proportional to $\lambda^3N^4$, where $\lambda$ is the wave-length of the incident radiation and N the atomic number of the absorber. This law has not so far been extended to include wave-lengths as short as those of gamma-rays.

A good deal of doubt exists as to whether the phenomenon of scattering observed with X-rays is of the same nature as that observed with gamma-rays. Experiment appears to show that the scattering laws governing the former do not hold for the latter. THOMSON'S classical theory, which explains satisfactorily the scattering of X-rays by light elements when radiations of moderate wave-lengths are employed, fails to account for

Digitized by Google

the results observed with gamma-rays. For instance, the total mass absorption coefficient for hard gamma-rays has been found to be of the order of 0·05, whilst the minimum value of the scattering alone predicted by the classical theory is 0·2. The theory also fails to account for the excess amount of scattered radiation on the emergent side of a screen irradiated by X- or gamma-radiation.

Recently COMPTON* has put forward a quantum theory of scattering, which appears to explain the above facts satisfactorily. It is assumed that when an X-ray or a gamma-ray quantum is scattered, it spends all its energy and momentum upon a single electron which scatters the quantum in some particular direction. If the direction of propagation of the scattered ray is different from that of the incident ray, a change in momentum of the gamma-ray quantum takes place which results in the recoil of the scattering electron. The energy of the scattered quantum will, therefore, be less than that of the primary quantum by the kinetic energy of recoil of the scattering electron. In other words, the scattered radiation will have a longer wave-length than the primary radiation. On this view it is evident that the wave-length of the incident radiation must be less than the distance between two adjacent scattering electrons. If this be not the case, a group of electrons will take part in the scattering and, since their combined mass is comparatively great, no appreciable amount of energy is lost by recoil and the wave-length of the scattered ray will be the same as that of the incident ray. On this theory the total energy removed from the primary beam by scattering is less than that given by THOMSON'S theory in the ratio of $1 : (1 + 2\alpha)$ where $\alpha = h/mc\lambda$, $\lambda$ being the wave-length of the incident radiation, $h$ PLANCK'S constant, and $m$, the mass of the scattering electron. A part of this energy appears as scattered radiation and the remainder is truly absorbed and transformed into the kinetic energy of recoil of the scattering electron.

It will be assumed that gamma-rays lose energy by traversing matter in the following ways: (1) By the emission of corpuscular radiation, which is accompanied by characteristic radiations of the absorbing material, (2) by scattering, *i.e.* the emission of electromagnetic radiation which may or may not be of the same wave-length as the primary radiation, and (3) by the absorption of energy by electrons either resulting in their emission with the full quantum of energy of the incident radiation but unaccompanied by the emission of characteristic radiation of the traversed material (in which case the electrons emitted would come from the outer layers of the atom), or, appearing as kinetic energy of recoil of the scattering electrons in accordance with COMPTON'S views.

Turning now to our present experiments, the absorption measured when the absorbing screens are situated inside the lead block is an accurate determination of the *total* absorption, including the loss of energy by all the processes above mentioned. Thus if $\tau$ is the fluorescent absorption coefficient, $\sigma_s$ the true scattering absorption coefficient, and $\sigma_a$ the corpuscular absorption coefficient under (3) above, then

$$\mu_1 = \tau + \sigma_s + \sigma_a. \quad \ldots\ldots\ldots\ldots \quad (2)$$

* 'Phys. Rev.', vol. 21, p. 483, 1923. See also 'Bull. Nat. Res. Council', No. 20, 1922.

Digitized by Google

When the screens are situated inside the inner sphere of the ionisation chamber, the truly scattered radiation enters the ionisation chamber. If there is no change of wave-length on scattering, then the same percentage of this radiation is absorbed in the wall of the inner sphere as of the primary radiation when the screens are not interposed in the beam. Even on COMPTON'S theory, which involves a change in wave-length on scattering, the difference between the amount absorbed in the wall in the two cases will be small, since the main portion of the scattered radiation for gamma-rays is contained within an angle of about 45° with the direction of the primary beam, and over this range of angle the change in wave-length on scattering is small.

The absorption under $\tau$ has associated with it the emission of characteristic radiation, which may or may not be of such short wave-length as to penetrate appreciably the wall of the chamber. Thus the measurements made when the absorbing screens are situated in the inner sphere of the ionisation chamber may be represented by the equation

$$\mu_2 = K\tau + \sigma_a, \quad \ldots \ldots \ldots \ldots \quad (3)$$

where K has a value not greater than unity.

## ANALYSIS OF THE EXPERIMENTAL RESULTS.

The experiments of different investigators on the absorption of X-rays of short wave-length in light elements point to the conclusion that this absorption is due almost entirely to scattering and is proportional to the atomic number of the absorber. It will be assumed that this holds for gamma radiation and that, in addition, the scattering in the heavy elements is proportional to the atomic number. Referring to Fig. 4, we may on these assumptions draw the straight line OC through the origin and the experimentally determined points for the total absorption of magnesium and aluminium, to represent the total scattering. The observed curve A departs very appreciably from the line OC for the heaviest elements examined. On the view we are adopting, this divergence is due to excitation of the characteristic radiations of the heavy elements and the difference in the ordinates of the two curves will give the values of the atomic fluorescent absorption coefficients. It will be assumed for the moment that the characteristic radiations emitted are those of the K, L, . . . series of the absorbing elements. The fluorescent absorption will be considered at a later stage in the paper.

The equation to the line OC in Fig. 4, which represents the total scattering, is

$$\frac{\sigma}{\rho} w \text{ (total atomic scattering coefficient)} = 1{\cdot}93 \times 10^{-25} N. \quad \ldots \ldots \quad (4)$$

Curve B of Fig. 4 represents the experimental results obtained when the screens are situated at the centre of the spherical ionisation chamber. In this case $\mu_2 = K\tau + \sigma_a$, where K has the value unity when the characteristic radiation excited in the absorbing

Digitized by Google

screen is so soft that it does not penetrate the wall of the inner sphere of the chamber to any appreciable extent. The wall of the inner sphere is of lead 2·8 mms. thick, and calculation shows that the amount of the K characteristic radiation of tin (wave-length 0·49Å) which enters the ionisation chamber is negligible, so that for tin $\mu_2 = \tau + \sigma_a$. This relation also holds for zinc radiation. Taking the values of $\frac{\tau}{\rho} . w$ for tin and zinc from curve A and decreasing the ordinates of curve B by these amounts, it is found that the resulting points lie very approximately on a straight line through the origin and through the observed value of $\mu_2$ for aluminium. The difference between the ordinate of this straight line and that of curve B for lead is, however, 3·2 instead of 5·8, as observed in curve A. This difference is due to the fact that the characteristic radiation excited in lead penetrates the wall of the inner sphere. HULL found that $\frac{\mu}{\rho}$ for K characteristic

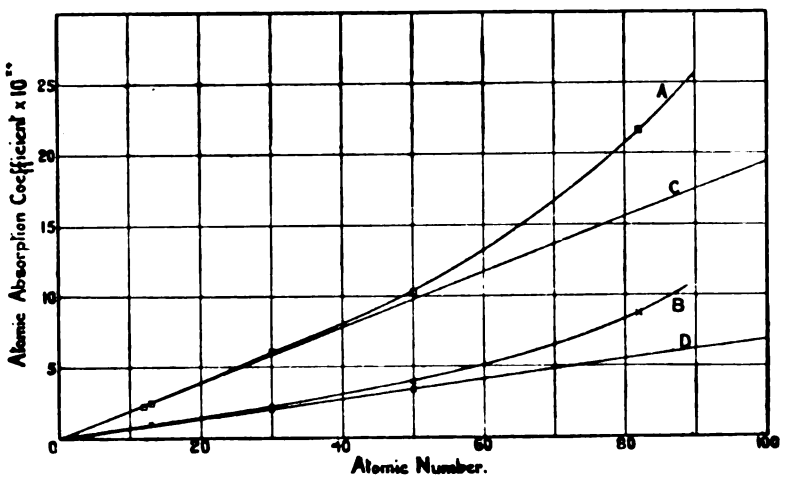


FIG. 4.

radiation of lead in lead is 1·51 approximately, so that about 0·7 per cent. of the radiation will be transmitted through the wall of the inner sphere. Correcting for this effect the difference between the ordinates of the curves B and D at the point corresponding to lead becomes equal within the error of measurement to the value of $\frac{\tau}{\rho} . w$ found for lead from the curves A and C.

The straight line OD (Fig. 4) represents the absorption of energy by electrons according to assumption (3) on p. 430. Its equation is

$$\frac{\sigma_a}{\rho} . w = 0{\cdot}68 \times 10^{-25} \mathrm{N} . . . . . \quad (5)$$

In the absence of definite data regarding the effective wave-length of gamma radiation from radium filtered through 23 mms. of lead, a satisfactory comparison of the

Digitized by Google

experimental results with the theoretical formulæ for scattering deduced by COMPTON or with the modified formulæ put forward by JAUNCEY is impossible. It may, however, be of interest to calculate from these theoretical formulæ what the mean wave-length should be to account for the scattering observed in the present investigation.

According to COMPTON's theory, the total scattering is given by the equation

$$\frac{\sigma}{\rho} \cdot w = \frac{\sigma_s + \sigma_a}{\rho} \cdot w = \frac{\sigma_0}{\rho} \cdot \frac{w}{1 + 2\alpha} = \frac{8\pi}{3} \cdot \frac{Ne^4}{m^2c^4} \cdot \frac{1}{1 + 2\alpha}, \quad \ldots \ldots \quad (6)$$

where $\alpha = h/mc\lambda$, $\lambda$ being the wave-length of the incident radiation, $c$ the velocity of light, N the atomic number, and $e$ the charge on the scattering electron measured in electrostatic units. This equation gives the value $1 \cdot 93 \times 10^{-25}$ N found by experiment for the total scattering when the wave-length is 0·020 Å.

Similarly, the absorption due to the kinetic energy of recoil of the scattering electron is given by the equation

$$\frac{\sigma_a}{\rho} \cdot w = \frac{\sigma_0}{\rho} \cdot w \cdot \frac{\alpha}{(1 + 2\alpha)^2}, \quad \ldots \ldots \ldots \quad (7)$$

which gives the experimental value $0 \cdot 68 \times 10^{-25}$ N when the wave-length is also 0·020 Å.

A mean wave-length of 0·020 Å would, therefore, account for the experimental results on COMPTON'S formulæ.

In deducing the above expressions for the intensity of scattered radiation, COMPTON reasoned from analogy with the Doppler effect in a manner which, as he himself points out, is not rigorous. JAUNCEY* has attempted to avoid this uncertainty by assuming that " quanta of X-rays in the form of corpuscles are deflected by the electrons according to a law of force such that, for corpuscles of small momentum (low-frequency quanta), the distribution of the scattered rays is that expressed by the classical theory ". He thus obtains a relation between the angle of deflection of the quantum and the distance of its undeviated path from the scattering electron and uses this relation to calculate the intensity of the scattered radiation in the case of high-frequency quanta. His expressions for the scattering differ only by second and higher powers of $\alpha$ ($\equiv h/mc\lambda$) from those of COMPTON, and in the region of X-rays ($\alpha < 0 \cdot 1$) the difference amounts at most only to a few per cent. For gamma-rays of short wave-length, however, the difference is appreciable.

According to JAUNCEY, the total scattering is given by the equation

$$\frac{\sigma}{\rho} \cdot w = \frac{8\pi}{3} \cdot \frac{Ne^4}{m^2c^4} \cdot \frac{1}{(1 + \alpha)^2}, \quad \ldots \ldots \quad (8)$$

which would require the wave-length of the incident radiation to be 0·029Å to give the experimental value for the total scattering.

* ' Phys. Rev.', vol. 22, p. 233, 1923.



Digitized by Google

Since the radiation is filtered through 23 mms. of lead, it consists mainly of the gamma radiation emitted by radium C. The highest energy lines so far observed by ELLIS* in the β-ray spectrum of radium C correspond to gamma radiations of wave-lengths 0·025, 0·021 and 0·020 Å. TUOMIKOSKI† found that the absorption coefficient of gamma radiation from radium showed little change for thicknesses of lead varying from 22 mms. to 120 mms. Thus, for a range of thickness of lead from 22 mms. to 54 mms. $\mu$ is 0·52, and for thicknesses between 54 mms. and 120 mms. $\mu$ is 0·50. This small change in the value of the absorption coefficient over such a great thickness of material would indicate that if, as is probable, radiations of shorter wave-lengths than those already recorded by ELLIS are emitted, they must be of small intensity compared with the three lines mentioned.

Since the line 0·020 Å is the most intense of these three lines, it would not be unreasonable to take 0·021 Å as the mean effective wave-length of the radiation dealt with in the present investigation, and, on this assumption, COMPTON'S theoretical formulæ for the scattering represent the experimental results very satisfactorily.

TABLE III.

| Absorber. | $\frac{\tau}{\rho} \cdot w \times 10^{24}$. | |
|---|---|---|
| | Observed. | Calculated. |
| Zn | 0·2 | 0·1 |
| Sn | 0·7 | 0·8 |
| Pb | 5·8 | 5·8 |

Returning now to the consideration of the fluorescent absorption, the differences between the ordinates of the curve A and the straight line OC in Fig. 4 give the values of the atomic fluorescent absorption coefficients. These are set out in column 2 of Table III. The values relative to lead, calculated on the assumption that the atomic fluorescent absorption coefficient is proportional to the fourth power of the atomic number, are given in column 3 of the same table. It will be observed that the observed and calculated values are in tolerable agreement, from which we conclude that the absorption in excess of that due to scattering obeys the same relation as that found for X-rays as far as the atomic number of the absorber is concerned. If, as has already been assumed, this fluorescent absorption is associated with the K, L, M, ... characteristic radiations of the absorbing element, and the absorption coefficient varies as the cube of the wave-length as with X-rays, a knowledge of the absorption coefficient for a radiation of any given wave-length enables us to calculate its value for gamma-rays. This procedure is possible only if the absorption is in the region between the same absorption bands for the wave-

* 'Roy. Soc. Proc.', A, vol. 101, p. 6, 1922.

† 'Phys. Zeits.', vol. 10, p. 372, 1909.

Digitized by Google

lengths considered. The necessary data for the calculation are available for lead and zinc. HULL and RICE* found the value of $\frac{\tau}{\rho}$ in lead for a wave-length 0·122Å to be 2·88. Hence the atomic fluorescent absorption coefficient in lead for a wave-length 0·021 Å is

$$2{\cdot}88 \times \frac{207{\cdot}2 \times 1{\cdot}664}{1{\cdot}008} \times \left(\frac{0{\cdot}021}{0{\cdot}122}\right)^3 \times 10^{-24} = 5{\cdot}1 \times 10^{-24},$$

the observed value being $5{\cdot}8 \times 10^{-24}$. The value of $\frac{\tau}{\rho} . w$ in zinc for radiation of wave-length 0·586 Å measured by OWEN† is $32{\cdot}8 \times 10^{-24}$, so that the atomic fluorescent absorption coefficient in zinc for gamma radiation of wave-length 0·021 Å, calculated as above, is $0{\cdot}16 \times 10^{-24}$, as against the observed value of $0{\cdot}2 \times 10^{-24}$ given in Table III. The values of the absorption coefficients of X-rays on which the above calculations are based are those in the K region. Considering the wide range of extrapolation, the calculated values show very good agreement with the observed values. These results support the following conclusions :—

When gamma-rays are absorbed by matter, the characteristic radiations of the absorbing medium are excited. The atomic fluorescent absorption coefficient depends upon the wave-length of the incident radiation and atomic number of the absorber according to the law

$$\frac{\tau}{\rho} . w = \mathrm{K} . \lambda^3 \mathrm{N}^4, \quad \ldots \ldots \ldots \ldots \quad (9)$$

which holds for X-rays. The radiations which accompany this fluorescent absorption are the characteristic radiations of the K, L, M, ... series of the absorbing elements.

The values of the absorption coefficients $\tau$, $\sigma_s$ and $\sigma_a$ and the corresponding mass and atomic absorption coefficients derived from the foregoing results are included in Table IV.‡

TABLE IV.—Absorption Coefficients for Gamma Radiation from Radium filtered through 23 mms. of Lead.

| Absorber. | $\tau$ | $\sigma_s$ | $\sigma_a$ | $\frac{\tau}{\rho}$ | $\frac{\sigma_s}{\rho}$ | $\frac{\sigma_a}{\rho}$ | $10^{24}$ | | |
|---|---|---|---|---|---|---|---|---|---|
| | | | | | | | $\frac{\tau}{\rho} . w$ | $\frac{\sigma_s}{\rho} . w$ | $\frac{\sigma_a}{\rho} . w$ |
| Mg | ... | 0·06 | 0·03$_5$ | ... | 0·035 | 0·020 | ... | 1·4 | 0·8 |
| Al | ... | 0·10 | 0·05 | ... | 0·036 | 0·020 | ... | 1·6 | 0·9 |
| Zn | 0·013 | 0·25 | 0·13 | 0·0019 | 0·035 | 0·019 | 0·2 | 3·8 | 2·0 |
| Sn | 0·026 | 0·23 | 0·13 | 0·0036 | 0·032 | 0·017 | 0·7 | 6·2 | 3·4 |
| Pb | 0·19 | 0·34 | 0·19 | 0·017 | 0·030 | 0·016 | 5·8 | 10·2 | 5·6 |

* ' Phys. Rev.', vol. 8, p. 836, 1916.

† ' Roy. Soc. Proc.', A, vol. 94, p. 522, 1918.

‡ The densities throughout have been taken from KAYE and LABY's ' Physical and Chemical Constants ', 4th ed., 1921, p. 22.



Digitized by Google

The fluorescent absorption is a measure of the loss of energy of the primary beam due to the emission of electrons from different energy levels in the atom. This emission of electrons gives rise to characteristic radiations in accordance with BOHR's views. In addition, the dislodged electrons produce secondary radiation by impact with atoms in their paths. It should be noted that these secondary effects are included in the measurement of the fluorescent absorption.

It has been suggested that the coefficient $\sigma_a$, which we called the corpuscular absorption coefficient, may possibly be due to the energy absorbed in the emission of electrons from the lowest energy levels in the atom. Since the work done by these electrons in getting free of the atom is negligible, their energy is equal to that of a full quantum of incident radiation in accordance with the relation $\frac{1}{2}mv^2 = h\nu$, $v$ being the velocity of the expelled electron. The fact that no electrons having a velocity corresponding to the value given by the above relation have been observed in $\beta$-ray experiments, disposes of the possibility of the emission of electrons from the outer electronic layers of the atom with the energy of a full quantum. We are therefore left with the second alternative that $\sigma_a$ represents the kinetic energy of recoil of the scattering electrons, as put forward by COMPTON.

There is a good deal of ground for the assumption that the absorption of gamma-rays in light elements is due entirely to scattering. BARKLA and WHITE,* for instance, infer from their work on the absorption and scattering of X-rays of short wave-length that "the absorption of gamma-rays in substances of low atomic weight is almost entirely absorption by scattering, which is proportional to the number of electrons in the substance traversed". That the proportionality between the scattering coefficient and the atomic number extends to the heavy elements departs from the generally accepted view, although, up to the present, the fluorescent absorption and the absorption by scattering for very short wave-length radiation have not been separated in the way attempted here.

The experiments are being extended to include a larger number of the elements.

* 'Phil. Mag.', vol. 34, p. 270, 1917.

Digitized by Google

# REVERBERATION EQUATIONS FOR TWO ADJACENT ROOMS CONNECTED BY AN INCOMPLETELY SOUNDPROOF PARTITION

BY

A. H. DAVIS, D.Sc.,
ASSISTANT IN THE PHYSICS DEPARTMENT.

Digitized by Google

## ABSTRACT.

The subject of the paper is related to a method of measuring the transmission of sound through partitions. Equations have been derived for the decay of reverberant sound in each of two chambers connected by an incompletely soundproof partition, when a source in one of the chambers is suddenly stopped. While in general the relations are complicated, they are considerably simplified if the receiving chamber has adequate absorbing power compared with the transmitting power of the partition, and if it is sufficiently less reverberant than the source room.


Digitized by Google

# REVERBERATION EQUATIONS FOR TWO ADJACENT ROOMS CONNECTED BY AN INCOMPLETELY SOUNDPROOF PARTITION.

By A. H. DAVIS, D.Sc., Assistant in the Physics Department.

[Reprinted from the 'Philosophical Mazagine', Vol. 50, 1925.]

The subject of this paper is closely related to a method of measuring the transmission of sound through a partition of a given material. In such a test the partition is built between two otherwise soundproof chambers. In one of the rooms, which is large and reverberant, an organ-pipe is sounded and after a time is suddenly stopped. Note is made of the length of time for which the residual sound is audible both in the source room and in that separated from it by the test partition.

W. C. Sabine* and P. E. Sabine† working on these lines have determined the difference in intensity in two such rooms when different thicknesses of various partitions were used. The present paper, on the basis of a reverberation hypothesis, investigates the manner in which the general duration of audibility in the two rooms in such a test may depend upon the circumstances of the experiment and the transmission factor for the partition.

The decay of sound in a single room has been considered by W. C. Sabine‡ and by Jäger§. More recently Eckhardt|| has published a treatment due to Buckingham. In all cases it is recognised that a sound suffers some two or three hundred reflections before it finally dies away, and in consequence, by random arrangement, the sound energy rapidly becomes uniformly distributed throughout the enclosure. Interference phenomena are ignored, and so results are valid only to the extent to which this is justifiable.

Buckingham assumes that the sound energy is divided up into a large number of equal parts, and that in the steady state these energy units are uniformly distributed throughout the room, both with regard to position and direction of motion. Each is assumed to move with the velocity $v$ of sound. He shows that if the intensity of sound in the room be I (*i.e.* I energy units per unit volume) the number reaching any element of boundary surface $dS$ in unit time is $\frac{1}{4}v \cdot dS \cdot I$. Of this energy a fraction will be absorbed or transmitted and the remainder reflected back into the room.

Using this result, we may readily derive differential equations governing the general intensity of sound in two adjacent rooms connected by an imperfectly soundproof partition when a source is sounded in one of them.

Let W represent the area of the test partition; $k$ the (unknown) fraction of incident

* 'Collected Papers', p. 237, 1922.

† 'Phys. Rev.', vol. 21, p. 480, 1923. 'Amer. Architect', July 28, 1920; Sept. 28, 1921; July 4, 1923.

‡ 'Collected Papers', p. 3, 1922.

§ 'Ber. Akad. Wiss. Wien.', No. 120, p. 613, 1911. See 'Science Abstracts', p. 17, 1912.

|| 'J. Franklin Inst.', vol. 195, p. 799, 1923.

Digitized by Google

energy which is transmitted through the partition on incidence; V, $V_1$ the volumes of the source and test rooms respectively; S, $S_1$ the respective total areas of exposed surface (including the partition area); $a$, $a_1$ the mean* fractions of incident energy which are lost by the room at each reflection through absorption or through transmission elsewhere; E the energy emission from the source in unit time.

Then, on the basis of the above reverberation theory, if the intensities in the two rooms be I and $I_1$ respectively, the diminution of energy in the source room due to its total surface S is $\frac{1}{4}vaSI$ units per second; the energy received in the second room in unit time by transmission through the partition area W is $\frac{1}{4}vkWI$; the energy transmitted back to the source room from the second room in unit time is $\frac{1}{4}vkWI_1$; the rate of diminution of energy in the second room is $\frac{1}{4}va_1S_1I_1$. Consequently, the following differential equations represent the energy growth in the rooms at any instant.

$$\text{Source Room} \qquad V\frac{dI}{dt}+\frac{vaS}{4}I=E+\frac{vkW}{4}I_1, \quad . \quad . \quad . \quad . \quad . \quad . \quad . \quad . \quad . \quad (1)$$

$$\text{Second Room} \qquad V_1\frac{dI_1}{dt}+\frac{va_1S_1}{4}I_1=\frac{vkW}{4}I. \quad . \quad . \quad . \quad . \quad . \quad . \quad . \quad . \quad . \quad (2)$$

*Conditions attained in Steady State under Constant Emission* E.—From the above equations we find that when the conditions become steady (i.e. $dI/dt = 0 = dI_1/dt$) the intensities have maximum values given by

$$I_{max.}=\frac{4E}{vaS\left(1-\frac{k^2W^2}{aSa_1S_1}\right)}, \quad . \quad . \quad . \quad . \quad . \quad . \quad . \quad . \quad . \quad (3)$$

$$I_{1\,max.}=I_{max.}\left(\frac{kW}{a_1S_1}\right). \quad . \quad . \quad . \quad . \quad . \quad . \quad . \quad . \quad . \quad (4)$$

*Emission stopped after Steady State has been reached.*—If through prolonged use of the source E the intensity has reached the steady values given in (3) and (4), and if the source is then suddenly stopped, the subsequent decay of sound (with E = 0) is given by the following solutions of the differential equations (1) and (2), viz.:—

$$I=I_{max.}\left\{\frac{1-\frac{4V_1\lambda_1}{va_1S_1}}{1-\frac{\lambda_1}{\lambda_2}}e^{-\lambda_1 t}+\frac{1-\frac{4V_1\lambda_2}{va_1S_1}}{1-\frac{\lambda_2}{\lambda_1}}e^{-\lambda_2 t}\right\}, \quad . \quad . \quad . \quad . \quad . \quad . \quad (5)^*$$

* If in the room there are surfaces S′, S″, S‴, etc., having respectively coefficients $a'$, $a''$, $a'''$, etc., then $aS = a'S' + a''S'' + a'''S''' +$. We may note here that for highly absorbent surfaces or highly transmissive openings, with dimensions which are small compared with the wave-length of the sound, effective areas may differ somewhat from actual values owing to diffraction effects (*cf.* P. E. SABINE, 'Phys. Rev.', vol. 19, p. 402, 1922).

† If (5) and (6) be written $I = AI_{max.}$ and $I_1 = A_1I_{1max.}$ respectively, then the solution of equations (1) and (2) corresponding to uniform sound emission beginning at zero time is

$$I = I_{max.}(1 - A) \text{ and } I_1 = I_{1max.}(1 - A_1).$$

Digitized by Google

$$I_1 = I_{1\,max.}\left\{\frac{1}{1-\frac{\lambda_1}{\lambda_2}}e^{-\lambda_1 t} - \frac{1}{\frac{\lambda_2}{\lambda_1}-1}e^{-\lambda_2 t}\right\}, \quad \ldots\ldots\ldots \quad (6)$$

where

$$\lambda_1 = \frac{v}{8}\left(\frac{aS}{V}+\frac{a_1S_1}{V_1}\right) - \frac{v}{8}\sqrt{\left(\frac{a_1S_1}{V_1}-\frac{aS}{V}\right)^2+\frac{4k^2W^2}{VV_1}}, \quad \ldots\ldots \quad (7)$$

$$\lambda_2 = \frac{v}{8}\left(\frac{aS}{V}+\frac{a_1S_1}{V_1}\right) + \frac{v}{8}\sqrt{\left(\frac{a_1S_1}{V_1}-\frac{aS}{V}\right)^2+\frac{4k^2W^2}{VV_1}} \quad \ldots\ldots \quad (8)$$

These expressions give the general conditions under which reverberant sound dies away in the two rooms when the source is stopped. It remains to ascertain the conditions to be fulfilled in the design of the chambers in order that simpler relations may be obtained.

*Conditions for Simpler Formulæ.*—(i) The expressions (7) and (8) defining $\lambda_1$ and $\lambda_2$ are much simplified if $k^2W^2/VV_1$ be small compared with $(aS/V - a_1S_1/V_1)^2$.

Since, as we shall see later, V should be larger than $V_1$, and $a_1S_1/V_1$ should be several times as great as $aS/V$, the above condition would be satisfied if, in addition, $kW$ were sufficiently small compared with $a_1S_1$.

With the condition fulfilled we have the great simplification

$$\lambda_1 = \frac{vaS}{4V}, \quad \ldots\ldots\ldots\ldots\ldots \quad (9)$$

$$\lambda_2 = \frac{va_1S_1}{4V_1}, \quad \ldots\ldots\ldots\ldots\ldots \quad (10)$$

and equation (5) reduces to $I = I_{max.}e^{-\lambda_1 t}$.

(ii) Within the brackets of (6) the term remaining in $e^{-\lambda_2 t}$ rapidly becomes negligible compared with that in $e^{-\lambda_1 t}$ provided $\lambda_2$ be several times as great as $\lambda_1$, *i.e.* if the absorbing power per unit volume for the second chamber $(a_1S_1/V_1)$ be sufficiently great compared with that $(aS/V)$ for the source room. Even a moderate ratio of, say, 2 or 3 may be sufficient in suitable cases. To this end the second room should be smaller than the first (since area per unit volume is greater for small rooms) and its surface should be more absorbent.

Possibly it is unnecessary to simplify further, but if $\lambda_2$ be as much as fifty times as great as $\lambda_1$, then the coefficient of $e^{-\lambda_1 t}$ within the brackets of (6) differs from unity by only 2 per cent., an amount which would not be perceptible in ordinary reverberation work. The higher absorptive power necessary for this would be advantageous in damping any tendency for the room to act as a resonator.



Digitized by Google

*Simplified Formulæ.*—With all the conditions fulfilled, the residual intensities in the rooms rapidly attain the values

$$I = I_{max.} e^{-vaSt/4V}, \quad . \quad . \quad . \quad . \quad . \quad . \quad . \quad . \quad . \quad . \quad (11)$$

$$I_1 = I_{1max.} e^{-vaSt/4V}, \quad . \quad . \quad . \quad . \quad . \quad . \quad . \quad . \quad . \quad . \quad (12)$$

where

$$\frac{I_{max.}}{I_{1max.}} = \frac{a_1 S_1}{kW}. \quad . \quad . \quad . \quad . \quad . \quad . \quad . \quad . \quad . \quad . \quad (13)$$

The quantity $(I_{max.}/I_{1max.})$ may be called the reduction factor for the partition, under the conditions considered.

If now T and $T_1$ be respectively the times which elapse in the two rooms before the reverberant sound dies away from its initial maximum value to the threshold of audibility, we have

$$I_{max.} e^{-vaST/4V} = I_{min.\,aud.} = I_{1max.} e^{-vaST_1/4V}, \quad . \quad . \quad . \quad . \quad . \quad . \quad . \quad (14)$$

whence

$$\log \left(\frac{a_1 S_1}{kW}\right) = \frac{vaS}{4V} (T - T_1), \quad . \quad . \quad . \quad . \quad . \quad . \quad . \quad . \quad (15)$$

a simple equation involving $k$.

The factor $\frac{vaS}{4V}$ determining the rate of decay of the sound can be obtained from a preliminary calibration of the room. For this the duration of reverberation would be determined first with a source of intensity E, and then with another of intensity $n$E: the difference in duration is the time taken for $n$-fold decay of sound in the room, and is a measure of $va$S/4V.

The simplified formulæ given above will not generally apply to the case (presumably $k = 1$) of an uncovered aperture, owing to conditions which have been introduced in the analysis. However, on extrapolating a curve of experimental results to which the formulæ apply—say for a series of diminishing thicknesses of porous non-resonant material—it is towards the value $a_1 S_1/W_1$ that the reduction factor tends as the condition of an uncovered aperture is approached, and not towards unity as might be conjectured at first glance. It is interesting, therefore, that P. E. Sabine,* working with various musical notes, found a reduction factor of about $2\frac{1}{2}$ to be indicated on an average for zero thickness of felt. While he suggests that this result may be due to surface phenomena in transmission by felt, the above analysis indicates that, apart from such a cause, factors greater than unity may arise from the circumstances of the experiment.

*Audibility at Special Points in the Second Room.*—In some conditions the above equations for reverberant sound may not represent the sound actually heard at a given point in the second room. For instance, if the room were very large and completely absorbent, there would be no general reverberation within it, but an ear situated close to the partition would detect transmitted sound. An estimate may be made of the intensity in this case.

* 'Amer. Architect', Sept. 28, 1921.

Digitized by Google

According to the above considerations, the energy transmitted in unit time through unit area of the partition would be $\frac{1}{4}kv\mathrm{I}$, which, in a simple progressive wave, corresponds to an intensity of $\frac{1}{4}k\mathrm{I}$ energy units per unit volume. With the sound in the source room decaying exponentially according to equation (11), the intensity of the entrant sound just near the partition would be

$$\mathrm{I}_e = \tfrac{1}{4}k\mathrm{I}_{max.}e^{-vaSt/4V}, \quad \ldots\ldots\ldots\ldots \quad (16)$$

a quantity which differs from the reverberant sound of equation (12) in the ratio $\frac{1}{4} : \mathrm{W}/a_1\mathrm{S}_1$.

Consequently, in some circumstances it may depend upon the position of the hearer whether (12) or (16) more nearly represents the audibility observed in the second room. However, if the chamber be suitably designed, both entrant and reverberant sound should die away at the same rate as that in the source room, and reduction factors obtained should bear a simple relation to $k$. The actual relation in a given case should be the subject of experiment.

Printed under the authority of His Majesty's Stationery Office, by Harrison and Sons, Ltd.
Printers in Ordinary to His Majesty, St. Martin's Lane, London, W.C. 2.
(B 34-2879)z Wt. 17886—1061/910 750 11/26 H & S Ltd. Gp. 34

Digitized by Google

Digitized by Google

# NATIONAL PHYSICAL LABORATORY PUBLICATIONS.

| | Price Net. s. d. | With Postage. s. d. |
|---|---|---|
| REPORTS for the years :— | | |
| 1909. (With plates) ... ... ... ... ... ... ... ... ... ... | 2 6 | 2 9 |
| 1910. (With plates and text-figures) ... ... ... ... ... ... ... | 2 6 | 2 9 |
| 1911. (With plates and plan of new Wernher Building) ... ... ... ... | 2 6 | 2 9 |
| 1912. (With plate) ... ... ... ... ... ... ... ... ... ... | 2 6 | 2 9 |
| 1913-14. (With plates, diagrams and text-figures) ... ... ... ... ... | 2 6 | 2 10 |
| 1914-15. (With plates and text-figures) ... ... ... ... ... ... ... | 2 6 | 2 10 |
| 1915-16. (With plans, plates and text-figures) ... ... ... ... ... ... | 2 6 | 2 9 |
| 1916-17. (With plans of the New Gauge Testing Laboratory) ... ... ... ... | 2 6 | 2 9 |
| 1917-18. (With plates) ... ... ... ... ... ... ... ... ... | 2 6 | 2 8 |
| 1918. (Supplementary, with scheme of work for 1919-20) ... ... ... ... | 1 6 | 1 8 |
| 1919. (With plates and text-figures) ... ... ... ... ... ... ... | 5 0 | 5 5 |
| 1920. (With plans, plates and text-figures) ... ... ... ... ... ... | 5 0 | 5 4 |
| 1921. (With plans, plates, text-figures and index) ... ... ... ... ... | 6 6 | 6 11 |
| 1922. (With plates, text-figures and index) ... ... ... ... ... ... | 9 0 | 9 6 |
| 1923. (With plates, text-figures and index) ... ... ... ... ... ... | 13 6 | 14 0 |
| 1924. (With plates, text-figures and index) ... ... ... ... ... ... | 8 6 | 9 0 |
| 1925. (With plates, text-figures and index) ... ... ... ... ... ... | 8 6 | 9 0 |
| SCREW GAUGES. Notes on, by the Staff of the Gauge Testing Department. (Enlarged issue II.) Nov., 1917, with diagrams ... ... ... ... ... ... ... *(Revised edition in preparation.)* | 2 6 | 2 8½ |
| SMALL TELESCOPE OBJECTIVES :— | | |
| Constructional Data ... ... ... ... ... ... ... ... ... ... | 2 6 | 2 8 |
| Additional Constructional Data ... ... ... ... ... ... ... ... ... | 5 0 | 5 3 |

*(Continued on p. 4 of cover.)*

Digitized by Google

# NATIONAL PHYSICAL LABORATORY PUBLICATIONS.

| COLLECTED RESEARCHES | | Price Net. s. d. | With Postage. s. d. |
|---|---|---|---|
| Vol. I. | *(Out of print)* | — | — |
| Vol. II. 1906 | | 15 0 | 16 0 |
| Vol. III. 1907 | | 25 0 | 26 0 |
| Vol. IV. 1908 | | 15 0 | 15 8½ |
| Vol. V. 1909 | | 20 0 | 21 0 |
| Vol. VI. 1910 | | 17 6 | 18 1 |
| Vol. VII. 1911 | | 18 0 | 18 8½ |
| Vol. VIII. 1912 | | 20 0 | 21 0 |
| Vol. IX. 1913 | | 18 0 | 18 8½ |
| Vol. X. 1913 | | 18 0 | 19 0 |
| Vol. XI. 1914 | | 20 0 | 21 0 |
| Vol. XII. 1915 | | 12 0 | 12 7 |
| Vol. XIII. 1916 | | 20 0 | 21 0 |
| Vol. XIV. 1920 | | 20 0 | 21 0 |
| Vol. XV. 1920 | | 20 0 | 21 0 |
| Vol. XVI. 1922 | | 20 0 | 20 9 |
| Vol. XVII. 1923 | | 17 6 | 18 3 |
| Vol. XVIII. 1924 | | 17 6 | 18 9 |
| Vol. XIX. 1926 | | 18 6 | 19 6 |
| Vol. XX. | *(In preparation)* | — | — |

Details of the papers in the volumes may be obtained from the Laboratory or H.M. Stationery Office.

The Technical Reports of the Aeronautical Research Committee from the year 1909-10 onwards may be obtained from H.M. Stationery Office, to whom application should be made for particulars. The papers contained in these reports may also be purchased separately.

The Laboratory publications may be purchased direct from H.M. Stationery Office at the following addresses:—

Adastral House, Kingsway, London, W.C.2; 120, George Street, Edinburgh; York Street, Manchester; 1, St. Andrew's Crescent, Cardiff; 15, Donegall Square West, Belfast; or through any bookseller.

*(Continued from p. 3 of cover.)*

Digitized by Google

Digitized by Google

Digitized by Google

Digitized by Google

Digitized by Google

Digitized by Google